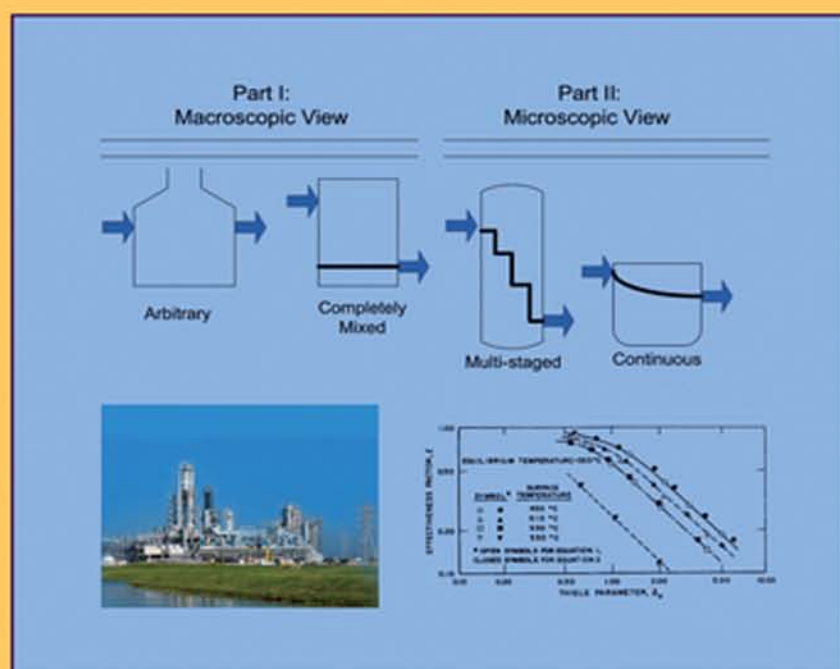


Principles of Chemical Engineering Practice

George DeLancey



WILEY

PRINCIPLES OF CHEMICAL ENGINEERING PRACTICE

PRINCIPLES OF CHEMICAL ENGINEERING PRACTICE

GEORGE DELANCEY

WILEY

Cover image reprinted with permission of BASF: The Chemical Company. All rights reserved. Graph image reprinted with permission of Elsevier, Kovenklioglu and DeLancey, 1979.

Copyright © 2013 by John Wiley & Sons, Inc. All rights reserved.

Published by John Wiley & Sons, Inc., Hoboken, New Jersey.

Published simultaneously in Canada.

No part of this publication may be reproduced, stored in a retrieval system, or transmitted in any form or by any means, electronic, mechanical, photocopying, recording, scanning, or otherwise, except as permitted under Section 107 or 108 of the 1976 United States Copyright Act, without either the prior written permission of the Publisher, or authorization through payment of the appropriate per-copy fee to the Copyright Clearance Center, Inc., 222 Rosewood Drive, Danvers, MA 01923, (978) 750-8400, fax (978) 750-4470, or on the web at www.copyright.com. Requests to the Publisher for permission should be addressed to the Permissions Department, John Wiley & Sons, Inc., 111 River Street, Hoboken, NJ 07030, (201) 748-6011, fax (201) 748-6008, or online at <http://www.wiley.com/go/permission>.

Limit of Liability/Disclaimer of Warranty: While the publisher and author have used their best efforts in preparing this book, they make no representations or warranties with respect to the accuracy or completeness of the contents of this book and specifically disclaim any implied warranties of merchantability or fitness for a particular purpose. No warranty may be created or extended by sales representatives or written sales materials. The advice and strategies contained herein may not be suitable for your situation. You should consult with a professional where appropriate. Neither the publisher nor author shall be liable for any loss of profit or any other commercial damages, including but not limited to special, incidental, consequential, or other damages.

For general information on our other products and services or for technical support, please contact our Customer Care Department within the United States at (800) 762-2974, outside the United States at (317) 572-3993 or fax (317) 572-4002.

Wiley also publishes its books in a variety of electronic formats. Some content that appears in print may not be available in electronic formats. For more information about Wiley products, visit our web site at www.wiley.com.

Library of Congress Cataloging-in-Publication Data:

DeLancey, George, 1940-

Principles of chemical engineering practice / George DeLancey.

pages cm

Includes index.

ISBN 978-0-470-53674-2 (hardback)

1. Chemical engineering. I. Title.

TP155.D425 2012

660—dc23

2012047056

Printed in the United States of America

10 9 8 7 6 5 4 3 2 1

This book is dedicated to my darling wife, Lynn, who nurtured every page and every moment with her generosity, encouragement, and unfaltering support.

CONTENTS

PREFACE	xix
PART I MACROSCOPIC VIEW	1
1 Chemical Process Perspective	3
1.1 Some Basic Concepts in Chemical Processing,	3
1.2 Acrylic Acid Production,	5
1.2.1 Catalysis,	7
1.2.2 Feed Section—Pumps and Compressors,	8
1.2.3 Reactor Section—Reactor, Heat Exchangers, and Gas Absorption,	12
1.2.4 Downstream Processing—Distillation and Extraction,	16
1.2.5 Storage,	19
1.2.6 Safety,	20
1.2.7 Overview of Typical Process,	20
1.3 Biocatalytic Processes—Enzymatic Systems,	21
1.3.1 Biotransformation,	22
1.3.2 Examples of Industrial Processes,	23
1.3.3 Alkyl Glucosides,	23
1.4 Basic Database,	24
Problems,	26
2 Macroscopic Mass Balances	28
2.1 Chemical Processing Systems,	28
Example 2.1-1: Active Units in Acrylic Acid Separation Train,	29
2.1.1 Input and Output Rates of Flow,	29
2.1.1.1 Some Equations of State,	31
Example 2.1.1.1-1: Calculate the Molar Volume of Methane at -250°F ,	32
2.1.1.2 Mass Rate of Production,	36

- 2.2 Steady-State Mass Balances Without Chemical Reactions, 37
 - 2.2.1 Degrees of Freedom, 37
 - Example 2.2.1-1: Manufacture of Sugar, 39
 - Example 2.2.1-2: Air Separation Plant, 40
- 2.3 Steady-State Mass Balances with Single Chemical Reactions, 41
 - 2.3.1 Degrees of Freedom: Reaction Rate and Key Component, 42
 - Example 2.3.1-1: Production of Formaldehyde, 42
 - Example 2.3.1-2: Manufacture of Nitroglycerin, 44
- 2.4 Steady-State Mass Balances with Multiple Chemical Reactions, 46
 - 2.4.1 Degrees of Freedom and Reaction Extents, 46
 - Example 2.4.1-1: Mass Balance on Acrylic Acid Reactor R-301, 46
 - 2.4.2 Test for Independent Reactions, 47
 - Example 2.4.2-1: Independent Reactions in the Acrylic Acid System, 47
 - Example 2.4.2-2: Selection of Independent Reactions, 48
 - 2.4.3 Construction of Independent Reactions, 48
 - Example 2.4.3-1: Independent Reactions in the Acrylic Acid System, 49
- Problems, 50

3 Macroscopic Energy and Entropy Balances 53

- 3.1 Basic Thermodynamic Functions, 53
 - 3.1.1.1 Gibbs–Duhem Equation, 55
- 3.2 Evaluation of H and S for Pure Materials, 55
 - 3.2.1 Gases—Departure Functions, 55
 - Example 3.2.1-1: Departure Functions for H and S Using the Redlich–Kwong–Soave (RKS) Equation of State, 57
 - Example 3.2.1-2: Evaluation of an Enthalpy Change for Ethylene, 57
 - 3.2.2 Liquids and Solids, 58
 - Example 3.2.2-1: Enthalpy Change in the Injection Molding of Polystyrene, 59
- 3.3 Evaluation of H and S Functions for Mixtures, 59
 - 3.3.1 Ideal Gas Mixture, 59
 - 3.3.2 Ideal Solution, 60
 - 3.3.3 Nonideal Gas Mixtures, 60
 - 3.3.4 Nonideal Liquid Solutions: Heat of Solution, 60
 - Example 3.3.4-1: Partial Molar Enthalpies for HCl–Water System, 62
- 3.4 Energy Flows and the First Law, 62
 - 3.4.1 Degrees of Freedom, 63
- 3.5 Energy Balances Without Reaction, 64
 - 3.5.1 Utilization of the Second Law, 64
 - Example 3.5.1-1: Minimum Work Required for Isothermal Pumping of a Liquid, 64
 - 3.5.2 System Definition for Duty and Flow Rate Calculation, 64
 - Example 3.5.2-1: Calculation of Heat Duty and Stream Flow Rate for Exchanger E-309, 65
 - 3.5.3 Arbitrariness of Reference State for Unreactive Systems, 66
 - Example 3.5.3-1: Energy Balance on T-303 Extraction Unit. Feed Reference State, 66
 - Example 3.5.3-2: Calculation of Net Heat Duty for Distillation Tower T-304. Feed Reference State, 67

- 3.5.4 Mixing of Nonideal Liquids; Use of Partial Molar Quantities, 68
 - 3.5.4.1 Mixing Two Liquid Streams at Different Temperatures and Concentrations, 68
 - Example 3.5.4.1-1: Dilution of an HCl Mixture, 69
- 3.6 Energy Balances with Reaction-Ideal Solution, 70
 - 3.6.1 Single Reaction-Ideal Solution, 70
 - 3.6.1.1 Reference States for Reactive Systems—Standard Heat of Reaction, 71
 - 3.6.1.2 Heat Duty and Adiabatic Operation, 72
 - Example 3.6.1.2-1 Energy Balances on Methanol Oxidation Reactor, 72
 - 3.6.2 Single Reactions—Neutralization of Acids, 74
 - 3.6.3 Multiple Reactions, 74
 - Example 3.6.3-1: Heat Duty for Acrylic Acid Reactor R-301, 75
 - Example 3.6.3-2: Feed Temperature Required in Methanol Synthesis, 76
- 3.7 Entropy Balances, 77
 - 3.7.1 Macroscopic Entropy Balance, 78
 - 3.7.2 Thermodynamic Models, 78
 - Example 3.7.2-1: Thermodynamic Models for Membrane Outlet Temperature, 78
 - 3.7.3 The Availability and Lost Work, 80
 - 3.7.4 Process Efficiency, 81
 - 3.7.4.1 Heat Exchanger with Saturated Heat Source, 81
 - Example 3.7.4.1-1: Heating Water from 25 to 95°C Using Steam at 0.125 MPa (106°C), 82
 - 3.7.4.2 Distillation, 82
 - Example 3.7.4.2-1: Column Efficiency Evaluation for Acylation Reactor Effluent in Ibuprofen Manufacture, 83

Problems, 83

4 Macroscopic Momentum and Mechanical Energy Balances 86

- 4.1 Momentum Balance, 86
 - Example 4.1-1: Force on a U-Bend, 87
- 4.2 Mechanical Energy Balance, 88
- 4.3 Applications to Incompressible Flow Systems, 89
 - 4.3.1 Flow of Liquids in Piping Systems, 89
 - 4.3.1.1 Flow in Pipes—The Friction Loss Factor, 89
 - 4.3.1.2 Sudden Expansion—Calculation of Friction Loss Factor, 91
 - 4.3.1.3 Fittings and Valves, 91
 - 4.3.1.4 Pump Sizing, 91
 - Example 4.3.1.4-1: Power Required for P-301 A/B: Acrylic Acid Plant, 91
 - Example 4.3.1.4-2: NPSH Consideration in Pumping *o*-Dichlorobenzene from Temporary Storage to Process Storage, 93

Problems, 94

5 Completely Mixed Systems—Equipment Considerations 95

- 5.1 Mixing and Residence Time Distributions—Definitions, 95
 - Example 5.1-1: Production of *n*-Hexyl Glucoside—Residence Time and Reactor Volume, 96

- 5.2 Measurement and Interpretation of Residence Time Distributions, 97
- 5.3 Basic Aspects of Stirred Tank Design, 99
 - 5.3.1 Tank Dimensions and Impeller Specifications, 99
 - Example 5.3.1-1 Mixer Dimensions for T-303 Alternative Solution, 100
 - 5.3.2 Heuristics for Mixing and Agitation, 102
 - 5.3.2.1 Power Requirements, 102
 - 5.3.2.2 Gas–Liquid Systems, 103
 - 5.3.2.3 Liquid–Liquid Systems, 103
 - Example 5.3.2.3-1 Power Required for T-303 Alternative, 104
 - 5.3.2.4 Solid Suspensions, 104
 - Example 5.3.2.4-1 Sizing of Hexyl Glucoside Slurry Adsorber, 105
- Problems, 106

6 Separation and Reaction Processes in Completely Mixed Systems 107

- 6.1 Phase Equilibrium: Single-Stage Separation Operations, 107
- 6.2 Gas–Liquid Operations, 109
 - 6.2.1.1 Gas Absorption and Stripping, 109
 - 6.2.1.2 Flash Vaporization, 110
 - 6.2.2 Vapor–Liquid Equilibrium, 111
 - 6.2.2.1 Equation of State Method, 112
 - 6.2.2.2 Activity Coefficient Method, 115
 - 6.2.2.3 Summary of VLE Expressions and Data, 125
 - Example 6.2.2.3-1: Comparison of Several Methods for Obtaining the K Values for an Equimolar Mixture of Ethane, Propane, and n -Butane at -70°F and 300 psi, 125
 - 6.2.3 Gas Absorption and Stripping, 126
 - 6.2.3.1 Mass Balance—Constant Total Flows, 128
 - 6.2.3.2 Mass Balances—Nondiffusing Components, 130
 - Example 6.2.3.2-1: Acetone Absorption, 130
 - Example 6.2.3.2-2: Determine the Solvent Requirements for Single-Stage Version of Tower 302: Off-Gas Absorber in Acrylic Acid Process, 132
- 6.3 Flash Vaporization, 133
 - 6.3.1 Mass Balances, 133
 - 6.3.2 Energy Balance, 134
 - 6.3.3 Equilibrium, 134
 - 6.3.4 Common Problem Specifications, 134
 - 6.3.5 Distribution Function—Limitations, 135
 - 6.3.6 Bounds on Bubble and Dew Points, 135
 - 6.3.7 Solution for $\mathcal{N}^{(V)}/\mathcal{N}^{(F)} = 0$, P —Bubble-Point Temperature, 135
 - Example 6.3.7-1: Calculate the Bubble Point of the Following Mixture at 2 atm, 136
 - Example 6.3.7-2: Saturation Temperature for IPA–Water System, 136
 - 6.3.8 Solution: for $\mathcal{N}^{(V)}/\mathcal{N}^{(F)} = 1$, P Specified: Dew-Point Temperature, 137
 - Example 6.3.8-1: Calculate the Dew Point of the Mixture in the Preceding Example, 137
 - Example 6.3.8-2: Calculate the Dew Point of an Equimolar Mixture of Propylene and Isobutane at 20 atm Assuming an Ideal Liquid and Application of the Peng–Robinson Equation of State for the Vapor, 137

- Example 6.3.8-3: Repeat Example 6.3.8-2 but Use the DePriester Charts to Formulate the Equilibrium Relations, 139
- 6.3.9 Solution for T, P Specified: Isothermal Flash, 140
 - Example 6.3.9-1: Isothermal Flash Calculation, 141
 - Example 6.3.9-2: Flash of the Extract from the Acid Extractor (Tower 303), Stream 13, 141
- 6.3.10 General Isothermal Flash Iteration, 143
- 6.3.11 Sizing of Flash Drum, 143
 - Example 6.3.11-1: Size the Flash Drum for Example 6.3.9-1, 144
- 6.4 Liquid–Liquid Extraction, 145
 - 6.4.1 Equilibrium in Ternary Systems, 145
 - 6.4.1.1 Solvent Selection, 146
 - 6.4.1.2 Data Collection and Representation, 146
 - 6.4.1.3 Interpolation, 147
 - 6.4.2 Single-Stage Operation, 147
 - 6.4.2.1 Equipment, 147
 - 6.4.2.2 Mixture Rule, 148
 - 6.4.2.3 Mass Balances, 148
 - Example 6.4.2.3-1: Extraction of HAc from Chloroform with Water, 149
 - Example 6.4.2.3-2: T-303 Acid Extractor—Solvent Flow for Single Equilibrium Stage, 150
- 6.5 Adsorption, 151
 - 6.5.1 Adsorbents, 152
 - 6.5.2 Gas Adsorption, 154
 - 6.5.2.1 Equilibrium Relations for a Single Adsorbate, 156
 - 6.5.3 Liquid Adsorption, 157
 - 6.5.3.1 Equilibrium, 157
 - 6.5.3.2 Liquid Adsorption Operations, 157
- 6.6 Single-Phase Stirred Tank Reactors, 159
 - 6.6.1 Continuous Stirred Tank Reactors, 160
 - 6.6.1.1 Liquid Phase Systems—Temperature Specified, 160
 - 6.6.1.2 Gas Phase Systems—Temperature Specified, 161
 - Example 6.6.1.2-1: Multiple Second-Order Reactions and Sizing of R-301, 162
 - 6.6.1.3 Selection of Reactor Temperature, 163
 - Example 6.6.1.3-1: Temperature Selection for Acrylic Acid Reactor, 164
 - 6.6.1.4 CSTR—Energy Balance, 165
 - Example 6.6.1.4-1: *A Priori* Calculation of Heat Load on Acrylic Acid Reactor R-301, 165
 - 6.6.1.5 Autothermal Operation, 166
 - 6.6.1.6 Heuristics, 168
 - 6.6.2 Isothermal Batch Reactor, 168
 - 6.6.2.1 Mass Balance, 168
 - 6.6.2.2 Liquid Phase Reactions at Constant Density, 169
 - 6.6.2.3 Some Background for Example 6.6.2.3-1, 169

- Example 6.6.2.3-1: Production of L-Tyrosine-Feed Stock to L-Dopa Plant, 170
 - 6.6.2.4 Gas Phase Reactions and Equation of State at Constant Volume, 172
 - Example 6.6.2.4-1: Reaction Order for Sulfuryl Chloride Oxidation, 173
 - 6.7 Chemical Reaction Equilibrium, 174
 - Example 6.7-1: Equilibrium Constant for the Synthesis of Hexyl Glucoside by Condensation, 176
 - Example 6.7-2: Check on Methanol Conversion to Formaldehyde, 176
 - Example 6.7-3: Phase Equilibrium with Chemical Reaction—Synthesis of Hexyl Glucoside, 178
 - Problems, 179

PART II MICROSCOPIC VIEW 181

7 Multistage Separation and Reactor Operations 183

- 7.1 Absorption and Stripping, 183
 - 7.1.1 Isothermal Binary Gas Absorption, 184
 - 7.1.2 Countercurrent Cascade-Tray Tower, 185
 - 7.1.3 Graphical Procedures for Single Components, 186
 - Example 7.1.3-1: Butane Recovery—Fixed Number of Stages, 190
 - 7.1.4 Isothermal Liquid Stripping, 191
 - Example 7.1.4-1: Stripping of Acetone from Water, 193
 - 7.1.5 Dilute Multicomponent Absorption and Stripping, 194
 - Example 7.1.5-1: Methane Purification, 195
 - 7.1.6 Column Efficiency, 196
 - 7.1.7 Column Diameter and Height, 197
 - Example 7.1.7-1: Tower 303: Off-Gas Absorber in Acrylic Acid Process, 197
 - 7.1.8 Heuristics for Absorption, 199
- 7.2 Distillation, 200
 - 7.2.1 Construction of Distillation Operation, 200
 - 7.2.2 Equipment for Distillation, 201
 - 7.2.3 Application of Material and Energy Balances to Feed Tray, 203
 - 7.2.4 Degrees of Freedom, 204
 - 7.2.5 Material Balance for Enriching or Rectifying Section, 205
 - 7.2.6 Material Balance for Stripping Section, 206
 - 7.2.7 Intersection of Operating Lines, 206
 - Example 7.2.7-1: Operating Lines in Acetic Acid–Water Distillation, 207
 - 7.2.8 Number of Stages, 208
 - Example 7.2.8-1: Number of Stages for Acetic Acid–Water Distillation, 210
 - 7.2.9 High Purity Products, 210
 - Example 7.2.9-1: Stages Required for Acetic Acid–Water Distillation Using the Recursion Relations, 211
 - 7.2.10 Energy Requirements, 212
 - 7.2.10.1 Total Condenser, 212
 - 7.2.10.2 Partial Condenser, 212
 - 7.2.10.3 Reboiler, 212

Example 7.2.10.3-1: Energy Loads on the Acetic Acid Distillation Tower, 213	
7.2.11 Efficiency and Column Height, 213	
Example 7.2.11-1: Height of Acetic Acid–Water Column, 214	
7.2.12 Summary of Calculations and Setting Process Operating Conditions, 214	
Example 7.2.12-1: Determine the Minimum Number of Stages for the Acetic Acid–Water Distillation, 215	
Example 7.2.12-2: Determine the Minimum Reflux Ratio for the Acetic Acid–Water Distillation, 215	
7.2.13 Heuristics for Distillation Towers, 217	
Example 7.2.13-1: Tower 305, 218	
7.3 Liquid–Liquid Extraction, 221	
7.3.1 Multistage Cross-Flow Cascade, 221	
7.3.2 Multistage Countercurrent Operation, 222	
Example 7.3.2-1: Extraction of Acetone from MIBK with Water, 224	
Example 7.3.2-2: T-303 Acid Extractor—Number of Equilibrium Stages and Solvent Flow Required, 229	
7.3.3 Extraction Equipment, 232	
7.3.4 Height and Efficiency of Sieve Tray Towers, 233	
Example 7.3.4-1: Height and Number of Trays on Tower 303 with Unagitated Sieve Tray Design, 233	
7.3.5 Mixer–Settler Units, 234	
Example 7.3.5-1: Typical Settler Size for Mixer–Settler Alternative to Tower 303, 234	
7.3.6 Heuristics for Liquid–Liquid Extraction, 234	
7.4 Multiple Reactor Stages, 235	
7.4.1 Comparison with Batch Reactor, 235	
7.4.2 Comparisons with Plug Flow Reactor, 235	
7.4.3 Number of Stages Required for a Given Conversion, 236	
Example 7.4.3-1: Number of Stages for a Diels–Alder Reaction, 236	
7.4.4 Temperature Programs for CSTR Stages, 237	
7.4.4.1 Single Reactions, 237	
7.4.4.2 Multiple Reactions, 238	
7.5 Staged Fixed-Bed Converters for Exothermic Gas Phase Reaction, 238	
Example 7.5-1: Staged Fixed-Bed Converter for SO ₂ Oxidation, 240	
Problems, 241	

8 Microscopic Equations of Change

243

8.1 Mass Flux: Average Velocities and Diffusion, 244
8.1.1 Mass Flow Rates Used in Material Balances, 245
8.1.2 Average Velocities and Diffusion Flows, 246
8.1.3 Superficial Velocities, 248
Example 8.1.3-1 Slip Velocity in Liquid–Liquid and Gas–Liquid Systems, 248
8.2 Momentum Flux: Stress Tensor, 249
8.3 Energy Flux: Conduction, 250
8.4 Balance Equations, 251
8.4.1 Mass Conservation, 251
8.4.2 Linear and Angular Momentum Balance, 252
8.4.3 Conservation of Energy, 252

8.5	Entropy Balance and Flux Expressions, 254
8.5.1	σ_0 : Scalar Processes, 255
8.5.1.1	Volume Flow, 255
8.5.1.2	Homogeneous Reaction Kinetics, 255
8.5.1.3	Heterogeneous Catalytic Kinetics, 256
8.5.2	σ_1 : Vector Processes: Diffusion and Conduction, 260
8.5.3	Viscous Momentum Flux, 261
8.5.4	Estimation of Transport Coefficients, 261
8.5.4.1	Diffusivities, 261
	Example 8.5.4.1-1 Estimation of Methane Diffusivity in Nitrogen for Application to Effective Diffusion in Honeycomb Monolith Reactor, 261
8.5.4.2	Thermal Conductivities, 261
8.5.4.3	Viscosity, 265
8.6	Turbulence, 265
8.6.1	Time-Averaged Mass Balance, 266
8.6.2	Turbulent Flux Expressions, 267
8.6.2.1	Empty Tubes, 267
8.6.2.2	Radial Dispersion in Packed Beds, 268
8.6.2.3	Axial Dispersion, 268
8.7	Application of Balance Equations, 269
8.7.1	Boundary Conditions, 269
8.7.2	Reduction to Scalar Equations: Laminar Flow in Tubes, 270
8.7.3	Introduction to Dimensionless Numbers and Characteristic Times, 272
8.7.4	Dual Geometry and Boundary Conditions for Fixed Beds, 274
	Problems, 275

9 Nonturbulent Isothermal Momentum Transfer 276

9.1	Rectangular Models, 276
9.1.1	Slit Flow: Extrusion of Plastics Through Narrow Dies, 276
	Example 9.1.1-1: Average Velocity and Volumetric Flow Rate, 280
9.2	Cylindrical Systems, 280
9.2.1	Axial Flow—Flow in Pipes and Tubes, 280
	Example 9.2.1-1: Volumetric Flow Rate, 281
	Example 9.2.1-2: Average Velocities, 281
9.2.1.1	Friction Factor, 281
9.2.1.2	Pump Requirements, 281
9.2.1.3	Distribution of Residence Times, 282
9.2.1.4	Laminar Flow Reactor (and Substantial Derivative), 282
	Example 9.2.1.4-1: Application of Microscopic Mass Balance to Laminar Flow Reactor, 282
9.2.1.5	Wetted Wall Towers, 283
	Example 9.2.1.5-1: Error in Film Thickness Approximation, 285
9.2.2	Angular Flow, 286
9.2.2.1	Couette Viscometer, 286
9.3	Spherical Systems, 287
9.3.1	Creeping Flow Around a Solid Sphere, 287

- 9.3.1.1 Application to Decanter Design, 289
 - Example 9.3.1.1-1: Separation of an Oil Water Mixture, 289
- 9.4 Microfluidics—Gas Phase Systems, 289
 - 9.4.1 A Model of Gas Flow in Microchannels, 290
 - 9.4.1.1 Momentum and Mass Balances, 290
 - 9.4.1.2 Mass Balance: Axial Velocity Distribution, 291
 - 9.4.1.3 Pressure Distribution, 292
 - Example 9.4.1.3-1: Helium Flow in a Long Microchannel, 294
- Problems, 294

10 Nonturbulent Isothermal Mass Transfer 296

- 10.1 Membranes, 296
 - 10.1.1 Material Balance for Generic Membrane, 297
 - 10.1.2 Gas Separations, 298
 - Example 10.1.2-1: Greenhouse Gas Removal from Power Station Flue Gas—Completely Mixed Membrane Model with No Sweep, 300
 - 10.1.3 Liquid Separations—Reverse Osmosis, 301
 - Example 10.1.3-1: Regeneration of Pulp Feed Solution in Paper Production, 304
 - 10.1.4 Porous Asymmetric and Composite Membranes—Overall Mass Transfer Coefficient, 305
- 10.2 Diffusion Models for Porous Solids, 307
 - 10.2.1 Effective Diffusivity of Porous Catalysts, 307
 - 10.2.1.1 Pore Diffusion, 307
 - 10.2.1.2 Surface Diffusion, 308
 - 10.2.2 Tortuosity Factor Model, 309
 - 10.2.3 Parallel Pore Model, 309
 - Example 10.2.3-1: Evaluation of Tortuosity in Parallel Pore Model for Honeycomb-Type Monolith Catalyst, 310
- 10.3 Heterogeneous Catalysis, 311
 - 10.3.1 Effectiveness of a Single Closed Pore, 311
 - Example 10.3.1-1: Key Component Kinetics for SO_2 Oxidation, 313
 - 10.3.2 Effectiveness of Catalyst Particle, 314
- 10.4 Transient Adsorption by Porous Solid, 316
 - Example 10.4-1: The Recovery of Hexyl Glucoside, 317
- 10.5 Diffusion with Laminar Flow, 318
 - 10.5.1 Wetted Wall Tower—Short Contact Time, 318
 - 10.5.1.1 Physical Absorption, 318
 - 10.5.1.2 Chemical Absorption, 319
 - 10.5.2 Laminar Flow in a Tube with Catalytic Walls, 320
- Problems, 322

11 Energy Transfer Under Nonturbulent Conditions 324

- 11.1 Conduction in Solids—Composite Walls, 325
 - Example 11.1-1: Insulated Firebox for Steam Reforming, 326
- 11.2 Thermal Effects in Porous Catalysts, 327
 - 11.2.1 Temperature Rise due to Single Chemical Reaction, 327
 - 11.2.2 Effectiveness Factor for Single Irreversible Reaction with Heat Effect, 328

- 11.3 Heat Transfer to Falling Film—Short Contact Times, 330
- 11.4 Moving Boundary Problem, 332
- Example 11.4-1: Onset of Freezing in a Pipe, 333
- Problems, 334

12 Isothermal Mass Transfer Under Turbulent Conditions 335

- 12.1 Intraphase Mass Transfer Coefficients, 335
 - 12.1.1 Film-Penetration Theory, 335
 - 12.1.2 Penetration Theories, 337
 - 12.1.3 Film Theory, 338
- 12.2 Interphase Mass Transfer Coefficients—Controlling Resistances, 338
- 12.3 Measurement and Correlation of Mass Transfer Coefficients, 339
 - 12.3.1 Measurement of Mass Transfer Coefficients, 339
 - 12.3.2 Correlation of Mass Transfer Coefficients, 340
 - Example 12.3.2-1: Determination of Liquid Mass Transfer Coefficients in a Fixed Bed, 341
- 12.4 Fixed Beds, 342
 - 12.4.1 Fixed-Bed Adsorption, 342
 - 12.4.1.1 Ideal Case, 342
 - 12.4.1.2 More General Model, 343
 - 12.4.1.3 Gas Phase, 343
 - 12.4.1.4 Intraparticle Diffusion, 344
 - 12.4.1.5 LDF (Linear Driving Force) Model, 344
- 12.5 Pipes, 345
 - 12.5.1 Turbulent Flow in a Pipe with Catalytic Walls, 345
- 12.6 Particles, Drops, and Bubbles in Agitated Systems, 346
 - 12.6.1 Slurry Adsorption—External Mass Transfer Control, 347
 - Example 12.6.1-1 Adsorption Time and Batch Integration in Continuous Processes, 348
- 12.7 Packed Towers—Gas Absorption, 349
 - 12.7.1.1 Heuristics for Packed Towers, 349
 - 12.7.2 Mass Transfer Correlations, 350
 - 12.7.3 Mass Balances, 351
 - 12.7.3.1 For the Liquid, 352
 - 12.7.3.2 For the Gas, 352
 - 12.7.3.3 Unreactive Case with Henry's Law, 353
 - Example 12.7.3.3-1: Sulfur Dioxide Absorber, 355
- 12.8 Application of Experimental Mass Transfer Coefficients, 357
 - 12.8.1 Free Fluxes, 357
 - 12.8.2 Constrained Fluxes, 358
 - 12.8.2.1 Diffusion Through a Stagnant Film: Absorption with Constant Flows, 358
 - Example 12.8.2.1-1: Height of Packed Bed in SO₂ Absorption Using Method Suitable for Nonlinear Equilibrium Data, 359
 - 12.8.2.2 Equimolar Counter-Diffusion, 360
 - 12.8.2.3 Heterogeneous Chemical Reaction, 360
 - 12.8.2.4 Kinetics Experiments, 361

12.8.2.5	Fixed-Bed Reactor Modeling, 362	
12.8.3	Homogeneous Chemical Reaction, 362	
12.8.3.1	Irreversible First-Order Kinetics, 363	
12.8.3.2	Surface Renewal Theory, 364	
12.8.3.3	Instantaneous Reactions, 364	
12.8.3.4	Linearized Kinetics, 365	
	Problems, 365	
13	Interphase Momentum Transfer Under Turbulent Conditions	367
13.1	Pressure Drop in Conduits and Fixed Beds, 368	
13.1.1	Turbulent Flow of Gases in Pipelines, 369	
13.1.1.1	Isothermal Flow in Pipelines, 370	
	Example 13.1.1.1-1: Pressure Drop and Pipe Size for Gas Supply Line, 370	
13.1.1.2	Compressors, 372	
13.1.2	Pressure Drop in Fixed Beds, 375	
13.2	Flow Over Submerged Spheres, 376	
13.2.1	Momentum Balance for Single Particle, 377	
	Example 13.2.1-1: Diameter of Gas-Liquid Separators, 377	
13.2.2	Terminal Velocities in Newtonian Fluids: Solid Suspensions, 377	
	Example 13.2.2-1: Slurry Adsorption of Hexyl Glucoside, 378	
13.2.3	Fluidization Velocities: Diameter of Fluidized Beds, 379	
	Example 13.2.3-1: Diameter of R-301 Reactor, 380	
13.2.4	Flooding Velocity in Packed Towers: Tower Diameter and Pressure Drop, 381	
	Example 13.2.4-1: Sulfur Dioxide Absorber, 382	
	Problems, 383	
14	Interphase Energy Transfer Under Turbulent Conditions	384
14.1	Heat Transfer Coefficients—Analogy with Mass Transfer, 384	
14.2	Heat Exchangers, 385	
14.2.1	Double Pipe Exchangers, 387	
	Example 14.2.1-1 Cooling of HCl Product from Adiabatic Mixing, 389	
14.2.2	Shell and Tube Heat Exchangers, 390	
14.2.2.1	Constant Wall Temperature, 390	
	Example 14.2.2.1-1: Exchanger 309—Solvent Endings, 392	
14.3	Multi-Tubular Catalytic Reactors, 395	
14.3.1	Fixed-Bed Constant Wall Temperature One-Dimensional Model, 395	
14.3.1.1	Bulk Phase Mass Balance (Molar Units), 396	
14.3.1.2	Particle Phase Mass Balance (Molar Units), 397	
14.3.1.3	Particle Phase Energy Balance, 397	
14.3.1.4	Bulk Phase Energy Balance, 397	
14.3.1.5	Momentum Balance on Interstitial Fluid, 398	
14.3.2	Some Operational Considerations, 398	
	Problems, 399	
15	Microscopic to Macroscopic	400
15.1	Macroscopic Mass Balance, 400	

15.2 Macroscopic Energy Balance,	401
15.3 Macroscopic Mechanical Energy Balance,	402
15.3.1 Unsteady-State Form,	403
15.3.2 Steady-State Systems,	403
Problems,	404

APPENDIX A	PERIODIC TABLE	405
APPENDIX B	CONVERSION FACTORS	406
APPENDIX C	PARTIAL DATABASE FOR ACRYLIC ACID PROCESS	409
APPENDIX D	SOME MATHEMATICAL RESULTS	414
APPENDIX E	MASS BALANCE IN CYLINDRICAL COORDINATES AND LAMINAR FLOW IN Z DIRECTION	418
NOMENCLATURE		419
REFERENCES		423
INDEX		427

PREFACE

This book is about the application of scientific principles and engineering experience to chemical processing. Major chemical engineering operations are organized under the principles of analysis in order to facilitate the consideration of new technologies from a chemical engineering point of view.

New applications have emerged in chemical engineering practice. Microchemical systems, for example, require attention to design parameters not important at larger scales. The shift from commodity chemicals to chemical products by many smaller companies is creating a demand for chemical engineers with a broader view of design than the traditional capstone design experience (Cussler and Moggridge, 2001). Biocatalysis and the chiral technology industry call for the support of undergraduate curricula. Opportunities for the chemical engineering graduate in the development of medical devices and drug manufacture call for more emphasis on the life sciences and physiology.

There is therefore a call to introduce a degree of flexibility into traditional undergraduate chemical engineering curricula for those who wish to serve a broader industrial base. An alternative is to concentrate the basic chemical engineering training in a minimal core designed to secure the distinguishing technical character of the chemical engineer and to provide the ground both for further specialization in traditional chemical engineering and for coherent studies in other areas. The minimization decisions regarding the required topics and the depth of coverage are local decisions that reflect the mission of the program.

This text can support such a local decision process as a consolidation of normally separate courses in material and energy balances, transport phenomena, reactor design, and separations. While not a replacement for these courses, it is

a functional treatment of the underlying skills that characterize them. The selection of major operations reflects the intention of establishing a minimum competency level required to be differentiated as a chemical engineer in an undergraduate engineering curriculum.

Although the book is primarily meant for chemical engineering undergraduates, it may be appropriate for conversion programs designed to prepare graduates of other engineering and science programs for matriculation in chemical engineering master's programs.

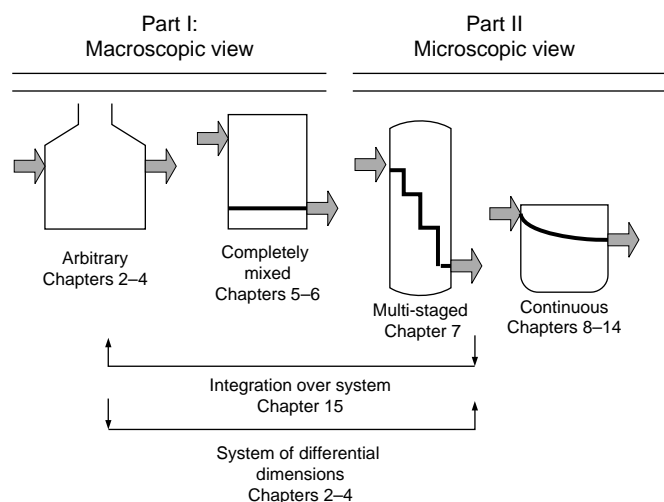
Graduate engineers in both academic and industrial positions may find it convenient to have a single resource with wide coverage.

CONTENT

The principles referred to above consist of the conservation of mass, energy, and momentum at the macroscopic and microscopic levels as well as the principle of the increase of entropy and characterization of equilibrium states by equilibrium thermodynamics. The production of entropy provides an important measure of process efficiency and underpins the conservation laws by providing a theoretical foundation for the nonconvective flows. In addition, the balance equations and equilibrium relations are used to develop models of the chemical process operations from the rate or equilibrium stage point of view, respectively. Efficiency is a link between the two.

The chemical engineering operations that are discussed in the text are as follows:

- Separators
- Heat exchangers.



Organization.

A process flow diagram for the manufacture of acrylic acid is presented at the outset and used for an introduction to chemical processing and equipment. Reference to the acrylic acid process is continued thereafter for presentation of new material in a process context. Example calculations in the text are compared with simulator results pertaining to equipment sizes and operating conditions in the acrylic acid plant.

Heuristics are regarded as fundamental tools and are stated extensively. They are used in calculations and are compared with some independent calculations. Degrees of freedom are employed throughout the earlier sections of the book.

Process control, economics, and safety are not included.

ORGANIZATION

Two major divisions of the subject matter in the text are made on the basis of a macroscopic and a microscopic view: The balance equations for mass, energy, momentum, and entropy are applied at the macroscopic level confined to the equipment ports, through completely mixed and staged systems to the continuous variations within equipment (see Organization).

The “macroscopic view” ensures the conservation of mass, energy, and momentum at the equipment and process levels with consideration only of the conditions at the entrances and exits of the process equipment. The exception is completely mixed systems where the uniform interior conditions appear at the outlet. The macroscopic view is taken at the level of process synthesis where the conditions are consistently set for each processing step to establish the

overall process design and economics. The microscopic view is subsequently adopted to arrive at the detailed design of the processing equipment and the final economics. This viewpoint can provide conditions at every location within the equipment boundaries. For multistaged systems consisting of completely mixed subsystems, the conditions vary stepwise throughout the equipment. The microscopic view ensures the local conservation of mass, energy, and momentum. The macroscopic view is therefore the net effect of this local role, which can be seen by integration over the system volume, thereby “closing the circle.”

CALCULATIONS

Many examples are provided within the chapters throughout the text to elucidate the discussion. Two process-related threads are carried through the examples (see Tables 1.7 and 1.8) in order to provide a broad process perspective for the calculations. Questions for discussion and encouragement to complete the argument or calculation appear periodically. A variety of problems are suggested at the end of chapters in order to initiate the problem-solving activity as a learning tool and to provide experience with scientific and engineering databases. The collection can be augmented to meet specific course objectives or a desired orientation without modifications to the chapters.

Scientific Notebook (MacKichan Software) and Microsoft Excel are primarily used in the example calculations. Scientific Notebook was chosen because the students who used the notes had prior experience with this software in their mathematics courses and they preferred this software over others that were available to them. Moreover, this

software is particularly compatible with the notation used throughout this book.

Excel was used because the ease with which objects could be moved on graphs, the magnification options, and the ability to construct multifunctional plots greatly facilitated stepping off stages and other graphical constructions. The

tabular formulation of recursive calculations is readily accomplished in Excel.

Some experience with the use of this software in an introductory course is available in DeLancey (1999).

GEORGE DELANCEY

PART I

MACROSCOPIC VIEW

CHEMICAL PROCESS PERSPECTIVE

The objective of this chapter is to provide an introduction to chemical processing and chemical processing equipment and to establish a realistic context for much of the more quantitative developments of the same topics appearing in the remaining chapters. A preliminary design of an acrylic acid process (Turton et al., 2003) with a complete flow sheet and stream table provides this context. A connected set of examples and exercises concerned with equipment sizing, material and energy balances, or stream and operating conditions threaded throughout the text are related to the acrylic acid process. The location and nature of these examples are summarized in Table 1.7.

Catalytic aspects of chemical processing are raised in the acrylic acid process and in biocatalytic systems with an introduction to enzyme catalysis. Industrial biotransformations are discussed and the production of hexyl glucoside is selected to provide the context for a second connected thread of examples and exercises throughout the text. In contrast to the acrylic acid thread, this selection is based on a proposed new process with much less information. The examples are therefore in the categories of scale up and process development. The location and nature of the examples in the subsequent chapters are summarized in Table 1.8.

1.1 SOME BASIC CONCEPTS IN CHEMICAL PROCESSING

It will be useful in the following discussion to have in mind what is meant by equilibrium, the steady state, and driving force. These ideas primarily underpin the steps in chemical

processing and fall into the three thermodynamic categories: thermal, chemical, and mechanical. The first two categories are discussed below. The third is left to the reader (see Problem 1.1).

Thermal Refer to Figure 1.1a. Here we imagine that two fluids not necessarily of the same phase are introduced into the two chambers of a rigid insulated container with impermeable walls. The two chambers are separated by a rigid dimensionless barrier (to allow the transfer of heat without mass transfer) and the fluids fill the two mixed chambers. The temperature of the hot fluid (A) will decrease and the temperature of the cold fluid (B) will increase, each approaching the same temperature at the equilibrium state.

If, on the other hand, the fluids are drawn at the same rate they are fed, they will reach a **steady-state** temperature that is constant throughout each phase except for a narrow region near the dimensionless diathermal wall where the temperature decreases continuously from the high to the low value. The same equilibrium temperature is approached from either side of the interface. The two phases are prevented from reaching the intermediate state by the continual replacement and removal of the transferred energy.

If the flows are stopped, the system will equilibrate as in Figure 1.1a. We therefore think of the steady state being subjected to a **driving force** proportional to the distance from equilibrium as in Figure 1.1c where the flux of thermal energy is the response to the force. Since each approaches zero together, we take the linear approximation that the flux is proportional to the force.

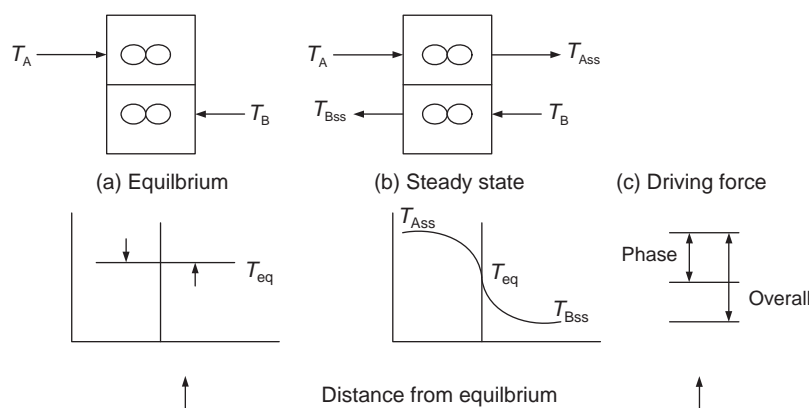


FIGURE 1.1 Rate and equilibrium in thermal processes.

We can focus on one phase and think of the driving force as the distance from the equilibrium value or we can think of the overall driving force as the difference between the phase temperatures. Both driving forces refer to the same flow of energy at steady state and each approaches zero at equilibrium.

Chemical—Unreactive Reaction Refer to Figure 1.2a. We again consider an insulated container with rigid impermeable walls. Here we charge the container with two immiscible liquid phases containing components that are partially soluble in both phases. We will assume for simplicity that the dissolution process of any one of the components in either phase involves no heat effect. Otherwise we would need to repeat the “thermal” discussion. We also assume that no reactions take place. Chemical reactions will be discussed separately.

Similar to the temperature in thermal phenomena, the concentration of each species will increase or decrease until a steady value is reached in each phase. This is a state of **interphase chemical equilibrium**. A fundamental

difference from the thermal case is that the values are not the same in each phase. Whereas the potential for the transfer of thermal energy is the temperature, thermodynamics tells us that the chemical potential is a function of the temperature, pressure, and composition in each phase.

If, as above, the fluids are withdrawn at the same rate they are fed, the concentrations will reach steady-state values that are constant throughout each phase, except for a narrow region near the dimensionless open barrier where the concentrations change stepwise to the values in the companion phase.

If the flows are stopped, the system will equilibrate as in Figure 1.2a. We therefore think of the steady state being subjected to a **driving force** proportional to the distance from equilibrium as in Figure 1.2c where the flux of mass is the response to the force. Since each approaches zero together, we take the linear approximation that the flux of mass is proportional to the driving force.

We can focus on one phase and think of the driving force as the distance from the equilibrium value for that phase or we can think of the overall driving force as the difference

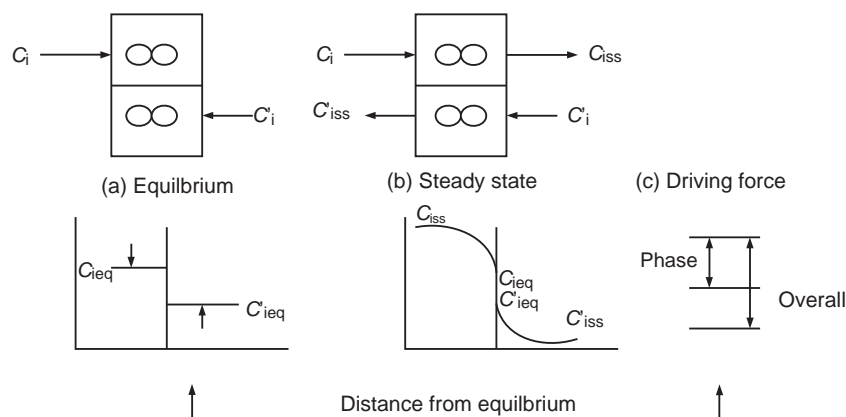


FIGURE 1.2 Rates and equilibrium in chemical processes—interphase phenomena.

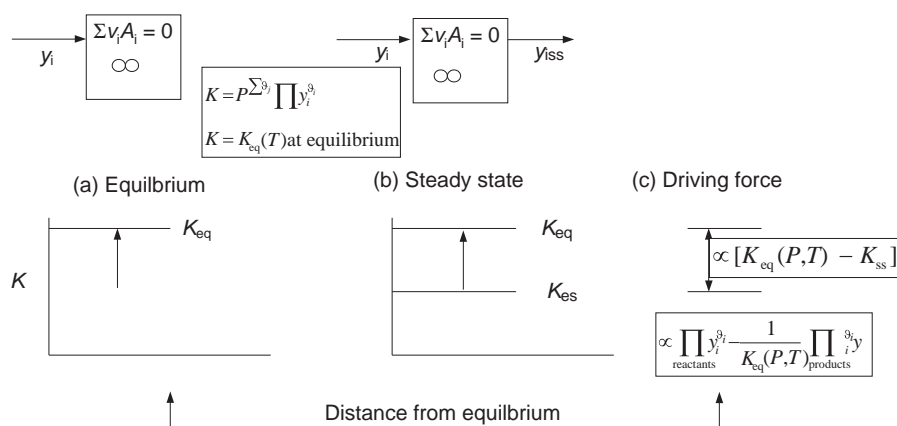


FIGURE 1.3 Reaction rates and equilibrium.

between the phase compositions. Since the interphase equilibrium compositions are not the same, the overall driving force will need to be modified slightly to assure that the rate is the same as that calculated in either phase.

Chemical—Single Ideal Gas-Phase Reaction The case of chemical reaction equilibrium is a bit more complicated in that reaction equilibrium is characterized by the chemical affinity, a linear combination of the chemical potentials mentioned in the preceding paragraph. We can, however, arrive at reaction kinetics, which are at least qualitatively correct and sufficient to understand some basic behavior of chemical reactors. We will consider a single ideal gas-phase reaction for which thermodynamics tells us that the ratio K in Figure 1.3a has a specific value at equilibrium $K_{eq}(T)$.

We again consider a container with rigid impermeable walls. Here we take the walls to be diathermal in order to begin and end the reaction process at the same temperature. We charge the container with a reactive ideal gas mixture. The value of K will increase as shown in Figure 1.3a until the equilibrium value is attained after which no further change will take place. This is the **intrapphase chemical equilibrium** condition. For irreversible reactions, the value of K is extraordinarily large.

If gases are withdrawn at the same rate they are fed as illustrated in Figure 1.3b, the products will be prevented from accumulating and therefore the value of K_{eq} will be prevented from being reached. The concentrations T and P will reach **steady-state** values that are constant throughout. If the flows are stopped, the system will equilibrate as in Figure 1.3a. We therefore think of the steady state being subjected to a **driving force** proportional to the distance from equilibrium as in Figure 1.3c where the rate of reaction is the response to the force. Since each approaches zero together, we take the linear approximation that the flux of mass is proportional to the driving force. The result shown in Figure 1.3c is the law of mass action.

1.2 ACRYLIC ACID PRODUCTION

Figure 1.4 is a process flow diagram of a continuous process for the manufacture of 50,000 metric ton/year of 99.9 mol% acrylic acid from a one-step oxidation of propylene. One reactor is therefore used, which stands in contrast to the commonly used dual reactor system. The process is based upon the 1986 AIChE Student Contest Problem. The process conditions and equipment sizes are reported by Turton et al. (2003).

There are a number of commercial software packages that are known to produce accurate designs of chemical processes in the hands of experienced engineers (Aspen Plus, Aspen Hysys, Chemcad, etc.). Turton et al. (2003) used Chemcad and expected the results to represent a preliminary process design. We will use the calculated results as if they were actual plant data. Actual plant data at this level of detail are neither available nor needed in light of the sophistication of the software to gain a familiarity with process concepts as well as equipment and basic ideas in chemical engineering analysis and design. However, any comparisons of approximate calculations with these calculations are comparisons with more rigorous calculation procedures, not actual data.

Continuous processes are common in the chemical industry where such products as organic chemicals, plastics, and solvents are produced in large quantities to meet market demands. These products are referred to as bulk or commodity chemicals. Batch processes on the other hand are commonly used by the pharmaceutical industry to produce a wide variety, but small amounts, of pharmaceuticals. These products fall under the category of fine chemicals. Semicontinuous process is the combination of batch and continuous processing, in which the chemical state of one or more chemical compounds is altered stepwise toward a well-defined target. A process flow diagram (PFD) is a schematic representation of the process.

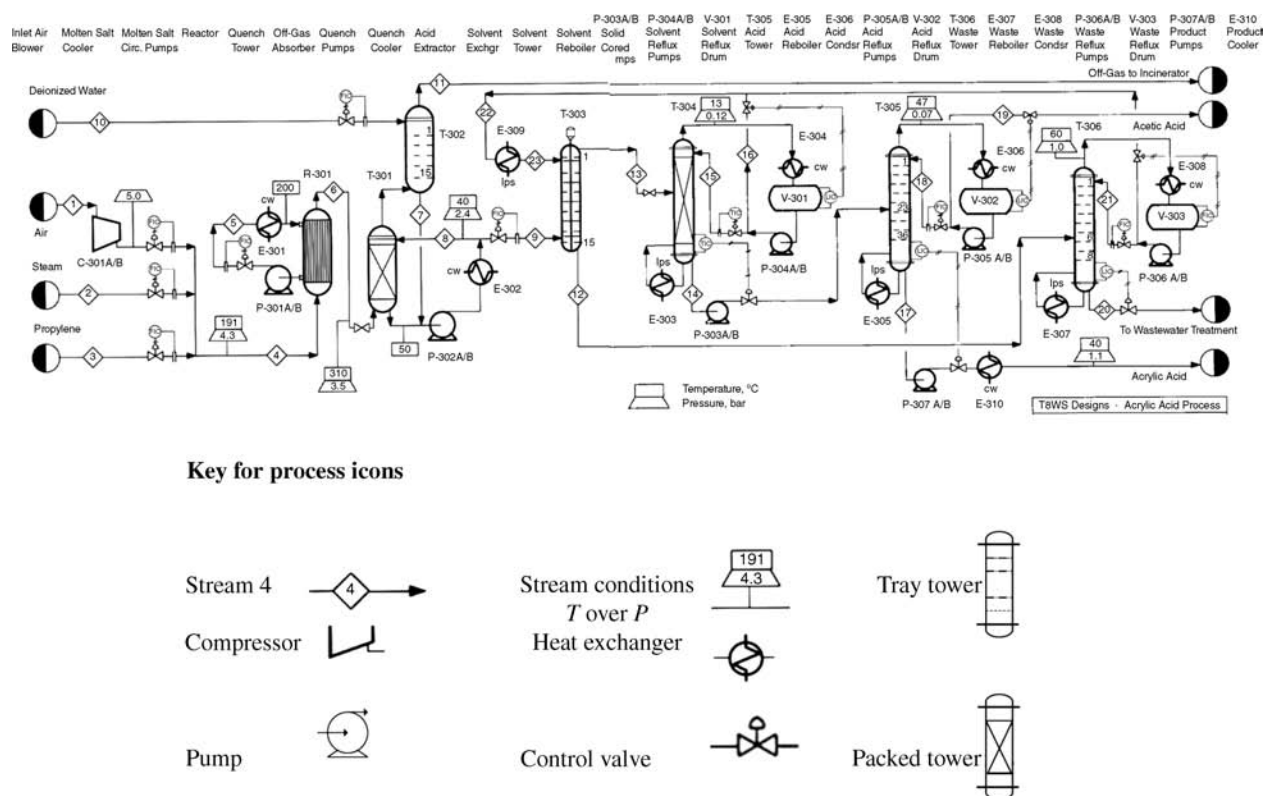


FIGURE 1.4 Process flow diagram for acrylic acid production plant (Turton et al., 2003). Reprinted with permission of Pearson.

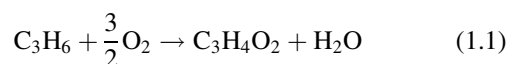
In a chemical process, material is moved in streams by mechanical devices such as pumps and compressors from one process unit to another. A summary of the schematic representations of these items is given in Figure 1.4.

The streams are connected to the process units by pipes and ducts for fluids and by screw or belt conveyors in the case of solids, for example. The process units perform operations on the content of the streams to change their temperature, pressure, phase, and/or composition. These units are often referred to as unit operations and are carefully configured by the chemical engineer to transform raw materials into the desired products, economically and safely. Some units are combinations of unit operations.

All of these processes consist of a sequence of operations in which the process streams begin at raw material storage and end with product storage. There are other streams called utilities, which are employed by the process units as sources or sinks of thermal energy. The supply and regeneration of the utility streams may be part of the process or these services may be supplied by a separate facility. In the latter case, the utility streams arrive and are returned after use to the utility site for regeneration.

We will look more carefully into each of these aspects of chemical processing for the production of 50,000 metric ton/year of acrylic acid via the process given in the flow diagram

(Figure 1.4). Normally, the adopted chemical route is the result of an intensive search involving technical, economic, and safety considerations. More than one route may be simulated to better evaluate the economics of the final competitors. A two-step process comprised of the oxidation of propylene to acrolein followed by the oxidation of acrolein to acrylic acid (Speight, 2002) is the common industrial choice. In the present case, the partial oxidation of propylene has been selected from other alternative routes to acrylic acid, which may be viewed as an alternative proposition for a single-step process over a new catalyst.



An economic view can be initiated at the outset of process development by considering only the raw material costs and product sales price. The net change for the chemical reaction must, of course, be positive or “economically endothermic” before the reaction is even considered to be a possibility for adoption. Some chemical prices are available in the *Chemical Market Reporter*, available online by subscription. Professional publications such as *Chemical and Engineering News* and *Chemical Engineering Progress* publish limited pricing information. In general, there is a cost associated

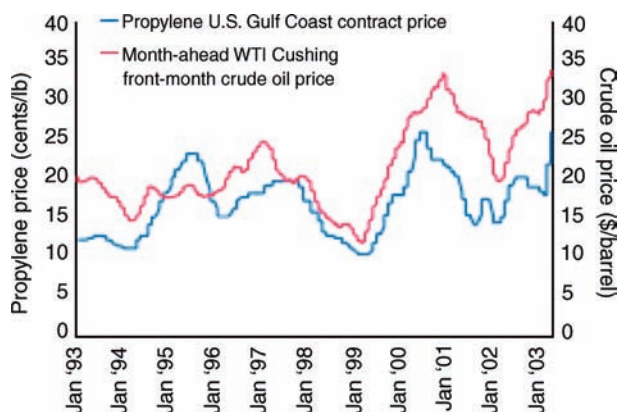


FIGURE 1.5 Propylene versus crude oil spot price: 1993–2003 (*Market Watch*, May 2003). Reprinted with permission of Platts and Global view.

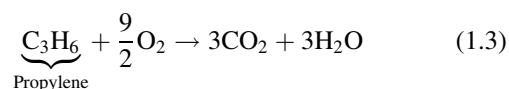
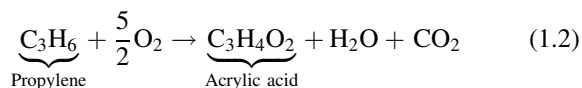
with obtaining chemical prices. Economic studies can also be a source of historical pricing. For example, the correlation between the price of propylene and the cost of crude oil is shown in Figure 1.5.

These results agree with the data published by TIG (<http://www.the-innovation-group.com/welcome.htm>) for propylene, which report a high of \$0.225/lb and a low of \$0.145/lb over the period from 1994 to 1999. The TIG profile for acrylic acid (propenoic acid) reports a high of \$0.49/lb and a low of \$0.41/lb over the period from 1997 to 2002. In the economic valuation of a sulfur dioxide generation process (Schendel, 1993), the price of oxygen was estimated at \$35/tonne.

Based on the conservative side of these figures, we can use the following prices to develop an approximate, albeit dated, economic evaluation of the partial oxidation of propylene as shown in Table 1.1.

The gross return per lb of propylene is \$0.473. This means that for a 50,000 metric ton/year production of acrylic acid, there is \$13,780/h available for all of the costs associated with manufacturing the chemicals, such as paying off loans, salaries, taxes, shipping, and certainly profit. Can you think of other costs? An analysis such as this is an important consideration in the selection of a chemical route from alternative possibilities.

We have not considered the full reaction system. The main reaction is accompanied by two undesirable side reactions [see Equations (1.2) and (1.3)]:



With some knowledge of the relative extent of the second two reactions, we could refine the economic evaluation. The second reaction [Equation (1.2)] has some economic compensation because acetic acid is a salable by-product. The third reaction [Equation (1.3)] is a complete liability.

The reactions are catalyzed by a single catalyst deposited on the interior walls of a porous solid support.

1.2.1 Catalysis

The conversion of reactants to products is often more than simply mixing the ingredients. Reactants are, in some limited sense, stable raw materials and must pass through some reactive intermediate state before the transformation to products can take place. A catalyst is a material that repeatedly promotes this intermediate condition from a renewed initial state with each repetition. The availability of a catalyst that, for example, acts only on the desirable reaction (chemoselective) and on a particular site within a molecule (regioselective) can determine whether or not a process is commercialized. Consequently, catalytic processes are common throughout the chemical industry. In addition, natural processes in living organisms are replete with examples of catalytic systems and chemical engineers are learning to use these sophisticated catalysts as a resource.

The action of catalysis in both cases can be simply characterized as follows (after Denbigh, 1971).

Consider the hypothetical reaction



and refer to Figure 1.6.

TABLE 1.1 Economic Analysis of Propylene Oxidation

Species	Cost (\$/lb)	Molecular Weight	Cost (\$/lb mole)	Reaction Contribution
Propylene	0.2250	42.081	9.47	−9.47
Oxygen	0.0175	16.000	0.28	−0.142
Acrylic acid	0.4100	72.065	29.55	29.55
Total lb mole				\$19.94

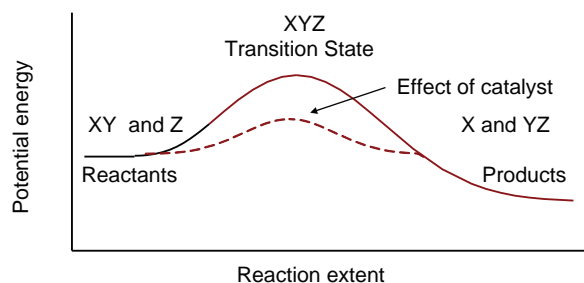


FIGURE 1.6 Potential energy path for a simple reaction.

Let us suppose that the potential energy of the system can be represented in three dimensions associated with distances between the reactant and product molecules. Three dimensions limits the number of atoms involved in the reaction to two molecules, say one free (Z) and one (Y) combined with others in a reactant (XY). There will be troughs in the surface at short atomic distances between the reactant and product molecules corresponding to stable molecular configurations (XY and YZ). Before reaching these troughs, the potential energy of the system will pass through very high peaks due to the repulsive forces between the reactants. These peaks are associated with the formation of molecular configuration in a *transition state* composed of both the original and final atoms (XYZ), the original (X) in a state of repulsion. The system falls into a trough when the transitory intermediates fall into the stable product configurations (YZ). The peak represents an energy barrier the system must overcome. A catalyst lowers that barrier.

A catalyst can be present in the same phase as the reactants or it may be in a separate phase. The first case, referred to as homogeneous catalysis, is found often in liquids. For example, the absorption of carbon dioxide into carbonate–bicarbonate solutions is catalyzed by arsenite (Danckwerts, 1970). The second case is referred to as heterogeneous catalysis where the catalyst is often solid. For example, vanadium pentoxide catalyzes the gas-phase oxidation of sulfur dioxide in sulfuric acid manufacture. Solid catalysts are most often supported on porous solids with very high internal surface areas, which serve primarily to retain the catalyst in the reactor with high availability. An internal area of 250 m²/g or approximately six football fields/quarter pound is common.

Catalysis accounts for approximately 60% of chemical products and 90% of the chemical processes (Vision 2020 Catalyst Report, 1997). In order to meet environmental regulations, for example, the chemical industry must desulfurize gas and diesel fuels (Bianchini et al., 2004). Much of the sulfur in fossil fuels is contained in thiophenic molecules of which benzothiophene (BT) is an example.

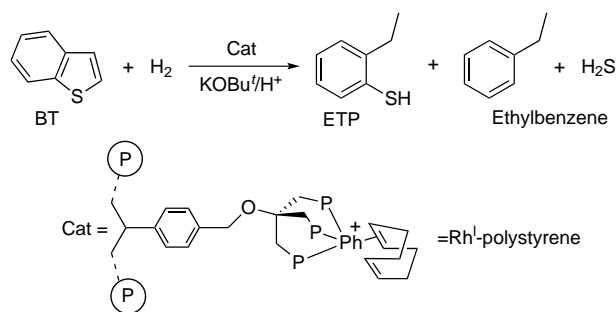


FIGURE 1.7 Hydrogenolysis of benzothiophene (Bianchini et al., 2004).

The hydrogenolysis of BT to 2-ethylthiophenol (ETP) and ethylbenzene with an Rh^I-polystyrene catalyst is shown in Figure 1.7.

The catalyst is bound to a flexible polystyrene matrix, which allows the cooperation between two adjacent metal sites, as shown in Figure 1.8.

Many catalysts in the petrochemical industry are simply composed of a metal on a porous support. Figure 1.9 is an example of Pt catalyst particles on alumina. Additional examples of nonenzymatic commercial catalytic processes are shown in Table 1.2.

Returning now to the acrylic acid process, the raw materials are propylene and oxygen, which is supplied by air.

1.2.2 Feed Section—Pumps and Compressors

Propylene and air are introduced in streams 1 and 3 on the left of the flow diagram shown in Figure 1.10. An important and ever present concern is safety. In this case, a hydrocarbon is present with oxygen, which can lead to ignition or explosive conditions. For this reason, steam is introduced in stream 2 in

RhI-polystyrene catalyst with two adjacent Rh atoms indicated (M)

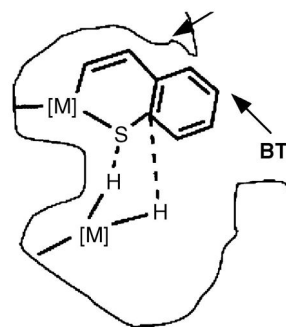


FIGURE 1.8 Adjacent metal sites in an Rh^I-polystyrene catalyst (Bianchini et al., 2004). Reprinted with permission of Elsevier.

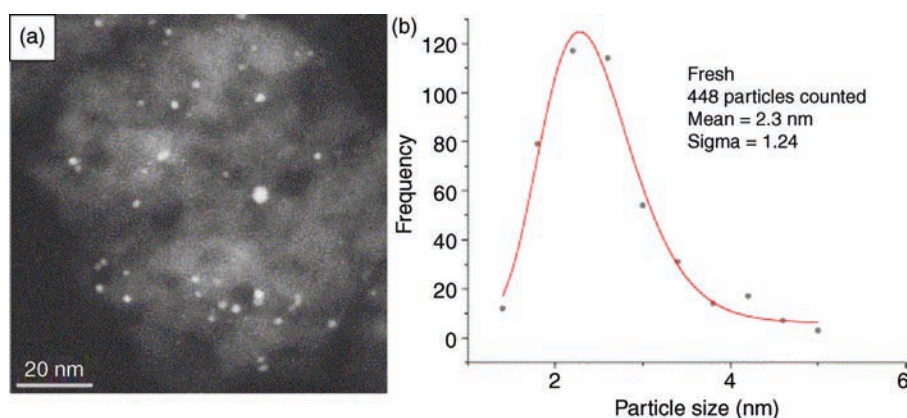


FIGURE 1.9 Stem image (a) and particle size distribution (b) of Pt on Al₂O₃ (Abhay et al., 2006). Reprinted with permission of Elsevier.

TABLE 1.2 Examples of Commercial Catalysts (Smith, 1981)

Process	Typical Catalysts	Poisons
Alkylation of hydrocarbons	H ₂ SO ₄ (l), HF(l), AlCl ₃ + HCl, H ₃ PO ₃ /kieselguhr	Substances that reduce acidity
Hydrocarbon cracking	Crystalline synthetic SiO ₂ –Al ₂ O ₃ (zeolites)	Nitrogen compounds, metals (Ni, V, Cu), coke deposition
Chlorination of hydrocarbons	CuCl ₂ /Al ₂ O ₃	
Dehydration	γ-Al ₂ O ₃ , SiO ₂ –Al ₂ O ₃ , WO ₃	Coke deposition
Dehydrogenation	Cr ₂ O ₃ /Al ₂ O ₃ , Fe, Ni, Co, ZnO, Fe ₂ O ₃	H ₂ O
Desulfurization of petroleum fractions	Sulfided Co–Mo/Al ₂ O ₃	
Fischer–Tropsch process	Ni/kieselguhr, Fe + Fe ₂ C + Fe ₃ O ₄	
Hydrogen from naphtha, coal	Ni/refractory	Sulfur, arsenic, coke deposition
Hydrogenation	Ni/kieselguhr, NiO, Ni–Al (Raney nickel), Pt/Al ₂ O ₃ , Pd/Al ₂ O ₃ , Ru/Al ₂ O ₃	Sulfur, chlorine compounds
Hydrocracking of coal, heavy oil	NiS, Co ₂ O ₃ –MoO ₃ /Al ₂ O ₃ , W ₂ O ₃ , ZnCl ₂	
Isomerization	AlCl ₃ + HCl, Pt/Al ₂ O ₃	
Oxidation, inorganic	Pt, V ₂ O ₅ , Rh, CuCl ₂ (HCl to Cl ₂)	Arsenic, chlorine compounds
Oxidation, organic (liquid phase)	CuCl ₂ (aq) + PdCl ₂ , Pd/Al ₂ O ₃ , Co + Cu, acetates	
Oxidation, organic (gas phase)	V ₂ O ₅ /Al ₂ O ₃ , Ag–AgO, CuO, bismuth molybdate	
Polymerization	Al(C ₂ H ₅) ₃ , P ₂ O ₅ /kieselguhr, MoO ₃ –CoO/Al ₂ O ₃ , CrO ₃ /(SiO ₂ > Al ₂ O ₃), TiCl ₃ –Al(CH ₃) ₃	H ₂ O, O ₂ , sulfur compounds, CO, CO ₂

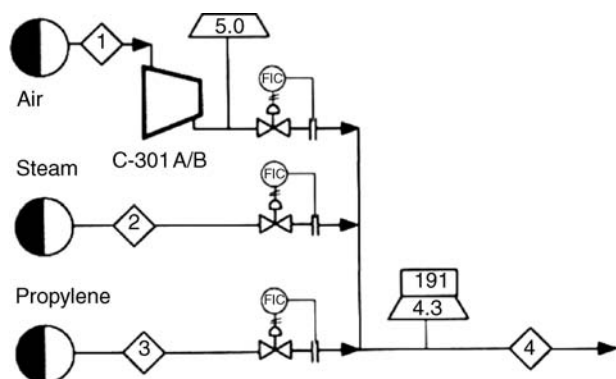


FIGURE 1.10 Feed section for the acrylic acid process.

parallel with the raw materials. The subsection shown in Figure 1.10 is then the primary feed section for the process.

The two product streams are shown at the end of the process on the right of the diagram.

The introduction of raw materials into the process and in fact the movement of all materials through the process requires suitable equipment. The movement of solids can be accomplished with conveyors. The equipment for gases and liquids provides the work required to overcome pressure differences. In both cases, the outlet pressure is higher than the inlet pressure. Blowers and compressors are used for gases and pumps are used for liquids.

The centrifugal pump is popular for both commercial and domestic applications. A centrifugal pump is illustrated in

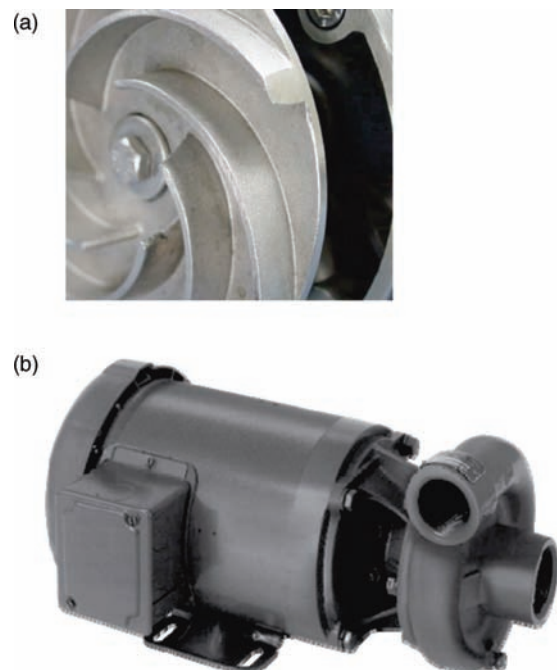


FIGURE 1.11 Centrifugal pump. (a) Vanes in volute casing of centrifugal pump. Reprinted with permission of MTH Tool Company/MTH Pumps. (b) Standard centrifugal pump with motor.

Figure 1.11, which includes a cutout side view (b) and an annotated picture of an actual installation (c). The liquid enters through the nozzle and the eye of the impeller. The impeller is composed of cavities formed by spiral-like vanes (see Figure 1.11a). The rotating cavities periodically communicate with the discharge nozzle as the impeller rotates with the shaft driven by the motor (see Figure 1.11b). The liquid is discharged by the accompanying centrifugal force. A suction is produced at the eye of the impeller, which admits more fluid. Other types of pumps are available to meet the demands of pressure head and flow.

Compressors are used to move gases. A reciprocating compressor, illustrated in Figure 1.12, uses the reciprocating action of a piston inside a cylinder to move a gas from a low to a high pressure. When the piston moves down, gas is sucked into the cylinder. When the piston moves upward, the intake valve closes and the gas in the cylinder is compressed. The exhaust valve opens when the pressure in the cylinder exceeds the pressure on the exhaust side and the gas is discharged. The following items are located on Figure 1.12.

1. Intercooler relief valve
2. Centrifugal, suction valve, or bleeder type unloader
3. Stainless steel disk and spring valve assemblies

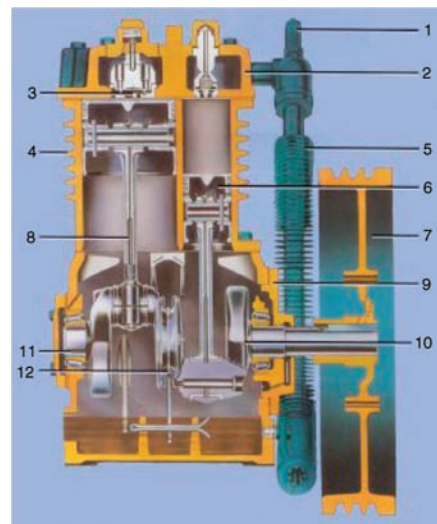


FIGURE 1.12 Reciprocating compressor. Reprinted with permission of Curtis Toledo.

4. Deep finned cylinders
5. Intercooler
6. High-pressure pistons
7. Flywheel
8. Connecting rods
9. Crankcase
10. Crankshaft
11. Main roller bearings
12. Pressure lubrication

When the compression ratio (outlet pressure/inlet pressure) is 2 or less, a blower is used instead of a compressor. A centrifugal blower, for example, resembles a centrifugal pump in appearance, except that the dimensions of the gas handling volumes are larger. A multistage centrifugal blower is shown in Figure 1.13.

The air stream in the acrylic acid process, stream 1, is compressed (with the compressor C-301A/B) and combined with the steam and propylene before being blown into the reactor (R-301) in stream 4. The flow of all these streams is controlled and indicated (FIC) in the control room for the process. The mass flow rate of each stream and the individual components of the stream is not changed by the compressor, the connecting pipes, or the valves. All that arrives in streams 1, 2, and 3 appears in stream 4. This can be seen in the stream table, Table 1.3 in the present case, which normally accompanies a PFD. Check that the sum of the individual flows across streams 1, 2, and 3 equals the flow in stream 4.

A stream table describes the state of each stream. The state variables are pressure, temperature, and flow rate of

TABLE 1.3 Stream Table for Acrylic Acid Process

Stream No.	1	2	3	4	5	6	7	8	9
Temperature (°C)	25	159	25	191	200	310	63	40	40
Pressure (bar)	1.0	6.0	11.5	4.3	3.0	3.5	2.0	2.4	2.4
Vapor fraction	1.0	1.0	1.0	1.0	0.0	1.0	0.0	0.0	0.0
Mass flow (tonne/h)	39.05	17.88	5.34	62.27	1075.0	62.27	3.08	1895	27.46
Mole flow (kmol/h)	1362.9	992.3	127.0	2482.2	—	2444.0	148.5	85200.0	1249.6
Component mole flow (kmol/h)	Hitec molten salt								
Propylene	—	—	127.0	127.0	—	14.7	—	—	—
Nitrogen	1056.7	—	—	1056.7	—	1056.7	—	—	—
Oxygen	280.9	—	—	280.9	—	51.9	—	—	—
Carbon dioxide	—	—	—	—	—	60.5	—	—	—
Water	25.3	992.3	—	1017.6	—	1165.9	140.9	78870	1156.7
Acetic acid	—	—	—	—	—	6.54	0.65	415	6.08
Acrylic acid	—	—	—	—	—	87.79	6.99	5915	86.81
Solvent (diisopropyl ether)	—	—	—	—	—	—	—	—	—

Stream No.	10	11	12	13	14	15	16	17	18
Temperature (°C)	25	48	40	40	90	13	13	89	47
Pressure (bar)	5.0	1.0	2.4	2.4	0.19	0.12	3.0	0.16	0.07
Vapor fraction	0.0	1.0	0.0	0.0	0.0	0.0	0.0	0.0	0.0
Mass flow (tonne/h)	2.54	37.35	20.87	143.0	6.63	155.3	136.4	6.26	5.28
Mole flow (kmol/h)	141.0	1335.4	1156.9	1591.2	93.19	1705.7	1498.0	86.85	90.49
Component mole flow (kmol/h)									
Propylene	—	14.7	—	—	—	—	—	—	—
Nitrogen	—	1056.7	—	—	—	—	—	—	—
Oxygen	—	51.9	—	—	—	—	—	—	—
Carbon dioxide	—	60.5	—	—	—	—	—	—	—
Water	141.0	150.2	1156.6	198.8	0.30	226.0	198.5	—	4.28
Acetic acid	—	0.46	0.03	6.08	6.08	—	—	0.05	86.07
Acrylic acid	—	0.98	—	86.81	86.81	—	—	86.80	0.14
Solvent (diisopropyl ether)	—	—	0.30	1299.5	—	1479.7	1299.5	—	—

Stream No.	19	20	21	22	23
Temperature (°C)	47	102	60	13	40
Pressure (bar)	1.1	1.1	1.0	3.0	2.8
Vapor fraction	0.0	0.0	0.0	0.0	0.0
Mass flow (tonne/h)	0.37	20.84	37.37	136.4	136.4
Mole flow (kmol/h)	6.34	1156.43	470.2	1498.5	1498.5
Component mole flow (kmol/h)					
Propylene	—	—	—	—	—
Nitrogen	—	—	—	—	—
Oxygen	—	—	—	—	—
Carbon dioxide	—	—	—	—	—
Water	0.30	1156.4	126.8	198.7	198.7
Acetic acid	6.03	0.03	—	—	—
Acrylic acid	0.01	—	—	—	—
Solvent (diisopropyl ether)	—	—	343.4	1299.8	1299.8

each species. These variables are the individual standard bearers for the conservation of momentum, energy, and mass referred to in the introduction. For example, the pressure, temperature, and compositions can be used to calculate the entropy that is used in studies of energy conservation and

efficiency. In most cases, these variables constitute all that is needed for process considerations. Note that the temperature of stream 4 is higher than that of any of the streams from which it was formed. From thermodynamics you know that this is due to the work done by the blower.



FIGURE 1.13 Centrifugal blower. Reprinted with permission of Gardner Denver, Inc.

1.2.3 Reactor Section—Reactor, Heat Exchangers, and Gas Absorption

The reaction and preliminary separation section is shown in Figure 1.14 and comes immediately after the feed section.

The reactants are introduced in the gas phase into reactor R-301 in stream 4. The products of the reactions with the unreacted reagents and nitrogen, the only inert material, are removed in stream 6. Note that the flow rate of nitrogen is the same in both stream 1 and stream 6.

The total rate of reaction in the reactor for each species can be computed from the difference between the input and

output flow rates. In a steady flow process for which there can be no accumulation in the vessel, there would be no other possibility. You can verify the results shown in Table 1.4.

We can scrutinize the reaction rates a little more carefully as follows. A single rate of reaction $R_j^{(V)}$ for each reaction over the volume V of the system under consideration ($j = 1, 2, 3, \dots$) can be determined by dividing the rate of reaction for any species that participates in the reaction (only) by its stoichiometric coefficient, reckoned positive for product and negative for reactants. This is what we mean by the proportions indicated by the coefficients. Since acrylic acid and

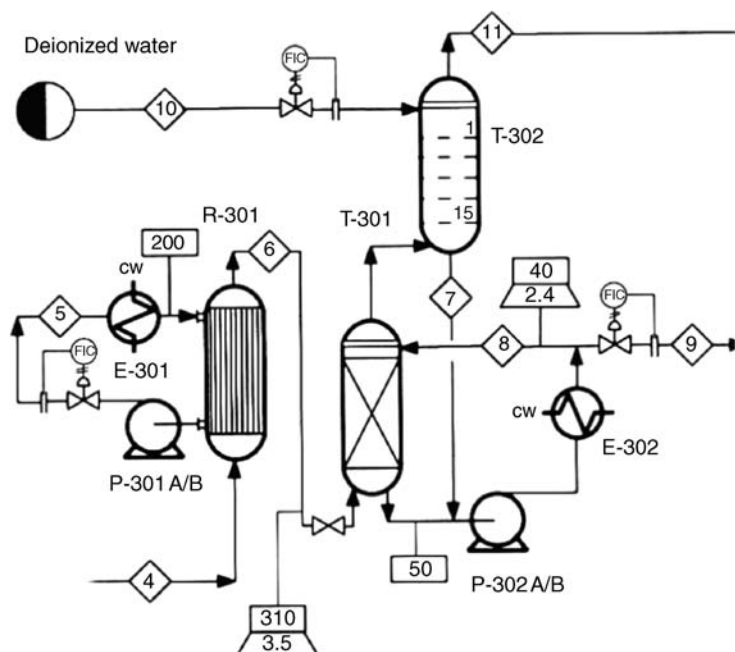


FIGURE 1.14 Reactor section. Reprinted with permission of Pearson.

TABLE 1.4 Reaction Rates in R-301

<i>I</i>	Species	Input Stream (4 kmol/h)	Output Stream (6 kmol/h)	Input – Output = Reaction Rate (kmol/h)
1	C ₃ H ₆	127	14.7	–112.3
2	O ₂	280.9	51.9	–229.0
3	C ₃ H ₄ O ₂	0	87.79	87.9
4	C ₂ H ₄ O ₂	0	6.54	6.54
5	H ₂ O	1017.6	1165.9	148.3
6	CO ₂	0	60.5	60.5
7	N ₂	1056.7	1056.7	0.0

acetic acid only participate in the first and second reactions, respectively, and their stoichiometric coefficients are unity, the reaction rate for the first two reactions on the preceding page can be taken directly from the table of reaction rates (Table 1.4):

$$\mathcal{R}_1^{(V)} = 87.9 \text{ kmol/h}$$

$$\mathcal{R}_2^{(V)} = 6.54 \text{ kmol/h}$$

Since 1 mol of water is produced in each of the first two reactions, these rates may be subtracted from the total rate of production of water, leaving the rate of water production by the third reaction (where the stoichiometric coefficient is 3). Consequently,

$$\mathcal{R}_3^{(V)} = \frac{148.3 - 87.9 - 6.54}{3} = 17.953 \text{ kmol/h} \quad (1.5)$$

The total reaction rates for carbon dioxide, oxygen, and propylene can then be generated as follows (making use of the constant ratio of rate to stoichiometric coefficient for each reaction):

$$R_{\text{CO}_2} = \mathcal{R}_2^{(V)} + 3\mathcal{R}_3^{(V)} = 60.400 \text{ kmol/h}$$

$$R_{\text{O}_2} = -\frac{3}{2}\mathcal{R}_1^{(V)} - \frac{5}{2}\mathcal{R}_2^{(V)} - \frac{9}{2}\mathcal{R}_3^{(V)} = -228.99 \text{ kmol/h}$$

$$R_{\text{C}_3\text{H}_6} = -\mathcal{R}_1^{(V)} - \mathcal{R}_2^{(V)} - \mathcal{R}_3^{(V)} = -112.39 \text{ kmol/h} \quad (1.6)$$

Check these values against the values calculated from the steam table and summarized in Table 1.4.

A well-mixed reactor has been provided here that consists of a bed of catalyst particles fluidized by the flowing gas mixture and a common wall shared with a flowing molten salt, which removes the thermal energy conducted through the wall and transfers it to cooling water in the heat exchanger E-301. A possible arrangement of a circulating fluid bed is illustrated in Figure 1.15 with heat transfer to an external fluid.

The “Reactants” and “Products” streams in Figure 1.15 correspond to Streams 4 and 6, respectively, in Figure 1.4.

The exchanger E-301 corresponds to the heat exchanger in the circulating salt loop, outside of the reactor. Stream 5 corresponds to the inlet of this exchanger for the salt. The rate of thermal energy transfer from the reaction mixture to the circulating salt is denoted by Q , which is released to the cooling water in E-301.

The circulating salt Hitec[®] is currently sold (Coastal Chemical Co.) as a mixture of sodium nitrate (60 wt%) and potassium nitrate (40 wt%). It has the advantage of being able to store thermal energy at relatively low volumes: 42 BTU/(ft³ °F).

Fixed-bed reactors where the catalyst is held stationary in a straight round tube is also used for gas–solid reactions. Multiple units are often arranged in the configuration of a shell and tube heat exchanger consisting of many tubes surrounded by a single shell containing a heat exchange fluid.

A heat exchanger permits the efficient transfer of thermal energy between two streams without material mixing of the streams. Energy is transferred as heat between the two fluids that seek to reach thermal equilibrium during their time of contact. Because of energy conservation, the energy lost by one fluid must be gained by the other. A common type of

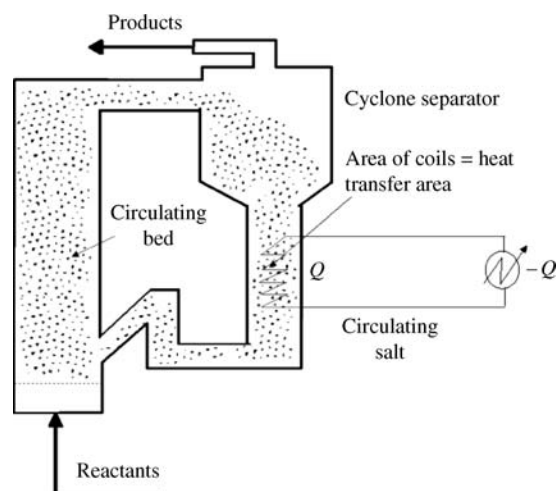


FIGURE 1.15 Circulating fluid bed reactor.

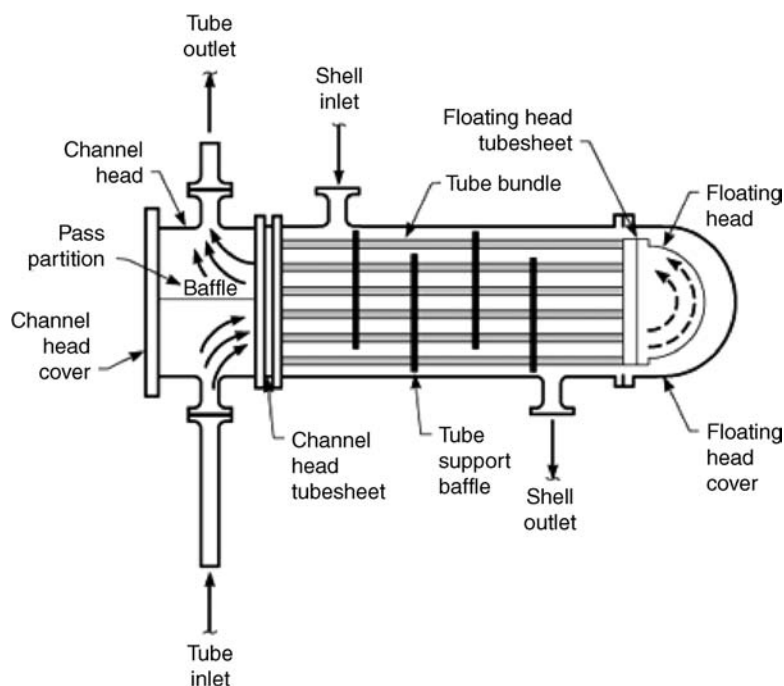


FIGURE 1.16 1-2 Shell and tube heat exchanger. Reprinted with permission of The Society of Naval Architects and Marine Engineers.

heat exchanger is the shell and tube exchanger illustrated in Figure 1.16.

One fluid is confined to the shell side outside of the tubes, normally the cold fluid. The second fluid, normally the corrosive or hot fluid, travels in the tubes. The area of the tubes represents the heat transfer area. The shell side fluid enters the nozzle and flows across the tubes in the transverse direction because of the baffles located along the tube bank at regular intervals. The tubes are mounted on tube sheets that are mounted on the shell with the heads at each end such that the shell fluid cannot escape. In the exchanger illustrated in Figure 1.16, the inlet head contains two chambers, each of which communicates with one half of the tubes; note there is no division at the opposite end of the exchanger. The fluid passes through one bank of tubes and returns through the other, thus providing two tube passes. Other similar arrangements are possible.

In the reactor, energy is conducted through the solid wall that separates the molten salt from the reaction mixture and is represented entirely by an energy debit to the reaction mixture and a credit to the molten salt. There is, of course, no material motion or convection in solids. At the inlets and outlets, however, the convective term is much more important and conduction can be neglected.

From a macroscopic view of the reactor, the net energy flow must be zero; that is, the energy flow into the reactor by the inlet streams 4 and 5 (upon exit from E-301) must be equal to the energy flow by the stream 6 and the outlet from

the pump, P-301 A/B. The heat exchanger, E-301, is provided to remove the thermal energy taken from the reaction mixture by the salt.

Cooling water is a utility in the plant whereby cold water at approximately 90 °F is supplied at a cost by a central facility. The water is returned at a maximum temperature of 120–130 °F after use. The facility cools the water to 90 °F for reuse as a coolant. Cooling often takes place in towers by partial evaporation of droplets sprayed into a warm air stream moving countercurrently to the droplets. The heat of evaporation is taken from the droplet. You can see the effect by spinning a wet cloth in the air. You also experience this cooling effect when you emerge from warm water into dry air.

Heat exchange takes place very efficiently by the direct contact of two fluids called quenching. Mixing of the two fluids must of course be acceptable from a safety, as well as economic, point of view. Economics would be important if a subsequent and expensive separation step would be required in the process.

In the present case, the liquid product from the gas absorber T-302 is used to further cool the reaction products (Figure 1.17). The gas absorber is used as the first step in the process of retrieving a pure product from the process. The absorber takes advantage of the much higher water solubility of the acids in the reaction products than the light gases. Water serves as the (mass) separating agent in the absorber and is supplied by the deionized water feed in stream 10.

TABLE 1.5 Mass Balance on Tower 302

	Stream 7 (kmol/h)	Stream 11 (kmol/h)	Stream 10 (kmol/h)	Gas Feed (kmol/h)	y in Gas Feed
N ₂		1056.7		1056.7	0.7868
O ₂		51.9		51.9	0.0386
C ₃ H ₆		14.7		14.7	0.0109
CO ₂		60.5		60.5	0.0450
H ₂ O	140.9	150.2	141	150.1	0.1118
C ₃ H ₄ O ₂	6.99	0.98		7.97	0.0059
C ₂ H ₄ O ₂	0.65	0.46		1.11	0.0008

Absorption equipment provides a large interfacial area between the water introduced at the top of the tower and the gaseous reaction products that flow countercurrently up the tower. Packing is present to create the required interfacial area as illustrated below.

The gas leaving the top of the tower consists of the light components (C₃H₆, N₂, O₂, CO₂) in the gaseous feed to the bottom of the tower and water. The streams are trying to equilibrate as they move through the tower. We might estimate the water flow rate overhead from this point of view, for example, by assuming that the gas product is saturated with water. The vapor pressure of water at the gas temperature of 48 °C is approximately 1.61 psia. A saturated ideal gas phase would have a mole fraction of 0.110975. The corresponding water flow rate would therefore be 148.2 kmol/h, which compares favorably with the value of 150.2 kmol/h given in Table 1.3.

From a microscopic view at each vertical position in the tower, an interfacial mass transfer process is taking place between gas and liquid phases, which are being mixed by the tortuous routes provided by the packing and the counter-current flow of the two fluids.

The interfacial mass transfer rate is proportional to a distance from equilibrium, the solubility limit. The liquid

will be saturated when the concentration reaches the solubility limit. The mass transfer rate ultimately determines the linear dimension of the equipment containing the flowing fluid on the basis of a desired amount of absorption.

The product losses to the overhead gas stream may be computed. The inlet gas flowing to the tower from the quench tower can be determined by a macroscopic mass balance over the absorber. What leaves in streams 7 and 11, less what comes in stream 10, equals what comes in the gas feed since there are no chemical reactions (Table 1.5).

The product losses to the overhead off-gas being sent to an incinerator are seen to be 12.2% for acrylic acid and 41.4% for acetic acid. Depending on the market price for acetic acid, it may be worthwhile to increase the recovery of acetic acid. The product stream at this juncture is stream 9.

Note that if the quench tower (T-301), the absorber (T-302), the heat exchanger (E-302), and the pump (P-302 A/B) are considered as one processing unit, streams 6 and 10 and the cooling water inlet to the exchanger would be inlets and streams 9 and 11 and the cooling water outlet would be outlets. All other streams begin and end on one of the process units in the group and therefore cannot upset the accumulated mass in the system. Note that streams are combined and separated in process units called mixers and splitters, respectively.



FIGURE 1.17 Packed tower gas absorber. Reprinted with permission of Branch Environmental Corp.

From a mass balance point of view, the cooling water inlet and outlet can be considered separately, since they do not materially communicate with the other streams. Since there are no chemical reactions in the units, the individual flow rates in streams 6 and 10 must sum to the individual rates in streams 9 and 11.

Water and carbon dioxide are produced as undesirable by-products and must be removed continuously to avoid accumulation in the process. Also, nitrogen is an inert gas that is introduced with the oxygen and must also be removed for the same reason. The off-gas purge stream 11 consists mostly of these materials. The environment is a primary concern in the disposition of waste streams. The water introduced in stream 10 captures the reaction products, acrylic and acetic acid. The outlet stream 9 consists primarily of water and the acid products. The other streams that enter or leave the process are utility streams required by the unit operations: low-pressure steam (lps) and cold water (cw), for example.

1.2.4 Downstream Processing—Distillation and Extraction

The product stream from the reaction and primary separation section stream 9 is the primary feed for the “separation” or “downstream processing” section. This section consists of a solvent loop, an acid tower and a waste tower.

The solvent loop consists of Towers 303 and 304 (see Figure 1.18).

The loop primarily recovers the acids from the water solvent and returns pure diisopropyl ether (DIPE) to the extractor.

The product stream 9 also contains the by-product acetic acid and a large amount of water. One basis of separation of

TABLE 1.6 Boiling Points of Acids and Water (Green and Maloney, 1997)

Species	N.B.P. (°F)	ΔH_{vap} (cal/(g mol))
Water	212	9745
Acetic acid	244	5713
Acrylic acid	285	6784

mixtures is volatility: The application of heat to a mixture can produce a vapor phase that is richer in the more volatile components than the residual liquid. The normal boiling points and latent heat of evaporation for these components are given in Table 1.6.

The difference in boiling points indicates that water is the most volatile and therefore the potential exists for driving off the water and leaving a residual liquid containing only the acids. However, the energy required would be extensive because of both the very large heat of vaporization for water and the very large quantity of water that must be removed. This translates into a large operating cost.

Another possibility and the one adopted here is to make use of a difference in solubility in a solvent that forms a separate phase with a high affinity for the desirable component(s) and from which these can be easily removed and the solvent recycled. The process is called extraction and takes place in Tower 303: acid extractor.

The solvent DIPE forms a second (organic) phase with water, has a low solubility in water, and has a high affinity for acrylic and acetic acids. The extraction equipment is designed to facilitate the transfer of the acid products to the DIPE phase. The DIPE phase is lighter than the water phase and will, analogous to the gas phase in the absorber, rise through the heavier organic solvent in a vertical tower. An

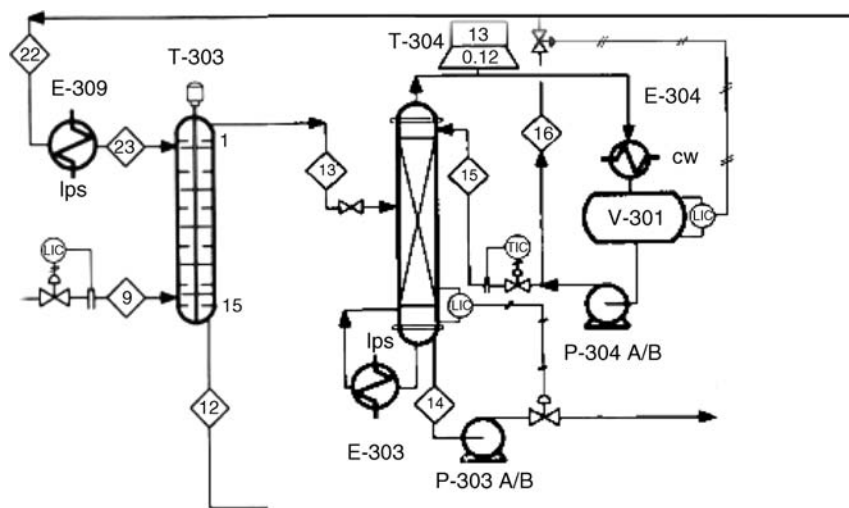


FIGURE 1.18 Distillation and extraction units—downstream processing. Reprinted with permission of Pearson.

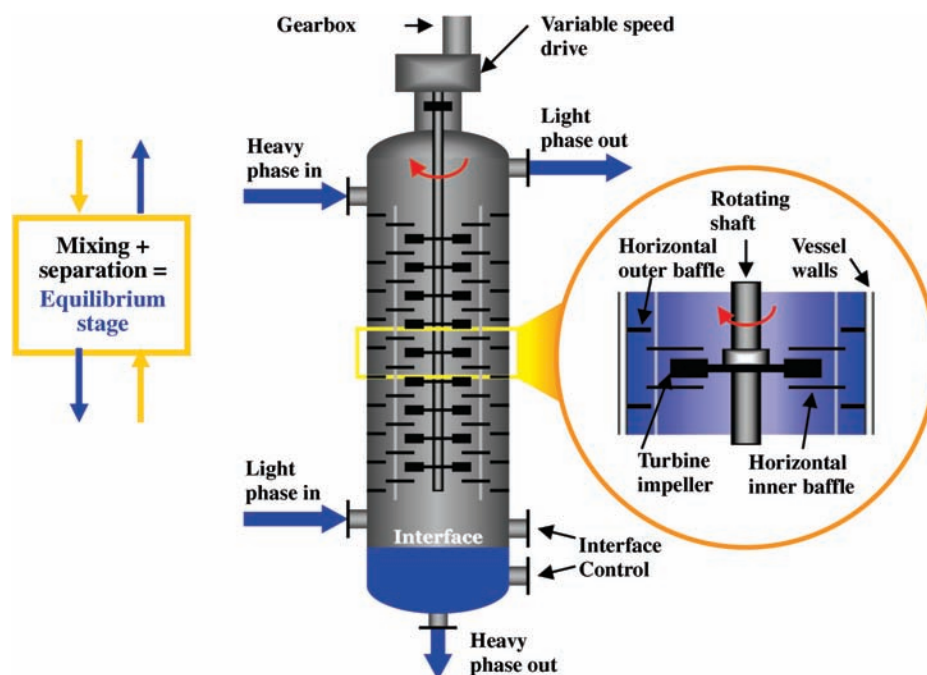


FIGURE 1.19 Scheibel extraction column (www.liquid-extraction.com). Reprinted with permission of Koch Modular Process Systems.

extraction column is illustrated in Figure 1.19, where the heavy liquid is dispersed at the top of the tower.

The column can be envisioned to consist of a series of equilibrium stages whereby the exiting streams from each stage are assumed to be in complete thermodynamic equilibrium (thermal, mechanical, and chemical). The ideal equilibrium stage provides sufficient time for the interfacial mass transfer rates to transfer the material required for equilibrium. The average contact time can be estimated as the volume of the stage divided by the flow rate. The interfacial area is the surface of the dispersed phase.

Each equilibrium stage provides mixing and surface area generation to enhance the mass transfer process. In some cases this is done mechanically and in some cases, such as in Figure 1.17, a packing material is used. The equipment is sized on the basis of providing the volume necessary for the required holding time and a phase disengagement. In the equilibrium stage analysis, the number of stages is determined. In the rate analysis, a size or dimension is calculated. Note that an inefficient equilibrium stage can be analyzed from a rate point of view, and the rate process is limited by equilibrium.

The solvent DIPE is returned to the column in stream 23 after the products have been removed and the low temperature resulting from the removal process is increased in the heat exchanger E-309. Stream 22 includes a recycle stream of recovered solvent from a downstream operation. Heat exchanger E-309 condenses low-pressure saturated steam to

a saturated liquid, making the latent heat of condensation available to the heating process.

Like cooling water, saturated steam is a utility. It is normally supplied by an offsite boiler operation to which the steam condensate is returned for re-evaporation. Low-pressure steam is approximately 5 barg, medium pressure is 10 barg, and high pressure is approximately 40 barg. The cost of process steam increases substantially with pressure.

The inlet for stream 23 is shown at the top of the tower in the flow diagram, shown in Figure 1.4. It should be interchanged with the inlet of the water or feed stream 9. The outlet water stream, stream 12, is nearly devoid of the acid products that have been transferred to the solvent stream, stream 13, which exits at the top of the tower. Since there are no chemical reactions, the inlet flow rates in streams 9 and 23 of each component must equal the sum of the output flow rates in streams 12 and 13. For example, for water,

$$1156.7 + 198.7 = 1156.6 + 198.8 \text{ (kmol/h)} \quad (1.7)$$

The solvent (DIPE) phase, stream 13, exiting from the top of the tower contains the acid products and a small amount of water. The products need to be retrieved and the solvent returned to the extractor. The boiling point of DIPE is 156 °F, which makes this compound much more volatile than the other constituents of stream 13 as can be seen from Table 1.6. The removal of DIPE can therefore also be accomplished by exploiting the difference in volatility, as

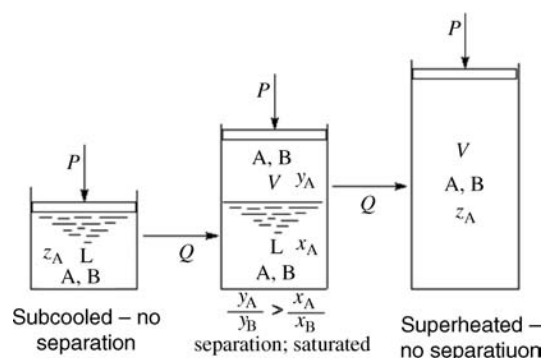


FIGURE 1.20 Physical state and separation.

mentioned above where this alternative was rejected in favor of extraction.

Consider a binary mixture composed of A and B where A is more volatile than B. A more quantitative statement is that the vapor pressure of A is greater than B or that the relative volatility of A to B is greater than 1. The relative volatility is defined as

$$\alpha_{AB} = \frac{P_A^{\text{sat}}(T)}{P_B^{\text{sat}}(T)} \quad (1.8)$$

Both vapor pressures increase with T , which makes α much less sensitive to temperature than either one of the vapor pressures.

We wish to produce a pure A and a pure B stream where purity provides a limit on the second component but does not exclude it. If we fix the pressure and apply heat to the mixture, we can produce a vapor that is richer in A than the liquid. Of course, if too much heat is applied, we obtain the same mixture but in vapor form. This situation is illustrated in Figure 1.20. Distillation is a separation operation based on this principle but applied many times to obtain saturated product streams at the operating pressure.

The overhead product from a distillation unit is referred to as the distillate and the bottom product as the residue. If possible, the column is operated at a pressure where the boiling point of the distillate is near 130 °F so that relatively inexpensive cooling water may be used in the reflux condenser. Recall that cooling water is generally available at 90 °F and can therefore be used as a heat sink under these circumstances.

Tower 304 is provided to return essentially pure DIPE as the overhead product and to deliver the acid products for purification. Note that T-304 is a packed tower that provides for continuous contact. It therefore calls for a rate-limited analysis as discussed above for the gas absorption column, T-302. This completes the solvent loop.

Stream 12, the bottoms product of Tower 304, is a product of this loop and is nearly pure water. It contains a trace

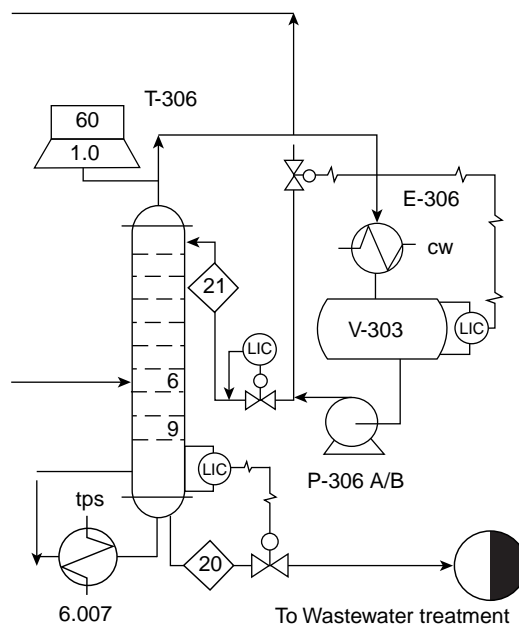


FIGURE 1.21 Waste tower—downstream processing. Reprinted with permission of Pearson.

amount of acetic acid (0.000026 mole fraction) and a small amount of DIPE (about 10 times the acetic acid). Except for the dissolved organic, this stream could be sent directly to the waste treatment facility. A separation step must be provided to remove the ether and recycle it to the extraction column. The boiling point of DIPE makes this compound much more volatile than acetic acid or water. This difference in volatility can be exploited with distillation to provide a separation. This is accomplished by the waste tower T-306, shown in Figure 1.21. The waste tower (Tower 306) returns trace amounts of acid and DIPE to the process and discharges the process water to the water treatment facility.

The distillate from T-304, stream 16, contains the two most volatile compounds, water and DIPE. These are returned to the extraction unit. There is no loss of DIPE to the bottom stream so that no makeup is required.

The bottoms product, stream 14, contains the acid products and a trace amount of water. Acrylic acid is present at 93 mol%. Acrylic acid may dimerize at high temperatures or rapidly polymerize with a large release of thermal energy resulting in an explosion (Center for Process Safety, 1995). Although effective inhibitors are used, the temperature is kept low in the separation operations involving the acid. The solvent tower (Tower 304) and acid tower (Tower 305), shown in Figure 1.22, are therefore operated at reduced pressures to keep the temperature low in the reboiler. The flash point of glacial acetic acid is 54 °C (Center for Process Safety, 1995). The overhead from the acid tower is the by-product acetic acid stream and the bottoms is the acrylic acid product stream.

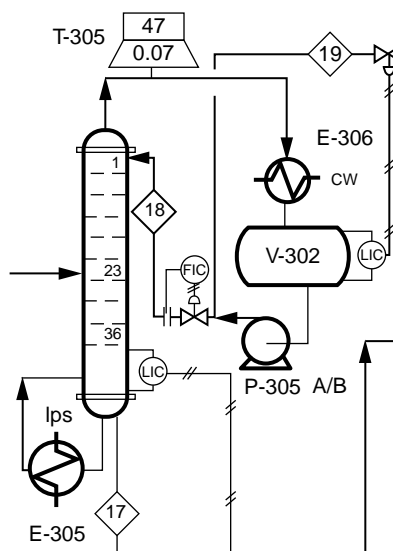


FIGURE 1.22 Acid tower—downstream processing. Reprinted with permission of Pearson.

1.2.5 Storage

Storage is provided in processing systems for the most part to compensate for variability in, for example, delivery and shipment schedules, upsets caused by shutdowns for routine and emergency maintenance and repairs, off-grade materials, and intermediate products. Storage tanks are often arranged in tank farms such as that shown in Figure 1.23.

Solids can be stored in silos, while liquids with vapor pressures less than 1.5 psia (Amrouche et al., 2002) are stored in tanks with fixed roofs of various shapes including flat, conical, and dome shaped. Solid products may be stored in the packaging used for distribution.



FIGURE 1.24 External floating roof of large diameter storage tank (www.hghouston.com). Reprinted with permission of The Hendrix Group, Inc.

Floating roofs are used for storing liquids with vapor pressures up to 11 psia. An external floating roof floats directly on the surface of the liquid with a sealing system attached to the roof (see Figure 1.24). Inside floating roofs also rest on the surface of the liquid but are under a fixed roof.

Small quantities of gases are stored as gases at ambient temperature, while larger quantities are stored as liquids. This requires pressurized facilities and refrigeration. Refrigeration may also be required to condense vent gases during filling. As an example of storage tank design considerations, refer to Figure 1.25.

- Net working capacity contained between the high and low liquid level controls. The volume for an in-process tank is determined by the desired hold-up time for the



FIGURE 1.23 Oil tank farm.

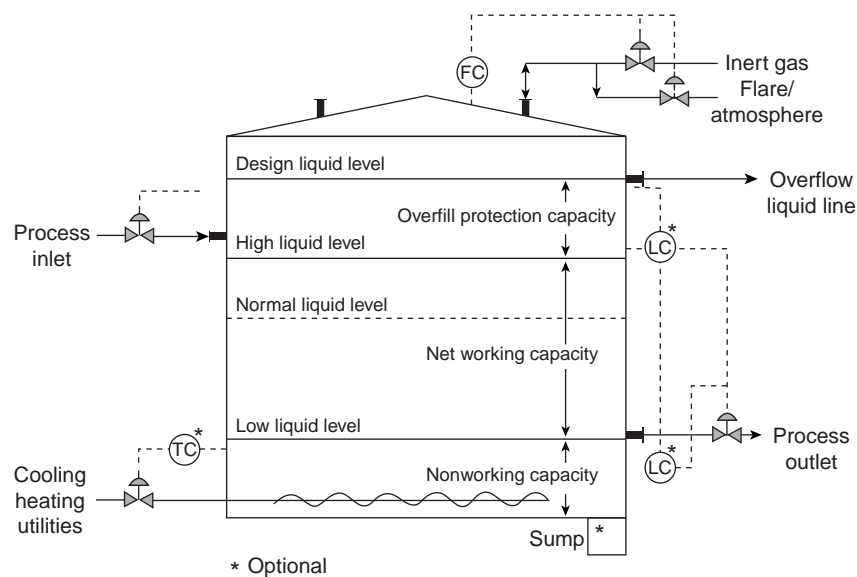


FIGURE 1.25 Design considerations for aboveground storage tanks (Amrouche et al., 2002).

liquid multiplied by its flow rate. For off-site storage, the shipment schedule is a major factor.

- Nonworking capacity below the low liquid level control situated 10 in. above the bottom seam to avoid weld interference.
- Overfill protection capacity above the high liquid level control. This volume is filled with vapor under normal operating conditions when the liquid level is between the level controls.

Other design considerations include the following:

- Tank temperature and pressure and the need for heat exchange or phase separation equipment.
- Materials of construction.
- Wind and seismic loadings.
- Size and position of accessories.
- Emission controls.
- Foundation type.
- Pressure, temperature, and level controls.

1.2.6 Safety

As noted in the introduction, the subject of process safety is not treated in this book. However, because of its extreme importance, special note of its omission is made here. Chemical engineers design and operate plants with huge capacities of hazardous materials. Therefore, they must be ever vigilant that these materials do not pose a threat to the operating personnel, the surrounding community, or

the environment. An excellent starting place for this topic is the Center for Chemical Process Safety, operated by the American Institute of Chemical Engineers.

1.2.7 Overview of Typical Process

To conclude with an overview of the process organization, consider the typical organization shown in Figure 1.26.

Raw materials in sufficient quantity to supply the process in the face of a discreet delivery schedule are stored near the process under the mildest possible conditions of temperature and pressure. These materials, A and B in Figure 1.26, will invariably need to be brought to the process temperature and pressure and there may be a need for some purification steps at this juncture. Any sensitivity, for example, of the catalyst to even trace amounts of a contaminant, will require that the contaminants be reduced to an acceptable level. Otherwise a costly catalyst replacement program may be required and process interruptions may be necessary.

Reactor products may be recycled to preheat the feed and thereby make use of the chemical energy that has been converted to thermal energy by the reaction process. Common reactor configurations are packed beds, fluidized beds, stirred tank reactors, and single and multi-tubular reactors. The reactors may be operated adiabatically or heat may be exchanged with a circulating fluid. Regeneration of the circulating fluid must be provided in this case, which will, in most applications, involve a heat source or sink.

A separation section follows the reactor and is designed to provide product streams at the purity levels required by the market or to recycle reactants used in excess to compensate for incomplete conversions in the reactor. It is also

TABLE 1.7 Acrylic Acid Process Calculations

Object Identification	Example Calculations	Example
Examples in Part I		
Separation train	Inactive units and system definitions	2.1-1
Reactor 301	Mass balances	2.4.1-1
Reactor 301	Test for independent reactions	2.4.3-1
Exchanger 309	Heat duty and steam rate	3.5.2-1
T-303 extraction unit	Heat duty	3.5.3-1
T-304 distillation unit	Heat duty	3.5.3-2
Reactor 301	Heat duty	3.6.3-1
P-301 A/B: molten salt pump	Power requirement	4.3.1.4-1
T-303 alternative	Power required	5.3.2.3-1
T-302: single-stage version	Solvent requirements	6.2.2-2
Stream 13	Single-stage flash	6.3-7
T-303	Solvent flow for single stage	6.4.2-2
R-301	Multiple second-order reactions and sizing	6.6.1.2-1
R-301	Temperature selection	6.6.1.3-1
R-301	<i>A priori</i> calculation of heat duty	6.6.1.4-1
Examples in Part II		
T-302	Solvent rate, stages, and diameter	7.1.7-1
T-305	Number of stages and solvent flow using constant relative volatility	7.2.13-1
T-303	Number of stages and solvent flow	7.3.2-2
T-303	Unagitated sieve tray requirements	7.3.4-1
T-303	Settler size for mixer settler alternative to T-303	7.3.5-1
Reactor 301	Reactor size	13.2.3-1
Exchanger 309	Size	14.2.2.1-1

necessary to provide exits for inert materials present in the feed and nonsalable reaction products. The separation section consists of absorbers, extraction units, distillation towers, adsorbers, membranes, and so on. Some streams may be sent directly to waste treatment and others to product storage (Table 1.7).

1.3 BIOCATALYTIC PROCESSES—ENZYMATIC SYSTEMS

The distinction between the action of catalysts in living systems and in chemical plants is rapidly diminishing with the commercial utilization of enzymes.

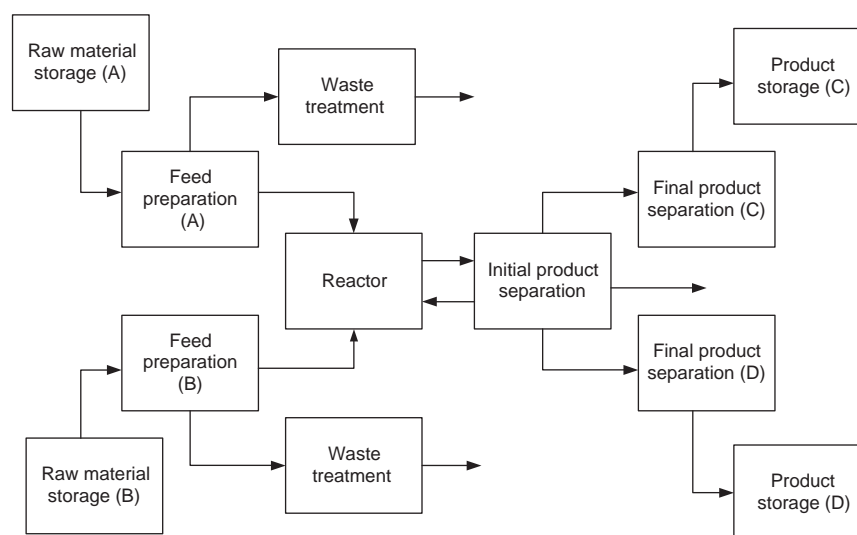

FIGURE 1.26 Generic chemical processing system (adapted from Luyben and Wenzel, 1988).



FIGURE 1.27 Schematic structures of the enzyme, subtilisin Carlsberg. The position of the catalytic triad in the active site (Ser221, His64, and Asp32) is indicated. (García-Junceda et al., 2004). Reprinted with permission of Elsevier Limited.

Enzymes are high molecular weight proteins that are produced and used by living organisms as catalysts. We will refer to the action of enzymes as biocatalysis and to the catalytic action of other materials as chemocatalysis.

Enzyme catalysts are named according to their primary function. For example, urease catalyzes the cleavage of urea. However, enzymes will accelerate the rates of many other reactions. They may be used in a pure state or in a whole cell system. The pure enzyme systems are better defined, but the whole cell system is attractive when a cascade of reactions is required, all of which the cell can supply. An example is cofactor regeneration in *Saccharomyces cerevisiae* (baker's yeast).

Figure 1.27 is an example of the enzyme subtilisin Carlsberg (SC). SC is a serine protease whose physiological role is to hydrolyze proteins. The ratio of the catalyzed to uncatalyzed rate can reach 10^{17} (García-Junceda et al., 2004). Enzymes are very selective relative to substrates (chemoselective), and to locations within the substrate molecule (regioselective). They are highly stereoselective.

1.3.1 Biotransformation

The number of industrial biotransformations involving the conversion of a preformed precursor has increased by approximately 400% over the last 20 years to nearly 150. More than one half of these are in the pharmaceutical industry (Straathof et al., 2002), followed by the food and agriculture sectors. The distribution of products is illustrated in Figure 1.28.

Chirality is an overriding concern in most biotransformations and refers to the following molecular considerations concerning isomers. There are two kinds of isomers,

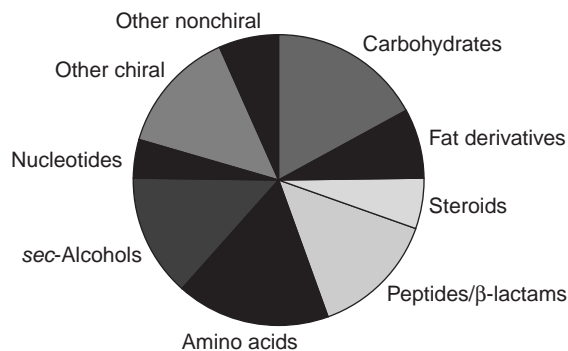


FIGURE 1.28 Distribution of products from industrial processes (Straathof et al., 2002). Reprinted with permission of Elsevier.

compounds with the same molecular constitution: constitutional isomers and stereoisomers. Constitutional isomers have a different connectivity or molecular arrangement. The connectivity of stereoisomers is the same. Stereoisomers fall into two categories. In the case of enantiomers, the stereoisomers are the mirror image of each other. In the second category, called diastereomers, this is not the case.

Enantiomers are said to possess the property of chirality or handedness. Chirality can be a very important consideration in the action of a drug in the human body. One enantiomer can be beneficial and the other actually a poison. The drug thalidomide is a case in point. Enzymatic transformations invariably produce one enantiomer, while purely chemical transformations produce a racemate composed of equal proportions of each enantiomer. The racemate is hard to separate because of its very nature of similarity. There are very little differences on which to base a separation; certainly there is no chemical difference between the constituents.

Yet another feature attraction of enzymes is that they produce only one of the enantiomeric forms, which has, of course, a major impact on the downstream processing. A system that is part of the IUPAC system for naming chemicals has been devised for naming the enantiomers. An *R* or an *S* is added in unique way to the ordinary chemical name. It is therefore an overriding imperative in most biotransformations that the desirable form, *R* or *S*, be obtained. The enantiomeric purity is measured by a quantity called the enantiomeric excess (*ee*) defined by

$$ee = \frac{\text{moles of one enantiomer} - \text{moles of the other enantiomer}}{\text{moles of both enantiomers}}$$

Chirality is achieved in most cases at present by starting with enantiopure precursors, but other methods are being used as illustrated in Figure 1.29. If the precursors are pure enantiomeric forms of the desired configuration, then the reaction will necessarily yield the desired products.

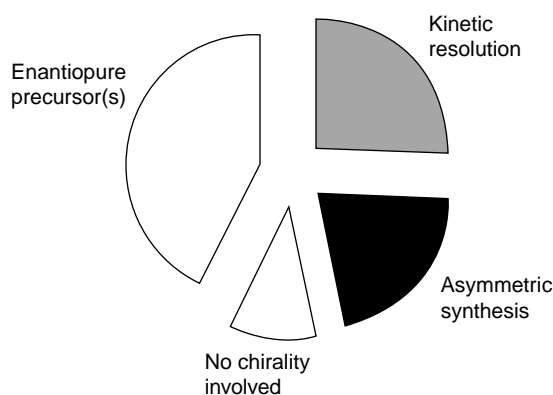


FIGURE 1.29 Source of chirality in current industrial processes (Straathof et al., 2002). Reprinted with permission of Elsevier.

An **asymmetric reaction** is one in which one or more new elements of chirality are formed in a substrate molecule and one that produces the stereoisomeric products in unequal amounts.

An example is the preparation of L-aspartic acid from fumaric acid and ammonia using aspartase in whole cells of *Escherichia coli* as shown in Figure 1.30. In an enzyme-catalyzed **kinetic resolution** of a racemate, one enantiomer is preferentially converted. The maximum yield is then 50%. If, however, the undesired enantiomer can be racemized, it may be recycled and the yield substantially increased. For example, Figure 1.31 illustrates that the isomerization of 1-phenethyl alcohol by a Ru catalyst (promotes racemization) and enzymatic acylation with 4-chlorophenyl acetate as an acyl donor results in the transformation of the racemic alcohol to enantiomerically pure acetate. There are also other approaches to the resolution of racemates (García-Junceda et al., 2004).

1.3.2 Examples of Industrial Processes

Examples of industrial processes using enzymes ranges from commodity chemicals (>20,000 tonne/year), such as acrylamide, fructose, and maleic and aspartic acids, to intermediates (100–20,000 tonne/year) to fine chemicals (<100 tonne/year), such as pharmaceutical intermediates and drugs. Fine chemical production is predominantly

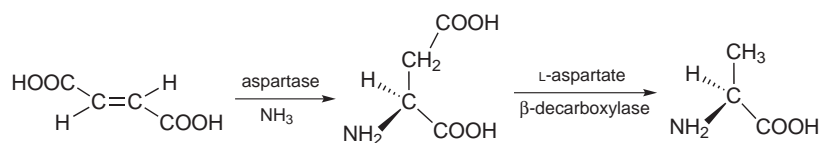


FIGURE 1.30 Enzymatic synthesis of L-aspartic acid and L-alanine (Van Balken et al., 1997). Reprinted with permission of Elsevier.

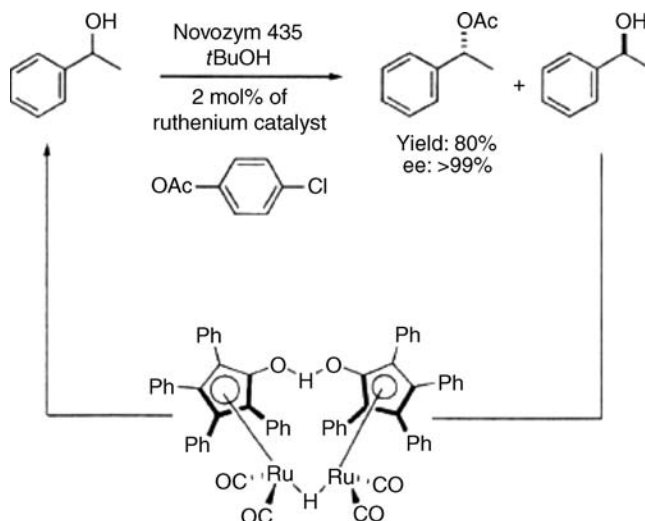


FIGURE 1.31 Dynamic kinetic resolution of 1-phenethyl alcohol (García-Junceda et al., 2004).

carried out in batch reactors and commodity chemical production is mostly done with continuous reactors.

The **synthesis of L-aspartic acid and L-alanine** discussed above (Van Balken et al., 1997) has been carried out on an industrial scale by Tanabe Seiyaku Co. Ltd., Japan. A continuous process was developed with the *Pseudomonas dacunhae* immobilized on χ -carrageenan.

Because of carbon dioxide evolution inhibiting plug flow, a closed column was designed (approximately 4 bar). The *E. coli* immobilized on χ -carrageenan showed a half-life of 680 days at 37 °C. The continuous process is shown in Figure 1.32.

One of the first bioconversion processes that produced a commodity chemical was the **manufacture of acrylamide** by Nitto Chemical Industry Company, Ltd., Japan. A schematic is shown in Figure 1.33. The feed is acrylonitrile (AN) and the product is a 50% solution of acrylamide (AA). The only detectable impurity is acrylic acid and that is less than 5 ppm.

1.3.3 Alkyl Glucosides

Alkyl glucosides are a group on nonionic surfactants that are antimicrobial and biodegradable. They have been used in

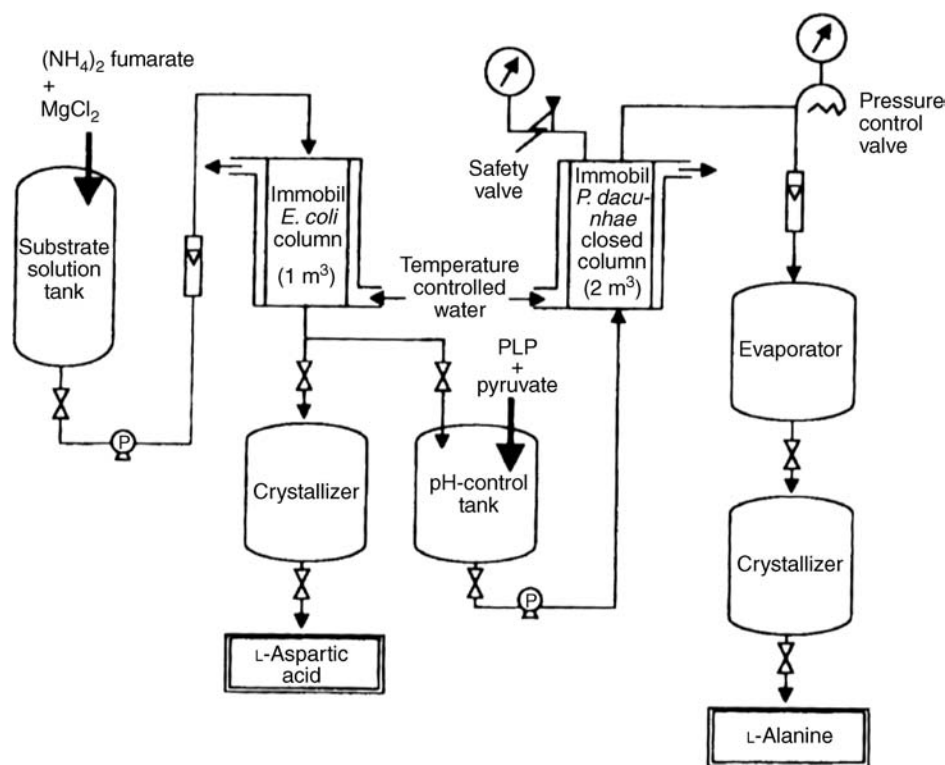


FIGURE 1.32 Continuous production of L-aspartic acid and L-alanine (Van Balken et al., 1997). Reprinted with permission of Elsevier.

detergents, foods, and pharmaceuticals. A glucoside is an acetal of glucose, which refers to the replacement of an $-OH$ group with an $-OR$ group. In contrast to the chemical method, an enzymatic synthesis method is available, which is regio- and stereoselective and does not require resolution of anomers. This is accomplished by a condensation reaction of glucose in aqueous solution with the appropriate alcohol to give the glucoside and water (Figure 1.34). A series of exercises, beginning with Problem 1.1 and continuing in Chapters 2, 5, 6, 10, and 13, are concerned with “engineering” the process for the synthesis of *n*-hexyl- β -D-glucoside through the condensation of glucose and *n*-hexanol using the enzyme β -glucosidase from almonds (Table 1.8).

1.4 BASIC DATABASE

It is important that you become familiar with the data resources that are available to you. These resources form the foundation for accurate engineering calculations, which in turn support sound economic decisions and safe, trouble-free operation of plants that meet the operating projections expected of them.

Process calculations require basic rate and equilibrium data, as well as economic and safety information. Rate data include, for example, thermal conductivities (heat conduction), diffusivities (nonconvective mass flows), and reaction kinetics (rate parameters). Equilibrium data include phase and chemical reaction equilibrium.

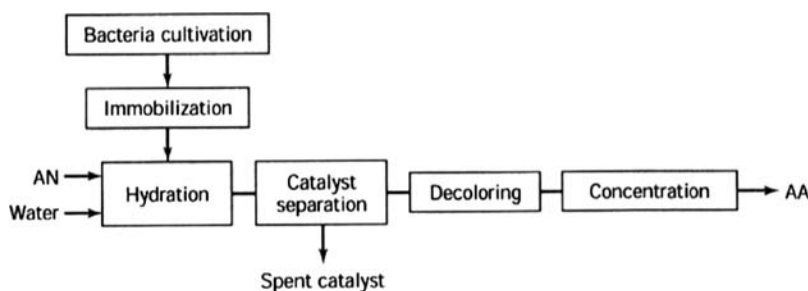


FIGURE 1.33 Manufacture of acrylamide using nitrile hydratase.

TABLE 1.8 Problems and Examples Concerning the Synthesis of Hexyl Glucoside

Equipment	Topic	Problem or Example Number
Part I		
All	Preliminary flow sheet and database	1.1
All	Process formation and material balances	2.3
Reactor	Volume and residence time	5.1-1
Batch adsorber	Power required to mix slurry	5.2.3-1
Adsorber	Adsorbent requirement	6.5.3-1
Reactor	Equilibrium constant	6.7-1
Reactor	Phase equilibrium with chemical reaction	6.7-3
Part II		
Adsorber	Recovery of hexyl glucoside	10.4-1
Adsorber	Slurry adsorption of hexyl glucoside	13.2.1-1

Online data resources are often organized into categories. Some categories of important process data are the following:

- Analytical Chemistry
- Catalysis
- Dispersion and Aggregation
- Electrochemistry
- Environmental Chemistry
- Industrial Chemistry and Chemicals
- Industrial Safety
- Physical Chemistry
- Plant Design, Operation, and Energy Efficiency
- Polymer Chemistry
- Separation
- Transport Processes

Some specific titles of interest to chemical engineers are the following:

- *Chemical Properties Handbook*
- *Chemical Tradename Dictionary*
- *DIPPR 882—Transport Properties and Related Thermodynamic Data of Binary Mixtures*, Parts 1–4

- *DIPPR Project 801—Full Version*
- *Dean's Analytical Chemical Handbook* (2nd Edition)
- *Dean's Handbook of Organic Chemistry* (2nd Edition)
- *Encyclopaedia of Scientific Units, Weights and Measures*
- *Handbook of Applied Surface and Colloid Chemistry*, Vols. 1–2
- *Handbook of Hydroxyacetophenones*
- *Handbook of Inorganic Chemicals*
- *Hawley's Condensed Chemical Dictionary* (14th Edition)
- *Heterocyclic Chemistry* (4th Edition)
- *International Critical Tables of Numerical Data, Physics, Chemistry and Technology* (1st Electronic Edition)
- *Knovel Critical Tables*
- *Lange's Handbook of Chemistry*
- Periodic Table of the Elements
- *Perry's Chemical Engineers' Handbook* (7th Edition)
- *Purification of Laboratory Chemicals*
- *Reservoir Engineering Handbook* (2nd Edition)
- *Smithsonian Physical Tables* (9th Revised Edition)

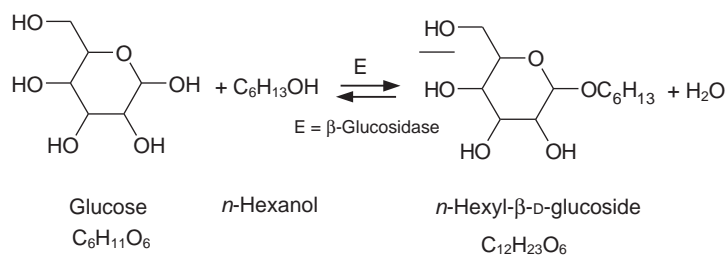


FIGURE 1.34 Synthesis of alkyl glucosides by enzymatic method (de Roode et al., 2001). Reprinted with permission of Elsevier.

- *Wiley Guide to Chemical Incompatibilities* (2nd Edition)
- *Yaws' Handbook of Antoine Coefficients for Vapor Pressure* (Electronic Edition)
- *Yaws' Handbook of Thermodynamic and Physical Properties of Chemical Compounds*

The titles above may be found, for example, in the *Knovel Engineering and Scientific Online References* electronic database.

Technical publications, especially those in the area of concern, offer data that may have not yet appeared in the summary publications. A few examples are the following:

- *Journal of the American Institute of Chemical Engineers*
- *Chemical Engineering Journal*
- *Journal of Biotechnology*
- *Journal of Membrane Science*
- *Fluid Phase Equilibrium*

A partial database for the acrylic acid process is given in Appendix C.

Invariably, it will be necessary to estimate data. A comprehensive summary of estimation methods is available in *The Properties of Gases and Liquids* (Poling et al., 2001).

PROBLEMS

1.1. A recent proposal has been made for the synthesis of alkyl glucosides by an enzymatic method rather than by the chemical method (de Roode et al., 2001). The reaction is shown in Figure 1.34. E is the enzyme. At high glucose concentrations it is possible that β -glucobioses will also form. The reaction is thermodynamically controlled (Van Rantwijk et al., 1999). The synthesis is limited by the low solubility of the alcohol in water, but the reaction

can be fine-tuned by the prudent selection of operating conditions and product removal.

The reaction was carried out in the laboratory followed by separation and purification steps. The aqueous phase contained the enzyme and glucose and was buffered to pH 6 with 0.16 M citrate/phosphate. The almond β -glucosidase activity was 0.2 U/ml (or approximately 1.2 mg/ml) of buffer solution. A unit of catalyst activity is the amount of enzyme required to convert one micromole of substrate per minute.

The details of the individual steps are available in de Roode et al. (2001). A continuous version of the process based on these individual steps is shown in Figure 1.35.

The process was assembled with the following considerations:

- Since water is produced in the process, it must be removed from the process. If the product stream does not provide this function, a purge must be provided.
- Since the enzyme is in the water phase, it will be part of the purge and will need to be replenished, either as part of the glucose feed or separately.
- The alcohol, being soluble also in the water phase, will need to be replenished in the alcohol feed.
- The reaction takes place in the water phase, which contains the enzyme catalyst, while the product and alcohol distribute between the two phases. The mixture is assumed to have reached equilibrium upon leaving the reactor in stream 5.
- The membrane separation is assumed to provide a perfect separation of the organic (stream 6) and aqueous (stream 7) phases.
 - a. Provide a short description of the function of each block on the PDF above.
 - b. List the ingredients of each stream if the enzyme is ignored.
 - c. Construct a database for the process.

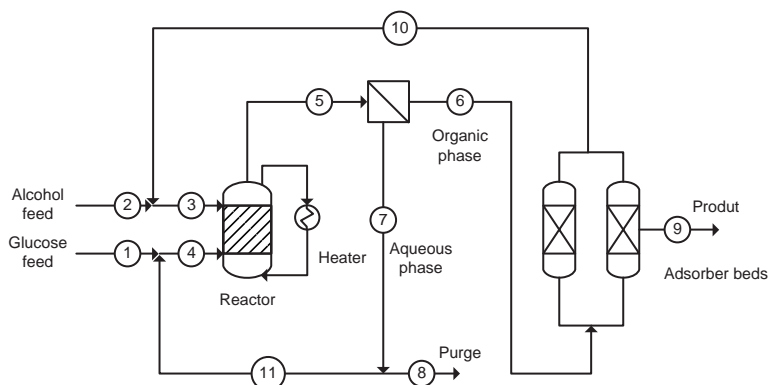


FIGURE 1.35 Continuous version of individual steps.

1.2. Find a chemical process in which you have some interest. It could be from the pharmaceutical industry, the food industry, the petrochemical industry, and so on. Prepare a report on the process assuming that a typical classmate will be the reader. The report should include the following items:

- Chemical formula and form/state of product.
- Uses and market price.
- Historical industry development.
- Common methods of production with raw material sources and side products.
- Major companies, production methods, and production levels.
- Details for a common production method: process chemistry with implications for the most favorable process conditions; flow sheet(s); operating conditions and problems; environmental considerations; production costs; utility requirements; hazards; handling of waste and side products.
- Relevant patents issued since 1971 (or earlier): number, title, abstracts of the most relevant patents.
- Discussion of competing technologies based on technical information in patents and/or other resources. Supply figures from patents wherever needed in the discussion or representations.
- References.

Distribution to the class would be relevant component of this exercise.

1.3. Prepare a report on a specific item or category of chemical processing equipment assuming that a typical classmate will be the reader.* Some examples of this topic are the following:

- Fixed beds
- Fluidized beds
- Furnaces
- Heat exchangers
- Packed towers
- Stirred tanks
- Tray towers

The report should address the following items (and others at your discretion):

- Purpose and operating principle(s)
- Historical background
- Construction—schematic/illustrations
- Pictures of actual equipment
- Range of duties—sizes
- Maintenance required
- Utilities required
- (Some) design equations
- References

2

MACROSCOPIC MASS BALANCES

Chapter 1 provides some experience with viewing and interpreting flow sheets for chemical processes and with some aspects of mass and energy conservation in such systems. These experiences with mass conservation are formalized in this chapter along with the introduction of some derivative ideas. In so doing, may arrive at system of equations may result of larger dimensionality than would otherwise be present when insight is used along the way. The methodology does not rely on insight and may therefore be abbreviated in some cases with this advantage.

We take the macroscopic view throughout this chapter and therefore do not consider local conditions within the process equipment. The macroscopic view is the first level of design and sets many of the conditions to be met in the design of the individual units from the microscopic view at the next design level.

Let us begin with what is probably an acceptable statement of mass conservation for all of us and follow this with a relatively detailed discussion of the terms used so that the statement can define a procedure for applications.

Mass Conservation: For each chemical species in a chemical processing system, the

$$\begin{aligned} &\text{input mass rate of flow} - \text{output mass rate of flow} \\ &+ \text{rate of mass production from chemical reactions} \\ &= \text{rate of mass accumulation} \end{aligned} \quad (2.1)$$

A chemical species refers here to a molecular entity. If the components being traced were taken to be atoms

instead, there would be no production term. Also, we can substitute molar rates for mass rates since moles are also a measure of quantity. An important difference will arise, however, when we discuss a total mass or molar balance rather than for only one component since mass and atoms are conserved in chemical reactions, but moles may not be. In the following discussion, we will refer primarily to mass units.

2.1 CHEMICAL PROCESSING SYSTEMS

A chemical processing system is defined by a specific set of process units and the streams that connect them, the collection being represented on a process flow sheet. We assume that changes taking place in the process piping are accounted for with process units. No changes are therefore associated with the streams that connect the process units on a flow sheet. A process unit is any operation that alters the flow, composition, temperature, or pressure of any stream. Active process units are those that change flow rates or compositions such as separators, reactors, splitters, and mixers. Inactive process units do not change flows or compositions but may change pressures or temperatures such as pumps, compressors, and heat exchangers without phase change. Active units must be identified as components of the chemical processing systems but inactive ones can be excluded from the viewpoint of the mass balance.

Example 2.1-1: Active Units in Acrylic Acid Separation Train

As far as macroscopic mass balances are concerned, the flow diagram in Figure 2.1 could have been constructed for the separation train that treats stream 9 in the acrylic acid process.

The inactive units will become active when energy and momentum balances are considered, which may be necessary when flow rates are based on volume. This necessity will be discussed below.

The set of process units is isolated from other equipment or operations by imaginary breaks in the interconnecting streams. Input streams are defined as those that begin at an imaginary break and end on a process unit within the system. Output streams begin on a process unit within the system and terminate at an imaginary break. All other streams that are connected to any process unit within the system must begin and end with a process unit. Otherwise, the system is ill defined. Only input and output streams are considered in the mass balance.

Recall that there may be isolated streams in the systems that do not communicate with the process streams other than to enable transfer of thermal energy. A cooling water stream to a chemical reactor or a combustion gas stream to a furnace heater are examples. These streams may be cautiously excluded since they individually satisfy a mass balance. Also, it may be noted that one may define a global system and progressively write mass balances on different subsystems, the smallest of which are single units, to construct an overall analysis.

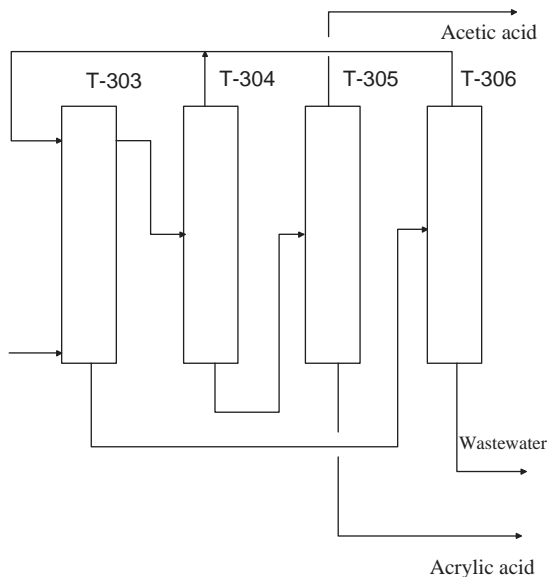


FIGURE 2.1 Active units in acrylic acid separation train.

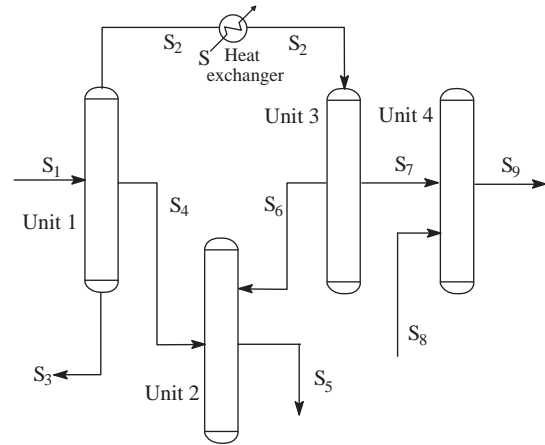


FIGURE 2.2 Inputs, outputs, and subsystem definition.

Consider for example, the process flow sheet in Figure 2.2. The units are active with arbitrary functions and an inactive heat exchanger with an isolated stream is included. Except for stream S , all streams are labeled with S and a single subscript. We can designate an imaginary break in stream S_i by B_i to construct the following examples:

System	Breaks	Units in System	Input Streams	Output Streams
1	B_1, B_3, B_5, B_8, B_9	1, 2, 3, 4	S_1, S_8	S_3, S_5, S_9
2	B_1, B_3, B_5, B_7	1, 2, 3	S_1	S_3, S_5, S_7
3	B_7, B_8, B_9	4	S_7, S_8	S_9
4	B_2, B_6, B_8, B_9	3, 4	S_2, S_8	S_6, S_9

Note that stream 7 is an input in system 3 and an output in system 2; streams 2 and 6 do not appear in the first three systems; systems 2, 3, and 4 are subsystems of system 1; the heat exchanger has been ignored and its inlet and outlet streams are considered to be the same from a mass balance point of view. What other observations can you make?

The application of mass conservation is not limited to the macroscopic chemical processing systems defined here. It must also apply to microscopic systems enclosed within the processing units such as stages in a distillation tower or a single catalyst particle, for example.

2.1.1 Input and Output Rates of Flow

Input and output rates of flow refer to the rate at which mass of a species is introduced or removed from the system in an input or output stream, respectively. The units of the flow rate are therefore mass of i per unit time where i stands for an arbitrary numeric or alphanumeric label assigned to the

species in question. Species may be labeled arbitrarily, but uniquely, for your convenience. However, your scheme must be clearly explained for your work to be comprehensible. Streams must also be uniquely labeled and defined.

Suppose that $\mathcal{W}_i^{(j)}$ refers to the mass rate of flow of species i in stream j . Input or output designations streams will generally change when different (sub)systems are considered and superscripts (j) may not be sequential over the input or output set. Therefore, it is safe to say that

$$\sum_{\text{input streams}(j)} \mathcal{W}_i^{(j)} = \text{Input mass rate of flow of species } i \quad (2.2)$$

$$\sum_{\text{output streams}(j)} \mathcal{W}_i^{(j)} = \text{Output mass rate of flow of species } i \quad (2.3)$$

Notation is a complicating issue in our applications since we deal with many streams and many components. The number of variables can be quite large. For example, there are 50 variables in a system with only 4 components and 10 streams, and 10 flow rates and 4 compositions in each stream. We may avoid the superscript, not necessarily complexity, by labeling the stream flow rates with letters only and thereby reserving a single subscript to denote the component. This is often done in simple cases such as a single input and a single output, which contrasts to our approach here where we identify a total flow rate with a single superscript:

$$\sum_{\text{all components}(i)} \mathcal{W}_i^{(j)} = \text{Total mass rate of flow of stream } j = \mathcal{W}^{(j)} \quad (2.4)$$

The possible ambiguity in the meaning of a single subscript highlights again the need for clarity in defining the notation for each application.

Note that if stream j consists of more than one phase, $\mathcal{W}^{(j)}$ refers to the total of all phases. An example is the feed to the drum in flash vaporization.

We do not generally meter individual mass flows. We meter the total volume or mass flow rates, for example, and measure the concentrations. We can generalize our notion of flow rates to be used in the mass balance to include these cases and others and to gain a better understanding of input and output flows as follows.

Consider an elapse of time, δt , during which an element of mass, δm , from stream j leaves a process unit through a circular conduit with cross-sectional area A as depicted in Figure 2.3. We will assume that all of the constituents of the mixture move with the same velocity and that this velocity is uniform over the cross section.

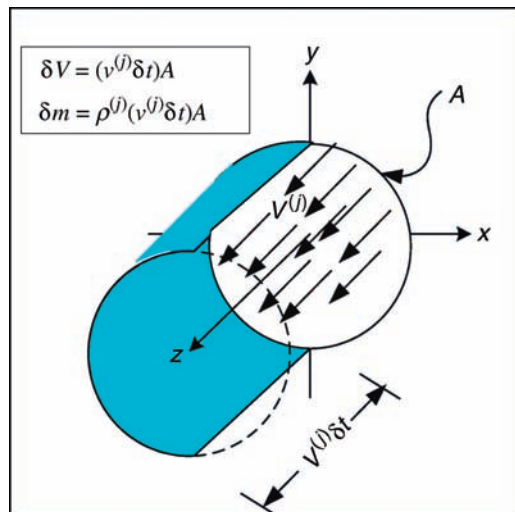


FIGURE 2.3 Idealized exit from process to cylindrical conduit S_j .

The assumption of a uniform velocity field neglects the retarding effect of the wall on the fluid motion in that vicinity. The assumption that all species have the same velocity neglects the small velocity of each species relative to the average velocity motion called diffusion. By neglecting diffusion we postpone consideration of process units or entities where the inputs or outputs are restricted, for example, by a membrane or by a porous structure such as a catalyst. These applications are found most often inside process equipment and are not normally important at the entrances and exits. They are considered in Part II.

All of the mass that passes through the surface A is contained in the cylindrical volume element swept out by the velocity. The volume element is indicated in Figure 2.3 from which the mass is obtained by introducing the stream density. The mass flow rate is then given by

$$\mathcal{W}^{(j)} = \frac{\delta m}{\delta t} = \rho^{(j)} v^{(j)} A \quad (2.5)$$

The product of density and velocity is the mass flow rate per unit area and is called the mass flux. The flux is an important quantity and is often used as a basis for scaling up small-scale operations such as pilot plants.

If $\omega_i^{(j)}$ is the fraction of δm that is species i , then

$$\omega_i^{(j)} \frac{\delta m}{\delta t} = \omega_i^{(j)} \mathcal{W}^{(j)}$$

The mass fraction, $\omega_i^{(j)}$, reflects the conditions at the entrance to the process unit. Concentrations in general refer only to conditions existing at an inlet or outlet of a process unit. A uniformly mixed unit is a special case where the outlet concentration is also the concentration throughout the

process unit. The product of concentration and flow rate can be used in the mass balance by substitution into Equation (2.4).

Note the interaction of the units in Equation (2.6),

$$\frac{\text{mass } i}{\text{total mass}} \times \frac{\text{total mass}}{\text{time}} = \frac{\text{mass } i}{\text{time}} \quad (2.6)$$

is such that the concentration units and the units of the total flow are related. Their product must give the units required for the mass balance. For example, we could use the mole ratio concentration unit (moles i /mole of constituent s) and use the flow rate of species s in place of the total flow. The validity of the mass balance would not be upset by substitution of the alternate flow and concentration variables.

$$\mathcal{V}^{(j)} = \frac{\delta V_j}{\delta t} = v^{(j)} A \quad (2.7)$$

$$\mathcal{W}^{(j)} = \rho^{(j)} \mathcal{V}^{(j)} \quad (2.8)$$

The velocity is seen to be a volume flux. Note that any property may be followed by combining its volume concentration with the velocity.

The density, $\rho^{(j)}$, is an equation of state for the fluid in stream j . It generally depends on the pressure, temperature, and concentration. Some examples are given in the following section.

2.1.1.1 Some Equations of State There is a wide variety of equations of state that apply to classes of materials over specific ranges of operating conditions. A particularly important class is the cubic equations of state that are explicit in pressure. Some of these cubic equations can describe both liquid and gas behavior. An application to a pure liquid is given in Example 2.1.1.1-1. Applications to liquid mixtures will be discussed further in Chapter 6 in the context of phase equilibrium.

Two popular examples of cubic equations are listed in Table 2.1. The truncated virial equation from statistical mechanics is also listed. A number of equations of state can be cast in the form of the virial equation. The composition dependence of the parameters in the cubic equations of state finds its roots in statistical mechanics.

The parameters in the cubic equations of state are typically functions of the critical parameters, the temperature and the acentric factor, ω . The critical parameters appear from the thermodynamic stability requirement that the first and second derivatives of pressure with respect to volume vanish at the critical point.

The acentric factor was introduced to account for the deviations that were observed for molecules with asymmetric force fields. The theory of corresponding states implies that among other things a plot of reduced vapor pressure against reduced temperature should be the same for all molecules. Referring to Figure 2.4, this conclusion is true

TABLE 2.1 Examples of Equations of State

Equation	Parameters	Example Applications
Redlich–Kwong–Soave (#) $P = \frac{RT}{V - b} - \frac{a}{V(V + b)}$	$a = 0.42747 \frac{R^2 T_c^2}{P_c} [1 + (1 - T_r^{0.5})\alpha(\omega, T_r)]^2$ $b = 0.08664 \frac{RT_c}{P_c}$ $\alpha(\omega, T_r) = 0.48508 + 1.5517\omega - 0.15613\omega^2$	Plant simulations: ^a • Ammonia • Ethylene • Acrylonitrile
Peng–Robinson $P = \frac{RT}{V - b} - \frac{a}{V^2 + 2bV - b^2}$	$a = 0.45724 \frac{R^2 T_c^2}{P_c} [1 + (1 - T_r^{0.5})\alpha(\omega, T_r)]^2$ $b = 0.07780 \frac{RT_c}{P_c}$ $\alpha(\omega, T_r) = 0.37464 + 1.5422\omega - 0.26992\omega^2$	Plant simulations: ^a • Vinyl chloride monomer • Refinery lube oil unit • Ethyl benzene
Truncated virial equation $Z = \frac{PV}{RT} = 1 + B \frac{1}{V}$	$B = \frac{RT_c}{P_c} (B^{(0)} + \omega B^{(1)})$ $B^{(0)} = 0.083 - 0.422T_r^{-1.6}$ $B^{(1)} = 0.139 - 0.172T_r^{-4.2}$	Fugacity coefficients of gases up to several atmospheres

Source: Walas (1985).

#Multiply a by $1.202 \exp(-0.30288T_r)$ for hydrogen.

^aAspen Technology (2000).

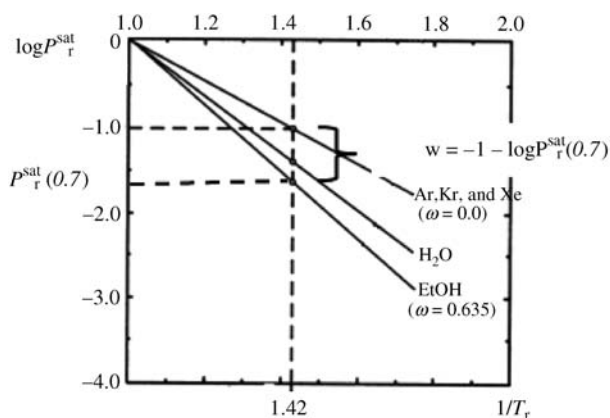


FIGURE 2.4 Determination of acentric factor from reduced vapor pressure. (Adapted from Tester and Modell, 1997.)

for the symmetric molecules, but significant deviations occur for those molecules with asymmetric force fields.

The acentric factor is the vertical distance between the line for the symmetric molecules and the molecule in question at a value of reduced temperature where the reduced vapor pressure is 0.1. This occurs at a reduced temperature of 0.7, which is near the boiling point for many compounds. Consequently, the vapor pressure is likely to be available. Otherwise, any reasonable measure of the distance from the line for the symmetrical molecules would do.

Example 2.1.1.1-1: Calculate the Molar Volume of Methane at -250°F

The critical temperature and pressure of CH_4 are 343 R and 665.73 psia and the ω acentric factor is given by 0.011

(Yaws, 1999). The parameters for the RKS equation of state in Table 2.1 are therefore given by

$$a = 0.42747 \frac{(10.73 \times 343.02)^2}{665.73} \left[1 + \left(1 - \sqrt{\frac{310}{343.02}} \right) \right]$$

$$(0.48508 + (1.5517 \times 0.011) - (0.15613 \times 0.011^2)) = 9135$$

$$b = 0.08664 \frac{10.73 \times 343.02}{665.73} = 0.479$$

The equation for the isotherm is then

$$P(V) = \frac{10.73 \times 310}{V - 0.479} - \frac{9135}{V(V + 0.479)}$$

which is plotted in Figure 2.5.

There is clearly a range of pressures for each of which there are three intersections or roots of the isotherm. The smallest can be interpreted as the molar volume of the liquid and the largest as the molar volume of the gas at the temperature of the isotherm. The pressure is the vapor pressure at this temperature. The question is which pressure to choose since any in the range of multiple intersections will provide the aforementioned behavior. Thermodynamic arguments (e.g., Sandler, 1999) conclude that the saturation pressure is the average pressure between the two molar volumes. The net area between the average pressure and the isotherm is zero. An algorithm for finding the saturation pressure is as follows:

1. Assume an average pressure.
2. Determine the roots.
3. Evaluate the integral.

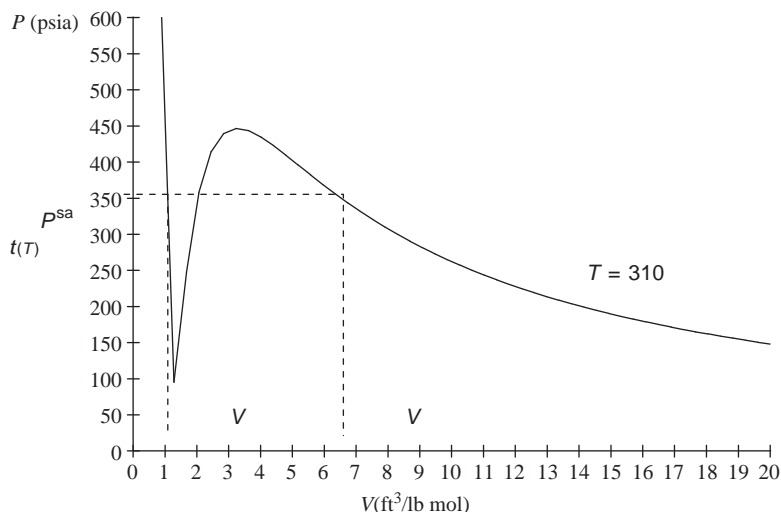


FIGURE 2.5 -150°F isotherm for methane: RKS equation of state.

4. Determine average pressure from the integral.
5. Reset the average pressure to the calculated value.
6. Go to step 2 and repeat until the pressure converges.

Application of the algorithm (root calculation is shown only for the first step):

Assume the saturation pressure = 355 psia.

$$355 = \frac{10.73 \times 310}{V - 0.479} - \frac{9135}{V(V + 0.479)}, \quad V \in (0, 2)$$

Solutions are $\{V = 0.94341\}$ and $\{V = 6.3780\}$

$$\frac{1}{6.3780 - 0.94341} \int_{0.94341}^{6.3780} P(v) dv = 368.93$$

$$\frac{1}{5.9574 - 0.93942} \int_{0.93942}^{5.9574} P(v) dv = 369.53$$

$$\frac{1}{5.9397 - 0.93925} \int_{0.93925}^{5.9397} P(v) dv = 369.53$$

$$V_L = 0.9393 \text{ lb mol/ft}^3$$

$$V_G = 5.9397 \text{ lb mol/ft}^3$$

The form of a cubic equation of state is generally retained for mixtures. The definition of an arbitrary parameter, p , in the equation of state is extended to the multicomponent case through the following mixture rule:

$$p = \sum_{i,j} x_i x_j p_{ij} \quad (2.9)$$

This is based on the results of molecular theory and applies exactly to the second virial coefficient, B , for example in Table 2.1. The p_{ij} are replaced with combination rules

$$p_{ij} = f(p_i, p_j), \quad \text{where } p_{ii} = p_i \quad (2.10)$$

A modified root mean square value is used for f to evaluate the a parameter in the Redlich–Kwong–Soave and Peng–Robinson equations of state:

$$a = \sum_{i,j=1}^C x_i x_j a_{ij} \quad (2.11)$$

$$a_{ij} = \sqrt{a_i a_j} (1 - k_{ij}) \quad k_{ii} = 0, \quad k_{ji} = k_{ij} \quad (2.12)$$

The k parameter is needed to correct the root mean square value for some specific systems. It is called a binary interaction parameter since it depends on the specific binary pair (i, j). Values of this parameter are given in Tables 2.2 and 2.3.

TABLE 2.2 Binary Interaction Parameters k_{ij} for the Redlich–Kwong–Soave Equation of State

	H ₂ S	CO ₂	N ₂	CO
H ₂ S	—	0.1020	0.1400	—
CO ₂	0.1020	—	−0.0220	−0.0640
N ₂	0.1400	−0.0220	—	0.0460
CO	—	−0.0640	0.0460	—
Methane	0.0850	0.0973	0.0319	0.0300
Ethane	0.0829	0.1346	0.0388	0.0000
<i>n</i> -Propane	0.0831	0.1018	0.0807	0.0200
2-Methylpropane	0.0523	0.1358	0.1357	—
<i>n</i> -Butane	0.0609	0.1474	0.1007	—
2-Methylbutane	—	0.1262	—	—
<i>n</i> -Pentane	0.0697	0.1278	—	—
<i>n</i> -Hexane	—	—	0.1444	—
<i>n</i> -Heptane	0.0737	0.1136	—	—
<i>n</i> -Octane	—	—	—	0.1000
<i>n</i> -Nonane	0.0542	—	—	—
<i>n</i> -Decane	0.0464	0.1377	0.1293	—
Propylene	—	0.0914	—	—
Cyclohexane	—	0.1087	—	—
Isopropylcyclohexane	0.0562	—	—	0.0100
Benzene	—	0.0810	0.2131	—
1,3,5-Trimethylbenzene	0.0282	—	—	—

Source: Walas (1985).

TABLE 2.3 Binary Interaction Parameters k_{12} for the Peng–Robinson Equation of State

	C ₂ H ₄	C ₂ H ₆	C ₃ H ₆	C ₃ H ₈	<i>i</i> -C ₄ H ₁₀	<i>n</i> -C ₄ H ₁₀	<i>i</i> -C ₅ H ₁₂	<i>n</i> -C ₅ H ₁₂	<i>n</i> -C ₆ H ₁₄	C ₆ H ₆	<i>c</i> -C ₆ H ₁₂	<i>n</i> -C ₇ H ₁₆	<i>n</i> -C ₁₀ H ₂₂	N ₂	CO	CO ₂	SO ₂	H ₂ S
CH ₄	0.022	−0.003	0.033	0.016	0.026	0.019	−0.006	0.026	0.040	0.055	0.039	0.035	0.049	0.030	0.030	0.09	0.136	0.08
C ₂ H ₄		0.010				0.092				0.031		0.014	0.025	0.086	−0.022	0.056		
C ₂ H ₆			0.089	0.001	−0.007	0.010		0.008	−0.04	0.042	0.018	0.007	0.014	0.044	0.026	0.130		0.086
C ₃ H ₆				0.007	−0.014									0.09	0.026	0.093		0.08
C ₃ H ₈					−0.007	0.003	0.011	0.027	0.001	0.023		0.006	0.0	0.078	0.03	0.12		0.08
<i>i</i> -C ₄ H ₁₀						0.0								0.10	0.04	0.13		0.047
<i>n</i> -C ₄ H ₁₀								0.017	−0.006			0.003	0.008	0.087	0.04	0.135		0.07
<i>i</i> -C ₅ H ₁₂							0.06							0.092	0.04	0.121		0.06
<i>n</i> -C ₅ H ₁₂										0.018	0.004	0.007		0.10	0.04	0.125		0.063
<i>n</i> -C ₆ H ₁₄										0.010	−0.004	−0.008		0.15	0.04	0.11		0.06
C ₆ H ₆											0.013	0.001	0.1	0.164	0.11	0.077	0.015	
<i>c</i> -C ₆ H ₁₂														0.14	0.10	0.105		
<i>n</i> -C ₇ H ₁₆														0.1	0.04	0.10		0.06
<i>n</i> -C ₁₀ H ₂₂														0.11	0.04	0.114		0.033
N ₂															0.012	−0.02	0.08	0.17
CO																0.03		0.054
CO ₂																	0.136	0.097
SO ₂																		
H ₂ S																		

Source: Adapted from Sandler (1998).

An *arithmetic mean* is used for f to evaluate the value of b in the Redlich–Kwong–Soave and Peng–Robinson equations of state:

$$b = \sum_{i,j=1}^C x_i x_j b_{ij} \quad (2.13)$$

$$b_{ij} = \frac{1}{2}(b_i + b_j) \quad (2.14)$$

$$b = \sum_{i=1}^C x_i b_i \quad (2.15)$$

The virial coefficient is extended to mixtures by using these expressions in Table 2.1 with pseudocritical properties for the binary pairs in the mixture (Walas, 1985):

$$B = \sum_{i,j} x_i x_j B_{ij} \quad (2.16)$$

$$B_{ij} = \frac{RT_{cij}}{P_{cij}} (B_{ij}^{(0)} + \omega_{ij} B_{ij}^{(1)}) \quad (2.17)$$

$$\omega_{ij} = \frac{1}{2}(\omega_i + \omega_j) \quad (2.18)$$

$$Z_{cij} = \frac{1}{2}(Z_{ci} + Z_{cj}) \quad (2.19)$$

$$V_{cij}^{1/3} = \frac{1}{2}(V_{ci}^{1/3} + V_{cj}^{1/3}) \quad (2.20)$$

$$T_{cij} = (1 - k_{ij})(T_{ci} T_{cj})^{1/2} \quad (2.21)$$

$$P_{cij} = z_{cij} RT_{cij} / V_{cij} \quad (2.22)$$

The value of the binary interaction parameter is given by Tsonopoulos (in Walas, 1985) in number or correlations. For methane (i)–hydrocarbon (j) mixtures, for example,

$$k_{ij} = 0.0279(\ln n_{cj})^2 \quad (2.23)$$

where n_c is the number of carbon atoms.

As mentioned above, the change in volume of a liquid or solid with pressure or temperature is not substantial. When this is not the case, the following approximation can be used. The change in volume resulting from changes in pressure and temperature is given by

$$dV = \left(\frac{\partial V}{\partial T} \right)_P dT + \left(\frac{\partial V}{\partial P} \right)_T dP \quad (2.24)$$

or

$$d \ln V = \alpha_T dT - \kappa dP \quad (2.25)$$

where the coefficient of thermal expansion and isothermal compressibility are defined respectively by

$$\alpha_T = \frac{1}{V} \left(\frac{\partial V}{\partial T} \right)_P \quad (2.26)$$

$$\kappa = -\frac{1}{V} \left(\frac{\partial V}{\partial P} \right)_T \quad (2.27)$$

We will take the equation of state for the pure condensed states to be the integral of Equation (2.26) where the coefficient of thermal expansion and isothermal compressibility are assumed constant:

$$V = V_0 e^{\alpha_T(T-T_0)} e^{-\kappa(P-P_0)} \quad (2.28)$$

Typical values of these parameters are, respectively, 10^{-5} (K^{-1}) and 10^{-6} (bar^{-1}) for solids and 10^{-3} (K^{-1}) and 10^{-4} (bar^{-1}) for liquids.

A variable density will give rise to a nonconstant volumetric flow rate, which will require energy and momentum balances to determine the temperature and pressure in the density function or equation of state.

We can express the flow rate of species i as the product of a concentration and total flow rate for use in the mass balance as

$$\rho_i^{(j)} \mathcal{V}^{(j)} = \mathcal{W}_i^{(j)} \quad (2.29)$$

The concentration $\rho_i^{(j)}$ is the mass of i per unit volume in the differential element of steam j in consistent units and is related to the mass fraction by

$$\frac{\rho_i^{(j)}}{\rho^{(j)}} = \omega_i^{(j)} \quad (2.30)$$

Note that the units of the concentration and total flow in Equation (2.22) are related as in Equation (2.7):

$$\frac{\text{mass } i}{\text{total volume}} \times \frac{\text{total volume}}{\text{time}} = \frac{\text{mass } i}{\text{time}} \quad (2.31)$$

It is often expedient if the total stream flows are approximately constant between inlets and outlets. The volumetric flow of gases is very sensitive to changes in temperature and pressure and the total mass flow will change significantly if a concentrated component is transferred to another phase, which is not uncommon in separation processes. A convenient flow unit in many such applications is the mass flow of a solvent or, more generally, of a nontransferring component, say species s , $\mathcal{W}_s^{(j)}$. The concentration unit required in the mass balance is the mass ratio of species i to species s :

$$\omega_{i/s} = \frac{\text{mass } i}{\text{mass } s} = \frac{\omega_i}{\omega_s} = \frac{\omega_i}{1 - \sum_{\text{all species } (k \neq s)} \omega_k} \quad (2.32)$$

where the solvent must be clearly identified and understood. The mass flow rate expression to be used in the mass balance for species i is then

$$\omega_{i/s}^{(j)} \mathcal{W}_s^{(j)} = \mathcal{W}_i^{(j)} \quad (2.33)$$

Note again that the units of the concentration and total flow in Equation (2.26) are related as in Equation (2.6):

$$\frac{\text{mass } i}{\text{mass } s} \times \frac{\text{total mass } s}{\text{time}} = \frac{\text{mass } i}{\text{time}} \quad (2.34)$$

This must always be the case. We are free to express the total flow in any units or terms that we wish as long as the concentration unit is consistent, that is, the product of the flow and the concentration gives $\mathcal{W}_i^{(j)}$:

$$\frac{\text{mass } i}{\text{flow unit}} \times \frac{\text{flow unit}}{\text{time}} = \frac{\text{mass } i}{\text{time}} \quad (2.35)$$

Recall that molar units may also be used. Conversions between different measures of flow and concentration measures can be developed. The relation between mass and molar concentrations is given by:

$$\frac{\rho_i^{(j)}}{M_i} = c_i^{(j)} \quad (2.36)$$

where $c_i^{(j)}$ and M_i are the moles per unit volume in stream j and the molecular weight of species i , respectively. Mass and mole fractions are related by

$$x_i^{(j)} = \frac{\omega_i^{(j)} / M_i}{\sum_{\text{all species } (k)} \omega_k^{(j)} / M_k} \Rightarrow \sum_{\text{all species } (i)} x_i^{(j)} = 1 \quad (2.37)$$

where the mole fraction of i in stream j is $x_i^{(j)}$. Mole ratios and mole fractions are related similarly to their analogues in mass units by

$$x_{i/s}^{(j)} = \frac{x_i^{(j)}}{x_s^{(j)}} = \frac{x_i^{(j)}}{1 - \sum_{\text{all species } (k \neq s)} x_k^{(j)}} \quad (2.38)$$

Total flow rates can also be related. Note that

$$\sum_{\text{all species } (i)} \rho_i^{(j)} = \rho^{(j)} \quad (2.39)$$

and refer, for example, to Equation (2.30) summed over all species for the relation of the total mass to volume flows. The total molar flow, $\mathcal{N}^{(j)}$, and total mass flows are related by

$$\mathcal{N}^{(j)} = \frac{\mathcal{W}^{(j)}}{M^{(j)}} \quad (2.40)$$

where the molecular weight of the mixture in stream j is

$$M^{(j)} = \sum_{\text{all species } (i)} x_i^{(j)} M_i \quad (2.41)$$

The following would be used in the mole balance in the case of a total molar flow unit:

$$x_i^{(j)} \mathcal{N}^{(j)} = \mathcal{N}_i^{(j)} \quad (2.42)$$

The units required are moles i /time. The total volume flow would be used in the molar case as

$$c_i^{(j)} \mathcal{V}^{(j)} = \mathcal{N}_i^{(j)} \quad (2.43)$$

Note that in concert with the mass units,

$$\sum_{\text{all species } (i)} c_i^{(j)} = c^{(j)} \quad (2.44)$$

and

$$x_i^{(j)} = \frac{c_i^{(j)}}{c^{(j)}} \quad (2.45)$$

The molar equation of state for the mixture in stream j is $c^{(j)}$, a function of temperature, pressure, and concentrations.

Other examples can be devised, but all have similar bases. Note that with this notation, the species and stream indices are separated by one line, making it easy to check a mass balance for a common species. The stream numbers are easily checked if an overall mass balance is done first, since all streams must appear.

2.1.1.2 Mass Rate of Production The mass rate of production of species i by chemical reactions is the net result of all chemical reactions taking place in the chemical processing system. The location of the reactions with respect to the individual units in the system is not recognized in the mass balance, except by finer definitions of the system that include fewer process units. We will limit the discussion to single reactions expressed as follows:

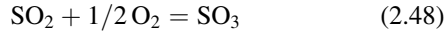
$$\sum_{\text{all species } (i)} \vartheta_i A_i = 0 \quad (2.46)$$

where the stoichiometric coefficients have the following signs:

$$\left. \begin{array}{ll} \vartheta_i = 0, & i = \text{inert} \\ \vartheta_i < 0, & i = \text{reactant} \\ \vartheta_i > 0, & i = \text{product} \end{array} \right\} \quad (2.47)$$

and A_i is the chemical symbol for species i . As an example, consider the oxidation of SO_2 (A_1) in air, N_2 (A_2), and

O₂ (A₃), to produce SO₃ (A₄), a step in H₂SO₄ production:



In the above scheme, $\vartheta_1 = -1$, $\vartheta_2 = 0$, $\vartheta_3 = -1/2$, and $\vartheta_4 = 1$.

Conservation of total mass in the reaction is expressed as

$$\sum_{\text{all species}(i)} \vartheta_i M_i = 0 \quad (2.49)$$

which is the motivation for the expression of the reaction stoichiometry as a mathematical equality. In the SO₂ example, the preceding result states that the molecular weight of SO₃ is the molecular weight of SO₂ plus half the molecular weight of O₂.

The molar rates of production of each species, R_i , are related by the stoichiometric coefficients:

$$\frac{R_i}{\vartheta_i} = \mathcal{R}^{(V)} \succ 0, \quad \text{for all components } (i) \quad (2.50)$$

In the SO₂ example, the rate of production of SO₃ is the rate of production of O₂ (negative) divided by $-1/2$, or oxygen must be depleted at twice the rate sulfur trioxide is formed. Check the implications for sulfur dioxide and alter the equation so that it works for nitrogen.

In some circumstances, such as in level one design calculations, we will know the molar reaction rate of a particular reactant, say A_{key} , by knowing its conversion. In this case, all of the reaction rates are known by

$$\frac{R_{\text{key}}}{\vartheta_{\text{key}}} = \mathcal{R}^{(V)} \quad (2.51)$$

$$R_i = \vartheta_i \frac{R_{\text{key}}}{\vartheta_{\text{key}}} \quad (2.52)$$

The preceding two relations are true also if A_{key} is a product whose production rate is known. Specifications regarding reaction rates are for the purposes of specifying operating conditions and material flows for the processing system. Equipment sizing in level-two design calculations follow these steps, which may need to be refined based on the results of the individual designs.

The above expressions must be scaled by the molecular weights to use mass units for the reaction rates. Note that

$$\sum_{\text{all species}(i)} R_i = \left\{ \sum_{\text{all species}(i)} \vartheta_i \right\} \mathcal{R}^{(V)} \quad (2.53)$$

where

$$\sum_{\text{all species}(i)} \vartheta_i = \text{mole change for the reaction} \quad (2.54)$$

Equation (2.54) expresses the fact that moles may not be conserved in the reaction. The sum of the mass rate of production for each species would, of course, be zero. Molar units are the most expedient ones to employ when chemical reactions are present.

The rate of mass accumulation refers to the rate at which the mass of species i is increasing throughout all of the units contained in the system. Like the reaction rate, the accumulation rate can only be localized by a less expansive definition of the system. At steady-state conditions, none of the system characteristics change in time, which requires that all rates of accumulation vanish. We will be concerned mostly with steady-state conditions.

2.2 STEADY-STATE MASS BALANCES WITHOUT CHEMICAL REACTIONS

Steady-state mass balances without chemical reactions can be expressed for each species as follows:

$$\sum_{\text{all input streams}(j)} \mathcal{W}_i^{(j)} = \sum_{\text{all output streams}(j)} \mathcal{W}_i^{(j)}, \quad i = 1, 2, \dots, N \quad (2.55)$$

These relations are used to determine the unknown flows and compositions that are the result of process decisions we have made to reach our objectives. The relations may be applied to a multiphase system since there can be no net interchanges of mass between the phases at steady state. On the other hand, they may be applied to a single phase in a multiphase application, but provision must then be made for interphase mass transfer in addition to the input and output streams for the process. Such interfacial mass transfer rates are considered in Chapter 12.

2.2.1 Degrees of Freedom

The variables in the macroscopic mass balances are flows and concentrations. The mass balances represent relations between these variables. If the number of equations is equal to the number of unknown flows and concentrations, we cannot, or need not, make any (additional) specifications; that is, there are no degrees of freedom. Only in this circumstance can the set of mass balances be solved. If the number of unknowns exceeds the number of equations, the degrees of freedom are positive and the mass balances cannot be solved. We must make additional process decisions or specifications. If the number of mass balances

exceeds the number of unknowns, the mass balance again cannot be solved. The problem is overconstrained in this case and we must leave some of our expressed needs to fate. The degrees of freedom must be zero before any attempt is made to solve the mass balances. The degrees of freedom can be investigated as follows.

The number of components in the system is taken to be N_C and either mass or molar units may be used. If the number of input streams is N_F and the number of output streams is N_P , there are $(N_F + N_P)N_C$ unknown flow rates in Equation (2.55). Since there are only N relations, the number of degrees of freedom in the system is

$$\Phi = (N_F + N_P - 1)N_C \quad (2.56)$$

This expresses the requirement that Φ flow rates must be specified or, more generally, Φ independent relations between the flow rates must be specified, in order that the mass balances in Equation (2.55) can be used to solve for the remainder.

The system may be expanded or diminished on the basis of exposing streams whose flow rates are desired, but the degrees of freedom may always be used to check that sufficient specifications are present. If the number of subsystems is N_u , which must always be less than the total number of active units, the degrees of freedom will be

$$\Phi = (N_s - N_u)N_C \quad (2.57)$$

where the number of streams entering or leaving the subsystems, N_s , has replaced N_P and N_F to avoid repetition. This result does not account for restrictions on the process flows, temperature, and pressure that are inherent in the process equipment or operation and therefore decrease the degrees of freedom. For example, we do not expect to find process materials in the coolant stream from a heat exchanger. However, these flows are counted as unknowns in the preceding expression for the degrees of freedom and are specified when satisfying the degrees of freedom in a particular application. We will account for stream splitters explicitly and leave other equipment to examples.

Consider the stream splitter shown in Figure 2.6. The degrees of freedom are reduced because of the splitter property that the concentrations in the daughter streams are the same as the parent stream. A fraction ϵ_j of the feed is sent to the daughter stream S_j , where

$$\sum_{j=1}^{N_D} \epsilon_j = 1 \quad (2.58)$$

Consequently,

$$\begin{aligned} \mathcal{W}_i^{(j)} &= \epsilon_j \mathcal{W}_i^{(0)} & j = 1, 2, \dots, N_D \\ & & i = 1, 2, \dots, N_C \end{aligned} \quad (2.59)$$

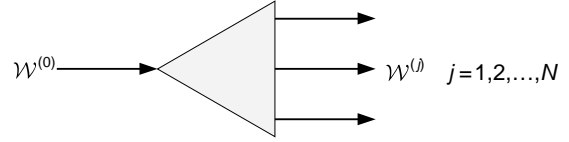


FIGURE 2.6 Splitter.

These $N_C N_D$ equations are not independent of the mass balances. The last set, $j = N_D$, can be derived from the mass balances as follows: adding,

$$\sum_{j=1}^{N_D-1} \mathcal{W}_i^{(j)} = \mathcal{W}_i^{(0)} \sum_{j=1}^{N_D-1} \epsilon_j, \quad i = 1, 2, \dots, N_C \quad (2.60)$$

$$\begin{aligned} \mathcal{W}_i^{(0)} - \mathcal{W}_i^{(N_D)} &= \mathcal{W}_i^{(0)} (1 - \epsilon_{N_D}), \quad i = 1, 2, \dots, N_C \\ \mathcal{W}_i^{(N_D)} &= \epsilon_{N_D} \mathcal{W}_i^{(0)}, \quad i = 1, 2, \dots, N_C \end{aligned} \quad (2.61)$$

We have therefore added $N_C(N_D - 1)$ equations, and N_D unknowns with one relation between them, stating that they must sum to unity. The total degrees of freedom can then be adjusted as follows:

$$\begin{aligned} \Phi &= (N_s - N_u)N_C - N_C(N_D - 1) - 1 + N_D \\ \Phi &= (N_s - N_u)N_C - (N_C - 1)(N_D - 1) \end{aligned} \quad (2.62)$$

If more than one splitter is present,

$$\Phi = (N_s - N_u)N_C - (N_C - 1)(N_{D,\text{total}} - N_{\text{splitters}}) \quad (2.63)$$

This expression represents the degrees of freedom when splitters are present and requires that the splitter mass balances be written as well as the equations above.

Concentrations and total flows may be used in place of the individual flows. The number of degrees of freedom will, however, remain the same. Consider stream j , for example. There is one total flow and N_C concentrations to give $(N_F + N_P)(N_C + 1)$ variables. To the N_C possible mass balances, we must add a relation for the concentrations. Stream concentrations in fractional units must sum to unity, those in volume units must obey an equation of state and the mole ratio for a nontransferring component is unity by definition. The number of equations is then $N_C + N_F + N_P$, which must be subtracted from the number of variables. The result reduces to Equation (2.59). The relation between the concentrations must be explicitly defined when using software to solve the mass balances. Software is not aware that mole fractions must sum to unity, for example, even though you may apply this automatically. The relation between the concentration units is equivalent to the total mass balance. Also, specifications for the process must be consistent with the mass balances and concentration relations. If all mass

fractions for a stream are specified, for example, they must sum to unity.

The individual species balances in mass fraction units and total flows are given by

$$\sum_{\text{all input streams}(j)} \omega_i^{(j)} \mathcal{W}^{(j)} = \sum_{\text{all output streams}(j)} \omega_i^{(j)} \mathcal{W}^{(j)},$$

$$i = 1, 2, \dots, N_C \quad (2.64)$$

The total mass balance is the addition of these over the individual components:

$$\sum_{\text{all species}(i)} \sum_{\text{all input streams}(j)} \omega_i^{(j)} \mathcal{W}^{(j)}$$

$$= \sum_{\text{all species}(i)} \sum_{\text{all output streams}(j)} \omega_i^{(j)} \mathcal{W}^{(j)} \quad (2.65)$$

or

$$\sum_{\text{all input streams}(j)} \left[\sum_{\text{all species}(i)} \omega_i^{(j)} \right] \mathcal{W}^{(j)}$$

$$= \sum_{\text{all output streams}(j)} \left[\sum_{\text{all species}(i)} \omega_i^{(j)} \right] \mathcal{W}^{(j)} \quad (2.66)$$

or

$$\sum_{\text{all input streams}(j)} \mathcal{W}^{(j)} = \sum_{\text{all output streams}(j)} \mathcal{W}^{(j)} \quad (2.67)$$

One individual species balance may therefore be eliminated in favor of a total mass balance. The total mass balance may not be added to a full set of species balances and the concentration relation is explicitly required.

Note that it is generally preferable to use the individual flows since in this case the mass balances are linear. Also in making process specifications, we presume that at the next level of process design it will be possible to configure that process units to meet the process specifications. Adjustments may therefore be needed in the process specifications and the material balances may need to be redone.

Example 2.2.1-1: Manufacture of Sugar

A simplified flow sheet for the manufacture of sugar is shown in Figure 2.7.

Sugar cane (S_1) is fed to a mill where a syrup is squeezed out, and the resulting gases (S_2) contain 80% pulp. The syrup (S_3) containing finely divided pieces of

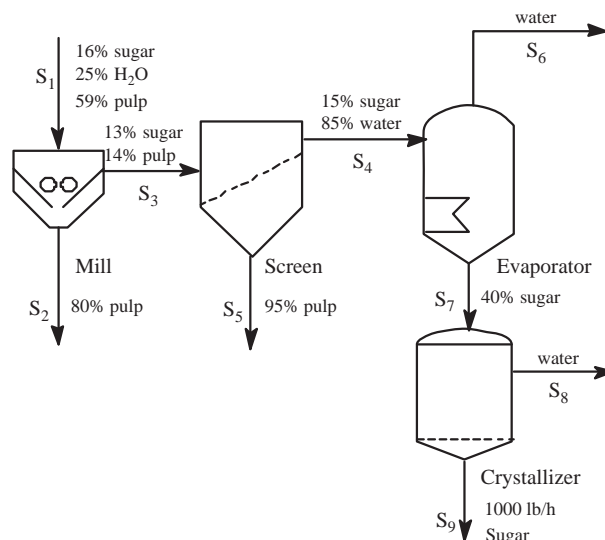


FIGURE 2.7 Sugar manufacture.

pulp is fed to a screen, which removes all of the pulp in a waste stream (S_5) and produces a clear syrup (S_4) containing 15% sugar and 85% water. The evaporator produces water (S_6) and a heavy syrup (S_7) containing 40% sugar. The crystallizer produces water (S_8) and 1000 lb/h of pure sugar crystals (S_9).

The objective is to determine all unknown flow rates and compositions and to calculate a process efficiency as lb of sugar obtained per lb of sugar cane. Can you think of another meaningful definition of efficiency for the process?

Define each unit as a processing system in order to expose all streams for analysis. Following is summary for all of the systems using mass fractions and total mass flow rates as the variables:

Sugar = component 1, water = component 2,

pulp = component 3

Number of units (N_u) = 4

Number of streams (N_s) = 9

Number of components (N_c) = 3

Number of unknowns = $9 \times (1 + 3) = 36$

Number of equations = 4×3 (mass balances) + 9 (concentration relations) = 21

Degrees of freedom (no splitters) = $\Phi = (9 - 4)3 - 0 = 15$

Specifications (total = 15)

$$\omega_1^{(1)} = 0.16, \quad \omega_2^{(1)} = 0.25$$

$$\omega_3^{(2)} = 0.80$$

$$\omega_1^{(3)} = 0.13, \quad \omega_3^{(3)} = 0.14$$

$$\omega_1^{(4)} = 0.15, \quad \omega_2^{(4)} = 0.85$$

$$\omega_3^{(5)} = 0.95$$

$$\omega_1^{(6)} = 0.0, \quad \omega_2^{(6)} = 1.0$$

$$\omega_1^{(7)} = 0.40$$

$$\omega_1^{(8)} = 0.0, \quad \omega_2^{(8)} = 1.0$$

$$\omega_1^{(9)} \mathcal{W}^{(9)} = 1000, \quad \omega_2^{(9)} = 0.0$$

Consequently, the problem is completely specified. “Normally,” one would write the mass balances and the required concentration relations and check that the degrees of freedom are zero.

Mass balances around each unit can be used to determine all of the unknown flow rates and compositions. These balances are summarized below and account for the specifications so that not all concentrations appear as variables. Note that there is no pulp present after the screen so it does not need to be introduced in the mass balances for the evaporator and crystallizer. This could be done, however, allowing the mass balances to conclude that the pulp concentrations are zero for streams 6 through 9. Try it.

$$0.16\mathcal{W}^{(1)} = \omega_1^{(2)}\mathcal{W}^{(2)} + 0.13\mathcal{W}^{(3)} \quad \text{mill, sugar}$$

$$0.25\mathcal{W}^{(1)} = \omega_2^{(2)}\mathcal{W}^{(2)} + \omega_2^{(3)}\mathcal{W}^{(3)} \quad \text{mill, water}$$

$$0.5\mathcal{W}^{(1)} = 0.80\mathcal{W}^{(2)} + 0.14\mathcal{W}^{(3)} \quad \text{mill, pulp}$$

$$\omega_1^{(2)} + \omega_2^{(2)} + 0.80 = 1 \quad \text{stream 2}$$

$$0.13 + \omega_2^{(3)} + 0.14 = 1 \quad \text{stream 3}$$

$$0.13\mathcal{W}^{(3)} = 0.15\mathcal{W}^{(4)} + \omega_1^{(5)}\mathcal{W}^{(5)} \quad \text{screen, sugar}$$

$$\omega_2^{(3)}\mathcal{W}^{(3)} = 0.85\mathcal{W}^{(4)} + \omega_2^{(5)}\mathcal{W}^{(5)} \quad \text{screen, water}$$

$$0.14\mathcal{W}^{(3)} = 0.95\mathcal{W}^{(5)} \quad \text{screen, pulp}$$

$$\omega_1^{(5)} + \omega_2^{(5)} + 0.95 = 1 \quad \text{stream 5}$$

$$0.15\mathcal{W}^{(4)} = 0.40\mathcal{W}^{(7)} \quad \text{evaporator, sugar}$$

$$0.85\mathcal{W}^{(4)} = \mathcal{W}^{(6)} + 0.60\mathcal{W}^{(7)} \quad \text{evaporator, water}$$

$$0.40\mathcal{W}^{(7)} = 1000 \quad \text{crystallizer, sugar}$$

$$0.60\mathcal{W}^{(7)} = \mathcal{W}^{(8)} \quad \text{crystallizer, water}$$

Unknown flows: $\mathcal{W}^{(1)}, \mathcal{W}^{(2)}, \mathcal{W}^{(3)}, \mathcal{W}^{(4)}, \mathcal{W}^{(5)}, \mathcal{W}^{(6)}, \mathcal{W}^{(7)}, \mathcal{W}^{(8)}$

Unknown concentrations: $\omega_1^{(2)}, \omega_2^{(2)}, \omega_2^{(3)}, \omega_1^{(5)}, \omega_2^{(5)}$

Total unknowns = 13

Total equations = 13

Solution is

$$\mathcal{W}^{(1)} = 2457.4, \quad \mathcal{W}^{(2)} = 1675.5, \quad \mathcal{W}^{(3)} = 7818.9,$$

$$\mathcal{W}^{(4)} = 6666.7$$

$$\mathcal{W}^{(5)} = 1152.3, \quad \mathcal{W}^{(6)} = 4166.7, \quad \mathcal{W}^{(7)} = 2500.0,$$

$$\mathcal{W}^{(8)} = 1500.0$$

$$\omega_1^{(2)} = 0.174, \quad \omega_2^{(2)} = 0.026$$

$$\omega_2^{(3)} = 0.73$$

$$\omega_1^{(5)} = 1.4286 \times 10^{-2}, \quad \omega_2^{(5)} = 3.5714 \times 10^{-2}$$

$$\text{Efficiency} = 1000/\mathcal{W}^{(1)} : 4.0693 \times 10^{-2} \text{ lbs sugar/lb sugarcane}$$

Example 2.2.1-2: Air Separation Plant

Adapted from Luyben and Wenzel (1988).

A typical separation plant is represented in Figure 2.8 and consists of two distillation columns (1 and 3) and a heat exchanger (2):

The pressures in the two columns is adjusted so the heat of condensation of the light component in the first column is at a sufficiently high temperature to be used to boil up the heavy component i in the second column. The condensation and boiling take place on the two sides of the heat exchanger.

Process specifications:

1. The reflux to the second column is three times that of the first column.
2. The plant produces 2500 ft³/h of oxygen product at 350 psia and -100°F .

Determine the stream flows and the unknown concentrations.

Degrees of Freedom

$N_C = 2, N_u = 3$ (includes one splitter with two daughter streams and excludes the heat exchanger).

$N_S = 7$ There is insufficient information to determine the unlabeled stream (Why?).

$\Phi = (7 - 3)2 - (2 - 1)(2 - 1) = 7$ There are five specified concentrations (count them) and two process specifications: The reflux relation above and the oxygen production rate, $N^{(7)}$. The problem is therefore well defined.

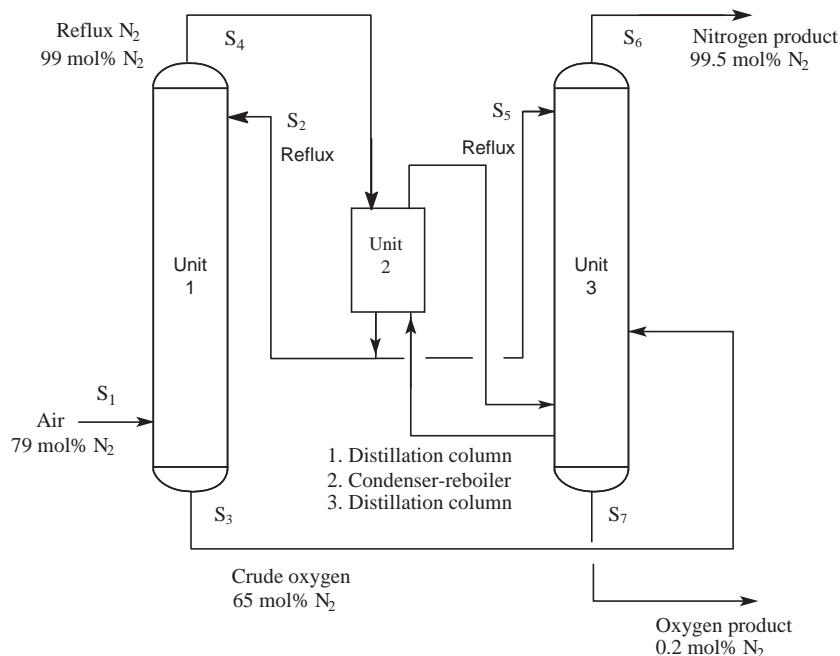


FIGURE 2.8 Air separation plant.

Define species 1 = nitrogen and 2 = oxygen and assume that air is an ideal gas consisting of 79 mol% N_2 and 29 mol% O_2 .

The unspecified concentrations may be easily established since the sum of the mole fractions is one (Equation 2.38):

$$x_2^{(1)} = 0.21, \quad x_2^{(3)} = 0.35,$$

$$x_2^{(4)} = 0.01 = x_2^{(2)} = x_2^{(5)} \text{ (Why?)},$$

$$x_2^{(6)} = 0.005, \quad x_2^{(7)} = 0.998$$

There are three process units: two distillation columns and a stream splitter. The heat exchanger is not significant from an overall mass balance point of view since it only adds/subtracts thermal energy. A set of independent mass balances can be written around each of these or two of these and the overall. You might try a combination other than the one we have chosen. Finally, we have the process specifications.

$$\mathcal{N}^{(1)} = \mathcal{N}^{(6)} + \mathcal{N}^{(7)}$$

$$0.79\mathcal{N}^{(1)} = 0.995\mathcal{N}^{(6)} + 0.002\mathcal{N}^{(7)}$$

$$\mathcal{N}^{(1)} + \mathcal{N}^{(2)} = \mathcal{N}^{(4)} + \mathcal{N}^{(3)}$$

$$0.79\mathcal{N}^{(1)} + 0.99\mathcal{N}^{(2)} = 0.99\mathcal{N}^{(4)} + 0.65\mathcal{N}^{(3)}$$

$$\mathcal{N}^{(4)} = \mathcal{N}^{(2)} + \mathcal{N}^{(3)}$$

$$\mathcal{N}^{(5)} = 3\mathcal{N}^{(2)}$$

$$\mathcal{N}^{(7)} = \frac{2500(350/14.7)}{0.7302(460 - 100)}$$

Solution (lb mol/h):

$$\mathcal{N}^{(1)} = 1096.8$$

$$\mathcal{N}^{(2)} = 150.55$$

$$\mathcal{N}^{(3)} = 645.20$$

$$\mathcal{N}^{(4)} = 602.18$$

$$\mathcal{N}^{(5)} = 451.64$$

$$\mathcal{N}^{(6)} = 870.40$$

$$\mathcal{N}^{(7)} = 226.44$$

2.3 STEADY-STATE MASS BALANCES WITH SINGLE CHEMICAL REACTIONS

The addition of a single reaction amounts to another contribution to the total output flow. In molar units

$$\sum_{\text{all output streams}(j)} \mathcal{N}_i^{(j)} = \sum_{\text{all input streams}(j)} \mathcal{N}_i^{(j)} + R_i, \quad i = 1, 2, \dots, N_C \quad (2.68)$$

Overall material (total) balance

Overall nitrogen balance

Total material balance around column 1

Nitrogen balance around column 1

Total material balance around splitter

Process specification

Process specification

R_i is the rate of production of species i taking place in the selected processing system due to all of the reactions, in which A_i participates. The addition of the reaction rates increases the degrees of freedom by at most N , which can be satisfied, for example, by specifying the conversion rates of all reactive components. We will limit our discussion to cases where it is possible to define subsystems in which there is at most a single reaction taking place. In such systems, we can use the reaction stoichiometry as expressed in Equation (2.46):

$$\sum_{\text{all output streams}(j)} \mathcal{N}_i^{(j)} = \sum_{\text{all input streams}(j)} \mathcal{N}_i^{(j)} + \vartheta_i \mathcal{R}^{(V)}, \quad i = 1, 2, \dots, N_C \quad (2.69)$$

2.3.1 Degrees of Freedom: Reaction Rate and Key Component

The degrees of freedom are increased by 1 over the unreactive case because of \mathcal{R} .

$$\Phi = (N_s - N_u)N_C - (N_C - 1)(N_{D,\text{total}} - N_{\text{splitters}}) + 1 \quad (2.70)$$

We will normally have a specification of the reaction rate of a key component, which may change if we focus on another subsystem with a different chemical reaction. This specification can be used to remove the additional degree of freedom introduced by the single reaction.

The reaction rate may be fixed by a specific fractional conversion of a key reactant, x_{key} ($0 \leq x_{\text{key}} \leq 1$):

$$\sum_{\text{all output streams}(j)} \mathcal{N}_{\text{key}}^{(j)} = (1 - x_{\text{key}}) \sum_{\text{all input streams}(j)} \mathcal{N}_{\text{key}}^{(j)} \quad (2.71)$$

The freedom to choose the reaction rate or conversion is only apparent. In fact, the reaction rate is a local variable that depends on the local state of the system (see Chapter 8). The net reaction rate for the key component referred to here is the integral result of the local rates, the integral depending on the system configuration. Aside from the case where the local conditions are uniform throughout the system, a microscopic analysis is required (see Part II). Local conditions are uniform throughout the system in the case of completely mixed systems (see Chapter 6). We will proceed here under the assumption that our specification of the net reaction rate or conversion is physically realizable.

Substitution into the mass balance for the key component and using the definition of \mathcal{R} in Equation (2.50) gives

$$\mathcal{R}^{(V)} = x_{\text{key}} \left[\frac{1}{-\vartheta_{\text{key}}} \right] \sum_{\text{all input streams}(j)} \mathcal{N}_{\text{key}}^{(j)} = \frac{R_{\text{key}}}{\vartheta_{\text{key}}} \quad (2.72)$$

or

$$R_{\text{key}} = -x_{\text{key}} \sum_{\text{all input streams}(j)} \mathcal{N}_{\text{key}}^{(j)} \quad (2.73)$$

The mass balances then consist of the preceding equation and

$$\sum_{\text{all output streams}(j)} \mathcal{N}_i^{(j)} = \sum_{\text{all input streams}(j)} \mathcal{N}_i^{(j)} + \frac{\vartheta_i}{\vartheta_{\text{key}}} R_{\text{key}}, \quad i = 1, 2, \dots, N_C \quad (2.74)$$

Equations (2.73) and (2.74) organize the reactive mass balances for single reactions and incorporate all of the implications of stoichiometry in this respect. Note that the mass balance for inerts reduces to the unreactive case and that complete conversion of a key reactant results in no output flows for this species.

Often the *key reactant* is a *limiting reactant* in the sense that it is materially or stoichiometrically possible to consume this component completely by chemical reaction. There can be more than one limiting reactant. For a single reaction, the index of the limiting reactant, say l , is given by

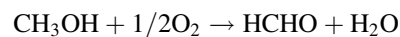
$$l = \text{Min}_{i \in \text{reactants}} \left[\frac{\sum_{\text{all input streams}(j)} \mathcal{N}_i^{(j)}}{-\vartheta_i} \right] \quad (2.75)$$

Example 2.3.1-1: Production of Formaldehyde

Adapted from Luyben and Wenzel (1988).

A condensed version of the process for the manufacture of formaldehyde is shown in Figure 2.9.

Methanol is oxidized to formaldehyde using air as the source of oxygen.



The reactor is a fixed bed containing an iron–molybdenum oxide catalyst. The reactor feed, stream 4, contains 8 mol% methanol and 10 mol% oxygen. The methanol is completely converted in the reactor. A purge stream for nitrogen is taken off the overhead product from the separator. The purge contains no water. The bottom product from the separator is a 37 wt% solution of formaldehyde in water. The additional water required for this product is supplied to the separator in stream 5.

Calculate the flow rates of the streams that have labels.

Since we are not concerned with the unlabeled streams, we may group together the two splitters and the reactor together with the separator. Therefore, we can make mass

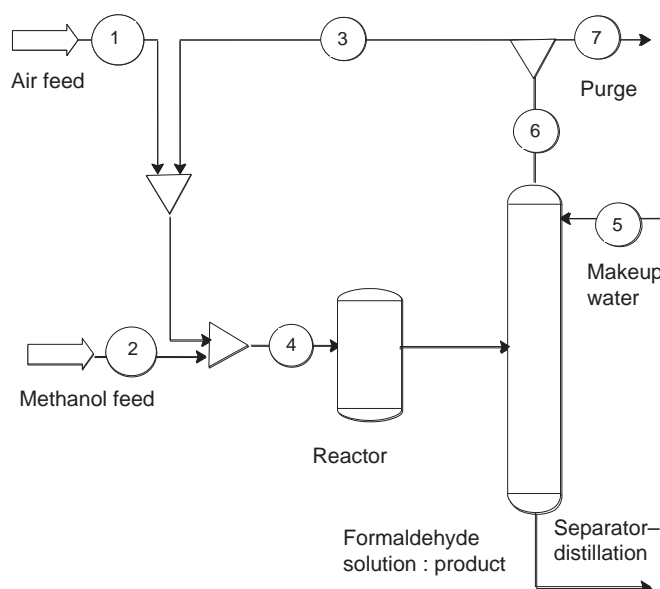


FIGURE 2.9 Manufacture of formaldehyde.

balances on three equipment groups. Note that stream 3 and stream 7 have the same composition, but possibly different flows and that stream 7 is the only exit for nitrogen. Stream 4 therefore contains no water or formaldehyde.

Degrees of freedom:

N_u = three degrees of freedom including one splitter (before purge stream) and two combinations: the two mixers and the reactor-separator combination

$N_{\text{splitters}}$ = one degree of freedom

N_s = eight degrees of freedom including the product stream leaving the bottom of the distillation column

N_C = five degrees of freedom

Therefore, the degrees of freedom may be calculated with Equation (2.70):

$$\Phi = (8 - 3)5 - 1(5 - 1) + 1 = 22$$

Specifications:

1. Methanol and oxygen content of stream 4 = two degrees of freedom.
2. Conversion of methanol = one degree of freedom.
3. No water in purge = three degrees of freedom (since there can be no water in streams 3 and 6).

4. Product stream flow and composition = four degrees of freedom.
5. Pure water makeup = four degrees of freedom.
6. Pure methanol feed = four degrees of freedom.
7. Pure air feed = four degrees of freedom.

The total number of specifications is 22, the number of degrees of freedom arrived at above. Consequently, the system is well defined.

Species labels:

1 = CH_3OH

2 = O_2

3 = HCHO

4 = H_2O

5 = N_2

Stoichiometry:

$\vartheta_1 = -1$

$\vartheta_2 = -1/2$

$\vartheta_3 = 1$

$\vartheta_4 = 1$

$\vartheta_5 = 0$

Air and reactor feed compositions:

$$x_2^{(1)} = 0.21$$

$$x_5^{(1)} = 0.79$$

$$x_1^{(4)} = 0.08$$

$$x_2^{(4)} = 0.10$$

Mass balances with preceding specifications incorporated:

$$\mathcal{N}^{(2)} = x_1^{(4)} \mathcal{N}^{(4)}$$

$$x_2^{(1)} \mathcal{N}^{(1)} + x_2^{(3)} \mathcal{N}^{(3)} = x_2^{(4)} \mathcal{N}^{(4)}$$

$$x_5^{(1)} \mathcal{N}^{(1)} + x_5^{(3)} \mathcal{N}^{(3)} = x_5^{(4)} \mathcal{N}^{(4)}$$

$$x_1^{(4)} + x_2^{(4)} + x_5^{(4)} = 1.0$$

$$x_2^{(3)} + x_5^{(3)} = 1$$

$$\frac{0.37(3000)}{30} = R_3$$

$$0 = x_1^{(4)} \mathcal{N}^{(4)} + \frac{\vartheta_1}{\vartheta_3} R_3$$

$$\frac{0.63(3000)}{18} = \mathcal{N}^{(5)} + \frac{\vartheta_4}{\vartheta_3} R_3$$

$$x_2^{(3)} \mathcal{N}^{(6)} = x_2^{(4)} \mathcal{N}^{(4)} + \frac{\vartheta_2}{\vartheta_3} R_3$$

$$x_5^{(3)} \mathcal{N}^{(6)} = x_5^{(4)} \mathcal{N}^{(4)}$$

$$\mathcal{N}^{(3)} + \mathcal{N}^{(7)} = \mathcal{N}^{(6)}$$

Mixers before reactor: CH₃OH

Mixers before reactor: O₂

Mixers before reactor: N₂

Definition

Definition

Reactor + separator: HCHO (key)

Reactor + separator: CH₃OH

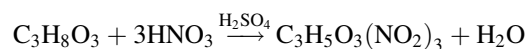
Reactor + separator: H₂O

Reactor + separator: O₂

Reactor + separator: N₂

Splitter after separator

with nitration acid, an aqueous solution of nitric and sulfuric acid.



Refer to the schematic in Figure 2.10.

1. Stream 1 is 100 wt% glycerin.
2. The nitration acid is stream 2, which consists of 43% nitric acid, 50% sulfuric acid, and the balance water.

Solution (flows in lb mol/min):

$$x_2^{(3)} = 0.068182$$

$$x_5^{(3)} = 0.93182$$

$$x_5^{(4)} = 0.82$$

$$\mathcal{N}^{(1)} = 121.55$$

$$\mathcal{N}^{(2)} = 37.0$$

$$\mathcal{N}^{(3)} = 303.95$$

$$\mathcal{N}^{(4)} = 462.5$$

$$\mathcal{N}^{(5)} = 68.0$$

$$\mathcal{N}^{(6)} = 407.0$$

$$\mathcal{N}^{(7)} = 103.05$$

$$R_3 = 37.0$$

Example 2.3.1-2: Manufacture of Nitroglycerin

Nitroglycerin, C₃H₅O₃(NO₂)₃, a widely known high explosive, is made by mixing high-purity glycerin C₃H₈O₃

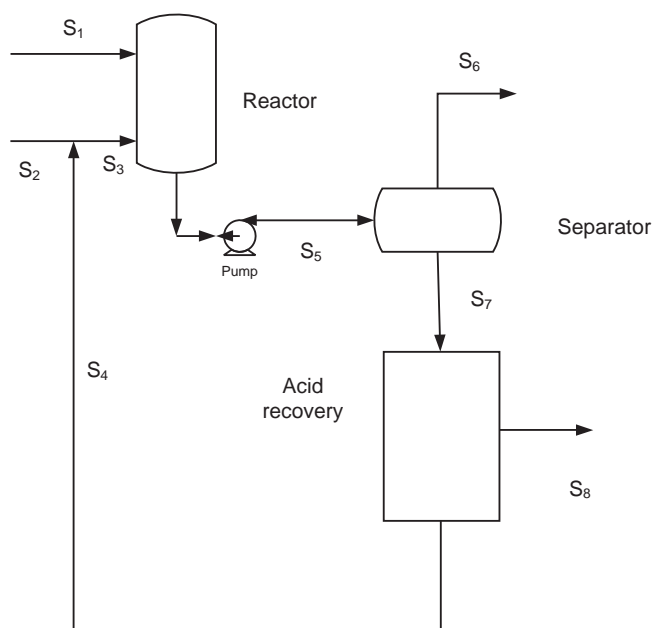


FIGURE 2.10 Manufacture of nitroglycerin.

- The sulfuric acid does not take part in the reaction, but is present to “catch” the water that is formed.
- The mixed acid entering the nitrator in stream 3 contains 20% excess nitric acid.
- After nitration, the mixture of nitroglycerin and the acid solution goes to a separator. In stream 5, the less dense and insoluble nitroglycerin rises to the top and is removed entirely with some water in stream 6. Stream 6 is 96.5% nitroglycerin and the remainder is water.
- The aqueous acid solution in stream 7 is sent to an acid recovery tank where the sulfuric and nitric acids are completely separated. The sulfuric acid stream (8) is concentrated and sold for industrial purposes. A 70% nitric acid stream (4) is returned as recycle to the reactor.

Compute the flows and compositions of all streams if 1000 kg/h of glycerin are fed to the nitrator.

Setup:

Species A_i	Index i	Molecular Weight, M_i	Stoichiometric Coefficient, ν_i
$C_3H_8O_3$	1	92.11	-1
HNO_3	2	63.01	-3
$C_3H_5O_3(NO_2)_3$	3	227.09	1
H_2O	4	18.02	1
H_2SO_4	5	98.08	0

Process stipulations and balance equations:

$$\mathcal{W}^{(1)} = 1000$$

$$\omega_1^{(3)} = 0$$

$$\omega_3^{(3)} = 0$$

$$\omega_1^{(5)} = 0$$

$$\omega_1^{(7)} = 0$$

$$\omega_3^{(7)} = 0$$

$$\omega_1^{(8)} = 0$$

$$\omega_2^{(8)} = 0$$

$$\omega_3^{(8)} = 0$$

$\frac{\omega_2^{(3)}\mathcal{W}^{(3)}}{63.01} = \frac{\mathcal{W}^{(1)}}{92.11}(3)(1.20)$	Component 3 fed in excess
$0.43\mathcal{W}^{(2)} + 0.70\mathcal{W}^{(4)} = \omega_2^{(3)}\mathcal{W}^{(3)}$	Nitric acid balance around feed mixer
$0.07\mathcal{W}^{(2)} + 0.30\mathcal{W}^{(4)} = \omega_4^{(3)}\mathcal{W}^{(3)}$	Water balance around feed mixer
$0.50\mathcal{W}^{(2)} = \omega_5^{(3)}\mathcal{W}^{(3)}$	Sulfuric acid balance around feed mixer
$\omega_1^{(3)} + \omega_2^{(3)} + \omega_3^{(3)} + \omega_4^{(3)} + \omega_5^{(3)} = 1$	Definition
$\frac{\omega_2^{(5)}\mathcal{W}^{(5)}}{63.01} = \frac{\omega_2^{(3)}\mathcal{W}^{(3)}}{63.01} + \frac{(-3)\mathcal{W}^{(1)}}{92.11}$	Nitric acid balance around reactor
$\frac{\omega_3^{(5)}\mathcal{W}^{(5)}}{227.09} = \frac{\mathcal{W}^{(1)}}{92.11}$	Nitroglycerin balance around reactor
$\frac{\omega_4^{(5)}\mathcal{W}^{(5)}}{18.02} = \frac{\omega_4^{(3)}\mathcal{W}^{(3)}}{18.02} + \frac{(3)\mathcal{W}^{(1)}}{92.11}$	Water balance around reactor
$\omega_5^{(5)}\mathcal{W}^{(5)} = \omega_5^{(3)}\mathcal{W}^{(3)}$	Sulfuric acid balance around reactor
$\omega_1^{(5)} + \omega_2^{(5)} + \omega_3^{(5)} + \omega_4^{(5)} + \omega_5^{(5)} = 1$	Definition
$\omega_3^{(5)}\mathcal{W}^{(5)} = 0.965\mathcal{W}^{(6)}$	Nitroglycerin balance around separator
$\omega_2^{(5)}\mathcal{W}^{(5)} = \omega_2^{(7)}\mathcal{W}^{(7)}$	Nitric acid balance around separator
$\omega_4^{(5)}\mathcal{W}^{(5)} = 0.035\mathcal{W}^{(6)} + \omega_4^{(7)}\mathcal{W}^{(7)}$	Water balance around separator
$\omega_5^{(5)}\mathcal{W}^{(5)} = \omega_5^{(7)}\mathcal{W}^{(7)}$	Sulfuric acid balance around separator
$\omega_1^{(7)} + \omega_2^{(7)} + \omega_3^{(7)} + \omega_4^{(7)} + \omega_5^{(7)} = 1$	Definition
$\omega_2^{(7)}\mathcal{W}^{(7)} = 0.70\mathcal{W}^{(4)}$	Nitric acid balance around acid recovery
$\omega_4^{(7)}\mathcal{W}^{(7)} = 0.30\mathcal{W}^{(4)} + \omega_4^{(8)}\mathcal{W}^{(8)}$	Water balance around acid recovery
$\omega_5^{(7)}\mathcal{W}^{(7)} = \omega_5^{(8)}\mathcal{W}^{(8)}$	Sulfuric acid balance around acid recovery
$\omega_1^{(8)} + \omega_2^{(8)} + \omega_3^{(8)} + \omega_4^{(8)} + \omega_5^{(8)} = 1$	Definition

Solution:

$$\mathcal{W}^{(2)} = 4772.6$$

$$\omega_5^{(8)} = 0.74158$$

$$\omega_5^{(7)} = 0.62728$$

$$\omega_4^{(8)} = 0.25842$$

$$\omega_4^{(7)} = 0.26483$$

$$\omega_5^{(5)} = 0.37526$$

$$\omega_4^{(5)} = 0.17249$$

$$\begin{aligned}
\omega_2^{(7)} &= 0.10789 \\
\omega_3^{(5)} &= 0.3877 \\
\omega_5^{(3)} &= 0.44529 \\
\omega_2^{(5)} &= 6.4545 \times 10^{-2} \\
\omega_5^{(3)} &= 9.5165 \times 10^{-2} \\
\omega_2^{(3)} &= 0.45954 \\
\mathcal{W}^{(8)} &= 3217.9 \\
\mathcal{W}^{(7)} &= 3804.2 \\
\mathcal{W}^{(6)} &= 2554.8 \\
\mathcal{W}^{(5)} &= 6359.1 \\
\mathcal{W}^{(4)} &= 586.35 \\
\mathcal{W}^{(3)} &= 5359.0
\end{aligned}$$

2.4 STEADY-STATE MASS BALANCES WITH MULTIPLE CHEMICAL REACTIONS

With single reactions we used the notion of conversion of a key reactant to measure the extent of the reaction. It is not possible to build on this approach since we cannot rely on any single component participating in all the reactions.

2.4.1 Degrees of Freedom and Reaction Extents

We can instead focus on the reaction and make use of the property that the change in molar flow for any component due to the j th reaction divided by the stoichiometric coefficient in that reaction is independent of the species:

$$\frac{1}{\vartheta_{ik}} d \sum_{\substack{\text{all output} \\ \text{streams}(j)}} \mathcal{N}_i^{(j)} = d\xi_k \quad i = 1, 2, \dots, N_c; \quad k = 1, 2, \dots, N_r \quad (2.76)$$

The output flow rate for all of the components can then be written as

$$\sum_{\text{output streams}(j)} \mathcal{N}_i^{(j)} = \sum_{\text{inlet streams}(j)} \mathcal{N}_i^{(j)} + \sum_{k=1}^{N_r} \vartheta_{ik} \xi_k \quad (2.77)$$

which is an extension of Equation (2.69) to multiple reactions. In the case of single reactions, Equations (2.69) and (2.77) show the correspondence of extent to reaction rate:

$$\vartheta_i \mathcal{R}^{(V)} = \vartheta_i \xi \quad \text{or} \quad \vartheta_i \mathcal{R}^{(V)} = \vartheta_i \xi \quad (2.78)$$

It is true in general since

$$\sum_{j=1}^{j=R} \vartheta_{ij} \mathcal{R}_j = \sum_{j=1}^{j=R} \vartheta_{ij} \xi_j \quad (2.79)$$

implies the equality $\mathcal{R}_j^{(V)} = \xi_j$ if the reactions are independent. Independent reactions are discussed in the following section.

The degrees of freedom are increased by N_r over the unreactive case so that we will need to have an additional N_r specification, assuming that the reactions are independent. Equation (2.62) then becomes

$$\Phi = (N_s - N_u)N_c - (N_c - 1)(N_{D, \text{total}} - N_{\text{splitters}}) + N_r \quad (2.80)$$

Example 2.4.1-1: Mass Balance on Acrylic Acid Reactor R-301

The acrylic acid reactor and the associated heat exchange loop are shown in Figure 2.11, which was extracted from Figure 1.4.

The heat exchange loop is included in the chemical processing system under consideration by specifying the stream breaks to be only 4 and 6. The heat duty for the reactor is considered in the following chapter (Example 3.6.3-1).

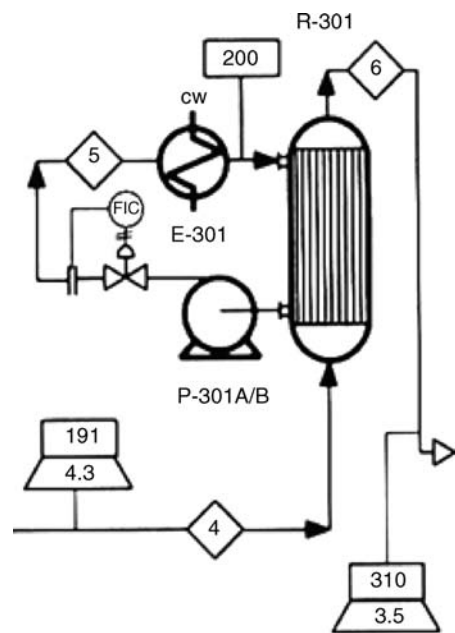


FIGURE 2.11 Reactor R-301. Reprinted with permission of Pearson.

Solution:

Indices for all components:

Component	Index
C ₃ H ₆	1
O ₂	2
C ₃ H ₄ O ₂	3
C ₂ H ₄ O ₂	4
H ₂ O	5
CO ₂	6
N ₂	7

Degrees of freedom:

$$N_s = \text{two degrees of freedom}$$

$$N_u = \text{one degree of freedom}$$

$$N_c = \text{seven degrees of freedom}$$

$$N_r = \text{three degrees of freedom}$$

$$N_{\text{splitters}} = \text{zero degree of freedom}$$

$$\Phi = (2 - 1)7 - 0 + 3 = 10 \text{ degrees of freedom}$$

Mass balances: Refer to Equation (2.77)

$$\mathcal{N}_1^{(6)} = \mathcal{N}_1^{(4)} - \xi_1 - \xi_2 - \xi_3$$

$$\mathcal{N}_2^{(6)} = \mathcal{N}_2^{(4)} - \frac{3}{2}\xi_1 - \frac{5}{2}\xi_2 - \frac{9}{2}\xi_3$$

$$\mathcal{N}_3^{(6)} = \mathcal{N}_3^{(4)} + \xi_1$$

$$\mathcal{N}_4^{(6)} = \mathcal{N}_4^{(4)} + \xi_2$$

$$\mathcal{N}_5^{(6)} = \mathcal{N}_5^{(4)} + \xi_1 + \xi_2 + 3\xi_3$$

$$\mathcal{N}_6^{(6)} = \mathcal{N}_6^{(4)} + \xi_2 + 3\xi_3$$

$$\mathcal{N}_7^{(6)} = \mathcal{N}_7^{(4)}$$

There are 17 variables here and 7 equations. We must therefore fix 10 variables, which checks with the calculations above.

Let us fix all the feeds and the first three outputs. We can solve for the three extents with this scheme using the first three equations and the remaining output.

Summary and solution:

$$14.7 = 127.0 - \xi_{1,1} - \xi_{1,2} - \xi_{1,3} \quad \mathcal{N}_4^{(6)} = 6.54$$

$$52.0 = 280.9 - \frac{3}{2}\xi_{1,1} - \frac{5}{2}\xi_{1,2} - \frac{9}{2}\xi_{1,3} \quad \xi_{1,1} = 87.79$$

$$87.79 = 0 + \xi_{1,1} \quad \mathcal{N}_4^{(6)} = 1165.8$$

$$\mathcal{N}_4^{(6)} = 0 + \xi_{1,2} \quad \xi_{1,3} = 17.97$$

$$\mathcal{N}_4^{(6)} = 1017.6 + \xi_{1,1} + \xi_{1,2} + 3\xi_{1,3} \quad \xi_{1,2} = 6.54$$

$$\mathcal{N}_4^{(6)} = 0 + \xi_{1,2} + 3\xi_{1,3} \quad \mathcal{N}_7^{(6)} = 1056.7$$

$$\mathcal{N}_7^{(6)} = 1056.7 \quad \mathcal{N}_6^{(6)} = 60.45$$

The output flows were fixed at the values given in Table 1.3. The calculated flows are seen to agree with this table. Also note that the three extents are the reaction rates calculated in Section 1.1.3, which we noted above is true for independent reactions.

2.4.2 Test for Independent Reactions

The reaction extents must be independent variables if we are to have independent relations between them. This in turn requires that the reactions be independent, by which we mean that no reaction can be written as a linear combination of the others. Another way of stating the same requirement is that the columns of the matrix of stoichiometric coefficients, $[\vartheta]$, be independent vectors (Dettman, 1962). These vectors can span at most an N_c or N_r dimensional space, whichever is smaller. The dimension of the space that is spanned is called the rank of the matrix (Perlis, 1958). If the rank is equal to $\min(N_c, N_r)$, then the matrix is fully ranked. Otherwise, it is rank deficient. We want to be certain that the matrix of stoichiometric coefficients is fully ranked.

By performing elementary column operations, $[\vartheta]$ may be reduced to column echelon form: for the first r columns, there is a one in the j th position, j being the column number, and all zeroes above. The remaining columns contain only zeroes. The rank of the matrix is r .

Elementary column operations are as follows:

- Interchange of any two columns
- Multiplication of any column by a nonzero scalar
- Addition of a scalar multiple of one column to another

Example 2.4.2-1: Independent Reactions in the Acrylic Acid System

The matrix of stoichiometric coefficients can be constructed as follows:

$$[\vartheta] = \begin{array}{c} \text{Reaction} \\ \text{C}_3\text{H}_6: \\ \text{O}_2: \\ \text{C}_3\text{H}_4\text{O}_2: \\ \text{C}_2\text{H}_4\text{O}_2: \\ \text{H}_2\text{O}: \\ \text{CO}_2 \end{array} \begin{bmatrix} 1 & 2 & 3 \\ -1 & -1 & -1 \\ -3/2 & -5/2 & -9/2 \\ 1 & 0 & 0 \\ 0 & 1 & 0 \\ 1 & 1 & 3 \\ 0 & 1 & 3 \end{bmatrix} \quad (2.81)$$

This matrix can be reduced to -2 with the following column (col) operations:

- Replace col2 with $(-1\text{col1} + \text{col2})$
- Replace col2 with $(1\text{col1} + \text{col3})$

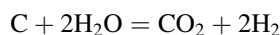
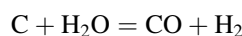
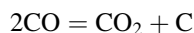
- Replace col3 with $(-3\text{col2} + \text{col3})$
- Multiply col1 and col2 by -1 and col3 by $1/2$

The rank of the matrix is 3, indicating that indeed we have three independent reactions.

If the reactions are not independent, one can select the independent set as the nonzero column vectors resulting from elementary column operations.

Example 2.4.2-2: Selection of Independent Reactions

Consider the following set of reactions. Determine the independent reactions that are present.



Solution:

The matrix of stoichiometric coefficients is

$$[\vartheta] = \begin{bmatrix} \text{Reaction} & 1 & 2 & 3 \\ \text{C} & 1 & -1 & -1 \\ \text{CO} & -2 & 1 & 0 \\ \text{CO}_2 & 1 & 0 & 1 \\ \text{H}_2 & 0 & 1 & 2 \\ \text{H}_2\text{O} & 0 & -1 & -2 \end{bmatrix} \quad (2.82)$$

The following steps

- Add the first column to the second and third columns.
- Subtract twice the second column from the third.

Reduce the stoichiometric coefficient matrix to

$$\begin{bmatrix} 1 & 0 & 0 \\ -2 & -1 & 0 \\ 1 & 1 & 0 \\ 0 & 1 & 0 \\ 0 & -1 & 0 \end{bmatrix} \quad (2.83)$$

This indicates that the third reaction is not independent. These calculations have not established that the first two reactions form a complete set of independent reactions. Also, it should be noted that the preceding discussion could have been focused on rows instead of columns. The rank is the same from both points of view.

Now suppose that we have the species present in the system identified and we set out to determine *all* of the independent reactions.

2.4.3 Construction of Independent Reactions

The column vectors in the matrix of stoichiometric coefficients are N_c dimensional. The coefficients are used to balance the system reactions from the viewpoint of conserving the number of atoms of each type that is present in each chemical reaction. Since we are presuming to know the chemical species that are present, we have information that can establish relationships between the stoichiometric coefficients. In fact, if there are N_l elements, we can write N_l balances for the elements. The column vectors formed by the stoichiometric coefficients are N_c dimensional but given the N_l balances, there can only be $N_c - N_l$ independent quantities remaining. The rank of $[\vartheta]$ is then $N_c - N_l$. The N_l balances can be written as

$$[d][\vartheta] = [0] \quad (2.84)$$

where d_{ij} is the number of elements in compound j . The $[d]$ matrix is then $N_l \times N_c$. The rank of $[d]$ must be 1 since the elemental balances are independent. The dimensions of $[\vartheta]$ are $N_c \times N_r$. The objective is to use Equation (2.84) to generate a set of independent column vectors for $[\vartheta]$, which span the $N_c - N_l$ dimensional space.

The $[d]$ matrix can be transformed into an upper triangular matrix using elementary row operations (equivalent row point of view referred to in the preceding section) to give

$$[u][\vartheta] = [0] \quad (2.85)$$

The first N_l columns of $[u]$ span a one-dimensional space. This means that $N_c - N_l$ of the elements of each column vector of $[\vartheta]$ must be set in order to solve for the remaining elements. We can guarantee the independence of the column vectors if these $N_c - N_l$ elements are specified as the unit vectors in $N_c - N_l$ dimensional space. Since the operation of $[d]$ on $[\vartheta]$ is accomplished column-wise, we may focus attention on one arbitrary column (reaction).

The m th column vector of $[\vartheta]$ can then be expressed with the m th unit vector appended to the elements, which are determined by the elemental balance

$$\vartheta_m = \begin{bmatrix} \vartheta_{1m} \\ \vartheta_{2m} \\ \vdots \\ \vartheta_{lm} \\ 0 \\ 0 \\ \vdots \\ \vartheta_{l+m,m} = 1 \\ \vdots \\ 0 \end{bmatrix} \quad (2.86)$$

The stoichiometric relation then reads as follows, since $[\vartheta]$ operates on the columns of $[u]$:

$$\sum_{i=1}^{N_l} \vartheta_{im} \mathbf{u}_i + \mathbf{u}_{l+m} = 0, \quad m = 1, 2, \dots, (N_c - N_l) \quad (2.87)$$

where the \mathbf{u}_i are the column vectors of $[u]$.

The preceding equation can generally be solved by standard algorithms. If the number of components is not large, the method employed in Example 2.4.3-1 might be applied.

Example 2.4.3-1: Independent Reactions in the Acrylic Acid System

Define an independent set of reactions for the acrylic acid system based on the species present and show the relationship between the given reactions and the derived set.

Solution:

Define the $[d]$ matrix based on the assumed species population:

$$[d] = \begin{bmatrix} & \text{C}_3\text{H}_6 & \text{O}_2 & \text{C}_3\text{H}_4\text{O}_2 & \text{H}_2\text{O} & \text{CO}_2 & \text{C}_2\text{H}_4\text{O}_2 \\ \text{C} & 3 & 0 & 3 & 0 & 1 & 2 \\ \text{H} & 6 & 0 & 4 & 2 & 0 & 4 \\ \text{O} & 0 & 2 & 2 & 1 & 2 & 2 \end{bmatrix} \quad (2.88)$$

The rank of $[d]$ can be verified as 3. Also $N_c = 6$, $l = 3$. The number of independent reactions is the $6 - 3 = 3$.

Reduce $[d]$ to the upper triangular form using elementary row operations:

1. Add -2 row 1 to row 2
2. Interchange row 2 and row 3
3. Divide row 1 by 3, and rows 2 and 3 by 2

The result is

$$[u] = \begin{bmatrix} 1 & 0 & 1 & 0 & 1/3 & 2/3 \\ 0 & 1 & 1 & 1/2 & 1 & 1 \\ 0 & 0 & -1 & 1 & -1 & 0 \end{bmatrix} \quad (2.89)$$

The equation for the m th column of $[\vartheta]$ is then

$$\vartheta_{1m} \begin{bmatrix} 1 \\ 0 \\ 0 \end{bmatrix} + \vartheta_{2m} \begin{bmatrix} 0 \\ 1 \\ 0 \end{bmatrix} + \vartheta_{3m} \begin{bmatrix} 1 \\ 1 \\ -1 \end{bmatrix} = -\bar{u}_{3+m}, \quad m = 1, 2, 3 \quad (2.90)$$

where

$$\mathbf{u}_4 = \begin{bmatrix} 0 \\ 1/2 \\ 1 \end{bmatrix}, \quad \mathbf{u}_5 = \begin{bmatrix} 1/3 \\ 1 \\ -1 \end{bmatrix}, \quad \mathbf{u}_6 = \begin{bmatrix} 2/3 \\ 1 \\ 0 \end{bmatrix} \quad (2.91)$$

For $m = 1$,

$$\vartheta_{11} + \vartheta_{31} = 0 \quad (2.92)$$

$$\vartheta_{21} + \vartheta_{31} = -1/2 \quad (2.93)$$

$$-\vartheta_{31} = -1 \quad (2.94)$$

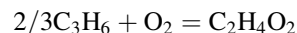
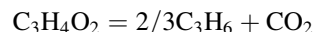
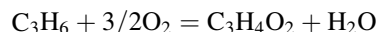
The solution is $\vartheta_{11} = -1$, $\vartheta_{21} = -3/2$, $\vartheta_{31} = 1$. The first column of $[\vartheta]$ is then

$$\vartheta_1 = \begin{bmatrix} -1 \\ -3/2 \\ 1 \\ 1 \\ 0 \\ 0 \end{bmatrix} \quad (2.95)$$

The remaining two columns can be obtained in a similar way to give

$$[\vartheta] = \begin{bmatrix} 1 & 2/3 & -2/3 \\ -3/2 & 0 & -1 \\ 1 & -1 & 0 \\ 1 & 0 & 0 \\ 0 & 1 & 0 \\ 0 & 0 & 1 \end{bmatrix} \quad (2.96)$$

The derived independent set of reactions is then



To relate these to the given set of reactions, the problem is to determine, for each reaction in the given set, what linear combination of the derived set will produce the stoichiometric coefficients. You can multiply the three derived equations, respectively, by the coefficients for H_2O , CO_2 , and $\text{C}_2\text{H}_4\text{O}_2$ in the given equation and add the equations. This is possible because the identity matrix forms a lower portion of $[\vartheta]$. The remaining coefficients must match if the results are correct.

The first reaction is the same in both sets. The second equation in the given set can be obtained by adding the derived equations in the following proportions: 1, 1, 1. The third reaction in the given set can be obtained by adding the derived equations in the following proportions: 3, 3, 0.

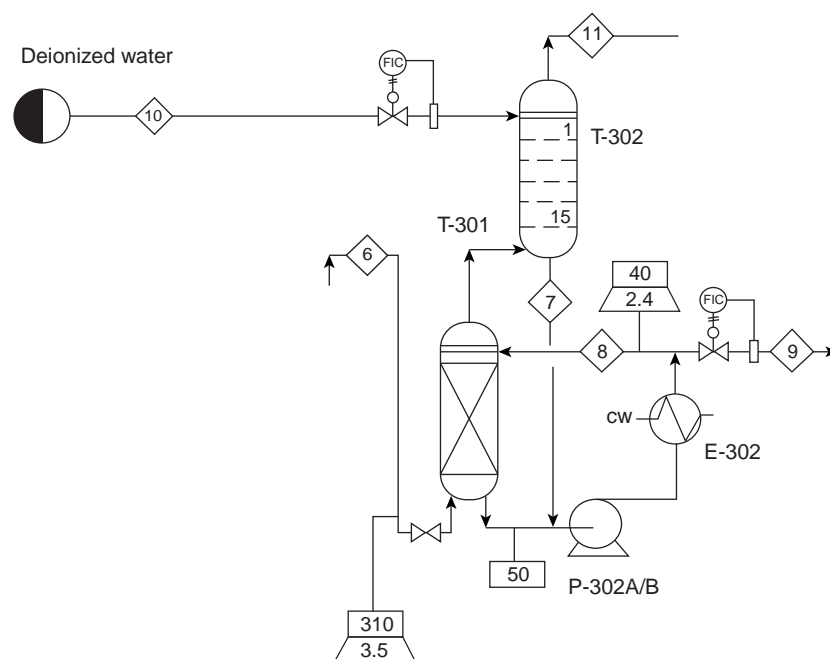


FIGURE 2.12 Section from acrylic acid flow sheet. Reprinted with permission of Pearson.

PROBLEMS

2.1. The flow sheet in Figure 2.12 was selected from the acrylic acid flow sheet (Figure 1.4).

- List the inactive units vis à vis the mass balance.
- Fix the number of components (see streams in Table 1.3.). Define a number of mass balances by selecting the chemical system and satisfying the degrees of freedom with values from the stream table (Table 1.3).
- Solve (some of) the mass balances that you have constructed.

2.2. Carry out a degree of freedom analysis for the nitroglycerin manufacturing process in Example 2.3.1-2.

2.3. Flow rates for the continuous biocatalytic synthesis of hexyl glucoside.

A bench scale process for the production of hexyl glucoside is discussed in Chapter 1. A continuous version of the process (shown Figure 1.35) is subject to the accompanying considerations. The objective here is to calculate the unknown flow rates for a modest production rate of 5000 lb/year of hexyl glucoside.

The process may be assumed to operate 8000 h/year with a glucose conversion per pass (stream 4 to stream 5) of 20 mol%.

Assumptions and additional process information:

- Ignore the enzyme for now (see the comment at the end of the problem statement) and label the remaining species as follows:

Component	Label (<i>i</i>)
Glucose	1
Hexanol	2
Glucoside	3
Water	4

- The product stream from the reactor (5) consists of an organic phase and an aqueous phase, which are perfectly separated in the membrane separator into an organic stream (6) and an aqueous stream (7). The two phases are illustrated in Figure 2.13.

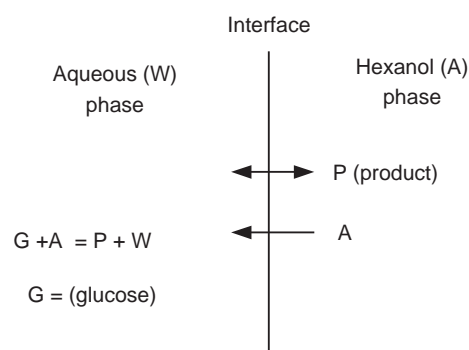


FIGURE 2.13 Exit phase characteristics at exit to membrane separator. (deRoode, et al. 2001).

- The aqueous phase reaction is assumed to be in equilibrium. This requires (see Example 6.7-1) that the concentrations be related by

$$\frac{C_3^{(7)} C_4^{(7)}}{C_1^{(7)} C_2^{(7)}} = 1.90$$

Phase equilibrium refers to the final redistribution of components between both of two phases placed in contact for a sufficiently long time that further change is not likely. If the streams leaving a processing operation are in equilibrium, the processing operation is called an equilibrium stage. Single equilibrium stages are discussed in Chapter 6 and multiple equilibrium stages are discussed in Chapter 7.

- The present case is considered in Example 6.7-3 with the result that the molar concentrations of the product in the two phases are related by

$$\frac{C_3^{(6)}}{C_3^{(7)}} = 109.091 C_3^{(7)} + 3.80$$

It may be useful to express the molar concentrations as the ratio of the molar flow rate to the volumetric flow rate where

$$\mathcal{V}^{(j)} = \sum_i \tilde{V}_i \mathcal{N}_i^{(j)}$$

The \tilde{V}_i are partial molar volumes. They represent the contribution of each component to the total volume and allow for the possibility that they may be a function of concentration and not equal to the value for the pure component. The notion of partial molar properties is generally very useful in the construction of properties for mixtures and they are discussed

in Chapter 3. They are approximated by the value for the pure component for ideal solutions.

- The solubility of the alcohol in the glucose solution may be neglected.
- The volumetric flows of the feed and product streams from the reactor may be considered equal.

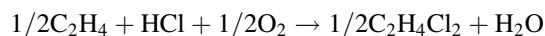
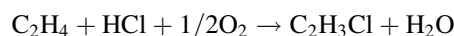
Discuss the disposition of the enzyme.

Solutions to Problem 2.3 are provided after the last problem statement.

2.4. A process is described in patent WO013872 for the manufacture of vinyl chloride monomer from ethane and ethylene. The chemical species that are present in the oxydehydrochlorination reactor are

{ethylene (C_2H_4), ethane (C_2H_6), oxygen (O_2), hydrogen chloride (HCl), vinyl chloride monomer or VCM (C_2H_3Cl), water (H_2O), chlorine (Cl_2), chloroethane or Et (C_2H_5Cl), carbon monoxide and carbon dioxide (CO , CO_2), carbon tetrachloride (CCl_4), and ethylene dichloride or DCE ($C_2H_2Cl_2$)}

- Formulate the independent reactions for this system
- Show that the following oxydehydrochlorination reactions can be expressed as a linear combination of reactions from the independent reaction set.



2.5. The production capacity for hydrogen peroxide in the United States totaled more than one billion pounds per year in 1998 (cheresources.com). It is used, for example, for bleaching in the textile, and pulp and paper industries

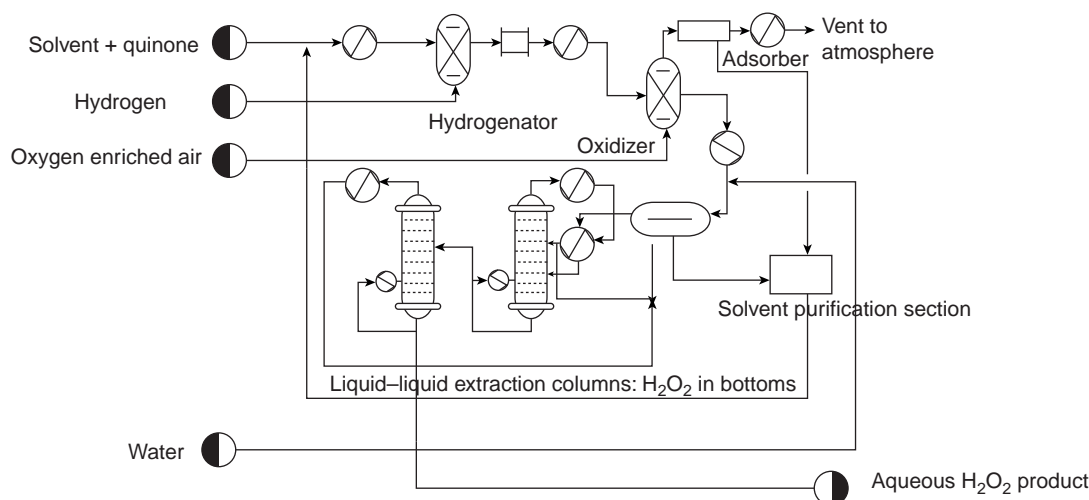
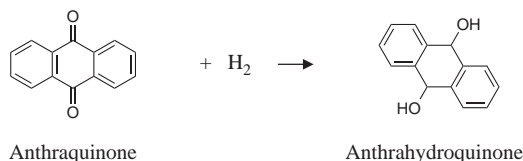


FIGURE 2.14 Auto-oxidation process for hydrogen peroxide (cheresources.com).

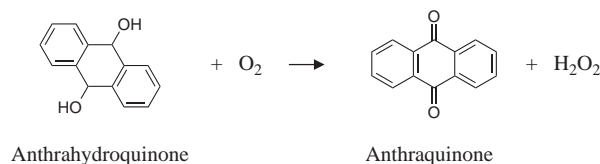
(Ullmann, 1994). The chemical industry uses hydrogen peroxide for the production of peroxy compounds.

The most widely used production method is the auto-oxidation process. In this process a solvent stream traverses a loop through the process. A hydroquinone dissolved in the solvent orchestrates the combination of hydrogen and oxygen in the loop and returns to its original state at the beginning of the loop. The auto-oxidation process is outlined in Figure 2.14. The hydroquinone is shown as anthraquinone but 2-ethyl-anthraquinone is normally used. The reactions are

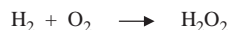
Hydrogenator:



Oxidizer:



Overall:



Consider the following approximations:

- There are no side reactions or losses.
- All hydrogen reacts; 80% of oxygen reacts.
- All oxygen and nitrogen are vented after the adsorber.
- Extractor removes all water and peroxide from the vacuum column(s), which produces the desired solution and a water recycle. The solvent is not soluble in water.

If, on a solvent-free basis, the concentration change across the hydrogenator is from 90 mol% anthraquinone and 10 mol% anthrahydroquinone to 15 mol% anthraquinone and 85 mol% anthrahydroquinone, calculate the feeds and vent rates for a 500,000 tonne per year plant producing a 50 wt% solution of hydrogen peroxide.

2.6. A gas mixture flowing at 2000 psia and 250 °C consists of 65 mol% nitrogen and 35% ammonia. Determine the molar density of the gas in order that the volumetric flow may be calculated from the molar flow rate.

Solutions to Problem 2.4:

$$\mathcal{N}_1^{(7)} = \mathcal{N}_1^{(4)} + \mathcal{R}$$

$$\mathcal{N}_2^{(6)} + \mathcal{N}_2^{(7)} = \mathcal{N}_2^{(3)} + \mathcal{N}_2^{(4)} + \mathcal{R}$$

$$\mathcal{N}_3^{(6)} + \mathcal{N}_3^{(7)} = \mathcal{N}_3^{(4)} - \mathcal{R} \quad \epsilon = 1.2608 \times 10^{-2}$$

$$\mathcal{N}_4^{(7)} = \mathcal{N}_4^{(4)} - \mathcal{R} \quad \mathcal{R} = -1.0776$$

$$\frac{\mathcal{N}_3^{(6)}}{\mathcal{N}_3^{(7)}} = \alpha \left(109.09 \frac{\mathcal{N}_3^{(7)}}{\mathcal{V}^{(7)}} + 3.80 \right) \quad \alpha = 30.744$$

$$\mathcal{N}_4^{(11)} = 84.412$$

$$\frac{\mathcal{V}^{(6)}}{\mathcal{V}^{(7)}} = \alpha \quad \mathcal{N}_3^{(11)} = 8.1997 \times 10^{-3}$$

$$\mathcal{V}^{(6)} = 0.120 \mathcal{N}_2^{(3)} \quad \mathcal{N}_2^{(11)} = 8.5594 \times 10^{-2}$$

$$\mathcal{V}^{(7)} = 0.018 \mathcal{N}_4^{(4)} + 0.118 \mathcal{N}_1^{(4)} \quad \mathcal{N}_1^{(11)} = 4.2561$$

$$\frac{\mathcal{N}_3^{(7)}}{\mathcal{N}_1^{(7)}} = 1.900(0.001014) \quad \mathcal{N}_4^{(8)} = 1.0776$$

$$\mathcal{N}_3^{(8)} = 1.047 \times 10^{-4}$$

$$\frac{\mathcal{N}_4^{(7)}}{\mathcal{N}_2^{(7)}} = \frac{1}{0.001014} \quad \mathcal{N}_4^{(7)} = 85.49$$

$$\mathcal{N}_2^{(8)} = 1.0927 \times 10^{-3}$$

$$\frac{\mathcal{N}_2^{(4)}}{\mathcal{N}_4^{(4)}} = 0.001014 \quad \mathcal{N}_3^{(7)} = 8.3044 \times 10^{-3}$$

$$\mathcal{N}_1^{(8)} = 5.4346 \times 10^{-2}$$

$$\frac{\mathcal{N}_1^{(4)}}{\mathcal{V}^{(7)}} = 2.5 \quad \mathcal{N}_2^{(7)} = 8.6686 \times 10^{-2}$$

$$\mathcal{N}_3^{(4)} = \mathcal{N}_3^{(7)} - \mathcal{N}_3^{(8)} \quad \mathcal{N}_3^{(6)} = 1.0775$$

$$\mathcal{N}_4^{(8)} = \mathcal{N}_4^{(7)} - \mathcal{N}_4^{(4)} \quad \mathcal{N}_2^{(6)} = 551.08$$

$$\mathcal{N}_1^{(11)} = (1 - \epsilon) \mathcal{N}_1^{(7)} \quad \mathcal{N}_4^{(4)} = 84.412$$

$$\mathcal{N}_2^{(11)} = (1 - \epsilon) \mathcal{N}_2^{(7)} \quad \mathcal{N}_3^{(4)} = 8.1997 \times 10^{-3}$$

$$\mathcal{N}_3^{(11)} = (1 - \epsilon) \mathcal{N}_3^{(7)} \quad \mathcal{N}_2^{(4)} = 8.5594 \times 10^{-2}$$

$$\mathcal{N}_4^{(11)} = (1 - \epsilon) \mathcal{N}_4^{(7)} \quad \mathcal{V}^{(7)} = 2.1552$$

$$\mathcal{N}_1^{(8)} = \epsilon \mathcal{N}_1^{(7)} \quad \mathcal{N}_2^{(3)} = 552.16$$

$$\mathcal{N}_2^{(8)} = \epsilon \mathcal{N}_2^{(7)} \quad \mathcal{V}^{(6)} = 66.259$$

$$\mathcal{N}_3^{(8)} = \epsilon \mathcal{N}_3^{(7)}$$

$$\mathcal{N}_4^{(8)} = \epsilon \mathcal{N}_4^{(7)}$$

MACROSCOPIC ENERGY AND ENTROPY BALANCES

Material and energy balances carried out during the creation and synthesis of a chemical process result in the calculation of stream compositions, temperature, and pressure. The energy balances require evaluation of changes in the thermodynamic enthalpy function over the range of the process conditions. Extensive experimental enthalpy data are available for relatively few substances. Much attention has therefore been focused on equations of state, which provide PVT (pressure, volume, and temperature) relationships as functions of composition that can meet these specific needs with a minimum of physical and chemical data. Other thermodynamic state functions and derived quantities are important to limitations on product compositions and processing requirements.

Process efficiencies in conjunction with the thermodynamic limits form the basis of staged equipment design and provide the distance from equilibrium, which form the basis of the rate processes governing nonequilibrium processes. Process efficiencies can also be viewed from the heat and work interactions that it undergoes with the environment. Such considerations lead to the need to extend the notion of macroscopic balances to the entropy and the Gibbs free energy.

We will begin here with a brief summary of the theory and practice of evaluating the enthalpy and entropy functions, followed by the formulation and application of energy and entropy balances.

3.1 BASIC THERMODYNAMIC FUNCTIONS

If we begin with the First Law for systems that do $P dV$ work and generalize it to mixtures, the result for the internal energy (U) is that

$$d\mathcal{U} = T d\mathcal{S} - P d\mathcal{V} + \sum_{i=1}^c \left(\frac{\partial \mathcal{U}}{\partial N_i} \right)_{\mathcal{S}, \mathcal{V}, N_j} dN_i \quad (3.1)$$

or

$$\mathcal{U} = \mathcal{U}(\mathcal{S}, \mathcal{V}, N_1, N_2, \dots, N_C) \quad (3.2)$$

The underscore indicates an extensive variable whose value in a composite is the sum of its values in the component parts. Note that Equation (3.1) refers to only sequences of equilibrium states.

The internal energy function is called the fundamental equation of thermodynamics in that it contains all of the thermodynamic information about the system. It is through the work term(s) that we define the intensive and extensive variables that distinguish our system from others. Surface effects could be included, for example, with a work term σdA where σ is surface tension. A similar work term will be included for adsorption equilibrium below.

Note in Equation (3.1) that the first derivative gives the pressure and temperature and that the extensive functions are additive over multiple phases. An equilibrium state is one for which the internal energy function is a minimum at a

constant S and V . It is known from experience that stable equilibrium states exist for closed systems devoid of imposed constraints and that these states can be characterized by two independently variable properties of the system in addition to the masses of the species charged to the system (Tester and Modell, 1997).

The internal energy function is called the energy representation. Interchange of S and U gives the entropy representation. The energy representation can be transformed into other completely equivalent forms that contain exactly the same thermodynamic information. These are thermodynamic potential functions, two of which are the enthalpy and the Gibbs free energy:

$$\text{Enthalpy: } H(S, P, N, \dots) = U + PV \quad (3.3)$$

$$\text{Gibbs free energy: } G(T, P, N, \dots) = H - TS \quad (3.4)$$

The variables designated for each function are important and are called the natural variables for that function. At constant composition, the dependence on the natural variables is given by

$$dU = T dS - P dV \quad (3.5)$$

$$dH = T dS + V dP \quad (3.6)$$

$$dG = -S dT + V dP \quad (3.7)$$

These alternative representations are the result of the method (Legendre transformations) of forming the potential function from the fundamental energy function in such a way that no information is lost in the transformation process.

The enthalpy, entropy, and Gibbs functions each have particular importance in applications. For example, the enthalpy function underpins the First Law, often referred to as the “enthalpy balance.” The analogous entropy balance can locate sources of entropy in a process system and thus uncover inefficiencies due to lost work in contrast to inefficiencies due to lost heat uncovered by the First Law. The Gibbs function represents the potential for doing work in a system that begins and ends at the same temperature and pressure.

In chemical engineering applications, it is changes in the thermodynamic functions rather than the values of the thermodynamic functions that are of interest. In this respect

it is important to note in using tables of compiled values of enthalpy, for example, that the words “relative to . . .” be added to the column heading, if not already present. The reference state is quite arbitrary and may be different for each species as long as the choice is consistent throughout the applications. However, when chemical reactions are present, a measure of arbitrariness is removed since the enthalpy change of the reaction involves a number of the components and can be measured by a calorimeter.

The reference states most often used for unreactive circumstances are as follows:

Gases: The pure gas at 1 bar in the ideal gas state. Strictly speaking, this is an arbitrary state since the real gas may not be ideal. However, in most circumstances, the difference is negligible.

Liquids: The pure liquid at 1 bar.

Solids: The pure solid at 1 bar.

The temperature is taken to be the temperature of the system but often the reference temperature of the available data basis is 25 °C.

In the case of reactive systems, the reference state is taken to be the elements at 25 °C. A compilation of formation or combustion reactions then provides enthalpies and Gibbs free energies of formation of all the components in the reactive systems that form the basis of free energy and enthalpy changes.

Changes in the thermodynamic state functions take place because of changes in composition, pressure, and temperature. Depending on the equation of state, it may be more convenient to replace pressure with molar or specific volume.

Several relations are most useful for expression of changes in H and S with respect to T and V or P .

Definitions, for example, for specific heat:

$$\frac{\partial}{\partial x} \left(\frac{\partial F(x, y)}{\partial y} \right) \bigg|_y = \frac{\partial}{\partial y} \left(\frac{\partial F(x, y)}{\partial x} \right) \bigg|_x \quad (3.8)$$

$$dF = F_x dx + F_y dy \Rightarrow \frac{\partial F}{\partial z} \bigg|_t = F_x \frac{\partial x}{\partial z} \bigg|_t + F_y \frac{\partial y}{\partial z} \bigg|_t \quad (3.9)$$

These relations were used in compiling Table 3.1.

TABLE 3.1 Useful Relations of H and S to the Equation of State

$\left(\frac{\partial H}{\partial T} \right)_p = C_p$	$\left(\frac{\partial H}{\partial P} \right)_T = V - T \left(\frac{\partial V}{\partial T} \right)_P$
$\left(\frac{\partial S}{\partial T} \right)_p = \frac{C_p}{T}$	$\left(\frac{\partial S}{\partial P} \right)_T = - \left(\frac{\partial V}{\partial T} \right)_P$
$\left(\frac{\partial H}{\partial T} \right)_V = C_V; \quad C_p - C_V = - \frac{TV \left[(1/V)(\partial V/\partial T)_P \right]_2}{(1/V)(\partial V/\partial P)_T}$	$\left(\frac{\partial H}{\partial V} \right)_T = V \frac{\partial P}{\partial V} + T \left(\frac{\partial P}{\partial T} \right)_V$
$\left(\frac{\partial S}{\partial T} \right)_V = \frac{C_V}{T}$	$\left(\frac{\partial S}{\partial V} \right)_T = \left(\frac{\partial P}{\partial T} \right)_V$

Note that changes in the Gibbs function due to temperature changes,

$$\left(\frac{\partial G}{\partial T}\right)_p = -S \quad \text{and} \quad \left(\frac{\partial G}{\partial T}\right)_v = -S + v\left(\frac{\partial P}{\partial T}\right)_v \quad (3.10)$$

have no physical significance since the reference state for entropy is arbitrary.

In general, the effect of composition on the thermodynamic properties can be expressed in terms of partial molar quantities. For any thermodynamic function, say F , the total value for a mixture is given by

$$E = E(T, P, N_1, N_2, N_3, \dots) \quad (3.11)$$

If the amount of the mixture increased by a factor of λ , it follows on physical grounds that

$$\lambda E(T, P, N_1, N_2, N_3, \dots) = E(T, P, \lambda N_1, \lambda N_2, \lambda N_3, \dots) \quad (3.12)$$

Differentiating with respect to λ gives

$$E(T, P, N_1, N_2, N_3, \dots) = \sum_{\text{all species}} N_i \tilde{F}_i \quad (3.13)$$

where

$$\tilde{F}_i = \left(\frac{\partial E}{\partial N_i}\right)_{T, P, N_{j \neq i}} \quad (3.14)$$

The \tilde{F}_i are called partial molar quantities. (Note that a mass basis is just as good.) Dividing Equation (3.13) by the total number of moles

$$F = \sum_{\text{all species}} y_i \tilde{F}_i \quad (3.15)$$

The partial molar quantities are therefore important thermodynamic quantities because they reflect the contribution of the individual components to the mixture value.

3.1.1.1 Gibbs–Duhem Equation The partial molar quantities are not independent, which can be seen by equating the general differential of the extensive property defined in Equation (3.11) to that obtained from Equation (3.13):

$$\begin{aligned} \left(\frac{\partial E}{\partial T}\right)_{p, N} dT + \left(\frac{\partial E}{\partial P}\right)_{T, N} dP + \sum_i \left(\frac{\partial E}{\partial N_i}\right)_{T, P, N_{j \neq i}} dN_i \\ = \sum_i (N_i d\tilde{F}_i + \tilde{F}_i dN_i) \end{aligned} \quad (3.16)$$

Therefore,

$$-\left(\frac{\partial E}{\partial T}\right)_{p, N} dT - \left(\frac{\partial E}{\partial P}\right)_{T, N} dP + \sum_i N_i d\tilde{F}_i = 0 \quad (3.17)$$

This is the general form of the Gibbs–Duhem equation. As a consequence, for example,

$$dE = \sum_i \tilde{F}_i dN_i \quad \text{at constant } T \text{ and } P \quad (3.18)$$

The partial molar properties are often measured in liquids by adding a small quantity of one component to the mixture and measuring the property change at a fixed temperature and pressure. In so doing, both partial molar properties are reported and the Gibbs–Duhem relation is used to check the thermodynamic consistency of the data. For a binary system, the Gibbs–Duhem equation requires that (see Example 3.3.4-1)

Slope Test: The slopes of the partial molar quantities versus the mole fraction of one of the components have opposite signs and each slope approaches zero with the mole fraction of the associated component.

Area Test: The area under the curve of a partial molar property relative to the pure component value for one component is equal that for the other.

Because of the linear appearance of temperature and pressure in the definitions of the parent functions, the partial quantities also obey relations analogous to the parent functions, for example,

$$\tilde{G}_i = \tilde{H}_i - T\tilde{S}_i \quad (3.19)$$

and

$$d\tilde{G}_i = -\tilde{S}_i dT + \tilde{V}_i dP \quad \text{at constant } x \quad (3.20)$$

The partial molar quantities can be evaluated with simplified models of solution behavior and experimental measurements, and evaluated with equations of state. We will consider each of these approaches below.

3.2 EVALUATION OF H AND S FOR PURE MATERIALS

3.2.1 Gases—Departure Functions

Changes in the thermodynamic state functions are determined by the PVT equation of state for the material. Since these changes are path independent, they can be evaluated at low pressure where the fluid is in the ideal gas state and corrections made with the equation of state in order to reach

and return from the ideal state. The ideal gas is one that obeys the ideal gas law and whose internal energy depends only on N and T .

We can write for the ideal gas, designated with the superscript 0,

$$\frac{dU^0}{dT} = C_V^0(T) \Rightarrow U^0(T_2) - U^0(T_1) = \int_{T_1}^{T_2} C_V^0(T) dT \quad (3.21)$$

It follows from the expression of the First Law above that

$$\left(\frac{\partial S^0}{\partial T}\right)_V = \frac{C_V^0(T)}{T} \quad (3.22)$$

The enthalpy of the ideal gas is also only a function of temperature since

$$H^0 = U^0(T) + RT \quad (3.23)$$

A heat capacity at constant pressure can be defined as

$$\frac{dH^0}{dT} = C_P^0(T) = C_V^0(T) + R \Rightarrow C_P^0(T) - C_V^0(T) = R \quad (3.24)$$

$$H^0(T_2) - H^0(T_1) = \int_{T_1}^{T_2} C_P^0(T) dT \quad (3.25)$$

Since the real gas approaches ideal behavior as the pressure approaches zero, the above property changes for the ideal gas apply to the real gas in this limit. The entropy change may be included as

$$S^0(T_2, V_2) - S^0(T_1, V_1) = \int_{T_1}^{T_2} \frac{C_V^0(T)}{T} dT + R \ln \frac{V_2}{V_1} \quad (3.26)$$

Regarding F as the internal energy, enthalpy, or entropy functions, the difference in the value of F between the real and ideal gas states may be expressed in terms of departure functions, F' , defined as

$$\begin{aligned} F'(T, V) &= F(T, V) - F^0(T, V^0) \\ &= F(T, V) - F(T, V \rightarrow \infty) + F(T, V \rightarrow \infty) - F^0(T, V^0) \end{aligned} \quad (3.27)$$

$$F'(T, V) = \int_{\infty}^V \left(\frac{\partial F}{\partial V}\right)_T dV + \left[\int_{V^0}^{\infty} \left(\frac{\partial F}{\partial V}\right)_T dV \right]_{\text{ideal}} \quad (3.28)$$

$$\begin{aligned} F'(T, V) &= \int_{\infty}^V \left(\frac{\partial F}{\partial V}\right)_T dV + \left[\int_V^{\infty} \left(\frac{\partial F}{\partial V}\right)_T dV \right]_{\text{ideal}} \\ &\quad - \left[\int_V^{V^0} \left(\frac{\partial F}{\partial V}\right)_T dV \right]_{\text{ideal}} \end{aligned} \quad (3.29)$$

$$F'(T, V) = \int_{\infty}^V \left[\left(\frac{\partial F}{\partial V}\right)_T - \left(\frac{\partial F}{\partial V}\right)_{T, \text{ideal}} \right] dV - \int_V^{V^0} \left(\frac{\partial F}{\partial V}\right)_{T, \text{ideal}} dV \quad (3.30)$$

A property change can then be expressed in terms of the change for the ideal gas and the corresponding departures.

$$\begin{aligned} F(T_2, V_2) - F(T_1, V_1) &= F^0(T_2, V_2^0) - F^0(T_1, V_1^0) \\ &\quad + F'(T_2, V_2) - F'(T_1, V_1) \end{aligned} \quad (3.31)$$

Note that no phase changes are considered. Also note that the derivatives appearing in the integrals may always be expressed in terms of P , V , and T and their derivatives. Leaving the internal energy as an exercise, the result may be applied to the internal enthalpy and entropy functions as follows:

a. *Enthalpy Departure Function:*

$$\begin{aligned} H'(T, V) &= \int_{\infty}^V \left[\left(\frac{\partial H}{\partial V}\right)_T - \left(\frac{\partial H}{\partial V}\right)_{T, \text{ideal}} \right] dV \\ &\quad - \int_V^{V^0} \left(\frac{\partial H}{\partial V}\right)_{T, \text{ideal}} dV \end{aligned} \quad (3.32)$$

$$\left(\frac{\partial H}{\partial V}\right)_T = T \left(\frac{\partial S}{\partial V}\right)_T + V \left(\frac{\partial P}{\partial V}\right)_T \text{ from Equation (3.6) for } dH \quad (3.33)$$

$$\left(\frac{\partial S}{\partial V}\right)_T = \left(\frac{\partial P}{\partial T}\right)_V \text{ from the differential of the Helmholtz free energy (Sandler, 1999)} \quad (3.34)$$

$$\begin{aligned} H'(T, V) &= \int_{\infty}^V \left[T \left(\frac{\partial P}{\partial T}\right)_V + V \left(\frac{\partial P}{\partial V}\right)_T \right] dV \\ &= PV|_{\infty}^V + \int_{\infty}^V \left[T \left(\frac{\partial P}{\partial T}\right)_V - P \right] dV \end{aligned} \quad (3.35)$$

$$H'(T, V) = pV - RT + \int_V^{\infty} \left[p - T \left(\frac{\partial p}{\partial T}\right)_V \right] dV \quad (3.36)$$

If a volume explicit equation of state, $V = V(P, T)$, was available, an analogous development would be followed with the pressure in place of the volume as the independent variable. The result would be

$$H_i(T, P) - H_i^0(T, P) = -RT^2 \int_0^P \left(\frac{\partial Z}{\partial T} \right)_P \frac{dP}{P} \quad (3.37)$$

where

$$Z = \frac{PV}{RT} \quad (3.38)$$

b. *Entropy Departure Function:*

$$S'(T, V) = \int_{\infty}^V \left[\left(\frac{\partial S}{\partial V} \right)_T - \left(\frac{\partial S}{\partial V} \right)_{T, \text{ideal}} \right] dV - \int_V^{V^0} \left(\frac{\partial S}{\partial V} \right)_{T, \text{ideal}} dV \quad (3.39)$$

$$\left(\frac{\partial S}{\partial V} \right)_T = \left(\frac{\partial P}{\partial T} \right)_V. \text{ See reference in Equation (3.34);}$$

$$\left(\frac{\partial S}{\partial V} \right)_{T, \text{ideal}} = \frac{R}{V} \quad (3.40)$$

$$S'(T, V) = \int_{\infty}^V \left[\left(\frac{\partial P}{\partial T} \right)_V - \frac{R}{V} \right] dV - \int_V^{V^0} \frac{R}{V} dV \quad (3.41)$$

$$S'(T, V) = \int_{\infty}^V \left[\left(\frac{\partial P}{\partial T} \right)_V - \frac{R}{V} \right] dV + R \ln Z \quad (3.42)$$

Example 3.2.1-1: Departure Functions for H and S Using the Redlich–Kwong–Soave (RKS) Equation of State

Refer to Table 2.1 for the RKS equation of state. The required derivatives are given by

$$\left(\frac{\partial P}{\partial T} \right)_V = \frac{R}{V-b} - \frac{da}{dT} \frac{1}{V(V+b)} \quad (3.43)$$

where

$$\frac{da}{dT} = -0.653812R \sqrt{\frac{T_c}{P_c}} \alpha(\omega) \sqrt{\frac{a(T)}{T}} \quad (3.44)$$

a. *Enthalpy Departure Function:*

$$H'(T, V) = PV - RT + \int_V^{\infty} \left[\left(P - T \frac{\partial p}{\partial T} \right)_V \right] dV \quad (3.45)$$

$$= PV - RT + \int_V^{\infty} \left(\frac{RT}{V-b} - \frac{a(T)}{V(V+b)} - \frac{RT}{V-b} + \frac{T da/dT}{V(V+b)} \right) dV \quad (3.46)$$

$$= PV - RT - \frac{a - T da/dT}{b} \left(\int_V^{\infty} \left[\frac{1}{V} - \frac{1}{V+b} \right] dV \right) \quad (3.47)$$

$$= PV - RT + \frac{(a - T da/dT)}{b} \ln \left[1 + \frac{b}{V} \right] \quad (3.48)$$

b. *Entropy Departure Function:*

$$S'(T, V) = \int_{\infty}^V \left[\left(\frac{\partial P}{\partial T} \right)_V - \frac{R}{V} \right] dV + R \ln Z \quad (3.49)$$

$$S'(T, V) = \int_{\infty}^V \left[\frac{R}{V-b} - \frac{da}{dT} \frac{1}{V(V+b)} - \frac{R}{V} \right] dV + R \ln Z \quad (3.50)$$

$$S'(T, V) = R \ln \left[Z \left(1 - \frac{b}{V} \right) \right] + \frac{1}{b} \frac{da}{dT} \ln \left[1 + \frac{b}{V} \right] \quad (3.51)$$

Example 3.2.1-2: Evaluation of an Enthalpy Change for Ethylene

Evaluate the enthalpy change for ethylene between (25 °C, 100 psia) and (250 °C, 250 psia) using the RKS equation of state.

Data (Poling et al., 2001)

$$C_p(T(K))/R = 4.221 - 8.782 \times 10^{-3}T + 5.795 \times 10^{-5}T^2 - 6.729 \times 10^{-8}T^3 + 2.511 \times 10^{-11}T^4$$

$$T_c = 282.34 \text{ K} = 282.34 \times 1.8 = 508.21 \text{ R}$$

$$T_c = 508.21$$

$$P_c = 50.41 \text{ bar} = 50.41 \frac{14.696}{1.01325} = 731.14 \text{ psia}$$

$$P_c = 731.14$$

$$\omega = 0.087$$

Process conditions:

$$T_1 = 1.8(273.16 + 25) = 536.69 \text{ R}$$

$$T_2 = 1.8(273.16 + 250) = 941.69 \text{ R}$$

$$T_1 = 536.69$$

$$T_2 = 941.69$$

$$P_1 = 100$$

$$P_2 = 300$$

$$R = 10.73 \text{ ft}^3 \text{ psia}/(\text{lb mol R})$$

Refer to Table 2.1.

$$a(T) = 0.42747 \frac{R^2(T_c)^2}{P_c} \left(1 + \left(1 - \left(\frac{T}{T_c} \right)^{0.5} \right) \right) \times (0.48508 + 1.5517\omega - 0.15613\omega^2)^2$$

$$b = 0.08664 \frac{RT_c}{P_c}$$

$$P(V, T) = \frac{RT}{V - b} - \frac{a(T)}{V(V + b)}$$

Molar volumes at process conditions:

$$P(V_1, T_1) = P_1, \text{ Solution is } \{[V_1 = 193.64], [V_1 = 1.1426 + 0.77548i], [V_1 = 1.1426 - 0.77548i]\}$$

$$P(V_2, T_2) = P_2, \text{ Solution is } \{[V_2 = 33.319], [V_2 = 0.18123 + 0.80295i], [V_2 = 0.18123 - 0.80295i]\}$$

Calculation of departures:

$$H'_1 = P_1 V_1 - RT_1 - \frac{a(T_1) - T_1 a'(T_1)}{b} \ln \left(1 + \frac{b}{V_1} \right) = -209.84 \text{ ft}^3 \text{ psia}/(\text{lb mol})$$

$$H'_1 = -209.84 \times 144 \times (1.2851 \times 10^{-3}) = -38.832 \text{ Btu}/(\text{lb mol})$$

$$H'_2 = P_2 V_2 - RT_2 - \frac{a(T_2) - T_2 a'(T_2)}{b} \ln \left(1 + \frac{b}{V_2} \right) = -758.23 \text{ ft}^3 \text{ psia}/(\text{lb mol})$$

$$H'_2 = -758.23 \times 144 \times (1.2851 \times 10^{-3}) = -140.31 \text{ Btu}/(\text{lb mol})$$

$$\Delta H = \Delta H^0 + H'_2 - H'_1$$

$$\Delta H^0 = 1449.9(8.314) = 12,054 \text{ J/mol}$$

$$\Delta H^0 = 1449.9(8.314)454 \times (9.486 \times 10^{-4}) = 5191.4 \text{ Btu}/(\text{lb mol})$$

$$\Delta H = \Delta H^0 + H'_2 - H'_1 = 5191.4 - 140.3 + 38.8 = 5089.9 \text{ Btu}/(\text{lb mol})$$

The departure at the high pressure is approximately 2.7% of the ideal value, while the departure at the lower pressure and temperature is approximately 0.75% of the ideal value.

3.2.2 Liquids and Solids

The enthalpy at (T, P) relative to T_0, P_0 can be obtained by computing the enthalpy change along the low-pressure isobar at P_0 until the final temperature is reached, followed by integration of the enthalpy along the isotherm at T until the final pressure is reached. Throughout the process, the equation of state provides the accompanying enthalpy changes. For liquids and solids, the equation of state is taken to be Equation (2.29).

$$H = H(T_0, P_0) + \int_{T_0}^T \left[\frac{\partial H}{\partial T} \right]_P dT + \int_{P_0}^P \left[\frac{\partial H}{\partial P} \right]_T dP \quad (3.52)$$

The derivative with respect to temperature and pressure can be obtained from Table 3.1.

$$H = \underbrace{\int_{T_0}^T C_p dT}_{P=\text{constant}=P_0} + \underbrace{\int_{P_0}^P \left[V - T \left(\frac{\partial V}{\partial T} \right)_P \right] dP}_{T=\text{constant}=T} : H(T_0, P_0) = 0 \quad (3.53)$$

$$H = \int_{T_0}^T C_p dT + \int_{P_0}^P V[1 - \alpha_T T] dP \quad (3.54)$$

where

$$\alpha_T = \frac{1}{V_T} \left(\frac{\partial V}{\partial T} \right)_P \equiv \text{coefficient of thermal expansion} \quad (3.55)$$

Substitution of the PVT relation and integrating gives

$$H = \int_{T_0}^T C_p dT + \frac{V_0}{\kappa} e^{\alpha_T(T-T_0)} [1 - \alpha_T T] \left[1 - e^{-\kappa(P-P_0)} \right] \quad (3.56)$$

where

$$\kappa = -\frac{1}{V_T} \left(\frac{\partial V}{\partial P} \right)_T \equiv \text{isothermal compressibility} \quad (3.57)$$

The heat capacity is to be evaluated at P_0 . Note that its variation with pressure is needed to obtain the equivalent negative enthalpy change if the path is reversed.

Similarly, the entropy relative to the value at T_0, P_0 may be obtained as follows:

$$S = \int_{T_0}^T \frac{C_p}{T} dT - \alpha_T V (P - P_0) \left[\frac{e^{\kappa(P-P_0)} - 1}{\kappa(P - P_0)} \right] \quad (3.58)$$

Incompressibility is often a very good approximation for liquids and solids. In this case, the internal energy is a function only of temperature and can be evaluated with the specific heat. The internal energy and enthalpy are approximately equal because the pV product is small. The change in entropy is proportional to the change in internal energy and can therefore be evaluated only with the specific heat. A case of significant compressibility effects is shown in Example 3.2.2-1.

Example 3.2.2-1: Enthalpy Change in the Injection Molding of Polystyrene

During the injection molding of polymers (see Chapter 8), an element of polymer melt undergoes a large temperature and pressure change when injected into a cooled mold from the extruder barrel. The following values are typical for the injection molding of polystyrene (Gogos, personal communication). The data were taken from Brandrup (2005). The calculation shows that a large correction is required when calculating the enthalpy of the fluid element relative to the mold conditions:

$$\Gamma = \frac{V_0}{C_p(T - T_0)\kappa} \exp(\alpha(T - T_0))(1 - \alpha T)(1 - \exp(-\kappa(P - P_0)))$$

= correction factor to enthalpy change to account for the compressibility

$$T = 250 + 273 \text{ K}$$

$$T_0 = 50 + 273 \text{ K}$$

$$P_0 = (20/14.7)1.01325 \times 10^5 \text{ Pa(N m)}$$

$$P = (12,000/14.7)1.01325 \times 10^5 \text{ Pa(N m)}$$

$$\alpha = 1.9 \times 10^{-4} \text{ K}^{-1}$$

$$\kappa = 2.20 \times 10^{-10} (\text{N m})^{-1}$$

$M = 50,000$. Correction does not depend on M

$$V_0 = 1.0 \times \frac{M}{10^6} \text{ m}^3/\text{mol}$$

$$C_p = 1.8 \text{ MJ}/(\text{mol K})$$

$$\Gamma = 0.21265 \text{ or } 21\%$$

3.3 EVALUATION OF H AND S FUNCTIONS FOR MIXTURES

3.3.1 Ideal Gas Mixture

An ideal gas is imagined to be composed of molecules that are completely devoid of any interactions. The properties of an ideal gas mixture are therefore presumed to be the sum of the individual contributions of the components at the same temperature and volume as the mixture—Gibbs theorem (Smith et al., 2005).

Thus, for the enthalpy of the ideal gas mixture

$$NH^0 = \sum_{\text{all components}} N_i H_i^0(T) \quad (3.59)$$

since the enthalpy of the pure component does not depend on pressure. Similarly for the internal energy

$$U^0 = \sum_{\text{all components}} y_i U_i^0(T) \quad \text{or} \quad \tilde{U}_i^0(T) = U_i^0(T) \quad (3.60)$$

However, the entropy of the individual components does depend on pressure

$$dS_i^0 = -R d \ln P \quad \text{at constant } T \quad (3.61)$$

$$S_i^0(T, P_i) = S_i^0(T, P) - R \ln \frac{P_i}{P} \quad (3.62)$$

$$S_i^0(T, P_i) = S_i^0(T, P) - R \ln y_i \quad (3.63)$$

or

$$\tilde{S}_i^0(T, y_i) = S_i^0(T, P) - R \ln y_i \quad (3.64)$$

Therefore, there is a mixing effect for entropy for the ideal gas mixture:

$$S^0 - \sum_{\text{all components}} y_i S_i^0(T, P) = -R \sum_{\text{all components}} y_i \ln y_i \geq 0 \quad (3.65)$$

Since $G^0 = H^0 - TS^0$, it follows that

$$G_i^0(T, P_i) = G_i^0(T, P) + RT \ln y_i \quad (3.66)$$

$$G^0 = \sum_{\text{all components}} y_i G_i^0(T, P) + RT \sum_{\text{all components}} y_i \ln y_i \quad (3.67)$$

In terms of partial molar quantities, we then have for the ideal gas mixture:

$$\tilde{H}_i^0 = H_i^0(T, P) \quad (3.68)$$

$$\tilde{U}_i^0 = U_i^0(T, P) \quad (3.69)$$

$$\tilde{S}_i^0 = S_i^0(T, P) - R \ln y_i \quad (3.70)$$

$$\tilde{G}_i^0 = G_i^0(T, P) + RT \ln y_i \quad (3.71)$$

These expressions can be used with the corresponding departure functions to express the property change in the ideal gas state. This approach is most often applied to gas mixtures. The ideal solution is developed on a broader basis and is applied to both liquids and gases.

3.3.2 Ideal Solution

Motivated by the results for an ideal gas mixture, the ideal solution is imagined as one composed of mixtures of like molecules where the effect of mixing may be described by processes similar to the mixing of ideal gases. A mixture of isomers is a limiting example. Adjacent members of an homologous series is another example. The resulting expressions for the ideal solution are therefore

$$\tilde{H}_i^{\text{id}} = H_i(T, P) \quad (3.72)$$

$$\tilde{U}_i^{\text{id}} = U_i(T, P) \quad (3.73)$$

$$\tilde{S}_i^{\text{id}} = S_i(T, P) - R \ln y_i \quad (3.74)$$

The pure component values indicate that both pressure and temperature dependence and the pure component need not be ideal. In borrowing the features of the ideal gas mixture, the constituents of the ideal solution are presumed to be in the same state of aggregation as the mixture at the mixture temperature and pressure. This is too restrictive and does not apply, for example, to sparingly soluble gases in liquid solvents. A broader definition of the ideal solution will be discussed below and will include such cases. For now, we

will limit the discussion of systems where the individual species exist in the same state of aggregation as the mixture. Liquid–liquid extraction systems are replete with examples of such systems. Note that $\tilde{V}_i = V_i$.

Mixing functions in liquids, discussed in Section 3.3.4, are analogous to departure functions for gases and can be used for the evaluation of partial molar quantities in nonideal liquid systems.

3.3.3 Nonideal Gas Mixtures

Departure functions can be used for mixtures in the same manner as for pure components, except that the equation of state must be evaluated for the mixture. The cubic equations of state (refer to Table 2.1; see key prepared in Chapter 2), for example, have been adapted to mixtures.

The effect of a composition change on the property can be evaluated for the mixture in the ideal gas state and the departure functions can be employed with constant but different compositions to reach and return from the ideal states of the mixture.

3.3.4 Nonideal Liquid Solutions: Heat of Solution

Mixing in liquids, which are not ideal mixtures, may be accompanied by a significant heat effect. Measured data of the magnitude of the heat effect can be analyzed with mixing functions to generate the partial molar enthalpies that underpin the enthalpy at the process conditions.

Mixing functions in general represent the change in a thermodynamic property resulting from mixing of the constituents in their reference states. Reference states are chosen for convenience and could, for example, be the pure components at the temperature and pressure of the solution and the same state of aggregation. More general reference states are needed to account for such systems as a dissolved solid or gas. A general ideal solution is then one in which the partial properties are evaluated at the reference state.

Since functions like the Gibbs free energy experience changes even when forming the ideal solution as discussed above, excess functions are defined to reflect the amount beyond that observed for the ideal solution. In the case of enthalpy, the mixing and excess functions are the same since the ideal heat of mixing is zero. Excess functions will be used later in the discussion of liquid phase equilibria.

The enthalpy mixing function applies to heat of solution data and is defined as

$$\Delta H_{\text{mixing}} = H - \sum_i x_i \tilde{H}_i^+(T, P) \quad (3.75)$$

It represents the heat absorbed when a solution is formed from the pure components in their standard states of aggregation denoted by $+$. Mixing is done isothermally and at

TABLE 3.2 Heat of Solution for the HCl–H₂O System at 25 °C (T^*)

r (mol water/mol HCl)	$Q_{\text{soln}}(T^*, r)$ (kcal/mol HCl)
1	–6.268
2	–11.668
5	–15.308
10	–16.608
20	–17.155
40	–17.448
50	–17.509
100	–17.650
200	–17.735
400	–17.796
1,000	–17.850
5,000	–17.909
10,000	–17.924
100,000	–17.949
∞	–17.960

Source: Whitwell and Toner (1969).

constant pressure. Heat of solution data are available for a number of binary systems in the form of the heat evolved per mole or unit mass of solute, $Q_{\text{soln}}(T^*, r)$, at a particular temperature, T^* , when a mixture is formed from the components in their standard states in varying ratios of the solvent to solute (r).

For example, heat of solution or mixing data for the HCl–H₂O system at 25 °C (T^*) is given in Table 3.2.

The reference states here are HCl gas and liquid water at 25 °C and 1 atm.

We will use a to denote the solute and w to denote the solvent in general so that the discussion will not be limited to the HCl–H₂O system. The mixing function for enthalpy, the heat of solution, and the enthalpy of the solution are then related by an energy balance on the liquid mixing process.

$$N_a Q_{\text{soln}} = (N_a + N_w) \Delta H_{\text{mixing}} = (N_a + N_w) H - N_a H_a^+ - N_w H_w^+ \quad (3.76)$$

It is the enthalpy of the mixture, H , at the process conditions that we are seeking to evaluate with the heat of solution data. The effect of pressure on liquid properties is generally negligible and will be neglected here. If the process temperature T is different from the temperature of the data, T^* , the specific heat of the solution is needed to make the adjustment:

$$H(x, T) = H(x, T^*) + \int_{T^* \text{ at constant } x}^T C_{p, \text{soln}}(x, T) dT \quad (3.77)$$

Consequently, we will formulate the enthalpy of the mixture at the experimental temperature and pressure as a function of composition using partial molar enthalpies.

The reference states H_a^+ and H_w^+ must correspond to the reference states for enthalpy used for the process or the difference accounted for in the energy balance. If for this or other reasons we wished to change the reference state for the solvent from a pure liquid at the experimental temperature to the vapor at its normal boiling point ($>T^*$), T_b , the new reference state would be given by

$$H_{w, \text{new}}^+ = H_w^+ + \int_{T^*}^{T_b} C_{pw}(T) dT + \Delta H_{w, \text{vap}}(T_b) \quad (3.78)$$

The effect of pressure is neglected. The new heat of solution then becomes

$$N_a Q_{\text{soln}, \text{new}} = N_a Q_{\text{soln}} - N_w \int_{T^*}^{T_b} C_{pw}(T) dT - N_w \Delta H_{w, \text{vap}}(T_b) \quad (3.79)$$

where

$$\begin{aligned} N_a Q_{\text{soln}, \text{new}} &= (N_a + N_w) \Delta H_{\text{mixing}} \\ &= (N_a + N_w) H - N_a H_a^+ - N_w H_{w, \text{new}}^+ \end{aligned} \quad (3.80)$$

If the heat of solution data are correlated against the value of $r = N_w/N_a$, the preceding equation may be differentiated to provide the partial molar quantities:

$$\left(\frac{\partial N_a Q_{\text{soln}}}{\partial N_a} \right)_{N_w, T, P} = \frac{\partial N H}{\partial N_a} - H_a^+ \quad (3.81)$$

or

$$\tilde{\Delta} H_{\text{mixing}, a} = \tilde{H}_a - H_a^+ = \left(\frac{\partial N_a Q_{\text{soln}}}{\partial N_a} \right)_{N_w, T, P} \quad (3.82)$$

$$\tilde{\Delta} H_{\text{mixing}, w} = \tilde{H}_w - H_w^+ = \left(\frac{\partial N_a Q_{\text{soln}}}{\partial N_w} \right)_{N_a, T, P} \quad (3.83)$$

The mole numbers may be transformed to mole fractions in the final result. The enthalpy as a function of composition at the temperature and pressure of the data can then be constructed from

$$H = x_a \tilde{H}_a + x_w \tilde{H}_w \quad (3.84)$$

$$H = x_a \tilde{\Delta} H_{\text{mixing}, a} + x_w \tilde{\Delta} H_{\text{mixing}, w} + x_a H_a^+ + x_w H_w^+ \quad (3.85)$$

Example 3.3.4-1: Partial Molar Enthalpies for HCl–Water System

The data for the HCl–water system given in Table 3.2 are plotted as the negative inverse of the heat of solution versus the inverse mole ratio of water to acid in Figure 3.1.

The data are fit by the quadratic function shown on the graph in Figure 3.1 with a correlation coefficient of 0.9991. Therefore,

$$Q_{\text{soln}} = -\frac{1}{0.0821(N_a/N_w)^2 + 0.0208(N_a/N_w) + 0.0563}$$

The partial molar properties follow from Equations (3.82) and (3.83) as

$$\begin{aligned}\tilde{H}_1 - H_1^+ &= -\frac{-0.0821x^2(1-x)^2 + 0.0563(1-x)^4}{(0.0821x^2 + 0.0208x(1-x) + 0.0563(1-x)^2)^2} \\ \tilde{H}_2 - H_2^+ &= -\frac{2(0.0821)x^3(1-x) + 0.0208x^2(1-x)^2}{(0.0821x^2 + 0.0208x(1-x) + 0.0563(1-x)^2)^2}\end{aligned}$$

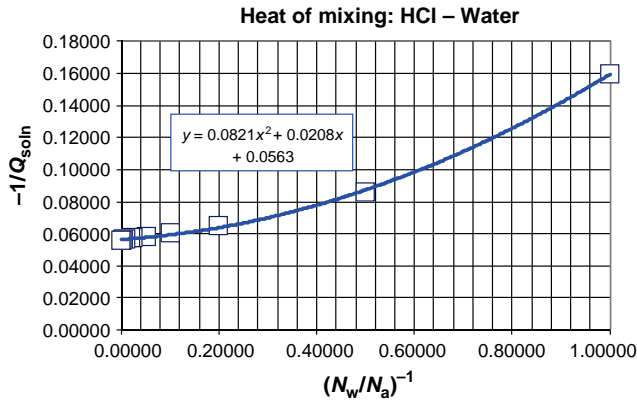


FIGURE 3.1 Quadratic fit of heat of solution data.

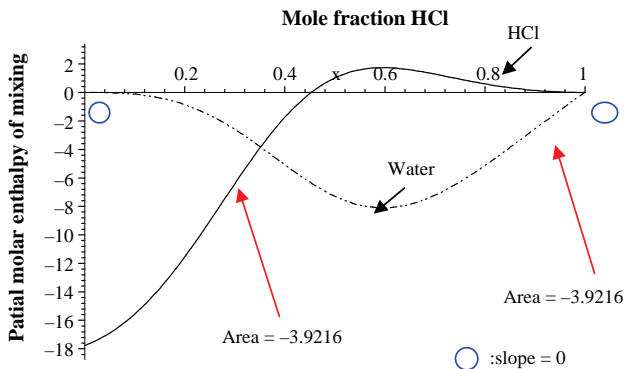


FIGURE 3.2 Partial molar enthalpies of water and hydrochloric acid.

Note that the area and slope tests referred to in Section 3.1 are satisfied by these results (see Figure 3.2).

3.4 ENERGY FLOWS AND THE FIRST LAW

The enthalpy function underpins the expression of energy conservation in flow systems. We can rationalize the total flow of energy in a mixture by identifying those contributions of which we are already aware and thereby arrive at the definition of a residual by difference that must be addressed in phenomenological terms. Consider first a pure fluid moving with a uniform velocity v in one direction. The flow field is depicted in Figure 2.3 without reference to a stream or equipment connection, although these are the applications we have in mind. The circular cross section implies flow in a conduit but is irrelevant under the assumption of uniform flow.

After the elapse of time, δt , all of the material that flows through an element of area, A , perpendicular to the direction of flow is contained in a volume element swept out by the area along the perpendicular direction of flow of length $v \delta t$.

The mass, δm , which has entered the volume element, has also carried with it the internal energy arising from molecular phenomena discussed in thermodynamics plus kinetic and potential energy because of the bulk motion of the element and its location in a potential field:

$$\left[u + \frac{1}{2}v^2 + g\mathcal{L} \right] \rho v \delta t A \quad (3.86)$$

We have taken the field to be gravity and h as the height above a datum plane. Mass units have been used for the internal energy because of the kinetic and potential energy terms.

In addition, the mass elements have encountered the normal pressure force, which does work on the element as it crosses the area:

$$PA v \delta t \quad (3.87)$$

We are assuming a unidirectional motion and therefore do not need to account for the shear type forces that can exist with the presence of velocity gradients. These will be important only in special circumstances and will never amount to more than several degrees.

Denoting the total energy flux (flow per unit area) as J_e , we then have

$$J_e A \delta t = \left[u + \frac{1}{2}v^2 + g\mathcal{L} + \frac{P}{\rho} \right] A v \delta t + q A \delta t \quad (3.88)$$

or

$$J_e = \rho \left[h + \frac{1}{2}v^2 + g\mathcal{L} \right] v + q \quad (3.89)$$

The flux q has been added to be certain of the equality since the flux of energy has meaning independent of our identifications. It is useful because we have been able to account for the convective flow component leaving q as a nonconvective flow called conduction.

The conduction term is similar to the diffusional flow of mass, as pointed out in Chapter 2 in the discussion of the macroscopic mass balance. Like diffusion, it can safely be ignored at inlets and outlets to chemical processing equipment. However, whereas diffusional flows through the walls of process equipment are normally unimportant, conduction in solids is very effective and cannot be neglected. In fact, heat exchange with the surroundings can be the primary objective of the system as, for example, in heat exchangers or an important component as in chemical reactors.

If more than one component is present, each species will have an average velocity, v_i , and the mass flux of species i through the area in Figure 2.3 is $\rho_i v_i$. Each component of the mixture will make a contribution to the enthalpy of the mixture, as discussed in Section 3.3. In general, this contribution is expressed by the partial molar or specific enthalpy.

The flux of energy for the pure component case can therefore be extended to the case of many components as

$$J_e = \sum_{\text{all components}} \rho_i \left(\bar{h}_i + \frac{1}{2} v^2 + g\mathcal{A} \right) v_i + q \quad (3.90)$$

where \bar{h}_i is the partial specific enthalpy of species i . The kinetic energy per unit mass associated with the individual mass flows has been calculated with the average velocity in lieu of using the individual values, $v_i^2/2$. This leads to a slight theoretical discrepancy between the two calculations of the kinetic energy, but the approximation is of no significant practical value. Also, the potential field has been limited to gravity for all components.

We can use the preceding results to express conservation of energy from a macroscopic point of view. We refer to the same “chemical processing systems” that were subjected to the conservation of mass (see Section 2.1). Energy will accompany all of the convective mass flows into and out of the system. In addition, energy may flow into the system as heat interactions or out of the system as work interactions, the former being negligible and the latter being approximated in the inlet and outlet streams:

$$\begin{aligned} Q + \sum_{\substack{\text{all inlets } (j) \\ \text{all species } (i)}} \mathcal{W}_i^{(j)} \left[\bar{h}_i + \frac{1}{2} v^2 + g\mathcal{A} \right]_{\text{stream } j} \\ = \sum_{\substack{\text{all outlets } (k) \\ \text{all species } (i)}} \mathcal{W}_i^{(k)} \left[\bar{h}_i + \frac{1}{2} v^2 + g\mathcal{A} \right]_{\text{stream } k} + W_s \end{aligned} \quad (3.91)$$

The kinetic and potential energy terms are not normally important when nonisothermal conditions are present in chemical systems and will therefore not be included in the discussion that follows in the present chapter. They will, however, be the focus of attention in the chapter that follows.

The summations account for convection at inlets and outlets and the work done by the system is expressed by W_s . The possibility of a volumetric energy generation by sources outside of the system, such as from a microwave, is not included. Chemical reactions do not have to be accounted for separately, but no advantage has yet been taken of the associated stoichiometries. Multiphase systems may be analyzed with this result since there is no net interchange of energy between the phases at steady state. The consideration of one phase in a multiphase system requires the evaluation of Q for an interphase energy transfer process, which will be considered in Chapter 15.

The meaning of Q depends on the subsystem chosen for analysis. It may be an actual heat stream if a single unit is selected as the system. It may be the net result of a number of identifiable heat streams.

3.4.1 Degrees of Freedom

With the introduction of energy conservation, temperature and pressure have been introduced as variables for each inlet and outlet stream and Q and W_s are new variables. This amounts to $2(N_s + N_u)$ new variables, a temperature and pressure for each stream and a heat stream and work term for each subunit. Note that the relation between heat or work interactions between two subunits will be counted in the process specifications. We will, however, in the present chapter assume that the pressures and work terms are specified. In the following chapter, this restriction will be removed with the mechanical energy balance.

We will retain the explicit consideration of splitters and specify that the daughter streams are at the temperature and pressure of the feed.

These provide $2N_D$ relations for a total of $2N_D + N_u$ relations with the energy balance for each subunit.

The degrees of freedom in the isothermal case can then be extended to the nonisothermal case as follows:

$$\Phi = (N_s - N_u)N_c - (N_c - 1)(N_{D,\text{total}} - N_{\text{splitters}}) + R + 2(N_s + N_u) - 2N_{D,\text{total}} - N_u \quad (3.92)$$

$$\Phi = (N_s - N_u)(N_c + 1) - (N_c - 1)(N_{D,\text{total}} - N_{\text{splitters}}) + R + N_s + 2N_u - 2N_{D,\text{total}} \quad (3.93)$$

$$\Phi = (N_s - N_u - N_{D,\text{total}})(N_c + 1) + (N_c - 1)N_{\text{splitters}} + N_s + 2N_u + R \quad (3.94)$$

The need for data has also increased the enthalpy for each inlet and outlet stream.

3.5 ENERGY BALANCES WITHOUT REACTION

Energy balances alone are not sufficient to calculate both the heat and work interactions for a given change of state. The mechanical energy balance, discussed in the following chapter, is normally used for the calculation of work, while the energy balance, or the First Law, is used to evaluate the associated heat effect or heat exchanger duty. However, in many cases involving heat exchange, the part that is due to work is negligible and the energy balance becomes the “heat balance.” On the other hand, the entropy balance (see Section 3.8) may be used in conjunction with the First Law for a minimum work calculation. In this case, the entropy balance supplies the (reversible) heat effect and the First Law supplies the work. This latter case will be illustrated with the isothermal pumping of a liquid (Example 3.5.1).

Energy balances are an integral part of sizing heat exchange equipment. The sizing of heat exchangers is considered in Chapter 13. We will illustrate the evaluation of heat exchanger duties for several cases involving ideal fluids with and without phase change in unreactive systems. Several examples involving mixing and evaporation of non-ideal liquids will illustrate the use of partial molar enthalpies in the energy balance.

3.5.1 Utilization of the Second Law

As noted above, it is not possible to evaluate both the heat and work terms with a single energy balance. In those cases where a limiting value of the work is satisfactory, the Second Law may be employed to evaluate the heat effect for a reversible process, thus, providing the minimum work required or the maximum work available from the Second Law.

Example 3.5.1-1: Minimum Work Required for Isothermal Pumping of a Liquid

The application of the energy balance to the pumping of a liquid solution is illustrated in Figure 3.3.

Equation (3.91) for this application becomes

$$Q + \sum_{\text{all } i} \mathcal{W}_i^{(0)} \bar{h}_i^{(0)} = \sum_{\text{all } i} \mathcal{W}_i^{(1)} \bar{h}_i^{(1)} + W_s$$

Conservation of mass requires that the individual flows be equal so that

$$Q = \sum_{\text{all } i} \mathcal{W}_i [\bar{h}_i^{(1)} - \bar{h}_i^{(0)}] + W_s$$

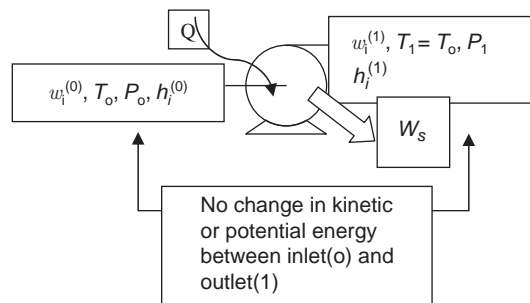


FIGURE 3.3 Energy balance—isothermal liquid pump.

or in molar units

$$Q = \mathcal{N} \Delta H + W_s$$

The enthalpy change is given by Equation (3.56) applied to an isothermal change of state:

$$\Delta H = \frac{V_0}{\kappa} [1 - \alpha_T T_0] [1 - e^{-\kappa(P-P_0)}]$$

For the minimum work required, the heat effect can be obtained from the entropy change associated with a reversible heat interaction:

$$\mathcal{N} \Delta S = \frac{Q_{\text{rev}}}{T} = \frac{Q}{T_0}$$

where the entropy change is given by the isothermal version of Equation (3.58).

$$\Delta S = -\alpha_T V_0 \left[\frac{1 - e^{-\kappa(P-P_0)}}{\kappa} \right]$$

Consequently, the minimum pumping work is given by

$$(-W_s)_{\min} = \mathcal{N} V_0 (P - P_0) \left[\frac{1 - e^{-\kappa(P-P_0)}}{\kappa(P-P_0)} \right]$$

The bracketed factor in the preceding equation is unity for a compressibility factor of zero.

Note that the minimum work required is independent of the coefficient of thermal expansion to which the heat transferred is directly proportional.

3.5.2 System Definition for Duty and Flow Rate Calculation

Heat exchanger E-309 in the acrylic acid process (see Figure 1.1) is used to reheat the solvent, stream 22, which

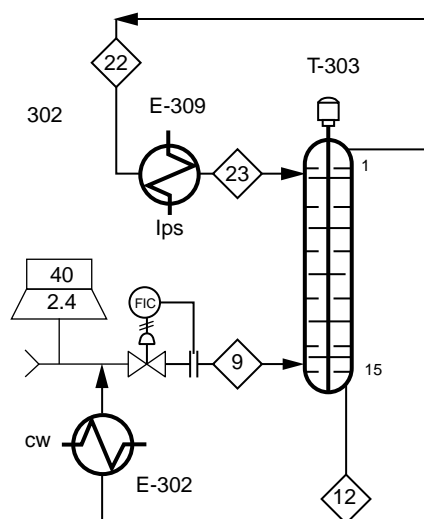


FIGURE 3.4 Solvent exchanger E-309 and extraction tower T-303. Reprinted with permission of Pearson.

is recycled from the product recovery section at 13 °C. The exchanger and extraction column are shown in Figure 3.4.

The extraction unit is designed to operate at 40 °C so that the recycled solvent must be heated to this temperature. Low-pressure saturated steam at 5 barg is available as a utility. The saturation temperature of the steam is 151.8 °C. This means that the steam will enter and leave at 151.8 °C. The minimum temperature difference between the two fluids is therefore 111.8 °C or 201.4 °F. This is far beyond the heuristic of a 10 °F minimum (Couper et al., 2005) and is likely to result in a condition known as film boiling. This refers a condition at the heat transfer surface where the rate of heat transfer is so high that the liquid evaporates and forms a gas film over the heat transfer surface. The gas film presents a large resistance to heat transfer. A shell and tube heat exchanger illustrated in Figure 1.16 will be used with the condensing steam in the shell.

We will use two different definitions of the system in carrying out the energy balance in order to calculate the heat duty and the flow rate of the steam that will be needed.

Case 1: Heat Duty

The interchange of thermal energy takes place across the internal surface that is shared by the process fluid and the steam. If we take the process fluid and the exchanger as the system, this surface is exposed to analysis. Refer to Figure 3.5.

A degree of freedom analysis is as follows: $N_c = 1$ (ether), $N_s = 2$, $N_u = 1$, and there are no splitters or chemical reactions. Consequently,

$$\Phi = (2 - 1 - 0)(2 + 1) + 2 + 2 = 7 \quad (3.95)$$

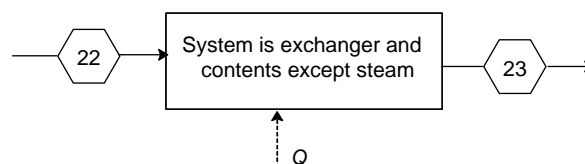


FIGURE 3.5 System for calculation of Q .

Fix the flow, temperature, and pressure of streams 22 and 23 and set the work to zero. Solve the energy balance for Q .

Case 2: Steam Flow Rate

When the steam is made part of the system, the steam flow rate is introduced as a system variable and the desired heat interaction disappears. The heat interaction for the combined system is in fact zero for sufficiently insulated equipment. Refer to Figure 3.6.

A degree of freedom analysis of this case is as follows: $N_c = 2$ (DIPE and water), $N_s = 4$, $N_u = 1$. Again there are no splitters or reactions. Consequently,

$$\Phi = (4 - 1 - 0)(2 + 1) - 0 + 4 + 2 = 15 \quad (3.96)$$

We can impose the equipment specifications that there is no mass communication between the two streams. This requires the specification of four zero component flows. There are four pressure specifications and both Q and W are zero. The process stream inlet and outlet temperatures are specified as well as the steam outlet temperature and physical state (liquid). The latter specification is a condition on the enthalpy. Fixing the process stream inlet rate finishes the required specifications. The energy and mass balance may then be solved for the steam flow rate and the outlet process stream flow rate.

Example 3.5.2-1: Calculation of Heat Duty and Stream Flow Rate for Exchanger E-309

Species indices:

Diisopropyl ether = 1; water = 2

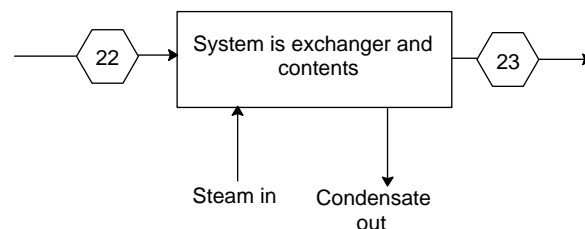


FIGURE 3.6 System for calculation of steam flow rate.

Specific heats:

Water (Green and Maloney, 1997); Ether (Yaws, 1999)

$$[a] = \begin{bmatrix} 73.085 \times 10^3 & 1.1235 \times 10^3 & -3.7356 \\ 2.7637 \times 10^5 & -2.0901 \times 10^3 & 8.125 \\ 5.2200 \times 10^{-3} & 0 & \\ -1.4116 \times 10^{-2} & 9.3701 \times 10^{-6} & \end{bmatrix}$$

$$C_p(i, T) = \sum_{j=1}^{j=5} a_{ij} T^{j-1} \text{ J/(kmol K)}$$

Enthalpy relative to feed

$$H(i, T) = \int_{13+273.16}^T C_p(i, x) dx$$

Definition of flows and application of energy balance:

$$[\mathcal{N}] = \begin{bmatrix} 1299.8 \\ 198.7 \end{bmatrix}$$

Case 1:

Excluding steam from the definition of the system, we get the heat transferred.

$$Q = \sum_{i=1}^{i=2} \mathcal{N}_i H(i, 40 + 273.16) = 7.94384 \times 10^9 = 7944 \text{ MJ/h}$$

The simulator reported a value of 8000 MJ/h.

Case 2:

If we include the steam, we get the flow rate, noting that the enthalpy of the steam condensate relative to the vapor feed is -906.2 Btu/lb or -956.05 kJ/lb steam. We keep the lb unit and therefore calculate the steam flow (m) in lb/h:

$$0 = \sum_{i=1}^{i=2} \mathcal{N}_i H(i, 40 + 273.16) - 956050 \mathcal{W}_{\text{steam}}$$

Solution is $\mathcal{W}_{\text{steam}} = 8309.02 \text{ lb low-pressure (5 barg) steam per hour.}$

3.5.3 Arbitrariness of Reference State for Unreactive Systems

The choice of a reference state for enthalpy in unreactive systems is arbitrary. This fact can be easily demonstrated for ideal mixtures as follows: The reference states for each

species are defined as

$$H_i^{(j)} = H_i^+ + \Delta H_i^{(j)} \quad (3.97)$$

Substitution of Equation (3.97) into the energy balance gives

$$\begin{aligned} & \sum_{\text{all species } (i)} H_i^+ \sum_{\text{all inlets } (j)} \mathcal{N}_i^{(j)} + \sum_{\text{all inlets } (j)} \sum_{\text{all species } (i)} \mathcal{N}_i^{(j)} \Delta H_i^{(j)} + Q \\ &= \sum_{\text{all species } (i)} H_i^+ \sum_{\text{all outlets } (j)} \mathcal{N}_i^{(j)} + \sum_{\text{all outlets } (j)} \sum_{\text{all species } (i)} \mathcal{N}_i^{(j)} \Delta H_i^{(j)} + W_s \end{aligned} \quad (3.98)$$

The first term on the right-hand side of Equation (3.98) is identical to the first term on the left-hand side because of the conservation of mass. Consequently,

$$\sum_{\text{all inlets } (j)} \sum_{\text{all species } (i)} \mathcal{N}_i^{(j)} \Delta H_i^{(j)} + Q = \sum_{\text{all outlets } (j)} \sum_{\text{all species } (i)} \mathcal{N}_i^{(j)} \Delta H_i^{(j)} + W_s \quad (3.99)$$

The calculations show that the enthalpies of all of the components may be individually translated by an arbitrary amount without compromising their application to the energy balance. A convenient reference is the feed state, which can be illustrated by considering extraction tower T-303 a bit further and the distillation tower.

Example 3.5.3-1: Energy Balance on T-303 Extraction Unit (see Figure 1.4a). Feed Reference State

The inlet streams, 9 and 23, to the extractor are at 40°C , as can be seen in Table 1.10. The reference state for enthalpy can therefore be set as liquid at 40°C and 1 atm. Since we have assumed that the solutions are ideal, the enthalpy of streams 9 and 23 are zero. The energy balance, neglecting kinetic and potential energy effects, for the extraction column is then

$$0 = \sum_i \mathcal{N}_i^{(12)} H_i(T^{(12)}) + \sum_i \mathcal{N}_i^{(13)} H_i(T^{(13)})$$

assuming adiabatic operation. The enthalpies are relative to the feeds and are either equal or one is greater than the other. If the former is the case, the enthalpies are equal to zero, since the sum of the flows is nonzero, or the outlet temperatures are equal to the feed temperature. If the latter is the case, a violation of the Second Law could be constructed whereby work could be created by allowing the two streams to equilibrate through a cyclic heat engine. The two streams could then be brought to 40°C by contact with a reservoir. The result is the production of work with the interchange of heat with a single reservoir, which is a violation of the Second Law. The simulator also reports no temperature change across the extraction unit.

One heat interaction is considered in the energy balance for each subsystem under consideration. If there are more than one, the net effect is determined by the energy balance.

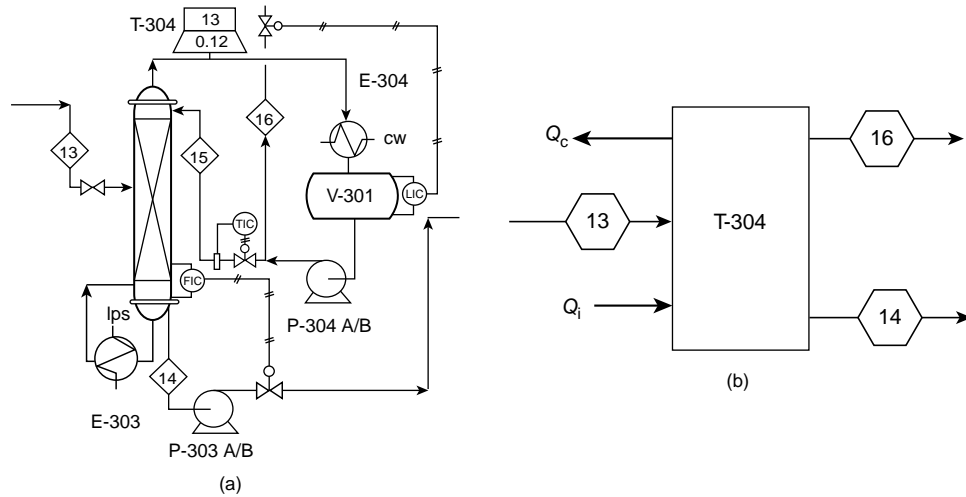


FIGURE 3.7 Tower T-304 and connections: (a) flow sheet, Reprinted with permission of Pearson. (b) block diagram.

A distillation tower, for example, has a reboiler and a condenser. An energy balance over the complete distillation unit provides the difference between the energy added to reboiler and that removed from the condenser. This is illustrated in Example 3.5.3-2, which also sets the feed as the reference for enthalpy.

Example 3.5.3-2: Calculation of Net Heat Duty for Distillation Tower T-304 (see Figure 3.7a and b). Feed Reference State

Consider the distillation tower, T-304, following the extractor and include the condenser and the reboiler in

complete the bottoms flow rates and the energy balance will give the net heat effect. The latter calculation is given below.

Label	Species
1	Water
2	Acetic acid
3	Acrylic acid
4	Diisopropyl ether

Specific heats {liquids}J/(mol K):

Water (Green and Maloney, 1997); Ether (Yaws, 1999)

$$\text{Chemical } [a] = \begin{bmatrix} 2.7637 \times 10^2 & -2.0901 & 8.1250 \times 10^{-3} & -1.4116 \times 10^{-5} & 9.3701 \times 10^{-9} \\ -18.944 & 1.0971 & -2.8921 \times 10^{-3} & 2.9275 \times 10^{-6} & 0.0 \\ -18.242 & 1.2106 & -3.1160 \times 10^{-3} & 3.1409 \times 10^{-6} & 0.0 \\ 73.085 & 1.1235 & -3.7356 \times 10^{-3} & 5.22 \times 10^{-6} & 0.0 \end{bmatrix}$$

the definition of the system but not the cooling water or the steam (see Figure 3.7).

Degrees of freedom analysis:

$$N_s = 3, \quad N_u = 1 \frac{\partial^2 \Omega}{\partial u^2}, \quad N_{\text{splitters}} = 0, \quad N_c = 4, \quad N_r = 0$$

$$\Phi = (3 - 1 - 0)(4 + 1) + 3 + 2 + 0 = 15$$

Set the temperature and pressure of all streams, the flows of the feed and distillate, and the work to zero for 15 specifications. The four mass balances can be used to

Flow rates—all liquids—kmol/h:

$$\mathbf{D} = \begin{bmatrix} 198.5 \\ 0 \\ 0 \\ 1299.5 \end{bmatrix} \text{ at } 13^\circ \text{C}$$

$$\mathbf{B} = \begin{bmatrix} 0.30 \\ 6.08 \\ 86.81 \\ 0 \end{bmatrix} \text{ at } 90^\circ\text{C with the feed at } 40^\circ\text{C}$$

Enthalpies relative to the feed—all liquids:

$$H(i, T) = \int_{40+273.16}^T C_p(i, x) dx$$

Energy balance must convert from kilomoles to moles

$$Q = 1000 \sum_{i=1}^{i=4} (D_i H(i, 13 + 273.16) + B_i H(i, 90 + 273.16)) \\ = -7.2213 \times 10^9$$

or 7221 MJ/h more energy removed than input to the reboiler. The simulator result is -7300 MJ/h.

3.5.4 Mixing of Nonideal Liquids; Use of Partial Molar Quantities

A common example of nonisothermal behavior is mixing and evaporation of liquids and their counterpart operations of condensation and separation. In this section, we will consider a number of examples of the calculations required to determine the heat effect associated with these processes in nonideal liquid systems composed of two components. The construction of the liquid phase enthalpies required in the energy balance from heat of mixing data for such systems is discussed in Section 3.3.4.

3.5.4.1 Mixing Two Liquid Streams at Different Temperatures and Concentrations Here we consider the mixing of two binary liquid streams to produce a third with molar flow rates $\mathcal{N}^{(j)}$ and temperatures $T^{(j)}$ (see Figure 3.8).

We assume that a vapor is not formed. Thermodynamic evaluation of the conditions for phase equilibrium (see

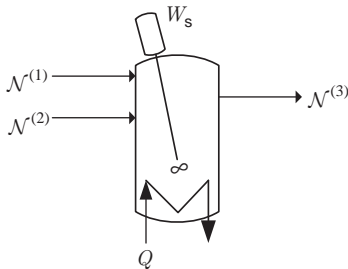


FIGURE 3.8 Mixing of nonideal liquids.

Chapter 6, Phase Equilibrium) would be required to verify this assumption.

The contribution of the mechanical work to the thermal effects produced by the heat of mixing in the energy balance can generally be neglected. Except possibly for very viscous liquids without other heat effects, this omission will most likely be justified. The energy balance can be solved using binary heat of solution data consisting of the heat released when r moles of solvent are mixed with 1 mol of solute, each in its reference state. Partial molar enthalpies developed from the heat of solution data are discussed in Section 3.3.4. The heat of solution data may be used directly in the energy balance.

Using partial molar quantities, the energy balance may be written

$$Q = \sum_{i=1}^2 \left(\mathcal{N}_i^{(3)} \tilde{H}_i^{(3)} - \mathcal{N}_i^{(1)} \tilde{H}_i^{(1)} - \mathcal{N}_i^{(2)} \tilde{H}_i^{(2)} \right) \quad (3.100)$$

If the enthalpy of species i in its pure reference state for the heat of solution data is denoted by H_i^+ , the energy balance can be modified as follows:

$$Q = \sum_{i=1}^2 \left[\mathcal{N}_i^{(3)} (\tilde{H}_i^{(3)} - H_i^+) - \mathcal{N}_i^{(1)} (\tilde{H}_i^{(1)} - H_i^+) - \mathcal{N}_i^{(2)} (\tilde{H}_i^{(2)} - H_i^+) \right] \quad (3.101)$$

since the mass balances must be satisfied.

Since each stream is possibly at a different temperature, the energy balance can be written in terms of the available data, say at T^* , as follows:

$$Q = \sum_{i=1}^2 \left[\mathcal{N}_i^{(3)} (\tilde{H}_i^{(3)*} - H_i^+) - \mathcal{N}_i^{(1)} (\tilde{H}_i^{(1)*} - H_i^+) - \mathcal{N}_i^{(2)} (\tilde{H}_i^{(2)*} - H_i^+) \right] \\ + \mathcal{N}^{(3)} \int_{T^*}^{T_3} C_p^{(3)} dT - \mathcal{N}^{(1)} \int_{T^*}^{T_1} C_p^{(1)} dT - \mathcal{N}^{(2)} \int_{T^*}^{T_2} C_p^{(2)} dT \quad (3.102)$$

The superscript (*) indicates evaluation at T^* . The specific heats refer to the liquid mixtures in the respective numbered streams. The partial molar quantities found from heat of solution data by the methods in Section 3.3.4 may be substituted into this result.

The heat of solution data may also be substituted directly. If this data is referred to component 1 as the solute, then

$$Q = \mathcal{N}_1^{(3)} Q_{\text{soln}}(T^*, r_3) - \mathcal{N}_1^{(1)} Q_{\text{soln}}(T^*, r_1) - \mathcal{N}_1^{(2)} Q_{\text{soln}}(T^*, r_2) \\ + \mathcal{N}^{(3)} \int_{T^*}^{T_3} C_p^{(3)} dT - \mathcal{N}^{(1)} \int_{T^*}^{T_1} C_p^{(1)} dT - \mathcal{N}^{(2)} \int_{T^*}^{T_2} C_p^{(2)} dT \quad (3.103)$$

where r is the ratio of solvent to solute that depends on the stream and Q^* is the heat of solution at the temperature of the data, T^* .

Example 3.5.4.1-1: Dilution of an HCl Mixture

Pure water at 20 °C is to be used to dilute an HCl mixture at the same temperature containing 70 mol% HCl to 35 mol% HCl. Heat of solution data and the resulting partial molar enthalpies may be found in Example 3.3.4-1.

Determine

- the cooling required for isothermal operation,
- the temperature of the mixture for adiabatic operation.

Specific heat data (Yaws, 1999): J/(mol K)

Component 1 = HCl; component 2 = water

$$[a] = \begin{bmatrix} 73.993 & -1.2946 \times 10^{-1} & -7.8980 \times 10^{-5} & 2.6409 \times 10^{-6} \\ 92.053 & -3.9953 \times 10^{-2} & -2.1103 \times 10^{-4} & 5.3469 \times 10^{-7} \end{bmatrix}$$

$$C_p(i, T) = \sum_{j=1}^{j=4} a_{ij} T^{j-1}$$

Mass balances:

Stream 1 = pure water, stream 2 = 70 mol% HCl,
stream 3 = 35 mol% HCl

$$\begin{aligned} \mathcal{N}_1^1 + \mathcal{N}_1^2 &= \mathcal{N}_1^3 \\ \mathcal{N}_2^1 + \mathcal{N}_2^2 &= \mathcal{N}_2^3 \\ \mathcal{N}_1^2 &= 0.70(\mathcal{N}_1^2 + \mathcal{N}_2^2) \\ \mathcal{N}_1^3 &= 0.35(\mathcal{N}_1^3 + \mathcal{N}_2^3) \\ \mathcal{N}_1^1 &= 0 \\ \mathcal{N}_1^2 + \mathcal{N}_2^2 &= 1 \end{aligned} \quad \text{Solution is } \left\{ \begin{array}{l} \mathcal{N}_1^1 = 0 \\ \mathcal{N}_2^2 = 0.3 \\ \mathcal{N}_1^3 = 0.7 \\ \mathcal{N}_2^3 = 1.3 \\ \mathcal{N}_2^1 = 1.0 \\ \mathcal{N}_1^2 = 0.7 \end{array} \right.$$

Using partial molar quantities: see Equation (3.100).

The partial molar heats of mixing are given by Example 3.3.4-1:

$$\begin{aligned} \tilde{H}_2(x) - H_2^+ &= \\ &= \frac{2(0.0821)x^3(1-x) + 0.0208x^2(1-x)^2}{(0.0821x^2 + 0.0208x(1-x) + 0.0563(1-x)^2)^2} \\ \tilde{H}_1(x) - H_1^+ &= \\ &= \frac{-0.0821x^2(1-x)^2 + 0.0563(1-x)^4}{(0.0821x^2 + 0.0208x(1-x) + 0.0563(1-x)^2)^2} \end{aligned}$$

which may be substituted into the general result.

Isothermal operation:

$$\begin{aligned} Q &= 0.7 \times [\tilde{H}_1(0.35) - H_1^+] + 1.3 \times [\tilde{H}_2(0.35) - H_2^+] \\ &\quad - 1.0 \times [\tilde{H}_2(0) - H_2^+] - 0.7 \times [\tilde{H}_1(0.7) - H_1^+] \\ &\quad - 0.3 \times [\tilde{H}_2(0.7) - H_2^+] \\ &\quad + (0.7 + 1.3) \int_{298.16}^{293.16} 0.00023901 \frac{0.7C_p(1, T) + 1.3C_p(2, T)}{0.7 + 1.3} dT \\ &\quad - \int_{298.16}^{293.16} 0.00023901 C_p(2, T) dT \\ &\quad - \int_{298.16}^{293.16} 0.00023901 \frac{0.7C_p(1, T) + 0.3C_p(2, T)}{0.7 + 0.3} dT \end{aligned}$$

Solution is $\{Q = -6.3982\}$, or 6398 cal/mol of acid feed must be removed to maintain isothermal conditions.

Adiabatic operation:

$$\begin{aligned} 0 &= 0.7 \times [\tilde{H}_1(0.35) - H_1^+] + 1.3 \times [\tilde{H}_2(0.35) - H_2^+] \\ &\quad - 1.0 \times [\tilde{H}_2(0) - H_2^+] - 0.7 \times [\tilde{H}_1(0.7) - H_1^+] \\ &\quad - 0.3 \times [\tilde{H}_2(0.7) - H_2^+] \\ &\quad + (0.7 + 1.3) \int_{298.16}^x 0.00023901 \frac{0.7C_p(1, T) + 1.3C_p(2, T)}{0.7 + 1.3} dT \\ &\quad - \int_{298.16}^{293.16} 0.00023901 C_p(2, T) dT \\ &\quad - \int_{298.16}^{293.16} 0.00023901 \frac{0.7C_p(1, T) + 0.3C_p(2, T)}{0.7 + 0.3} dT \end{aligned}$$

Solution is $\{x = -675.22\}$, $\{x = 409.49\}$, or final temperature is $(409.49 - 273.16) = 136.33$ °C.

Using the heat of solution directly:

From Section 3.3.4, the heat of solution per mole of acid is given by $Q_{\text{soln}}(r)$ where r is the moles of water per mole of acid added:

$$Q(r) = - \frac{1}{(0.0821/r^2) + (0.0208/r) + 0.0563}$$

$$r_1 = \infty$$

$$\frac{1}{1 + r_2} = 0.70, \text{ Solution is } \{r_2 = 0.428571\}$$

$$\frac{1}{1 + r_3} = 0.35, \text{ Solution is } \{r_3 = 1.85714\}$$

$$Q(r_1, 298) = q(10,000,000) = -17.762$$

$$Q(r_2, 298) = q(0.428571) = -1.8122$$

$$Q(r_3, 298) = q(1.85714) = -10.952$$

Substitution into general result: Equation (3.103).

Isothermal operation:

$$\begin{aligned} Q &= 0.7(-10.952) - 0.7(-1.8122) \\ &+ (0.7 + 1.3) \int_{298.16}^{293.16} 0.00023901 \frac{0.7c_p(1, T) + 1.3c_p(2, T)}{0.7 + 1.3} dT \\ &- \int_{298.16}^{293.16} 0.00023901 c_p(2, T) dT \\ &- (0.7 + 0.3) \int_{298.16}^{293.16} 0.00023901 \frac{0.7c_p(1, T) + 0.3c_p(2, T)}{0.7 + 0.3} dT \end{aligned}$$

Solution is $\{Q = -6.3979\}$ or 6398 cal/mol of acid feed must be removed.

Adiabatic operation:

$$\begin{aligned} 0 &= 0.7(-10.952) - 0.7(-1.8122) \\ &+ (0.7 + 1.3) \int_{298.16}^x 0.00023901 \frac{0.7c_p(1, T) + 1.3c_p(2, T)}{0.7 + 1.3} dT \\ &- \int_{298.16}^{293.16} 0.00023901 c_p(2, T) dT - (0.7 + 0.3) \int_{298.16}^{293.16} 0.00023901 \\ &\quad \frac{0.7c_p(1, T) + 0.3c_p(2, T)}{0.7 + 0.3} dT \end{aligned}$$

Solution is $\{x = -675.22\}$, $\{x = 409.49\}$, or 136.3°C .

3.6 ENERGY BALANCES WITH REACTION-IDEAL SOLUTION

Energy flows in chemically reactive systems are often crucial considerations for the safe and efficient operation of the

$$\begin{aligned} Q + \chi_A \mathcal{N}_A^{(F)} \left[- \sum_{\text{all species}} \vartheta_i H_i(T, P) \right] &= \sum_{\text{all species}} \mathcal{N}_i^{(F)} \left[H_i(T, P) - H_i(T^{(F)}, P^{(F)}) \right] \\ \text{Input by} & \quad \text{Conversion of} & \quad \text{Energy required to raise} \\ \text{conduction} & \quad \text{chemical to thermal} & \quad \text{reactants from feed to} \\ \text{across solid} & \quad \text{energy at outlet} & \quad \text{outlet temperature} \\ \text{surfaces} & \quad \text{conditions} & \end{aligned} \quad (3.106)$$

system. The area-to-volume ratio is an important parameter in these considerations as it is a measure of the ability of the

system to transfer energy as heat relative to its capacity to generate heat. This ratio is large in microchemical systems. For very large systems, the ratio may be so small that lagging is not necessary.

We will first consider flow systems where the feeds, if more than one for each component, are at the same temperature and pressure, $T^{(F)}$ and $P^{(F)}$. The total molar feed rate of each component will then be designated by $\mathcal{N}_i^{(F)}$.

We will make the same assumption about the outlet flows, \mathcal{N}_i , at T and P . If these assumptions regarding the inlet and outlet flows are not valid in any particular application, it will be evident how the calculations should be modified from the discussion below.

3.6.1 Single Reaction-Ideal Solution

If the discussion is limited to single chemical reactions and the key or limiting reactant is labeled A, the mass balances may be written as

$$\mathcal{N}_i = \mathcal{N}_i^{(F)} + \frac{\vartheta_i}{-\vartheta_A} \chi_A \mathcal{N}_A^{(F)} \quad (3.104)$$

where χ_A is the conversion of A. Recall that the stoichiometric coefficient of an inert is zero. Also note that the preceding equation is a combination of Equations (2.73) and (2.74) and constitutes the mass balances for the system. There are $2N_c$ flows and one conversion. Since there are N_c equations, fixing $N_c + 1$ variables will determine the remainder. That is not to say, however, that the result is physically realizable without a microscopic view and/or consideration of the equilibrium limitations. See the discussion following Equation (2.71).

The energy balance as a result appears as

$$\begin{aligned} Q + \sum_{\text{all species at inlets}} \mathcal{N}_i^{(F)} H_i(T^{(F)}, P^{(F)}) \\ = \sum_{\text{all species at outlets}} \left[\mathcal{N}_i^{(F)} + \frac{\vartheta_i}{-\vartheta_A} \chi_A \mathcal{N}_A^{(F)} \right] H_i(T, P) \end{aligned} \quad (3.105)$$

or, after rearrangement, as

Note that it was not necessary to reformulate the energy balance to account for the chemical reaction. The sensible

and reactive heat effects are separated in the energy balance equation by the stoichiometry that appears in the mass balances. However, the evaluation of the enthalpies in the energy balance requires some modification of the procedure followed for unreactive systems. The result, shown in the following section, is that

$$\sum_{\text{all species}} \vartheta_i H_i(T, 1 \text{ bar}) = \underbrace{\Delta H_R^0(T, 1 \text{ bar})}_{\text{standard heat of reaction at } T} \quad (3.107)$$

If a pressure correction is called for, it may be evaluated for each component with,

$$\begin{aligned} \sum_{\text{all species}} \vartheta_i H_i(T, P) &= \sum_{\text{all species}} \vartheta_i H_i(T, 1 \text{ bar}) \\ &+ \sum_{\text{all species}} \vartheta_i \underbrace{\left\{ \int_1^P \left[V_i - T \left(\frac{\partial V_i}{\partial P} \right)_T \right] dP \right\}}_{\text{at constant temperature}} (T) \end{aligned} \quad (3.108)$$

The change in enthalpy with respect to pressure was obtained from Equation (3.53). An adjustment of approximately 5% was required for ammonia synthesis to correct the standard heat of reaction from the value at 400 °C and 1 atm to 400 °C and 200 atm (Kramers and Westerterp, 1963). A pressure correction for the specific heat may be obtained, if necessary, by the methods followed in making the pressure correction for the enthalpy. We will assume that the pressure correction is not needed.

The right-hand side of Equation (3.106) may be evaluated with values of the specific heats. Reported values of the specific heats for liquids and solids do not depend on pressure. For gases, the reported values are at the ideal gas limit. In all cases, the specific heat may be regarded as a function only of temperature:

$$\sum_{\text{all species}} \mathcal{N}_i^{(F)} \left[H_i(T, P) - H_i(T^{(F)}, P^{(F)}) \right] \approx \sum_{\text{all species}} \mathcal{N}_i^{(F)} \int_{T^{(F)}}^T C_{pi}(T) dT \quad (3.109)$$

$$= \mathcal{N}^{(F)} \langle C_P^{(F)} \rangle (T - T^{(F)}) \quad (3.110)$$

where the average specific heat is defined by

$$\langle C_P^{(F)} \rangle = \frac{1}{T - T^{(F)}} \int_{T^{(F)}}^T \sum_{\text{all species}} x_i^{(F)} C_{pi}(T) dT \quad (3.111)$$

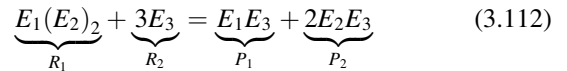
3.6.1.1 Reference States for Reactive Systems—Standard Heat of Reaction In the unreactive case, we found that an arbitrary reference state could be set for each component

where the enthalpy of that component could be set to zero. The energy balance was insensitive to the selection since only changes of enthalpy between thermodynamic states were involved. In the case of chemical reactions, not only changes of state are involved but the presence of chemical reactions with well-defined heat effects must be accounted for. Here, there must be coherence of enthalpies in the reference states with measured heats of reaction. Clearly, arbitrary reference states for the reactants and products will not reproduce all measured heats of reaction. On the other hand, it is not possible to measure the heat effects associated with all reactions. Instead, the following procedure is applied for reactive systems.

The chemical pool of all the elements is shared by all chemical reactions, and represents a convenient dead state or reference state on which to base the enthalpy of chemical compounds formed from the elements. This enthalpy is what a chemical compound brings to all chemical reactions in which it participates. To be more precise, a value of zero is assigned to each atomic species in its most stable form at 25 °C and 1 bar. The base state for hydrogen, for example, is gaseous, while the base state for carbon is solid graphite.

The enthalpy of chemical compounds in their standard states defined as their most stable form at 25 °C and 1 bar can then be determined from measurements of heats of reaction. The chemical reactions most often used are formation reactions and combustion reactions. From these data, a standard heat of reaction can be defined that can be applied to the reactive energy balance in equations and to chemical equilibrium calculations as well (see Section 6.7).

For example, suppose that the stoichiometry of the reaction under consideration is



where the products P_i and reactants R_i are formed from the elements, E_i . The enthalpy of each compound relative to the elements in their standard states can be obtained from heat of formation data. For example, consider the formation reaction for the product P_1 :

$$E_1(298 \text{ K}, 1 \text{ bar}) + E_3(298 \text{ K}, 1 \text{ bar}) = E_1E_3(298 \text{ K}, 1 \text{ bar}) \quad (3.113)$$

The heat effect for this reaction is the heat of formation $\Delta H_{f,E_1E_3}^0$. Consequently,

$$\begin{aligned} H_{E_1E_3}(298 \text{ K}, 1 \text{ bar}) &= \Delta H_{f,E_1E_3}^0 + H_{E_3}(298 \text{ K}, 1 \text{ bar}) \\ &+ H_{E_1}(298 \text{ K}, 1 \text{ bar}) \end{aligned} \quad (3.114)$$

with similar expressions for the other reactants and products. A standard heat of reaction for the original reaction can then

be written as

$$\begin{aligned}\Delta H_R^0 &= H_{E_1 E_3}(298 \text{ K}, 1 \text{ bar}) + 2H_{E_2 E_3}(298 \text{ K}, 1 \text{ bar}) \\ &\quad - 3H_{E_3}(298 \text{ K}, 1 \text{ bar}) - H_{E_1(E_2)_2}(298 \text{ K}, 1 \text{ bar})\end{aligned}\quad (3.115)$$

Substitution of the heat of formation data

$$\begin{aligned}\Delta H_R^0 &= [\Delta H_{f,E_1 E_3}^0 + H_{E_3}(298 \text{ K}, 1 \text{ bar}) + H_{E_1}(298 \text{ K}, 1 \text{ bar})] \\ &\quad + 2[\Delta H_{f,E_2 E_3}^0 + H_{E_2}(298 \text{ K}, 1 \text{ bar}) + H_{E_3}(298 \text{ K}, 1 \text{ bar})] \\ &\quad - 3[H_{E_3}(298 \text{ K}, 1 \text{ bar})] \\ &\quad - [\Delta H_{f,E_1(E_2)_2}^0 + H_{E_1}(298 \text{ K}, 1 \text{ bar}) + 2H_{E_2}(298 \text{ K}, 1 \text{ bar})]\end{aligned}\quad (3.116)$$

or, canceling terms,

$$\begin{aligned}\Delta H_R^0(298 \text{ K}, 1 \text{ bar}) &= \Delta H_{f,E_1 E_3}^0(298 \text{ K}, 1 \text{ bar}) \\ &\quad + 2\Delta H_{f,E_2 E_3}^0(298 \text{ K}, 1 \text{ bar}) - \Delta H_{f,E_1(E_2)_2}^0(298 \text{ K}, 1 \text{ bar})\end{aligned}\quad (3.117)$$

In general,

$$\Delta H_R^0(298 \text{ K}, 1 \text{ bar}) = \sum_{\text{all species}} \vartheta_i \Delta H_{f,i}^0(298 \text{ K}, 1 \text{ bar})\quad (3.118)$$

The same result is obtained when heat of (complete) combustion data is used to generate the enthalpy data, which replaces the heat of formation in the preceding equation.

The standard heat of reaction may be evaluated at another temperature, such as the reactor outlet temperature referred to in Section 3.6.1, with specific heat data:

$$\begin{aligned}\Delta H_R^0(T, 1 \text{ bar}) &= \sum_{\text{all species}} \vartheta_i \Delta H_{f,i}^0(298 \text{ K}, 1 \text{ bar}) \\ &\quad + \sum_{\text{all species}} \vartheta_i \int_{298 \text{ K}}^T C^{pi}(T, 1 \text{ bar}) dT\end{aligned}\quad (3.119)$$

If a phase change occurs between 298 K and T , the heat effect must be added to the right-hand side of Equation (3.105) and the specific heat changed accordingly before proceeding with the integration. The specific heat data used in this calculation is the same as that referred to in the discussion of Equation (3.109).

3.6.1.2 Heat Duty and Adiabatic Operation From an energy consumption point of view, it is desirable to use

the thermal energy generated by an exothermic reaction to supply the energy required to raise the feed temperature to the levels required for acceptable reaction rates in reaction equipment. In such cases, the temperature will increase throughout the converter unless sufficient cooling is provided. The equilibrium limitation will at the same time shift in the direction of the reactants and therefore present a continuously decreasing upper bound on the conversion. The equilibrium limitation is discussed in Chapter 6. Here, we will consider two situations.

First, the calculation of the heat duty required for a given conversion and outlet temperature can be explicitly extracted from the energy balance.

$$\begin{aligned}Q &= \sum_{\text{all species}} \mathcal{N}_i^{(F)} [H_i(T, P) - H_i(T^{(F)}, P^{(F)})] \\ &\quad - \chi_A \mathcal{N}_A^{(F)} [-\Delta H_R^0(T, 1 \text{ bar})]\end{aligned}\quad (3.120)$$

Under these circumstances all quantities on the right-hand side are known. The first term accounts for the heat required to reach the outlet conditions and the second term is the contribution of thermal energy provided by the conversion of chemical to thermal energy. For endothermic reactions, the second term is an additional deficit.

On the other hand, if the heat duty is known, such as in the adiabatic case, the feed and inlet temperatures both appear explicitly in the integrals of specific heat for the enthalpy calculations.

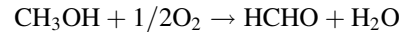
$$\begin{aligned}\sum_{\text{all species}} \mathcal{N}_i^{(F)} [H_i(T, P) - H_i(T^{(F)}, P^{(F)})] \\ = \chi_A \mathcal{N}_A^{(F)} [-\Delta H_R^0(T, 1 \text{ bar})]\end{aligned}\quad (3.121)$$

A trial-and-error procedure is therefore generally required to calculate the adiabatic value of either temperature.

Example 3.6.1.2-1 includes both of these cases.

Example 3.6.1.2-1 Energy Balances on Methanol Oxidation Reactor

Consider the process for the manufacture of formaldehyde presented in Example 2.3.1.1-1. Methanol is oxidized to formaldehyde using air as the source of oxygen.



The reactor is a fixed bed containing an iron–molybdenum oxide catalyst. The reactor feed contains 8 mol% methanol and 10 mol% oxygen in nitrogen. If methanol is completely converted in the reactor and the outlet temperature is to be 425 °C, determine the feed temperature required for adiabatic operation. Also calculate the heat duty per mole of methanol fed for an inlet temperature of 150 °C.

Definitions:

Species	Reference No.
CH ₃ OH	1
O ₂	5
HCHO	3
H ₂ O	4
N ₂	5

Heats of formation—kJ/mol (Yaws, 2003):

$$[H_f] = \begin{bmatrix} -200.6 \\ 0 \\ -108.6 \\ -241.8 \\ 0 \end{bmatrix}$$

Specific heats—J/(mol K) (Sandler, 1999):

$$[a] = \begin{bmatrix} 19.038 & 9.146 \times 10^{-2} & -1.218 \times 10^{-5} & -8.034 \times 10^{-9} \\ 25.460 & 1.519 \times 10^{-2} & -0.715 \times 10^{-5} & 1.311 \times 10^{-9} \\ 22.791 & 4.075 \times 10^{-2} & 0.713 \times 10^{-5} & -8.695 \times 10^{-9} \\ 28.883 & -0.157 \times 10^{-2} & 0.808 \times 10^{-5} & -2.8712 \times 10^{-9} \\ 32.218 & 0.192 \times 10^{-2} & 1.055 \times 10^{-5} & -3.593 \times 10^{-9} \end{bmatrix}$$

$$C_p(k, T) = a_{k,1} + \sum_{j=2}^4 a_{k,j} T^{j-1}$$

Stoichiometric coefficients and feed mole fractions:

$$[\vartheta] = \begin{bmatrix} -1 \\ -0.5 \\ 1 \\ 1 \\ 0 \end{bmatrix} \quad [y] = \begin{bmatrix} 0.08 \\ 0.10 \\ 0 \\ 0 \\ 0.82 \end{bmatrix}$$

Adiabatic energy balance with variable feed temperature and outlet temperature of 425 °C:

$$y_{1,1} \left(- \sum_{i=1}^{i=5} \vartheta_{i,1} (H_f)_{i,1} - 0.001 \sum_{i=1}^{i=5} \vartheta_{i,1} \int_{298}^{425+273} C_p(i, T) dT \right) - 0.001 \sum_{i=1}^{i=5} y_{i,1} \int_{x+273}^{425+273} C_p(i, T) dT = 0, \text{ Solution is}$$

$$\{x = 103.95\}, \{x = 4834.8\}.$$

Feed temperature required = 104 °C.

Energy balance per mole of methanol fed with 150 °C feed temperature and outlet temperature of 425 °C

$$q + y_{1,1} \left(- \sum_{i=1}^{i=5} \vartheta_{i,1} (H_f)_{i,1} - 0.001 \sum_{i=1}^{i=5} \vartheta_{i,1} \int_{298}^{425+273} C_p(i, T) dT \right) - 0.001 \sum_{i=1}^{i=5} y_{i,1} \int_{150+273}^{425+273} C_p(i, T) dT = 0, \text{ Solution is}$$

$\{q = -1.6367\}$ or 1637 J/mol of methanol fed to the reactor.

An approximation to the energy balance for adiabatic operation is often very useful. The energy balance for adiabatic operation is given by Equation (3.115). Using the absolute values of the stoichiometric coefficients, the heat of reaction is seen to be the difference between the enthalpy of the reactants and products, the reactants having the larger value for exothermic reactions and the lower for endothermic reactions:

$$\Delta H_R^0(T, 1 \text{ bar}) = \sum_{\text{products}} |\vartheta_i| \left[\Delta H_{f,i}^0(298 \text{ K}, 1 \text{ bar}) + \int_{298 \text{ K}}^T C_{pi}^0(T, 1 \text{ bar}) dT \right] - \sum_{\text{reactants}} |\vartheta_i| \left[\Delta H_{f,i}^0(298 \text{ K}, 1 \text{ bar}) + \int_{298 \text{ K}}^T C_{pi}^0(T, 1 \text{ bar}) dT \right] \quad (3.122)$$

Both the reactant and the product contributions increase with temperature, which tends to stabilize the net effect making the heat of reaction nearly constant in many cases. For example, the two contributions are plotted in Figure 3.9 for the methanol oxidation reaction considered in Example 3.6.1.2-1.

A constant heat of reaction is then a reasonable approximation. In addition, the average specific heat is not much

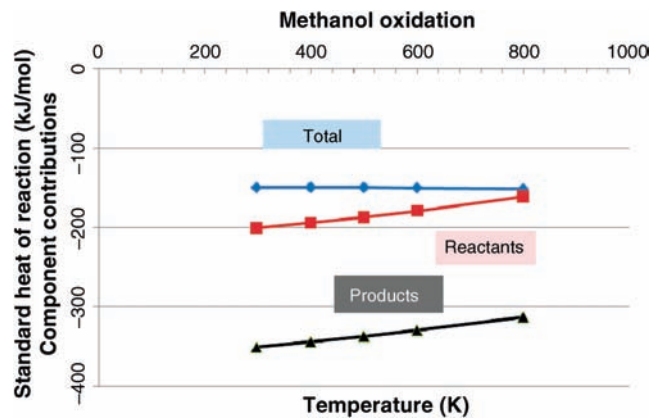


FIGURE 3.9 Heat of reaction and reactant and product contributions for methanol oxidation (see Example 3.6.1.2-1).

different than the value at the feed conditions. For the methanol oxidation in Example 3.6.1.2-1, the average value of the specific heat at the feed conditions is given by

$$\langle C_{Pf}(377, 1 \text{ bar}) \rangle = 0.0352 \text{ kJ}/(\text{mol K}) \quad (3.123)$$

The average value between the feed temperature and the outlet temperature varies from 0.0354 to 0.0376 kJ/(mol K). It should be noted that approximately 80% of the mixture is composed of the inert nitrogen. It is not uncommon to operate an exothermic reactor with an inert diluent for temperature control.

With the preceding approximations, the energy balance is represented by a linear relation between outlet temperature and conversion:

$$T = T^{(F)} + \frac{x_A^{(F)} [-\Delta H_R^0(298 \text{ K}, 1 \text{ bar})]}{\langle C_{Pf}(T_0, 1 \text{ bar}) \rangle} \chi_A \quad (3.124)$$

3.6.2 Single Reactions—Neutralization of Acids

Here we continue the introduction to systems that display a significant heat effect on mixing but at the same time can undergo chemical reaction. However, we will retain the same restrictions to the solution where binary mixing data may be applied. Neutralization of strong acids falls into this category. If, for example, component 1 is an acid and component 2 is the hydroxide, both in aqueous solutions, then the neutralization reaction can be written

$$\sum_i \vartheta_i A_i = 0, \quad i = 1, 2, 3, 4 \quad (3.125)$$

where 3 is the salt and 4 is the aqueous solvent. Referring to Figure 3.8, stream 1 can be considered the acid, stream 2 the base, and stream 3 the salt, all aqueous solutions. We assume that the feeds are stoichiometric so that all three streams are binary mixtures. The energy balance is given by

$$\mathcal{N}^{(1)} H^{(1)} + \mathcal{N}^{(2)} H^{(2)} + Q = \mathcal{N}^{(3)} H^{(3)} \quad (3.126)$$

We assume that the reference states for all components are the same for both the heat of solution data and the standard enthalpy of reaction. If the streams are at temperatures different than the reference temperature, $T^+ = 298.16 \text{ K}$, Equation (3.125) becomes

$$\begin{aligned} & \mathcal{N}^{(1)} \int_{T^+}^{T_1} C_P^{(1)}(T) dT + \mathcal{N}^{(2)} \int_{T^+}^{T_2} C_P^{(2)}(T) dT - \mathcal{N}^{(3)} \int_{T^+}^{T_3} C_P^{(3)}(T) dT \\ & \left\{ \mathcal{N}_1^{(1)} H_1^+ + \mathcal{N}_4^{(1)} H_4^+ + \mathcal{N}_1^{(1)} Q_{\text{soln}}^{(1)} \right\} \\ & + \left\{ \mathcal{N}_2^{(2)} H_2^+ + \mathcal{N}_4^{(2)} H_4^+ + \mathcal{N}_2^{(2)} Q_{\text{soln}}^{(2)} \right\} \\ & - \left\{ \mathcal{N}_3^{(3)} H_3^+ + \mathcal{N}_4^{(3)} H_4^+ + \mathcal{N}_3^{(3)} Q_{\text{soln}}^{(3)} \right\} + Q = 0 \end{aligned} \quad (3.127)$$

The mass balances with complete neutralization and stoichiometric feeds are given by

$$\mathcal{N}_1^{(3)} = \mathcal{N}_2^{(3)} = 0 \quad (3.128)$$

$$\mathcal{N}_3^{(3)} = \frac{\vartheta_3}{\vartheta_2} \mathcal{N}_2^{(2)} \quad (3.129)$$

$$\mathcal{N}_4^{(3)} = \mathcal{N}_4^{(1)} + \mathcal{N}_4^{(2)} + \frac{\vartheta_4}{\vartheta_2} \mathcal{N}_2^{(2)} \quad (3.130)$$

$$\mathcal{N}_2^{(2)} = \frac{\vartheta_2}{\vartheta_1} \mathcal{N}_1^{(1)} \quad (3.131)$$

$$\mathcal{N}_3^{(3)} = \frac{\vartheta_3}{\vartheta_1} \mathcal{N}_1^{(1)} \quad (3.132)$$

Equation (3.126) becomes

$$\begin{aligned} & \mathcal{N}^{(1)} \int_{T^+}^{T_1} C_P^{(1)}(T) dT + \mathcal{N}^{(2)} \int_{T^+}^{T_2} C_P^{(2)}(T) dT - \mathcal{N}^{(3)} \int_{T^+}^{T_3} C_P^{(3)}(T) dT \\ & + \frac{\mathcal{N}_1^{(1)}}{\vartheta_1} \left\{ [H_1^+ + Q_{\text{soln}}^{(1)}] + \vartheta_2 [H_2^+ + Q_{\text{soln}}^{(2)}] - \vartheta_3 [H_3^+ + Q_{\text{soln}}^{(3)}] - \vartheta_4 [H_4^+] \right\} \\ & + Q = 0 \end{aligned} \quad (3.133)$$

Under the circumstances that we have created, the heat of solution must be added to the heats of formation in order to account for the total heat effect produced by the solution process and the chemical reaction.

3.6.3 Multiple Reactions

The energy balance in Equation (3.91) applies in general, including the case of single or multiple reactions. If the inlet and outlet flows are known, the energy balance may be used to determine the value of Q that is required. The calculations are illustrated in the following example for the acrylic acid reactor with the stream flows given in Table 1.10.

Example 3.6.3-1: Heat Duty for Acrylic Acid Reactor R-301

The acrylic acid reactor and attached cooling loop are shown in Figure 3.10.

The reactor inlet and outlet flows, streams 4 and 6, respectively, are given in Table 1.10. Thermal energy is removed from the reactor by the circulating molten salt. The salt is cooled to 200 °C in the heat exchanger E-301 before

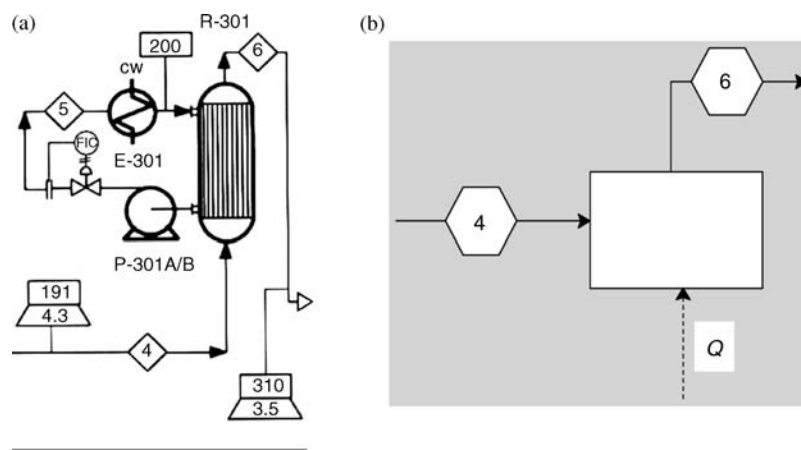


FIGURE 3.10 Acrylic acid reactor and cooling loop. Reprinted with permission of Pearson (a) with block diagram (b).

being returned to the reactor. A schematic that includes all of the material above except the cooling water (the heat transfer surface in E-301 forms part of the boundary between the system and the surroundings) is shown in Figure 3.10b. The value of Q is needed.

Solution: See Appendix C for data.

Definition of numerical references—hydrogen not needed

Species	Index
Propylene	1
Acetic acid	2
Hydrogen	3
Oxygen	4
Nitrogen	5
Water	6
Carbon dioxide	7
Acrylic acid	8

Specific heats: (DIPPR, 2009). Acrylic acid from Yaws, 2003.

4339×10^5	1.52×10^5	1.4250×10^3	0.7860×10^5	623.9	0
0.4020×10^5	1.3765×10^5	1.2620×10^3	0.7003×10^5	569.7	0
0.2762×10^5	0.0956×10^5	2.4660×10^3	0.0376×10^5	567.6	0
0.2910×10^5	0.1004×10^5	2.5265×10^3	0.0936×10^5	1153.8	0
0.2911×10^5	0.0861×10^5	1.7016×10^3	0.001×10^5	909.79	0
0.3336×10^5	0.2679×10^5	2.6105×10^3	0.0890×10^5	1169	0
0.2937×10^5	0.3454×10^5	1.4280×10^3	0.2640×10^5	588	0
7.7550	2.9386×10^{-1}	2.0878×10^{-4}	7.159×10^{-8}	9.0960×10^{-12}	1

Rows correspond to the species index. The first five columns correspond to coefficients in a specific heat function. The last column refers to units as follows:

$s = 0$: C_p in J/(kmol K), $s = 1$: C_p in J/(mol K) adjusted below to kmol basis

$$c_p(i, T) = (1 - s_{i,1}) \left(a_{i,1} + a_{i,2} \left(\frac{a_{i,3}/T}{\sinh(a_{i,3}/T)} \right)^2 + a_{i,4} \left(\frac{a_{i,5}/T}{\cosh(a_{i,5}/T)} \right)^2 + s_{i,1} \left(\sum_{j=1}^8 a_{8,j} T^{j-1} \right) / 1000 \text{ J}/(\text{kmol K}) \right)$$

Inlet (column 1) and outlet (column 2) flows in kmol/h from stream (see Table 1.10):

$$[\mathcal{N}] = \begin{bmatrix} 127.0 & 14.7 \\ 0 & 6.54 \\ 0 & 0 \\ 280.9 & 51.9 \\ 1056.7 & 1056.7 \\ 1017.6 & 1165.9 \\ 0 & 60.5 \\ 0 & 87.79 \end{bmatrix}$$

Heats of formation for gases at 1 atm and 25 °C:

$$[f] = \begin{bmatrix} 1.9710 \\ -43.280 \\ 0 \\ 0 \\ 0 \\ -57.7979 \\ -94.052 \\ -77.3197 \end{bmatrix} \text{ kcal/mol: adjusted to J/kmol below in enthalpy formation}$$

Formation of enthalpy function based on elements at standard conditions:

$$H(i, x) = f_{i,1} \frac{1000 \times 1000}{0.23901} + \int_{298.16}^x C_p(i, T) dT$$

Energy balance:

$$Q = \sum_{i=1}^{i=8} (N_{i,2} H(i, 310 + 273.16) - N_{i,1} H(i, 191 + 273.16))$$

$Q = -8.2007 \times 10^{10}$ J/h or 82,007 MJ/h must be removed from the exchanger.

The result from the process simulator 83,400 MJ/h or 1.96×10 and 7 kcal/h.

The result using Aspen with all pressures set at atmospheric is 1.9963998 kcal/h. The Redlich–Kwong–Soave equation of state was used. If the pressures of the stream are adjusted to the values given in Table 1.10, the result is 1.9958819 kcal/h. The assumptions of an ideal mixture without any pressure dependence are therefore quite good in the present case.

In general, the energy and mass balances are solved simultaneously. The mass balances for the case of multiple reactions were written in terms of the extents (see Section 2.4). The extents may be introduced into the energy balance as follows. By definition,

$$\mathcal{N}_i = \mathcal{N}_i^{(F)} + \sum_{j=1}^{N_r} \vartheta_{ij} \xi_j \quad (3.134)$$

which is Equation (2.77) in terms of the cumulative flows introduced in Section 3.6. Substitution into the energy balance, Equation (3.91) gives

$$\begin{aligned} Q + \sum_{\text{all species at inlets}} \mathcal{N}_i^{(F)} H_i(T^{(F)}, P^{(F)}) \\ = \sum_{\text{all species at outlets}} \left[\mathcal{N}_i^{(F)} + \sum_{j=1}^{N_r} \vartheta_{ij} \xi_j \right] H_i(T, P) \end{aligned} \quad (3.135)$$

$$Q + \sum_{j=1}^{N_r} \xi_j [-\Delta H_{Rj}] = \sum_{\text{all species}} \mathcal{N}_i^{(F)} [H_i(T, P) - H_i(T^{(F)}, P^{(F)})] \quad (3.136)$$

where

$$\Delta H_{Rj} = \sum_{i=1}^{N_c} \vartheta_{ij} H_i(T, P) \quad (3.137)$$

The discussion given earlier for the case of single reaction applies to each of the N_r reactions here.

Example 3.6.3-2: Feed Temperature Required in Methanol Synthesis

Methanol can be synthesized by the following vapor phase reactions [unless noted, all data are taken from Bartholomew and Farrauto (2006)]

1. $\text{H}_2 + \text{CO}_2 = \text{CO} + \text{H}_2\text{O}$ $\Delta H_{R1}^0 = 41,200$ J/mol
2. $\text{CO} + 2\text{H}_2 = \text{CH}_3\text{OH}$ $\Delta H_{R1}^0 = -100,500$ J/mol

The reaction mixture is at equilibrium at the reactor outlet, which means that the mole fractions at the outlet obey the following relationships (T in K, P in atm):

$$K_1(T) = \frac{y_{\text{CO}} y_{\text{H}_2\text{O}}}{y_{\text{H}_2} y_{\text{CO}_2}}$$

$$K_2(T) = \frac{y_{\text{CH}_3\text{OH}}}{y_{\text{CO}} y_{\text{H}_2}^2} \frac{1}{P^2}$$

where

$$\begin{aligned} K_1(T) = 1.4286 \exp \left(13.148 - \frac{5639.5}{T} - 1.077 \ln(T) \right) \\ + 5.44 \times 10^{-4} T - 1.125 \times 10^{-7} T^2 + \frac{49170}{T^2} \end{aligned}$$

$$\begin{aligned} K_2(T) = 1.6233 \times 10^{-4} \exp \left(21.225 + \frac{9143.6}{T} - 7.492 \ln(T) \right) \\ + 4.076 \times 10^{-3} T - 7.161 \times 10^{-8} T^2 \end{aligned}$$

A correction for nonideality has been made using the charts reported in Bartholomew and Farrauto (2006).

If the feed to the reactor consists of 19 mol% CO, 76% H₂, and 5% CO₂, determine the feed temperature required for an outlet temperature of 180 °C under adiabatic operating conditions and a pressure of 150 atm.

Solution:

We must determine the extent of each reaction since each contributes to the total heat effect with different intensity. The mass balances are therefore required. The energy balance is required to establish the desired sensible heat effect given the thermal energy released by the reactions.

Mass balance:

Species	Index
CO	1
H ₂ O	2
H ₂	3
CO ₂	4
CH ₃ OH	5

Take the basis of 100 mol/time for which the outlet molar flows are given in terms of the extents [see Equation (2.77)]:

$$N_1 = 19 + \xi_1 - \xi_2$$

$$N_2 = \xi_1$$

$$N_3 = 76 - \xi_1 - 2\xi_2$$

$$N_4 = 10 - \xi_1$$

$$N_5 = \xi_2$$

$$N_T = 100 - 2\xi_2$$

Chemical equilibrium in lieu of kinetics:

$$P = 150 \text{ atm}$$

$$T = 453 \text{ K}$$

$$y_1(\xi_1, \xi_2) = \frac{19 + \xi_1 - \xi_2}{100 - 2\xi_2}$$

$$y_2(\xi_1, \xi_2) = \frac{\xi_1}{100 - 2\xi_2}$$

$$y_3(\xi_1, \xi_2) = \frac{76 - \xi_1 - 2\xi_2}{100 - 2\xi_2}$$

$$y_4(\xi_1, \xi_2) = \frac{5 - \xi_1}{100 - 2\xi_2}$$

$$y_5(\xi_1, \xi_2) = \frac{\xi_2}{100 - 2\xi_2}$$

Substitution into the equilibrium expressions provides the two independent equations required for determining the extents.

Energy balance:

Assuming no temperature dependence of the heat of reaction and estimating the average specific heat as 29 J/(mol K), the energy balance may be written as quoted in the following summary:

$$K_1(T) = \frac{y_1(\xi_1, \xi_2)y_2(\xi_1, \xi_2)}{y_3(\xi_1, \xi_2)y_4(\xi_1, \xi_2)}$$

$$K_2(T) = \frac{y_5(\xi_1, \xi_2)}{y_1(\xi_1, \xi_2)(y_3(\xi_1, \xi_2))^2} \frac{1}{150 \times 150} \\ -41,200\xi_1 + 100,500\xi_2 = 100(29.5)(T - \theta)$$

The solution is

$$\theta = 367.82, \quad \xi_1 = 0.13079, \quad \xi_2 = 2.5538$$

The inlet temperature is θ , which has the value of 95 °C. The outlet gas composition is given by

$$y_1(0.13079, 2.5538) = 0.17469$$

$$y_2(0.13079, 2.5538) = 1.3783 \times 10^{-3}$$

$$y_3(0.13079, 2.5538) = 0.7457$$

$$y_4(0.13079, 2.5538) = 5.1313 \times 10^{-2}$$

$$y_5(0.13079, 2.5538) = 2.6913 \times 10^{-2}$$

This is the beginning of a multistage operation in which the system is cooled between stages to permit a fresh approach to equilibrium as the conversion accumulates (see Chapter 6).

The energy balance in Equation (3.136) can be viewed as providing the adjustment Q to the difference between the heat generated by the reactions and the heat removed by convection in order to maintain a desired temperature level in the reactor. The temperature appearing in the energy balance is the outlet temperature, which is not necessarily the temperature in the reactor. A limiting case is completely mixed systems where the output temperature is the system temperature. The completely mixed system is an important model, which is taken up in Chapter 5.

3.7 ENTROPY BALANCES

Primary concerns in the design of new processes and the evaluation of existing ones is the process effectiveness and the process efficiency. The notion of process effectiveness has to do with the achievement of a goal relative to the possible outcomes of the process variables. For example, we might say that a chemical reactor that produces a conversion of 80% under conditions where it was designed to achieve 90% conversion is 89% effective. On the other hand, if the reactor achieved 90% conversion, it may have done so with a

huge loss of thermal energy to the environment. In that case, we might say that the reactor is highly effective but inefficient with respect to its utilization of thermal energy.

The utilization of energy is within the purview of the First Law, which differentiates between heat and work, but counts them equal in the balance. A loss of energy as work that is retained by the process as heat is adequate compensation under the First Law to leave the efficiency unchanged. Consequently, if a premium is placed on work over heat, the definition of efficiency must involve the Second Law as well as the First. The Second Law limits the amount of heat that can be converted into work but places no limit on the reverse so that in this sense the work interaction is a stronger indicator of energy efficiency than heat interactions. Moreover, the irreversibilities in the system and thus the inefficiencies in the system are directly reflected in the entropy production, which appears in the entropy balance.

3.7.1 Macroscopic Entropy Balance

A steady-state entropy balance for a chemical processing system can be established by recognizing the entropy flows that accompany the material flows at the inlets and outlets and the exchange of energy as heat with R reservoirs, the zeroth being the environment.

$$\sum_{\text{input streams } (j)} \sum_{\text{all species } (i)} \tilde{S}_i^{(j)} \mathcal{N}_i^{(j)} + \sigma + \sum \frac{Q_R}{T_R} = \sum_{\text{output streams } (j)} \sum_{\text{all species } (i)} \tilde{S}_i^{(j)} \mathcal{N}_i^{(j)} \quad (3.138)$$

or

$$\sum_{\text{input streams } (j)} S^{(j)} \mathcal{N}^{(j)} + \sigma + \sum \frac{Q_R}{T_R} + \frac{Q_0}{T_0} = \sum_{\text{output streams } (j)} S^{(j)} \mathcal{N}^{(j)} \quad (3.139)$$

A slight modification will be necessary in the results to account for those circumstances where the temperature of the heat source (sink) is not constant. The irreversibilities in the exchanges with the reservoirs are charged to the system. The temperature associated with the transfer is at the system boundary where the transfer takes place. All irreversibilities are collected a single term, σ .

The entropy generation term reflects the irreversible nature of the processes taking place in the system. It is, of course, zero for the reversible case. In fact for the reversible process, there are no gradients in the system. Gradients, for example, temperature gradients, are therefore the building blocks for the entropy generation expression. A microscopic analysis shows that the entropy generation is a function of the fluxes and gradients of potentials in the system and has been used to identify the relationship between them.

This entropy generation term above is the integrated consequence of the local entropy generation associated with the microscopic mass, energy, and momentum transport processes.

Partial molar enthalpies and entropies are given by Equations (3.72) and (3.74), respectively, for ideal solutions. Since

$$\tilde{G}_i = \tilde{H}_i - T\tilde{S}_i \quad (3.140)$$

It follows that

$$\tilde{G}_i = G_i + RT \ln x_i \quad (3.141)$$

for ideal solutions.

We can use these results to carry out entropy balances in processes involving ideal solutions.

3.7.2 Thermodynamic Models

By making some stipulations concerning the locations of the generation term in the various subsystems, the entropy balance can become an additional relation between system variables and thereby provide some limiting process conditions (see Example 3.5.1-1). The generation term may be set to zero, thereby assuming all processes in the system to be reversible. It may be divided into representations for each part of the system when there is more than one subsystem and the individual values are set to zero, thereby specifying reversibility in one or more subsystem. In each of these cases the stipulation provides an additional relationship.

Example 3.7.2-1: Thermodynamic Models for Membrane Outlet Temperature

A gas at 16.7 MPa and 40°C, containing the following components in kmol/h: 42.4 H₂, 7.0 CH₄, and 0.5 N₂, is separated into a retentate gas at 16.2 MPa and a permeate gas at 4.56 MPa. The membrane is not permeable to nitrogen, the membrane separation index (SP) for hydrogen relative to methane is 34.13, and the split fraction for hydrogen relative to methane is 0.6038, calculate kmol/h of each component and the total flow of the retentate and the permeate. Estimate the temperature of each outlet stream (see Figure 3.11).

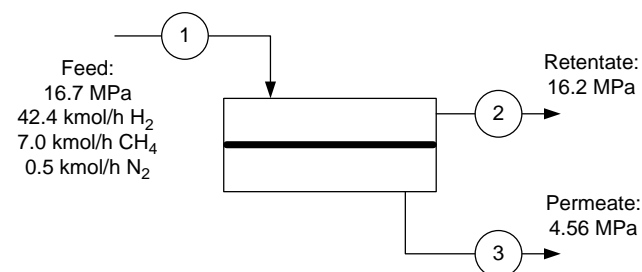


FIGURE 3.11 Membrane separation of gas mixture.

Solution:

Mass balances:

1 = hydrogen, 2 = methane, 3 = nitrogen

$$[N^{(1)}] = \begin{bmatrix} 42.4 \\ 7.0 \\ 0.5 \end{bmatrix}$$

$$N_1^{(2)} + N_1^{(3)} = N_1^{(1)}$$

$$N_2^{(2)} + N_2^{(3)} = N_2^{(1)}$$

$$N_3^{(2)} = N_3^{(1)}$$

$$N_1^{(3)} = 0.6038 N_1^{(1)}$$

$$N_2^{(2)} N_1^{(3)} = 34.13 N_1^{(2)} N_1^{(3)}$$

$$\text{Solution is } [N^{(3)}] = \begin{bmatrix} 25.6011 \\ 0.299205 \\ 0 \end{bmatrix} \quad [N^{(2)}] = \begin{bmatrix} 16.7989 \\ 6.70080 \\ 0.5 \end{bmatrix}$$

First Law:

$$0 = \sum_{i=1}^3 \mathcal{N}_i^{(2)} C_{vi} (T^{(2)} - T^{(1)}) + \sum_{i=1}^3 \mathcal{N}_i^{(3)} C_{vi} (T^{(3)} - T^{(1)})$$

or for approximately equal specific heats

$$\sum_{i=1}^3 \mathcal{N}_i^{(2)} (T^{(2)} - T^{(1)}) + \sum_{i=1}^3 \mathcal{N}_i^{(3)} (T^{(3)} - T^{(1)}) = 0$$

Entropy balance:

$$\gamma + \sum_{i=1}^3 \mathcal{N}_i^{(1)} \tilde{S}_i^{(1)} = \sum_{i=1}^3 \mathcal{N}_i^{(2)} \tilde{S}_i^{(2)} + \sum_{i=1}^3 \mathcal{N}_i^{(3)} \tilde{S}_i^{(3)}$$

$$\gamma = \sum_{i=1}^3 \mathcal{N}_i^{(2)} (\tilde{S}_i^{(2)} - \tilde{S}_i^{(1)}) + \sum_{i=1}^3 \mathcal{N}_i^{(3)} (\tilde{S}_i^{(3)} - \tilde{S}_i^{(1)}) = \gamma_R + \gamma_P$$

$$\gamma_R = \sum_{i=1}^3 \mathcal{N}_i^{(2)} (\tilde{S}_i^{(2)} - \tilde{S}_i^{(1)}), \quad \gamma_P = \sum_{i=1}^3 \mathcal{N}_i^{(3)} (\tilde{S}_i^{(3)} - \tilde{S}_i^{(1)})$$

Partial molar entropies:

$$\tilde{S}_i = S_i - R \ln x_i$$

$$R = 1.987$$

$$x_j^{(1)} = \frac{\mathcal{N}_j^{(1)}}{\sum_{i=1}^3 \mathcal{N}_i^{(1)}}, \quad x_j^{(2)} = \frac{\mathcal{N}_j^{(2)}}{\sum_{i=1}^3 \mathcal{N}_i^{(2)}}, \quad x_j^{(3)} = \frac{\mathcal{N}_j^{(3)}}{\sum_{i=1}^3 \mathcal{N}_i^{(3)}}$$

$$\gamma = 1.4$$

Final expressions for entropy production:

$$\gamma_R = \sum_{i=1}^3 \mathcal{N}_i^{(2)} \left[(\tilde{S}_i^{(2)} - \tilde{S}_i^{(1)}) - R \ln \frac{x_i^{(2)}}{x_i^{(1)}} \right]$$

$$= \sum_{i=1}^3 \mathcal{N}_i^{(2)} \left[\left(C_{pi} \ln \frac{T^{(2)}}{T^{(1)}} + R \ln \frac{P^{(1)}}{P^{(2)}} \right) - R \ln \frac{x_i^{(2)}}{x_i^{(1)}} \right]$$

$$\gamma_R = R \sum_{i=1}^3 \mathcal{N}_i^{(2)} \left(\left(\frac{\gamma}{\gamma-1} \ln \frac{T^{(2)}}{313.6} + \ln \frac{16.7}{16.2} \right) - \ln \frac{x_i^{(2)}}{x_i^{(1)}} \right)$$

$$\gamma_P = \sum_{i=1}^3 \mathcal{N}_i^{(3)} \left[(\tilde{S}_i^{(3)} - \tilde{S}_i^{(1)}) - R \ln \frac{x_i^{(3)}}{x_i^{(1)}} \right]$$

$$= \sum_{i=1}^3 \mathcal{N}_i^{(3)} \left[\left(C_{pi} \ln \frac{T^{(3)}}{T^{(1)}} + R \ln \frac{P^{(1)}}{P^{(3)}} \right) - R \ln \frac{x_i^{(3)}}{x_i^{(1)}} \right]$$

$$\gamma_P = R \sum_{i=1}^3 \mathcal{N}_i^{(3)} \left(\left(\frac{\gamma}{\gamma-1} \ln \frac{T^{(3)}}{313.16} + \ln \frac{16.7}{4.56} \right) - \ln \frac{x_i^{(3)}}{x_i^{(1)}} \right)$$

Case 1: Permeate Reversible

$$\sum_{i=1}^3 \mathcal{N}_i^{(2)} (T^{(2)} - 313.16) + \sum_{i=1}^3 \mathcal{N}_i^{(3)} (T^{(3)} - 313.16) = 0$$

$$\sum_{i=1}^3 \mathcal{N}_i^{(3)} \left(\left(\frac{\gamma}{\gamma-1} \ln \frac{T^{(3)}}{313.16} + \ln \frac{16.7}{4.56} \right) - \ln \frac{x_i^{(3)}}{x_i^{(1)}} \right) = 0$$

$$\text{Solution: } \{T^{(2)} = 409.704, T^{(3)} = 223.7\}$$

Case 2: Retentate Reversible

$$\sum_{i=1}^3 \mathcal{N}_i^{(2)} (T^{(2)} - 313.16) + \sum_{i=1}^3 \mathcal{N}_i^{(3)} (T^{(3)} - 313.16) = 0$$

$$\sum_{i=1}^3 \mathcal{N}_i^{(2)} \left(\left(\frac{\gamma}{\gamma-1} \ln \frac{T^{(2)}}{313.6} + \ln \frac{16.7}{16.2} \right) - \ln \frac{x_i^{(2)}}{x_i^{(1)}} \right) = 0$$

$$\text{Solution: } \{T^{(2)} = 317.326, T^{(3)} = 309.3\}$$

Case 3: Reversible Process

$$\sum_{i=1}^{i=3} \mathcal{N}_i^{(2)} (T^{(2)} - 313.16) + \sum_{i=1}^{i=3} \mathcal{N}_i^{(3)} (T^{(3)} - 313.16) = 0$$

$$\sum_{i=1}^{i=3} \mathcal{N}_i^{(2)} \left(\left(\frac{\gamma}{\gamma-1} \ln \frac{T^{(2)}}{313.6} + \ln \frac{16.7}{16.2} \right) - \ln \frac{x_i^{(2)}}{x_i^{(1)}} \right)$$

$$+ \sum_{i=1}^{i=2} \mathcal{N}_i^{(3)} \left(\left(\frac{\gamma}{\gamma-1} \ln \frac{T^{(3)}}{313.16} + \ln \frac{16.7}{4.56} \right) - \ln \frac{x_i^{(3)}}{x_i^{(1)}} \right) = 0$$

Solution: $\{T^{(2)} = 489.587, T^{(3)} = 149.679\}$

Case 4: Reversible Adiabatic Expansion in Retentate

$$\sum_{i=1}^{i=3} \mathcal{N}_i^{(2)} (T^{(2)} - 313.16) + \sum_{i=1}^{i=3} \mathcal{N}_i^{(3)} (T^{(3)} - 313.16) = 0$$

$$\frac{\gamma}{\gamma-1} \ln \frac{T^{(2)}}{313.6} + \ln \frac{16.7}{16.2} = 0$$

Thermodynamic Model (Case)	Retentate Temperature (K)	Permeate Temperature (K)
Permeate reversible (I)	409.7	223.7
Retentate reversible (II)	317.3	309.3
Reversible process (III)	489.6	149.7
Reversible adiabatic expansion		
Retentate (IV)	310.9	315.3
Permeate (V)	417.9	216.2

Solution: $\{T^{(3)} = 315.265, T^{(2)} = 310.888\}$

Case 5: Reversible Adiabatic Expansion in Permeate

$$\sum_{i=1}^{i=3} \mathcal{N}_i^{(2)} (T^{(2)} - 313.16) + \sum_{i=1}^{i=3} \mathcal{N}_i^{(3)} (T^{(3)} - 313.16) = 0$$

$$\left(\frac{\gamma}{\gamma-1} \ln \frac{T^{(3)}}{313.16} + \ln \frac{16.7}{4.56} \right) = 0$$

Solution: $\{T^{(3)} = 216.120, T^{(2)} = 417.885\}$
Which model do you think gives the best solution?

3.7.3 The Availability and Lost Work

The entropy generation can also be shown to be proportional to the loss of the potential of the system to do useful work.

This can be seen in a reformulation of the entropy balance that includes the First Law. The First Law, given in Equation (3.91), can be adapted to the system under consideration as follows:

$$\sum Q_R + Q_0 + W_t = \sum_{\text{outlets } (j)} \mathcal{W}^{(j)} u^{(j)} - \sum_{\text{inlets } (j)} \mathcal{W}^{(j)} u^{(j)} \quad (3.142)$$

We have neglected the kinetic and potential energies, but they may be readily inserted in the final result, if needed. Also, the work interactions at the system inlets and outlets have been included in the total work term, W_t . Two approaches have been taken regarding the formulation of a useful work term. The first discounts the work against the atmosphere [e.g., Denbigh (1971)] and defines the useful work as

$$W_t = W_s + (P_{\text{in}} - P_0)V_{\text{in}} - (P_{\text{out}} - P_0)V_{\text{out}} + P_0(V_{\text{in}} - V_{\text{out}}) \quad (3.143)$$

The pressure–volume products in Equation (3.143) are to be included for each inlet and outlet stream. In summary,

$$W_t = W_u + P_0(V_{\text{in}} - V_{\text{out}}) \quad (3.144)$$

The First Law in terms of useful work is then

$$\sum Q_R + Q_0 + W_u = \sum_{\text{outlets } (j)} \mathcal{W}^{(j)} (u^{(j)} + P_0 v^{(j)}) - \sum_{\text{inlets } (j)} \mathcal{W}^{(j)} (u^{(j)} + P_0 v^{(j)}) \quad (3.145)$$

The Second Law does not discount the work against the medium (Dodge, 1944):

$$W_t = W'_u + P_{\text{in}} V_{\text{in}} - P_{\text{out}} V_{\text{out}} \quad (3.146)$$

$$W'_u = W_s \quad (3.147)$$

This approach results in

$$\sum Q_R + Q_0 + W'_u = \sum_{\text{outlets } (j)} \mathcal{W}^{(j)} (u^{(j)} + P^{(j)} v^{(j)}) - \sum_{\text{inlets } (j)} \mathcal{W}^{(j)} (u^{(j)} + P^{(j)} v^{(j)}) \quad (3.148)$$

The latter reduces to the first for nonflow systems and is easier to apply. We will retain the second definition and

substitute the resulting value of Q_0 into the entropy balance to give

$$\begin{aligned} \sum (Q_R + T_0 \Delta S_R) + W'_u &= \sum_{\text{outlets } (j)} \mathcal{W}^{(j)} (h^{(j)} - T_0 s^{(j)}) \\ &- \sum_{\text{inlets } (j)} \mathcal{W}^{(j)} (h^{(j)} - T_0 s^{(j)}) + T_0 \sigma \end{aligned} \quad (3.149)$$

The left-hand side of Equation (3.149) includes in the first term the reversible work required to restore the reservoirs at the expense of the environment (and allows a reservoir to be replaced with a nonisothermal heat source or sink). The work term is the shaft work done on the system. The work done on the system at the inlets and outlets is included in the enthalpy functions on the right-hand side. The left-hand side represents the total work required, with the recognition that the restoration of the reservoirs must be charged to the process in any evaluation of the process efficiency.

$$W'_t = \sum (Q_R + T_0 \Delta S_R) + W'_u \quad (3.150)$$

The right-hand side of Equation (3.149) reflects a change in thermodynamic function called the Availability,

$$\mathcal{A} = h - T_0 s \quad (3.151)$$

and a strictly positive term proportional to the total entropy production in the system. In summary,

$$W'_t = \mathcal{W} \Delta \mathcal{A} + T_0 \sigma \quad (3.152)$$

Consequently, if the value of $\Delta \mathcal{A}$ is positive, it represents the minimum amount of useful work required to affect the change. If $\Delta \mathcal{A}$ is negative, it represents the maximum amount of useful work that could be extracted. In this sense, the function \mathcal{A} represents the available useful work in the system. In summary,

$$\begin{aligned} W'_t &\geq \mathcal{W} \Delta \mathcal{A} \quad \Delta \mathcal{A} \geq 0 \\ -\mathcal{W} \Delta \mathcal{A} &\geq -W'_t \quad \Delta \mathcal{A} \leq 0 \end{aligned} \quad (3.153)$$

3.7.4 Process Efficiency

It is often possible to adopt the following definitions of efficiency:

$$\eta = \frac{\mathcal{W} \Delta \mathcal{A}}{W'_t} \quad \Delta \mathcal{A} \geq 0 \quad (3.154)$$

$$\eta = \frac{-W'_t}{-\mathcal{W} \Delta \mathcal{A}} \quad \Delta \mathcal{A} \leq 0 \quad (3.155)$$

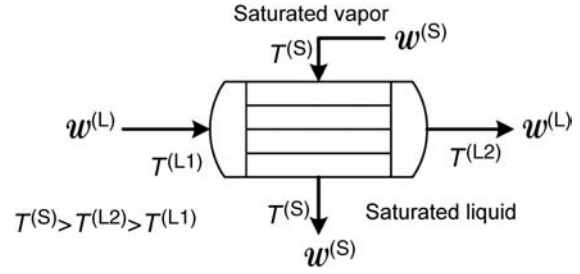


FIGURE 3.12 Shell and tube heat exchanger.

The same change in availability can accompany various levels of the lost work, depending on how the process was carried out. Efficiency calculations would therefore be done with operating data when such data are available. However, the efficiency may be estimated with models of the process in question, the validity of the results depending on the accuracy of the process model. In this section, we will calculate the efficiency of some of the various process steps and end with an evaluation of a complete process.

3.7.4.1 Heat Exchanger with Saturated Heat Source Here we consider the heating of a liquid in the tube side of a shell and tube heat exchanger with a condensing fluid in the shell. Refer to Figure 3.12. We will assume that the specific heat of the cold liquid is constant.

$$\Delta \mathcal{A} = c_{PL} (T^{(L2)} - T^{(L1)}) \quad (3.156)$$

$$\Delta s = c_{PL} \ln \frac{T^{(L2)}}{T^{(L1)}} \quad (3.157)$$

$$\Delta \mathcal{A} = c_{PL} (T^{(L2)} - T^{(L1)}) - T_0 c_{PL} \ln \frac{T^{(L2)}}{T^{(L1)}} \quad (3.158)$$

$$Q_R = \mathcal{W}^{(S)} \Delta h_{\text{vap}} \quad (3.159)$$

$$\Delta S_R = \mathcal{W}^{(S)} \frac{(-\Delta h_{\text{vap}})}{T^{(S)}} \quad (3.160)$$

$$W'_u = 0 \quad (3.161)$$

$$W'_t = \mathcal{W}^{(S)} (\Delta h_{\text{vap}}) \left[1 - \frac{T_0}{T^{(S)}} \right] \quad (3.162)$$

$$\eta = \frac{\mathcal{W}^{(L)} \Delta \mathcal{A}}{W'_t} = \frac{\mathcal{W}^{(L)} c_{PL} [(T^{(L2)} - T^{(L1)}) - T_0 \ln(T^{(L2)}/T^{(L1)})]}{\mathcal{W}^{(S)} (\Delta h_{\text{vap}}) [1 - (T_0/T^{(S)})]} \quad (3.163)$$

$$\eta = \frac{[1 - (T_0/(T^{(L2)} - T^{(L1)})) \ln(T^{(L2)}/T^{(L1)})]}{[1 - (T_0/T^{(S)})]} \quad (3.164)$$

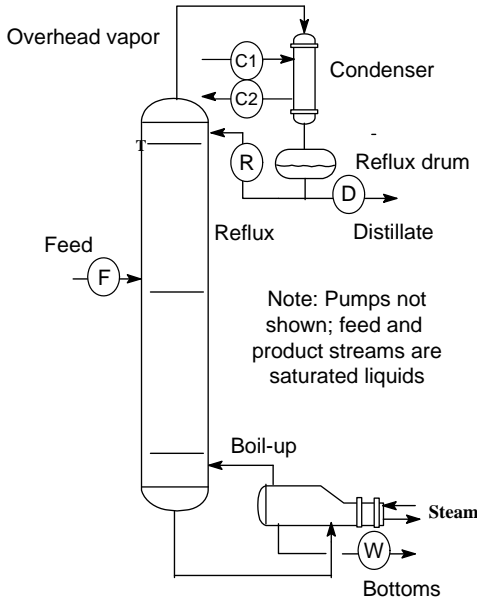


FIGURE 3.13 Distillation tower.

Example 3.7.4.1-1: Heating Water from 25 to 95 °C Using Steam at 0.125 MPa (106 °C)

Substitution into the preceding efficiency relation gives

$$\eta = \frac{1 - ((22 + 273.16)/(95 - 25)) \ln((95 + 273.16)/(25 + 273.16))}{1 - ((22 + 273.16)/(106 + 273.16))} = 0.50003 = 50\%$$

3.7.4.2 Distillation Refer to Figure 3.13 for the stream designations for a standard distillation column configuration. Chapters 1 and 6 provide a more detailed discussion of distillation than is needed here.

A saturated liquid feed is separated into two saturated liquid products: the distillate at a lower temperature and the bottoms or residue at a higher temperature. The distillate contains the lower boiling components and the residue components with the higher boiling points.

There are two reservoirs with which the system interacts aside from the environment. The condenser at the top of the column is a low-temperature heat sink. It employs a variable temperature sensible heat transfer fluid, water in many cases. The high-temperature reservoir is the boiler at the bottom of the tower. The boiler employs a saturated heat transfer fluid, steam in many cases. Assuming that the streams are ideal solutions, the enthalpy and entropy changes for the system may be expressed as

$$\mathcal{N}^{(F)} \Delta H = \sum_i \mathcal{N}_i^{(D)} (\tilde{H}_i^{(D)} - \tilde{H}_i^{(F)}) + \sum_i \mathcal{N}_i^{(W)} (\tilde{H}_i^{(W)} - \tilde{H}_i^{(F)}) \quad (3.165)$$

$$\tilde{H}_i = H_i \quad (3.166)$$

$$\mathcal{N}^{(F)} \Delta H = \mathcal{N}^{(D)} C_p^{(D)} (T^{(D)} - T^{(F)}) + \mathcal{N}_i^{(W)} C_p^{(W)} (T^{(W)} - T^{(F)}) \quad (3.167)$$

$$\mathcal{N}^{(F)} \Delta S = \sum_i \mathcal{N}_i^{(D)} (\tilde{S}_i^{(D)} - \tilde{S}_i^{(F)}) + \sum_i \mathcal{N}_i^{(W)} (\tilde{S}_i^{(W)} - \tilde{S}_i^{(F)}) \quad (3.168)$$

$$\tilde{S}_i = S_i - R \ln x_i \quad (3.169)$$

$$\begin{aligned} \mathcal{N}^{(F)} \Delta S &= \sum_i \mathcal{N}_i^{(D)} (S_i^{(D)} - S_i^{(F)}) + \sum_i \mathcal{N}_i^{(W)} (S_i^{(W)} - S_i^{(F)}) \\ &- R \sum_i \mathcal{N}_i^{(D)} (\ln x_i^{(D)} - \ln x_i^{(F)}) - R \sum_i \mathcal{N}_i^{(W)} (\ln x_i^{(W)} - \ln x_i^{(F)}) \end{aligned} \quad (3.170)$$

The pure component reference state has been used as well as an average specific heat. Pressure effects are not being considered. The entropy changes can be completed as

$$\begin{aligned} \mathcal{N}^{(F)} \Delta S &= \mathcal{N}^{(D)} C_p^{(D)} \ln \frac{T^{(D)}}{T^{(F)}} + \mathcal{N}^{(W)} C_p^{(W)} \ln \frac{T^{(W)}}{T^{(F)}} \\ &- R \mathcal{N}^{(D)} \sum_i x_i^{(D)} \ln \frac{x_i^{(D)}}{x_i^{(F)}} - R \mathcal{N}^{(W)} \sum_i x_i^{(W)} \ln \frac{x_i^{(W)}}{x_i^{(F)}} \end{aligned} \quad (3.171)$$

$$\mathcal{N}^{(F)} \Delta S = \ln \frac{(T^{(D)}/T^{(F)})^{\mathcal{N}^{(D)} C_p^{(D)}} (T^{(W)}/T^{(F)})^{\mathcal{N}^{(W)} C_p^{(W)}}}{\left[\prod_i (x_i^{(D)}/x_i^{(F)})^{x_i^{(D)}} \right]^{R \mathcal{N}^{(D)}} \left[\prod_i (x_i^{(W)}/x_i^{(F)})^{x_i^{(W)}} \right]^{R \mathcal{N}^{(W)}}} \quad (3.172)$$

The change in Availability may be calculated with the entropy and enthalpy changes.

$$\begin{aligned} \Delta \mathcal{B} &= \mathcal{N}^{(D)} C_p^{(D)} (T^{(D)} - T^{(F)}) + \mathcal{N}_i^{(W)} C_p^{(W)} (T^{(W)} - T^{(F)}) \\ &- T_0 \ln \frac{(T^{(D)}/T^{(F)})^{\mathcal{N}^{(D)} C_p^{(D)}} (T^{(W)}/T^{(F)})^{\mathcal{N}^{(W)} C_p^{(W)}}}{\left[\prod_i (x_i^{(D)}/x_i^{(F)})^{x_i^{(D)}} \right]^{R \mathcal{N}^{(D)}} \left[\prod_i (x_i^{(W)}/x_i^{(F)})^{x_i^{(W)}} \right]^{R \mathcal{N}^{(W)}}} \end{aligned} \quad (3.173)$$

The work term consists of the restoration of the high-temperature reservoir and the extraction of work from the low-temperature reservoir. Mechanical pumping is being neglected.

$$W'_t = \left[Q_R - T_0 \frac{Q_R}{T_R} \right] + \left[Q_C + T_0 c_{PC} W_C \ln \frac{T_{C2}}{T_{C1}} \right] \quad (3.174)$$

For nearly pure products in a binary distillation,

$$\begin{aligned} Q_R &= \beta \mathcal{N}^{(W)} (-\Delta H_{\text{vap}W}) = (RR + 1) \mathcal{N}^{(D)} (-\Delta H_{\text{vap}W}) \\ Q_C &= -(-\Delta H_{\text{vap}D})(RR + 1) \mathcal{N}^{(D)} = -W_C c_{PC} (T^{(C2)} - T^{(C1)}) \end{aligned} \quad (3.175)$$

$$\begin{aligned} W'_t &= (RR + 1) \mathcal{N}^{(D)} \left\{ (-\Delta H_{\text{vap}W}) \left[1 - \frac{T_0}{T_R} \right] \right. \\ &\quad \left. + (-\Delta H_{\text{vap}D}) \left[1 - \frac{T_0}{T^{(C2)} - T^{(C1)}} \ln \frac{T^{(C2)}}{T^{(C1)}} \right] \right\} \end{aligned} \quad (3.176)$$

$$\mathcal{N}^{(F)} \Delta S = \ln \left(\frac{\left(\frac{(328.1+460)}{(328.4+460)} \right)^{90.8752(5.76)} \left(\frac{(607.85+460)}{(328.4+460)} \right)^{0.30001(78.58)}}{\left(\frac{(0.00392)}{(0.00391)} \right)^{0.00392} \left(\frac{(0.9958916)}{(0.9926152)} \right)^{0.9958916} \left(\frac{(0.0000584)}{(0.00335)} \right)^{0.0000584} \left(\frac{(1.987 \times 90.8752)}{(0.0000003)} \right)^{0.0000003} \left(\frac{(0.000183)}{(0.9926152)} \right)^{0.000183} \left(\frac{(0.000000173)}{(0.000129)} \right)^{0.000000173} \left(\frac{(0.9998163)}{(0.00335)} \right)^{0.9998163} \left(\frac{(1.987 \times 0.30001)}{(0.00335)} \right)^{1.987 \times 0.30001}} \right)$$

Example 3.7.4.2-1: Column Efficiency Evaluation for Acylation Reactor Effluent in Ibuprofen Manufacture

The following distillation is being considered for the separation of the acylation product, isobutylacetophenone, in the first of a three-step process for the manufacture of ibuprofen:

	Feed	Bottoms	Distillate
Mole flow (lb mol/h)			
Acetic acid	0.3563185	9.01E-09	0.3563185
Acetic anhydride	90.5019	5.50E-05	90.50185
Isobutylbenzene	0.0117332	5.19E-08	0.0117332
Isobutylacetophenone	0.3052585	0.2999548	5.30E-03
Mole fraction			
Acetic acid	3.91E-03	3.00E-08	3.92E-03
Acetic anhydride	0.9926152	1.83E-04	0.9958916
Isobutylbenzene	1.29E-04	1.73E-07	1.29E-04
Isobutylacetophenone	3.35E-03	0.9998163	5.84E-05
Temperature (°F)	328.4	607.8	328.2
$Q_R = 4471500$ Btu/h		$Q_C = 4464700$ Btu/h	
$T_R = 621.2$ °F		$T_{C1} = 75$ °F,	
		$T_{C2} = 120$ °F	
		$W_C = 99215.6$ lb/h	

Evaluate the efficiency of the separation.

Estimate $C_p^{(D)}$ is nearly that for acetic anhydride at 328 °F = 55.76 Btu/(lb mol °F) from *Yaws' Handbook* (2003).

$$\mathcal{N}^{(D)} = 90.8752 \text{ lb mol/h}$$

$$T^{(D)} = 328.1 \text{ °F}$$

Estimate $C_p^{(W)}$ as that for isobutylbenzene = 78.58 Btu/(lb mol °F) from *Yaws' Handbook*

$$\mathcal{N}^{(W)} = 0.30001 \text{ lb mol/h}$$

$$T^{(W)} = 607.85 \text{ °F}$$

$$\begin{aligned} \mathcal{N}^{(F)} \Delta H &= 90.8752 \times 55.76(328.1 - 328.4) + 0.30001 \\ &\times 78.58(607.85 - 328.4) = 5067.8 \text{ Btu/h} \end{aligned}$$

$$\mathcal{N}^{(F)} \Delta S = 3.0061 \text{ Btu/(h °R)}$$

$$T_0 = 300 \text{ K} = 540 \text{ °R}$$

$$\mathcal{N}^{(F)} \Delta B = 5067.8 - 540(3.0061) = 3444.5 \text{ Btu/h}$$

$$\begin{aligned} Q_R - T_0 \frac{Q_R}{T_R} &= 4.4715 \times 10^6 \left(1 - \frac{540}{621.2 + 460} \right) \\ &= 2.2382 \times 10^6 \text{ Btu/h} \end{aligned}$$

$$\begin{aligned} Q_C + T_0 c_{PC} W_C \ln \frac{T_{C2}}{T_{C1}} \\ &= -4,464,700 + 540(99,216)(1.00) \ln \frac{120 + 460}{75 + 460} \\ &= -1.3780 \times 10^5 \text{ Btu/h} \end{aligned}$$

$$W'_t = 2.2382 \times 10^6 - 1.3780 \times 10^5 = 2.1004 \times 10^6 \text{ Btu/h}$$

$$\eta = \frac{3444.5}{2.1004 \times 10^6} 100 = 0.16399\%$$

The efficiency of this distillation is seen to extraordinarily low. To obtain a very small quantity of the desired component, 0.3 lb mol/h, it is necessary to vaporize approximately 91 lb mol/h. In addition, the reboiler is operated at a high temperature. It is necessary to consider other means of product separation, such as liquid extraction or adsorption.

PROBLEMS

3.1. An example of a thermodynamic diagram is shown in Figure 3.14. Thermodynamic diagrams are normally constructed for pure substances when a repeated need for the

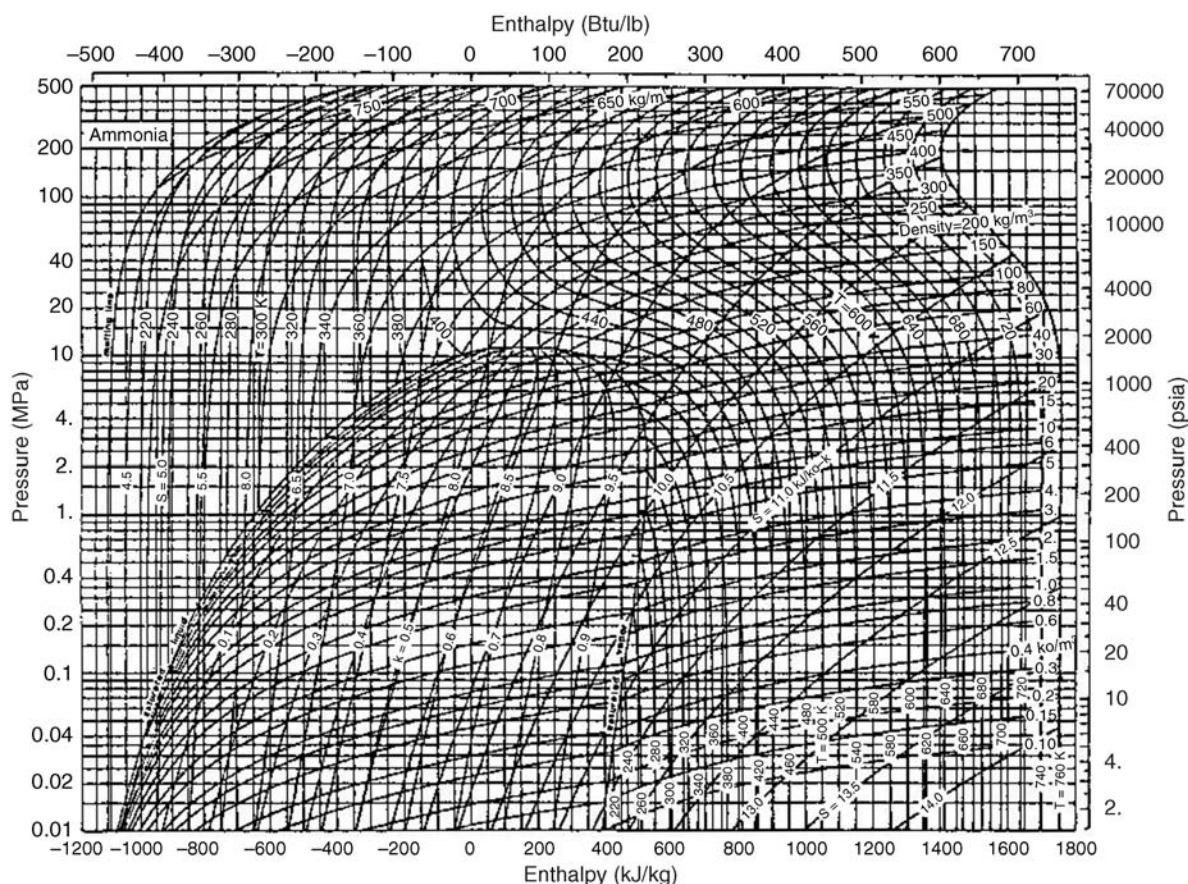


FIGURE 3.14 Pressure-enthalpy diagram for NH₃ (Green and Maloney, 1997). Reprinted with permission of McGraw Hill.

values of a thermodynamic function occurs, for example, or for clarity in representing a thermodynamic process. Common examples are the PH, TS, and HS diagrams. This problem is concerned with the construction of an isotherm on the PH chart (see Figure 3.14).

Some observations are as follows:

- Note the saturated liquid and saturated vapor lines (labeled on the graph). They intersect at the critical point and enclose a two-phase region.
- Saturation refers to phase equilibrium, in this case, between liquid and vapor. Consequently, each point on the saturated liquid line corresponds to a point on the saturated vapor line at the same temperature (thermal equilibrium), therefore, on the same isotherm and pressure (mechanical equilibrium). The pressure is the vapor pressure. The difference in enthalpy is the latent heat of vaporization.

Choose a reference state on the saturated liquid curve and use the values at that point for your reference conditions.

Construct the isotherm that passes through your reference state. Use the RKS equation of state for the gas phase and Equation (2.29) for the liquid phase. Compare your results with those on the graph.

3.2. Throttling is a process operation by which the pressure of a flowing fluid is reduced without a significant change in the kinetic or potential energy. It is realized by placing a restriction in the conduit such as a partially open valve. No shaft work is done and the process takes place so rapidly that there is no significant heat transferred to the surroundings.

- Apply the energy balance to this process assuming that no phase change takes place. Suppose that the process stream is a pure gas that obeys the volume explicit form of the virial equation:

$$Z = \frac{PV}{RT} = 1 + \frac{B(T)}{RT}P$$

where B is given in Table 2.1.

b. Show that the enthalpy departure is given by

$$H'(T, P) = PT \left[\frac{B}{T} - \frac{dB}{dT} \right]$$

Substituting the departures into the energy balance producing a single, nonlinear algebraic equation for the outlet temperature, given the inlet conditions and the outlet pressure.

c. Solve the energy balance for the outlet temperature that appears in the ideal gas term:

$$T_2 = T_1 + \frac{H'(T_2, P_2) + H'(T_1, P_1)}{\langle C_p^0(T_1, T_2) \rangle}$$

This may be solved iteratively for the outlet temperature

$$T_{2,n} = T_1 + \frac{H'(T_{2,n-1}, P_2) + H'(T_1, P_1)}{\langle C_p^0(T_1, T_{2,n-1}) \rangle}$$

$$T_{2,0} = T_1 + \frac{H'(T_1, P_1)}{C_p^0(T_1)}$$

provided that the temperature change is not too large and the outlet is nearly ideal.

Propane at 20 bar and 400 K is throttled at steady state to bar. Estimate the final temperature with the volume explicit virial equation truncated after one added term.

3.3. The throttling process can produce a decrease or an increase in temperature depending on the sign of the Joule–Thompson coefficient defined by

$$\alpha_J = \left(\frac{\partial T}{\partial P} \right)_H$$

a. Show that

$$\alpha_J = \frac{T(\partial V / \partial T)_P - V}{C_p^0 - \int_0^P (\partial^2 V / \partial T^2) dP}$$

where the second term in the denominator is the departure for the specific heat (Tester and Modell, 1997). The numerator may be obtained by first applying Equation (3.9) to $H(T, P)$. The derivative that appears there can be obtained by applying Equation (3.9) to Equation (3.6). The entropy derivative that results can be expressed in terms of the independent variables applying Equation (3.9) to Equation (3.7).

b. Determine the Joule–Thompson coefficient for propane at the conditions specified in Problem 3.2b.

MACROSCOPIC MOMENTUM AND MECHANICAL ENERGY BALANCES

The macroscopic momentum and mechanical energy balances complete the basic equations that are available for analyzing the states of streams at the entrances and exits of process equipment. The macroscopic momentum balance provides the means to evaluate forces on the equipment and the macroscopic mechanical energy balance provides the means to evaluate pressure at the entrances and exits.

4.1 MOMENTUM BALANCE

We are accustomed to applying Newton's law to rigid bodies where the sum of the forces acting on the body is the time rate of change of its momentum. The forces in Newton's law are interpreted as momentum flows or stresses as momentum fluxes to provide the viewpoint of a conservation principle. We are now concerned with applying this conservation principle to a flowing fluid in a fixed volume where convective momentum flows must be accounted for and the fluid elements may deform during the momentum transfer process. Moreover, the containing surface may move as in cases where mechanical work is transferred between the system and surroundings.

Consider a fluid contained between two coaxial cylinders as illustrated Figure 4.1.

The ends are closed so that no material may be introduced or withdrawn from the fluid in the volume element under consideration. The axis of the cylinders is aligned with gravity so that a pressure or normal force distribution is established throughout the fluid to resist motion in the axial

direction; that is, the ends of the cylinder must support the fluid. Consequently, a normal force is exerted on the fluid over the entire containing surface. If the outer cylinder is set in motion, the adjacent fluid layer begins to move with exactly the same velocity. Except for some rare circumstances, this nonslip condition will apply at solid–fluid interfaces. There is then a transfer of momentum, θ (the direction tangent to the cylindrical surfaces) momentum, in the radial direction. The next fluid layer also begins to move because of frictional interactions due to fluid viscosity. This radial flux of momentum continues throughout the radial direction and is ultimately transmitted to the wall of the inner cylinder. Unless supported, the inner cylinder will begin to move in the θ direction because of the influx of this momentum. In addition, the radial movement of the fluid will, through the viscous effect, actually persist to the ends of the cylinder and will transmit θ momentum in the axial direction to these surfaces as well. As a result of the rotation of the outer cylinder, momentum flows appear at all of the containing surfaces.

The momentum transfer process is more effective the more viscous the fluid. If you stir honey in a cup, the cup will spin. A cup of coffee will not. Viscosity refers to the proportionality between momentum flux and the associated velocity gradient. If the annular gap between the coaxial cylinders in Figure 4.1 is very narrow, we can neglect the curvature and call the radial direction x and the circumferential direction y in a rectangular coordinate system. The flux of y momentum in the x direction is proportional to the velocity gradient for many fluids called

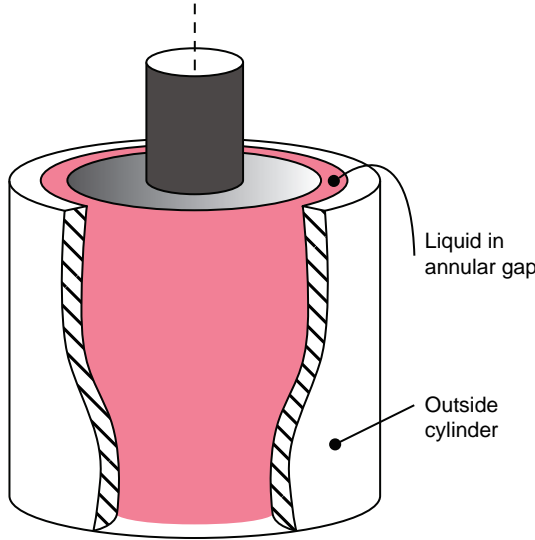


FIGURE 4.1 Fluid contained between coaxial cylinders.

Newtonian fluids.

$$\tau_{xy} = -\eta \frac{dv_y}{dx} \quad (4.1)$$

The viscosity is η . This viscous flux of momentum is analogous to the diffusional flow in mass transfer and the conductive flux in energy transfer.

The convective flux of y momentum in the present case is $\rho v_y v_y$, the product of the momentum concentration and the carrying velocity. If we denote the gap distance by d , a measure of the relative importance of the convective transport of momentum, the viscous transport process is given by the dimensionless Reynolds number:

$$N_{\text{Re}} = \frac{\rho v_y v_y}{\eta((v_y - 0)/d)} = \frac{\rho v d}{\eta} \quad (4.2)$$

The Reynolds number is used in the same way in geometrically similar circumstances. In these applications, v is a characteristic velocity and d is a characteristic length. In pipe flow for example, d is the pipe diameter and v is the average axial velocity. Dimensionless numbers are effectively used in many circumstances to consolidate the roles of multiple parameters. They appear naturally in the microscopic analyses of Part II and can be formulated on the basis of a dimensional analysis (Zlokarnik, 1991).

In contrast to the mass balance, the surfaces that define a macroscopic volume element are all active in the momentum transfer process and involve the viscous flux of momentum and the normal pressure forces. Whereas chemical reactions pay an important role in the conservation of mass principle, they have no direct effect on the momentum transfer process since mass is conserved in a chemical reaction. However,

body forces such as gravity represent sources in the momentum balance but do not affect the mass balance.

In systems with inlet and outlet flows, the transport of mass is accompanied by a transport of momentum. Consider an inlet with cross-sectional area $S^{(1)}$ and outwardly directed unit normal $\mathbf{n}^{(1)}$. We suppose that the inlet flow is everywhere normal to $S^{(1)}$ and that the normal direction does not vary over the inlet. The concentration of momentum everywhere on the inlet surface is therefore $\rho^{(1)}\mathbf{v}^{(1)}$, where

$$\rho^{(1)}\mathbf{v}^{(1)} = -\rho^{(1)}v^{(1)}\mathbf{n}^{(1)} \quad (4.3)$$

If the concentration is constant but the magnitude of the velocity varies over the surface,

$$\begin{aligned} \text{Inlet momentum flow rate} &= \int_{A^{(1)}} [-\rho v \mathbf{n}] v dA \\ &= -\rho^{(1)} \left[\frac{1}{A^{(1)}} \int_{A_1} v^2 dA \right] \mathbf{n}^{(1)} A^{(1)} = \rho^{(1)} \langle v^{(1)^2} \rangle \mathbf{A}^{(1)} \end{aligned} \quad (4.4)$$

The vector $\mathbf{S}^{(1)}$ has the magnitude of the surface area and the direction of the flow. Similarly at an outlet surface, $\mathbf{A}^{(2)}$,

$$\text{Outlet momentum flow rate} = \rho^{(2)} \langle v^{(2)^2} \rangle \mathbf{A}^{(2)} \quad (4.5)$$

A pressure acts normal to the surface at the inlet and outlet, adding momentum to the system at the inlet,

$$-P^{(1)}\mathbf{n}^{(1)}A^{(1)} = P^{(1)}\mathbf{A}^{(1)} \quad (4.6)$$

and removing it at the outlet,

$$-P^{(2)}\mathbf{n}^{(2)}S^{(2)} = -P^{(2)}\mathbf{A}^{(2)} \quad (4.7)$$

The net result at steady state is

$$0 = \rho^{(1)} \langle v_1^2 \rangle \mathbf{A}^{(1)} - \rho^{(2)} \langle v_2^2 \rangle \mathbf{A}^{(2)} + P^{(1)}\mathbf{A}^{(1)} - P^{(2)}\mathbf{A}^{(2)} + mg - \mathbf{F} \quad (4.8)$$

where the gravitational body force per unit mass, g , and the force, \mathbf{F} , of the fluid on the system surface other than at the inlets and outlets have been added. Note that \mathbf{F} is a momentum flow out of the fluid and g is a momentum flow into the fluid. As noted above, a flow of momentum into a body is a force on that body. The momentum balance clearly provides the means to calculate the force exerted by the fluid on the equipment. On the other hand, if a reliable estimate can be made of the force, the momentum balance provides a relationship between velocity and pressure. Examples of both applications will be presented in the following sections.

Example 4.1-1: Force on a U-Bend

A liquid is flowing with a uniform velocity through a pipe segment consisting of a U-bend. Refer to Figure 4.2. The inlet flow is in the direction of gravity and there is no

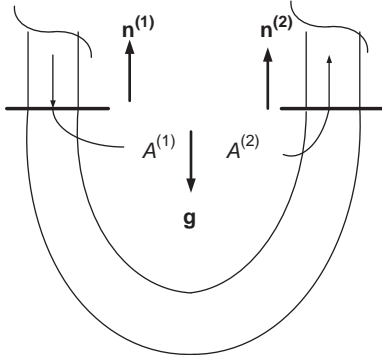


FIGURE 4.2 Flow of a liquid through a U-bend.

change in the pipe diameter across the bend. Calculate the vertical force on the U-bend.

The mass balance gives:

$$\rho^{(1)} v^{(1)} A^{(1)} = \rho^{(2)} v^{(2)} A^{(2)} = \rho v A$$

Set the x direction equal to the direction of gravity and write the x component of Equation (4.6).

$$F_x = \rho v^2 A(+1) - \rho v^2 A(-1) + P^{(1)} A(+1) - P^{(2)} A(-1) + \rho V_{\text{bend}} g$$

Note that the direction of the surface vector is in the positive x direction at the inlet and in the negative x direction at the outlet, the direction of flow in both cases. Collecting terms

$$F_x = 2\rho v^2 S + [P^{(1)} + P^{(2)}] S + \rho V_{\text{bend}} g$$

where V_{bend} is the volume of the U-bend.

4.2 MECHANICAL ENERGY BALANCE

The macroscopic energy balance requires the simultaneous consideration of the heat and work effects or the thermal and mechanical aspects of the energy transfer process. It is often convenient when evaluating work requirements to separate the two. The mechanical component can be isolated as follows.

The macroscopic energy balance written per unit mass of throughput and accounting for potential and kinetic energy contributions follows from Equation (3.91) as

$$\Delta \left(h + \frac{1}{2} v^2 + g\mathcal{L} \right) = Q_m - W_{\text{sm}} \quad (4.9)$$

One inlet and one outlet have been accounted for. No other open surface is represented. If this equation is applied to a

differential element in a single-phase system, there results

$$d \left(h + \frac{1}{2} v^2 + g\mathcal{L} \right) = dQ_m - dW_{\text{sm}} \quad (4.10)$$

We arrive at this differential element by progressively moving the inlet and outlet into the system at each juncture capturing all of the fluid elements that have just entered the system and discarding a portion of the system boundary. We are consequently following the lines of flow. We consider the system properties to be averages over each cross section. Allowing for an irreversible transfer of the thermal energy, dQ_m , and the consequent production of entropy results in

$$d \left(h + \frac{1}{2} v^2 + g\mathcal{L} \right) = T ds - T d\sigma - dW_{\text{sm}} \quad (4.11)$$

where T is the local system temperature. Rearranging Equation (4.11) provides

$$du + d(P\hat{V}) + d \left(\frac{1}{2} v^2 + g\mathcal{L} \right) = T ds - T d\sigma - dW_{\text{sm}} \quad (4.12)$$

$$\hat{V} dP + d \left(\frac{1}{2} v^2 + g\mathcal{L} \right) + T d\sigma + dW_{\text{sm}} = 0 \quad (4.13)$$

where the local system temperature has been used with the average local values of the thermodynamic state functions. Integrating this result from the conditions at the inlet to those at the outlet gives

$$\Delta \left(\frac{1}{2} \langle v \rangle^2 + g\mathcal{L} \right) + \int_{P^{(10)}}^{P^{(2)}} \frac{dP}{\rho} + W_{\text{sm}} + E_{\text{vm}} = 0 \quad (4.14)$$

where E_v is a lost work due to the irreversible transfer of thermal energy. A microscopic analysis is given in Chapters 13 and 15 where the lost work will be more clearly seen as the degradation of mechanical energy into heat and where the relation of both the work and viscous dissipation terms to the local flows will be expressed. The result is particularly applicable to turbulent flow where cross-sectional values can be nearly constant. The correction required for laminar flow is discussed in Chapter 15.

The integral in Equation (4.14) generally depends on the path and an average value is used.

The fluid may be gas or liquid, the essential difference being the influence of pressure on the density. For the flow of gases in pipes, the equation must be written in differential form and an equation of state introduced for the gas. This requires a microscopic view of the system and is discussed in Chapter 13.

4.3 APPLICATIONS TO INCOMPRESSIBLE FLOW SYSTEMS

One of the most important applications of the mechanical energy balance is to flow systems that supply the interconnections between process equipment or plant and entails the specification of pumps, compressors, fans, flow meters, valves, pipe sizes, and so forth. In all cases, some mix of the initial and final conditions is imposed.

We will consider the turbulent flow of liquids in piping systems containing valves and fittings and the sizing of pumps. The calculations for piping systems will apply also to gases if the density variations are on the order of 10–15%. In these applications, the mechanical energy balance is divided into intervals containing straight lengths of piping, flow obstacles, and pumps:

$$\Delta\left(\frac{1}{2}\langle v \rangle^2 + g\mathcal{L}\right) + \frac{\Delta P}{\rho} + \sum_{\text{pumps}} W_{\text{sm}} + \sum_{\text{straight lengths}} E_{\text{vm}} + \sum_{\text{flow obstacles}} E_{\text{vm}} = 0 \quad (4.15)$$

4.3.1 Flow of Liquids in Piping Systems

In these applications, the means for evaluating the loss of mechanical energy must be available if this loss is important. Evaluation of the loss term can be accomplished first by application of the momentum balance, which provides a relationship between pressure and velocity if an experimental result or theoretical estimate is available for \mathbf{F} . Substitution of this relationship between pressure and velocity into the mechanical energy balance then provides a relation of \dot{E} to velocity. This relationship is expressed as

$$E_{\text{vm}} = e_v \frac{1}{2} \langle v \rangle^2 \quad (4.16)$$

where e_v is called the “friction loss factor.” This form can be rationalized at this juncture from the fact that E_v is measured by the portion of the average momentum flux that is lost to the production of useful work.

4.3.1.1 Flow in Pipes—The Friction Loss Factor Some useful rules of thumb pertaining to piping systems are given by Couper et al. (2005):

- Line velocities and pressure drops (line diameter = D in inches).
Liquid pump discharge velocities are approximately $(5 + D/3)$ ft/s.
Pressure drops are approximately 2.0 psi/100 ft.

Liquid pump suction velocities are about $(1.3 + D/6)$ ft/s with pressure drops of approximately 0.4 psi/100 ft.

For steam or gas, typical values are 20 D ft/s and 0.5 psi/100 ft.

- Control valves require at least 10 psi drop for good control.
Globe valves are used for gases, for control, and whenever tight shutoff is required.
Gate valves are for most other services.
- Screwed fittings are used only on sizes 1.5 in. and smaller. Flanges or welding are used otherwise.
Flanges and fittings are rated for 150, 300, 600, 900, 1500, or 2500 psig.
- Pipe schedule number = $1000P/S$, approximately, where P is the internal pressure psig and S is the allowable working stress (about 10,000 psi for A120 carbon steel at 500 °F).

Schedule 40 is most common (see Table 4.1).

The diameter of pipelines and the velocity of the fluid may be related in an optimal way on the basis of cost. For a given mass flow rate, the velocity decreases with increasing pipe diameter and the cost of pumping or compression correspondingly decreases. On the other hand, the cost of the piping increases. This opposing interplay results in an optimal diameter. Extensive results are given by Peters et al. (2003). For example, if the following stipulations are made:

1. Efficiency of pumps and motors = 0.50.
2. Yearly hours of operation = 8760 h.
3. Frictional loss due to fittings and bends expressed as equivalent frictional loss in straight round pipe = 0.35.
4. Electric energy cost: 80.05 \$/kwh.
5. Annual fixed charges = 20% of installed equipment cost.
6. Ratio of total cost for fittings and installation to purchase cost of new pipe = 1.4.
7. Purchase cost of new pipe per meter of length of 0.025 m I.D. steel pipe.

The optimum diameter may be calculated with

$$D_{\text{opt}}[\text{m}] = 0.363 \mathcal{V}[\text{m}^3/\text{s}]^{0.45} \rho[\text{kg}/\text{m}^3]^{0.13} \eta[\text{Pa s}]^{0.0235} \quad (4.17)$$

or turbulent flow: $N_{\text{Re}}(\text{dimensionless}) = (\rho D v / \eta) \geq 2100$ and $D_{\text{opt}} \geq 0.0254 \text{ m}$

The result is, of course, a function of the variables stipulated above; however, the relationship is very weak and the same values may be used over a range of industrial

TABLE 4.1 Dimensions of Standard Steel Pipe (ASA Standards B36.10–1939)

Nominal Pipe Size (in.)	Outside Diameter (in.)	Schedule No.	Wall Thickness (in.)	Inside Diameter (in.)	Cross-Sectional Area of Metal (in. ²)	Inside Sectional Area (ft ²)	Circumference (ft) or Surface (ft ² /ft) of Length	
							Outside	Inside
1/8	0.405	40	0.06800	0.26900	0.07200	0.00040	0.10600	0.07050
		80	0.09500	0.21500	0.09300	0.00025	0.10600	0.05630
1/4	0.540	40	0.08800	0.36400	0.12500	0.00072	0.14100	0.09540
		80	0.11900	0.30200	0.15700	0.00050	0.14100	0.07920
3/8	0.675	40	0.09100	0.49300	0.16700	0.00133	0.17700	0.12930
		80	0.12600	0.42300	0.21700	0.00098	0.17700	0.11100
1/2	0.840	40	0.10900	0.62200	0.25000	0.00211	0.22000	0.16300
		80	0.14700	0.54600	0.32000	0.00163	0.22000	0.14300
3/4	1.050	40	0.11300	0.82400	0.33300	0.00371	0.27500	0.21580
		80	0.15400	0.74200	0.43300	0.00300	0.27500	0.19420
1	1.315	40	0.13300	1.04900	0.49400	0.00600	0.34400	0.27450
		80	0.17900	0.95700	0.63900	0.00499	0.34400	0.25050
1 1/4	1.660	40	0.14000	1.38000	0.66900	0.01040	0.43500	0.36200
		80	0.19100	1.27800	0.88100	0.00891	0.43500	0.33500
1 1/2	1.900	40	0.14500	1.61000	0.79900	0.01414	0.49800	0.42200
		80	0.20000	1.50000	1.06800	0.01225	0.49800	0.39300
2	2.375	40	0.15400	2.06700	1.07500	0.02330	0.62200	0.54200
		80	0.21800	1.93900	1.47700	0.02050	0.62200	0.50800
2 1/2	2.875	40	0.20300	2.46900	1.70400	0.03322	0.75300	0.64700
		80	0.27600	2.32300	2.25400	0.02942	0.75300	0.60900
3	3.500	40	0.21600	3.06800	2.22800	0.05130	0.91700	0.80400
		80	0.30000	2.90000	3.01600	0.04587	0.91700	0.76000
3 1/2	4.000	40	0.22600	3.54800	2.68000	0.06870	1.04700	0.93000
		80	0.31800	3.36400	3.67800	0.06170	1.04700	0.88200
4	4.500	40	0.23700	4.02600	3.17300	0.08840	1.17800	1.05500
		80	0.33700	3.82600	4.40700	0.07986	1.17800	1.00200
5	5.563	40	0.25800	5.04700	4.30400	0.13900	1.45600	1.32200
		80	0.37500	4.81300	6.11200	0.12630	1.45600	1.26300
6	6.625	40	0.28000	6.06500	5.58400	0.20060	1.73400	1.59000
		80	0.43200	5.76100	8.40500	0.18100	1.73400	1.51000
8	8.625	40	0.32200	7.98100	8.39600	0.34740	2.25800	2.09000
		80	0.50000	7.62500	12.76000	0.31710	2.25800	2.00000
10	10.750	40	0.36500	10.02000	11.90000	0.54750	2.81400	2.62000
		80	0.59300	9.56400	18.92000	0.49890	2.81400	2.50300
12	12.750	40	0.40600	11.93800	15.77000	0.77730	3.33800	3.13000
		80	0.68700	11.37600	26.03000	0.70580	0.35972	2.98000

Source: Foust et al. (1960).

conditions. See Example 13.1.1.1-1: This section contains pipe sizing calculations.

With gravity in the direction of flow:

- The momentum balance in the flow direction is given by

$$\rho^{(1)} \langle v^{(1)^2} \rangle A^{(1)} - \rho^{(2)} \langle v^{(2)^2} \rangle A^{(2)} + P^{(1)} A^{(1)} - P^{(2)} A^{(2)} + mg - F = 0 \quad (4.18)$$

Position 1 is the inlet, position 2 is the outlet, and m is the mass of fluid contained in the length L between the inlet and outlet.

- The mass balance is given by

$$\rho^{(1)} \langle v^{(1)} \rangle A^{(1)} = \rho^{(2)} \langle v^{(2)} \rangle A^{(2)} \quad (4.19)$$

For constant density fluids and pipes of constant cross section, the momentum balance reduces to

$$F = P^{(1)} A - P^{(2)} A + \rho A L g \quad (4.20)$$

- The steady-state mechanical energy balance is given for these circumstances as

$$E_{vm} = gL + \frac{P^{(1)} - P^{(2)}}{\rho} \quad (4.21)$$

The value of F is expressed in terms of the Fanning friction factor as

$$F = \pi DL \left(\frac{1}{2} \rho v^2 \right) f \quad (4.22)$$

The friction factor (divided by 2) is the fraction of the characteristic momentum flux ($\rho v v$), which is transmitted to the wall. For turbulent flow in tubes or pipes, experimental results are available for f in Section 13.1.1.2. Theoretical results are available for laminar flow in Chapter 9. Solving the preceding three equations for the friction loss gives

$$e_V = \frac{4L}{D} f(N_{Re}) \quad (4.23)$$

4.3.1.2 Sudden Expansion—Calculation of Friction Loss Factor A sudden enlargement in cross section is an example where an estimate of F can be made. Refer to the sudden enlargement in Figure 4.3.

The flow direction is axial, which is perpendicular to the direction of gravity. The inlet surface is placed just to the left of the enlargement, before the resulting disturbances in the flow. The outlet surface is fixed at the point where fully developed flow has just been reinstituted. The lateral surface between the inlet and outlet constitutes the remainder of the surface.

Mass balance: Same as Equation (4.18) without the gravity term.

For incompressible flow, the velocity ratio is therefore

$$\beta = \frac{v^{(2)}}{v^{(1)}} = \frac{A^{(1)}}{A^{(2)}} \quad (4.24)$$

z -Momentum balance: Same as Equation (4.17) without the gravity term.

F is the force of the fluid on the walls, in this case the lateral wall between the inlet and outlet as well as the ring-shaped surface at the division of the two cross sections. We

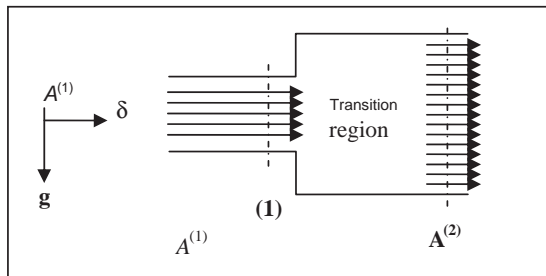


FIGURE 4.3 Sudden expansion of flow cross section.

can estimate the value of F by assuming that the normal pressure force on the ring-shaped surface is the governing ingredient. The pressure on the surface should not be much different than what exists at the inlet so that

$$F \approx -P^{(1)}(A^{(2)} - A^{(1)}) \quad (4.25)$$

Substitution of this estimate into the momentum balance and using the mass balance to eliminate the upstream velocity provides

$$P^{(2)} - P^{(1)} = \Delta P = \rho v^{(2)^2} \left[\frac{1}{\beta} - 1 \right] \quad (4.26)$$

Note that the pressure increases! The mechanical energy balance,

$$\Delta \left(\frac{1}{2} v^2 \right) + \frac{1}{\rho} (P^{(2)} - P^{(1)}) + E_{vm} = 0 \quad (4.27)$$

may now be solved for the friction loss factor:

$$e_V = \left[\frac{1}{\beta} - 1 \right]^2 \quad (4.28)$$

Recall that the characteristic velocity is the downstream velocity.

4.3.1.3 Fittings and Valves Table 4.2 is a partial list of friction loss factors for valves and fittings.

4.3.1.4 Pump Sizing Given the choice, it is more economical to increase the pressure of a liquid than to increase the pressure of a gas so that pumping should precede vaporization rather than vaporization preceding compression.

The power required for pumping is independent of the pump aside from the pump efficiency in delivering the required power to the fluid. The ability of the pump to deliver the required power depends on its particular operational characteristics, which must be examined when selecting a pump.

Example 4.3.1.4-1: Power Required for P-301 A/B: Acrylic Acid Plant

A centrifugal pump is used to circulate a molten salt through the heat transfer tubes mounted in the fluidized bed reactor system. The flow rate of the salt is 1075 tonne/h as recorded for stream 5 in Table 1.3. Properties of Hitec are included in the Preliminary Database at the conclusion of Chapter 1. The pump must compensate for the pressure drop across the heat exchanger (E-301) as well as the reactor (R-301). The salt is a dense, high viscosity liquid so that we might estimate the pressure drop as 12 psi for each of the heat transfer units for 24 psi or 1.632 atm. This is somewhat higher than the 9 psi suggested by Couper et al. (2005). Calculate the power requirement for the pump.

TABLE 4.2 Friction Loss Factors

Flow Obstacle	e_v
45° ell, standard	0.35
45° ell, long radius	0.2
90° ell, standard	0.75
Long radius	0.45
Square or miter	1.3
180° bend, close return	1.5
Tee, standard, along run, branch blanked off	0.4
Used as ell, entering run	1.0
Used as ell, entering branch	1.0
Branching flow	1.0
Coupling	0.04
Union	0.04
Gate valve, open	0.17
3/4 open	0.9
1/2 open	4.5
1/4 open	24.0
Diaphragm valve, open	2.3
3/4 open	2.6
1/2 open	4.3
1/4 open	21.0
Globe valve	
Bevel seat, open	6.0
1/2 open	9.5
Composition seat, open	6.0
1/2 open	8.5
Plug disk, open	9.0
3/4 open	13.0
1/2 open	36.0
1/4 open	112.0
Check valve, swing	2.0
Disk	10
Ball	70

Source: Green and Maloney (1997).

Solution:

$$-W_{sm} = \frac{\Delta P}{\rho} = \frac{(24/14.7)1.01325 \times 10^6 \text{ dyn/cm}^2}{(112/62.4) \text{ g/cm}^3}$$

$$= 9.2167 \times 10^5 \text{ dyn cm/g}$$

$$-W_s = (9.2167 \times 10^5) \times (1075) \times (2204.62)$$

$$\times (454) = 9.9168 \times 10^{14} \text{ dyn cm/h}$$

$$-W_s = (9.9168 \times 10^{14}) \times (2.778 \times 10^{-14})$$

$$= 27.549 \text{ kW } 00\% \text{ efficiency}$$

$$\mathcal{V} = 1075 \times 2204.62 \times (1/60) \times (1/112)$$

$$\times (264.17/35.3145) = 2638.2 \text{ gpm}$$

Estimate efficiency from data in Table 4.3:

$$\frac{\eta - 0.7}{0.8 - 0.7} = \frac{2638.2 - 500}{10000 - 500}$$

Solution is $\{\eta = 0.72251\}$ or 72.3% efficiency.

$$-W_s = 27.549/0.723 = 38.104 \text{ kW}$$

Some heuristics for pumps (Couper et al., 2005) are given below:

- Power for pumping liquids: $hp = (\text{gpm})(\text{psi difference})/(1714)$ (fractional efficiency).
- The pressure at the suction side of a pump decreases somewhat upon entering the pump due to friction losses. If the pressure drops below the vapor pressure of the liquid, bubbles will form (boiling), which will be absorbed when the pressure inside the pump increases. The reabsorption process causes noisy and irregular behavior of the pump. This undesirable condition is called cavitation, which can severely damage the pump if left unchecked. Cavitation can be avoided if the net positive suction head (NPSH) equals the pressure at the pump inlet minus the vapor pressure of the liquid at the suction side exceeds a value that depends upon the pump design and the liquid rate. The common range is 4–20 ft. The actual value must be supplied by the manufacturer.
- See Table 4.3.

We will consider the sizing of a single-stage centrifugal pump. A centrifugal pump is illustrated in Figure 1.11. A general problem is illustrated in Figure 4.4. A fluid is available at pressure P_{in} and the fluid is to pass through a flow system and emerge at P_{out} at a specified flow rate.

The pipe sizes connected to the pump and the system outlet are all the same and the sizes within the flow system are determined. If we apply the mechanical energy balance

TABLE 4.3 Pump Applications

Pump	gal/min	Max. Head (ft)	Efficiency
Centrifugal-single stage	15–5,000	500	45% at 100 gpm, 70% at 500 gpm, 80% at 10,000 gpm
Centrifugal-multistage	20–11,000	5,500	
Axial	20–100,000	40	65–85%
Rotary	1–5,000	50,000	50–80%
Reciprocating	10–10,000	1,000,000	70% at 10 hp, 85% at 50 hp, 90% at 500 hp

Source: Couper et al. (2005).

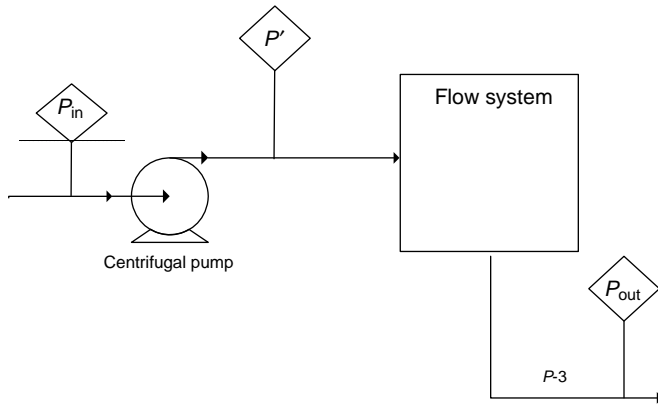


FIGURE 4.4 General flow system pump.

to the entire process between the pump inlet and the flow system output, the work required of the pump is given by

$$W_{\text{pump}} = -W_{\text{sm}} = \Delta(g\mathcal{L}) + \frac{P_{\text{out}} - P_{\text{in}}}{\rho} + E|_{\text{vm}} \quad (4.29)$$

if, for simplicity, we do not consider changes in kinetic energy.

The pump work does not determine if a specific pump can deliver the desired flow rate under the imposed process conditions. The performance curve for a centrifugal pump is supplied by the manufacturer and provides the output of the pump as a function of the pressure increase across the pump. This same relation can be developed from the system point of view. A viable pump has been selected when these two views are the same.

The system view in the preceding problem can be quantified as follows: consider the result of applying the mechanical energy balance only to the flow system:

$$\frac{P' - P_{\text{out}}}{\rho} = \Delta(g\mathcal{L}) + E_{\text{vm}} = \frac{P' - P_{\text{in}} + P_{\text{in}} - P_{\text{out}}}{\rho} \quad (4.30)$$

$$\frac{P' - P_{\text{in}}}{\rho} = \frac{P_{\text{out}} - P_{\text{in}}}{\rho} + \Delta(g\mathcal{L}) + E_{\text{vm}} \quad (4.31)$$

The first and second terms on the right-hand side of the preceding equations are fixed by the flow system construction and the required pressures. The friction loss was seen above to be proportional to the square of the flow velocity through the system. The right-hand side is therefore a parabolic function of velocity.

The right-hand side must match the view of the manufacturer whose pump will deliver a particular flow rate or at a given pressure increase across the pump. In contrast to the system view, the flow rate will decrease as the pressure increases across the pump. The situation is summarized in Figure 4.5.

Example 4.3.1.4-2: NPSH Consideration in Pumping *o*-Dichlorobenzene from Temporary Storage to Process Storage

The piping arrangement in Figure 4.6 is being considered for the transfer of *o*-dichlorobenzene (adapted from Towler

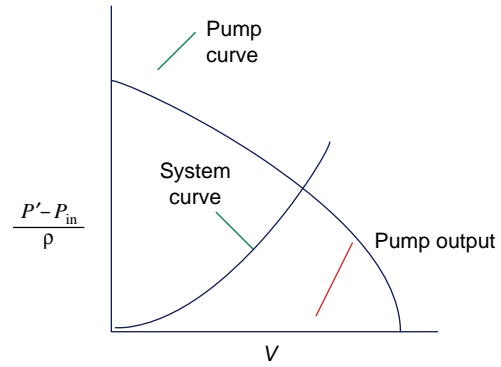


FIGURE 4.5 Pump and system curves for sizing.

and Sinnott, 2008). You are asked to consider the location of the pump.

Solution:

An important issue is whether not the available net positive suction head will meet the manufacturer's requirement for the pump. This question can be addressed by considering the piping design on the suction side of the pump.

Optimum pipe size:

$$V = \frac{10,000}{1,306 \times 3,600} = 2.1269 \times 10^{-3} \text{ m}^3/\text{s}$$

$$D = 0.363(2.1269 \times 10^{-3})^{0.45} (1,306)^{0.13} = 5.7872 \times 10^{-2} \text{ m} = 5.8 \text{ cm} = 2.28 \text{ in.}$$

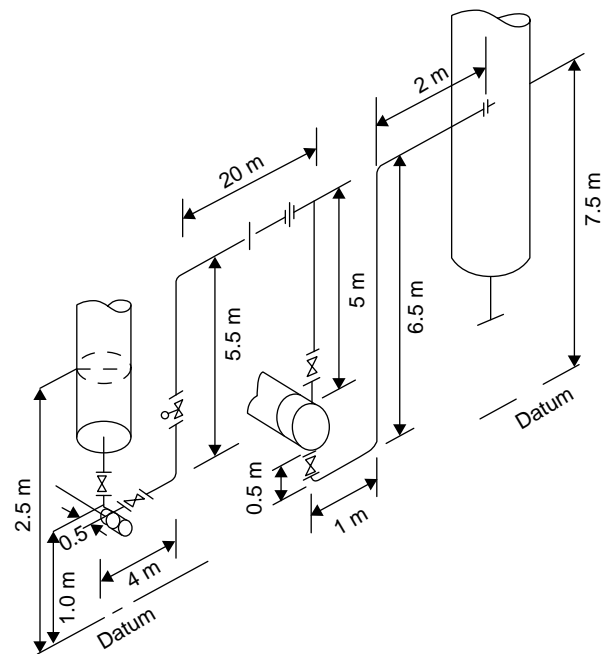


FIGURE 4.6 Piping system for transfer of *o*-dichlorobenzene (not to scale).

$$v = 0.0021368 / (3.1468 \times 0.058 \times (0.058/4)) = 0.80742 \text{ m/s}$$

$$N_{\text{Re}} = \frac{1,306(.058)(0.80742)}{0.9(0.001)} = 67,956$$

Conditions on calculation of optimum diameter are met.

Choose 2.5 in Schedule 40 pipe—inside diameter = 2.469 in. = 0.0627126 m

Suction side of pump—beginning with tank outlet (2 m elevation):

1. Pipe length = 1.5 m

$$v = 0.0021269 / (3.1468 \times 0.062713 \times (0.062713/4)) = 0.68742 \text{ m/s}$$

$$N_{\text{Re}} = \frac{1,306(.0627126)(0.68742)}{0.9(0.001)} = 62,557$$

Friction factor (Figure 13.3) = 0.006

$$\text{Friction loss factor} = \frac{2 \times 1.5}{0.0627} 0.006 = 0.28708$$

2. Gate valve (1/2 open)

Friction loss factor = 4.5

3. 90° ell (standard)

Friction loss factor = 0.75

Total friction loss factors for suction side = 0.287 + 4.5 + 0.75 = 5.537.

Total friction loss for suction side = $5.537 \times \frac{1}{2} \times 0.68742^2 = 1.3082 \text{ (m/s)}^2$.

Note that we have not considered the contraction at the tank outlet or the frictional loss at the pump entrance so that we will be on the conservative side of the question.

Application of mechanical energy balance to suction side of the pump gives:

$$P_{\text{suction}} = P_{\text{tank outlet}} + \rho g(h_{\text{tank outlet}} - h_{\text{suction}}) - 1.3082\rho$$

If the liquid is stored under its vapor pressure, then at the point where the liquid height in the tank is h_{liquid} .

$$P_{\text{suction}} = P_{\text{vapor}} + (1306)(9.80665)h_{\text{liquid}} + (1,306)(9.80665)(2 - 1) - 1.3082(1306)$$

$$P_{\text{suction}} = P_{\text{vapor}} + (1,306)(9.80665)h_{\text{liquid}} + 11,099$$

$$\text{NPSH(N/m}^2\text{)} = 12,807h_{\text{liquid(m)}} + 11,099$$

If the pump requires 10 m, then the liquid level in the tank must satisfy $h_{\text{liquid}} > 9.134 \text{ m}$ or the pump will cavitate.

It is probably too much to expect the liquid height to be kept above this value. A combination of raising the tank height, raising the tank pressure, and locating the pump in a pit should be considered.

PROBLEMS

4.1. Figure 4.7 illustrates a liquid-fuel rocket being fired while rigidly attached to a test stand. Exhaust gas is exiting the 7 m² nozzle at a pressure of 35,000 N/m². Determine the force on the support arms.

4.2. Information on the system containing two vessels shown in Figure 4.8 is as follows:

Parameter	Vessel 1	Vessel 2
P_{max}	20 psig	81 psig
P_{min}	8 psig	47 psig
Maximum liquid level above $z = 0$	43 ft	127 ft
Minimum liquid level above $z = 0$	21 ft	100 ft

The system connecting the two vessels is a 3 in. I.D. pipe, 650 ft in total length. It contains six elbows (rounded 90°), four gate valves, and one globe valve. The flow rate range is 150–200 gal/min of water ($k = 62.4 \text{ lb/ft}^3 = 1.0 \text{ cp}$). You are ordering the pump. Determine the work value to be specified in hp.

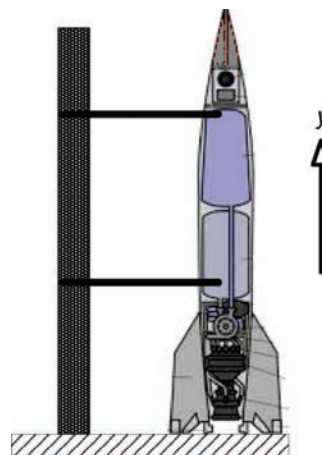


FIGURE 4.7 Test firing of rocket attached to test stand.

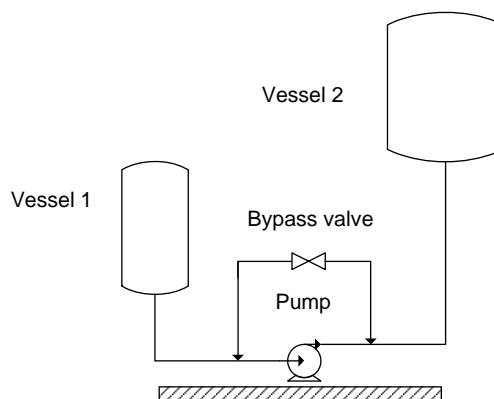


FIGURE 4.8 Pump location between process vessels.

COMPLETELY MIXED SYSTEMS—EQUIPMENT CONSIDERATIONS

In completely mixed systems, at least one phase within the system is at a uniform temperature and composition and is maintained in this condition either by mechanical stirring or by the motion of the fluid medium itself with momentum gained in a previous step. Other phases, if present, may or may not contain gradients, in composition for example, and these phases are dispersed uniformly throughout the otherwise homogeneous phase. The characteristic dimension of the dispersed phase is much less than the characteristic dimension of the containing vessel. If an output from either phase is present, its temperature, pressure, and composition are those that persist throughout the system.

We will consider at most two-phase systems in the current chapter with the objective of determining the size and power requirements to achieve complete mixing in stirred tanks for gas–liquid, liquid–liquid, and solid–liquid systems. In Chapter 6, we will introduce the separation operations of gas absorption, flash vaporization, extraction, and slurry adsorption in stirred tanks where the phases emerge in equilibrium. The stirred tank operations serve as models for the individual components of the multistage versions of the same separation operations where the product streams do not directly reflect the internal state(s) of the system (Chapter 7). The application of the completely mixed tank to single-phase chemical reactions in Chapter 6 introduces the CSTR (continuous stirred tank reactor), a building block of chemical reaction engineering.

Some other examples of completely mixed systems are

- Pharmacokinetic models used in bioengineering to follow the kinetics of a drug or anesthetic agent as it

is metabolized or biotransformed by the body (Ritter et al., 2005).

- Box models in environmental engineering used, for example, to follow contaminant elution from polluted lakes (Clark, 1996).

It will be useful to see in more quantitative terms what is meant by complete mixing and the manifestations of some systems that fall short of this condition. For a completely mixed system, we expect that all the materials in the system at some instant have the same probability of leaving in the next instant, regardless of how long it has been in the system. We have in mind a steady homogeneous flow system consisting of a single input and output. The results will be more generally applicable but that will be apparent after the discussion with these restrictions in force.

5.1 MIXING AND RESIDENCE TIME DISTRIBUTIONS—DEFINITIONS

Based on our exit scenario from a completely mixed fluid, what we need is the distribution or intensity function, $\Lambda(t)$, where

$$\Lambda(t)dt = \text{volume fraction of material in the system with age } t \text{ that will exit the system in the next instant, that is, at } t + dt \quad (5.1)$$

The volume fraction is small with respect to the system dimensions, but not so small that the continuity of physical properties is lost. The length of time that a fluid element has been in the system is its age.

In addition to the intensity function defined above, it will be useful to have several other functions that can be extracted relatively easily from measurements:

$$f(t)dt = \text{volume fraction of material at the outlet with age between } t \text{ and } t + dt \quad (5.2)$$

$$F(t) = \text{volume fraction of material at the outlet with age less than or equal to } t \quad (5.3)$$

The former is called the “residence time frequency distribution” and the latter is referred to as the “cumulative residence time frequency distribution.” They have the following properties:

$$\int_0^{\infty} f(t)dt = 1 \quad (5.4)$$

$$F(t) = \int_0^t f(\tau)d\tau \quad F(0) = 0, F(\infty) = 1 \quad (5.5)$$

Note that the average residence time is given by

$$\langle t \rangle = \int_0^{\infty} tf(t)dt \quad (5.6)$$

The average residence time defined by this relation can be related to the system volume and flow rate as follows: A volume element, $\mathcal{V}dt$, that emerges from the outlet between t and $t + dt$ contains a fraction $F(t)$ that entered the system between 0 and t time units earlier. The remainder, $1 - F(t)$, must be counted as still in the system. The total volume of the system must then be comprised of the contributions from all the volume elements at the outlet or

$$V = \int_0^{\infty} [1 - F(t)]\mathcal{V} dt \quad (5.7)$$

Set $t = 0$. In t time units later, a fraction $F(t)$ of the entering fluid will have left the system and $1 - F(t)$ will still be in the system

Integrating by parts,

$$\frac{V}{\mathcal{V}} = \lim_{t \rightarrow \infty} t[1 - F(t)] - \int_0^{\infty} t \frac{d}{dt}[1 - F(t)]dt \quad \text{or} \quad (5.8)$$

$$\frac{V}{\mathcal{V}} = \int_0^{\infty} tf(t)dt$$

The limit is presumed to exist so that the average residence time is the volume of the system divided by the volumetric throughput. This simple, but important relation can form a basis for estimating the size of equipment.

Example 5.1-1: Production of *n*-Hexyl Glucoside—Residence Time and Reactor Volume

A preliminary process for the production of 25,000 lb/year *n*-hexyl glucoside is illustrated in Figure 1.35. The product stream from the reactor, stream 5, is separated into a water phase, stream 7, and an organic phase, stream 6, in a membrane separator. Assuming no volume changes in the reactor, the volumetric throughput of the reactor was determined in the overall mass balance as

$$\mathcal{V}^{(6)} + \mathcal{V}^{(7)} = 66.259 + 2.1552 = 68.414 \text{ L/h} \quad (5.9)$$

A residence time of approximately 3.5 days is required in the reactor to reach equilibrium as can be seen in Figure 5.1.

This requires a reactor volume of 5.747 m^3 . This volume could be provided in a cylindrical vessel 1.94 m in diameter and a height of 1.94 m.

We can bring the intensity function into the accounting scheme by recognizing that the fraction of the emerging volume element with residence times from t to $t + dt$ must come from the elements still in the system, the fraction being the intensity function:

$$f(t)d\mathcal{V}dt = [1 - F(t)]\mathcal{V}dt\Lambda(t)dt \quad (5.10)$$

$$\Lambda(t) = \frac{f(t)}{1 - F(t)} \quad (5.11)$$

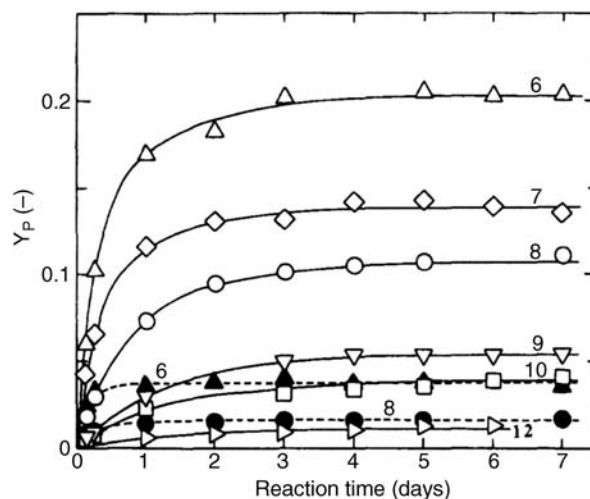


FIGURE 5.1 Transient changes in yield of *n*-hexyl glucoside (Panintrarux et al., 1995). Reprinted with permission of Butterworth Heinemann.

Also,

$$\int_0^{\infty} \Lambda(t) dt = 1 \quad (5.12)$$

5.2 MEASUREMENT AND INTERPRETATION OF RESIDENCE TIME DISTRIBUTIONS

The functions $f(t)$ and/or $F(t)$ can be determined from measurements at the outlet of the concentration of a tracer injected earlier in the feed stream. A tracer is a substance that does not disappear during the course of the experiment by chemical reaction, adsorption, or settling and whose concentration can be easily and accurately measured without disturbing the system.

Suppose that the mass concentration of tracer at the inlet is $c_0(t)$ and at the outlet is $c(t)$. The tracer flow rate at the outlet is composed of all the inlet flows with residence times increasingly longer as we move further back in time to place the element at the outlet on time:

$$c(t) = \underbrace{\int_0^{\infty} c_0(t - \tau) f(\tau) d\tau}_{\substack{\text{fluid arriving at } t - \tau \text{ that will} \\ \text{exit the system between } \tau \text{ and } \tau \\ + d\tau \text{ time units later}}} \quad (5.13)$$

One view of this result is toward the determination of the distribution function from an imposed input concentration of tracer and a measured outlet concentration. The step and impulse functions are convenient input functions from this point of view because the measured output concentration in each case provides a distribution function directly.

a. Step input

$$c_0(t) = \begin{cases} c_0^+, t > 0 \\ c_0^-, t < 0 \end{cases} \quad (5.14)$$

The outlet tracer composition for the step input function is

$$c(t) = \int_0^t c_0^+ f(\tau) d\tau + \int_t^{\infty} c_0^- f(\tau) d\tau \quad (5.15)$$

$$= c_0^+ F(t) + c_0^- [1 - F(t)] \quad (5.16)$$

$$F(t) = \frac{c(t) - c_0^-}{c_0^+ - c_0^-} \quad (5.17)$$

The normalized outlet composition is in fact the cumulative distribution function for the system.

b. Impulse

$$c_0(t) = \begin{cases} c_0, 0 < t < \varepsilon \\ 0, \text{ otherwise} \end{cases} \quad (5.18)$$

This amounts to a mass, m_0 , of tracer being injected over a very short time period, ε . The value of the concentration is then $m_0/(\mathcal{V}\varepsilon)$. The corresponding outlet response is

$$c(t) = \int_0^{\infty} c_0(t - \tau) f(\tau) d\tau = \int_{t-\varepsilon}^t c_0 f(\tau) d\tau \quad (5.19)$$

$$c(t) = c_0 [F(t) - F(t - \varepsilon)] = c_0 \varepsilon \frac{[F(t) - F(t - \varepsilon)]}{\varepsilon} \quad (5.20)$$

$$f(t) = \frac{\mathcal{V}}{m_0} c(t) \quad (5.21)$$

In this case, the outlet composition of tracer is proportional to the frequency distribution.

From another point of view, Equation (5.19) can provide the output concentration associated with a known distribution function, or better, a known or better understood state of mixing. This view provides ideal distribution functions, which can be used to reveal the salient traits of a nonideal distribution.

Ideal Cases We can construct RTD (residence time distribution) for any flow configuration that we can describe theoretically from the dynamic response to one of the tracer inputs defined in the previous section. For example, at the limit of no mixing, we have the ideal of plug flow in a conduit. All fluid elements that arrive together in this case leave together. The flow is completely segregated. All elements have the same residence time, which is therefore the average residence time:

$$f(t) = \delta(t - \langle t \rangle) \equiv \text{Dirac delta function} \quad (5.22)$$

$$F(t) = \mathcal{U}(t - \langle t \rangle) \equiv \text{Unit step function} \quad (5.23)$$

From the definition it must also be true that

$$\Lambda(t) = \delta(t - \bar{t}) \quad (5.24)$$

An example at the other end of the mixing spectrum is the completely mixed system, consisting of an ideally stirred tank. To obtain the cumulative RTD, we suppose that a fluid is passing through the tank at steady state when the mass concentration of a tracer is suddenly raised to c_0^+ , a step input. We need to determine the output concentration as a

function of time, since from it we gain the cumulative distribution function by simple proportion according to Equation (5.17). An unsteady-state mass balance on the tracer will do what amounts to adding the rate of mass accumulation to the steady-state mass balance to meet the statement of mass conservation in Chapter 2, Equation (2.1):

$$\text{rate of accumulation} = \text{input flow rate} - \text{output rate} \quad (5.25)$$

or

$$\frac{d(V_f c)}{dt} = V(c_0 - c) \quad (5.26)$$

The tracer concentration in the tank and in the output stream is c and we have maintained the steady-state flow rate. If we ignore any slight change in volume of the tank contents from the addition of the tracer and note that there is no tracer present initially, we have

$$\begin{aligned} \langle t \rangle \frac{dx}{dt} &= 1 - x, & x &= \frac{c}{c_0} \\ x(0) &= 0 \end{aligned} \quad (5.27)$$

The cumulative distribution function is $x(t)$, the solution to the differential equation:

$$F(t) = 1 - e^{-t/\langle t \rangle} \quad (5.28)$$

From this result, we can obtain directly from Equations (5.5) and (5.11):

$$f(t) = \frac{e^{-t/\langle t \rangle}}{\langle t \rangle} \quad (5.29)$$

$$\Lambda(t) = \frac{1}{\langle t \rangle} \quad (5.30)$$

Note that all elements have the same probability of leaving in the next instant. Newly arrived elements quickly disperse and can leave immediately or spend a very short time in the system. The frequency distribution is consequently nonzero at short times (see Figure 5.2).

In summary, the frequency and intensity function have the general shapes at the extremes and intermediate states of mixing as illustrated in Figure 5.3a and b, respectively:

- Two common nonideal flow characteristics are “bypassing” and “dead space.”
- Bypassing refers to the situation when a significant amount of fluid passes through the system in a time less than the average residence time (see Figure 5.4).

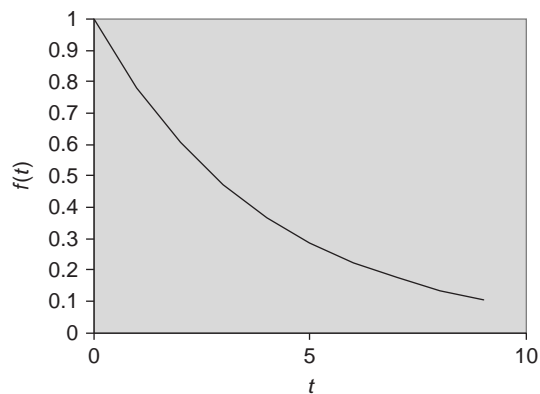


FIGURE 5.2 RTD for ideally stirred tank.

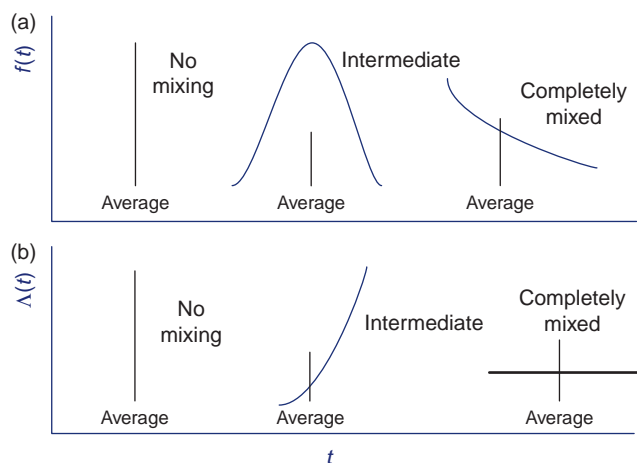


FIGURE 5.3 General characteristics of frequency (a) and intensity (b).

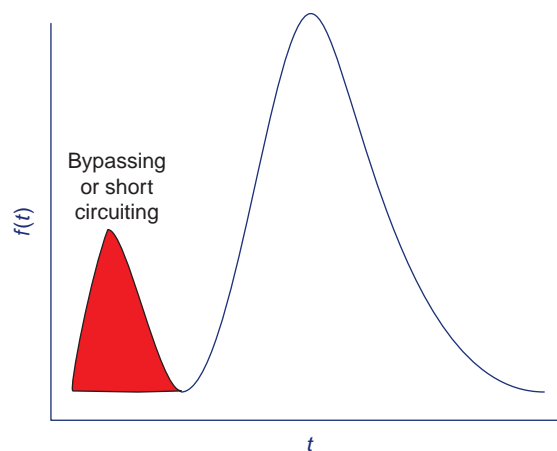


FIGURE 5.4 Evidence of bypassing.

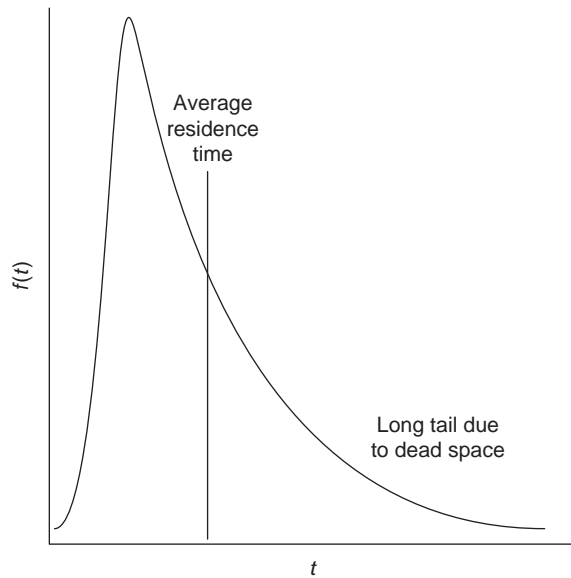


FIGURE 5.5 Evidence of dead space.

Dead space refers to regions within the equipment where the fluid elements may become trapped for considerable periods of time. The frequency distribution has a long tail due to these fluid elements as illustrated in Figure 5.5.

The effect of mixing on the total time spent in the vessel by the fluid elements is reflected by the RTD. However, the RTD does not provide the time at which the fluid elements arriving at the exit were formed. For example, the configurations shown in Figure 5.6 of the two ideal cases discussed above have the same RTD.

The cumulative distribution for example is that for an ideally stirred tank with a delay equal to the residence of

time for plug flow, t_{pf} :

$$F(t) = \left[1 - e^{-\frac{t-t_{pf}}{t_{pf}}} \right] U(t - t_{pf}) \quad (5.31)$$

An RTD alone is therefore considered to be information of the macromixing (Danckwerts, 1953) but not the associated micromixing.

Zwietering (1959) has shown that an RTD admits two extremes of micromixing: one where the mixing comes as early as possible and one where it occurs as late as possible. The first is called segregated flow where the mixing occurs at the outlet and the age within each volume element is the same. The latter is called “maximum mixedness” where the elements that make up the RTD are formed as early as possible.

The limiting cases are shown by Zwietering (1959) to provide bounds on the actual conversion in a reactive system, but not the actual conversion, except for a first-order reaction. The effect of mixing on chemical reactions can be illustrated by considering a specific case. Suppose that A undergoes an irreversible first-order reaction of order n . We can compare reaction rates in two volume elements with and without mixing: r_s and r_m , respectively. The behavior of the ratio is illustrated in Figure 5.7.

The calculations in Figure 5.7 infer that there is no effect of mixing on reaction rate for $n = 1$, that mixing is beneficial for $n < 1$, and that the segregated case is superior for $n > 1$.

5.3 BASIC ASPECTS OF STIRRED TANK DESIGN

In many cases, the selection and sizing of agitated tanks is done on the basis of experience with similar mixing operations. In this section, some methods for the preliminary sizing of mixers for gas–liquid, liquid–liquid, and liquid–solid systems will be summarized (Couper et al., 2003). In addition to the design applications, these methods can also be used as guidelines in adapting and scaling experience with similar systems to a new installation.

5.3.1 Tank Dimensions and Impeller Specifications

A typical stirred tank geometry is shown in Figure 5.8. The dimensions were taken from the heuristics given below for stirred tanks (Couper et al., 2005).

The tank diameter can be determined by the holdup required by the physical or chemical rate processes taking place in the tank. An estimate of the tank volume for liquid–liquid extraction systems can be made as follows. If the viscosity of the liquids is less than 5 cP and the specific gravity difference is greater than approximately 0.1, a residence time of no more than 5 min will provide a stage efficiency of at least 90% with a power input of 4 hp/1000 gal (Seader and Henley, 2006).

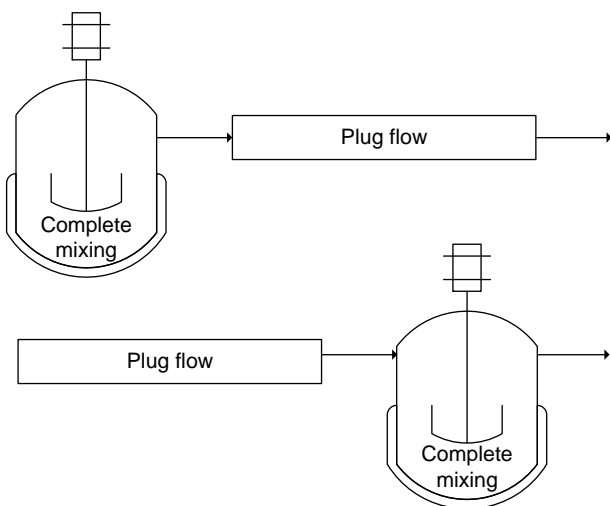


FIGURE 5.6 Equivalent RTD.

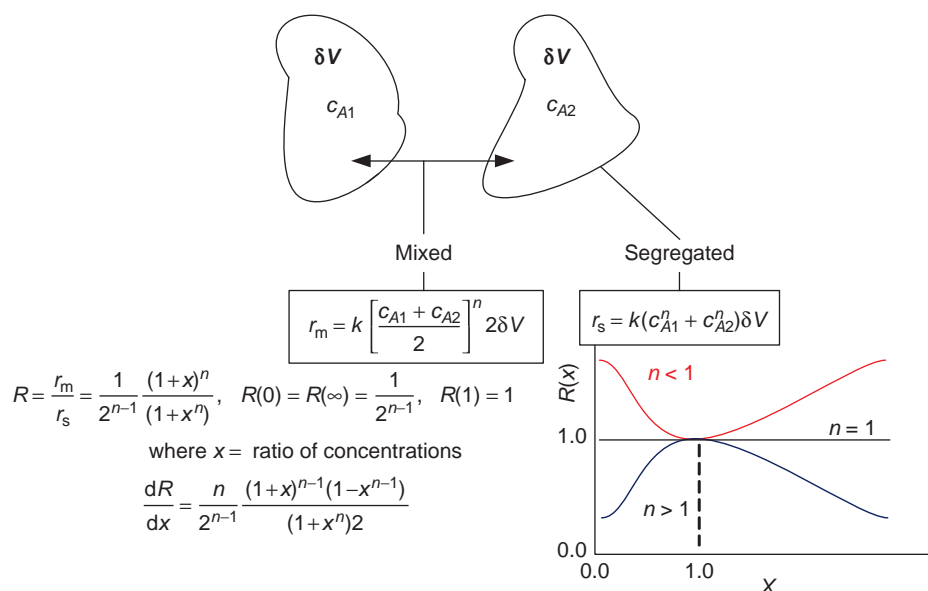


FIGURE 5.7 Effect of mixing on reaction rate.

Example 5.3.1-1 Mixer Dimensions for T-303**Alternative Solution**

In Example 7.3.2-2, the liquid flows in a countercurrent chain of equilibrium stages for liquid–liquid extraction are determined. The objective is to decrease the acrylic acid concentration in the product stream from the reactor. The solvent is diisopropyl ether (DIPE). An approximate tank size is needed to compare a mixer–settler arrangement with other means of contacting.

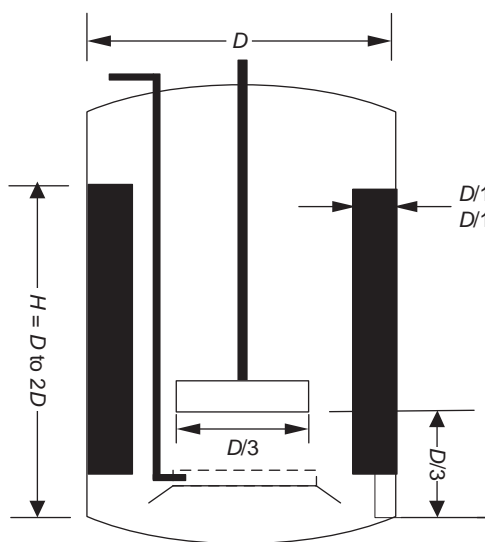


FIGURE 5.8 Basic stirred tank geometry.

The average flows for the two phases are

$$\text{raffinate} : \frac{27,463 + 21,089}{2} = 24,276 \text{ kg/h}$$

$$\text{extract} : \frac{145,114 + 151,490}{2} = 1.48302 \times 10^5 \text{ kg/h}$$

Assume for the purpose of estimating the volumetric flow rate that the raffinate is pure water and the extract is pure DIPE. The densities are available in the acrylic acid data-bank in Appendix C.

At 40 °C,

Water:

$$\left. \begin{aligned} A &= 0.3471 \\ B &= 0.274 \end{aligned} \right\}$$

$$T = 40 + 273.16 \quad \rho = AB^{-(1-\frac{T}{T_c})^n} = 1.0136 \text{ g/cm}^3$$

$$T_c = 647.13$$

$$n = 0.28571$$

DIPE:

$$A = 0.2621 = 0.2621 \quad \rho = AB^{-(1-\frac{T}{T_c})^n} = 0.70483 \text{ g/cm}^3$$

$$B = 0.2697$$

$$T_c = 500.05$$

The volumetric flow rate is then

$$\mathcal{V} = \left(\frac{148,302}{0.70483} + \frac{24,276}{1.0137} \right) \frac{1000}{28,317} \frac{1}{60} = 137.936 \text{ cfm}$$

Assuming a residence time of 3 min:

$V = \mathcal{V}t_{\text{res}} = 137.936 \times 3 = 413.808 \text{ ft}^3 = 413.808 \times 7.4805 = 3095.491$ or a 3100 gal tank $\pi \frac{D^2}{4} H = \pi \frac{D^3}{4} = 413.808$, Solution is:

$$\{D = -4.038372 - 6.994666i\},$$

$$\{D = -4.038372 + 6.994666i\}, \{D = 8.076744\}$$

Result:

$$D = 8.1 \text{ ft}, H = 8.1 \text{ ft}$$

Impeller diameter = 2.7 ft located 2.7 ft from bottom
Baffle 0.675 ft wide over full height of tank

For gas–liquid operations, a gas inlet is shown in Figure 5.8 at the top of the tank, which supplies gas to the sparger at the bottom of the tank. The sparger admits the gas in the form of bubbles. An axial and a radial impeller (see below) may also be provided and headspace for vapor–liquid disengagement. These items are not present for liquid systems. It should be noted that the energy provided by the gas in the expansion from the bottom of the tank to the top in comparison to that input by the impeller can have a significant effect on the operation of the gas–liquid system. There will be a more uniform distribution of small gas bubbles and a more rigorous dispersion if the power input by the impeller is 10–100 times the expansion energy. On the other hand, if the input by the impeller is less, there will be considerable entrainment and violent explosions of the gas bubbles at the surface.

There are many impeller designs available for a myriad of applications. Three typical designs are shown in Figure 5.9 for the applications under consideration here: gas–liquid, liquid–liquid, and solids suspended in liquids.

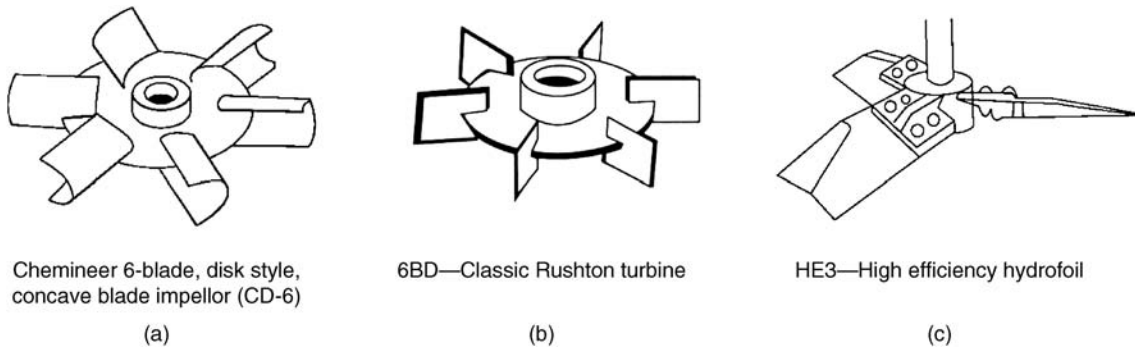


FIGURE 5.9 Representative impellers for gas–liquid, liquid–liquid, and solid–liquid applications (Couper et al., 2003). Reprinted with permission of Elsevier.

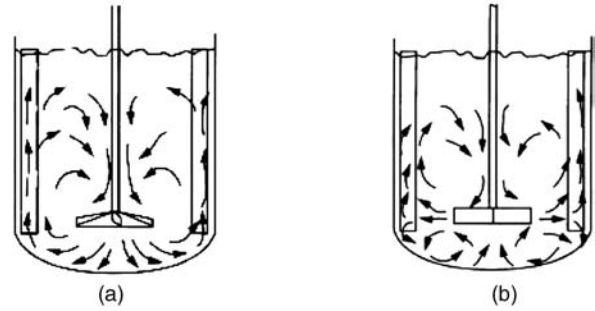


FIGURE 5.10 Basic flow patterns: (a) axial flow (propeller) and (b) radial flow. (Paul et al., 2004). Reprinted with permission of John Wiley and Sons.

The CD-6 is very good for gas dispersions in large vessels. The Rushton turbine is the preferred impeller for gas–liquid dispersions at low rates in small vessels. It is also used to create liquid–liquid dispersions. The hydrofoil is used for solid suspensions and other applications as well.

Axial flow impellers have blades that strike an angle less than 90° with the plane of rotation. Radial flow impellers have blades that are parallel to the axis of the drive shaft. Typical flow patterns for axial and radial flow impellers are illustrated in Figure 5.10 (Paul, 2004).

The impellers in Figure 5.9a and b are radial flow impellers and Figure 5.9c is an axial flow impeller. Note that there are two mixing compartments for the radial flow impeller, while there is only one for the axial flow.

A key feature of an impeller is the rate that it can discharge material through its flow area. This feature is characterized by the pumping number, N_V , defined by

$$V = N_V N D_i^2 \quad (5.32)$$

Some pumping numbers for commonly used impellers are given in Table 5.1.

TABLE 5.1 Pumping Number under Turbulent Conditions for Various Impellers

Impeller Type	N_V
Propeller	0.4–0.6
Pitched blade turbine	0.79
Hydrofoil impellers	0.55–0.73
Retreat curved blade	0.3
Flat-blade turbine	0.7
Disk flat-blade turbine (Rushton)	0.72
Hollow-blade turbine (Smith)	0.76

5.3.2 Heuristics for Mixing and Agitation

1. Mild agitation is obtained by circulating the liquid with an impeller at superficial velocities of 0.1–0.2 ft/s, and intense agitation at 0.7–1.0 ft/s. [Refer to the pumping number for the impeller (Couper et al., 2005).]

For most installations, the superficial gas velocity based on the tank cross section does not exceed 0.25 ft/s (Treybal, 1980).

2. Intensities of agitation with impellers in baffled tanks are measured by power input, hp/1000 gal, and impeller tip speeds (Couper et al., 2005) (Table 5.2).
3. Proportions of a stirred tank relative to the diameter D : liquid level = D ; turbine impeller diameter = $D/3$; impeller level above bottom = $D/3$; impeller blade width = $D/15$; four vertical baffles with width = $D/10$.
4. Propellers are made a maximum of 18 in., turbine impellers to 9 ft.
5. Gas bubbles sparged at the bottom of the vessel will result in mild agitation at a superficial gas velocity of 1 ft/min, and severe agitation at 4 ft/min.
6. Suspension of solids with a settling velocity of 0.03 ft/s is accomplished with either turbine or propeller impellers, but when the settling velocity is above 0.15 ft/s intense agitation with a propeller is needed.
7. Power to drive a mixture of a gas and a liquid can be 25–50% less than the power to drive the liquid alone.

TABLE 5.2 Impeller Tip Speeds and Power Input

Operation	kW/m ^{2a}	Tip Speed (m/s)
Blending	0.05–0.1	
Homogeneous reaction	0.1–0.3	2.5–3.3
Reaction with heat transfer	0.3–1.0	3.5–5.0
Liquid–liquid mixtures	1	5
Liquid–gas mixtures	1–2	5–6
Slurries	2–5	

^akW/m² = 5.08 hp/1000 gal

8. In-line blenders are adequate when a second or two contact time is sufficient, with power inputs of 0.1–0.2 hp/gal.

5.3.2.1 Power Requirements Integration of the microscopic momentum flows over the equipment surfaces (see Chapter 15) shows that for geometrically similar tanks the dimensionless power required is a function of the Reynolds number:

$$N_P = f(N_{Re}, N_{Fr}) \quad (5.33)$$

where the power number, the Reynolds number, and the Froude number are defined respectively by

$$N_P = \frac{\mathcal{P}g_c}{N_{\text{rpm}}^3 D_{\text{imp}}^5 \rho_M} \quad (5.34)$$

$$N_{Re} = \frac{D_i^2 N_{\text{rpm}} \rho_M}{\mu_M} \quad (5.35)$$

and

$$N_{Fr} = \frac{N^2 D_i}{g} \quad (5.36)$$

We can rationalize these expressions as follows. The velocity of the impeller, say at the tip, is a reasonable choice for a characteristic velocity and the diameter of the impeller is therefore a natural for the dimensionless length. The Reynolds number is the ratio of the characteristic convective flux of momentum to the characteristic viscous flux:

$$N_{Re} = \frac{(\rho_M v)v}{\mu_M \frac{D_{\text{imp}} - 0}{D_{\text{imp}} - 0}} \quad \text{where } v = N_{\text{rpm}} D_{\text{imp}} \quad (5.37)$$

$$N_{Re} = \frac{D_{\text{imp}}^2 N_{\text{rpm}} \rho_M}{\mu_M}$$

The Froude number is a measure of the convective flow of momentum relative to the input of the gravitational body force:

$$N_{Fr} = \frac{\rho v v \frac{\pi D_{\text{imp}}^2}{4}}{g \rho \frac{\pi D_{\text{imp}}^2}{4} D_{\text{imp}}} = \frac{v^2}{g D_{\text{imp}}} \quad (5.38)$$

Power, on the other hand, is an energy flow. In this case, we are concerned with the flow of kinetic energy, a flux times an area. The tank cross section is a good choice for the area because of the major circulation patterns from top to bottom that exist in the tank:

$$N_P = \frac{\mathcal{P}}{(\frac{1}{2} \rho_M v^2) v \frac{\pi D_{\text{imp}}^2}{4}} \propto \frac{\mathcal{P}g_c}{N_{\text{rpm}}^3 D_{\text{imp}}^5 \rho_M} \quad (5.39)$$

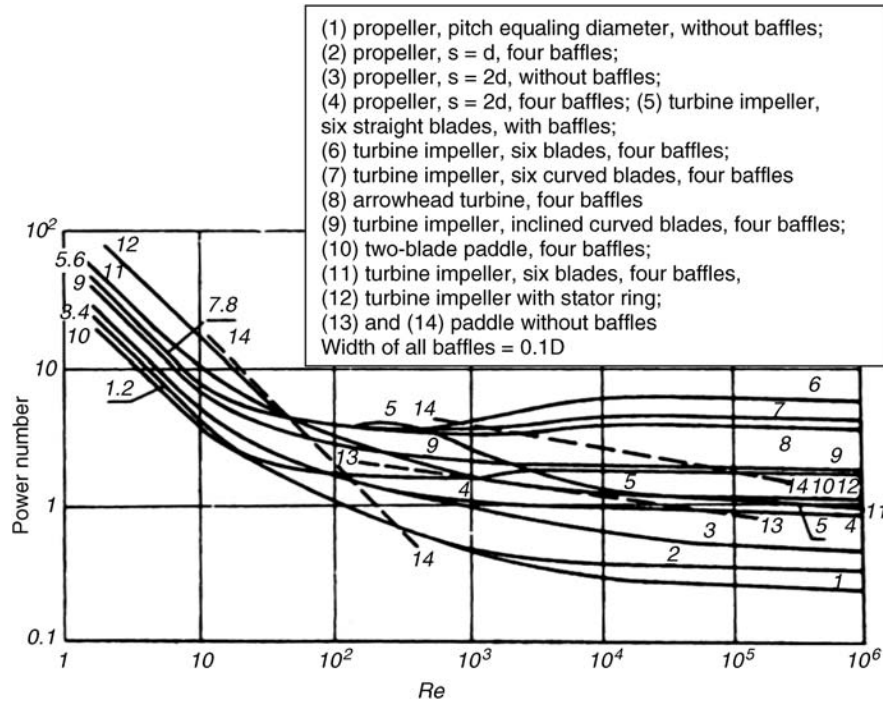


FIGURE 5.11 Power number versus Reynolds number for various equipment configurations (Couper et al., 2005). Reprinted with permission of Elsevier.

(from Figure 5.1). The conversion factor g_c has been included. A correlation is given in Figure 5.11. This is the ungassed power requirement and refers to gas–liquid and liquid–liquid dispersions. For a single-phase liquid:

1. propeller, pitch equaling diameter, without baffles
 2. propeller, $s = d$, four baffles
 3. propeller, $s = 2d$, without baffles
 4. propeller, $s = 2d$, four baffles
 5. turbine impeller, six straight blades, with baffles
 6. turbine impeller, six blades, four baffles
 7. turbine impeller, six curved blades, four baffles
 8. arrowhead turbine, four baffles
 9. turbine impeller, inclined curved blades, four baffles
 10. two-blade paddle, four baffles
 11. turbine impeller, six blades, four baffles
 12. turbine impeller with stator ring
 13. and 14. paddle without baffles
- Width of all baffles = 0.1D

5.3.2.2 Gas–Liquid Systems The ratio of gassed to ungassed power is given by (Couper et al., 2006)

$$\frac{\mathcal{P}_g}{\mathcal{P}_u} = [1 - (b - a\eta)]N_{Fr}^d \tanh cN_A \quad (5.40)$$

where the aeration number is given in terms of the gas flow rate as

$$N_A = \frac{V_g}{N_{rpm} D_{imp}^3} \quad (5.41)$$

And the parameters for the CD-6 and 6BD impellers shown in Figure 5.9 are given in Table 5.3.

The RPM can be approximately set from the ranges given in the heuristics for gas–liquid systems: tip speed 5–6 m/s.

5.3.2.3 Liquid–Liquid Systems The ungassed power correlation may be used with the liquid–liquid dispersions provided that the mixture density and viscosity be calculated as follows for the six bladed, flat-blade turbine in a baffled vessel (Treybal, 1980):

$$\rho^{(M)} = \rho^{(C)}\phi^{(C)} + \rho^{(D)}\phi^{(D)} \quad (5.42)$$

$$\eta^{(M)} = \frac{\eta^{(C)}}{\phi^{(C)}} \left[1 + 1.5 \frac{\eta^{(D)}\phi^{(D)}}{\eta^{(D)} + \eta^{(D)}} \right] \quad (5.43)$$

TABLE 5.3 Parameters for Equation (5.40)

Impeller	a	b	c	d
6BD	0.72	0.72	24	0.26
CD-6	0.12	0.44	12	0.37

For estimation purposes, the RPM can be set from the ranges given in the heuristics for liquid–liquid systems: tip speed approximately 5 m/s.

Example 5.3.2.3-1 Power Required for T-303 Alternative

Refer to Example 5.3-1 for flows. The dispersed phase hold up can be estimated as its fraction of the feed:

$$\varphi^{(D)} = \frac{(148,302/0.70483)}{(148,302/0.70483) + (24,276/1.0136)} = 0.8978$$

$$\varphi^{(C)} = 1 - 0.8978 = 0.1022$$

The density is then:

$$\begin{aligned}\rho^{(M)} &= 0.8978 \times 0.705 + 0.1022 \times 1.0136 = 0.73654 \text{ g/cm}^3 \\ &= 45.939 \text{ lbm/ft}^3\end{aligned}$$

The viscosities can be estimated as the values for the pure components

Refer to the database at the end of Appendix C.

$$\begin{aligned}\eta^{(D)} &= 10^{-5.535 + \frac{748.94}{273.16 + 40} + 0.013145(273.16 + 40) - 1.5557 \times 10^{-5}(273.16 + 40)^2} \\ &= 0.28015 \text{ cP}\end{aligned}$$

$$\begin{aligned}\eta^{(C)} &= 10^{-10.2158 + \frac{1792.5}{273.16 + 40} + 0.017730(273.16 + 40) - 1.2631 \times 10^{-5}(273.16 + 40)^2} \\ &= 0.66332 \text{ cP}\end{aligned}$$

The mixture viscosity is calculated using Equation (5.42):

$$\begin{aligned}\eta^{(M)} &= \frac{0.66332}{0.1022} \left(1 + 1.5 \frac{0.28015 \times 0.8978}{0.28015 + 0.66332} \right) \\ &= 9.0858 \text{ cP}\end{aligned}$$

The tip velocity of 5 m/s given in Table 5.2 corresponds to an rpm value as follows: $\pi(2.7)N = 5 \left(\frac{100 \times 60}{2.54 \times 12} \right)$, Solution

is: $\{N = 116.04\}$ The Reynolds number is then

$$N_{Re} = \frac{(2.7)^2 \left(\frac{116}{60} (45.939) \right)}{9.0858 \times 6.7197 \times 10^{-4}} = 1.0605 \times 10^5$$

$N_P = 6$ (approximate from Figure 5.11)

Solving for the required power

$$P = 6 \frac{(116/60)^3 (2.7)^5 (45.939)}{32.14} 5.0505 \times 10^{-7} \times 3600 = 16.168 \text{ hp}$$

This is $\frac{16.168}{3.1} = 5.2155/1000$ gal, which is close to the rule of thumb; 4 hp/1000 gal.

5.3.2.4 Solid Suspensions The hp required can be calculated with (Gates et al., 1976)

$$D_{\text{imp}} = 394 \left[\frac{P}{\sigma_{\text{gm}} N_{\text{rpm}}^3 n} \right]^{0.2}$$

n = number of impellers (spacing $\succ D$)
 D_{imp} = impellor diameter in inches
 P = horsepower
 N_{rpm} = number of revolutions per minute
 σ_{gm} = specific gravity of mixture

The density of the mixture may be approximated with

$$\rho_m = \frac{100}{c_w/\rho + 100 - c_w/\rho_f}$$

c_w = concentration of solids in weight percent
 ρ_m, ρ, ρ_f = density of medium, solid, and fluid, respectively

This result will provide the means to calculate the specific gravity of the mixture.

The revolutions per minute can be found from Figure 5.12 once the scale of agitation is selected –1d from Table 5.4.

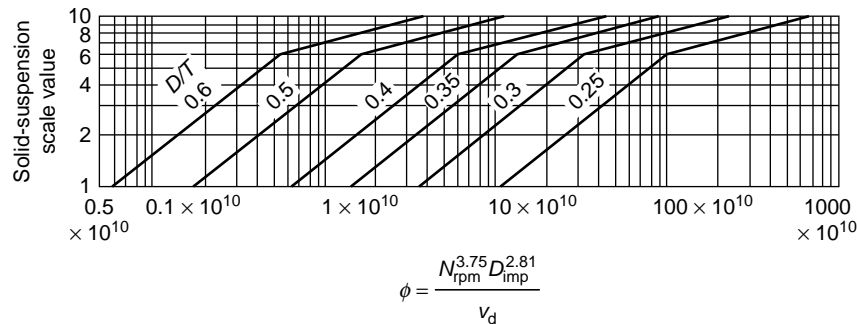


FIGURE 5.12 Solid-suspension scale value. Abulnaga (2002). Reprinted with permission of McGraw-Hill.

TABLE 5.4 Chemineer Scale for Agitation of Solids in Suspension

Scale of Agitation	Description
1–2	At levels 1–2, agitation is required for minimal suspension of solids. Agitators capable of working at an agitation level of 1 will: <ul style="list-style-type: none"> • Produce motion of all of the solids of the design-settling velocity in the vessel • Permit moving fillets of solids on the bottom, which are periodically suspended
3–5	Agitation levels 3–5 characterize most chemical process industries solids suspension applications. This scale range is typically used for dissolving solids. Agitators capable of working at an agitation level of 3–5 will: <ul style="list-style-type: none"> • Suspend all of the solids of design velocity completely off the vessel bottom • Provide slurry uniformity to at least one-third of the fluid batch height • Be suitable for slurry draw-off at low exit-nozzle elevations
6–8	Agitation levels 6–8 characterize applications where the solids suspension level approaches uniformity. Agitators capable of scale level 6 will: <ul style="list-style-type: none"> • Provide concentration uniformity of solids to 95% of the fluid batch height • Be suitable for slurry draw-off up to 80% of the fluid batch height
9–10	Agitation levels 9–10 characterize applications where the solids suspension uniformity is the maximum practical. Agitators capable of scale 9 will: <ul style="list-style-type: none"> • Provide concentration uniformity of solids to 98% of the fluid batch height • Be suitable for slurry draw-off by means of overflow

The scale of agitation was defined by Chemineer in order to have a quantitative measure of the agitation objective.

With the scale of agitation and the ratio of the impeller diameter to the tank diameter (D/T), the value of ϕ can be read from the following graph. The impeller diameter (inches) can be slightly larger for suspended solids (0.33–0.4).

The value of Φ will provide the rpms required with a value of the design velocity v_d , the terminal velocity of the particles (ft/min) multiplied by factor f_w , which is a function of the solids concentration (see Table 5.5). The terminal velocity is discussed in Chapter 12.

TABLE 5.5 Correction Factor f_w versus Weight Concentration

Solids Weight Concentration (%)	Factor f_w
2	0.80
5	0.84
10	0.91
15	1.00
20	1.10
25	1.20
30	1.30
35	1.42
40	1.55
45	1.70
50	1.85

Example 5.3.2.4-1 Sizing of Hexyl Glucoside Slurry Adsorber

Slurry adsorption is considered in Example 6.5.3-1 for the recovery of hexyl glucoside. The size of the mixer is considered here.

Solid weight = 438 lbs ($438 \times 0.454 = 198.8$ kg) see Example 6.5.3-1.

Apparent density of solids $\rho_p = 1028.2$ kg/m see Example 13.2.

$$\text{Solid volume} = \frac{438 \times 0.454}{1028.2} = 0.19340 \text{ m}^3$$

Hexanol volume (see the solution to Problem 2.3 and use the fill time of 4 h) $4 \times 551.088 \times 264.3 \times \frac{0.001}{793.6} = 0.73414 \text{ m}^3$

$$\text{Weight of hexanol} = 793.6 \times 0.73414 = 582.61 \text{ kg}$$

$$\text{Weight fraction solids} = \frac{198.85}{198.85 + 582.61} = 0.25446$$

$$f_w = 1.2 + \frac{0.446}{5} \times 0.1 = 1.2089 \text{ from Table 5.5}$$

$v_d = 1.21 \times 8.027 = 9.7127$ ft/min: Definition of design velocity see Example 13.2.1-1 for terminal velocity.

$$\rho_m = \frac{1}{0.25446 \times 2.3 \times 3.3 / 1028.2 + 1 - 0.25446 / 793.6}$$

842.5 kg/m of slurry

$$\text{Slurry volume} = 0.73414 + 0.1934 = 0.92754 \text{ m}^3 \quad 245.03 \text{ ft}^3$$

Tank volume = $245.3 / 0.9 = 272.56$ ft³ assuming 90% “occupancy”

$$\pi D^2 \frac{h}{4} = \pi D^3 \frac{1}{4} = 272.56, \text{ Solution is: } \{D = 7.0273\}$$

Tank diameter = 7 ft

Impeller diameter = $0.40D = 2.8$ ft

See Chemineer agitation scale = 5

$$\varphi = 4 \times 10^{10} = N_{\text{rpm}}^{3.75} (2.8 \times 12)^{2.81} \frac{1}{9.7127} \text{ from Figure 5.12.}$$

Solution is: $\{N_{\text{rpm}} = 88.465\}$

$$2.8 \times 12 = 394 \left(\frac{P}{0.8408 \times 89^3 \times 1} \right)^{0.2}, \text{ from Equation (5.44).}$$

Solution is: $P = 2.6735$ hp

PROBLEMS

5.1. A mass of tracer was injected very quickly into the inlet stream of a system of unknown volume. The inlet stream had a steady flow of $2.0 \text{ m}^3/\text{h}$. The concentration of tracer was measured in the outlet stream as a function of the elapsed time from the injection (adapted from Clark, 1996):

Time (min)	conc (mg/l)	Time (min)	conc (mg/l)
0.00	0.00	13.00	5.00
0.50	0.10	13.50	4.20
1.00	1.60	14.00	3.40
1.50	3.00	14.50	3.10
2.00	6.40	15.00	2.80
2.50	8.30	15.50	2.60
3.00	9.70	16.00	2.50
3.50	10.70	16.50	2.20
4.00	12.80	17.00	1.90
4.50	13.20	17.50	1.60
5.00	13.30	18.00	1.40
5.50	13.20	18.50	1.20
6.00	13.10	19.00	1.00
6.50	12.20	19.50	0.90
7.00	11.80	20.00	0.80
7.50	10.70	20.50	0.70
8.00	10.10	21.00	0.50
8.50	9.10	21.50	0.40
9.00	8.80	22.00	0.20
9.50	8.40	22.50	0.10

10.00	8.10	23.00	0.00
10.50	7.40	23.50	0.00
11.00	6.60	24.00	0.00
11.50	6.20	24.50	0.00
12.00	5.90	25.00	0.00
12.50	5.40		

Plot the residence time frequency distribution, the cumulative residence time frequency distribution, and the intensity function. Determine the volume of the system and the average residence time. Interpret your results and note any assumptions that you have made (especially in the volume calculation).

5.2. The textile industry uses dyes for coloring fibers. Studies have shown that these dyes, which are present in the effluent from the colorization process, can cause cancer, allergic reactions, eye and skin disorders, and other maladies. Consequently, many countries require the industry to remove the dyes before discharging the waste streams into the environment. Adsorption is an effective separation process. To reduce costs, a textile manufacturer is evaluating the possibility of using waste carbon slurries, resulting from the partial combustion of fuel in industries that generate their energy from fuel oil (Gupta et al., 2007).

In one such application, treatment of a carbon slurry yielded carbon particles for adsorption applications with the following properties:

diameter = 50 mm

surface area = $629 \text{ m}^2/\text{g}$

density = 1.30 g/cm^3

porosity = 0.78

Determine dimensions for a stirred tank (1000 gal) and the power required for stirring if the adsorbent loading is $.5 \text{ g adsorbent}/300 \text{ cm}^3$ of effluent. The effluent properties can be taken as the values for water. The terminal velocity of the particles is 41.0 ft/min .

6

SEPARATION AND REACTION PROCESSES IN COMPLETELY MIXED SYSTEMS

The descriptions of the major chemical engineering operations of chemical separation and chemical reaction have represented two points of view. These points of view arise from the common ground of processes being driven by rates proportional to distances from equilibrium. The rate point of view regards equilibrium as a target present in the rate expression and configures the process conditions to achieve a product state at an economic distance from the target. On the other hand, the equilibrium stage point of view assumes that the process has reached equilibrium consistent with the imposed operating conditions. An efficiency correction determined by recorded experience is then applied. To the extent that the records reflect the experience at hand, and the models are complete, the two approaches are equivalent in completely mixed systems. For completely mixed systems, the equilibrium stage approach applies extensively in the major separation operations. The rate approach applies to the design and analysis of the continuous stirred tank reactor (CSTR) and the batch reactor. These applications will be considered in this chapter.

6.1 PHASE EQUILIBRIUM: SINGLE-STAGE SEPARATION OPERATIONS

The major separation operations in chemical engineering: distillation (multistage flash vaporization), gas absorption, liquid–liquid extraction (LLE), and adsorption are considered below in single equilibrium stages with the following common characteristics.

All processes are conducted at a specified temperature. A general representation of the equilibrium stages considered here is presented in Figure 6.1.

There can be one or two feed streams and one or two product streams, each containing many components. There can be two product streams of different phase so that if there is one feed, a separate phase is created as, for example, the creation of a vapor phase from a liquid feed by the addition of heat at rate Q . There is sufficient mixing and sufficient residence time for the mass and energy transfer processes and any chemical reactions to be completed.

If there are two product streams, they are drawn from two separate phases existing within the equipment so that the interstream equilibrium at the outlet is a reflection of the uniform equilibrium conditions within the equipment. A single feed and a single product will then be a reactive system.

In order to analyze the equilibrium stages discussed above, we need to express phase equilibrium for gas–liquid, liquid–liquid, and solid–liquid systems in terms of the system variables: concentration, temperature, and pressure. Phase and chemical equilibrium in general (Callen, 1960; Tester and Modell, 1997) can be stated in terms of the fundamental equation of thermodynamics, Equation (3.2), as follows:

In an isolated system of constant entropy, volume, and mass, the equilibrium state is characterized by a minimum in the total internal energy.

This condition requires the equality of temperature and pressure throughout the system for thermal and mechanical equilibrium as well as $(\partial U / \partial N_i)_{S, V, N_{j \neq i}}$ for chemical equilibrium. The conditions for thermal and mechanical

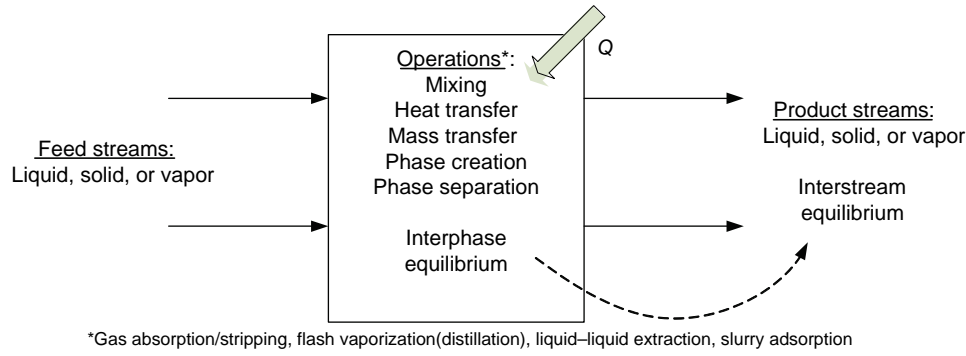


FIGURE 6.1 Equilibrium stage.

equilibrium, being known *a priori*, may be regarded as a confirmation of the theory. The condition for chemical equilibrium is in terms of an apparently inconvenient derivative. If, instead of the energy representation, the equivalent representation in terms of the Gibbs free energy, Equation (3.4), is used, the equilibrium criterion becomes

In a system at constant temperature, pressure, and total mass, the equilibrium state is characterized by a minimum in the Gibbs free energy.

Now changes in the Gibbs free energy follow from Equations (3.7) and (3.14) as

$$d\mathcal{G} = -\mathcal{S}dT + \mathcal{V}dP + \sum \tilde{G}_i dN_i \quad (6.1)$$

where

$$\tilde{G}_i = \left(\frac{\partial \mathcal{G}}{\partial N_i} \right)_{T,P,N_j} \quad (6.2)$$

It can be shown that the minimum in the Gibbs function at equilibrium in a multiphase system at uniform temperature and pressure (thermal and mechanical equilibrium, respectively) requires that the partial molar Gibbs free energy for each component be equal in all of the phases. For this reason, these quantities have been given the special name of chemical potentials:

$$\mu_i = \tilde{G}_i \quad (6.3)$$

Remember, the chemical potential is not a new thermodynamic variable. It is just another name for an existing variable. The conditions for chemical equilibrium between two phases (' and ') in thermal and mechanical equilibrium can then be stated as

$$\mu_i' = \mu_i'', \quad i = 1, 2, \dots, N_c \quad (6.4)$$

It turns out that the chemical potential is not well behaved. In dilute systems, for example, it becomes infinite at infinite dilution. An equivalent quantity that is more convenient in

the calculations, called the fugacity, is used in place of the chemical potential.

The fugacity is defined and calculated as follows. For an ideal solution, Equation (3.141) states

$$\tilde{G}_i^{\text{id}} = G_i(T, P) + RT \ln y_i \quad (6.5)$$

Therefore,

$$\begin{aligned} d\tilde{G}_i^{\text{id}} &= d\mu_i = dG_i(T, P) + RT d \ln y_i \\ &= V dP + RT d \ln y_i \quad \text{at constant } T \end{aligned} \quad (6.6)$$

or

$$d\mu_i^{\text{id}} = RT d \ln P_i \quad \text{at constant } T \quad (6.7)$$

On this basis, the fugacity of species *i* in a mixture, \hat{f}_i , is defined by a differential equation as

$$d\mu_i = RT d \ln \hat{f}_i \quad \text{at constant } T \quad (6.8)$$

where

$$\hat{f}_i \rightarrow y_i P \quad \text{as } P \rightarrow 0$$

Note that the boundary or initial condition at very low pressures provides a starting point for the evaluation of fugacity at all other conditions. To reach other states, the changes in fugacity with respect to the accompanying changes in composition, temperature, and pressure must be expressed in term of measured thermodynamic functions: equation of state, vapor pressure, and specific heat (a similar statement can be made for all of the thermodynamic functions!).

The simplicity of the phase equilibrium criteria *i* terms of the chemical potential carries over directly to the fugacities. This can be seen by integrating the preceding expression between any two phases that are at the same temperature and pressure. The result is that

$$\underbrace{\mu_i(T, P, x') - \mu_i(T, P, x'')}_{\text{equals 0 if phases ' and '' are in equilibrium}} = RT \ln \frac{\hat{f}_i'}{\hat{f}_i''} = 0 \quad (6.9)$$

$$\hat{f}_i' = \hat{f}_i'' \quad (6.10)$$

Since the phases denoted by ' and '' are arbitrary, the fugacity, like the chemical potential, is uniform throughout the phases at equilibrium for each component. It is important that we be able to evaluate the fugacity in order to determine the compositions of the equilibrium phases. Let us see how much we need to specify.

For each phase (suppose there are N_π) there are N_C unknown mole fractions. The temperature and pressure are unknown throughout the system. The number of unknowns is therefore $N_\pi N_C + 2$. The mole fractions in each phase must sum to unity and there are $N_C (N_\pi - 1)$ fugacity equalities. The number of relations between the unknowns is therefore $N_C (N_\pi - 1) + N_\pi$. The degrees of freedom in the set of unknowns consisting of the mole fractions in each phase and the temperature and pressure is therefore

$$\phi = N_C + 2 - N_\pi \quad (6.11)$$

which is an expression of Gibbs phase rule. For our two-phase systems, there are N_C degrees of freedom.

6.2 GAS-LIQUID OPERATIONS

The terms *gas* and *vapor* are sometimes used interchangeably, both referring to the noncondensed state. In other cases, the term *vapor* is reserved for the presence of components that are condensable under the prevailing conditions. We are using the terms interchangeably.

6.2.1.1 Gas Absorption and Stripping

In gas absorption, a gas is contacted with a liquid (solvent) phase that has been selected on the basis that it has a high affinity for one or more undesirable components in the gas phase and that it has a low volatility. In addition, the solvent should be nontoxic, noncorrosive, and nonflammable. The most common solvents are water, high molecular weight hydrocarbon oils, and ionic solutions. Gas stripping is the analogous operation where a solute is stripped from a liquid phase by a gaseous solvent or stripping agent. Steam, heated air, and inert gases are commonly employed as stripping agents. The nature of the equilibrium is the same for both stripping and absorption.

Generally speaking, the pressures should be high for absorption, whereas the reverse is true for stripping. Care must be taken not to condense the feed to the absorber or vaporize the feed to the stripper when fixing the operating pressure.

The liquid absorbs the soluble gas phase components and thereby produces a gas of higher purity. In stripping, the undesirable components are present in the liquid

phase and are taken up by the gas phase. The two operations are analyzed in a similar fashion and are often carried out sequentially since the solvent phase in the initial separation operation will normally be purified and recirculated.

Gas absorption falls into two categories based on the processes at play during the absorption process.

- Physical absorption refers to the case when the gas phase component dissolves in the solvent and subsequently maintains its chemical integrity. Heat effects in physical absorption are usually negligible.
- Chemical absorption refers to the case when the dissolved gas undergoes a reaction with an ingredient of the liquid phase. The mass transfer system is analyzed in much the same way as physical absorption but the simultaneous reaction increases both the rate of absorption (higher concentration gradient) and the capacity (solute "hides" in reaction products). Heat effects in chemical absorption can be large. Examples of each operation are given in Table 6.1.

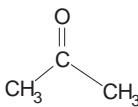

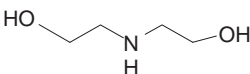
A typical distribution of material for a ternary gas absorption system is illustrated in Figure 6.2.

The basic elements of the illustration from a somewhat more general material viewpoint than the indicated ternary mixture are as follows:

- A gas stream (V) consisting of undesirable components (A) that are soluble in the liquid absorbent and one or more components that are not soluble to any appreciable extent (C). The collection of insoluble components (C) represents the maximum purity of the gas phase.
- A liquid stream (L) consisting of solvent (B) in which there is preferential solubility of the undesirable element (A) of the gas phase. A small amount of A may be present in the solvent at the inlet if the solvent is being recycled.
- The very small concentrations reflect a low volatility of the solvent and a small solubility of the nontargeted components of the gas phase. These concentrations are often ignored in the calculations, giving rise to a gas phase solvent (C) and a liquid phase solvent (B).

The outlet streams are in equilibrium. Gibbs phase rule for three components and two phases indicates that there are three degrees of freedom. Consequently, if the temperature and pressure are fixed, the gas phase concentration of A at equilibrium may be plotted against the liquid phase concentration of A.

TABLE 6.1 Examples of Gas Absorption Systems

Solvent (Absorbent)	Solute (Absorbate)	Type
Water (H ₂ O)	Acetone 	Physical Solubility at 85.4 mmHg = 0.117 mole fraction (Geankopolis, 2003)
Hydrocarbon oil 3–10 carbons beyond lightest component	Benzene 	Physical (Branan, 1994)
Sodium hydroxide (NaOH)	Hydrogen sulfide (H ₂ S)	Chemical (irreversible) H ₂ S + NaOH → NaHS + H ₂ O Instantaneous (Danckwerts, 1970)
Diethanolamine 	Carbon dioxide (CO ₂)	Chemical (reversible) CO ₂ + 2R ₂ NH = R ₂ NCOO ⁻ + R ₂ NH ⁺ K _c = 2.3 × 10 ⁻⁴ g mol/l at 25 °C (Danckwerts, 1970)

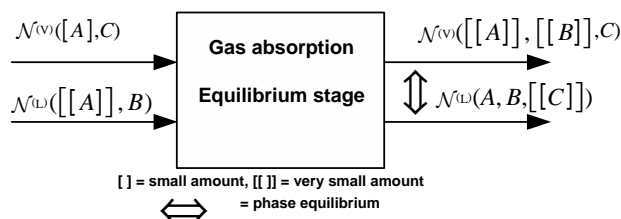


FIGURE 6.2 Material distribution in gas absorption system.

A similar situation arises if the liquid contains the impurities (*A*) in the feed instead of the gas. In that case, the final phase equilibrium state will be primarily a redistribution of *A* to the gas phase and the operation is called stripping. The analyses of these processes have no essential differences.

6.2.1.2 Flash Vaporization

Flash vaporization is another example of a gas–liquid unit operation. It differs from gas absorption in that the separating agent is heat rather than mass. All of the components are normally volatile and may be present in substantial amounts in both phases. This is often referred to as vapor–liquid equilibrium (VLE) as opposed to gas–liquid equilibrium in the case of noncondensable components, although the distinction is more convenient than real.

In this single-stage separation operation, illustrated in Figure 6.3, a liquid process stream contains one or more components (say *A* and *B*) with vapor pressures much greater than the others (*C* and *D*).

This difference may be sufficient to effectively remove these components in a vapor phase produced by reducing the pressure and/or by increasing the temperature, both of which take advantage of their greater volatility. Of course, it is pointless to vaporize the entire liquid since we will be left with a vapor with the same composition. A partial vaporization process will favor the most volatile components.

The partial vaporization equipment and the unit for separating the resulting two-phase mixture are combined in Figure 6.3 and the combination referred to as an equilibrium stage. A more detailed view including the individual steps is available in Figure 6.22.

The separation agent is energy and the expansion valve, if the valve is present.

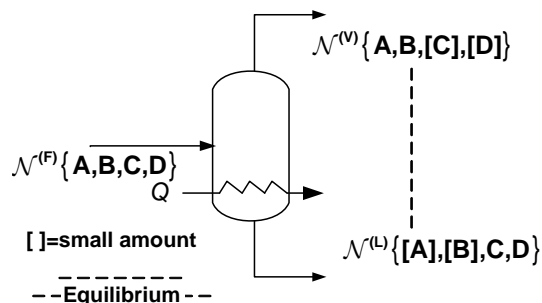


FIGURE 6.3 Flash vaporization.

A similar situation arises with a vapor stream that contains a group of components with very low volatilities. The idea in that case is to partially condense the vapor. The analyses of these processes have no essential differences.

The final equilibrium states achieved in gas absorption (stripping) and flash vaporization (partial condensation) have the same features (what are they?) and can therefore be studied under one heading: vapor–liquid equilibrium.

6.2.2 Vapor–Liquid Equilibrium

In a pure system, there one degree of freedom. The system must be at its boiling point under the imposed pressure; in other words, the system temperature is that value at which the vapor pressure is equal to the imposed pressure. Also, the system is said to be saturated.

In a binary system, there are two degrees of freedom. If the temperature is fixed, the vapor and liquid mole fractions are determined by the equilibrium conditions. If the vapor composition is fixed, the system temperature and liquid mole fraction are determined by the equilibrium conditions.

Vapor–liquid equilibrium data at a fixed pressure in binary systems often take the graphical form shown in Figure 6.4. This form is typical of many binary flash vaporization and distillation applications and provides a framework for multi-component applications. The two-phase region may disappear or become restricted at other pressures $P^{\text{sat}}(T_B)$.

- Suppose the mixture is at a very high temperature—no liquid in sight. We know that there is a temperature at which this mole fraction persists in the gas phase at equilibrium with a liquid. We say that the gas is superheated (see Figure 6.4) and that, if cooled, will eventually reach a temperature called the dew point where a minute droplet of liquid will form at the same temperature with a mole fraction that satisfies the

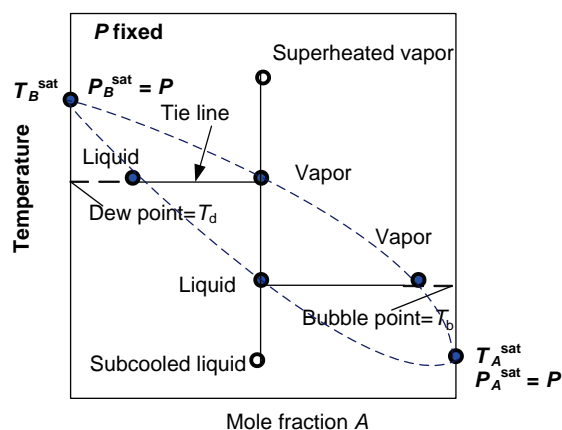


FIGURE 6.4 Typical VLE data in a binary system.

vapor–liquid equilibrium condition or the state of VLE. If the mole fraction corresponds to the more volatile component, the liquid mole fraction will generally be less than the vapor, but not always. The vapor and liquid points can be connected by a “tie line.”

- If, on the other hand, the mixture is at a very low temperature, no liquid (or solid) in sight, we say that the mixture is subcooled (see Figure 6.4). If heated, the mixture will reach a temperature at which a small bubble of gas will form, which is the physical state of VLE.

The solid points in Figure 6.4 represent qualitative equilibrium conditions for a binary system composed of *A* and *B*. *A* is more volatile than *B* ($T_A^{\text{sat}} < T_B^{\text{sat}}$). A curve through the vapor points is the dew-point curve. A curve through the liquid points is called the bubble-point curve. Corresponding vapor–liquid equilibrium compositions ranging from pure *B* to pure *A* on the two curves are connected by a line at constant temperature called a tie line. Some specific examples are the acetic acid–water system shown in Figure 6.5 and the isopropyl alcohol (IPA)–water (W) system shown in Figure 6.6.

An azeotrope occurs in the IPA–water system at an alcohol mole fraction of 0.6854 where the vapor and liquid mole fractions are identical. The system will boil at these conditions like a pure fluid. At this point, the relative positions of bubble and dew-point curves shift.

These data are of course for binary systems and are the result of experimental measurements of vapor and liquid compositions at equilibrium. Such data are needed not only for many binary systems but also for never ending combinations in multicomponent mixtures. The possibility

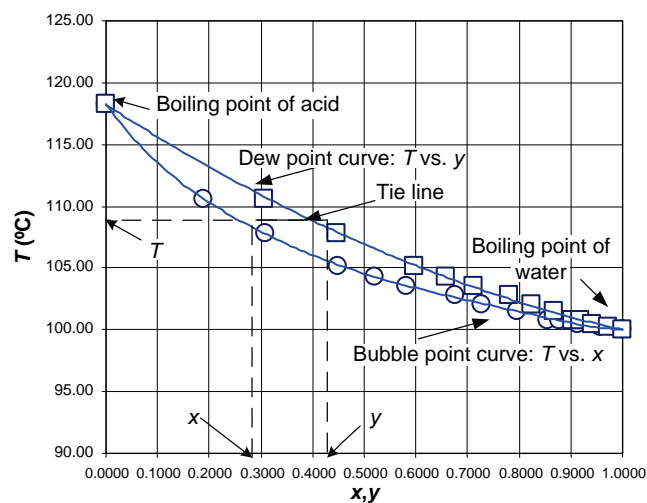


FIGURE 6.5 VLE data for acetic acid–water system at 1 atm (Green and Maloney, 1997). Reprinted with permission of McGraw-Hill.

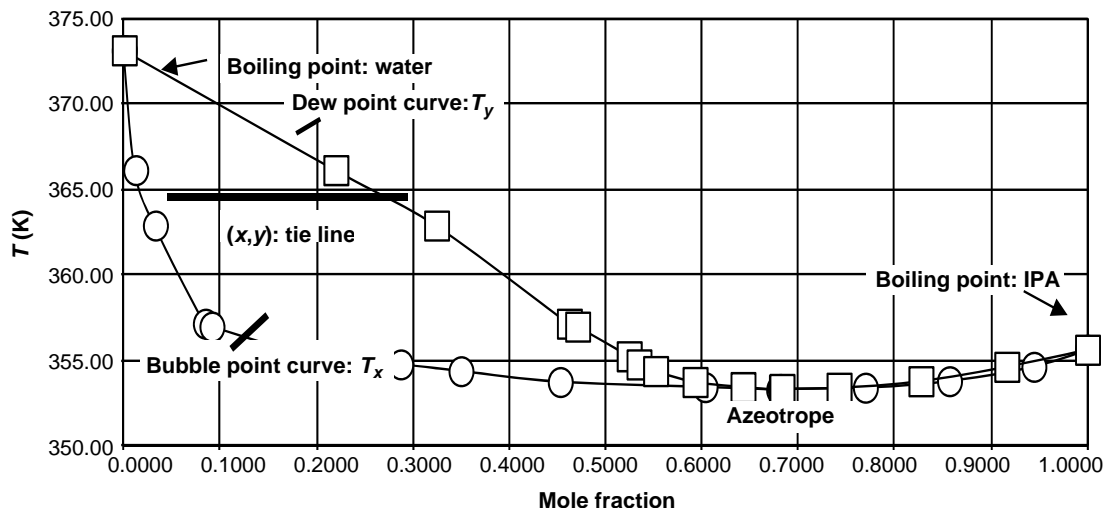


FIGURE 6.6 VLE data for isopropyl alcohol (IPA)–water system at 1 atm (Green and Maloney, 1997). Reprinted with permission of McGraw-Hill.

of accurately producing these data through the phase equilibrium equalities is therefore an important capability.

We need to transform the fugacity equalities into terms of pressure, temperature, and composition in order for them to be useful in process calculations. There are essentially two methods for accomplishing this.

6.2.2.1 Equation of State Method In those cases where an equation of state is available for both the liquid and vapor phases, the fugacity can be obtained directly from the equation of state. Such cases include mixtures of hydrocarbons and dissolved gases such as carbon dioxide and nitrogen.

6.2.2.1.1 Pure Component Fugacity The partial molar Gibbs free energy (or chemical potential) for a pure component is the molar Gibbs free energy [see Equation (3.15)]. Consequently, using Equation (3.7)

$$d\mu = dG = V dP \quad \text{at constant } T \quad (6.12)$$

From the definition of fugacity in Equation (6.8)

$$d \ln f = \frac{V}{RT} dP \quad \text{at constant } T \quad (6.13)$$

$$d \ln f = \frac{PV}{RT} d \ln P = \left[\frac{PV}{RT} - 1 \right] d \ln P + d \ln P \quad (6.14)$$

$$d \ln \left(\frac{f}{P} \right) = \frac{1}{RT} \left[V - \frac{RT}{P} \right] dP \quad \text{at constant } T \quad (6.15)$$

The integration at constant T is performed after substituting a volume explicit equation of state for the material. The integration may be changed to volume if a pressure explicit equation of state is used. Both possibilities are included below.

The integral over pressure is shown graphically in Figure 6.7 along a predefined isotherm ending at the desired system state.

In spite of the fact that (in this case) a liquid phase fugacity is needed, the integration begins in the very low-pressure region. In this region, the material behaves like an ideal gas so that the kernel of the integral vanishes to give the fugacity equal to the pressure.

As the pressure increases, an equation of state may be needed, depending on the material, to represent the molar volume in the integral. The integration proceeds in this fashion until the vapor pressure is reached at the fixed temperature. The liquid phase fugacity may be set equal to the gas

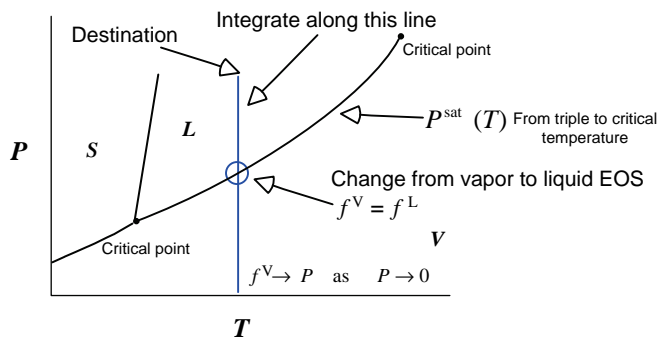


FIGURE 6.7 Integration path for pure component fugacity (ideal gas to nonideal gas to liquid).

phase fugacity at this juncture (why?) and the integration continued with a liquid phase molar volume. If the same equation of state applied to both phases, there would be no need to make the adjustments at the vapor pressure.

The integration is stopped at the desired pressure. Note that in general, an equation of state is required for the gas phase, and possibly for the liquid or solid phases depending on the destination and the pressure at each phase change along the isotherm. The equation of state and the vapor pressure are representative of the physical data that drive thermodynamics.

Consequently, for $P \leq P^{\text{sat}}$, Equation (6.15) becomes for a volume explicit equation of state for the gas region

$$\ln \frac{f}{P} = -\frac{1}{RT} \int_0^P \left[\frac{RT}{P} - V \right]_{\text{constant } T} dP \quad (6.16)$$

For a pressure explicit equation of state for the gas region, Equation (6.15) becomes

$$\ln \frac{f}{P} = Z - 1 - \ln Z - \frac{1}{RT} \int_{\infty}^P \left[P - \frac{RT}{V} \right]_{\text{constant } T} dV \quad (6.17)$$

Equation (6.16) can be used to evaluate the fugacity at $P = P^{\text{sat}}$.

$$f^{\text{sat}} = P^{\text{sat}} e^{-\frac{1}{RT} \int_0^{P^{\text{sat}}} \left[\frac{RT}{P} - V \right] dP} \quad (6.18)$$

The fugacity at saturation is nearly equal to the vapor pressure at moderate pressures where ideal behavior applies to the vapor pressure. The exponential correction factor in this case differs little from unity.

Using the liquid phase equation of state in Equation (2.29) with the reference conditions at saturation, the integration may be continued into the liquid region.

For $P \geq P^{\text{sat}}$,

$$\ln \frac{f}{P} - \ln \frac{f^{\text{sat}}}{P^{\text{sat}}} = -\frac{1}{RT} \int_{P^{\text{sat}}}^P \left[\frac{RT}{P} - V^{\text{sat}} e^{-\kappa(P-P^{\text{sat}})} \right] dP \quad (6.19)$$

or

$$\ln \frac{f}{f^{\text{sat}}} = \frac{V^{\text{sat}}}{\kappa RT} \left[1 - e^{-\kappa(P-P^{\text{sat}})} \right] \quad (6.20)$$

In the limit of zero isothermal compressibility,

$$f = f^{\text{sat}} e^{\frac{V^{\text{sat}}(P-P^{\text{sat}})}{RT}} \quad (6.21)$$

The exponential factor in Equation (6.21) is referred as the Poynting factor. Except for very high pressures, it is near unity and the liquid phase fugacity is taken to be the value at saturation at the prevailing temperature.

Example 6.2.2.1.1-1 illustrates the integration over the gas region for a basic equation of state and refers to the integrals in Equations (6.16) and (6.17).

Fugacity coefficients for pure components obeying the equations of state listed in Table 2.1 are given in Table 6.2.

Example 6.2.2.1.1-1: Pure Component Gas Phase Fugacity: Berthelot Equation of State

Equation of state: $PV = RT + [b - (a/RT^2)]P$; a and b are constants with values depending upon the material

$$\begin{aligned} \text{a. Pressure explicit: } P &= \frac{RT}{V - b + (a/RT^2)} \quad \text{and} \\ Z &= \frac{V}{V - b + (a/RT^2)} \end{aligned}$$

Substitution into Equation (6.17) gives

$$\begin{aligned} \ln \frac{f}{P} &= \frac{V}{V - b + (a/RT^2)} - 1 - \ln \left[\frac{V}{V - b + (a/RT^2)} \right] \\ &\quad - \frac{1}{RT} \int_{\infty}^V \left[\frac{RT}{V - b + (a/RT^2)} - \frac{RT}{V} \right] dV \\ &= \frac{b - (a/RT^2)}{V - b + (a/RT^2)} - \ln \left[\frac{V}{V - b + (a/RT^2)} \right] \\ &\quad - \ln \left[\frac{V - b + (a/RT^2)}{V} \right] = \frac{b - (a/RT^2)}{V - b + (a/RT^2)} \end{aligned}$$

TABLE 6.2 Fugacity Coefficient Expressions for Pure Components

Equation of State	Fugacity Coefficient of Pure Component $= \frac{f}{P} = \phi$	Reference
Redlich-Kwong-Soave	$\ln \phi = z - 1 - \ln \left[z \left(1 - \frac{b}{V} \right) \right] - \frac{a}{bRT} \ln \left(1 + \frac{b}{V} \right)$	Walas (1985)
Peng-Robinson	$\ln \phi = z - 1 - \ln \left(z - \frac{bP}{RT} \right) - \frac{a}{2\sqrt{2}RTb} \ln \left[\frac{z + (1 + \sqrt{2})(bP/RT)}{z + (1 - \sqrt{2})(bP/RT)} \right]$	Sandler (1999)
Virial	$\ln \phi = \frac{2PB}{zRT} - \ln z$	Sandler (1999)

b. Volume explicit: $V = \frac{RT}{P} + b - \frac{a}{RT^2}$

Substitution into Equation (6.15)

$$\begin{aligned} \ln \frac{f}{P} &= \frac{1}{RT} \int_0^P \left[b - \frac{a}{RT^2} \right] dP \\ &= \frac{1}{RT} \left[b - \frac{a}{RT^2} \right] P = \frac{b - (a/RT^2)}{V - b + (a/RT^2)} \end{aligned}$$

If we think in terms of the typical VLE displayed in Figure 6.4, the equality of pure component fugacities applies at the two extremes of composition: pure *A* at the right and pure *B* at the left of the diagram. In each case, the fugacity of the liquid must equal the fugacity of the gas. If pressure is fixed, the equality defines the temperature as the only remaining variable. At intermediate compositions, we need the fugacities as functions of composition in order to express the equilibrium criterion.

6.2.2.1.2 Mixture Fugacities The form of the equation of state is retained for mixtures and the composition dependence is placed entirely in the parameters, for example, the values of *a* and *b* in the Redlich–Kwong–Soave and the Peng–Robinson equations of state in Table 2.1. The evaluation of fugacity for a mixture begins with the definition and the fact that the partial molar quantities obey the same differential relations as the parent functions for constant composition solutions, so,

$$d\tilde{G}_i = -\tilde{S}_i dT + \tilde{V}_i dP \quad \text{at constant composition} \quad (6.22)$$

The starting point is then the differential equation that defines the fugacity, Equation (6.8), with the added restriction of constant composition:

$$d\mu_i = RT d\ln \hat{f}_i = d\tilde{G}_i = \tilde{V}_i dP \quad \text{at constant } T \text{ and composition}$$

where $\hat{f}_i \rightarrow y_i P$ as $P \rightarrow 0$ (6.23)

or

$$RT \ln \frac{\hat{f}_i}{y_i P^*} = \int_{P^*}^P \tilde{V}_i dP \quad \text{at constant } T \text{ and composition} \quad (6.24)$$

Writing the same equation for the pure component and subtracting gives

$$RT \ln \frac{\hat{f}_i}{y_i \hat{f}_i} = \int_{P^*}^P (\tilde{V}_i - V_i) dP = \int_0^P (\tilde{V}_i - V_i) dP - \int_0^{P^*} (\tilde{V}_i - V_i) dP$$

at constant *T* and composition (6.25)

The last integral is in the ideal gas region where the integrand is identically zero. Therefore,

$$RT \ln \frac{\hat{f}_i}{y_i \hat{f}_i} = \int_0^P (\tilde{V}_i - V_i) dP \quad \text{at constant } T \text{ and composition} \quad (6.26)$$

Note that for an ideal solution the integrand vanishes [see Equations (3.72) and (3.73)] so that,

$$\hat{f}_i^{\text{id}} = y_i \hat{f}_i \quad (6.27)$$

For an ideal solution, therefore, the fugacity of the pure component is sufficient to evaluate the fugacity in the mixture. This relation is called the Lewis–Randall rule.

Substituting the expression for the pure component fugacity obtained earlier into Equation (6.16) gives

$$RT \ln \frac{\hat{f}_i}{y_i P} = \int_0^P \left(\tilde{V}_i - \frac{RT}{P} \right) dP \quad \text{at constant } T \text{ and composition} \quad (6.28)$$

The partial molar volumes are obtained from the equation of state. The result transformed to the case where the equation of state is pressure explicit gives

$$\hat{f}_i = y_i P \exp \left\{ \frac{1}{RT} \int_{\underline{V}}^{\infty} \underbrace{\left[\left(\frac{\partial P}{\partial N_i} \right)_{T, \underline{V}, N_{j \neq i}} - \frac{RT}{\underline{V}} \right]}_{\text{at constant } T \text{ and composition}} d\underline{V} - \ln Z \right\} \quad (6.29)$$

Example 6.2.2.1.2-1: Calculation of the Mixture Fugacity of a Component Obeying the van der Waals Equation of State

$$P = \frac{RT}{V - b} - \frac{a}{V^2}$$

$$a = \left(\sum_j y_j \sqrt{a_j} \right)^2$$

$$P = RT \frac{N}{\underline{V} - Nb} - \frac{(\sum_j N_j \sqrt{a_j})^2}{\underline{V}^2}$$

$$\left(\frac{\partial P}{\partial N_i} \right)_{T, \underline{V}, N_{k \neq i}} = RT \frac{\underline{V}}{(\underline{V} - Nb)^2} - \frac{2\sqrt{a_i} (\sum_j N_j \sqrt{a_j})}{\underline{V}^2}$$

$$\begin{aligned}
& \int_V \left[\left(\frac{\partial P}{\partial N_i} \right)_{T, V, N_{k \neq i}} - \frac{RT}{V} \right] dV \\
&= \int_V \left[RT \frac{V}{(V - Nb)^2} - \frac{2\sqrt{a_i} \left(\sum_j N_j \sqrt{a_j} \right)}{V^2} - \frac{RT}{V} \right] dV \\
&= \left[RT \ln(V - Nb) - \frac{NbRT}{V - Nb} + \frac{2N\sqrt{a_i}\sqrt{a}}{V} - RT \ln V \right]_V^\infty \\
&= -RT \ln \frac{V - Nb}{V} + \frac{NbRT}{V - Nb} - \frac{2N\sqrt{a_i}\sqrt{a}}{V} \\
\ln \hat{\phi}_i &= -\ln \frac{V - Nb}{V} + \frac{Nb}{V - Nb} - \frac{2N\sqrt{a_i}\sqrt{a}}{RTV} - \ln z \\
\ln \hat{\phi}_i &= \frac{b}{V - b} - \ln \left[z \left(1 - \frac{b}{V} \right) \right] - \frac{2\sqrt{a_i}\sqrt{a}}{RTV}
\end{aligned}$$

Fugacity coefficients for components of a mixture obeying the equations of state listed in Table 6.1 are given in Table 6.3.

If the equation of state can be applied to gas and liquid states, the preceding results can be used to evaluate a distribution coefficient for each species, K_i , that reflects the consequences in Equation (6.31) in terms of concentrations, temperature, and pressure within the system. Starting with the equality of fugacities in Equation (6.31) with the ' phase as the vapor phase and the liquid as the '' phase as follows,

$$x'_i P \hat{\phi}'_i = x''_i P \hat{\phi}''_i \quad (6.30)$$

$$x'_i = K_i x''_i \quad (6.31)$$

where

$$K_i(T, P, x', x'') = \frac{\hat{\phi}''_i}{\hat{\phi}'_i} \quad (6.32)$$

Note that if a cubic equation of state is used, the smaller molar volume applies to the liquid. Simplifications of the

distribution coefficient using a cubic equation of state included in Figure 6.8.

Example 6.2.2.1.2-2: Distribution Coefficients for Ethane-Propylene System Using the RKS Equation of State

A liquid at 261 K and 10 bar contains 40 mol% ethane and 60 mol% propylene. The distribution coefficient for each component is desired for determining the equilibrium vapor composition over the liquid. Calculate values of the distribution coefficient corresponding to various assumptions of ideality in the two phases. Use the RKS equation of state.

Solution:

The distribution coefficients require the fugacity coefficients for the mixtures and the pure components. The possibilities are summarized in Figure 6.8 along the path originating with the cubic equation of state for the liquid.

A summary of the fugacity calculations is included here in Table 6.4. These results are assembled into distribution coefficients and reported in Figure 6.9 in the format of Figure 6.8.

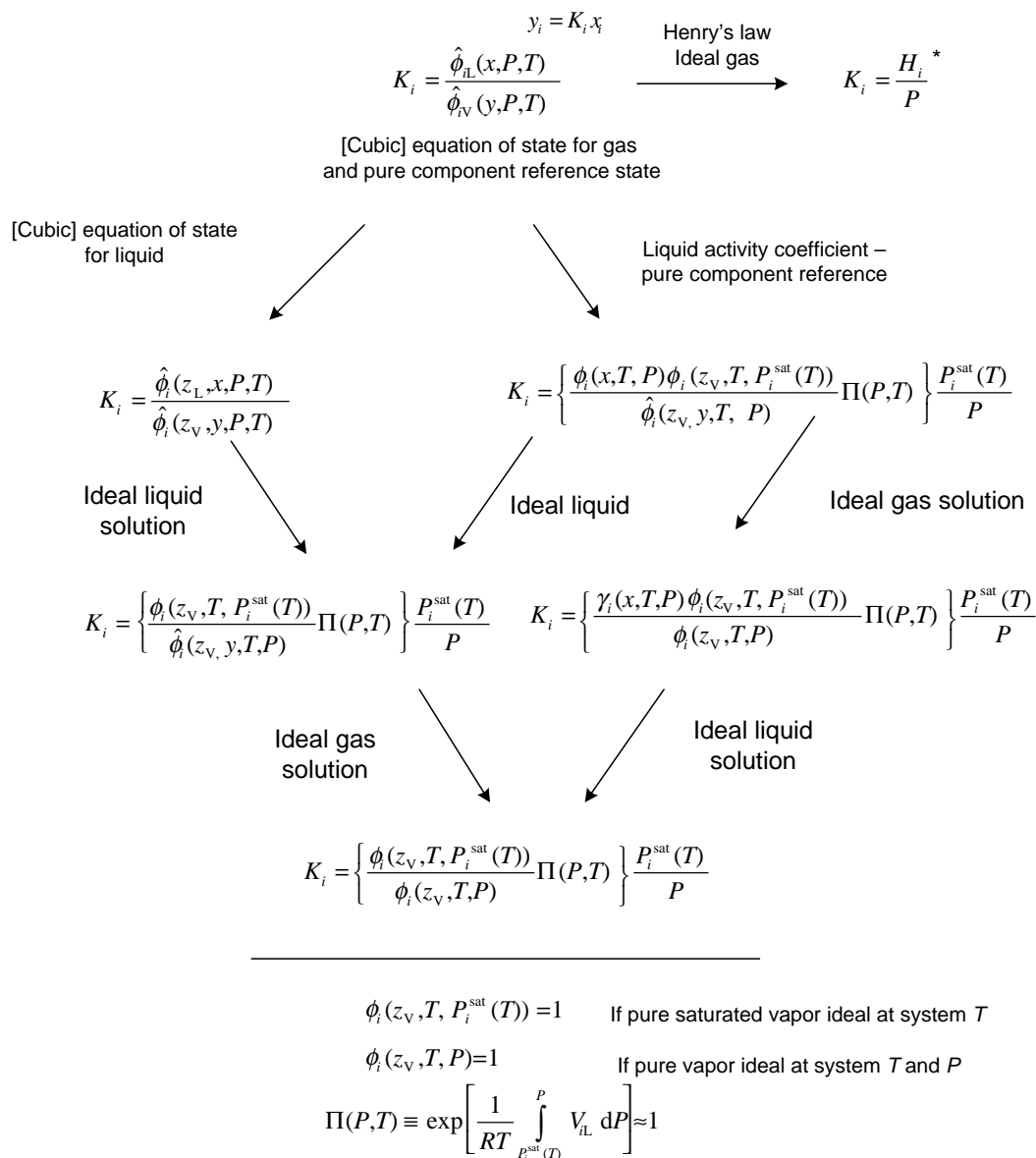
Note that both the vapor and the liquid compositions are needed to evaluate the distribution coefficients, which are not known. A direct substitution method is generally followed where Raoult's law is used to provide an initial estimate of the vapor composition and subsequent trials use new vapor fractions from the previous trial. The calculations here are the first trial.

This approach concentrates the need for data into the area of PVT measurements in pure systems and relies on the ability of the equation of state models to predict multi-component behavior in both liquids and gases.

6.2.2.2 Activity Coefficient Method Another approach to the evaluation of fugacity in liquid mixtures has been used often because of the inability of the equation of state to reflect behavior of both the vapor and the liquid state. The activity coefficient method is applied, for example, to mixtures containing alcohols, acids, and electrolytes. A standard state is chosen on the basis that the fugacity can be

TABLE 6.3 Fugacity Coefficient Expressions for Mixture Components

Equation of State	Fugacity Coefficient of Component of a Mixture = $\frac{\hat{f}_i}{y_i P} = \hat{\phi}_i$	Reference
Redlich-Kwong-Soave	$\ln \hat{\phi}_i = (z - 1) \frac{b_i}{b} - \ln \left[z \left(1 - \frac{b}{V} \right) \right] - \frac{a}{bRT} \left[\frac{b_i}{b} - \frac{2}{a} \sum_j y_j a_{ij} \right] \ln \left(1 + \frac{b}{V} \right)$	Walas (1985)
Peng-Robinson	$\ln \hat{\phi}_i = (z - 1) \frac{b_i}{b} - \ln \left(z - \frac{bP}{RT} \right) - \frac{a}{2\sqrt{2}RTb} \left[\frac{2\sum_j y_j a_{ij}}{a} - \frac{b_i}{b} \right] \ln \left[\frac{z + (1 + \sqrt{2})}{z + (1 - \sqrt{2})(bP/RT)} \right]$	Sandler (1999)
Virial	$\ln \hat{\phi}_i = \frac{2P}{zRT} \sum_j y_j B_{ij} - \ln z$	Sandler (1999)



* See some selected data for organic compounds in water in Table 6.11. Also see Figure 6.20.

FIGURE 6.8 Summary of VLE expressions.

determined and the state is consistent with the physical application. The fugacity at all other conditions is expressed as a deviation from this standard state. Attempts are then made to provide models that can

- correlate this data with a minimal set of parameters or
- produce multicomponent data on the basis of data correlation of the binary pairs or
- predict the deviations from the reference state on the basis of molecular structure.

From the definition of fugacity in Equation (6.8),

$$\tilde{G}_i(T, P, x) - \tilde{G}_i^+(T, P^+, x^+) = RT \ln \frac{\hat{f}_i(T, P, x)}{\hat{f}_i^+(T, P^+, x^+)} \quad (6.33)$$

The fugacity in Equation (6.33) and throughout this section refers to the liquid phase unless otherwise stated. The + sign indicates the reference state. Note that the reference state is at the temperature of the mixture but is otherwise arbitrary.

TABLE 6.4 Calculation of Fugacity Coefficients for Ethane–Propylene Equilibrium (Example 6.2.2.1.2-2)

Item	Units	C ₂ H ₆	C ₃ H ₆	Reference/Notes
X		0.4	0.6	Given
P	bar	10	10	Given
T	K	261	261	Given
T _c	K	305.42	364.76	<i>Chemical Properties Handbook</i> (Yaws, 1999)
P _c	bar	48.8	46.13	
Z _c		0.284	0.275	
Ω		0.099	0.142	
k ₁₂		0	0	Approximation
T _r		0.854560932	0.715538985	Definition at given temperature
P _r		0.204918033	0.216778669	Definition at given pressure
A		0.63716807	0.702273195	Table 2.1
a _i	l ² atm/g mol ²	6.188735473	10.34175572	Table 2.1
b _i	l/g mol	0.045108238	0.056990434	Table 2.1
V _{vi}	l/g mol	1.9019	1.5957	Largest root of pure component equations of state
V _{Li}	l/g mol	0.07755	0.079043	Smallest root of pure component equations of state
Z _{vi}		0.875966306	0.734938448	Definition at given temperature and pressure
Z _{Li}		0.035717539	0.036405176	Definition at given temperature and pressure
b _i P/(RT)		0.020775696	0.026248331	Intermediate convenience result
φ _v		0.888975613	0.804203579	Pure component vapor fugacity coefficient: Table 6.2
φ _L		1.355009785	0.3784647	Pure component liquid fugacity coefficient: Table 6.2
P _i ^{sat} (T)	atm	17.35	3.964	<i>Chemical Properties Handbook</i> (Yaws, 1999)
y _{est}		0.703196	0.240991	Raoult's law
Y		0.744763	0.255237	Normalize approximations from Raoult's law
a _L	l ² atm/g mol ²	8.553301	8.553301	Equation (2.13); Mixture with liquid composition
b _L	l/g mol	0.052238	0.052238	Equation (2.16); Mixture with liquid composition
V _L	l/g mol	0.076768	0.076768	Largest root of mixture (liquid x) equations of state
V _V	l/g mol	1.7592	1.7592	Smallest root of mixture (liquid x) equation of state
Z _V		0.810242	0.810242	Definition at given temperature and pressure
Z _L		0.035357	0.035357	Definition at given temperature and pressure
φ _{iL}		1.387452	0.381072	Table 6.3 fugacity coefficient in mixture with liquid composition
a _v	l ² atm/g mol ²	7.147955	7.147955	Walas (1985)
b _v	l/g mol	0.048141	0.048141	Equation (2.16); mixture with vapor composition
V _V	l/g mol	1.8472	1.8472	Largest root of mixture (vapor y) equations of state
V _L	l/g mol	0.076146	0.076147	Smallest root of mixture (vapor y) equation of state
Z _V		0.850773	0.844878	Definition at given temperature and pressure
Z _L		0.035071	0.035071	Definition at given temperature and pressure
φ _{iV}		0.900907	0.815223	Table 6.3 fugacity coefficient in mixture with vapor composition
V _V ^{sat}	l/g mol	0.93316	4.9374	Use pure component EOS for each (above) with P = saturation
Z _V ^{sat}		0.755565	0.913373	Definition at given temperature and saturation pressure
φ _{iV} ^{sat}		0.805049	0.921645	Pure component vapor fugacity coefficient: Table 6.2 at P ^{sat}

However, it is almost always the case that the reference and system pressures are the same and that the reference state is the pure component. Before evaluating the fugacity at two common reference states, we introduce some convenient definitions:

$$a_i = \frac{\hat{f}_i}{\hat{f}_i^+} \equiv \text{activity of species } i \quad (6.34)$$

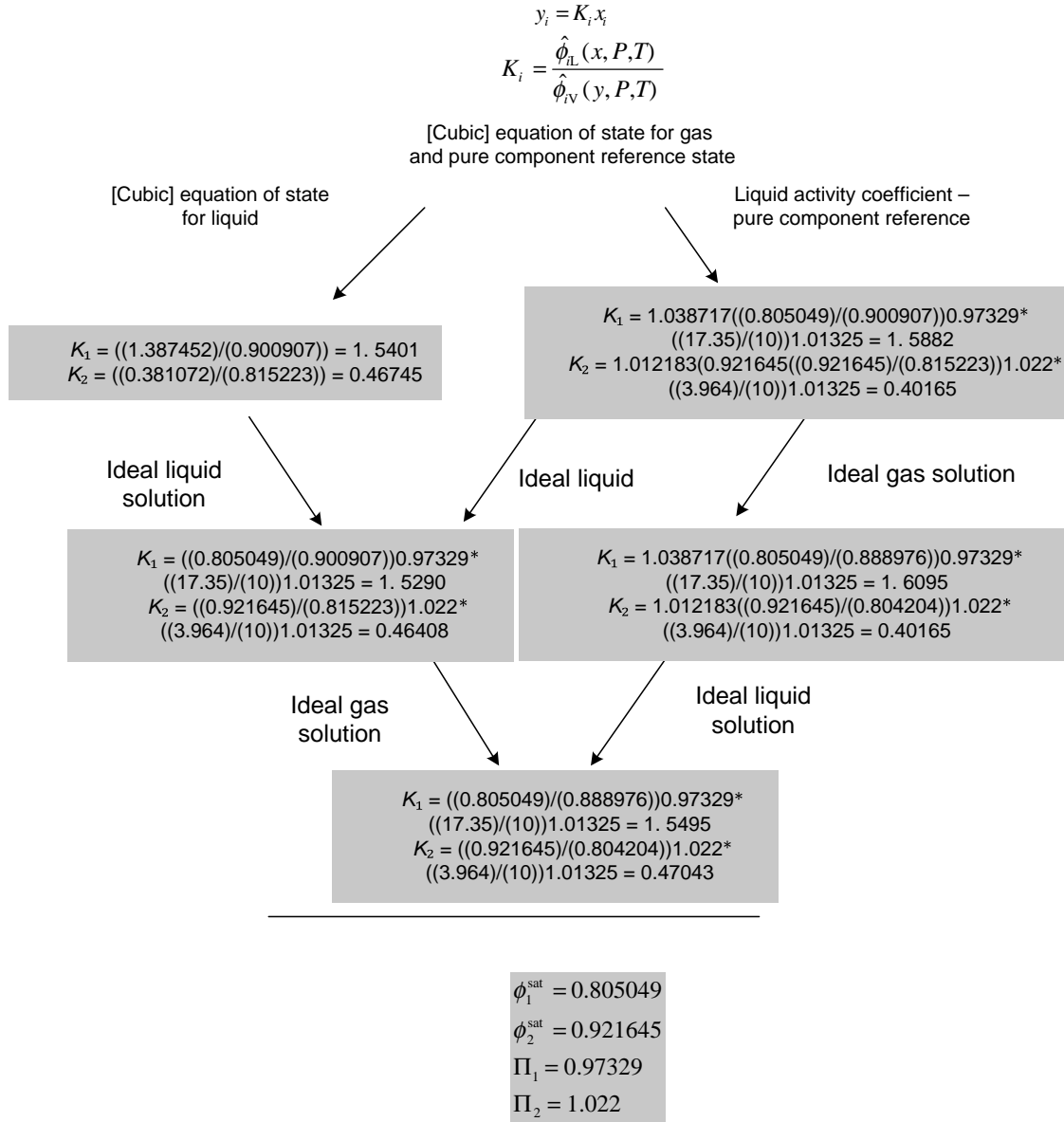
$$\hat{f}_i^{\text{id}} = x_i \hat{f}_i^+ \quad \text{ideal solution} \quad (6.35)$$

$$\gamma_i = \frac{a_i}{x_i} \equiv \text{activity coefficient} = \text{deviation from ideal behavior} \quad (6.36)$$

Note that the activity of a component in an ideal solution is the mole fraction. The liquid phase fugacity is then stated as

$$\hat{f}_i = \gamma_i x_i \hat{f}_i^+ \quad (6.37)$$

Remember that the activity coefficient and the reference state fugacity are not independent quantities.



*Ethane–propylene system at 10 bar and 261 K. The liquid mole fraction of ethane is 0.40.

FIGURE 6.9 Summary of K values from Examples 6.2.2.1.2-1 and 6.2.2.1.2-2.

Two common examples of the reference state are the pure component and infinite dilution. These reference states are discussed below for binary systems with species i as the solute under consideration.

- *Pure Component Reference State*

When the pure component at the temperature and pressure of the mixture is in the same state of aggregation, which is often the case in liquid–liquid extraction, for example, the reference state is chosen as this pure material.

$$\hat{f}_i^+(x_i^+ = 1, T, P) = f_i(T, P) \quad (6.38)$$

The fugacity of the pure liquid was calculated in Section 6.2.1.1.1. From Equation (6.21),

$$\hat{f}_i^+ = f_i^{\text{sat}} e^{(V_i^{\text{sat}}(P - P^{\text{sat}}))/RT} \quad (6.39)$$

which assumes that the molar volume of the liquid is constant at the saturation value. A slightly more general

result can be obtained that makes use of Equation (6.12) to give

$$\hat{f}_i^+ = f_i^{\text{sat}} e^{(1/RT) \int_{p^{\text{sat}}}^P V_L dP} \quad (6.40)$$

Either of the preceding two equations for the reference state fugacity may be used, but, as pointed out earlier, neither is important in almost all cases.

The fugacity of the liquid at saturation in Equation (6.40) may be replaced with the value for the gas phase, which we are assuming can be calculated from an equation of state (see, e.g., Table 6.2). In summary,

$$\hat{f}_i^+ (x_i^+ = 1, T, P) = \phi_i^{\text{sat}} P_i^{\text{sat}}(T) e^{(1/RT) \int_{p_i^{\text{sat}}(T)}^P V_{iL} dP} \quad (6.41)$$

The ideal solution definition is a generalization of the Lewis–Randall rule stated earlier in Equation (6.38) for gas mixtures:

$$\hat{f}_i^{\text{id}} = x_i f_i(T, P) \quad (6.42)$$

The limiting value of the activity coefficient as the pure solute is approached must be unity in order for the liquid fugacity to approach the correct value:

$$\lim_{x_i \rightarrow 1} \gamma_i = 1 \quad (6.43)$$

• Infinite Dilution Reference State

Another common reference state is the infinite dilution state reached by extrapolating from the dilute region to the concentrated region:

$$\hat{f}_i^+ (x_i^+ = 1, T, P) = \left. \frac{d\hat{f}_i}{dx_i} \right|_{x_i=0} \quad (6.44)$$

The tangent at the origin is extended to the pure solute to obtain the value of the reference state fugacity. The ideal solution definition for this reference state is

$$\hat{f}_i^{\text{id}} = \left. \frac{d\hat{f}_i}{dx_i} \right|_{x_i=0} x_i \quad (6.45)$$

The limiting value of the activity coefficient as the pure solvent is approached is (note the unsymmetrical comparison with Equation (6.43))

$$\lim_{x_i \rightarrow 0} \gamma_i = \lim_{x_i \rightarrow 0} \frac{\hat{f}_i}{\hat{f}_i^{\text{id}}} = \lim_{x_i \rightarrow 0} \frac{d\hat{f}_i/dx_i}{d\hat{f}_i^{\text{id}}/dx_i} = 1 \quad (6.46)$$

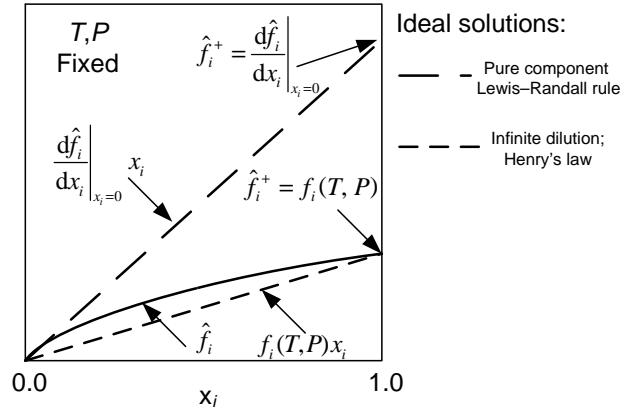


FIGURE 6.10 Features of pure component and infinite dilution reference states. (Adapted from Tester and Modell, 1997.)

A summary of the two reference states is given in Figure 6.10.

Either reference state may be used when the mutual solubility extends over the complete range as indicated in Figure 6.10. When the solubility is limited, as for gases above their critical point, the liquid phase fugacity curve does not extend to the pure solute. In these cases, Henry's law is normally employed:

$$\hat{f}_i = \gamma_i \left(\frac{d\hat{f}_A}{dx_A} \right)_{x_A=0} y_i \approx H_i(T, P) x_i \quad (6.47)$$

The derivative in the preceding equation depends only on temperature and the activity coefficient is close to unity in the dilute region. The combination is referred to as Henry's constant at a particular temperature and pressure. However, close attention must be paid in any particular application since other concentrations may be employed at the reference state as well as the inverse of Henry's constant Equation (6.47).

A primary objective in this approach is to calculate values of the activity coefficients in multicomponent mixtures from models of the liquid phase containing parameters related to the various binary pairs in the mixture. This limits data collection to only binary systems. A liquid phase model provides values of the excess Gibbs free energy, defined below, in terms of physical parameters related to the model. These parameters can then be directly related to the activity coefficients, which form the excess Gibbs free energy.

The excess Gibbs free energy is the amount remaining in the real solution after accounting for the free energy in the ideal solution. Refer to Figure 6.11 where a comparison between mixing and excess functions is given. Mixing functions were introduced in Section 3.3.4.

The excess free energy function is given by

$$G^{\text{ex}} = \sum x_i (\tilde{G}_i - \tilde{G}_i^{\text{id}}) = RT \sum x_i \ln \frac{\hat{f}_i}{\hat{f}_i^{\text{id}}} = RT \sum x_i \ln \gamma_i \quad (6.48)$$

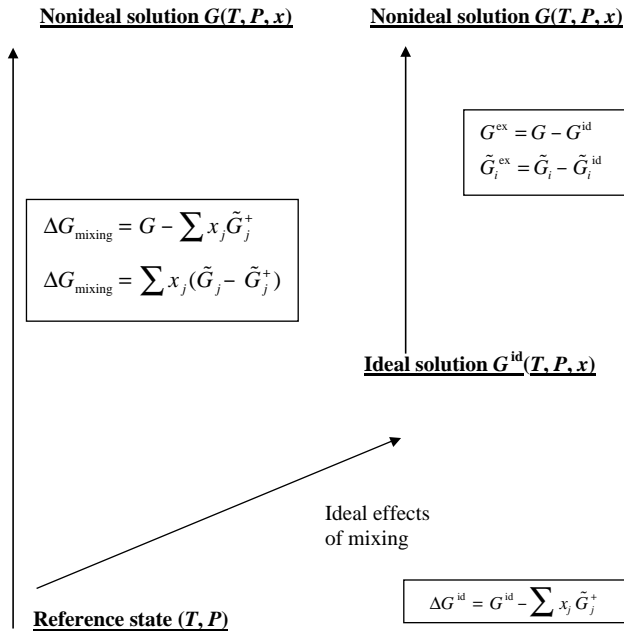


FIGURE 6.11 Mixing and excess functions.

which implies that

$$\tilde{G}_i^{\text{ex}} = RT \ln \gamma_i \quad (6.49)$$

or

$$\underbrace{\gamma_i(x, T, P)}_{\text{Experimental}} = \underbrace{e^{(1/RT)\tilde{G}_i^{\text{ex}}(\text{parameters: } x, T, P)}}_{\text{Liquid phase model}} \quad (6.50)$$

As noted above, the theoretical models generally provide an expression for the excess Gibbs free energy, which, according to Equation (6.50), provides equations for the activity coefficients that are obtained experimentally (see below). Curve fitting of the experimental data will then provide values for the model parameters, which can be used in the construction of multicomponent models or simply for binary applications.

A number of the common correlations for the activity coefficients are given in Table 6.5.

The van Laar and Margules equations represent empirical correlations. The Wilson and NRTL models provide a mechanism for constructing values of the activity coefficients in a multicomponent mixture from the binary parameters. The multicomponent generalizations are shown in Table 6.6:

TABLE 6.5 Equations for Correlating Binary Activity Coefficient Data^a

$\ln \gamma_1$ (Interchange Subscripts for Second Activity Coefficient)	Correlation; Notes
Ax_2^2	Margules
$x_2^2[A_{12} + 2x_1(A_{21} - A_{12})]$	Margules—two constant
$\frac{A_{12}}{[1 + x_1A_{12}/(x_2A_{21})]^2}$	van Laar—two constant
$-\ln(x_1 + \Lambda_{12}x_2) + x_2 \left[\frac{\Lambda_{12}}{x_1 + \Lambda_{12}x_2} - \frac{\Lambda_{21}}{x_2 + \Lambda_{21}x_1} \right]$	Wilson—two constant
$\frac{x_2^2\tau_{21}G_{21}^2}{(x_1 + G_{21}x_2)^2} + \frac{x_2^2\tau_{12}G_{12}}{(x_2 + G_{12}x_1)^2}$	NRTL—three constant $\ln G_{ij} = -\alpha\tau_{ij}$

Source: Sandler (1999).

^aThe important UNIQUAC (Universal Quasi-Chemical Equation) is available elsewhere (e.g., Poling et al., 2001).

TABLE 6.6 Multicomponent Generalizations of Binary Correlation Function (Sandler, 1999; Tester and Modell, 1997)

$\ln \gamma_i =$	
Wilson: $1 - \ln \left(\sum_{j=1}^{N_c} x_j \Lambda_{ij} \right) - \sum_{j=1}^N \frac{x_j \Lambda_{ji}}{\sum_{k=1}^{N_c} x_k \Lambda_{jk}}$	$\Lambda_{ii} = \Lambda_{jj} = 1$ $\Lambda_{ij} = \frac{V_j}{V_i} \exp \left(\frac{\lambda_{ij}}{RT} \right)$
NRTL: $\frac{\sum_{j=1}^{N_c} \tau_{ji} G_{ji} x_j}{\sum_{j=1}^{N_c} G_{ji} x_j} + \sum_{j=1}^{N_c} \frac{x_j G_{ij}}{\sum_{k=1}^{N_c} x_k G_{kj}} \left[\tau_{ij} - \frac{\sum_{k=1}^{N_c} x_k \tau_{kj} G_{kj}}{\sum_{k=1}^{N_c} x_k G_{kj}} \right]$	$\tau_{ji} = \frac{g_{ji} - g_{ii}}{RT}$ $\tau_{ii} = \tau_{jj} = 0$ $G_{ji} = \exp(-\alpha_{ji} \tau_{ji}) \sum_{i=1}^n X_i$ $G_{ji} = G_{jj} = 0$

6.2.2.2.1 Determination of Model Parameters from VLE Data Activity coefficients can be determined experientially in a number of ways. Osmotic pressure measurements can yield activity coefficients (see Section 10.3). A common approach to extract experimental values of the activity coefficients extracted from a full set of vapor-liquid equilibrium data (T, P, x, y) and an equation of state for the vapor phase. For example, with the pure component reference state,

$$\hat{f}_i^V = \hat{f}_i^L = \gamma_i x_i \hat{f}_i^L \quad (6.51)$$

The activity coefficient is the only unknown in the preceding equation since the compositions, temperature, and pressure are presumed to be measured and the fugacity in the vapor phase can be calculated from the equation of state. For example, suppose the gas phase is ideal ($\hat{f}_i^V = y_i P$). The expression for the liquid phase fugacity can be obtained from Equation (6.41), assuming that the Poynting correction factor is negligible. Consequently,

$$y_i P = \gamma_i x_i P_i^{\text{sat}}(T) \quad (6.52)$$

Suppose that *VLE data* are obtained at a fixed pressure in a binary system. This means that a full set of x, y, T data are obtained. The pressure in most cases can be selected so that ideal behavior in the gas phase may be assumed. Also it can be noted that liquid phase properties are not significantly affected by pressure. The vapor pressures can be added to the data or extracted from the data at the concentration extremes. Vapor pressure data are often correlated with a variation of the extended Antoine equation:

$$\ln P^{\text{sat}} = k_1 + \frac{k_2}{k_3 + T} + k_4 T + k_5 \ln T + k_6 T^{k_7} \quad (6.53)$$

The Gibbs phase rule states that we have two degrees of freedom in this case. Consequently, if, for example, x and P are fixed, then the equilibrium relationships provide the means to calculate the vapor phase mole fractions and the temperature if the parameters associated with the activity coefficients were known. Comparison of the calculated values with the measured values of the vapor phase mole fractions and the temperature for various values on the parameters in the model leads to their best values in terms of data correlation. This means that the model parameters are determined to minimize the residuals.

$$\sum_{\text{data points}} (y - y^+)^2, \quad \sum_{\text{data points}} (T - T^+)^2 \quad (6.54)$$

where $+$ indicates a calculated value and its absence indicates a measured value.

A minimal set of data can be used in some cases to estimate the model parameters, but each case is an attempt to represent a full range of behavior from a single interior or boundary value. For example, if an azeotrope is present, the

activity coefficients for the two components are given at the azeotrope by

$$\gamma_i^{\text{az}} = \frac{P}{P_i^{\text{sat}}(T_{\text{az}})} \quad (6.55)$$

These values are sufficient to determine the model parameters, in those cases where there are only two and their temperature dependence is ignored. For example, the two parameters in the van Laar equation can be evaluated in this fashion with the azeotropic data.

$$A_{12} = \ln \gamma_1^{\text{az}} \left[1 + \frac{x_2^{\text{az}} \ln \gamma_2^{\text{az}}}{x_1^{\text{az}} \ln \gamma_1^{\text{az}}} \right]^2; \quad A_{21} = \ln \gamma_2^{\text{az}} \left[1 + \frac{x_1^{\text{az}} \ln \gamma_1^{\text{az}}}{x_2^{\text{az}} \ln \gamma_2^{\text{az}}} \right]^2 \quad (6.56)$$

Activity coefficients at vanishingly small concentrations, “infinite dilution” values, can be used in a similar fashion since the models take on simpler forms under these dilute conditions. For example, for the Wilson equation

$$\begin{aligned} \lim_{x_1 \rightarrow 0} (\ln \gamma_1) &= \ln \gamma_1^\infty = 1 - \ln \Lambda_{12} - \Lambda_{21} \\ \lim_{x_2 \rightarrow 0} (\ln \gamma_2) &= \ln \gamma_2^\infty = 1 - \ln \Lambda_{21} - \Lambda_{12} \end{aligned} \quad (6.57)$$

and the van Laar equation:

$$\begin{aligned} A_{ij} &= \ln \gamma_i^\infty \quad x_i = 0 \\ A_{ji} &= \ln \gamma_j^\infty \quad x_j = 0 \end{aligned} \quad (6.58)$$

Finally, reported data for activity coefficients can be tested for thermodynamic consistency. This amounts to applying the slope and area properties of all partial molar quantities specified by the Gibbs–Duhem equation (3.17). In the present case, the thermodynamic function is the excess Gibbs free energy for which the Gibbs–Duhem equation is given by

$$x_1 d\tilde{G}_1^{\text{ex}} + x_2 d\tilde{G}_2^{\text{ex}} = 0 \quad \text{at constant } T \text{ and } P \quad (6.59)$$

The activity coefficients must comply with this relation since

$$d\tilde{G}_i^{\text{ex}} = d(\tilde{G}_i - \tilde{G}_i^{\text{id}}) = RT d \ln \frac{\hat{f}_i}{\hat{f}_i^{\text{id}}} = RT d \ln \gamma_i \quad (6.60)$$

which, when substituted into the preceding equation, gives

$$x_1 d \ln \gamma_1 + x_2 d \ln \gamma_2 = 0 \quad \text{at constant } T \text{ and } P \quad (6.61)$$

or

$$x_1 \frac{d \ln \gamma_1}{d x_1} = -x_2 \frac{d \ln \gamma_2}{d x_1} \quad \text{at constant } T \text{ and } P \quad (6.62)$$

This result implies that the slopes of the $\ln \gamma$ versus x curves

- have opposite signs and
- the slope of each approaches zero as the associated mole fraction approaches one.

Also, at constant T and P , Equation (3.18) written in terms of intensive quantities and applied to the excess Gibbs free energy gives

$$dG^{\text{ex}} = \tilde{G}_1^{\text{ex}} dx_1 + \tilde{G}_2^{\text{ex}} dx_2 \quad (6.63)$$

Since the excess Gibbs free energy vanishes at the composition extremes, integration of this result gives

$$0 = \int_0^1 \tilde{G}_1^{\text{ex}} dx_1 - \int_0^1 \tilde{G}_2^{\text{ex}} dx_1 \quad (6.64)$$

or

$$\int_0^1 \ln \gamma_1 dx_1 = \int_0^1 \ln \gamma_2 dx_1 \quad (6.65)$$

which requires that the areas under the two curves be equal.

Example 6.2.2.1-1: Wilson Parameters for Isopropyl Alcohol (OH)–Water (W) System

Estimate the parameters in the Wilson equation for both components at 1 atm (Tables 6.7 and 6.8). The following VLE and vapor pressure data are available (Seader and Henley, 2006):

Composition of azeotrope: $x = y = 0.6854$.

Boiling point of azeotrope = 80.22 °C.

A Txy diagram of the data is given in Figure 6.6. A $y-x$ diagram is given below in Figure 6.12. Assuming an ideal

TABLE 6.7 Vapor Pressures of OH and W

P^s (Torr)	200.00	400.00	760.00
OH (°C)	53.00	67.80	82.50
W (°C)	66.50	83.00	100.00

TABLE 6.8 Vapor–Liquid Equilibrium for the OH–W System at 1.0 atm

t (°C)	$100x_{\text{OH}}$	$100y_{\text{OH}}$
100.00	0.00	0.00
93.00	1.18	21.95
89.75	3.22	32.41
84.02	8.41	46.20
83.85	9.10	47.06
82.12	19.78	52.42
81.64	28.68	53.44
81.25	34.96	55.16
80.62	45.25	59.26
80.32	60.30	64.22
80.16	67.94	68.21
80.21	68.10	68.26
80.28	76.93	74.21
80.66	85.67	82.70
81.51	94.42	91.60
82.50	100.00	100.00

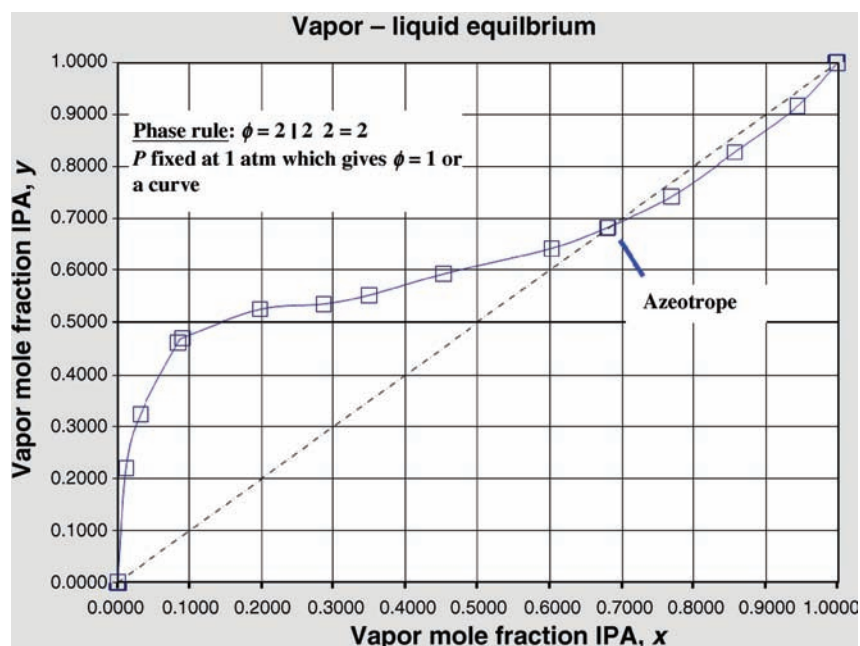


FIGURE 6.12 Equilibrium data for isopropyl alcohol (IPA)–water (W) system at 1 atm.

TABLE 6.9 Antoine Constants for OH-W System

Parameter in Equation (6.35)	OH	W
k_1	25.017	18.485
k_2	-8010	-3922
k_3	80.078	-42.45

gas, we can compute the activity coefficients for each component using Equation (6.33) (Table 6.9)

$$yP = \gamma x P^{\text{sat}}$$

The pure component reference state can be used for each component. We need to fit the vapor pressure data to a function of temperature in order to interpolate at intermediate points.

Using first two terms of the extended Antoine equation [Equation (6.33)].

The activity coefficients at infinite dilution can be used to calculate the parameters in the Wilson model [see Equation (6.33)]. These values are, however, indeterminate from Equation (6.33) at the composition extremes. The values may be estimated on the basis that fit of Wilson equation to the data is maximized. We will carry out this process visually by observing the goodness of fit graphically at selected values of the activity coefficients at infinite dilution.

Calculations using Excel

Plot activity coefficients and estimate values at infinite dilution. Calculate model parameters using Equation (6.49). Repeat until a “good” fit is obtained.

Approximate values are

$$\gamma_{\text{OH}}^{\infty} = 12.75$$

$$\gamma_{\text{W}}^{\infty} = 3.5$$

Wilson parameters using the preceding estimates for the values at infinite dilution are given by

$$\ln 12.75 = 1 - \ln \Lambda_{12} - \Lambda_{21}$$

$$\ln 3.50 = 1 - \ln \Lambda_{21} - \Lambda_{12}$$

$$\Lambda_{12} = 0.10603, \quad \Lambda_{21} = 0.69852$$

The Wilson model with these parameters was used to calculate the activities in Table 6.10 and Figure 6.13.

The azeotropic data may also be used to correlate the data. At the azeotrope, Equation (6.37) applies to each component:

$$\gamma_{\text{OH}}^{\text{az}} = \frac{P}{P_{\text{OH}}^{\text{sat}}} = \frac{760}{\exp \left[25.017 - \left(\frac{8010.6}{88.078 + 273.16 + 80.22} \right) \right]} = 1.1019$$

t (°C)	100 x_{OH}	100 y_{OH}	x_{OH}	y_{OH}	T (K)	$P_{\text{OH}}^{\text{sat}}$	γ_{OH}	$P_{\text{W}}^{\text{sat}}$	γ_{W}
100.00	0.00	0.00	0.0000	0.0000	373.16	1545.097	$\gamma_{\text{OH}}^{\infty}$	759.6325	1.0005
93.00	1.18	21.95	0.0118	0.2195	366.16	1170.976	12.0731	587.9832	1.0209
89.75	3.22	32.41	0.0322	0.3241	362.91	1026.481	7.4522	520.0768	1.0206
84.02	8.41	46.20	0.0841	0.4620	357.18	809.910	5.1549	416.3136	1.0723
83.85	9.10	47.06	0.0910	0.4706	357.01	804.160	4.8874	413.5229	1.0704
82.12	19.78	52.42	0.1978	0.5242	355.28	747.677	2.6938	386.0047	1.1678
81.64	28.68	53.44	0.2868	0.5344	354.80	732.645	1.9329	378.6483	1.3103
81.25	34.96	55.16	0.3496	0.5516	354.41	720.631	1.6640	372.7583	1.4056
80.62	45.25	59.26	0.4525	0.5926	353.78	701.594	1.4186	363.4066	1.5562
80.32	60.30	64.22	0.6030	0.6422	353.48	692.688	1.1685	359.0232	1.9078
80.16	67.94	68.21	0.6794	0.6821	353.32	687.979	1.1091	356.7037	2.1127
80.21	68.10	68.26	0.6810	0.6826	353.37	689.447	1.1049	357.4272	2.1156
80.28	76.93	74.21	0.7693	0.7421	353.44	691.508	1.0602	358.4421	2.3703
80.66	85.67	82.70	0.8567	0.8270	353.82	702.789	1.0439	363.9944	2.5207
81.51	94.42	91.60	0.9442	0.9160	354.67	728.621	1.0119	376.6763	3.0373
82.50	100.00	100.00	1.0000	1.0000	355.66	759.771	1.0003	391.9133	$\gamma_{\text{W}}^{\infty}$

TABLE 6.10 Calculated Values of Activity Coefficients

$z\gamma_{\text{OH}}, \text{ calc}$	$\gamma_{\text{w}}, \text{ calc}$
12.7498 ^b	1.0000
10.5405	1.0011
8.0233	1.0072
4.8918	1.0374
4.6464	1.0426
2.6317	1.1437
1.9705	1.2534
1.6953	1.3442
1.4093	1.5200
1.1790	1.8521
1.1093	2.0648
1.1081	2.0696
1.0534	2.3649
1.0198	2.7221
1.0029	3.1633
1.0000	3.5000 ^b

^aEstimated-visual fit.

Similarly for water

$$\gamma_{\text{w}}^{\text{az}} = \frac{P}{P_{\text{sat}}^{\text{w}}} = \frac{760}{\exp\left[18.485 - \left(\frac{3922.0}{-42.25 + 273.16 + 80.22}\right)\right]} = 2.1254$$

Solving for the two Wilson parameters that will produce the preceding two values at the azeotrope ($x = 0.6854$)

$$\begin{aligned} \ln 1.1019 &= -\ln(x + a(1-x)) \\ &+ (1-x)\left(\frac{a}{x + a(1-x)} - \frac{b}{(1-x) + bx}\right) \\ \ln 2.1254 &= -\ln(1-x + bx) \\ &-x\left(\frac{a}{x + a(1-x)} - \frac{b}{(1-x) + bx}\right) \end{aligned}$$

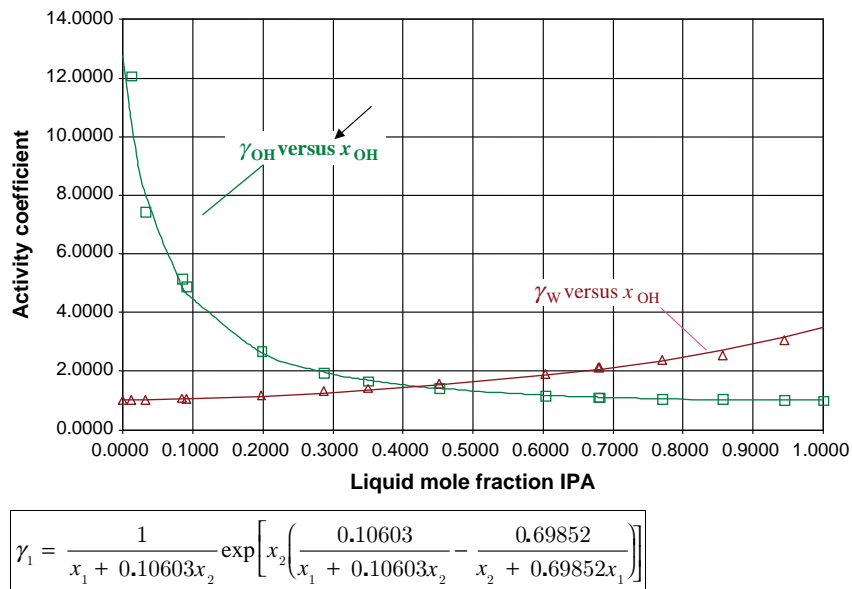
Solution: $a = 0.07256$ and $b = 0.71921$.

The correlation with the data is shown in Figure 6.14. The correlations shown in Figures 6.13 and 6.14 are remarkable when it is considered that only one point per curve was used.

However, the first correlation does not pinpoint the azeotrope (Where does it predict the azeotrope will occur?) and the second is inferior with respect to the values at infinite dilution (What values does it predict?).

The calculations presented here are more to the point of preparing for analysis that uses all of the data and, for example, minimizes the residuals shown in Equation (6.36). This preparation involves the selection of candidate models and approximate initial values for search routines. It may also be the case that only approximate values are needed.

In predictive models, the regular solution model for liquids assumes that the excess entropy and excess volume vanish and results in an expression for the excess Gibbs free energy as in terms of the volume fractions and solubility parameters. A correction for molecular size differences is included.

**FIGURE 6.13** Data correlation using estimated activities at infinite dilution.

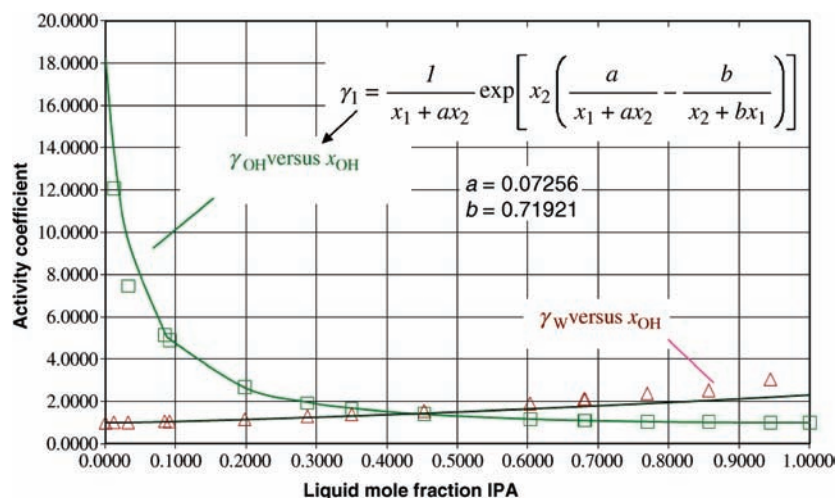


FIGURE 6.14 Data correlation using activities at azeotrope.

The UNIFAC (UNIQUAC Functional Group Activity Coefficients) method uses the UNIQUAC correlation for the activity coefficients. The idea is to use phase equilibrium data to determine parameters that characterize interactions between structural groups and then to use these parameters in unknown systems with the same functional groups (Poling et al., 2001).

Example 6.2.2.1-2: Distribution Coefficients of Ethane–Propylene System Using the RKS Equation of State and Wilson Model

Refer to the conditions in Example 6.2.2.1.2-1. Recalculate the distribution coefficient using the Wilson model for the activity coefficient.

Solution: The activity coefficients for ethane (1) and propylene (2) for the conditions stated in Example 6.2.2.1.2-1 are

$$\begin{aligned}\gamma_1 &= 1.038717 \\ \gamma_2 &= 1.012183\end{aligned}$$

These values were obtained with Aspen using the UNIFAC estimates for the Wilson parameters.

The calculations of the distribution coefficients using these estimates and the results in Table 6.4 are shown in Figure 6.9.

6.2.2.3 Summary of VLE Expressions and Data The expressions in Figure 6.8 are a summary of the discussion in Section 6.2.1 on VLE. The summary can be judiciously used to express the equilibrium relations in terms of concentration, temperature, and pressure, which were originally expressed as the equality of the chemical potentials and subsequently as equality of the individual fugacities between phases. Although the current focus is on vapor–liquid systems, some aspects will be seen to carry over to liquid–liquid and

fluid–solid systems. Some data for particular circumstances are presented in Figure 6.15a and b and Table 6.11.

The charts (called Depriester charts) in Figure 6.15a and b were prepared with an average composition allowance and provide good engineering approximations. If the molecular force fields for light hydrocarbons are simple and not significantly interactive, the resulting K values are weak functions of composition. More extensive charts are also available (e.g., Hadden and Grayson, 1961). Table 6.11 contains solubility data and Henry’s law parameters for a variety of compounds.

Example 6.2.2.3-1: Comparison of Several Methods for Obtaining the K Values for an Equimolar Mixture of Ethane, Propane, and n -Butane at -70°F and 300 psi

Solution: Aspen Plus was used for the last three rows of the following table. In those cases, the first reference is to the liquid phase model and the second is to gas phase model. Peng–Robinson was used for both phases. The largest discrepancy is for n -butane. Can you offer an explanation?

Component	C_2H_6	C_3H_8	$n\text{-C}_4\text{H}_{10}$
$P = 200 \text{ psi}, T = -70^\circ\text{F}, x_i = 0.333333$			
$P^{\text{sat}} (\text{psi})^a$	62.5300	7.3380	0.9071
P^{sat}/P	0.31270	0.03669	0.00454
Chart	0.37000	0.04000	0.00750
W–RK	0.38220	0.71570	0.01320
U–RK	0.36700	0.07144	0.01280
PR–WS	0.33220	0.07340	0.01555

W–RK = Wilson–Redlich–Kwong; U–RK = UNIQUAC–Redlich–Kwong; PR–WS = Peng–Robinson–Woo–Sandler mixing rules.

^a Green and Maloney (1997).

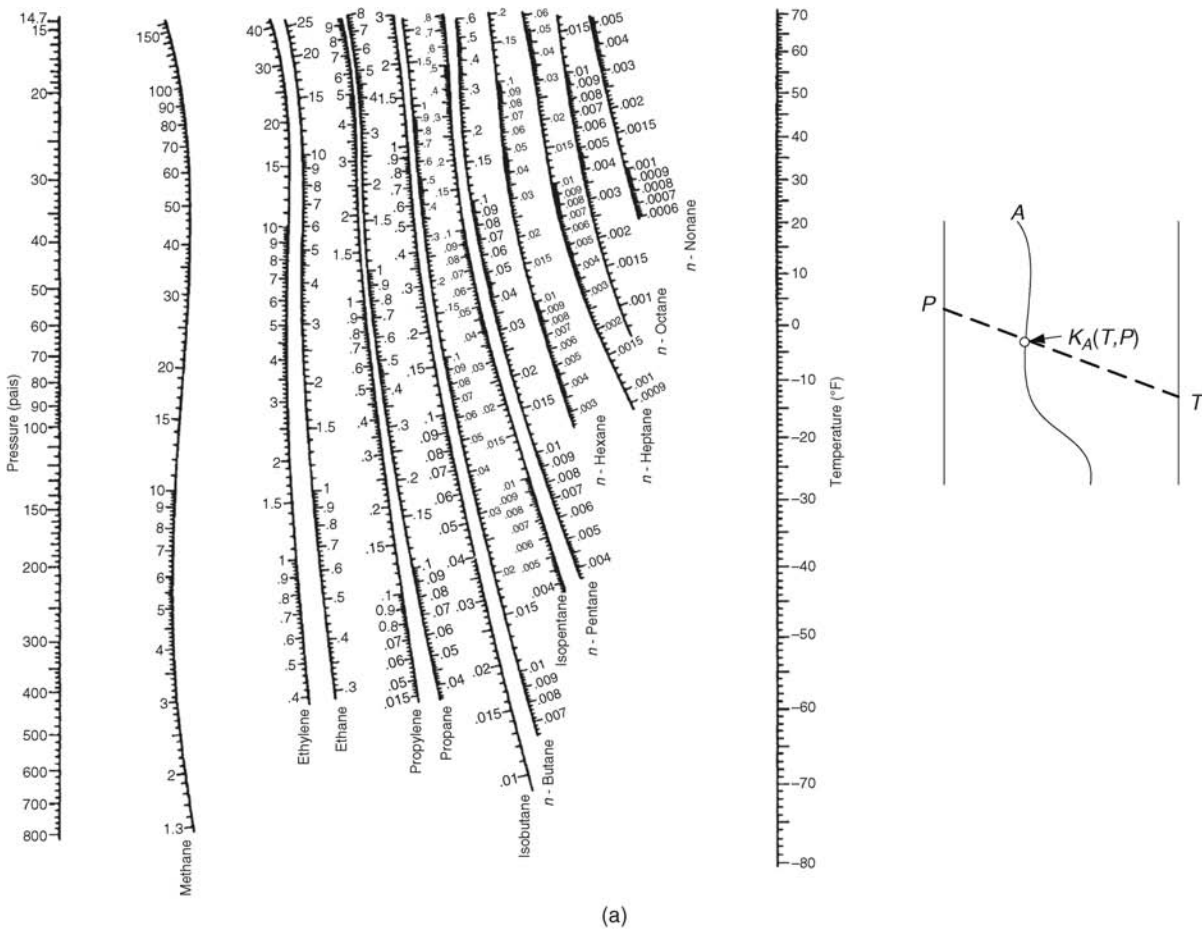


FIGURE 6.15 DePriester chart (Green and Maloney, 1997). K values for light hydrocarbon systems (a) at low temperatures and (b) at high temperatures. Reprinted with permission of McGraw-Hill.

$$\phi_1^{\text{sat}} = 0.805049$$

$$\phi_2^{\text{sat}} = 0.921645$$

$$\Pi_1 = 0.97329$$

$$\Pi_2 = 1.022$$

We are now prepared to describe the equilibrium state that under ideal conditions is reached in a single equilibrium stage, which is generally described in Figure 6.1 and in Figures 6.2 and 6.3 for the particular operations of gas absorption and stripping and flash vaporization and condensation.

6.2.3 Gas Absorption and Stripping

An equilibrium stage for gas absorption is illustrated in Figure 6.2. In the limit that the gas phase solvent (C) is insoluble in the liquid phase solvent (B) and the liquid phase solvent is nonvolatile, only the gas phase impurity crosses the gas-liquid interface. Under these circumstances, the

equilibrium relation may be expressed in terms of mole fractions for A :

$$y_A = K_A x_A \quad (6.66)$$

where, for example,

$$K_A = \frac{\gamma_A^{\text{sat}} P_A^{\text{sat}}(T)}{\hat{\phi}_A P} \quad (6.67)$$

which neglects the Poynting correction factor and assumes that the pure component vapor is ideal at saturation. The integrity of the gas and liquid phases is otherwise maintained by

$$y_A + y_C = 1 \quad (6.68)$$

and

$$x_A + x_B = 1 \quad (6.69)$$

respectively.

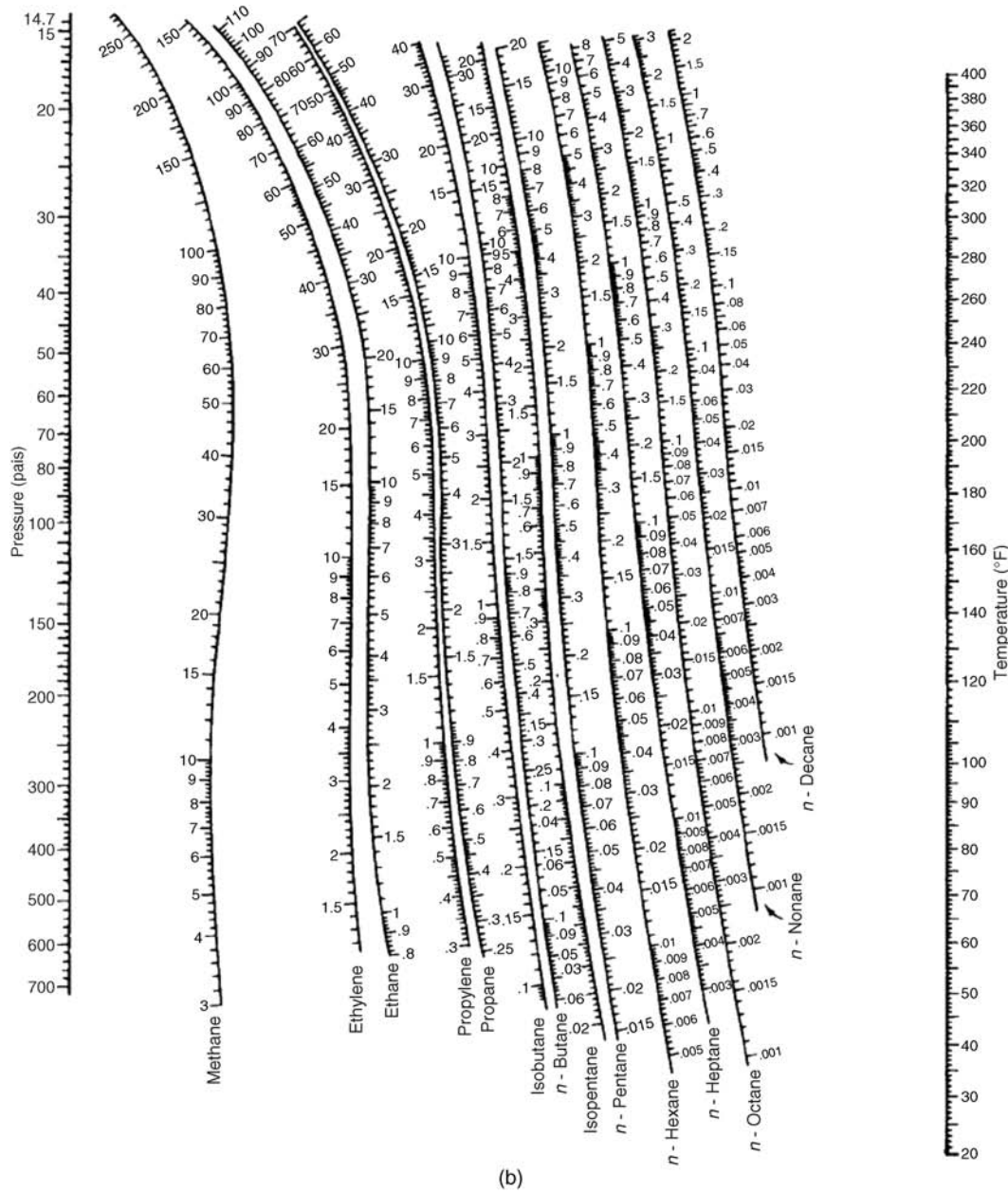


FIGURE 6.15 (Continued)

If C is soluble in B or if B is volatile, the corresponding mole fraction stipulation must in general be replaced with a phase equilibrium expression analogous to that for A . When considering if this replacement is necessary, the following approximations may be helpful:

- If C is slightly soluble in the liquid and the gas phase is ideal and consists mostly of C then

$$x_C \approx \frac{P}{\gamma_C^\infty P_C^{\text{sat}}(T)} \quad (6.70)$$

- If the liquid solution is dilute, B is slightly volatile, and the gas phase is ideal, then

$$y_B \approx \frac{P_B^{\text{sat}}}{P} \quad (6.71)$$

We are considering an equilibrium stage at a fixed temperature and pressure. The pressure may be fixed by the condition of the inlet streams or the pressure may be augmented with pumping and compression. The mechanical energy balance will be needed for these calculations. The

TABLE 6.11 Selected Solubility Data and Henry's Constants in Water (Yaws, 1999)

Substance	Molecular Weight	Boiling Point (K)	Temperature (°C)	Henry's Law Constant		Solubility Mass Basis (ppmw)
				Mole Fraction Basis: (atm/mole fraction)	Mole Basis (atm m ³ /mol)	
Acetone	58.08	329.44	25	3.6505	0.000065709	1,000,000
Acrolein	56.064	325.84	20	4.557	0.000082025	211,000
Acrylic acid	72.064	414.15	25	0.022397	4.0314E-07	1,000,000
Benzene	78.114	353.24	25	308.26	0.0055486	1,755
<i>n</i> -Butyl mercaptan	90.189	371.61	25	499.32	0.0089877	600
Carbon dioxide	44.01	194.67	25	1212.2	0.02182	1,950
Carbon disulfide	76.143	319.37	25	5817.4	0.10471	1,879
Carbon monoxide	28.01	81.7	25	63364	1.1405	23.77
Carbon tetrachloride	153.822	349.79	25	1629.9	0.029338	785.7
Chloroform	119.377	334.33	25	227.84	0.0041011	7,500
Cumene	120.194	425.56	25	798.42	0.014371	50
Cyclohexane	84.161	353.87	25	10785	0.19412	56.1
<i>n</i> -Decane	142.285	447.3	25	285080	5.1314	0.052
Diethylamine	73.138	328.6	25	3.9376	0.000070875	1,000,000
Diethyl ether	74.123	307.58	25	45.412	0.00081741	60,880
Dimethyl ether	46.069	248.31	18	36.909	0.00066435	65,180
<i>n</i> -Dodecane	170.338	489.47	25	456190	8.2113	0.0037
Ethane	30.07	184.55	25	26770	0.48186	60.4
Ethyl acrylate	100.117	372.65	25	13.874	0.00024973	73720
Ethylamine	45.084	289.73	20	1.4442	0.000025995	1,000,000
Ethylene glycol	62.068	470.45	25	0.00010506	1.8911E-09	1,000,000
Ethyl mercaptan	62.136	308.15	25	160.77	0.0028938	14,780
1-Heptene	98.188	366.79	25	22220	0.39996	18.16
1-Hexanol	102.177	430.15	25	1.1721	0.000021097	5,875
Isopropanol	60.096	355.41	25	0.68936	0.000012408	1,000,000
Methane	16.043	111.66	25	35356	0.6364	24.4
Methanol	32.042	337.85	25	0.28851	5.1932E-06	1,000,000
Nitroglycerine	227.088	523	20	0.0054644	9.8359E-08	1,380
<i>n</i> -Pentane	72.15	309.22	25	70302	1.2654	38.5
Phenol	94.113	454.99	25	0.042199	7.5958E-07	80,190
Propane	44.096	231.11	25	37998	0.68396	62.4
Propylene	42.081	225.43	25	11313	0.20363	200
Tetrahydrofuran	72.107	338	20	2.9242	0.000052635	1,000,000
Vinyl acetate	86.09	345.65	25	27.631	0.00049735	25,530
Vinyl chloride	62.499	259.78	25	1243.7	0.022387	2,697
<i>m</i> -Xylene	106.167	412.27	25	376.53	0.0067775	174

Note: Pressure in mmHg. Do not use for CO₂ and H₂S above 1 atm. ppmw = parts per million by weight; ppmm = parts per million by mole.

energy balance may be solved separately to determine the heat duty required to maintain the specified temperature. We are concerned here only with the mass balances.

6.2.3.1 Mass Balance—Constant Total Flows Consider a single stage consisting of a stirred vessel with internals that distribute the gas, promote mixing, and minimize the quantity of liquid that is carried overhead. The situation is depicted in Figure 6.16.

As implied in Figure 6.16, the total molar flow rates of the liquid and gas streams are assumed constant. The inevitable change is assumed to be a small fraction of

the total flow. This assumption will be alleviated later. The liquid phase mole fractions are denoted by x and y denotes a gas phase mole fraction. These mole fractions pertain to any component so that every component is being absorbed or stripped.

The degrees of freedom based for an equilibrium stage that satisfies the mass balances are computed as follows in terms of total molar flows and mass fractions:

- Unknowns = $2 + 4 N_c$ (N_c mole fractions in each stream and two flows)
- Mass balances = N_c

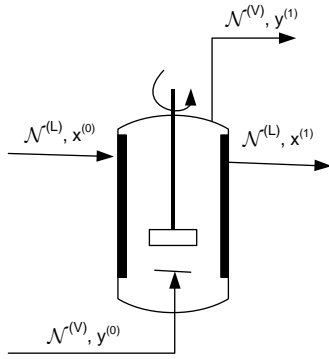


FIGURE 6.16 Single-stage gas absorption.

- Mole fraction summations = 2 (2 are automatically satisfied by constant flow assumptions)
- Equilibrium between outlet streams = N_c

$$\text{Degrees of freedom} = 2N_c$$

The degrees of freedom for a typical absorption problem are satisfied as follows:

- Gas feed: flow (1) and mole fractions $(N_c - 1) = N_c$
- Solvent composition (mole fractions) = $N_c - 1$
- Desired mole fraction of key component in gas product = 1

$$\text{Total specifications} = 2N_c$$

A mass (molar) balance on the key component is given by

$$y^{(1)} = -\frac{N^{(L)}}{N^{(V)}}x^{(1)} + \left[y^{(0)} + \frac{N^{(L)}}{N^{(V)}}x^{(0)} \right] \quad (6.72)$$

This result states that the outlet mole fractions lie on a straight line of slope $-N^{(L)}/N^{(V)}$ that passes through the inlet point $(x^{(0)}, y^{(0)})$. Refer to Figure 6.17. The straight line represents the material balance and is called the “operating line” for the single stage. Equilibrium requires that the point representing the outlet concentrations must also fall on the equilibrium curve. The intersection of the mass balance and the equilibrium curve is then provided by the value of $y^{(1)}$, since this value is specified.

The slope will give the liquid flow rate required to achieve the desired outlet mole fraction of the key component. This flow rate can then be used to determine the remaining mole fractions with the same graphical construction, except that the slope is known and the intersection with the equilibrium curve is unknown. If a component is being stripped, the input point will lie below the equilibrium curve.

Note that the absorption of the key component increases with a relative increase of the liquid rate. However, the result

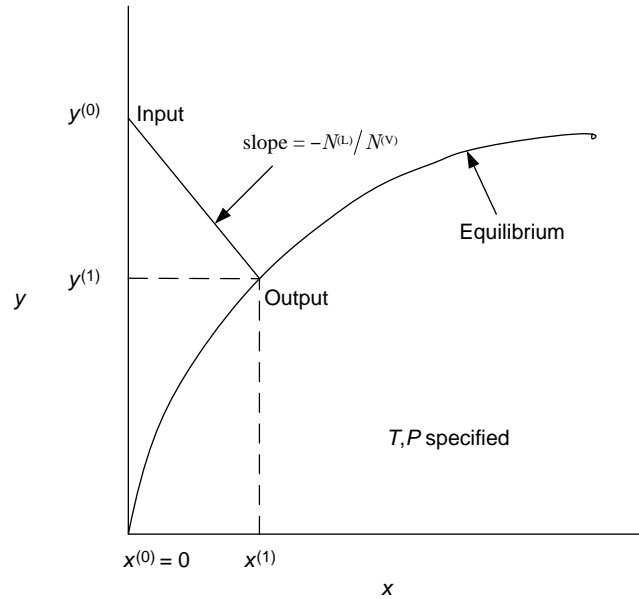


FIGURE 6.17 Graphical solution for single equilibrium stage.

is that more solvent must be treated before reuse in the absorption stage and the cost of this treatment increases with both the quantity of solvent and the dilution of the impurity. The reader might consider how to represent a second equilibrium stage in series with the first.

We are presuming that the equilibrium curve primarily depends on the concentration of a single species. If the equilibria can be expressed as a straight line, that is,

$$y_i = K_i x_i, \quad K_i \approx \text{constant} \quad (6.73)$$

Equation (6.72) can be solved for the outlet conditions:

$$\phi_{Ai} = \frac{1}{1 + A_i} + \frac{x_i^{(0)} N^{(L)}}{y_i^{(0)} N^{(V)}} \frac{1}{1 + A_i} \quad (6.74)$$

where ϕ_{Ai} is the fraction of species i that is not absorbed and A_i is the absorption factor for species i defined by

$$A_i = \frac{N^{(L)}}{K_i N^{(V)}} \quad (6.75)$$

Large values of A correspond to large absorption rates but also to large liquid flows and the unfavorable economics noted above. A reasonable practical compromise is approximately 1.4 (see Couper et al., 2005).

For components that are stripped, the fraction not stripped follows from Equation (6.72) as

$$\phi_{Si} = \frac{1}{1 + S_i} + \frac{y_i^{(0)} N^{(V)}}{x_i^{(0)} N^{(L)}} \frac{1}{1 + S_i} \quad (6.76)$$

where ϕ_{S_i} is the fraction of species i that is not absorbed and S_i is the absorption factor for species i defined by

$$S_i = \frac{K_i \mathcal{N}_S^{(V)}}{\mathcal{N}_S^{(L)}} \quad (6.77)$$

The stripping factor has an interpretation to the absorption factor and an optimal value of around 1.4 as well (see Couper et al., 2005).

6.2.3.2 Mass Balances—Nondiffusing Components If there are one or more components in each phase that do not cross the gas–liquid interface (see discussion in Section 6.2), their flows may be combined in each phase to provide a constant flow basis for the gas and liquid phases: $\mathcal{N}_S^{(V)}$ and $\mathcal{N}_S^{(L)}$, respectively. These flows will be referred to as the solvent flows. The solvent flows may be used in the mass balances instead of the total molar flows if the concentration measures are changed from mole fractions to mole ratios (see Section 2.1.1.1). For example, consider the flow of a component i at the liquid inlet or outlet:

$$x_i \mathcal{N}^{(L)} = \underbrace{\frac{x_i}{\sum_{k \in S} x_k}}_{\text{Mole ratio} = x_{i/s} = X_i} \underbrace{\left[\sum_{k \in S} x_k \right] \mathcal{N}^{(L)}}_{\text{Flow rate of nondiffusing components} = \mathcal{N}_S^{(L)}} = X_i \mathcal{N}_S^{(L)} \quad (6.78)$$

The collection of indices for the nondiffusing components in the phase under consideration is denoted by S in each phase. Since the form remains the same, all of the results in the preceding section may be replaced with mole ratios and solvent flows. Changes in the total flows are of no consequence in this framework. However, the equilibrium relations must be transformed into the new system, which will not conserve linearity. For example,

$$y = f(x) \Rightarrow \frac{Y}{1+Y} = f\left(\frac{X}{1+X}\right) \Rightarrow Y = F(X) \quad (6.79)$$

where the phase equilibrium relation in terms of mole fractions is f and in terms of mole ratios is F . If the mole fraction relation is linear,

$$y = Kx \Rightarrow Y = \frac{KX}{1 + (K-1)X} \quad (6.80)$$

The operating line (material balance) for each diffusing species,

$$Y^{(1)} = -\frac{\mathcal{N}_S^{(L)}}{\mathcal{N}_S^{(V)}} X^{(1)} + \left[Y^{(0)} + \frac{\mathcal{N}_S^{(L)}}{\mathcal{N}_S^{(V)}} X^{(0)} \right] \quad (6.81)$$

is a straight line on Y – X coordinates. The fractions not absorbed or not stripped are transformed in a similar fashion. Note that the linearity in the equilibrium relation is preserved in the region where

$$X \ll \frac{1}{K-1} \quad (6.82)$$

The size of the vessel cannot be determined without additional information such as an estimate of the gas residence time required for the gas and liquid stream to equilibrate. An approximate diameter may be calculated on the basis of limiting the superficial gas velocity to 0.25 ft/s based on the tank diameter (Treybal, 1980).

Example 6.2.3.2-1: Acetone Absorption

The acetone mole fraction in an air stream is to be reduced from 0.15 to 0.05 by contact with pure water in stirred tank. The unit will operate at 20 °C and 101 kPa pressure and may be assumed to be completely mixed. The NRTL parameters for acetone (1) in water (2) are given by (Aspen, 2000):

$$A_{12} = 6.3981 \quad B_{12} = -3256.18$$

$$A_{21} = 0.0544 \quad B_{21} = 755.949$$

where

$$\tau_{ij} = A_{ij} + B_{ij}/T \text{ (}^\circ\text{R)}$$

$$\ln G_{ij} = -0.30\tau_{ij}$$

Equilibrium data:

Assuming an ideal gas phase and a nonideal liquid phase described by the activity coefficient model discussed above may be applied for acetone (1):

$$y_1 = \frac{\gamma_1 P_1^{\text{sat}}(T)}{P} x_1$$

The NRTL model for the activity coefficient is given in Table 5.3.

$$\ln \gamma_1 = \frac{x_2^2 \tau_{21} G_{21}^2}{(x_1 + G_{21} x_2)^2} + \frac{x_2^2 \tau_{12} G_{12}}{(x_2 + G_{12} x_1)^2}$$

The parameters are given by the equations above as

$$\tau_{12} = 0.2311$$

$$\tau_{21} = 1.4861$$

$$G_{12} = 0.9330$$

$$G_{21} = 0.6403$$

The vapor pressures at 20 °C are (Yaws et al., 2005)

$$P_1^{\text{sat}} = 3.545 \text{ psi}$$

$$P_2^{\text{sat}} = 0.3393 \text{ psi}$$

so that

x_1	x_2	$\ln \gamma_1$	γ_1	y_1
0.0000	1.0000	1.7017	5.4835	0.0000
0.0250	0.9750	1.5795	4.8527	0.0294
0.0500	0.9500	1.4648	4.3268	0.0523
0.0750	0.9250	1.3572	3.8852	0.0705
0.1000	0.9000	1.2561	3.5118	0.0850
0.1250	0.8750	1.1613	3.1940	0.0966
0.1500	0.8500	1.0723	2.9220	0.1060
0.1750	0.8250	0.9888	2.6879	0.1138
0.2000	0.8000	0.9104	2.4854	0.1203

These results are plotted in Figure 6.18.

The slope of the mass balance can be interpreted as the ratio of the inlet liquid to the inlet gas flow since the liquid and gas flows are assumed to be the same at the inlet and outlet. To estimate the effect of this assumption, we can carry out the same calculations using mole ratios of acetone instead of mole fractions but retaining water as the nonvolatile liquid

solvent and air as the insoluble gas phase solvent. The converted equilibrium data is

x_1	y_1	X_1	Y_1
0.0000	0.0000	0.0000	0.0000
0.0250	0.0294	0.0256	0.0302
0.0500	0.0523	0.0526	0.0552
0.0750	0.0705	0.0811	0.0758
0.1000	0.0850	0.1111	0.0928
0.1250	0.0966	0.1429	0.1069
0.1500	0.1060	0.1765	0.1186
0.1750	0.1138	0.2121	0.1284
0.2000	0.1203	0.2500	0.1367

$$Y_{1,\text{in}} = 0.176471$$

$$Y_{1,\text{out}} = 0.052632$$

See Figure 6.19.

The ratio of the inlet flows is obtained by dividing the slope by $(1 + 0.176471)$ to give 0.2111 mol liquid/mol inlet gas. Consequently, it was indeed not necessary to consider a change in the liquid and gas rates due to the transfer of acetone.

The mole fraction of water vapor may be estimated as $0.3393/14.7 = 0.02308$ (the vapor pressure of water is given above) or approximately 2%. Using Henry's law ($1/H$ for nitrogen = 1.3×10^{-5} from Figure 6.20), the dissolved air in the exit water is approximately $1.3 \times 10^{-5} (0.85)760 = 0.0084$ or less than 1 mol%.

The water requirement is then $0.2105 \times 454 \times (1/1000) \times (1/3.7854) \times 293/273 = 9.73$ gal water/ft³ gas. A much more efficient multistage arrangement is applied in Problem 6.1. A large quantity of water is needed here because all of the solvent must contain the solute at a concentration in

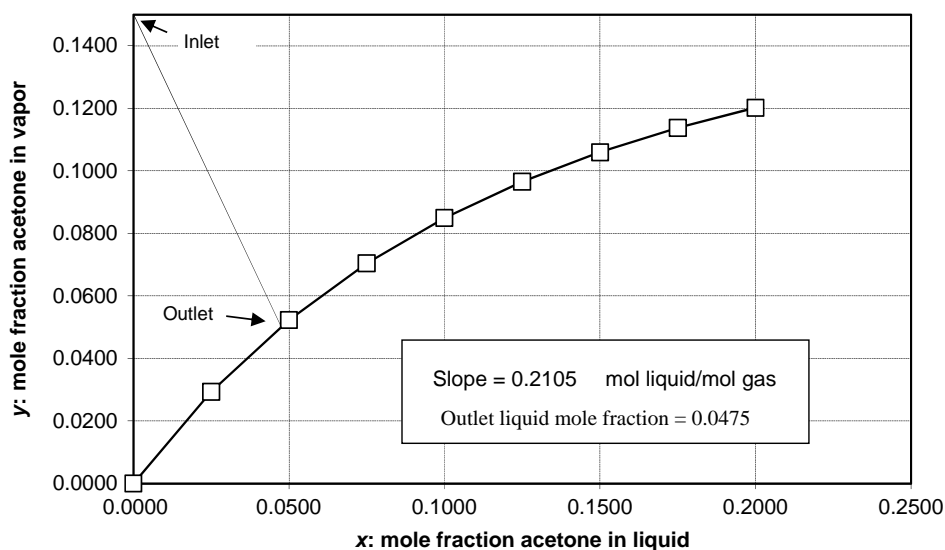


FIGURE 6.18 Single-stage construction using mole fractions.

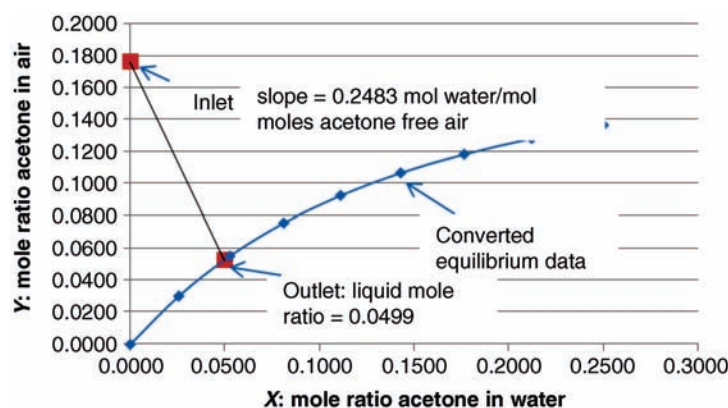
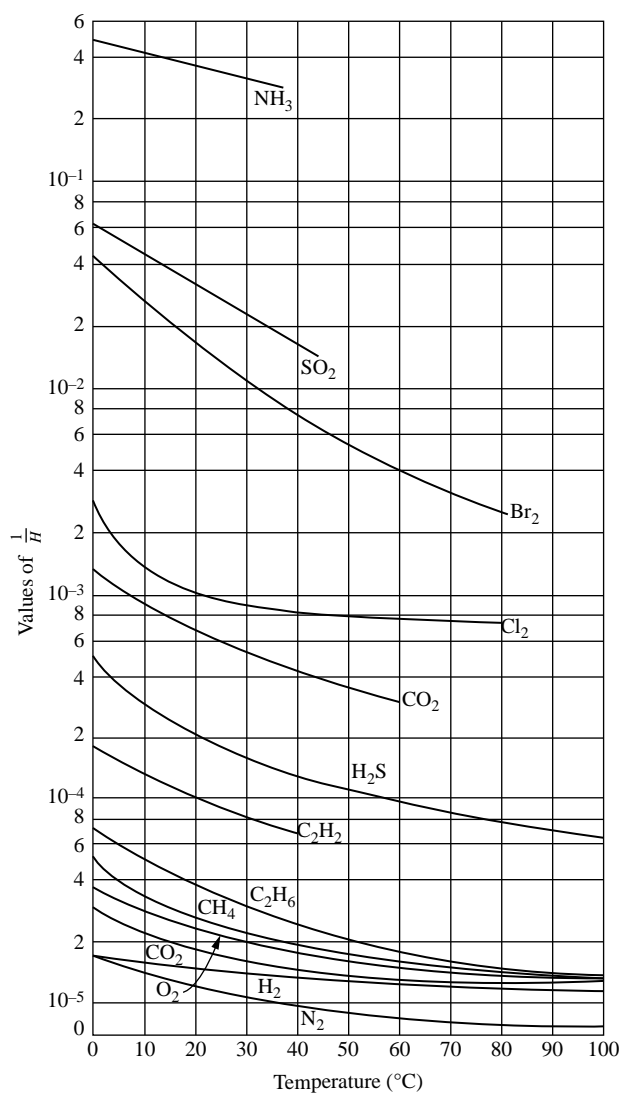


FIGURE 6.19 Single-stage construction using mole ratios.

FIGURE 6.20 Henry's law ($P_i = H_i x_i$) parameter. Reprinted from Hougen et al. (1954) with permission of John Wiley.

equilibrium with the outlet gas, which is, by the nature of the problem, quite low.

Example 6.2.3.2-2: Determine the Solvent Requirements for Single-Stage Version of Tower 302: Off-Gas Absorber in Acrylic Acid Process

The exit stream from the acrylic acid reactor is rapidly quenched to prevent deeper oxidation to side products (refer to Section 1.2.3). The product stream is subsequently contacted in T-302 with an aqueous solvent to separate the acid solution from the light gases. Refer to Figure 6.21.

The stream temperatures are considerably different so that a nonisothermal analysis is called for but we will assume isothermal conditions at 30 °C and 29 psia for illustration. The problem is to select a water rate required to remove the light gases and retain the acids in the exit solvent stream.

The infinite dilution activity coefficients for acetic and acrylic acid are 2.8256 and 4.2563, respectively. These values were obtained from Aspen Plus using the UNIQUAC model with UNIFAC estimation.

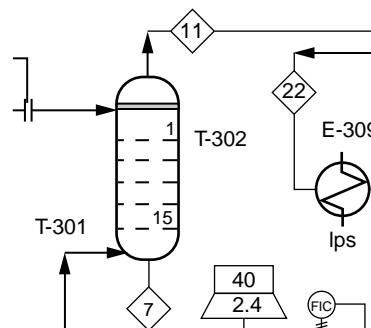


FIGURE 6.21 Tower T-302. Reprinted with permission of Pearson.

Solution:

We will assume that propylene, nitrogen, oxygen, and carbon dioxide follow Henry's law that the water and acids are ideal is ideal, and that the acids are corrected with the activity coefficients at infinite dilution.

Equation (6.74) is applied in the following table to estimate the fraction not absorbed for each component. The calculations are carried out with the suggested value of the optimal absorption factor. This value primarily applies to multistage operations and is seen here to be totally inadequate for the single stage leaving more than 405 of the acetic acid in the gas phase and approximately a quarter of the acrylic acid.

Care must be taken to include all of the equipment in the process flow diagram, especially in process simulators. The value of Q , for example, refers to the heat exchanger. The value of Q for the drum is most often zero.

There are a number of common problems associated with the flash operation. These are defined by the nature of the process specifications that are used to satisfy the degrees of freedom resulting from the application of the mass and energy balances and the conditions of phase equilibrium. The number of variables is $3(N_C + 3) + 1$, three streams each with a flow, a temperature, and pressure, and C mole fractions, and the heat duty. The temperature (T) and pressure (P) of streams L and V are equal in Figure 6.22, which anticipates the application of thermal and mechanical equilibrium and which will be imposed below.

Species	$1/H$ @ 30 °C mole fraction/atm ^a	P^{sat} (30 °C) psia ^b	γ_{∞}	K	$x_i^{(0)}$	$y_i^{(0)} \mathcal{N}^{(V)}$	$y_i^{(0)}$	A	ϕ_{Ai}
C ₃ H ₆	8.84E-05			5734.7726	0.00	14.7000	0.0109	9.4717E-06	1.0000
N ₂	1.10E-05			46081.5047	0.00	1056.7000	0.7865	1.1787E-06	1.0000
O ₂	2.10E-05			24137.9310	0.00	51.9000	0.0386	2.2503E-06	1.0000
CO ₂	5.30E-04			956.4086	0.00	60.5000	0.0450	5.6793E-05	0.9999
H ₂ O		0.6165		0.0213	1.00	150.1000	0.1117	2.5551E+00	0.2813
HAc		0.3982	2.8256	0.0388	0.00	1.6100	0.0012	1.4000	0.4167
HAcr		0.1006	4.7563	0.0165	0.00	7.9700	0.0059	3.2921	0.2330

^a See Figure 6.20.

^b See Appendix C.

Increasing the solvent rate by a factor of approximately 15 still leaves a substantial amount of the acids in the gas phase.

Species	$1/H$ @ 30 °C mole fraction/atm ^a	P^{sat} (30 °C) psia ^b	γ_{∞}	K	$x_i^{(0)}$	$y_i^{(0)} \mathcal{N}^{(V)}$	$y_i^{(0)}$	A	ϕ_{Ai}
C ₃ H ₆	8.84E-05			5734.7726	0.00	14.7000	0.0109	1.3531E-04	0.9999
N ₂	1.10E-05			46081.5047	0.00	1056.7000	0.7865	1.6839E-05	1.0000
O ₂	2.10E-05			24137.9310	0.00	51.9000	0.0386	3.2147E-05	1.0000
CO ₂	5.30E-04			956.4086	0.00	60.5000	0.0450	8.1134E-04	0.9992
H ₂ O		0.6165		0.0213	1.00	150.1000	0.1117	3.6501E+01	0.0267
HAc		0.3982	2.8256	0.0388	0.00	1.6100	0.0012	20.0000	0.0476
HAcr		0.1006	4.7563	0.0165	0.00	7.9700	0.0059	47.0300	0.0208

^a See Figure 6.20.

^b See Appendix C.

6.3 FLASH VAPORIZATION

The flash vaporization unit includes the equipment for vaporizing the mixture, achieving the pressure reduction, and separating the resulting two-phase mixture. The short-hand configuration used in Figure 6.3 does not include these items. A more detailed view is shown in Figure 6.22 as well its relation to the short-hand version.

6.3.1 Mass Balances

We have cut the F, L, V, and Q lines with the envelope that defines the equilibrium stage and the boundary for the material balance. The heat transfer medium will not affect the material balance since it does not communicate with the process. If we take the expansion across the valve as adiabatic, any Q that we calculate will be assigned to the heat exchanger design. The material balance for C

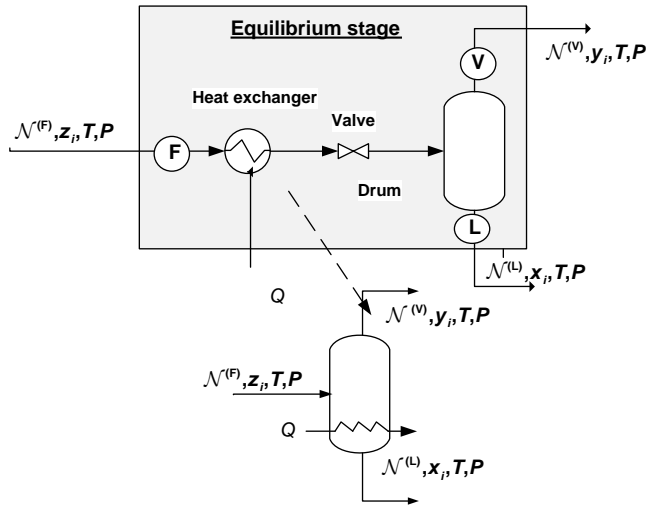


FIGURE 6.22 Short-hand representation of flash vaporization.

components can then be written in molar units as

$$x_i^{(F)} \mathcal{N}^{(F)} = x_i^{(L)} \mathcal{N}^{(L)} + x_i^{(V)} \mathcal{N}^{(V)}, \quad i = 1, 2, \dots, N_C \quad (6.83)$$

where

$$\sum_{i=1}^{N_C} x_i^{(L)} = 1, \quad \sum_{i=1}^{N_C} x_i^{(V)} = 1, \quad \sum_{i=1}^{N_C} x_i^{(F)} = 1 \quad (6.84)$$

The number of mass balances and mole fraction relations is $N_C + 3$.

6.3.2 Energy Balance

Kinetic and potential energies are not important in these circumstances and there is no work performed within the boundaries that we have defined. Consequently, the energy balance in Equation (3.91) reduces in molar units to

$$H^{(F)} \mathcal{N}^{(F)} + Q = H^{(V)} \mathcal{N}^{(V)} + H^{(L)} \mathcal{N}^{(L)} \quad (6.85)$$

The stream enthalpies are presumed to be known functions of the stream variables (see the discussion of departure functions in Chapter 3) and therefore do not in themselves introduce any new variables. The energy balance brings the total equations to $N_C + 4$.

6.3.3 Equilibrium

We are assuming that the heat and mass transfer rates are sufficiently high, and therefore that the mixing process in the unit are sufficiently effective so that the conditions of streams L and V satisfy the thermodynamic conditions of

thermal, mechanical, and chemical equilibrium. This means, respectively, that in addition to the temperatures and pressures of the two streams being equal, the chemical potential of each component is the same in the two streams. We have learned how to express the equality of chemical potentials in terms of the distribution coefficient:

$$x_i^{(V)} = K_i(\mathbf{x}^{(L)}, \mathbf{x}^{(V)}, T, P) x_i^{(L)}, \quad i = 1, 2, \dots, N_C \quad (6.86)$$

The equality of chemical potentials has been expressed as the proportionality of the liquid and vapor mole fractions as discussed above. These equilibrium expressions increase the number of equations by $N_C + 2$ to give $2N_C + 6$.

The number of unknowns is $3N_C + 10$ so that $N_C + 4$ specifications are needed.

If the feed is completely known, an additional $N_C + 2$ specifications are available leaving two degrees of freedom. This implies that if any two of the following variables or relations between them are specified, the equations listed above can be used to determine the others: $T, P, \mathbf{x}^{(L)}, \mathbf{x}^{(V)}, \mathcal{N}^{(V)}, \mathcal{N}^{(L)}$, and Q .

6.3.4 Common Problem Specifications

Although it is arbitrary how we set the degrees of freedom, some combinations arise much more than others. A list of common problem specifications is given below (Seader and Henley, 2006):

1.	$\mathcal{N}^{(V)} / \mathcal{N}^{(F)} = 0, P$	Bubble-point temperature
2.	$\mathcal{N}^{(V)} / \mathcal{N}^{(F)} = 1, P$	Dew-point temperature
3.	$\mathcal{N}^{(V)} / \mathcal{N}^{(F)} = 0, T$	Bubble-point pressure
4.	$\mathcal{N}^{(V)} / \mathcal{N}^{(F)} = 1, T$	Dew-point pressure
5.	T, P	Isothermal flash
6.	$Q = 0, P$	Adiabatic flash
7.	Q, P	Nonadiabatic flash
8.	$\mathcal{N}^{(V)} / \mathcal{N}^{(F)}$	Percent vaporization flash

The first four specifications refer to bubble- and dew-point calculations. A discussion of bubble and dew points may be found in Section 6.2.1, which includes a graphical illustration in Figure 6.4. The operating temperature must be between the bubble and dew points of the feed. If the dew point is exceeded, a superheated vapor will result with no liquid. If the bubble point is not reached, a subcooled liquid will result with no vapor. The calculation of bubble and dew points will be incorporated in the calculations for flash vaporization as they correspond to the onset of the conditions of no vapor or no liquid flow (at equilibrium).

The specification of a vapor fraction of one, for example, in the current context, does not include the possibility of a superheated vapor (refer to Section 6.2.1). The current context calls for saturated outputs so that an infinitesimally small amount of liquid must remain to form the equilibrium liquid

phase. The vapor has the feed composition in this case. The fifth and eighth specifications consider operating conditions within the boundaries determined by the first four.

All of the specifications thus far mentioned refer to the drum feed stream (unlabelled in Figure 6.22) and must be achieved by the action of the heat exchanger and valve on the feed stream F . Specification 7 is primarily on the input side of the heat exchanger.

We will consider some applications from the first five categories. It will be convenient to adopt the notation used in the discussion of vapor–liquid equilibrium in Section 6.2.1:

$$\left. \begin{array}{l} x_i = x_i^{(L)} \\ y_i = x_i^{(V)} \\ z_i = x_i^{(F)} \end{array} \right\}, \quad i = 1, 2, \dots, N_C \quad (6.87)$$

The input stream to the drum will be referred to as the feed.

6.3.5 Distribution Function—Limitations

We will consider cases where the distribution function depends only on the temperature and pressure, either because of the problem specifications or the assumed phase behavior of the mixture. A summary is given in Table 6.12.

The form of the equilibrium relation expressed in Table 6.12 will be used in all of the flash vaporization calculation that remain in this section

6.3.6 Bounds on Bubble and Dew Points

It is very useful to be aware of the bounds on the bubble and dew points. We can bracket the bubble and dew points for K , a function of T and P as follows. In all VLE applications, the sum of the vapor mole fractions must be one, so that

$$\sum_{i=1}^{N_C} K_i(T, P) x_i = 1 \quad (6.88)$$

Since the mole fractions are positive and between 0 and 1, it is not possible for all of the distribution coefficients in Equation (6.88) to be either greater than 1 or less than 1. We can use this fact to determine an allowable range of temperatures for Equation (6.87)

Since the distribution coefficients are positive increasing functions of temperature, we can define a temperature for each component where the value of K is 1:

$$T_i \ni K_i(T_i, P) = 1 \quad (6.89)$$

If T_{\max} and T_{\min} are the temperatures above which and below which all of the K 's are greater or less than 1, respectively, it follows that

$$\begin{array}{l} \text{Min}_i \{T_i\} = T_{\min} \\ \text{Max}_i \{T_i\} = T_{\max} \end{array} \quad (6.90)$$

Consequently,

$$T_{\min} < T_b < T_d < T_{\max} \quad (6.91)$$

Note that if either the bubble point or the dew point is available, it may be used as a bound for the other.

6.3.7 Solution for $\mathcal{N}^{(V)}/\mathcal{N}^{(F)} = 0, P$ —Bubble-Point Temperature

Under these conditions, the liquid will be at the feed composition and flow rate, a trivial solution of the mass balance under the above conditions. Substitution of the equilibrium conditions into the vapor mole fraction summation gives

$$\sum_{i=1}^{N_C} K_i(T, P) z_i = 1 \quad (6.92)$$

The N_C equilibrium relations and Equation (6.92) are the $N_C + 1$ equations needed for the vapor mole fractions and the bubble-point temperature. A graphical representation of the problem for the binary case is given in Figure 6.23.

The problem amounts to finding the root of the following nonlinear function:

$$f(T) = \sum_{i=1}^{N_C} K_i(T, P) z_i - 1 \quad (6.93)$$

The root can be bounded by the method described above, which can greatly facilitate the calculations, whatever numerical technique is used.

TABLE 6.12 Conditions Where $y = K(P, T)x$: Application to Flash Specifications

Liquid Phase	Gas Phase	K Variables	Specifications
Ideal	Ideal	T, P	All
Ideal solution	Nonideal	y, T, P — y given	Dew-point calculations: 2, 4
Nonideal	Ideal solutions	x, T, P — x given	Bubble-point calculations: 1, 3
Nonideal	Nonideal	x, y, T, P — x and y given	Iterative calculations where x and y taken from previous trials
Weak dependence on concentration	Weak dependence on concentration	T, P (DePriester charts—Figures 6.15 and 6.26)	All

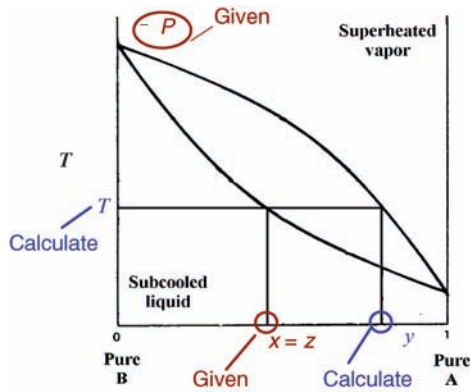


FIGURE 6.23 Bubble-point temperature problem for a binary system.

Example 6.3.7-1: Calculate the Bubble Point of the Following Mixture at 2 atm

Assume ideal behavior.

Component	Mole Fraction	Vapor Pressure at 80 °C (kPa)	α_{i,C_3H_8}
CH ₄	0.20	3000	333.33
C ₃ H ₆	0.20	9	1.000
C ₃ H ₈	0.35	7	0.78
C ₄ H ₁₀	0.25	0.55	0.061

The relative volatility values indicate that it would not be difficult to remove most of the benzene in a single flash without significant losses of the other components. See Example 6.3.9-1.

Solution:

Feed composition—species ordered as listed in preceding table:

$$\mathbf{z} = \begin{bmatrix} 0.2 \\ 0.2 \\ 0.35 \\ 0.25 \end{bmatrix}, P = 2 \text{ atm}$$

Vapor pressure data (Green and Maloney, 1997); P in Pa, T in K

$$[c] = \begin{bmatrix} 39.205 & -1324.4 & -3.4366 & 3.10195 \times 10^{-5} & 2 \\ 57.263 & -3382.4 & -5.7077 & 1.0431 \times 10^{-5} & 2 \\ 59.078 & -3492.6 & -6.0669 & 1.0919 \times 10^{-5} & 2 \\ 66.343 & -4363.2 & -7.046 & 0.94509 \times 10^{-5} & 2 \end{bmatrix}$$

$$P^{\text{sat}}(i, T) = \exp\left(c_{i,1} + \frac{c_{i,2}}{T} + c_{i,3} \times \ln T + c_{i,4} \times T^{c_{i,5}}\right)$$

Form distribution coefficient—ideal case; P in atm

$$K(i, T) = \frac{P^{\text{sat}}(i, T)}{P} \times 9.869233 \times 10^{-6}$$

Bounds on equilibrium temperature (K)

$$K(1, T) - 1 = 0, \text{ Solution is } T_1 = 120.81 = T_{\min}$$

$$K(2, T) - 1 = 0, \text{ Solution is } T_2 = 233.46$$

$$K(3, T) - 1 = 0, \text{ Solution is } T_3 = 248.06$$

$$K(4, T) - 1 = 0, \text{ Solution is } T_4 = 292.35 = T_{\max}$$

Solve for bubble point

$$f(T) = \sum_{i=1}^{i=4} K(i, T)z_{i,1} - 1$$

$$\left. \begin{array}{l} f(T) = 0 \\ T \in (120, 293) \end{array} \right\}, \text{ Solution is } T = 149.42$$

$$\sum_{i=1}^{i=4} K(i, 149.42)z_{i,1} = 1.0 \text{ Checks!}$$

Check range of vapor pressure validity. See reference above.

Species	Range	
CH ₄	90.69	190.56
C ₃ H ₆	87.89	365.57
C ₃ H ₈	85.47	369.83
C ₄ H ₁₀	134.86	425.12

Example 6.3.7-2: Saturation Temperature for IPA–Water System

Calculate the equilibrium or saturation temperature at 1 atm in the IPA–water system at a liquid mole fraction of 0.118 for IPA. Use the data and activity coefficients from Example 6.2.2.2.1-1.

Solution:

Activity coefficients and vapor pressures from Example 6.2.2.2.1-1:

$$\gamma_1(x) = \frac{1}{x + 0.10603} \exp\left((1-x) \left(\frac{0.10603}{0.89397x + 0.10603} - \frac{0.69852}{1 - 0.30148x} \right)\right)$$

$$\gamma_2(x) = \frac{1}{1 - x + 0.69852x}$$

$$\times \exp\left(x\left(\frac{0.69852}{1 - x + 0.69852x} - \frac{0.10603}{x + 0.10603(1 - x)}\right)\right)$$

$$P_1^{\text{sat}}(T) = \exp\left(25.017 - \frac{8010.6}{80.078 + T}\right)$$

$$P_2^{\text{sat}}(T) = \exp\left(18.485 - \frac{3922.0}{-42.25 + T}\right)$$

Bounds on bubble and dew points at $x = 0.118$:

$$K_1 = \gamma_1(0.118) \frac{P_1^{\text{sat}}(T)}{760} = 1, \text{ Solution is } T = 306.38$$

$$K_2 = \gamma_2(0.118) \frac{P_2^{\text{sat}}(T)}{760} = 1, \text{ Solution is } T = 371.44$$

Iteration function

$$f(x, T) = \gamma_1(x)x \frac{P_1(T)}{760} + \gamma_2(x)(1 - x) \frac{P_2(T)}{760} - 1$$

Solution for $x = 0.118$

$$\left. \begin{array}{l} f(0.118, T) = 0 \\ T \in (306, 371) \end{array} \right\}, \text{ Solution is } \{T = 367.38\}$$

Experimental value = 366.16 K. Check some other points.

6.3.8 Solution: for $\mathcal{N}^{(V)}/\mathcal{N}^{(F)} = 1, P$ Specified: Dew-Point Temperature

The vapor will be at the flow rate and composition of the feed, a trivial solution of the mass balance. The liquid mole fraction summation and equilibrium condition gives the $N_C + 1$ equations needed for the liquid mole fractions and the dew-point temperature. The calculations are similar to those for the bubble point. A graphical summary for the binary case is given in Figure 6.24.

Again, the problem amounts to finding the root of a nonlinear algebraic equation for the temperature:

$$f(T) = \sum_{i=1}^{N_C} x_i - 1 = \sum_{i=1}^{N_C} \frac{y_i}{K_i(x, y, T, P)} - 1 \quad (6.94)$$

The root can be bounded by the temperatures shown in Equation (6.90). Note that the bubble point could be used if it were available.

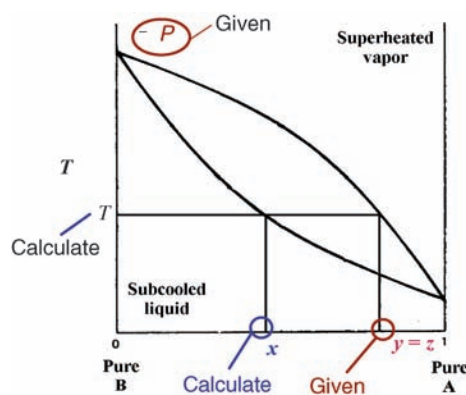


FIGURE 6.24 Dew-point temperature problem for a binary system.

Example 6.3.8-1: Calculate the Dew Point of the Mixture in the Preceding Example

Assume ideal behavior.

Solve for dew point:

$$\left. \begin{array}{l} g(T) = \sum_{i=1}^4 \frac{z_i}{K_i(T)} - 1 \\ g(T) = 0 \\ 120 \leq T \leq 293 \end{array} \right\} T = 263.16;$$

$$\sum_{i=1}^4 \frac{z_i}{K_i(T)} = 0.99985 \quad \text{Checks!}$$

Check range of vapor pressure validity. See reference above.

Species	T_{\min} (K)	T_{\max} (K)
CH ₄	90.69	190.56
C ₃ H ₆	87.89	365.57
C ₃ H ₈	85.47	369.83
C ₄ H ₁₀	134.86	425.12

The solution is out of vapor pressure range for methane. What is the next step?

The next example is again concerned with calculating the dew point of a mixture but with an equation of state.

Example 6.3.8-2: Calculate the Dew Point of an Equimolar Mixture of Propylene and Isobutane at 20 atm Assuming an Ideal Liquid and Application of the Peng-Robinson Equation of State for the Vapor

Physical properties:

$$1 = \text{propylene (C}_3\text{H}_6); \quad 2 = \text{isobutane (C}_4\text{H}_{10})$$

	1	2
T_c (K)	365	408
P_c (atm)	45.60	36.00
ω	0.148	0.176
V_L (G/L)	612	557
T_{REF} (K)	223	293

$$k_{12} = -0.014 \text{ (see Table 2.5)}$$

$$P_1^{\text{sat}}(T) = \frac{1}{101,325} \exp \left(-0.2495796 \times 10^4 + \frac{0.1179981 \times 10^6}{T + 0.9407885 \times 100} - 0.8528422T + 0.4267405 \times 10^3 \ln T + 0.0003578286T^2 \right)$$

$$P_2^{\text{sat}}(T) = \frac{1}{101,325} \exp \left(-0.2280513 \times 10^4 + \frac{0.1370518 \times 10^6}{T + 0.1219671 \times 1000} - 0.4689486T + 0.3691451 \times 10^3 \ln T + 0.137195 \times 10^{-6}T^3 \right)$$

$$R = 0.08206 \text{ l atm / (mol K)}$$

$$P = 20 \text{ atm}$$

Equation of state: Peng–Robinson (Table 2.1).

$$1 = \frac{1}{Z - (bP/RT)} - \frac{a(T)}{P \left(((RT/P)Z)^2 + 2b(RT/P)Z - b^2 \right)}$$

$$\alpha(\omega) = 0.37464 + 1.5422\omega - 0.26992\omega^2$$

$$a_1(T) = 0.45724 \frac{R^2 365^2}{45.60} \left(1 + \left(1 - \sqrt{\frac{T}{365}} \right) \alpha(0.148) \right)^2$$

$$a_2(T) = 0.45724 \frac{R^2 408^2}{36} \left(1 + \left(1 - \sqrt{\frac{T}{408}} \right) \alpha(0.176) \right)^2$$

$$b_1 = 0.07780 \frac{365R}{45.60}$$

$$b_2 = 0.07780 \frac{408R}{36}$$

$$a(T) = \frac{1}{2} \left(\sqrt{a_1(T)} \sqrt{a_1(T)} + 2\sqrt{a_1(T)} \sqrt{a_2(T)} (1.014) + \sqrt{a_2(T)} \sqrt{a_2(T)} \right)$$

$$b = \frac{1}{2} (b_1 + b_2)$$

$$f(z, T) = \frac{1}{Z - (bP/RT)} - \frac{a(T)}{P \left((RT/P)Z^2 + 2b(RT/P)Z - b^2 \right) - 1}$$

Component fugacity coefficients (Table 6.3):

$$\phi_1(z, T) = \exp(Z - 1) \frac{b_1}{b} - \ln \left(Z - \frac{20b}{RT} \right) - \frac{a(T)}{2\sqrt{2}RTb} \left(\frac{\sqrt{a_1(T)} \sqrt{a_1(T)} + \sqrt{a_1(T)} \sqrt{a_2(T)}}{a(T)} - \frac{b_1}{b} \right)$$

$$\ln \left(\frac{Z + (1 + \sqrt{2})(20b/RT)}{Z + (1 - \sqrt{2})(20b/RT)} \right)$$

$$\phi_2(z, T) = \exp(Z - 1) \frac{b_2}{b} - \ln \left(Z - \frac{20b}{RT} \right) - \frac{a(T)}{2\sqrt{2}RTb} \left(\frac{\sqrt{a_2(T)} \sqrt{a_1(T)} + \sqrt{a_2(T)} \sqrt{a_2(T)}}{a(T)} - \frac{b_2}{b} \right) \ln \left(\frac{Z + (1 + \sqrt{2})(20b/RT)}{Z + (1 - \sqrt{2})(20b/RT)} \right)$$

Pure component fugacity coefficients pressure = ξ

$$\varphi_1(z, T, \xi) = \exp(z - 1) - \ln \left(z - \frac{b_1 \xi}{RT} \right) - \frac{a_1(T)}{2\sqrt{2}RTb_1} \ln \left(\frac{z + (1 + \sqrt{2})(b_1 \xi/RT)}{z + (1 - \sqrt{2})(b_1 \xi/RT)} \right)$$

$$\varphi_2(z, T, \xi) = \exp(z - 1) - \ln \left(z - \frac{b_2 \xi}{RT} \right) - \frac{a_2(T)}{2\sqrt{2}RTb_2} \ln \left(\frac{z + (1 + \sqrt{2})(b_2 \xi/RT)}{z + (1 - \sqrt{2})(b_2 \xi/RT)} \right)$$

Iteration function for dew point:

Use distribution coefficient expression from Figure 6.8, assuming liquid is an ideal solution:

$$K_i = \frac{\phi_i^L(T, P_i^{\text{sat}}(T))}{\hat{\phi}_i^V} \frac{P_i^{\text{sat}}(T)}{P} \exp \left[\frac{1}{RT} \int_{P_i^{\text{sat}}(T)}^P V_L dp \right]$$

The iteration function for an equimolar vapor is then as follows:

Assume the Poynting correction factor = 1. Check value at end of calculations:

$$\text{Set } z^V = V \text{ and } z^L = L$$

$$h(V, L, T) = 0.5 \left(\phi_1(V, T) \frac{20}{\phi_1(L, T, P_1(T)) P_1(T)} + \phi_2(V, T) \frac{20}{\phi_2(L, T, P_2(T)) P_2(T)} \right) - 1$$

where Φ is the fugacity coefficient of the pure liquid.

Calculation procedure:

1. Assume a value for T between saturation temperatures at 20 atm.
2. Compute value of z for liquid and vapor using

$$\boxed{\begin{matrix} f(z, T) = 0 \\ z \in (0.3, 1) \end{matrix}} \text{ for the vapor and}$$

$$\boxed{\begin{matrix} f(z, 336.66) = 0 \\ z \in (0, 0.2) \end{matrix}} \text{ for the liquid. See Figure 6.25 to}$$

rationalize the ranges.

3. Calculate new value for T with $\boxed{h(z^V, z^L, T) = 0}$
 $T \in (320, 375)$

4. Repeat until value of temperature converges.

Calculation results:

T	z^V	z^L	T_{new}
347.5	0.663 78	0.078625	343.28
343.28	0.642 60	0.07713 5	342.97
342.97	0.640 90	0.07703 8	343.1
343.1	0.641 95	0.07709 7	342.96
342.96	0.640 86	0.07703 5	342.94
342.94	0.640 75	0.07 02 9	342.94

Values at dew point:

Poynting correction factor:

$$\Pi_1(T, V) = \exp\left(\frac{1}{RT} V(20 - P_1(T))\right)$$

$$\Pi_2(T, V) = \exp\left(\frac{1}{RT} V(20 - P_2(T))\right)$$

$$\Pi_1(343.94, 42.08/612) = 0.97349$$

$$\Pi_2(343.94, 58.124/557) = 1.034$$

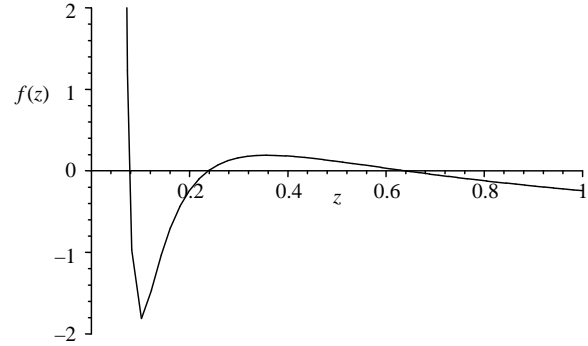


FIGURE 6.25 Roots of typical isotherm for Peng–Robinson equation of state.

Fugacity coefficients:

Vapor:

$$\phi_1(0.64075, 342.94) = 0.82315$$

$$\phi_2(0.64075, 342.94) = 0.67104$$

Liquid:

$$\phi_1(0.077029, 342.94) = 1.0658$$

$$\phi_2(0.077029, 342.94) = 0.46904$$

Example 6.3.8-3: Repeat Example 6.3.8-2 but Use the DePriester Charts to Formulate the Equilibrium Relations

Read two values from the chart in Figure 6.15b and determine constants in $\ln K = A/T + B$ for each component.

Recall that component 1 is propylene and component 2 is isobutane.

$$\begin{aligned} \ln 2.1 &= \frac{A_1}{212 + 460} + B_1 \\ \ln 1.9 &= \frac{A_1}{200 + 460} + B_1 \\ \ln 0.62 &= \frac{A_2}{212 + 460} + B_2 \\ \ln 0.375 &= \frac{A_2}{200 + 460} + B_2, \end{aligned}$$

Solution is $\{A_2 = -18583, B_2 = 27.176, A_1 = -3699.1, B_1 = 6.2465\}$:

$$K_1(T) = \exp\left(\frac{-3699.1}{T + 460} + 6.2465\right)$$

$$K_2(T) = \exp\left(\frac{-18583}{T + 460} + 27.176\right)$$

$$f(T) = 0.5 \left(\frac{1}{K_1(T)} + \frac{1}{K_2(T)} \right) - 1$$

$K_1(t) = 1$, Solution is $t = 132.19$

$K_2(t) = 1$, Solution is $\{t = 223.8\}$

$$\boxed{f(T) = 0, T \in (130, 224)}, \text{ Solution is } T = 213.29^\circ\text{F} = \frac{213.29 - 32}{1.8} +$$

$$273.16 = 373.88 \text{ K}$$

This temperature is close but outside the range of the two data points. Repeat the example with points in a higher range and compare the result with that obtained in Example 6.3.8-2.

6.3.9 Solution for T, P Specified: Isothermal Flash

The liquid fraction in this case may be eliminated from the mass balance since the vapor and liquid fractions must sum to 1. The vapor phase mole fractions may be removed by using the equilibrium conditions. The results are that

$$x_i = \frac{z_i}{1 + (\mathcal{N}^{(V)}/\mathcal{N}^{(F)})[K_i(T, P) - 1]} \quad (6.95)$$

and therefore that

$$y_i = K_i x_i = \frac{K_i(T, P) z_i}{1 + (\mathcal{N}^{(V)}/\mathcal{N}^{(F)})[K_i(T, P) - 1]} \quad (6.96)$$

Since the mole fractions must sum to 1 and the distribution functions are known, either one of these results may be used to form a single nonlinear function of the vapor fraction ($\vartheta = \mathcal{N}^{(V)}/\mathcal{N}^{(F)}$) representing the difference between the sum and unity. However, better convergence properties are obtained; if use is made instead, then the difference must vanish:

$$\sum_{i=1}^{N_c} \frac{[K_i(T, P) - 1] z_i}{1 + \vartheta [K_i(T, P) - 1]} = 0 \quad (6.97)$$

The unknown is ϑ , the vapor fraction in Equation (6.97). In this case, determination of ϑ gives the vapor and liquid mole fractions from the preceding two equations. The heat duty and liquid fraction are given by

$$\mathcal{N}^{(L)}/\mathcal{N}^{(F)} = 1 - \vartheta \quad (6.98)$$

and

$$\frac{Q}{\mathcal{N}^{(F)}} = H^{(V)} \vartheta + H^{(L)} (1 - \vartheta) - H^{(F)} \quad (6.99)$$

The conditions under which there is a fractional solution for the vapor fraction may be derived as follows (although we

know the result!). Note that

$$g(\vartheta) = \sum_{i=1}^C \frac{[K_i(T, P) - 1] z_i}{1 + \vartheta [K_i(T, P) - 1]} \quad (6.100)$$

The function g is a monotonic decreasing function since all of the terms that make up its derivative are negative:

$$g'(\vartheta) = - \sum_{i=1}^{N_c} \frac{[K_i(T, P) - 1]^2 z_i}{\{1 + \vartheta [K_i(T, P) - 1]\}^2} \leq 0 \quad (6.101)$$

The conditions for the fractional solution (in the $[0, 1]$ range) are therefore

$$g(0) = \sum_{i=1}^{N_c} (K_i - 1) z_i = \sum_{i=1}^{N_c} K_i(T, P) z_i - 1 \geq 0 \quad (6.102)$$

or the temperature must be greater than the bubble point of the feed and

$$g(1) = \sum_{i=1}^{N_c} \frac{(K_i - 1) z_i}{K_i} = 1 - \sum_{i=1}^{N_c} \frac{z_i}{K_i(T, P)} \leq 0 \quad (6.103)$$

or the temperature must be less than the dew point of the feed. The possibilities are illustrated in Figure 6.26.

The problem is therefore to find the root of g over the unit interval after determining that the root exists. If the test fails at the origin, $g(0) < 0$, the solution is that a subcooled liquid results. If the test fails at unity, $g(1) > 0$, the solution is a superheated vapor with the feed composition.

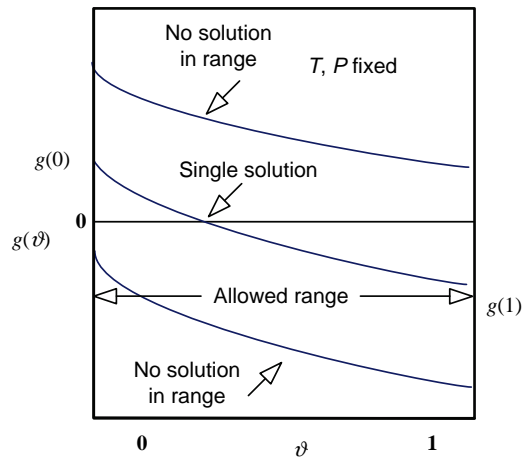


FIGURE 6.26 Behavior of objective function for determining vapor fraction.

Example 6.3.9-1: Isothermal Flash Calculation

Flash the mixture given in Example 6.3.7-1 at 2 atm. Find a temperature where the mole fraction of methane in the gas phase is greater than 0.99. Again assume ideal behavior.

Check on the vapor content at conditions in Example 6.3.7-1:

1. Formulate K function from vapor pressure data.

$$K(i, T) = \frac{9.869233 \times 10^{-6}}{P} \exp \left[c_{i,1} + \frac{c_{i,2}}{T} + c_{i,3} \ln T + c_{i,4} T^{c_{i,5}} \right]$$

2. Formulate g function and solve for current ($T = 190$) split

$$g(\vartheta) = \sum_{i=1}^4 \frac{[K(i, T) - 1]z_{i,1}}{1 + \vartheta[K(i, T) - 1]}$$

$$g(0) = 3.4921$$

$$g(1) = -67.188$$

$$\vartheta = 0.17247$$

$$y(i) = \frac{K(i, T)z_{i,1}}{[1 + \vartheta(K(i, T) - 1)]} \quad y(1) = 0.9545$$

Try lower T (say, 170) will condense less methane because of high volatility.

$$\vartheta = 0.12582$$

$$y(1) = 0.99076$$

Check that the solution is in the range of vapor pressure data (equations):

The following are the results are from a rigorous process simulator—Aspen Plus. The Peng–Robinson equation of state with Boston–Mathias modifications was used for both the liquid and gas phases.

Aspen Plus results for Example 6.3.9-1

$X(I)$	$Y(I)$	$K(I)$
0.79249 E – 01	0.99038	12.497
0.22991	0.42394 E – 02	0.18440 E – 01
0.40268	0.51703 E – 02	0.12840 E – 01
0.28816	0.21494 E – 03	0.74589 E – 03
Vapor fraction		0.13253

$$[a] = \begin{bmatrix} 15.9552 & -2.0276 \times 10^{+03} & -2.8551 & 2.7660 \times 10^{-04} & -9.9111 \times 10^{-14} \\ 2.9861 \times 10^{+01} & -3.1522 \times 10^{+03} & -7.3037 & 2.4247 \times 10^{-09} & 1.8090 \times 10^{-06} \\ 2.8376 \times 10^{+01} & -2.9734 \times 10^{+03} & -7.0320 & -1.5051 \times 10^{-09} & 2.1806 \times 10^{-06} \\ 2.3067 \times 10^{+01} & -3.1437 \times 10^{+03} & -4.8813 & 4.3690 \times 10^{-04} & -4.9161 \times 10^{-13} \end{bmatrix}$$

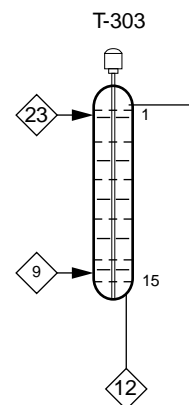


FIGURE 6.27 Acid extraction Tower 300. Reprinted with permission of Pearson.

Example 6.3.9-2: Flash of the Extract from the Acid Extractor (Tower 303), Stream 13

Refer to Figure 6.27. The objective is to return the DIPE solvent to the extractor and to subsequently separate the acrylic and acetic acid products.

Flash vaporization is to be considered as a first step in meeting this objective. Because of the reactive properties of acrylic acid, the flash is to be evaluated at 90 °C and at a more conservative value of 40 °C. At least 90% of the DIPE in the feed stream 13 is to be taken overhead in the vapor product.

The isothermal flash solution may be used in a trial-and-error fashion by fixing the temperature and iterating on pressure until the desired split is achieved. Raoult's law will be used since the pressures will be low:

Component 1 = diisopropyl ether

Component 2 = water

Component 3 = acetic acid

Component 4 = acrylic acid

Vapor pressure data—see Appendix C:

where the vapor pressure in mmHg is given by

$$P(i, T) = 10^{a_{i,1} + a_{i,2}/T + a_{i,3} \log_{10} T + a_{i,4}T + a_{i,5}T^2}$$

where T is in K nits.

Ideal distribution coefficient and feed rates:

$$K(i, T, \Pi) = P(i, T) / \left(\frac{\Pi}{1.01325} \times 760 \right)$$

where Π is the applied pressure in bar.

$$\mathcal{N}^{(13)} = \sum_{i=1}^4 \mathcal{N}_{i,1}^{(13)} \text{ kmol/h}$$

$$\left[\mathcal{N}^{(13)} \right] = \begin{bmatrix} 1299.5 \\ 198.8 \\ 6.08 \\ 86.81 \end{bmatrix}$$

$$\left| z(i) = \frac{\mathcal{N}_{i,1}^{(13)}}{\mathcal{N}^{(13)}} \right|$$

Flash equations:

$$g(\vartheta, T, \Pi) = \sum_{i=1}^4 \frac{(K(i, T, \Pi) - 1)z(i)}{1 + \vartheta(K(i, T, \Pi) - 1)}$$

$$y(i, \vartheta, T, \Pi) = \frac{K(i, T, \Pi)z(i)}{1 + \vartheta(K(i, T, \Pi) - 1)}$$

$$x(i, \vartheta, T, \Pi) = \frac{z(i)}{1 + \vartheta(K(i, T, \Pi) - 1)}$$

Fraction of feed appearing in vapor product:

$$\text{for component } 1 = \frac{y(1)\vartheta}{z(1)} = \Omega$$

Set flash temperature and determine pressure by trial and error that will take 90% of the DIPE overhead.

(a) Say $T = 40^\circ\text{C}$

$$T = 273.16 + 40$$

Solve following for pressure range (set $j = 1, 2, 3, 4$):

$$K(j, T, \Pi) = 1$$

$$\Pi \in (0.01, 10)$$

$$0.012809 \leq \Pi \leq 0.36848$$

Solve isothermal flash equation over allowable pressure range until 90% condition on DIPE is attained.

Solution:

$$\Pi = 0.2$$

$$\vartheta = 0.83216$$

$$\Omega = \frac{y(1, \vartheta, T, \Pi)\vartheta}{z(1)} = 0.90133$$

$$y \left(\begin{bmatrix} 1 \\ 2 \\ 3 \\ 4 \end{bmatrix}, \vartheta, T, \Pi \right) \vartheta F = 1324.1 \begin{bmatrix} 0.88457 \\ 9.7166 \times 10^{-2} \\ 2.4647 \times 10^{-3} \\ 0.0158 \end{bmatrix} \begin{bmatrix} 1171.3 \\ 128.66 \\ 3.2635 \\ 20.921 \end{bmatrix} \begin{bmatrix} 1299.5 \\ 198.8 \\ 6.08 \\ 86.81 \end{bmatrix}$$

(b) Say $T = 90^\circ\text{C}$

$$\Pi = 1.28$$

$$\vartheta = 0.85853$$

$$\Omega = \frac{y(1, \vartheta, T, \Pi)\vartheta}{z(1)} = 0.90198$$

$$y \left(\begin{bmatrix} 1 \\ 2 \\ 3 \\ 4 \end{bmatrix}, \vartheta, T, \Pi \right) \vartheta F = 1366.1 \begin{bmatrix} 0.85802 \\ 0.11191 \\ 2.9054 \times 10^{-3} \\ 2.7172 \times 10^{-2} \end{bmatrix} \begin{bmatrix} 1172.1 \\ 152.88 \\ 3.9691 \\ 37.120 \end{bmatrix}$$

The required pressures are therefore 0.20 bar and 1.28 bar, corresponding to 40 and 90°C operating temperatures. In the first case, the vapor contains 54% of the acetic acid in the feed and 24% of the acrylic acid in addition to 90% of the DIPE. In the second case where the pressure is higher, 65% of the acetic acid is in the vapor and 43% of the acrylic acid as well as 90% of the DIPE. The difference in vapor pressures is not sufficient to provide a good separation in one step.

Note that the pressure has no effect on the separation factor for the ideal case:

$$S_{ij} = \frac{y_i/y_j}{x_i/x_j} = \frac{P_i}{P_j}$$

The preceding problem was also solved using Aspen Plus with the UNIQUAC model for the liquid phase under an ideal vapor phase. The pressures obtained were 0.23 and 1.38 bar, respectively, which are close to the values obtained above. The vapor and liquid compositions and flows from the Aspen simulation are shown below for comparison.

Aspen Plus Results for Example 6.3.9-2

	Feed	$T = 90\text{ }^{\circ}\text{C}$		$T = 40\text{ }^{\circ}\text{C}$	
		Vapor	Liquid	Vapor	Liquid
Mole flow (kmol/h)					
DIISO-01	1299.5	1170.027	129.4729	1169.591	129.9088
Water	198.8	182.6619	16.13811	165.47	33.33001
ACETI-01	6.08	3.273491	2.806509	2.312824	3.767176
ACRYL-01	86.81	19.71348	67.09652	8.318573	78.49143
Mole fraction					
DIISO-01	0.8166844	0.8505107	0.6007631	8.69E-01	0.5291656
Water	0.1249379	0.1327797	0.0748819	0.1229627	0.1357652
ACETI-01	3.82E-03	2.38E-03	0.0130224	1.72E-03	0.015345
ACRYL-01	0.0545566	0.01433	0.3113325	6.18E-03	0.3197241
Total flow (kmol/h)	1591.19	1375.676	215.514	1345.693	245.4974
Pressure (atm)	1	1.32987	1.32987	0.2273336	0.2273336

6.3.10 General Isothermal Flash Iteration

In the more general case, the distribution function depends on composition and the preceding algorithm will not work as it stands. A problem is that we do not know the values of x and y to use in the distribution function. We can, however, calculate approximate values by carrying out the flash, assuming Raoult's law applies. These values can be used in the first trial to calculate the K values in the iterations for the vapor fraction. Refer to Figure 6.28.

Based on the value of the vapor fraction, new values of x and y can be calculated, still using the assumed values to calculate the K 's. If the new values agree with the old, we effectively have a solution to the problem by using the correct values in the iterations or the vapor fraction. Otherwise, we can replace the old values with the new and repeat the same procedure until the mole fractions agree. Detailed algorithms are available for a variety of applications [see, for example, King (1980) and Sandler (1999)].

6.3.11 Sizing of Flash Drum

The following heuristics (Couper et al., 2005) may be used to size the flash drum: a gas-liquid separator:

- Gas-liquid separators are vertical.
- Optimum length to diameter is 3, but a range of 2.5–5.0 is common.
- Holdup time is 5 min half full for reflux drums, 5–10 min for product feeding another tower.
- Gas velocity in gas/liquid separators is given by

$$v = k \sqrt{\left(\frac{\rho_{\text{Liquid}}}{\rho_{\text{Vapor}}} - 1 \right)} \quad (6.104)$$

See Section 13.2 for basis of Equation (6.104) in interphase momentum transfer.

The value of k is given by

$k = 0.10\text{ ft/s}$ without a mesh de-entrainer

$k = 0.35\text{ ft/s}$ with a mesh de-entrainer

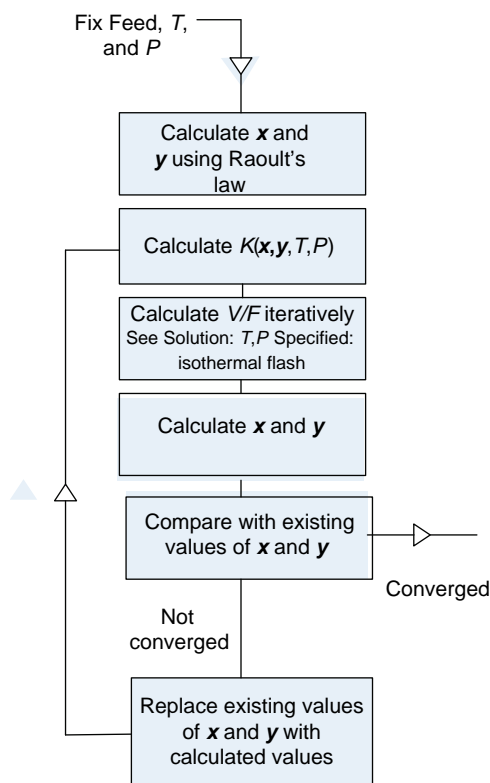


FIGURE 6.28 Isothermal flash iteration.

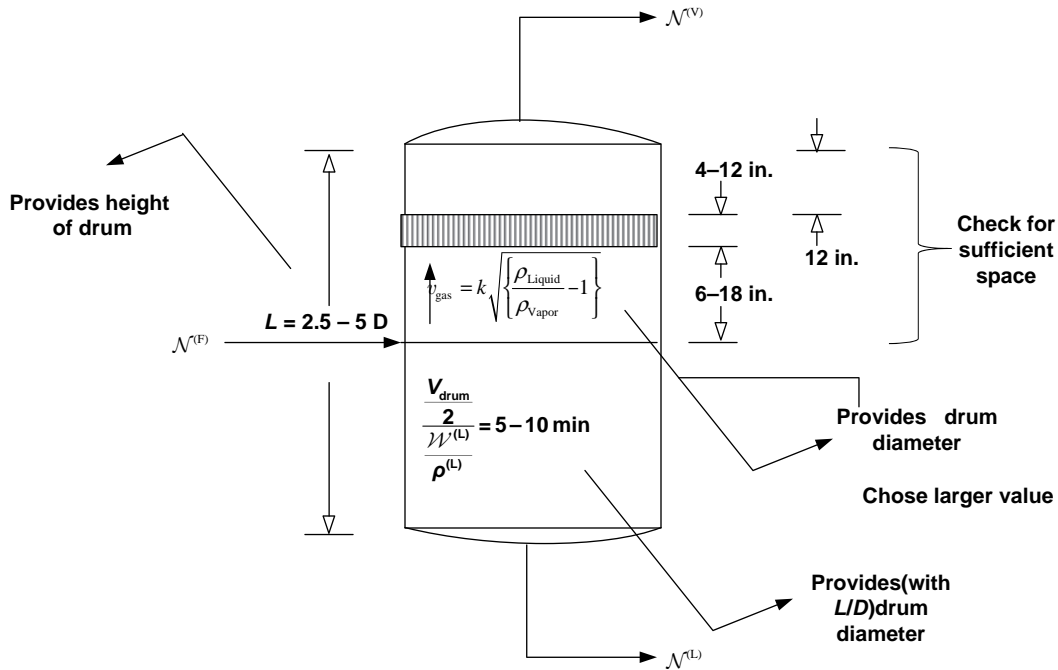


FIGURE 6.29 Summary of sizing method for flash drum.

For vertical pads, the value of k is reduced by a factor of 2/3. Good performance can be expected at velocities of 30–100% of those calculated with the given k ; 75% is popular.

- 99% entrainment removal is attained with mesh pads of 4–12 in. thickness; 6 in. is popular.
- Disengaging spaces of 6–18 in. ahead of the pad and 12 in. above the pad are suitable.

A summary is given in Figure 6.29.

Example 6.3.11-1: Size the Flash Drum for Example 6.3.9-1

The feed flow rate is 500 lb mol/h and the density of the liquid and vapor phases are 43.359 and 0.1495 lb/ft³, respectively.

Vapor flow rate:

$$\begin{aligned} \mathcal{W}^{(V)} &= [\sum y_i M_i] \mathcal{N}^{(V)} = [\sum y_i M_i] \mathcal{N}^{(F)} \vartheta \\ &= [(0.9906(12.011 + 4 \times 1.008) \\ &\quad + 0.004782(3 \times 12.011 + 6 \times 1.008) \\ &\quad + 0.004315(3 \times 12.011 + 8 \times 1.008) \\ &\quad + 0.0001653(4 \times 12.011 + 10 \times 1.008))] 500 \\ &\quad \times 0.12582 \end{aligned}$$

$$\mathcal{W}^{(V)} = 1025.0 \text{ lb/h}$$

Liquid flow rate:

$$\begin{aligned} \mathcal{W}^{(L)} &= [\sum x_i M_i] \mathcal{N}^{(L)} = [\sum x_i M_i] \mathcal{N}^{(F)} (1 - \vartheta) \\ &= (0.086187(12.011 + 4 \times 1.008) \\ &\quad + 0.2281(3 \times 12.011 + 6 \times 1.008) \\ &\quad + 0.39975(3 \times 12.011 + 8 \times 1.008) \\ &\quad + 0.28596(4 \times 12.011 + 10 \times 1.008)) 500 \\ &\quad \times (1 - 0.12582) \end{aligned}$$

$$\mathcal{W}^{(L)} = 19770.0 \text{ lb/h}$$

Drum volume based on 5 min holdup:

$$\frac{V_d}{2} = \frac{L}{43.359} \frac{5}{60}, \text{ Solution is } V_d = 75.993$$

$$\text{Drum diameter for } H/D = 4: D = \left(\frac{75.993}{\pi} \right)^{1/3} = 2.8921 \text{ ft}$$

Gas velocity required for disengagement (75%) and corresponding diameter:

$$0.75 \times 0.35 \left(\frac{43.359}{0.1495} - 1 \right)^{1/2} = 4.4627$$

$\frac{1025}{3600} = 0.1495 \times 4.4627 \times \pi \times \frac{D^2}{4}$, Solution is $D = 0.73713$ $D = -0.73713$ Less than 2.89 ft so use 2.89 ft diameter and 11.56 ft height. Height above liquid is then 5.78 ft.

Say mesh is 1 ft. The disengaging space is 1.5 ft ahead and 1 ft above, giving 3.5 ft. Consequently, there adequate space above the liquid.

6.4 LIQUID-LIQUID EXTRACTION

Liquid-liquid extraction is a separation operation whereby specific components dissolved in a liquid are selectively removed by contact with a second liquid, ideally immiscible with the first, which has a higher affinity for the specific components. Refer to Figure 6.30.

The mixture containing the components targeted for removal is the feed to an extraction process. The liquid with the higher affinity for the targeted components is the solvent. The feed is thereby refined and is referred to as the raffinate.

The solvent that contains the extracted components is referred to as the extract. The operation shares some general features with gas-liquid operations. Like flash vaporization, a second phase needs to be formed from the same constituents. However, unlike flash vaporization, the formation of the second phase is not one of our prerogatives and we must theoretically and/or experimentally investigate the compliance of candidate systems. This amounts, in the simplest case, to finding an immiscible solvent that can selectively remove the solute from a binary mixture.

Immiscibility in binary systems (e.g., the pure feed and solvent streams above) depends on the temperature, pressure, and composition. Three possibilities are illustrated in Figure 6.31.

In the center drawing of Figure 6.31, a closed region bounded above by the upper consolute temperature and below by the lower consolute temperature defines the region where two phases exist. Equilibrium concentrations in the two phases (1 and 2) are connected by a horizontal tie line since both phases must be at the same temperature for thermal equilibrium. Vapor-liquid equilibrium appears at higher temperatures and liquid-solid equilibrium appears at lower temperatures. If the two-phase region merges with the

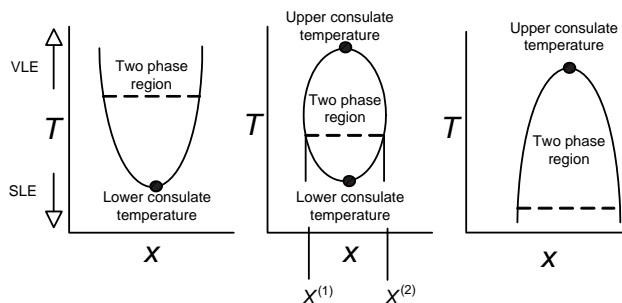


FIGURE 6.31 Examples of binary phase equilibria.

VLE region, the upper consolute temperature does not exist (see the left-hand drawing in Figure 6.31). If the two-phase region merges with the SLE region, the lower consolute temperature does not exist (see the right-hand drawing in Figure 6.31).

The two concentrations at either end of the tie line correspond to phase equilibrium at the temperature of the tie line and the pressure for the figure. As discussed in Section 6.1, this corresponds to an extremum in the Gibbs free energy for the system and is represented by equal chemical potentials (and fugacities) between the two phases. The complete thermodynamic analysis of phase splitting includes not only that $dG = 0$ at a fixed temperature and pressure but also that $d^{(2)}G > 0$ at the two equilibrium states or phase.

6.4.1 Equilibrium in Ternary Systems

Liquid (1)-liquid equilibrium is generally characterized by the equality of chemical potentials [Equation (6.4)], which translates into the equality of fugacities [see Equation (6.10)] or

$$\gamma_i^{(1)} x_i^{(1)} = \gamma_i^{(2)} x_i^{(2)} \quad (6.105)$$

since the same standard state applies to each phase. The implementation of Equation (6.105) requires that the parameters of the activity coefficients be known experimentally or estimated. The ASOG (Analytical Solution of Groups) and UNIFAC are group contribution methods that provide estimates of activity coefficients based on the Wilson and UNIQUAC expressions of the excess Gibbs Free energy, respectively. If sufficient binary are available, the multi-component generalizations of binary models in Table 6.6 can be used.

The equilibrium data may be generated by following the consequences of adding N_i moles of species i to the mixture. At equilibrium, both the equilibrium and the following material balances must be satisfied:

$$N_i = N_i^{(1)} + N_i^{(2)} \quad (6.106)$$

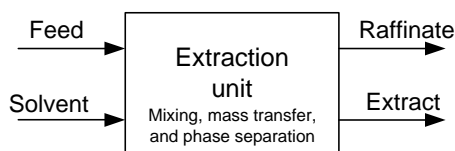


FIGURE 6.30 Stream identification in an extraction unit.

Note that the distribution coefficient is given by the ratio of activity coefficients

$$K_i = \frac{x_i^{(1)}}{x_i^{(2)}} = \frac{\gamma_i^{(2)}}{\gamma_i^{(1)}} \quad (6.107)$$

Equations (6.105) and (6.106) have been used often in determining the value of the parameters in the activity coefficient model to minimize the difference between the calculated and experimental mole fractions (e.g., Arce and Blanco, 1998; Kao and Lin, 1999).

In the following section, we will consider only ternary systems for which experimental data or the results of reliable calculations are available. The objective is to determine the solvent requirements and size of a single-stage extraction unit that will provide a desired degree of separation.

6.4.1.1 Solvent Selection The activity coefficient data can play a significant role in solvent selection. For example, as noted at the outset, the selectivity of the solvent for the solute should be high. We might say that the selectivity has several ingredients:

- *High Affinity of Solvent (3) for Solute (1) Relative to Carrier (2)*
The ratio

$$\begin{aligned} \gamma_1^{(3)} x_1^{(3)} &= \gamma_1^{(2)} x_1^{(2)} \\ \frac{x_1^{(2)}}{x_1^{(3)}} &= \frac{\gamma_1^{(3)}}{\gamma_1^{(2)}} \end{aligned} \quad (6.108)$$

should be as low as possible.

- *Low Affinity of Solvent (3) for Carrier (2)*
The ratio

$$\begin{aligned} \gamma_2^{(3)} x_2^{(3)} &= \gamma_2^{(2)} x_2^{(2)} \\ \frac{x_2^{(3)}}{x_2^{(2)}} &= \frac{\gamma_2^{(2)}}{\gamma_2^{(3)}} \end{aligned} \quad (6.109)$$

should be as low as possible.

The ratio of the preceding two characteristics provides a meaningful definition of selectivity:

$$S = \frac{\gamma_1^{(2)}/\gamma_1^{(3)}}{\gamma_2^{(2)}/\gamma_2^{(3)}} \quad (6.110)$$

which should be as high as possible. See Kao and Lin (1999) for an example of the use of selectivity in solvent selection.

More sophisticated use of the activity coefficients in the selection of solvents has been proposed (Cusack et al., 1991). In addition, the solvent should be easy to recover, nontoxic, have low flammability limits, and a low vapor

pressure. Dispersion and coalescence are also considerations. The following discussion is carried out with mass units, but molar units may also be used. Recall that mole fractions may be obtained from mass fractions with Equation (2.38).

6.4.1.2 Data Collection and Representation The following discussion of a hypothetical experiment raises some important features of ternary LLE data and its graphical representation. We begin with a mixture of the pure solvent and the pure feed and note the concentration of each in the other phase, which we presume has formed. We will consider a ternary system consisting of three species numbered as follows:

- 1 = impurity
- 2 = pure feed: raffinate phase
- 3 = pure solvent: extract phase

The Gibbs phase rule [Equation (6.11)] gives three degrees of freedom ($\Phi = N_C + 2 - N_\pi = 3$). This means that we could fix the temperature and pressure and have one degree of freedom to generate the solubility curve.

Small amounts of the impurity are added to the mixture stepwise thereafter with the mass fraction of two independent components measured in each phase. Concentration measurements are taken repeatedly until constant results are obtained at each step. The situation is depicted in Figure 6.32.

The collection of concentration pairs collected in this way can be tabulated as illustrated in Table 6.13, which constitutes a sampling of the conditions where equality of chemical potentials is present.

On a rectangular diagram, the collection of points under each column (phase) in Table 6.13 will yield a curve that is part of the total solubility curve. Each point on the raffinate

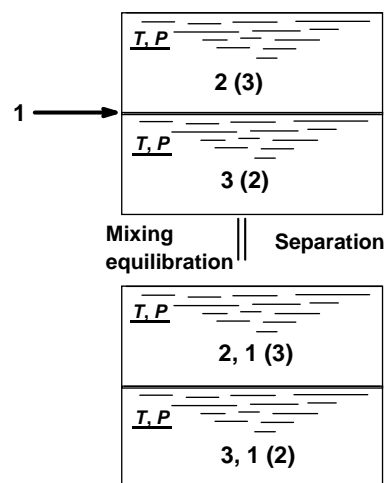


FIGURE 6.32 Ternary LLE data collection.

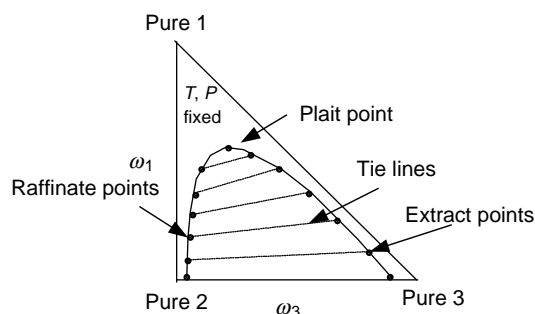
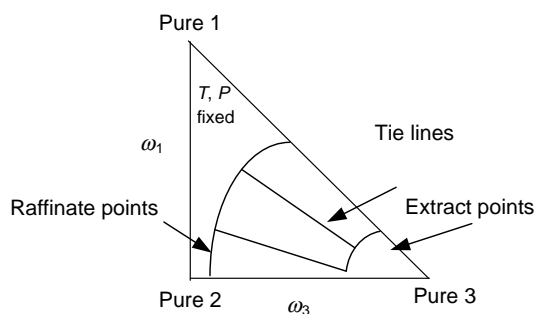
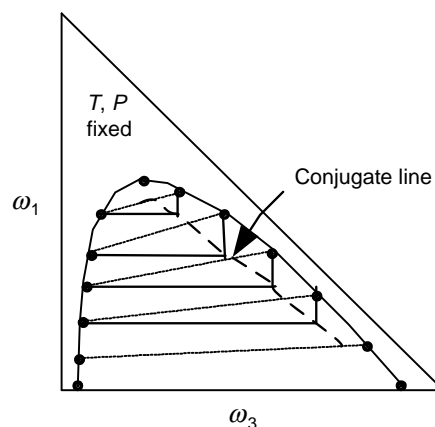
TABLE 6.13 Tabulation of Ternary Equilibrium Data

Solvent Phase—Extract		Feed Phase—Raffinate	
$\omega_1^{(E)} = \omega_1^{(S)}$	$\omega_3^{(E)} = \omega_3^{(S)}$	$\omega_1^{(R)}$	$\omega_3^{(R)}$
(ω_1, ω_3) points at extract end of tie line		(ω_1, ω_3) points at raffinate end of tie line	

curve corresponds to one point on the extract curve. The points may be connected with a tie line, indicating that phase equilibrium is present under these conditions. A possible scenario is given in Figure 6.33.

With the progressive addition of component 1 in the manner indicated above, a condition is reached where the phase boundary disappears with the addition of a very small additional amount of the impurity (1). The two phases are of course identical at this point and have gradually reached this condition as seen by the progressive approach of the two end points of the tie lines.

The apexes of the right triangle represent the pure compounds. Although not needed, the concentration of component 2 can be scaled along the perpendicular drawn from the hypotenuse to the right angle.

**FIGURE 6.33** Graphical ternary equilibrium data—one pair mutually soluble.**FIGURE 6.34** Example of ternary data—two pairs mutually soluble.**FIGURE 6.35** Conjugate line for tie line interpolation.

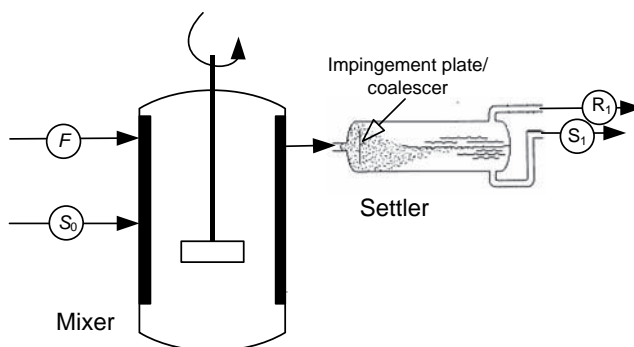
The equilibrium data can take other forms. The form presented here falls under the category of “one pair mutually soluble.” Another type is “two pairs mutually soluble,” an example of which is shown in Figure 6.34. There is no plait point in this case (see Arce and Blanco, 1998).

6.4.1.3 Interpolation Interpolation between tie lines is often required. To accomplish this, conjugate line is used. The conjugate line is the locus of points representing the intersection of a horizontal line through the raffinate point and a vertical line through the extract point of each relevant tie line (Luyben and Wenzel, 1998) (see Figure 6.35).

6.4.2 Single-Stage Operation

6.4.2.1 Equipment The extraction equipment consists of a well-mixed vessel and a settler following the tank to separate the emulsion as illustrated in Figure 6.36. The streams leaving the settler presume that the raffinate is the light phase. The mixer is a baffled vessel as discussed in Chapter 5. The settler is a horizontal cylindrical vessel.

The emulsion enters the settler (Treybal, 1980) and strikes a vertical impingement plate, which minimizes disturbances

**FIGURE 6.36** Single-stage mixer-settler arrangement.

to the main section of the settler where the drops coalesce and settle by gravity. A coalescer may also be provided at the entrance to the settler to aid in the formation of larger droplets, which settle faster. The interface is at the center of the vessel.

The settler may be sized approximately (Treybal, 1980) by taking the L/D to be 4 where the diameter is given by

$$D(\text{ft}) = 0.22 \sqrt{\mathcal{V}^{(R)}(\text{gal/min}) + \mathcal{V}^{(S)}(\text{gal/min})} \quad (6.111)$$

The extract and raffinate phases leaving the settler are the exit streams for the mixer–settler configuration as an equilibrium stage and are therefore considered to be in equilibrium.

The mixer–settler configuration is a single-stage version of the multistage configuration illustrated in Figure 1.10 for the acrylic acid process. In that case, the pure feed is water, the solvent is DIPE, and the solutes (two in this case) are acrylic and acetic acids.

6.4.2.2 Mixture Rule The mass balances associated with the addition of two mixtures to form a third possess a useful property when represented on the same graph. Namely, the concentration of the third mixture lies on a straight line connecting the concentration of the two original mixtures. This rule is illustrated in Figure 6.37.

There are three mass balances that can be written for this mixing operation since it is a ternary system.

$$\begin{aligned} \omega_1^{(M_1)} \mathcal{W}^{(M_1)} + \omega_1^{(M_2)} \mathcal{W}^{(M_2)} &= \omega_1^{(M)} \mathcal{W}^{(M)} \\ \omega_3^{(M_1)} \mathcal{W}^{(M_1)} + \omega_3^{(M_2)} \mathcal{W}^{(M_2)} &= \omega_3^{(M)} \mathcal{W}^{(M)} \\ \mathcal{W}^{(M_1)} + \mathcal{W}^{(M_2)} &= \mathcal{W}^{(M)} \end{aligned} \quad (6.112)$$

The mixing rule can be proved using similar triangles and these three equations.

Note that the same equations apply if a mixture M_2 is extracted from a mixture M . The mole fractions in M_1 may be negative if the operation removes something that is not there. The region enclosed by the (0,1) axes represents what is physically realizable, but the validity of the mixture rule extends beyond these limits.

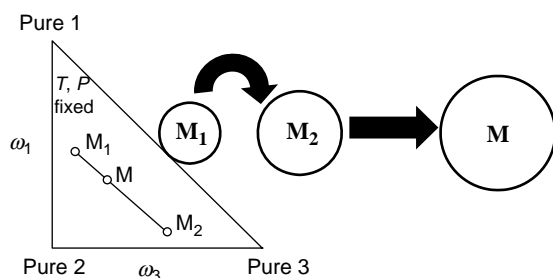


FIGURE 6.37 Mixture rule (comprised of two figures).

The distances from M to the two components are in proportion to the respective quantities. This is known as the Lever rule, but it is primarily useful conceptually. It is more convenient to read the concentrations and use the equations to solve for the amounts of the mixtures. It is convenient to remember that the larger the fraction of the mixture taken by one of the two ingredients, the more the mixture must look like that ingredient. The mixture point is therefore closer to the end point representing the dominant ingredient.

As noted above, the collection of points constituting the extremes of the tie lines is called the solubility curve. A mixture falling within this envelope will split into two phases, the concentrations of which are connected by the line through the mixture composition according to the mixture rule. A single phase exits outside the solubility curve.

6.4.2.3 Mass Balances There are four streams associated with the mixer–settler in Figure 6.36 and for each there are two independent mass fractions. There is one mass balance for each component. We choose to write the individual balances for species 1 and 3 to maintain consistency with the graphical coordinates and replace the balance for species 2 with the overall balance. The degrees of freedom for this system are shown below to be six.

$$\text{Variables}(12) : 4 \text{ streams}(1 \text{ rate}) = 2 \text{ compositions}$$

Mass balances (3)

$$\omega_1^{(F)} \mathcal{W}^{(F)} + \omega_1^{(S_0)} \mathcal{W}^{(S_0)} = \omega_1^{(R_1)} \mathcal{W}^{(R_1)} + \omega_1^{(S_1)} \mathcal{W}^{(S_1)} \quad (6.113)$$

$$\omega_3^{(F)} \mathcal{W}^{(F)} + \omega_3^{(S_0)} \mathcal{W}^{(S_0)} = \omega_3^{(R_1)} \mathcal{W}^{(R_1)} + \omega_3^{(S_1)} \mathcal{W}^{(S_1)} \quad (6.114)$$

$$\mathcal{W}^{(F)} + \mathcal{W}^{(S_0)} = \mathcal{W}^{(R_1)} + \mathcal{W}^{(S_1)} \quad (6.115)$$

Equilibrium (3):

$$\mu_i^{(R_1)} = \mu_i^{(S_1)}, \quad i = 1, 2, 3 \Rightarrow \text{Graph} \quad (6.116)$$

$$\Phi = 12 - 3 - 3 = 6 \quad (6.117)$$

The graph of the equilibrium solubility data is the full expression of chemical equilibrium at the specified T and P and is therefore equivalent to the three equalities of the chemical potential between the raffinate and the extract. There are consequently six degrees of freedom (number of variables–mass balances–equilibrium relations).

We are required then to fix six of the variables or relations between them before we use the mass balance and equilibrium data to determine the unknown values. It makes good sense that we would know the feed and the purity of the solvent, which amounts to four concentrations and one flow

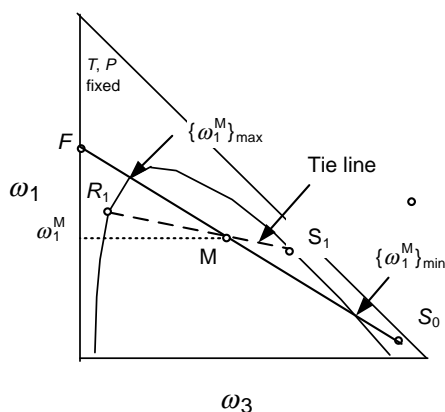


FIGURE 6.38 Limits on solvent-to-feed ratio.

or five variables, and the desired purity of the feed, that is, the concentration of species 1 in the raffinate, which completes the specifications. We can now solve for the quantity of solvent required and the concentrations and amounts of the resulting phases. Refer to Figure 6.38.

The points representing the concentration of the feed, stream F, the concentration of the solvent, stream S₀, and the composition of the raffinate, stream R₁, can all be located on the graph of the equilibrium data. The single concentration specified for the raffinate is sufficient to locate it on the graph since it must lie on the solubility curve. It is limited by the location of M within the solubility curve as indicated by the maximum and minimum values of the impurity concentration in M. The ideal target for the raffinate is the intersection of the solubility curve with the solvent axis representing complete removal of the impurity.

The extract composition must lie at the opposite end of the tie line connecting it to the desired raffinate composition. This can be accomplished by estimating the location of the desired tie line between the two that bracket the raffinate composition. The tie line through the raffinate can be graphically located with the conjugate line.

The tie line connecting the raffinate and extract intersects the line that connects the feed and the solvent since each combination is the same mixture M. The composition of M can be read from the graph and the amount of solvent calculated as follows:

$$\mathcal{W}^{(M_1)} = \mathcal{W}^{(F)} + \mathcal{W}^{(S_0)} = \mathcal{W}^{(R_1)} + \mathcal{W}^{(S_1)} \quad (6.118)$$

$$\omega_1^{(M_1)} (\mathcal{W}^{(F)} + \mathcal{W}^{(S_0)}) = \omega_1^{(F)} \mathcal{W}^{(F)} + \omega_1^{(S_0)} \mathcal{W}^{(S_0)} \quad (6.119)$$

$$\frac{\mathcal{W}^{(S_0)}}{\mathcal{W}^{(F)}} = \frac{\omega_1^{(F)} - \omega_1^{(M)}}{\omega_1^{(M)} - \omega_1^{(S_0)}} \quad (6.120)$$

The maximum and minimum solvent flows within the region of two-phase operation can be obtained by substituting the

minimum and maximum values of the mixture composition ($\omega_1^{(M)}_{\min}$, $\omega_1^{(M)}_{\max}$, respectively). These values correspond to the intersections of the feed solvent line with the solubility envelope as indicated in Figure 6.38. A tie line connects the intersection corresponding to the maximum solvent flow to the minimum possible raffinate composition in the single-stage operation.

With the feed and solvent streams completely specified, then the compositions of the extract and raffinate streams can be read from the graph and the material balances used to calculate the flows. The procedure may be repeated using the raffinate as the new feed. This is called cross-flow extraction and results in substantial solvent requirements.

Example 6.4.2.3-1: Extraction of HAc from Chloroform with Water (Seader and Henley, 2006)

A mixture of chloroform, CHCl₃, and acetic acid at 1 atm (101.3 kPa) is to be extracted with water to recover the acid. LLE data are given below.

- 45 kg of a mixture containing 35 wt% chloroform and 65 wt% acid, which is treated with 22.75 kg of water at 18 °C in a simple one-stage batch extraction. What are the weights and compositions of the raffinate and extract layers produced?
- If the raffinate layer from the above treatment is extracted again with half of its weight of water, what will be the compositions and weights of the new layers?
- If all the water is removed from this final raffinate layer, what will its composition be?

Heavy Phase (wt%)			Light Phase (wt%)		
CHCl ₃	H ₂ O	CH ₃ COOH	CHCl ₃	H ₂ O	CH ₃ COOH
99.01	0.99	0.00	0.84	99.16	0.00
91.85	1.38	6.77	1.21	73.69	25.10
80.00	2.28	17.72	7.30	48.58	44.12
70.13	4.12	25.75	15.11	34.71	50.18
67.15	5.20	27.65	18.33	31.11	50.56
59.99	7.93	32.08	25.20	25.39	49.41
55.81	9.58	34.61	28.85	23.28	47.87

Solution:

The solubility data (complete set) were selected and used to make a new chart (xy scatter with grid) on a separate sheet. The series (solubility envelope) was formatted with a smooth solid line. It may be easier in what follows to remove the data symbols (Marker—None) from the solubility envelope data series. They will be identified again with the tie lines.

The tie lines can be plotted on top of this chart as follows: Select the tie line end points (two sets) using the ctrl key. Since the data are ordered there will be one set near the top of

the preceding table and a corresponding set the same distance from the bottom. Select copy under the edit menu followed by paste special under the edit menu on the chart (choose new data series with x values in the first column). Click on the new data series (two points) that will be on top of the previously plotted series. When selected, only two points should be highlighted. Format the series with a dotted line and a convenient color (same as solubility envelope, for instance). The plait point is not included in this step. It is equivalent to a *collapsed* tie line.

3			1		
Heavy Phase (wt%)			Light Phase (wt%)		
CHCl ₃	H ₂ O	CH ₃ COOH	CHCl ₃	H ₂ O	CH ₃ COOH
99.01	0.99	0.00	0.84	99.16	0.00
91.85	1.38	6.77	1.21	73.69	25.10
80.00	2.28	17.72	7.30	48.58	44.12
70.13	4.12	25.75	15.11	34.71	50.18
67.15	5.20	27.65	18.33	31.11	50.56
59.99	7.93	32.08	25.20	25.39	49.41
55.81	9.58	34.61	28.85	23.28	47.87

Plot the equilibrium data and the inlet compositions

Feed	Feed	
0.00	65.00	65.00
Solvent		
100.00	0.00	0.00

Compute M; read composition of M from chart:

$$\begin{aligned}\mathcal{W}^{(S_0)} &= 22.75 \\ \mathcal{W}^{(F)} &= 45 \\ \mathcal{W}^{(M)} \omega_1^{(M)} &= 0.65 \mathcal{W}^{(F)} \\ \mathcal{W}^{(M)} &= \mathcal{W}^{(F)} + \mathcal{W}^{(S_0)} \\ \omega_1^{(M)} &= 0.43173 \\ \mathcal{W}^{(M)} &= 67.75\end{aligned}$$

	ω_3	ω_1	
1	0.99	0.00	Raffinate
2	1.38	6.77	Raffinate
3	2.28	17.72	Raffinate
4	4.12	25.75	Raffinate
5	5.20	27.65	Raffinate
6	7.93	32.08	Raffinate
7	9.58	34.61	Raffinate
7	23.28	47.87	Extract
6	25.39	49.41	Extract
5	31.11	50.56	Extract
4	34.71	50.18	Extract
3	48.58	44.12	Extract
2	73.69	25.10	Extract
1	99.16	0.00	Extract

43.173

Location of M by trial (34) with 43.173 fixed

Read product stream compositions from graph and compute amounts from material balances

$$\omega_1^{(R)} = 0.23$$

$$\omega_1^{(S)} = 0.475$$

$$0.23\mathcal{W}^{(R)} + 0.475\mathcal{W}^{(S)} = 0.43173(67.75)$$

$$\mathcal{W}^{(R)} + \mathcal{W}^{(S)} = 67.75$$

$$\text{Solution : } \mathcal{W}^{(R)} = 11.965, \quad \mathcal{W}^{(S)} = 55.785$$

New feed

$$\begin{aligned}\omega_3^{(R)} &= 0.035 \\ \omega_1^{(R)} &= 0.23 \\ \omega_2^{(R)} &= 1 - 0.2 - 0.035 = 0.735 \\ 0.23\mathcal{W}^{(R)} &= \omega_1^{(M)}\mathcal{W}^{(M)} \\ 0.5\mathcal{W}^{(R)} + \mathcal{W}^{(R)} &= \mathcal{W}^{(M)} \\ \omega_1^{(M)} &= 0.15333 \\ \mathcal{W}^{(M)} &= 17.948\end{aligned}$$

pure solvent at 1/2 the mass of the new feed (R)

Read product compositions and compute amounts as above.

$$\omega_{(3)}^{(R)} = 0.0138 \quad \omega_{(3)}^{(S)} = 0.736 \quad \mathcal{W}^{(R)} + \mathcal{W}^{(E)} = 17.948$$

$$\omega_{(1)}^{(R)} = 0.0677 \quad \omega_{(1)}^{(S)} = 0.251 \quad 0.0677\mathcal{W}^{(R)} + 0.251\mathcal{W}^{(S)} = 0.1533(17.948)$$

$$\omega_{(2)}^{(R)} = 0.915 \quad \omega_{(2)}^{(S)} = 0.0121 \quad \text{Solutions : } \mathcal{W}^{(R)} = 9.5664, \quad \mathcal{W}^{(S)} = 8.3816$$

Extend line from S through R to vertical axis to find 8% HAC as shown in Figure 6.39.

Example 6.4.2.3-2: T-303 Acid Extractor—Solvent Flow for Single Equilibrium Stage

Just after the reaction section in the manufacture of acrylic acid, the product stream (9) at 27,463 kg/h consists essentially of 23 wt% acrylic acid and 77 wt% water. The actual stream contains about 1% acetic acid. The product stream is to be fed to an extraction column (see Figure 6.27) and contacted with a recycled diisopropyl ether stream (23) that contains 2.6 wt% water. The objective is to reduce the acid concentration in the water stream to 0.5 wt% (12). The acid is therefore recovered before the water stream is sent to the waste tower.

Determine the solvent requirement for a single equilibrium stage.

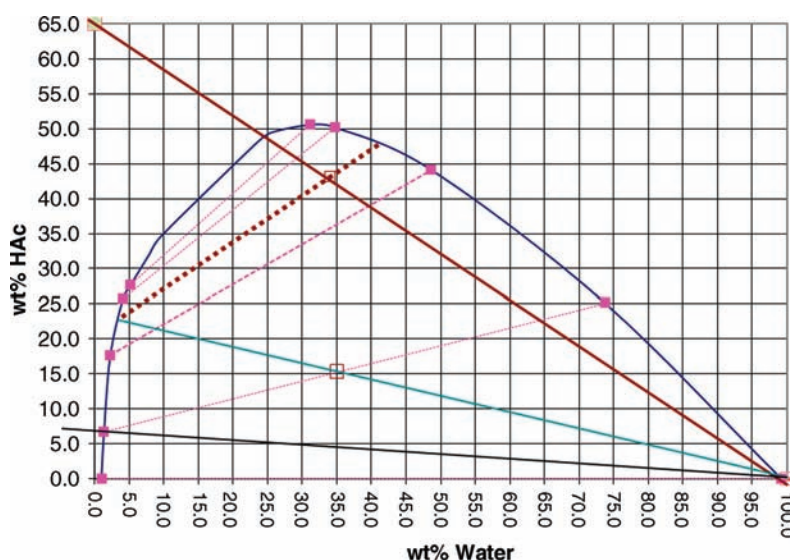


FIGURE 6.39 Determination of water-free concentration.

Equilibrium data are available at 40 °C and 2 bar but most of the data are outside the range of operating conditions. The results will therefore be approximate.

Water Phase		Ether Phase	
ω_D	ω_A	ω_D	ω_A
0.00125	0.00000	0.99676	0.00000
0.00146	0.06694	0.97586	0.02067
0.00263	0.32750	0.93628	0.05981
0.00404	0.64690	0.91333	0.08274
0.00400	0.73712	0.90082	0.09542
0.00389	0.77622	0.89262	0.10379
0.00380	0.79814	0.88686	0.10968
0.00374	0.81218	0.88260	0.11404
0.00369	0.82194	0.87934	0.11738
0.00366	0.82911	0.87676	0.12003
0.00363	0.83460	0.87468	0.12217

ω = weight fraction: D, diisopropyl ether; A, acrylic acid.

Only the lowest tie lines have any significance in this application. The first here are plotted in the following figure. The feed, solvent (pure), and the desired raffinate composition are located on the plot. A tie line with R as an end point is then estimated (an understatement!) and the intersection with the line connecting F and S is drawn. The flow rate of stream S can then be estimated giving a solvent to feed ratio of 75.6 or 2,078,034 kg/h.

For an estimation of M for single-stage solvent requirement (see Figure 6.40).

In Example 7.3-2, it is found that six equilibrium stages and a solvent flow rate of 145,114 kg/h are required for this

separation if a countercurrent arrangement (see Chapter 7) is used. If the countercurrent arrangement is a series of mixer-settlers, the calculations in Example 5.3-1 show that the volume of the mixers must be 3100 gal.

If 3100 gal tanks are used in the present example, we calculate the number by using a residence time of 3 min. In this case, the flow to each mixer should be

$$\mathcal{N}^{(F)} \left[\frac{1}{\rho^{(F)}} + \frac{75.6}{\rho^{(S)}} \right] = \frac{3100}{3} \text{ gpm}$$

$$\rho^{(F)} = 1.0137 \text{ kg/l, see Example 5.3-1}$$

$$\rho^{(S)} = 0.70183 \text{ kg/l}$$

$$\mathcal{N}^{(F)} \text{ kg/h} \left[\frac{1}{1.0137} + \frac{75.6}{0.70183} \right] \frac{7.4805}{28.317} \left[\frac{1}{60} \right] = \frac{3100}{3}$$

$$\mathcal{N}^{(F)} = 2159 \text{ kg/h}$$

It requires 13 tanks acting as single stages.

In summary, the single-stage operation requires 14.3 times as much solvent as the countercurrent arrangement of mixer-settlers and more than twice the number of stages.

6.5 ADSORPTION

The surface of particular porous solids plays a vital role in a number of important chemical engineering operations. In the separation of gas mixtures and liquid mixtures, for example, a surface that preferentially adsorbs either the desirable or the undesirable components can provide the required purity. In the case of catalytic reactions, the surface hosts the reaction process by providing a large number of sites that bind the catalyst and possibly one or more reactants or products. In

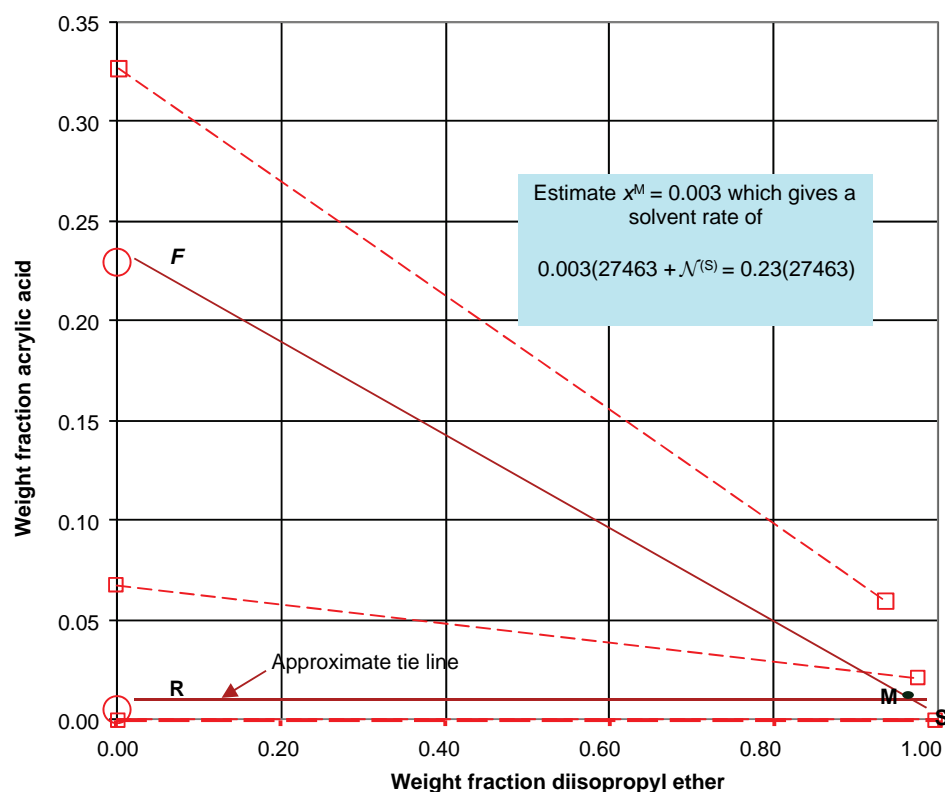


FIGURE 6.40 Estimation of M for single-stage solvent requirement.

both cases, a large surface per unit volume is often provided by a highly porous solid. Consequently, molecular participants must diffuse into and out of the particle as well as interact with the surface. The diffusion process is analyzed in Chapter 10.

Adsorption processes consist of the selective uptake of one or more components, called adsorbates, from a gas or liquid mixture by a porous solid referred to as the adsorbent. The adsorbates are bound to the internal surface of the adsorbent, which is measured in hundreds of square meters per gram. The internal surface of most adsorbents is produced by the expulsion of water vapor.

The forces of interaction between the diffusants and the solid can be primarily van der Waals forces or they may involve chemical bonds. The former is referred to as physical adsorption and the latter as chemical adsorption. Figure 6.41 illustrates both types for the adsorption of hydrogen on N_i .

As a molecule of hydrogen approaches the surface, it is trapped by shallow potential energy well characteristic of physical adsorption and as an enthalpy of adsorption (ΔH_p in Figure 6.41). This process can result in the formation of more than one layer of physically adsorbed molecules.

The deep well next to the surface represents the chemisorption of hydrogen atoms in this case and has an enthalpy change (ΔH_c in Figure 6.41). There is an activation barrier to chemisorption (equal to E in Figure 6.41). Since the

hydrogen molecule dissociates into hydrogen atom, this is called dissociative chemisorption. Not all chemisorption is dissociative.

The heat released in physical adsorption is of the order of the heat of condensation where the heat effect of chemisorption is larger and in the range of heats of reaction. Chemisorption is normally irreversible and takes place in catalytic systems. Industrial adsorbents rely on physical adsorption, which is reversible.

During the transient period, the adsorbate diffuses into the adsorbent and progressively saturates the solid surface. The saturation process is completed when the concentration on the solid surface is uniform throughout at the value associated with the gas phase conditions. The exterior and interior gas phase conditions are the same at equilibrium or saturation. The saturation process is illustrated in Figure 6.42.

The mass transfer processes, which are an important feature of these operations, is discussed in Chapters 10 and 12.

6.5.1 Adsorbents

Characterization of a porous region is often limited to the basic parameters defined and illustrated in Table 6.14.

Other parameters used to characterize porous solids are the specific surface area, S_g , defined as the internal surface area per unit mass of solid, and the external surface area per

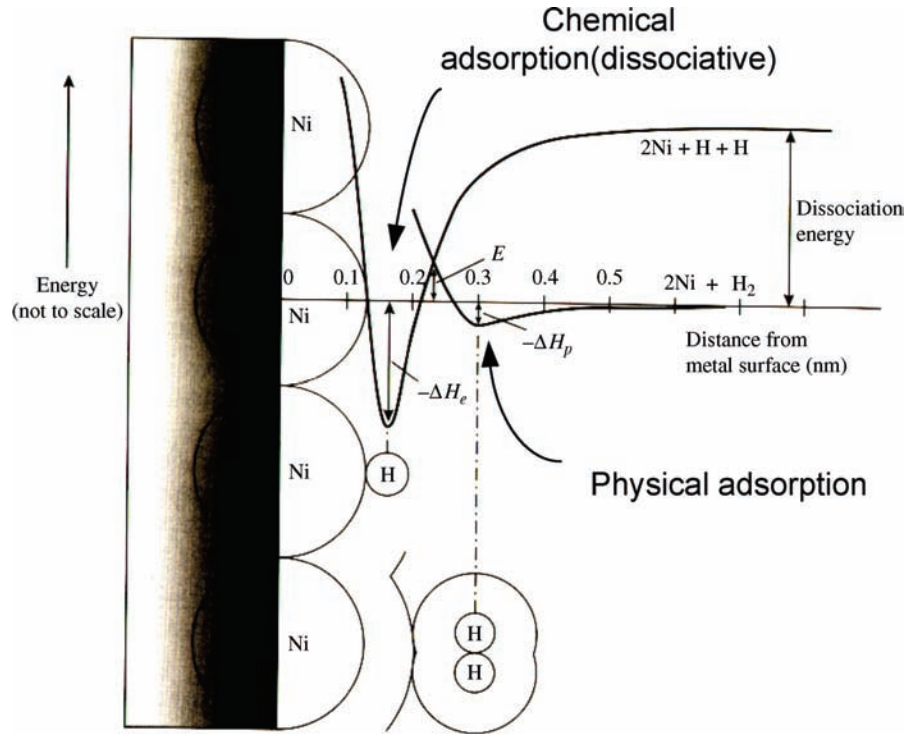


FIGURE 6.41 Adsorption of hydrogen on nickel (Davis and Davis, 2003). Reprinted with permission of McGraw-Hill.

unit mass S_m , which is the boundary between the inside and outside of the particle.

The surface area can be measured by the BET (Brunauer–Emmet–Teller) method, which determines the amount of a gas, usually nitrogen required for a monolayer coverage. Knowledge of the cross-sectional area of the adsorbed gas molecule then gives the surface area. The method is discussed in Ruthven (1984).

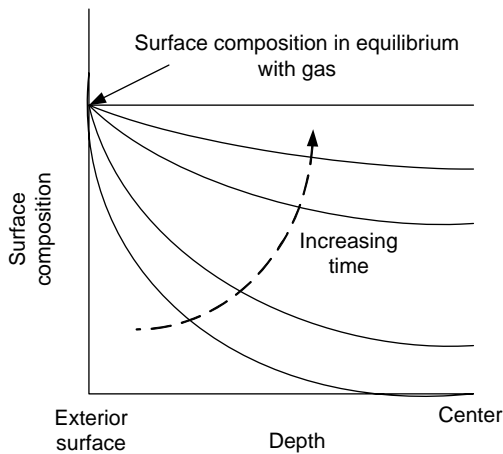


FIGURE 6.42 Concentration profiles during adsorbent saturation.

A finer description of the porous structure is given by the pore size distribution, $f(r)$, where $f(r)dr$ is the fraction of the particle volume that is made up of pores with radii between r and $r + dr$. The pore size distribution can be measured by nitrogen adsorption and mercury porosimetry (Satterfield, 1970).

Mercury porosimetry makes use of the relationship of the pressure, P , required to force mercury into a pore of radius r :

$$r = \frac{1 - 2\sigma \cos \theta}{P} \quad (6.121)$$

where σ is the surface tension of Hg and θ is the contact angle.




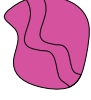

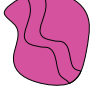


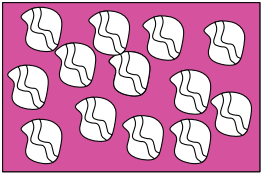
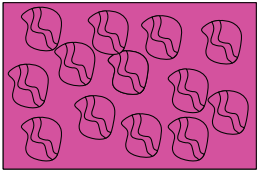
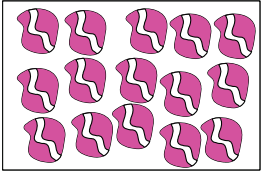
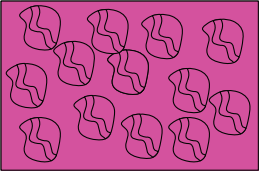
Because of the definition of the pore size distribution,

$$\varepsilon_p = \int_0^\infty f(r)dr \quad (6.122)$$

The surface area per unit volume for a pore of radius r is $2/r$ so that

$$\rho_p S_g = \int_0^\infty \frac{2}{r} f(r)dr \quad (6.123)$$

TABLE 6.14 Characterization of Porous Solids

Mass or Volume =Numerator	Mass or Volume =Denominator	Parameter Definition Relations
		Solid or true density = mass/volume
		ρ_s Apparent density=mass/volume
		ρ_p Porosity = volume/volume
		ε_p Void volume = volume/mass
		V_g $\rho_p = \rho_s(1 - \varepsilon_p)$; $V_g = \frac{\varepsilon_p}{\rho_p}$ Bed porosity = volume/volume
		ε_b $\varepsilon_b = 1 - \frac{\rho_b}{\rho_p}$ Bulk density = mass/volume
		ρ_b $\rho_b = \rho_p(1 - \varepsilon_b)$

Note: The shaded regions in the first and second columns represent the region whose mass or volume is being used in the numerator or denominator of the definition in the third column.

If a single pore size exists,

$$f(r) = \varepsilon \delta(r - r_0) \quad (6.124)$$

It follows from the preceding equation that

$$r_0 = \frac{2\varepsilon}{\rho_p S_g} = \frac{2V_g}{S_g} \quad (6.125)$$

This value can be used as the average pore radius when the pore size distribution is not known.

The most important industrial adsorbents are summarized in Table 6.15. The oxygen containing compounds have hydrophilic properties and the materials with carbon as the major component have hydrophobic properties. The zeolites and molecular sieves have specific pore diameters and the zeolites have interconnected cage-like structures that will exclude molecules larger than a specific size. These materials are highly selective.

Adsorption operations are divided into purification operations and bulk separations. The dividing point is a feed composition of approximately 10 wt% adsorbate.

6.5.2 Gas Adsorption

In Chapter 3, we noted with the introduction of Equation (3.2) that the extensive variables (ξ) and the associated intensive variables (Ξ) that describe a thermodynamic chemical system are introduced through work terms in the differential of the internal energy function or the First Law.

$$dU(\underline{S}, \dots, N_i, \dots, \dots, \Xi_k, \dots) = T d\underline{S} + \sum \mu_i dN_i + \sum \xi_k d\Xi_k \quad (6.126)$$

The intensive variables are the first derivatives of the internal energy function and are therefore functions of the extensive variables. For the PVT systems we have studied thus far, the

TABLE 6.15 Industrially Important Adsorbents

Adsorbent		Major Component	Shape ^a and Size	True Density (kg/m ³)	Apparent Density (kg/m ³)	Packing Density (kg/m ³)	Micropore Volume (cm ³ /g)	Macropore Volume (cm ³ /g)	Specific Surface (m ² /g)	Specific Heat Capacity (J/(kg K))	Thermal Conductivity (W/(m K))	Porosity
Oxygen-containing adsorbents	Silica gel	SiO ₂	P, S (1–8 mm)	2200	750–1250	300–850	0.30–1.15	<0.10–0.25	100–850	0.92–1.0	0.14–0.20	0.45–0.65
	Activated alumina	Al ₂ O ₃	G, S (2–10 mm)	3000–3100	1200–2400	700–950	0.40–0.60	0.10–0.15	100–400	0.88–1.05	0.12	0.13–0.6
	Zeolites and molecular sieves	SiO ₂ Al ₂ O ₃	P, S (1–5 mm), HC (6–7 mm), CP (2–4 mm)	2100–2600	1100–1500	400–900	0.20–0.30	0.30–0.70	350–1100	0.80–1.05	0.13–0.58	0.5–0.6
	MCM	SiO ₂ Al ₂ O ₃	HC		550 (min)	170–450	Mesopore: 0.21–1.00	450–1200			0.20–0.52	
	Clay mineral and pillared clays	SiO ₂ Al ₂ O ₃	P, G	2200	1600–1700	500–700	~150	0.19–0.40	120–500			0.20–0.35
Carbon adsorbents	Activated carbon	C	P, G (1–10 mm), CP	1880–2200	440–900	250–550	0.20–0.50	0.40–1.5	200–4000	0.76–0.92	0.65–0.1	0.45–0.77
	Activated coke	C	P, G	~1900	~900	450–600	0.01–0.10	0.20–0.30	15–400			~0.35
	Carbon molecular sieves	C	P, S, CP	1800–2100	900–1290	600–900	~0.18	0.38–0.60	100–1500	0.84–1.00	0.65	0.35–0.57
	Carbon nanotubes	C	P				Mesopore: 0.05–0.45	150–650				
	Polymeric resins	C, H SiO ₂ , C, Cu, Ag	S, G P, G, CP	1000–1300	400–900	300–750	<0.10–0.43	0.37–1.50 0.20–1.60	80–1500 50–670	0.33–1.5 ^b	0.06–0.07 ^b	0.35–0.65

Source: Ullmann (1994).

^aP, fine powder; S, spheres; G, granules; HC, hollow cylinder (external diameter); CP, cylindrical pellets (diameter).

^bIn dry state.

work term is $-P(=\xi)(dV)(=\Xi)$. Other systems such as magnetic and electric systems (Callen, 1960) are incorporated into the thermodynamic framework in this manner.

6.5.2.1 Equilibrium Relations for a Single Adsorbate (see Smith et al., 2005) Here we consider a unit mass of adsorbent and assume that it is completely inert. Consequently, only the adsorbate and the single the equilibrium gas phase will contribute to the calculations. The adsorbed component of the gas phase forms a two-dimensional phase resting on the adsorbent surface. The adsorbed species does work against a spreading pressure Π in order to increase the occupied area on the surface Δ . In general,

$$dU = T dS - \Pi d\Delta + \mu dN \quad (6.127)$$

and

$$-\Delta d\Pi + N d\mu = 0 \quad \text{at constant } T \quad (6.128)$$

which is the Gibbs–Duhem equation at a constant temperature. In this case, the area is per unit mass of the adsorbent and may be taken as S_g , a characteristic of the adsorbent.

The chemical potential in the condensed state is equal to the chemical potential of the component in the gas phase equilibrium. Using the definition of fugacity in Equation (6.8) and assuming that the gas phase is ideal, the preceding equation may be written as

$$a d\Pi = RT d \ln yP \quad \text{at constant } T \quad (6.129)$$

where $a = S_g/N$ and y is the gas phase mole fraction of the adsorbate. This relation can be used to generate an isothermal plot of the gas phase pressure versus the amount adsorbed with an equation of state for the adsorbed phase. Suppose that the following analogue of the compressibility factor applies to the adsorbed phase:

$$Z = \frac{\Pi a}{RT} \quad (6.130)$$

Differentiating this expression and using the expression for the molar area and Equation (6.129),

$$\begin{aligned} dZ &= \frac{\Pi}{RT} da + \frac{a}{RT} d\Pi \\ &= \frac{\Pi}{RT} da + d \ln yP = \frac{\Pi}{RT} \left[-S_g \frac{dN}{N^2} \right] + d \ln yP \\ &= -Z \frac{dN}{N} + d \ln yP \end{aligned} \quad (6.131)$$

Or integrating from a fresh surface ($N = 0, P = 0, Z = 1$) to an arbitrary quantity of adsorption—at a constant temperature,

$$\int_0^N d \ln \frac{N}{yP} dN = \int_0^N (1 - Z) \frac{dN}{N} - \int_{N=0}^{N=N} dZ \quad (6.132)$$

The ideal value of 1 is taken for Z for a fresh surface with the expectation that the adsorbed species will exhibit ideal behavior under these conditions.

$$\ln \frac{N}{yP} - \lim_{yP \rightarrow 0} \frac{N}{yP} = \int_0^N (1 - Z) \frac{dN}{N} - (Z - 1) \quad (6.133)$$

The limit is indeterminate and can be evaluated with l'Hopital's rule:

$$\lim_{yP \rightarrow 0} \frac{N}{yP} = \lim_{yP \rightarrow 0} \frac{dN}{d(yP)} = \frac{1}{k} \quad (6.134)$$

where k is the slope of the isotherm (yP vs. N at constant T) at the origin. The isotherm is then given in terms of the equation of state as follows:

$$N = kyP \exp \left[\int_0^N (1 - Z) \frac{dN}{N} - (Z - 1) \right] \quad (6.135)$$

Some useful special cases are given below. Note that N may be replaced with w , the mass of adsorbed material per unit mass of adsorbent. Other units are also possible with the associated changes in the parameters.

Case 1: $Z = 1$

This is the ideal case that results in Henry's law:

$$N = kyP \quad (6.136)$$

When the amount of adsorption is small, all isotherms obey Henry's law:

$$\text{Case 2: } Z = \frac{-\ln \left[1 - \left(\frac{N}{N_{\max}} \right) \right]}{\left(\frac{N}{N_{\max}} \right)} \text{ where } N_{\max} \text{ is a constant}$$

This is the ideal–lattice-gas equation (Smith et al., 2005). The integral yields the isotherm

$$\frac{N}{N_{\max}} = \frac{kyP}{N_{\max} + kyP} \quad (6.137)$$

This is referred to as the Langmuir isotherm.

Other:

There is no equation of state that will describe the full range of adsorption data. Equations in addition to the ones above that have been useful in correlating adsorption data are the Freundlich equation,

$$N = \alpha(yP)^{1/\beta} \quad (6.138)$$

and the Toth equation,

$$N = \frac{yP}{(b + (yP)^t)^{1/t}} \quad (6.139)$$

If the adsorbent is highly selective, the small amount of adsorption over the target species can be neglected and the data for the single component can be used to describe the adsorption. The case of multicomponent adsorption where the adsorption of two or more species is appreciable has been treated with extensions of the Langmuir and Freundlich isotherms. We will consider applications involving significant adsorption of one component only.

Gas adsorption is most often carried out in fixed beds of adsorbent particles, which gradually become saturated with adsorbate and must be regenerated while a fresh bed is placed on stream. Fixed-bed adsorbers are discussed in Chapter 12. Equilibrium considerations can be used to estimate the time at which the bed will become saturated (see Chapter 12) in the cases of both gas and liquid adsorption.

6.5.3 Liquid Adsorption

6.5.3.1 Equilibrium In the case of liquids, many applications involve the selective adsorption of one or more components dissolved in a solvent. In the case of a single component, the equilibrium isotherms used in the case of gas adsorption are applied with the partial pressure replaced with the concentration of the adsorbate in the liquid over the surface. For example,

$$w = \alpha\rho^{1/\beta} \quad (6.140)$$

and

$$w = \frac{w_{\max}\rho}{(w_{\max}/k) + \rho} \quad (6.141)$$

for the Freundlich and Langmuir isotherms, respectively.

6.5.3.2 Liquid Adsorption Operations Batch operations for the purification of liquids can be carried out in stirred tanks where the liquid to be treated is placed in contact with a powdered adsorbent in a stirred tank of suitable size. Such operations are called slurry adsorption and the equilibrium

stage view of the batch mode is discussed below. The transient period is discussed in Chapter 12 as well as adsorption in fixed beds.

6.5.3.2.1 Batch Operation We want to reduce the mass concentration of a solute from $\rho^{(F)}$ to a fraction φ of this value in a volume \mathcal{V}_L of feed by introducing a mass \mathcal{W}_{ads} of solid adsorbent. The object is to determine the amount of adsorbent to use. The methods to follow for sizing the tank and agitator system are discussed in Section 5.1.

A material balance at any point during the process must state that whatever solute has disappeared from the fluid phase must be found in the solid phase. We can use the average value for the adsorbate loading, $\langle w \rangle$ (mass of adsorbate per unit mass of adsorbent), to express the mass of adsorbate in the solid:

$$\langle w \rangle \mathcal{W}_{\text{ads}} = \int_{\text{Adsorbent particle}} w \rho_{\text{ads}} dV \quad (6.142)$$

The integral is generally represented by the area under the curve in Figure 6.42 at the corresponding time in question. At equilibrium, the local concentrations and the average concentration are equal.

The material balance is given by

$$\begin{aligned} \rho \mathcal{V}_L + \langle w \rangle \mathcal{W}_{\text{ads}} &= \rho^{(F)} \mathcal{V}_L \\ \text{or} \\ \langle w \rangle &= -\frac{\mathcal{V}_L}{\mathcal{W}_{\text{ads}}} (\rho - \rho^{(F)}) \end{aligned} \quad (6.143)$$

which is a straight line of slope $-\mathcal{V}_L/\mathcal{W}_{\text{ads}}$ that passes through the point $(0, \rho^{(F)})$ in $(\rho, \langle w \rangle)$ coordinates and intersects the equilibrium curve at the conclusion of the ideal (equilibrium stage) process.

At the conclusion of the process, the fluid and solid phases are at equilibrium at a fraction of the original concentration, $\varphi\rho^{(F)}$. This is represented graphically at the intersection of the equilibrium curve and the material balance or operating line on Figure 6.43.

A multistage operation results from filtering the product and introducing fresh adsorbent. This is illustrated by the dashed line in Figure 6.43. Each step involves emptying and recharging one or more vessels while charging others. The number of vessels needed for treating a continuous feed depends upon the time required for each of these steps in addition to the time required for the separation to take place. The separation time requires a transient analysis of the mass transfer operation (see Example 12.6.1-1), which tracks the time required to pass from the feed composition to the equilibrium curve (or near to it!). At this juncture, we can, for example, carry out an equilibrium stage analysis and compute the amount of adsorbent required for a given

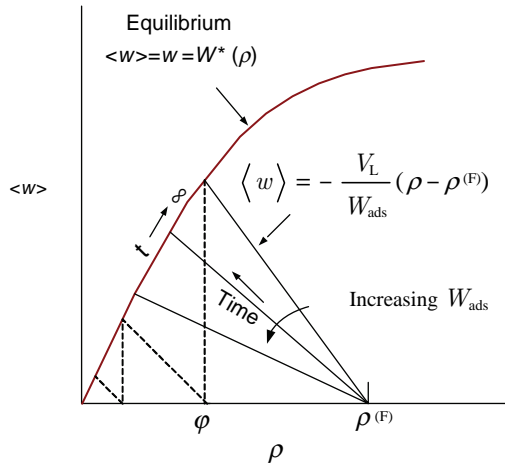


FIGURE 6.43 Single-stage batch adsorption (slurry).

policy. The amount of adsorbent required to reduce the concentration to a fraction of the feed is given by

$$\text{Linear isotherm : } W_{\text{ads}} = \frac{V_L}{\alpha} \left[\frac{1 - \phi}{\phi} \right] \quad (6.144)$$

$$\text{Langmuir : } W_{\text{ads}} = \frac{V_L \rho^{(F)} (1 - \phi)}{w_{\text{max}}} \left[\frac{1}{k \phi \rho^{(F)}} + 1 \right] \quad (6.145)$$

The linear and Langmuir isotherms are discussed above.

Example 6.5.3.2.1-1: Adsorption Step in the Production of Hexyl Glucoside

The material balance for a proposed continuous process is given in Problem 4 in Chapter 2. The adsorber feed consists of hexanol ($N_2^{(6)} = 551.08 \text{ g mol/h}$) and hexyl glucoside ($N_3^{(6)} = 1.0775 \text{ g mol/h}$) at a total volumetric flow rate of $V^{(6)} = 66.2591 \text{ h}$. Determine the amount of adsorbent required for a batch adsorption system for a final concentration in the hexanol effluent 0.5% of the feed.

Storage must be provided to accumulate the feed over the time required to process the amount accumulated. If the adsorption is done in stages, the tank size is determined by the time required to complete all of the stages, which includes filling, processing, emptying, filtering, and cleaning. Allowance must also be made to accommodate disruptions in the process. In this example, we will assume that 4 h is required for the adsorption process.

The adsorption isotherm for the glucoside is (de Roode et al., 2001)

$$w = \frac{w_{\text{max}} k \rho}{1 + k \rho}$$

$$w_{\text{max}} = 0.1295 \text{ g/g}$$

$$k = 2.141/\text{g}$$

For a fill time of 4 h,

$$V_L = 4 \times 66.259 = 265.0361 = 70 \text{ gal}$$

The initial concentration is

$$\rho^{(F)} = \frac{1.0775}{66.259} 263.3 = 4.2823 \text{ g/l}$$

The amount of adsorbent required is given by Equation (6.145):

$$W_{\text{ads}} = \frac{265.036(4.2823)(1 - 0.005)}{0.1295} \left[\frac{1}{2.14(0.005)4.2823} + 1 \right] = 199,036 \text{ g} = 438.4 \text{ lb}$$

Graphical construction:

The graphical solution begins with a plot of the given equilibrium data (w vs. ρ) and locating the charging conditions and final equilibrium conditions. These steps are shown in Figure 6.44.

The slope of the operating line is so small (see inset) that it appears to coincide with the horizontal axis. The inset portrays the situation near the output, which is found by locating the point on the equilibrium curve corresponding to the desired purity of the adsorbate. The quantity of adsorbent required can be calculated from the slope (see Equation (6.143)):

$$\frac{V_L}{W_{\text{ads}}} = 0.001332 \text{ or } W_{\text{ads}} = \frac{265.036}{0.001332} = 198,976 \text{ g} = 438 \text{ lb}$$

This large adsorbent requirement (estimate the volume) is typical of single-stage operations, which must equilibrate at the low concentrations required of the output. For example, if the adsorption operation were carried out in two steps with equal concentration drops, the adsorbent requirement would be

$$(W_{\text{ads}})_1 = \frac{265.036(4.2823)(1 - 0.498)}{0.1295} \left[\frac{1}{2.14(0.498)4.2823} + 1 \right] = 5,362 \text{ g}$$

$$(W_{\text{ads}})_2 = \frac{265.036(4.2823)0.498(1 - 0.01004)}{0.1295} \left[\frac{1}{2.14(0.498)4.2823(0.01004)} + 1 \right] = 98,619 \text{ g}$$

$$\text{Total} = 103,981 \text{ g} = 229 \text{ lb}$$

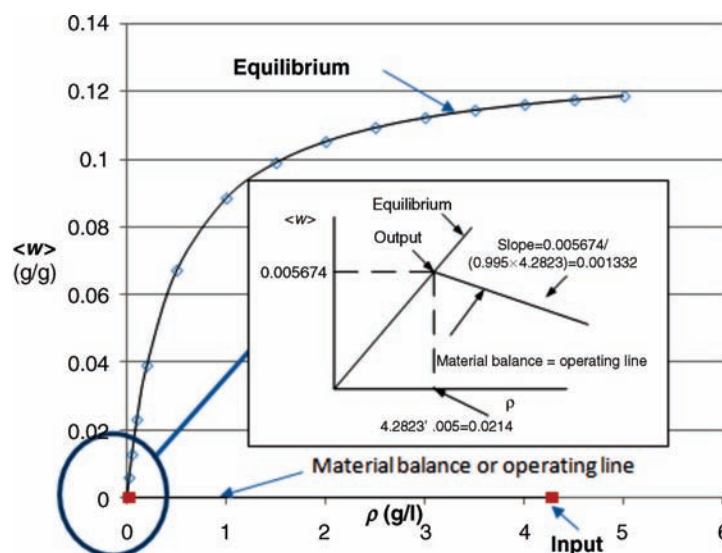


FIGURE 6.44 Equilibrium and operating lines for hexyl glucoside adsorption.

The adsorbent requirement is nearly halved; however, the number of operations has doubled.

6.6 SINGLE-PHASE STIRRED TANK REACTORS

In contrast to the completely mixed systems considered thus far, a stirred tank reactor is a completely mixed system in which the contents may not be in equilibrium. Here we are referring to chemical reaction equilibrium. We will consider first the case where the reaction processes have not yet equilibrated when the products are withdrawn. Chemical reaction equilibrium is considered in conclusion.

The single-phase stipulation generally excludes, for example, such operations as gas absorption and liquid extraction with reaction. A CSTR is illustrated in Figure 6.45.

A steady feed is supplied. The molar discharge rate prevents any accumulation in the tank due to flow or chemical reaction. Any remnants of the unsteady conditions associated with a startup program are assumed to have been washed away.

The conditions in the exit stream are identical with those in the tank. The volume of the reaction mixture, V_R , is equal to the volume of the vessel in the case of gases. The temperature of the contents is established by the supply or removal of heat accomplished by a submerged heat exchanger, by circulation through an external heat exchanger, or through the vertical walls of a jacketed reactor. Heat supplied to the reactor is counted as a positive value of Q .

The CSTR responds immediately to changes in the feed or tank conditions and may be chosen on this basis for process control implementation. The CSTR is also applied to systems where there is a kinetic/selectivity advantage to low

reactant compositions (see Chapter 7), which at the same time is a drawback since the rate is at its lowest value here.

Without the feed and product streams, the stirred tank is a batch reactor that supplies the holding time required for an initial charge of reactive components to reach a desired level of conversion. The batch reactor is an unsteady-state reactor where all of the elements in the system have exactly the same age. There is, therefore, no mixing of elements of different ages.

The CSTR and the batch reactors are related to the ideal plug flow reactor (PFR), a conduit of circular cross section through which all of the fluid elements flow with the same velocity. An observer moving with the velocity of the fluid in the PFR would experience the same conditions in time as a stationary observer recording conditions in a stationary batch reactor. Also, it may be shown that if a series of CSTRs with all outlets, save the last, attached to the inlet of the succeeding member of the series, the series will converge to the PFR (Denbigh, 1966).

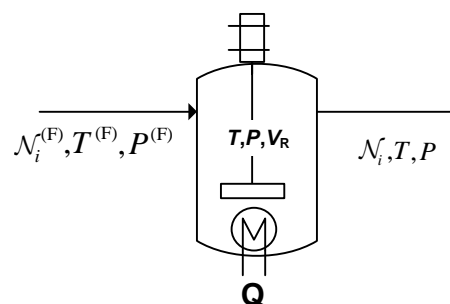


FIGURE 6.45 Continuous stirred tank reactor.

The reaction rates in the following discussion will be expressed as

$$\text{Reaction rate} = \underbrace{k(T)}_{\substack{k(T) = \text{rate constant} = k_0 e^{-(E/RT)} \\ k_0 = \text{preexponential factor} \\ E = \text{activation energy} \\ \frac{dk(T)}{dT} = \frac{E}{RT^2} > 0}} \underbrace{F(\text{concentrations})}_{\text{Distance from equilibrium}} \quad (6.146)$$

except for the biocatalytic production of L-tyrosine. Additional discussion of chemical kinetics may be found in Chapter 8.

6.6.1 Continuous Stirred Tank Reactors

Multiple chemical reactions, N_r in number, are accounted for with the following stoichiometry:

$$\sum_{\text{all } i} \vartheta_{ij} A_i = 0 \quad j = 1, 2, \dots, N_r \quad (6.147)$$

If the molar rate per unit volume of the j th reaction is \mathcal{R}_{vj} , the mass balances for the CSTR may be written in molar units as

$$\mathcal{N}_i = \mathcal{N}_i^{(F)} + \sum_{j=1}^{N_r} \vartheta_{ij} \mathcal{R}_{vj} V_R \quad i = 1, 2, \dots, N_c \quad (6.148)$$

where

$$\mathcal{R}_j = \int_{V_R} \mathcal{R}_{vj} dV = \mathcal{R}_{vj} V_R \quad j = 1, 2, \dots, N_r \quad (6.149)$$

is used in Section 2.4. Following the approach used for the macroscopic mass balances with multiple reactions in Section 2.4, the reaction extents may be introduced as follows:

$$\mathcal{N}_i = \mathcal{N}_i^{(F)} + \sum_j \vartheta_{ij} \xi_j \quad \text{for all } i \quad (6.150)$$

Substitution of Equation (6.150) into the mass balance, Equation (6.148), gives

$$\sum_j \vartheta_{ij} (\xi_j - \mathcal{R}_{vj} V_R) = 0 \quad \text{for all } i \quad (6.151)$$

$$\xi_j = \mathcal{R}_{vj} V_R \quad \text{for all } j \quad (6.152)$$

since the reactions are independent (see Section 2.4.2).

In general, Equation (6.152) with an equation of state represents a system of algebraic equations with two degrees

of freedom if the feed composition is fixed. An expedient approach to the sizing problem is to fix the reactor temperature and volume and solve for the extents until a desired product distribution is obtained.

Note in particular that the energy and mass transfer problems are uncoupled by specifying the value of the reactor temperature. The solution to the mass balance will in this case provide the means to evaluate the heat load, which must be met to maintain the specified value of the reactor temperature.

For liquid systems, the reaction rates depend, in many cases, on the molar compositions. For gas phase reactions, the prevalent composition variables are partial pressures or mole fractions. The composition variables in both cases must be expressed in terms of extents to close the system of algebraic equations [Equation (6.152)], for the extents. In general, the kinetics for both liquid and gas phase systems will be nonlinear so that a numerical solution to the system of equations will generally be required. Some analytical solutions can however be obtained for particular cases.

6.6.1.1 Liquid Phase Systems—Temperature Specified For liquid phase reactions, the small difference in density between the inlet and outlet can be neglected. The flow rates in terms of the extents can be replaced with molar compositions:

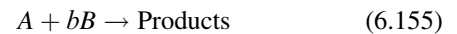
$$c_i = c_i^F + \sum_{j, \text{all reactions}} \vartheta_{ij} \frac{\xi_j}{\mathcal{V}} \quad (6.153)$$

where \mathcal{V} is the volumetric flow rate. Upon substitution of Equation (6.153), the balance equations, Equation (6.151) for the extents become:

$$\left[\frac{\xi_j}{\mathcal{V}} \right] = R_j \left(c_i \left(\mathbf{c}^{(F)}, \frac{\xi}{\mathcal{V}} \right), T \right) \tau_R \quad \text{for all } j \quad (6.154)$$

The extents have been scaled by the volumetric flow rate. A dependence of the reaction rate on pressure has not been expressed since it is not normally important for liquids. The average residence time is denoted by τ_R .

6.6.1.1.1 Single Irreversible First-Order Reactions Suppose we have a single liquid phase reaction with the following stoichiometry that we wish to carry out in a CSTR:



The reaction is irreversible in the sense that the equilibrium conversion is nearly complete at the conditions we plan to carry it out. If we suppose that the feed to the CSTR is very

concentrated in B ,

$$c_B^{(F)} \gg bc_A^{(F)} \quad (6.156)$$

then we can expect no noticeable change in the concentration of B across the reactor. If in addition the reaction order with respect to A is 1, the kinetics can be expressed in the linear form regardless of the order with respect to B , β .

$$\mathcal{R}_v = kc_B^{(F)\beta} c_A = kc_B^{(F)\beta} \left(c_A^{(F)} - \frac{\xi}{V} \right), \quad \xi \leq \mathcal{V}c_A^{(F)} \quad (6.157)$$

The mass balance

$$\frac{\xi}{V} = kc_B^{(F)\beta} \left(c_A^{(F)} - \frac{\xi}{V} \right) \tau \quad (6.158)$$

or

$$\xi = \frac{\mathcal{V}c_A^{(F)}}{1 + (\mathcal{V}c_A^{(F)} / (kc_A^{(F)} c_B^{(F)\beta} V_R))} \quad (6.159)$$

The extent, relative to its maximum value, depends on the ratio of two rates: the feed rate of A relative to a measure of its reaction rate, actually the maximum possible. If the ratio is large, the reaction rate is small relative to the feed rate of A and the extent will therefore be proportionally small. Note that the relative conversion of A is given by

$$x = \frac{\mathcal{V}c_A^{(F)} - \mathcal{V}c_A}{\mathcal{V}c_A^{(F)}} = \frac{\xi}{\mathcal{V}c_A^{(F)}} \frac{\mathcal{V}c_A^{(F)} - \mathcal{V}c_A}{\mathcal{V}c_A^{(F)}} = \frac{\xi}{\mathcal{V}c_A^{(F)}} \quad (6.160)$$

and that the volume for a specified conversion is given by

$$V_R = \frac{\mathcal{V}c_A^{(F)}}{kc_A^{(F)} c_B^{(F)\beta}} \frac{\xi / \mathcal{V}c_A^{(F)}}{1 - (\xi / \mathcal{V}c_A^{(F)})} \quad (6.161)$$

Bear in mind that the fractional conversion for a single reaction is generally $-\nu_A(\xi / \mathcal{V}c_A^{(F)})$.

6.6.1.1.2 Single Irreversible Second-Order Reactions If the kinetics of the single reaction considered in the previous section are second order, Equation (6.157) becomes instead

$$R_v = kc_B^{(F)\beta} c_A^2 = kc_B^{(F)\beta} \left(c_A^{(F)} - \frac{\xi}{V} \right)^2, \quad \xi \leq \mathcal{V}c_A^{(F)} \quad (6.162)$$

The mass balance is

$$\frac{\xi}{\mathcal{V}c_A^{(F)}} = \frac{\left(1 - (\xi / \mathcal{V}c_A^{(F)}) \right)^2}{\left[\mathcal{V}c_A^{(F)} / (kc_A^{(F)2} c_B^{(F)\beta} V_R) \right]} \quad (6.163)$$

The solutions to this quadratic equation are

$$\begin{aligned} \frac{\xi}{\mathcal{V}c_A^{(F)}} &= \frac{1}{2} \left[\frac{\mathcal{V}c_A^{(F)}}{kc_A^{(F)2} c_B^{(F)\beta} V_R} + 2 \right] \\ &\pm \frac{1}{2} \sqrt{\left[\frac{\mathcal{V}c_A^{(F)}}{kc_A^{(F)2} c_B^{(F)\beta} V_R} + 2 \right] \frac{\mathcal{V}c_A^{(F)}}{kc_A^{(F)2} c_B^{(F)\beta} V_R}} \end{aligned} \quad (6.164)$$

Since

$$\sqrt{\left[\frac{\mathcal{V}c_A^{(F)}}{kc_A^{(F)2} c_B^{(F)\beta} V_R} + 2 \right] \frac{\mathcal{V}c_A^{(F)}}{kc_A^{(F)2} c_B^{(F)\beta} V_R}} > \frac{\mathcal{V}c_A^{(F)}}{kc_A^{(F)2} c_B^{(F)\beta} V_R} \quad (6.165)$$

the positive root is greater than 1 and therefore unacceptable since the extent is bounded by the feed rate of A with the prevailing stoichiometry. The solution for the extent is then

$$\begin{aligned} \frac{\xi}{\mathcal{V}c_A^{(F)}} &= \frac{1}{2} \left[\frac{\mathcal{V}c_A^{(F)}}{kc_A^{(F)2} c_B^{(F)\beta} V_R} + 2 \right] \\ &- \frac{1}{2} \sqrt{\left[\frac{\mathcal{V}c_A^{(F)}}{kc_A^{(F)2} c_B^{(F)\beta} V_R} + 2 \right] \frac{\mathcal{V}c_A^{(F)}}{kc_A^{(F)2} c_B^{(F)\beta} V_R}} \end{aligned} \quad (6.166)$$

The interpretation of the ratio of flow rate to reaction rate discussed above applies here as well. The volume for a given conversion can be obtained for an arbitrary order as

$$V_R = \frac{\mathcal{V}c_A^{(F)}}{kc_A^{(F)\alpha} c_B^{(F)\beta}} \frac{\xi / \mathcal{V}c_A^{(F)}}{\left(1 - (\xi / \mathcal{V}c_A^{(F)}) \right)^\alpha} \quad (6.167)$$

In the present case, of course, $\alpha = 2$.

6.6.1.2 Gas Phase Systems—Temperature Specified For gas phase reactions, the mole fractions need to be related to the extents. The total molar flow rate can be calculated from the addition of the individual flows in Equation (6.151):

$$\mathcal{N} = \mathcal{N}^{(F)} + \sum_{j, \text{all reactions}} \xi_j \Delta n_j \quad (6.168)$$

where the mole change for the j th reaction is

$$\Delta n_j = \sum_{i, \text{all components}} \vartheta_{ij} \quad (6.169)$$

The sum of the stoichiometric coefficients for each reaction gives the mole change associated with that reaction, Δn_j .

The contribution to the change in the total molar flow rate is scaled by the extent for each reaction. The mole fractions in the system are given by

$$y_i = \frac{\mathcal{N}_i}{\mathcal{N}} = \frac{\mathcal{N}_i^{(F)} + \sum_{j, \text{all reactions}} \vartheta_{ij} \xi_j}{\mathcal{N}^{(F)} + \sum_{j, \text{all reactions}} \xi_j \Delta n_j}$$

$$= \frac{y_i^{(F)} + \sum_{j, \text{all reactions}} \vartheta_{ij} \left(\xi_j / \mathcal{N}^{(F)} \right)}{1 + \sum_{j, \text{all reactions}} \left(\xi_j / \mathcal{N}^{(F)} \right) \Delta n_j} \quad (6.170)$$

The balance equations (6.152) for the extents become

$$\mathcal{N}^{(F)} \left[\frac{\xi_j}{\mathcal{N}^{(F)}} \right] = R_j \left(\mathbf{y} \left(\mathbf{y}_0; \left(\frac{\xi}{\mathcal{N}^{(F)}} \right), T, P \right) V_R \right) \text{ for all } j \quad (6.171)$$

The extents have been scaled by the total molar flow rate at the inlet. The pressure has been reintroduced into the rate expression to reflect the usual case for kinetics in gas phase systems.

Example 6.6.1.2-1: Multiple Second-Order Reactions and Sizing of R-301

The reactions in the production of acrylic acid (see Section 1.1) form a series of three second-order reactions between propane and oxygen in the gas phase. The reactor is a fluid bed containing small suspended catalyst particles (see Figure 1.15). The product is withdrawn from a cyclone overhead. The remainder of the circulating gas is returned along with particles removed from the product stream through the heat exchange section. We want to estimate the volume of the fluid bed reactor (see Figure 6.46).

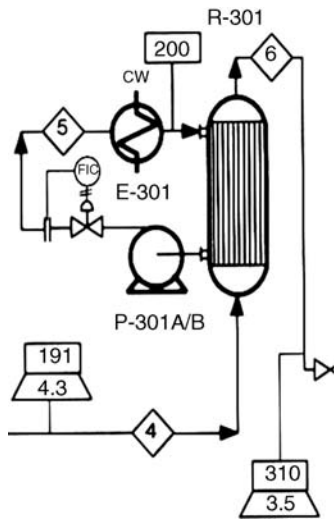


FIGURE 6.46 Reactor R-301 and heat transfer loop. Reprinted with permission of Pearson.

	Stream No.	
	4	6
Temperature (°C)	191	310
Pressure (bar)	4.3	3.5
Mole flow (kmol/h)	2482.2	2444.0
Component mole flow (kmol/h)		
Propylene	127.0	14.7
Nitrogen	1056.7	1056.7
Oxygen	280.9	51.9
Carbon dioxide	—	60.5
Water	1017.6	1165.9
Acetic acid	—	6.54
Acrylic acid	—	87.79

The stream data is reproduced from Table 1.3.

Pressure and temperature: $P = 350 \text{ kPa}$, $T = 310 + 273.16 \text{ K}$

Components are labeled as follows:

Species	Label
C_3H_8	1
O_2	2
N_2	3
CO_2	4
H_2O	5
HAc	6
AAc	7

Stoichiometric coefficients:

(Verify that reactions are independent.)

$$\mathbf{v} = \begin{bmatrix} -1 & -1 & -1 \\ 3 & 5 & 9 \\ -\frac{3}{2} & -\frac{5}{2} & -\frac{9}{2} \\ 0 & 0 & 0 \\ 0 & 1 & 3 \\ 1 & 1 & 3 \\ 0 & 1 & 0 \\ 1 & 0 & 0 \end{bmatrix}; \quad \Delta n_1 = \Delta n_2 = -\frac{1}{2}, \Delta n_3 = \frac{1}{2}$$

Kinetics (see Appendix B):

$$R_{vj} = K_j(T) y_1 y_2 P^2$$

where

$$K(i, T) = k_{i,1} \exp\left(-\frac{E_{i,1}}{RT}\right) \text{ kmol}/(\text{m}^3 \text{ reactor h kPa}^2)$$

and

$$E = \begin{bmatrix} 15,000 \\ 20,000 \\ 25,000 \end{bmatrix} \quad k = \begin{bmatrix} 1.59 \times 10^5 \\ 8.83 \times 10^5 \\ 1.81 \times 10^8 \end{bmatrix} \text{ kcal/kmol}$$

with $R = 1.987 \text{ kcal/(kmol K)}$

The kinetic constants are the product of the true kinetic constants per unit mass of the catalyst and the bulk density of the fluidized catalyst. The reactor volume in the mass balance therefore includes both gas and catalyst.

Reactor inlet flows are considered to be 90% of total flow in stream 4, the reactive channel. The remaining 10% will pass through the unreactive channel to account for known bypassing. Define flows and inlet mole fractions and reaction rate:

$$\mathcal{N}^{(F)} = 0.90 \begin{bmatrix} 127 \\ 280.9 \\ 1056.7 \\ 0 \\ 1017.6 \\ 0 \\ 0 \end{bmatrix} = \begin{bmatrix} 114.3 \\ 252.81 \\ 951.03 \\ 0 \\ 915.84 \\ 0 \\ 0 \end{bmatrix} \quad \text{with } y^{(F)}(i) = \frac{\mathcal{N}_i^{(F)}}{\sum_{j=1}^7 \mathcal{N}_j^{(F)}}$$

$$R_1 = K(1, T) \frac{y^{(F)}(1) + \left(-(\xi_1/\mathcal{N}^{(F)}) - (\xi_2/\mathcal{N}^{(F)}) - (\xi_3/\mathcal{N}^{(F)}) \right)}{1 + \left(-(1/2)(\xi_1/\mathcal{N}^{(F)}) - (1/2)(\xi_2/\mathcal{N}^{(F)}) + (1/2)(\xi_3/\mathcal{N}^{(F)}) \right)} \\ \times \frac{y^{(F)}(2) + \left(-(3/2)(\xi_1/\mathcal{N}^{(F)}) - (5/2)(\xi_2/\mathcal{N}^{(F)}) - (9/2)(\xi_3/\mathcal{N}^{(F)}) \right)}{1 + \left(-(1/2)(\xi_1/\mathcal{N}^{(F)}) - (1/2)(\xi_2/\mathcal{N}^{(F)}) + (1/2)(\xi_3/\mathcal{N}^{(F)}) \right)} P^2$$

Ratio of mass balances: $\frac{\xi_j}{\xi_1} = \frac{R_j}{R_1} = \frac{K(j, T)}{K(1, T)}$

$$\text{Set } \varphi = \frac{\xi_1}{\mathcal{N}^{(F)}}$$

$$R_1(\varphi) = r(\varphi) = K(1, T)$$

$$\times \frac{(y_0(1) - \varphi((1/1) + ((K(2, T))/(K(1, T)))) + ((K(3, T))/(K(1, T))))(y_0(2) - \varphi(3/2) + (5/2)((K(2, T))/(K(1, T))) + (9/2)((K(3, T))/(K(1, T))))}{(1 - (\varphi/2)((1/1) + ((K(2, T))/(K(1, T)))) - ((K(3, T))/(K(1, T))))^2} P^2$$

Establish limiting reactant:

Outlet molar flows:

$$\mathcal{N}_j = \mathcal{N}_j^{(F)} + \left(\sum_{i=1}^i \mathcal{N}_i^{(F)} \right) \varphi \left(\sum_{s=1}^{s=3} v_{j,s} \right) \left(\frac{K(s, T)}{K(1, T)} \right) \\ 0 = \mathcal{N}_j^{(F)} + \left(\sum_{i=1}^{i=7} \mathcal{N}_i^{(F)} \right) \varphi \left(\sum_{s=1}^{s=3} v_{j,s} \right) \left(\frac{K(s, T)}{K(1, T)} \right)$$

Solution is $\{\varphi = 4.0047 \times 10^{-2}\}$

= Maximum value of φ for depletion of 1

Solution is $\{\varphi = 4.3513 \times 10^{-2}\}$

= Maximum value of φ for depletion of 2

Reactor volume:

Say $\varphi = 0.98 \times 4.0047 \times 10^{-2} = 3.9246 \times 10^{-2}$ for 98% of maximum

$$Vr(\phi) = \left(\sum_{i=1}^{i=7} \mathcal{N}_i^{(F)} \right) \phi, \text{ Solution is } V = 160.32 \text{ m}^3$$

$$\text{Output flows from reactive channel : } \begin{bmatrix} \mathcal{N}_1 \\ \mathcal{N}_2 \\ \mathcal{N}_3 \\ \mathcal{N}_4 \\ \mathcal{N}_5 \\ \mathcal{N}_6 \\ \mathcal{N}_7 \end{bmatrix} = \begin{bmatrix} 2.2868 \\ 24.791 \\ 951.03 \\ 59.999 \\ 1063.5 \\ 6.5079 \\ 87.675 \end{bmatrix}$$

Total output flow: reactive channel with bypass

$$\begin{bmatrix} 2.2868 \\ 24.791 \\ 951.03 \\ 59.999 \\ 1063.5 \\ 6.5079 \\ 87.675 \end{bmatrix} + 0.10 \begin{bmatrix} 127 \\ 280.9 \\ 1056.7 \\ 0 \\ 1017.6 \\ 0 \\ 0 \end{bmatrix} = \begin{bmatrix} 14.987 \\ 52.881 \\ 1056.7 \\ 59.999 \\ 1165.3 \\ 6.5079 \\ 87.675 \end{bmatrix} \text{ kmol/h}$$

Compare with stream 6 in Table 1.3 (reproduced above).

The total volume is then $(10/9)160.32 = 178.13 \text{ m}^3$.

This does not include the heat exchange equipment (tubes). We can think of the gas circulating through a heat exchange chamber with some circulation of the catalyst particles.

See Example ccc in Chapter 13 for diameter calculation ($D = 3.46 \text{ m}$).

The height is given by $3.1416 \frac{3.46^2}{4} (H) = 178.13$, Solution is $H = 18.945 \text{ m}$

6.6.1.3 Selection of Reactor Temperature The Arrhenius dependence of rate parameters on temperature is given in Equation (6.146). Temperature is an effective process variable for influencing the relative rates of competing processes provided that the activation energies of the processes are significantly different. Temperature will have the

strongest effect on the process with the highest activation energy.

For single irreversible reactions, the highest possible temperature should be implemented. This is also the case for reversible endothermic reactions since the equilibrium is shifted toward the products with an increase in temperature. If the reaction is exothermic, there is a competition between the increase in the rate parameter and the shift of the equilibrium toward the reactants. This competition leads to an optimum operating temperature (Aris, 1965).

For multiple reactions, the question of yield comes into play along with conversion. For example, a low temperature may be desirable from a selectivity point of view (undesirable reactions have higher activation energy but may result in low productivity (conversion) if adopted without compensation in the latter stages of reaction (see Table 7.3).

In the acrylic acid system, the first reaction is the most desirable of the three reactions that take place (see Section 1.2). It is the least sensitive to temperature having the lowest activation energy (see Appendix to Chapter 1). A low temperature would therefore be favorable in the early stages of conversion when the concentration dependence of the reaction rates are greatest and the rates of the undesirable reactions would be affected by temperature to a greater extent. A high temperature would be desirable in the later stages of the reaction from the viewpoint of conversion. We might expect an optimum temperature therefore at intermediate conditions. The required calculations follow.

Example 6.6.1.3-1: Temperature Selection for Acrylic Acid Reactor

Definition of Numerical References		Inlet Flows in kmol/h From Stream Table
Propylene	1	127.0
Acetic acid	2	0
Hydrogen	3	0
Oxygen	4	$\mathcal{N}^{(F)} = 280.9$
Nitrogen	5	1056.7
Water	6	1017.6
Carbon dioxide	7	0
Acrylic acid	8	0

Kinetic parameters—see Appendix C:

$$E = \begin{matrix} 15,000 \\ 20,000 \text{ kcal/kmol} \\ 25,000 \end{matrix} \quad k = \begin{matrix} 1.59 \times 10^5 \\ 8.83 \times 10^5 \\ 1.81 \times 10^8 \end{matrix} \quad R = 1.987 \text{ kcal/(kmol K)}$$

$$K(i, T) = k_{i,1} \exp\left(-\frac{E_{i,1}}{RT}\right) \text{ kmol}/(\text{m}^3 \text{ reactor h kPa}^2)$$

Recall that $\xi_j = R_j V$ so that

$$\frac{\xi_j}{\xi_j} = \frac{K(j, T)}{K(1, T)}, \quad j = 2, 3$$

and

$$\xi_j = K(1, T) P^2 y_{1,y4}$$

The reactor volume is considered in Example 6.6.1.2-1 where account is taken of some nonidealities in mixing. An ideal value of 178 m^3 will be assumed here. The operating pressure is 350 kPa.

Therefore, we may determine the dependence of the reaction rates on the temperature with

$$V = 178 \text{ m}^3$$

$$P = 350 \text{ kPa}$$

$$T = 300 \text{ K}$$

$$\xi_3 = \xi_1 \frac{K(3, T)}{K(1, T)}$$

$$\xi_2 = \xi_1 \frac{K(2, T)}{K(1, T)}$$

$$\xi_1 = K(1, T)$$

$$\frac{(127.0 - \xi_1 - \xi_2 - \xi_3)(280.9 - 1.5\xi_1 - 2.5\xi_2 - 4.5\xi_3)P^2}{(2482.2 - \xi_1/2 - \xi_2/2 + \xi_3/2)^2} V$$

The result is

T	ξ_1	T	ξ_2	T	ξ_3
300	0.23601	300	2.9832×10^{-4}	300	1.3919×10^{-5}
325	1.6064	325	3.8712×10^{-3}	325	3.4433×10^{-4}
350	7.7741	350	3.2570×10^{-2}	350	5.0366×10^{-3}
375	25.288	375	0.17110	375	4.2729×10^{-2}
400	53.17	400	0.54718	400	0.20785
425	79.597	425	1.1860	425	0.65224
450	97.341	450	2.0152	450	1.5400
475	106.54	475	2.9604	475	3.0363
500	109.60	500	3.9691	500	5.3055
575	99.571	575	6.9520	575	17.916
600	92.332	600	7.736	600	23.924

The results in graphical form are given in Figure 6.47.

The optimum temperature is seen to be approximately 500 K under the assumed ideal conditions. The design temperature is 583 K.

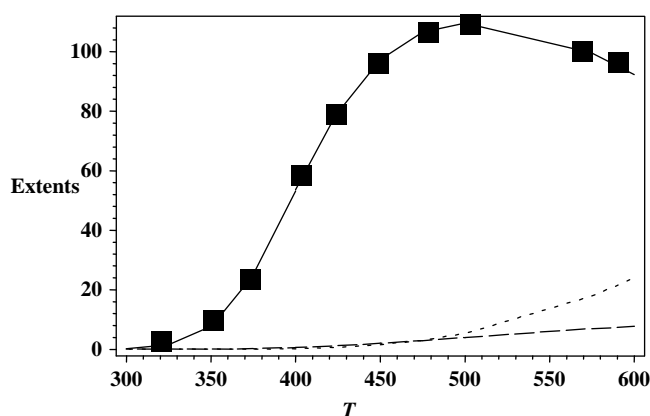


FIGURE 6.47 Reaction extents versus reactor temperature in acrylic acid system: solid line, species 1; dashed line, 2; and dotted line, species 3.

6.6.1.4 CSTR—Energy Balance Once having established the operating temperature by, for example, chemical considerations (see problems) or by equilibrium limitations (see Section 6.3.3), the heat load on the heat exchange system may be calculated with the energy balance, Equation (3.6.3-3), which may be written as

$$Q_r = Q + Q_g \quad (6.172)$$

Calculations for the acrylic acid reactor follow in Example 6.6.1.4-1.

Example 6.6.1.4-1: A Priori Calculation of Heat Load on Acrylic Acid Reactor R-301

The heat load on acrylic acid reactor was calculated in Example 3.6.3-1 using reaction extents based on a full knowledge of the reactor effluent. Here we calculate the reaction extents (and the reactor effluent) from knowledge of the temperature and reactor volume. The heat load is then the difference of the removal and generation term from Equation (6.173).

Following the preceding example:

Definition of numerical references—hydrogen not needed:

Propylene	1
Acetic acid	2
Hydrogen	3
Oxygen	4
Nitrogen	5
Water	6
Carbon dioxide	7
Acrylic acid	8

Specific heats:

$$[a] = \begin{bmatrix} 0.4339 \times 10^5 & 1.52 \times 10^5 & 1.4250 \times 10^3 & 0.7860 \times 10^5 & 623.9 \\ 0.4020 \times 10^5 & 1.3675 \times 10^5 & 1.2620 \times 10^3 & 0.7003 \times 10^5 & 569.7 \\ 0.2762 \times 10^5 & 0.0956 \times 10^5 & 2.4660 \times 10^3 & 0.0376 \times 10^5 & 567.6 \\ 0.2910 \times 10^5 & 0.1004 \times 10^5 & 2.5265 \times 10^3 & 0.0936 \times 10^5 & 1153.8 \\ 0.2911 \times 10^5 & 0.0861 \times 10^5 & 1.7016 \times 10^3 & 0.001 \times 10^5 & 909.79 \\ 0.3336 \times 10^5 & 0.2679 \times 10^5 & 2.6105 \times 10^3 & 0.0890 \times 10^5 & 1169 \\ 0.2937 \times 10^5 & 0.3454 \times 10^5 & 1.4280 \times 10^3 & 0.2640 \times 10^5 & 588 \\ 7.7550 & 2.9386 \times 10^{-1} & 2.0878 \times 10^{-4} & 7.159 \times 10^{-8} & 9.0960 \times 10^{-12} \end{bmatrix} s = \begin{bmatrix} 0 \\ 0 \\ 0 \\ 0 \\ 0 \\ 0 \\ 0 \\ 1 \end{bmatrix}$$

The generation of thermal energy is defined as,

$$Q_g = \sum_{j=1}^R \xi_j [-\Delta H_{Rj}] \quad (6.173)$$

and the removal rate by the reactor effluent as

$$Q_r = \sum_{\text{all species}} \left[N_i^{(F)} (H_i - H_i^{(F)}) \right] \quad (6.174)$$

$s = 0$: c_p in J/(kmol K); $s = 1$: c_p in J/(mol K) adjusted below to kmol basis

$$c_p(i, \theta) = (1 - s_{i,1}) \left(a_{i,1} + a_{i,2} \left(\frac{a_{i,3}/\theta}{\sinh(a_{i,3}/\theta)} \right)^2 + a_{i,4} \left(\frac{a_{i,3}/\theta}{\cosh(a_{i,5}/\theta)} \right)^2 \right) + 1000 s_{i,1} \left(\sum_{j=1}^{j=5} a_{8,j} \theta^{j-1} \right) \text{ J/(kmol K)}$$

Inlet flows in kmol/h from stream table and heats of formation for gases at 1 atm and 25 °C in kcal/mol:

$$\mathcal{N}^{(4)} = \begin{array}{cc} 127.0 & 20.42 \\ 0 & -434.84 \\ 0 & 0 \\ 280.9 & 0 \\ 1056.7 & 0 \\ 1017.6 & -241.8 \\ 0 & -393.5 \\ 0 & -336.23 \end{array} \quad \Delta H_f =$$

Units are kJ/mol; adjusted to J/kmol below in enthalpy formation.

Formation of enthalpy function based on elements at standard conditions:

Elements at standard conditions:

$$H(i, x) = 10^6 \Delta H_{f,i,1} + \int_{298.16}^x c_p(i, \theta) d\theta$$

$$Q_r = \sum_{i=1}^{i=6} \mathcal{N}^{(4)} \times (H(i, 583) - H(i, 191 + 273)) = 1.0552 \times 10^{10} \text{ J/h}$$

$$\vartheta = \begin{array}{ccc} -1 & -1 & -1 \\ 0 & 1 & 0 \\ 0 & 0 & 0 \\ -\frac{3}{2} & -\frac{5}{2} & -\frac{9}{2} \\ 0 & 0 & 0 \\ 1 & 1 & 3 \\ 0 & 1 & 3 \\ 1 & 0 & 0 \end{array} \quad \begin{array}{cc} & \\ & \\ & \\ 15,000 & 1.59 \times 10^5 \\ E = 20,000 \text{ kcal/kmol} & k = 8.83 \times 10^5 \\ 25,000 & 1.81 \times 10^8 \end{array}$$

$$R = 1.987 \text{ kcal}/(\text{kmol K})$$

$$K(i, T) = k_{i,1} \exp\left(-\frac{E_{i,1}}{RT}\right) \text{ kmol}/(\text{m}^3 \text{ reactor h kPa}^2)$$

$$V = 178$$

$$P = 350$$

$$T = 583$$

$$\Delta(X) = \sum_{i=1}^{i=8} \vartheta_{i,1} H(i, X) + \sum_{i=1}^{i=8} \vartheta_{i,2} H(i, X) \frac{K(2, X)}{K(1, X)} + \sum_{i=1}^{i=8} \vartheta_{i,3} H(i, X) \frac{K(3, X)}{K(1, X)}$$

$$\xi_3 = \xi_1 \frac{K(3, T)}{K(1, T)}$$

$$\xi_2 = \xi_1 \frac{K(2, T)}{K(1, T)}$$

$$\xi_1 = K(1, T)$$

$$\times \frac{(127.0 - \xi_1 - \xi_2 - \xi_3)(280.9 - 1.5\xi_1 - 2.5\xi_2 - 4.5\xi_3)P^2}{(2482.2 - \xi_1/2 - \xi_2/2 + \xi_3/2)^2} V$$

$$\text{Solution is } \{\xi_1 = 97.459, \xi_2 = 7.2256, \xi_3 = 19.773\}$$

$$-\xi_1 \Delta(T) \times 10^{-9} \text{ generation rate} \times 10^{-9}$$

$$Q_g = 10.176 \times 10^{10} \text{ Btu/h}$$

$$Q = (1.0552 - 10.176) \times 10^{10} = -9.1208 \times 10^{10}$$

This result indicates that 9.120×10^{10} J/h must be removed from the reaction medium in order to maintain a steady temperature of 583 K. This result differs from the value of 8.2007×10^{10} J/h obtained in Example 3.6.3-1 by approximately 10% due to the kinetic modeling and reactor sizing included in the present calculations.

If the convective removal of thermal energy by the reactor effluent matches the generation rate, the reactor can be operated without heat exchange with the surroundings. The operation in this case is called autothermal.

6.6.1.5 Autothermal Operation We can discuss the major characteristics of autothermal operation within the context of the acrylic acid reactor R-301. Continuing with the preceding example and the results of Example 6.6.2-1 used to construct Figure 6.47, the generation term as a function of temperature can be determined. The generation term is given by Equation (6.173). The results are given in Table 6.16.

These results are plotted in Figure 6.48.

The behavior of the generation curve in Figure 6.48 is generally what we can expect in other situations. Generation curves will generally increase rapidly from low to intermediate values of temperature because of the exponential dependence of the rate constants. Instead of leveling out for complete conversion, they may decrease to zero at reaction equilibrium. If the reactor volume were increased, these features would be enhanced.

The removal term due to flow of the process stream is given by Equation (6.6.3-3). Assuming no phase changes in the reactor, the removal term can be written as

$$Q_r = \mathcal{N}^{(F)} \langle C_p^{(F)} \rangle (T - T^{(F)}) \quad (3.110)$$

TABLE 6.16 Thermal Energy Generation in R-301

$Q_g(T, \xi_1) = -\xi_1 \Delta(T) \times 10^{-9}$ Generation rate $\times 10^{-9}$							
T	ξ_1	T	ξ_2	T	ξ_3	T	$Q_g(T, \xi_1)$
300	0.23601	300	2.9832×10^{-4}	300	1.3919×10^{-5}	300	0.14157
325	1.6064	325	3.8712×10^{-3}	325	3.4433×10^{-4}	325	0.96432
350	7.7741	350	3.2570×10^{-2}	350	5.0366×10^{-3}	350	4.6783
375	25.288	375	0.17110	375	4.2729×10^{-2}	375	15.302
400	53.17	400	0.54718	400	0.20785	400	32.515
425	79.597	425	1.1860	425	0.65224	425	49.580
450	97.341	450	2.0152	450	1.5400	450	62.468
475	106.54	475	2.9604	475	3.0363	475	71.54
500	109.60	500	3.9691	500	5.3055	500	78.511
575	99.571	575	6.9520	575	17.916	575	99.218
600	92.332	600	7.736	600	23.924	600	107.13

where the average specific heat of the mixture and each component are defined respectively by

$$\langle C_p^{(F)} \rangle = \sum y_{i0} \langle C_{pi}^{(F)} \rangle (T - T^{(F)}) \quad (6.175)$$

$$\langle C_p^{(F)} \rangle = \frac{1}{T - T^{(F)}} \int_{TT^{(F)}}^T C_{pi} dT \quad (6.176)$$

If we assume that the average specific heat of the mixture is constant, then the removal rate is linear in temperature with slope proportional to the flow rate.

A number of possibilities can be illustrated for the intersection of the generation and removal curves, the intersection being the solution to the energy balance. Some of these are illustrated in Figure 6.49 and depend on the slope of the removal line and inlet temperature. The slope is varied in Figure 6.49 but the same behavior can be demonstrated by varying the inlet temperature. If the maximum slope of the generation curve is less than the slope of the removal curve, one intersection can exist at a temperature depending upon the inlet temperature.

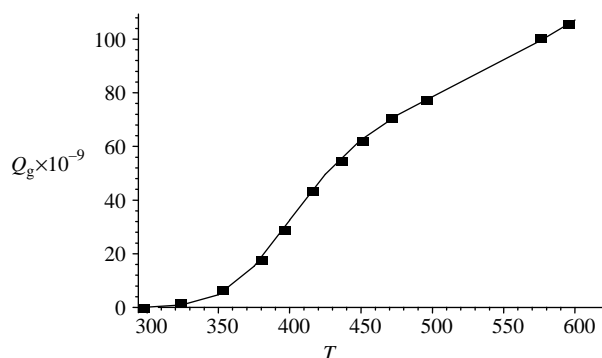


FIGURE 6.48 Energy generation in acrylic acid reactor.

If, on the other hand, the maximum slope of the generation curve is greater than the slope of the removal line, more than one intersection is possible with the final temperature of the reactor depending upon the startup procedure.

Consider the removal curves labeled Q_r in Figure 6.49a and begin with one whose slope is relatively large because of a relatively high throughput. A single intersection at a low temperature would result since a significant reaction rate could not be sustained with such a high removal rate. As the throughput is gradually decreased, the situation would be slightly improved with the reactor temperature rising slightly along the lower portion of the generation curve until the “ignition” temperature is reached at the illustrated position of Q_r . Even though additional intersections are possible, we expect that the system will go to the nearest stable state. A slight decrease in the flow rate will result in a very large increase in temperature ($\Delta T_{\text{ignition}}$) and conversion.

Now consider the removal curves labeled Q_r in Figure 6.49b and begin with one whose slope is relatively small because of a relatively small throughput. A single intersection at a high temperature would result with a significant reaction rate and conversion. As the throughput is gradually increased, the reactor temperature would decrease along the upper portion of the generation curve until the “extinction” temperature is reached at the illustrated position of Q_r . Even though additional intersections are possible, we again expect that the system will go to the nearest stable state. A slight decrease in the flow rate at the extinction point will result in a relatively large decrease in temperature ($\Delta T_{\text{extinction}}$) and conversion.

Multiple steady states are accompanied by the notion of stability: Under what, if any, disturbances to the system will the system travel to another steady state? The middle (circled) state is unstable, since, for example, a small temperature rise would be reinforced by the generation rate exceeding the removal rate. The system would therefore

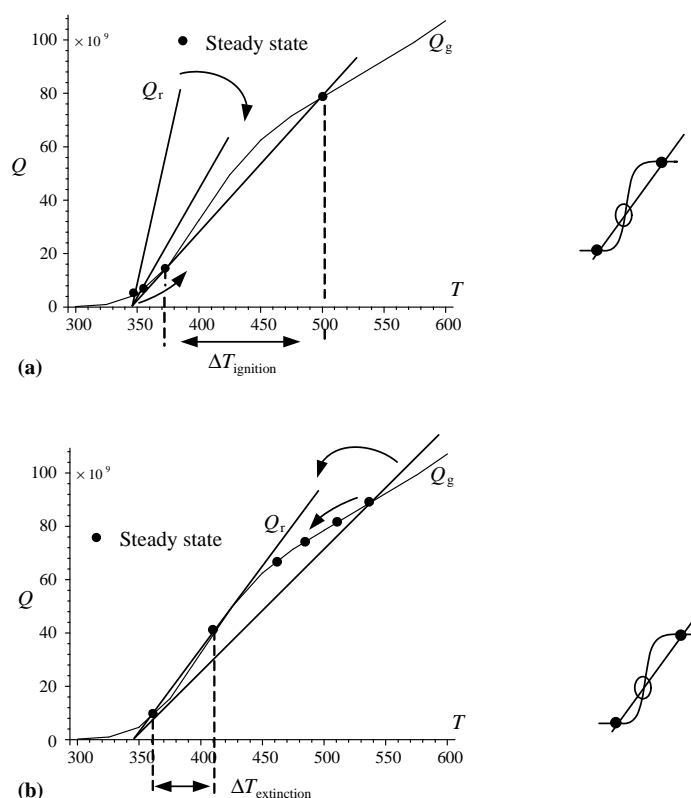


FIGURE 6.49 Multiple steady states, ignition (a) and extinction (b) in well-mixed acrylic acid reactor.

travel to the steady state at the higher temperature. A small temperature decrease would similarly cause the system to move to the lower steady state. Similar arguments can be made in support of the stability of the remaining two states.

Note that the system could be taken through a sequence of steady states that begin with the ignition states discussed above and return along the extinction route, a different sequence of reactor conditions. The system is consequently said to exhibit hysteresis.

6.6.1.6 Heuristics Some heuristics for single CSTRs are as follows (Couper et al., 2005):

- The reaction rate must be established in the laboratory.
- The residence time and product distribution eventually must be found in a pilot plant.
- The optimum proportions of stirred tank reactors are with liquid level equal to the tank diameter. At high pressures, slimmer proportions are economical.
- Power input to a homogeneous reaction stirred tank is 0.5–1.5 hp/1000 gal but three times this amount applies when heat is transferred.

- Ideal behavior is approached when the residence time is 5–10 times the time required to achieve homogeneity.
- Homogeneity is obtained with 500–2000 revolutions of the properly designed stirrer.

6.6.2 Isothermal Batch Reactor

A batch reactor is a stirred tank that is initially charged with reactants and maintains uniform conditions as the reaction proceeds without product withdrawal or further addition of reactants. Calculation of the production rate for the reactor must therefore account for the charge time, the drain or product removal time, and the time required for any other operation such as cleaning or sterilization in addition to the reaction time.

6.6.2.1 Mass Balance Since there are no inlets or outlets to the batch reactor, the statement of mass conservation at the beginning of Chapter 2, implies that the time rate of change of the total amount (i mass or moles) for each

species (i) in the batch reactor is due only to chemical reaction:

$$\frac{dN_i}{dt} = \sum_{j=1}^{N_c} \vartheta_{ij} R_{vj} V_R \quad \text{with } N_i = N_i(0) \text{ at } t = 0; i = 1, 2, \dots, N_c \quad (6.177)$$

where the number of moles of species i in the mixture is $N_i(t)$ at time t . The charge to reactor is given by $N_i(0)$. V_R is the empty volume of the vessel in the case of gases and the mixture volume in the case of liquids. For liquid phase reactions, we will consider only those cases where the gas phase, as well as variations in the volume of liquid, may be neglected in accounting for mass variations.

Introducing extents

$$N_i(t) = N_i(0) + \sum_j \vartheta_{ij} \xi_j \quad \text{for all } i \quad (6.178)$$

and substitution into the mass balance gives

$$\sum_j \vartheta_{ij} \left(\frac{d\xi_j}{dt} - R_{vj} V_R \right) = 0 \quad \text{for all } i \quad (6.179)$$

or

$$\frac{d\xi_j}{dt} = R_{vj} V_R \quad \xi_j(0) = 0 \quad \text{for all } j \quad (6.180)$$

6.6.2.2 Liquid Phase Reactions at Constant Density Here we assume that the kinetics for each reaction are of the form: $\mathcal{R}(\mathbf{c}, T)$. The molar concentrations may be expressed as

$$\frac{N_i}{V_R} = c_i = c_{i0} + \sum_j \vartheta_{ij} \left(\frac{\xi_j}{V_R} \right) \quad \text{for all } i \quad (6.181)$$

which, when substituted into the kinetic expression, provides

$$\frac{d\xi_j'}{dt} = \mathcal{R}_j(\xi', T), \quad \xi_j'(0) = 0 \quad \text{for all } j \quad (6.182)$$

where

$$\xi_j' = \left(\frac{\xi_j}{V_R} \right) \quad (6.183)$$

With a specified temperature and charge, there are no degrees of freedom.

6.6.2.3 Some Background for Example 6.6.2.3-1 Levodopa (L-dopa) is used to treat Parkinson's disease and has the molecular structure shown in Figure 6.50. It is produced *in vivo* from L-tyrosine where it is subsequently converted to dopamine, a neuron transmitter (see Figure 6.51).

The ability of cells to communicate with one another is essential to reflexes and local responses and therefore to homeostasis (the notion of an internal environment and the necessity of maintaining its composition as relatively constant). Most nerve cells communicate with each other by means of chemical agents called neurotransmitters. One nerve cell alters the activity of the next by releasing a neurotransmitter from its ending that diffuses through the extra cellular fluid separating the nerve cells and acts upon the second.

Dopamine is a catecholamine (nomenclature basis see Figure 6.52) neurotransmitter; it is found predominantly in three major pathways in the central nervous system. One of the most important dopamine paths projects from the substantia nigra pars compacta to the neostriatum composed of the caudate nucleus and putamen. These are part of the basal ganglia located deep within the each cerebral hemisphere just above the spinal cord (see Figure 6.53).

This pathway controls movement and balance and coordinates motor function. In Parkinson's disease, the amount of dopamine delivered to the basal ganglia is diminished

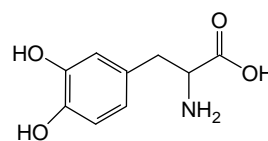


FIGURE 6.50 $C_9H_{11}NO_4$, L-3,4-dihydroxyphenylalanine.

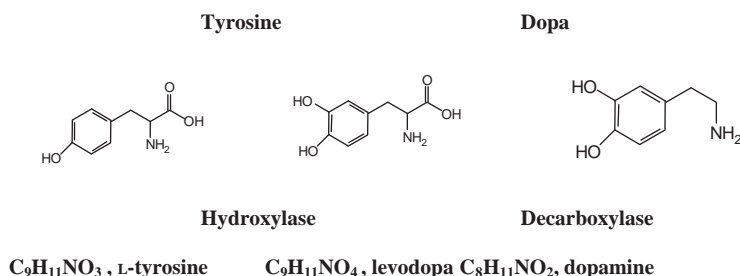


FIGURE 6.51 *In vivo* production of dopamine.

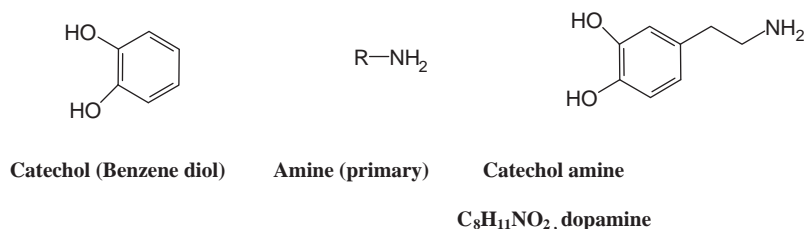


FIGURE 6.52 Nomenclature basis.

resulting in a loss of motor control. Symptoms include tremor, muscular rigidity, and dyskinesia or involuntary movements. Each year about 50,000 Americans are diagnosed with Parkinson's disease and over one million may presently have the disease. That means that you probably know, or know of, someone who has the disease.

Dopamine does not cross the blood-brain barrier and it therefore cannot be used therapeutically. However, L-dopa does cross the blood-brain barrier and is subsequently converted to dopamine; L-dopa can therefore be used as a therapeutic agent.

Example 6.6.2.3-1: Production of L-Tyrosine-Feed Stock to L-Dopa Plant

Your company is planning to produce L-dopa from tyrosine and to produce tyrosine in-house. You are required to size the reactor(s) and determine the operating conditions to meet an L-dopa production rate of 1% of the total market.

A literature search uncovered an experimental study (Lloyd-George and Chang, 1995) where microencapsulated whole cells of *Erwinia herbicola* are used to catalyze the reaction:

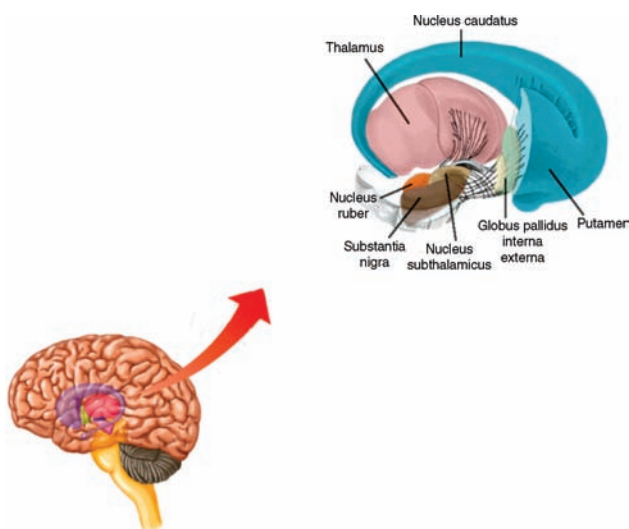


FIGURE 6.53 Location of substantia nigra.

The cells that contain the necessary cofactors and enzymes are made available in microcapsules consisting of the cell suspension in a buffered environment and surrounded by an alginate-polysine-alginate. The batch reactor environment is illustrated in Figure 6.54.

The K_s are equilibrium constants associated with steps in the underlying molecular mechanism.

The experimental conditions we will duplicate in order to be consistent with the kinetic data are as follows:

Stirring rate = 240 rpm

Temperature = 37 °C

Reaction medium:

Solution 1: Solution 2: Solution 3 = 8:1:1 by volume

Solution 1: Phosphate buffer (0.1 M, pH = 8) containing

$A = 80$ mM, $B = 80$ mM, $C = 40$ mM

$A =$ ammonia, $B =$ pyruvate, $C =$ phenol

Solution 2: Microcapsules containing 6.6 mg of protein/ml of microcapsules

Solution 3: Phosphate buffer

The kinetic parameters were found to be

$$K_P = 0.28 \text{ mM}$$

$$K_C = 0.47 \text{ mM}$$

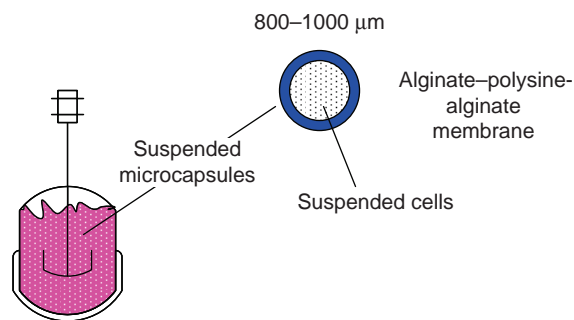


FIGURE 6.54 Batch reactor configuration for tyrosine production.

$K_A K_B = 1871 \text{ mM}^2$ with K_A for saturation with phenol and tyrosine

$$V_{\max} = 4.34 \text{ mM/h}$$

Using the batch reactor equations, the time required achieve a desired extent, ξ'_f , is given by

$$t = \int_0^{\xi'_f} \frac{dz}{\mathcal{R}(z, T)}$$

where

$$\frac{1}{\mathcal{R}(z, T)} = \frac{1}{V_{\max}} \left\{ \frac{K_A K_B K_C}{(C_0 - z)^2 (C_{c0} - z)} + \frac{K_B K_C}{(C_0 - z)(C_{c0} - z)} + \frac{K_C}{(C_{c0} - z)} + 1 + \frac{(K_A K_B K_C / K_P) z}{(C_0 - z)^2 (C_{c0} - z)} \right\}$$

The kinetic model is based upon the ternary mechanism with all steps occurring much faster than the product forming step. The concentrations in the reaction rate expression have been replaced with their representations in terms of the extent per unit volume (expressed as z for the integration variable). The initial concentration of A and B are both equal to C_0 and the initial concentration of C is equal to C_{c0} . We assume that the initial concentration of C is strictly less than the initial concentrations of A and B . These restrictions suit the experimental conditions stated above. The limiting reactant [see Equation (2.75)] is C since

$$0 = C_{i0} + \nu_i \xi_{i, \max} \Rightarrow \xi_{C, \max} = C_{c0} < \xi_{A, \max} = \xi_{B, \max} = C_0$$

The integration may be accomplished with partial fraction expansions applied to the individual terms in the expression above for the inverse of the reaction rate:

Functions of z to be integrated and the result are bolded.

$$\begin{aligned} \frac{1}{(C_0 - z)^2 (C_{c0} - z)} &= \frac{1}{(C_0 - C_{c0})^2} \left[\frac{z - (2C_0 - C_{c0})}{(z - C_0)^2} - \frac{1}{(z - C_{c0})} \right] \\ &= \frac{1}{(C_0 - C_{c0})^2} \left[\frac{1}{(z - C_0)} - \frac{1}{(z - C_{c0})} - \frac{(C_0 - C_{c0})}{(z - C_0)^2} \right] \\ \frac{1}{(C_0 - z)(C_{c0} - z)} &= \frac{1}{(C_0 - C_{c0})} \left[\frac{1}{(z - C_0)} - \frac{1}{(z - C_{c0})} \right] \\ \frac{z}{(C_0 - z)^2 (C_{c0} - z)} &= -\frac{1}{(C_0 - z)^2} + \frac{C_{c0}}{(C_0 - z)^2 (C_{c0} - z)} \\ &= -\frac{1}{(z - C_0)^2} + \frac{C_{c0}}{(C_0 - C_{c0})^2} \\ &\times \left[\frac{1}{(z - C_0)} - \frac{1}{(z - C_{c0})} - \frac{(C_0 - C_{c0})}{(z - C_0)^2} \right] \\ &= \frac{C_{c0}}{(C_0 - C_{c0})^2} \left[\frac{1}{(z - C_0)} - \frac{1}{(z - C_{c0})} - \frac{(C_0 - C_{c0})}{(z - C_0)^2} \frac{C_0}{C_{c0}} \right] \end{aligned}$$

Substitution into the kernel of the integral gives

$$\begin{aligned} \frac{1}{\mathcal{R}(z, T)} &= \frac{1}{V_{\max}} \\ &\times \left\{ \frac{K_A K_B K_C}{(C_0 - C_{c0})^2} \left[\frac{1}{(z - C_0)} - \frac{1}{(z - C_{c0})} - \frac{(C_0 - C_{c0})}{(z - C_0)^2} \right] \right. \\ &\quad + \frac{K_B K_C}{(C_0 - C_{c0})} \left[\frac{1}{(z - C_0)} - \frac{1}{(z - C_{c0})} \right] \\ &\quad - \frac{K_C}{(z - C_{c0})} + 1 + \frac{C_{c0}(K_A K_B K_C / K_P)}{(C_0 - C_{c0})^2} \\ &\quad \left. \times \left[\frac{1}{(z - C_0)} - \frac{1}{(z - C_{c0})} - \frac{(C_0 - C_{c0})}{(z - C_0)^2} \frac{C_0}{C_{c0}} \right] \right\} \end{aligned}$$

Combining terms

$$\begin{aligned} \frac{V_{\max}}{\mathcal{R}(z, T)} &= 1 - \frac{K_C}{(z - C_{c0})} + \left[\frac{1}{(z - C_0)} - \frac{1}{(z - C_{c0})} \right] \\ &\times \left[\frac{K_A K_B K_C}{(C_0 - C_{c0})^2} + \frac{K_B K_C}{(C_0 - C_{c0})} + \frac{C_{c0}(K_A K_B K_C / K_P)}{(C_0 - C_{c0})^2} \right] \\ &- \left[\frac{1}{(z - C_0)^2} \right] \left[\frac{K_A K_B K_C}{(C_0 - C_{c0})} + \frac{(K_A K_B K_C)}{K_P} \frac{C_0}{(C_0 - C_{c0})} \right] \end{aligned}$$

Integrating

$$\begin{aligned} \int_0^{\xi'_f} \frac{V_{\max}}{\mathcal{R}(z, T)} dz &= \xi'_f - K_C \ln \frac{C_{c0} - \xi'_f}{C_{c0}} \\ &+ \left[\frac{K_A K_B K_C}{(C_0 - C_{c0})^2} + \frac{K_B K_C}{(C_0 - C_{c0})} + \frac{C_{c0}(K_A K_B K_C / K_P)}{(C_0 - C_{c0})^2} \right] \\ &\times \left[\ln \frac{C_{c0} - \xi'_f}{C_{c0}} - \frac{C_{c0} - \xi'_f}{C_{c0}} \right] \\ &+ \left[\frac{K_A K_B K_C}{(C_0 - C_{c0})} + \frac{(K_A K_B K_C)}{K_P} \frac{C_0}{(C_0 - C_{c0})} \right] \left[\frac{1}{C_{c0}} - \frac{1}{C_0 - \xi'_f} \right] \end{aligned}$$

or

$$\begin{aligned} \int_0^{\xi'_f} \frac{V_{\max}}{\mathcal{R}(z, T)} dz &= \xi'_f - \left[K_C + \frac{K_B K_C}{(C_0 - C_{c0})} + \frac{K_A K_B K_C}{(C_0 - C_{c0})^2} \left(1 + \frac{C_{c0}}{K_P} \right) \right] \\ &\times \ln \frac{C_{c0} - \xi'_f}{C_{c0}} + \left[\frac{K_B K_C}{(C_0 - C_{c0})} + \frac{K_A K_B K_C}{(C_0 - C_{c0})^2} \left(1 + \frac{C_{c0}}{K_P} \right) \right] \end{aligned}$$

$$\times \left[\ln \frac{C_0 - \xi'_f}{C_0} \right] + \left[\frac{K_A K_B K_C}{(C_0 - C_{c0})} \left(1 + \frac{C_0}{K_P} \right) \right] \left[\frac{1}{C_0} - \frac{1}{C_0 - \xi'_f} \right]$$

or

$$\begin{aligned} \int_0^{\xi'_f} \frac{dz}{R(z, T)} &= t \\ &= \frac{1}{V_{\max}} \left\{ \xi'_f - \left[K_C + \frac{K_B K_C}{(C_0 - C_{c0})} + \frac{K_A K_B K_C}{(C_0 - C_{c0})^2} \left(1 + \frac{C_{c0}}{K_P} \right) \right] \right. \\ &\quad \times \ln \frac{C_{c0} - \xi'_f}{C_{c0}} + \left[\frac{K_B K_C}{(C_0 - C_{c0})} + \frac{K_A K_B K_C}{(C_0 - C_{c0})^2} \left(1 + \frac{C_{c0}}{K_P} \right) \right] \\ &\quad \times \left[\ln \frac{C_0 - \xi'_f}{C_0} \right] + \left[\frac{K_A K_B K_C}{K_P} + \frac{K_A K_B K_C}{(C_0 - C_{c0})} \left(1 + \frac{C_{c0}}{K_P} \right) \right] \\ &\quad \times \left. \left[\frac{1}{C_0} - \frac{1}{C_0 - \xi'_f} \right] \right\} \end{aligned}$$

The reaction time required to reach 99% conversion of phenol can be computed with this result using the data provided and allowing the rapid equilibrium constant for ammonia to become large enough to have no effect on the results:

$$\begin{aligned} t(t) &= \frac{1}{4.34} \left(40x - \left(0.47 + \frac{(1871/K_A)0.47}{40} + \left(\frac{1871 \times 0.47}{40^2} \right) \right. \right. \\ &\quad \times \left. \left(1 + \frac{40}{0.28} \right) \right) \ln(1 - x) \left(\left(\frac{1871 \times 0.47}{40^2} \right) \times \left(1 + \frac{40}{0.28} \right) \right. \\ &\quad + \frac{(1871/K_A)0.47}{40} \ln \left(\frac{80 - 40x}{80} \right) + \left(\frac{1871 \times 0.47}{0.28} \right) \\ &\quad \left. + \left(\frac{1871 \times 0.47}{40} \right) \left(1 + \frac{40}{0.28} \right) \right) \left(\frac{1}{80} - \frac{1}{80 - 40x} \right) \end{aligned}$$

$$K_A = 10,000 \quad t(0.99) = 63.280$$

$$K_A = 20,000 \quad t(0.99) = 63.279$$

$$K_A = 40,000 \quad t(0.99) = 63.279$$

Note that the fractional amount of phenol converted is given by

$$x = \frac{\xi'_f}{C_{c0}}$$

The reaction time is therefore 63.279 h. If 7 h are required to drain, clean, and recharge the reactor, the production rate of

the reactor is

$$\begin{aligned} \frac{0.99 C_{c0} V}{63.279 + 7} &= \frac{0.99(40 \times 0.001 \times (19,720/454))V(1)}{63.279 + 7} \\ &= 2.4476 \times 10^{-4} V(1) \text{ lb tyrosine/h} \end{aligned}$$

If 1% of the L-dopa market of 250 tonne/year is the target, the desired production rate of tyrosine is

$$\begin{aligned} \frac{0.10 \times 250 \times 2000 \times (197.21/187.21)}{0.90 \times 365 \times 24} \\ = 6.6807 \text{ lb tyrosine/h assuming 90\%} \end{aligned}$$

efficiency with respect to operating hours

The reaction volume is then

$$2.4476 \times 10^{-4} V = 6.6807,$$

Solution is $V = 27,295$ l or 7211 gal

6.6.2.4 Gas Phase Reactions and Equation of State at Constant Volume

Here we presume that the kinetics for each reaction is of the form $\mathcal{R}_v(\mathbf{y}, P, T)$. In order to use the mass balances in Equation (6.180), we need to express the mole fractions in terms of the extents and we need the pressure in terms of the extents.

The total number of moles in the tank at any time is given by adding Equation (6.180)

$$N = N(0) + \sum_{j=1}^{N_r} \xi_j \Delta n_j \quad (6.184)$$

where

$$\Delta n_j = \sum_{i=1}^{N_c} \vartheta_{ij} \quad (6.185)$$

The sum of the stoichiometric coefficients for each reaction gives the mole change associated with that reaction, Δn_j . The contribution to the change in the total molar flow rate is scaled by the extent for each reaction.

The mole fractions in the system are given by

$$\begin{aligned} y_i &= \frac{N_i}{N} = \frac{N_i(0) + \sum_{j, \text{all reactions}} \vartheta_{ij} \xi_j}{N(0) + \sum_{j, \text{all reactions}} \xi_j \Delta n_j} \\ &= \frac{c_i(0) + \sum_{j, \text{all reactions}} \vartheta_{ij} (\xi_j/V_R)}{c(0) + \sum_{j, \text{all reactions}} (\xi_j/V_R) \Delta n_j} \end{aligned} \quad (6.186)$$

The balance equations for the extents become

$$\left[\frac{d\xi_j'}{dt} \right] = R_j(\xi', T, P), \quad \xi_j'(0) = 0 \quad \text{for all } j \quad (6.187)$$

where

$$\xi_j' = \left(\frac{\xi_j}{V_R} \right) \quad \text{and} \quad c(0) = \frac{N(0)}{V_R} = \text{initial molar density}$$

The pressure P can be obtained from a pressure explicit equation of state into which the mole fractions have been expressed in terms of the reaction extents:

$$P = P(T, V_R, N) = P(T, V_R, \xi') \quad (6.188)$$

Provided that the mole changes in the reactions are significant, the total pressure is a direct measure of the progress of the reactions. Its time profile is determined by

$$\frac{dP}{dt} = \sum_j \left(\frac{\partial P}{\partial \xi_j'} \right)_{T, V_R, \xi_{k \neq j}'} R_{vj} \quad (6.189)$$

For an ideal gas, the preceding result is easily valuated using the expression above for the total number of moles in the system. The result is

$$\frac{dP}{dt} = RT \sum_j \Delta n_j R_j$$

Example 6.6.2.4-1: Reaction Order for Sulfuryl Chloride Oxidation

Smith (1981) measured the total pressure during the constant volume decomposition of sulfuryl chloride at 279.2 °C. The decomposition products are sulfur dioxide and chlorine. Suggest a reaction order from the following measurements:

t (min)	P (mmHg)
3.4	325
15.7	335
28.1	345
41.1	355
54.5	365
68.3	375
82.4	385
96.3	395

Eventually all of the sulfuryl chloride decomposed.

Assume that the rate of decomposition is given by

$$R_v = k(T) y_A^n P^n$$

where A designates sulfuryl chloride. Using Equation (6.6.2.2-3) for the mole fraction

$$\frac{dP}{dt} = k(T) RT \left[\frac{c_A(0) - \xi'}{c(0) + \xi'} \right]_A^n P^n$$

We, therefore, need to know the composition of the mixture at some time. It is reasonable to assume that the initial charge was pure sulfuryl chloride. The initial pressure can be recovered by extrapolation of the pressure–time data. Consult the reference for the data to determine the validity of this assumption.

Since there is a single reaction, the ideal gas law can be easily inverted to obtain the extent in terms of pressure; refer to Equation (6.184). Otherwise, it would be necessary to solve for the extent profiles followed by substitution into the equation of state to obtain the pressure profile:

$$\frac{P}{RT} = c(0) + \xi' \Rightarrow \xi' = \frac{P}{RT} - c(0) = \frac{1}{RT} (P - P(0))$$

Substitution into the pressure differential equation yields

$$\frac{dP}{dt} = kRT(2P(0) - P)_0^n$$

or

$$\ln \left[2 - \frac{P}{P(0)} \right] = -kRTt, \quad n = 1$$

$$\frac{1}{[2 - (P/P_0)]^{n-1}} = 1 + kRT(n-1)P(0)^{n-1}t, \quad n > 1$$

Refer to Figure 6.55. Linear extrapolation to $t = 0$ provides an initial pressure of 323.41 mmHg. Linear plots of the data indicate that the first-order model provides better fit of the data.

t	p	$n = 1$	$n = 2$
		$\ln(2 - P/P(0))$	$1/(2 - P/323.41) - 1$
3.4	325	-0.00493	0.00494
15.7	335	-0.03649	0.03717
28.1	345	-0.06909	0.07153
41.1	355	-0.10278	0.10825
54.5	365	-0.13765	0.14758
68.3	375	-0.17378	0.18979
82.4	385	-0.21126	0.23524
96.3	395	-0.25021	0.28429

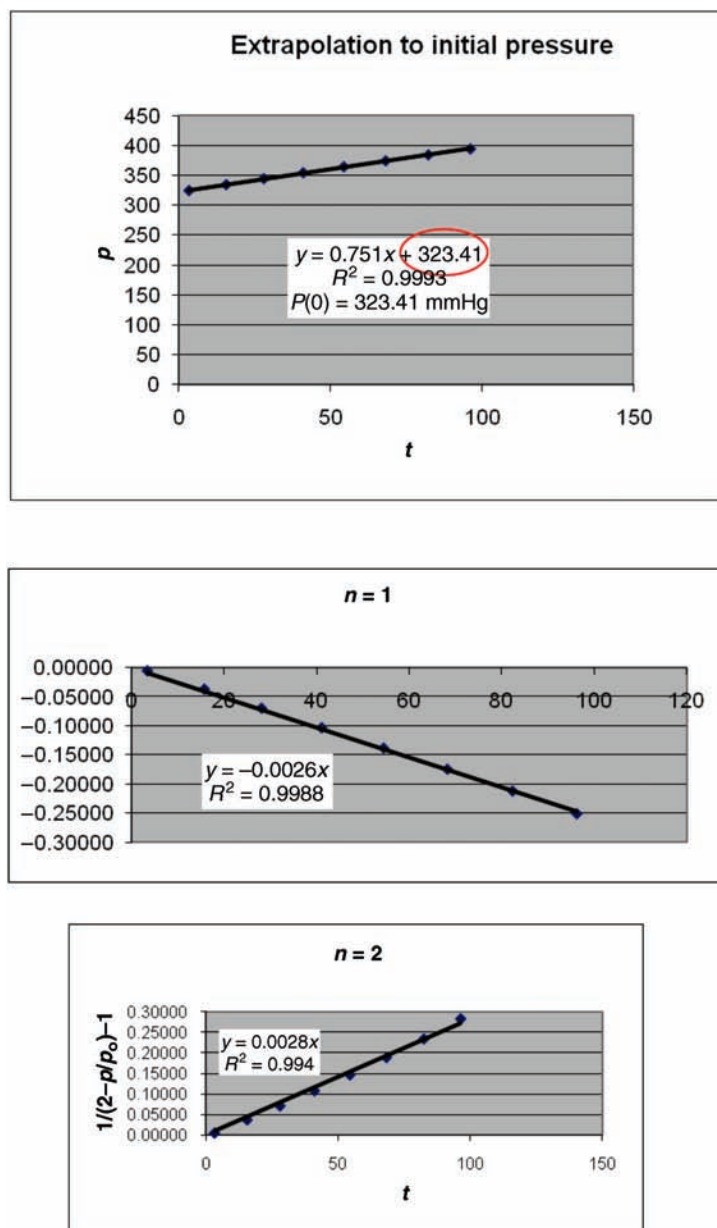


FIGURE 6.55 Linear plots of data.

6.7 CHEMICAL REACTION EQUILIBRIUM

Chemical reaction equilibrium appears as an important consideration even at the very beginning stages of process design. It establishes the limiting reactor conditions necessary to achieve a desired conversion or the conversion limit at a specified set of process conditions. From a macroscopic point of view, these conditions exist at the equipment outlet and are the result of the microscopic rate processes experienced by the process materials prior to reaching the outlet. Reaction rates that are applied near the chemical equilibrium state need to vanish at the limiting condition.

For completely mixed systems, the equilibrium persists throughout the system. Phase equilibrium is a separate consideration and therefore may or may not be present.

The Gibbs free energy is a minimum in a reactive single-phase system at a specified temperature and pressure. At the equilibrium point, therefore,

$$dG = \sum \tilde{G}_i dN_i = \sum \mu_i dN_i = 0 \quad (6.190)$$

For a single reaction, $\sum \nu_i A_i = 0$, the mole numbers must change in proportion to each other and to the limiting

reactant (A),

$$dG = \sum \tilde{G}_i \frac{\vartheta_i}{(-\vartheta_A)} dN_A = 0 \quad (6.191)$$

or

$$\sum_{i=1}^{N_c} \vartheta_i \tilde{G}_i = 0 \quad (6.192)$$

From Equation (6.8), the chemical potential in the mixture can be written in terms of the value for the each component in a standard state at the temperature of the system.

$$\tilde{G}_i - G_i^0 = RT \ln \frac{\hat{f}_i}{f_i^0} \quad (6.193)$$

As discussed in Section 3.6.1.1, the reference state or thermodynamic dead state for all chemical species is the elements in their most stable form at 25 °C and 1 bar. The standard state for all chemical compounds is at 25 °C and 1 bar and then as follows: for gases, it is the ideal gas; for liquids and solids, it is that state of aggregation; for solutes in aqueous solution, the standard state is the hypothetical 1 molal solution of the solute in water. These standard states translated to the temperature of the system can be taken as the standard states in Equation (6.193). Substitution of Equation (6.193) into Equation (6.192) gives

$$\sum_{i=1}^{N_c} \vartheta_i G_i^0 + RT \sum_{i=1}^{N_c} \vartheta_i \ln \frac{\hat{f}_i}{f_i^0} = 0 \quad (6.194)$$

The first term is called the standard Gibbs free energy change (or better, the Gibbs free energy change for the standard reaction) at the temperature of the system. The second term can therefore only be a function of temperature:

$$\frac{\Delta G_R^0}{RT} + \ln K(T) = 0 \quad (6.195)$$

where

$$\Delta G_R^0(T, 1 \text{ bar}) = \sum \vartheta_i G_i^0 \quad (6.196)$$

and

$$K(T) = \prod \left[\frac{\hat{f}_i}{f_i^0} \right]^{\vartheta_i} = \prod a_i^{\vartheta_i} \quad (6.197)$$

The ratio of fugacities in Equation (6.197) is called the equilibrium constant. (It is not constant! It depends on temperature.) The individual fugacities depend on pressure and concentration as well as temperature. At equilibrium, the equilibrium constant K provides a functional relationship between the reaction extent and the temperature and pressure that must be satisfied. In order to make use of this relationship, we need to know the Gibbs free energy change for the standard reaction at the temperature in question as shown in Equation (6.195).

From the definition of the Gibbs function,

$$\Delta G_R^0 = \Delta H_R^0 - T \Delta S_R^0 \quad (6.198)$$

In Section 3.6.1, the experimental basis for the tabulation of heats of formation was discussed as well as their relationship to the standard heat of reaction.

$$\Delta H_R^0(298 \text{ K}, 1 \text{ bar}) = \sum_{\text{all species}} \vartheta_i \Delta H_{f,i}^0(298 \text{ K}, 1 \text{ bar}) \quad (3.118)$$

At the same time, these tabulations can include calculations of the entropy change for the standard reaction based on specific heat data and of the *Third Law of Thermodynamics: The entropy of all perfect crystalline substances is zero at absolute zero* (Smith et al., 2005). The standard Gibbs free energy change is then evaluated with Equation (6.198). One such tabulation is in Yaws (2003).

Using these tabulated values, the equilibrium constant may be evaluated at 298 K:

$$K(T) = e^{-(\Delta G_R^0/RT)} \quad \text{at } T = 298 \text{ K} \quad (6.199)$$

Equation (6.195) provides the temperature dependence of the equilibrium constant:

$$\ln K(T) - \ln K(298) - \int_{298}^T \frac{d}{dT} \left[\frac{\Delta G_R^0}{RT^2} \right] dT \quad (6.200)$$

Using the thermodynamic identity

$$\frac{\partial(G/T)}{\partial T} = -\frac{H}{T^2} \quad (6.201)$$

we arrive at the working relationship:

$$\ln K(T) = \ln K(298) + \int_{298}^T \frac{\Delta H_R^0}{RT^2} dT \quad (6.202)$$

where

$$\Delta H_R^0(T, 1 \text{ bar}) = \sum_{\text{all species}} \nu_i \Delta H_{f,i}^0(298 \text{ K}, 1 \text{ bar}) + \sum_{\text{all species}} \nu_i \int_{298 \text{ K}}^T C_{pi}(T, 1 \text{ bar}) dT \quad (3.119)$$

is the standard enthalpy change for the reaction. The H_i^0 are the enthalpies of the pure components at the standard reaction states.

If the standard heat of reaction is nearly constant over the temperature range of interest, Equation (6.202) can be integrated to give

$$\ln K(T) = \ln K(298.16) + \frac{(-\Delta H_R^0)}{R} \left[\frac{1}{T} - \frac{1}{298.16} \right] \quad (6.203)$$

This assumption may not be as bad as one may think on the basis that the enthalpy is a strong function of temperature. The point here is that the heat of reaction is a difference of enthalpies, each of which increases with temperature, at possibly the same rate.

Example 6.7-1: Equilibrium Constant for the Synthesis of Hexyl Glucoside by Condensation

The condensation reaction between *n*-hexanol and glucose can be used to synthesize hexyl glucoside with the aid of an enzyme catalyst, β -glucosidase. See discussion in Chapter 2 and the summary of related examples. The synthesis reaction takes place in an aqueous phase at 60 °C:



The idea here is to find the equilibrium relation that will be useful in the material balances in process synthesis.

Solution:

We want to apply Equations (6.199) and (6.202) for which we require enthalpy and Gibbs free energy of formation data. The data are summarized below:

Component	Standard State (<i>T</i> , <i>P</i>)	G_f^0 (kJ/mol)	H_f^0 (kJ/mol)	Source
Glucoside (P)	Solid	-940.04	-1079	Aspen Plus ^a
Water (W)	Liquid	-237.14	-285.83	Langes
Hexanol (A)	Liquid	-152.30	-372.5	Langes
Glucose (G)	Solid	-910.40	-1273.3	Langes

^aThis estimate was made with the process simulator, Aspen Plus, Property Estimation.

The standard Gibbs free energy change for the reaction is

$$\Delta G_R^0 = -940.04 - 237.14 - (-152.3) - (-910.4) = -114.48 \text{ kJ/mol}$$

The equilibrium constant can be evaluated with this result and Equation (6.199).

This is clearly a very large equilibrium constant. According to Equation (6.203), its value at 60 °C may be obtained with the standard heat of reaction. The standard heat of reaction at 25 °C is

$$\Delta H_R^0 = -1079 - 285.83 - (-377.5) - (-1273.3) = 285.97 \text{ kJ/mol}$$

Assuming this to be constant,

$$\ln K(333.16) = 46.185 - \frac{285,970(0.23901)}{1.987} \times \left[\frac{1}{333.16} - \frac{1}{298.16} \right] = 58.305$$

Now this equilibrium constant can be expressed as

$$K(333.16) = \frac{a_P a_W}{a_G a_A} = \frac{\gamma_P \gamma_W x_P x_W}{\gamma_G \gamma_A x_G x_A} = K_\gamma K_x = K_\gamma K_c$$

The value of K_c was measured to be constant at 1.90 over a range of conditions that will be preserved in the scale up. This result obviates the need to evaluate the activity coefficients, but it can be noted that, in this case, there are some activity coefficients that deviate substantially from one!

Example 6.7-2: Check on Methanol Conversion to Formaldehyde

In Examples 2.3.1.1-1 and 3.6.1.2-1, material and energy balances were carried out on the methanol oxidation reactor described in the former example. It was assumed that the conversion of methanol was 100% at an outlet temperature of 425 °C. We can determine the validity of that assumption.

Formaldehyde reactor:

Data from Sandler-TRC tables.

Definitions:

Species	Reference
CH ₃ OH	1
O ₂	2
HCHO	3
H ₂ O	4
N ₂	5

The standard states for the reaction system can be taken as the pure components in the gaseous state at 1 atm. Assuming ideal behavior, all of the f_i^0 are unity. The heats and free energies of formation will be taken for the gaseous state at 298 K.

Heats of formation (kJ/mol):

$$\Delta H_f = \begin{matrix} -200.6 \\ 0 \\ -108.6 \\ -241.8 \\ 0 \end{matrix}$$

Specific heats (J/(mol K)):

$$[a] = \begin{bmatrix} 19.038 & 9.146 \times 10^{-2} & -1.218 \times 10^{-5} & -8.034 \times 10^{-9} \\ 25.460 & 1.519 \times 10^{-2} & -0.715 \times 10^{-5} & 1.311 \times 10^{-9} \\ 22.791 & 4.075 \times 10^{-2} & 0.713 \times 10^{-5} & -8.695 \times 10^{-9} \\ 28.883 & -0.157 \times 10^{-2} & 0.808 \times 10^{-5} & -2.8712 \times 10^{-9} \\ 32.218 & 0.192 \times 10^{-2} & 1.055 \times 10^{-5} & -3.593 \times 10^{-9} \end{bmatrix}$$

$$C_p(k, T) = a_{k,1} + \sum_{j=2}^4 a_{k,j} T^{j-1}$$

Stoichiometric coefficients and feed mole fraction

$$[\vartheta] = \begin{bmatrix} -1 \\ -0.5 \\ 1 \\ 1 \\ 0 \end{bmatrix} \quad [y] = \begin{bmatrix} 0.08 \\ 0.10 \\ 0 \\ 0 \\ 0.82 \end{bmatrix} \quad y_{5,1} = 0.82$$

Standard heat of reaction:

$$\Delta H_R(T) = \sum_{i=1}^{i=5} \vartheta_{i,1} (\Delta H_f)_{i,1} + 0.001 \sum_{i=1}^{i=5} \vartheta_{i,1} \int_{298}^T c_p(i, x) dx$$

$$H_R(298) = -149.8$$

$$H_R(400) = -149.53$$

Gibbs free energy change (kJ/mol) and equilibrium constant at 298:

$$\Delta G_f = \begin{matrix} -162.0 \\ 0 \\ -102.5 \\ -228.6 \\ 0 \end{matrix}$$

$$\Delta G_R^0 = \sum_{i=1}^{i=5} \vartheta_{i,1} (\Delta G_f)_{i,1} = -169.1$$

$$K(298) = \exp\left(\frac{169.1}{0.008314 \times 298}\right) = 4.3813 \times 10^{29}$$

Equilibrium constant as a function of temperature:

$$K(T) = \exp\left(\ln(4.3813 \times 10^{29}) + \int_{298}^T \frac{\Delta H_R(T)}{0.008314 T^2} dT\right)$$

$$K(298) = 4.3813 \times 10^{29}$$

$$K(600) = 2.7398 \times 10^{16}$$

The equilibrium conversion will be essentially 100% at this value of the equilibrium constant.

Equilibrium constant as a function of composition and pressure:

Assuming that the gas is ideal, the fugacities are equal to (see discussion on evaluation of fugacities) yP . Since the reference state fugacities are unity, the equilibrium constant becomes

$$K = \Pi(y_i P)^{\vartheta_i}$$

Taking methanol as the key reactant (A), the mass balances for the reactor are given in terms of conversion as

$$n_i = n_{i0} + \vartheta_i x_A n_{A0}$$

The mole fractions are then

$$y_i = \frac{y_{i0} + \vartheta_i x_A y_{A0}}{1 + x_A y_{A0}/2}$$

The equilibrium constant can then be formed as follows for no product in the reactor feed:

$$y_i = \frac{y_{i0} + \vartheta_i x_A y_{A0}}{1 + x_A y_{A0}/2}$$

$$K(T) = \frac{y_{A0}^{0.5} x_A^2 P^{0.5}}{(1 - x_A)(r - 0.5x_A)^{0.5}(1 + 0.5x_A y_{A0})^{0.5}}$$

where r is the ratio of the oxygen to the methanol mole fraction in the feed.

Calculation of conversion:

$$r = 10/8$$

$$P = 1$$

$$x_0 = 0.08$$

$$\frac{x_o^{0.5} x^2 P^{0.5}}{(1 - x)(r - 0.5x)^{0.5}(1 + 0.5xx_0)^{0.5}}$$

$$= K(425 + 273) = 3.9764 \times 10^{14}$$

$$g(x) = \frac{x_0^{0.5} x^2 P^{0.5}}{(1-x)(r-0.5x)^{0.5}(1+0.5xx_0)^{0.5}}$$

$$g(x) = 3.9764 \times 10^{14}, \quad x \in (0.9999999, 1), \quad \text{Solution is } \{x = 0.99999999999999\}$$

Example 6.7-3: Phase Equilibrium with Chemical Reaction—Synthesis of Hexyl Glucoside

The synthesis of hexyl glucoside (P) can take place in a biphasic system as described in Chapter 1. The condensation reaction between hexyl alcohol (A) and glucose (G) takes place in the aqueous phase and produces water (W) and hexyl glucoside (P) (see Figure 6.56).

Biphasic condensation of glucose and hexanol using almond β -glucosidase:

The product P distributes between the aqueous phase and the organic phase. In the organic phase, it is supposed that P forms aggregates containing m molecules of P and that these aggregates do not partition between the two phases. The organic phase becomes saturated with water and the liquid phase becomes saturated with the alcohol. When the product is removed from the organic phase, the aggregates decompose to form the monomer so that there is no loss of product due to the aggregation. It will be convenient then to not deal with the aggregates in the material balances but just the total product in the organic phase. This will require the use of an apparent phase equilibrium constant in terms of the total product in the organic phase that accounts for both phase and chemical equilibrium. Data were taken for various alcohols (Panintrarux et al., 1995) from which the data shown in Figure 6.57 for hexanol was highlighted.

Calculate the aggregation and phase equilibrium constants and the size (m) of the aggregates.

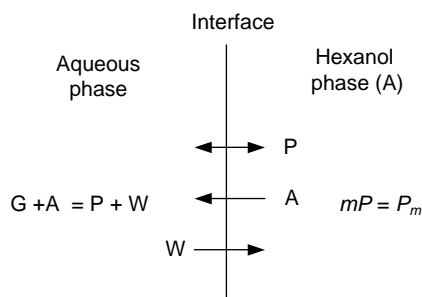


FIGURE 6.56 Biphasic condensation of glucose and hexanol using almond β -glucosidase.

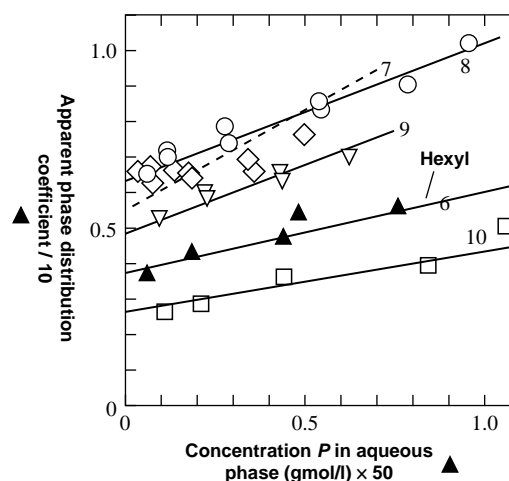


FIGURE 6.57 Apparent phase distribution coefficient for hexyl glucoside (solid points); scaling factors on axes apply only to this compound.

Solution:

Define the aggregation and phase equilibrium constants as

$$K_m = \frac{[P_m]_{\text{org}}}{[P]_{\text{org}}^m}, \quad K_p = \frac{[P]}{[P]_{\text{aq}}}$$

The apparent, or total, composition of P in the organic phase is

$$[P]_{\text{org,app}} = [P]_{\text{org}} + m[P]_{\text{org}}^m$$

or

$$K_{\text{ap}} = K_p + m$$

$$[P]_{\text{org,app}} = [P]_{\text{org}} + m[P]_{\text{org}}$$

or

$$[P]_{\text{org,app}} = [P]_{\text{org}} + mK_m[P]_{\text{org}}^m$$

This relation can be cast in terms of phase equilibrium constants as follows:

$$\frac{[P]_{\text{org,app}}}{[P]_{\text{aq}}} = \frac{[P]_{\text{org}}}{[P]_{\text{aq}}} + mK_m \frac{[P]_{\text{org}}^m}{[P]_{\text{aq}}^m} \frac{[P]_{\text{aq}}^m}{[P]_{\text{aq}}}$$

$$K_{\text{ap}} = K_p + mK_m K_p^m [P]_{\text{aq}}^{m-1}$$

This result in light of the fact that the plot of K_{ap} versus $[P]_{\text{aq}}$ in Figure 6.57 is linear leads us to believe that, over the range

of compositions covered in the experiments, both the phase and aggregation coefficients are constant and $m = 2$.

The equation of the straight line is approximately

$$\frac{K_{ap}}{10} = \frac{0.620 - 0.380}{1.1} (50[P]_{aq} + 0.380)$$

$$K_{ap} = 109.091[P]_{aq} + 3.80$$

$$\frac{[P]_{org,app}}{[P]_{aq}} = 109.091[P]_{aq} + 3.80$$

PROBLEMS

6.1. Calculate the bubble point for an equimolar mixture of *n*-pentane and *n*-propionaldehyde at 1.5 atm. Assume that the vapor is ideal and the liquid follows the van Laar equation (see Problem 6.2).

6.2. Equilibrium measurements in the *n*-pentane (1) propionaldehyde (2) system have shown that $\gamma_1^\infty = 3.848$ and $\gamma_2^\infty = 3.979$. Using the van Laar equation, compute the values of y_1 and P for the values of x_1 listed in the following table. The experimental values are listed for comparison and for providing the vapor pressure data. The temperature is 40 °C.

x_1	Experimental		Calculated	
	y_1	P (bar)	y_1	P (bar)
0.0000	0.0000	0.7609		
0.0503	0.2121	0.9398		
0.1014	0.3452	1.0643		
0.1647	0.4288	1.1622		
0.2212	0.4685	1.2173		
0.3019	0.5281	1.2756		
0.3476	0.5539	1.2949		
0.4082	0.5686	1.3197		
0.4463	0.5877	1.3354		
0.5031	0.6146	1.3494		
0.5610	0.6311	1.3568		
0.6812	0.6827	1.3636		
0.7597	0.7293	1.3567		
0.8333	0.7669	1.3353		
0.9180	0.8452	1.2814		
1.0000	1.0000	1.1541		

6.3. Formulate the K function for a component of a vapor-liquid mixture under the following circumstances

- Ideal vapor-ideal liquid.
- Vapor is ideal solution (Lewis-Randall rule)—liquid phase follows Margules two constant model.
- Vapor is nonideal mixture—liquid component obeys Henry's law.

If an equation of state is required, use the Virial equation of state. The only variables are T , P , and the liquid and vapor mole fractions. This means that you must define all parameters in these terms and list sources of data.

6.4. A number of selective solvent systems have been tested to improve the separation of carboxylic acids from fermentation broths. Methylcyclohexanol ($C_6H_{13}CH_3OH$) has been found to be particularly effective for the extraction of levulinic acid ($CH_3OC_3H_4COOH$) from water (Senol, 2005). A 40 wt% aqueous solution of levulinic acid flowing at 2000 lb/h is available for extraction with methylcyclohexanol. The final acid concentration is to be no more than 2.5 wt%. The separation operation is to take place at 25 °C. Equilibrium data are available at 25 °C (Senol, 2005):

Water Phase		Methylcyclohexanol Phase	
Water	Levulinic Acid	Water	Levulinic Acid
0.9865	0.0000	0.0782	0.0000
0.9231	0.0625	0.0750	0.0465
0.8354	0.1434	0.0848	0.1126
0.7203	0.2502	0.0961	0.2142
0.6170	0.3473	0.1120	0.3157
0.5070	0.4340	0.1585	0.4232

Some useful pure component liquid data that may be used in approximating the mixture values are as follows (Yaws, 1999, 2003):

	Density (g/cm ³)	Viscosity (cP)
Water	1.018	0.7399
Levulinic acid	1.127	4.501
Methylcyclohexanol	0.913	10.88

- What are the maximum and minimum solvents to feed ratios for a single cross-flow extraction?
- What are the limiting amounts and solvent concentrations in the extract and raffinate for the minimum solvent to feed ratio in part a?

6.5. In the production of acetone by the dehydrogenation of isopropyl alcohol, a stream containing 35 kmol/h hydrogen, 35 kmol/h acetone, and 20 kmol/h water is to be flashed at 2 bar and 20 °C.

Assume that there is no hydrogen in the liquid product. The distribution coefficient for hydrogen is very large.

- Using VLE data, find an equation for the activity coefficients acetone and water as a function of composition. You may choose the Wilson equation or any

other that you feel is more applicable. The fit to the data may be obtained by trial and error based on critical observations.

Assume that the activity coefficients are independent of temperature and pressure.

- b. Find an expression for the distribution coefficient of both acetone and water assuming that the vapor phase fugacity of these components (\hat{f}_i) obeys the Lewis–Randal rule $\hat{f}_i = y_i f_i(T, P)$ where $f_i(T, P)$ is the fugacity of the pure component (i) at the temperature and pressure of the mixture, and y_i is the mole fraction. You may choose any nonideal model for the vapor phase and you may use an integrated form for the fugacity. If you use an integrated form, set up the integral that has to be evaluated to obtain the result.
- c. Compute the bubble point of the feed at 2 bar if there were no hydrogen present.
- d. Compute the flow rates and compositions in the vapor and liquid product streams shown assuming that the vapor and liquid mixtures are ideal. Remember that the hydrogen mole fraction in the liquid is zero. You might consider the effect of this in the expressions that you want to use as the distribution coefficient of hydrogen becomes very large.

6.6. Oil is to be extracted from meal using benzene in a single equilibrium stage mixer–settler. The unit is to treat

2000 lb of completely exhausted meal. The untreated meal contains 800 lb of oil and 50 lb benzene. The fresh solvent contains 20 lb of oil and 1310 lb of benzene. The underflow is to contain all of the meal, 120 lb of unextracted oil, and retained solution. Experimental data acquired at the same conditions indicate that the concentration of the retained solution depends on the amount retained:

Concentration lb Oil/lb Solution	Amount Retained lb/lb Solid
0.0	0.500
0.1	0.505
0.2	0.515
0.3	0.530
0.4	0.550
0.5	0.571
0.6	0.595
0.7	0.620

Determine the

- a. amount of overflow,
- b. concentration of oil in the overflow and in the retained solution,
- c. amount of retained solution per lb of exhausted meal.

PART II

MICROSCOPIC VIEW

MULTISTAGE SEPARATION AND REACTOR OPERATIONS

The stages discussed in Chapter 6 will not, in many cases, be sufficiently practical to implement because of excessive material and/or equipment requirements. In this chapter, the multistage analogs of those single-stage operations will be developed. The same principles will be used, but the development will lead to single items of equipment that offer a multistage separation capability rather than to a direct multiplication of the single-stage steps. The stagewise component will remain so that the stream conditions will change stepwise throughout the equipment, but the outlet conditions will not be the same as the interior conditions. This progressive *stepwise* change is an intermediate condition between completely mixed systems where the output and interior conditions coincide and the processing systems where the interior states *continuously* change from inlet to outlet. Since our viewpoint must change focus to reach the interior conditions of the equipment, we place multiple equilibrium stage systems in the microscopic category.

In the limiting case of continuous variation throughout the equipment, the macroscopic equilibrium stage notion is carried into the microscopic notion of local equilibrium. The balance equations for mass, energy, and momentum become differential equations, since the conservation principles must be applied to differential elements in order to bring the local variations into view. The interactions of the processing equipment with the surroundings will appear in the boundary conditions associated with the differential balance equations: for example, interfacial mass transfer rates in absorption, heat transfer rates to reactors, momentum transfer rates to suspended droplets at flooding. Such rates determine, for example, equipment sizes when coupled

with a net macroscopic requirement. The complications of turbulence in these circumstances have led to the definition of the interfacial transport coefficients based on experimental determination organized by the microscopic balance equations.

To improve upon the separations achieved in the single-stage arrangements developed in Chapter 6, it will be argued that the most efficient arrangement is a countercurrent flow of the two phases, where the separating agent for one stage is provided by the output from the previous stage. In every case, the equilibrium relations discussed in Chapter 6 can be expressed graphically and the graphical construction provides the number of stages required for the separation. The two central features of the single or multistage graphical constructions are the equilibrium relation and the material balance or operating line.

We will consider the case of multicomponent systems for gas absorption only. Except for distillation, we will assume isothermal operation. Isobaric operation will also be assumed. Aside from the real applications that are included within our purview, we will gain substantial insight into those applications that are not.

Pressure drop calculations and equipment diameters based on flooding are considered in Chapter 13 where turbulent momentum transfer is discussed.

7.1 ABSORPTION AND STRIPPING

The basic aspects of absorption and stripping are discussed in Sections 1.2.3 and 6.2.3. The basic aspects consist

primarily of the equilibrium relations and the material balances for isothermal operation as well as the typical applications.

7.1.1 Isothermal Binary Gas Absorption

As pointed out earlier, the gas of stripping components from a liquid is treated in the same way as absorbing components from a gas phase. The form of the equations is exactly the same. The distinction will be made in the examples so that the discussion will be framed primarily for the application to gas absorption.

Refer to the single-stage analysis in Section 6.2.2 and consider improving the amount of absorption. For example, a second stage operating similarly to the first stage may be added as illustrated in Figure 7.1 where a separate fresh solvent flow to the second stage is provided to effect additional absorption.

The fresh solvent provides a fresh equilibrium state for the output of the second stage. The mass balance for the second stage and its interaction with the equilibrium curve are the same as the first stage. If the same liquid to gas ratio is used, the graphical representation is given in Figure 7.2.

We are assuming that, aside from the target species (impurity), there is no appreciable interphase mass transfer and that the impurity is present in sufficiently small quantities such that its transfer has no noticeable effect on the total flow. This latter assumption can be easily

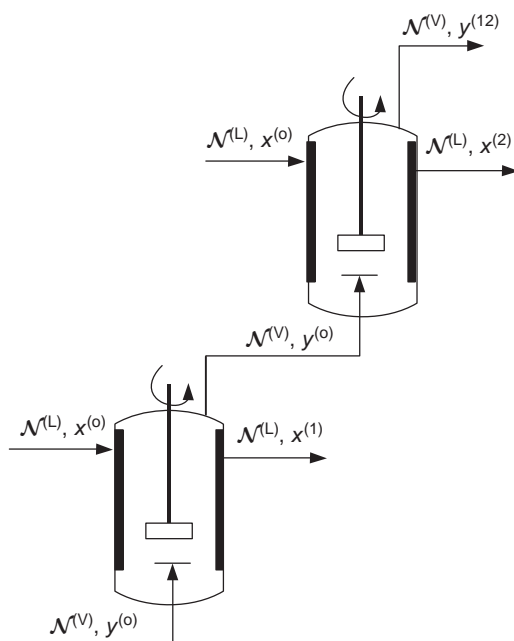


FIGURE 7.1 Addition of a second absorption step.

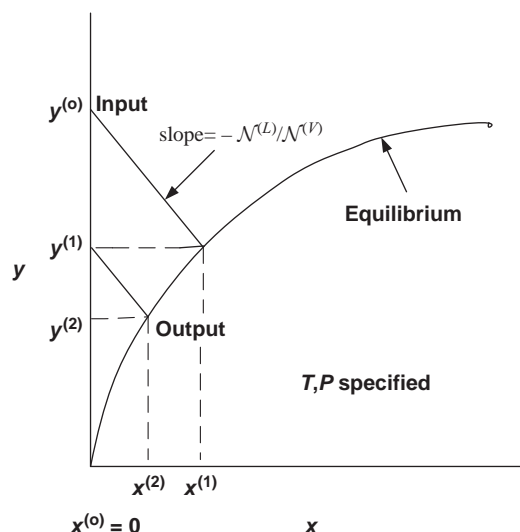


FIGURE 7.2 Graphical solution for the cross-flow cascade.

removed with the use of mole ratios, which were introduced in Chapter 1 and applied to gas absorption in Section 6.2.2.

The purity of the gas product increases with the second stage and will continue to do so with the addition of even more stages as well as fresh solvent. The arrangement is called a cross-flow cascade. A major drawback of this cross-flow arrangement is that there is an ever-increasing quantity of solvent to be treated and it is becoming more and more dilute. The gradual dilution can be seen from the fact that

$$y^{(j+1)} < y^{(j)} \quad (7.1)$$

implies that

$$x^{(j+1)} < x^{(j)} \quad (7.2)$$

We take this to be a property of the equilibrium relation.

The liquid leaving each stage can consequently act as a solvent, less efficient to be sure since it is not fresh, for the preceding stage. Taking advantage of this by reintroducing the liquid product from each stage, beginning with the last, will therefore increase the number of stages required but will result in a disproportionately large savings in solvent regeneration or purchase costs. We are thereby led to the countercurrent contacting arrangement shown in Figure 7.3.

Gas absorption may also be carried out in a continuous contacting fashion where the intermediate steps of phase separation are bypassed. The packed tower is an example of a continuous contacting device for lower capacity operations, for example, and will be discussed in Chapter 12. We

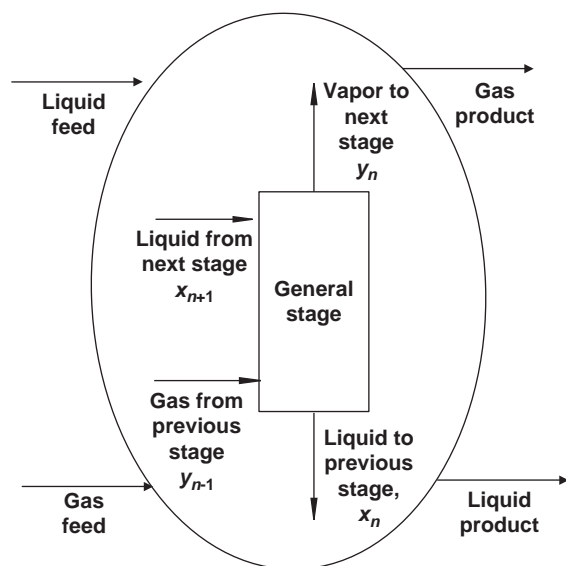


FIGURE 7.3 Stage in countercurrent cascade.

will continue here with the countercurrent arrangement of equilibrium stages.

7.1.2 Countercurrent Cascade-Tray Tower

A sequence of stirred tanks becomes less attractive as the stages increase in number since each step requires a new vessel with mechanical mixing as well as liquid-pumping and gas-moving equipment. A better operation that exploits gravity to mix and move fluids within the contacting operation can be arranged in a vertical cylindrical tower as illustrated in Figure 7.4.

Liquid travels down the tower and gas travels up. The two streams are kept separate, except for regular intervals where the two are mixed and separated. The liquid flows down between trays in a closed channel called a downcomer. At the end of a downcomer, there is an opening that directs the

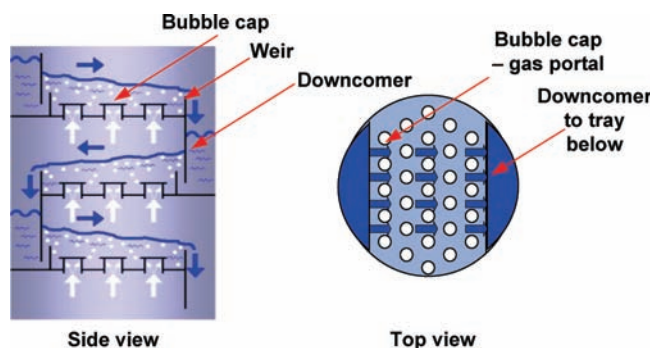


FIGURE 7.4 Schematic of flow in a tray tower for gas-liquid contracting. Courtesy of Koch Modular Process Systems.

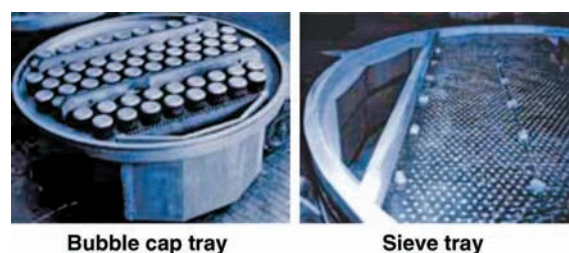


FIGURE 7.5 Bubble-cap and sieve tray. (Courtesy of SGL Group.)

liquid flow across a tray or plate. The plate is outfitted with portals that allow the upward passage of gas and promote mixing and interfacial mass and energy transfer. The liquid falls to the plate below through the next downcomer after flowing over a retainer designed to hold up liquid on the plate. The retainer is called a weir.

The liquid is prevented from falling through the portals on the plate by the upcoming vapor stream and the design of the portals. Two popular designs are shown in Figure 7.5.

Mixing and separation take place above the plate to the extent that the exiting gas and liquid streams are in equilibrium. The plate functions as the stirred tank in the countercurrent construction discussed above. The correspondence between the two is shown in Figure 7.6.

A picture of a tray tower used for absorption is shown in Figure 7.7.

The first steps in the approximate design or sizing of the absorption equipment involves the determination of the number of stages and the solvent flow rate that is required. We presume that the following are given:

- Inlet gas flow rate, composition, and pressure.
- Desired purity of the outlet gas.
- Solvent composition.
- Operating pressure and temperature for isothermal operation.

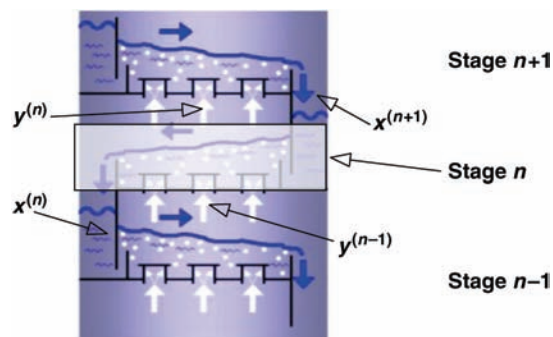


FIGURE 7.6 Transition from a stirred tank to a tray tower. Courtesy of Koch Modular Process Systems.



FIGURE 7.7 Absorption tower. Courtesy of Clean Gas Systems.

We will take a graphical approach to determine the number of equilibrium stages for systems that entail the transfer of a single component. An algebraic method will be used for dilute multicomponent systems. The actual stage requirement will be obtained through use of an empirical efficiency that accounts for the lack of reaching equilibrium in the stage. The actual number of stages will be used to estimate height of the tower. The tower diameter will be determined in Chapter 13.

7.1.3 Graphical Procedures for Single Components

Refer to the tower illustration in Figure 7.8. Allowance is made for changes in the liquid and gas flows from stage to stage.

Note that we are numbering the trays from the bottom to the top. This is not always the case, so care must be taken to establish the scheme being used. It is also helpful to be aware of the physical associations when interpreting the results, as these interpretations are independent of the numbering scheme.

Each stage is an equilibrium stage, so the streams leaving the stage are in equilibrium. We are assuming that each phase consists of a solvent and a solute and that the solvent is not taken up to any appreciable extent by the other phase.

Therefore, there are +1 liquid flows, $N_s + 1$ vapor flows, $N_s + 1$ liquid, and $N_s + 1$ vapor mole fractions, or $4(N_s + 1) + 1$ unknowns, including the number of stages.

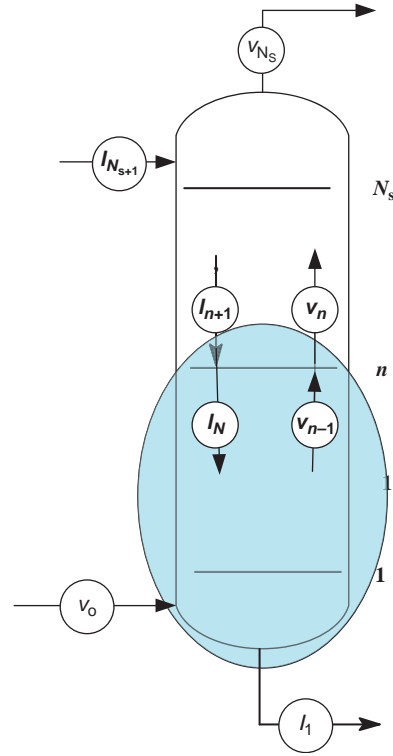


FIGURE 7.8 Stream labels.

There are N_s stages, each a chemical processing unit, each of which must satisfy conservation of mass. There are N balances for the solute. A subscript on the mole fractions will not be necessary, since there is only one solute. These balances may be taken in a number of ways. This most obvious is to consider a single stage (n):

$$x^{(l_{n+1})} \mathcal{N}^{(l_{n+1})} + y^{(v_{n-1})} \mathcal{N}^{(v_{n-1})} = x^{(l_n)} \mathcal{N}^{(l_n)} + y^{(v_n)} \mathcal{N}^{(v_n)} \quad (7.3)$$

The most convenient, however, is to begin with the bottom (or top) stage and progressively add a stage at a time as indicated in: Figure 7.8

$$y^{(v_n)} \mathcal{N}^{(v_n)} + x^{(l_1)} \mathcal{N}^{(l_1)} = x^{(l_{n+1})} \mathcal{N}^{(l_{n+1})} + y^{(v_0)} \mathcal{N}^{(v_0)} \quad (7.4)$$

Since the solvent flows are assumed constant for each phase, we have the $2N_s$ relations:

$$\mathcal{N}^{(l_n)} (1 - x^{(l_n)}) = \mathcal{N}^{(l_{N_s+1})} (1 - x^{(l_{N_s+1})}), \quad n = 1, 2, \dots, N_s \quad (7.5)$$

$$\mathcal{N}^{(l_{v_n})} (1 - y^{(v_n)}) = \mathcal{N}^{(0)} (1 - y^{(0)}), \quad n = 1, 2, \dots, N_s \quad (7.6)$$

There is one equilibrium expression for each stage for the solute:

$$\mu_1^{(l)} = \mu_1^{(v)}, \quad n = 1, 2, \dots, N_s \quad (7.7)$$

In total, there are $4N_s$ relationships between the unknowns. There are, therefore, five degrees of freedom.

In a gas absorption problem, we would generally know the inlet gas conditions, the solvent composition, and the gas purity required. Consequently we can count $\mathcal{N}^{(v_0)}$, $y^{(v_0)}$, $x^{(l_{N_s+1})}$, and $y^{(v_0)}$ as given leaving one degree of freedom. We will assume that the solvent flow is fixed for now and return to the question about how best to do this later.

The number of unknowns can be substantially reduced if the liquid and vapor flows are constant. This is the case, or nearly the case, in two circumstances that can be seen by taking a closer look Equations (7.5) and (7.6). These relations state the condition that only one component is crossing the gas-liquid interface or the equivalent that the solvent flow is constant throughout the column in each phase.

For dilute systems, where

$$y^{(0)} \ll 1 \quad \text{and} \quad x^{(1)} \ll 1 \quad (\Rightarrow x^{(N_s+1)} \ll 1) \quad (7.8)$$

the equations above reflecting the invariability of the solvent flows reduce to

$$\mathcal{N}^{(l_n)} = \mathcal{N}^{(l_{N_s+1})} = \mathcal{N}^{(l)}, \quad n = 1, 2, \dots, N_s \quad (7.9)$$

$$\mathcal{N}^{(v_n)} = \mathcal{N}^{(v_0)} = \mathcal{N}^{(v)}, \quad n = 1, 2, \dots, N_s \quad (7.10)$$

In this case, the solvent conditions are satisfied to a very close approximation by constant total molar rates of the liquid and vapor rates. The mass balances written above for the solute can then be rearranged as

$$y^{(v_n)} = \frac{\mathcal{N}^{(l)}}{\mathcal{N}^{(v)}} x^{(l_{n+1})} + (y^{(v_0)} - \frac{\mathcal{N}^{(l)}}{\mathcal{N}^{(v)}} x^{(l_1)}), \quad n = 1, 2, \dots, N_s \quad (7.11)$$

This result, called the operating line, states that the *inter-stage* composition pairs $\{x^{(l_{n+1})}, y^{(v_n)}\}$ lie on a straight line of constant slope $\frac{\mathcal{N}^{(l)}}{\mathcal{N}^{(v)}}$ that passes through the mole fractions at the bottom of the tower $\{x^{(l_1)}, y^{(v_0)}\}$ as well as the mole fractions at the top $\{x^{(l_{N_s+1})}, y^{(v_{N_s})}\}$. Note that both the liquid and vapor flows decrease with the height of the tower, which is a stabilizing feature of the constant slope assumption.

If the system is not dilute, we can introduce the mole ratio composition measure (see Section 2.1.1.1) and again obtain a straight operating line since the use of this composition measure requires the use of the constant nonsolute flows expressed in Equations (7.5) and (7.6):

$$x^{(l_n)} \mathcal{N}^{(l_n)} = \frac{x^{(l_n)}}{1 - x^{(l_n)}} \underbrace{\left(1 - x^{(l_n)}\right) \mathcal{N}^{(l_n)}}_{\text{Constant liquid phase solvent flow: See Equation (7.5)}} = X^{(l_n)} \mathcal{N}_S^{(l)} \quad (7.12)$$

$$y^{(v_n)} \mathcal{N}^{(v_n)} = \frac{y^{(v_n)}}{1 - y^{(v_n)}} \underbrace{\left(1 - y^{(v_n)}\right) \mathcal{N}^{(v_n)}}_{\text{Constant gas phase solvent flow: See Equation (7.6)}} = Y^{(v_n)} \mathcal{N}_S^{(v)} \quad (7.13)$$

Substitution into the mass balances gives

$$Y^{(v_n)} = \frac{\mathcal{N}_S^{(l)}}{\mathcal{N}_S^{(v)}} X^{(l_{n+1})} + (Y^{(0)} - \frac{\mathcal{N}_S^{(l)}}{\mathcal{N}_S^{(v)}} X^{(l_1)}) \quad n = 1, 2, \dots, N_s \quad (7.14)$$

a straight line called the operating line with the properties stated above for the case of dilute systems.

In conclusion, assuming that only one component is absorbed, we must use mole ratios and nonsolute (solvent) molar stream rates that are constant in each phase in order to obtain a straight material balance line that passes through the stream conditions at the top and bottom of the tower. For dilute systems, we may use mole fractions and total molar stream rates that are constant in each phase in order to obtain a straight material balance line that passes through the stream conditions at the top and bottom of the tower.

The equilibrium data in each case must be expressed in the same concentration scale used in the mass balances. If, for example, the equilibrium data are given in terms of mole fractions, we may use the definitions to convert the data to the mole ratio scale. If the data are given in terms of mole ratios, we may convert it to mole fraction scale with their relationship implied by Equations (7.13) and (7.14).

We will continue the discussion in the mole fraction scale but with the similarity to the mole ratio scale very much in mind. The mole fraction scale is common in multi-component systems where the equilibrium data are seldom if ever expressed in the mole ratio scale.

The equilibrium line can be plotted on mole fraction coordinates. The operating line can be located on the same coordinates. It will always fall above the equilibrium line for a self-consistent application. This can be seen

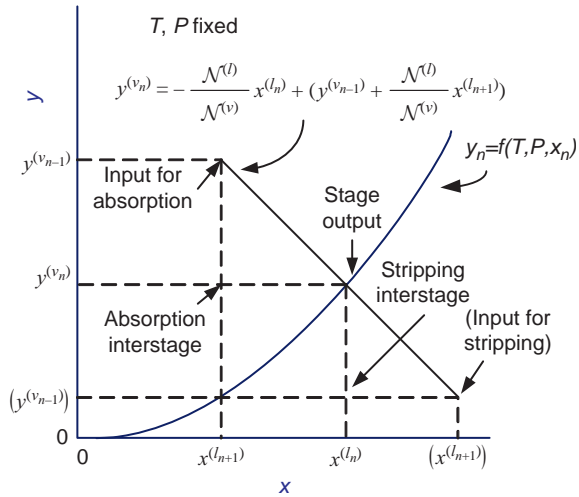


FIGURE 7.9 Relative location of liquid and vapor mole fractions.

as follows: First, consider the mass balance for a single stage:

$$y^{(v_n)} = -\frac{N^{(l)}}{N^{(v)}} x^{(l_n)} + (y^{(v_{n-1})} + \frac{N^{(l)}}{N^{(v)}} x^{(l_{n+1})}) \quad n = 1, 2, \dots, N_s \quad (7.15)$$

This relation states that the outlet compositions $\{x^{(l_n)}, y^{(v_n)}\}$ fall on a straight line of slope $-\frac{N^{(l)}}{N^{(v)}}$ that passes through the point representing the inlet liquid and gas flow compositions $\{x^{(l_{n+1})}, y^{(v_{n-1})}\}$. In gas absorption, the gas composition must decrease from inlet to outlet. In a stripping operation where a solute is removed from the liquid phase, the gas phase composition must increase from inlet to outlet (refer to Figure 7.9).

The interstage composition pair $\{x^{(l_{n+1})}, y^{(v_n)}\}$ is seen to fall above the equilibrium curve for absorption. The interstage

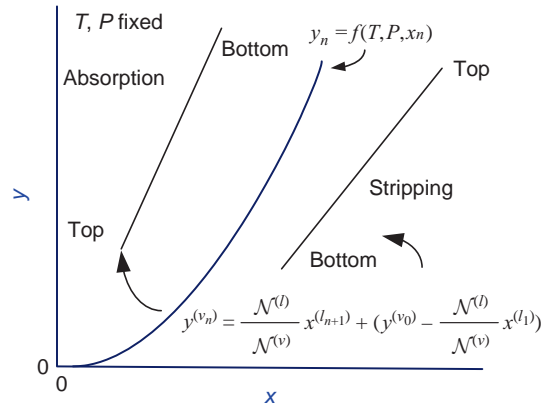


FIGURE 7.10 Relative location of operating lines and the equilibrium curve.

composition pair represented as $\{x^{(l_n)}, y^{(v_{n-1})}\}$ is seen to fall below the equilibrium curve for stripping.

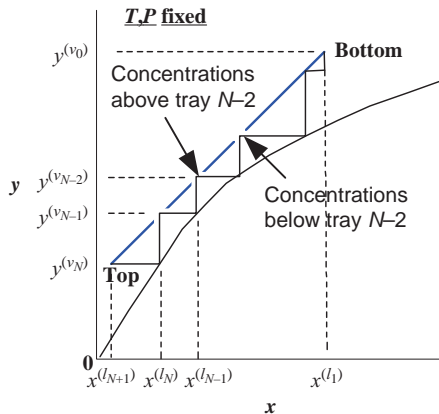
These considerations place the operating line for absorption above the equilibrium line and the operating line for stripping below the equilibrium line. The two cases are illustrated in Figure 7.10.

The solvent flow fixes the outlet liquid composition by an overall material balance:

$$N^{(l)}(x^{(l_1)} - x^{(l_{N+1})}) = N^{(v)}(y^{(v_0)} - y^{(v_N)}) \quad \text{or} \quad (7.16)$$

$$x^{(l_1)} = x^{(l_{N+1})} + \frac{N^{(v)}}{N^{(l)}}(y^{(v_0)} - y^{(v_N)}) \quad (7.17)$$

The inlet and outlet conditions can then be used to locate the operating line by fixing the end points. The remaining gas phase compositions as well as the liquid compositions on all of the stages may be determined by alternating between the equilibrium curve and the operating line while recalling what the composition pairs mean on each (see Figure 7.11).



Stage stepping;

Starting at the top of the column, a horizontal line from y_N to the equilibrium curve gives x_N . A vertical line from the equilibrium curve to the operating line gives the interstage gas composition associated with x_N , y_{N-1} . Must end on operating line. Can also start at bottom of column

FIGURE 7.11 Stage stepping for gas absorption.

Note that the last step is a partial one, but one that must end on the operating line. This means that we have justifiably sacrificed the assumption of an equilibrium stage on the last step in order to satisfy the material balance. Also note that the indicated concentrations above or below the stage are what this theory predicts you would measure if you sampled the liquid and vapor streams at that location in an operating tower.

We now have a graphical technique to solve the problem that we defined at the outset. The graphical technique is described in terms of mole fractions. In these terms, it applies to dilute systems. However, the same graphical technique may be followed with mole fractions replaced with mole ratios and total molar flow rates replaced with nonsolute molar flows without the assumption of dilute systems.

It is clear from the construction method that many liquid flows will provide the required gas purity, since the same procedure may be followed for a range of slopes. The question of which to choose is therefore not a technical problem for the most part. The choice is an economic one.

Without the specification of the liquid flow, we may still draw the equilibrium curve, locate the top of the tower, and define the line through the inlet gas composition on which the outlet liquid composition must fall (refer to Figure 7.12).

Starting with a very large flow rate where the operating line is vertical and progressively decreasing the liquid flow, we see that the number of stages can be determined for each flow condition until the operating line touches the equilibrium curve at what is called a pinch point. This may occur at the inlet gas composition or at an intermediate point between the inlet and outlet gas composition. The latter is illustrated in Figure 7.12.

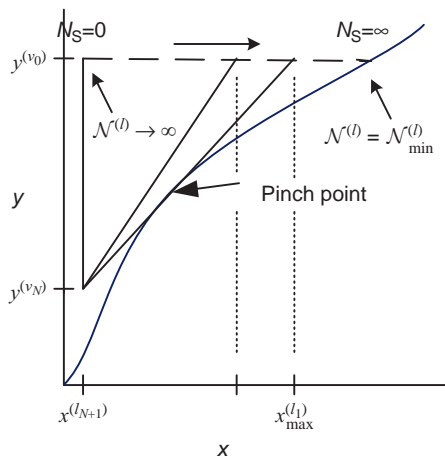


FIGURE 7.12 Effect of solvent flow on the operating line.

As the pinch point is approached, the number of stages approaches an infinitely large number, and the liquid flow cannot be decreased further. The minimum solvent flow is therefore determined by

$$N_{\min}^{(l)} = N^{(v)} \frac{y^{(v_0)} - y^{(v_N)}}{x_{\max}^{(l_1)} - x^{(l_{N+1})}} \quad (7.18)$$

The liquid rate must be larger than this minimum value in order to have a finite number of stages.

There is an economic interplay between the solvent flow and the number of stages that gives rise to an optimum selection of the liquid rate. There is an operating cost associated with the solvent flow that reflects regeneration cost and a depreciated investment cost associated with the number of stages or the column. At low liquid rates, the operation is close to equilibrium; therefore, a large number of stages are required, which results in a costly column. At high solvent flows, the distance from equilibrium is increased by a more dilute liquid, so a large investment is not needed for the column. However, the cost of regenerating the solvent increases with the solvent flow. Consequently, at both high and low solvent flows, we are faced with high costs that suggest an intermediate minimum. A graphical representation of the total cost is given in Figure 7.11.

The optimum is found under constant economic conditions to be nearly proportional to the minimum flow for a wide range of operating conditions. In this case, the cost calculations are replaced with a value for α defined in Figure 7.13.

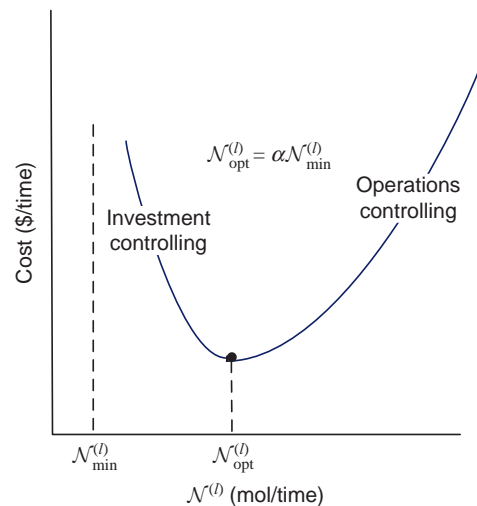


FIGURE 7.13 Costs versus solvent flow.

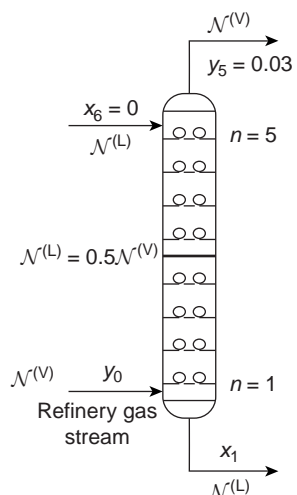


FIGURE 7.14 Butane recovery column.

Example 7.1.3-1: Butane Recovery—Fixed Number of Stages

Butane ($n\text{-C}_4\text{H}_{10}$) in a refinery gas stream is recovered by absorbing it in a liquid, heavy-oil stream. A five-tray gas-liquid countercurrent absorber column is used. Measurements of the mole fractions in the exit gas stream

from the absorber indicate 3 mol% C_4H_{10} . Fifty moles of liquid, containing no C_4H_{10} , are fed into the top of the absorber for every 100 mol of gas fed to the bottom of the absorber.

Calculate the concentration of n -butane in (a) the gas stream fed to the absorber assuming constant liquid and vapor flows in a dilute system and (b) the outlet gas composition using the inlet mole fraction obtained in part (a) but using mole ratios (see Figure 7.14).

Solution: (a)

The K value for n -butane at 40°F and 35 psia is approximately 0.50 (refer to the DePriester charts in Chapter 5). The equilibrium curve is therefore the straight line with slope = 0.50 drawn in Figure 7.15.

The slope of the operating line is the specified liquid to gas ratio, also 0.50. The conditions at the top of the absorber are given as (0, 0.03). With the slope and this point, the operating line may be drawn.

Beginning at the top of the tower, exactly five stages may be stepped off. The conditions at the bottom of the tower may be read from the graph. The result is

$$x^{(I_1)} = 0.296$$

$$y^{(V_0)} = 0.178$$

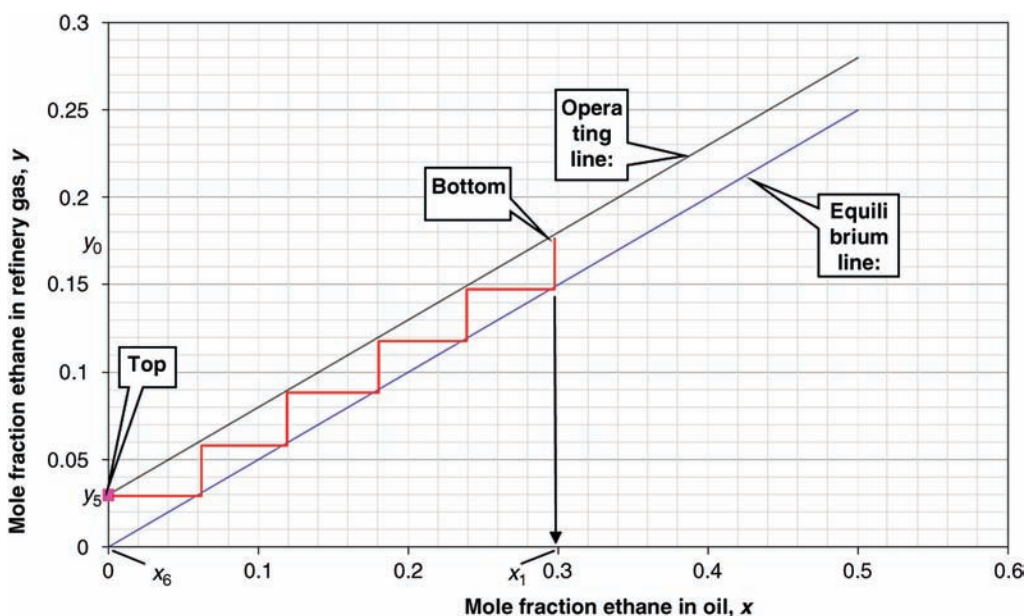


FIGURE 7.15 Graphical solution to the butane recovery problem.

Solution: (b) Mole ratios

$$Y^{(0)} = y^{(0)}(1 - y^{(0)}) = 0.216545$$

$$X^{(6)} = 0$$

$$N^{(1)}_s / N^{(v)}_s = 0.5(1 + Y^{(0)}) = 0.589$$

$Y^{(0)}$ and $X^{(6)}$ specified
 $N^{(1)}_s / N^{(v)}_s$ specified
 Assume $Y^{(5)}$
 Calculate $X^{(1)}$
 Determine N_s
 Iterate on $Y^{(5)}$ until $N_s = 5$

$Y^{(5)}$	$X^{(1)}$	N_s
0.01	0.350671	6.6
0.025	0.325204	3.9
0.019	0.335391	4.75
0.017	0.338786	5

$$y^{(0)} = 0.016716 \quad 0.6000$$

Equilibrium data: $y = 0.5x$ or $Y = 0.5X / (1 + 0.5X)$	
X	Y
0.0000	0.0000
0.0500	0.0244
0.1000	0.0476
0.1500	0.0698
0.2000	0.0909
0.2500	0.1111
0.3000	0.1304
0.3500	0.1489
0.4000	0.1667
0.4500	0.1837
0.5000	0.2000
0.5500	0.2157
0.6000	0.2308
0.7000	0.2593

Apparently, the assumption of a dilute solution underestimates the effectiveness of the column and provides a conservative estimate of the allowable feed composition. For the feed composition arrived at by using the dilute phase assumption, the outlet mole fraction was 0.03 mole ratios the outlet mole fraction is estimated to be 0.016.

The last trial is shown in Figure 7.16.

7.1.4 Isothermal Liquid Stripping

In stripping, one or more components are removed by contacting with an unsaturated gas phase. The mass balances

are the same as those in absorption but the direction of the interfacial mass transfer is in the opposite direction so that the operating line falls below the equilibrium line. The number of degrees of freedom are the same but different selections are made that are suitable to stripping: the inlet

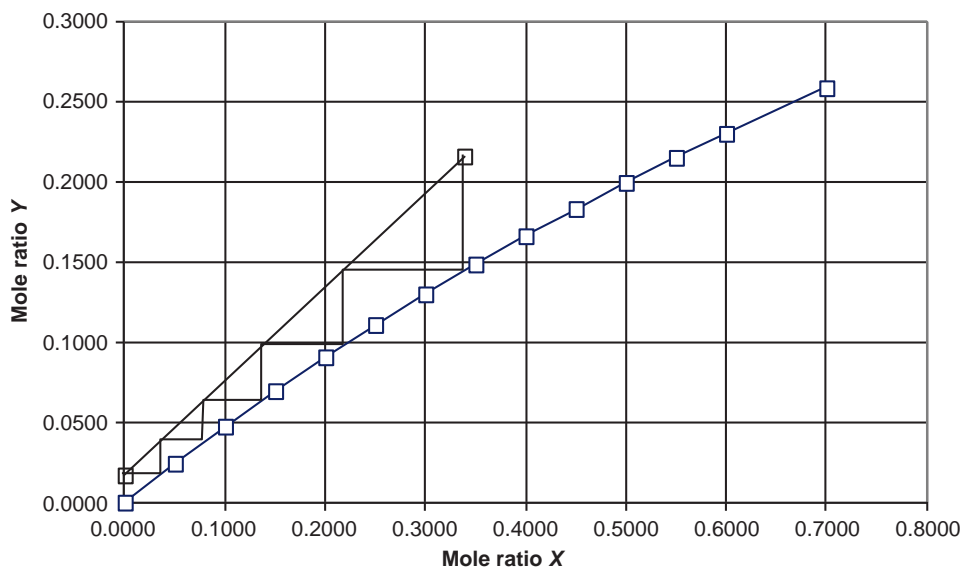


FIGURE 7.16 Outlet mole fractions for five stages.

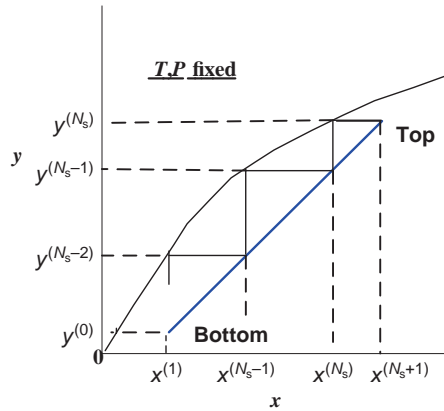


FIGURE 7.17 Stage stepping for liquid stripping.

liquid conditions ($\mathcal{N}^{(L_{Ns+1})}, x^{(L_{Ns+1})}$), the gas phase purity ($y^{(0)}$), and the desired purity of the liquid ($x^{(1)}$) are known. The final degree of freedom is taken by the gas flow, which will be determined by the same economic arguments as the liquid flow in absorption. The gas flow fixes the outlet liquid composition by an overall material balance:

$$\mathcal{N}^{(L)}(x^{(1)} - x^{(Ns+1)}) = \mathcal{N}^{(V)}(y^{(0)} - y^{(Ns)}) \quad \text{or} \quad (7.19)$$

$$y^{(Ns)} = y^{(0)} + \frac{\mathcal{N}^{(L)}}{\mathcal{N}^{(V)}}(x^{(Ns+1)} - x^{(1)}) \quad (7.20)$$

The inlet and outlet conditions can be conveniently used to plot the operating line. Given any single gas phase composition, the remaining gas phase compositions as well as the liquid compositions on all of the stages may be determined (see Figure 7.17).

The discussion has again been in the mole fraction frame but can be cast directly in the mole ratio frame, which is necessary for the case of relatively large mass transfer rates. We have a graphical technique to solve the stripping problem for a specified gas flow. It is clear from the construction method that, like the liquid flow in gas absorption, many input gas flows will provide the required liquid purity. The question about which to choose is therefore not a technical problem for the most part. The choice is again an economic problem. Without the specification of the gas flow, we may still draw the equilibrium curve, locate the bottom of the tower, and define the line through the inlet liquid composition on which the outlet gas composition must fall (refer to Figure 7.18).

To find the minimum gas flow, begin with a very large value where the slope is near zero and decrease the flow progressively until any part of the operating line touches the equilibrium curve. This may occur before the inlet flow is reached, which is shown in Figure 7.18. During the progression, the operating line becomes closer to the equilibrium

Stage stepping:

Starting at the top of the column, a horizontal line from $x^{(Ns+1)}$ on the operating line where the associated interstage composition is $y^{(Ns)}$ to the equilibrium curve. The value of $x^{(Ns)}$ is obtained from the equilibrium curve. The step represents stage N_s . The stepwise descent along the operating line is continued with the last step ending precisely on the operating line at the outlet liquid composition.

curve so the number of stages increases and approaches an infinitely large number as the pinch point is approached. The minimum solvent flow is therefore determined by

$$\mathcal{N}^{(v)} = \mathcal{N}^{(l)} \frac{x^{(Ns+1)} - x^{(1)}}{y^{(Ns)} - y^{(0)}} \quad (7.21)$$

where

$$y^{(Ns)} = f(T, P, x^{(Ns+1)}) = \text{equilibrium function} \quad (7.22)$$

There is an interplay between the gas solvent flow and the number of stages that gives rise to an optimum gas flow rate. There is an operating cost associated with the gas flow that reflects recirculation cost and a depreciated investment cost associated with the number of stages or the column. The situation is analogous to the optimum liquid flow in absorption. Again, the optimum is found under constant economic conditions to be nearly proportional to the minimum flow.

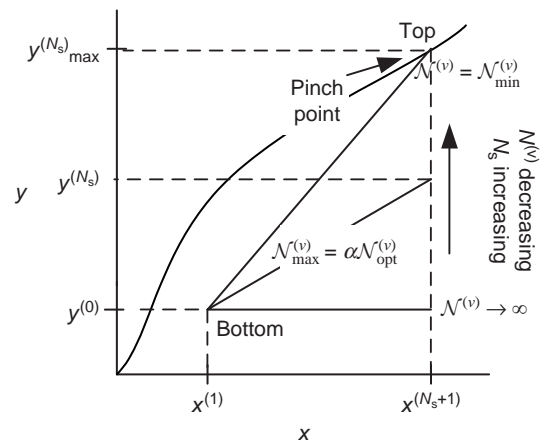


FIGURE 7.18 Effect of gas flow on the operating line.

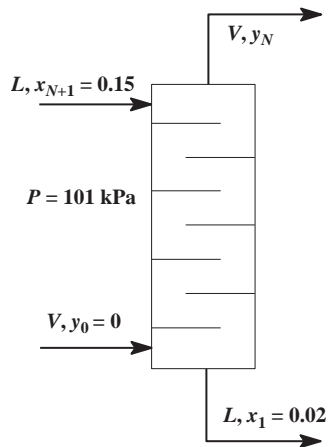


FIGURE 7.19 Stripping of acetone from water.

Example 7.1.4-1: Stripping of Acetone from Water

A water stream containing 15 mol% acetone is to be stripped to an acetone content of 2 mol% using a pure air stream (see Figure 7.19). Countercurrent contact in a perforated tray tower at 101 kPa will be employed. Air may be considered insoluble and water may be assumed nonvolatile. Assuming constant liquid and gas rates, determine the

- minimum gas flow per unit of liquid feed
- number of stages required

Equilibrium data:

x	y
0.033	0.03959
0.072	0.08288
0.117	0.11271
0.171	0.13594

where

x = mole fraction acetone in water

y = mole fraction acetone in air

Solution:

- Draw an equilibrium curve with mole fractions. Locate the inlet gas point (0.02,0). Draw the line from the inlet gas point to the vertical line through the inlet liquid mole fraction (0.15). Increase the slope until the line touches the equilibrium curve (refer to Figure 7.20).

This occurs at $y = 0.128$. The maximum slope is therefore

$$\left(\frac{\mathcal{N}^{(l)}}{\mathcal{N}^{(v)}} \right)_{\max} = \frac{0.128 - 0}{0.15 - 0.02} = 0.98462$$

or the minimum moles of gas per mole of liquid

$$\left(\frac{\mathcal{N}^{(v)}}{\mathcal{N}^{(l)}} \right)_{\min} = \frac{1}{0.98462} = 1.0156$$

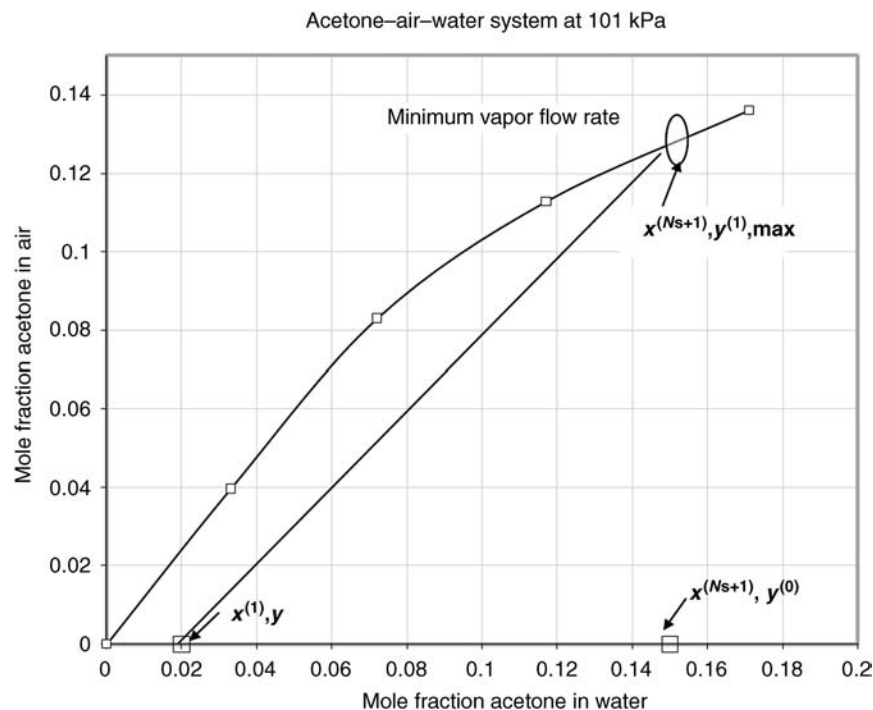


FIGURE 7.20 Minimum gas flow for acetone stripping.

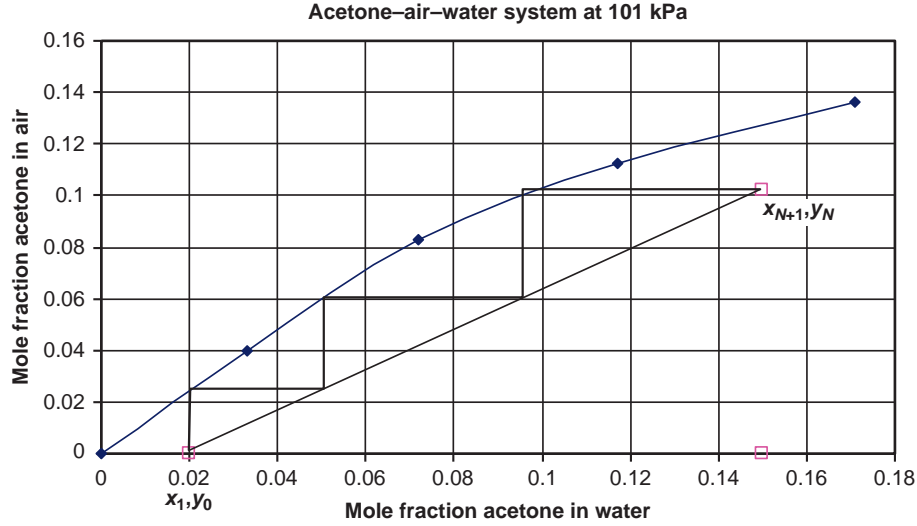


FIGURE 7.21 Graphical solution to the acetone stripping problem.

The actual gas rate must of course be smaller. We will assume an economic factor of 1.25 (see Figure 7.21).

Plot operating line and step off the stages.

The number of equilibrium stages is seen to be three.

7.1.5 Dilute Multicomponent Absorption and Stripping

In the case of multicomponent systems, it is often necessary to use a detailed model of the unit in order to properly account for the variation in the individual flows. If, however, the system is sufficiently dilute in the soluble or volatile compounds that the total liquid and vapor flows remain close to their inlet values and the distribution coefficient for each species is constant, the group method devised by Kremser can be used. The method may also be used effectively for providing the starting values in a rigorous iterative procedure.

In the following calculations, we will follow an individual component and use the notation illustrated in Figure 7.8. Since the subscript, j , will appear on every element, we do not need to carry it through the calculations. However, we will do so in order that this fact is clear.

Mass balance on a single tray see Equation (7.3):

$$\mathcal{N}_j^{(v_{n-1})} + \mathcal{N}_j^{(l_{n+1})} = \mathcal{N}_j^{(l_n)} + \mathcal{N}_j^{(v_n)} \quad (7.23)$$

Assuming that the individual ratios of the component flows leaving each stage are constant, as well as the equilibrium distribution coefficient.

$$A_j = \mathcal{N}_j^{(l_n)} / \mathcal{N}_j^{(v_n)} = \mathcal{N}_j^{(l_1)} / [K_j \mathcal{N}_j^{(v_1)}] \quad (7.24)$$

The change in the vapor rates across the trays may be written in the following recursive format obtained by eliminating the

liquid flows from the mass balance given in Equation (7.23)

$$\mathcal{N}_j^{(v_n)} \mathcal{N}_j^{(v_{n-1})} = \mathcal{N}_j^{(l_{n+1})} - \mathcal{N}_j^{(l_n)} = A_j (\mathcal{N}_j^{(v_{n+1})} - \mathcal{N}_j^{(v_n)}) \quad (7.25)$$

The change in the vapor rate over the column is

$$\begin{aligned} \mathcal{N}_j^{(v_{N_s})} - \mathcal{N}_j^{(v_0)} &= [\mathcal{N}_j^{(v_{N_s})} - \mathcal{N}_j^{(v_{N_s-1})}] \\ &+ [\mathcal{N}_j^{(v_{N_s-1})} - \mathcal{N}_j^{(v_{N_s-2})}] + \dots + [\mathcal{N}_j^{(v_1)} - \mathcal{N}_j^{(v_0)}] \end{aligned} \quad (7.26)$$

$$= [A_j^{N_s-1} + A_j^{N_s-2} \dots + A_j] [\mathcal{N}_j^{(v_{N_s})} - \mathcal{N}_j^{(v_{N_s-1})}] \quad (7.27)$$

$$\frac{\mathcal{N}_j^{(v_{N_s})} - \mathcal{N}_j^{(v_0)}}{\mathcal{N}_j^{(v_{N_s})} - \mathcal{N}_j^{(v_{N_s-1})}} = \left[\frac{A_j^{N_s} - 1}{A_j - 1} \right] \quad \text{where } \mathcal{N}_j^{(l_0)} \equiv A_j \mathcal{N}_j^{(v_0)} \quad (7.28)$$

Substitution of the fraction not absorbed,

$$\varphi_{na,j} = \left[\frac{\mathcal{N}_j^{(v_{N_s})}}{\mathcal{N}_j^{(v_0)}} \right] \quad (7.29)$$

and noting that from the mass balance on the top tray

$$\mathcal{N}_j^{(v_{N_s-1})} = \mathcal{N}_j^{(v_{N_s})} (1 + A) - \mathcal{N}_j^{(l_{N_s+1})} \quad (7.30)$$

give

$$\varphi_{na,j} = \left[\frac{A_j - 1}{A_j^{N_s+1} - 1} \right] + \frac{\mathcal{N}_j^{(l_{N_s+1})}}{A_j \mathcal{N}_j^{(v_0)}} \left[\frac{A_j^{N_s+1} - A_j}{A_j^{N_s+1} - 1} \right] \quad (7.31)$$

In place of $\varphi_{na,j}$, we could solve for the fraction not stripped,

$$\varphi_{ns,j} = \left[\frac{\mathcal{N}_j^{(l_1)}}{\mathcal{N}_j^{(l_{N_s+1})}} \right] \quad (7.32)$$

In terms of the stripping factor

$$S_j = A_j^{-1} = \mathcal{N}_j^{(v_n)} / \mathcal{N}_j^{(l_n)} = [K_j \mathcal{N}^{(v_n)}] / \mathcal{N}^{(l_n)} \quad (7.33)$$

the result is

$$\varphi_{ns,j} = \left[\frac{S_j - 1}{S_j^{N_s+1} - 1} \right] + \frac{\mathcal{N}_j^{(v_0)}}{S_j \mathcal{N}_j^{(l_{N_s+1})}} \left[\frac{S_j - S_j^{N_s+1}}{1 - S_j^{N_s+1}} \right] \quad (7.34)$$

In the application of these results to absorption, we assume that the inlet liquid and gas flows are known for each component as well as the number of trays and the operating temperature and pressure. The calculations may be carried out as follows:

1. Evaluate A or S for each component using inlet/outlet flows for the vapor and liquid rates. Evaluate A for those components that for the most part enter in the gas phase. Evaluate S for those components that for the most part enter in the liquid phase. It may be necessary to iterate on these values, since it will normally not be possible to use the values for the same tray at the beginning. Experience indicates that the values of A and S should be in the range of 1.25–2.00 with 1.4 being a good target.
2. Determine the fraction not absorbed or not stripped for each species and use the results to calculate outlet flows for each component.
3. Add the results to determine outlet flows and compositions.
4. Repeat the calculations if the calculation of A and S with new flow rates gives significantly different results.

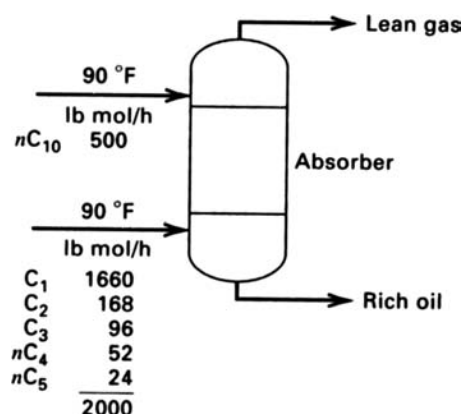


FIGURE 7.22 Tower for methane purification.

Example 7.1.5-1: Methane Purification (Seader and Henley, 2006)

Determine by the Kremser method the separation that can be achieved for the absorption operation indicated in Figure 7.22 for the following combinations of conditions:

- (a) Six equilibrium stages and 75 psia operating pressure,
- (b) Three equilibrium stages and 150 psia operating pressure,
- (c) Six equilibrium stages and 150 psia operating pressure.

At 90 °F and 75 psia, the K -value of $n\text{-C}_{10}\text{H}_{22} = 0.0011$
 K -values from Figure 2.8

Species	75 psia	150 psia
		in C7 to C12
1	41.0000	18.5000
2	7.5000	3.6000
3	2.3000	1.0500
4	0.6600	0.3200
5	0.2100	0.1000
10	0.0011	given

$P=75$ psia,
 $N_s=6$

0.9306

Values obtained using calculated flows...compare with values used to calculate the flows at left.

Species	$\mathcal{N}^{(v_0)}$	$\mathcal{N}^{(l_0)}$	S	A	φ_{na}	φ_{ns}	$\mathcal{N}^{(v_{N_s})}$	$\mathcal{N}^{(l_{N_s})}$	$1\varphi_{ns}$	$1\varphi_{ns}$	S	A
1	0.0000	1660.0000		0.0061	0.9939		1649.8780	10.1220	0.0061			0.006305
2	0.0000	168.0000		0.0333	0.9667		162.4000	5.6000	0.0333			0.034466
3	0.0000	96.0000		0.1087	0.8913		85.5652	10.4348	0.1087			0.112388
4	0.0000	52.0000		0.3788	0.6219		32.3392	19.6608	0.3781			0.391654
5	0.0000	24.0000		1.1905	0.0797		1.9137	22.0863	0.9203			1.230914

10	500.0000	0.0000	0.0044	0.9956	2.2000	497.8000	0.0044	0.003889
	500.0000	2000.0000			1934.2962	565.7038		

P=150 psia,
N=3

Species	$\mathcal{N}^{(l_{N+1})}$	$\mathcal{N}^{(v_0)}$	S	A	φ_{na}	φ_{ns}	$\mathcal{N}^{(v_{N_1})}$	$\mathcal{N}^{(l_1)}$	$1-i\varphi_{ns}$	$1-i\varphi_{ns}$
1	0.0000	1660.0000		0.0135	0.9865		1637.5676	22.4324	0.0135	
2	0.0000	168.0000		0.0694	0.9306		156.3370	11.6630	0.0694	
3	0.0000	96.0000		0.2381	0.7644		73.3787	22.6213	0.2356	
4	0.0000	52.0000		0.7813	0.3486		18.1283	33.8717	0.6514	
5	0.0000	24.0000		2.5000	0.0394		0.9458	23.0542	0.9606	
10	500.0000	0.0000	0.0022			0.9978	1.1000	498.9000		0.0022
	500.0000	2000.0000					1887.4574	612.5426		

P=150 psia,
N=6

Species	$\mathcal{N}^{(l_{N+1})}$	$\mathcal{N}^{(v_0)}$	S	A	φ_{na}	φ_{ns}	$\mathcal{N}^{(v_{N_1})}$	$\mathcal{N}^{(l_1)}$	$i\varphi_{ns}$	$i\varphi_{ns}$
1	0.0000	1660.0000		0.0135	0.9865		1637.5676	22.4324	0.0135	
2	0.0000	168.0000		0.0694	0.9306		156.3333	11.6667	0.0694	
3	0.0000	96.0000		0.2381	0.7619		73.1460	22.8540	0.2381	
4	0.0000	52.0000		0.7813	0.2660		13.8321	38.1679	0.7340	
5	0.0000	24.0000		2.5000	0.0025		0.0591	23.9409	0.9975	
10	500.0000	0.0000	0.0022			0.9978	1.1000	498.9000		0.0022
	500.0000	2000.0000					1882.0381	617.9619		

7.1.6 Column Efficiency

We have assumed that the output streams for each stage are in equilibrium. This means that the residence time and mixing on the stage is sufficient for the interphase mass transfer rate in all of the fluid elements to provide the required material transfer. This may not be the case in practice and there are a number of ways that we can account for this.

Consider the material balance around a single stage and the fact that it must be satisfied whether or not equilibrium is achieved at the outlet. The balance represented graphically in Figure 7.23 is a straight line that passes through the inlet stream compositions, $(x^{(l_{n+1})}, y^{(v_{n-1})})$ at the outlet.

For an equilibrium stage, the outlet compositions must also fall on the equilibrium curve, which is denoted by y^* on the figure. If equilibrium is not achieved, then the outlet compositions will fall short of the equilibrium curve and the

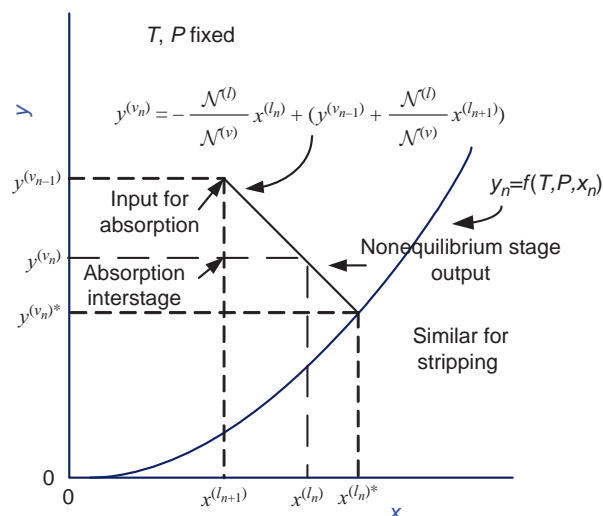


FIGURE 7.23 Molar balance for the stage showing inefficiencies.

efficiency defined below will be less than one:

$$E_{MV} = \frac{y^{(v_{n+1})} - y^{(v_n)}}{y^{(v_{n+1})} - y^{(v_n)*}} \quad (7.35)$$

This is called the Murphree vapor-phase efficiency. A similar approach will clearly result in the analogous Murphree liquid-phase efficiency. If these values were known *a priori*, the equilibrium curve could be shifted in the appropriate direction to give a pseudoequilibrium curve that would be used in the same way as the equilibrium stage analysis uses the true equilibrium curve for determining the number of stages. We will discuss the local efficiency after we have developed a broader base in mass transfer theory. Another definition of efficiency very often employed is the overall efficiency defined by

$$E_0 = \frac{N_s}{N_{s,\text{actual}}} \quad (7.36)$$

that is, the total number of equilibrium stages divided by the actual number of stages. Its value is available for a wide range of operating conditions in the O'Connell correlation (1946) shown graphically in Figure 7.24. A correlation for Figure 7.24 is given in Seider and Henley (2006).

$$\log E_0 = 1.987 - 0.199 \log \left[\frac{K_\alpha M_\alpha \eta_L}{\rho_L} \right] - 0.0896 \left\{ \log \left[\frac{K_\alpha M_\alpha \eta_L}{\rho_L} \right] \right\}^2 \quad (7.37)$$

7.1.7 Column Diameter and Height

The spacing between trays must be sufficient to limit entrainment and carry over from the tray below. However,

the spacing is commonly set on the basis of accessibility for servicing. This requires 20–24 in. The tower height required for the trays can be set on this basis for atmospheric and high-pressure operation but 30 in. should be allowed for vacuum operation (Silla, 2003). Approximately 4 ft should be allowed above the top tray for vapor disengagement (see heuristics) and 6 ft at the bottom for gas inlet nozzles.

The tower diameter is based on flooding considerations where the transfer of momentum to the falling liquid must be sufficiently below the point where the liquid drops are suspended in the rising gas. The calculation of column diameter on this basis is considered in Chapter 13. A not unrelated approximation is based on tray efficiency (see the next section). The linear gas velocity obtained from

$$F_G = u_G(\text{ft/s}) \sqrt{\rho_G(\text{lb/ft}^3)} \quad (7.38)$$

provides maximum tray efficiencies with values of F_G between 0.75 and 1.0 (Couper et al., 2005). The density of the gas is denoted by ρ_G .

Example 7.1.7-1: Tower 303: Off-Gas Absorber in Acrylic Acid Process

The exit stream from the acrylic acid reactor is rapidly quenched to prevent deeper oxidation to side products. The product stream is subsequently contacted in T-303 with an aqueous solvent to separate the acid solution from the light gases. The situation is depicted in the diagram. The problem is to determine the solvent rate, the number of stages, and an estimate of the column diameter to remove

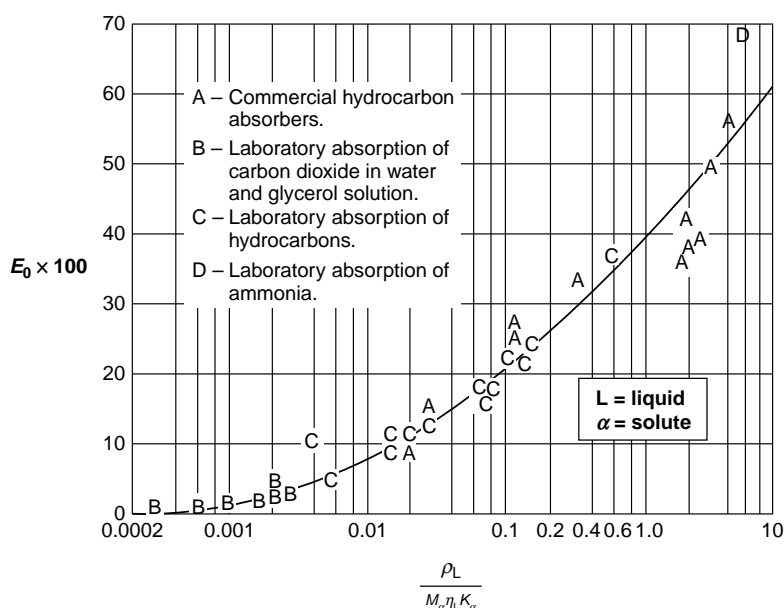


FIGURE 7.24 Overall efficiency for absorbers. Reprinted with permission of McGraw-Hill.

the light gases and retain the acids in the exit solvent stream (see Figure 7.25).

The infinite dilution activity coefficients for acetic and acrylic acid are 2.8256 and 4.2563, respectively. These values were obtained from Aspen Plus using the UNIQUAC model with UNIFAC estimation.

The stream temperatures are considerably different so that a nonisothermal analysis may be considered. We will assume isothermal conditions at 30 °C for illustration. The solvent rate may be fixed in order to obtain an absorption factor of 1.4 for acetic acid and then adjusting the number of stages to obtain the desired separation.

Species	Vapor Pressure at 30 °C	Units	Source	Ideal K	Activity Coefficient at Infinite Dilution
Water	0.6165	psia	Perrys Green and Maloney,1997	0.021247	
Acetic	0.3982	psia	Perrys Green and Maloney,1997	0.013724	2.8256
Acrylic	0.1006	psis	Yaws,2003	0.003467	4.7563

Species	1/Henry's Constant at 30 °C	Units	Source	K
Propylene	8.83939E-05	mole fract/atm	Table 6.2.1.3-1	5731.449
Nitrogen	0.000011	mole fract/atm	Fig. 6-17	46056.82
Oxygen	0.000021	mole fract/atm	Fig. 6-17	24125
Carbon dioxide	0.00053	mole fract/atm	Fig. 6-17	955.8962

Equilibrium stages=	9.5	Efficiency =	62.6333%
Actual stages =	15.16765047		

K	$N^{(L_{N+1})}$	$N^{(V_0)}$	A	Fraction not Absorbed	Outlet Gas Flows	New A	New Fraction not Absorbed	New Outlet Flows, $N^{(V_{N+1})}$	New A	Outlet Liquid Flow $N^{(L_1)}$	
Propylene	5731.4		14.7	9.29E-06	0.999991	14.69986	1.029E-05	0.99999	14.699849	9.457E-06	0.0002
Nitrogen	46056.81818		1056.7	1.16E-06	0.999999	1056.699	1.28E-06	0.999999	1056.6986	1.177E-06	0.0014
Oxygen	24125		51.9	2.21E-06	0.999998	51.89989	2.445E-06	0.999998	51.899873	2.247E-06	0.0001
Carbon dioxide	955.8962264		60.5	5.57E-05	0.999944	60.49663	6.17E-05	0.999938	60.496267	5.67E-05	0.0037
Water	0.021247232	71.5	150.1	2.504797	0.190254	28.55712	2.7756634	0.902042	135.39648	2.5508947	86.2035
Acetic	0.038776254		1.61	1.372489	0.013906	0.022388	1.5209093	0.006457	0.0103957	1.3977485	1.5996
Acrylic	0.016490602		7.97	3.227293	1.01E-05	8.06E-05	3.5762894	3.98E-06	3.173E-05	3.2866873	7.9700
Sum =		71.5	1343.48			1212.375			1319.2015		

Adjusted the inlet liquid flow and the number of stages to obtain an absorption factor of 1.4 for HAc and a loss of HAc to the vapor less than 1%. The number of stages was 9.5 with an efficiency of approximately 31.7 % or 30 stages. The heuristic efficiency is slightly less - see section 7.1.8

The simulator gives 15 stages and a water rate twice that found here. Refer to the stream tables given earlier for the acrylic acid process and compare all of the outlet flow rates continue with "Diameter based on maximizing the stage efficiency"

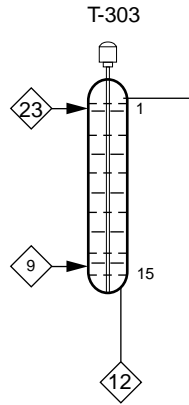


FIGURE 7.25 Tower 303 with feed rates.

The water rate is considerably underestimated at 71.5 kmol/h in comparison to 141 kmol/h (refer to stream tables). Compare the outlet streams.

The number of stages found by the simulator is 15, which compares well with the 16 found here. The stage efficiency found above, 62.6%, is higher than expected (see heuristic 1, Section 7.1.8)

Diameter based on maximizing stage efficiency:

Use conditions at the bottom of the tower since the maximum vapor rate occurs here.

14.69999931	$3 \times 12.01 + 6 \times (1.008)$	42.078
1056.7	2×14.01	28.02
51.9	2×16	32.0
$\mathcal{N}^{(V)} = 60.5$	$12.01 + 32$	$= 44.01$
150.1	$2 \times 1.008 + 16$	18.016
1.61	$2 \times 12.01 + 3 \times 1.008 + 32$	59.044
7.97	$3 \times 12.01 + 4 \times 1.008 + 32$	72.062

$$\mathcal{N}^{(V)} = \sum_{i=1}^{i=7} \mathcal{N}_{i,1}^{(V)} = 1343.5 \text{ kmol/h}, \quad M = \frac{\sum_{i=1}^{i=7} M_{i,1} \mathcal{N}_{i,1}^{(V)}}{\mathcal{N}^{(V)}} = 28.228$$

$$P = 2, \quad T = 460 + 32 + 30 \times 1.80 = 546.0$$

$$\rho_G = \frac{M_g P}{0.7302 \times T} \text{ lb/ft}^3$$

$$u_G \sqrt{\rho_G} = F_G \text{ where } u_G(A - A_d) = \frac{VM_g}{\rho_G}$$

$$D = \sqrt{\frac{4}{\pi} \frac{VM_g}{\sqrt{\frac{M_g P}{0.7302 \times T} (1 - A_d/A) F_G}}}$$

$$= \sqrt{\frac{4}{3.1416} \frac{\frac{1343.5}{3600} \frac{1000}{454} 28.228}{\sqrt{\frac{28.228 \times 2}{0.7302 \times 546} (1 - 0.1) 0.75}}}$$

Using a fractional downcomer area of 0.1 (see heuristics at end of the section)

$$D = 10.785 \text{ ft} = 10.785(12)(2.54)/100 = 3.2873 \text{ m}$$

Use this result since it is greater than the diameter based on flooding. The simulated value is 3.5 m.

The column height = $(16 - 1) 2 + 4 + 6 = 40 \text{ ft} = 12.2 \text{ m}$. The simulator result is 11 m.

Reconcile the differences and similarities between the simulator and the results found here. What would you do differently?

7.1.8 Heuristics for Absorption

(Couper et al., 2005)

1. Tray efficiencies for light hydrocarbons and aqueous solutions in absorption and stripping are in the range of 10–20%.
2. The optimum value of the Kremser–Brown absorption factor is in the range of 1.25–2.0.
3. A safety factor of 10% of the number of trays calculated by the best means is advisable.
4. Tower height: For reasons of accessibility, tray spacings are made 20–24 in.
5. Tower diameter: Peak efficiency of trays is at values of the vapor factor $F_G = u \rho_G^{1/2}$, in the range 1.0–2.0 (ft/s) $(\text{lb/ft}^3)^{1/2}$. This range of F_s establishes the diameter of the tower. Roughly, linear velocities are 2 ft/s at moderate pressures and 6 ft/s in vacuum.
6. Pressure drop per tray is of the order of 3 in. of water or 0.1 psi.
7. Sieve trays have holes 0.25–0.50 in. diameter, the hole area being 10% of the active cross section.
8. Valve trays have holes 1.5 in. diameter each provided with a liftable cap, 12–14 caps/ft² of active cross section. Valve trays usually are cheaper than sieve trays.
9. Bubble-cap trays are used only when a liquid level must be maintained at low turndown ratio; they can be designed for lower pressure drop than either sieve or valve trays.
10. Weir heights are 2 in., weir lengths about 75% of tray diameter, liquid rate a maximum of about 8 gpm/in. of weir; multipass arrangements are used at high liquid rates.
11. For towers about 3 ft in diameter, add 4 ft at the top for vapor disengagement and 6 ft at the bottom.
12. Limit the tower height to about 175 ft max because of wind load and foundation considerations. An additional criterion is that *LID* be less than 30.

7.2 DISTILLATION

We have seen that a single flash vaporization will suffice to meet a stringent separation standard when one of the components of interest has a very high relative volatility. A multistage version of flash vaporization can be applied when this relative volatility condition is not necessarily met. The multistage version is called distillation.

7.2.1 Construction of Distillation Operation

Suppose that we begin with the flash vaporization of a binary mixture of A and B, A being the most volatile (refer to Figure 7.26). The vapor stream will be called the A stream and it will be our objective to make this stream pure A. The liquid stream will be called the B stream and we will focus on making this stream pure B. Remember we are assuming that the A and the B streams are in equilibrium.

Consider first the A stream. If we add a condenser, it will be possible to condense a relatively small amount of the vapor to obtain an enriched A stream and an equilibrium liquid stream as illustrated in Figure 7.26.

We could then repeat this condensation a number of times, obtaining a richer A stream at each step of the way until we reached the required purity (or an azeotrope).

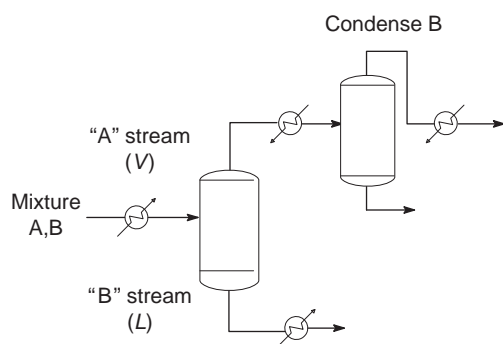


FIGURE 7.26 Purification step for A stream.

Suppose, for example, that an additional two steps will suffice as illustrated in Figure 7.27.

The situation, however, is not that bright because our A stream is diminished in quantity at each step. Also each condensation has produced a sequentially colder liquid that contains valuable product we have not accounted for. These liquid streams will be costly in terms of both capital expenditures and operating expenses. We need to take steps to improve the situation.

The liquid product from the last condensation illustrated in Figure 7.27 is colder than the overhead from the first and is richer in A than the liquid in equilibrium with the overhead vapor from the second. It makes sense from a heat transfer point of view then to increase the duty of the last condenser, remove the second condenser, and introduce the final liquid directly into the second condensation. It also makes sense from a mass transfer point of view since the recycled streams will be richer in A than required for equilibrium, resulting in a release of A to the vapor and an enrichment of the A stream. The same reasoning could be applied to the first and second condensation. The net effect is shown in Figure 7.28.

The A product can be as pure as we like by adding more condensation steps and by adjusting the duty on the last condenser. Remember that the condenser is responsible for returning cold liquid to the process, which in turn provides the enriching operation in the sequence of partial vaporizations and condensations. Note that our A product can be saturated vapor or liquid, a combination of the two, or a subcooled liquid depending on how we operate the condenser. The same ideas can be applied to the B stream with vaporizations in place of the condensations. The idea is to strip A from the liquid to obtain a pure liquid product. Try it! The result is shown in Figure 7.29.

The boiler in the last step is responsible for returning hot vapor to the operation, which in turn produces the vaporizations required to strip the A from the B product stream. The B purity can be as high as we are willing to supply the necessary number of steps. It may suffice in some cases

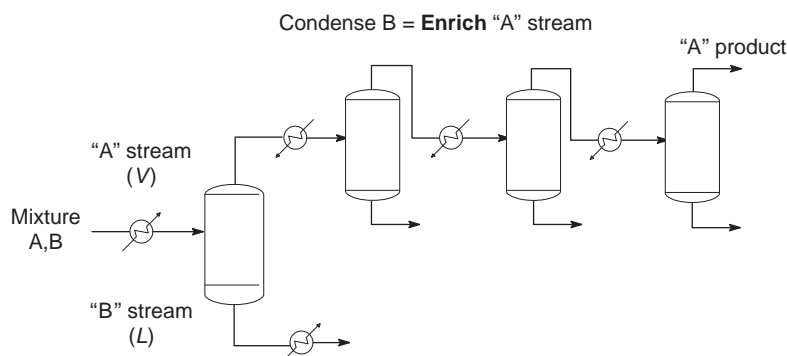


FIGURE 7.27 Multistep enrichment of A stream.

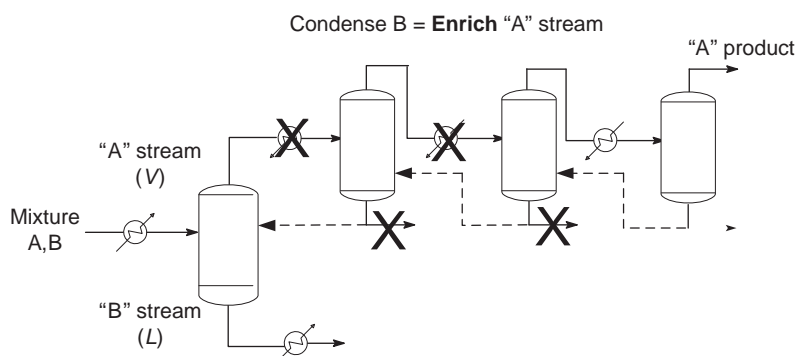


FIGURE 7.28 Energy and mass conservation using recycle (reflux).

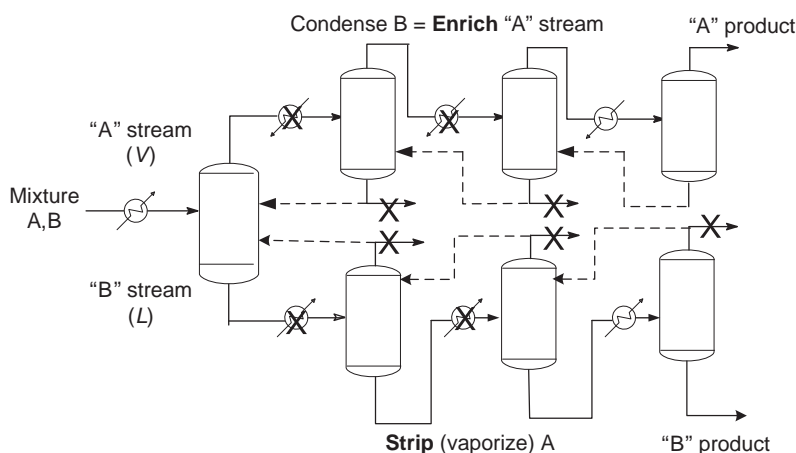


FIGURE 7.29 Stripping of the B stream with energy and mass conservation.

where only a pure B steam is desired to keep only the stripping operation and omit the enriching steps entirely.

With a sufficient number of steps, we can obtain two arbitrarily pure streams. Remember that the following:

- At each stage, we assumed that the mixing is sufficiently intense and the residence time sufficiently long for the required amount of energy and mass transfer to take place to essentially establish thermal and chemical equilibrium. This also requires that the separation of liquid and vapor is complete.
- The A stream was processed through an enriching operation focused on obtaining the more volatile component (A) in pure form. The B stream was processed through a stripping operation focused on obtaining the less volatile component (B) in pure form.
- The reflux liquid in the enriching operation is required to condense B from the A stream and carry it to the B stream.
- The boil-up vapor in the stripping section is required to strip A from the B stream and carry it to the A stream.

- The enriching and stripping sections are separated by a feed stage where a saturated feed stream is introduced.
- The temperature increases from the B product stage to the A product stage.

With the addition of pumps and compressors to move the liquid and vapor streams, the operation just described could be accomplished. However, by taking advantage of gravity, a more efficient and less costly construction can be provided to accomplish the same operations as summarized above. Note that the distillation operation can be carried out in a continuous fashion without the introduction of discrete stages.

7.2.2 Equipment for Distillation

The equipment used for contacting the gas and liquid stream in distillation is the same as the equipment used for that purpose in gas absorption and stripping shown in Figures 7.4–7.7. The vapor in those figures is the A stream and the liquid is the B stream. After providing separately for a condenser and reboiler

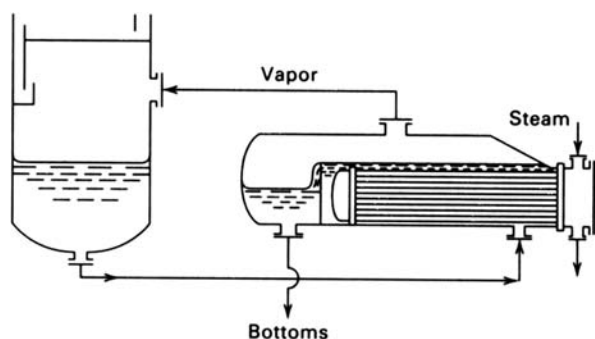


FIGURE 7.30 Kettle reboiler.

outside of the column and an opening for a feed, the arrangement provides all of the features discussed in the original construction.

A common partial reboiler (last step in stripping section) is shown in Figure 7.30.

This is a kettle reboiler that vaporizes the liquid feed and produces a vapor and bottoms stream that are in equilibrium. It is an equilibrium stage as we discussed during the construction of the stripping operations in Section 7.1.4. The modifications to a tray tower for gas absorption/stripping for distillation service are illustrated in Figure 7.31.

Note that the enriching section has been labeled as the rectifying section. The two terms are used interchangeably. Tray labels are the same. The distillate may be a saturated liquid, a saturated vapor, or a saturated two-phase mixture. We will not consider the possibility of a subcooled distillate. Multiple feeds and side stream withdrawals are common in

multicomponent systems. They are not considered here (see, for example, Kister, 1992).

The problem: The problem we want to consider for binary systems is as follows:

Given:

- Feed rate, $\mathcal{N}^{(F)}$, composition, $z^{(F)}$, and fraction liquid.
- Distillate composition $x^{(D)}$ and thermal state.
- Bottoms composition $x^{(B)}$.
- Equilibrium data and physical properties.
- Coolant temperature for the condenser.
- Thermal state of the reflux.

Determine:

- Operating pressure
- Number of stages
- Location of the feed tray
- Reflux rate
- Column height and diameter
- Pressure drop across the unit
- Condenser and reboiler loads

The solution (McCabe–Thiele analysis): We have at our disposal the balance equations for mass, energy, and momentum, and thermodynamics including physical and chemical properties. Before applying these tools, let us make a few observations of what we can expect.

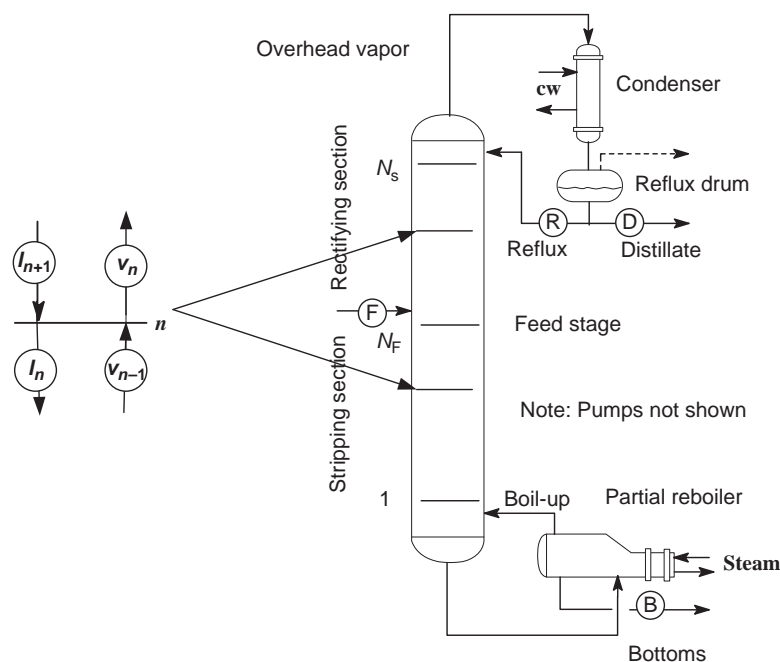


FIGURE 7.31 Distillation equipment.

the fraction liquid, q) of the saturated values. The enthalpy in the subcooled region is considered relative to the saturated liquid with a constant heat capacity. The enthalpy in the superheated region is considered similarly relative to the saturated vapor. Note the correspondence to the Txy diagram and that the graph will change numerically from the bottom to the top of the tower but the general behavior will be the same.

We assume that the enthalpies of the liquid and vapor do not change appreciably across the feed tray and again that there is no heat loss from the column. The system is defined by breaking the feed stream and the liquid and vapor streams above and below the tray. The energy and total mass balances respectively are

$$\mathcal{N}^{(F)}H_F + \mathcal{N}^{(vs)}H_V + \mathcal{N}^{(lr)}H_L = \mathcal{N}^{(ls)}H_L + \mathcal{N}^{(vr)}H_V \quad (7.43)$$

$$\mathcal{N}^{(F)} + \mathcal{N}^{(vs)} + \mathcal{N}^{(lr)} = \mathcal{N}^{(ls)} + \mathcal{N}^{(vr)} \quad (7.44)$$

If we take the changes in the vapor and liquid flows across the feed tray as the unknowns, these two independent equations give:

$$\mathcal{N}^{(vr)} = \mathcal{N}^{(vs)} + \mathcal{N}^{(F)}(1 - q^*) \quad (7.45)$$

$$\mathcal{N}^{(ls)} = \mathcal{N}^{(lr)} + q^*\mathcal{N}^{(F)} \quad (7.46)$$

where

$$q^* = \frac{H_V - H_F}{H_V - H_L} \quad (7.47)$$

The value of q^* depends on the state of the feed. The possibilities are summarized in Table 7.1.

The entry for the saturated feed indicates that the liquid and vapor portions augment the corresponding internal saturated flows. This is illustrated in Figure 7.33.

In the case of the subcooled feed, the vapor flow result with the value of q^* from the subcooled entry gives

$$[\mathcal{N}^{(vs)} - \mathcal{N}^{(vr)}]\Delta H_V = C_{PL}(T_B - T_F)\mathcal{N}^{(F)} \quad (7.48)$$

TABLE 7.1 Values of Feed Thermal Parameter

Feed Condition	Value of q^*
Subcooled liquid: $H = H_L - C_{PL}(T_B - T)$	$q^* = 1 + \frac{C_{PL}(T_B - T_F)}{\Delta H_V}$
Saturated mixture: $H_F = qH_L + (1-q)H_V$	$q^* = q$, the fraction liquid
Superheated vapor: $H_F = H_V + C_{PV}(T_F - T_D)$	$q^* = -\frac{C_{PV}(T_F - T_D)}{\Delta H_V}$

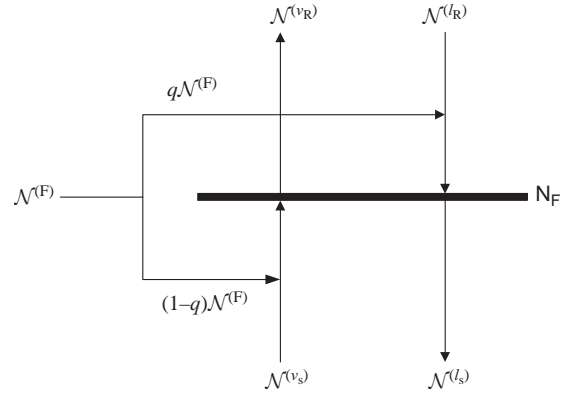


FIGURE 7.33 Stream splitting at the feed tray for saturated feed.

which indicates that sufficient vapor condenses to raise the liquid feed to its bubble point. In the last case, the superheated vapor vaporizes sufficient liquid to be cooled to its dew point.

The energy balance will be needed again for the heat duties. Before proceeding, let us check the degrees of freedom to be certain that there is sufficient information.

7.2.4 Degrees of Freedom

Unknowns:

x, y : $2(N_s + 1)$ – stages + reboiler

$x^{(D)}, D, \mathcal{N}^{(R)}, z_F, \mathcal{N}^{(F)}, q^*, \mathcal{N}^{(B)}, \mathcal{N}^{(vR)}, \mathcal{N}^{(vS)}, \mathcal{N}^{(lR)}, \mathcal{N}^{(lS)}, N_s, Q_C, Q_R$: 14

Total = $2N_s + 16$

Relations:

Equilibrium relations: $N_s + 1$

Mass balances: $N_s + 1 + 2 + 2 = \text{stages}(\text{component}) + \text{stages}(\text{total}) + \text{condenser}$

Total condenser: 1: $x^{(D)} = y^{(vNs)}$

Energy balance: 1(used) + condenser and reboiler: 3

Total = $2N_s + 10$

Degrees of freedom = 6

Specify: $\mathcal{N}^{(F)}, z^{(F)}, x^{(D)}, RR, x^{(B)}, q^*$. The reflux ratio has been specified for convenience. A method for its evaluation depends on being able to determine the solution when its value is known.

7.2.5 Material Balance for Enriching or Rectifying Section

We are entitled to write one material balance for each internal stage since the total is already satisfied. However, if we include the condenser, as indicated in the Figure 7.34, two balances may be written.

It is convenient to choose the total and the light component balances for the subsystems defined by the boundaries shown in Figure 7.34. The boundary is progressively shrunk from the stage above the feed to the top stage in the tower. The results are

$$\mathcal{N}^{(v_R)} = \mathcal{N}^{(l_R)} + \mathcal{N}^{(D)} \quad (7.49)$$

$$\mathcal{N}^{(v_R)} y^{(v_{n-1})} = \mathcal{N}^{(l_R)} x^{(l_n)} + \mathcal{N}^{(D)} x^{(D)}, \quad n = N_F + 1, \dots, N_S \quad (7.50)$$

In the last step, the boundary includes the overhead condenser, the reflux drum, and the splitter. We will assume for the time being that there is no vapor product, that is, that the condenser is a total condenser. A partial condenser will be considered shortly. In both cases, the distillate is saturated at its bubble point. In summary, the material balance for the condenser is

$$\mathcal{N}^{(v_R)} = \mathcal{N}^{(R)} + \mathcal{N}^{(D)} \quad (7.51)$$

Note that the reflux, distillate, and overhead vapor all have the same composition, a condition that is satisfied by

the preceding equation. The reflux is saturated liquid and an analysis similar to the one carried out for the feed tray will verify that the liquid flow in the enriching section is equal to the reflux rate.

$$\mathcal{N}^{(l_R)} = \mathcal{N}^{(D)} \quad (7.52)$$

Since the top streams will be nearly pure, the bubble point and dew points will be nearly equal.

Equations (7.50) to (7.52) imply that

$$y^{(v_{n-1})} = \frac{RR}{RR + 1} x^{(l_n)} + \frac{x^{(D)}}{RR + 1} \quad (7.53)$$

where the reflux ratio is defined as

$$RR = \frac{\mathcal{N}^{(R)}}{\mathcal{N}^{(D)}} \quad (7.54)$$

Equation (7.53) states that every interstage composition pair, $\{x^{(l_n)}, y^{(v_{n-1})}\}$ in the enriching section, falls on a straight line of slope $RR/(RR + 1)$ and intercept $x^{(D)}/(RR + 1)$. This is called the *enriching section operating line (EOL)*. The slope is positive and less than 1 and the line intersects the $y = x$ line at $x^{(D)}$. Furthermore, every intra-stage composition pair $\{x^{(l_n)}, y^{(v_n)}\}$ must fall on the equilibrium curve. The equilibrium curve and operating line can be plotted from the given information and the assumption that the reflux ratio is given. The result (EOL) is

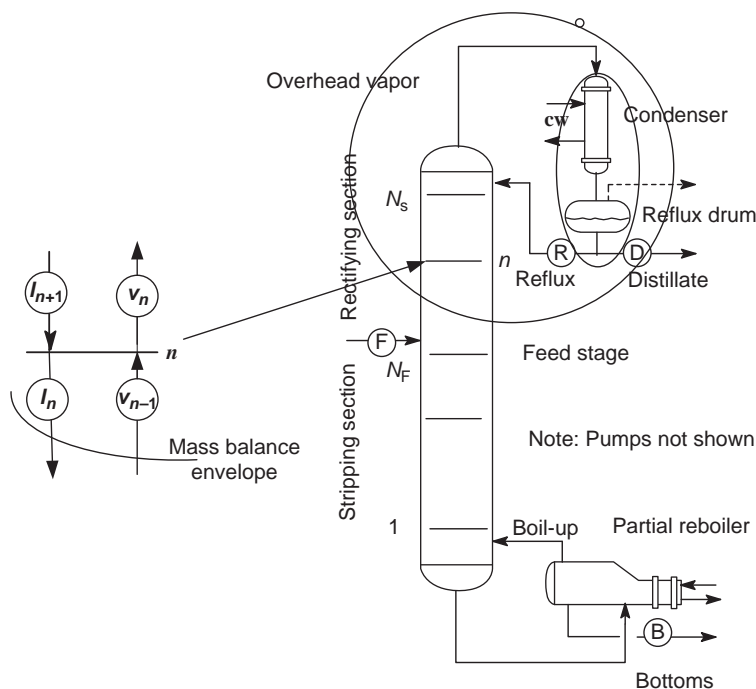


FIGURE 7.34 Material balance boundaries in the enriching section.

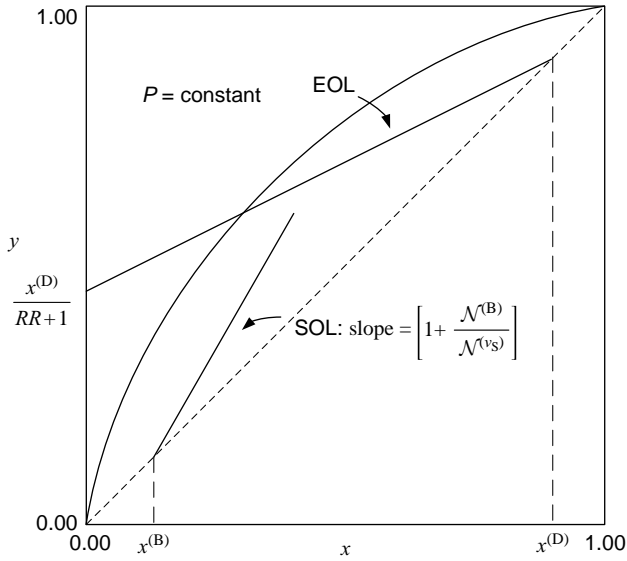


FIGURE 7.35 Operating lines for stripping and enriching sections.

illustrated in Figure 7.35 along with the analogous result for the stripping section operating line (the SOL).

7.2.6 Material Balance for Stripping Section

Similar to the enriching section, a mass transfer boundary capturing all trays below the feed tray and the reboiler can be progressively shrunk to the reboiler. A mass balance at each step yields the SOL relating the interstage compositions in that section.

$$y^{(v_n)} = \left[1 + \frac{\mathcal{N}^{(B)}}{\mathcal{N}^{(v_S)}} \right] x^{(l_{n+1})} - \frac{\mathcal{N}^{(B)}}{\mathcal{N}^{(v_S)}} x^{(B)} \quad n = 1, 2, \dots, N_{F-1} \quad (7.55)$$

The interstage compositions in the stripping section therefore fall on the straight line of slope $\left[1 + \frac{\mathcal{N}^{(B)}}{\mathcal{N}^{(v_S)}} \right]$, which intersects the $y = x$ line at $x^{(B)}$. This EOL is in Figure 7.35.

The vapor return from the reboiler is saturated and establishes the vapor rate in the stripping section. Note that the boil-up ratio (BR) is defined as $\frac{\mathcal{N}^{(v_S)}}{\mathcal{N}^{(B)}}$ and is related to the reflux ratio as follows:

$$\mathcal{N}^{(v_R)} = \mathcal{N}^{(I_R)} + \mathcal{N}^{(D)} = \mathcal{N}^{(D)}(RR + 1) \quad (7.56)$$

$$\mathcal{N}^{(v_S)} = \mathcal{N}^{(v_R)} - \mathcal{N}^{(v_F)} = \mathcal{N}^{(v_R)} - (1 - q)\mathcal{N}^{(F)} \quad (7.57)$$

$$BR = \frac{\mathcal{N}^{(v_S)}}{\mathcal{N}^{(B)}} = \frac{\mathcal{N}^{(D)}(RR + 1) - (1 - q)\mathcal{N}^{(F)}}{\mathcal{N}^{(B)}} \quad (7.58)$$

With the assumed value of the reflux ratio and the given data, the SOL may be fixed. The operating line in the stripping section may be located by the slope and intercept, but it is easier to use its intersection with the EOL.

7.2.7 Intersection of Operating Lines

The locus of intersection points may be obtained from the expression for the same point (x', y') on each operating line:

$$\mathcal{N}^{(v_R)} y' = \mathcal{N}^{(I_R)} x' + \mathcal{N}^{(D)} x^{(D)} \quad (7.59)$$

$$\mathcal{N}^{(v_S)} y' = \mathcal{N}^{(I_S)} x' - \mathcal{N}^{(B)} x^{(B)} \quad (7.60)$$

Subtracting and using the results for the changes in the internal flows from the feed tray analysis gives

$$y' = \left[\frac{q^*}{q^* - 1} \right] x' + \frac{z^{(F)}}{1 - q^*} \quad (7.61)$$

This straight line, called the q line, is the locus of possible intersections of the two operating lines. Its slope, $\left[\frac{q^*}{q^* - 1} \right]$, and intersection with the $y = x$ line, $z^{(F)}$, are known from the given conditions. Since the EOL is fixed, it in turn fixes the intersection point. Since the SOL intersection with the $y = x$ line is given, the location of this operating line is completed with the intersection point. See Figure 7.36.

The q line can be found in the region swept out by rotating it clockwise from the $y = x$ line to the $y = x$ line. These two limiting positions arise from very large negative and positive values for q^* , respectively, where the slope of the q line is

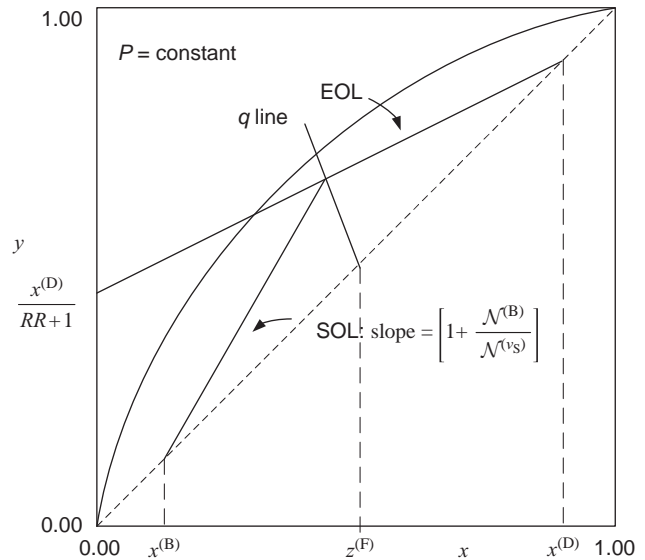


FIGURE 7.36 Intersection of operating lines—the q line.

unity. Within this region, three subregions can be identified corresponding to the values of q^* associated with the three thermal states of the feed discussed above.

Example 7.2.7-1: Operating Lines in Acetic Acid–Water Distillation

A saturated mixture of acetic acid in water flowing at 100 lb-mol/h is to be separated into two streams, one 98 mol% acid and the other 98 mol% water, by distillation. The feed is 52 mol% acid and is at 101.3 kPa. The vapor fraction of the feed is 0.63.

Locate the operating lines if the reflux ratio is 3.72.

Solution:

VLE data are available in Green and Maloney (1997).

x_{water}	y_{water}	$t^{\circ}\text{C}$
0.0000	0.0000	118.30
0.1881	0.3063	110.60
0.3084	0.4467	107.80
0.4498	0.5973	105.20
0.5195	0.6580	104.30
0.5824	0.7112	103.50
0.6750	0.7797	102.80
0.7261	0.8239	102.10
0.7951	0.8671	101.50
0.8556	0.9042	100.80
0.8787	0.9186	100.80
0.9134	0.9409	100.50
0.9578	0.9708	100.20
1.0000	1.0000	100.00

A chart was constructed in Excel consisting of the $y = x$ data for water (the more volatile component). The $y = x$

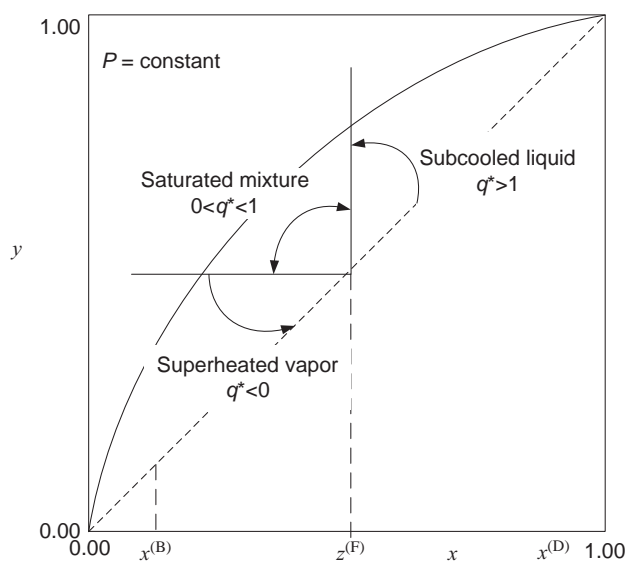


FIGURE 7.37 Feed status and the q -line location.

line containing the top and bottom compositions were plotted on the same chart, each as a new data series.

x_B :	0.0200	0.0200	Top and bottom concentrations
x_D :	0.9800	0.9800	
	0.0000	0.0000	$y = x$ line
	1.0000	1.0000	

The q line was plotted with the feed mole fraction (0.48) and q (0.37) fixed. Two points were used: the feed and a variable x with the y computed from Equation (7.61). The plot was extended beyond the equilibrium line by visually observing the results (see Figures 7.37 and 7.38).

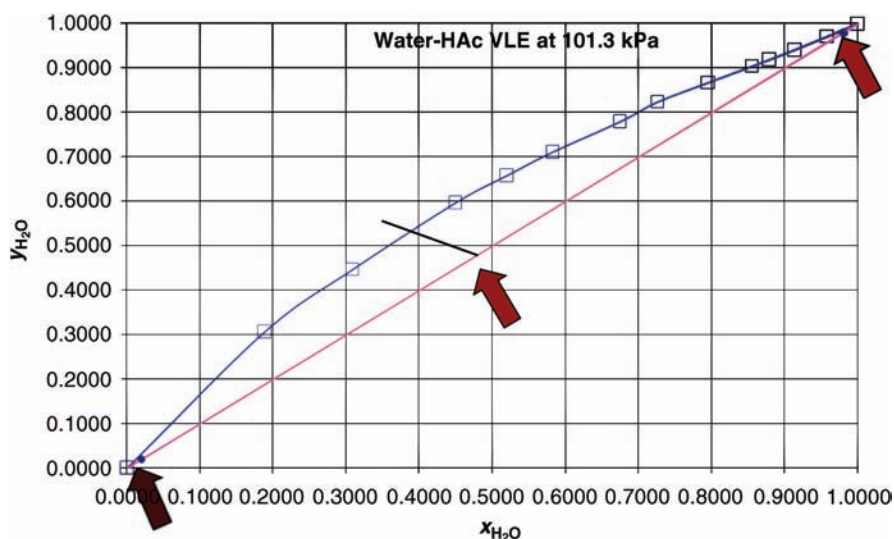


FIGURE 7.38 Location of the feed and bottoms product.

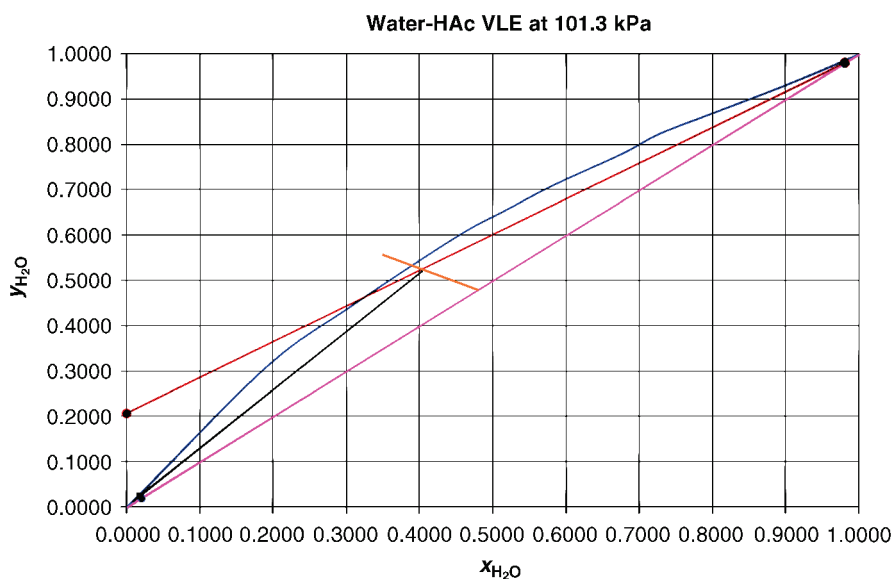


FIGURE 7.39 Location of EOL.

	0.3700	0.4800	q line
z :	0.4800	0.4800	
	0.3500	0.5563	

The EOL was also drawn as a new series with two points: the distillate on the 45° line and the y intercept calculated from Equation (7.2.5-5) (see Figure 7.39).

$RR =$	3.7200		EOL at actual reflux
	0.9800	0.9800	
	0.0000	0.2076	

The SOL was drawn with the Excel drawing tool from the y intercept to the intersection of the EOL with the q line.

7.2.8 Number of Stages

We can now determine the number of stages associated with the value of the reflux ratio that is being used by applying the properties of the equilibrium data and the operating lines. We will begin at the reboiler and progress up the tower. It is equally valid to begin at the top of the column. We will consider a total condenser and leave the other configurations to the problems (refer to Figure 7.40).

A vertical line drawn from the intersection point of the SOL with the $y=x$ line, $x^{(B)}$ to the equilibrium curve gives the value of the mole fraction of the equilibrium vapor that is being returned to the column, $y^{(B)}$. This vapor and the liquid leaving tray 1 at mole fraction $x^{(t_1)}$ form an interstage composition pair that must fall on the SOL. The point and therefore $x^{(t_1)}$ are determined by a horizontal line

from the equilibrium curve found prior to the SOL. The composition of the equilibrium vapor $y^{(v_1)}$ leaving tray 1 is found by drawing a vertical line from the SOL at $x^{(t_1)}$ to the equilibrium curve. The stream compositions and flows on the first tray and reboiler are also shown in Figure 7.40.

It is possible to proceed through the stripping section in this manner.

Note that the interstage composition above each tray is determined by a horizontal line from the equilibrium curve to the SOL. If instead the horizontal line is extended to the EOL, then above the tray is the enriching section and below the tray is the stripping section. This is by definition the feed tray. The least number of trays will be obtained if the switch to the EOL is made as soon as possible since a larger step will be made.

This stepping algorithm is applied until a horizontal line can be drawn to $x^{(D)}$. This stage is the top tray in the tower with a total condenser (with no subcooling) where the distillate and reflux compositions are equal to the overhead vapor composition. It will not be a full equilibrium stage if the horizontal line did not originate on the equilibrium curve. It is necessary to begin and end on the operating lines since they represent the material balances. The equilibrium assumption may be sacrificed, but not the material balances.

The stream compositions and flows on the top tray and condenser are depicted in Figure 7.41 for this case of the total condensation of a liquid to its bubble point. In this case, the overhead vapor, the distillate, and the reflux, all have the same composition,

The last step in the tray-counting procedure above is the top tray and the condenser is counted separately.

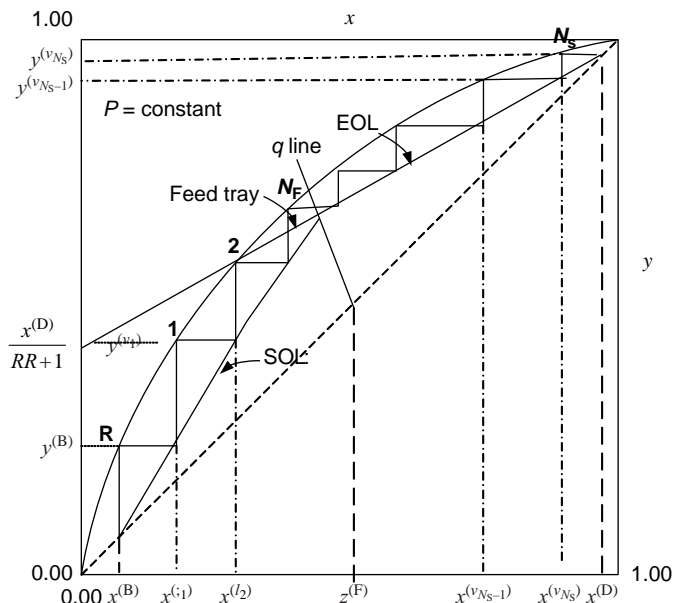
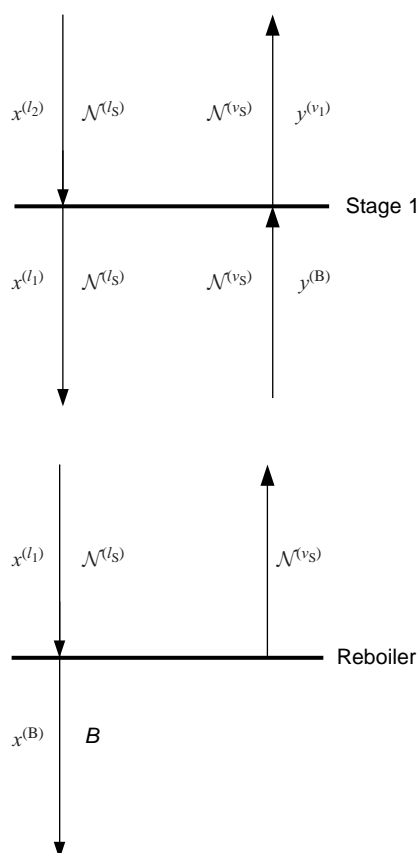


FIGURE 7.40 Stage stepping—bottom up.

The situation for a vapor distillate is somewhat different, as illustrated in Figures 7.42 and 7.43. The operating line remains the same with the vapor distillate mole fraction replacing the liquid distillate mole fraction.

The distillate and overhead vapor compositions are different and the last liquid phase mole fraction in the enriching section falling on the operating line will be the reflux composition. The projection to the equilibrium line will be the condenser.

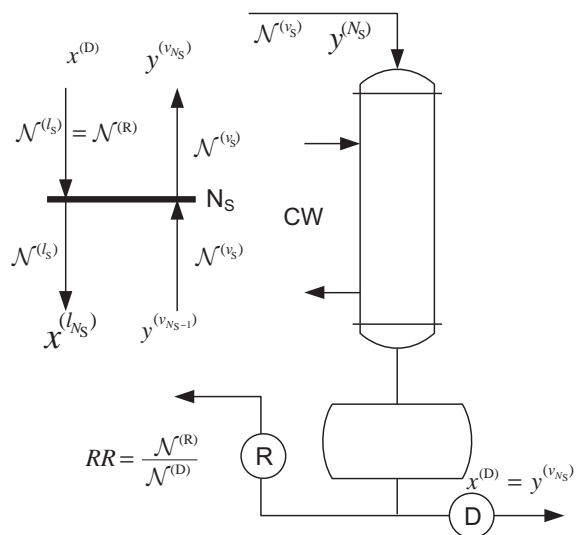


FIGURE 7.41 Flows at the top of the column for a liquid distillate.

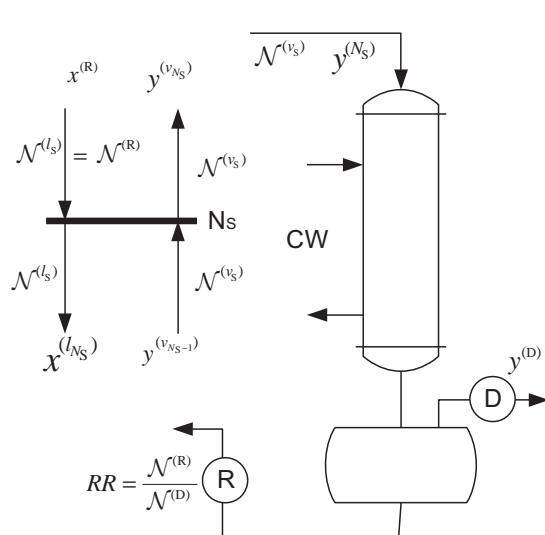


FIGURE 7.42 Flows at the top of the column for a vapor distillate.

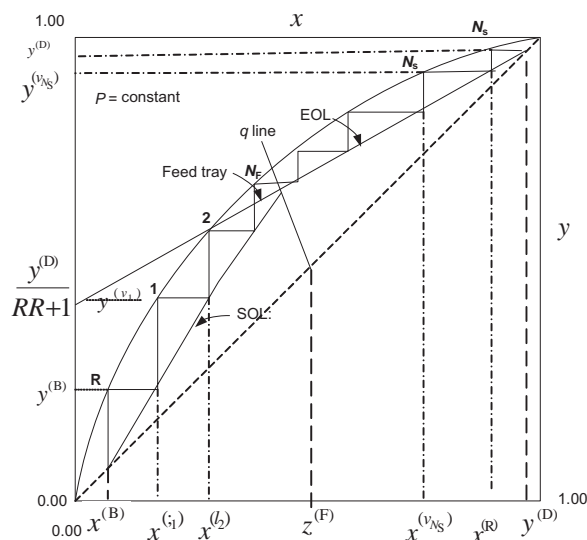


FIGURE 7.43 Steps in the enriching section for a vapor distillate.

Example 7.2.8-1: Number of Stages for Acetic Acid–Water Distillation

Use the graph prepared in Example 7.2.7-1. Use the autoshapec, lines, freeform, and zoom tool (for the narrow region at the top of the column) in Excel. (See Figure 7.44.)

The number of stages was determined to be 36 with the feed tray being tray 13. There are 12 trays in the stripping

section and 23 trays in the enriching section. The number of trays in the top of the column is less reliable because of the restricted space between the operating and equilibrium curves. See Example 7.2.9-1.

7.2.9 High Purity Products

In the case of a very high purity product, it may not be practical to visually step off the stages in the regions of the 45° line where the products are located: near $x^{(B)}$ equal to zero and $x^{(D)}$ equal to one. In these cases, a recursion relation can be used until the visual process can be resumed or initiated. We presume that the equilibrium line can be approximated until that point with a constant relative volatility but other forms could be used. The volatility should be evaluated at an average temperature over the range of conditions encountered in the calculations. A good value at the bottom of the tower is the reboiler temperature (refer to Figure 7.45). The form of the equilibrium relation is not important for this section of the tower as long as it adequately represents the data. It is more important at the top of the tower where an inverse is required.

During the process of counting stages from the bottom up, we have the point $x^{(l_n)}, y^{(v_{n-1})}$ on the operating line and we wish to locate the next point $x^{(l_{n+1})}, y^{(v_n)}$. The y -coordinate is can be calculated from the assumed equilibrium relation:

$$y^{(v_n)} = \frac{\alpha x^{(l_n)}}{1 + (\alpha - 1)x^{(l_n)}} \quad (7.62)$$

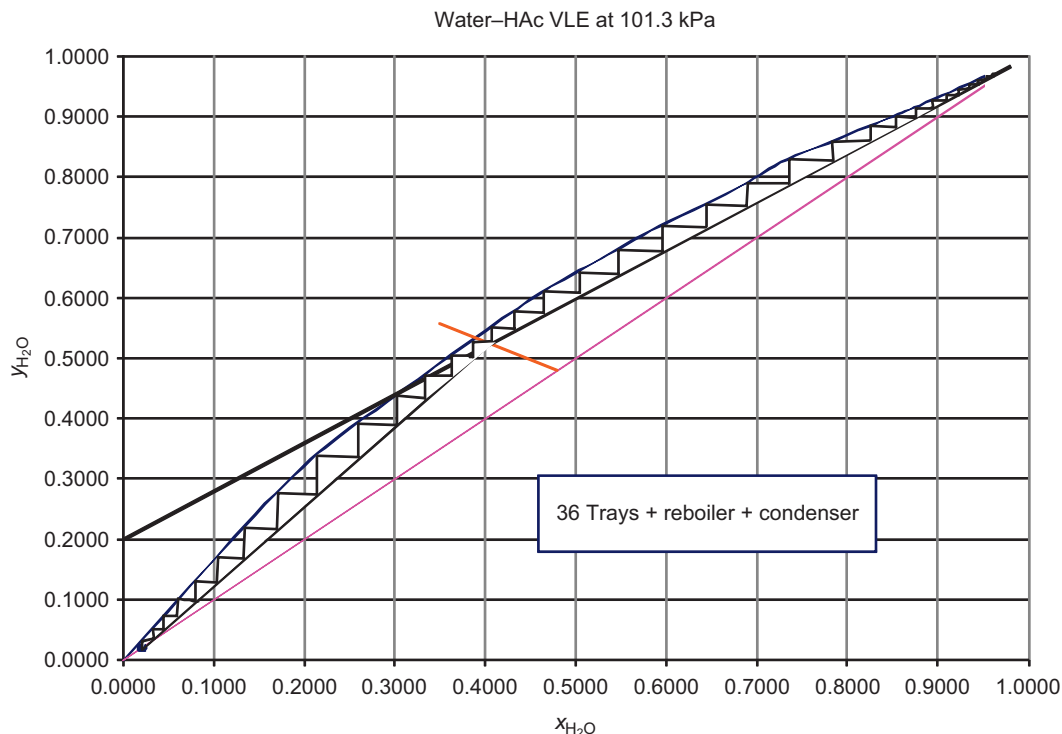


FIGURE 7.44 Water–HAc VLE at 101.3 kPa.

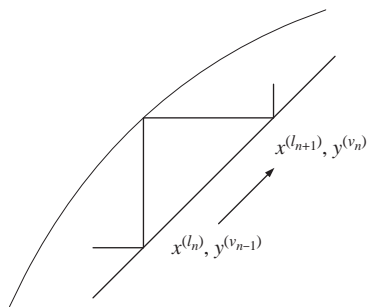


FIGURE 7.45 Stage construction from the bottom.

The associated value of the liquid phase mole fraction can be obtained from the operating line for the stripping section, Equation (7.55).

$$x^{(l_{n+1})} = \frac{y^{(v_n)} + \mathcal{N}^{(B)} x_B / \mathcal{N}^{(v_s)}}{[1 + \mathcal{N}^{(B)} / \mathcal{N}^{(v_s)}]} = \frac{y^{(v_n)} + x_B / BR}{[1 + 1/BR]} \quad (7.63)$$

The value of the boil-up ratio is given in Equation (7.58).

Given a point on the operating line, we can, with the preceding equations, locate the next point. The process is initiated by

$$x^{(l_0)} = x^{(B)} \quad (7.64)$$

$$y^{(v_{-1})} = y^{(v_0)} = x^{(B)} \quad (7.65)$$

Equations (7.64) and (7.65) start the SOL at the reboiler composition on the y - x line. This process must be stopped when the approximation for the equilibrium line fails or soon after the intersection of the operating line, before the intersection with the equilibrium curve. The graphical technique for stepping off the stages is initiated with the last calculated point on the operating line.

If starting at the top of the tower (refer to Figure 7.46), the procedure can be restated as follows. Given the point $x^{(l_{n+1})}, y^{(v_n)}$ on the enriching section operating line, determine the next point $x^{(l_n)}, y^{(v_{n-1})}$ with:

$$x^{(l_n)} = \frac{1}{(\alpha/y^{(v_n)}) - (\alpha - 1)} \quad (7.66)$$

The corresponding value of y comes from the enriching section operating line: Equation (7.2.5-5):

$$y^{(v_{n-1})} = \frac{RR}{RR + 1} x^{(l_n)} + \frac{x^{(D)}}{RR + 1} \quad (7.67)$$

The calculations are initialized with

$$x^{(l_{N_s+1})} = y^{(v_{N_s})} = x^{(D)} \quad (7.68)$$

for a total condenser. As with these calculations, this process must be terminated when the approximation for the equilibrium

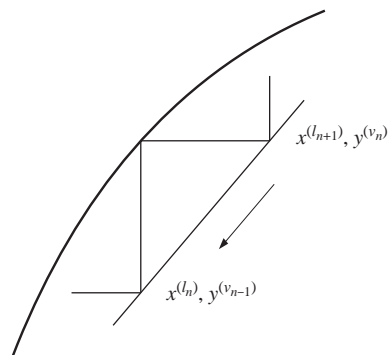


FIGURE 7.46 Stage construction from the top.

line fails or soon after the intersection of the operating line, before the intersection with the equilibrium curve.

Utilization of the recursion relations is also useful when the relative volatility is near unity over the entire operation. It is of course possible to impose different values of the volatility over concentration intervals. On the other hand, the ability to magnify in graphics software can greatly facilitate the graphical procedure (see Examples 7.2.11-1 and 7.2.11-2).

Example 7.2.9-1: Stages Required for Acetic Acid–Water Distillation Using the Recursion Relations

Determine the number of trays in the acetic acid–water distillation tower using the recursion relation in both sections of the tower.

Solution:

An overall material balance provides the distillate and bottoms flow rates:

$$\begin{aligned} 48 &= 0.02\mathcal{N}^{(B)} + 0.98\mathcal{N}^{(D)} \\ 100 &= \mathcal{N}^{(D)} + \mathcal{N}^{(B)} \\ \mathcal{N}^{(D)} &= 47.917 \text{ lb mol/h} \\ \mathcal{N}^{(B)} &= 52.083 \text{ lb mol/h} \end{aligned}$$

Value of BR from Equation (7.56) = 3.13285

Starting at the bottom of the tower, the recursion relations in Equations (7.62) and (7.63) will give the interstage compositions in the stripping section. The first is the reboiler. The feed tray has been reached when the x -coordinate of the intersection of the operating line.

The intersection is given by the solution to

$$y = \frac{3.72}{3.72 + 1} x + \frac{0.98}{3.72 + 1} \quad (7.47)$$

$$y = \frac{0.37}{0.37 - 1} x + \frac{0.48}{1 - 0.37} \quad (7.64)$$

Solution: $x = 0.40298$, $y = 0.52523$

A relative volatility of 1.8 is able to represent the equilibrium data in the stripping section:

x_{water}	Data y_{water}	$\alpha = 1.8$ y_{water}
0	0	0
0.1881	0.3063	0.294295
0.3084	0.4467	0.445264
0.4498	0.5973	0.595394

The recursion relation gives

$x^{(l_{n+1})}$	$y^{(v_n)}$	Stage
0.02	0.02	
0.031699	0.035433	REBOILER
0.047022	0.055647	1
0.066673	0.08157	2
0.091205	0.113934	3
0.120823	0.153005	4
0.155167	0.198312	5
0.19318	0.248459	6
0.233144	0.301179	7
0.272949	0.35369	8
0.310521	0.403254	9
0.344225	0.447717	10
0.373108	0.48582	11
0.396906	0.517214	12
0.415886	0.542252	Feed

This result agrees with the graphical result. However, in the more restricted region at the top of the tower, the results from the two methods are different.

The values of the relative volatility used in the enriching section are given by

x_{water}	y_{water}			
	Data	1.45	1.75	1.8
0.0000	0.0000			0
0.1881	0.3063			0.294295
0.3084	0.4467			0.445264
0.4498	0.5973			0.595394
0.5195	0.6580		0.654223	
0.5824	0.7112		0.709354	
0.6750	0.7797		0.784232	
0.7261	0.8239		0.82267	
0.7951	0.8671		0.871643	
0.8556	0.9042	0.895742		
0.8787	0.9186	0.913072		
0.9134	0.9409	0.938626		
0.9578	0.9708	0.97051		
1.0000	1.0000	1		

The recursion relation gives

$x^{(l_{n+1})}$	$y^{(v_n)}$	Stage
0.98	0.98	
0.971259	0.973111	31
0.961477	0.965401	30
0.950601	0.956829	29
0.938595	0.947368	28
0.925449	0.937006	27
0.911177	0.925758	26
0.895829	0.913662	25
0.879492	0.900786	24
0.862288	0.887227	23
0.818038	0.852352	22
0.767376	0.812423	21
0.712225	0.768957	20
0.65539	0.724163	19
0.60003	0.680532	18
0.548993	0.640308	17
0.497229	0.599511	16
0.45404	0.565473	15
0.419608	0.538335	14
0.393137	0.517472	Feed

There are 18 trays in the stripping section, a significant difference from the graphical method, and more reliable. Can you improve on the graphical solution in this case?

7.2.10 Energy Requirements

As discussed in Section 7.2.2, the application of the First Law and the total material balance to the reflux drum will complete the application of these principles to our distillation model.

7.2.10.1 Total Condenser (See Figure 7.41.)

$$\mathcal{N}^{(v_s)} H_V = \mathcal{N}^{(R)} H_L + \mathcal{N}^{(D)} H_L + Q_c \quad (7.69)$$

$$\mathcal{N}^{(v_s)} = \mathcal{N}^{(R)} + \mathcal{N}^{(D)} = (RR + 1) \mathcal{N}^{(D)} \quad (7.70)$$

$$Q_c = \mathcal{N}^{(D)} (RR + 1) \Delta H_v \quad (7.71)$$

7.2.10.2 Partial Condenser (See Figure 7.41.)

$$Q_c = \mathcal{N}^{(D)} (RR) \Delta H_v \quad (7.72)$$

7.2.10.3 Reboiler (See Figure 7.30.)

$$Q_R = (BR) B \Delta H_v \quad (7.73)$$

This energy requirement is usually fulfilled by the saturated steam utility in the plant with the lowest possible pressure (temperature). If possible, the pressure in the

column is selected so that this energy may be removed with cooling water, which is normally a relatively low-cost utility that is available in the plant. See Section 7.2.12.

Example 7.2.10.3-1: Energy Loads on the Acetic Acid Distillation Tower

Specific heats of the pure liquids in J/(kmol K)—see Green and Maloney (1997)

T in K units

1 = water

2 = HAc

$$[c] = \begin{bmatrix} 2.7637 \times 10^5 & 1.3964 \times 10^5 \\ -2.0901 \times 10^3 & -3.2080 \times 10^2 \\ 8.125 & 0.89850 \\ -1.4116 \times 10^{-2} & 0 \\ 9.3201 \times 10^{-6} & 0 \end{bmatrix}$$

$$C(k, T) = \sum_{i=1}^{i=5} c_{i,k} \times T^{i-1}$$

Latent heats of vaporization in J/kmol for pure components—see Green and Maloney (1997)

$$d = \begin{matrix} 5.2053 \times 10^7 & 2.0265 \times 10^7 \\ 0.3199 & 0.11911 \\ -0.212 & -1.3487 \\ 0.25795 & 1.4227 \end{matrix}$$

$$\lambda = 646.75 \quad 594.41$$

These are the critical temperatures in K, which are needed to calculate the reduced temperature in the expression for the latent heat:

$$\Delta(k, T) = d_{1,k} \times (1 - T/\lambda_{1,k})^{d_{2,k} + d_{3,k} \times T/\lambda_{1,k} + d_{4,k} \times (T/\lambda_{1,k})^2}$$

Condenser load

$$\Delta(k, T) = d_{1,k} \times (1 - T/\lambda_{1,k})^{d_{2,k} + d_{3,k} \times T/\lambda_{1,k} + d_{4,k} \times (T/\lambda_{1,k})^2}$$

With heats of mixing, we could formulate the enthalpy of the liquid and vapor for substitution into the condenser heat balance.

The vaporization term is the difference between the enthalpy of the distillate as a vapor at its dew point and the liquid (same composition) at its bubble point. In many cases, the distillate is nearly pure, so the bubble point and dew point are approximately equal. The sensible heat effect can be neglected in such cases and the latent heat for the pure component or an average, weighted by the mole fractions, of the two latent heats.

$$Q_c = 47.917 \times 0.454 \times (3.72 + 1) \times (0.98 \times \Delta(1, 373.16) + 0.02 \times \Delta(2, 373.16)) = 4.1535 \times 10^9 \text{ J/h}$$

$$4.1535 \times 10^9 / (4.1840 \times 252.16) = 3.9368 \times 10^6 \text{ Btu/h}$$

$$Q_c = 3,936,800 \text{ Btu/h}$$

Reboiler duty

$$\beta = (RR \times D + qF)/B - 1$$

$$\beta = (3.72 \times 47.9170 + 0.37 \times 100)/52.083 - 1 = 3.1329$$

$$Q_R = 3.1329 \times 52.083 \times 0.454 \times (0.98 \times \Delta(2, 118 + 273) + 0.02 \times \Delta(1, 118 + 273)) = 1.7917 \times 10^9 \times 252.16 = \text{Btu/h}$$

$$Q_R = 1.6757 \times 10^6 \text{ Btu/h}$$

7.2.11 Efficiency and Column Height

As discussed for gas absorption and stripping, an overall tray efficiency for fractionators may be defined. An extension of the correlation earlier for absorbers (see Section 7.1.6) is given in Figure 7.47.

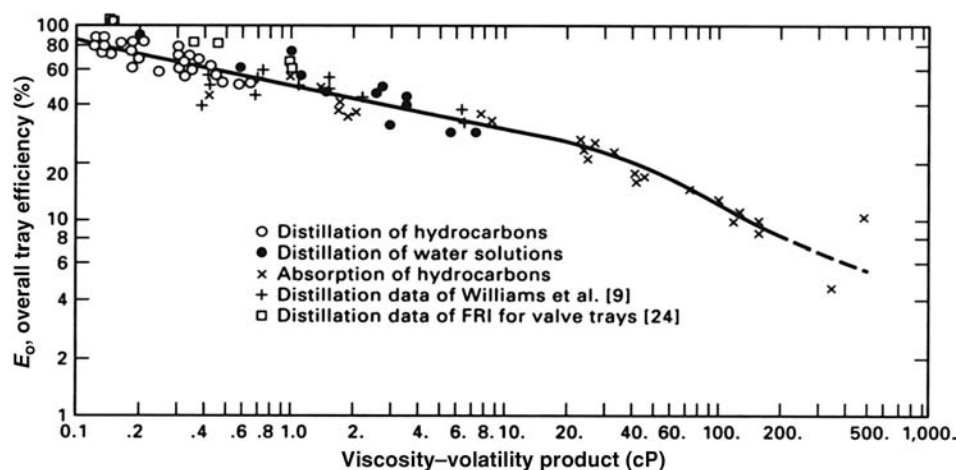


FIGURE 7.47 Overall column efficiency (Seader and Henley, 2006). Reprinted with permission of John Wiley & Sons.

The overall column efficiency is a function of the product of the average volatility and the liquid viscosity that may be determined at the feed stage conditions.

$$E_o = 50.3(\alpha\eta)^{-0.226} \quad (7.74)$$

Example 7.2.11-1: Height of Acetic Acid–Water Column

Example 7.2.7-1 are plotted in Figure 7.48 as well as the curve representing a constant relative volatility of water to acetic acid equal to 1.8. Recall that distillation may be practical with volatilities as low as 1.2.

$$\begin{aligned} \eta_{\text{H}_2\text{O}} &= 0.0265 \text{ cP at } 100^\circ\text{C} & \eta_{\text{HAc}} &= 0.465 \text{ cP at } 100^\circ\text{C} \\ \eta &= 0.98(0.0265 + 0.02(0.465)) = 0.03527 \text{ cP} \\ y_{\text{H}_2\text{O}} &E_o = 50.3(1.8 \times 0.03527)^{-0.226} = 93.791 \\ \text{Total trays} &= 31/0.93791 = 33.05 \text{ or } 34 \text{ plus} \\ &\text{a condenser and reboiler} \end{aligned}$$

Height = 68 ft for a 24 in. tray spacing + 3 ft at top for vapor disengagement and 5 ft at bottom for liquid level and reboiler return = 76 ft $L/D = 31.6$ (near 30: see Heuristics in Section 7.2.13).

Note: The reflux drum may be sized by following the procedures for flash drums (see Section 6.3).

7.2.12 Summary of Calculations and Setting Process Operating Conditions

- Specifications: We are considering the design of a new column for the separation of a given binary mixture into two defined product streams. The following variables are fixed at the outset: $\mathcal{N}^{(F)}$, $z^{(F)}$, $x^{(D)}$, $x^{(B)}$.

Set P and retrieve/compile/calculate equilibrium data. The most economical cooling medium in the plant is water. It is supplied approximately at 90°F , and is to be returned at not higher than approximately 120°F for cooling and recirculation. The column pressure is then set at the bubble-point pressure of the distillate at 120°F , which is essentially the vapor pressure of the nearly pure overhead product. If this calls for vacuum operation, the column pressure may be set at several pounds above atmospheric pressure for a base-case design. An intermediate pressure equal to the dew point of the distillate might be tried for multicomponent overhead products. Further reductions in the operating pressure can be achieved with the use of increasingly cooler heat transfer media: chilled water, chilled brine, and so on. The imposition of higher pressures results in higher reboiler temperatures, which may have a deleterious effect on the bottom product, for example, the bottom product may decompose. The maximum temperature normally found for reboilers is approximately 500°F . Furthermore, the cost of high-pressure equipment can be prohibitive.

- The value of q^* may be set at a saturation value by the designer in order to avoid extensive vaporization or condensation at the feed plate. Setting this value at a value different than the existing one in the feed means that the column must be preceded by a heat exchanger. The feed must be saturated when it enters the column or the energy required to do so must be supplied by the reboiler or condenser.

- Plot equilibrium data and the 45° line on mole fraction coordinates.
- Locate the feed, distillate, and bottoms composition on the 45° line.

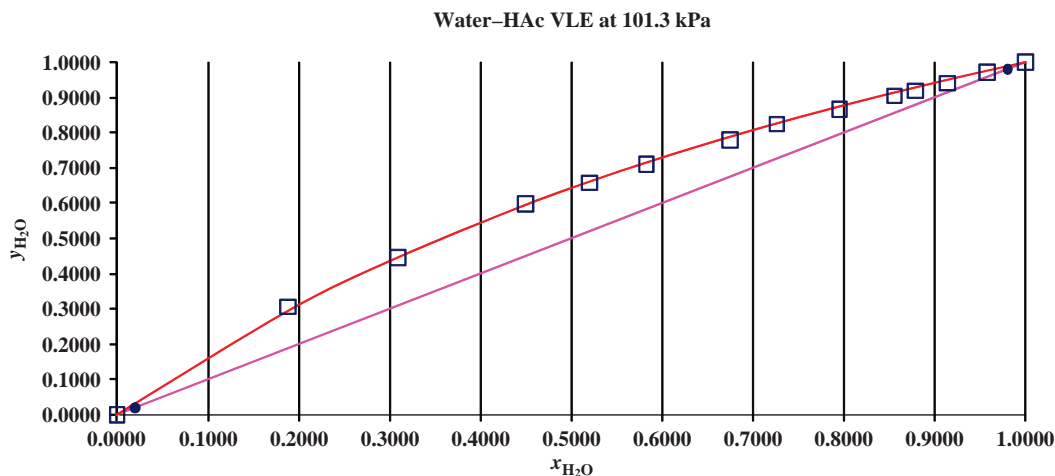


FIGURE 7.48 Representation of acetic acid–water equilibrium with a relative volatility of 1.8.

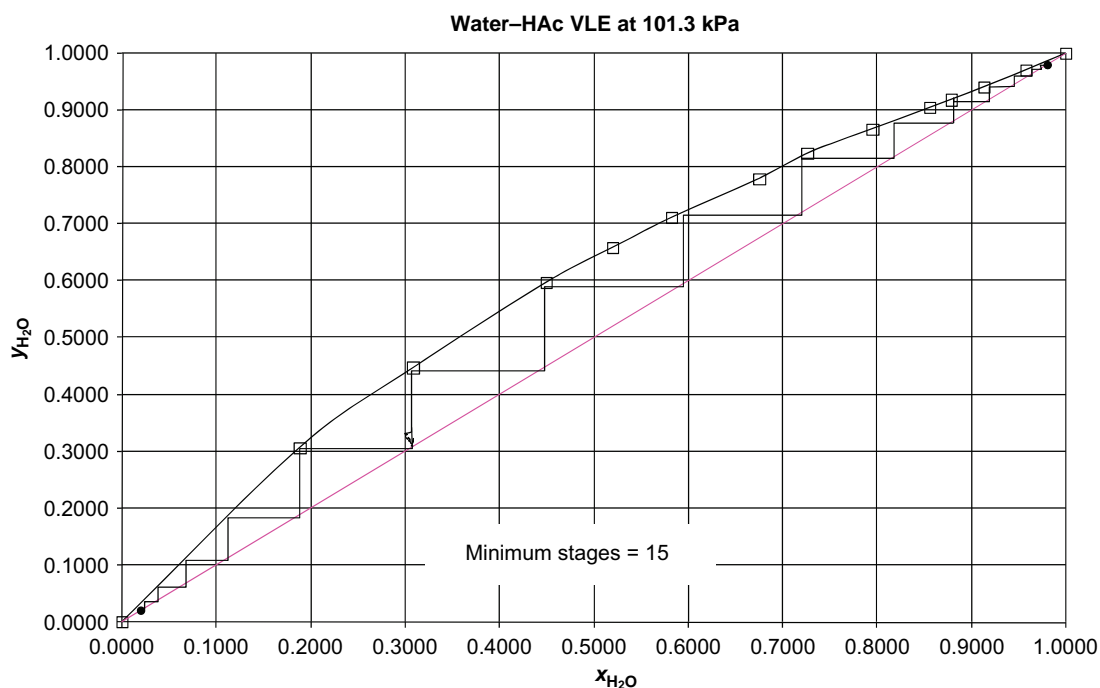


FIGURE 7.50 Minimum stage construction for water-HAc distillation.

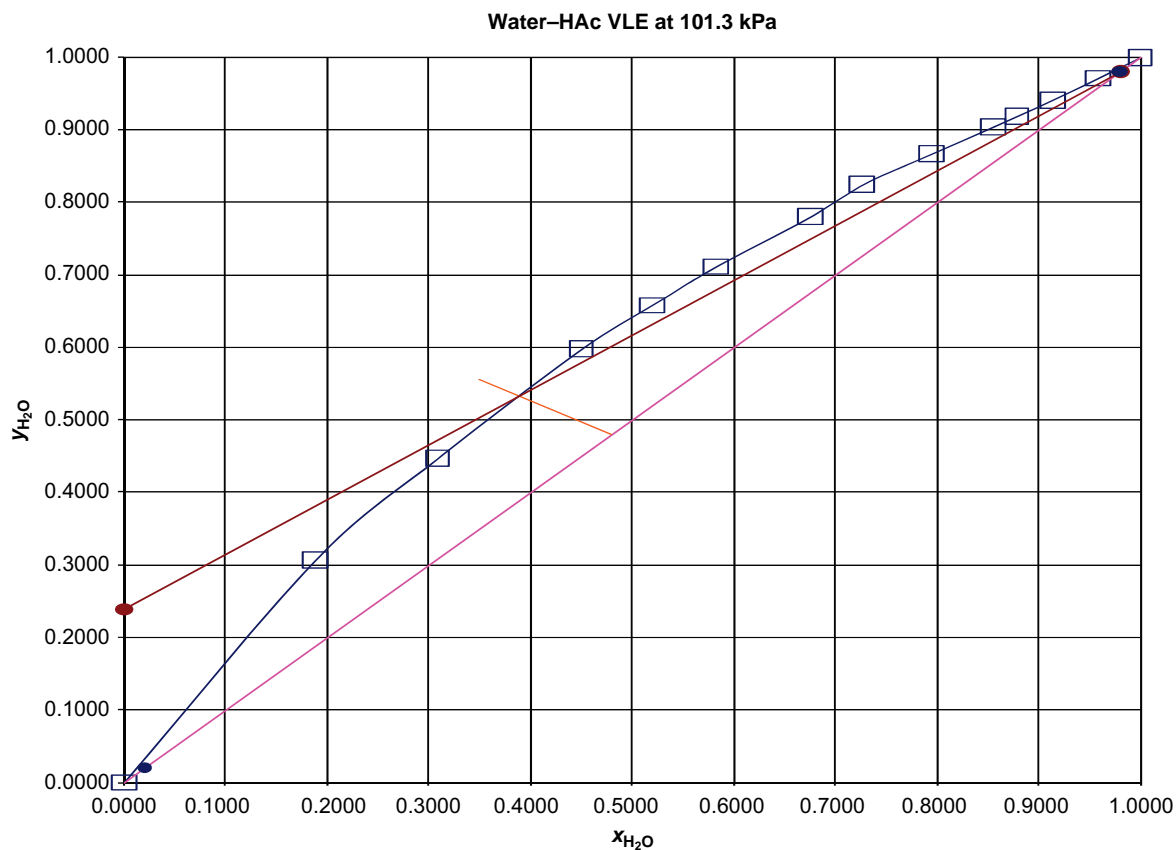


FIGURE 7.51 Determination of the minimum reflux ratio.

Using an extended grid scale in Excel, the value of the y -intercept was found to be 0.2390, so that, from Equation 7.2.5-5:

$$\frac{x^{(D)}}{RR_{\min} + 1} = 0.2390 \Rightarrow RR_{\min} = 3.1$$

This value conforms to the heuristic (see Section 7.2.13) that the minimum reflux ratio should be given by

$$RR_{\min} = \frac{1}{\alpha - 1} \frac{1}{\left[\mathcal{N}^{(D)} / \mathcal{N}^{(F)} \right]} = 2.609$$

$$RR_{\min} = \frac{\alpha}{\alpha - 1} \frac{1}{\left[\mathcal{N}^{(D)} / \mathcal{N}^{(F)} \right]} - 1 = 3.696$$

for a bubble-point feed and a dew-point feed, respectively.

7. Step off the stages, being certain to interpret the number in the column correctly.
 8. Determine the condenser and reboiler duties.
 9. Determine the capital and operating costs for the current value of RR . This will require the sizing of the reboiler, the condenser, the reflux pump, and so on. Pump sizing is discussed in Chapter 4. Heat exchangers are considered in Chapter 14. The height and diameter of the distillation column will be discussed presently. Also, it can be noted that software such as Aspen Icarus Process Evaluator can do both sizing and cost estimation.
 10. Return to step 4 until the important features of the plot are revealed.
- The general features of a yearly cost versus reflux ratio plot are contained in the particular case of benzene–toluene.

At the high reflux ratios, the cost of operating the column will be high both because of the higher demand for cooling in the condenser and because of the correspondingly large call for heating in the reboiler. Recall the proportionality between the BR and RR in Equation (7.58). The diameter will be large to accommodate the large internal flows.

On the other hand, as the reflux is decreased, the number of stages increases without limit. This implies that an arbitrarily large capital investment is approached, no matter the cost per unit height. The column will be tall to accommodate the large number of stages. These competing features give an optimum value for the reflux ratio, as illustrated in Figure 7.52.

Instead of evaluating the economics as a function of the reflux ratio, a shortcut is often employed whereby the optimum reflux ratio is calculated as a proportion of the minimum reflux ratio, the proportionality factor being rooted in the economics. Consequently the value of the economic factor must be part of the specifications for the design problem. A typical value is 1.2 (see Section 7.2.13).

7.2.13 Heuristics for Distillation Towers

(Couper et al., 2005)

1. Tower operating pressure is determined most often by the temperature of the available condensing medium, 100–120 °F if cooling water; or by the maximum allowable reboiler temperature, 150 psig steam, 366 °F.
2. Sequencing of columns for separating multicomponent mixtures: (a) perform the easiest separation first, that is, the one least demanding of trays and reflux, and leave

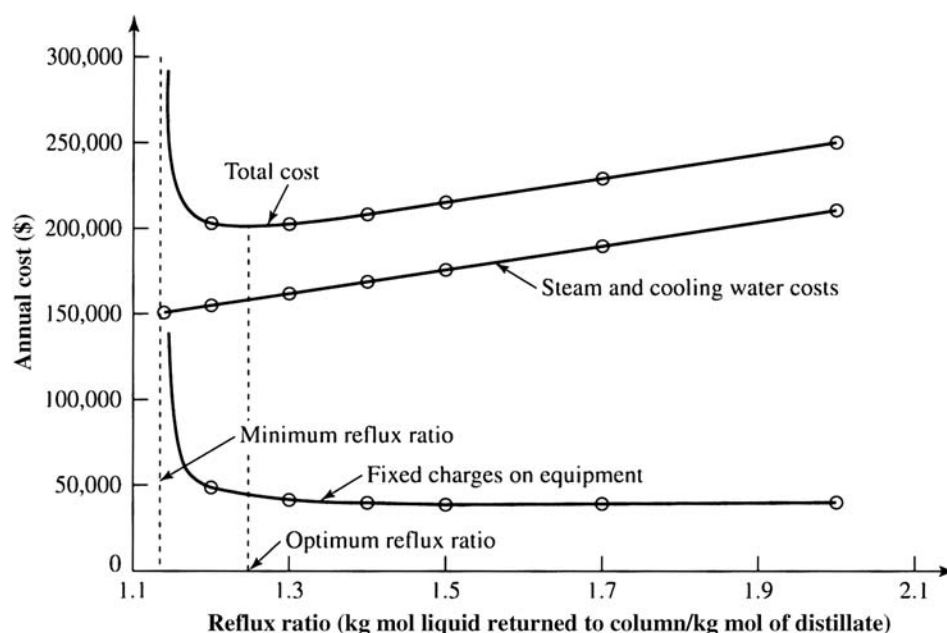


FIGURE 7.52 Optimum reflux ratio for a benzene–toluene distillation (from Peters et al., 2003). Reprinted with permission of McGraw-Hill.

the most difficult to the last; (b) when neither relative volatility nor feed concentration vary widely, remove the components one by one as overhead products; (c) when the adjacent ordered components in the feed vary widely in relative volatility, sequence the splits in the order of decreasing volatility; (d) when the concentrations in the feed vary widely, but the relative volatilities do not, remove the components in the order of decreasing concentration in the feed.

3. Economically optimum reflux ratio is about 1.2 times the minimum reflux ratio.
4. The economically optimum number of trays is near twice the minimum value.
5. The minimum number of trays is found with the Fenske equation (Henley and Staffin, 1963) (see Problem 7.4 for a derivation).
- 6.

$$N_{s,\min} = \frac{\log(x^{(D)}/1 - x^{(D)})(1 - x^{(B)}/x^{(B)})}{\sqrt{\alpha^{(D)}\alpha^{(B)}}} \quad (7.75)$$

7. Minimum reflux for binary or pseudobinary mixtures is given by the following when separation is essentially complete ($x_D \sim 1$):

$$\frac{RR_{\min} \mathcal{N}^{(D)}}{\mathcal{N}^{(F)}} = \frac{1}{\alpha - 1} \quad (7.76)$$

when feed is at the bubble point and

$$\frac{[RR_{\min} + 1] \mathcal{N}^{(D)}}{\mathcal{N}^{(F)}} = \frac{\alpha}{\alpha - 1} \quad (7.77)$$

when feed is at the dew point.

8. A safety factor of 10% of the number of trays calculated by the best means is advisable.
9. Reflux pumps are made at least 25% oversize.
10. For reasons of accessibility, tray spacings are made 20–24 in.
11. Peak efficiency of trays is at values of the vapor factor $F_s = u\rho_v^{1/2}$, in the range 1.0–1.2 (ft/s) (lb/ft³)^{1/2}. This range of F_s establishes the diameter of the tower. Roughly, linear velocities are 2 ft/s at moderate pressures and 6 ft/s in vacuum.
12. Pressure drop per tray is of the order of 3 in. of water or 0.1 psi.
13. Tray efficiencies for distillation of light hydrocarbons and aqueous solutions are 60–90%.
14. Sieve trays have holes 0.25–0.50 in. in diameter, the hole area being 10% of the active cross section.
15. Valve trays have holes 1.5 in. diameter, each provided with a liftable cap, 12–14 caps/ft² of active cross section. Valve trays usually are cheaper than sieve trays.

16. Bubble-cap trays are used only when a liquid level must be maintained at low turndown ratio; they can be designed for a lower pressure drop than either sieve or valve trays.
17. Weir heights are 2 in., weir lengths about 75% of tray diameter, liquid rate a maximum of about 8 gpm/in. of weir; multipass arrangements are used at high liquid rates.
18. Reflux drums usually are horizontal, with a liquid holdup of 5 min half full. A takeoff pot for a second liquid phase, such as water in hydrocarbon systems, is sized for a linear velocity of that phase of 0.5 ft/s, minimum diameter of 16 in.
19. For towers about 3 ft in diameter, add 4 ft at the top for vapor disengagement and 6 ft at the bottom for liquid level and reboiler return.
20. Limit the tower height to about 175 ft max because of wind load and foundation considerations. An additional criterion is that *LID* be less than 30.

Example 7.2.13-1: Tower 305

The last separation step in the process for the manufacture of acrylic acid (see Section 7.1.2 and Figure 7.53) is the separation of a process stream containing 86.8 kmol/h of acrylic acid and 6.1 kmol/h of acetic acid. The small amount of water is being neglected. Distillation in a tray tower is used to obtain a 99.9 mol% acrylic acid stream and a 95 mol% acetic acid stream. Acrylic acid will dimerize significantly above 90 °C or so. The operating pressure must be chosen accordingly. Estimate the number of trays required for a constant relative volatility (see Figure 7.53).

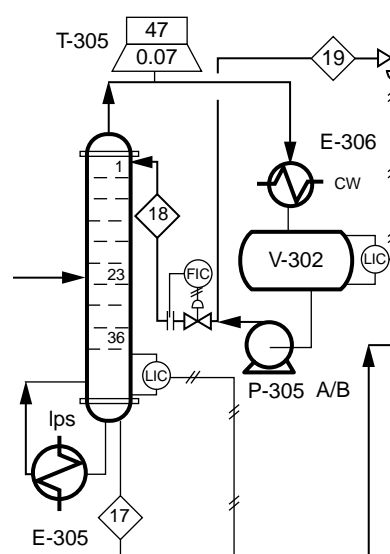


FIGURE 7.53 Waste tower in the acrylic acid process.

Solution:

Need to estimate top and bottom temperatures to get average volatility. Set bottom at 89 °C, just below limit.

See database for vapor pressures"

$$\log P^{\text{sat}} = A + B/T + C \log T + DT + ET^2$$

Coeff.	HAc	HAcr	log α	T (°C)	T (K)	log α	α
<i>A</i>	2.8376E+01	2.3067E+01	5.3086E+00	89	362.16	4.0319E-01	2.53038092
<i>B</i>	-2.9734E+03	-3.1437E+03	1.7030E+02	51.5	324.66	5.1982E-01	3.30992914
<i>C</i>	-7.0320E+00	-4.8813E+00	-2.1507E+00	Average volatility = 2.92			
<i>D</i>	-1.5051E-09	4.3690E-04	-4.3690E-04				
<i>E</i>	2.1806E-06	-4.9161E-13	2.1806E-06				

Calculation of operating pressure at 1.1325E+02mm Hg Vapor pressure of HAcr at 90 °C 89 °C

Bottom of tower assuming pure HAcr: 1.5099E-01bar
-8.6226E-01 barg

Estimated pressure drop with 10 trays at 0.1 psi/tray = 51.70068 mmHg = 0.06892857 bar

Top pressure = 61.55 mmHg or 0.0821 bar. Note that stream 18 is at 0.07 bar.

Top temperature is then approximately, assuming pure HAc :

51.5 324.66 61.17475421

Used above to calculate average relative volatility.

Equilibrium data and enriching section: Column pressure at approximately -1 barg

x_{HAc}	y_{HAc}						
0	0						
0.01	0.02865						
0.02	0.05624	$x_B =$	0.001				
0.06	0.157102	$x_D =$	0.95				
0.1	0.244966						
0.2	0.421965	$x_F =$	0.065662			mole fraction HAc in feed	
0.3	0.555838						
0.4	0.660633	$x_D = 0.95$					
0.5	0.744898	$\frac{x_D}{R_m + 1} = 0.105$, Solution is: $\{[R_m = 8.0476]\}$					
0.6	0.814126	$RR = 1.75 \times 8.0476 = 14.083$					
0.7	0.872014	$R = 14.083 \times 6.3299 = 89.144$					
0.8	0.921136						
0.9	0.963343						
1	1						
		$\frac{x_D}{14.083 + 1} = 6.2985 \times 10^{-2}$					

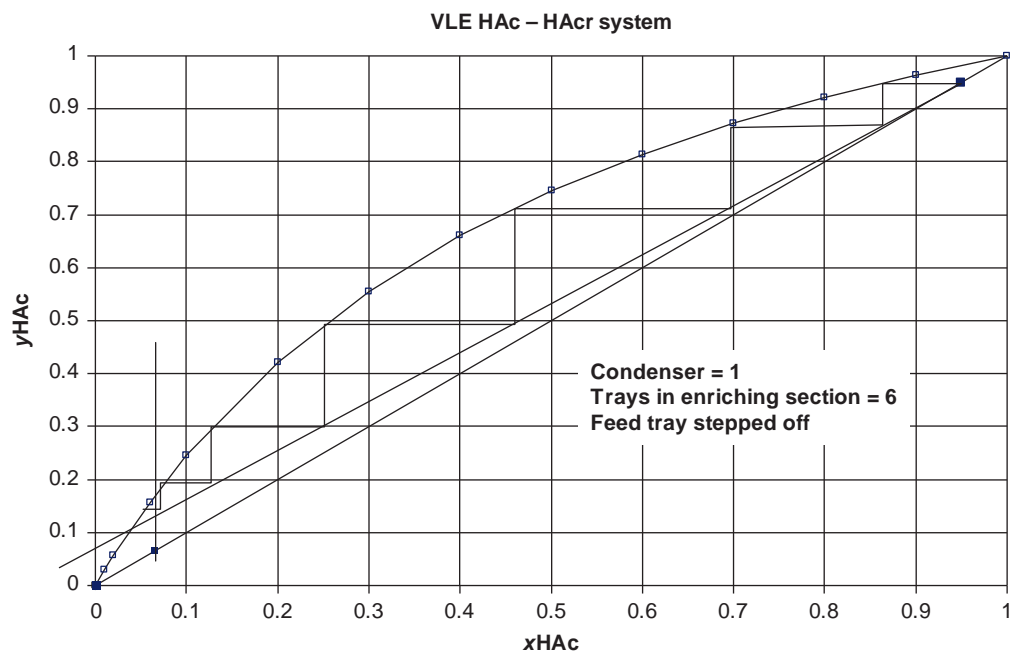
(see Figure 7.54).

Stripping section:

Use recursion relation since graph too constricted

$RR=$	14.083	y_{n+1}	x_n
$B=$	86.57	0.001	0.001
$D=$	6.3299	0.002914	0.002004
$F=$	92.9	0.005829	0.003533
$q=$	1	0.010246	0.005849
$\alpha=$	2.92	0.01689	0.009334
		0.026774	0.014517
		0.041241	0.022105
		0.061918	0.032949
		0.090486	0.047932

Reboiler + 7 stages

**FIGURE 7.54** Equilibrium trays in the enriching section.

Summary

Total trays;
 condenser = 1
 enriching section = 5
 feed tray = 1
 stripping section = 7
 reboiler = 1

Viscosity of HAc at 51.5°C = 0.7980 cP

Viscosity of HAc at 89°C = 0.4603 cP

$$\text{Eff at top} = 50.3(3.31 \times 0.7980)^{-0.226} = 40.386$$

$$\text{Eff at bottom} = 50.3(2.53 \times 0.4603)^{-0.226} = 49.988$$

Say efficiency = 0.40
 Number of stages in tower = 33

$$\text{Height} = 2 \times 32 + 4 + 6 = 74 \text{ ft} = 22 \text{ m.}$$

The number of trays and the height in the rigorous design are 36 and 25 m.

7.3 LIQUID-LIQUID EXTRACTION

The single-stage extraction operation introduced in Section 6.4.2 may not provide the purity required without excessive use of solvent and equipment volumes for large-scale operations. The purity issue might be alleviated by successive treatments of the same batch with fresh solvent at each step. The solvent issue can be alleviated by using spent solvent from later stages in earlier ones, since there is residual capacity for doing so. The former configuration is referred to as a cross-flow cascade. The latter refers to countercurrent operation. Recall that the solvent phase is also called the extract.

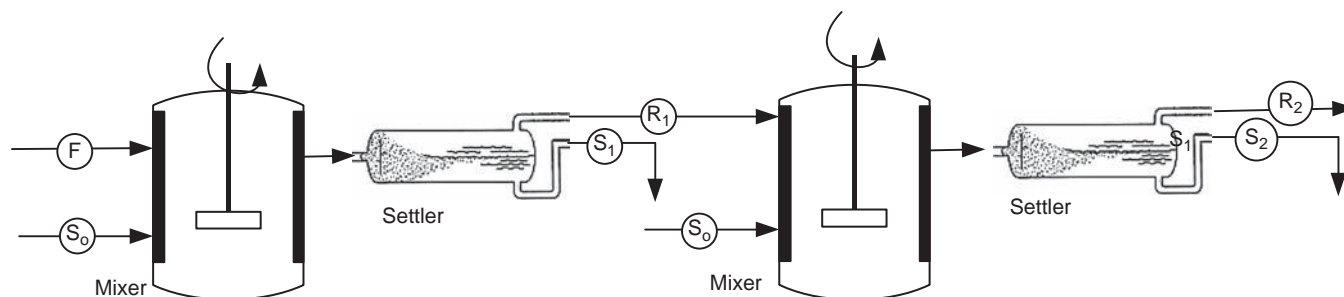


FIGURE 7.55 Cross-flow cascade—the first two stages.

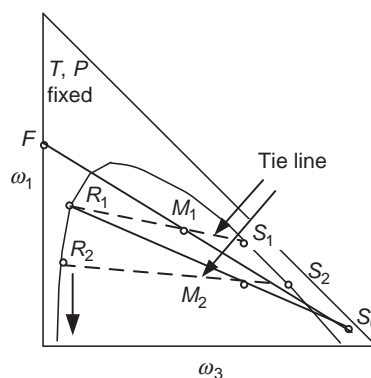


FIGURE 7.56 Second extraction step.

7.3.1 Multistage Cross-Flow Cascade

The first two stages in a cross-flow cascade are illustrated in Figure 7.55. Each stage is a mixer-settler arrangement to emphasize the more general characteristic of mixing and separation. The feed to the second stage is the raffinate from the first stage. Otherwise, the second stage is operated in the same way as the first. The graphical procedure is the same as the first, except that the feed location has changed. The same solvent is used, but at a possibly different flow rate.

The graphical procedure used for the single stage in Section 6.4.2 can therefore be repeated as illustrated in Figure 7.56.

Additional stages may be added in the same way as the first addition. The raffinate from stage $n - 1$ becomes the feed to stage n . The raffinate is retained as the product. The idea is to lower the concentration of the impurity, which brings the raffinate closer to the 2-rich phase of the 2-3 binary systems. The cross-flow cascade therefore has the ultimate capacity to meet any purity requirement. The issue of requiring large volumes of solvent to do so is aggravated with each additional stage. This drawback is addressed by countercurrent operation.

7.3.2 Multistage Countercurrent Operation

The cross-flow cascade is converted to countercurrent operation by fixing the source of solvent for each stage to be the solvent flow or extract from the succeeding stage. Material from stage n is in equilibrium with a raffinate of lower concentration than the solvent from stage $n - 1$. It can therefore serve as a solvent for that stage. This will be less efficient than the pure solvent. It will considerably reduce the solvent flow (Figure 7.57).

The solvent feed to the process therefore comes from an imaginary (N_{s+1}) stage in stream S_{N_s+1} . The degrees of freedom can be calculated by extending the results from the single stage to N stages.

Unknowns:

$$\mathcal{W}^{(R_1)}: (N_s + 1)(1 + 2) = 3(N_s + 1)$$

$$\mathcal{W}^{(S_1)}: (N_s + 1)(1 + 2) = 3(N_s + 1)$$

$$N_s: 1$$

Equations:

$$\text{Mass balances} = 3N_s$$

$$\text{Equilibrium} = 3N_s$$

$$\Phi = 3(N_s + 1)_s + 3(N_s + 1)_s + 1 - 3N_s - 3N_s = 7$$

$$\text{Fix } \mathcal{W}_i^{(F)} \text{ and } \mathcal{W}^{(S_{N+1})} \text{ completely and } x_1^{R_N}$$

In solving for the remaining variables, we will repeatedly use the mixture rule, introduced in Chapter 6.

The total mass balance for system consisting of the first n stages is

$$\mathcal{W}^{(F)} + \mathcal{W}^{(S_{n+1})} = \mathcal{W}^{(R_n)} + \mathcal{W}^{(S_1)} \quad n = 1, 2, \dots, N_s \quad (7.78)$$

Note that the feed (F) point is known in the preceding equation. If two of the remaining streams can be specified, the fourth will follow from the application of the mixture

rule. For example, for stage N_s , Equation (7.78) gives

$$\mathcal{W}^{(F)} + \mathcal{W}^{(S_{N_s+1})} = \mathcal{W}^{(R_{N_s})} + \mathcal{W}^{(S_1)} \quad (7.79)$$

This means that the mixture formed by the feed and fresh solvent is the same as the mixture formed by the raffinate and the exit solvent. All of the concentrations required to locate the streams graphically are known, except for the exit solvent concentration. The mixture is located at the intersection of the lines connecting the solution pairs. The mixture composition is given by the mass balance based on the streams with known compositions:

$$x_1^{(M)} = \frac{x_1^{(F)} \mathcal{W}^{(F)} + x_1^{(S_{N_s+1})} \mathcal{W}^{(S_{N_s+1})}}{\mathcal{W}^{(F)} + \mathcal{W}^{(S_{N_s+1})}} \quad (7.80)$$

A line drawn through the raffinate point and the preceding mixture composition will pass through the final solvent concentration. This point must be located on the equilibrium curve, since it represents a stream leaving an equilibrium stage. The companion stream R_1 falls at the opposite end of a tie line from S_1 . The steps are summarized in Figure 7.58.

Rearranging the mass balance, Equation (7.78)

$$\mathcal{W}^{(F)} - \mathcal{W}^{(S_1)} = \mathcal{W}^{(R_n)} - \mathcal{W}^{(S_{n+1})} \quad (7.81)$$

The left-hand side of Equation (7.81) does not vary with the stage number and the right-hand side links the raffinate from the current stage to the solvent flow from the next stage. This relationship between interstage streams is analogous to the material balance in gas absorption and distillation, which also linked the interstage compositions. The linkage was called an operating line. We call the left-hand side of Equation (7.81) an operating point, Δ , which represents the removal of S_1 from F .

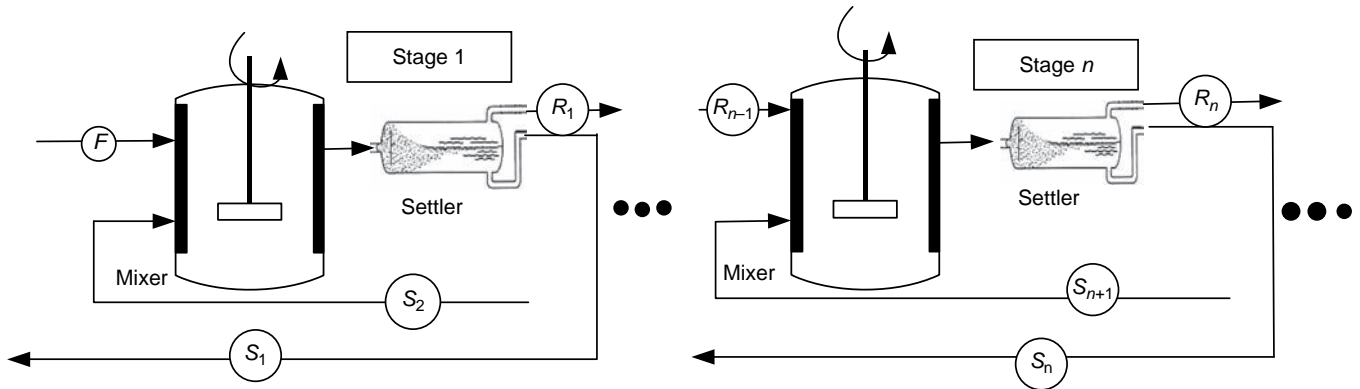


FIGURE 7.57 Countercurrent configuration.

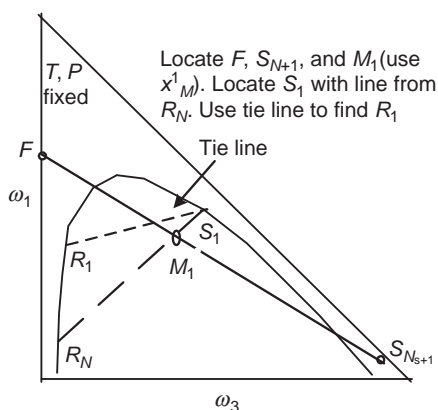


FIGURE 7.58 Location of stage 1 product streams.

Let us consider the fate of component 3 in this removal process:

$$\omega_3^{(\Delta)} \mathcal{W}^{(\Delta)} = \omega_3^{(F)} \mathcal{W}^{(F)} - \omega_3^{(S_1)} \mathcal{W}^{(S_1)} \quad (7.82)$$

$$\text{or if } \omega_3^{(F)} = 0, \quad \omega_3^{(\Delta)} = \frac{\omega_3^{(S_1)} \mathcal{W}^{(S_1)}}{\mathcal{W}^{(S_1)} - \mathcal{W}^{(F)}} \quad (7.83)$$

$$\text{If } \mathcal{W}^{(S_1)} > \mathcal{W}^{(F)}, \text{ but small, } \omega_3^{(\Delta)} > 1. \text{ If } \mathcal{W}^{(S_1)} < \mathcal{W}^{(F)}, \text{ but small, } \omega_3^{(\Delta)} < 0 \quad (7.84)$$

Therefore, there are circumstances under which the generalized mixture, Δ , will not find itself within the range of realizable mass fractions and will in fact lie either to the left or to the right of this triangular space.

The mass balance equations allow for whatever deficits or credits are necessary for a solution. The triangular space defined by the values of 0–1 merely represents the region of realizable mixtures. Points outside this region are mathematical, not physical, possibilities.

The operating point may be located on the basis that it lies on two known lines: the line through F and S_1 and the line through

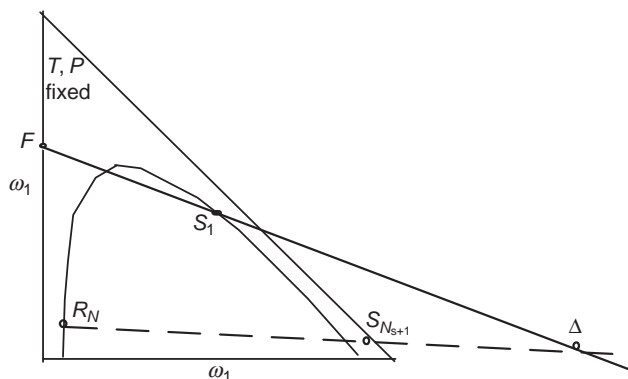


FIGURE 7.59 Location of the operating point.

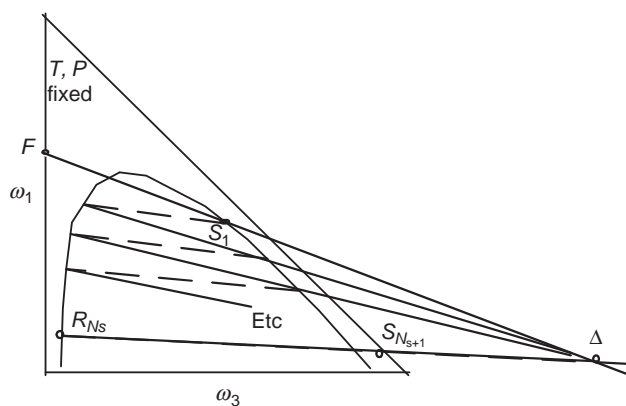


FIGURE 7.60 Stepping off the stages.

R_{Ns} and S_{Ns+1} . The result is shown below in Figure 7.59 for the case when the operating point falls on the right side of the diagram.

The solvent flow from the next stage is obtained by drawing a line from the operating point to the raffinate from the current stage. The raffinate and solvent flow from the same stage are connected by a tie line as shown in Figure 7.60.

The raffinate associated with each solvent flow is located with a tie line from the solvent point to the raffinate side of the equilibrium diagram.

Note in the construction of the equilibrium stages in Figure 7.60 that the slope of this operating line is greater than the slope of the tie lines. Should these slopes be equal at any point in the operating range, a pinch point will be encountered, which will prevent further reduction in the concentration of the impurity. An infinite number of stages will be accumulated as the point is approached. We can locate this point and demonstrate that it constitutes the minimum solvent flow rate by first considering the effect of the solvent rate on the operating point.

Consider the situation is depicted in Figure 7.61.

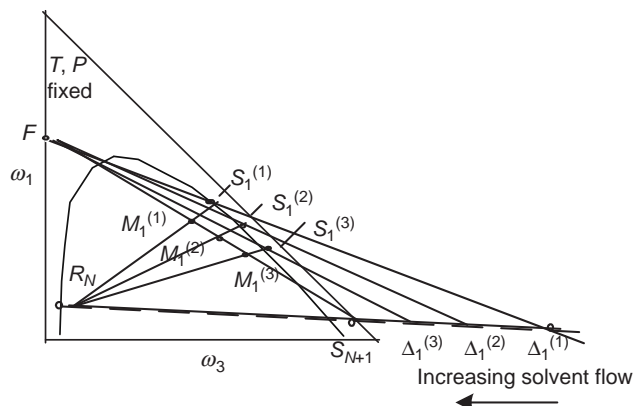


FIGURE 7.61 Effect of solvent flow on the operating point.

The feed, raffinate, and inlet solvent points in Figure 7.61 are considered fixed. The solvent rate is progressively increased through three values. The mixture point travels along the line connecting the feed and the inlet solvent, becoming closer to the solvent as the solvent rate or proportion increases. This can be argued on physical grounds and can also be seen from the expression for the mole fraction of component 1 in the mixture.

$$x_1^{(M)} = x_1^{(S_0)} + \left[\frac{x_1^{(F)} - x_1^{(S_0)}}{1 + \frac{\mathcal{W}^{(S_{N_s+1})}}{\mathcal{W}^{(F)}}} \right] \quad (7.85)$$

We can therefore be assured that the slope of all tie lines encountered during the stage stepping operation will be less than the slope of the operating line if the operating point is to the left of the intersection of the steepest relevant tie line with the line through the raffinate and fresh solvent points. This intersection is labeled Δ_{\min} in Figure 7.62.

The relevant tie lines begin with the uppermost one that when extended goes through the feed point and ends with the tie line whose extension goes through the raffinate point.

The solvent flow associated with the minimum operating point is obtained by finding the corresponding mixing point graphically as illustrated in Figure 7.63.

The minimum solvent flow can then be calculated from the mixture point found graphically.

$$x_1^{(M_{\min})} = \frac{x_1^{(F)} + x_1^{(S_0)} (\mathcal{W}^{(S_{N_s+1})} / \mathcal{W}^{(F)})_{\min}}{1 + (\mathcal{W}^{(S_{N_s+1})} / \mathcal{W}^{(F)})_{\min}} \quad (7.86)$$

Similar calculations are carried out when the operating point falls on the left side of the diagram. As on the right-hand side of the diagram, the operating point travels to the left as the solvent flow increases. We again want the actual operating point to be to the left of the region containing the intersections

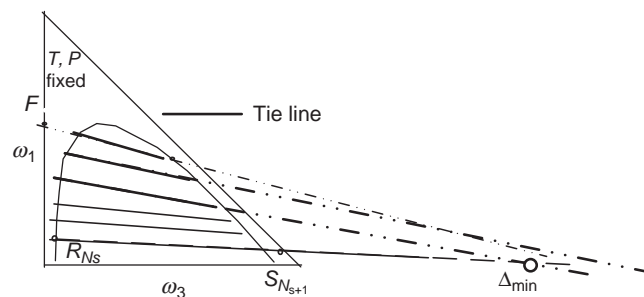


FIGURE 7.62 Location of the operating point for the minimum solvent.

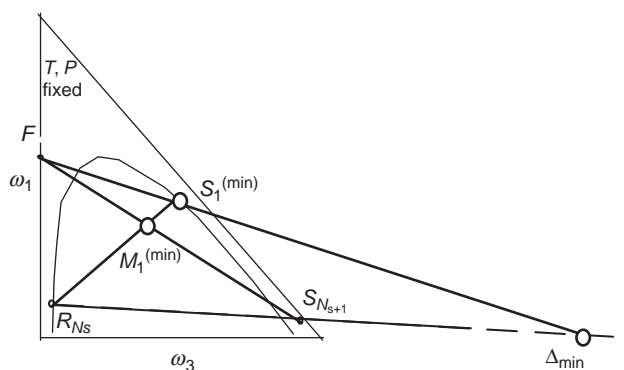


FIGURE 7.63 Determination of the minimum solvent flow.

of all relevant tie lines with the solvent factor as in the case of gas absorption and stripping.

Example 7.3.2-1: Extraction of Acetone from MIBK with Water (This example will discuss the use of Excel to solve extraction problems. The version of Excel will almost certainly not coincide with that of the reader. However, there may be enough similarities that the benefits will outweigh the inconvenience of making the required transition.)

A liquid–liquid extraction column, operating at 25 °C, is fed 20,000 lb/h of a mixture of 40 wt% acetone, 55 wt% methyl isobutyl ketone (MIBK), and 5 wt% water (see Figure 7.64). A solvent stream fed to the top of the column contains 95 wt% water, 2.5 wt% acetone, and 2.5 wt% ketone.

The raffinate-rich product stream from the top of the extractor has a composition of 89.5 wt% ketone, 7.5 wt% acetone, and 3 wt% water. The solvent-rich product stream from the bottom of the column contains 81 wt% water, 16 wt% acetone, and 3 wt% ketone.

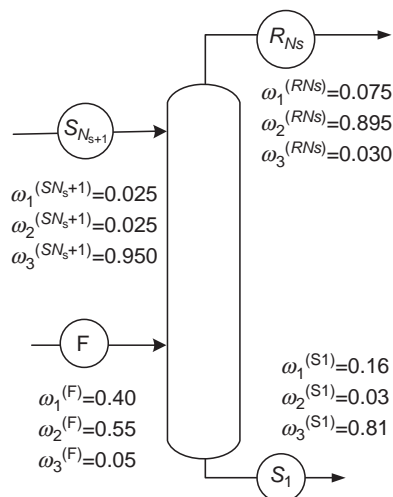


FIGURE 7.64 Acetone extraction.

Calculate the solvent flow rate, the minimum solvent rate, the number of theoretical stages in the extractor, and the amount of acetone recovered.

Component 1 = acetone, component 2 = MIBK,
component 3 = water

Solution: (with discussion of Excel application)

The equilibrium data are available at 25 °C as follows:

Raffinate			Extract		
ω_1	ω_2	ω_3	ω_1	ω_2	ω_3
0.0000	0.9700	0.0300	0.0000	0.0250	0.9750
0.0590	0.9110	0.0300	0.0255	0.0255	0.9490
0.1000	0.8700	0.0300	0.0580	0.0270	0.9150
0.1500	0.8200	0.0300	0.0880	0.0270	0.8850
0.2000	0.7650	0.0350	0.1150	0.0350	0.8500
0.2500	0.7100	0.0400	0.1600	0.0370	0.8030
0.3058	0.6442	0.0500	0.1980	0.0370	0.7650
0.3500	0.5900	0.0600	0.2450	0.0400	0.7150
0.4000	0.5200	0.0800	0.2950	0.0500	0.6550
0.4550	0.4200	0.1250	0.3550	0.0750	0.5700
0.4730	0.1820	0.3450	0.4730	0.1820	0.3450

The (all) solubility data were selected and used to construct a new chart (xy scatter with grid) on a separate sheet. The data may have to be placed in two columns for plotting. The series (solubility envelope) was formatted with a smooth solid line. It may be easier in what follows to remove the data symbols (Marker=None) from the solubility envelope data series. They will be identified again with the tie lines. The tie lines can be plotted on top of this chart as follows: Select the tie line end points (two sets) using the ctrl key. Since the data are ordered, there will be one set near the top of the preceding table and a corresponding set the same distance from the bottom. Select copy under the Edit menu followed by Paste special under the Edit menu on the chart (choose new data series with x values in the first column). Click on the new data series (two points), which will be on top of the previously plotted series. When selected, only two points should be highlighted. Format the series with a dotted line and a convenient color (same as the solubility envelope, for instance). The plait point is not included in this step. It is equivalent to a collapsed tie line. Figure 7.65 will result.

Inclusion of Stream Points: See Figure 7.66. Note that the symbol S_o is used in place of S_{N+1} throughout the calculations in this example.

		Phase
Stream points:	0.0300	0.0000
	0.0300	0.0590
	0.0300	0.1000
	0.0300	0.1500
	0.0350	0.2000
	0.0400	0.2500
	0.0500	0.3058
	0.0600	0.3500
	0.0800	0.4000
	0.1250	0.4550
	0.3450	0.4730
	0.5700	0.3550
	0.6550	0.2950
	0.7150	0.2450
	0.7650	0.1980
	0.8030	0.1600
	0.8500	0.1150
	0.8850	0.0880
	0.9150	0.0580
	0.9490	0.0255
	0.9750	0.0000
	x_3	x_1
	0.0500	0.4000
	0.9500	0.0250
	0.0300	0.0750
	0.8100	0.1600
		Feed(F)
		Fresh solvent($S_o=S_{N+1}$)
		Final raffinate(R_N)
		Final solvent(S_1)

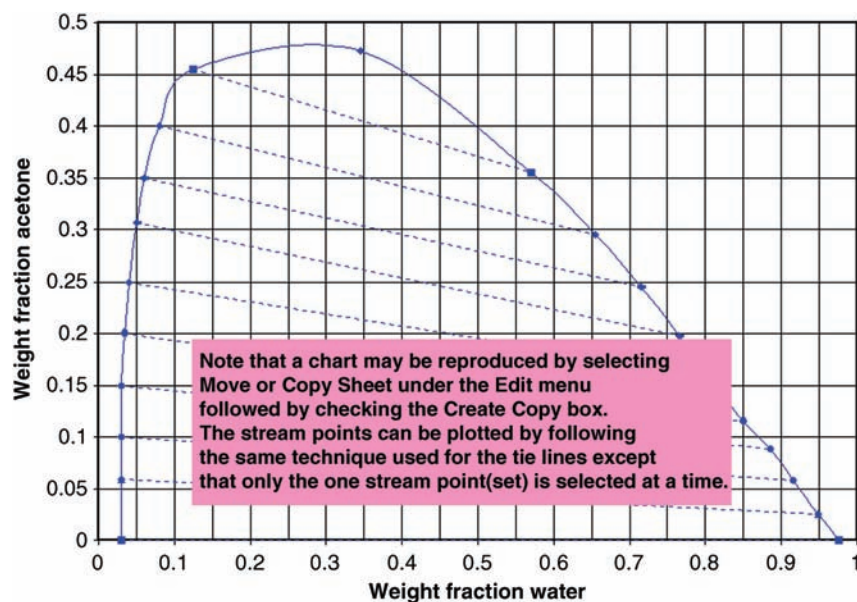


FIGURE 7.65 Equilibrium data for acetone–water–MIBK.

Determination of Solvent Flow: The solvent flow can be calculated from a material balance. This calculation can be illustrated by using the M (mixture) point. The mixture of the feed and fresh solvent is the same as the mixture of the final raffinate and spent solvent. The lines can be drawn using the line drawing tool. See Figure 7.67.

Minimum Solvent Flow: See Figure 7.68. The chart with the solubility data can be used to calculate the minimum delta point. Beginning with a tie line that passes through F if extended and continuing down to the one passing through R, extend all tie lines to the line passing through R_N and S_0 . Just draw lines over the tie lines (which

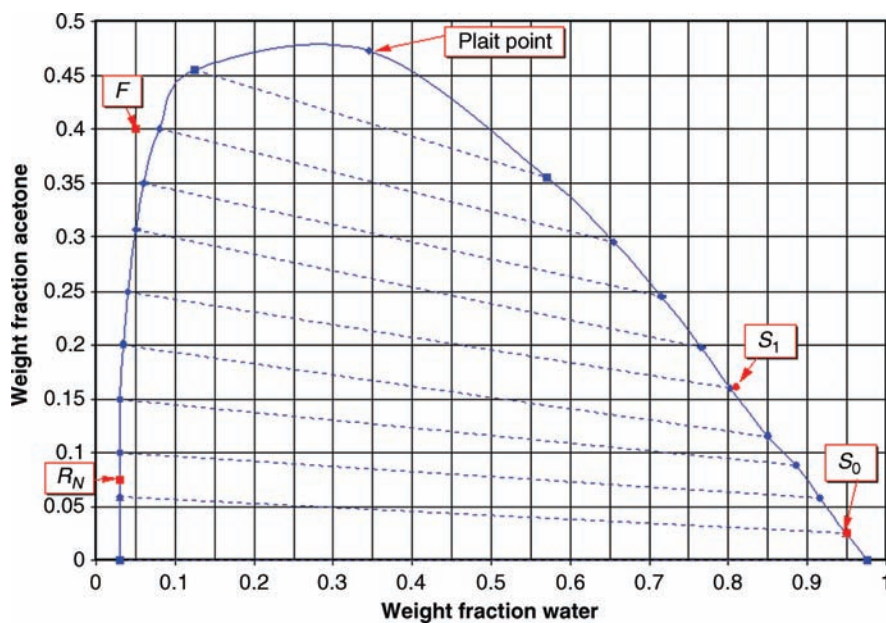


FIGURE 7.66 Location of the stream points.

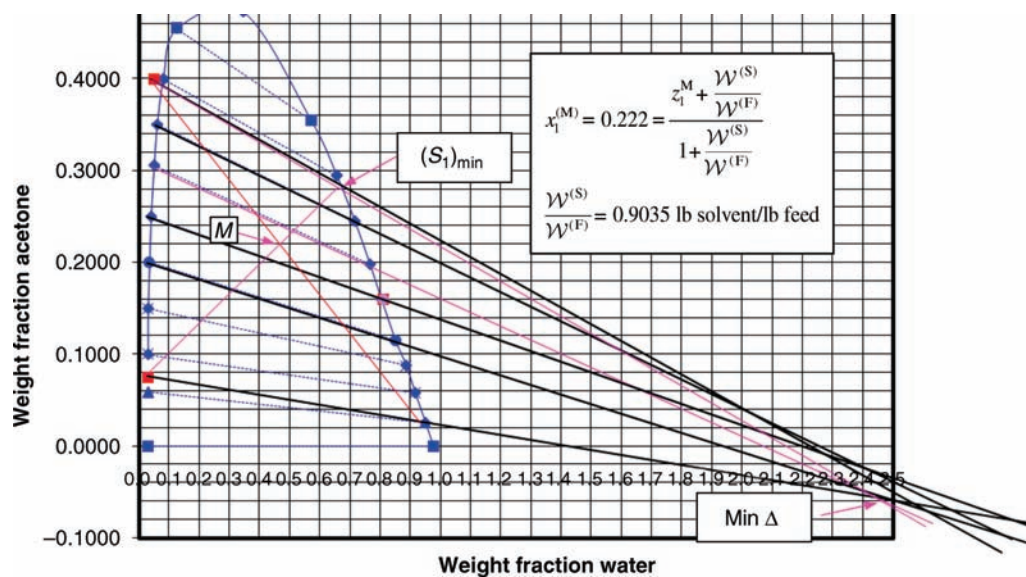


FIGURE 7.69 Determination of the minimum solvent flow.

Location of Actual D Point: The actual flow calculated above is 2.55 lb solvent/lb feed. The actual delta point can be located by extending the line through F and the S_1 . See Figure 7.70.

First Stage: See Figure 7.71. The first stage may now be represented by fixing R_1 using the tie line at S_1 . A step

to the next stage can be taken by fixing S_2 as the intersection of a line from R_1 to the delta point with the solubility envelope.

Remaining Stages: The remaining stages may be stepped off in this manner. Four equilibrium stages are needed for the separation (rounding up) (see Figure 7.72).

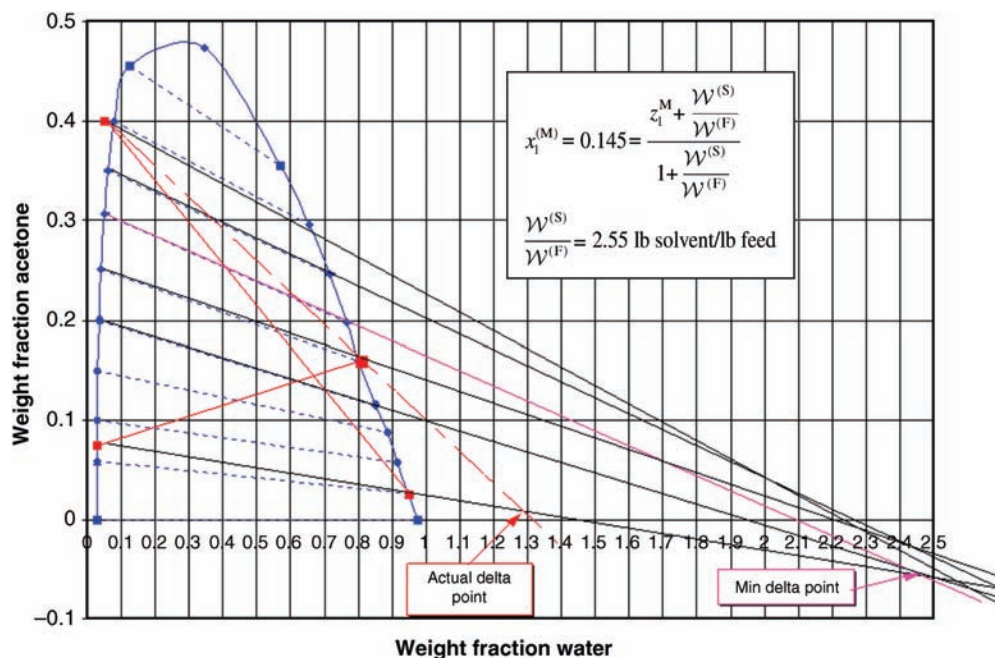


FIGURE 7.70 Location of the operating point.

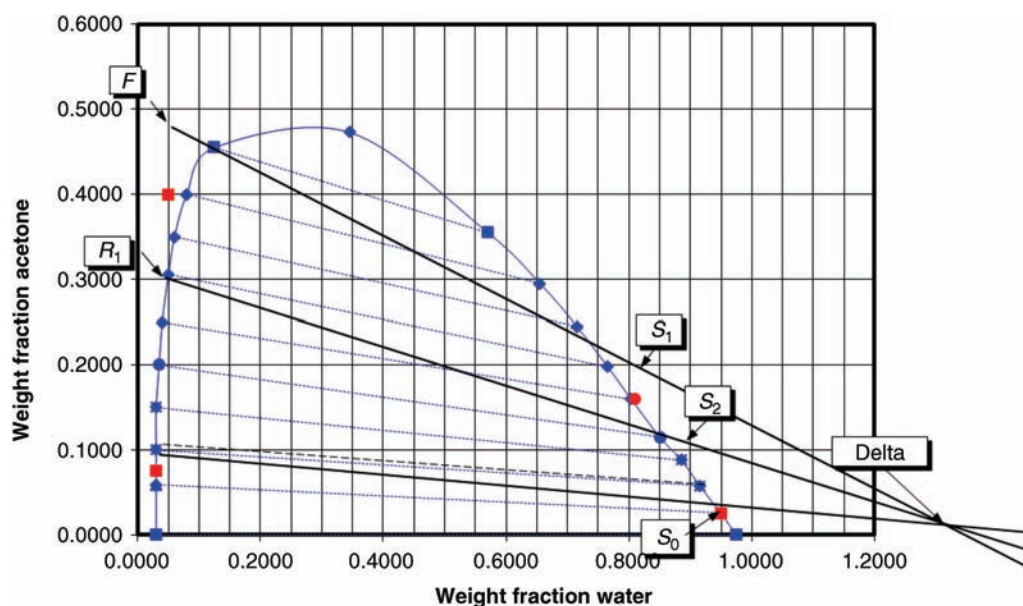


FIGURE 7.71 Location of the first stage.

Example 7.3.2-2: T-303 Acid Extractor—Number of Equilibrium Stages and Solvent Flow Required

This example is the multistage version of Example 6.4.2-2. A comparison of the solvent requirements is made there.

Just after the reaction section in the manufacture of acrylic acid, the product stream (9) at 27463 kg/h

consists essentially of 23 wt% acrylic acid and 77 wt% water. The actual stream contains about 1% acetic acid. The product stream is to be fed to an extraction column and contacted with a recycled diisopropyl ether stream (23) that contains 2.6 wt% water (see Figure 7.73). The objective is to reduce the acid concentration in the water stream (12) to 0.5 wt%. The acid is therefore

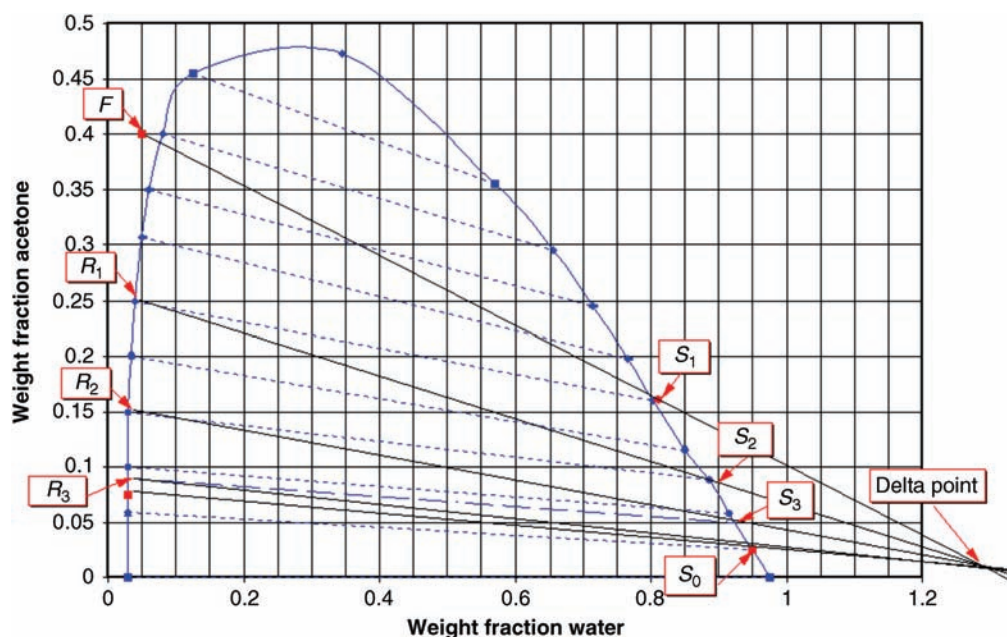


FIGURE 7.72 Location of the remaining stages.

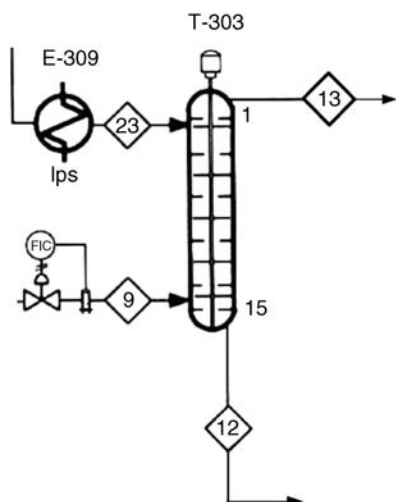


FIGURE 7.73 T-303 acid extractor.

recovered before the water stream is sent to the waste tower.

Recall from the discussion in Chapter 1 that this separation route was chosen largely because the direct distillation of stream 9 would require that water be taken overhead, a large energy cost.

Determine the solvent requirements, the outlet raffinate and extract flows and compositions, and the number of equilibrium stages required.

The equilibrium data at 40 °C, the operating temperature, are given in Example 6.4.2-2. The data are reproduced here for convenience. Most of the data are outside the range of operating conditions. The results will therefore be approximate.

Water Phase		Ether Phase	
ω_D	ω_A	ω_D	ω_A
0.00125	0.00000	0.99676	0.00000
0.00146	0.06694	0.97586	0.02067
0.00263	0.32750	0.93628	0.05981
0.00404	0.64690	0.91333	0.08274
0.00400	0.73712	0.90082	0.09542
0.00389	0.77622	0.89262	0.10379
0.00380	0.79814	0.88686	0.10968
0.00374	0.81218	0.88260	0.11404
0.00369	0.82194	0.87934	0.11738
0.00366	0.82911	0.87676	0.12003
0.00363	0.83460	0.87468	0.12217

D = diisopropyl ether; A = acrylic acid

Only the data in the lower concentration range will be used. This amounts to using only the bottom three tie lines.

See Example 7.3.2-1 for application of Excel to liquid-liquid extraction problems.

Plot equilibrium data		Given stream locations		Draw portion (extract) of solubility curve	
0.00125	0.00000	0.00125	0.00500	raffinate	0.00125 0.00000
0.00146	0.06694				0.00146 0.06694
0.00263	0.32750	0.00000	0.23000	feed	0.00263 0.32750
0.00404	0.64690				0.93628 0.05981
0.00400	0.73712	0.97400	0.00000	solvent	0.97586 0.02067
0.00389	0.77622				0.99676 0.00000
0.00380	0.79814				
Location of M point-plot as new series (1 point)					
0.00374	0.81218				
0.00369	0.82194				
0.00366	0.82911				
0.00363	0.83460	0.83	0.0366		
0.87468	0.12217				
0.87676	0.12003				
0.87934	0.11738				
0.88260	0.11404				
0.88686	0.10968				
0.89262	0.10379				
0.90082	0.09542				
0.91333	0.08274				
0.93628	0.05981				
0.97586	0.02067				
0.99676	0.00000				

The data are plotted in Figure 7.74. The minimum solvent flow appears to be defined by the tie line extension that passes through F.

stream F = stream 9
stream S₁ = stream 12
stream S_{Ns+1} = stream 23
stream R_{Ns} = stream 13

The calculations for the minimum solvent rate are shown on the graph and are based on the value of ω_1^{\min} read from the graph. Using an economic factor of 1.25, the solvent flow is calculated and used in Figure 7.75 to locate the extract from the first stage and the operating point.

The stages may now be stepped off (see Figure 7.76).

With six stages operated countercurrently, the desired separation can be achieved with a solvent to feed ratio of 5.28. A single stage required a solvent to feed ratio of more than 75 (see Example 6.4.2-2).

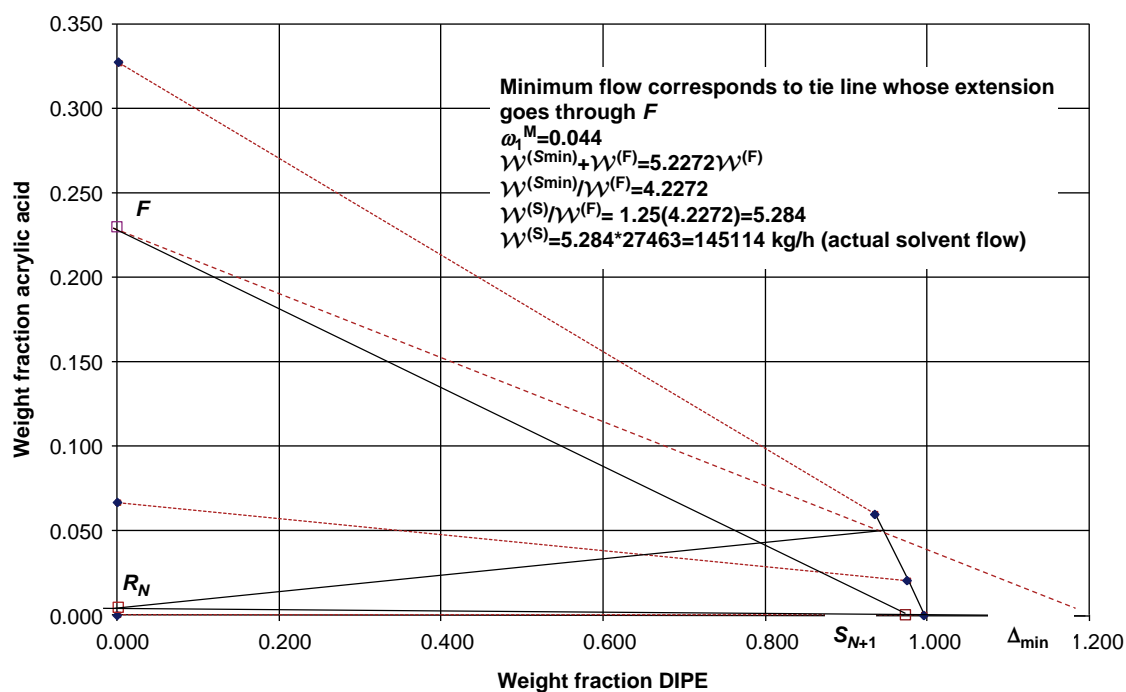


FIGURE 7.74 Minimum solvent flow for acrylic acid extraction.

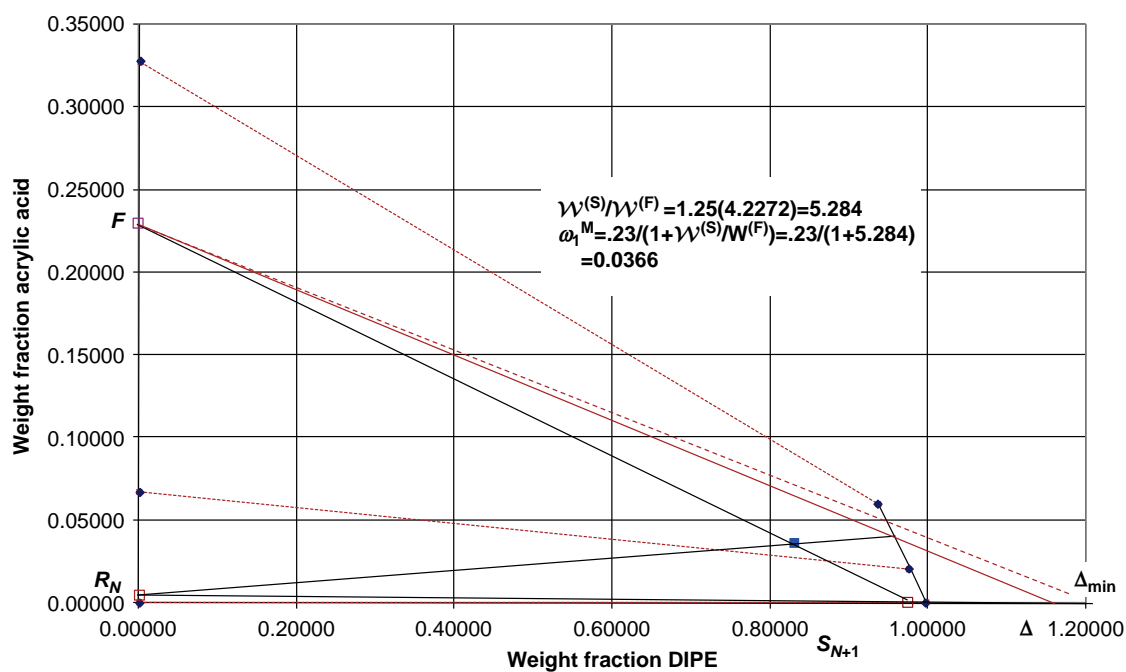


FIGURE 7.75 Operating point for acrylic acid extraction.

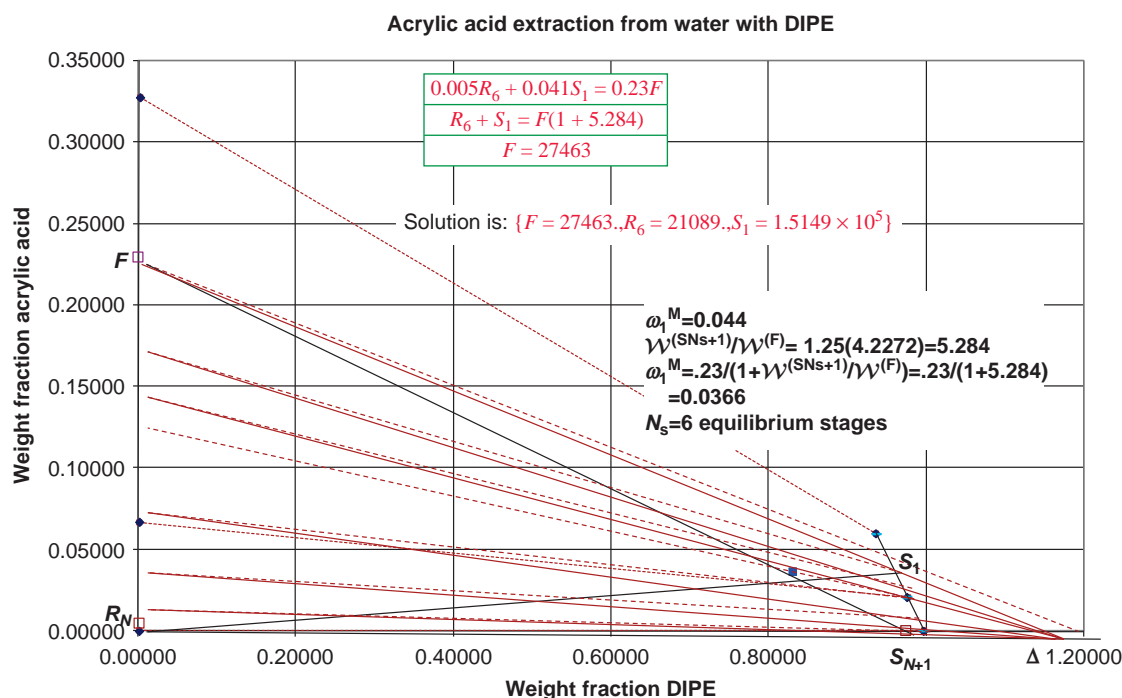


FIGURE 7.76 Stages for acrylic acid extraction.

7.3.3 Extraction Equipment

There exists a wide range of equipment for multistage countercurrent extraction ranging from a train of mixer-settlers (see Figures 7.57 and 7.77).

Through sieve plate towers with complex plate designs, to large variety of mechanically assisted designs such as the Scheibel column (see Figure 1.19), some attributes of the various equipment types are given in Table 7.2.

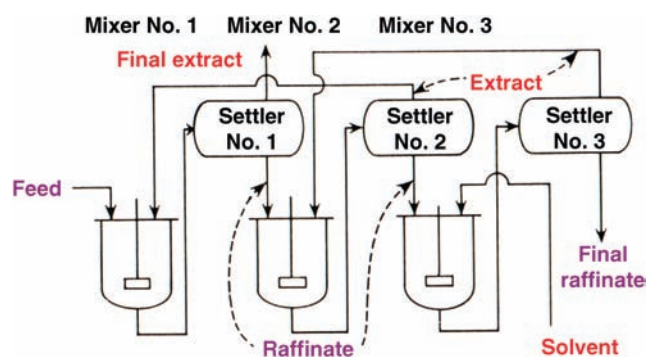


FIGURE 7.77 Mixer-settler train. (Adapted from liquidextraction.com.)

The mixer-settler arrangement is a clear expression of an equilibrium stage configuration. Although arrangements such as the Scheibel column appear to be a series of equilibrium stages, they are closer to a continuous contacting device. However, many of the designs of continuous contacting equipment are based on the height equivalent to a theoretical stage (HETS), a value that is best obtained in the laboratory or may be available from the manufacturer. The basis of the HETS is rate based and is discussed in Chapter 12. In all of these cases where the HETS approach is taken, the number of equilibrium stages is obviously required.

The equilibrium stage approach applies directly to the sizing of tray towers for liquid-liquid extraction. The sieve tray or perforated plate tower is usually selected for liquid-liquid extraction. By using some heuristics and common values, the actual number of trays and the height of an unagitated sieve tray tower may be obtained. The equilibrium stage approach also applies directly to the mixer-settler configuration. We will follow each of these possibilities and apply each to the extraction operation of Tower 303 in the acrylic acid process. Some heuristics for liquid-liquid extraction are given at the end of this section.

TABLE 7.2 Features and Industrial Applications of Liquid-Liquid Extractors

Types of Extractors	General Features	Fields of Industrial Applications
Unagitated columns	Low capital, operating and maintenance cost Simplicity in construction Handles corrosive material High-stage efficiency	Petrochemical Chemical
Mixer-settlers	Good flexibility High capacity Handles liquids with high viscosity Handles wide solvent ratios Reliable scale-up Low NETS	Petrochemical Nuclear Fertilizer Metallurgical
Pulsed columns	No internal moving parts Many stages possible Reasonable capacity Reasonable NETS	Nuclear Petrochemical Metallurgical
Rotary-agitation columns	Many stages possible Reasonable construction cost Low operating and maintenance cost High throughput	Petrochemical Metallurgical Pharmaceutical Fertilizer
Reciprocating plate columns	Low NETS Great versatility and flexibility Handles liquids containing suspended solids Handles liquids containing suspended solids Simplicity in construction Handles mixtures with emulsifying tendencies	Pharmaceutical Chemical Petrochemical Metallurgical
Centrifugal extractors	Short contacting time for unstable material Limited space required Handles easily emulsified material Handles system with little liquid density difference	Pharmaceutical Nuclear Petrochemical

Source: Couper et al. (2005).

7.3.4 Height and Efficiency of Sieve Tray Towers

An approximate tray efficiency can be evaluated with the following correlation originally due to Treybal (Couper et al., 2005):

$$E_o = 0.35 \frac{Z \ell_{ts}^{0.5}}{\sigma D_0^{0.35}} \left(\frac{v^{(D)}}{v^{(C)}} \right)^{0.42} \quad (7.87)$$

ℓ_{ts} = tray spacing, ft
 σ = surface tension, dyn/cm
 D_0 = hole diameter, ft
 $v^{(D)}$ = superficial velocity of dispersed phase
 $v^{(C)}$ = superficial velocity of continuous phase

With the number of equilibrium stages determined, the height of the tower can be estimated with

$$\ell_t = \left(\frac{N_s}{E_o} - 1 \right) \ell_{ts} + 2\ell_s, \text{ ft} \quad (7.88)$$

where ℓ_{ts} = height of settling zone, ft

A settling zone of 3–4 ft may be used. These estimates are valid to within approximately 25%.

Example 7.3.4-1: Height and Number of Trays on Tower 303 with Unagitated Sieve Tray Design

ℓ_{ts} = 2.0 ft, see heuristics

$$D_0 = 3 \text{ mm} = \left[\frac{0.3}{12 \times 2.54} \right] = 0.0098425 \text{ ft, see heuristics}$$

σ = 17.34 dyn/cm(25 °C). Corrected to 40 °C with data (Yaws, 2003) for propyl isopropyl ether = factor of approximately (18.13/19.76):

$$= 15.91 \text{ dyn/cm}$$

$$\frac{v^{(D)}}{v^{(C)}} = \frac{m^{(D)}}{m^{(C)}} \left(\frac{\rho}{\rho^{(C)}} \right)^{-1}$$

where $\rho = AB^{-(1-(T/T_c))^n}$ from Yaws (1999). Dispersed phase = solvent since it is the highest throughput

$$\rho^{(D)} = 0.26218(0.26974)^{(1-(313/500.05))^{0.28571}} = 0.705 \text{ g/cc}$$

$$\rho^{(C)} = 0.34710(0.274)^{(1-(313/647.13))^{0.28571}} = 1.0137 \text{ g/cc}$$

$$E_o = 0.35 \frac{2^{0.5}}{15.91 \times (0.0098425)^{0.35}} \left[\frac{139310 \times 1.0137}{27463 \times 0.705} \right]^{0.42}$$

$$= 0.36$$

Number of actual trays = $6/0.36 = 17$ trays

$$\mathcal{A}_1 = 32 + 6 = 38 \text{ ft}$$

The rigorous simulation arrived at a height of 32 ft and 15 trays.

7.3.5 Mixer–Settler Units

The mixer or stirred tank design basis is discussed in Chapter 5. An illustration of a gravity settler is shown in Figure 6.37. The settler is cylindrical in shape with an L/D ratio of approximately 4 (a common range values for cylindrical drums is 2.5–5). This value and the total flux from the disengaging area, 5 gal/min ft², are due to Happel and Jordan (1975) and Ryon et al. (1959). The disengaging area is the intersection of a parallel plane with the cylindrical settler. The maximum disengaging area is therefore L/D. The settler may in fact be larger than the mixer.

Example 7.3.5-1: Typical Settler Size for Mixer–Settler Alternative to Tower 303

We will illustrate the calculations with average values for the raffinate and extract flows as was done in Chapter 5.

The average flows for each of the two phases are

$$\mathcal{W}^{(\text{Raffinate})} = \frac{27463 + 21089}{2} = 24276 \text{ kg/h}$$

$$\mathcal{W}^{(\text{Extract})} = \frac{145144 + 151490}{2} = 148302 \text{ kg/h}$$

The average flow through the disengaging area is then

$$\mathcal{V} = \left[\frac{148302}{0.70483} + \frac{24276}{1.0137} \right] \frac{1000}{2831760} 7.485 = 1032.5 \text{ gpm}$$

The disengaging area can then be estimated as

$$A = \frac{103.5}{5} = 206.5 \text{ ft}^2$$

If the area is located at the midpoint of the horizontal drum,

$$DL = 4D^{23} = 206.5 \text{ ft}^2$$

$$D = 7 \text{ ft} \quad L = 28 \text{ ft}$$

The stirred tank dimension and horsepower are determined in Examples 5.3-1 and 5.3.2.2-1. The tank required is approximately 3100 gal with a diameter of 8 ft and a 16 hp motor. If we assume an efficiency of 90%, the number of stages becomes 7 (2 above the recommended limit). Each stage consists of an 8 ft × 8 ft mixer and a cylindrical settler 7 ft in diameter and 28 ft long.

7.3.6 Heuristics for Liquid–Liquid Extraction

(Couper et al., 2005)

- The dispersed phase should be the one that has the higher volumetric rate, except in equipment subject to backmixing where it should be the one with the smaller volumetric rate. It should be the phase that wets the material of construction less well. Since the holdup of continuous phase usually is greater, that phase should be made up of the less expensive or less hazardous material.
- Mixer–settler arrangements are limited to at most five stages. Mixing is accomplished with rotating impellers or circulating pumps. Settlers are designed on the assumption that droplet sizes are about 150 μm diameter. In open vessels, residence times of 30–60 min or superficial velocities of 0.5–1.5 ft/min are provided in settlers. Extraction stage efficiencies commonly are taken as 80%.
- Spray towers even 20–40 ft high cannot be depended on to function as more than a single stage.
- Packed towers are employed when 5–10 stages suffice. Pall rings of 1–1.5 in. size are best. Dispersed phase loadings should not exceed 25 gal/min (ft²). HETS of 5–10 ft may be realizable. The dispersed phase must be redistributed every 5–7 ft. Packed towers are not satisfactory when the surface tension is more than 10 dynes/cm.
- Sieve tray towers have holes of only 3–8 mm diameter. Velocities through the holes are kept below 0.8 ft/s to avoid formation of small drops. Redispersed of either phase at each tray can be designed for this purpose. Tray spacings are 6–24 in. Tray efficiencies are in the range of 20–30%.
- Pulsed packed and sieve tray towers may operate at frequencies of 90 cycles/min and amplitudes of 6–25 mm. In large diameter towers, HETS of about 1 m has been observed. Surface tensions as high as 30–40 dynes/cm have no adverse effect.

- Reciprocating tray towers can have holes of 126 in. in diameter, 50–60% open area, stroke length of 0.75 in., 100–150 strokes/min, plate spacing normally 2 in. but in the range of 1–6 in. In a 30 in. diameter tower, HETS is 20–25 in. and throughput is 2000 gal/(h)(sq ft). Power requirements are much less than of pulsed towers.
- Rotating disk contactors or other rotary agitated towers realize HETS in the range 0.1–0.5 m. The especially efficient Kuhni with perforated disks of 40% free cross section has HETS 0.2 m and a capacity of 50 ml/m² h.

7.4 MULTIPLE REACTOR STAGES

In this section, the progressive transition from completely mixed systems through systems formed by multiple completely mixed stages to the microscopic view is completed. The single CSTR is considered a step in a sequence of CSTRs whose limiting behavior is the ideal PFR with continuous gradients in concentrations and temperature. On the other hand, the single adiabatic PFR in which a reversible catalytic reaction ideally reaches equilibrium at the outlet is shown to be an effective member of the stage in a sequence of such reactors devised to further increase the conversion.

The sequence of CSTRs exposes finite stages in the reaction chemistry to external manipulation through such variables as temperature. Optimal temperature programs for a CSTR sequence are discussed in this context.

7.4.1 Comparison with Batch Reactor

A characteristic of the CSTR is that the reactions take place at the outlet conditions. This is advantageous, for example, when a side reaction of higher order is present and selectivity is an important issue. For single reactions, however, the low reaction rate is a burden and will result in a longer residence time in the CSTR than the batch reactor. This can be seen in Figure 7.78 where the extent per unit volume of feed is $\xi'' (= \xi/V)$.

The cross-hatched area under the curve is given by the integral of Equation (6.183). It is the batch reaction time required to reach the final extent, ξ''_f . The total solid area (above and below the curve) is given by Equation (6.153) to be the average residence time required in the CSTR for the same conversion. The extra holding time required in the CSTR is then the shaded area above the curve. The extra holding time can be greatly diminished by distributing the holding time for the CSTR over more than one tank. The material balance for the n th tank in a series of CSTRs is

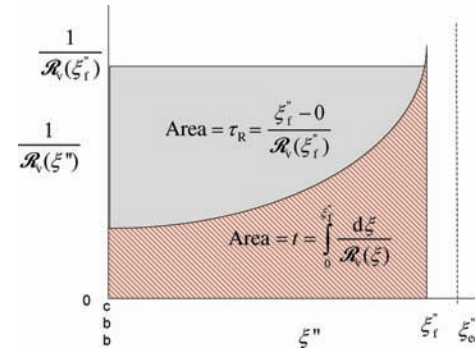


FIGURE 7.78 Comparison of residence time between batch and single CSTR.

given by a modification of Equation (6.154) to account for the accumulated extent in the feed:

$$\frac{\xi^{(n)} - \xi^{(n-1)}}{R_v(\xi^{(n)})} = \tau_{Rn} \quad (7.89)$$

An example of three tanks is illustrated in Figure 7.79. The total holding time for the three stages is the sum of the individual values, which are the rectangular areas in Figure 7.79. The extra holding time required in the CSTR has decreased and is again represented by the shaded area above the curve. Additional tanks will bring the two values even closer until there is no practical difference between them.

7.4.2 Comparisons with Plug Flow Reactor

The plug flow model was introduced in Chapter 5. It refers to the ideal case of flow of a fluid in a straight round conduit of uniform, circular cross section in which all of the fluid elements have the same axial velocity. The analogy with the batch reactor is clearly that the fluid elements entering

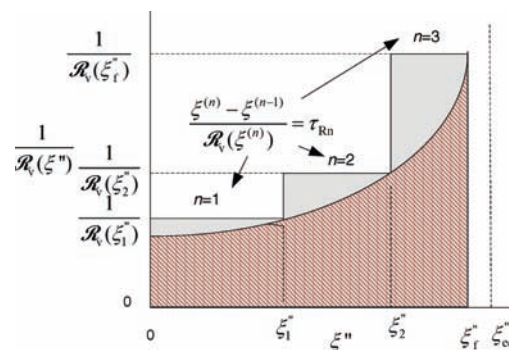


FIGURE 7.79 Comparison of residence time between batch and three CSTR.

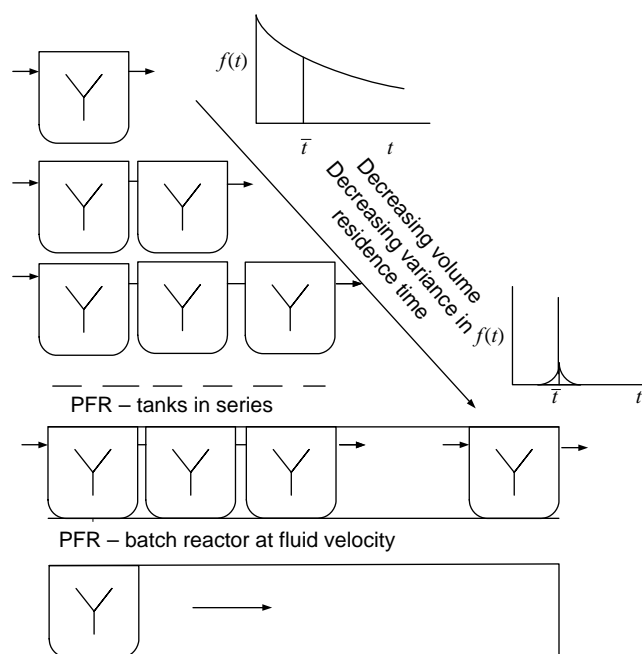


FIGURE 7.80 Summary comparison of ideal reactors.

the plug flow reactor experience the same history as their counterparts in the stirred batch with time measured by the distance traveled divided by the fluid velocity. In this case, extensive laboratory kinetic data are not needed. Only the time to reach a desired conversion is required, t_{batch} :

$$D = \left[4 \frac{t_{\text{batch}} \mathcal{V}^{(F)}}{(L/D)} \right]^{1/3} \quad (7.90)$$

These limiting cases are summarized in Figure 7.80.

Note also, the transition from multiple stages to a continuum.

7.4.3 Number of Stages Required for a Given Conversion

The number of stages required for a given conversion, residence time, and temperature can be determined with a graphical technique similar to those employed earlier in this chapter (Aris). The material balance in Equation (6.148) can be written as

$$\xi^{(n-1)} = \xi^{(n)} - \mathcal{R}_v(\xi^{(n)}) \tau_R \quad (7.91)$$

which emphasizes the point that it is easier to solve for the input given the output than vice versa. A plot of the input extent versus the output extent may be prepared as illustrated in Figure 7.81 using Equation (7.91).

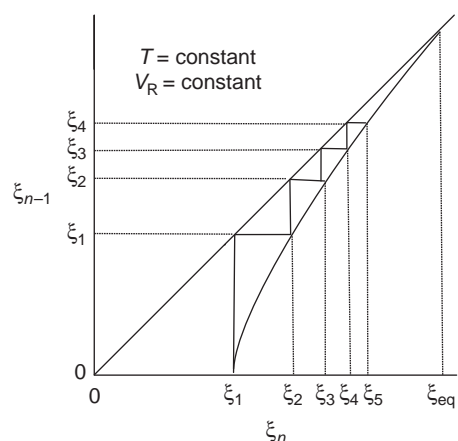


FIGURE 7.81 Stages in CSTR sequence of equal volume and temperature.

The 45° line is a construction aid. The material balance curve meets the 45° line at the equilibrium or complete conversion, since with either of these conditions at the input, there can be no further conversion.

The material balance curve crosses the horizontal axis at the output for no conversion at the input: ξ_1 . This output is reflected off the 45° line to become an input for which the output is ξ_2 . The stepping procedure stops when the desired extent is reached or exceeded along the horizontal axis. The number of stages is the number of intersections on the material balance curve. If the reactor volumes or temperatures are not equal, additional material balance curves may be drawn with these values and used for the output at the applicable step.

Example 7.4.3-1: Number of Stages for a Diels–Alder Reaction

Diels–Alder reactions refer to the very useful reactions of unsaturated carbonyl compounds with conjugated dienes. An example is the reaction of butadiene with benzoquinone shown in Figure 7.82.

The kinetics of this reaction are available (Wassermann, 1965) in the range of 25–55 °C:

$$\begin{aligned} R(\text{mol/L}) s &= k(T) c_A c_B \text{ with } k(T) \\ &= \exp(-E(\text{cal/mol})/RT(\text{K})) \end{aligned}$$

where A = butadiene and B = benzoquinone and the concentrations are in mol/L and

$$\log_{10} A(\text{L/mol}) = 5.2 \pm 0.6$$

$$E = 14.5 \pm 0.6 \text{ kcal/mol}$$

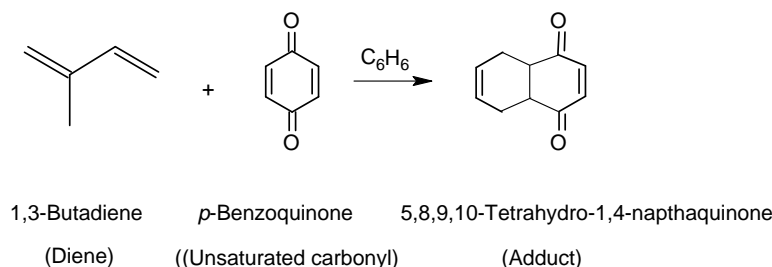


FIGURE 7.82 Diels–Alder reaction.

- Determine the size tank required for 50% conversion at 50 °C of a 1 m³/h feed containing 1.0 mol/L of each reactant.
- Determine the increase in conversion with the addition of one and two tanks, the same size as the first.

Solution: (a)

$$c_i = c_i^{(F)} + \vartheta_i \xi = 2 - \xi; \quad i = A, B$$

$$R_v(\xi) = 10^{5.2} e^{(-\frac{14500}{1.987 \times 323.16})} (2 - \xi)^2$$

$$\xi = 1$$

$$\xi = R_v(\xi) \tau_R, \text{ Solution is: } \{[\tau_R = 40459.]\} \text{ Equation (6.154)}$$

$$\tau_R = 40459.s = 40459/3600 = 11.239 \text{ h}$$

$$V_R = \tau_R V = 11.239 \times 1 = 11.239 \text{ m}^3$$

$$V_R = 11.239 \times 264.17 = 2969.0 \text{ gal}$$

Solution: (b)

Plot $\xi^{(n-1)}$ versus $\xi^{(n)}$ as per Equation (7.91) and step off stages (see Figure 7.83).

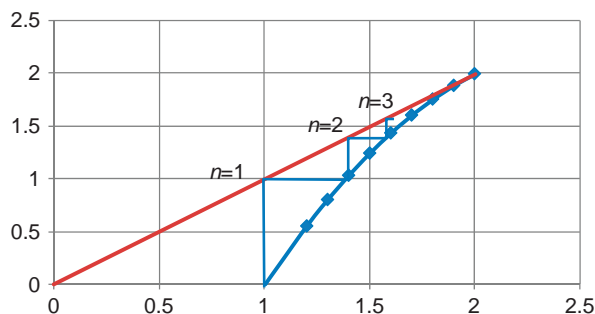


FIGURE 7.83 Increase in conversion with the number of stages.

$\xi^{(n)}$	$\xi^{(n-1)}$
1	-2.3742E-05
1.2	0.559984805
1.3	0.809988366
1.4	1.039991453
1.5	1.249994065
1.6	1.439996201
1.7	1.609997863
1.8	1.75999905
1.9	1.889999763
2	2

The addition of 1 tank increases the conversion by approximately 20%. The increase in conversion achieved with the third tank is only 5%.

Although there are incentives for employing unequal volumes in a cascade of CSTRs (Denbigh, 1966), the extra cost associated with design, construction, and spare parts inventory generally outweighs the advantages (Hill, 1977). Temperature selection for the individual tanks is discussed in following section.

7.4.4 Temperature Programs for CSTR Stages

It is realistic to presume that there are temperature limits within which the sequence of reactors can be safely and economically operated. The question of the best operating temperature is therefore confined to this range, that is, $T_* \leq T \leq T^*$. The determination of the optimal temperature most often involves numerical search routines (Nauman, 2008), which will not be discussed here. The objective of the following discussion is to raise some basic ideas that will aid in the recognition of the existence an optimal temperature and the elucidation of its features in a sequence of CSTRs. Rate expressions of the type given in Section 6.6 where the function of concentration is given by the mass action (Boudart, 1968) and expression for systems close to equilibrium (see Chapter 8).

7.4.4.1 Single Reactions For single reactions, the extent is an implicit function of temperature according to the

material balance, Equation (6.154). Differentiation of the material balance gives

$$\frac{d\xi}{dT} = \frac{[\partial \mathcal{R}_v(\xi, T)/\partial T]_{\xi} \tau_R}{1 - [(\partial \mathcal{R}_v(\xi, T)/\partial \xi) \tau_R]_T} \quad (7.92)$$

The sign of the derivative of extent is determined by the sign of the numerator in Equation (7.92).

For *irreversible reactions*, that is, those where the equilibrium is very far to the right, the equilibrium restraint is not present in the rate equation so that

$$\left[\frac{\partial \mathcal{R}_v(\xi, T)}{\partial T} \right]_{\xi} = \frac{E}{RT^2} \mathcal{R}_v(\xi, T) > 0 \quad (7.93)$$

Consequently, the reactors should be operated at the highest possible temperature, T^* .

For *endothermic reactions*, both the rate constant and the distance from equilibrium increase with temperature. The optimal temperature sequence is the same as that for irreversible reactions.

For *exothermic reactions*, the distance from equilibrium decreases with an increase in temperature while the rate constant increases. This competition leads to an optimum (extremum) temperature that maximizes the conversion. The simplest case in this category is



$$\mathcal{R}_v = k_f c_A - k_b c_B \quad (7.95)$$

The reaction extent per unit volume of feed follows from Equations (6.153, 6.154), and (7.96):

$$\xi'' = \frac{k_f c_A^{(F)} - k_b c_B^{(F)}}{1 + (k_f + k_b) \tau_R} \tau_R \quad (7.96)$$

The temperature at which the extent per unit volume of feed is a maximum (extremum) follows as

$$\begin{aligned} T_{max} \\ = \frac{E_b}{R \ln \left\{ \frac{(E_b - E_f)}{E_f} k_{of} \tau_R \right\} + R \ln \left\{ \frac{1 + (c_B^{(F)}/c_A^{(F)})}{1 - K_c (c_B^{(F)}/c_A^{(F)}) (E_b/E_f) \tau_R} \right\}} \end{aligned} \quad (7.97)$$

Note that the second term in the denominator is due entirely to the presence of B in the feed.

7.4.4.2 Multiple Reactions When more than one reaction is present, it is often the case that there are undesirable routes through the kinetic system that result in a loss of reactants to the primary objective. In addition to conversion, therefore, the yield or fraction of converted reactant that is converted to the desirable product is a primary objective. The two objectives often compete for attention and one must be attended to early in the reaction sequence while the other is treated later. The stages in a CSTR sequence are particularly well suited for implementing operating strategies at different stages of the reaction sequence. Some examples are presented below (see Denbigh (1966) and Hill (1977) for further discussion) (Table 7.3).

7.5 STAGED FIXED-BED CONVERTERS FOR EXOTHERMIC GAS PHASE REACTION

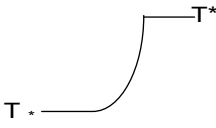

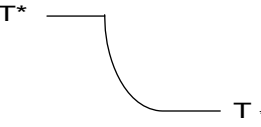
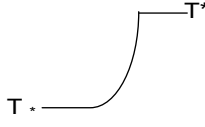
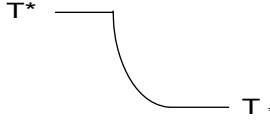
The adiabatic reactor is attractive because of the simplicity of its design. However, the temperature increase in the case of exothermic reactions may be prohibitive from a number of viewpoints: catalyst stability, process safety, the reaction chemistry, and chemical equilibrium. The temperature rise in such cases may be checked by the addition of an inert diluent, by distributing a cold feed along the reactor (cold shot cooling), by excess reactant, or by periodic cooling of the reaction mixture. The last case is the subject of this section.

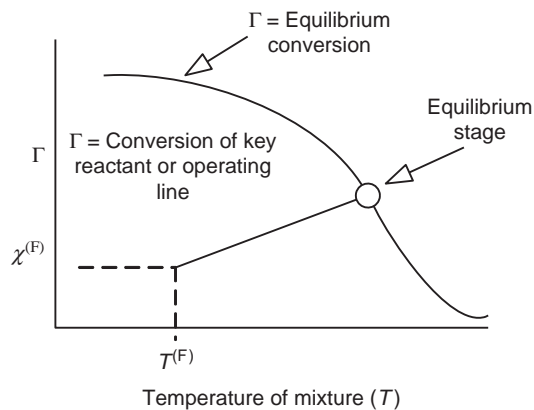
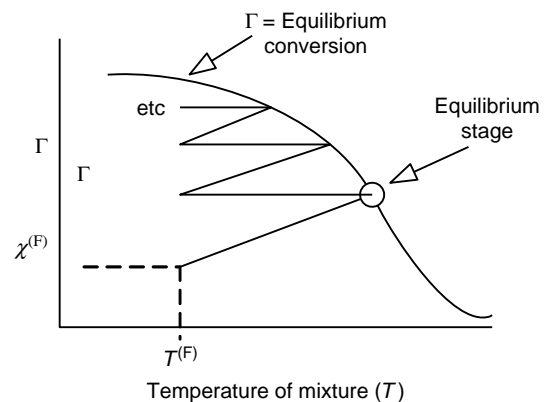
The temperature of the reaction mixture in a fixed bed increases approximately linearly with conversion indicated by Equation (3.124). At the same time, the equilibrium constant decreases with the rising temperature in the bed. An ideal equilibrium stage in this case is defined by their intersection (see Figure 7.84).

In order to increase conversion further, the reaction mixture can be cooled noncatalytically, say, to the feed temperature, and the equilibration process repeated until a satisfactory conversion is achieved. The stagewise process is illustrated graphically in Figure 7.85.

The slopes may change slightly due to changes in the average specific heat of the feed. Also an approach temperature may be set for each stage to account for deviations from equilibrium. The maximum conversion for the program in Figure 7.85 is $\chi_{eq}(T^{(F)})$. The interstage cooling temperatures and the number of stages are an optimization problem.

TABLE 7.3 Examples of Optimal Temperature Profiles (P = desired product)

Reactions	Conditions	Optimum Profile	Arguments
$A \xrightarrow{E_1} P$ $A \xrightarrow{E_2} X$	$E_2 > E_1$		Initially will decrease high initial rate of reaction 2 more than 1 (yield consideration). Increase temperature for conversion.
	$E_1 > E_2$		Increases rate of reaction 1 more than 2 throughout the reaction process.
$A \xrightleftharpoons[E_2]{E_1} P$ $A \xrightarrow{E_3} X$	$E_1 < E_2$ $E_3 > E_1$		High initially with regard to conversion. Cooling towards reactor outlet since rate of reactions 2 and 3 will be decreased more than reaction 1.
	$E_1 > E_2$ $E_3 > E_1$		Low initially since rate of reaction 3 will be decreased more than rate of reaction 1. Increase temperature for conversion since reaction 2 will be less impacted.
	$E_2 > E_1$ $E_3 < E_1$		High initially to increase in reaction 1 more than 3. Decrease toward outlet will decrease rate of reaction 2 more than in reaction 1.


FIGURE 7.84 Equilibrium stage in a fixed-bed adiabatic converter.

FIGURE 7.85 Multiple equilibrium stages in a fixed-bed adiabatic converter.

Example 7.5-1: Staged Fixed-Bed Converter for SO₂ Oxidation

Suppose that sulfur is burned in air to give a reaction mixture with the following composition:

SO ₂ :	10%
O ₂ :	20%
N ₂ :	70%

The mixture is fed to the converter at 415 °C and 1 atm. Neglect any pressure drop in the bed and assume that the reaction mixture is cooled to 415 before being introduced to the next stage. Determine the number of stages required.

Definitions

Species	Reference	$\vartheta = \begin{vmatrix} -1 \\ -0.5 \\ 1 \\ 0 \end{vmatrix}$
SO ₂	1	
O ₂	2	
SO ₃	3	
N ₂	4	

Heats and Free Energies of Formation kJ/mol

From Sandler (TRC tables)

$H_f = \begin{vmatrix} -296.8 \\ 0 \\ -395.7 \\ 0 \end{vmatrix}$	$G_f = \begin{vmatrix} -300.2 \\ 0 \\ -371.1 \\ 0 \end{vmatrix}$
--	--

Specific Heats at Low Pressure—Ideal Gas State J/(mol K)

$a = \begin{vmatrix} 25.762 & 5.791 \times 10^{-2} & -3.809 \times 10^{-5} & 8.607 \times 10^{-9} \\ 28.167 & 0.630 \times 10^{-2} & -0.075 \times 10^{-5} & 0 \\ 16.393 & 14.573 \times 10^{-2} & -11.193 \times 10^{-5} & 32.402 \\ 27.318 & 0.623 \times 10^{-2} & -0.095 \times 10^{-5} & 0 \end{vmatrix}$
--

Equilibrium Constant at 298 K and as a Function of Temperature

$$\ln K(298) = \frac{-1}{(0.00831434)(298)} \sum_{i=1}^{i=4} \vartheta_{i,1} (G_f)_{i,1} = 28.6156$$

$$K(298) = \exp(28.6156)$$

$$DHR = \sum_{i=1}^{i=4} \vartheta_{i,1} (H_f)_{i,1} = -98.9$$

Assuming a constant heat of reaction (see Example 6.7-2):

$$K(T) = \exp\left(28.6156 + \frac{98.9}{0.00831434} \left(\frac{1}{T} - \frac{1}{298}\right)\right)$$

$$K(298) = 2.67668 \times 10^{12}$$

$$K(800) = 35.4459$$

Mass Balance and Equilibrium Constant as a Function of Composition

Key reactant = SO₂

$$\mathcal{N}_i = \mathcal{N}_{io} + \frac{\vartheta_i}{-\vartheta_A} x \mathcal{N}_{ao}$$

or in terms of mole fractions, the basis being the feed composition,

$$y_i = \frac{y_{io} + \vartheta_i x y_{Ao}}{1 + \sum \vartheta_i x y_{Ao}}$$

Since pressure is 1 atm and the standard state fugacities are unity, the equilibrium constant in terms of compositions or conversion is given by

$$f(x) = \frac{(0.10x/1 - 0.5(0.1)x)}{(0.10(1-x)/1 - 0.5(0.1)x)((0.20 + (-0.5)0.10x)/(1 - 0.5(0.1)x))^{0.5}}$$

Equating the two forms provides the equilibrium curve:

$$K(T) = f(x)$$

400	1.000000
600	0.999501
700	0.991594
800	0.934270
850	0.856927
900	0.736566
925	0.663768
975	0.509813
1000	0.436057
1100	0.21186
1200	9.94720×10^{-2}
1225	8.28911×10^{-2}
1250	6.93627×10^{-2}
1300	4.92437×10^{-2}

Reactor Temperature

$$T = T_o + \frac{y_{Ao} [-\Delta H_R]}{\langle pf \rangle} x_A$$

$$T_o = 415^\circ \text{C}$$

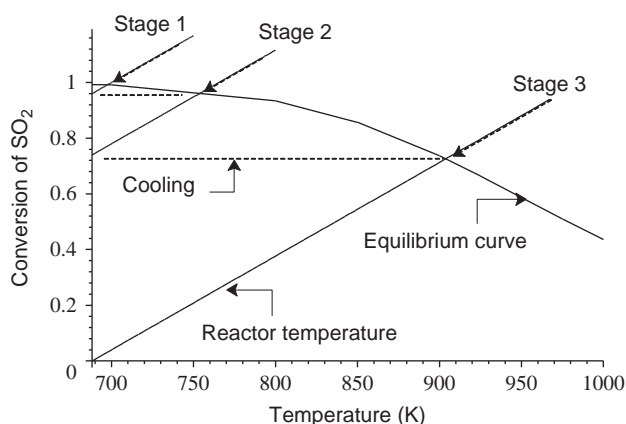


FIGURE 7.86 Stages in a sulfur dioxide converter with interstage cooling.

$$y = \begin{bmatrix} 0.10 \\ 0.20 \\ 0 \\ 0.70 \end{bmatrix}$$

$$c_p(i, T) = \sum_{j=1}^4 a_{ij} T^{j-1}$$

$$c_{pf} = \sum_{i=1}^4 y_{i,1} c_p(i, 415 + 273) = 33.2752$$

Need conversion as a function of T :

$$t = 415 + 273.16 + \frac{0.10(98900)}{33.2752} x, \quad \text{Solution is}$$

$$\{x = 3.36453 \times 10^{-3} t - 2.31533\}$$

$$x(t) = 3.36453 \times 10^{-3} t - 2.31533$$

Plot on the graph until the intersection with the equilibrium line completes an equilibrium stage. Then cool to the original inlet temperature without catalyst and allow the conversion to accumulate throughout the stage (refer to Figure 7.86).

$$y(t) = 3.36453 \times 10^{-3} t - 2.31533 + 0.74$$

PROBLEMS

7.1. A single-stage operation was considered in Problem 6.4 for the extraction of carboxylic acids from fermentation broths with methylcyclohexanol ($\text{C}_6\text{H}_{13}\text{CH}_3\text{OH}$). This

exercise considers the same problem from a multistage point of view.

- Determine the minimum flow rate of the solvent required to reach the desired raffinate composition with a multistage countercurrent cascade.
- Determine the number of equilibrium stages required for a solvent flow rate of 1478 lb/h in a multistage countercurrent cascade.
- Using the feed and solvent rates, size a typical mixer-settler unit for the countercurrent operation.
- Summarize a comparison of the single and multistage operations.

7.2. A gas analyzing 70 mol% CH_4 , 15% C_2H_6 , 10% $n\text{-C}_3\text{H}_8$, and 5% $n\text{-C}_4\text{H}_{10}$ at 70 °F and 30 psia is to be scrubbed in an isothermal tray absorber with a liquid containing 1 mol % $n\text{-C}_4\text{H}_{10}$ and 99% nonvolatile hydrocarbon oil. At least 70% of the propane in the entering gas is to be absorbed. If the column has three equilibrium stages, estimate with Kremser's group method the liquid to gas ratio that will be required and the composition of the exit streams. Note that the butane content of the inlet solvent stream may be significant regarding the mass balances.

7.3. Hydrogen peroxide is a widely used oxidizing agent. Over half of the production is used by the paper industry to bleach pulp. You probably have a container in your medicine chest at home. In the standard process for the manufacture of hydrogen peroxide, the reaction section is followed by an extraction unit that recovers the peroxide from an organic working solution. The extract is a 10 wt% solution of hydrogen peroxide in water at 60 °F and 1 atm. This stream is sent at a rate of 2000 lb/h to a distillation unit that recovers a 99 wt% water stream for recycle to the extraction unit and a 70 wt% hydrogen peroxide solution for stabilization and shipping. You are asked to size the column: height, diameter(s), calculate the major heat duties, and determine the dimensions of reflux drum.

7.4. As discussed in Section 7.2.1.2, the minimum number of distillation stages corresponds to the limit of an infinite reflux. At this limit, there is no feed to the column and no product is withdrawn. Assuming that the relative volatility is constant at the geometric mean of the top and bottom values, derive the Fenske equation (see Heuristic 6, page 65, Section 7.13).

7.5. Consider the absorption of acetone by water in a single equilibrium stage as described in Example 6.2.2-1. The objective is to reduce the mole fraction of acetone in an air stream from 0.15 to 0.05 by using pure water at 0 °C and 101 kPa. Compare the single-stage minimum water requirement with the water requirement for the multistage operation.

7.6. A 52 mol% solution of acetic acid in water flowing at 100 lb-mol/h is to be separated into two streams, a 98 mol% acid and a 98 mol% water stream. A two-step process is being considered. In the first step, ethyl acetate is to be used to extract the acetic acid and produce the desired water stream. Distillation is being considered for the second step whereby the spent solvent is to be purified and returned to the extraction unit.

- a. What is the minimum concentration of acetic acid in the water stream that can be achieved in a single-step extraction unit and what is the solvent rate required?
- b. Devise a two-step cross-flow extraction process. Report the purity of the water stream that you achieve

and the amount and concentration of the (mixed) solvent stream that results.

- c. Determine the number of equilibrium stages and solvent rate required for a multistage countercurrent extraction unit.
- d. What conclusions can you draw from the preceding calculations? Suppose a cascade of mixer-settler units are under consideration for the countercurrent cascade considered in part c.
- e. Determine one of the units for the dimensions of the mixer, a closed baffled vessel, and the settler diameter of a flat bladed impeller.
- f. Determine the minimum rate of rotation for uniform dispersion power requirement of the agitator.

8

MICROSCOPIC EQUATIONS OF CHANGE

The macroscopic view of chemical processing systems has, at this juncture, reached the interior of process equipment for completely mixed systems and for systems composed of completely mixed stages with the stepwise changes taking place inside the equipment. In the case of the staged fixed-bed converters, the concentrations and temperature in fact varied continuously through each bed with the stepwise changes taking place across the beds. In these cases, the macroscopic view was not sufficient to completely characterize the pointwise variation of the process variables. This chapter carries the analytical viewpoint to these interior regions of process equipment where the material properties can vary both spatially and temporally. The distinction of a staged system is not therefore any longer relevant as the continuous variations can be, for example, from the inlet to the outlet of a single nonequilibrium stage or across the entire bulk phase in a fixed-bed absorber as well. The microscopic balance equations, flux expressions, parameter estimations, with typical boundary conditions provide the tools necessary to develop the applications in Chapters 9–13.

It will be well to consider what is meant by continuous and microscopic in the face of the molecular theory of matter. Consider the following thought experiment. A container of gas with volume V_C is in contact with a volume and a heat reservoir. Locate a small volume element of molecular dimensions within the container. Suppose that the volume of the element is gradually and incrementally increased, capturing all molecules in its path. If the number of molecules that have been captured is plotted against the volume, a curve such as the one in Figure 8.1 may result.

Erratic behavior is expected when a relatively small number of molecules have been captured at low volumes where the characteristic dimension of the volume element is in the order of the distance between the molecules. If, however, the erratic behavior gradually decreases and finally disappears at some $V_{\max} \ll V_C$, the system can be treated as a continuum where statistical distributions such as the following may be used to deduce meaningful average properties for the system:

$f(\mathbf{r}, \mathbf{v}, t)$ = fraction of molecules in a small volume element about the point of the position vector $\bar{\mathbf{r}}$ which have velocities between $\bar{\mathbf{v}}$ and $\bar{\mathbf{v}} + d\bar{\mathbf{v}}$ at time t .

(8.1)

For example, the average velocity of a species i in a multi-component mixture

$$\mathbf{v}_i = \int_{-\infty}^{\infty} \int_{-\infty}^{\infty} \int_{-\infty}^{\infty} \mathbf{v} f_i(\mathbf{r}, \mathbf{v}, t) dv_x dv_y dv_z \quad (8.2)$$

Note that the molecular velocity under the integral sign is not attached to any single molecule. In order to carry out a local material balance, it will be necessary that the velocity vector and its first partial derivatives be continuous over the spatial coordinate. These requirements are what we mean by a thermodynamic phase so that a velocity field must be associated with each phase. All of the microscopic balance equations will be phase specific for this reason.

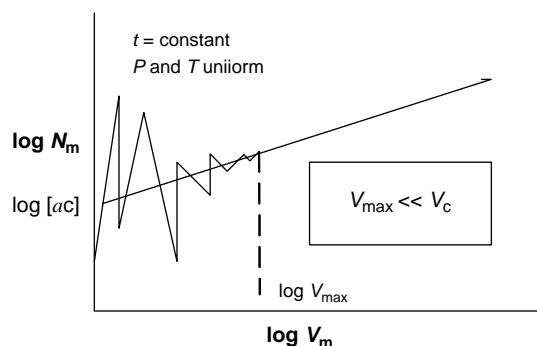


FIGURE 8.1 Molar density trial.

Full discussions of the molecular versus the continuum view may be found elsewhere (Hirschfelder et al., 1954). Our focus here is to express the laws of mass, momentum, and energy conservation in a continuum in coordinate-free representations and to express the conditions at the boundaries of such systems that permit the full description of the concentration, temperature, pressure, and velocity fields within.

The coordinate systems most often used in chemical engineering are the Cartesian rectangular, cylindrical, and spherical systems whose base vectors, $\delta_i (i = 1, 2, 3)$, are orthonormal. A review of these coordinate systems is given in the appendix with particular emphasis on the base vectors. A familiarity with the material in the appendix will facilitate the formulation of boundary conditions in the various coordinate systems and be of substantial help in the formulation of the conservation equations.

The conservation equations govern the distribution of mass, energy, and momentum. The distribution system is composed of the following fluxes.

8.1 MASS FLUX: AVERAGE VELOCITIES AND DIFFUSION

The velocity is an important variable because it is a major mechanism for the transport of mass, energy, and momentum in the system, but because, with a processing time, the velocity can lead to a equipment dimensions.

The velocity is a vector because its components in one system of coordinates can be obtained from those in another by a simple transformation law. The representation of the vector in one coordinate system is given by

$$\mathbf{v} = v_i \delta_i \quad (8.3)$$

where summation is indicated by the repeated subscript and δ_i is the base vector. There are two products defined for these

systems, the scalar or dot product and the vector or cross product. We will make use of the scalar product:

$$\delta_i \cdot \delta_j = \delta_{ij} \quad (8.4)$$

The components of a vector in one coordinate system (primed) can be obtained from those in another by the transformation law.

$$v_{i'} = \cos \theta_{i'i} v_i \quad (8.5)$$

where $\cos \theta_{i'i}$ is the cosine of the angle between the i' and the i directions.

We may also extract the components of a vector using the scalar product:

$$v_{i'} = \mathbf{v} \cdot \delta_{i'} = v_i \delta_i \cdot \delta_{i'} = \cos \theta_{i'i} v_i \quad (8.6)$$

The last step expresses the trigonometric result that the scalar product is the product of the magnitude of the vectors and the cosine of the angle between them.

In the sense that we know the elements of vector in all coordinate systems from those in one, the vector is an invariant whose picture we take with different cameras. The coordinate system is most often chosen to take advantage of physical symmetry in the system when expressing conditions on its behavior. We will revisit this idea when discussing boundary conditions.

The average species velocity defined above underpins the mass and molar flows that we have been using in the macroscopic view of the process streams. A key element of the relationship is the mass flux vector constructed as follows. Consider a small area δA with unit normal ξ through which component i is flowing with velocity \mathbf{v}_i . The area is illustrated in Figure 8.2.

The area may be located anywhere within a homogeneous region or phase of the fluid system. Homogeneity will provide the mathematical properties required for our calculations. The area may, for example, be within the pores of a supported catalyst particle, between the solid particles in a packed-bed absorber or a fixed-bed absorber or within a gas transmission line. The reader can generate some possibilities also.

If the unit normal vector is moved through various angles, the area will experience material flows ranging from a maximum when it is parallel to the velocity vector to

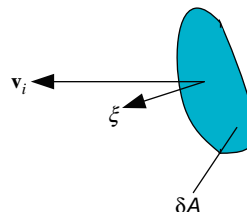


FIGURE 8.2 Flow through oriented surface.

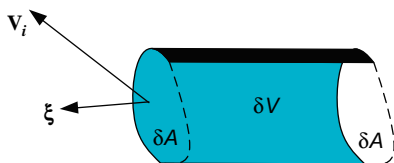


FIGURE 8.3 Volume element containing captured material flows.

zero when it is perpendicular. In any case, after the elapse of a small time δt , all of the material that has passed through δA is contained in the volume element δV illustrated in Figure 8.3.

The volume is given by

$$\delta V = (\mathbf{v}_i \cdot \boldsymbol{\xi}) \delta A \quad (8.7)$$

The mass of species i in the volume element is then

$$\delta m_i = \rho_i (\mathbf{v}_i \delta t \cdot \boldsymbol{\xi}) \delta A \quad (8.8)$$

We can note at this juncture that the accumulation of any property in the cylinder due to the mass velocity could be accounted for here by replacing the mass concentration with the property concentration. For example, the concentration of x momentum is ρv_x , which could replace the mass concentration in the preceding equation if we wished to account for the accumulation of x momentum.

The mass flow rate of species i per unit area or the flux of i in the ξ direction is obtained by dividing by the time and area increments.

$$\frac{\delta m_i}{\delta A \delta t} = (\rho_i \mathbf{v}_i) \cdot \boldsymbol{\xi} \quad (8.9)$$

The mass flux in a particular direction is the mass flow rate per unit area perpendicular to that direction. The vector $\rho_i \mathbf{v}_i$ is independent of the orientation of the area and has the property that the mass flux in any direction is its component in that direction. It is called the mass flux vector for this reason:

$$\mathbf{W}_i = \rho_i \mathbf{v}_i \quad (8.10)$$

The molar analog is

$$\mathbf{N}_i = c_i \mathbf{v}_i = \left[\frac{1}{M_i} \right] \mathbf{W}_i \quad (8.11)$$

8.1.1 Mass Flow Rates Used in Material Balances

The mass flow rates, which we have been using to express conservation of mass, are the macroscopic expression of these local flows. Consider flow of a process stream

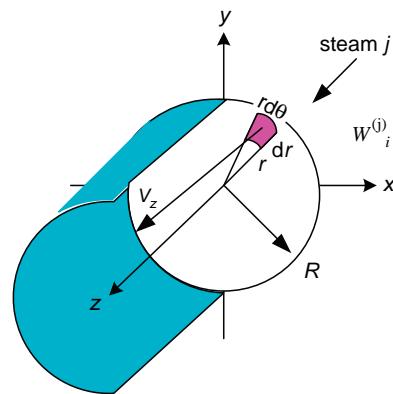


FIGURE 8.4 Cylindrical coordinates in a straight round tube.

j in a straight round tube of radius R , for example, and place a cylindrical coordinate system on the tube axis (see Figure 8.4).

The total mass flow rate of species i in the axial direction is given by adding the contributions from each area element over the total cross section of the pipe:

$$\mathcal{W}_i^{(j)} = \int_0^{2\pi} \int_0^R \underbrace{\rho_i \mathbf{v}_i \cdot \boldsymbol{\delta}_z}_{\substack{\text{axial} \\ \text{component} \\ \text{of mass} \\ \text{flux vector}}} \underbrace{h_r dr}_{\substack{ds_r \\ h_r = 1}} \underbrace{h_\theta d\theta}_{\substack{ds_\theta \\ h_\theta = r}} = \int_0^{2\pi} \int_0^R \rho_i v_{iz} r dr d\theta \quad (8.12)$$

where $\boldsymbol{\delta}_z$ is a unit vector in the axial direction and ds_q is a differential distance in the q coordinate direction. The mass flow rate through differential surfaces in other coordinate systems is expressed in similar fashion. Consider, as an example in a spherical system of coordinates, the mass flow rate of a reactant i to the surface of a catalytic particle coated on the exterior surface with active material illustrated in Figure 8.5.

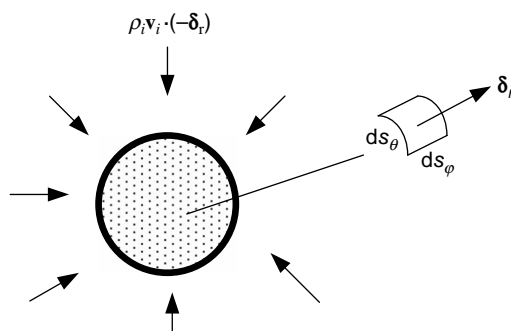


FIGURE 8.5 Radial flow of a reactant to a spherical catalytic surface.

$$\begin{aligned}
\mathcal{W}_i^{(\text{surface})} &= \int_0^\pi \int_0^{2\pi} \underbrace{\rho_i \mathbf{v}_i \cdot (-\mathbf{\delta}_r)}_{\substack{\text{radial component of} \\ \text{mass flux vector} \\ \text{in direction of} \\ \text{surface}}} \underbrace{h_\phi d\phi}_{\substack{ds_\phi \\ h_\phi = r \sin \theta}} \underbrace{h_\theta d\theta}_{\substack{ds_\theta \\ h_\theta = r}} \bigg|_{r=R} \\
&= - \int_0^{2\pi} \int_0^R \rho_i v_{iz}|_{r=R} R^2 \sin \theta d\theta d\phi \quad (8.13)
\end{aligned}$$

where ds_q is a differential distance in the q coordinate direction. In both cases, Equation (8.9) was used where the area factor is the product of the two differential distances normal to the ξ direction.

8.1.2 Average Velocities and Diffusion Flows

The mass flux of i is seen to be the mass of i per unit volume multiplied by the velocity by which it is propagated. If we carry this observation to the total flux of mass, we can express the result as the total mass concentration multiplied by a velocity.

$$\rho \mathbf{v} = \sum_{\text{all } i} \rho_i \mathbf{v}_i \quad (8.14)$$

The velocity, \mathbf{v} , is called the mass average velocity. It is a weighted average of the individual specie velocities. There is no flow of mass relative to this velocity. This can be seen by summing over the relative mass fluxes and using the definition of the mass average velocity provide by Equation (8.14):

$$\sum_{\text{all } i} \rho_i (\mathbf{v}_i - \mathbf{v}) = 0 \quad (8.15)$$

Consequently,

$$\mathcal{W} = \int_0^{2\pi} \int_0^R \rho \mathbf{v} \cdot \mathbf{\delta}_z r dr d\theta \quad (8.16)$$

If we collected the effluent from a pipe over a short (if flow is unsteady) time period and divided the collected mass by the time over which it was collected, we would have a measurement of the total mass flow rate expressed in Equation (8.16).

The velocity difference in each term of the summation in Equation (8.15) represents the flow of a component (i)

relative to the mass average velocity. An individual component can have a larger or smaller velocity with respect to the mass average velocity, but there is no net effect of these individual differences. Each component of the mixture is then seen to move at the mass velocity of the bulk fluid plus or minus some correction. The bulk movement is called convection and the relative movement is called diffusion.

$$\rho_i \mathbf{v}_i = \underbrace{\rho_i \mathbf{v}}_{\substack{\text{convection in mass} \\ \text{average reference frame}}} + \underbrace{\mathbf{j}}_{\substack{\text{diffusion in mass} \\ \text{average reference frame}}} \quad (8.17)$$

where

$$\mathbf{j}_i = \rho_i (\mathbf{v}_i - \mathbf{v}) \Rightarrow \sum_{\text{all } i} \mathbf{j} = 0 \quad (8.18)$$

and the molar analog is given by

$$\mathbf{n}_i = \left[\frac{1}{M_i} \right] \mathbf{j}_i \quad (8.19)$$

Note that the total mass flux vector is the concentration of momentum in the system so that this velocity will be important for expressing conservation of momentum.

Other average velocities may also be defined. The volume average velocity, for example, is defined by accumulating the underlying individual contributions of each species:

$$\mathbf{v}^\bullet = \sum_{\text{all } i} \rho_i \bar{V}_i \mathbf{v}_i \quad (8.20)$$

$$\text{Note that} \quad \sum_{\text{all } i} \rho_i \bar{V}_i = 1 \quad (8.21)$$

The \bar{V}_i are the partial specific volumes. The coefficient of the velocity of each species is the fractional volume contribution to the total volume of the system. There is no volume flow relative to the volume average velocity

$$\sum_{\text{all } i} \rho_i \bar{V}_i (\mathbf{v}_i - \mathbf{v}^\bullet) = 0 \quad (8.22)$$

so that \mathbf{v}^\bullet is the total volume flux.

$$\mathcal{V} = \int_0^{2\pi} \int_0^R \mathbf{v}^\bullet \cdot \mathbf{\delta}_z r dr d\theta \quad (8.23)$$

The volume average velocity is zero at a stationary phase boundary even though there may be a net flow of mass across the boundary. Volume changes on mixing that can take place in extraction and gas absorption, for example, can be reflected in the movement of a phase interface.

If we think of bulk fluid movement in terms of the volume average velocity, we can define the associated diffusion flows as follows:

$$\rho_i \mathbf{v}_i = \underbrace{\rho_i \mathbf{v}_i^\bullet}_{\text{convection in volume average reference frame}} + \underbrace{\mathbf{j}_i^\bullet}_{\text{diffusion in volume average reference frame}} \quad (8.24)$$

where

$$\mathbf{j}_i^\bullet = \rho_i (\mathbf{v}_i - \mathbf{v}^\bullet) \quad (8.25)$$

and

$$\sum_i \bar{V}_i \mathbf{j}_i^\bullet = 0 \quad (8.26)$$

The total mass flux is of course the same in both reference systems. The diffusional flows are therefore related. This relation and a generalization of the preceding discussion is summarized below.

The velocity and diffusive flows in an arbitrary reference frame are given by

$$\mathbf{v}^R = \frac{1}{W^R} \sum_i \rho_i w_i^R \mathbf{v} \quad (8.27)$$

$$\rho_i \mathbf{v}_i = \rho_i \mathbf{v}^R + \mathbf{j}_i^R \quad (8.28)$$

The diffusional flows are not independent since

$$\sum_k w_k^R \mathbf{j}_k^R = 0 \quad (8.29)$$

$$W^R = \sum_i \rho_i w_i^R \quad (8.30)$$

The definitions of the weights are given in Table 8.1.

Parameters for two other reference frames that have been used have been included in Table 8.1—the molar average frame and the solvent-fixed frame.

In many applications, simplifications are possible that essentially remove the distinction between the basic reference frames. For example, the assumption of constant mass density implies that the partial specific volume are all equal to its inverse and therefore that the mass average and volume

TABLE 8.1 Weighting Factors by Reference Frame

Reference (Frame)	w_i^R	W^R
Mass ()	1	ρ
Volume (°)	\hat{V}_i	1
Molar (N)	$1/M_i$	c
Solvent fixed	c	ρ_s

average reference frames are the same:

$$\rho \bar{V} = \sum_j m_j \Rightarrow \rho \bar{V}_i = \rho \left(\frac{\partial \bar{V}}{\partial m_i} \right)_{m_{k \neq i}} = 1 \quad (8.31)$$

$$\mathbf{v}^\bullet = \sum_i \rho_i \bar{V}_i \mathbf{v}_i = \sum_i \rho_i \frac{1}{\rho} \mathbf{v}_i \quad \text{or} \quad \rho \mathbf{v}^\bullet = \rho \mathbf{v} \quad (8.32)$$

$$\mathbf{v}^\bullet = \mathbf{v} \quad (8.33)$$

If the molar density is constant, the molar average velocity and the volume average velocity are the same:

$$c \bar{V} = \sum_j \frac{m_j}{M_j} \Rightarrow c \bar{V}_i = c \left(\frac{\partial \bar{V}}{\partial m_i} \right)_{m_{k \neq i}} = \frac{1}{M_i} \quad (8.34)$$

$$\mathbf{v}^* = \sum_i \rho_i \bar{V}_i \mathbf{v}_i = \sum_i \rho_i \frac{1}{M_i c} \mathbf{v}_i \quad (8.35)$$

$$\mathbf{v}^* = \frac{1}{c} \sum_i c_i \mathbf{v}_i = \mathbf{v}^N \quad (8.36)$$

In addition, for systems with components of equal molecular weight, the molar and mass average frames coincide.

In pure systems, there is of course no distinction (Table 8.2).

Another category of velocities called superficial velocities arises primarily in systems of more than one phase or more generally when the cross section being considered is not entirely available for flow.

TABLE 8.2 Conditions for Equality of Reference Frames

Assumption	Result
Constant mass density	$\mathbf{v} = \mathbf{v}^\bullet$
Constant molar density	$\mathbf{v}^N = \mathbf{v}^\bullet$
Equal molecular weights	$\mathbf{v} = \mathbf{v}^N$
Pure system	No distinction

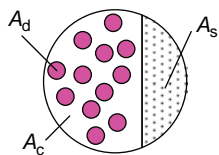


FIGURE 8.6 Multiphase cross section for flow.

8.1.3 Superficial Velocities

The area available to flow may not be connected in the sense that a line connecting two points in the flow area may not be contained completely in the flow area. For example, consider the flow of a fluid through the cross section in Figure 8.6.

The total cross section is made up of a connected closed portion that is not available to the fluid, A_s ; an unconnected portion that is also not available to the fluid, A_d , but with which the fluid may interact such as in extraction, adsorption, or catalytic systems; and a connected portion, A_c , made up of the fluid in question.

- In basic fixed-bed reactors, A_d is the stationary solid catalyst (assumed unavailable for bulk flow), A_s is not present, and A_c is the gas phase.
- In a distillation tower, A_s is a downcomer, A_c is the gas phase, and A_d is entrained liquid, if present.
- In a countercurrent extraction tower, A_s is not present, A_d represents the dispersed phase, A_c is the continuous phase, the two phases moving in opposite directions. The dispersed phase is itself a flowing fluid on which this discussion may therefore have been focused.

The total mass flow rate of the fluid through the cross section is given by

$$\mathcal{W} = \int_{A_c} \rho \mathbf{v} \cdot \boldsymbol{\xi} dA \quad (8.37)$$

where $\boldsymbol{\xi}$ represents the flow direction, normal to A_c . If the density is constant over the cross section, a common and useful approximation, then

$$\mathcal{W} = \rho \int_{A_c} \mathbf{v} \cdot \boldsymbol{\xi} dA = \rho A_c \langle v \rangle_{\text{int}} \quad (8.38)$$

$$\langle v \rangle_{\text{int}} = \frac{1}{A_c} \int_{A_c} \mathbf{v} \cdot \boldsymbol{\xi} dA \quad (8.39)$$

The average velocity of the fluid in the $\boldsymbol{\xi}$ direction is denoted by $\langle v \rangle_{\text{int}}$. It is referred to as the interstitial velocity in fixed-bed applications such as adsorption, absorption, and catalysis. It is real in the sense that the fluid would have this velocity if the velocity distribution over the connected area were constant.

Unreal or superficial velocities are defined for convenience as follows:

$$\mathcal{W} = \rho \langle v \rangle A \quad (8.40)$$

A can be the open area plus any one or the combination of the others. Since the density and mass flow rate are fixed, the average velocity and area are dependent, that is, their product is fixed. For example, we can define the following three superficial velocities:

$$\mathcal{W} = \rho \langle v \rangle_{\text{cds}} (A_c + A_d + A_s) \quad (8.41)$$

$$\mathcal{W} = \rho \langle v \rangle_{\text{cs}} (A_c + A_s) \quad (8.42)$$

$$\mathcal{W} = \rho \langle v \rangle_{\text{cd}} (A_c + A_d) \quad (8.43)$$

These velocities are all related by

$$\begin{aligned} \frac{\mathcal{W}}{\rho} &= \langle v \rangle_{\text{cds}} (A_c + A_d + A_s) = \langle v \rangle_{\text{cs}} (A_c + A_s) \\ &= \langle v \rangle_{\text{cd}} (A_c + A_d) = \langle v \rangle_{\text{int}} A_c \end{aligned} \quad (8.44)$$

Each is seen to be the product of a fractional area ratio and the interstitial velocity. Fluid area fractions are often approximated with the corresponding volume fractions. Care must be taken in the applications to discern what velocity is being employed.

Example 8.1.3-1 Slip Velocity in Liquid-Liquid and Gas-Liquid Systems

The slip velocity refers to the relative velocity of the dispersed and continuous phases in two-phase absorption and extraction towers (see Figure 8.7). To begin, we can focus on gas-liquid systems where the continuous phase is flowing downward and the dispersed phase is flowing up the column. Here, we are interested in the droplet rise velocity relative to the continuous phase in terms of the superficial velocities:

$$\langle v \rangle_c A_c = \langle v \rangle_{\text{cd}} (A_c + A_d)$$

$$\langle v \rangle_d A_d = \langle v \rangle_{\text{dc}} (A_d + A_c)$$

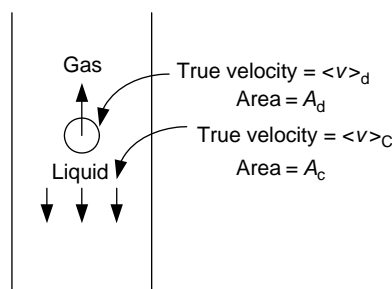


FIGURE 8.7 Gas-liquid dispersion.

or using volume fractions:

$$\langle v \rangle_c \phi_c = \langle v \rangle_{cd}$$

$$\langle v \rangle_d \phi_d = \langle v \rangle_{dc}$$

where

$$\phi_c + \phi_d = 1$$

$$v_{\text{droplet}} = \langle v \rangle_c + \langle v \rangle_d = \frac{\langle v \rangle_{cd}}{1 - \phi_d} + \frac{\langle v \rangle_{dc}}{\phi_d}$$

The result is easily modified for concurrent flow by changing the sign for the continuous phase velocity.

8.2 MOMENTUM FLUX: STRESS TENSOR

The mass flows were seen in the previous section to consist of a convection term and a diffusion term. The convective contribution consisted of two factors: the concentration of the conserved quantity and the velocity that propagated it for which a number of choices were discussed. These formats may be applied also to momentum transfer.

The most convenient convective velocity in the case of momentum transfer is the mass average velocity, since $\rho \mathbf{v}$ is already the concentration of momentum. The concentration of momentum in the system, say x momentum, is represented by ρv_x , the x component of the total mass flux vector. If instead of mass, x momentum were being followed in Figure 8.3, the resulting relation in Equation (8.10) would be $\rho v_x \mathbf{v}$, is the convective flux of x momentum with analogous expressions for y and z momentum.

Convection in the case of momentum transfer therefore consists of nine elements $v_i v_j$, ($i, j = x, y, z$) in the rectangular system. They are examples of the elements of a dyadic product:

$$\mathbf{v}\mathbf{v} = \begin{pmatrix} a_{11} & \dots & a_{1n} \\ \vdots & \ddots & \vdots \\ a_{m1} & \dots & a_{mn} \end{pmatrix}, \quad a_{ij} = v_i v_j \quad (8.45)$$

Because of the vector components, these quantities move between coordinate systems according to the following transformation law:

$$v_i' v_j' = v_i v_j \cos \theta_{i'i} \cos \theta_{j'j} \quad (8.46)$$

In the sense discussed above for the vector representation, the collection $v_i v_j$ constitutes an invariant between coordinate systems. The invariant is called a tensor, or more precisely in

our case, a second order Cartesian tensor. The counterparts of the unit vectors are the unit dyads, the dyadic products of \mathbf{i} :

$$\delta_i \delta_j = \begin{pmatrix} a_{11} & a_{12} & a_{13} \\ a_{21} & a_{22} & a_{23} \\ a_{31} & a_{32} & a_{33} \end{pmatrix}, \quad a_{nm} = \delta_{mi} \delta_{nj} \quad (8.47)$$

There are nine of these, one for each position occupied by 1 and the remaining positions with zeros. A tensor T can therefore be expressed as $T_{ij} \delta_i \delta_j$, that is,

$$\rho \mathbf{v}\mathbf{v} = \rho v_i v_j \delta_i \delta_j \quad (8.48)$$

There are two vector products, a tensor product, and a scalar product defined for the tensor:

$$\delta_i \delta_j \cdot \delta_k \delta_l = \delta_{jk} \delta_i \delta_l \quad (8.49)$$

$$\delta_i \delta_j \cdot \delta_k = \delta_{jk} \delta_i \quad (8.50)$$

$$\delta_i \cdot \delta_j \delta_k = \delta_{ij} \delta_k \quad (8.51)$$

$$\delta_i \delta_j : \delta_k \delta_l = \delta_{il} \delta_{jk} \quad (8.52)$$

They are so called because of their transformation properties and they are defined because they arise in applications. For example, the component of $\rho \mathbf{v}\mathbf{v}$ in the direction of a unit normal to an oriented surface is given by

$$\rho \mathbf{v}\mathbf{v} \cdot \mathbf{n} = \rho v_i v_j \delta_i \delta_j \cdot n_k \delta_k = \rho v_i v_j n_k \delta_i \delta_j \cdot \delta_k \quad (8.53)$$

$$= \rho v_i v_j n_k \delta_{jk} \delta_i = \rho (v_k n_k) v_i \delta_i \quad (8.54)$$

$$= \rho \mathbf{v} v_n \quad (8.55)$$

Consequently, $\rho \mathbf{v}\mathbf{v}$ is the convective flux of momentum in the same sense that $\rho \mathbf{v}$ is the mass flux vector, namely, that its component in any direction is the convective flux of momentum through an area oriented perpendicularly to that direction. We may say that the resulting force on the object into which the momentum flows is $\rho \mathbf{v}\mathbf{v} \cdot \mathbf{n} dA$.

This is not the total force on the surface. The thermodynamic pressure P , for example, exerts a normal stress on a surface, or a momentum flux in the normal direction. In the absence of convection, for example in solids, very strong stresses or momentum fluxes are known to be possible. If the small element of volume formed by a differential area cutting the coordinate plains and moving with the mass average velocity is subjected to Newton's First Law, the

following result is obtained. The element of area experiences a stress system or a momentum flux that can be represented by a second order Cartesian tensor. We can therefore express the total flux of momentum as

$$\Phi = \rho \mathbf{v} \mathbf{v} + \Pi \quad (8.56)$$

This expression is relative to the mass average velocity and corresponds to Equation (8.17) for the mass flux. It can be considered a definition of Π .

The average normal stress at a point in the medium can be obtained by integrating the normal force over the surface of a sphere of vanishingly small radius, ε :

$$4\pi\varepsilon^2 \langle P \rangle = \int_S \underbrace{\underbrace{(-\Pi \cdot \mathbf{n})}_{\text{Stress on surface with outward unit normal}} \cdot \underbrace{(-\mathbf{n})}_{\text{Unit normal to surface directed inward}}}_{\text{Normal stress on surface}} dS, \quad \mathbf{n} = \hat{\mathbf{d}}_r \quad (8.57)$$

The first factor in the integrand expresses the force on the surface and the second factor extracts the normal component of that force. The unit normal is the coordinate vector in the r direction: $\hat{\mathbf{d}}_r$. The momentum flux can be expanded in terms of a Taylor series about the center of the sphere. As the radius approaches zero, only the value at the center will contribute to the integral:

$$\langle P \rangle = \frac{1}{4\pi} \int_0^{2\pi} \int_0^\pi (\Pi(0) \cdot \hat{\mathbf{d}}_r \cdot \hat{\mathbf{d}}_r) \sin \theta d\theta d\phi \quad (8.58)$$

$$= \frac{1}{3} \text{tr} \Pi \quad (8.59)$$

where tr means to sum the diagonal elements.

The average normal stress is what we refer to as the pressure but it will be advantageous to maintain the distinction between P and $\langle P \rangle$. The total flux of momentum can be expressed in a finer grain as either

$$\Phi = \rho \mathbf{v} \mathbf{v} + \langle P \rangle \hat{\mathbf{d}} + \Pi_0 \quad (8.60)$$

or

$$\Phi = \rho \mathbf{v} \mathbf{v} + P \hat{\mathbf{d}} + \tau \quad (8.61)$$

The stress tensor Π_0 has zero trace and bears a similar relation to the total momentum flux as the diffusional flows bear to the total mass flows.

8.3 ENERGY FLUX: CONDUCTION

The energy content of an element of mass consists of the kinetic and potential energy of the element because of its motion and position in a potential field and of the “hidden” modes reflected by the temperature of the element. This latter constituent we identify with the internal energy of equilibrium thermodynamics and in so doing assume that the element of mass is in a state of “local equilibrium” with its neighbors in spite of the global nonequilibrium state of the system. Moreover, we will carry along all of the differential relationships for the thermodynamic functions. The title of “irreversible thermodynamics” is consequently often applied to the present subject.

The energy content per unit mass is therefore expressed as

$$e = u + \sum_i \left[\omega_i \left(\frac{1}{2} \mathbf{v}_i \cdot \mathbf{v}_i + \Psi_i \right) \right] \quad (8.62)$$

where Ψ_i is the potential energy per unit mass of species i . For example,

$$\text{Gravity:} \quad \Psi_i = g\mathcal{L} \quad (8.63)$$

$$\text{Electrochemical cell:} \quad \Psi_i = \frac{Z_i e^-}{M_i} \mathcal{F} \psi \quad (8.64)$$

\mathbf{J}_e , can be constructed incrementally as follows:

$$\text{Convection:} \quad \rho e \mathbf{v} \quad (8.65)$$

$$\text{Work against stress system:} \quad \Pi \cdot \mathbf{v} \quad (8.66)$$

Diffusion

$$\text{Internal, kinetic, and potential:} \quad \sum_i \left[\bar{U}_i + \frac{1}{2} \mathbf{v}_i \cdot \mathbf{v}_i + \Psi_i \right] \mathbf{j}_i \quad (8.67)$$

$$P dV \text{ work:} \quad \sum_i P \hat{V}_i \mathbf{j}_i \quad (8.68)$$

The remainder we call conduction relative to the mass average velocity, \mathbf{q} :

$$\mathbf{J}_e = \rho e \mathbf{v} + \Pi \cdot \mathbf{v} + \sum_i \left[\bar{U}_i + \frac{1}{2} \mathbf{v}_i \cdot \mathbf{v}_i + \Psi_i \right] \mathbf{j}_i + \sum_i P \hat{V}_i \mathbf{j}_i + \mathbf{q} \quad (8.69)$$

This constitutes a definition of the conductive flux. The terms may be combined to give

$$\mathbf{J}_e = \sum_i \left[\bar{H}_i + \frac{1}{2} \mathbf{v}_i \cdot \mathbf{v}_i + \Psi_i \right] \mathbf{W}_i + \tau \cdot \mathbf{v} + \mathbf{q} \quad (8.70)$$

where, from Equations (8.56) and (8.61),

$$\mathbf{\Pi} = P\mathbf{\delta} + \boldsymbol{\tau} \quad (8.71)$$

The energy flux associated with the shear stresses is rarely important in the nonisothermal chemical systems so that

$$\mathbf{J}_e = \sum_i \left[\bar{h}_i + \frac{1}{2} \mathbf{v}_i \cdot \mathbf{v}_i + \psi_i \right] \mathbf{W}_i + \mathbf{q} \quad (8.72)$$

Since all other terms are frame independent, the conduction term must also be independent of the reference frame. The kinetic and potential energy terms are also relatively unimportant in most applications so that the total energy flux in most chemical engineering applications is

$$\mathbf{J}_e = \sum_i [\bar{H}_i \mathbf{W}_i] + \mathbf{q} = \sum_i [\tilde{H}_i \mathbf{N}_i] + \mathbf{q} \quad (8.73)$$

The phrase “enthalpy balance” is often substituted for “energy balance” for obvious reasons.

8.4 BALANCE EQUATIONS

With the preceding definitions of the fluxes of mass, momentum, and energy, the associated conservation laws may be formulated in the microscopic scale. The goal is to arrive at a set of equations that govern the evolution of the state of the system in time and space coordinates. The state of the system is determined by the values of the concentrations, temperature, pressure, and velocity of its elements. This will not be possible until the fluxes are represented in these terms. To accomplish this in a rational manner, a microscopic entropy balance will be used to display the sources of irreversibilities in the system that will serve to identify the fluxes and the forces that drive them.

Consider a two-phase system and construct a small arbitrary, stationary, volume element in either phase that does not include the phase boundary (see Figure 8.8).

We exclude the phase boundary because we need to have continuity in the system properties in order to carry out the

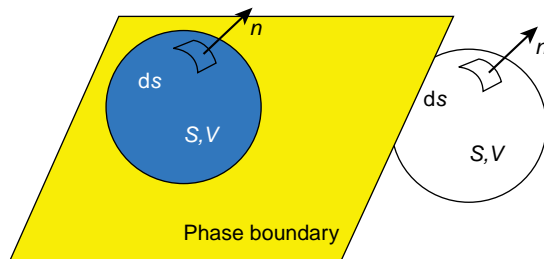


FIGURE 8.8 Intraphase location of volume element.

mathematical operations that follow. The result will be a differential equation for each conservation law and conditions at the phase boundary that connect the solutions to the phase-specific equations. The boundary conditions will be constructed to maintain the conservation laws and to express the assumption of local equilibrium that was expressed above. It calls for local thermal, mechanical, and chemical equilibrium at the phase boundary and supplies the needed continuity in the system properties in each phase.

8.4.1 Mass Conservation

The mass rate of flow of species i out of the volume element is given by adding the fluxes through the small differential elements with outwardly pointing normals that comprise the surface:

$$\iint_S \rho_i \mathbf{v}_i \cdot \mathbf{n} dS \quad (8.74)$$

The divergence theorem (see Appendix D) allows the expression to be converted from a surface to a volume integral, which will be more useful below:

$$\iiint_V \nabla \cdot (\rho_i \mathbf{v}_i) dV = \iint_S \rho_i \mathbf{v}_i \cdot \mathbf{n} dS \quad (8.75)$$

The continuity requirements for this conversion call for the volume to be within a single homogeneous phase.

The generation of species i inside the volume element produces a net accumulation rate for the element given by

$$\iiint_V r_{iv} dV \quad (8.76)$$

where r_{iv} is the local mass rate of production of species i per unit volume due to all of the chemical reactions that take place within the volume element. The molar analogue is R_{iv} so that

$$r_{iv} = M_i R_{iv} \quad (8.77)$$

The molar rate per unit volume of reaction j is R_j , then

$$R_{iv} = \sum_{\text{all } j} \vartheta_{ij} R_j \quad (8.78)$$

The rate of change of the mass of i inside the volume element is

$$\frac{\partial}{\partial t} \iiint_V \rho_i dV \quad (8.79)$$

The rate of change is equal to the rate of production less the loss through the surface or

$$\iiint_V \left[\frac{\partial \rho_i}{\partial t} + \nabla \cdot (\rho_i \mathbf{v}_i) - r_{iv} \right] dV = 0 \quad (8.80)$$

Since the volume element is arbitrary, the integrand must vanish everywhere in the homogeneous phase:

$$\frac{\partial \rho_i}{\partial t} + \nabla \cdot (\rho \mathbf{v}_i) = r_{iv} \quad (8.81)$$

$$\frac{\partial \rho_i}{\partial t} + \nabla \cdot (\rho_i \mathbf{v} + \mathbf{j}_i) = r_{iv} \quad (8.82)$$

By adding the individual mass balances, the equation of continuity (total mass) is obtained

$$\frac{\partial \rho}{\partial t} + \nabla \cdot (\rho \mathbf{v}) = 0 \quad (8.83)$$

The sum of the diffusional flows is zero and there is no net production of mass by chemical reaction.

Equations (8.82) and (8.83) must be augmented with initial and boundary conditions as well as expression of the reaction kinetics and diffusional flows in terms of the system variables. This will be addressed in Section 8.5.

8.4.2 Linear and Angular Momentum Balance

Calculations similar to those used for the mass balance will yield the momentum balance for the volume element that constitutes an expression of Newton's First Law for a convective system. The existence of body forces per unit mass such as gravity are admitted and play a role similar to chemical reactions in the expression of conservation of mass in that they express a generation of momentum per unit mass of the system. The result for the conservation of linear momentum is

$$\frac{\partial \rho \mathbf{v}}{\partial t} + \nabla \cdot \Phi^t = \rho \mathbf{f}_b \quad (8.84)$$

where

$$\Phi^t = \rho \mathbf{v} \mathbf{v} + \Pi^t \quad (8.85)$$

and

$$\mathbf{f}_b = \sum_i \omega_i \mathbf{f}_b \quad (8.86)$$

Chemical reactions do not appear here since they experience no change in mass.

The angular momentum or the moment of momentum balance is satisfied if Π is symmetric:

$$\Pi = \Pi^t \quad (8.87)$$

As with the mass balances, Equation (8.82), the momentum balances in Equations (8.84) and (8.85) need to be expressed in terms of system variables before they can be used to any significant extent. The issue will be addressed in Section 8.5.

8.4.3 Conservation of Energy

Following the same procedure as in the mass balance, conservation of energy may be written as

$$\frac{\partial \rho e}{\partial t} + \nabla \cdot \mathbf{J}_e = 0 \quad (8.88)$$

There is no source term for the energy balance and unlike the momentum and mass balances, the conserved quantity is not normally a state variable. To replace the total energy content with state variables, we can begin by separating the constituents of the total energy, the internal, kinetic, and potential energies, and arrive at balance equations for each one of them as follows:

$$\frac{\partial \rho e}{\partial t} = \underbrace{\frac{\partial \rho u}{\partial t}}_{\text{Internal energy}} + \underbrace{\frac{\partial}{\partial t} \frac{1}{2} \left[\sum_i \rho_i \mathbf{v}_i \cdot \mathbf{v}_i \right]}_{\text{Kinetic energy}} + \underbrace{\frac{\partial}{\partial t} \left[\sum_i \rho_i \psi_i \right]}_{\text{Potential energy}} \quad (8.89)$$

The kinetic energy of the mixture may be thought of in terms of bulk motion and diffusional flows. The diffusional flows are due to motion relative to the mass average velocity:

$$\text{Diffusional component} = \frac{1}{2} \rho_i (\mathbf{v}_i - \mathbf{v}) \cdot (\mathbf{v}_i - \mathbf{v}) \quad (8.90)$$

• Kinetic Energy

The kinetic energy term can be restructured as follows:

$$\frac{1}{2} \left[\sum_i \rho_i \mathbf{v}_i \cdot \mathbf{v}_i \right] = \frac{1}{2} \rho \mathbf{v} \cdot \mathbf{v} + \frac{1}{2} \left[\sum_i \rho_i (\mathbf{v}_i - \mathbf{v}) \cdot (\mathbf{v}_i - \mathbf{v}) \right] \quad (8.91)$$

The second term on the right-hand side is called the "kinetic energy of diffusion" and can be safely neglected. The derivative of the kinetic energy term is therefore given by

$$\frac{1}{2} \frac{\partial}{\partial t} \left[\sum_i \rho_i \mathbf{v}_i \cdot \mathbf{v}_i \right] \cong \frac{1}{2} \frac{\partial}{\partial t} \rho \mathbf{v} \cdot \mathbf{v} = \frac{1}{2} \mathbf{v} \cdot \frac{\partial \rho \mathbf{v}}{\partial t} + \frac{1}{2} \mathbf{v} \cdot \left[\frac{\partial \rho \mathbf{v}}{\partial t} - \mathbf{v} \frac{\partial \rho}{\partial t} \right] \quad (8.92)$$

The preceding identity is derived in the appendix. The equations of continuity and motion can be substituted into the preceding equation to arrive at the final expression for the derivative of the kinetic energy term:

$$\begin{aligned} \frac{\partial \rho(v^2/2)}{\partial t} + \nabla \cdot \rho(v^2/2)\mathbf{v} = & -\mathbf{v} \cdot \nabla p - \nabla \cdot (\boldsymbol{\tau} \cdot \mathbf{v}) \\ & - (-\boldsymbol{\tau} : \nabla \mathbf{v}) + \rho \mathbf{v} \cdot \mathbf{f}_b \end{aligned} \quad (8.93)$$

The required calculations are included in Appendix D. The term $(-\boldsymbol{\tau} : \nabla \mathbf{v})$ appears as a loss of kinetic energy above. It appears as a source term in the temperature explicit form of the internal energy balance. It may therefore be regarded as a degradation of mechanical energy into heat.

• Potential Energy

The mass conservation equations can be used directly in the derivative of the potential energy term and we assume that the individual potential functions are independent of time and produce the individual body forces: $\mathbf{f}_{bi} = -\nabla \Psi_i$. The result is that

$$\frac{\partial \rho \Psi}{\partial t} + \nabla \cdot \left(\sum \rho_i \Psi_i \mathbf{v} + \Psi_i \mathbf{j}_i \right) = - \sum \mathbf{w}_i \cdot \mathbf{f}_{bi} \quad (8.94)$$

where the following conservation relation for the potential functions has been applied:

$$\sum \vartheta_{ij} M_i \Psi_i = 0 \quad (8.95)$$

• Internal Energy

Substitution of the balance equations for kinetic and potential energy into the conservation equation for total energy gives

$$\frac{\partial \rho u}{\partial t} + \nabla \cdot \left[\rho u \mathbf{v} + \sum_i \bar{H}_i \mathbf{j}_i + \mathbf{q} \right] = \sum_i \mathbf{j}_i \cdot \mathbf{f}_{bi} - \boldsymbol{\Pi} : \nabla \mathbf{v} \quad (8.96)$$

Conservation of energy is expressed by the preceding three equations. However, the expression of energy conservation in terms of state variables is not accomplished by Equation (8.95) because of the appearance of the internal energy function.

The conservation of internal energy can be expressed in terms of temperature through the differential relationships available for nonflow systems in equilibrium thermodynamics on the basis of local equilibrium. The differentials in thermodynamic relations, for example,

$$du = T ds - P dv + \sum_i \hat{\mu}_i d\omega_i \quad (8.97)$$

where

$$ds = \left(\frac{\partial s}{\partial T} \right)_{p,\omega} dT + \left(\frac{\partial s}{\partial p} \right)_{T,\omega} dp + \sum_i \bar{S}_i d\omega_i \quad (8.98)$$

may be referred to as an element of mass moving with the mass average velocity in order to maintain the nonflow framework of equilibrium thermodynamics. There would be no net flow of mass across the surface of the element moving with the mass average velocity. The differentials in this case are given by the chain rule where the coordinates are moving with the mass average velocity:

$$\frac{df}{dt} = \frac{\partial f}{\partial t} + v_x \frac{\partial f}{\partial x} + v_y \frac{\partial f}{\partial y} + v_z \frac{\partial f}{\partial z} \quad (8.99)$$

The derivative is referred to as the substantial derivative to maintain this distinction:

$$\frac{df}{dt} = \frac{Df}{Dt} = \frac{\partial f}{\partial t} + \mathbf{v} \cdot \nabla f \quad (8.100)$$

The thermodynamic expression in Equation (8.96) is therefore written as

$$\frac{Du}{Dt} = T \frac{Ds}{Dt} + \frac{P}{\rho^2} \frac{D\rho}{Dt} + \sum_i \mu_i \frac{D\omega_i}{Dt} \quad (8.101)$$

If $\hat{\xi}$ is any quantity per unit mass, it can be shown using the equation of continuity that

$$\frac{\partial \rho \hat{\xi}}{\partial t} + \nabla \cdot \rho \hat{\xi} \mathbf{v} = \rho \frac{D\hat{\xi}}{Dt} \quad (8.102)$$

Therefore, the following substitutions from the balance equations can be made in the thermodynamic differential relations in Equation (8.100):

$$\rho \frac{Du}{Dt} = \frac{\partial \rho u}{\partial t} + \nabla \cdot [\rho u \mathbf{v}] = \sum_i \mathbf{j}_i \cdot \mathbf{f}_{bi} - \boldsymbol{\Pi} : \nabla \mathbf{v} - \sum_i \bar{H}_i \mathbf{j}_i + \mathbf{q} \quad (8.103)$$

$$\rho \frac{D\omega_i}{Dt} = \frac{\partial \rho_i}{\partial t} + \nabla \cdot [\rho_i \mathbf{v}] = r_{iv} \quad (8.104)$$

$$T \frac{Ds}{Dt} = \hat{c}_p \frac{DT}{Dt} - \frac{1}{\rho} \left[\frac{\partial \ln \rho}{\partial \ln T} \right]_{p,\omega} \frac{DP}{Dt} + \sum_i \mu_i S_i \quad (8.105)$$

$$\frac{D\rho}{Dt} = -\rho \nabla \cdot \mathbf{v} \quad (8.106)$$

The result is the temperature explicit form of the internal energy equation:

$$\rho \hat{c}_p \frac{DT}{Dt} + \nabla \cdot \mathbf{q} = -\tau : \nabla \mathbf{v} - \left[\frac{\partial \ln \rho}{\partial \ln T} \right]_{P,\omega} \frac{Dp}{Dt} + \sum_j (-\Delta H_{Rj}) \mathcal{R}_j - \frac{1}{M_i} \sum_i \mathbf{j}_i \cdot \nabla \tilde{H}_i + \sum_i \mathbf{j}_i \cdot \mathbf{f}_b \quad (8.107)$$

where

$$-\Delta H_{Rj} = \sum_i \vartheta_{ij} \tilde{H}_i \quad (8.108)$$

The two equations are completely equivalent but from a practical viewpoint the temperature explicit form is much preferred.

The term, $(-\tau : \nabla \mathbf{v})$, appears as a loss in the kinetic energy in Equation (8.92) and as a source in the internal energy balance in Equation (8.102), including the temperature explicit form Equation (8.106). It is therefore interpreted as a loss or degradation of kinetic to thermal energy. The term is largely influenced by velocity gradients, which are generated in the vicinity of solid walls. These interactions are found, for example, with conduits such as pipes and pipe bends and with submerged objects such as those encountered in packed beds. A pressure drop results in these cases, which must be compensated by the pressure of the process stream or by the intervention of a pump or compressor. Some examples are considered in Chapter 14 when the macroscopic view is readopted from the basis of the microscopic equations. Here, we take the opposite route.

8.5 ENTROPY BALANCE AND FLUX EXPRESSIONS

At this juncture, the microscopic balance equations form an open set in the sense that they are incomplete and cannot be solved until the reaction rates and the irreversible fluxes of mass, energy, and momentum relative to the mass average velocity have been expressed in terms of the dependent state variables: concentration, temperature, pressure, and velocity.

The generation of entropy is due to the irreversible processes that are taking place in the microscopic system. These irreversible processes are due to fluxes and forces that are not present at equilibrium. We expect the entropy generation, therefore, to identify these fluxes and the forces or imbalances that drive them.

An entropy balance may be struck by first rearranging Equation (8.100):

$$\rho \frac{Ds}{Dt} = \frac{1}{T} \underbrace{\rho \frac{Du}{Dt}}_{\text{Equation (8.102)}} - \frac{1}{T} \frac{P}{\rho} \underbrace{\frac{D\rho}{Dt}}_{\text{Equation (8.105)}} - \sum_i \frac{\mu_i}{T} \underbrace{\rho \frac{D\omega_i}{Dt}}_{\text{Equation (8.103)}} \quad (8.109)$$

Making the substitutions indicated in Equation (8.109) will yield an equation that can be put in the following format if the entropy flux is identified:

$$\rho \frac{Ds}{Dt} + \nabla \cdot \mathbf{j}_s = T\sigma \quad (8.110)$$

A suitable definition of the entropy flux in the mass average frame comprises the conductive flux at the local temperature as well as that carried by the diffusive flows:

$$\mathbf{j}_s = \frac{\mathbf{q}}{T} + \sum_i \tilde{S}_i \mathbf{j}_i \quad (8.111)$$

The balance of the terms comprise the generation term. The result for the generation term can be expressed as the sum of three contributions, each determined by a common scalar, vector, or tensorial nature of the processes that are represented. In each case, the processes appear in the form of a flux or rate multiplied by a force, that is,

$$\sum \mathcal{Q}_i \circ \{\mathcal{X}_i\}, \circ = \text{scalar product}$$

$$\sigma = \sigma_0(\text{scalar processes}) + \sigma_1(\text{vector processes}) + \sigma_2(\text{tensor process}) \quad (8.112)$$

$$\sigma_0 = (\langle P \rangle - P) \{-\nabla \cdot \mathbf{v}\} + \sum \mathcal{R}_{jv} \{\mathcal{A}_j\} \quad (8.113)$$

$$\sigma_1 = \mathbf{q} \cdot \{-\nabla \ln T\} + \sum_i \mathbf{j}_i \cdot \{-[\nabla_T \mu_i - \mathbf{f}_{bi}]\} \quad (8.114)$$

$$\sigma_3 = \mathbf{\Pi}_0 : \{-(\nabla \mathbf{v})_{os}\} \quad (8.115)$$

The subscript on the divergence in Equation (8.114) means differentiation at a constant T . The symmetric part of $(\nabla \mathbf{v})_0$ is $(\nabla \mathbf{v})_{os}$ where

$$(\nabla \mathbf{v})_0 = \nabla \mathbf{v} - \left(\frac{1}{3} \text{tr} \nabla \mathbf{v} \right) \delta \quad (8.116)$$

The chemical affinity of reaction j is defined by

$$\mathcal{A}_j = \sum_i \vartheta_{ij} \mu_i \quad (8.117)$$

The rates, forces, and flows vanish together at equilibrium. It is reasonable then to regard the fluxes as functions of the forces and to express this functionality in a Taylor series about the equilibrium condition:

$$\mathcal{Q}_i = 0 + \sum_j \mathcal{L}_{ij} (\mathcal{X}_j - 0) + \text{higher order terms} \dots \quad (8.118)$$

In an isotropic system, the forces must be of the same tensor order as the fluxes (Curie's principle). Otherwise the coefficients would need a directional character to resolve the difference. Therefore, the preceding series refers to each of the generation terms in Equation (8.112) separately.

If the system is not far removed from equilibrium, only the first term may be necessary and we arrive at the linear laws proposed by Onsager (1931), who showed that the coefficients need to be symmetric ($\mathcal{L}_{ij} = \mathcal{L}_{ji}$). The off-diagonal elements reflect the thermodynamic coupling of the microscopic processes. The major contribution in most circumstances, however, is given by the diagonal term that provides the flux expressions required to complete the formulation of the microscopic balance equations as discussed below.

8.5.1 σ_0 : Scalar Processes

The two scalar processes represented in the entropy production are volume flow and reaction kinetics.

8.5.1.1 Volume Flow A difference between the normal stress in a flow system ($\langle P \rangle$) and that which would persist in the absence of flow (hydrostatic or thermodynamic pressure, P) is predicted due to the local volume flow per unit volume of the system.

$$(\langle P \rangle - P) = -\kappa \nabla \cdot \mathbf{v} \quad (8.119)$$

The chemical affinities would also appear in the preceding equation if thermodynamically coupled flows were considered.

The phenomenological coefficient, κ , is called the bulk or volume viscosity. Measurements have found that the bulk viscosity is negligible for most fluids. It is zero for a low-density monatomic gases and is a small number for dense gases and liquids (Bird et al., 2002). It will be neglected here so that

$$\langle P \rangle = P \quad (8.120)$$

$$\Pi_0 = \tau \quad (8.121)$$

8.5.1.2 Homogeneous Reaction Kinetics A complete expression of the linear laws would have each reaction rate proportional to a linear combination of all the chemical affinities. The thermodynamically uncoupled expression of the linear laws does not include the accompanying affinities, that is,

$$\mathcal{R} = -\mathcal{L}A \quad (8.122)$$

where, from Equations (8.117) and (6.192),

$$\mathcal{A} = \sum \vartheta_i \mu_i^0 + RT \sum \vartheta_i \ln \frac{\hat{f}_i}{f_i^0} \quad (8.123)$$

Introducing the equilibrium constant from Equation (6.194)

$$\mathcal{A} = RT[-\ln K(T) + \ln K_a] \quad (8.124)$$

where

$$\ln K_a = \sum \vartheta_i \ln \frac{\hat{f}_i}{f_i^0} \quad (8.125)$$

The reaction rate is then given by

$$\mathcal{R} = -\mathcal{L}RT \ln \frac{K_a}{K(T)} \quad (8.126)$$

At equilibrium, $K_a = K$. Regarding the reaction rate as a function of the ratio, the logarithm in Equation (8.126) may be expressed as Taylor series for conditions not far removed from equilibrium.

$$\mathcal{R} \approx -\mathcal{L}RT \left(\left\{ 0 + (1) \left[\frac{K_a}{K(T)} - 1 \right] + \dots \right\} \right) \quad (8.127)$$

or

$$\mathcal{R}_v \approx k \left[\prod_{\text{Reactants}} a_i^{|\vartheta_i|} - \frac{1}{K(T)} \prod_{\text{Products}} a_i^{\vartheta_i} \right] \quad (8.128)$$

where

$$k = \mathcal{L}RT \frac{1}{\prod_{\text{Reactants}} a_i^{|\vartheta_i|}} \quad (8.129)$$

Equation (8.128) is the format of the familiar mass action expression representing a reversible reaction, the forward rate being the first term and the reverse rate being the second term. To be effectively incorporated into the microscopic balance equations, the activities need to be expressed in terms of concentrations, temperature, and pressure. For ideal gas phase reactions, for example, the activity can be replaced with the mole fraction times the total pressure. For ideal liquid phase reactions at a constant molar density, the activity may be replaced with the molar concentration.

In more general terms, the product factors need not contain only reactants or products as indicated. However, the resulting equilibrium ratio obtained by setting the rate to zero must be an integer power of the thermodynamic result, $K(T)$ (Aris, 1965; Denbigh, 1971) if the expression is to be applied near equilibrium. The power to which a concentration is raised is the order of the forward or reverse reaction with respect to that component. For elementary reactions where the stoichiometry represents the actual molecular events, the reaction order for each component is the unsigned stoichiometric coefficient. In any event, the order with respect to any of the reagents is rarely greater than 2.

TABLE 8.3 Rate Constant Temperature Dependence (Espenson, 1981)

<i>E</i>	<i>N</i>	Source
Activation energy	0	Arrhenius
Critical collision energy	$1/2$ Temperature dependence of collision frequency	Collision theory
Enthalpy of activation	1 Temperature dependence of universal frequency	Absolute rate theory

The reaction rate constant, k , has been found to represent a wide range of kinetic data with only the following temperature dependence:

$$k = k_0 T^n e^{-E/RT} \quad (8.130)$$

The parameters k_0 , n , and E must be determined experimentally. Recall Example 6.6.2-21 (Table 8.3).

If k is carried inside the parentheses in Equation (8.128), it is clear that the reverse rate constant is given by

$$k_- = \frac{k}{K(T)} \quad (8.131)$$

The temperature dependence of the equilibrium constant is given by Equation (6.201). Consequently,

$$E - E_r = \Delta H_R \quad (8.132)$$

Finally, it can be noted that homogeneous reactions in a fluid phase, the solution to the balance equations with reaction kinetics in the format discussed above provides the change in the state variables for the fluid stream between a reactor input and output. The change provides the information required to calculate, conversion, selectivity, and productivity.

8.5.1.3 Heterogeneous Catalytic Kinetics Heterogeneous catalytic kinetics refers to cases where the catalyst exists in a separate phase from the reaction components. Very few industrially important systems will be overlooked if we restrict the discussion to solid catalysts and fluid reaction mixtures. This will, for example, include the acrylic acid and hexyl glucoside processes that appear throughout this book and many other systems as well. Refer to Table 1.2 and Section 1.3.

The expressions for the reaction rate term in the microscopic balances for heterogeneous catalytic kinetics can be rationalized from an introduction to the tools available for formulating rate expressions that can correlate rate data, in addition to accounting for other data such as mass

spectrometry, nuclear magnetic resonance data, and so on, data obtained for such systems. The formation of a candidate rate expression generally entails:

- Formation of reaction mechanism.
- Expression of reaction rates in mechanism.
- Application of the steady-state approximation.
- An active center balance.
- Rate controlling step.

All of the preceding will be illustrated in the following two sections. A brief description is given here.

By reaction mechanism, we mean a closed sequence of elementary reactions, which lead from the reactants to the products of an overall reaction whose progress can be measured by a single extent (Boudart, 1968). Elementary reactions are closed sequences of molecular events between the stable species representing the overall stoichiometry, reactive intermediates, and active centers. Other species in a transition state between the species from which they are formed and the species they are about to become are also present. These intermediates cannot be isolated and are not explicitly represented in telemetry reactions. Elementary reactions follow mass action kinetics.

Active centers are the sites where a relatively stable species becomes highly reactive through interactions with the active center. Association of a reactant with an active center is a step in the closed sequence of elementary reactions. The sequence is closed when the depletion of an active center is followed by its release in the sequence.

The highly reactive intermediates are short-lived. The “steady-state approximation” states that after a short time of the same order of magnitude as the turnover frequency [see Equation (8.134)] the rates of reaction of the reactive intermediates may be set to zero, that is, the rates of formation are equal to the rates of depletion. This implies that the rates of all reactions in the closed sequence are equal.

It may be that one of the steps in the sequence of reactions is rate controlling in the sense that the other reactions are sufficiently close to equilibrium that their rates may be set to zero and the reaction rate set equal to the rate of the controlling step. This presumes that the other reactions are reversible. In more quantitative terms.

Rate determining step: Consider a single reaction with rate r , the result of a forward and a reverse rate, r_f and r_b , respectively. Given r and r_b , the forward rate could be calculated from $r_f = r_b(1 + r/r_b)$. If, however, the forward rate was judged to be equal to r_b , the relative error would be $[r_b(1 + r/r_b) - r_b]/r_b = r/r_b$, which approaches zero as r_b increases.

Refer to Table 1.2 for a variety of examples of heterogeneous catalytic systems from the petrochemical industry, and to Section 1.3 for examples of biocatalytic systems. Heterogeneous catalysts may be supported or freely suspended in

solution (see Chapter 5). Examples of the preceding discussion will be found in the following two sections.

8.5.1.3.1 Suspensions—Enzyme Kinetics Enzymes, although we may think of them as preferring the aqueous environment offered by the human body, have been found to function vigorously when freely suspended in organic solvents (Klibanov, 1986). This discovery has led to improvements in enzyme stability, reactant solubility, and diminished side reactions involving water. Whole cells, such as baker's yeast and *Escherichia coli*, may be suspended in aqueous solutions. Platinum may be suspended in the solvent for hydrogenation reactions. Therefore, although in this section we will refer to the case of suspended enzymes, they may be thought of in more general terms as active centers, which were defined above.

We will assume that the number of active units per unit volume of the reaction mixture is sufficiently large so that a limiting process such as that illustrated in Figure 8.1 is satisfied. Note, for example, that 10^8 cells/ml is representative for yeast and bacteria (Aiba et al., 1973). We define a pseudohomogeneous reaction rate for the microscopic mass balance (Equation 8.81) as

$$r_{iV} = \rho_{E0} r_{iE} \quad (8.133)$$

or in molar units

$$r_{iV} = M_i c_{E0} \mathcal{R}_{iE} \quad (8.134)$$

where the mass concentration of the active units in the solution is ρ_c and r_{iE} is the rate of production of species i per unit mass of active material. The product is the rate per unit volume of the bulk phase.

The determination of r_{iE} is the result of a kinetic study.

Example 8.5.1.3.1-1 Ping-Pong Bi-Bi mechanism

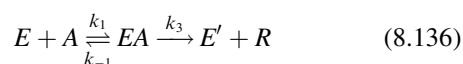
See Davis and Davis (2003).

Consider the bimolecular reaction between A and B to produce the products R and S :

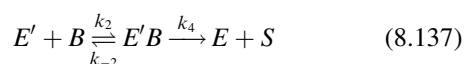


Elementary Reactions—Molecular Model:

Suppose that A combines with the enzyme to form a very reactive intermediate, EA .



The product R is released from EA with a fragment left behind to react with B :



B attaches to an enzyme containing a fragment, E' , to form yet another reactive intermediate $E'B$. The product S and the naked enzyme E detach from E' .

Elementary reaction rates:

These are molecular events and we apply the law of mass action:

$$r_A = -k_1 c_A c_E + k_{-1} c_{EA} \quad (8.138)$$

$$r_B = -k_2 c_{E'} c_B + k_{-2} c_{E'B} \quad (8.139)$$

$$r_R = k_3 c_{EA} \quad (8.140)$$

$$r_S = k_4 c_{E'B} \quad (8.141)$$

$$r_{EA} = k_1 c_A c_E - (k_{-1} + k_3) c_{EA} \quad (8.142)$$

$$r_{E'} = k_3 c_{EA} - k_2 c_{E'} c_B + k_{-2} c_{E'B} \quad (8.143)$$

$$r_{E'B} = k_2 c_{E'} c_B - (k_{-2} + k_4) c_{E'B} \quad (8.144)$$

$$r_E = k_4 c_{E'B} + k_{-1} c_{EA} - k_1 c_A c_E \quad (8.145)$$

Quasisteady-state approximation (QSSA):

$$c_E = \left(\frac{k_{-1} + k_3}{k_1} \right) \frac{c_{EA}}{c_A} \quad (8.146)$$

EA rate:

E' and $E'B$ rates

$$\left\{ c_{E'B} = \frac{k_3}{k_4} c_{EA} \right. \quad (8.147)$$

$$\left\{ c_{E'} = (k_{-2} + k_4) \frac{k_3}{k_2 k_4} \frac{c_{EA}}{c_B} \right. \quad (8.148)$$

Note that the QSSA will always provide one relation for each reactive intermediate. An additional relation is needed to account for the unknown enzyme concentration. This is provided by the enzyme balance.

Enzyme balance:

$$c_E + c_{E'} + c_{E'A} + c_{E'B} = c_{E0} \quad (8.149)$$

where c_{E0} is the initial free enzyme concentration. The value of c_{EA} may be obtained from this result and the preceding consequences of the quasisteady-state approximation.

$$c_{EA} = \frac{c_{E0}}{((k_{-1} + k_3)/k_1)(1/c_A) + (k_{-2} + k_4)(k_3/k_2 k_4)(1/c_B) + k_3/k_4 + 1} \quad (8.5.150)$$

Note that the QSSA and enzyme balance equations may be solved in any order that you find convenient.

Consequently,

$$c_E = \frac{((k_{-1} + k_3)/k_1)c_{E0}c_B}{((k_{-1} + k_3)/k_1)c_B + (k_{-2} + k_4)(k_3/k_2k_4)c_A + ((k_3/k_4) + 1)c_Ac_B} \quad (8.151)$$

Reaction rate:

Any one of the reactants or products (from the overall stoichiometry) may be selected to express the reaction rate

$$\mathcal{R}_{Rv} = \mathcal{R}_v = k_3c_{EA} = \frac{(k_3k_4/(k_3 + k_4))c_{E0}c_Ac_B}{c_Ac_B + (k_3/k_2)((k_{-2} + k_4)/(k_3 + k_4))c_A + (k_4/k_1)((k_{-1} + k_3)/(k_3 + k_4))c_B} \quad (8.152)$$

The turnover number or frequency for an enzyme is defined as the maximum number of molecules of product that can be produced per unit time per molecule of enzyme or the number of times that the catalytic cycle is completed per unit of time. The value depends on the reaction conditions:

$$f = \frac{\mathcal{R}_{v,\max}}{c_{E0}} \quad (8.153)$$

The turnover frequency for the system in Example 8.5.1.3.1-1 is

$$f = \frac{(k_3k_4)/(k_3 + k_4)}{1 + (k_3/k_2)((k_{-2} + k_4)/(k_3 + k_4))(1/c_B) + (k_4/k_1)((k_{-1} + k_3)/(k_3 + k_4))(1/c_A)} \quad (8.154)$$

Typical values of the turnover frequency are 10^{-3} – 10 s $^{-1}$ commercial catalysts, and 10^2 – 10^4 s $^{-1}$ for enzymes (Bartholomew and Farrauto, 2006).

8.5.1.3.2 Supported Catalysts Immobilization of cells and enzymes refers to the attachment of the catalyst to a solid surface (Rosevear et al., 1987). Immobilization, for example, prevents the loss of suspended biocatalysts in the product stream and, therefore, eliminates or greatly reduces the need for cell recovery and recycle operations. See Example 2.3.2-3 and Problem 2.3 for an example of enzyme loss in the manufacture of hexyl glucoside. Immobilization can also improve enzyme stability and prevent cell damage due to high shear fields in the bulk liquid.

The availability of expensive metal catalysts can be dramatically increased by dispersing small particles with a high surface to volume ratio on a support material. It is the surface atoms on a bulk metal that provide the catalytic action. The following discussion is concerned primarily with gaseous mixtures, although much also applies to liquids.

There are essentially two categories of supported catalysts:

NONPOROUS In the nonporous case, the reactive surface is directly exposed to the reaction mixture, which carries the

reactants and products and is therefore part of the reactor boundary (see Section 9.5.2). An example of the monolithic catalysts is illustrated in Figure 8.9.

The diameters of the monoliths are in the neighborhood of 15 cm. They contain multiple channels with equivalent diameters from approximately 0.5 to 10 mm. The catalyst is

deposited on the channel walls. The monoliths can be as long as 1 m. A well-known application of monoliths is the catalytic converter for the automobile.

In the nonporous case, the reaction occurs on the catalytic surface, not in the reaction mixture. Consequently, the reaction rate term vanishes from the microscopic balance equations for this case and reappears in a boundary condition (see Table 8.12):

POROUS Porous catalysts generally consist of a porous solid containing many convoluted pores of varying dimensions. They come in many different sizes and shapes as illustrated in Figure 8.9. Some typical properties are given in Table 8.4.

TABLE 8.4 Typical Catalyst Properties (Smith, 1981)

	Surface Area	Pure Volume	Mean Pore Radius
Catalyst	m ² /g	cm ³ /g	Å
Activated carbons	500–1,500	0.6–0.8	
Silica gels	200–600	0.4	15–100
SiO–Al ₂ O ₃ cracking Catalysts	200–500	0.2–0.7	33–150
Activated clays	150–225	0.4–0.52	100
Activated alumina	175	0.39	45
Celite (Kieselguhr)	4.2	1.1	11,000
Synthetic ammonia Catalysts, Fe		0.12	200–1,000
Pumice	0.38		
Fused copper	0.23		

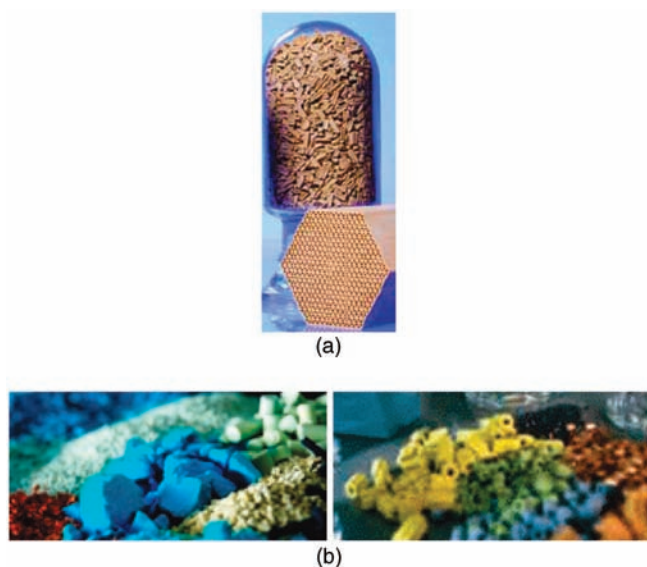


FIGURE 8.9 Examples of supported catalysts. (a) Monolithic catalysts and (b) variety of porous catalysts. Courtesy of BASF Corporation, Catalyst Division.

Refer also to Section 6.5.1 for a basic introduction to porous solids.

A characteristic dimension is approximately 1/16 to 1/4 in. Pore sizes range from less than 50 Å (micropores) to greater than 500 Å (macropores). Surface areas around 500 m²/g are typical (that's about 20 football fields per 1/4 lb).

The catalyst is deposited on the walls of the porous support so that the reaction conditions needed to calculate the reaction rate requires an analysis of external mass transfer and internal mass transfer with chemical reaction (Figure 8.10).

The objective at this juncture is the rate expression resulting from the three steps associated with the surface reaction at the internal reaction site.

The formulation of kinetic expressions for heterogeneous gas phase reactions is very much the same as that for enzymatic reactions introduced in Section 8.5.1.3.1 with the active center on the interior surface of the support replacing the role of the enzyme.

Example 8.5.1.3.2-1 Generic Hydrogenation with Surface Reaction Controlling

Consider the following reaction, which may be considered a generic form for a hydrogenation (A_2 hydrogen) reaction;

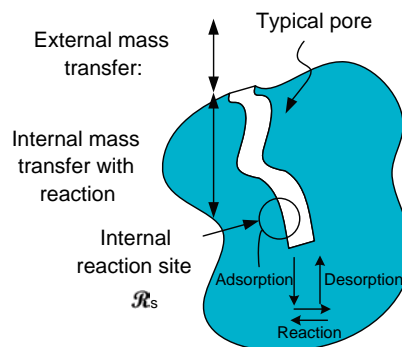
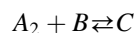
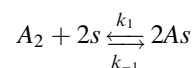


FIGURE 8.10 Illustration of the reaction site in porous support.

Mechanism: Elementary reactions:

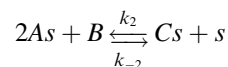
Adsorption (dissociative):

It is necessary for at least one component to be adsorbed for the catalytic action to take place. As noted earlier in Section 6.5, the catalytic adsorption step involves the formation of covalent bonds. An active site, for example, a Pt atom, will be denoted by s and adsorption is the result of a successful collision of a gas phase molecule with this site. These are considered elementary events to which mass action kinetics are employed. In many cases, a reactant will be adsorbed on a single sight. Here, we consider the case of dissociative adsorption as takes place with hydrogen (see Figure 6.42).

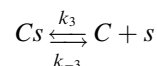


Surface reaction:

The B component may be adsorbed or it may remain in the gas phase and react with the adsorbed A . The latter is referred to as a Rideal mechanism.



Desorption:



Reaction rates:

$$\text{Adsorption: } r_1 = k_1 c_{A_2} c_s - k_{-1} c_{As}^2$$

$$\text{Surface reaction: } r_2 = k_2 c_{As}^2 c_B - k_{-2} c_{Cs} c_s$$

$$\text{Desorption: } r_3 = k_3 c_{Cs} - k_{-3} c_C c_s$$

Steady-state approximation:

The steady-state approximation is that the reaction rates are equal:

$$r_1 = r_2 = r_3$$

Site balance:

$$c_s^0 = c_s + c_{As} + c_{Cs}$$

The steady-state approximation provides for the elimination of the adsorbed species concentrations and the site balance in turn provides the concentration of vacant sites. The reaction rate, r_1 , r_2 , or r_3 thus formed, contains only the gas phase concentrations. However, in this example, the surface reaction is considered to be rate controlling. (see the discussion of the rate-controlled step in Section 8.5.1.3.) This means that we can set

$$r_1 \approx 0, r_3 \approx 0$$

$$r_1 \approx 0 \Rightarrow c_{As} = \sqrt{\frac{k_1}{k_{-1}}} c_{A_2} c_s$$

$$r_3 \approx 0 \Rightarrow c_{Cs} = \frac{k_{-3}}{k_3} c_C c_s$$

Substitution into the site balance gives

$$c_s = \frac{c_s^0}{1 + \sqrt{\frac{k_1}{k_{-1}}} c_{A_2} + \frac{k_{-3}}{k_3} c_C}$$

The reaction rate is then given by

$$r_2 = \frac{\frac{k_1}{k_{-1}} k_2 c_{so}^2 \left(c_{A_2} c_B - \frac{k_{-1}}{k_1} \frac{k_{-2}}{k_2} \frac{k_{-3}}{k_3} c_C \right)}{\left[1 + \sqrt{\frac{k_1}{k_{-1}}} c_{A_2} + \frac{k_{-3}}{k_3} c_C \right]^2} =$$

or

$$\mathcal{R}_s = \frac{k \left(c_{A_2} c_B - \frac{1}{K_{Cr}} c_C \right)}{[1 + \sqrt{K_{A_2} c_{A_2}} + K_{CC} c_C]^2}$$

Approximate homogeneous models of porous catalysts such as the one illustrated in Figure 8.10 are often employed. The surface kinetics are homogenized in such cases as follows (see Table 6.15 for definition of porous material properties).

$$\mathcal{R}_v = \mathcal{R}_s S_g \rho_p$$

See Section 10.3 for an example.

In the nonporous case, \mathcal{R}_s would appear in a boundary condition as discussed above. See Section 10.5.

8.5.2 σ_j : Vector Processes: Diffusion and Conduction

The vector processes are the independent molecular fluxes of mass and energy. Recalling that the sum of the mass diffusional flows is zero, the independent fluxes and forces are, respectively:

$$\begin{aligned} \mathcal{Q} &= \{\mathbf{j}_i, \mathbf{q}; i = 1, N_c - 1\}^T \text{ and} \\ \mathcal{X} &= \{[\nabla_T(\mu_j - \mu_{N_c}) - (\mathbf{f}_{bj} - \mathbf{f}_{bN_c})], \nabla \ln T; j = 1, N_c - 1\}^T \end{aligned} \quad (8.155)$$

The linear laws expressed by Equation (8.113) can be expressed here as

$$\mathcal{Q} = -\mathcal{L}\mathcal{X} \quad (8.156)$$

where \mathcal{L} is symmetric matrix of the scalar phenomenological coefficients. Carrying out the differentiations in the preceding equation, and considering the case where the body forces per unit mass are the same for all species (e.g., gravity), the preceding equation becomes

$$\mathcal{Q} = -\mathcal{D}\mathcal{F} \quad (8.157)$$

where

$$\mathcal{F} = \{\nabla \omega_1, \nabla \omega_2, \dots, \nabla \omega_{N_c-1}, \nabla P, \nabla T\}^T \quad (8.158)$$

The Soret effect (thermal diffusion) is the proportionality between the mass flux and the temperature gradient and the Dufour effect is the proportionality between the energy flux and the concentration gradient. These effects as well as the proportionality to the concentration gradients off the major diagonal are not important in most applications. Consequently, the linear laws reduce to

$$\mathbf{j}_i = -D_{ii} \nabla \omega_i \quad (8.159)$$

$$\mathbf{q} = -\lambda \nabla T \quad (8.160)$$

Equation (8.159) is a form of Fick's Law of diffusion. Equation (8.162) is known as Fourier's law of conduction. The thermal conductivity of the medium is denoted by λ .

If the diffusional flows are represented in other reference frames (refer to earlier discussion), the concentration field used in the flux expression is changed to preserve specific properties of the full matrix of diffusion coefficients. The concentration fields and reference frames are associated as follows:

$$\mathbf{j}_i = -\rho D_i^V \nabla \omega_i \quad (8.161)$$

$$\mathbf{j}_i^N = -c M_i D_i^V \nabla x_i \quad (8.162)$$

$$\mathbf{j}_i^V = -D_i^V \nabla \rho_i \quad (8.163)$$

The molar flux corresponding to \mathbf{j}_i is \mathbf{n}_i [see Equation (8.19)].

As noted earlier, it is seldom necessary to distinguish between the reference frames. We will therefore adopt the following form for the diffusional mass flux:

$$\mathbf{j}_i = -D_{im}\nabla\rho_i \quad (8.164)$$

The D_{im} is the diffusivity of species i in a mixture. If it is a binary mixture, the two components are identified. For example, D_{AB} is the binary diffusivity of A in B whose value at infinite dilution is given by

$$D_{AB}^0 = \lim_{\rho_A \rightarrow 0} D_{AB} \quad (8.165)$$

8.5.3 Viscous Momentum Flux

Since there are no other processes of the same tensorial order, the viscous transport of momentum is not thermodynamically coupled to another process and the momentum flux tensor may be expressed as

$$\Pi_0 = -2\eta(\nabla\mathbf{v})_{\text{os}} \quad (8.166)$$

$$\boldsymbol{\tau} = -2\eta\boldsymbol{\Delta} + \left(\frac{2}{3}\eta - \kappa\right)(\nabla \cdot \mathbf{v})\boldsymbol{\delta} \quad (8.167)$$

where the rate of deformation tensor is given by

$$\boldsymbol{\Delta} = \frac{1}{2}\{\nabla\mathbf{v} + (\nabla\mathbf{v})'\} = \frac{1}{3}(\nabla \cdot \mathbf{v})\boldsymbol{\delta} + (\nabla\mathbf{v})_{\text{os}} \quad (8.168)$$

Equation (8.167) represents the behavior of many fluids in which case they are called Newtonian. It is entirely possible that a fluid is Newtonian only over a specific range of shear. However, the linear law is not sufficient to represent momentum transfer in all fluids and, phenomenological approaches have therefore been employed to capture non-Newtonian behavior. In some sense, these may be regarded as efforts to include higher order terms in the expansion of the flux in terms of forces.

8.5.4 Estimation of Transport Coefficients

The goal of closing the microscopic balance equations that was announced at the beginning of Section 8.5 will be complete when the diffusivity, thermal conductivity, and viscosity are expressed in terms of the state variables. In this section, we will summarize a number of empirical correlations of experimental data that are known to give reasonable results over a wide variety of circumstances (Poling et al., 2001). However, errors greater than 15–20% can occur and the user would be wise to compare alternative methods and

certainly to use experimental data to the extent possible. Theoretical models (Chapman–Enskog) are also available. Note that the ratio of two predictions provides the means of extrapolating data. Measurements under mild laboratory conditions may be adjusted for application under extreme operating conditions.

8.5.4.1 Diffusivities Approximate values of the diffusivity are 10^{-9} cm²/s for solids, and 10^{-5} cm²/s for liquids, and 10^{-1} cm²/s for gases. Table 8.5 lists recommended correlations for liquids and low-pressure gases (Poling et al., 2001).

Example 8.5.4.1-1 Estimation of Methane Diffusivity in Nitrogen for Application to Effective Diffusion in Honeycomb Monolith Reactor

Diffusion data at 291 K and 1 bar in a catalytic monolith are reported by Hayes and Kolaczowski (1999). In order to analyze these data with the parallel pore model for effective diffusivities in porous catalysts, the binary molecular diffusivity of methane in nitrogen is required (see Example 10.2-31).

Solution:

$$A = \text{CH}_4, B = \text{N}_2$$

$$M_A = 16.043 = 12.011 + 4 \times 1.0079$$

$$M_B = 28.014 = 2 \times 14.007$$

Refer to Table 8.6:

$$\Sigma_A = 25.14 = 15.9 + 4(2.31)$$

$$\Sigma_A = 18.5$$

Refer to Table 8.5, “binary low pressure gases.”

$$D_{AB}(T, P) = \frac{0.00143T^{1.75}}{P \left[\frac{2}{(1/M_A) + (1/M_B)} \right]^{0.5} \left[(\Sigma_A)^{1/3} + (\Sigma_B)^{1/3} \right]^2}$$

$$D_{AB}(291, 1) = 0.20890 \text{ cm}^2/\text{s}$$

A value of 0.224 cm²/s has been reported for methane in air at 298 K and 1 atm (Yaws, 2003). This value generally supports the calculations above.

8.5.4.2 Thermal Conductivities Gases have thermal conductivities of the order 10^{-2} W/(m K). Liquids have thermal conductivities of the order 10^{-1} W/(m K) and solids 10 W/(m K). These are very crude estimates. Table 8.7 summarizes recommended correlations for liquids and low pressure gases (Poling et al., 2001) (Table 8.8).

TABLE 8.5 Correlations to Estimate Diffusion Coefficients for Nonelectrolytes

Correlation	Definitions and Units	Restrictions/Notes
Binary liquid phase diffusivity at infinite dilution: Hayduk and Minhas (1982) for $B = n$ -paraffin: $D_{AB}^0 = 13.3 \times 10^{-8} \frac{T^{1.47} \eta_B^{(9.58/V_A - 1.12)}}{V_A^{0.71}}$	$V_i(T_{\text{nbp}})$: cm^3/mol ; molar volume of i at n.b.p. $A = \text{solute}$, $B = \text{solvent}$ P_i : Parachor for species $i = V_i \sigma^{1/4}$ with molar volume (cm^3/mol) and surface tension (dyn/cm) at the same temperature; $\left[\frac{\sigma_B}{\sigma_A}\right]^{0.5} \approx 1$ for many organic liquids T : K η_B : viscosity of solvent (cP) Estimate: $V_i = 0.288 V_c^{1.045}$; cm^3/gmol	<ul style="list-style-type: none"> • $\eta_B < 20$ to 30 cP • $A = \text{water} \Rightarrow P_A = 2P_{\text{water}}$, $V_A = 2V_{\text{water}}$ • $A = \text{organic acid and } B \neq \text{H}_2\text{O}, \text{CH}_3\text{OH}, \text{ or } \text{C}_4\text{H}_9\text{OH} \Rightarrow P_A = 2P_{\text{water}}, V_A = 2V_{\text{water}}$ • $A = \text{nonpolar}$; $B = \text{monohydroxy alcohol} \Rightarrow$ multiply P_B and V_B by $8\eta_B$ See Example 10.4-1
Otherwise Tyn–Calus (1975) method: $D_{AB}^0 = 8.93 \times 10^{-8} \left(\frac{V_A}{V_B^2}\right)^{1/6} \left(\frac{P_B}{P_A}\right)^2 \frac{T}{\eta_B}$	T : K η_B : viscosity of solvent (cP) Estimate: $V_i = 0.288 V_c^{1.045}$; cm^3/gmol	Not good for systems where the component may solvate
Concentrated binary liquid solutions— Vignes (1966): $D_{AB} = (D_{AB}^0)^{x_B} (D_{BA}^0)^{x_A} \left[1 + \frac{\partial \ln \gamma_A}{\partial \ln x_A}\right]$		
Multicomponent liquid mixtures (Perkins and Geankoplis, 1969) $D_{Am}^0 \eta_m = \sum_{\substack{j=1 \\ j \neq A}}^N x_j D_{Aj}^0 \eta_j^{0.8}$	D^0 : cm^2/s x : mole fraction η : cP	$A \neq \text{CO}_2$
Binary low pressure gases (Fuller et al., 1966) $D_{AB} = \frac{0.00143 T^{1.75}}{P M_{AB}^{1/2} \left[(\sum \nu)_A^{1/3} + (\sum \nu)_B^{1/3} \right]^2}$	$M_{AB} = \frac{2}{(1/M_A) + (1/M_B)}$ P : bar $\sum \nu$: Summation of atomic diffusion volumes (see Table 8.6) D_{AB} : cm^2/s	Note: $D_{AB} P \propto T^{7/4}$
(see Example 8.5.4.1-1)		
Multicomponent dilute gas (Sandler and Mason, 1968) $D_{im} = \left[\sum_{\substack{j=1 \\ j \neq i}}^N \frac{x_j}{D_{ij}} \right]^{-1}$	D_{ij} : Binary diffusivity of i in j under ideal gas conditions; independent of composition; cm^2/s	Derived from Stefan–Maxwell equations for diffusion of species i through a stagnant medium Referred to as Blanc’s law
Knudsen diffusion of gases in small pores (Satterfield, 1970) $D_{KA} = 97.0 r \sqrt{\frac{T}{M_A}}, \quad r [\text{m}]$	R : radius of (cylindrical) pore; m T : K D_{Ki} : cm^2/s	Collisions with pore walls a significant fraction of the total number of collisions

TABLE 8.6 Atomic Diffusion Volumes

Atomic and structural diffusion volume increments			
C	15.9	F	14.7
H	2.31	Cl	21.0
O	6.11	Br	21.9
N	4.54	I	29.8
Aromatic ring	-18.3	S	22.9
Heterocyclic ring	-18.3		
Diffusion volumes of simple molecules			
He	2.67	CO	18.0
Ne	5.98	CO ₂	26.9
Ar	16.2	N ₂ O	35.9
Kr	24.5	NH ₃	20.7
Xe	32.7	H ₂ O	13.1
H ₂	6.12	SF ₆	71.3
D ₂	6.84	Cl ₂	38.4
N ₂	18.5	Br ₂	69.0
O ₂	16.3	SO ₂	41.8
Air	19.7		

TABLE 8.8 Correlation Parameters (Latini et al., 1989)

Family	A^*	α	β	γ
Saturated hydrocarbons	0.00350	1.2	0.5	0.167
Olefins	0.0361	1.2	1.0	0.167
Cycloparaffins	0.0310	1.2	1.0	0.167
Aromatics	0.0346	1.2	1.0	0.167
Alcohols	0.00339	1.2	0.5	0.167
Acids (organic)	0.00319	1.2	0.5	0.167
Ketones	0.00383	1.2	0.5	0.167
Esters	0.0415	1.2	1.0	0.167
Ethers	0.0385	1.2	1.0	0.167
Refrigerants				
R20, R21, R22, R23	0.562	0.0	0.5	-0.167
Others	0.494	0.0	0.5	-0.167

TABLE 8.7 Correlations to Estimate Thermal Conductivities

Correlation	Definitions and Units	Restrictions/Notes
Thermal conductivity of pure organic liquids below n.b.p. (Latini et al., 1989)	$\lambda = A \frac{(1 - T_r)^{0.38}}{T_r^{1/6}}$ $A = \frac{A^* T_b^\alpha}{M^\beta T_c^\gamma}$ $\lambda [=] \text{W}/(\text{m K})$ $T_b = \text{normal boiling point, K}$	$50 < M < 250$ A not N ₂ sulfur containing compounds, aldehydes
Nonaqueous liquid mixture	See Table 8.8 for A^* , α , β , γ ω = weight fraction	Neglect effect of pressure up to 60 bar except near critical point. Thermal conductivity of no component is more than twice another
Low pressure pure gases—nonpolar compounds (Chung et al., 1988)	λ : W/(m K) η : Ns/m ² C_v : J/mol K $R = 8.314 \text{ J}/(\text{mol K})$ $\Psi = 1 + \alpha \frac{0.215 + 0.28288\alpha - 1.061\beta + 0.26665Z}{0.6366 + \beta Z + 1.061\alpha\beta}$ $\alpha = \frac{C_v}{R} - \frac{3}{2}$ $\beta = 0.7862 - 0.7109\omega + 1.3168\omega^2$ $Z = 2.0 + 10.5T_r^2$	If polar compound, can use $\beta = 0.758$ if not available for specific compound
Low pressure gas mixtures—nonpolar (Mason and Saxena, 1958)	$\lambda_m = \sum_i \frac{y_i \lambda_i}{\sum_j y_j A_{ij}}$ $A_{ii} = 1, A_{ij} = \frac{\left[1 + \sqrt{\lambda_{tr_i}/\lambda_{tr_j}} (M_i/M_j)^{1/4}\right]^2}{\sqrt{8[1 + (M_i/M_j)]}}$ $\lambda_{tr_i} = \frac{\Gamma_i [\exp(0.0464T_{ri}) - \exp(-0.2412T_{ri})]}{\Gamma_i [\exp(0.0464T_{rj}) - \exp(-0.2412T_{rj})]}$ $\Gamma_i = 210 \left[\frac{T_{ci} M_i^3}{P_{ci}^4} \right]^{1/6}$ $\Gamma [=] (\text{W}/(\text{m K}))^{-1}$	

TABLE 8.9 Correlations to Estimate Viscosities

Correlation	Definitions and Units	Restrictions/Notes
Pure gases at low pressure (Lucas, 1980) $\eta\xi = [0.807T_r^{0.618} - 0.357 \exp(-0.449T_r) + 0.340 \exp(-4.058T_r) + 0.018]F_P^0 F_Q^0$ $\xi = 0.176 \left[\frac{T_c}{M^3 P_c^4} \right]$ $\xi: (\mu\text{P})^{-1}$ $T: \text{K}$ $M: \text{g/gmol}$ $P_c: \text{bar}$	Correction factors (F) for polarity (P) and quantum (Q) effects: Polarity P : $\mu_r = 52.46 \frac{\mu^2 P_c}{T_c^2}$ $F_P^0 = 1 \quad 0 \leq \mu_r \leq 0.022$ $F_P^0 = 1 + 30.55(0.292 - Z_c)^{1.72} \quad 0.022 \leq \mu_r \leq 0.075$ $F_P^0 = 1 + 30.55(0.292 - Z_c)^{1.72} [0.96 + 0.10(T_r - 0.7)] \quad 0.075 \leq \mu_r$ Quantum F : The quantum correction factor, F_Q^0 is used only for He, H ₂ , and D ₂ $F_Q^0 = 1.22Q^{0.15} \left\{ 1 + 0.00385(T_r - 12)^{2/M} \text{sign}(T_r - 12) \right\}$ $Q = 1.38(\text{He}), 0.76(\text{H}_2), 0.52(\text{D}_2)$ $\text{sign}(x) = +1, x \succ 0$ $\text{sign}(x) = -1, x \prec 0$	
Gas mixture at low pressure (Lucas, 1980) Use the pure gas equations with following rules for the values to be used for the mixture: $T_{cm} = \sum_i y_i T_{ci}$ $P_{cm} = RT_{cm} \frac{\sum_i y_i Z_{ci}}{\sum_i y_i V_{ci}}$ $M_m = \sum_i y_i M_i$ $F_{pm}^0 = \sum_i y_i F_{pi}^0$ $F_{Qm}^0 = \left[\sum_i y_i F_{Qi}^0 \right] A$	Use pure gas correlation $A = 1 - 0.01 \left[\frac{\text{Max}(M_i)}{\text{Min}(M_i)} \right]^{0.87} \text{ for } \frac{\text{Max}(M_i)}{\text{Min}(M_i)} > 9$ and $0.05 < \text{Max}(y_i) < 0.7$ $A = 1 \quad \text{otherwise}$	
Low temperature pure liquid viscosity $\ln \left[\frac{\eta}{\rho M} \right] = A + \frac{B}{T}$	$\rho(\text{g/cm}^3)$ at 20°C if n.b.p. $< 20^\circ\text{C}$ $\rho(\text{g/cm}^3)$ at melting point if freezing point $< 20^\circ\text{C}$	
Liquid mixtures (Grunberg and Nissan, 1949; Isdale et al., 1985) $\ln \eta_m = \sum_i x_i \ln \eta_i + \frac{1}{2} \sum_{i,j} x_i x_j G_{ij}$ $G_{ii} = 0$	Follow the procedure listed below: 1. For a binary of i and j , select i by the following priority rules (j then becomes the second component) i = an alcohol, if present i = acid if present i = the component with the most carbon atoms i = the component with the most hydrogen atoms i = the component with the most $-\text{CH}_3$ groups $G_{ii} = 0$ if none of these rules establish a priority 2. Once the decision has been made which component is i and which is j , calculate $\sum \Delta_i$ and $\sum \Delta_j$ from the group contributions in Table 8.11 3. Determine the parameter W . (If either i or j contains atoms other than carbon and hydrogen, set $W = 0$ and go to step 4.) Let the number of carbon atoms in i be N_i and that in j be N_j . $W = \frac{0.3161(N_i - N_j)^2}{N_i + N_j} - 0.11889(N_i - N_j)$ 4. Calculate G_{ij} from $G_{ij} = \sum \Delta_i + \sum \Delta_j + W$ G_{ij} is sometimes a function of temperature. However, existing data suggest that, for alkane-alkane solutions or for mixtures of an associated component with an unassociated one, G_{ij} is independent of temperature. However, for mixtures of nonassociated compounds (but not of only alkanes) or for mixtures of associating compounds, G , is a mild function of temperature. Isdale et al. (1985) suggest for these latter two cases $G_{ij}(T) = 1 - [1 - G_{ij}(298)] \frac{573-T}{275}$	

TABLE 8.10 Orrick and Ebar Group Contributions for A and B

Group	A	B
Carbon atoms	$-(6.95 + 0.21 N)$	$275 + 99 N$
$\text{R}-\text{C}-\text{R}$ \parallel R	-0.15	35
$\text{R}-\text{C}-\text{R}$ \mid R	-1.20	400
Double bond	0.24	-90
Five-membered ring	0.10	32
Six-membered ring	-0.45	250
Aromatic ring	0	20
<i>Ortho</i> substitution	-0.12	100
<i>Meta</i> substitution	0.05	-34
<i>Para</i> substitution	-0.01	-5
Chlorine	-0.61	220
Bromine	-1.25	365
Iodine	-1.75	400
-OH	-3.00	1600
-COO-	-1.00	420
-O-	-0.38	140
C=O	-0.50	350
-COOH	-0.90	770

TABLE 8.11 Group Contributions to G_{ij} at 298 K

Group	Notes	Value of A
-CH		-0.100
>CH_2		0.096
>CH-		0.204
>C<		0.433
Benzene ring		0.766
Substitutions		
<i>Ortho</i>		0.174
<i>Meta</i>		-
<i>Para</i>		0.154
Cyclohexane ring		0.887
-OH	Methanol	0.887
	Ethanol	-0.023
	Higher aliphatic alcohols	-0.443
>C=O	Ketones	1.046
-Cl		0.653-0.161 K
-Br		-0.116
-COOH	Acid with:	
	Nonassociated liquids	-0.411 + 0.06074 K
	Ketones	1.130
	Formic acid with ketones	0.167

8.5.4.3 Viscosity The viscosity of gases is of the order $10^{-4}P$, while liquids are of the order $10^{-3}P$. Again, these estimates are very crude and can perhaps only serve to detect the most serious errors in calculations. Table 8.9 summarizes recommended correlations for liquids and low pressure gases (Poling et al., 2001) (Tables 8.10 and 8.11).

8.6 TURBULENCE

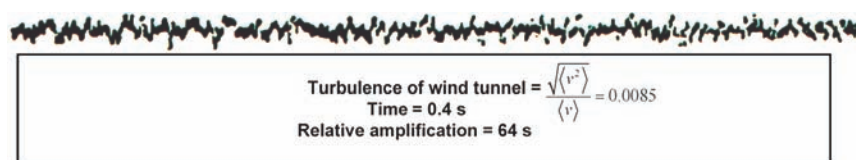
The conservation laws and flux expressions apply at each point in the homogeneous medium and, in the case of unsteady flows, at each instant of time. When we think of unsteady flows, the time scale that we have in mind may be of the order of hours. If there is no detectable change over a number of such time units, we begin to speak of steady flows or steady state.

If in the steady-state regime we take measurements of the velocity field, or other state variables that are sufficiently

accurate, we may find under some conditions, an unsteady component of the otherwise stable average velocity that changes over a very small time scale and has an oscillating statistical nature. This condition is called turbulence and has the characteristics displayed in Figure 8.11 of the “steady velocity” field measured in a wind tunnel.

Note that the average velocity is constant, that the average fluctuation about the mean velocity is about 0.85% of the mean velocity, and that the record is over an elapsed time of only 0.4 s. Turbulence may be defined as the irregular motion in which the various intensive quantities (concentration of mass or energy, temperature, pressure, and so on) vary randomly in both the time and spatial coordinates. Isotropic turbulence refers to the case where the statistical properties of the turbulence do not vary with direction. Flow in pipes becomes turbulent at a Reynolds number (see below) of approximately 2100.

The turbulent condition is also characterized by the eddy motions that accompany the condition of fluctuating

**FIGURE 8.11** Steady velocity field in a wind tunnel (Hinze, 1959). Reprinted with permission of McGraw-Hill.

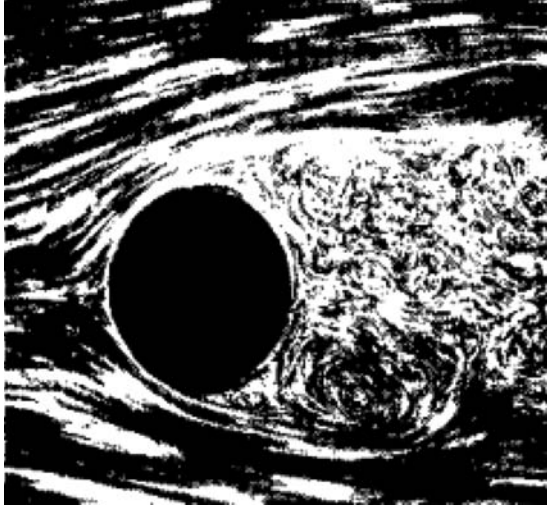


FIGURE 8.12 Flow behind a cylinder with lateral flow (Hinze, 1959). Reprinted with permission of McGraw-Hill.

velocity components. Eddies are clearly present in Figure 8.12, which shows the flow field behind a cylinder subjected to a high lateral flow.

This is an example of wall turbulence that has different characteristics than free turbulence that may be encountered in a free jet or when two fluid phases are contacted as in a liquid-liquid extractor.

The spatial scale of the eddies is approximately 1 mm. This eddy motion contributes another mechanism for transport of mass, momentum, and energy.

Although the transport equations may hold at each instant, the small scale of the turbulent fluctuations makes the average flow more interesting in practice where most flows are turbulent. Our objective is to cast the conservation equations in terms of the average flow (following Bird et al., 2002) (see Figure 8.13).

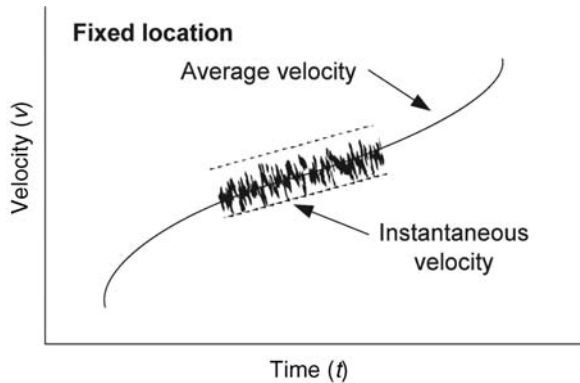


FIGURE 8.13 Average and instantaneous velocity.

By the average velocity component at a fixed position in a turbulent flow field, we mean as follows:

$$\langle v(t) \rangle = \frac{1}{T} \int_0^T v(t + \tau) d\tau \quad (8.169)$$

where the interval T is much larger than the time scale of the fluctuations in the flow due to turbulence but much less than the time scale of the average motion. When this is true, we can say that the average value is independent of time over a small time interval and write

$$\langle v(t + T) \rangle \approx \langle v(t) \rangle \quad (8.170)$$

The fluctuating component is then expressed as

$$v = \langle v \rangle + v' \quad (8.171)$$

where

$$\langle v' \rangle = 0 \quad (8.172)$$

The following properties of the averaging operation can be identified for the scalar functions, m and n :

$$\langle \langle m \rangle \rangle = \langle m \rangle \quad (8.173)$$

$$\langle \langle m \rangle n \rangle = \langle m \rangle \langle n \rangle \quad (8.174)$$

$$\langle m + n \rangle = \langle m \rangle + \langle n \rangle \quad (8.175)$$

$$\langle \partial m / \partial s \rangle = \partial \langle m \rangle / \partial s \quad (8.176)$$

where s is distance in the direction of the derivative. These properties will be used in the following calculations to reformulate the mass conservation equations in terms of average values.

8.6.1 Time-Averaged Mass Balance

The time average of the mass balance for species i in a mixture can be calculated as follows:

$$\left\langle \frac{\partial \rho_i}{\partial t} + \nabla \cdot (\rho_i \mathbf{v} + \mathbf{j}_i) \right\rangle = \langle r_{iv} \rangle \quad (8.177)$$

$$\frac{\partial \langle \rho_i \rangle}{\partial t} + \nabla \cdot (\langle \rho_i \mathbf{v} \rangle + \langle \mathbf{j}_i \rangle) = \langle r_{iv} \rangle \quad (8.178)$$

The flux term may be expressed in more useful terms as follows:

$$\langle \rho_i \mathbf{v} \rangle = \langle (\langle \rho_i \rangle + \rho'_i) (\langle \mathbf{v} \rangle + \mathbf{v}') \rangle \quad (8.179)$$

$$= \langle \rho_i \rangle \langle \mathbf{v} \rangle + \langle \rho'_i \mathbf{v}' \rangle \quad (8.180)$$

The first term is the familiar convective form, but in terms of time-averaged quantities. The second term represents an additional transport mechanism for the averaged quantities that is due entirely to the turbulent motion. It is an eddy transport mechanism, not a molecular-based phenomenon like molecular diffusion.

$$\mathbf{j}_i^t = \langle \rho_i \mathbf{v}' \rangle \quad (8.181)$$

The averaging process uncovers a contribution of the turbulent flow field to the reaction rate in terms of time-averaged quantities. Consider, for example, the case of an irreversible second order reaction under isothermal conditions:

$$\langle r_{iv} \rangle = k \langle c_i^2 \rangle = k \langle c_i \rangle^2 + k \langle c_i'^2 \rangle \quad (8.182)$$

The result is that the microscopic mass balance can be written in terms of time-averaged quantities if we add a turbulent transport mass transfer mechanism relative to the convective flow and we recognize a possible enhancement of the reaction rates. With the understanding that the intensive quantities are time averaged, the microscopic mass balance can be expressed with one additional term

$$\frac{\partial \rho_i}{\partial t} + \nabla \cdot (\rho_i \mathbf{v} + \mathbf{j}_i + \mathbf{j}_i^t) = r_{iv} \quad (8.183)$$

We assume that there is no net transport of mass by the turbulent mechanism

$$\sum_i \mathbf{j}_i^t = 0 \quad (8.184)$$

The equation of continuity is therefore not changed when passing to time-averaged quantities.

8.6.2 Turbulent Flux Expressions

Following the same procedure with the momentum and energy balance equations as for the mass balance yields a similar result. The balance equations are augmented by an additional flux relative to the mass average velocity but are otherwise unchanged when written in terms of the time-averaged quantities. The turbulent fluxes, to a first approximation, are empirically expressed in a form similar to their molecular-based counterparts:

$$\begin{aligned} \mathbf{j}_i^t &= -\rho D^t \nabla \omega_i \\ \mathbf{q}^t &= -\lambda^t \nabla T \end{aligned} \quad (8.185)$$

$$\boldsymbol{\tau}^t = -2\mu^t \nabla \mathbf{v}_{0s} \quad (8.186)$$

The turbulent transport coefficients are called the eddy diffusivity, the eddy conductivity, and the eddy viscosity. Note that the same eddy diffusivity applies to all components. Written in this way, the turbulent and molecular based

fluxes are proportional to the same gradients with one or the other predominating at the extremes of flow:

$$D_{im}^t = D_{im} + D^t \quad (8.187)$$

$$\lambda_m^t = \lambda_m + \lambda^t \quad (8.188)$$

$$\eta_m^t = \eta_m + \eta^t \quad (8.189)$$

It must be emphasized that the turbulent flux expressions in Equations (8.188) and (8.189) are very crude approximations. The turbulent components are known to be functions of the distance from submerged objects, the intensity of the turbulence, and so on. In general, the molecular-based components are properties of the fluid while the turbulent components depend on the characteristics of the fluid dynamics. This dependence has been a formidable impediment to obtaining solutions to practical problems.

The difficulties are most apparent in regions with large gradients that tend to occur near phase boundaries in chemical processing equipment. The processes that take place near these phase boundaries may, in fact, provide the basic functionality of the equipment. The transport phenomena in these regions are described with mass, momentum, and heat transfer coefficients (see Chapters 12, 13, and 14, respectively), which are based on experimental data and characteristic properties of the transport equations. The eddy transport coefficients, if needed, are applied outside of these regions, which is called the bulk phase.

8.6.2.1 Empty Tubes The behavior of the eddy diffusivity for flow in pipes of diameter D is shown in Figure 8.14.

Three dimensionless groups are employed in Figure 8.14. The Reynolds number is on the horizontal axis and is a measure of the convective flux of momentum to the viscous flux. Laminar flow takes place at Reynolds numbers less than 2100. The inverse of the Peclet number appears on the vertical axis and is a measure of the eddy transport of momentum to the convective transport. The Schmidt number is shown parametrically and is a measure of the rate at which momentum is transferred through the system by viscous effects relative to the molecular diffusion rate. The laminar regime is the result of an analysis of the spread of a pulse injection at the pipe entrance in terms of concentration averaged over the cross section.

Of most interest here is the turbulent flow regime beyond the Reynolds number of 2100. These results are experimental.

The eddy conductivity and viscosity are often approximated with

$$\frac{\lambda^t}{\rho c_p} \approx D_{im}^t \quad \text{and} \quad \frac{\eta^t}{\rho} \approx 1.0 - 2.0 \quad (8.190)$$

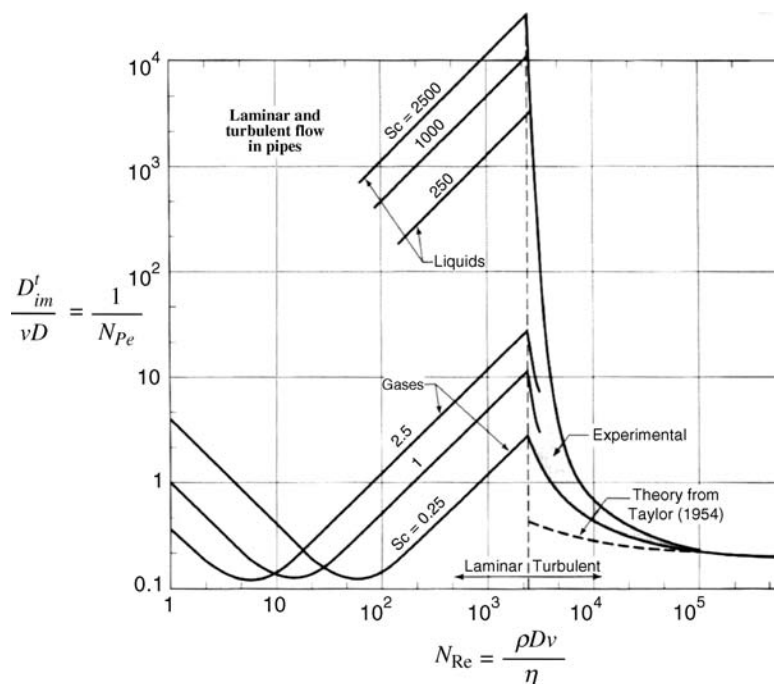


FIGURE 8.14 Correlation for dispersion of fluids flowing in pipes (Levenspiel, 1999). Reprinted with permission of McGraw-Hill.

8.6.2.2 Radial Dispersion in Packed Beds Consider the two-dimensional bed of spherical particles shown in Figure 8.15. The process may be modeled from a random walk (see Denbigh, 1966). Each time that a fluid element moves through a layer of particles, it undergoes a lateral movement of $D_p/2$ to the right or left.

The direction of the deflection is random. The result is a flux in the lateral direction in the same form as the molecular flux in Equation (8.151) but with a dispersion (to distinguish the process) coefficient, D_r , given by a value of 11 for the axial Peclet number. This is close to the experimental values shown in Figure 8.16. See Gunn (1987) for functional relationships.

8.6.2.3 Axial Dispersion In the axial or direction of flow, area open to flow first increases to a maximum value and

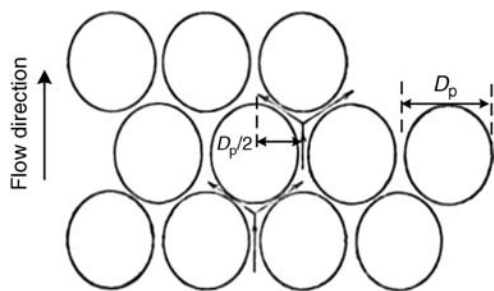


FIGURE 8.15 Radial dispersion process in a packed bed (Denbigh, 1966).

then decreases through the same values. The fluid can then be imagined to accelerate rapidly through areas of small voidage, and then to slow and mix in those regions of high voidage. The rapid acceleration through the low voidage areas provides the energy of mixing in the high voidage areas. This process as analyzed by Aris and Amundson (1957) who found an axial Peclet number of 2.0. This result is in good agreement with the data shown in Figure 8.17.

Lines replace a series of data points in Figure 8.17. See Gunn (1987) for functional relationships. Also refer to Section 8.7.4 for the influence of axial dispersion on boundary conditions for fixed-bed reactors.

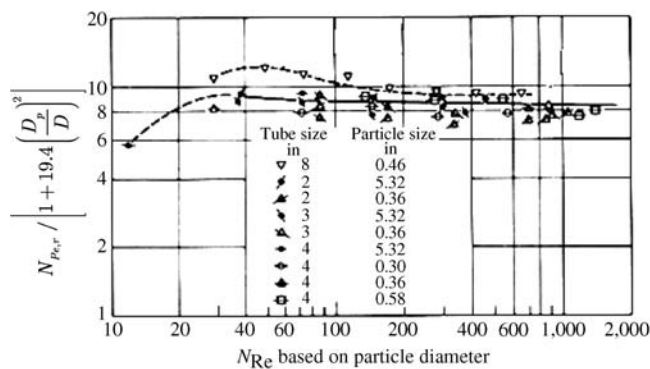


FIGURE 8.16 Radial dispersion coefficients in a packed bed (Smith, 1981). Reprinted with permission of McGraw-Hill.

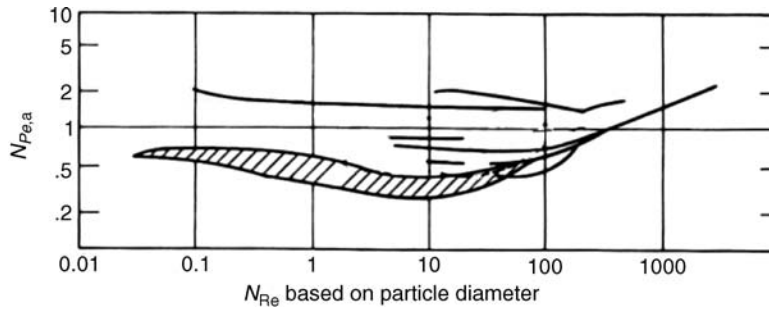


FIGURE 8.17 Axial dispersion coefficients (Froment and Bischoff, 1979). Reprinted with permission of John Wiley & Sons.

8.7 APPLICATION OF BALANCE EQUATIONS

The application of the conservation equations to physical circumstances invariably requires the selection of a coordinate system. The coordinate system is normally chosen so that one or more of the coordinate surfaces coincide with a surface over which we have specific knowledge of the physical conditions. These surfaces are normally system boundaries and the conditions are called boundary conditions.

The steady-state balance equations are summarized in Table 8.12. Two limiting regimes of flow are pointed out: The creeping flow regime where the viscous transport of momentum dominates the momentum flux (see Section 9.4.1) and the ideal region where the reverse is true. Ideal flows may be used as limits of solutions to flows around submerged objects as the distance from the object increases (Bird et al., 2002).

8.7.1 Boundary Conditions

The flux expressions derived above in conjunction with the balance equations for mass, energy, and momentum constitute a complete description of microscopic behavior in a homogeneous system of known material properties. The system is identified by the boundaries it forms with other systems within which microscopic phenomena are described in an identical way. The descriptions are linked by assuring that the physical laws that govern the processes in adjacent systems are preserved in exchanges and interactions at adjoining boundaries. We consider moving boundaries with surface tension so that systems that exhibit significant changes of volume on mixing, condensation, and evaporation, as well as melting and freezing and the influence of surface tension on mass transfer may be included at least approximately. A summary is given in Table 8.13.

The conditions at the boundary between two phases are considered for mass, energy, and momentum transfer. The

TABLE 8.12 Summary of Steady-State Microscopic Balances (Unsteady-State Accumulation Term Crossed Out)

Mass

$$\cancel{\frac{\partial \rho_i}{\partial t}} + \nabla \cdot (\rho_i \mathbf{v} + \mathbf{j}_i) = r_{iv} \Rightarrow \cancel{\frac{\partial \rho}{\partial t}} + \nabla \cdot (\rho \mathbf{v}) = 0 \text{ "Continuity" equation}$$

$$\mathbf{j}_i = -D_{im} \nabla \rho_i$$

Momentum

Newtonian fluid with bulk viscosity (κ) = 0

1. Navier–Stokes equations if ρ = constant

2. Euler's equation for $\nabla \cdot \boldsymbol{\tau} = 0$

$$\cancel{\frac{\partial \rho \mathbf{v}}{\partial t}} + (\rho \mathbf{v} \mathbf{v} + \mathbf{P} \boldsymbol{\delta} + \boldsymbol{\tau}) = \sum_i \rho_i \mathbf{f}_{bi}$$

$$\boldsymbol{\tau} = -2\eta \left[\Delta \mathbf{v} - \left(\frac{1}{3} \nabla \cdot \mathbf{v} \right) \boldsymbol{\delta} \right]$$

$$\text{and } \Delta \mathbf{v} = \frac{\nabla \mathbf{v} + (\nabla \mathbf{v})^t}{2}$$

Energy

Constant partial molar enthalpies

$$\cancel{\rho \hat{c}_p \frac{\partial T}{\partial t}} + \rho \hat{c}_p \mathbf{v} \cdot \nabla T + \nabla \cdot \mathbf{q} = -\boldsymbol{\tau} : \nabla \mathbf{v} - \left[\frac{\partial \ln \rho}{\partial \ln T} \right]_{P, \omega} [\mathbf{v} \cdot \nabla P] + \sum_j (-\Delta H_{Rj}) \mathcal{R}_{jv}$$

Specific body force same for all components

$$\mathbf{q} = -\lambda \nabla T$$

TABLE 8.13 Summary of Boundary Conditions for [Phase α] (See Table Notes for Additional Information)

Condition	Mass (M)	Energy (E)	Momentum (P)
1. Local equilibrium	$\mu_i^{(\alpha)} = \mu_i^{(\beta)}$ (see note)	$T^{(\alpha)} = T^{(\beta)}$	Young–Laplace equation: $P^{(\alpha)} = P^{(\beta)} + \sigma[R_{c1}^{-1} + R_{c2}^{-1}]$
2. Permeable No slip	$(\mathbf{W}_i^{(\alpha)} - \rho_i^{(\alpha)} \mathbf{v}_s) \cdot \mathbf{n}$ $= (\mathbf{W}_i^{(\beta)} - \rho_i^{(\beta)} \mathbf{v}_s) \cdot \mathbf{n}$	$(\mathbf{J}_e^{(\alpha)} - \rho_e^{(\alpha)} \mathbf{v}_s - P^\alpha \mathbf{v}_s) \cdot \mathbf{n}$ $= (\mathbf{J}_e^{(\beta)} - \rho_e^{(\beta)} \mathbf{v}_s - P^\beta \mathbf{v}_s) \cdot \mathbf{n}$	$(\boldsymbol{\tau}^{(\alpha)} - \rho^{(\alpha)} \mathbf{v}^{(\alpha)} \mathbf{v}_s) \cdot \mathbf{n}$ $= (\boldsymbol{\tau}^{(\beta)} - \rho^{(\beta)} \mathbf{v}^{(\beta)} \mathbf{v}_s) \cdot \mathbf{n}$ $\mathbf{v}^{(\alpha)} \cdot \mathbf{t} = \mathbf{v}^{(\beta)} \cdot \mathbf{t}$
3. Impermeable No slip diathermal	$(\mathbf{W}_i^{(\alpha)} - \rho_i^{(\alpha)} \mathbf{v}_s) \cdot \mathbf{n} = 0$	$\mathbf{J}_e = \rho h \mathbf{v}_s + \mathbf{q} \Rightarrow \mathbf{q}^{(\alpha)} \cdot \mathbf{n} = \mathbf{q}^{(\beta)} \cdot \mathbf{n}$	$\boldsymbol{\tau}^{(\alpha)} \cdot \mathbf{n} = \boldsymbol{\tau}^{(\beta)} \cdot \mathbf{n}$ $\mathbf{v}^{(\alpha)} \cdot \mathbf{t} = \mathbf{v}^{(\beta)} \cdot \mathbf{t}$
4. Impermeable No slip adiabatic	$(\mathbf{W}_i^{(\alpha)} - \rho_i^{(\alpha)} \mathbf{v}_s) \cdot \mathbf{n} = 0$	$\mathbf{q}^{(\alpha)} \cdot \mathbf{n} = 0$	$\boldsymbol{\tau}^{(\alpha)} \cdot \mathbf{n} = \boldsymbol{\tau}^{(\beta)} \cdot \mathbf{n}$ $\mathbf{v}^{(\alpha)} \cdot \mathbf{t} = \mathbf{v}^{(\beta)} \cdot \mathbf{t}$
5. Impermeable No slip velocity = 0 Single reaction	$\mathbf{W}_i^{(\alpha)} \cdot \mathbf{n} = 0 \Rightarrow \mathbf{v}^{(\alpha)} \cdot \mathbf{n} = 0$ $\Rightarrow \mathbf{j}_i^{(\alpha)} \cdot \mathbf{n} = \vartheta_i M_i \mathcal{R}_s$ Also, $\mathbf{N}_i^{(\alpha)} \cdot \mathbf{n} = \vartheta_i \mathcal{R}_s$	$\mathbf{W}_i^{(\alpha)} \cdot \mathbf{n} = 0 \Rightarrow \mathbf{v}^{(\alpha)} \cdot \mathbf{n} = 0,$ $\mathbf{J}_e^{(\alpha)} \cdot \mathbf{n} = 0,$ $\Rightarrow \mathbf{q}^{(\alpha)} \cdot \mathbf{n} = -[(-\Delta H_R)/(-\vartheta_A)] \mathbf{d}_A^{(\alpha)}$ A = key reactant	$\boldsymbol{\tau}^{(\alpha)} \cdot \mathbf{n} = \boldsymbol{\tau}^{(\beta)} \cdot \mathbf{n}$ $\mathbf{v}^{(\alpha)} \cdot \mathbf{t} = \mathbf{v}^{(\beta)} \cdot \mathbf{t}$

Notes: Symmetry may be used to set conditions; require finite solutions; concentrations are continuous between porous boundaries.

phases may be liquid, solid, or gas so that the conditions, for example, apply to extraction (liquid–liquid), distillation (vapor–liquid), absorption (gas–liquid), adsorption (gas–solid), and so on. It is assumed that boundary conditions are being formulated for phase α . The conditions arise from physical considerations alone and do not include, for example, discarding solutions that are unbounded in the region of interest or the need for derivatives to vanish at lines of symmetry.

The system is supposed to be in a state of “local equilibrium” as noted at the beginning of Section 8.3. It follows that the two adjoining phases must meet the conditions of thermal, mechanical, and chemical equilibrium at the interface. This implies that the temperature and chemical potentials be continuous across the phase boundary and that a step change in pressure occurs due to surface tension. The equality of chemical potentials translates into a relationship between the compositions in each phase. A summary is provided in Table 6.12 for gas–liquid systems.

The interface is presumed to have no mass so that the mass flux of each species, the energy flux, and the momentum flux are therefore continuous across the interface. The fluxes expressions formulated in Section 8.5 may be used but under turbulent conditions, the interphase transfer coefficients discussed in Chapters 11, 12, and 13 are used. For reactive interface, the mass flux must equal the rate of reaction to avoid any accumulation of material, and the thermal energy released by the reaction must be removed. There is, however, no change of momentum due to the reaction. The momentum transferred from a gas may be approximated as zero for gas–liquid or gas–solid systems.

Fluids cling to each other through the interface. Thus, we may say that the tangential velocity is continuous across the interface.

We will apply these conditions to a variety of situations in Chapters 9–13. It is rarely necessary in many typical applications to need more than two spatial directions to describe, at least to a good approximation, the physical and chemical changes that are actually taking place. Symmetry plays a central role in such considerations and can result in considerable simplification of the applicable balance equations. We consider the details of the simplification procedure for a typical application here and give the results for two-dimensional problems in the following chapters.

8.7.2 Reduction to Scalar Equations: Laminar Flow in Tubes

One approach to simplifying the coordinate-free microscopic balances is to begin with the general equations fully expressed on the coordinate system chosen for the application and to eliminate coordinate-dependent terms that are inconsistent with our physical view of the of the application. A full exposition of the microscopic balance equations on the rectangular, cylindrical, and spherical coordinate systems is available elsewhere (Bird et al., 2002) with many illustrations of simplifications to a variety of applications. Another approach is to couple the simplification and the coordinate representation steps. We take the latter approach here for laminar flow in tubes.

Consider the steady laminar flow of a pure, constant density liquid in a straight round pipe under isothermal conditions (see Figure 8.18).

In the terms of Table 8.13, [phase α] is the fluid and [phase β] is the pipe. The interface is the inside surface of the pipe. The system is most conveniently represented in cylindrical coordinates since the boundary is represented by an r coordinate surface ($r = \text{constant}$) if the cylindrical system is

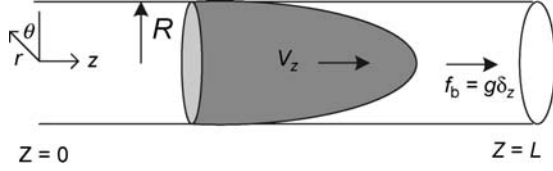


FIGURE 8.18 Laminar flow in a tube.

located at the center of the tube entrance. Also, we can see the symmetry in the angular direction in cylindrical coordinates since gravity is only acting in the z direction.

The fluid clings to the motionless wall and the wall is taken as impermeable. Consequently, the normal component of the velocity (M3) vanishes as well as the tangential component. Consequently, the velocity profile will be similar to that illustrated in Figure 8.18 where the fluid is anchored at the wall and allowed to respond to gravity otherwise.

The relations in Equations (8.49)–(8.52) will be of considerable utility in the adaption of the general equations to the tube flow. The velocity and del operator are given by

$$\mathbf{v} = v_z \delta_z \quad (8.191)$$

$$\nabla = \delta_r \frac{\partial}{\partial r} + \delta_\theta \frac{1}{r} \frac{\partial}{\partial \theta} + \delta_z \frac{\partial}{\partial z} \quad (8.192)$$

The equation of continuity (Table 8.12) at steady state and constant density is

$$\nabla \cdot \mathbf{v} = 0 \quad (8.193)$$

which reduces to the following for the current application:

$$\left(\delta_r \frac{\partial}{\partial r} + \delta_\theta \frac{1}{r} \frac{\partial}{\partial \theta} + \delta_z \frac{\partial}{\partial z} \right) \cdot v_z \delta_z = \frac{\partial v_z}{\partial z} = 0 \Rightarrow v_z = v_z(r) \quad (8.194)$$

The orthogonality of the coordinate vectors and the fact that the z -coordinate direction is constant have been used.

Conservation of momentum [see Equations (8.84)–(8.87)] for a Newtonian fluid at steady state and with gravity (z direction) as the only body force is expressed by

$$\nabla \cdot (\rho \mathbf{v} \mathbf{v} + P \delta - \eta [\nabla \mathbf{v} + (\nabla \mathbf{v})^t]) = g \delta_z \quad (8.195)$$

The bulk viscosity has been set to zero.

The first term in the preceding equation is reduced at constant density as follows:

$$\nabla \cdot \rho \mathbf{v} \mathbf{v} = \rho \nabla \cdot \mathbf{v} \mathbf{v} \quad (8.196)$$

$$\nabla \cdot \mathbf{v} \mathbf{v} = \left(\delta_r \frac{\partial}{\partial r} + \delta_\theta \frac{1}{r} \frac{\partial}{\partial \theta} + \delta_z \frac{\partial}{\partial z} \right) \cdot v_z v_z \delta_z \delta_z \quad (8.197)$$

$$\nabla \cdot \mathbf{v} \mathbf{v} = \delta_r \cdot \delta_z \delta_z \frac{\partial v_z v_z}{\partial r} + \delta_\theta \cdot \delta_z \delta_z \frac{1}{r} \frac{\partial v_z v_z}{\partial \theta} + \delta_z \cdot \delta_z \delta_z \frac{\partial v_z v_z}{\partial z} \quad (8.198)$$

Since the unit vector in the z direction is constant, the differentiation is carried into the velocity terms only. Referring to the appendix, the tensor products in the first and second terms vanish. The derivative in the second term vanishes as well and the third term reduces to

$$\nabla \cdot \mathbf{v} \mathbf{v} = \delta_{zz} \delta_z \frac{\partial v_z v_z}{\partial z} = \delta_z \frac{\partial v_z v_z}{\partial z} \quad (8.199)$$

This also vanishes because the velocity depends only on the radial coordinate because of the continuity equation. The vector components of the first term in the conservation equation are therefore all zero.

Since the pressure is multiplied by the unit tensor, the second term in Equation (8.195) becomes

$$\nabla \cdot P \delta = \left(\delta_r \frac{\partial P}{\partial r} + \delta_\theta \frac{1}{r} \frac{\partial P}{\partial \theta} + \delta_z \frac{\partial P}{\partial z} \right) \quad (8.200)$$

Further reductions are possible in this result but we will wait for a more informative point to affect them.

The third term in the conservation equation involves the evaluation of the velocity gradient:

$$\nabla \mathbf{v} = \left(\delta_r \frac{\partial}{\partial r} + \delta_\theta \frac{1}{r} \frac{\partial}{\partial \theta} + \delta_z \frac{\partial}{\partial z} \right) (\delta_z v_z) \quad (8.201)$$

Again, since the unit vector in the z direction is independent of position, the gradient of the velocity vector in the preceding equation reduces to

$$\nabla \mathbf{v} = \delta_r \delta_z \frac{\partial v_z}{\partial r} \quad (8.202)$$

Therefore,

$$(\nabla \mathbf{v})^t = \delta_z \delta_r \frac{\partial v_z}{\partial r} \quad (8.203)$$

At this juncture, the momentum balance, Equation (8.189) has been reduced to:

$$\begin{aligned} & \left(\delta_r \frac{\partial P}{\partial r} + \delta_\theta \frac{1}{r} \frac{\partial P}{\partial \theta} + \delta_z \frac{\partial P}{\partial z} \right) - \eta \nabla \cdot \left(\delta_z \delta_r \frac{\partial v_z}{\partial r} + \delta_r \delta_z \frac{\partial v_z}{\partial r} \right) \\ & = \rho g \delta_z \end{aligned} \quad (8.204)$$

The divergence term on the left side of the preceding equation is

$$\left(\delta_r \frac{\partial}{\partial r} + \delta_\theta \frac{1}{r} \frac{\partial}{\partial \theta} + \delta_z \frac{\partial}{\partial z} \right) \cdot \left(\delta_z \delta_r \frac{\partial v_z}{\partial r} + \delta_r \delta_z \frac{\partial v_z}{\partial r} \right) \quad (8.205)$$

Since the unit vectors do not depend on the radial coordinate, the first term of the operator provides

$$\left(\delta_r \frac{\partial}{\partial r}\right) \cdot \left(\delta_z \delta_r \frac{\partial v_z}{\partial r} + \delta_r \delta_z \frac{\partial v_z}{\partial r}\right) \quad (8.206)$$

$$= \delta_r \cdot \delta_z \delta_r \frac{\partial^2 v_z}{\partial r^2} + \delta_r \cdot \delta_r \delta_z \frac{\partial^2 v_z}{\partial r^2} \quad (8.207)$$

$$= \delta_{rz} \delta_r \frac{\partial^2 v_z}{\partial r^2} + \delta_{rr} \delta_z \frac{\partial^2 v_z}{\partial r^2} \quad (8.208)$$

The second term of the operator, however, involves changes in the unit vectors in the angular direction of the differentiation:

$$\left(\delta_\theta \frac{1}{r} \frac{\partial}{\partial \theta}\right) \cdot \left(\delta_z \delta_r \frac{\partial v_z}{\partial r} + \delta_r \delta_z \frac{\partial v_z}{\partial r}\right) \quad (8.209)$$

$$= \delta_\theta \frac{1}{r} \cdot \left(\delta_z \frac{\partial \delta_r}{\partial \theta} \frac{\partial v_z}{\partial r} + \frac{\partial \delta_r}{\partial \theta} \delta_z \frac{\partial v_z}{\partial r}\right)$$

noting that only the radial coordinate vector has an angular dependence. Substitution of the derivatives of the unit vectors (see Appendix) gives

$$\delta_\theta \frac{1}{r} \cdot \left(\delta_z \frac{\partial \delta_r}{\partial \theta} \frac{\partial v_z}{\partial r} + \frac{\partial \delta_r}{\partial \theta} \delta_z \frac{\partial v_z}{\partial r}\right) \quad (8.210)$$

$$= -\delta_\theta \cdot \delta_z \delta_\theta \left(\frac{1}{r} \frac{\partial v_z}{\partial r} + \delta_\theta \delta_z \frac{1}{r} \frac{\partial v_z}{\partial r}\right)$$

$$= -\delta_{\theta z} \delta_\theta \frac{1}{r} \frac{\partial v_z}{\partial r} - \delta_{\theta \theta} \delta_z \frac{1}{r} \frac{\partial v_z}{\partial r} = \delta_z \frac{1}{r} \frac{\partial v_z}{\partial r} \quad (8.211)$$

The third term of the operator is zero since there is no z dependence:

$$\left(\delta_z \frac{\partial}{\partial z}\right) \cdot \left(\delta_z \delta_r \frac{\partial v_z}{\partial r} + \delta_r \delta_z \frac{\partial v_z}{\partial r}\right) = 0 \quad (8.212)$$

Substitution of Equations (8.208), (8.211), and (8.212) into the divergence term in Equation (8.204) gives the vector form of the momentum balance:

$$\left(\delta_r \frac{\partial P}{\partial r} + \delta_\theta \frac{1}{r} \frac{\partial P}{\partial \theta} + \delta_z \frac{\partial P}{\partial z}\right) - \eta \left(\delta_z \frac{\partial^2 v_z}{\partial r^2} + \delta_z \frac{1}{r} \frac{\partial v_z}{\partial r}\right) = \rho g \delta_z \quad (8.213)$$

or, collecting terms,

$$\delta_r \left[\frac{\partial P}{\partial r}\right] + \delta_\theta \left[\frac{1}{r} \frac{\partial P}{\partial \theta}\right] + \delta_z \left[\frac{\partial P}{\partial z} - \eta \left(\frac{\partial^2 v_z}{\partial r^2} + \frac{1}{r} \frac{\partial v_z}{\partial r}\right) - \rho g\right] = 0 \quad (8.214)$$

The scalar equivalents to the preceding equation constitute the momentum balance in the three coordinate directions:

$$r: \quad \frac{\partial P}{\partial r} = 0 \quad (8.215)$$

$$\theta: \quad \frac{1}{r} \frac{\partial P}{\partial \theta} = 0 \quad (8.216)$$

$$z: \quad \frac{\partial P}{\partial z} - \eta \frac{1}{r} \frac{\partial}{\partial r} \left(r \frac{\partial v_z}{\partial r}\right) = \rho g \quad (8.217)$$

Similar considerations will give the internal energy balance as

$$\rho c_p v_z \frac{\partial T}{\partial z} - k \left[\frac{1}{r} \frac{\partial T}{\partial r} \left(r \frac{\partial T}{\partial r}\right) + \frac{\partial^2 T}{\partial z^2} \right] = -\tau : \nabla \mathbf{v} \quad (8.218)$$

Note that, except for the term on the right-hand side of Equation (8.216), a uniform temperature field would satisfy the energy balance. This term represents the degradation of kinetic to thermal energy and the energy balance requires that it be removed by convection and conduction in the axial direction and by conduction in the radial direction. The term is normally so small that the required temperature gradients are negligible, validating the assumption of an isothermal system.

We will return to the tube flow problem in the next chapter where applications involving nonturbulent momentum transfer are discussed. In that chapter and the following chapters, additional applications of the balance equations will be presented.

8.7.3 Introduction to Dimensionless Numbers and Characteristic Times

In the preceding discussion, we can intuitively recognize that laminar flow of all Newtonian fluids in straight round tubes displays similar hydrodynamic behavior and that adjustment in the flow conditions may compensate for changes in dimensions. We can quantify this intuition and at the same generalize the question somewhat by considering any collection of systems that share a common geometric configuration in the same coordinate system. Such systems differ only in the scale of the operation scale. Furthermore, we can consider energy and mass transfer from the same point of view. We will say that two systems are hydrodynamically or thermally or chemically similar if they obey the same microscopic balances in the domain of the scaled variables used to describe the system.

We will designate a scaled quantity by a superscript *. We first establish the length and velocity scales: (θ, L) and (θ, V) .

For the concentration, temperature, and pressure, we set the scales at (c_{Amin}, c_{Amax}) , (T_{min}, T_{max}) , and (P_{min}, P_{max}) . The minimum and maximum values are set for convenience and have no bearing other than to establish the individual scales with characteristic values. In fact, the value of V is often taken as the average value of the velocity in which event the scaled velocity can take on values greater than unity. A summary of the scaled variables is given by

$$x_i = Lx_i^* \Rightarrow \nabla = L^{-1}\nabla^* \quad (8.219)$$

$$c_i = c_{i,min} + c_i^*(c_{i,max} - c_{i,min}) \quad (8.220)$$

$$T = T_{min} + T^*(T_{max} - T_{min}) \quad (8.221)$$

$$P = P_{min} + P^*(P_{max} - P_{min}) \quad (8.222)$$

$$\mathbf{v} = \mathbf{v}^*V \quad (8.223)$$

The dimensionless microscopic balance equations can be obtained as follows:

- Assume a constant density, and specific heat, no bulk viscosity, a constant diffusivity, viscosity, and thermal conductivity.
- Substitute the flux expressions for mass, momentum, and energy with the preceding assumptions in to the unsteady-state balances in Table 8.12.
- Make the balance equations obtained in the preceding step dimensionless by substituting the variables defined in Equations (8.219)–(8.223).

The results are

$$\nabla^* \cdot \mathbf{v}^* = 0 \quad (8.224)$$

$$\begin{aligned} \frac{\partial \mathbf{v}^*}{\partial t^*} + \nabla^* \cdot \mathbf{v}^* \mathbf{v}^* = & -\nabla^* P^* - \frac{1}{N_{Re}} \nabla^* \cdot \Delta \mathbf{v}^* \\ & + \frac{1}{N_{Fr}} \mathbf{g}^* + \frac{N_{Gr,h}}{N_{Re}^2} \mathbf{g}^* T^* \end{aligned} \quad (8.225)$$

$$\frac{\partial c_A^*}{\partial t^*} + \mathbf{v}^* \cdot \nabla^* c_A^* = \frac{1}{N_{Re} N_{Sc}} \nabla^{*2} c_A^* \quad (8.226)$$

$$\frac{\partial T^*}{\partial t^*} + \mathbf{v}^* \cdot \nabla^* T^* = \frac{1}{N_{Re} N_{Pr}} \nabla^{*2} T^* \quad (8.227)$$

Notes: The momentum balance was modified to approximately account for free convection currents in spite of the assumption of constant density. Natural convection refers to the flows resulting from the replacement of fluid elements

with less dense elements produced by temperature gradients. The driving force is gravity that appears on the right side of the momentum balance. An approximation to the effects of natural convection can be included by assuming a linear variation of density with temperature in that term only:

$$\rho = \rho_0 + \left. \frac{\partial \rho}{\partial T} \right|_{T_0} (T - T_{min}) \quad (8.228)$$

The reference density is taken as the value at which the density has been assumed constant. With this understanding, the subscript 0 on the densities is omitted in the final equation.

The dimensionless equations, Equations (8.224)–(8.227) contain a number of dimensionless groups obtained by dividing each term of a balance equation by the coefficient of the convective term. This gives rise to a dimensionless time defined by

$$t^* = \frac{t}{\tau_c}, \quad \tau_c = \frac{L}{V} \quad (8.229)$$

where τ_c might be called a convective time constant, which is the unit of time in the dimensionless system. Note that an exponential decays by 10% after one-tenth of a time constant, by 50% after seven-tenths of a time constant, and by 95% after three time constants. Also note that the smaller the time constant, the faster the process. The convective time constant and others are discussed below.

The dimensionless group, $(P_{max} - P_{min})/(\rho V^2)$ was set equal to one. The dimensionless pressure is therefore

$$P^* = \frac{P - P_{min}}{\rho V^2} \quad (8.230)$$

The remaining dimensionless groups and their physical interpretation are delineated in Table 8.14.

We see that the differential equations describing the system differ among generic systems only in the dimensionless groups: N_{Re} , N_{Sc} , N_{Pr} , N_{Gr} , and N_{Fr} . This means, for example, that the correlation of data on system behavior need only be carried out with these dimensionless groups in lieu of the individual system parameters, a substantial savings. The Froude number can often be neglected, so that for an isothermal system only two groups remain N_{Re} and N_{Sc} . Note in particular the interchangeability of heat and mass transfer problems with the substitution of the Prandtl number for the Schmidt number. Additional dimensionless groups may appear in the boundary conditions required at the inlet, equipment boundaries, and phase interfaces. Geometric parameters associated with the equipment and interfaces may arise and we will group these in N_{Eq} . If the reference concentration and pressure are the inlet values, additional dimensionless groups will not be introduced to

TABLE 8.14 Dimensionless Numbers—Distinguishing Features of Mass, Energy, and Momentum Transfer in Similar Systems

Group Name	Definition	Interpretation	Typical Values (Approximate)
Reynolds = N_{Re}	$\frac{\rho LV}{\eta}$	Convection relative to viscous flux of momentum ^a	
Schmidt = N_{Sc}	$\frac{\eta}{\rho D_{Am}}$	Viscous flux of momentum relative to diffusional flux	0.1–1 for gases 100–10,000 for liquids
Prandtl = N_{Pr}	$\frac{c_p \eta}{\lambda}$	Viscous flux of momentum relative to thermal conduction	0.1–1 for liquids 1–10,000 for gases
Froude = N_{Fr}	$\frac{V^2}{gL}$	Momentum flux by convection relative to flux from characteristic height of liquid ^a	
Grashof = N_{Gr}	$\frac{\rho^2 L^3 g \zeta_T \Delta T}{\eta^2}$, $\zeta_T = -\frac{1}{\rho} \frac{\partial \rho}{\partial T} \Big _{T=T_o}$	Ratio of buoyancy force to viscous force in free convection	$N_{Pr} N_{Gr}$ from 10^{-5} to 10^{11}

^aSee Section 5.3.3 for application to power requirements for mixing.

account for these inlet conditions. Moreover in systems with two fluid phases the difference in density and viscosity may be important, for example. Power input to an agitated tank will have an important effect on interfacial areas, bubble breakup, and coalescence. These effects may be accounted for by the same general procedures being followed here. Applications to the correlation of mass and heat transfer data are considered in Chapters 11 and 14.

As noted above, τ_c is a convective time constant that is shared by the momentum, mass, and energy transfer processes represented in Equations (8.225)–(8.227), respectively. Superimposed on the convective flow are the molecular transport processes of viscous flow, diffusion, and conduction. Each of these processes is associated with a time constant arrived at by dividing through with the coefficient of its representation in the balance equation. The results are shown in Table 8.15.

The dimensionless groups can also be interpreted in terms of time constants. Diffusion in gases is faster than the viscous transport of momentum but the opposite is true for liquids as seen by the relative values of the Schmidt number.

Time constants can be very useful for establishing limiting conditions on outcomes in multiprocess systems. For example, consider a liquid flowing in a tube where the τ_c wall temperature is increased very rapidly to a new steady value. If

τ_v is much smaller than τ_q , we would not expect the fluid temperature to change except in a very thin layer near the wall.

8.7.4 Dual Geometry and Boundary Conditions for Fixed Beds

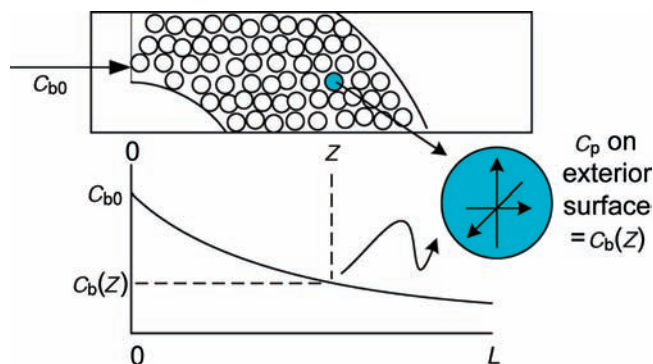
A fluid flowing through a bed of solid particles is a common occurrence in chemical engineering operations. Examples include catalytic reactors, fixed-bed adsorption, absorption, and distillation in packed towers. In the first two examples, there are transport processes taking place within or on the surface of the solid, while in the later two the solid is facilitating the intimate contact of two phases.

To enhance the interaction of the fluid and solid phases, the exposed surface of the solid is made large by utilizing small particles, but not so small that the pressure drop becomes excessive. The application of the conservation equations to these situations often involves two geometries as illustrated in Figure 8.19.

From the point of view of the solid, it is assumed that the surrounding fluid conditions do not change over the surface of the solid. A coordinate system is placed in the solid and the transport of mass and energy are described by the

TABLE 8.15 Time Constants for Mass, Energy, and Momentum Transfer

Process	Definition	Value Relative to τ_v	Typical Values (Approximate)
Momentum	$\tau_v = \frac{\rho L^2}{\eta}$	1.0	
Mass	$\tau_d = \frac{L^2}{D_{Am}}$	N_{Sc}	0.1–1 for gases 100–10,000 for liquids
Energy	$\tau_q = \frac{\rho c_p L^2}{\lambda}$	N_{Pr}	0.1–1 for liquids 1–10,000 for gases

**FIGURE 8.19** Dual geometries in a fixed bed.

balance equations subject to uniform boundary conditions at the outer boundary. These transport processes take place in porous media, which will require some modification of the homogeneous transport coefficients developed above. We will introduce these modifications in Chapter 10. They will include a homogenizing procedure similar to the one we are presently engaged in.

The solid regime interacts with the fluid by exchanging energy and mass. This interchange is viewed as a point source in the geometry of the fluid phase by scaling the surface fluxes of mass and energy from the solid geometry to the bed geometry by a factor equal to the surface area of the solid per unit volume of fluid. If the fraction of the bed volume that is empty (porosity) is ε , and the particles are spheres of diameter D_p the scaling factor is

$$\frac{6}{D_p} \frac{1 - \varepsilon}{\varepsilon}$$

The solid geometry is thereby relegated to a point in the fluid geometry. The reaction rate term in the mass balance is not a reaction rate at all in this case. It is a mass transfer rate:

$$\mathcal{R}_{iv} = \rho_p S_g \frac{1 - \varepsilon}{\varepsilon} \int_S \mathbf{j}_i \cdot (-\mathbf{n}) dS$$

where S is the surface that encloses the solid and the outward directed unit normal is \mathbf{n} .

A general discussion of area and volume averaging is available in Slattery (1972).

The appropriate boundary conditions to be applied to the fixed bed were found by Danckwerts (1953) and Wehner and Wilhelm (1956) to be

$$c_{b0} = c_b(0) - \frac{1}{N_{Pe}} \frac{dc_b}{dz} \bigg|_{z=0}$$

$$\frac{dc_b}{dz} \bigg|_{z=L} = 0$$

These results were obtained by providing a fore and an aft section within each of which there was axial dispersion but

no reaction. Continuity of concentration and flows at the entrance and exit of the bed were applied. The preceding boundary conditions produced same behavior in the isolated reactor.

PROBLEMS

8.1. Prove the following identities:

- $\nabla \cdot (\nabla \cdot \mathbf{v}) \delta = \nabla (\nabla \cdot \mathbf{v})$
- $\nabla \cdot (\nabla \mathbf{v})^t = \nabla \cdot (\nabla \cdot \mathbf{v}) \delta$

8.2. Find $\nabla \cdot \boldsymbol{\tau}$ for a compressible Newtonian fluid.

8.3. Formulate the momentum balance for a compressible Newtonian fluid and display the rectangular components.

8.4. Plot calculated values of the viscosity of benzene versus absolute temperature for the following conditions:

- Saturated liquid
- Saturated vapor
- Low pressure gas

The temperature should be varied over the temperature range for vapor pressures for benzene.

Spot check the calculated values with experimental values.

Explain the behavior of the curves.

Plot the logarithm of the kinematic viscosity of the saturated vapor and saturated liquid versus the absolute temperature. Note any special features and in what circumstances, if any, these features may be exploited.

8.5. Isopropyl alcohol is often referred to as the first petrochemical (Kent, 1983). Approximately one half of the current production is used to manufacture acetone. A large percentage of the remaining half is used as a solvent. One step in the production of isopropyl alcohol is distillation to the binary azeotrope (see Example 6.2.1.2-11).

Develop the concentration dependence of the diffusivity of isopropyl alcohol in water for use in estimating the tray efficiencies.

NONTURBULENT ISOTHERMAL MOMENTUM TRANSFER

Application of the microscopic balance equations for momentum transport generally requires the selection of an equation of state, a transport model for viscous momentum flow, a visualization of the major flow patterns, and a consideration of the boundary features with respect to momentum transfer. The equation of continuity and the equations of motion in all three directions can then be written and the boundary conditions associated with the flow field can be formulated.

As an introduction to this process, Newtonian fluids with constant viscosity and constant density will be considered. The equation of state and the transport model parameters are fixed at the imposed temperature. The equations of motion can be simplified for such applications with the calculations illustrated in Section 8.7.2. The results are summarized below in Table 9.1 for some unidirectional systems.

9.1 RECTANGULAR MODELS

9.1.1 Slit Flow: Extrusion of Plastics Through Narrow Dies

Plastics are generally available in the form of solids, which are melted and formed into plastic products. Formation of products takes place with a die or mold. The required melting and the required pressurization are usually accomplished in an extruder containing a rotating screw. An extruder is illustrated in Figure 9.1.

Raw polymer in the form of particulate solids (pellets, powder, etc.) is gravitationally fed onto the screw through a hopper. The solids are then conveyed forward, plasticated,

homogenized, and pressurized along the rotating screw. The screw is rotated by electric motors through a gear reducer. The barrel is heated electrically or by a fluid heat exchanger system. Thermocouples placed in the metal barrel wall record and help to control barrel temperature settings. Sections of barrel, however, are often cooled to remove the excessive heat generated by viscous dissipation. A uniformly molten polymer arrives fully pressurized at the extruder “head,” thus prepared for further processing.

The extruded polymer is fed to the die where the polymer is formed into a desired shape or product, followed by cooling and solidification of the newly formed product. A cylindrical die, illustrated in Figure 9.2, is a common shape that is used for tubes and blown film.

Flow Visualization The problem that we wish to address here is the relationship between pressurization by the extruder and the throughput of molten polymer through a cylindrical die. We will, for purposes of illustration, make some approximations. If the radius of the cylindrical die is very much greater than its thickness, we can approximate the natural cylindrical geometry with a rectangular one. The flow direction will be z . The radial direction will be replaced with y and the angular distance with x . A summary of the flow geometry is illustrated below in Figure 9.3. The center of the coordinate system is placed in a symmetrical position.

Additional assumptions are

- fully developed flow at the inlet,
- negligible effect of boundaries in x direction,
- negligible effects of gravity,

TABLE 9.1 Steady-State Momentum Balance, Unidirectional Velocity, Newtonian Fluid with Constant Density and Viscosity, Navier–Stokes Equations

Rectangular System: $\mathbf{v} = v_z \mathbf{\hat{e}}_z$	
Continuity	$\frac{\partial v_z}{\partial z} = 0$
Motion in x direction	$\frac{\partial P}{\partial x} = \rho g_x$
Motion in y direction	$\frac{\partial P}{\partial y} = \rho g_y$
Motion in z direction	$\frac{\partial P}{\partial z} - \eta \left[\frac{\partial^2 v_z}{\partial x^2} + \frac{\partial^2 v_z}{\partial y^2} \right] = \rho g_z$
Nonzero momentum fluxes	$\tau_{yz} = \tau_{zy} = -\eta \frac{\partial v_z}{\partial y}$ $\tau_{zx} = \tau_{xz} = -\eta \frac{\partial v_z}{\partial x}$
Cylindrical System: $\mathbf{v} = v_z \mathbf{\hat{e}}_z$	
Continuity	$\frac{\partial v_z}{\partial z} = 0$
Motion in r direction	$\frac{\partial P}{\partial r} = \rho g_r$
Motion in θ direction	$\frac{1}{r} \frac{\partial P}{\partial \theta} = \rho g_\theta$
Motion in z direction	$\frac{\partial P}{\partial z} - \eta \left[\frac{1}{r} \frac{\partial}{\partial r} \left(r \frac{\partial v_z}{\partial r} \right) + \frac{1}{r^2} \frac{\partial^2 v_z}{\partial \theta^2} \right] = \rho g_z$
Nonzero momentum fluxes	$\tau_{z\theta} = \tau_{\theta z} = -\frac{\eta}{r} \frac{\partial v_z}{\partial \theta}$ $\tau_{zr} = \tau_{rz} = -\eta \frac{\partial v_z}{\partial r}$
Cylindrical system: $\mathbf{v} = v_\theta \mathbf{\hat{e}}_\theta$	
Continuity	$\frac{1}{r} \frac{\partial v_\theta}{\partial \theta} = 0$
Motion in r direction	$-\rho \frac{v_\theta^2}{r} + \frac{\partial P}{\partial r} = \rho g_r$
Motion in θ direction	$\frac{1}{r} \frac{\partial P}{\partial \theta} - \eta \left[\frac{\partial}{\partial r} \left(\frac{1}{r} \frac{\partial r v_\theta}{\partial r} \right) + \frac{\partial^2 v_\theta}{\partial z^2} \right] = \rho g_\theta$
Motion in z direction	$\frac{\partial P}{\partial z} = \rho g_z$
Non zero momentum fluxes	$\tau_{r\theta} = \tau_{\theta r} = -\eta r \frac{\partial}{\partial r} \left(\frac{v_\theta}{r} \right)$ $\tau_{z\theta} = \tau_{\theta z} = -\eta \frac{\partial v_\theta}{\partial z}$
Spherical system: $\mathbf{v} = v_\theta(r, \theta) \mathbf{\hat{e}}_\theta$	
Continuity	$\frac{\partial}{\partial \theta} [v_\theta \sin \theta] = 0$
Motion in r direction	$-\rho \frac{v_\theta^2}{r} = -\frac{\partial P}{\partial r} + \eta \left[-\frac{2}{r^2} \frac{\partial v_\theta}{\partial \theta} - \frac{2}{r^2} v_\theta \cot \theta \right] + \rho g_r$
Motion in θ direction	$\frac{\rho v_\theta}{r} \frac{\partial r v_\theta}{\partial r} = -\frac{1}{r} \frac{\partial P}{\partial \theta} + \eta \left[\frac{1}{r^2} \frac{\partial}{\partial r} \left(r^2 \frac{\partial v_\theta}{\partial r} \right) + \frac{1}{r^2 \sin \theta} \frac{\partial}{\partial \theta} \left(\sin \theta \frac{\partial v_\theta}{\partial \theta} \right) + \frac{1}{r^2 \sin \theta} \left(\frac{\partial^2 v_\theta}{\partial \phi^2} \right) - \frac{v_\theta}{r^2 \sin \theta} \right] + \rho g_\theta$
Motion in ϕ direction	$0 = -\frac{1}{r \sin \theta} \frac{\partial P}{\partial \phi} + \rho g_\phi$
Nonzero momentum fluxes	$\tau_{\theta\theta} = -2\eta \frac{1}{r} \frac{\partial v_\theta}{\partial \theta}$ $\tau_{\phi\phi} = \tau_{\theta z} = -2\eta \frac{v_\theta \cot \theta}{r}$ $\tau_{r\theta} = \tau_{\theta r} = -\eta r \frac{\partial}{\partial r} \left(\frac{v_\theta}{r} \right)$

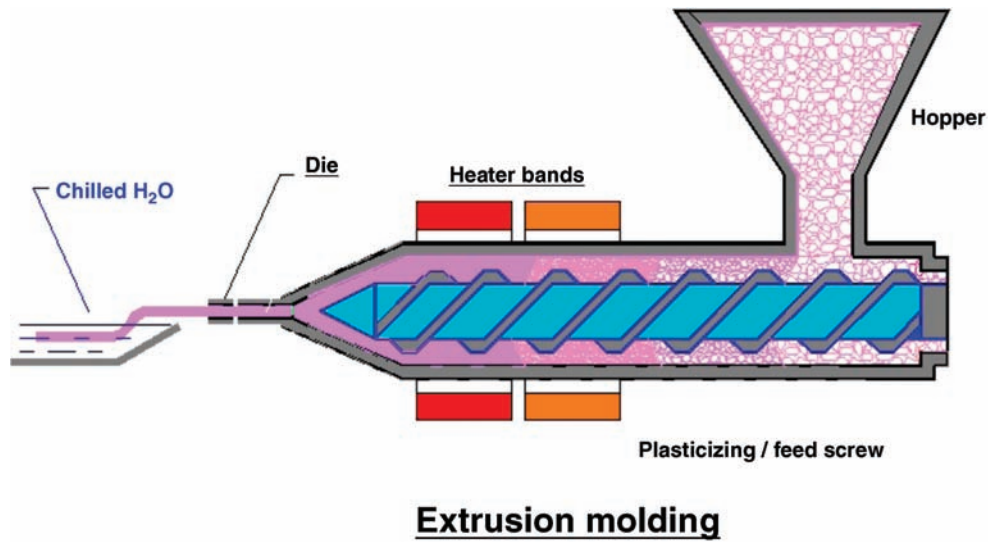


FIGURE 9.1 Extruder with exposed view of barrel. Reprinted with permission of Dr. Aaron Ball, Western Carolina University.

- and a Newtonian fluid with a viscosity. This assumption is perhaps the most restrictive one in the case of plastics.

The circumference of the extruded pipe is W and its wall thickness is H . We can readily see that the approximate flow

field has the following characteristics:

$$v_x = 0 \quad (9.1)$$

$$v_y = 0 \quad (9.2)$$

$$v_z = v_z(y, z) \quad (9.3)$$

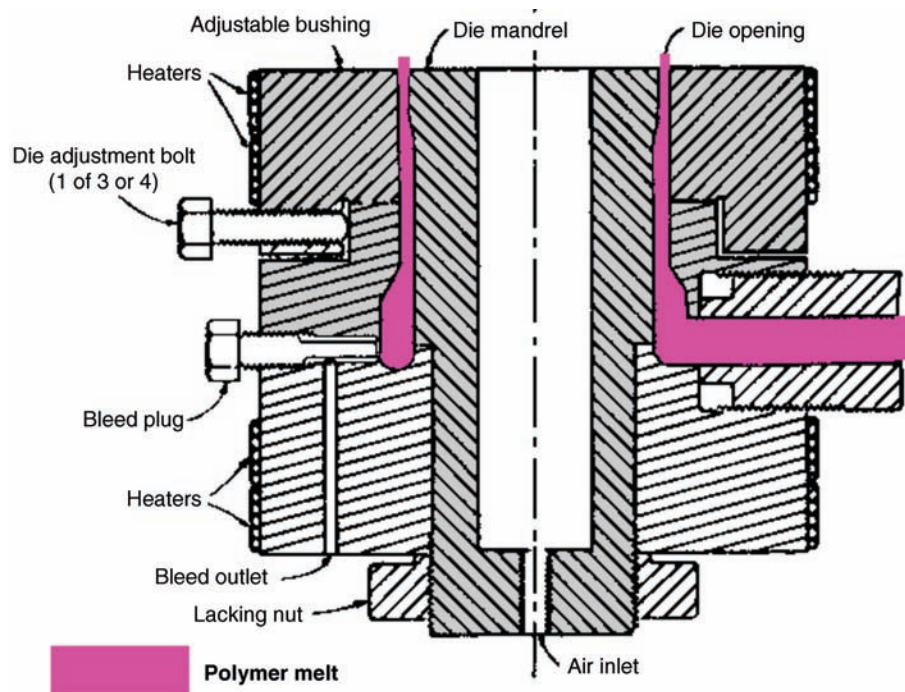


FIGURE 9.2 Cylindrical die.

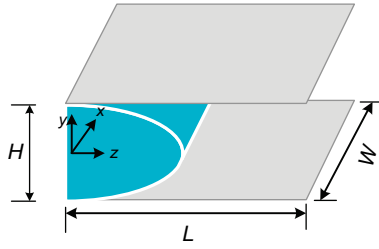


FIGURE 9.3 Approximate flow geometry.

with no variations in the x direction. The appropriate simplifications of the balance equations for this situation are therefore those summarized in Table 9.1 (rectangular coordinates) at the beginning of this chapter.

Continuity Equation

$$\frac{\partial v_z}{\partial z} = 0 \quad (9.4)$$

Momentum Balance

$$\frac{\partial P}{\partial x} = \rho g_x = 0 \quad (9.5)$$

$$\frac{\partial P}{\partial y} = \rho g_y = 0 \quad (9.6)$$

$$\frac{\partial P}{\partial z} - \eta \left[\frac{\partial v_z^2}{\partial x^2} + \frac{\partial v_z^2}{\partial y^2} \right] = \rho g_z = 0 \quad (9.7)$$

Boundary Conditions The boundary conditions associated with momentum transfer are in column M of Table 8.13. Here the α -phase is the polymer and the β -phase is the solid die. Curvature is not an issue and the die surface is not permeable so that M1 and M2 are not needed. The remaining boundary conditions (M3–M5) consist of a momentum flux condition for the β -phase and a no slip condition that can be applied to the α -phase. Since the die is stationary, the tangential component of the polymer velocity must vanish at the die surface.

$$v_z(y, z) = 0 \quad \text{at } y(\pm H/2) = 0 \quad (9.8)$$

There are no other boundaries to consider.

Solution The equations of motion in the x and y directions imply that P can at most depend on z . The equation of motion in the z direction with the flow imagined above not to

vary in the x direction is given by

$$\underbrace{\frac{\partial P}{\partial z}}_{f(z)} = \eta \underbrace{\left[\frac{\partial v_z^2}{\partial y^2} \right]}_{g(y)} \quad (9.9)$$

The flow visualization and the equation of continuity imply that v_z can depend only on y . The preceding equation calls for a function of z to be equal to a function of y , which can only be true if the function is constant:

$$\frac{\partial P}{\partial z} = \text{constant} = -\frac{P_0 - P_L}{L} \quad (9.10)$$

where P_0 and P_L are evaluated at $(0, 0, 0)$ and $(0, 0, L)$, respectively. The equation of motion in the z direction becomes

$$\frac{d^2 v_z}{dy^2} = -\frac{P_0 - P_L}{\eta L} \quad (9.11)$$

The general solution to the differential equation is given by

$$v_z(y) = -\frac{P_0 - P_L}{2\eta L} y^2 + C_1 y + C_2 \quad (9.12)$$

The constants, C_1 and C_2 , can be evaluated with the boundary conditions given above in Equation (9.1) to give

$$v_z(y) = v_{\max} \left[1 - \left(\frac{y}{H/2} \right)^2 \right] \quad (9.13)$$

where

$$v_{\max} = \frac{P_0 - P_L}{2\eta L} \left[\frac{H}{2} \right]^2 \quad (9.14)$$

The parabolic velocity distribution is a microscopic result in that the velocity is described pointwise throughout the die. The distribution is shown in Figure 9.4 in comparison to the average velocity.

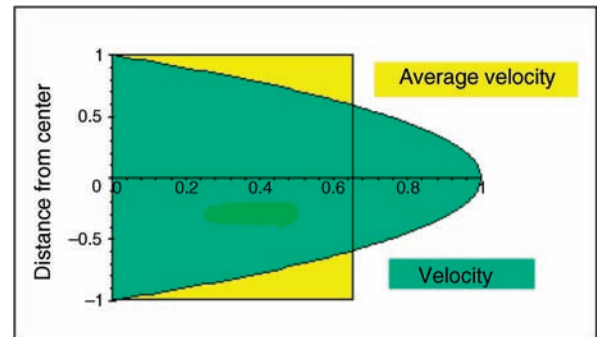


FIGURE 9.4 Velocity field in the die slit.

The average velocity is defined on the basis that it may be used to evaluate the total mass flow rate through the slit.

Example 9.1.1-1: Average Velocity and Volumetric Flow Rate

$$\rho \langle v \rangle WH = \int_{-H/2}^{H/2} \int_0^W \rho \mathbf{v} \cdot \hat{\mathbf{n}}_z dS_x dS_y = \text{total mass flow rate} \quad (9.15)$$

$$= \int_{-H/2}^{H/2} \int_0^W \rho v_z dx dy = \int_{-H/2}^{H/2} \int_0^W \rho v_{\max} \left[1 - \left(\frac{y}{H/2} \right)^2 \right] dx dy \quad (9.16)$$

$$\langle v \rangle = \frac{2}{3} v_{\max} \quad (9.17)$$

At constant density, the volume and mass average velocities are equal. The velocity is the volume flux so that the volume flow rate, \mathcal{V} , is the average velocity multiplied by the cross-sectional area:

$$\mathcal{R} = \frac{1}{12} \frac{P_0 - P_L}{\eta L} WH^3 \quad (9.18)$$

Note, for example, that \mathcal{V} increases linearly with the pressure drop and cubically with the slit thickness.

9.2 CYLINDRICAL SYSTEMS

9.2.1 Axial Flow—Flow in Pipes and Tubes

Flow in pipes and tubes is ubiquitous in chemical processing. Pipes transport fluids between units in a plant, across the country from wells to seaside distribution facilities. Tubes provide the heat exchange area in shell and tube heat exchangers and often provide the residence time for chemical reactions to take place.

The reduction of the general microscopic momentum balance equations to the case of tube flow was carried out in Section 8.7.2 to illustrate the steps involved.

Flow Visualization In summary, gravity was placed along the axis of the tube. No angular imbalances were imagined and the velocity was argued to vanish at the tube wall. Consequently, the flow field was imagined to be the paraboloid, shown in Figure 8.18, with the center of the coordinate system placed on the tube axis. The system boundary is then one the coordinate planes. The simplified balance equations in Table 9.1 for a cylindrical system with flow only in the z direction therefore apply.

Continuity With only a z component of velocity, the equation of continuity reduces to Equation (9.4).

Momentum The momentum balance is given by Equations (8.215)–(8.217).

Boundary Conditions The fluid must cling to the walls (M3–M6 in Table 8.13) or

$$v_z = 0 \quad \text{at } r = R \text{ for } 0 \leq z \leq L \quad (9.19)$$

Solution The equations of motion in the radial and angular directions imply that the pressure field can only be a function of z . The equation of motion in the z direction therefore contains the z -dependent pressure term and the r -dependent viscous term.

$$\underbrace{\frac{\partial P}{\partial z} - \rho g_z}_{f(z)} = \underbrace{\eta \left[\frac{1}{r} \frac{\partial}{\partial r} \left(r \frac{\partial v_z}{\partial r} \right) \right]}_{g(r)} \quad (9.20)$$

This is only possible if the functions are equal to the same constant:

$$\frac{d(P - \rho g z)}{dz} = A \quad (9.21)$$

The component of gravity in the positive z direction (axial flow direction) is g .

The constant A is therefore proportional to the pressure drop:

$$A = - \left[\frac{P_1 - P_2}{L} + \rho g \right] \quad (9.22)$$

The general solution to

$$\eta \left[\frac{1}{r} \frac{\partial}{\partial r} \left(r \frac{\partial v_z}{\partial r} \right) \right] = A \quad (9.23)$$

is

$$v_z = \frac{A r^2}{4\eta} + B \ln r + C \quad (9.24)$$

The constant B must be zero for a finite solution (see note in Table 8.13), since the center of the tube is in our purview. This solution would be retained in an annular flow problem (see also Sections 9.2.1.5 and 9.2.2.1). The value of C can be set to satisfy the boundary condition in Equation (9.19) to give the final result:

$$v_z = \frac{R^2}{4\eta} \left[\frac{P_1 - P_2}{L} + \rho g \right] \left[1 - \left(\frac{r}{R} \right)^2 \right] \quad (9.25)$$

The pressure drop must also be specified to determine the resulting flow. Note the similarities to slit flow.

Example 9.2.1-1: Volumetric Flow Rate

The volumetric flow rate in the z direction is obtained on the same basis as the volumetric flow in thin slits given above:

$$\begin{aligned} dV_z &= \mathbf{v} \cdot \mathbf{\delta}_z dS_r dS_\theta = v_z dr (rd\theta) \\ V &= 2\pi \int_0^R \left(\frac{R^2}{4\mu} \left[\frac{P_1 - P_2}{L} + \rho g \right] \left[1 - \left(\frac{r}{R} \right)^2 \right] \right) r dr \\ V &= \frac{\pi R^4}{8\mu} \left[\frac{P_1 - P_2}{L} + \rho g \right] \end{aligned}$$

Example 9.2.1-2: Average Velocities

In the application of the mechanical energy balance to pipe flow, the average velocity squared was used in place of the average square velocity, which is an approximation better suited to the relatively flat turbulent velocity profile than the parabolic laminar profile. The correction factor for laminar flow may be computed as follows:

$$\begin{aligned} \langle v \rangle &= \frac{1}{2\pi R^2} \int_0^{2\pi} \int_0^R v_z(r) r dr d\theta \\ \langle v \rangle &= \frac{1}{R^2} \int_0^R \frac{R^2}{4\mu} \left[\frac{P_1 - P_2}{L} + \rho g \right] \left[1 - \left(\frac{r}{R} \right)^2 \right] dr \\ \langle v \rangle &= \left[\frac{P_1 - P_2}{L} + \rho g \right] \frac{R^2}{8\mu} = \frac{v_{z,\max}}{2} \end{aligned}$$

Similarly,

$$\begin{aligned} \langle v^2 \rangle &= \frac{1}{R^2} \int_0^R \frac{R^2}{4\mu} \left[\frac{P_1 - P_2}{L} + \rho g \right] \left[1 - \left(\frac{r}{R} \right)^2 \right] dr \\ \langle v^2 \rangle &= \frac{2}{\pi R^2} \int_0^R \left\{ \frac{v_{z,\max}}{2} \left[1 - \left(\frac{r}{R} \right)^2 \right] \right\}^2 r dr d\theta \\ \langle v^2 \rangle &= \frac{v_{z,\max}^2}{2} = 2 \langle v \rangle^2 \end{aligned}$$

The large difference is due to the parabolic shape of the velocity field.

9.2.1.1 Friction Factor In the mechanical energy balance in Chapter 4, the force on the tube wall was expressed

as a fraction of a characteristic momentum flux. That fraction, called the Fanning friction factor, is developed for laminar flow as follows.

The force exerted by the fluid on the tube wall in the z direction is given by the z component of the momentum flow to the wall:

$$dF_z = [(\mathbf{\Pi} \cdot \mathbf{\delta}_r) dS_\theta dS_z] \cdot \mathbf{\delta}_z \quad \text{at } r = R \quad (9.26)$$

$$dF_z = [(P\delta_{ij}\mathbf{\delta}_i\mathbf{\delta}_j \cdot \mathbf{\delta}_r + \tau_{ij}\mathbf{\delta}_i\mathbf{\delta}_j \cdot \mathbf{\delta}_r)]_{r=R} \cdot \mathbf{\delta}_z R d\theta dz \quad (9.27)$$

$$dF_z = (P\mathbf{\delta}_r + \tau_{ir}\mathbf{\delta}_i)|_{r=R} \cdot \mathbf{\delta}_z R d\theta dz = \tau_{zr}|_{r=R} R d\theta dz \quad (9.28)$$

$$dF_z = -\eta \frac{dv_z}{dr} \bigg|_{r=R} R d\theta dz \quad (9.29)$$

$$F_z = -\eta \frac{dv_z}{dr} \bigg|_{r=R} R \int_0^L \int_0^{2\pi} d\theta dz = -2\pi R \eta L \frac{dv_z}{dr} \bigg|_{r=R} = 8\pi \eta L \langle v \rangle \quad (9.30)$$

Since the forces on the fluid due to the applied pressure drop and the fluid head must, at steady flow, exactly counter-balance the forces exerted by the tube walls.

$$F_z = [(P_1 - P_2) + \rho g L] \pi R^2 = 8\pi \eta L \langle v \rangle \quad (9.31)$$

The Fanning friction factor expresses the force on the tube wall as a fraction of a characteristic momentum flux and the wall area:

$$F_z = [(P_1 - P_2) + \rho g L] \pi R^2 \quad (9.32)$$

$$\frac{f}{2} (\rho \langle v \rangle^2) \pi D L = 8\pi \eta L \langle v \rangle \quad (9.33)$$

or

$$f = \frac{16}{N_{Re}} \quad (9.34)$$

This equation is valid up to a Reynolds number of approximately 2100 where the flow becomes turbulent.

9.2.1.2 Pump Requirements The pressure that must be developed by a pump placed at the pipe inlet for a given volumetric flow and outlet pressure for a pipe section of specified length is given by

$$P_1 = P_2 + \left[\frac{4\mu^2 L}{\rho R^3} \right] N_{Re} - \rho g L \quad (9.35)$$

See Chapter 13 for a discussion of pipe flow under turbulent conditions.

9.2.1.3 Distribution of Residence Times We can imagine that the fluid elements arrive at the tube entrance in all respects equal except for the radial location of their arrival, whereupon a parabolic velocity distribution is instantly formed or is formed over a distance very much shorter than the length of the tube. This assumption is questionable in many applications. The development of a fully parabolic velocity distribution may require as much as 50 pipe diameters (Denbigh, 1966). The individual elements traverse the length of the tube without mixing and without departing from the radius of their arrival

The residence time is therefore related to the radius as follows for a tube of length L :

$$\frac{L}{t} = v_{\max} \left[1 - \left(\frac{r}{R} \right)^2 \right] \quad (9.36)$$

$$\frac{L}{t_0} = v_{\max} \quad (9.37)$$

$$\frac{t_0}{t} = \left[1 - \left(\frac{r}{R} \right)^2 \right] \quad \text{and} \quad -\frac{t_0}{t^2} dt = -2 \left(\frac{r}{R} \right) \frac{1}{R} dr \quad (9.38)$$

The fraction of the fluid with residence times between t and $t + dt$ is given by the fraction of the fluid entering between the corresponding values of the radius:

$$f(t)dt = \frac{dV}{V} = \frac{v_{\max} \left[1 - \left(\frac{r}{R} \right)^2 \right] 2\pi r dr}{\int_0^R v_{\max} \left[1 - \left(\frac{r}{R} \right)^2 \right] 2\pi r dr} = \frac{\frac{t_0}{t} \frac{R^2}{2} \frac{t_0}{t^2} dt}{\frac{R^2}{4}} \quad (9.39)$$

$$f(t) = 2 \frac{t_0^2}{t^3}, \quad t \geq t_0 \quad (9.40)$$

The mean residence time is

$$\langle t \rangle = \int_{t_0}^{\infty} t f(t) dt = \int_{t_0}^{\infty} 2 \frac{t_0^2}{t^2} dt = 2t_0 \quad (9.41)$$

The contribution of the slower moving fluid elements is to increase the average residence time by a factor of 2!

The cumulative distribution is provided by the integral

$$F(t) = \int_{t_0}^t 2 \frac{t_0^2}{x^3} dx = 1 - \left(\frac{t_0}{t} \right)^2 \quad (9.42)$$

Some values of the cumulative distribution are listed in Table 9.2.

Here we see, for example, that a full 25% of the fluid has a residence time greater than twice the value at the center. Moreover, the residence times of this fraction are sufficient

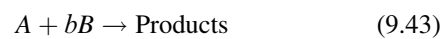
TABLE 9.2 Values of Cumulative Distribution

t/t_0	$F(t/t_0)$
1.0000	0.0000
1.2500	0.3600
1.5000	0.5556
1.7500	0.6735
2.0000	0.7500

to counterbalance the residence times of the 75% that have residence times less than the average.

9.2.1.4 Laminar Flow Reactor (and Substantial Derivative) The results of the preceding section can be applied to a reactive case with some additional assumptions. We suppose that the fluid arriving at the tube entrance is a reactive liquid mixture but that the extent of the ensuing reaction(s) will have no significant effect on the fluid density. We will assume that molecular diffusion is likewise insignificant and that the heat of reaction produces no noticeable change in temperature. Each arriving fluid element then arrives at the tube entrance in all respects equal and traverses the length of the tube in the time associated with point of arrival. While in the tube, each fluid element acts as an independent batch reactor.

Consider a reaction with the following stoichiometry:



When B is present very much in excess, the molar reaction rate per unit volume can be expressed as

$$\mathcal{R}_v = k c_{B0}^\beta c_A \quad (9.44)$$

The concentration of A depends on the residence time.

From Table 8.12:

$$\frac{dc_A}{dt} = -k c_{B0}^\beta c_A, \quad c_A(0) = c_{A0} \quad (9.45)$$

This result can be derived by developing a mass balance for a constant volume element with time counted from the point of arrival to the residence time at the arrival radius. On the other hand, we have a general microscopic mass balance in hand, so let us consider how it can be applied to this situation.

Example 9.2.1.4-1: Application of Microscopic Mass Balance to Laminar Flow Reactor

Our viewpoint here is by an observer moving with the mass average velocity of the fluid, while that of the microscopic balances (continuity and species) are by an observer fixed in space. The microscopic balances can be placed on the same basis as follows:

From Table 8.12

$$\frac{\partial \rho_i}{\partial t} + \nabla \cdot (\rho_i \mathbf{v} + \mathbf{j}_i) = r_{iv} = M_i \vartheta_i \mathcal{R}_v$$

but $\rho_i = \omega_i \rho$ so that substituting and differentiating gives

$$\omega_i \frac{\partial \rho}{\partial t} + \rho \frac{\partial \omega_i}{\partial t} + \rho_i \nabla \cdot \mathbf{v} + \mathbf{v} \cdot \nabla \rho_i + \nabla \cdot \mathbf{j}_i = M_i \vartheta_i \mathcal{R}_v$$

Differentiating again, collecting terms, and using the continuity equation

$$\omega_i \left[\frac{\partial \rho}{\partial t} + \rho \nabla \cdot \mathbf{v} \right] + \rho \frac{\partial \omega_i}{\partial t} + \mathbf{v} \cdot [\omega_i \nabla \rho + \rho \nabla \omega_i] + \nabla \cdot \mathbf{j}_i = M_i \vartheta_i \mathcal{R}_v$$

or

$$\rho \left[\underbrace{\frac{\partial \omega_i}{\partial t} + \mathbf{v} \cdot \nabla \omega_i}_{\frac{D\omega_i}{Dt}} \right] = M_i \vartheta_i \mathcal{R}_v - \nabla \cdot \mathbf{j}$$

A similar result would have been obtained in terms of the molar density and mole fraction. The bracketed term is the time derivative compiled by an observer moving with the mass average velocity (D/Dt). This is called the substantial derivative. The first term provides the changes due to the passage of time ($\partial/\partial t$) and the second term ($\mathbf{v} \cdot \nabla$) provides the changes due to the changes in position with respect to time, or the velocity. He attributes the changes in concentration to diffusion into his element (relative to his velocity) and to chemical reaction. If there is no diffusion and the kinetics follow the rate expressed above, we obtain at constant density

$$\frac{Dc_i}{Dt} = \vartheta_i R$$

The mass balance in Equation (9.45) is thus confirmed.

The solution to Equation (9.45) is

$$c_A = c_{A0} e^{-k_B t} \quad \text{where } k_B = k c_{B0}^\beta \quad (9.46)$$

The cup average outlet concentration is then

$$\langle c_A \rangle = \int_{t_0}^{\infty} f(t) c_{A0} e^{-k_B t} dt = \int_{t_0}^{\infty} 2 \frac{t_0^2}{t^3} c_{A0} e^{-k_B t} dt \quad (9.47)$$

The cup average is weighted by the flow field. It is convenient to express these results in terms of conversion:

$$x = 1 - \frac{1}{2} \int_{0.5}^{\infty} \frac{1}{\theta^3} e^{-N_{Da}\theta} d\theta \quad (9.48)$$

where

$$x = \frac{c_{A0} - \langle c_A \rangle}{c_{A0}} \quad \text{and } N_{Da} = \frac{2t_0}{1/k_B} \quad (9.49)$$

The Damköhler number, N_{Da} , is the ratio of the average residence time to the first-order time constant. Hence, large conversions are associated with large values of the Damköhler number.

Integrating the result for the conversion by parts gives

$$x = 1 - e^{-\frac{N_{Da}}{2}} \left[1 - \frac{N_{Da}}{2} \right] - \left[\frac{N_{Da}}{2} \right]^2 \int_{0.5}^{\infty} \frac{1}{\theta} e^{-N_{Da}\theta} d\theta \quad (9.50)$$

$$1 - e^{-\frac{N_{Da}}{2}} \left[1 - \frac{N_{Da}}{2} \right] + \left[\frac{N_{Da}}{2} \right]^2 Ei \left(-\frac{N_{Da}}{2} \right) \quad (9.51)$$

Values of the exponential integral are available in tabular form (Abramowitz and Stegun, 1965).

9.2.1.5 Wetted Wall Towers A wetted wall tower is a gas-liquid contacting device of known interfacial area. See Figure 9.5. A liquid flows by gravity down the inside of a circular pipe, while a gas flows up or down the center. Such arrangements have been used to study mass transfer to gases in pipes (see Chapter 12). Commercial applications include the absorption of hydrochloric acid, which is accompanied by a very large heat effect. In this case, cooling water is passed over the external surface of the tube, which is mounted in a multitube arrangement. In this way, the generation of thermal energy per unit volume in the thin film is well within the capacity of the large volume of coolant. As a first approximation, we will assume that the effects of energy and mass transfer on the flow field are small. The resulting flow field will be used in those calculations since the reverse is not a good assumption.

Fixing a cylindrical coordinate system on the axis at the top of the tower, it is clear that the velocity is only in the axial or z direction ($\mathbf{v} = v_z \delta_z$) and the cylindrical coordinate system captures the system boundaries. The equations in Table 9.1 therefore apply with gravity in the z direction only:

$$\text{Continuity Equation: } \frac{\partial v_z}{\partial z} = 0 \quad (9.52)$$

Equation of Motion:

$$\text{r direction: } \frac{\partial P}{\partial r} = 0 \quad (9.53)$$

$$\theta \text{ direction: } \frac{\partial P}{\partial \theta} = 0 \quad (9.54)$$

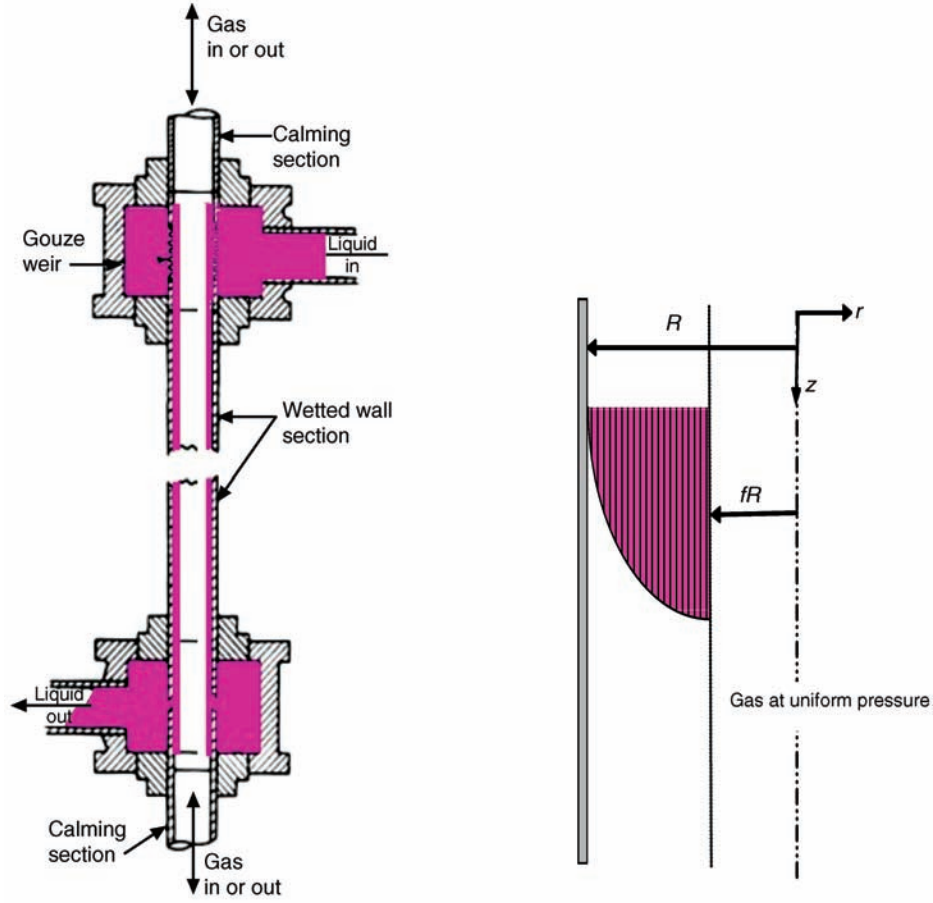


FIGURE 9.5 Wetted wall tower (McCabe et al., 2001). Reprinted with permission of McGraw-Hill.

$$z \text{ direction: } \frac{\partial P}{\partial z} - \frac{\eta}{r} \frac{\partial}{\partial r} \left(r \frac{\partial v_z}{\partial r} \right) = \rho g_z \quad (9.55)$$

or

$$\begin{aligned} \tau_{rr} &= 0 \\ \Rightarrow \tau_{\theta r} &= 0 \\ \tau_{zr} &= 0 \end{aligned} \quad (9.59)$$

The boundary conditions (see Table 8.13) are

1. Mechanical equilibrium exists at the gas–liquid interface (M1):

$$P(R, z) = P_0 = \text{uniform gas phase pressure} \quad (9.56)$$

2. There is no significant transfer of momentum by viscous mechanisms from the gas to the liquid (M3–M5 with $\boldsymbol{\tau}^{(B)} \cdot (-\boldsymbol{\delta}_r) = 0$). Consequently, at the gas–liquid interface

$$\boldsymbol{\tau} \cdot \boldsymbol{\delta}_r(R, z) = \mathbf{0} \quad (9.57)$$

Obtaining the vector product in Equation (9.57) gives

$$\tau_{ij} \boldsymbol{\delta}_i \boldsymbol{\delta}_j \cdot \boldsymbol{\delta}_r = \tau_{ij} \delta_{jr} \boldsymbol{\delta}_i = \tau_{ir} \boldsymbol{\delta}_i = \mathbf{0} \quad (9.58)$$

The first two of the three conditions in Equation (9.59) are satisfied because of the assumed velocity distribution. The third requires that

$$\tau_{zr} = -\eta \frac{\partial v_z}{\partial r} = 0 \text{ at } r = fR \quad (9.60)$$

The solution may be obtained as follows: The equation of continuity implies that the velocity in the z direction does not vary with z . Since there is angular symmetry, the axial velocity can only depend on the radius.

The pressure does not depend on the radius or the angle. Because of mechanical equilibrium, it is equal to

the gas pressure at each value of z . Since the gas pressure is assumed to be uniform, the system pressure does not depend on z .

The problem therefore reduces to

$$-\frac{\eta}{r} \frac{d}{dr} \left(r \frac{dv_z}{dr} \right) = \rho g_z \quad (9.61)$$

With the two boundary conditions

$$-\eta \frac{dv_z}{dr} = 0 \text{ at } r = fR \quad (9.62)$$

$$v_z = 0 \text{ at } r = R \quad (9.63)$$

The exact solution is

$$v_z(r) = \frac{\rho g R^2}{4\eta} \left(1 - \frac{r^2}{R^2} + 2f^2 \ln \frac{r}{R} \right) \quad (9.64)$$

Note that the solution is not required to be at the center of the tube.

The maximum velocity is clearly at the free surface of the liquid.

$$v_{\max} = \frac{\rho g R^2}{4} (1 - f^2 + 2f^2 \ln f) \quad (9.65)$$

The volumetric flow rate of the liquid is obtained as follows:

$$\mathcal{V} = \int_{fR}^R \int_0^{2\pi} v_z(r) r d\theta dr = 2\pi \int_{fR}^R v_z(r) r dr = \langle v \rangle \int_{fR}^R \int_0^{2\pi} r d\theta dr \quad (9.66)$$

or

$$\mathcal{V} = \frac{\pi \rho g R^4}{8\eta} H(f) \quad (9.67)$$

where

$$\langle v \rangle = \frac{\rho g R^2}{8\eta} \frac{H(f)}{1 - f^2} \quad (9.68)$$

and x

$$H(f) = 1 - 4f^2 + 3f^4 - 4f^4 \ln f \quad (9.69)$$

The function H is a monotonically decreasing function of the fraction f . The maximum value of the volumetric flow rate is then the value for a filled tube flowing under gravity alone as given above for flow in pipes and tubes (Example 9.2.1-1).

While this is reassuring, it has little practical value since the fraction f is near unity or if $f = 1 - \epsilon$, the value of ϵ is quite small. In this case, the value of H may be approximated by a Taylor series about the origin:

$$H(1 - \epsilon) = \frac{16}{3} \epsilon^3 + O(\epsilon^4) \quad (9.70)$$

The value of Q to a good approximation is then

$$\mathcal{V} \approx \frac{\pi \rho g R^4}{8\eta} \frac{16}{3} \epsilon^3 = \frac{\pi \rho g D}{3\eta} \delta^3 \quad (9.71)$$

where the film thickness, ϵR , is denoted by δ :

$$\delta \approx \left[\frac{3\eta \mathcal{V}}{\pi \rho g D} \right]^{1/3} \quad (9.72)$$

The error in this approximation depends on the value of ϵ or f . The solution is limited to laminar flow, which is conservatively restricted to a Reynolds number of 250 (Danckwerts, 1970).

Turbulence sets in at $Re = 250$ (Conservative)

$$N_{Re} = \frac{\rho \mathcal{V}}{\pi D \eta} \leq 250 \quad (9.73)$$

This provides a maximum value of the film thickness for which the solution can be applied

$$\frac{1}{v^2} \frac{g R^3}{16} H(f) \leq 250 \quad (9.74)$$

or

$$H(f_{\min}) = 4000 \frac{v^2}{g R^3} \quad (9.75)$$

where v is the kinematic viscosity.

Example 9.2.1.5-1: Error in Film Thickness Approximation

For water in a 1 in. column

$$\begin{aligned} H(f_{\min}) &= 0.000024882 \\ f_{\min} &= 0.9820 \end{aligned}$$

The percent error in the film thickness incurred by using the approximation is

$$E(f) = 100 \left(1 - \left(\frac{3}{16} \right)^{1/3} (H(f))^{1/3} / (1 - f) \right)$$

$$E(0.9820) = 1.235$$

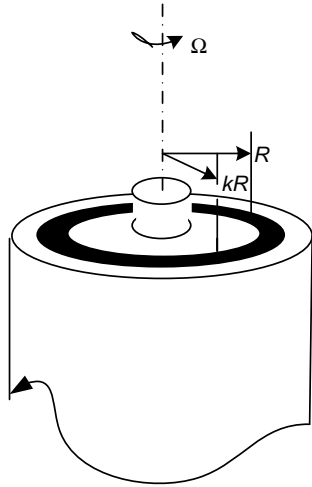


FIGURE 9.6 Couette viscometer.

The error in film thickness is quite small under these conditions and decreases with increasing f (decreasing film thickness).

9.2.2 Angular Flow

9.2.2.1 Couette Viscometer Viscosity measurements can be carried out in a Couette viscometer where the resistance of a fluid to motion in an annular gap is measured by the torque on the inner cylinder whose rotation drives the motion. Refer to Figure 9.6.

Flow Visualization The inner cylinder is made to rotate at an angular velocity Ω . The fluid whose viscosity is to be determined fills the annular region between R and κR over the length L . The ends of the cylinder are closed and we assume that the length is sufficiently large that the effect of the closed ends on the velocity field may be neglected over the entire length. Under these conditions, the only flow is in the angular direction of a cylindrical coordinate system whose z axis is the axis of the inner cylinder and whose coordinate planes capture the system boundaries. The equations of motion and continuity in Table 9.1 (cylindrical system, angular motion) therefore apply with gravity acting only in the z direction and the angular velocity independent of z .

The equation of continuity is consistent with our vision of the flow field. Gravity only acts in the z direction so that

$$\text{Motion in } r \text{ direction: } \frac{\partial P}{\partial r} = \rho \frac{v_\theta^2}{r} \quad (9.76)$$

Pressure variations in the angular direction are also inconsistent with our vision of the flow field so that the

equation of motion in the angular direction becomes

$$-\eta \left[\frac{\partial}{\partial r} \left(\frac{1}{r} \frac{\partial r v_\theta}{\partial r} \right) \right] = 0 \quad (9.77)$$

The pressure changes in the z direction are due to gravity as indicated by the simplified equation of motion in the z direction:

$$\text{Motion in } z \text{ direction: } \frac{\partial P}{\partial z} = \rho g_z \quad (9.78)$$

Boundary Conditions The boundary conditions (on the velocity) are that the fluid clings to both cylinder walls one of which is moving. See Table 8.13 (tangent condition in M2–M5) with the fluid sample as phase α and the cylinder walls as the β phase:

$$v_\theta(\kappa R) = \Omega \kappa R \quad (9.79)$$

$$v_\theta(R) = 0 \quad (9.80)$$

Solution The equation of motion in the angular direction with boundary conditions provides the velocity as a function of radial position. With the substitution this solution into equations of motion in the radial and axial directions, the pressure field can be obtained if the pressure is established at one axial and one radial position.

The general solution to Equation (9.77) is

$$v_\theta(r) = Ar + \frac{B}{r} \quad (9.81)$$

Note that in contrast to pipe flow, for example, the value of zero for the radius is outside the region over which the equation of motion is being applied. The parameter B may therefore be retained and, along with A , evaluated from the boundary conditions. The result is that the angular velocity depends on the radial position as follows:

$$v_\theta = \frac{\Omega \kappa R}{((1/\kappa) - \kappa)} \left[\frac{R}{r} - \frac{r}{R} \right] \quad (9.82)$$

The torque that must be applied to an element of area on the surface of the rotating cylinder is derived from the momentum flux to the surface multiplied by the area and the lever arm:

$$dT = - \underbrace{\left(\underbrace{\tau \cdot (-\delta \mathbf{r})}_{\text{momentum flux into surface}} \cdot \underbrace{\delta \mathbf{\theta}}_{\theta \text{ component of " "}} \right)}_{\text{distance on surface in angular direction}} \bigg|_{r=\kappa R} \underbrace{(\kappa R d\theta)}_{\text{lever arm}} dz \underbrace{(\kappa R)}_{\text{lever arm}} \quad (9.83)$$

$$T = \int_0^L \int_0^{2\pi} \tau_{r\theta}|_{r=\kappa R} \kappa^2 R^2 d\theta dz \quad (9.84)$$

$$T = 2\pi\kappa^2 R^2 L \tau_{r\theta}|_{r=\kappa R} \quad (9.85)$$

This result is independent of the fluid. For a Newtonian fluid, we may again refer to Table 9.1 to obtain

$$\tau_{r\theta} = -\eta r \frac{d}{dr} \left(\frac{v_\theta}{r} \right) \quad (9.86)$$

In this case, the torque is given by

$$T = 4\pi\mu R^2 L \frac{\kappa^2}{1 - \kappa^2} \Omega \quad (9.87)$$

A plot of the torque against the angular velocity will give a straight line through the origin whose slope is proportional to the viscosity. The proportionality constant is a function only of the instrument, which may therefore be calibrated with another Newtonian fluid of known viscosity.

9.3 SPHERICAL SYSTEMS

9.3.1 Creeping Flow Around a Solid Sphere

Flow around submerged objects has many applications in chemical engineering. Spherical or nearly spherical objects are shapes that can be applied to the dispersed phase for flooding calculations in absorption, distillation, and extraction towers. Fluidization and entrainment in moving beds and settling velocities in decanters are also important applications that involve flow around nearly spherical particles.

We will consider the limiting case of a small spherical solid, uninfluenced by its neighbors in a fluid that flows over the sphere in the opposite direction to gravity. We suppose that in the case of a fluid particle the surface tension is sufficient to maintain the spherical shape and to limit internal circulation (refer to Figure 9.7).

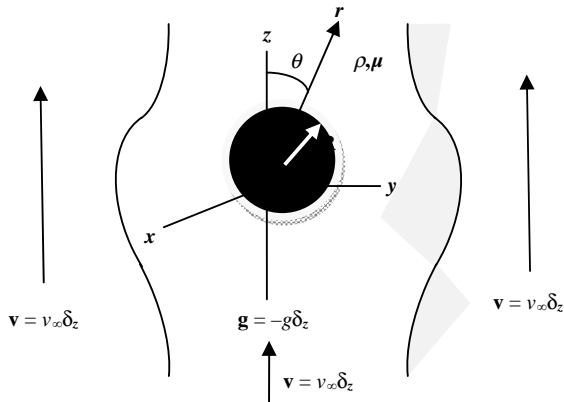


FIGURE 9.7 Axial flow over submerged sphere.

This fluid velocity far from the sphere is uniform at v_∞ . This velocity is required to suspend the sphere or it may be interpreted as the terminal velocity of the solid falling through the medium.

Flow Visualization We are interested in the flow field external to the sphere where we can make the following observations/visualizations:

- The system is symmetric with respect to the ϕ (see Appendix D) coordinate, which has therefore not been shown in Figure 9.7.
- There are two velocity components, each of which depends on r and θ : $v_r(r, \theta)$, $v_\theta(r, \theta)$
- The medium is undisturbed by the sphere if the distance from the sphere is sufficiently large:

$$\lim_{r \rightarrow \infty} \mathbf{v} = v_\infty \delta_z \quad (9.88)$$

- The limiting values of the velocity components are therefore given by

$$\lim_{r \rightarrow \infty} v_r = v_\infty \delta_z \cdot \delta_r = v_\infty \cos \theta \quad (9.89)$$

$$\lim_{r \rightarrow \infty} v_\theta = v_\infty \delta_z \cdot \delta_\theta = -v_\infty \sin \theta \quad (9.90)$$

Also, since the velocity field is uniform far from the sphere, the equation of motion can be used to solve for the pressure distribution since there are no other contributions to the gradient of the momentum flux. From Table 8.12

$$\nabla \cdot (\rho \mathbf{v} \mathbf{v} + P \delta + \boldsymbol{\tau}) = \nabla P = \rho \mathbf{g} \quad (9.91)$$

Substituting the expression for gravity gives

$$\frac{dP}{dz} = -\rho g \quad (9.92)$$

$$P = P_0 - \rho g z \quad (9.93)$$

where P_0 is the pressure in the $z = 0$ plane at large distances from the sphere.

- There is no flow of mass across the surface of the particle and the fluid does not slip at the solid surface (refer to boundary condition M5 in Table 8.13):

$$v_r(R, \theta) = 0 \quad 0 \leq \theta \leq \pi \quad (9.94)$$

$$v_\theta(R, \theta) = 0 \quad 0 \leq \theta \leq \pi \quad (9.95)$$

Because of the two-dimensional nature of this problem, it is somewhat harder to solve than the ones we have been

considering. We will focus on some ways that the solution can be used.

Solution For slow (creeping) flow, the solution is given by (Bird et al., 2002):

$$v_r(r, \theta) = v_\infty \left[1 - \frac{3}{2} \left(\frac{R}{r} \right) + \frac{1}{2} \left(\frac{R}{r} \right)^3 \right] \cos \theta \quad (9.96)$$

$$v_\theta(r, \theta) = -v_\infty \left[1 - \frac{3}{4} \left(\frac{R}{r} \right) - \frac{1}{4} \left(\frac{R}{r} \right)^3 \right] \sin \theta \quad (9.97)$$

$$P = P_0 - \rho g z - \frac{3}{2} \frac{\eta v_\infty}{R} \left(\frac{R}{r} \right)^2 \cos \theta \quad (9.98)$$

The reader can verify that these results meet the expectations that are outlined above. As stated at the outset, we are interested in the force exerted by the fluid on the sphere. The force in the z direction can be formulated as follows.

The flux of momentum from the fluid to the solid is $-\mathbf{\Pi} \cdot \mathbf{\delta_r}$ and the z component of that flux is $-\mathbf{\Pi} \cdot \mathbf{\delta_r} \cdot \mathbf{\delta_z}$. Both of these expressions are evaluated at the surface of the sphere where the unit area is $h_\theta d\theta h_\phi d\phi$. Multiplication of the flux by the area gives the force on the local area, which when accumulated over the entire surface gives the total force:

$$F_z = \int_0^{2\pi} \int_0^\pi (-\mathbf{\Pi} \cdot \mathbf{\delta_r} \cdot \mathbf{\delta_z})|_{r=R} R^2 \sin \theta d\theta d\phi \quad (9.99)$$

The integrand may be evaluated as follows:

$$(\mathbf{\Pi} \cdot \mathbf{\delta_r} \cdot \mathbf{\delta_z}) = (\Pi_{ij} \mathbf{\delta_i} \mathbf{\delta_j} \cdot \mathbf{\delta_r}) \cdot \mathbf{\delta_z} \quad (9.100)$$

$$(\mathbf{\Pi} \cdot \mathbf{\delta_r} \cdot \mathbf{\delta_z}) = (\Pi_{ij} \mathbf{\delta_i} \mathbf{\delta_{jr}}) \cdot \mathbf{\delta_z} = (\Pi_{ir} \mathbf{\delta_i}) \cdot \mathbf{\delta_z} \quad (9.101)$$

$$(\mathbf{\Pi} \cdot \mathbf{\delta_r} \cdot \mathbf{\delta_z}) = \Pi_{ir} \mathbf{\delta_i} \cdot \mathbf{\delta_z} = \Pi_{rr} \mathbf{\delta_r} \cdot \mathbf{\delta_z} + \Pi_{\theta r} \mathbf{\delta_\theta} \cdot \mathbf{\delta_z} \quad (9.102)$$

$$(\mathbf{\Pi} \cdot \mathbf{\delta_r} \cdot \mathbf{\delta_z}) = (P + \tau_{rr}) \cos \theta + \tau_{\theta r} (-\sin \theta) \quad (9.103)$$

The expression for the momentum flux in Equation (8.167) may be used to show that

$$\tau_{rr} = -2\eta \frac{\partial v_r}{\partial r} \quad (9.104)$$

$$\tau_{\theta r} = -\eta \left[\frac{\partial v_\theta}{\partial r} + \frac{1}{r} \frac{\partial v_r}{\partial \theta} - \frac{v_\theta}{r} \right] \quad (9.105)$$

Using the expressions for the velocity components provides the values on the surface of the sphere:

$$\tau_{rr}(R, \theta) = 0 \quad (9.106)$$

$$\tau_{\theta r}(R, \theta) = \frac{3}{2} \frac{\eta v_\infty \sin \theta}{R} \quad (9.107)$$

$$P(R, \theta) = P_0 - \rho g R \cos \theta - \frac{3}{2} \frac{\eta v_\infty \cos \theta}{R} \quad (9.108)$$

The force on the sphere may be evaluated with these results:

$$F_z = 2\pi \left\{ \int_0^\pi \left[\left(P_0 - \rho g R \cos \theta - \frac{3}{2} \frac{\eta v_\infty \cos \theta}{R} \right) \cos \theta - \left(\frac{3}{2} \frac{\eta v_\infty \sin \theta}{R} \right) \sin \theta \right] R^2 \sin \theta d\theta d\phi \right\} \quad (9.109)$$

or

$$F_z = \underbrace{\frac{4}{3} \pi R^3 \rho g}_{\text{Bouyancy}} + \underbrace{6\pi \eta R v_\infty}_{\text{Drag: Stoke's law}} \quad (9.110)$$

The first term in Equation (9.110) is the buoyancy force exerted by the fluid and the second is the drag force exerted by the fluid on the solid. The drag force is referred to as Stoke's law. Remember that this solution is for the case of creeping flow of an incompressible Newtonian fluid where the convective transport of momentum is neglected. Also note that we have not yet accounted for the balance of momentum for the solid, which may be written as follows:

$$\frac{4}{3} \pi R^3 \rho_s \frac{dv_\infty}{dt} = \frac{4}{3} \pi R^3 \rho g + 6\pi \eta R v_\infty - \frac{4}{3} \pi R^3 \rho_s g \quad (9.111)$$

The velocity required to suspend the sphere or the terminal velocity of a falling particle is then given by

$$0 = \frac{4}{3} \pi R^3 \rho g + 6\pi \eta R v_\infty - \frac{4}{3} \pi R^3 \rho_s g \quad (9.112)$$

$$\text{or} \quad v_\infty = \frac{2R^2 g}{9\eta} \{ \rho_s - \rho \} \quad (9.113)$$

The velocity is seen to be proportional to the first power of the density difference. This result is valid for

$$N_{Re} = \frac{2R\rho v_\infty}{\eta} \leq 0.01 \quad (9.114)$$

See Chapter 13 for higher values of the Reynolds number.

An approximate criterion that the particle is not be aware of its neighbors or the walls of the container is that the sphere be located at least 15 radii from these entities (Middleman, 1998). Fluid drops with radii less than approximately 1 mm are likely to be able to maintain their spherical shape with surface tension (Middleman, 1998).

9.3.1.1 Application to Decanter Design In Chapter 7, an approximate size of a decanter was obtained by specifying the value of the flux to the disengaging area. Another approach (see Schweitzer, 1979) is to specify the settling rate of the smallest drops of the dispersed phase to be greater than the overflow rate of the continuous phase.

Taking the disengaging area at a height h above the center of the horizontal cylinder, the diameter of the settler may be calculated on this basis:

$$LD\sqrt{\left[1 - 4\frac{h^2}{D^2}\right]}v_{\infty,\min} = V^{(c)} \quad (9.115)$$

$$\Rightarrow D = \sqrt{\frac{V^{(c)}}{\left(\frac{L}{D}\right)\sqrt{\left[1 - 4\frac{h^2}{D^2}\right]}v_{\infty,\min}}}$$

with $\frac{L}{D}$ between approximately 2.5 and 5

The reader is referred to Schweitzer (1979) for the completion. Our interest here is whether or not the bases of the two methods are comparable.

The flux to the disengaging area is then

$$\frac{V^{(c)} + V^{(d)}}{LD\sqrt{\left[1 - 4\frac{h^2}{D^2}\right]}} = \left[1 + \frac{V^{(d)}}{V^{(c)}}\right]v_{\infty,\min} \quad (9.117)$$

This result may be compared to the value of 5 gal/(ft² min) quoted in Section 7.3.5.

Example 9.3.1.1-1: Separation of an Oil Water Mixture

(See Schweitzer, 1979)

Oil Phase (Dispersed)

$$\mathcal{W} = 10000 \text{ lb/h}$$

$$\rho = 56 \text{ lb/ft}^3$$

$$\eta = 10 \text{ cP}$$

Water Phase (Continuous)

$$\mathcal{W} = 40000 \text{ lb/h}$$

$$\rho = 62 \text{ lb/ft}^3$$

$$\eta = 0.7 \text{ cP}$$

Using Equation (9.113) to calculate the settling velocity of 0.0005 ft diameter oil spheres

$$v_{\infty,\min} = \frac{(2)(0.00025)^2 32.17(56 - 62)}{9(0.7)6.7197 \times 10^{-4}} = -0.0057 \text{ f}$$

The total flux to the disengaging area is then

$$\left[1 + \frac{10000}{40000} \frac{62}{56}\right] 0.0057 \times 60 \times 7.4805 = 3.3 \text{ gal/(ft}^2\text{ min)}$$

9.4 MICROFLUIDICS—GAS PHASE SYSTEMS

Microfluidics is the application of transport phenomena (Bird et al., 2002) and engineering technology to systems with dimensions in the order of 1–1000 μm . It involves the manipulation of fluids in networks of channels that connect pumps, valves, filters, and other components that are required to fabricate complex systems. Microfluidic systems have features that are attractive to users in biology, chemistry, engineering, and medicine. These features include high surface to volume ratio, small volumes of samples and reagents, and direct scale-up (number up), which have grown out of the “lab on a chip” concept that was put forth by Manz et al. (1990) (see Figure 9.8 for some examples).

Both liquids and gases can comprise the fluid medium in a microchannel. Modeling the gas flow in microchannels can be accomplished on the basis of compressible Newtonian

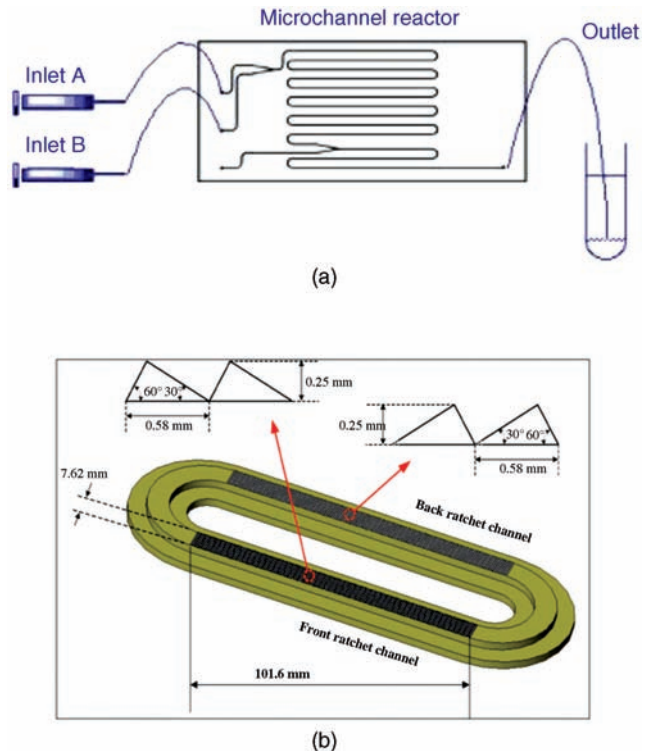


FIGURE 9.8 Examples of microchannels: (a) microchannel reactor (Professor S. Kobayashi, Department of Chemistry, University of Tokyo, Reprinted with permission of Professr S. Kobayashi) and (b) closed loop ASME International. Reprinted with permission of ASSEE.

fluid mechanics, provided that the continuum and local equilibrium assumptions remain valid. A key parameter in making this determination is the Knudsen number, N_{Kn} , which is defined for gases as the ratio of the mean free path to the characteristic macroscopic dimension, λ/L . The continuum assumption has been considered invalid for gases if the Knudsen number is greater than 0.1 (Gad-el-Hak, 2003). However, the applicability of the nonslip condition at the wall has been considered to fail if the Knudsen number is greater than 0.001 (Gad-el-Hak, 2003). We will discuss a model for gas flow in microchannels under conditions where the continuum approach is valid. It can be noted that liquid flows in microchannels can be purely pressure driven and modeled with the tools discussed earlier in this chapter. High pressures are normally required. A system of alternatives is electrokinetic phenomena (Hu and Li, 2007), which includes electroosmosis and electrophoresis.

9.4.1 A Model of Gas Flow in Microchannels

Consider a straight channel of length L and rectangular cross section of width W and height H (see Figure 9.9).

A gas flows along the length L . The channel has been formed in a solid material different from that which it is covered. Establish a rectangular coordinate system at the inlet cross section with z directed along the length and y along the height. The bottom face of the channel is in the $y = 0$ plane and the top face is in the $y = H$ plane. The two sides of the channel are in the $x = -W/2$ and $x = W/2$ planes. Note that the fully developed flow pattern is symmetric about the centerline of the channel.

Assumptions:

- The length of the channel is sufficiently large that the effects of introducing and removing the gas are confined to such a small fraction of the length that they be ignored in the analysis.
- $H \ll W$ so that changes in the x direction may be neglected in comparison to changes in the y direction.
- The shear stresses over the $x = W/2$ and $x = -W/2$ faces are very much smaller than those on the other faces.
- The viscous compressive stresses are negligible.
- The gas obeys the ideal gas law.
- Isothermal and steady conditions prevail.
- The pressure is uniform over each cross section.

The following analysis is primarily due to Dongari et al. (2007). The objective of the calculations is to determine the velocity and pressure distributions along the channel: $v_z(y, z)$, $v_y(y, z)$, $P(z)$.

9.4.1.1 Momentum and Mass Balances The velocity vector is expressed as

$$\mathbf{v} = v_y \delta_y + v_z \delta_z \quad (9.118)$$

The z -momentum balance for compressible flow (see Problem 8.3 in Chapter 8) is replaced with an approximate balance over an elemental volume of length dz illustrated in Figure 9.5. Recall the definition of momentum flux from Chapter 8:

$$\underbrace{-2}_{\substack{\text{Negative sign for} \\ \text{reactive force on} \\ \text{gas. Factor of 2} \\ \text{includes opposite} \\ \text{face}}} \int_{-W/2}^{W/2} \underbrace{\left[(\Phi \cdot \delta_y) \right]_{y=H}}_{\substack{\text{Total flux of} \\ \text{momentum} \\ \text{from gas to} \\ \text{wall at } y = H}} \cdot \underbrace{\delta_z}_{\substack{\text{Extracts } z \\ \text{component} \\ \text{of force}}} dx dz = \frac{d}{dz} \left\{ \underbrace{\int_0^H \int_{-W/2}^{W/2} \underbrace{[(\Phi \cdot \delta_z) \cdot \delta_z]}_{\substack{\text{Flux of } z \text{ momentum} \\ dA}} dx dy}_{\substack{\text{Net gain of } z \text{ momentum} \\ \text{by gas element}}} \right\} dz \quad (9.119)$$

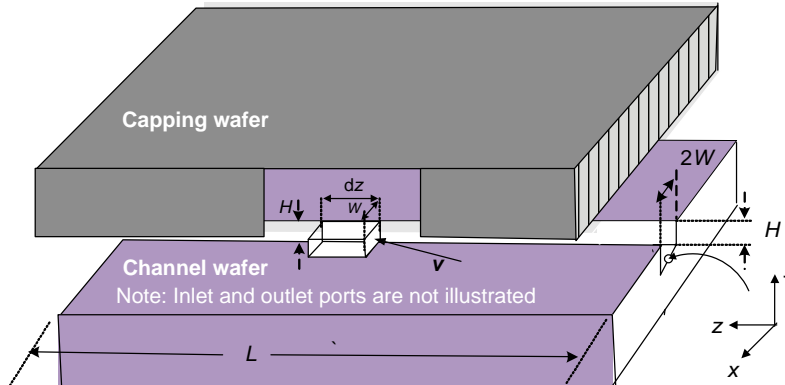


FIGURE 9.9 Illustration of channel dimensions and coordinate system.

The integral on the left-hand side of Equation (9.119) represents the force on the wall at $y=H$ and the negative sign provides the reaction of the fluid. The factor of two includes the identical situation at $y=0$. The integral may be simplified by inserting the definition of the total momentum flux and carrying out the indicated operations:

$$\int_{-W/2}^{W/2} \underbrace{[(\Phi \cdot \delta_y)]_{y=H}}_{\text{Total flux of momentum from gas to wall at } y=H} \cdot \underbrace{\delta_z}_{\text{Extracts } z \text{ component of force}} dx = W[(\rho \mathbf{v}\mathbf{v} + P\delta + \tau) \cdot \delta_y] \cdot \delta_z \quad (9.120)$$

$$\begin{aligned} \tau_W &= [(\rho \mathbf{v}\mathbf{v} + P\delta + \tau) \cdot \delta_y] \cdot \delta_z = [\rho v_y \mathbf{v} + P\delta_y + \tau_{iy} \cdot \delta_i] \cdot \delta_z \\ &= [\rho v_y v_z + \tau_{zy}]_{y=H} \end{aligned} \quad (9.121)$$

With a stationary and impermeable channel wall, the y component of the velocity vector must be zero (see M3 in Table 8.13).

$$(\rho v - 0) \cdot \delta_y = 0 \Rightarrow v_y = 0 \quad \text{at } y = H \quad (9.122)$$

The shear stress is given in terms of the velocity for compressible flow in Problem 8.2, Chapter 8:

$$\tau_{yz} = \tau_{zy} = -\eta \left[\frac{\partial v_y}{\partial z} + \frac{\partial v_z}{\partial y} \right] \quad (9.123)$$

The y component of the velocity is uniformly zero at the wall so that

$$\tau_W = -\eta \frac{\partial v_z}{\partial y}_{y=H} \quad (9.124)$$

The right-hand side of Equation (9.118) may be reduced as follows:

$$\begin{aligned} &\frac{d}{dz} \left\{ \underbrace{\int_0^H \int_{-W/2}^{W/2} [(\Phi \cdot \delta_z) \cdot \delta_z] dx dy}_{\text{Flux of } z \text{ momentum}} \right\} \\ &\quad \text{Net gain of } z \text{ momentum by gas element} \\ &= \frac{d}{dz} \int_0^H \underbrace{\int_{-W/2}^{W/2} [(\rho v_z \mathbf{v} + P\delta_z + \tau_{zi}\delta_i) \cdot \delta_z] dA}_{\text{Flux of } z \text{ momentum}} \quad (9.125) \end{aligned}$$

$$= \frac{d}{dz} \int_A (\rho v_z v_z) dA + PA\delta_z + \underbrace{\tau_{zz}}_{\substack{\text{Neglect-} \\ \text{see} \\ \text{assumptions}}} \cdot \delta_z \quad (9.126)$$

$$= \frac{d}{dz} \int_A (\rho v_z^2) dA + \frac{dP}{dz} A \quad (9.127)$$

The momentum balance on the differential element can therefore be expressed as

$$-2\tau_W W dz - A \frac{dP}{dz} dz = \frac{d}{dz} \int \rho v_z^2 dA dz \quad (9.128)$$

or

$$-\frac{2\tau_W A}{H} dz - AdP = d \int \rho v_z^2 dA \quad (9.129)$$

9.4.1.2 Mass Balance: Axial Velocity Distribution The equation continuity for steady compressible flow in two dimensions follows from Table 8.12 as

$$\frac{\partial \rho v_y}{\partial y} + \frac{\partial \rho v_z}{\partial z} = 0 \quad (9.130)$$

and constitutes a pointwise total mass balance for the gas in the channel. Note that if the z component of the velocity was known, the y component could be obtained from the equation of continuity and the pressure distribution from the z momentum balance.

Based on our experience with incompressible flows in slots (Section 9.1) and pipes (Section 9.2), it is reasonable to suppose that the axial velocity is a parabolic function of y at each location along the microchannel:

$$v_z(y, z) = A_2(z)y^2 + A_1(z)y + A_0(z) \quad (9.131)$$

We must narrow the choice of functions to one by designing the coefficients, $A_i(z)$, to meet the needs of the particular problem at hand.

The functions must have the symmetry that was pointed out earlier. The maximum in the axial velocity must therefore be at mid-height:

$$\frac{\partial v_z}{\partial y} = 0 \quad \text{at } y = \frac{H}{2} \quad \forall z \Rightarrow A_2 = -\frac{A_1}{H} \quad (9.132)$$

Under conditions where the mean free path of the gas is much smaller than the characteristic dimension of the system, molecular collisions with the walls of the container are a very small fraction of the total and the assumption that

the gas clings to the surface could be used to further restrict the parabolic form.

However, for large value of the mean free path (Hirschfelder et al., 1954) given by

$$\lambda(m) = \frac{0.0013804T(K)}{\sqrt{2}\pi d(A)^2 P(Pa)} \quad (\text{dimension in parentheses}) \quad (9.133)$$

the difference between the tangential velocity of the wall and the gas must be considered. A simplifying assumption is that a fraction of the molecules that strike the surface are absorbed and eventually return to the gas with the thermal velocity relative to the surface. The remaining fractions are reflected elastically. A number of models for the difference between the tangential velocity of the wall and gas fall in the general format:

$$v_{tw} = 2C_1 N_{Kn} \frac{\partial v_t}{\partial n} + 4C_2 N_{Kn}^2 \frac{\partial^2 v_t}{\partial n^2} \quad (9.134)$$

The tangential component of the gas velocity at the wall is denoted by v_t and v_{tw} is its value relative to the tangential velocity of the wall. The normalized direction n points from the gas phase into the wall. The Knudsen number is the mean-free path relative to a characteristic dimension of the system, in this case twice the depth of the channel:

$$N_{Kn} = \frac{\lambda}{2H} \quad (9.135)$$

Under isothermal conditions $N_{Kn}P = \text{constant}$

The constants C_1 and C_2 distinguish between the models. A summary is available in Dongari et al. (2007). An engineering approximation may be taken as $C_1 = 1$ and $C_2 = 0$ (Arkilic et al., 1997).

The parabolic velocity distribution must therefore satisfy Equation (9.134) at the upper and lower surfaces of the channel. Since the profile is symmetric, we can therefore assure both with

$$v_z(H, z) = -2C_1 N_{Kn} \frac{\partial v_z}{\partial y} \Big|_{y=H} - 4C_2 N_{Kn}^2 \frac{\partial^2 v_z}{\partial y^2} \Big|_{y=H} \quad (9.136)$$

$$\Rightarrow A_0 = (C_1 + 4C_2 N_{Kn}) 2HN_{Kn} A_1 \quad (9.137)$$

Finally, we expect the velocity distribution to reflect conservation of mass on the same scale as the momentum balance that can be expressed as

$$\mathcal{W} = \int_0^H \int_{-W/2}^{W/2} \rho \mathbf{v} \cdot \mathbf{\hat{d}}_z dx dy = \text{constant} \quad (9.138)$$

or, since changes in the x direction are not considered important,

$$\mathcal{W} = \rho W \int_0^H \mathbf{v} \cdot \mathbf{\hat{d}}_z dy = \rho WH \langle v_z \rangle = \text{constant} \quad (9.139)$$

The coefficient in the proposed velocity profile remaining to be evaluated, A_1 , can be replaced with the average velocity:

$$\frac{1}{H} \int_0^H v_z(y, z) dy = \langle v_z \rangle = \frac{1}{6} HA_1 [1 + 12C_1 N_{Kn} + 48C_2 N_{Kn}^2] \quad (9.140)$$

$$\Rightarrow A_1 = \frac{6}{H} \frac{\langle v_z \rangle}{[1 + 12C_1 N_{Kn} + 48C_2 N_{Kn}^2]} \quad (9.141)$$

In summary,

$$v_z(y, z) = \langle v_z \rangle \frac{\frac{y}{H} (1 - \frac{y}{H}) + 2C_1 N_{Kn} + 8C_2 N_{Kn}^2}{\frac{1}{6} + 12C_1 N_{Kn} + 48C_2 N_{Kn}^2} \quad (9.142)$$

The average velocity is not constant but the Reynolds number,

$$N_{Re} = \frac{\rho D_h \langle v_z \rangle}{\eta} \quad (9.143)$$

contains the product of the average velocity and density, which is constant [see Equation (9.139)]. The hydraulic diameter for the noncircular cross section is given by

$$D_h = \frac{\text{four cross-sectional areas}}{\text{wetted perimeter}} = \frac{2WH}{W + H} \approx 2H \quad (9.144)$$

The gas will therefore accelerate along the length of the channel to accommodate the decrease in density caused by the pressure drop.

9.4.1.3 Pressure Distribution The momentum balance in Equation (9.129) may be used to determine the pressure profile along the length of the channel. The shear stress at the wall may be determined from Equations (9.124) and (9.142):

$$\begin{aligned} \tau_w &= \frac{\partial}{\partial y} \left[-\eta \langle v_z \rangle \frac{\frac{y}{H} (1 - \frac{y}{H}) + 2C_1 N_{Kn} + 8C_2 N_{Kn}^2}{\frac{1}{6} + 12C_1 N_{Kn} + 48C_2 N_{Kn}^2} \right]_{y=H} \\ &= \frac{1}{\rho} \frac{3\eta^2 \frac{1}{H^2} N_{Re}}{1 + 12C_1 N_{Kn} + 48C_2 N_{Kn}^2} \end{aligned} \quad (9.145)$$

Setting

$$P(z_0) = P_0 \quad (9.146)$$

$$\vartheta = \frac{P_0}{P} \quad (9.147)$$

Then

$$\tau_w = \frac{\left[3\eta^2 \frac{1}{\rho_0 H^2} N_{Re}\right] \vartheta}{1 + 12C_1 N_{Kn0} \vartheta + 48C_2 N_{Kn0}^2 \vartheta^2} \quad (9.148)$$

Substitution into the momentum balance gives

$$\begin{aligned} & \frac{\left[3\eta^2 \frac{1}{\rho_0 H^2} N_{Re}\right] \vartheta}{1 + 12C_1 N_{Kn0} \vartheta + 48C_2 N_{Kn0}^2 \vartheta^2} + \frac{AP_0}{\vartheta^2} \frac{d\vartheta}{dz} \\ &= \frac{d}{dz} W \int_0^H \rho \langle v_z \rangle^2 \left[\frac{v_z}{\langle v_z \rangle} \right]^2 dy = WH \frac{\eta^2}{\rho_0 D_h^2} N_{Re}^2 \frac{d}{dz} \vartheta \Omega(\vartheta) \end{aligned} \quad (9.149)$$

where

$$\begin{aligned} \Omega(\vartheta) &= \frac{1}{H} \int_0^H \left[\frac{v_z}{\langle v_z \rangle} \right]^2 dy \\ &= \frac{1}{H} \int_0^H \left[\frac{\frac{y}{H} \left(1 - \frac{y}{H}\right) + 2C_1 N_{Kn0} \vartheta + 8C_2 N_{Kn0}^2 \vartheta^2}{\frac{1}{6} + 2C_1 N_{Kn0} \vartheta + 8C_2 N_{Kn0}^2 \vartheta^2} \right]^2 dy \end{aligned} \quad (9.150)$$

$$\Omega(\vartheta) = \frac{\frac{1}{30} + \frac{2}{3} C_1 N_{Kn0} \vartheta + \frac{8}{3} C_2 N_{Kn0}^2 \vartheta^2 + 4N_{Kn0}^2 C_1^2 \vartheta^2 + 32N_{Kn0}^3 C_1 C_2 \vartheta^3 + 64N_{Kn0}^4 C_2^2 \vartheta^4}{\left(\frac{1}{6} + 2C_1 N_{Kn0} \vartheta + 8C_2 N_{Kn0}^2 \vartheta^2\right)^2} \quad (9.151)$$

This function has been shown to have a negligible effect on pressure over a wide range of Knudsen numbers. We will use the value at the reference pressure. The momentum balance becomes

$$-\frac{4N_{Re}\beta}{MH} \left[\frac{\vartheta}{\frac{1}{6} + 2C_1 N_{Kn0} \vartheta + 8C_2 N_{Kn0}^2 \vartheta^2} \right] + \frac{1}{\vartheta^2} \frac{d\vartheta}{dz} = \Omega(1) N_{Re}^2 \frac{\beta}{M} \frac{d\vartheta}{dz} \quad (9.152)$$

where

$$\beta = \frac{\eta^2 RT}{P_0^2 D_h^2} \quad (9.153)$$

Separating the variables results in

$$\begin{aligned} \frac{8N_{Re}\beta}{MD_h} (z - z_0) &= \int_1^{\vartheta} \frac{1}{\vartheta} \left[\frac{1}{6} + 2C_1 N_{Kn0} \vartheta + 8C_2 N_{Kn0}^2 \vartheta^2 \right] \\ &\quad \left(\beta \frac{N_{Re}^2 \Omega(1)}{M} - \frac{1}{\vartheta^2} \right) d\vartheta \end{aligned} \quad (9.154)$$

The result can be written in the form of a quadratic equation for the Reynolds number:

$$\begin{aligned} & \underbrace{\left(\frac{1}{\vartheta^2} - 1 \right) + 24C_1 N_{Kn0} \left(\frac{1}{\vartheta} - 1 \right) - 96C_2 N_{Kn0}^2 (\ln \vartheta)}_{< 0} \\ &+ \frac{96\beta}{MD_h} (z - z_0) N_{Re} + \\ & \frac{2\beta \Pi(1)}{M} [12C_1 N_{Kn0} (\vartheta - 1) + 24(\vartheta^2 - 1) C_2 N_{Kn0}^2 \\ &+ (\ln \vartheta)] N_{Re}^2 = 0 \end{aligned} \quad (9.155)$$

A convenient reference point is the inlet in which case P_0 is the inlet pressure and $z_0 = 0$. In general, four of the five

variables ($z, \vartheta, H, W, \mathcal{W}$) must be fixed for a particular gas with the corresponding value for the last variable determined by Equation (9.155). The quadratic form in Equation (9.155) is convenient for preparing the inlet to outlet pressure ratio required for a given flow rate in a specified channel. In this case, it is easier to solve for the flow rate for a specified pressure ratio instead of the opposite, that is, $z = L, \vartheta, H, W$ are fixed and the flow rate, represented by the Reynolds number, is determined from Equation (9.155). The result is

$$\begin{aligned} N_{Re} &= \\ & -1 + \sqrt{1 - \frac{8MD_h^2 \Pi(1)}{(96)^2 \beta L^2} [12C_1 N_{Kn0} (\vartheta - 1) + 24(\vartheta^2 - 1) C_2 N_{Kn0}^2 + (\ln \vartheta)] \left[\left(\frac{1}{\vartheta^2} - 1 \right) + 24C_1 N_{Kn0} \left(\frac{1}{\vartheta} - 1 \right) - 96C_2 N_{Kn0}^2 (\ln \vartheta) \right]} \\ & \frac{\Pi(1) D_h}{96 \beta L} [12C_1 N_{Kn0} (\vartheta - 1) + 24(\vartheta^2 - 1) C_2 N_{Kn0}^2 + (\ln \vartheta)] \end{aligned}$$

Example 9.4.1.3-1: Helium Flow in a Long Microchannel

Helium mass flow rates were measured at 314 K in a microchannel with the following dimensions: $L = 7500 \mu\text{m}$, $W = 52.25 \mu\text{m}$, and $H = 1.33 \mu\text{m}$ (Arkilic et al., 1997). The outlet pressure was fixed at 100,000 Pa. Determine the inlet pressures required for mass flows of $1.6\text{E}-12$ and $1.23\text{E}-11 \text{ kg/s}$ (approximate extrapolations that bracket actual data). The outlet Knudsen number was 0.0775 in the experiments.

Solution:

$$C_1 = 1.466$$

$$C_2 = 0.9756$$

$$\eta = 20.66 \times 10^{-6} \text{ Ns/m}^2$$

$$M = 4.0026 \text{ kg/mol}$$

$$R = 8314 \text{ m}^3 \text{ Pa}/(\text{kmol K})$$

$$H = 1.33 \times 10^{-6} \text{ m}$$

$$W = 52.25 \times 10^{-6} \text{ m}$$

$$L = 7500 \times 10^{-6} \text{ m}$$

$$T = 314 \text{ K}$$

$$D = \frac{2WH}{W+H} \text{ m}$$

$$d = 2.18$$

$$K_0 = \frac{0.0013804T}{(3.14160)\sqrt{2}d^2P_0} \frac{1}{2H}$$

$$\beta = \frac{\eta^2 RT}{P_0^2 D^2}$$

$$a(\vartheta) = \frac{2\beta}{M} \Omega(\vartheta) (12C_1 K_0(\vartheta - 1) + 24(\vartheta^2 - 1)C_2 K_0^2 + \ln \vartheta)$$

$$b(\vartheta) = \frac{96\beta L}{MD}$$

$$c(\vartheta) = \left(\frac{1}{\vartheta^2} - 1\right) + 24C_1 K_0 \left(\frac{1}{\vartheta} - 1\right) - 96C_2 K_0^2 (\ln \vartheta)$$

$$\Omega(\vartheta) = \frac{\frac{1}{30} + \frac{2}{3}C_1 K_0 \vartheta + \frac{8}{3}C_2 K_0^2 \vartheta^2 + 4K_0^2 C_1^2 \vartheta^2 + 32K_0^3 C_1 C_2 \vartheta^3 + 64K_0^4 C_1^2 \vartheta^4}{\left(\frac{1}{6} + 2C_1 K_0 \vartheta + 8C_2 K_0^2 \vartheta^2\right)^2}$$

$$N(\vartheta) = \frac{(b(\vartheta)b(\vartheta) - 4a(\vartheta)c(\vartheta))^{1/2}}{2a(\vartheta)} - \frac{b(\vartheta)}{2a(\vartheta)}$$

$$w(\vartheta) = N(\vartheta) \frac{WH\eta}{D}$$

For a quick solution, select values of the inlet pressure until a satisfactory match between the calculated and measured mass flow rate is achieved. At this point, calculate the value of the output Knudsen number. A value of 0.0775 signifies complete agreement of model with the data

$$P_0 = 415000$$

$$w(4.2) = 1.2354 \times 10^{-11}$$

$$K_0(4.2) = 0.07810$$

$$P_0 = 155000$$

$$w(1.6) = 1.5926 \times 10^{-12}$$

$$K_0(1.6) = 0.07967$$

PROBLEMS

9.1. The basic design of a gear pump is shown in Figure 9.10.

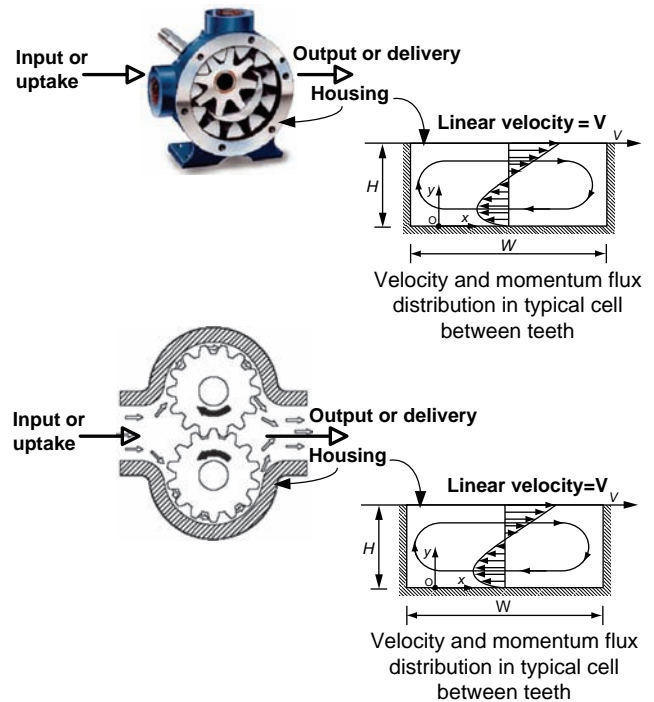


FIGURE 9.10 Gear pump.

The liquid enters and fills the compartments between the teeth, which rotate in contact with the housing. The liquid is thus transferred from the uptake to the delivery side. During the transfer process, the liquid circulates and mixes in each compartment without any loss or gain from other compartments. An idealization of the flow in a compartment is also shown in Figure 9.10.

Assume that the fluid is a Newtonian liquid at constant temperature/pressure and density.

- a. Neglecting the flow reversal at each end, simplify the equations of motion and continuity for the fluid in the cavity in a rectangular system with no variations in the z direction and motion only in the x direction. Note

any conclusions that you can draw with respect to the dependence of pressure on the x , y , and z coordinates.

- b. Establish the required boundary conditions for the equations of motion in part a and solve them for the velocity distribution.
- c. Evaluate the pressure gradient using the condition that there can be no net flow in the x direction, that is, over any cross section denoted by a fixed value of x , there cannot be any net flow.
- d. Calculate the torque per unit depth on the pump housing about the axis of the pump caused by the fluid in one compartment. Denote the radius of the pump housing by R_h .

NONTURBULENT ISOTHERMAL MASS TRANSFER

The term *mass transfer* generally refers to a process within a fluid or solid consisting of two or more components. Flow of a pure fluid in a conduit would not therefore be referred to as a mass transfer operation, although mass is indeed being transferred. Nonturbulent mass transfer refers to applications where either there is no forced flow or the flow is laminar. In both cases, the relevant microscopic balance equations are the steady-state form of the microscopic mass balance, the appropriate flux expression, and the momentum balance. The energy balance is not needed in the cases considered here where significant temperature changes are not expected. Also, if the density is approximately constant, the momentum balance is uncoupled from the mass balance and the forms given at the beginning of Chapter 8 can be applied to determine the velocity to be used in the mass balance.

The unsteady-state version of the microscopic mass balance is provided in Table 10.1 for some important unidirectional flow applications. In most cases, only the steady-state version is needed and the accumulation term may be omitted.

Note: Analogous expressions for molar basis:

$$\frac{\partial c_i}{\partial t} + \nabla \cdot \mathbf{N}_i = \mathcal{R}_{iV}, \quad \mathbf{N}_i = c_i \mathbf{v}^N + \mathbf{j}_i^N$$

For most applications, the flux expression given in Equation (8.164) can be used for the diffusional flux. The more general expression for the diffusional flow based on the linear laws and the entropy generation will be needed for the reverse osmosis example of membrane transport, which will be discussed below.

Nonflow mass transfer applications occur very often in both porous and nonporous solids. Membrane processes provide examples of diffusion through both solids. Heterogeneous catalysis is an example of diffusion through porous solids where the mass transfer process is accompanied by chemical reaction at the active sites on the surface of the pores. Adsorption is an unreactive example of the porous solid case. The plasma membrane is an example of diffusion with homogeneous reaction in liquid membranes.

We will consider examples of membranes, catalysis, adsorption, and examples of the relief offered by convection to a surface reaction constrained by diffusional limitations.

10.1 MEMBRANES

A membrane is a semipermeable barrier through which the constituents of a mixture pass at different rates. The membrane is potentially useful only if at least a subset of the constituents have significantly different rates from the remainder. A general scheme of membrane separations is shown in Figure 10.1.

The feed is separated into a retentate stream consisting of components that do not pass through the membrane and a permeate stream containing those components that do. A sweep gas is sometimes used and ideally does not penetrate the membrane. Membranes are generally isothermal, simple in construction and operation, require relatively low amounts of energy, and are ideal for process intensification

TABLE 10.1 Mass Balance $((\partial \rho_i / \partial t) + \nabla \cdot \mathbf{W}_i = r_{iv}, \mathbf{W}_i = \rho_i \mathbf{v} + \mathbf{j}_i)$ **Constant ρ and $D_{im} \cdot \mathbf{v} = v_z \delta_z$**

Rectangular system:

See Table 9.1 for steady-state momentum balance

$$\frac{\partial \rho_i}{\partial t} + v_z \frac{\partial \rho_i}{\partial z} = D_{im} \left(\frac{\partial^2 \rho_i}{\partial x^2} + \frac{\partial^2 \rho_i}{\partial y^2} + \frac{\partial^2 \rho_i}{\partial z^2} \right) + r_{iv}$$

Cylindrical system:

See Table 9.1 for momentum balance

See Appendix E for reduction of general mass balance

$$\frac{\partial \rho_i}{\partial t} + v_z \frac{\partial \rho_i}{\partial z} = D_{im} \left(\frac{1}{r} \frac{\partial}{\partial r} \left(r \frac{\partial \rho_i}{\partial r} \right) + \frac{1}{r^2} \frac{\partial^2 \rho_i}{\partial \theta^2} + \frac{\partial^2 \rho_i}{\partial z^2} \right) + r_{iv}$$

Spherical system:

No convection ($\mathbf{v} = 0$) or angular dependence

$$\frac{\partial \rho_i}{\partial t} = D_{im} \left(\frac{\partial^2 \rho_i}{\partial r^2} + \frac{2}{r} \frac{\partial \rho_i}{\partial r} \right) + r_{iv}$$

since they substantially decrease the equipment size–production capacity ratio (Drioli and Romano, 2001).

Membranes may be porous or nonporous. A combination of both properties is found in cases where a porous supporting structure is combined with a nonporous membrane to provide resistance to a large pressure difference. We will consider two specific examples: gas permeation and reverse osmosis. The membrane in both cases is solid. Gas permeation is a gas–gas operation and reverse osmosis is a liquid–liquid operation.

Some general aspects of membrane analysis are discussed in the following section.

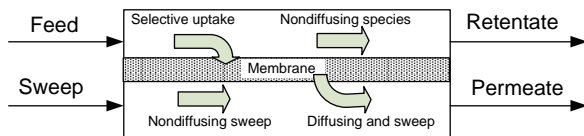
10.1.1 Material Balance for Generic Membrane

The stream concentrations and flows for the generic membrane process in Figure 10.1 are defined in Figure 10.2.

The total mass transfer rate across the membrane for each species (i), $\mathcal{W}_i^{(m)}$, is expressed in terms of an overall mass transfer coefficient, $\mathcal{K}_{i,ave}^{(m)}$, and an average driving force, $\mathcal{X}_{i,ave}$, over the active membrane contact area, A . The driving force is a characteristic of the membrane operation. One of the following two averages is commonly used:

Arithmetic:

$$\mathcal{X}_{i,ave} = \frac{1}{2} [\mathcal{X}_i|_{\text{feed side}} + \mathcal{X}_i|_{\text{f permeate side}}] \quad (10.1)$$

**FIGURE 10.1** Generic membrane process.

Log mean:

$$\mathcal{X}_{i,ave} = \frac{[\mathcal{X}_i|_{\text{feed side}} - \mathcal{X}_i|_{\text{f permeate side}}]}{\ln [\mathcal{X}_i|_{\text{feed side}} / \mathcal{X}_i|_{\text{f permeate side}}]} \quad (10.2)$$

Note: The log mean arises in the cases where the rate of change of the function is proportional to its current value. Consider present case an arbitrary function of a single variable, Wx :

$$\frac{dW}{dx} = \alpha W$$

We would like to compute the actual change in the function using an average value of the forcing function, that is,

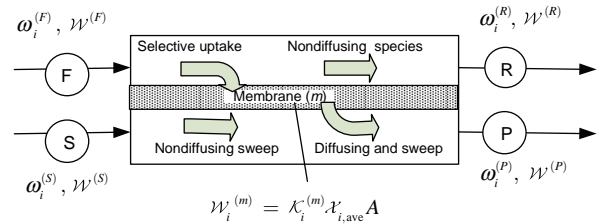
$$W(x_2) - W(x_1) = \alpha \langle W \rangle (x_2 - x_1)$$

The actual change is given implicitly by the integral of the differential equation:

$$\ln \frac{W(x_2)}{W(x_1)} = \alpha (x_2 - x_1)$$

Consequently, the desired result is obtained with

$$\langle W \rangle_{\log \text{ mean}} = \frac{W(x_2) - W(x_1)}{\ln(W(x_2)/W(x_1))}$$

**FIGURE 10.2** Mass flows in a generic membrane.

Mass transfer coefficients are discussed in Chapter 12. We will assume at this juncture that the mass transfer resistance rests entirely within the membrane and that an experimental value is available for the mass transfer coefficient can be evaluated with the defined variables for the membrane. More sophisticated models may consider the local conditions in the membrane unit.

A mass balance can be applied to each component:

$$\omega_i^{(F)}\mathcal{W}^{(F)} + \omega_i^{(S)}\mathcal{W}^{(S)} = \omega_i^{(R)}\mathcal{W}^{(R)} + \omega_i^{(P)}\mathcal{W}^{(P)}, \quad (10.3)$$

$$i = 1, 2, \dots, N_C$$

$$\sum_{i=1}^N \omega_i^{(E)} = 1, \quad E = F, S, P, R \quad (10.4)$$

The transmembrane fluxes are given by

$$\mathcal{W}_i^{(m)} = \mathcal{K}_i^{(m)} \mathcal{X}_{i,ave} A, \quad i = 1, 2, \dots, N_C \quad (10.5)$$

$$= \omega_i^{(P)}\mathcal{W}^{(P)} - \omega_i^{(S)}\mathcal{W}^{(S)}, \quad i = 1, 2, \dots, N_C \quad (10.6)$$

The degrees freedom may be determined as follows:

Assuming an isothermal operation, one temperature is needed.

Four pressures are required to allow for a pressure drop on each side of the membrane.

Unknowns:

$$\omega_i^{(E)} = 4N_C, \quad \mathcal{W}^{(E)} = 4, \quad \mathcal{W}_i^{(m)} = N_C$$

$$A = 1, \quad \mathcal{K}_i^{(m)} = N_C, \quad P^{(E)} = 4, \quad T = 1$$

$$\text{Total} = 6N_C + 10$$

Relations:

- Mole fraction summations = 4
- Transmembrane rates = N_C
- Overall mass balance = N_C
- Membrane mass balance = N_C
- Total = $3 N_C + 4$
- Degrees of freedom = $3(N_C + 2)$

Adjustments to the degrees of freedom may or may not be necessary in particular circumstances. For example, molar units may be substituted with no effect on the degrees of freedom.

If, however, there is no sweep, the number of unknowns is decreased by $N_C + 2$ and one relation (mass fraction summation) is lost leaving the degrees of freedom = $2 N_C + 5$.

10.1.2 Gas Separations

As mentioned above, the membrane employed in most gas separations is solid. Diffusion in solids is characterized by relatively small diffusion coefficients as seen in Section 8.5.4.1. If, however, we make an order of magnitude estimate of a concentration (solubility) ρ_{Ao} , we have a more comprehensive measure of the efficacy of a membrane

$$\frac{W_A^{(m)}}{A} \approx \frac{D_{Am}\rho_{Ao}}{L} \quad (10.7)$$

than with the diffusivity alone.

Industrial gas separations fall for the most part into the categories shown in Table 10.2.

The membrane is typically formed into a membrane module, containing a large internal surface area per unit volume. A hollow fiber construction for air separation is illustrated in Figure 10.3 where the membrane essentially forms the fiber walls.

TABLE 10.2 Principal Membrane Systems for Gas Separations

Principal Membrane Material	Module Type	Principal Market	Notes
Polysulfone Polyimide/polyaramide Tetrabromo polycarbonate Polyimide	Hollow fiber	Nitrogen from air separation and hydrogen separation	In the separation of nitrogen from air, the nitrogen product is obtained as the permeate and there is no sweep. The feed is compressed to 8–10 atm and oxygen/nitrogen. Selectivities of 7–8 are obtained
Cellulose acetate Cellulose acetate	Spiral wound Hollow fiber	Natural gas separations	Natural gas separations involve meeting the specifications required for delivery to the U.S. national pipeline grid for natural gas, which contains 10–25% impurities (ethane, propane, butane)
Polyphenylene oxide Polyimide Silicone rubber Silicone rubber	Hollow fiber Plate and frame Spiral wound	Vapor–gas separations and air dehydration	Vapor–gas separations can be accomplished with silicone rubber. Vapor recovery systems such as gasoline recovery are small capacity systems ideally suited for membrane installations

Source: Adapted from Baker (2001).



FIGURE 10.3 Hollow fiber for gas separation. Reprinted with permission of Air Liquide MEDAL.

Hollow fiber modules have surface areas in the range of $500\text{--}9000\text{ m}^2/\text{m}^3$ (Seader and Henley, 2006).

On either side of the membrane, at a particular point in the module, there exists a flow-mixing process that delivers the solute locally to the membrane surface at the feed side of the membrane and removes it at the permeate side. The situation is illustrated in Figure 10.4. Complete mixing is indicated on both sides of the membrane, but this is not important to the present discussion. Mass transfer to and from the membrane that results in fluid concentrations at the membrane surface, which differ from the bulk values will be discussed in Chapter 12. Note the change in concentration across the surface that implies a solution process.

Diffusion in the membrane is described by the uni-directional (x), nonflow ($v_z = 0$) version of the rectangular entry in Table 10.1:

$$\underbrace{\frac{\partial \rho_i}{\partial t}}_{=0} + \underbrace{v_z}_{=0} \underbrace{\frac{\partial \rho_i}{\partial z}}_{=0} = D_{im} \left(\underbrace{\frac{\partial^2 \rho_i}{\partial x^2} + \frac{\partial^2 \rho_i}{\partial y^2} + \frac{\partial^2 \rho_i}{\partial z^2}}_{=0} \right) + \underbrace{r_{iv}}_{=0} \quad (10.8)$$

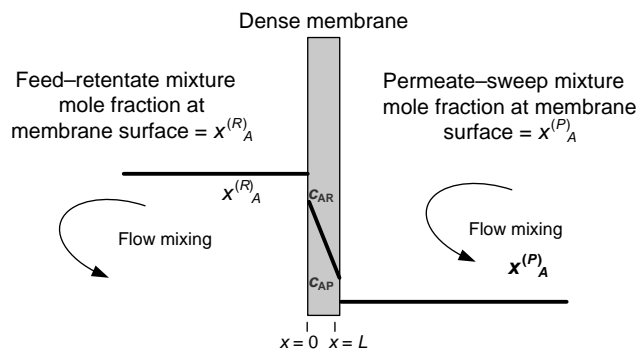


FIGURE 10.4 Gas membrane diffusion—local conditions.

or

$$M_A D_{Am} \frac{\partial^2 c_A}{\partial x^2} = 0 \quad (10.9)$$

Local thermodynamic equilibrium is presumed to exist throughout. This is expressed in the form of Henry's law at the two interfaces (see M1, Table 8.12):

$$\begin{aligned} c_A^{(R)} &= H_A x_A^{(R)} P^{(R)}, & x &= 0 \\ c_A^{(P)} &= H_A x_A^{(P)} P^{(P)}, & x &= L \end{aligned} \quad (10.10)$$

Note the form of Henry's law that is being used as per the comments associated with Equation (6.57).

For a porous membrane, the medium for diffusion is continuous across the pore mouths on membrane surface, the diffusional medium in the membrane being essentially limited to the porous matrix.

For the nonporous membrane, the concentration on either side of the surfaces are not equal in spite of the corresponding equality of the chemical potentials. The same value of Henry's constant is taken at both sides of the membrane. The solution is given by

$$c_A = \frac{c_A^{(P)} - c_A^{(R)}}{L} x + c_A^{(R)} \quad (10.11)$$

Evaluation of the mass flux using Equation (8.164).

$$j_A = -M_A D_{Am} \frac{\partial c_A}{\partial x} \quad (10.12)$$

$$j_A = -M_A D_{Am} \frac{c_A^{(P)} - c_A^{(R)}}{L} \quad (10.13)$$

$$\frac{\mathcal{W}_A^{(m)}}{A} = \underbrace{\frac{M_A D_{Am} H_A}{L}}_{\mathcal{K}_A^{(m)}} \underbrace{\left(y_A^{(R)} P^{(R)} - y_A^{(P)} P^{(P)} \right)}_{\mathcal{X}_A} \quad (10.14)$$

The mass flux is constant throughout the membrane (why?). These results conform to the solution-diffusion model for membrane transport (Wijmans and Baker, 1995).

The permeability of the membrane is defined by

$$P_{MA} = M_A D_{Am} H_A \quad (10.15)$$

and the permeance by

$$\bar{P}_{MA} = \frac{M_A D_{Am} H_A}{L} = \frac{P_{MA}}{L} = \mathcal{K}_A^{(m)} \quad (10.16)$$

Some permeability data are listed in Table 10.3. The ideal selectivity of A to B is the ratio of the respective permeabilities.

TABLE 10.4 Comparison of Membranes for “Greenhouse” Application

P_{MCO_2} (barrer)	α	θ	$x_1^{(P)}$	A (ft ²)
28,000	5.6	0.80702	0.17391	402.77
4,550	13.0	0.47296	0.26143	2984.7
520	14.5	0.44862	0.27291	27166
191	13.2	0.46939	0.26304	71482
171	16.6	0.422	0.28697	87104
153	16.2	0.42654	0.28445	96393
5.00	22.1	0.37616	0.31584	3.3809×10^6
12.4	23.8	0.3662	0.32307	1.4130×10^6
5.18	16.0	0.42889	0.28316	2.833×10^6
7.01	21.2	0.38206	0.31174	2.3647×10^6
75.7	19.9	0.3915	0.30543	2.1272×10^5
6.80	17.9	0.40866	0.2947	2.2604×10^6

Note: Purchase cost at CE Index 500 = \$45.00/ft² (Seader et al., 2009).

In summary:

Relations (use molar units): Total = 9

$$x_2^{(F)}, x_2^{(R)}, x_1^{(P)}, x_2^{(P)}, \mathcal{N}_1^{(m)}, \mathcal{N}_2^{(m)}, \mathcal{W}^{(R)}, A$$

Equations (10.4) and (10.5).

$$A = \frac{x_1^{(P)} \theta \mathcal{W}^{(F)}}{(P_{\text{MA}}/L) [x_1^{(R)} P^{(R)} - x_1^{(P)} P^{(R)}]}$$

Solution:

Mole fractions sum to 1.0

Ratio of transmembrane flux expressions:

$$\frac{x_1^{(P)}}{1 - x_1^{(P)}} = \frac{P_{\text{CO}_2}}{P_{\text{N}_2}} \frac{x_1^{(R)} - (P^{(P)}/P^{(R)})x_1^{(P)}}{(1 - x_1^{(R)}) - (P^{(P)}/P^{(R)})(1 - x_1^{(P)})}$$

Expand in powers of $x_1^{(P)}$ and solve the resulting quadratic for the positive root in the unit interval.

$$x_1^P = \frac{-[1 - (1 - \alpha)(x_1^{(R)} + r)] + \sqrt{[1 - (1 - \alpha)(x_1^{(R)} + r)]^2 - 4\alpha x_1^{(R)}}}{2r[1 - \alpha]}$$

where

$$\alpha = \frac{P_{\text{MCO}_2}}{P_{\text{MN}_2}} \quad \text{and} \quad r = \frac{P^{(P)}}{P^{(R)}}$$

Calculate the permeate flow (or cut) using the overall material balance for CO₂, Equation (10.3):

$$\theta = \frac{x_1^{(F)} - x_1^{(R)}}{x_1^{(P)} - x_1^{(R)}}$$

Calculate A using the transmembrane flux expression for CO₂

The results are summarized in Table 10.4.

Equation (10.3) = 2

Equation (10.4) = 3

Equation (10.5) = 2 with the driving forces in Equation (10.14)

Equation (1.6) = 2

Specified values: Total = 8

$$x_1^{(F)} = 0.15, \quad x_1^{(R)} = 0.05, \quad \in K_1^{(m)} \text{ and } K_2^{(m)}$$

from Table 10.3, $P^{(R)}$, $P^{(P)}$, $\mathcal{N}^{(F)}$, and $\mathcal{N}^{(P)} = \theta \mathcal{N}^{(F)}$

Unknowns: Total = 9

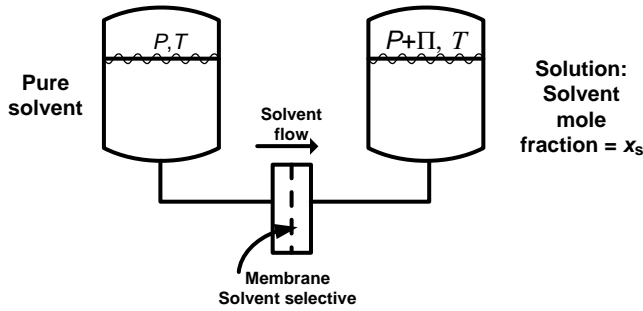
The poly[(trimethylsilyl)-*i*-propyne] membrane has the lowest area (402.77 ft²) and the highest permeability. However, it also requires the largest cut. A large cut as well as a small mole fraction of CO₂ in the permeate results in inefficient use of limited underground storage, the ideal being storage of pure carbon dioxide.

The cellulose acetate membrane has the highest ideal selectivity (31.7), but the mole fraction of CO₂ in the permeate is only 0.35. In fact, the mole fraction in the permeate is low for all of the membranes.

Can you propose a more efficient arrangement?

10.1.3 Liquid Separations—Reverse Osmosis

Whereas gas separations are gas–gas operations, reverse osmosis is a liquid–liquid operation. Osmosis refers to the

FIGURE 10.6 Osmotic pressure (Π) demonstration.

passage of solvent through a solvent selective membrane from a pure solvent to a solution containing a dissolved solute. An experimental determination of the osmotic pressure is illustrated in Figure 10.6. A pure solvent is indicated but may be replaced with a solution of lower concentration than the solution on the right.

Solvent passes from left to right, diluting the solution, until equilibrium is reached. At equilibrium, the pressure on the right is observed to be π units higher than the pressure above the pure solvent. The difference in pressure is called the osmotic pressure. An osmotic pressure of the order of 1000 psi is not uncommon. It can be evaluated as follows:

At equilibrium [refer to Equation (6.4)],

$$\mu_s(T, P, x_s = 1) = \mu_s(T, P + \Pi, x_s) \quad (10.17)$$

This equality can also be written in terms of fugacity. The change of fugacity (actually the natural logarithm of fugacity) with pressure is proportional to the partial molar volume. Using these results Equation (10.17) becomes

$$\ln f_s(T, P, x_s = 1) = \ln f_s(T, P, x_s) + \int_P^{P+\Pi} \frac{\tilde{V}_s}{RT} dP \quad (10.18)$$

The ratio of fugacities is proportional to the activity coefficient for the pure component reference state (see Section 6.2.1.2):

$$a_s = \frac{f(T, P, x_s)}{f(T, P, x_s = 1)} = \gamma_s x_s \quad (10.19)$$

Also in many cases the partial volume can be approximated by the value for the pure component so that

$$\ln \gamma_s x_s = - \int_P^{P+\Pi} \frac{V_s}{RT} dP \quad (10.20)$$

or

$$\Pi = - \frac{RT}{V_s} \ln \gamma_s x_s \quad (10.21)$$

if the molar density is nearly constant. This result provides the means of evaluating the activity of the solvent from osmotic pressure data, or the osmotic pressure from activity data. For a dilute solute, this relation may be approximated by

$$\Pi = - \frac{RT}{V_a} \ln \gamma_a x_a \approx RT c_B \text{ for dilute systems} \quad (10.22)$$

A membrane permeable only to water will pass water from a solution if the applied pressure is greater than the osmotic pressure of the solution. The realization of this inference in the desalination of brackish water has been at the origin of the interest in membrane operations and has had an impact on all of the progress in membrane development (Drioli and Romano, 2001).

The driving force (χ) for the passage of solvent through the membrane may be obtained by recalling that the driving forces for mass, energy, and momentum were identified in the entropy generation expression in Chapter 8. For systems not far removed from equilibrium, it was argued that the fluxes and forces approach zero in linear relationships. The result for the mass flux of species A,

$$\mathbf{j}_A = - \sum_k \mathcal{L}_{Ak} \nabla_T \mu_k \quad (10.23)$$

was further approximated with only the concentration gradient in the chemical potential gradients on the right-hand side. The result was Fick's law. We will continue here instead with the major gradient at the chemical potential level:

$$\mathbf{j}_A = - \mathcal{L}_{AA} \nabla_T \mu_A \quad (10.24)$$

Equation (10.8) expresses mass conservation under Fick's law in a thin (assumption of unidirectional transfer), solid membrane without convection. To see the result without the application of a flux expression, we may simplify the general balance given at the top of Table 10.1 with no velocity or chemical reaction:

$$\underbrace{\frac{\partial \rho_i}{\partial t}}_{=0} + \underbrace{\nabla \cdot \mathbf{n}_i}_{=\partial j_{ix}/\partial x} = \underbrace{r_{iv}}_{=0}, \quad \mathbf{n}_i = \underbrace{\rho_i \mathbf{v}}_{=0} + \underbrace{\mathbf{j}_i}_{=j_{ix}} \quad (10.25)$$

$$\frac{dj_{Ax}}{dx} = 0 \quad \text{or} \quad j_{Ax} = \text{constant} \quad (10.26)$$

Since the flux is constant, the x component of Equation (10.24) may be integrated over the membrane to give

$$j_{Ax} = -\frac{\mathcal{L}_{AA}}{L} \left[\mu_A(T, P^{(P)}, x_A^{(P)}) - \mu_A(T, P^{(R)}, x_A^{(R)}) \right] \quad (10.27)$$

This result may be written in terms of activity coefficients:

$$\begin{aligned} j_{Ax} = & -\frac{L_{mm}}{L} \left[\mu_A(T, P^{(P)}, x_A^{(P)}) - \mu_A(T, P^0, x_A = 1) \right. \\ & \left. - \mu_A(T, P^{(R)}, x_A^{(R)}) + \mu_A(T, P^0, x_A = 1) \right] \\ & + \left[\mu_A(T, P^{(P)}, x_A^{(P)} = 1) - \mu_A(T, P^{(R)}, x_A^{(R)} = 1) \right] \end{aligned} \quad (10.28)$$

$$j_{Ax} = -\frac{L_{mm}}{L} \left[RT \ln \gamma_A^{(P)} x_A^{(P)} - RT \ln \gamma_A^{(R)} x_A^{(R)} + V_A(P^{(P)} - P^{(R)}) \right] \quad (10.29)$$

The molar volume of A in the membrane has been assumed constant when evaluating the effect of pressure on the chemical potential. The standard state for the activity coefficients is the pure solvent at the temperature of the system and pressure P^0 , usually 1 atm.

If the fluxes were to vanish, the prevailing pressures would be the osmotic pressure on the respective sides of the membrane:

$$RT \ln \gamma_A^{(P)} x_A^{(P)} - RT \ln \gamma_A^{(R)} x_A^{(R)} + V_A(\Pi^{(P)} - \Pi^{(R)}) = 0 \quad (10.30)$$

$$\Pi^{(P)} = -\frac{RT}{V_A} \ln \gamma_A^{(P)} x_A^{(P)} \quad (10.31)$$

$$\Pi^{(R)} = -\frac{RT}{V_A} \ln \gamma_A^{(R)} x_A^{(R)} \quad (10.32)$$

The flux is then given by

$$j_{Ax} = -\frac{\mathcal{L}_{AA} V_A}{L} \left[-\Pi^{(P)} + \Pi^{(R)} + (P^{(P)} - P^{(R)}) \right] \quad (10.33)$$

$$j_{Ax} = -\frac{P_{MA}}{L} [\Delta P - \Delta \Pi] \quad (10.34)$$

or

$$\mathcal{K}_A^{(m)} = \frac{P_{MA}}{L} = \bar{P}_{MA} \quad (10.35)$$

$$\mathcal{X}_A = \Delta \Pi - \Delta P \quad (10.36)$$

The pressures are illustrated in Figure 10.7. The applied pressure difference must overcome the osmotic pressure difference in order for the solvent to flow from the more concentrated solution.

A convenient way to view the driving force is to regard the quantity, $P - \Pi$, as a potential for flow.

The flux of the solute, B (e.g., salt) is given by

$$j_{Bx} = \frac{P_{MB}}{L} (c_{BR} - c_{BP}) \quad (10.37)$$

which is independent of pressure. The selectivity of the membrane for water should therefore increase with pressure.

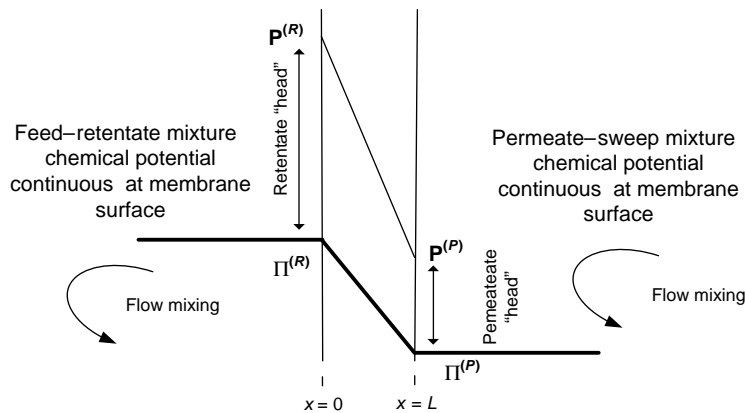


FIGURE 10.7 Pressure gradient in reverse osmosis membranes.

Example 10.1.3-1: Regeneration of Pulping Feed Solution in Paper Production

(Adapted from Seader and Henley, 2006.)

In an existing process for the production of paper, a pulping step to break down wood chips into cellulose and lignin results in a solution that is regenerated and subsequently recycled to the pulping step. Following the removal of pulp in the regeneration step, the pulping solution is concentrated from 15 wt% (dissolved solids) to 45–70 wt% by multieffect evaporation. It has been suggested that reverse osmosis might be used to perform an initial concentration to perhaps 25 wt%. Higher concentrations may not be feasible because of the very high osmotic pressure, which at 180 °F and 25 wt% solids is estimated to be 1700 psia. The osmotic pressure for other conditions can be scaled by assuming that the osmotic pressure is proportional to the weight percent solids.

A two-stage reverse osmosis process, shown in Figure 10.8, has been proposed to carry out this initial concentration for a feed rate of 1000 lb/h at 180 °F.

The permeance for water can be taken as 0.0134 lb/ft h psi in conjunction with an arithmetic-mean osmotic pressure for plug flow on the feed side. Complete the material balance for the process and estimate the required membrane area for each stage.

Solution:

Material balances around each stage (mixer included in first stage):

$$\begin{aligned} 0.15(1,000) + 0.026\mathcal{W}^{(8)} &= 0.25\mathcal{W}^{(4)} + 0.004\mathcal{W}^{(6)} \\ 1,000 + \mathcal{W}^{(8)} &= \mathcal{W}^{(4)} + \mathcal{W}^{(6)} \\ 0.004\mathcal{W}^{(6)} &= 0.026\mathcal{W}^{(8)} + \frac{300}{300 + 1,000,000}\mathcal{W}^{(7)} \\ \mathcal{W}^{(6)} &= \mathcal{W}^{(8)} + \mathcal{W}^{(7)} \end{aligned} \quad \left\{ \begin{array}{l} \mathcal{W}^{(6)} = 467.84 \\ \mathcal{W}^{(4)} = 599.52 \\ \mathcal{W}^{(7)} = 400.48 \\ \mathcal{W}^{(8)} = 67.355 \end{array} \right\} \text{ lb/h}$$

Osmotic pressure of feeds and product streams.

Correction of reported value to other concentrations—assume constant conversion factor from molality to wt% at same T :

$$\Pi(\omega) = \frac{\omega}{0.25} 1700 = 6800\omega$$

$$\Pi(\omega) = 6800\omega$$

Feed composition to stage 1:

$$0.15(1000) + 0.026(67.355) = x_1^{(3)}(1000 + 67.355), \text{ Solution}$$

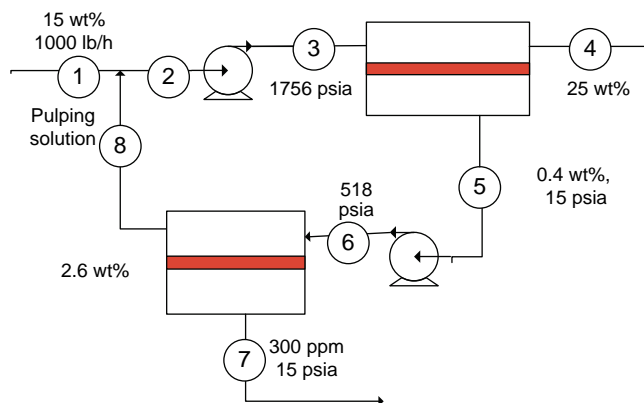


FIGURE 10.8 Proposed two-stage reverse osmosis process.

is $x_1^{(3)} = 0.14218$ Evaluation of osmotic pressures:

0.14218	966.82	
0.25	1700.0	
Π (0.004)	= 27.2	all psia
0.026	176.8	
300	2.0394	
<u>300 + 1,000,000</u>		

Calculation of membrane areas:

$$\mathcal{W}_i^{(m)} = 0.0134(\Delta P - \Delta \Pi)_{\text{ave}} A$$

Stage 1

$$(\Delta P)_{\text{ave}} = (1756 - 15) = 1741.0$$

$$(\Delta \Pi)_{\text{ave}} = 0.5((966.82 - 27.2) + (1700 - 27.2)) = 1306.2$$

$$(\Delta P - \Delta \Pi)_{\text{ave}} = 1741.0 - 1306.2 = 434.8 \Pi$$

$$\mathcal{W}_1^{(m)} = 0.996\mathcal{W}^{(6)} = 465.97 \text{ lb/h}$$

$$A_1 = \frac{465.97}{0.0134(434.79)} = 79.979 \text{ ft}^2$$

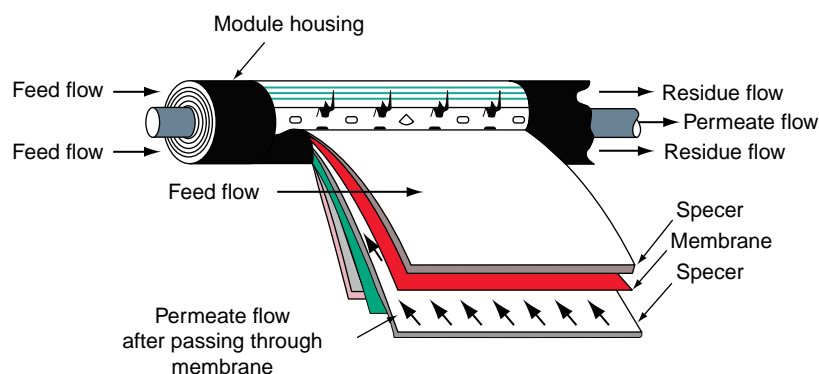


FIGURE 10.9 Spiral-wound module (www.lenntech.com). Courtesy of Membrane Technology and Research.

$$(\Delta P)_{\text{ave}} = (518 - 15) = 503.0$$

$$\Delta \Pi_{\text{ave}} = \frac{1}{2} \left(\left(\Pi(0.004) - \Pi \left(\frac{300}{300 + 1,000,000} \right) \right) + \left(\Pi(0.026) - \Pi \left(\frac{300}{300 + 1,000,000} \right) \right) \right) = 99.961$$

$$(\Delta P - \Delta \Pi)_{\text{ave}} = 503.0 - 99.961 = 403.04$$

$$\mathcal{W}_1^{(m)} = 0.996\mathcal{W}^{(6)} - 0.974\mathcal{W}^{(8)} = 0.996(467.84) - 0.974(67.355) = 400.3 \text{ lb/h}$$

$$A_1 = \frac{400.3}{0.0134(403.04)} = 74.120 \text{ ft}^2$$

Reverse osmosis membranes are often installed in spiral-wound modules, which are illustrated by the example in Figure 10.9.

The module consists of a membrane envelope wrapped around a central collecting tube. The module is placed in a pressurized tubular vessel and the feed is introduced axially through the membrane. The permeate flows in the central collection tube. Spiral-wound modules have surface areas in the range of $200\text{--}800 \text{ m}^2/\text{m}^3$.

10.1.4 Porous Asymmetric and Composite Membranes—Overall Mass Transfer Coefficient

Dense membranes tend to be thick for mechanical strength, which makes them selective at the expense of permeability. The so-called asymmetric membrane typically consists of a thin selective layer ($<2000 \text{ \AA}$) of a dense membrane material and a $50\text{--}100 \text{ }\mu\text{m}$ microporous layer for support as illustrated in Figure 10.10.

Diffusion through the dense skin layer was analyzed in Section 10.1.2. See Figure 10.4 where the permeate conditions persist up to the interface with the membrane. In the present case of a supported membrane, the diffusing species must pass through the porous support before reaching these conditions. The circumstances are called “series diffusion.”

Processes in series occur quite often in chemical engineering, especially in heat and mass transfer. A common feature of

these situations is that although the rate at which the process takes place may be expressed in terms of intermediate variables, these are not ordinarily the process or stream values that are being used to express the state of the processing system and calculations are carried out to meet this requirement.

The physical situation in Figure 10.10 is embellished in Figure 10.11 to reflect membrane diffusion in series with diffusion in the support.

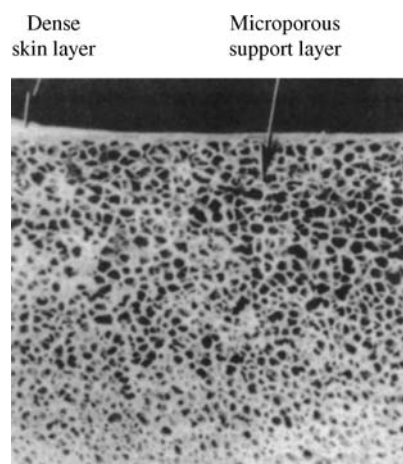


FIGURE 10.10 Scanning electron micrograph of an asymmetric Loeb–Sourirajan membrane (Baker et al., 1991). Reprinted with permission of Elsevier.

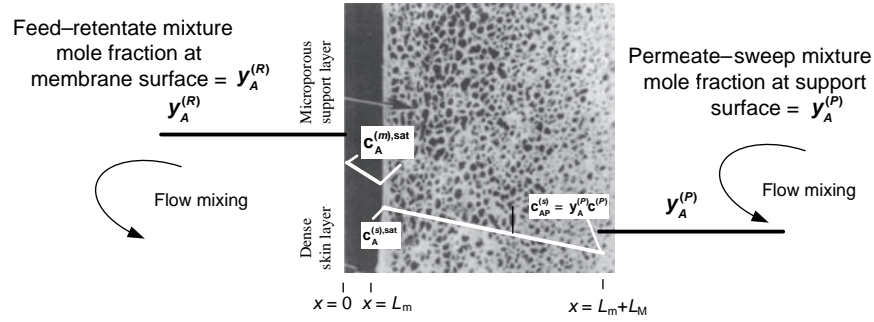


FIGURE 10.11 Series diffusion in asymmetric membrane: (m): dense skin layer; (s): support layer.

Diffusion in the membrane is governed by the same differential equation as that applied in Section 10.1.2 for unidirectional mass transfer without convection or chemical reaction [Equation (10.9)]. Because of the abrupt change in physical properties at the phase boundaries, the microscopic mass balance must be applied in each separate phase and then linked through the conditions applied at the phase boundaries.

On each side of the dense skin layer, we apply the condition of phase equilibrium between the dissolved solute in the solid membrane and the gas phase as it exists at the boundary. At the membrane-support interface, we assume that the mixing processes in the raffinate are sufficient to bring the bulk phase conditions to the interface.

At the interface between the skin layer and support, we again find the conditions of phase equilibrium between the dissolved solute and a gas phase. The gas phase in this case is contained in the pores of the support matrix (see Notes to Table 8.12) and the concentration level is that which will provide a diffusional flow in the support equal to that which arrives from the dense skin. Since the cross section of the support is not totally open (diffusion through the solid is assumed to be negligible), an “effective” diffusivity will be required. Diffusion in porous solids is discussed in the following section.

The open boundary between the support and the permeate provides a continuous passage for the dissolved solute so that the solute concentration on either side of the phase boundary are equal.

Summary in analytical terms for determination of membrane flux:

$$\text{Microscopic mass balance: } M_A D_A \frac{\partial^2 c_A}{\partial x^2} = 0 \quad \text{or} \quad \frac{\partial j_A}{\partial x} = 0 \quad (10.38)$$

$$\text{Membrane skin (m): } 0 \leq x \leq L^{(m)}$$

$$\text{General solution: } c_A^{(m)} = a^{(m)}x + b^{(m)} \quad (10.39)$$

$$\text{Boundary conditions: } c_A^{(m)}(0) = \frac{y_A^{(R)} P^{(R)}}{H'_A} \quad (10.40)$$

$$c_A^{(m)}(L^{(m)}) = \frac{RT}{H'_A} c_A^{(s)}(L^{(m)}) \quad (10.41)$$

$$\text{Evaluation of } a: \quad a^{(m)} = \frac{RT c_A^{(s)}(L^{(m)}) - y_A^{(R)} P^{(R)}}{H'_A L^{(m)}} \quad (10.42)$$

$$\text{Porous support (s): } L^{(m)} \leq x \leq L^{(m)} + L^{(s)}$$

$$\text{General solution: } c_A^{(s)} = a^{(s)}x + b^{(s)} \quad (10.43)$$

$$\text{Boundary conditions: } c_A^{(s)}(L^{(m)}) = c_A^{(m)}(L^{(m)}) \quad (10.44)$$

$$\text{To be chosen such that } j_A^{(m)}(L^{(m)}) = j_A^{(s)}(L^{(m)}) = j_A \quad (10.45)$$

$$c_A^{(s)}(L^{(m)} + L^{(s)}) = y_A^{(P)} \frac{P}{RT} \quad (10.46)$$

$$\text{Evaluation of } a: \quad a^{(s)} = \frac{y_A^{(P)} (P^{(P)}/RT) - c_A^{(s)}(L^{(m)})}{L^{(s)}} \quad (10.47)$$

Flux continuity at membrane-support interface (see M2 in Table 8.12),

$$-D_A^{(m)} a^{(m)} = -D_A^{(s)} a^{(s)} \quad (10.48)$$

provides

$$RT c_A^{(s)}(L^{(m)}) = \frac{(D_A^{(m)}/H'_A L^{(m)}) y_A^{(R)} + (D_A^{(s)}/RTL^{(s)}) y_A^{(P)} P^{(P)}}{(D_A^{(m)}/H'_A L^{(m)}) + (D_A^{(s)}/RTL^{(s)})} \quad (10.49)$$

Substitution of this result into the mass flux expression gives

$$j_A^{(m+s)} = \frac{D_A^{(m+s)}}{L^{(m)} + L^{(s)}} (y_A^{(R)} P^{(R)} - y_A^{(P)} P^{(P)}) \quad (10.50)$$

where the overall diffusivity is defined as

$$\underbrace{\frac{1}{D_A^{(m+s)}}}_{\text{Overall resistance}} = \underbrace{\frac{L^{(m)}}{L^{(m)} + L^{(s)}} \frac{H'_A}{D_A^{(m)}}}_{\text{Skin resistance}} + \underbrace{\frac{L^{(s)}}{L^{(m)} + L^{(s)}} \frac{RT}{D_A^{(s)}}}_{\text{Support resistance}} \quad (10.51)$$

The diffusivity is a conductance in electrical terminology. Its inverse is then a resistance. The preceding expression then states that the overall resistance is the sum of the two individual ones, thereby preserving the electrical analogy for a series configuration. The overall mass transfer coefficient can also be expressed in these terms:

$$\underbrace{\frac{1}{K_A^{(m+s)}}}_{\text{Overall resistance}} = \underbrace{\frac{L^{(m)}}{D_A^{(m)}}}_{\text{Skin resistance} = \frac{1}{K_A^{(m)}}} + \underbrace{RT \frac{L^{(s)}}{D_A^{(s)}}}_{\text{Support resistance} = \frac{1}{K_A^{(s)}}} \quad (10.52)$$

10.2 DIFFUSION MODELS FOR POROUS SOLIDS

The asymmetric membrane discussed above consists as part of a porous support through which the liquid or gas permeates must flow. Porous solids are used in many chemical engineering applications. In adsorption, chromatography, and ion exchange, for example, a solute is transferred to the surface of the solid from the surrounding fluid phase, diffuses through the solid, is adsorbed in the first two applications, and exchanges ions with the solid ion exchanger in the third. In adsorption, the solutes accumulate in the solid until the solid adsorbent is saturated and can no longer purify the surrounding fluid. In chromatography, the solutes are repeatedly adsorbed and desorbed at different rates, thereby affecting a separation in the exterior fluid after diffusing back to the surface of the solid and being transferred to the fluid phase. On the other hand, the products of the ion exchange in the solid carry the exchange to the surrounding fluid. Porous solids are used extensively to provide support for catalysts where the diffusants react at the interior catalytic sites on the solid. There are many more examples including the porous structures in living organisms, which govern the transport of water and vital solutes.

Characterization of the porous region is often limited to the basic parameters defined and illustrated in Table 6.16.

Mass transfer within a porous solid must satisfy the principle of mass conservation. However, the balance equations apply to homogeneous systems and therefore can be applied to each phase of a porous solid with boundary conditions at the pore surfaces. This level of complexity is not generally required since the contribution to the diffusional flow of the solid is small and the time for

the solid reach a steady-state saturation level is large relative to the timescale of most chemical processes. A pseudohomogeneous approach is therefore adopted where the mass flux is averaged over the cross section containing both open and solid features at the flux and balance equation levels.

10.2.1 Effective Diffusivity of Porous Catalysts

Diffusion in the porous solid takes place within the system of pores. The description of the diffusion process is accomplished by considering first a single pore and then adapting this result to the porous structure. We will have porous catalysts in mind but the approach applies equally as well to other porous structures.

We can begin with gases. It is assumed that

- the pores are sufficiently small as well as the pressure gradient that forced convection may be neglected. In spite of the large pressure differences that are applied across membranes, the mechanism of forced convection must be avoided since it does not differentiate between solutes.
- molecular sizes are too small for configurational effects to be important.

10.2.1.1 Pore Diffusion Under these circumstances, it can be shown on the basis of the kinetic theory of gases (Scott and Dullien, 1962) for a binary ideal gas mixture that at constant temperature and pressure

$$N_{Az} = -D_{Ap} \frac{dc_A}{dz} \quad (10.53)$$

where

$$\frac{1}{D_{Ap}} = \frac{1}{D_{KA}} + \frac{1 - \alpha y_A}{D_{AB}^V} \quad (10.54)$$

and

$$\alpha = 1 + \frac{N_{Bz}}{N_{Az}} \quad (10.55)$$

The Knudsen diffusivity is given by

$$D_A = \frac{2}{3} \sqrt{\frac{3RT}{M_A}} \quad (10.56)$$

and is important in small pores where the frequency of collisions with the walls is of the same order of magnitude as the frequency as intermolecular collisions. This applies to the molar average velocity, which is equal to the mass average velocity if the molar density is constant, which is at least approximately true in the present case.

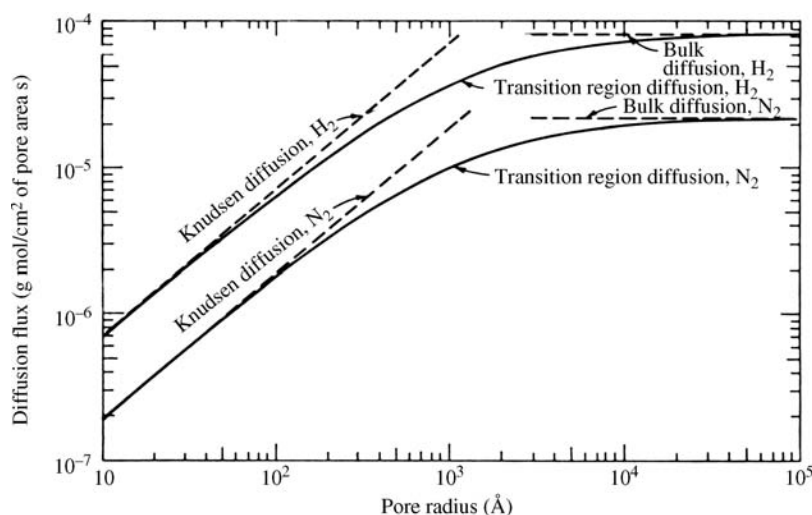


FIGURE 10.12 Knudsen and bulk flow regimes for the N₂-H₂ system (Satterfield, 1970).

The value of α is determined by the reaction stoichiometry (see below) or in the nonreactive case by the condition of no net transport of momentum to the walls:

$$\frac{N_{Bz}}{N_{Az}} = -\sqrt{\frac{M_A}{M_B}} \quad (10.57)$$

The generalization of these results to multicomponent mixtures is given by (Rothfeld, 1963).

$$\frac{1}{D_{ip}} = \frac{1}{D_{Ki}} + \sum_{j=1}^N y_j - \frac{[N_{jz}/N_{iz}]y_i}{D_{ij}^V} \quad (10.58)$$

This amounts to the superposition of Knudsen diffusion on bulk diffusion described by the Maxwell-Stefan equations (Bird et al., 2002). For small values of the pore radius, the diffusivity in the pore is the Knudsen value, while at large values of the pore radius it is the bulk diffusivity. Both are important at intermediate values. Figure 10.12 demonstrates this behavior for the nitrogen-hydrogen system (Satterfield, 1970).

Knudsen diffusion does not apply in the case of liquids in the pores. Without this term the previous equation applies to liquids, except that the diffusion terms are not the binary (Bird et al., 2002). The diffusivity in the pore can in this case be approximated by the bulk phase diffusivity in the mixture,

$$\begin{aligned} T &= 298 \text{ K} \\ P &= 1 \text{ atm} \end{aligned}$$

10.2.1.2 Surface Diffusion Another pathway by which material may progress through the porous solid is provided

by the adsorbed layer. This mechanism proceeds in parallel to those discussed above as illustrated in Figure 10.13.

The rate of flow per unit area of the adsorbed layer can be represented as

$$N_{As} = -D_{As} \frac{dc_{As}}{dz} \quad (10.59)$$

where c_{As} is the molar concentration on the surface. We first convert the surface concentration to the loading variable N (moles adsorbed per unit mass of adsorbent) used in the discussion of adsorption equilibrium (refer to Section 6.5.2):

$$c_{As} = N \frac{\rho_p}{\varepsilon_{ads}} \quad (10.60)$$

where ρ_p is the apparent density of the adsorbent particle and ε_{ads} is the volume fraction of the adsorbed phase. This result assumes that the void fraction on an area basis is the same on a volume basis. If, in addition, we assume a linear equilibrium relation between the surface and the pore [see Equation (6.136)].

$$c_{As} = \frac{\rho_p}{\varepsilon_{ads}} kRT c_{Ap} \quad (10.61)$$

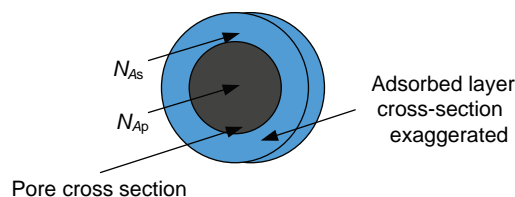


FIGURE 10.13 Surface diffusion.

The flux in Equation (10.59) can be scaled to the open pore area with ratio $\varepsilon_{\text{ads}}/\varepsilon_p$ (ε_p is the porosity of the particle) and the result added to the pore diffusion flux discussed in the previous section:

$$D_{Ap} = \frac{1}{(1/D_{KA}) + ((1 - \alpha y_A)/D_{AB}^V)} + D_{As} \frac{\rho_p K_A}{\varepsilon_p} \quad (10.62)$$

If the pressure is low and the temperature high, surface diffusion may be neglected. The low temperature and pressure favor a condensed state. Surface diffusion is usually neglected but the method by which it is included is instructive.

10.2.2 Tortuosity Factor Model

The extension of the pore diffusion model to the scale of the porous solid involves two major aspects. First, diffusion is based on the open area. The open area fraction is not normally available for porous materials and the fraction of the volume that is open is taken as a good approximation:

$$(dA)_{\text{pore}} = \varepsilon (dA)_{\text{particle}} \quad (10.63)$$

Second, as our coordinate system is now being transferred to the particle, the distance moved along the pore is greater than the unidirectional distance traveled in the particle. In a gross way we account for this by introducing a tortuosity factor

$$(dz)_{\text{pore}} = \tau (dz)_{\text{particle}} \quad (10.64)$$

where τ is greater than unity. These approximations give

$$N_{iz} = -D_{ie} \frac{dc_i}{dz} \quad (10.65)$$

where

$$D_{ie} = \frac{\varepsilon}{\tau} D_{ip} \quad (10.66)$$

The flux is referred to as the total cross section. The concentration represents the value in the void space. It must be noted that in translating this pore diffusivity to the total cross section, the tortuosity of the adsorbed layer may be different than the value for the pore, although as an approximation they may be considered equal.

The tortuosity factor must be measured. Its values normally fall in the range of 2.0–10.0 (Satterfield, 1970). A useful aspect of this model is that the tortuosity factor, as well as the void fraction, are functions of the internal geometry. Consequently, Equation (10.66) can be used to extrapolate data taken under convenient experimental conditions to processing conditions that may be much more severe.

As a pore size distribution function is not utilized in this simple model, the average pore radius in Equation (6.125) can be used calculating the pore diffusion coefficient.

10.2.3 Parallel Pore Model

In contrast to the tortuosity factor model of the diffusion process, the parallel pore model (Johnson and Stewart, 1965) makes use of the pore size distribution function and consequently is based upon a more refined view of the structure.

We again consider diffusion in the medium in the z direction only and assume that the pore under consideration is oriented with an angle θ to this direction. The situation is depicted in Figure 10.14.

It is assumed that this orientation applies to all rotations about the z direction. The contribution of the diffusional flow in the pore to the flux in the z direction is given by

$$N_{Ax}^z = N_{Ax} \cos \theta \quad (10.67)$$

This reduces to

$$N_{Ax}^{(z)} = -(\cos \theta)^2 D_{Ap} \frac{dc_A}{dz} \quad (10.68)$$

The contribution of all pores with different orientations about the z -axis can be obtained with a more refined distribution function as follows: define $F(\theta, r) dr d\theta$ = fraction of total area in plane of constant z , which consists of pore cross sections with inclinations between θ and $\theta + d\theta$

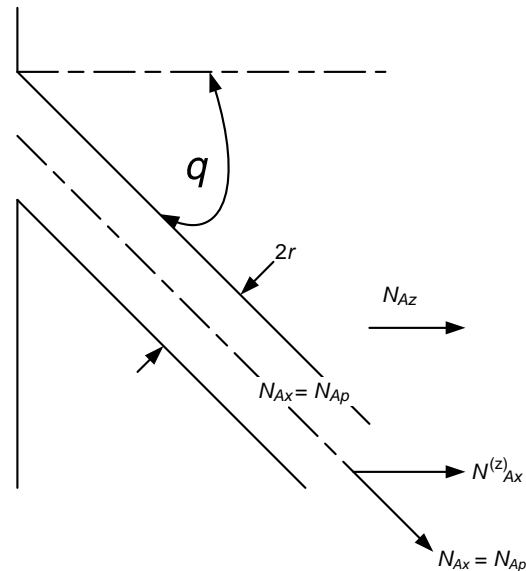


FIGURE 10.14 Open pore at an angle to the diffusion area.

and radii between r and $r + dr$. If the size and angle distributions are not correlated,

$$F(\theta, r) = g(\theta)f(r) \quad (10.69)$$

where g is the distribution of angular orientations. Furthermore, in the case of gases,

$$D_{ie} = \kappa \int_0^{\infty} D_{ip}(r)f(r)dr \quad (10.70)$$

where

$$D_{ie} = \kappa \int_0^{\infty} \frac{f(r)dr}{(3/2)r\sqrt{M_A/3RT}(1/r) + \sum_{j=1}^N \left((y_j - [N_{jz}/N_{iz}])y_i / D_{ij}^V \right)} \quad (10.71)$$

and

$$\kappa = \int_0^{\pi/2} (\cos \theta)^2 g(\theta) d\theta \quad (10.72)$$

Note that if

1. all of the pores are perpendicular to the z -axis, $g(\theta) = (2/\pi)\delta(\theta - \pi/2)$ and $\kappa = 0$,
2. all the pores are parallel to the z -axis, $g(\theta) = (2/\pi)\delta(\theta)$ and $\kappa = 1$,
3. g is a constant, $g(\theta) = (2/\pi)$ and $\kappa = 1/2$,
4. the pore system is isotropic, $\kappa = 1/3$ (Johnson and Stewart, 1965).

If the pore-size distribution consists of discrete peaks, the preceding integral becomes a summation of the values of the denominator evaluated at the corresponding values of the pore radii multiplied by the void fraction associated with each pore size. This result would also apply to the case of a single pore radius. It is useful when the pore volume is divided between macropores and micropores as may be the case in pelleted catalysts.

If the diffusion is entirely in the bulk phase regime, the first term in the denominator can be neglected. The resulting integrand becomes a constant factor and the resulting integral the void fraction. This is the case for liquids.

If the diffusion is entirely in the Knudsen regime, the integral can be replaced with the product of the void fraction and the Knudsen diffusivity evaluated at the average pore radius. In most other cases, the integral must be obtained numerically.

Tests of the parallel pore model, for example, Johnson and Stewart (1965) and Brown et al. (1969), have shown it to

give good results especially when the value of κ is obtained from one experimental measurement.

Other models of diffusion in porous media have been useful. An example is the random pore model (Wakao and Smith, 1962), which has also been applied to biocatalysts (Zhao and DeLancey, 2000).

Example 10.2.3-1: Evaluation of Tortuosity in Parallel Pore Model for Honeycomb-Type Monolith Catalyst

The diffusion of methane through nitrogen in a monolithic honeycomb catalyst has been studied experimentally at 291 K and 1 bar by Hayes and Kolaczowski (1999). Three formulations were investigated:

Monolith 1: Blank substrate (cordierite)

Monolith 6: Substrate coated with alumina wash coat

Monolith 2: Substrate coated with a wash coat containing alumina and a Pd catalyst

The monolith is shown in Figure 10.15.

Pore size distributions were obtained for all of the formulations. The distribution reported for Monolith 6 is shown in Figure 10.16.

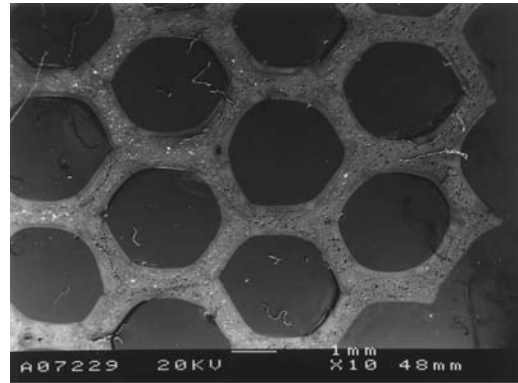


FIGURE 10.15 Scanning electron micrograph of Monolith 2 showing cell geometry, substrate, and wash coat. Reprinted with permission of Elsevier.

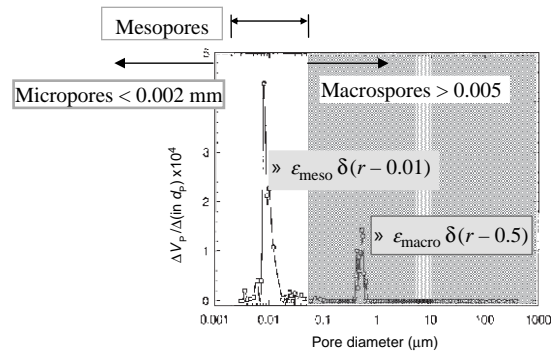


FIGURE 10.16 Pore size distribution for Monolith 6.

TABLE 10.5 Summary of Experimental Results and Tortuosity Calculations

Monolith	Mesopores				Macropores				Overall			
	$\langle r \rangle$ (nm)	ε	D_K	D_{Ap}	$\langle r \rangle$ (nm)	ε	D_K	D_{Ap}	D_{Ap}	$D_{Ae, \text{exp}}$	ε	τ
1					3500	0.360	14.459	0.220	0.220	0.009	0.360	8.605
6	10	0.580	0.041	0.035	500	0.100	2.066	0.202	0.059	0.005	0.680	8.074
2	10	0.410	0.041	0.035	400	0.060	1.652	0.197	0.056	0.002	0.350	12.146

The porous regions in Figure 10.16 are labeled according to the IUPAC definitions. Note that the pore-size distribution is bimodal with a set of mesopores and a set of macropores. The data are narrowly distributed about the mean in each case so the Dirac's delta function has been indicated as an approximation to the actual distribution. The experimental results and the tortuosity calculations are summarized in Table 10.5.

10.3 HETEROGENEOUS CATALYSIS

Catalytic systems were introduced in Chapter 2. In heterogeneous systems, by far the most prevalent, the catalyst is present as a separate phase in contrast to homogeneous catalysis. See Table 1.6 for examples of commercial catalysts and to Section 6.5.1 for the definitions of some basic parameters that are used to characterize porous solids.

In most cases, the catalyst is immobilized on a solid support whether it be a supported vanadium oxidation catalyst or an immobilized enzyme catalyst such as β -glucosidase or a whole cell such as *Saccharomyces cerevisiae*. The catalytic actions of adsorption of reactants, reaction over the catalyst, and desorption of products take place after the reactants reach the catalytic site and before the products are released. The reaction rate expression is formulated on the basis of mechanisms and tested against experimental

data as illustrated in Chapter 1. To reach the catalytic site, reactants normally must move through a bulk phase to the exterior surface of the support, after which they move through the support to the reactive sites. The products must, of course, follow the same path, but in the reverse sequence. The process is illustrated in Figure 10.17.

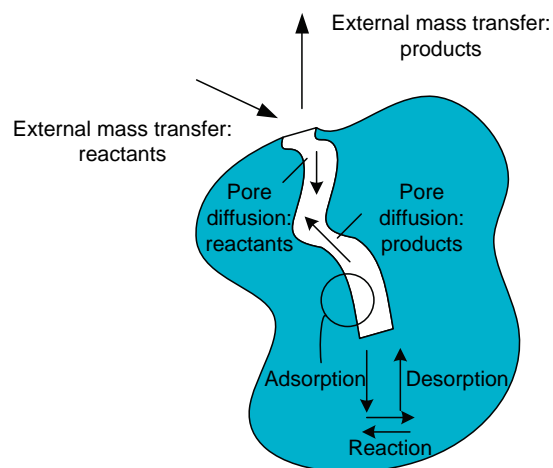
The walls of the pores in a catalytic particle are impregnated with materials that catalyze one or more desirable reactions. In the case of heterogeneous catalysis, there is no reaction term present in the transport equations that fully describes the behavior of the reactive mixture in the pore. The reaction representation appears in a boundary condition that equates the mass flux from the homogeneous phase to the surface reaction rate. However, under some circumstances, it is justified to scale the heterogeneous rate by the surface area per unit volume and thereby treat the heterogeneous reaction as a pseudohomogeneous rate per unit volume. Furthermore, there is often no difference in the model that distinguishes between, for example, enzyme catalysis and catalysis affected by the noble metals. This degree of generality should be kept in mind as we consider the case of diffusion and reaction in a single pore, followed by the extension to a porous particle.

10.3.1 Effectiveness of a Single Closed Pore

The thermal energy released by the reaction process in the pores is conducted to the exterior surface where it is released to the gas phase. Thermal energy is absorbed in the case of endothermic reactions. Because the thermal conductivity of solids is generally very high, it is generally acceptable to consider the reaction-diffusion process in the porous solid as isothermal. This approach will be taken here with the note that we will be able to estimate the maximum possible temperature rise in the catalyst.

We assume that the radius of curvature of the pore is much greater than its radius and, therefore, consider it to be cylindrical with radius r_0 and length L . It is convenient to select a cylindrical coordinate system placed at the entrance to the pore at the center of the cross section (see Figure 10.18). Typical values of the radius and length are 10,000 Å and 0.75 in.

There is no reason to expect gradients in the angular direction. Also, the reaction takes place on the walls of the

**FIGURE 10.17** Catalytic particle with a single pore emphasized.

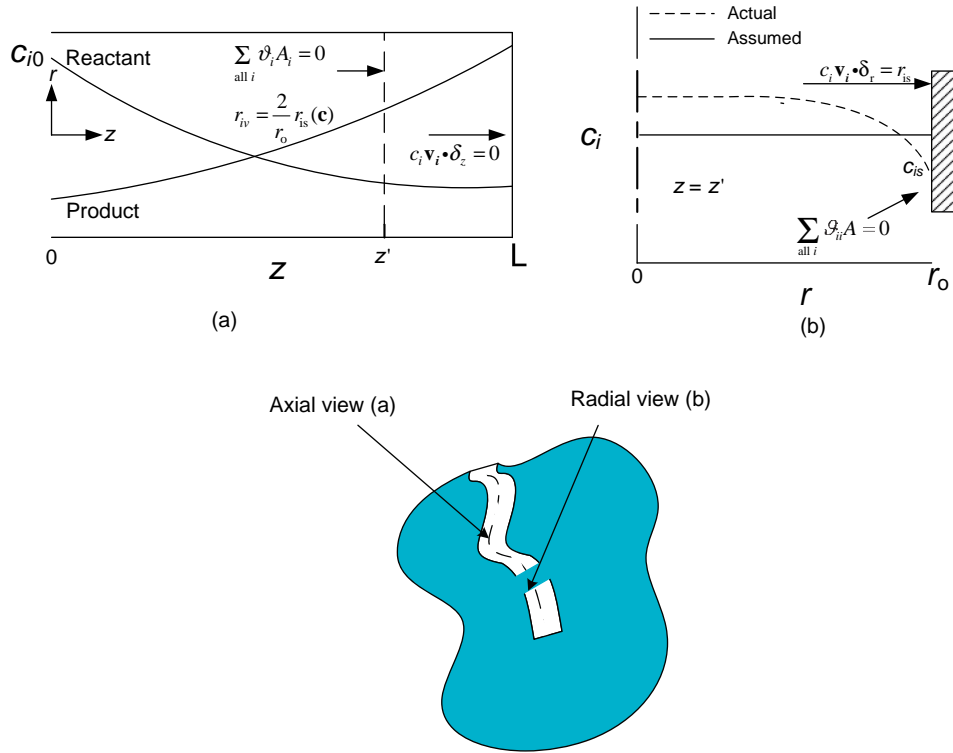


FIGURE 10.18 Concentration gradients in a single pore.

pore so that a reactant concentration will diminish in the radial direction as illustrated in Figure 10.18. The mass flux of a species to the catalyst surface is equal to its reaction rate per unit area:

$$\mathbf{N}_i \cdot \delta_r = \mathcal{R}_{is} \quad \text{at } r = r_0 \quad (10.73)$$

Concentration gradients will also exist in the axial direction because of the reaction as illustrated in Figure 10.18a. If we assume that the radial gradients may be neglected in proportion to the axial gradients, the surface reaction has no radial transport mechanism and must therefore be represented as a volumetric phenomenon. The scale factor from the unit pore area to the unit pore volume is $2/r_0$, giving a homogeneous reaction rate of $2\mathcal{R}_{is}/r_0$ when accounting only for axial gradients in concentration. The surface reaction rate expression is evaluated with the bulk phase compositions.

We have envisioned a unidirectional system in the pore. If we furthermore limit the calculations to a single reaction:

$$\sum_i \nu_i A_i = 0 \quad \text{where } r_{is} = M_i \nu_i \mathcal{R}_s \quad (10.74)$$

the mass balance for this situation may be obtained by reducing the more general form of the mass balance given

in Table 10.1 (see Note for molar form):

$$\underbrace{\frac{\partial c_i}{\partial t}}_{=0} + \underbrace{\nabla \cdot \mathbf{N}_i}_{=\frac{\partial N_{ix}}{\partial x}} = \underbrace{\mathcal{R}_{iv}}_{=\nu_i \mathcal{R}_s \frac{2\pi r_0}{\pi r_0^2}} \quad (10.75)$$

or

$$\frac{dN_i}{dz} = \frac{2}{r_0} \nu_i \mathcal{R}_s \quad (10.76)$$

Since the pore is closed and the reaction on the terminal surface can be neglected in comparison to that on the walls, a key reactant can be selected and the preceding equation integrated from the terminal surface to an arbitrary location in the pore to give

$$N_i = \frac{\nu_i}{\nu_\alpha} N_\alpha \quad (10.77)$$

The ratio of stoichiometric coefficients may be used in place of the flux ratios in Equation (10.58) for the diffusivity of the key reactant in the pore. The concentrations at the pore mouth may be used for this calculation.

Regarding the diffusivity as constant (in spite of the concentration dependence reflected in the multicomponent

generalization of the pore diffusion equation), the general mass balance above becomes

$$D_{ip} \frac{d^2 c_i}{dz^2} + \frac{2}{r_0} \vartheta_i \mathcal{R}_s = 0 \quad (10.78)$$

The reaction rate may be expressed as a function of the concentration of a single key component, say A , by noting that

$$\frac{D_{ip}}{\vartheta_i} \frac{d^2 c_i}{dz^2} = \frac{D_{Ap}}{\vartheta_A} \frac{d^2 c_A}{dz^2} \quad (10.79)$$

and therefore that

$$c_i = c_{i0} + \frac{D_{Ap}}{D_{ip}} \frac{\vartheta_i}{\vartheta_A} (c_A - c_{A0}) \quad (10.80)$$

where c_{i0} are the concentrations at the pore mouth. Substitution of this result into the reaction rate expression yields a function of a single variable, the key component concentration.

Example 10.3.1-1: Key Component Kinetics for SO_2 Oxidation

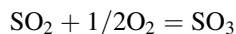
The chemical product of largest quantity the United States is sulfuric acid. It is manufactured by the contact or the lead chamber process. In both of these processes, SO_2 is oxidized to SO_3 using air as the source of oxygen.

The rate of oxidation over a V_2O_5 catalyst is given by Kadlec and Pour (1968) as

$$\mathcal{R}_s = k(T) \rho_P c_{SO_2} c_{O_2}^{1/2} \left[1 - \frac{c_{SO_3}}{c_{SO_2} c_{O_2}^{1/2} K_c(T, P)} \right]$$

The problem is to develop a rate expression in terms of the concentration of SO_2 that can be employed in the microscopic mass balance for SO_2 [Equation (10.78) with $i = SO_2$] for generating the concentration profiles in a pore coated with the V_2O_5 catalyst.

Equation (10.80) gives the concentration of all the components in terms of a key component (A), in this case, SO_2 .



Consequently,

$$\begin{aligned} \nu_{SO_2} &= -1, & \nu_{O_2} &= -1/2, & \nu_{SO_3} &= +1, \\ \nu_{\text{inerts}} &(\text{e.g., } N_2) &= 0 \end{aligned}$$

and

$$\begin{aligned} c_{SO_2} &= c_{SO_2} \\ c_{O_2} &= c_{O_2,0} + \frac{(-1/2) D_{SO_2,P}}{(-1) D_{O_2,P}} [c_{SO_2} - c_{SO_2,0}] \\ c_{SO_3} &= c_{SO_3,0} + \frac{(+1) D_{SO_2,P}}{(-1) D_{SO_3,P}} [c_{SO_2} - c_{SO_2,0}] \\ c_{\text{inert}} &= c_{\text{inert},0} \end{aligned}$$

The rate equation becomes,

$$\begin{aligned} \mathcal{R}_s(T, c_{SO_2}) &= \frac{(-1/2) D_{SO_2,P}}{(-1) D_{O_2,P}} [c_{SO_2} - c_{SO_2,0}] k(T) \rho_P S_g \\ &\times \left\{ 1 - \frac{c_{SO_3,0} - (D_{SO_2,P}/D_{SO_3,P}) [c_{SO_2} - c_{SO_2,0}]}{c_{SO_2} \sqrt{c_{O_2,0} + (1/2) (D_{SO_2,P}/D_{O_2,P}) [c_{SO_2} - c_{SO_2,0}] K_c(T, P)}} \right\} \end{aligned}$$

The concentrations at the pore mouth are considered to be given. If the heat effect is neglected, T is the isothermal temperature. If the heat effect is accounted for, the temperature also becomes a function of the key component concentration (see Section 11.2.1).

Finally, it can be noted that the concentrations at the pore mouth can be written in terms of the conversions based on the feed to the reactor (Kovenklioglu and DeLancey, 1979).

In general, the mass balance requires a numerical solution because of the complexity of the rate equation. However, the irreversible first-order case will display the essential features of a diffusion–reaction system and serve as a good approximation to some practical applications:

$$D_{Ap} \frac{d^2 c_A}{dz^2} + \frac{2}{r_0} \vartheta_A k_s c_A = 0 \quad (10.81)$$

$$c_A = c_{A0} \quad \text{at } z = 0 \quad (10.82)$$

$$-D_{Ap} \frac{dc_A}{dz} = 0 \quad \text{at } z = L \quad (10.83)$$

Remember that the pore is closed when considering the second boundary condition.

The solution to Equations (10.81)–(10.83) is given by

$$\Gamma_A = \cosh \Lambda \xi - [\tanh \Lambda] \sinh \Lambda \xi \quad (10.84)$$

$$\xi = \frac{z}{L}, \quad \Gamma_A = \frac{c_A}{c_{A0}} \quad (10.85)$$

$$\Lambda = L \sqrt{\frac{2k_s}{r_0 D_{Ap}}} = \sqrt{\frac{\text{Reaction rate per unit area} \times \text{Reaction area}}{\text{Diffusivity} \times \text{concentration gradient} \times \text{Diffusion area}}} \quad (10.86)$$

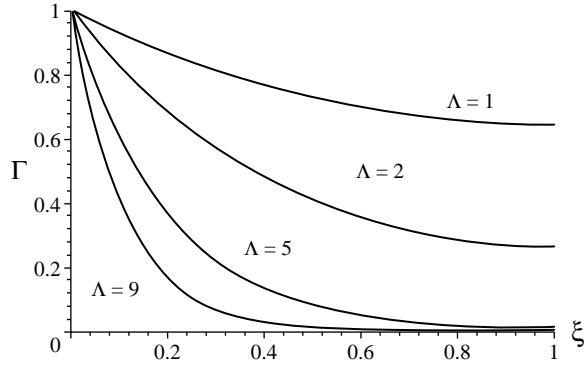


FIGURE 10.19 Dimensionless concentration profiles in a single pore.

Λ is called the Thiele parameter. It is a measure of the reaction rate in the pore relative to a measure of the diffusion rate as illustrated by the expanded equivalent under the square root in Equation (10.86). Typical dimensionless concentration profiles are shown in Figure 10.19 as a function of the dimensionless Thiele parameter.

At larger values of the Thiele parameter, the diffusion rate requires a large concentration gradient to supply the needed reactant. Diffusion and reaction are competing since the catalyst in the pore is not fully utilized in the sense that the concentration above the catalyst is less than the maximum available, the value at the pore mouth. We will see in Section 10.5 that diffusion augmented with forced convection in an open tube with catalytic walls will not suffer from this deficiency. Diffusion is up to the task for a relatively slow reaction characterized by smaller values of the Thiele parameter.

Using the conditions at the pore mouth to define a reaction standard, a pore effectiveness factor, E , can be defined as

$$E_p = \frac{\text{Actual reaction rate}}{\text{Rate at pore mouth conditions}} \quad (10.87)$$

Values of the pore effectiveness factor are generally between 0 and 1. However, values greater than 1 are possible for exothermic reactions where the increase in the reaction rate constant with temperature may nullify the decrease of the concentration dependent term with conversion. In quantitative terms,

$$\mathcal{E}_p = \frac{1}{\mathcal{R}_s(T_0, c_{A0})2\pi r_0 L} \int_0^L \mathcal{R}_s(T, c_A) \frac{2}{r_0} \pi r_0^2 dz \quad (10.88)$$

Note that the reaction rate in the pore must be the rate of diffusion into the pore mouth at steady state so that

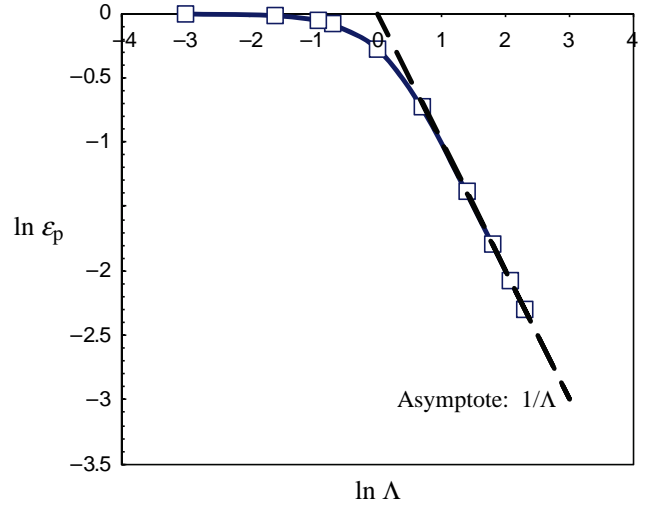


FIGURE 10.20 Pore effectiveness factor for irreversible first-order reaction.

$$\mathcal{E}_p = \frac{1}{\mathcal{R}_s(T_0, c_{A0})2\pi r_0 L} \int_0^{2\pi} \int_0^{r_0} -D_{pi} \left. \frac{dc_A}{dz} \right|_{z=0} r dr d\theta \quad (10.89)$$

In the case of the single irreversible reaction taking place isothermal conditions [see (Equations (10.81)–(10.83)],

$$\mathcal{E}_p = -\frac{1}{\Lambda^2} \left. \frac{d\Gamma_A}{d\xi} \right|_{\xi=0} \quad (10.90)$$

Substitution of the solution in Equation (10.84) into Equation (10.90) gives

$$\mathcal{E}_p = \frac{\tanh \Lambda}{\Lambda} \quad (10.91)$$

which is asymptotic to $1/\Lambda$ for fast reactions. The asymptotic limit and the preceding expression are shown graphically in Figure 10.20.

10.3.2 Effectiveness of Catalyst Particle

Our interest for the most part is focused on the behavior of a catalyst particle. A catalyst particle contains many interconnected pores of various dimensions. A large porosity is beneficial from the viewpoint of reaction rate but not from the viewpoint of mechanical strength. For a given porosity, the reaction rate is always served by increasing the surface coverage, except possibly for whole cell catalysts. In these cases, the addition of biocatalyst will adversely affect the diffusivity and thereby create a competition between

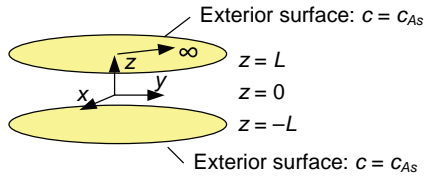


FIGURE 10.21 Semi-infinite flat slab.

reaction and diffusion that may lead to an optimal loading (Zhao and DeLancey, 2000).

We suppose that the surface area per unit volume of a small volume element contained within the particle reaches a constant value during a limiting process as the volume element shrinks to zero or to a dimension very much smaller than the particle. In fact, we assume the validity of a number of limiting processes such as

$$\lim_{V \rightarrow 0} \frac{1}{V} \int_0^\infty \int_0^\infty f(V, r, L) \langle \mathcal{R}_s(r, L) \rangle 2\pi r L dr dL = \mathcal{R}_s \rho_p S_g \quad (10.92)$$

where f is the fraction of the particle volume V consisting of pores with radius between r and $r + dr$ and length between L and $L + dL$, and $\langle R \rangle$ is the average reaction rate in the included pores. Under such conditions we might scale the surface reaction to the particle volume as was done for the single pore, and write a pseudohomogeneous model for the catalyst particle similar to Equation (10.76) for the single pore as

$$\frac{dN_i}{dz} = \rho_p S_g \vartheta_i \mathcal{R}_s \quad (10.93)$$

for a unidirectional system. As illustrated in Figure 8.9, catalyst particles come in a variety of shapes and sizes. Fortunately,

the flat slab geometry illustrated in Figure 10.21 can serve as a very good approximation by using an appropriate surface-to-volume ratio (Aris, 1965).

The thickness of the slab is very much smaller than the remaining dimensions so that we can safely consider only gradients in this dimension. The preceding mass balance with the surface concentration specified and symmetry at the center becomes for an irreversible first-order reaction:

$$D_{Ae} \frac{d^2 c_A}{dz^2} + \rho_p S_g \vartheta_A k_s c_A = 0 \quad (10.94)$$

$$c_A = c_{As} \quad \text{at } z = L \quad (10.95)$$

$$-D_{Ae} \frac{dc_A}{dz} = 0 \quad \text{at } z = 0 \quad (10.96)$$

For more complicated kinetic expressions, all of the concentrations may be expressed in terms of the concentration of a key component (see Section 11.2.1) including temperature. The linear kinetic term in Equation (10.94) is replaced with a highly nonlinear function of c_A .

In the present case, the solution for the concentration profile is

$$\Gamma_A = \frac{c_A}{c_{As}} = \frac{\cosh \Lambda \xi}{\cosh \Lambda} \quad (10.97)$$

where the Thiele parameter is

$$\Lambda = L \sqrt{\frac{k_s \rho_p S_g}{D_{Ae}}} = \frac{\text{apparent volume of pellet}}{\text{external area of pellet}} \times \sqrt{\frac{\text{reaction rate measure}}{\text{diffusion rate measure}}} \quad (10.98)$$

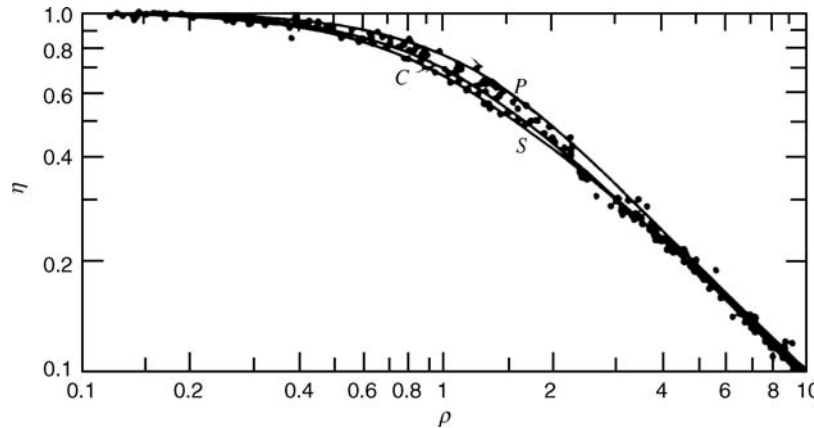


FIGURE 10.22 Consolidation of geometry effect on effectiveness factor (Rester and Aris, 1969). Reprinted with permission of Elsevier.

The total reaction rate in the slab in terms of the catalyst effectiveness is then

$$\text{Total reaction rate} = \mathcal{E} k_s c_{As} \rho_p S_g A_c (2L) \quad (10.99)$$

$$\mathcal{E} = \frac{\tanh \Lambda}{\Lambda} \quad (10.100)$$

Therefore, the graph of catalysts effectiveness in Figure 10.20 also applies to the flat slab shape. In fact, it has been shown that there is little difference between many particle geometries if the characteristic length is taken as the ratio of the volume to the exterior surface (references), for example, $R/3$ for the sphere. See Figure 10.22 for an example.

Catalyst particles are primarily found in fixed and fluidized beds where energy and mass transfer from and to the particle surface are promoted by a turbulent flow field. Some applications are considered in Chapter 12.

10.4 TRANSIENT ADSORPTION BY POROUS SOLID

Adsorption of solutes in porous solids (see Chapter 6) has a number of transport features that are similar to those in the catalytic particles discussed above. However, there are two not unrelated differences. Adsorption is a transient process with the objective of selectively expanding the condensed surface phase. The microscopic mass balance will reflect these two features, which are not present in the microscopic balance for the catalytic particle [see Equation (10.93)].

Consider the microscopic view of a porous adsorbent in Figure 10.23.

It is assumed that only gradients in the s coordinate direction are significant. The perpendicular area generated by the remaining two coordinates is denoted by A_c . A differential volume element in this system contains the adsorbate (A) fluid, the adsorbate on the adsorbent surface, and the adsorbent. The differential volume is divided in accordance with the particle porosity (assumed to be unaffected by the adsorbed layer). The adsorbate passes through the volume element, is taken to the adsorbed layer

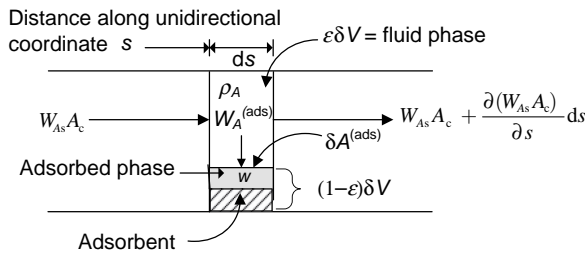


FIGURE 10.23 Microscopic unidirectional adsorption in a porous solid.

by the flux $W_A^{(ads)}$ through the solid–fluid interface, $\delta A^{(ads)}$, or accumulates in the volume element. Conservation of mass [Equation (2.1)] in the fluid and adsorbed phases requires that

Fluid phase:

$$\underbrace{W_{As} A_c}_{\text{Input by flow}} = \underbrace{W_{As} A_c + \frac{\partial(W_{As} A_c)}{\partial s} \delta s}_{\text{Output by flow}} + \underbrace{W_A^{(ads)} \delta A^{(ads)}}_{\text{Output by interfacial mass transfer}} + \underbrace{\varepsilon \delta V \frac{\partial \rho_A}{\partial t}}_{\text{Accumulation}} \quad (10.101)$$

Adsorbed phase:

$$\underbrace{W_A^{(ads)} \delta A^{(ads)}}_{\text{Input by interfacial mass transfer}} = \underbrace{\frac{\partial w}{\partial t} \rho_s (1 - \varepsilon) \delta V}_{\text{Accumulation}} \quad (10.102)$$

Adding the two mass balances eliminates the interfacial mass transfer term:

$$0 = \frac{\partial(W_{As} A_c)}{\partial s} \delta s + \frac{\partial w}{\partial t} \rho_s (1 - \varepsilon) \delta V + \varepsilon \delta V \frac{\partial \rho_A}{\partial t} \quad (10.103)$$

If the interfacial mass transfer process is very fast in comparison to the changes in the fluid and solid bulk phase concentrations, the two phases may be assumed to be in equilibrium (see Section 6.5.2). Assuming this to be the case, we will approximate the equilibrium relationship with Henry's law:

$$w_A = K_A \rho_A \quad (10.104)$$

Assuming that the equilibrium constant is independent of concentration, substitution of Equation (10.104) into Equation (10.103) gives

$$\frac{\partial w_A}{\partial t} = - \frac{K_A}{\rho_s (1 - \varepsilon) K_A + \varepsilon} \frac{\partial(W_{As} A_c)}{\partial s} \frac{\delta s}{\delta V} \quad (10.105)$$

If the particle is spherical with only radial gradients and an effective diffusivity is introduced,

$$\delta s = \delta r \quad (10.106)$$

$$\delta V = 4\pi r^2 \delta r \quad (10.107)$$

$$W_{As} = -D_{Ac} \frac{\partial \rho_A}{\partial r} \quad (10.108)$$

Equation (10.105) becomes

$$\frac{\partial w_A}{\partial t} = \frac{D_{Ac}}{[\varepsilon + \rho_s (1 - \varepsilon) K_A]} \left[\frac{\partial^2 w_A}{\partial r^2} + \frac{2}{r} \frac{\partial w_A}{\partial r} \right] \quad (10.109)$$

We can gain some insight into the behavior of adsorbers by considering a single spherical adsorbent after the concentration of the adsorbate at its surface is suddenly raised. The surface concentration will be approximately constant thereafter if the capacity of the adsorbent is very much less than the availability of adsorbate in the surroundings.

If the loading is uniform at the instant the surface concentration is increased,

$$w_A(r, 0) = w_{A0} \quad 0 \leq r \leq \frac{D_p}{2} \quad (10.110)$$

$$\left\{ w_A\left(\frac{D_p}{2}, t\right) = w_A^s \quad t \geq 0 \right\} \quad (10.111)$$

The solution must be finite at the center of the particle so that

$$w_A(0, t) < \infty \quad (10.112)$$

The solution may be obtained (Ruthven, 1984) with the separation of variables method:

$$\frac{\langle w_A \rangle - w_{A0}}{w_A^{(s)} - w_{A0}} = 1 - \frac{6}{\pi^2} \sum_{n=1}^{\infty} \frac{1}{n^2} \exp\left[-\frac{4n^2\pi^2 D_A}{D_p^2} t\right] \quad (10.113)$$

$$D_A = \frac{D_{Ac}}{[\varepsilon + \rho_s(1 - \varepsilon)K_A]} \quad (10.114)$$

where the average loading is given by

$$\langle w_A \rangle = \frac{1}{(4/3)\pi[D_p/2]^3} \int_0^{2\pi} \int_0^\pi \int_0^{D_p/2} w_A(r, t) r^2 \sin \theta \, dr \, d\theta \, d\phi \quad (10.115)$$

$$= \frac{24}{D_p^3} \int_0^{D_p/2} w_A(r, t) r^2 \, dr \quad (10.116)$$

Note that the elapsed time is measured in units of $D_p^2/(\pi^2 D)$. This means for example that if the surface concentration changed in units of time much larger than this value, the particle may be considered to be at equilibrium, that is, fully loaded at the surface value.

Example 10.4-1: The Recovery of Hexyl Glucoside

The recovery of hexyl glucoside in the production process described in Chapter 2 is accomplished in an adsorption process. A two-step batch operation is considered in Example 5.1-1. Determine a lower bound on the time required in the first stage. Assume that the particles are 5 mm spheres of activated alumina with 0.56 porosity and a tortuosity of 4.

Solution:

A conservative estimate can be obtained by calculating the time required for the adsorbent to uptake the required amount of the glucoside with the surface concentration at its initial value. The concentration gradient at the exterior surface of the particle will be lower in the actual process since the bulk phase composition is decreasing while that of the particle is increasing. The uptake flux of the glucoside at the particle surface is given by

$$-W_{Ar}\left(\frac{D_p}{2}, t\right) = D_{Ac} \frac{\partial \rho_A}{\partial r} \Big|_{r=\frac{D_p}{2}} = D_{Ac} \frac{1}{K_A} \frac{\partial w_A}{\partial r} \Big|_{r=\frac{D_p}{2}}$$

The time estimate may be obtained from Equation (10.113) with a value for the left-hand side and a linear form for the adsorption equilibrium.

For the purposes of illustration only, we will use the Freundlich isotherm, Equation (6.140), with $\alpha = 0.201 \text{ g}$, $\beta = 1$, and $w_{\max} = 0.1295$ or in summary, $K_A = 0.0295$.

Fresh adsorbent is added so that $w_{A0} = 0$

The concentration at the end of the first stage = 2.1326 g/l for a reduction of 50%. Consequently, the amount of adsorbent required for a single equilibrium stage is given by Equation (6.144):

$$W_{\text{ads}} = \frac{265.036}{0.0259} = 10233 \text{ g}$$

$$w_A^{(s)} = 0.0259(4.2823) = 0.11091$$

The average loading is given by the material balance for the 50% reduction.

$$\langle w \rangle W_{\text{ads}} = 265.036(0.50)4.2823$$

$$\langle w \rangle = \frac{265.036(0.50)4.2823}{10233} = 5.5456 \times 10^{-2}$$

The left-hand side of Equation (10.113) is then given by

$$\frac{\langle w \rangle}{w_A^{(s)}} = \frac{5.5456 \times 10^{-2}}{0.11091} = 0.50001$$

Diffusivity calculation: $A = \text{glucoside}$, $B = \text{hexanol}$.

Assuming that the square root of the surface tensions is near unity, the Tyne–Callus method in Table 8.5 is calculated as follows:

$$D_{AB}^0 = 8.93 \times 10^{-8} \frac{V_B^{5/3} T}{V_A^{11/6} \eta_B}$$

$$V_A \approx 0.1181/\text{mol} = 118 \text{ cm}^3/\text{mol} \varepsilon$$

$$V_B \approx \frac{1}{1.043} \text{ cc/g} = \frac{60.054}{1.043} = 57.578 \text{ cc/mol}$$

$$\eta_B = 10^{-9.7166+2006/T+0.0159 \times T-1.2286 \times 10^{-5} \times T^2} = 4.3085 \text{ cP}$$

$$D_{AB}^0 = 8.93 \times 10^{-8} \frac{(57.58)^{5/3}}{(118)^{11/6}} \frac{300}{4.3085} = 8.4915 \times 10^{-7} \text{ cm}^2/\text{s}$$

$$D_{Ac} = \frac{\varepsilon}{\tau} D_{AB}^0 = \frac{0.56}{4} 8.4915 \times 10^{-7} = 1.1888 \times 10^{-7} \text{ cm}^2/\text{s}$$

Substitution into Equation (10.113)

$$D_A = \frac{1.1888 \times 10^{-7}}{0.56 + 1.8(1 - 0.56)0.0259} = 2.0478 \times 10^{-7}$$

where ρ_s is estimated to be 1.8 g/cc from the values for activated alumina in Table 6.16.

The right-hand side of Equation (10.113) is only a function of time:

$$F(t) = 1 - \frac{6}{\pi^2} \sum_{n=1}^{\infty} \frac{1}{n^2} \exp\left(-\frac{4\pi^2(2.0478 \times 10^{-7})}{0.25} 3600 n^2 t\right)$$

for t in hours

$$F(t) = 1 - \frac{6}{\pi^2} \sum_{n=1}^{\infty} \frac{1}{n^2} \exp(-0.116425 n^2 t)$$

$$F(0) = 0$$

$$F(\infty) = 1.0$$

By repetitive calculation:

$$F(2.589) = 0.49996. \text{ At least 2.5 h are required.}$$

10.5 DIFFUSION WITH LAMINAR FLOW

Although the preceding examples did not include forced convection in the subsystems that we were concerned with, convection was an important feature of the mechanism by which the interfacial or boundary conditions were established. Forced convection will almost always be the predominant mechanism for mass transfer in the direction of the convective velocity vector, and in the case of turbulent flow, convection can make a significant lateral contribution. In the case of laminar flow, there is no lateral contribution and a pure diffusion process can be envisioned normal to the velocity vector. An example is the wetted wall tower discussed in Section 9.2.1.5.

10.5.1 Wetted Wall Tower—Short Contact Time

The basic construction of a wetted wall tower is illustrated in Figure 9.5 and the velocity distribution of a nonvolatile,

constant density liquid is derived there in a cylindrical coordinate system. Here we consider a liquid with these characteristics that is contacted with a pure gas, A . The gas flows into the wetted wall tower with the liquid and is soluble in the liquid. We want to know the rate at which A is taken up by the liquid in the tower under two circumstances: first, physical absorption, where there is no reaction, and second, chemical absorption, where A undergoes a reaction in the liquid phase. A comparison of these two cases will demonstrate the efficacy of chemical absorption and therefore the reason for the widespread use of chemical absorption in the chemical industry.

10.5.1.1 Physical Absorption By assuming that the liquid is nonvolatile and that the gas feed is pure, the gas remains at nearly uniform conditions, and we can focus attention on the liquid phase. Refer to Figure 10.24.

We suppose that the concentration of A in the liquid at the inlet is c_{Ab} , which is less than the solubility of the gas in the liquid at the prevailing conditions. The gas–liquid interface immediately equilibrates with the gas. The interfacial concentration is consequently uniform throughout the tower at the solubility, c_{Ai} and the concentration distribution in the liquid at the entrance undergoes a step change at the interface from the bulk value to the solubility.

Suppose we accompany an element of liquid as it travels down the column. Species A gradually diffuses into the liquid in the radial direction, which is reflected by the penetration of the concentration distribution deeper into the liquid. If the diffusion rate is slow relative to the velocity of the fluid, two simplifications can be made. First, the only velocity experienced by the diffusion process is essentially the maximum velocity, the fluid velocity at the interface. Consequently, the diffusion process is unaware of the wall. This is what we mean by short contact times. Second, the effects of curvature are negligible. We can make this stipulation of a short contact time quantitative if we consider

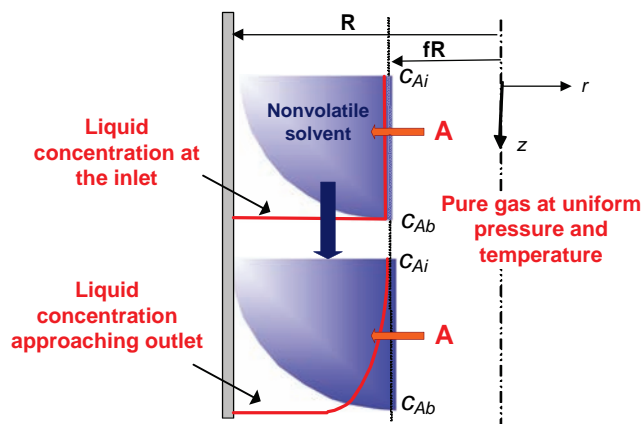


FIGURE 10.24 Concentration gradients in a wetted wall tower.

the unidirectional, unsteady-state, diffusion process that we experience as passengers on the fluid element. Since the effects of curvature are negligible, we may begin with the mass balance in rectangular coordinates in Table 10.1, the origin fixed at the fluid surface:

$$\underbrace{\frac{\partial \rho_i}{\partial t} + v_z \frac{\partial \rho_i}{\partial z}}_{\leftarrow \text{diffusion}} = D_{im} \underbrace{\left(\frac{\partial^2 \rho_i}{\partial x^2} + \frac{\partial^2 \rho_i}{\partial y^2} + \frac{\partial^2 \rho_i}{\partial z^2} \right)}_{\approx 0} + \underbrace{r_{iv}}_{=0} \quad (10.117)$$

This reduces to

$$\frac{\partial \Gamma}{\partial \tau} = \frac{\partial^2 \Gamma}{\partial \eta^2} \quad (10.118)$$

where

$$\Gamma = \frac{c_A}{c_{Ai}}, \quad \eta = \frac{x}{\delta}, \quad \tau = \frac{t}{\delta^2/D_{Am}} \quad (10.119)$$

Recall that the film thickness is denoted by δ . Temporal changes in this system are most significant when measured in increments of the time constant δ^2/D_{Am} . By short contact times we then mean that

$$\frac{L}{v_{\max}} \ll \frac{\delta^2}{D_{Am}} \quad (10.120)$$

where L is the height of the liquid film. This result may be rearranged to give

$$\frac{L}{D} \ll 0020153 N_{\text{Fr}}^{1/3} N_{\text{Sc}} \quad (10.121)$$

The Froude number is based on the maximum velocity.

We may solve the diffusion problem in the time domain but to be consistent with the steady-state thread that we are following, let us switch back to the fixed coordinates and reapply the general form:

$$\underbrace{\frac{\partial \rho_i}{\partial t}}_{=0} + \underbrace{v_z}_{\approx v_{\max}} \frac{\partial \rho_i}{\partial z} = D_{im} \underbrace{\left(\frac{\partial^2 \rho_i}{\partial x^2} + \frac{\partial^2 \rho_i}{\partial y^2} + \frac{\partial^2 \rho_i}{\partial z^2} \right)}_{\approx 0} + \underbrace{r_{iv}}_{=0} \quad (10.122)$$

or in molar units

$$v_{\max} \frac{\partial c_A}{\partial z} = D_{Am} \frac{\partial^2 c_A}{\partial x^2} \quad (10.123)$$

$$c_A = c_{Ai} \quad x = 0 \quad \text{and} \quad z \rightarrow \infty \quad (10.124)$$

$$c_A = c_{Ab} \quad x \rightarrow \infty \quad \text{and} \quad z = 0 \quad (10.125)$$

This formulation would not apply to the case where diffusion as well as convection takes place in the z direction.

These equations may be solved with the Boltzmann substitution, which combines the variables as follows:

$$\eta = \frac{x}{\sqrt{4D_{Am}z/v_{\max}}} \quad (10.126)$$

The solution may be shown to be

$$\frac{c_A - c_{Ai}}{c_{Ab} - c_{Ai}} = \frac{2}{\sqrt{\pi}} \int_0^\eta e^{-\xi^2} d\xi = \text{erf}(\eta) \quad (10.127)$$

The local molar flux of A from the gas to the liquid can be evaluated with this result:

$$N_{Ai} = -D_{Am} \left. \frac{\partial c_A}{\partial x} \right|_{x=0} = D_{Am}(c_{Ai} - c_{Ab}) \left[\frac{2}{\sqrt{\pi}} e^{-\eta^2} \frac{\partial \eta}{\partial x} \right]_{x=0} \quad (10.128)$$

$$N_{Ai} = \sqrt{\frac{D_{Am} v_{\max}}{\pi z}} (c_{Ai} - c_{Ab}) = k_{cA}(c_{Ai} - c_{Ab}) \quad (10.129)$$

A mass transfer coefficient, k_{cA} , based on the overall concentration driving force has been defined. In terms of the dimensionless Sherwood number (or the Nusselt number for mass transfer), the definition amounts to

$$N_{\text{Sh}} = \frac{k_{cA} z}{D_{Am}} = \sqrt{\frac{v_{\max} z}{D_{Am} \pi}} \quad (10.130)$$

Referring to Section 9.2.1.5, the Sherwood number can also be expressed in terms of the average velocity:

$$N_{\text{Sh}} = [0.691 + 0.0576\epsilon + O(\epsilon^2)] \sqrt{\frac{\langle v \rangle z}{D_A^V}} \quad (10.131)$$

The first term agrees with form presented by Cussler (1984). Recall that the film thickness is ϵR and that this result holds for values of the Reynolds number up to approximately 250. If ripples are present, that mass transfer coefficient can be increased by 50% (Geankopolis, 2003).

Let us now repeat the analysis but include a chemical reaction and compare the resulting mass transfer coefficient with the one above for the unreactive case.

10.5.1.2 Chemical Absorption Before we do the analysis, let us consider what to expect. Our interest is primarily

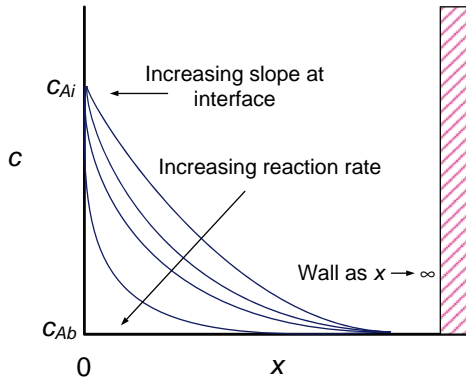


FIGURE 10.25 Effect of the reaction on concentration gradients.

in the interfacial mass transfer rate, which is proportional to

$$\left. \frac{\partial c_A}{\partial x} \right|_{x=0}$$

as discussed above for the case of physical absorption. To be fair in making a comparison, we will fix the same boundary conditions in each case, that is, those stated for the unreactive case in the preceding section. We will consider a single chemical reaction whereby *A* disappears at rates we can control catalytically with no appreciable effect on the flow field. The concentration field must be increasingly diminished as we increase the rate of consumption of *A*. Refer to Figure 10.25.

The beneficial effect of the reaction on the interfacial mass transfer rate is apparent from the increasing slope.

Consider now a second-order reaction of *A* with a component *B* present in excess so that the reaction rate depends only on the concentration of *A*:

$$\mathcal{R}_{Av} = -k_r c_A^\alpha c_B^\beta = -k c_A^\alpha = -k_1 c_A \quad (10.132)$$

An example is the absorption of chlorine (*A*) in water (*B*) (Brian et al., 1962).

Adding the reaction rate to the equations describing the unreactive case gives

$$v_{\max} \frac{\partial c_A}{\partial z} = D_{Am} \frac{\partial^2 c_A}{\partial x^2} - k_1 c_A \quad (10.133)$$

$$c_A = c_{Ai} \quad x = 0 \quad \text{and} \quad z \rightarrow \infty \quad (10.134)$$

$$c_A = c_{Ab} \quad x \rightarrow \infty \quad \text{and} \quad z = 0 \quad (10.135)$$

The solution for a zero bulk phase composition (Danckwerts, 1970) is

$$\frac{c_A}{c_{Ai}} = \frac{1}{2} e^{-x\sqrt{k_1/D_{Am}}} \operatorname{erfc} \left[\frac{x}{2\sqrt{D_{Am}t}} - \sqrt{k_1 t} \right] + \frac{1}{2} e^{x\sqrt{k_1/D_{Am}}} \operatorname{erfc} \left[\frac{x}{2\sqrt{D_{Am}t}} + \sqrt{k_1 t} \right] \quad (10.136)$$

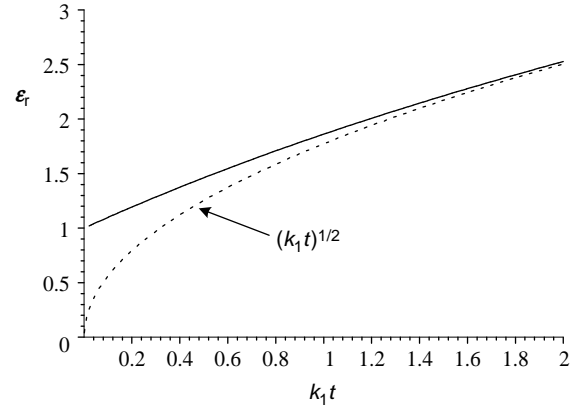


FIGURE 10.26 Mass transfer enhancement due to first-order kinetics.

where

$$t = \frac{z}{v_{\max}} \quad (10.137)$$

The corresponding interfacial mass transfer rate is

$$N_{Ai} = -D_{Am} \left. \frac{\partial c_A}{\partial x} \right|_{x=0} = c_{Ab} \sqrt{k_1 D_{Am}} \left[\operatorname{erf} \sqrt{k_1 t} - \frac{e^{-k_1 t}}{\sqrt{\pi k_1 t}} \right] \quad (10.138)$$

Note that only the diffusion component of the flux is used. A convective term would be present, for example, if there were a substantial volume change accompanying the absorption. Ammonia absorption is a case in point.

Division of this result by the rate of absorption for the unreactive case gives

$$\mathcal{E}_r = \sqrt{\pi k_1 t} \left[\operatorname{erf} \sqrt{k_1 t} - \frac{e^{-k_1 t}}{\sqrt{\pi k_1 t}} \right] \quad (10.139)$$

\mathcal{E}_r is the enhancement factor or the correction to the mass transfer coefficient for physical absorption required to account for the reaction. Refer to Figure 10.26 and note that the asymptotic limit is $\sqrt{\pi k_1 t}$.

Many reactive systems have been investigated. The results can be used to adjust the values of mass transfer coefficients that are measured under nonreactive conditions when the penetration theory of interfacial mass transfer is applicable.

10.5.2 Laminar Flow in a Tube with Catalytic Walls

In Section 10.3, we saw that the effectiveness of a catalytic surface could be quite small under circumstances where the reactants are supplied by a diffusional process. We now want

to learn on quantitative grounds the effect of a convective supply of reactants, while at the same time extending our experience with the microscopic mass balance.

The effectiveness of the catalytic surface can be considerably increased in general for single reactions by providing a convective supply mechanism for the reactants and removal for the products. A straight round tube with a coated surface provides this mechanism as an open conduit for convective flow under an imposed pressure gradient. Laminar flow of a Newtonian fluid at constant density and isothermal conditions was discussed in the previous chapter. These conditions can be applied here and include gas phase systems if the pressure drop is not large and the surface-to-volume ratio is sufficiently high to remove the thermal energy released by the reaction. The heat removal rate is proportional to the lateral area of the tube, while thermal energy is produced at a rate per unit volume. The surface-to-volume ratio for the tube of diameter D is $4/D$. This is a very attractive feature of small-scale systems.

If the effect of composition on the viscosity is also neglected, the momentum and mass balances are uncoupled and convective velocity profile can therefore be obtained separately. We will use the results from Chapter 8 for flow in tubes.

$$v_z = v_{\max} \left[1 - \left(\frac{r}{r_0} \right)^2 \right] \quad (10.140)$$

There are no angular upsets and diffusion in the convective (z) direction can be neglected, except possibly near the tube wall. However, because of the large radial gradients at the wall, diffusion in the radial direction is expected to be the major mechanism there.

The mass balance for this model is then obtained from the cylindrical component of Table 10.1.

$$\underbrace{\frac{\partial \rho_i}{\partial t}}_{=0 \text{ (s.s.)}} + \underbrace{v_z}_{=f(r) \text{ see Chapter 8}} \frac{\partial \rho_i}{\partial z} = D_{im} \left(\frac{1}{r} \frac{\partial}{\partial r} \left(r \frac{\partial \rho_i}{\partial r} \right) + \underbrace{\frac{1}{r^2} \frac{\partial^2 \rho_i}{\partial \theta^2}}_{=0 \text{ symmetry}} + \underbrace{\frac{\partial^2 \rho_i}{\partial z^2}}_{\ll \text{convection}} \right) + \underbrace{r_{iv}}_{=0: \text{ surface reaction}} \quad (10.141)$$

or

$$\left[1 - \left(\frac{r}{r_0} \right)^2 \right] \frac{\partial c_A}{\partial z} = D_A \left[\frac{\partial}{\partial r} \frac{\partial c_A}{\partial r} + \frac{1}{r} \frac{\partial c_A}{\partial r} \right] \quad (10.142)$$

Note that there is no reaction represented in the mass balance, which applies to the homogeneous fluid phase in

the tube. The reaction appears only in the boundary condition (M5 in Table 8.12):

$$\begin{aligned} \mathbf{j}_A \cdot \mathbf{\delta}_r &= \left[-M_A D_A \nabla c_A \cdot \mathbf{\delta}_r = -M_A D_A \frac{\partial c_A}{\partial r} = M_A k_s c_A \right] \\ &= \vartheta_A M_A \mathcal{R}_s \quad \text{at } r = r_0 \end{aligned} \quad (10.143)$$

Note that the mass average velocity normal to the wall must be zero since the tube wall is closed and mass is preserved in chemical reactions. Therefore, the diffusional flow to the wall must be equal to the reaction rate for each species.

The radial derivative of the concentration vanishes at the center of the tube because of symmetry (or to keep the differential equation within bounds):

$$\frac{\partial c_A}{\partial r} = 0 \quad \text{at } r = r_0, \forall z \quad (10.144)$$

Because of the axial derivative, a boundary condition on the z -axis is needed. Here we will specify a concentration distribution in the radial direction that satisfies the radial boundary conditions and has the value c_{A0} specified at the center. Using the first three terms of a powers series gives,

$$c_A(r, 0) = c_{A0} \left[1 - \frac{k_s}{2D_A r_0 + k_s r_0^2} r^2 \right] \quad (10.145)$$

A summary of the model in dimensionless form is given by

$$(1 - \xi^2) \frac{\partial \Gamma}{\partial \eta} = \left[\frac{\Lambda_l}{\Lambda_c} \right] \frac{1}{\xi} \frac{\partial}{\partial \eta} \xi \frac{\partial \Gamma}{\partial \eta} \quad (10.146)$$

$$\frac{\partial \Gamma}{\partial \xi} = - \left[\frac{\Lambda_r}{\Lambda_l} \right]^2 \Gamma, \quad \xi = 1, \forall \eta \quad (10.147)$$

$$\frac{\partial \Gamma}{\partial \xi} = 0, \quad \xi = 0, \forall \eta \quad (10.148)$$

$$\Gamma(\xi, 0) = 1 - \left[\frac{\Lambda_r^2}{\Lambda_l^2 + \Lambda_r^2} \right] \xi^2 \quad (10.149)$$

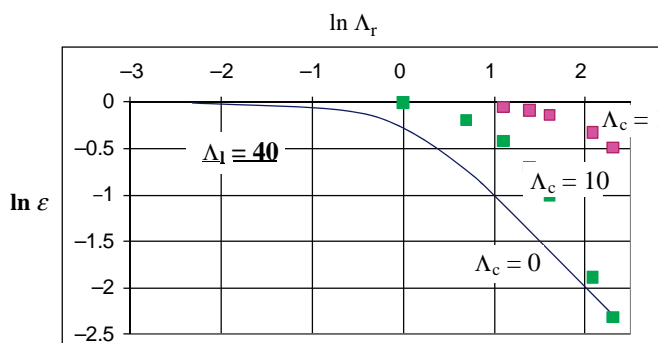
The dimensionless radial and axial coordinates as well as the dimensionless concentration, $\xi = r/r_0$, $\eta = z/L$, and $\Gamma = c_A/c_{A0}$, respectively, all lie between 0 and 1. Recall that the radius and length of the tube are 0 and L , respectively. The Λ_l are dimensionless groups defined in Table 10.6 with the indicated interpretations.

Mathematica was used to solve the dimensionless equations and to calculate the effectiveness factor defined by

$$\begin{aligned} E &= \frac{1}{k_s c_{A0} 2\pi r_0 L} \int_0^L k_s c_A(r_0, x) 2\pi r_0 dx \\ &= \int_0^1 \Gamma(1, \eta) d\eta \end{aligned}$$

TABLE 10.6 Dimensionless Groups for Laminar Flow Reactor

Dimensionless Group	Interpretative Form	Interpretation
$\Lambda_1 = \frac{L}{r_0}$		Tube length in radius units
$\Lambda_c = \frac{r_0 v_{\max}}{D_A}$	$\frac{r_0 v_{\max}}{D_A} = \frac{c_{A0} v_{\max}}{(D_A/r_0)(c_{A0} - 0)}$	Axial convection relative to radial diffusion flux
$\Lambda_r = L \sqrt{\frac{k_s}{D_A r_0}}$	$L \sqrt{\frac{k_s}{D_A r_0}} = \sqrt{\frac{k_s c_{A0} 2\pi r_0 L}{(D_A/L)(c_{A0} - 0)\pi r_0^2}}$	Reaction rate relative to axial diffusion rate

**FIGURE 10.27** Effect of convective velocity on the enhancement factor.

The values of the effectiveness factor calculated with convection are compared below to those values obtained above for the closed pore in Figure 10.27. The results were obtained with Mathematica.

The values with convection are higher or, more precisely, increasing the velocity will increase the catalyst effectiveness, except possibly for some very fast reactions.

PROBLEMS

10.1. A vapor recovery system is shown in Figure 10.28 for the treatment of off gases generated from the storage, handling, and distribution of benzene.

Three separation units are used to recover the benzene from the benzene–air stream, which arrives at the input to the compressor. Benzene is absorbed in the tray tower using benzene from the tank storage as the solvent. The air is not absorbed and goes overhead with a benzene mole fraction of 0.1316. The final separation is accomplished in two steps.

First, the benzene mole fraction is reduced to 0.0055 in a membrane unit. Air does not penetrate the membrane, which is composed of a material similar to the FAU-type zeolite membranes (Jeong et al., 2003). The pressure on the permeate side is maintained at 0.01 atm by a vacuum pump,

which also provides the means for periodically regenerating the saturated fixed-bed adsorber. The permeance of benzene in the membrane is $9.5 \times 10^{-8} \text{ mol}/(\text{m}^2 \text{ s Pa})$.

The two-bed adsorption unit is used to reduce the benzene concentration to 0.1% of the feed value. The adsorbents activated carbon of the type designated by M3 (Carrot et al., 2000) with a particle diameter of 0.50 cm. The equilibrium data in the dilute gas phase region is given by

$$q(\text{mol}/\text{m}^3) = 18,708c(\text{mol}/\text{m}^3)$$

- Determine the area of the membrane.
- Assuming a reasonable packing density and an L/D ratio of 5, determine the size of a cylindrical unit that could house the membrane.
- Assuming that the adsorption operation involves only two regions in the bed (one fully saturated and the other fresh adsorbent), determine the bed volume required for a saturation time of 0.5 h. Compute the diameter and length for an L/D of 6 and use the calculated diameter for the following calculations.
- Determine the breakthrough time for the calculated length.

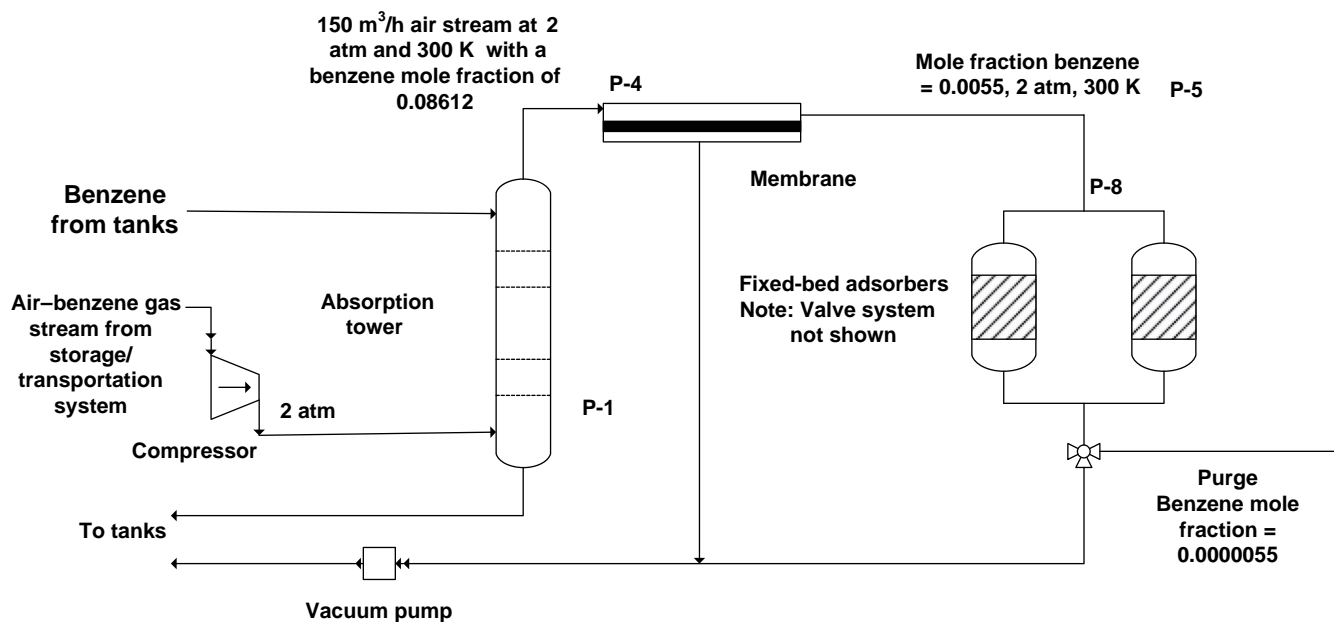


FIGURE 10.28 Problem 10.1.

- Provide the breakthrough curve.
- Provide the gas phase concentration in the bed at breakthrough.

10.2. Suppose that the single (elementary) reversible reaction, $A = B$, can take place on a particular macroporous support with a forward rate constant per unit mass equal to k_{if} on the microporous support and k_{af} on the macroporous support. The two support powders are to be pressed into pellets in proportions to maximize the reaction rate.

- If the supports have the same shape, show that the apparent pellet density is given by

$$\rho_p = \frac{\rho_i(1 - \varepsilon_s)}{\omega_i + \rho_p(\rho_i/\rho_a)(1 - \omega_i)}$$

where ρ , ε , and ω are mass concentration, porosity, and mass concentration, respectively, p refers to the pellet; and i and a refer to the microporous and macroporous powders; and s refers to the interparticle spaces in the pellet.

- If the effective diffusivity of A in the pellet is the average of the diffusivities in the three pellet regimes weighted by the respective void fractions, show that

$$D_{Ap} = \frac{\omega_i(1 - \varepsilon_s)}{\omega_i + \rho_p(\rho_i/\rho_a)(1 - \omega_i)} D_{Ai} + \frac{\rho_i(1 - \varepsilon_s)(1 - \omega_i)}{\omega_i + \rho_p(\rho_i/\rho_a)(1 - \omega_i)} D_{Aa} + \varepsilon_s D_{As}$$

- Using the pore diffusion model in Section 10.2.1.1 for the interparticle spaces with an average pore radius of

$$r_s = \frac{2v}{a} \frac{\varepsilon_s}{1 - \varepsilon_s}$$

where v and a are the apparent volume and external surface of the support particles, the parallel pore model can be used to give

$$\frac{D_{Ap}}{D_{Ai}} = \alpha(\omega_i)(1 - \varepsilon_s) + \beta(\varepsilon_s)$$

$$\alpha(\omega_i) = \frac{D_{Ab} \varepsilon_s + (D_{Aa}/D_{Ai})(\rho_i/\rho_a)(1 - \varepsilon_s)}{D_{Ai} \varepsilon_s + (\rho_i/\rho_a)(1 - \varepsilon_s)} \varepsilon_s^2$$

$$\beta(\varepsilon_s) = \frac{\rho_i(1 - \varepsilon_s)(1 - \omega_i)}{\omega_i + (D_{Ab}/D_{AK})(1 - \omega_i)} D_{Aa}$$

$$D_{AK} = K_A \frac{2v}{a} = \text{Knudsen diffusivity}$$

- Set up and solve the diffusion-reaction problem in a flat slab and from this result determine an optimal value for the microporous mass fraction assuming that

$$\frac{D_{Aa}}{D_{Ai}} \gg 1 \quad \text{and} \quad \frac{\rho_a k_a S_a}{\rho_a k_a S_a} \ll 1$$

11

ENERGY TRANSFER UNDER NONTURBULENT CONDITIONS

The exchange of energy as heat between a hot and a cold body occurs throughout many chemical processes. Review the acrylic acid process in Figure 1.1 for instances of heat exchange. The reasons for this are many but a number of the common ones are summarized below:

- The temperature level is an agent by which an operation is executed, for example, flash vaporization/distillation, thermal diffusion, freeze drying, and melting.
- Material limitations for process vessels or process materials, for example, sintering of catalyst and cost.
- Effect on rates and equilibrium, for example, equipment size.
- Effect on relative rates, for example, yield and selectivity considerations.
- Production of work, for example, production of electricity and air conditioning.

The intentional transfer of thermal energy to a process mixture almost invariably takes place through solid walls or heat transfer surfaces (refer to Figure 14.1). The mixing of process and heat transfer fluids is generally undesirable. There are exceptions. Steam, for example, can be injected directly into the bottom of a tower for distillation of an aqueous mixture where water is the heavy component. A rapid change in temperature can be achieved by the direct contact of a cold with a hot fluid, a process known as

quenching. Refer to tower T-301 in the acrylic acid process. Examples such as these aside, the exchange of thermal energy to or from process equipment takes place through solid walls (see Section 11.1).

Transfer of thermal energy in the process fluid takes place primarily by turbulent mechanisms, but possibly beginning with generation and conduction through a porous solid such as a catalyst or adsorption particle. A nonisothermal porous catalyst is considered in Section 11.2.

Analogous to mass transfer, conduction normal to a laminar flow field discussed in terms of the wetted wall tower is presented in Section 11.3. The similarity of the microscopic mass and energy balances make it possible to draw analogies between the two processes. However, it must be remembered that the two processes take place in very different time scales. Referring to Table 8.15, the time constant for diffusion is orders of magnitude higher for liquids and solids than the time constant for conduction. Temperature gradients, therefore, disappear much faster than concentration gradients. The situation is reversed when comparing the two time constants for gases.

The chapter closes with an example of a moving boundary application of a conduction-controlled process.

Only unidirectional systems in rectangular and cylindrical coordinates are included. The simplified energy balance is given in Table 11.1. The corresponding momentum and mass balance equations under similar limitations may be found in Tables 9.1 and 10.1, respectively.

TABLE 11.1 Steady-State Energy Balance

Unidirectional velocity $\mathbf{v} = v_z \delta_z$
 Newtonian fluid with constant density and thermal conductivity
 Rectangular and cylindrical systems:

$$\sum_i \mathbf{j}_i \cdot \nabla \bar{H}_i \approx 0 \quad \mathbf{v} = v_z \delta_z, \quad \bar{\mathbf{F}}_i = \mathbf{g}, \quad \tau : \nabla \mathbf{v} = 0$$

See Table 9.1 for momentum balance

Rectangular system

$$\rho c_P v_z \frac{\partial T}{\partial z} = k \left(\frac{\partial^2 T}{\partial x^2} + \frac{\partial T}{\partial y^2} + \frac{\partial^2 T}{\partial z^2} \right) + \sum_j (-\Delta H_{Rj}) \mathcal{R}_{jv}$$

Cylindrical system

$$\rho c_P v_z \frac{\partial T}{\partial z} = k \left(\frac{1}{r} \frac{\partial}{\partial r} \left(r \frac{\partial T}{\partial r} \right) + \frac{1}{r^2} \frac{\partial^2 T}{\partial \theta^2} + \frac{\partial^2 T}{\partial z^2} \right) + \sum_j (-\Delta H_{Rj}) \mathcal{R}_{jv}$$

11.1 CONDUCTION IN SOLIDS–COMPOSITE WALLS

Convection is not present in solid phases. Energy is transferred by conduction only. An important application of conduction through solids is the calculation of heat losses from insulated equipment, such as a process furnace. Considering the equipment and insulation, there are at least two layers through which the energy is conducted. A multilayer rectangular configuration is illustrated in Figure 11.1.

We assume that there are no sources or sinks of thermal energy other than what is needed to maintain the temperatures at either end of the narrow dimension (illustrated in Figure 11.1) of the composite wall. Furthermore, we assume that the dimensions in all directions appear infinite in comparison to the narrow directions. We are left with conduction in only one dimension (say, z) to consider. The microscopic energy balance can then be simplified as follows in each layer:

$$\underbrace{\rho c_P v_z \frac{\partial T}{\partial z}}_{\text{velocity}=0} = \lambda \left(\underbrace{\frac{\partial^2 T}{\partial x^2} + \frac{\partial T}{\partial y^2}}_{=0 \text{ negligible gradients}} + \frac{\partial^2 T}{\partial z^2} \right) + \underbrace{\sum_j (-\Delta H_{Rj}) \mathcal{R}_{jv}}_{=0 \text{ no reactions}} \quad (11.1)$$

Therefore,

$$\lambda \frac{\partial^2 T}{\partial z^2} = 0 \quad \text{or} \quad \frac{\partial T}{\partial z} = \text{constant or } q = \text{another constant} \quad (11.2)$$

where λ refers to the material of the layer. Remember, because of the continuity requirements imposed during the derivation of the transport equations, we cannot include a phase boundary in the domain of the differential equation.

Since the energy flux must be continuous across each interface, the energy flux is constant throughout all of the layers (see boundary condition E3 in Table 8.12). In addition, since there is thermal equilibrium at each interface, the temperature profile is continuous as indicated in Figure 11.1. We are not concerned at this juncture with the source of the energy flux at the surface of the first layer nor are we concerned with how this energy is removed from the N th phase. These mechanisms are presumed to establish the two surface temperatures T_0 and T_N . We wish to calculate the heat flux through the composite given the value of these two temperatures and the dimensions of the layers. Considering an arbitrary layer,

$$\lambda_i \frac{\partial^2 T^{(i)}}{\partial z^2} = 0 \quad (11.3)$$

$$T^{(i)}(L_i) = T_i \quad (11.4)$$

$$T^{(i)}(L_{i-1}) = T_{i-1} \quad (11.5)$$

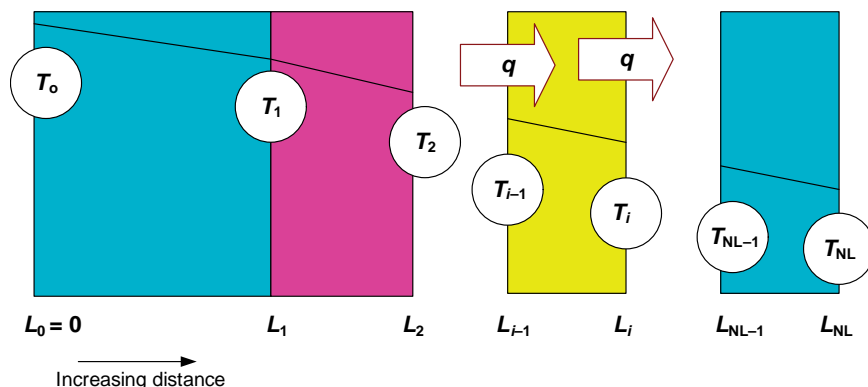


FIGURE 11.1 Heat conduction through a composite wall.

The solution is

$$T^{(i)} = \frac{T_i - T_{i-1}}{L_i - L_{i-1}} z + \frac{L_i T_{i-1} - T_i L_{i-1}}{L_i - L_{i-1}} \quad \text{at } z \in (L_{i-1}, L_i) \quad (11.6)$$

$$\text{and } q = \frac{\lambda_i}{L_i - L_{i-1}} (T_{i-1} - T_i) \quad (11.7)$$

The intermediate temperatures may be eliminated by adding the individual temperature drops.

$$\sum_{i=1}^{N_L} q \frac{L_i - L_{i-1}}{\lambda_i} = \sum_{i=1}^{N_L} (T_{i-1} - T_i) \quad (11.8)$$

$$q \sum_{i=1}^{N_L} \frac{L_i - L_{i-1}}{\lambda_i} = T_0 - T_N \quad (11.9)$$

$$q = U(T_0 - T_N) \quad \text{where} \quad (11.10)$$

$$\frac{1}{U} = \sum_{i=1}^{N_L} \frac{L_i - L_{i-1}}{\lambda_i} \quad (11.11)$$

The thickness of the i th layer is $(L_i - L_{i-1})$. Whereas λ_i ($L_i - L_{i-1}$) is a conductivity, the inverse may be thought of as a resistance. The overall resistance is the sum of these individual resistances and defines an overall heat transfer coefficient or conductivity. Note the close analogy of this interpretation with that given for the overall mass transfer coefficient in Equations (10.51) and (10.52).

Note that a resistance may be neglected in the overall sum if the thermal conductivity is much larger than in the other layers. In this event, the temperature gradient in that layer may be neglected and the energy transfer takes place as if the layer were not present. By the same token, a layer may have a very small thermal conductivity that would require a large temperature difference to support the heat flux. In the extreme case, this layer may be the only important resistance and the others may be neglected. An example of this situation is a single layer or multiple layers of insulation covering a thin metal wall.

Example 11.1-1: Insulated Firebox for Steam Reforming

Synthesis gas, a mixture of CO and H₂, is the starting material that begins the route to many petrochemical products. Synthesis gas can be derived from the steam reforming of CH₄, which can be carried out over a promoted iron catalyst in tubes arranged in a fire box with provisions for the heat of reaction to be provided by the direct combustion of methane. The components of the firebox are illustrated in Figure 11.2.

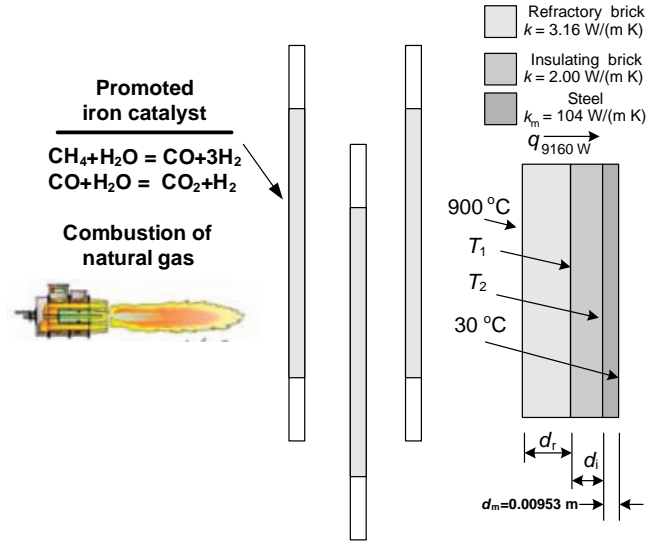


FIGURE 11.2 Firebox wall in steam reforming of methane.

The outside surface of the metal wall is set at 30 °C primarily for safety reasons. A consideration of the environmental conditions leads, with this surface temperature, to an estimate of the energy flux from the outside surface, q (value given in Figure 11.2). Suppose that through the processes of radiation and convection, the inside wall of the furnace reaches a temperature 900 °C. What must be the thicknesses of the refractory brick and the insulating brick if the thickness of the metal wall is 0.00953 m?

Solution:

The problem as stated is underspecified since equating the fluxes gives three equations but four unknowns (T_1, T_2, d_r, d_i):

$$q = \frac{k_r(900 - T_1)}{d_r} = \frac{k_i(T_1 - T_2)}{d_i} = \frac{k_m(T_2 - 30)}{d_m} \quad (11.12)$$

where d_r and d_i are defined in Figure 11.2. The insulating brick has a maximum operating temperature so that it is convenient to consider T_1 as the independent variable.

The total dimension of the insulation applied to the metal is given by

$$d_r + d_i = - \left[\frac{\lambda_r - \lambda_i}{q} \right] T_1 + \frac{\lambda_r}{q} 900 - \frac{\lambda_i}{q} \left[30 + q \frac{d_m}{k_m} \right]_{=T_2} \quad (11.13)$$

The coefficient of T_1 is clearly negative so that the total dimension of the insulation is a minimum if T_1 is set at its maximum of 600. Taking this as a basis, the insulation

dimensions are

$$d_r = \frac{\lambda_r}{q} (900 - 600) = 0.10349 \text{ m} \quad (11.14)$$

$$d_r + d_i = 0.22776 \text{ m} \quad (11.15)$$

$$d_i = 0.12427 \text{ m} \quad (11.16)$$

with T_2 given by

$$T_2 = 30 + q \frac{d_m}{k_m} = 30.8^\circ \text{C} \quad (11.17)$$

The overall resistance is given by the sum of the three individual resistances:

$$\underbrace{\frac{1}{U}} = \underbrace{\frac{d_r}{k_r}} + \underbrace{\frac{d_i}{k_i}} + \underbrace{\frac{d_m}{k_m}} \quad (11.18)$$

0.09462	0.03275	0.06178	0.00009163
100%	34.6%	65.3%	0.1%

Note that the metal wall offers no significant resistance and could have been ignored in the calculations.

If the layers in Figure 11.1 are cylindrical, which would be the case for an insulated pipe, for example, the thickness could be represented by the difference between the radial dimensions of each layer.

$$d_n = r_n - r_{n-1} \quad (11.19)$$

where r_0 is the beginning of the first layer and the dimension of the cylindrical core of the multilayer arrangement. Conduction through the layers is then governed by the equation for cylindrical coordinates in Table 10.1 and the same boundary conditions. The reader may show that in this case

$$Q = U_0(T_0 - T_N)(2\pi r_0 L) \quad (11.20)$$

$$\frac{1}{r_0 U_0} = \sum_{i=1}^N \frac{1}{\lambda_i} \ln \left[\frac{r_i}{r_{i-1}} \right] \quad (11.21)$$

Note that the area increases with the radius so that energy conservation requires the product of the energy flux and the radius, or the rate of energy flow, to be constant through the layers.

11.2 THERMAL EFFECTS IN POROUS CATALYSTS

Diffusion in porous solids, and specifically, porous catalysts, is discussed in Chapter 10. The point is made that the mass

transfer process is limited to the void space, since the diffusivity in solids is orders of magnitude less than diffusivities in liquids and gases (see Chapter 8). In all three cases, matter in the form of molecules for the most part must move through a material medium. Thermal energy on the other hand is transferred through solids by the movement of free electrons and vibrational waves through the lattice structure, a much faster process than the diffusion of matter. Consequently, both the fluid in the pores and the material in the solid matrix will contribute the average thermal conductivity of the medium. An approximate effective thermal conductivity of the medium is given by Smith (1981):

$$\lambda_{eff} = \lambda_{solid} \left(\frac{\lambda_{fluid}}{\lambda_{solid}} \right)^{1-\varepsilon} \quad (11.22)$$

With an estimate of the value of the effective thermal conductivity of the porous medium, we can calculate the maximum possible temperature rise due to a single reaction and with this value make a decision concerning the need to incorporate nonisothermal effects in our analysis.

11.2.1 Temperature Rise due to Single Chemical Reaction

The effective thermal conductivity can be used in a pseudohomogeneous model of the porous catalyst in the same manner that the effective diffusivity was used in Section 10.3 for the isothermal model of diffusion in the particle. We will use the semi-infinite slab model that was shown in Figure 10.21, but the results can be used for any shape. The thermal energy balance for a rectangular system is taken from Table 11.1

$$\underbrace{\rho c_P v_z \frac{\partial T}{\partial z}}_{v_z=0} = \lambda_{eff} \left(\underbrace{\frac{\partial^2 T}{\partial x^2} + \frac{\partial T}{\partial y^2} + \frac{\partial^2 T}{\partial z^2}}_{\substack{=0 \\ \text{only gradients} \\ \text{in } z \text{ direction}}} \right) + \underbrace{\sum_j (-\Delta H_{Rj}) \mathcal{R}_{jv}}_{\text{single reaction}} \quad (11.23)$$

or

$$\lambda_e \frac{d^2 T}{dz^2} + (-\Delta H_R) \rho_p S_g \mathcal{R}_s = 0 \quad (11.24)$$

Similar considerations with the microscopic mass balance in Table 10.1 gives [refer to Equation (10.78) for the same result for a single pore]

$$D_{ie} \frac{d^2 c_i}{dz^2} + \vartheta_i \rho_p S_g \mathcal{R}_s = 0 \quad (11.25)$$

The boundary conditions associated with Equations (11.24) and (11.25) are

$$T = T_s \quad z = L \quad (11.26)$$

$$c_i = c_{is} \quad z = L \quad (11.27)$$

$$\frac{dT}{dz} = \frac{dc_i}{dz} = 0 \quad z = 0 \quad (11.28)$$

The reaction term is present in each microscopic balance so that the temperature and all of the concentrations may be related to the concentration of a single key reactant (A):

$$\frac{\lambda_e}{(\Delta H_R)} \frac{d^2 T}{dz^2} = \frac{D_{Ae}}{(-\vartheta_A)} \frac{d^2 c_A}{dz^2} = \rho_p S_g \mathcal{R}_s \quad (11.29)$$

$$T - T_s = \frac{D_{Ae}(-\Delta H_R)}{\lambda_e(-\vartheta_A)} (c_{As} - c_A) \quad (11.30)$$

$$c_i = c_{is} + \frac{D_{Ae}\vartheta_i}{D_{ie}(-\vartheta_A)} (c_{As} - c_A) \quad (11.31)$$

The effective thermal conductivity and diffusivity as well as the enthalpy change for the reaction have been assumed constant.

The maximum temperature in the catalyst is therefore related to the minimum value of the key reactant concentration. For irreversible reactions, the key reactant can be completely reacted thereby providing a minimum concentration of zero. It is possible that the reaction reaches equilibrium in advance of the depletion of the key reactant. To include this possibility, the reaction rate expression

$$\mathcal{R}_s(c_1, c_2, \dots, c_N, T, P)$$

may be used to determine the limiting value of the concentration of A after substituting the relationship of the

concentrations and temperature to the concentration of the key reactant from Equations (11.30) and (11.31):

$$\mathcal{R}_s(c_A) = 0. \quad c_A = c_{Ae} \quad (11.32)$$

The maximum temperature rise in the porous catalyst can then be stated in more accurate terms as

$$\frac{(\Delta T)_{\max}}{T_s} = \frac{D_{Ae}(-\Delta H_R)c_{As}}{\lambda_e(-\vartheta_A)T_s} \left[\frac{c_{As} - c_{Ae}}{c_{As}} \right] \leq \frac{D_{Ae}(-\Delta H_R)c_{As}}{\lambda_e(-\vartheta_A)T_s} \quad (11.33)$$

See Table 11.2 for some typical values of the maximum temperature rise.

The values of the maximum temperature rise in the table are relatively small in most cases but may be large enough in others to be considered in kinetic studies and design calculations.

When thermal effects are important, the catalyst effectiveness may be calculated as if there were a single reactant under isothermal conditions with the consolidated rate expression: $\mathcal{R}_s^*(c_A)$. An example follows in the next section.

11.2.2 Effectiveness Factor for Single Irreversible Reaction with Heat Effect

The catalyst effectiveness factor was discussed in Section 10.3.2 as the reaction rate in a catalyst pellet relative to the rate that would persist if the surface conditions existed throughout the pellet. The concentration of the key reactant decreases with distance into the pellet, which has a deleterious effect on the reaction rate and therefore on the catalyst effectiveness factor as discussed in Chapter 10. The effect of temperature in the case of endothermic reactions is to reinforce this behavior. For exothermic reactions, on the other hand, the temperature is higher inside than on the exterior surface. Under conditions where this effect on the rate exceeds the concentration effect, the

TABLE 11.2 Values of Maximum Relative Temperature Rise in Pellet

Reaction	$\frac{(\Delta T)_{\max}}{T_s} = \frac{D_{Ae}(-\Delta H_R)c_{As}}{\lambda_e(-\vartheta_A)T_s}$
Synthesis of higher alcohols from CO and H ₂	0.00085
Oxidation of CH ₃ OH to CH ₂ O	0.0109
Synthesis of vinyl chloride from acetylene and HCl	0.25
Hydrogenation of ethylene	0.066
Oxidation of H ₂	0.10
Oxidation of ethylene to ethylene oxide	0.13
Dissociation of N ₂ O	0.64
Hydrogenation of benzene	0.12
Oxidation of SO ₂	0.012

Source: Adapted from Froment and Bischoff (1979).

catalyst effectiveness factor will increase. Example calculations follow below.

Equations (11.30) and (11.31) show that the temperature as well as all concentrations in the pellet may be expressed in terms of the concentration of a single key reactant (A). The concentration and temperature distributions can then be obtained from the mass balance of the key reactant, again using the semi-infinite slab model shown in Figure 10.21. Equation (11.25) becomes

$$D_{Ae} \frac{d^2 c_A}{dz^2} + \vartheta_A \rho_p S_g \mathcal{R}_s(c_A) = 0 \quad (11.34)$$

where

$$\mathcal{R}_s(c_A) = k_0 e^{\frac{E/R}{T_s + \frac{D_{Ae}(-\Delta H_R)}{\lambda_e(-\vartheta_A)}(c_{As} - c_A)}} c_A \quad (11.35)$$

for a single irreversible reaction with Arrhenius kinetics. The exponential factor in the reaction rate is often approximated under the supposition that the value of

$$\frac{T - T_s}{T_s}$$

is small. In this case,

$$\begin{aligned} e^{-E/RT} &= e^{-(E/(RT_s(1+(T-T_s)/(T_s))))} \approx e^{-(E/RT_s)(1-((T-T_s)/T_s))} \\ &= e^{-(E/RT_s)} e^{E((T-T_s)/RT_s^2)} = e^{-(E/RT_s)} e^{\delta(1-(c_A/c_{As}))} \end{aligned} \quad (11.36)$$

where

$$\delta = \frac{ED_{Ae}(-\Delta H_R)c_{As}}{\lambda_e(-\vartheta_A)RT_s^2} \begin{cases} > 0 & \text{Exothermic} \\ = 0 & \text{Isothermal} \\ < 0 & \text{Endothermic} \end{cases} \quad (11.37)$$

The reaction rate expression in Equation (11.35) becomes with this approximation

$$\mathcal{R}_s(c_A) = k(T_s) e^{\delta(1-(c_A/c_{As}))} c_A \quad (11.38)$$

Finally, it is convenient to transfer the origin to the surface since at high reaction rates relative to the diffusion rate, the reaction is completed in a narrow region near the exterior surface and the behavior for all shapes is that of a semi-infinite medium. The translation is affected with

$$\xi = \frac{L - z}{L}$$

With these alterations, the dimensionless form of Equations 11.35 and 11.36 become

$$\frac{d^2 \Gamma_A}{d\xi^2} + \Lambda^2 e^{\delta(1-\Gamma_A)} \Gamma_A = 0 \quad (11.39)$$

$$\Gamma_A = 1 \quad \xi = 0 \quad (11.40)$$

$$\frac{d\psi_A}{d\xi} = 0 \quad \xi = 1 \quad (11.41)$$

The dimensionless concentration and the Thiele parameter are defined in Equations (10.97) and (20.98). The effectiveness factor, is given by

$$\mathcal{E} = \frac{1}{\Lambda^2} \frac{d\Gamma_A}{d\xi} \Big|_{\xi=0} = \mathcal{E}(\delta; \Lambda) \quad (11.42)$$

The solution must be obtained numerically and is shown in Figure 11.3.

As noted above, the effectiveness factor is considerably greater than one in some regions, since the internal temperature is greater than the surface temperature for exothermic reactions. Also, the possibility of multiple steady states is evident from the inset. The curve for $\delta = 9.8$ contains a region of values for the Thiele parameter where there are three possibilities for the effectiveness. The question of stability always accompanies the multiplicity of available steady states. In the present case, two of the three states are stable, as indicated in the inset. This behavior is similar to what is observed for the CSTR in Section 6.6.1.2. In fact, the catalyst pellet is the distributed version in the CSTR. The conditions required for multiple steady states in the catalytic pellet are unlikely to be encountered in practice (Froment and Bischoff, 1979).

Each of the curves is seen to approach a linear asymptote at high reaction rates. The asymptotes may be found by noting that at high values of the Thiele parameter, the boundary at the center may be replaced with

$$\frac{d\Gamma_A}{d\xi} = 0 \quad \Gamma_A = 0 \quad \text{as } \xi \rightarrow \infty \quad (11.43)$$

Setting

$$p = \frac{d\Gamma_A}{d\xi} \Rightarrow p \frac{dp}{d\Gamma_A} = \frac{d^2 \Gamma_A}{d\xi^2} \quad (11.44)$$

Equation (11.29) may be integrated as

$$\frac{1}{2} p(\infty)^2 - \frac{1}{2} p(0)^2 = \int_1^0 e^{\delta(1-\Gamma_A)} \Gamma_A d\Gamma_A \quad (11.45)$$

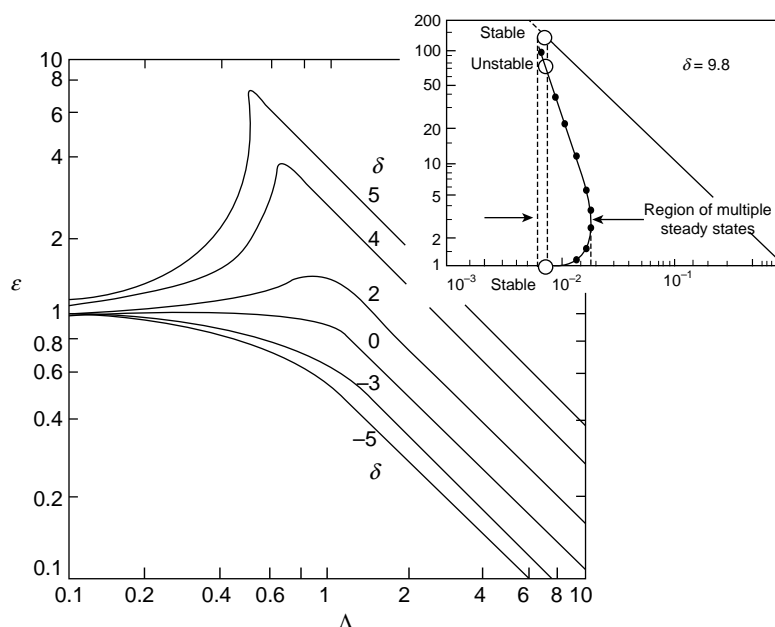


FIGURE 11.3 Effectiveness factor for nonisothermal irreversible reaction in a flat slab (adapted from Petersen, 1965). Inset (adapted from Drott and Aris, 1969). Reprinted with permission of Elsevier.

where

$$\mathcal{E} = -\frac{p(0)}{\Lambda^2} = \frac{\frac{\sqrt{2}e^{\frac{\delta}{2}}}{|\delta|} \sqrt{1 - e^{-\delta}(1 + \delta)}}{\Lambda}, \quad \delta \neq 0 \quad (11.46)$$

11.3 HEAT TRANSFER TO FALLING FILM—SHORT CONTACT TIMES

The wetted wall tower was introduced in Chapter 10 as a mass transfer device. As is mentioned there, the mass transfer process may be nonisothermal. The heat effect may take place to the extent that the solubility of the solute is seriously compromised and/or significant evaporation of the solvent results. Both conditions erode the efficiency of the mass transfer operation. In these cases, such as in the HCl–water system, the liquid film is cooled by heat exchange through the wall with a heat exchange fluid. The heat transfer process is considered in this section.

We will ignore the interfacial mass transfer processes that would inevitably be taking place and assume that a nonvolatile liquid enters the top of the tower at temperature T_0 and encounters a wall at a higher temperature T_s . With these stipulations attention is focused on the heat transfer process, which is illustrated in Figure 11.4.

The illustration is for short contact times where only the thin layer of fluid next to the wall undergoes a significant change in temperature. In just the same way that we considered only the region at the interface for the mass transfer

process in Chapter 10, we can consider the thin region at the, Drott and Aris, 1969 wall for this heat transfer process.

The velocity field in this region may be approximated by a Taylor series expansion from the value at the wall. If we therefore say that the velocity in the z direction is a function of the distance y from the wall, the functional dependence on y may be determined as follows.

The velocity distribution determined earlier in Equation (9.64) is given by

$$v_z(y) = \frac{\rho g R^2}{4\eta} \left[1 - \frac{(R - y)^2}{R^2} + 2f^2 \ln \frac{(R - y)}{R} \right] \quad (11.47)$$

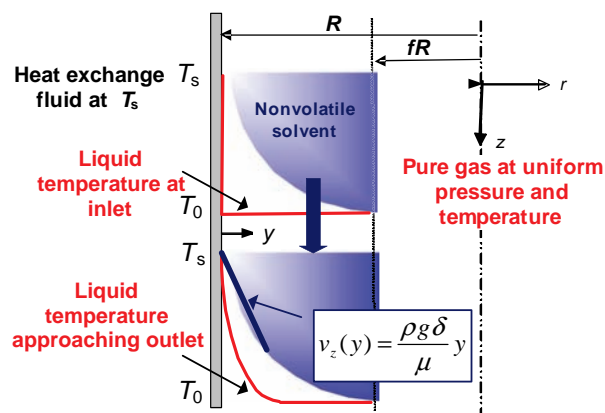


FIGURE 11.4 Heat transfer to a falling film.

in terms of the distance from the wall, $y = R - r$. This assumes that the density and viscosity are not significantly affected by the increase in temperature and therefore that the momentum transfer process may be considered separately.

A Taylor series approximation for the velocity,

$$v_z(y) \approx v_z(0) + v_z'(0)(y - 0) \quad (11.48)$$

can be used for distances not too far from the wall. The result is

$$v_z(y) \approx \frac{\rho g R^2}{4\eta} \left[\frac{(1-f)^2}{R} \right] y \approx \frac{\rho g R^2}{4\eta} \left[\frac{2(1-f)R}{R^2} \right] y = \frac{\rho g \delta}{\eta} y \quad (11.49)$$

Substitution of Equation (9.72) for the film thickness, $(1-f)R$ gives:

$$v_z(y) = \left[\frac{3\rho^2 g^2 Q}{\pi \eta^2 D} \right]^{1/3} y \quad (11.50)$$

We will use this result for the velocity field near the tube wall.

We have a two-dimensional process for energy transfer: conduction in the y direction and convection in the z direction. Keeping only these terms in the entry for the energy balance for rectangular coordinates in Table 11.1,

$$\underbrace{\rho c_P v_z \frac{\partial T}{\partial z}}_{\substack{\neq 0 \\ \text{Convection down} \\ \text{column}}} = \underbrace{\lambda \left(\frac{\partial^2 T}{\partial x^2} + \frac{\partial T}{\partial y^2} + \frac{\partial^2 T}{\partial z^2} \right)}_{= \frac{\partial T}{\partial y^2} \text{ Conduction only in } y \text{ direction}} + \underbrace{\sum_j (-\Delta H_{Rj}) \mathcal{R}_s}_{=0 \text{ No reactions}} \quad (11.51)$$

for an unreactive system, results in

$$\rho c_P v_z \frac{\partial T}{\partial z} = \lambda \frac{\partial T}{\partial y^2} \quad (11.52)$$

Substituting for the velocity distribution and expressing the boundary condition for the shallow penetration of the thermal effect gives

$$y \frac{\partial T}{\partial z} = \beta \frac{\partial T}{\partial y^2}, \quad \beta = \frac{\lambda}{\rho c_P} \left[\frac{\pi \mu^2 D}{3\rho^2 g^2 Q} \right]^{1/3} \quad (11.53)$$

$$T = T_s \quad \text{at} \quad y = 0 \quad \forall z \quad (11.54)$$

$$T = T_0 \quad \text{as} \quad y \rightarrow \infty \quad \forall z \quad (11.55)$$

$$T = T_0 \quad \text{at} \quad z = 0 \quad \forall y \quad (11.56)$$

This problem may be expressed in terms of a single variable:

$$\zeta = \frac{y}{(3\beta z)^{1/3}} \quad (11.57)$$

The differential equation and boundary conditions are given in terms of the combined variable as

$$\frac{d^2 T}{d\zeta^2} + \zeta^2 \frac{dT}{d\zeta} = 0 \quad (11.58)$$

$$T = T_s \quad \zeta = 0 \quad (11.59)$$

$$T = T_0 \quad \zeta \rightarrow \infty \quad (11.60)$$

The solution is given by

$$\frac{T - T_0}{T_s - T_0} = \frac{\int_0^\infty e^{-x^3/3} dx}{\int_0^\infty e^{-x^3/3} dx} \quad (11.61)$$

Of particular interest is the energy flux into the falling film, which can be used with the mass transfer analysis in Section 10.5 to size the column. The local flux of energy into the falling film can be evaluated as

$$q_o = -\lambda \frac{\partial T}{\partial y} \Big|_{y=0} = -\lambda \frac{d}{d\zeta} \left[\frac{\int_0^\infty e^{-x^3/3} dx}{\int_0^\infty e^{-x^3/3} dx} (T_s - T_0) \right] \frac{\partial \zeta}{\partial y} \Big|_{y=0} \quad (11.62)$$

$$= \lambda \frac{e^{-\eta^3/3}}{\left[\int_0^\infty e^{-x^3/3} dx \right]} \Big|_{y=0} \frac{1}{(3\beta z)^{1/3}} (T_s - T_0) = h(T_s - T_0) \quad \text{where} \quad (11.63)$$

$$h = \frac{\lambda}{(3\beta z)^{1/3}} \frac{1}{\left[\int_0^\infty e^{-x^3/3} dx \right]} \quad (11.64)$$

The parameter h is a local heat transfer coefficient that gathers together the contributions of convection and conduction of thermal energy and expresses the flux in terms of the overall driving force or temperature difference. Its value relative to conduction over a distance equal to the column diameter under the same temperature difference is the Nusselt number for this case:

$$Nu = \frac{hD}{k} = \frac{1}{3^{1/3} \left[\int_0^\infty e^{-x^3/3} dx \right]} \frac{1}{\left(\frac{z}{D} \right)^{1/3}} \frac{1}{\left(\frac{\beta}{D^2} \right)^{1/3}} \quad (11.65)$$

The Froude and Reynolds numbers introduced in Chapter 8 (see Table 8.14) may be uncovered here to give

$$\frac{\beta}{D^2} = \left[\frac{N_{Fr}^2}{3N_{Pr}^3 N_{Re}^5} \right]^{1/3}, \quad \text{where} \quad V = \frac{Q}{\pi D^2} \quad (11.66)$$

$$N_{Nu} = \frac{1}{3^{2/9} \left[\int_0^\infty e^{-x^3/3} dx \right]} \frac{N_{Fr}^{-2/9} N_{Pr}^{1/3} N_{Re}^{5/9}}{(z/D)^{1/3}} \quad (11.67)$$

$$N_{Nu} = 1.644 \frac{N_{Fr}^{-2/9} N_{Pr}^{1/3} N_{Re}^{5/9}}{(z/D)^{1/3}} \quad (11.68)$$

The Prandtl number ($N_{Pr} = c_p \eta / \lambda$) is a measure of the rate of molecular conduction of momentum to molecular conduction of thermal energy.

11.4 MOVING BOUNDARY PROBLEM

Moving boundary problems are encountered in a variety of industries. In the steel industry (reference), for example, the progressive dimension of the solid skin formed in steel ingots, while cooling on the tracks between steelmaking and the blooming mills, determines the reheating program for the ingots in the soaking pits prior to rolling in the blooming mill. Energy storage as the latent heat of fusion involves a similar moving boundary. In the food industry, the freezing and thawing of foodstuffs are important considerations. In the chemical industry, the regeneration of coked catalysts with oxygen-containing gases is accompanied by a moving boundary between the fouled catalyst and the restored region (Froment and Bischoff, 1979). In the absorption of ammonia by water, the effect of the temperature rise (17°C) is nearly completely offset by the volume change in the liquid (Chiang and Toor, 1964; Verma and DeLancey, 1975).

In this section, we will consider a simple example of a freezing process that will not meet all of the demands of the

applications mentioned above but will reflect some of the major components of the more general cases.

In Figure 11.5, a liquid is being frozen by removal of heat from one of the faces held at a temperature T_0 , which is less than the freezing temperature, T_M .

The dimensions of the liquid are very large except in the dimension of the freezing process (x). There is no substantial energy transfer in the large dimensions (e.g., y).

We assume that the liquid is initially at the freezing point when the surface is suddenly lowered to T_0 . The liquid at the surface freezes as well as each subsequent layer as time advances. The boundary between liquid and solid thereafter moves into the system, while the energy released in the formation of fresh solid is conducted through the solid region to the surface at T_0 the temperature of the unfrozen liquid is presumed to be constant.

If we locate ourselves on the moving surface along with the origin of the coordinate system and look into the unfrozen phase, it will be evident that unfrozen liquid is flowing toward us and similarly frozen solid is flowing away. The velocity in both phases is the volume average velocity, which is the same as the mass average velocity since the densities are assumed to be constant. The continuity equation applied to the solid phase implies that the velocity cannot depend on the distance coordinate and therefore can at most be a function of time.

$$\underbrace{\frac{\partial \rho}{\partial t}}_{=0} + \underbrace{\frac{\partial \rho v_x}{\partial x}}_{=0} + \underbrace{\frac{\partial \rho v_y}{\partial y}}_{=0} + \underbrace{\frac{\partial \rho v_z}{\partial z}}_{\rho=\text{const}} = 0$$

$\rho = \text{const}$ $\rho = \text{const}$ $\rho = \text{const}$ $\rho = \text{const}$
 No change No change No change No change
 in x direction in y direction

$$\Rightarrow \frac{\partial v_z}{\partial z} = 0 \Rightarrow v_z = v_z(t) \quad (11.69)$$

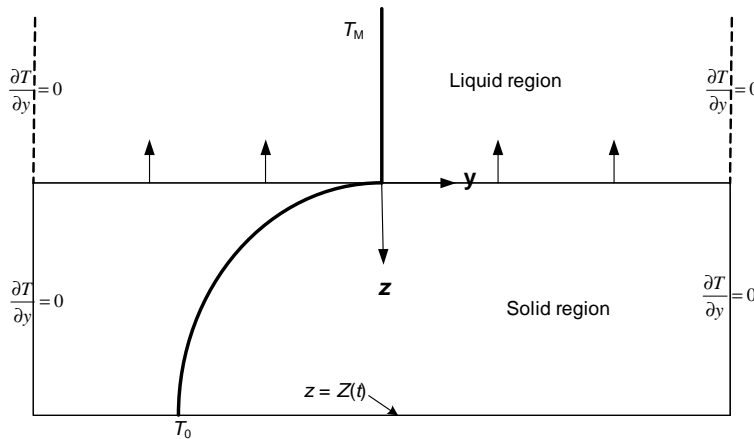


FIGURE 11.5 Freezing of a semi-infinite liquid: moving boundary.

The microscopic thermal energy balance in Table 11.1 written for the z direction and including the unsteady state accumulation term is then given by

$$\frac{\partial T}{\partial t} + v_z(t) \frac{\partial T}{\partial z} = \alpha_D \frac{\partial^2 T}{\partial z^2} \quad (11.70)$$

where α_D is the thermal diffusivity.

Returning now to the moving boundary, the continuity of mass across the boundary requires that

$$\rho_L v_{Lz} = \rho_s v_{sz} \quad \text{at } z = 0 \quad (11.71)$$

Conservation of energy requires that

$$\rho_L v_{Lz} h_L = \rho_s v_{sz} h_s - \lambda_s \frac{\partial T}{\partial z} \quad \text{at } z = 0 \quad (11.72)$$

The combination of the preceding two conditions is

$$-\lambda_s \frac{\partial T}{\partial z} = \rho_s v_{sz} \Delta H_f \quad \text{at } z = 0 \quad (11.73)$$

where the thermal energy released at freezing is denoted by ΔH_f . Conduction of thermal energy through the solid region is therefore described by the differential equation given in Equation (11.70) with boundary and initial conditions given by Equations (11.73)–(11.76).

$$\begin{aligned} T(z, 0) &= T_M \\ T(0, t) &= T_M \end{aligned} \quad (11.74)$$

$$T(Z(t), t) = T_0 < T_M \quad (11.75)$$

The solution may be obtained by the method of combination of variable used in the falling film problem discussed in the previous section:

$$\zeta = \frac{z}{\sqrt{t}} \quad (11.76)$$

Substitution into Equation (11.70) gives a differential equation in a single variable,

$$\alpha_D \frac{d^2 T}{d\zeta^2} + \frac{1}{2}(\zeta - 2\lambda) \frac{dT}{d\zeta} = 0 \quad (11.77)$$

only if a value for λ can be found for

$$v_z(t) = \frac{\lambda}{\sqrt{t}} \quad (11.78)$$

Integration of Equation (11.78) using the boundary condition in Equation (11.73) gives

$$\frac{dT}{d\zeta} = \frac{\rho_s(-\Delta H_f)}{\lambda_s} \lambda e^{\frac{\lambda^2}{\alpha_D}} e^{-\frac{1}{4\alpha_D}(\zeta-2\lambda)^2} \quad (11.79)$$

Integration of the velocity provides the location of the solid boundary

$$Z(t) = 2\lambda\sqrt{t} \quad \text{or} \quad \zeta = 2\lambda \quad (11.80)$$

Integration of Equation (11.80) over the solid region provides the required value of λ as the solution to

$$F(\lambda) = \lambda e^{\frac{\lambda^2}{\alpha_D}} \int_0^{2\lambda} e^{-\frac{1}{4\alpha_D}(\zeta-2\lambda)^2} d\zeta - \frac{\lambda_s(T_M - T_0)}{\rho\Delta H_f} = 0 \quad (11.81)$$

Example 11.4-1: Onset of Freezing in a Pipe

Suppose that water has been left standing in a 1 in. diameter pipe and has equilibrated with the surroundings at a temperature slightly above freezing. If the surrounding temperature were to drop below freezing, say 1°C , estimate the time for a ring of ice to form with thickness equal to 5% of the pipe diameter.

Solution:

$$f(\lambda) = \lambda \exp\left(\frac{\lambda^2}{\alpha_D}\right) \int_0^{2\lambda} \exp\left(-\frac{1}{4\alpha_D}(\eta - 2\lambda)^2\right) d\eta$$

$$\lambda_s = 0.0214 \text{ J/(s m K)} \quad (\text{Sleeh, 1980})$$

$$\Delta H_f = 6002 \text{ J/mol} \quad (\text{DIPPR, 2009})$$

$$\rho_s = 50.8 \text{ kmol/m}^3 = 50800 \text{ mol/m}^3 \quad (\text{DIPPR, 2009})$$

$$\begin{aligned} c_P &= 20.11 \text{ Btu/lb mol } ^\circ\text{F} = \frac{20.11}{454} \frac{1}{9.486 \times 10^{-4}} \\ &= 46.695 \text{ J/mol} \quad (\text{DIPPR, 2009}) \end{aligned}$$

$$T_M - T_0 = 0 - (-1) = 1\text{K}$$

$$A = \frac{0.0214(1)}{50800(6002)} = 7.0187 \times 10^{-11} \text{ m}^2/\text{s}$$

$$= 7.0187 \times 10^{-5} \text{ mm}^2/\text{s}$$

$$\alpha_D = \frac{0.0214}{50800 \times 46.695} = 9.0215 \times 10^{-9} \text{ m}^2/\text{s}$$

$$= 9.0215 \times 10^{-3} \text{ mm}^2/\text{s}$$

$$A = 7.0187 \times 10^{-5} \text{ mm}^2/\text{s}$$

$$\alpha_D = 0.0090215 \text{ mm}^2/\text{s}$$

$$f(0.005) = 5.0092 \times 10^{-5}$$

$$f(0.006) = 7.2192 \times 10^{-5}$$

Solution is: $[\xi = 5.9163 \times 10^{-3}]$

$$t = \left(\frac{0.05 \times \frac{25.4}{2}}{2 \times 0.0059163} \right)^2 \frac{1}{60} = 47.999 \text{ min}$$

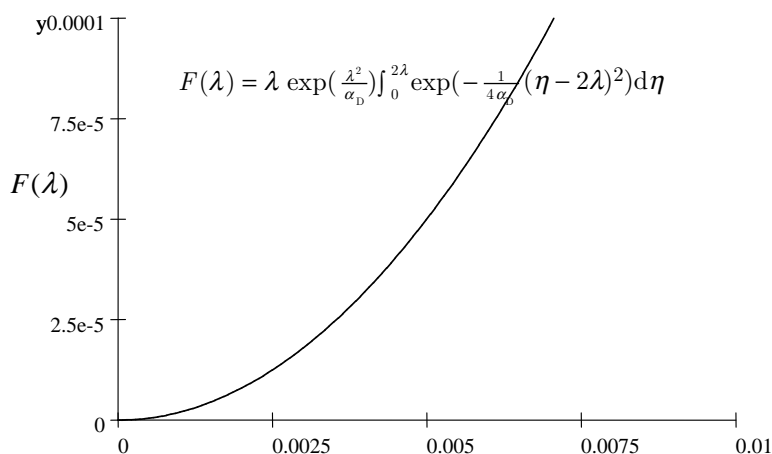


FIGURE 11.6 Variation of velocity parameter with temperature difference.

See Figure 11.6.

PROBLEMS

11.1. A cylindrical vessel, vented to the atmosphere, is used to store a liquefied gas. The vessel is metal, covered on the outside with a layer of insulation. The inner and outer radii of the insulation are r_i and r_o , respectively. The length of the tank is L . The normal boiling point of the liquefied gas is T_b and the ambient temperature is T_a .

The vessel is outside and is subjected to a transverse wind velocity of v_∞ . The thermal conductivity of the metal is very large and the thermal conductivity of the insulation, λ , is independent of temperature.

Determine an expression for the

- surface temperature of the tank and
- rate of heat input to the tank, Q .
- Describe how you would obtain a value for the outside heat transfer coefficient.
As more insulation is added (r_i increases), the resistance to heat transfer increases, which tends to diminish Q . On the other hand, the heat transfer area increases, which tends to increase Q .
- Show that this competition leads to an optimum value of the insulation thickness and comment on its practical significance by employing typical values of the parameters involved.

ISOTHERMAL MASS TRANSFER UNDER TURBULENT CONDITIONS

As the interfacial mass transfer rate is proportional to the interfacial area, the creation of a large interfacial area is of paramount importance in operations involving mass transfer. In fluid–fluid systems, a large interfacial area is often achieved by intense mixing, which naturally entails the creation of a highly turbulent and thereby highly complicated flow field. In solid–fluid systems, the surface area of the solid is made as large as possible and intimate contact of the solid with the fluid phase(s) again involves intense mixing of the two phases either by external means or indirectly by forced flow through a convoluted interstitial area presented by the matrix of solid particles. In both fluid–fluid and fluid–solid systems, intense mixing is also important from the viewpoint of the intraphase concentration gradients near the interface, which is the second important factor in the interfacial mass transfer rate. Consequently, the analysis of mass transfer operations involves the consideration of complicated fluid hydrodynamics.

12.1 INTRAPHASE MASS TRANSFER COEFFICIENTS

The computational effort involved in the simultaneous solution of the momentum and mass balance equations, and often the energy balance in such situations, is, for the most part, unrealistic. However, in the case of a turbulent fluid flowing around submerged objects, there must be a laminar region where the fluid velocity changes from zero to the value in the bulk liquid. The bulk liquid velocity is

considered to be a potential flow field (no viscosity, constant density, and irrotational) (see Figure 12.1). The solution for the flow field provides the limiting value for the solution of the boundary layer equations obtained by eliminating unimportant terms in the transport equations.

An alternate approach and the one that we will adopt here is to effectively relegate the hydrodynamics to experimental determination with efficient correlation of the results followed by superposition of the mass and energy transfer processes by the analyst. The isolation of the hydrodynamic processes is accomplished in the following manner.

12.1.1 Film-Penetration Theory

The film-penetration theory developed by Toor and Marchello (1958) is a unification of two theories: the film theory originally proposed by Whitman (1923) and the penetration theory originally proposed by Higbie (1935) and modified later by Danckwerts (1951).

The film-penetration theory views the interfacial region between two turbulent fluids as consisting of two regions, one in each phase, within which all concentration gradients are localized by the mixing process. The phenomena that take place in each of these regions are identical so that we can focus on one. The situation is depicted in Figure 12.2.

Assume for the time being that the fluid is a binary mixture of *A* and *B* and that species *A* alone is being transferred across the interface from a pure gas phase. The depth *L* is presumed to be the result of the turbulent mixing process alone and therefore to be independent of any

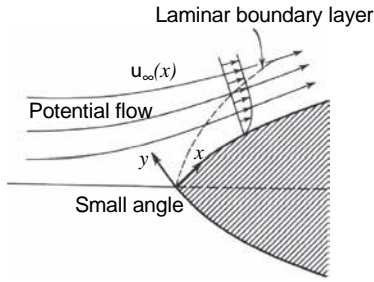


FIGURE 12.1 Two-dimensional flow around a submerged object. (Adapted from Bird, et al., 2002).

other physical or chemical process, which may be taking place in the fluid. The bulk region of the fluid, the region beyond L , is considered to be homogenous in all respects. The molar concentration of species A in the bulk region is c_{Ab} . The interface is in equilibrium with the gas phase and therefore remains at the concentration, c_{Ai} .

Material is transferred between the bulk region and the film region by an eddy transfer process that is sufficiently effective to maintain the concentration at the film boundary at the bulk value. Furthermore, the fluid elements transferred to the film region by this process are uniform in concentration at the bulk value. A fluid element once transferred to the film region undergoes continual bombardment by eddies in the bulk region, while it is stabilized to some extent by surface tension. This bombardment process eventually provides an extra large kick, which results in the complete replacement of a surface element of fluid with an element of fluid from the bulk region, and the process is repeated.

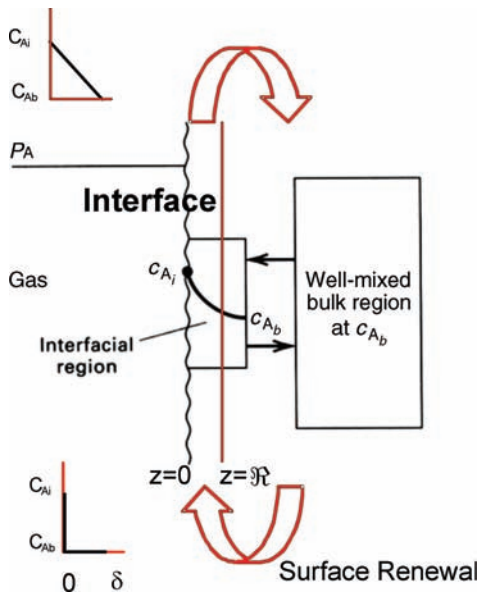


FIGURE 12.2 Intraphase mass transfer—film-penetration theory.

The time scale of the replacement process is assumed to be very much smaller than the time scale of the processes that affect the bulk fluid conditions. Consequently, during the lifetime of an element in the film region, the concentrations at its boundaries do not change. The interphase mass transfer process takes place under these conditions, while the fluid element resides in the film region.

The situation in the fluid phase at a fluid–solid interface is considered to be essentially the same as that described above for the fluid–fluid interface. The fluid adjacent to the solid is considered to be a laminar film of thickness L , which is completely replaced at various intervals by the bulk fluid by disturbances from the surrounding fluid. The mixing intervals are assumed to be sufficiently frequent that the bulk concentration in the fluid does not change appreciably in the distance between two successive mixings. The implied velocity gradient in this situation is not explicitly considered by the film-penetration theory. The concentration at the fluid–solid interface is also assumed to be constant during the lifetime of an element in the film region. This concentration need not be an equilibrium value but may be determined by continuity requirements as would be the case for a porous catalyst.

In both the fluid–fluid and fluid–solid cases, the interphase mass transfer process for each fluid element is described for low mass rates by the unsteady-state microscopic mass balance without reaction. The mass flux is due to diffusion alone. Assuming constant density in the film region,

$$\mathbf{j}_A = -D_A^V M_A \frac{\partial c_A}{\partial z} \delta_z \quad (12.1)$$

We will carry the designation of the volume average reference frame because of the assumption of constant density. The mass balance and boundary conditions may be obtained from Tables 8.12 and 10.1. The components of the model are nonturbulent.

$$\frac{\partial c_A}{\partial t} = D_A^V \frac{\partial^2 c_A}{\partial z^2} \quad (12.2)$$

$$c_A = c_{Ab} \quad t = 0, 0 < z \leq L \quad (12.3)$$

$$c_A = c_{Ai} \quad z = 0, 0 \leq t \quad (12.4)$$

$$c_A = c_{Ab} \quad z = L, 0 \leq t \quad (12.5)$$

The molar flux of A into a surface element whose age is t is given by

$$N_A(0, t) = n_A(0, t) = -D_A^V \frac{\partial c_A}{\partial z} \Big|_{z=0} \quad (12.6)$$

According to the above discussion, the interface is considered to be a mosaic of elements of different ages. The preceding expression denotes the contribution of those elements of age t . If the area fraction of the interface that consists of elements of age between t and $t + dt$ is denoted by $\phi(t)$, the net flux across the interface can be expressed as

$$N_A = \int_0^{\infty} -D_A^V \frac{\partial c_A}{\partial z} \bigg|_{z=0} \phi(t) dt \quad (12.7)$$

The mass transfer coefficient is defined as a conductivity associated with the concentration difference across the film as the driving force:

$$N_A = k_{cA}^o (c_{Ai} - c_{Ab}) \quad (12.8)$$

where

$$k_{cA}^o = \frac{D_A^V}{L} \int_0^{\infty} -\frac{\partial c_A^*}{\partial z^*} \bigg|_{z=0} \phi(t) dt \quad (12.9)$$

The subscript c denotes the concentration driving force. Other concentration measures are used such as the mole fraction y where $ck_{yA} = k_{cA}$. The use of the superscript o serves as a reminder that the value of the mass transfer coefficient refers to the basic conditions associated with the mass transfer model. For example, there is no convective contribution to the mass flux and that there are no chemical reactions in the film.

The dimensionless concentration and distance into the film are defined as

$$c_A^* = \frac{c_A - c_{Ab}}{c_{Ai} - c_{Ab}}, \quad z^* = \frac{z}{L} \quad (12.10)$$

The superscript on the mass transfer coefficient indicates the base condition of only diffusion (no convection) in the film and the subscript indicates the molar concentration as the driving force.

The age distribution function and the depth of the film are the hydrodynamic parameters required to calculate the interfacial mass transfer rate. These two quantities must ultimately be determined experimentally. The film theory and the penetration theory are two limiting cases where only one of the quantities is required.

12.1.2 Penetration Theories

If the lifetime of the fluid elements at the interface is very short, the influence of the boundary with the bulk phase will not be important and the mass transfer process will

essentially be one of diffusion into a semi-infinite medium. This process is described by the Equations (9.1)–(9.6) with the dimension L in Equations (9.2) and (9.3) replaced with ∞ . The solution was obtained earlier for short contact times in wetted wall towers (Section 9.5.1.1) if z/v_{\max} is replaced with t .

$$N_a(0, t) = \sqrt{\frac{D_A^V}{\pi t}} (c_{Ai} - c_{Ab}) \quad (12.11)$$

If the ages according to Higbie (1935) are equally distributed between 0 and t_0 , the interfacial flux becomes

$$N_a(0, t) = 2\sqrt{\frac{D_A^V}{\pi t_0}} (c_{Ai} - c_{Ab}) \quad (12.12)$$

The concentration difference is referred to as the driving force. Its coefficient is referred to as a mass transfer coefficient:

$$k_{cA}^0 = 2\sqrt{\frac{D_A^V}{\pi t_0}} \quad (12.13)$$

The value of the maximum age must be determined experimentally as a function of the hydrodynamic conditions. Having done so for one system, the preceding result implies that the mass transfer coefficient for another under the same hydrodynamic conditions can be determined by scaling with the $1/2$ power of the diffusivity.

Danckwerts (1951) obtained a similar result but by assuming that the chance of a fluid element being replaced with fresh fluid is independent of its age and that the fractional rate of replacement is s . The distribution function in this case is

$$\phi(t) = se^{-st} \quad (12.14)$$

Note that this distribution function, the integral in Equation (12.7) can be evaluated with the Laplace transform of the concentration. The mass transfer coefficient according to this surface renewal theory is given by

$$k_{cA}^0 = \sqrt{D_A^V s} \quad (12.15)$$

The hydrodynamic parameter in this case is s , which must be determined experimentally. Having done so for one system, the mass transfer coefficient may be scaled to another system as in the Higbie model. In both cases, chemical reactions may be superimposed on the hydrodynamics and the mass transfer coefficient corrected accordingly for their presence. This will be discussed below.

The $1/2$ power dependence on the diffusivity is not always found to be the case experimentally. The film theory limit of the film-penetration theory admits a first power dependence, thereby bounding most mass transfer data.

12.1.3 Film Theory

As the age of the element increases, the concentration distribution approaches its steady-state value. This limit is the film theory, which is the steady-state solution to Equations (12.2)–(12.5):

$$N_a(0, \infty) = \frac{D_A^V}{L} (c_{Ai} - c_{Ab}) \quad (12.16)$$

The hydrodynamic parameter in this theory is L , which must be determined by an experimental measurement of the mass transfer coefficient, is

$$k_{cA}^0 = \frac{D_A^V}{L} \quad (12.17)$$

Having done so for one system, the preceding result implies that the mass transfer coefficient for another under the same hydrodynamic conditions can be determined by scaling with the first power of the diffusivity.

The first power is indicative of the film theory and the square root is indicative of the penetration and surface renewal theories. Intermediate values of the dependence may be obtained with the film-penetration theory but with the requirement that two hydrodynamic parameters be measured. The use of the mass transfer theories at the two limits and the experimental correlation of mass transfer data are discussed below.

12.2 INTERPHASE MASS TRANSFER COEFFICIENTS—CONTROLLING RESISTANCES

Consider now the case of a gas–liquid system where a component A is soluble in both phases and in the process of reaching equilibrium is transferring from the gas to the liquid phase. A section of the interface according to the film-penetration theory is shown in Figure 12.3.

The mass flux from the gas phase is governed by a mass transfer coefficient, which is available from a mass transfer correlation founded in the gas-phase conditions and the particular equipment:

$$a_V N_{AG} = k_{yA}^o a_V (y_{Ab} - y_{Ai}) \quad (12.18)$$

Similarly for the liquid phase:

$$a_V N_{AL} = k_{cA}^o a_V (c_{Ai} - c_{Ab}) \quad (12.19)$$

Changes in the bulk-phase concentrations under isothermal conditions are governed by the mass conservation equations written in terms of the bulk-phase concentrations. The interfacial conditions are a necessity for evaluating the

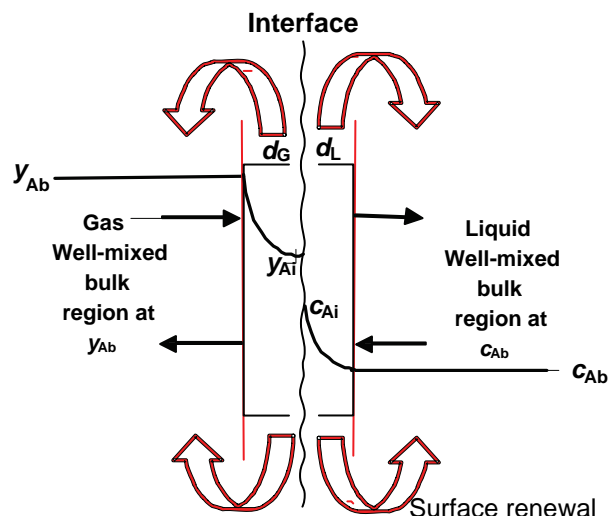


FIGURE 12.3 Interphase mass transfer—film-penetration theory.

mass fluxes, but they are extraneous otherwise. The need to determine the interfacial concentration under reactive conditions is considered in Section 12.5.1.

Since the mass fluxes must be equal across the interface and the two phases are considered to be in local thermodynamic equilibrium, two independent relations are available to eliminate the interfacial concentrations:

$$k_{yA}^o a_V (y_{Ab} - y_{Ai}) = k_{cA}^o a_V (c_{Ai} - c_{Ab}) \quad (12.20)$$

$$y_{Ai} = m c_{Ai} + b \quad (12.21)$$

The linear equilibrium relation can be replaced with any algebraic relationship between the interfacial concentrations, which would require a graphical or numerical solution. An analytical result can be obtained with the linear relationship, which may, of course, be adjusted to meet changing conditions through the equipment by suitably changing the values of m and b .

Elimination of the interfacial liquid concentration gives the mass transfer rate in terms of an overall gas-phase transfer coefficient and bulk-phase gas concentrations:

$$N_A a_V = K_{Gy}^o a_V (y_{Ab} - y_{Ab}^*) \quad (12.22)$$

$$y_{Ab}^* = m c_{Ab} + b \quad (12.23)$$

$$\frac{1}{K_{Gy}^o} = \frac{1}{k_{yA}^o} + \frac{m}{k_{cA}^o} \quad (12.24)$$

The last equation expresses the overall resistance in terms of a gas and a liquid has resistance to use the voltage

(concentration difference)—current (mass flux) analogy. Recall the inverse of a conductance (mass transfer coefficient) is a resistance. Elimination of the interfacial gas-phase concentration gives an equivalent result in liquid terms:

$$N_A a_v = K_{Lc}^o a_v (c_{Ab}^* - c_{Ab}) \quad (12.25)$$

$$c_{Ab}^* = \frac{y_{Ab} - b}{m} \quad (12.26)$$

$$\frac{1}{K_{Lc}^o} = \frac{1}{m k_{yA}^o} + \frac{1}{k_{cA}^o} \quad (12.27)$$

If the value of m is small, a low concentration of A in the gas phase will result in a large concentration in the liquid. In this case, A is very soluble in the liquid phase and the major resistance is in the gas phase:

$$\frac{1}{K_{Gy}^o} \approx \frac{1}{k_{yA}^o} \quad \text{Gas phase controlled} \quad (12.28)$$

If, on the other hand, m is very large, A is not very soluble in the liquid and the major resistance is in the liquid phase:

$$\frac{1}{K_{Lc}^o} \approx \frac{1}{k_{cA}^o} \quad \text{Liquid phase controlled}$$

These limiting cases are illustrated in Figure 12.4.

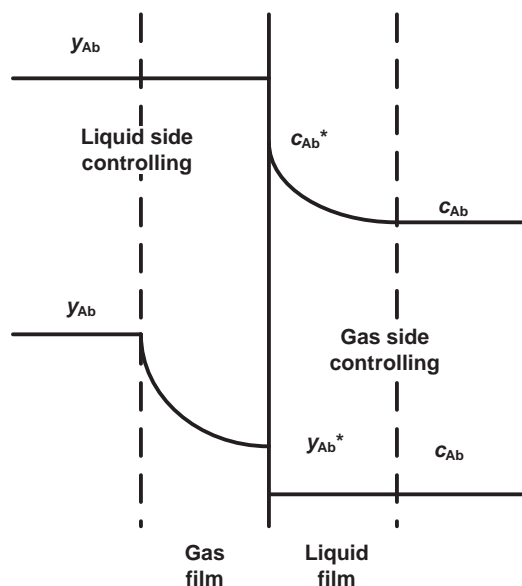


FIGURE 12.4 Controlling resistances.

12.3 MEASUREMENT AND CORRELATION OF MASS TRANSFER COEFFICIENTS

The following is a generalization that is meant to present some basic principles that are considered in all experimental determinations of mass transfer coefficients. The mass transfer coefficient is associated with a particular phase in, for the most part, a two-phase system. One of the phases must be fluid since the turbulent mass transfer process occurs in a fluid phase. The second phase may be fluid or solid. One approach to the measurement of mass transfer coefficient is to restrict the mass transfer process to that fluid phase. The mass transfer coefficient is not measured directly but is the result of calculations that use measurements of concentration and inlet and outlet flows to calculate the mass transfer coefficient. The dependence of the mass transfer coefficient on the system parameters is deduced from the microscopic mass balance for the particular circumstances of the experiment. As we have seen above, the solution to the microscopic mass balance in terms of dimensionless variables exposes the relative effects of the combinations of the physical parameters that affect the system behavior. The mass transfer coefficients can thereby be expressed most efficiently in the terms of these dimensionless variables.

12.3.1 Measurement of Mass Transfer Coefficients

It is important to know the concentration of the solute at the mass transfer interface in order to extract the mass transfer coefficient from an overall rate measurement. To this end, we may construct a mass transfer system from two phases, one of which, and the one in which the mass transfer process takes place, is a fluid phase. The situation is illustrated in Figure 12.5.

This phase we suppose is composed of a material B , which may be soluble in the second phase A , but only to a very small extent. This will limit the mass transfer process to the B phase. The second phase, which may be solid or fluid, is comprised of material A , which is only slightly soluble in phase B . The limited solubility of A is meant to guarantee a low mass transfer rate and thereby exclude convection from consideration. The mass transfer interface is the interface between these two phases and the interfacial concentration is constant over the entire surface at the equilibrium solubility of species A . In some cases, the area is known, such as the mass transfer inside pipes. In other cases, such as fixed beds, it is not.

We assume that there is only one inlet and one outlet. We also assume that the hydrodynamics at the mass transfer surface is the same over the entire surface and that the concentration change is not sufficient to significantly affect the mass transfer coefficient. Finally, we take the z direction to be the direction of net flow of the binary phase through the equipment and define the bulk concentration as the cup

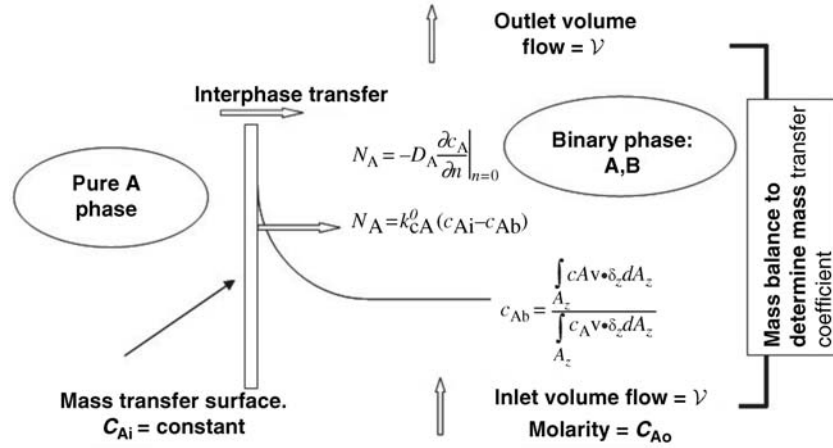


FIGURE 12.5 General scheme of mass transfer coefficient measurements.

average as indicated in the figure. This is the concentration that would be measured if a sample of the flow over the entire cross-section perpendicular to the net flow were collected, mixed, and analyzed. A mass balance over a differential volume element covering a full cross section of flow at constant volumetric flow rate is given by

$$\lim_{x \rightarrow \infty} dc_{Ab} = k_{cA}^o (c_{Ai} - c_{Ab}) \frac{dA_m}{dV} dV \quad (12.29)$$

The mass transfer surface per unit volume of equipment is normally constant. If it is known, the mass balance may be integrated to give

$$V(c_{Af} - c_{Ao}) = k_{cA}^o (c_{Ai} - c_{Ab})_{LM} A_m \quad (12.30)$$

the driving force over the mass transfer surface is defined as

$$(c_{Ai} - c_{Ab})_{LM} = \frac{(c_{Ai} - c_{Ao}) - (c_{Ai} - c_{Af})}{\ln[(c_{Ai} - c_{Ao})/(c_{Ai} - c_{Af})]} \quad (12.31)$$

If the mass transfer surface per unit volume of equipment is not known, it is combined with the mass transfer coefficient and the product evaluated with

$$V(c_{Af} - c_{Ao}) = k_{cA}^o a_v (c_{Ai} - c_{Ab})_{LM} V \quad (12.32)$$

where the equipment volume is V .

The mass transfer coefficient may be calculated with the overall mass balance for various experimental conditions such mass transfer surface per unit volume, equipment parameters such as the aspect ratio but keeping the same geometry and fluid properties. How to vary these quantities in an independent fashion and to present the mass transfer

results in the most compact way can be determined by examining the transport equations.

12.3.2 Correlation of Mass Transfer Coefficients

The dimensionless transport equations are formulated in Section 8.7.3. The mass transfer coefficient, assumed to be constant over the mass transfer surface, may be computed from the solution as follows:

$$k_{cA}^o \Delta c_A a_v = \int_V D_A^v \nabla c_A \cdot \mathbf{n}_v dV \quad (12.33)$$

This result offers some useful information even without a solution for the concentration field. Following the calculations in Section 8.7.3, Equation (12.33) can be expressed in dimensionless form as follows:

$$N_{Sh} = \frac{k_{cA}^o L}{D_A^v} = \frac{1}{V} \int_V \nabla^* c_A^* \cdot \mathbf{n} dV \quad (12.34)$$

left side of the Equation (12.34) is a dimensionless mass transfer coefficient called the Sherwood number. The right-hand side comes from the solution to the dimensionless transport equations, which depends on position and the values of the dimensionless parameters appearing in the differential equations and boundary conditions. Integration over the volume removes the dependence on position but may introduce dimensionless geometric parameters required for the integration limits. The result is that we expect experimental data for mass transfer coefficients to be effectively correlated by

$$N_{Sh} = F(N_{Re}, N_{Sc}, N_{Gr}, N_{Fr}, N_{Eq}, \dots) \quad (12.35)$$

The functional form, F , comes from the correlation of experimental data arranged in the form of the dimensionless groups

delineated in Equation (12.35). The validity of this expectation is generally evident in mass transfer correlations.

Note that the thermal energy equation, Equation (8.227), is the same differential equation as the mass balance in Equation (8.226) if the Schmidt number is replaced with the Prandtl number. This means that the same solution will apply to both if the boundary conditions are the same form. A dimensionless heat transfer coefficient will be defined (see Section 14.1) that will result in a number of heat transfer problems where this comparison is valid. In such cases, the dimensionless heat transfer coefficient, called the Nusselt number, and the Prandtl number in the heat transfer correlation, may be replaced, respectively, with the Sherwood and Schmidt numbers to obtain a valid mass transfer correlation.

The analogy between the heat and the mass transfer is also expressed by the empirical Chilton–Colburn relations:

$$j_D = \frac{N_{Sh}}{N_{Re} N_{Sc}^{1/3}} = j_H = \frac{N_{Nu}}{N_{Re} N_{Pr}^{1/3}} = F(N_{Re}) \quad (12.36)$$

for geometrically similar systems and the same boundary conditions.

Example 12.3.2-1: Determination of Liquid Mass Transfer Coefficients in a Fixed Bed

In a mass transfer experiment, 50 cc/s(?) of pure water at 27 °C was passed over a fixed bed of benzoic acid spheres maintained at 27 °C (see Figure 12.6), which is based on Figure 8.19.

Benzoic acid (A) was chosen because of its limited solubility in water (501.53 ppm on a molar basis at 20 °C) (Yaws, 2003). The limited solubility assured a stable interface for mass transfer and that there was no convective component to the mass flux in the film surrounding the benzoic acid spheres. Its concentration can be easily measured, for example, by titration.

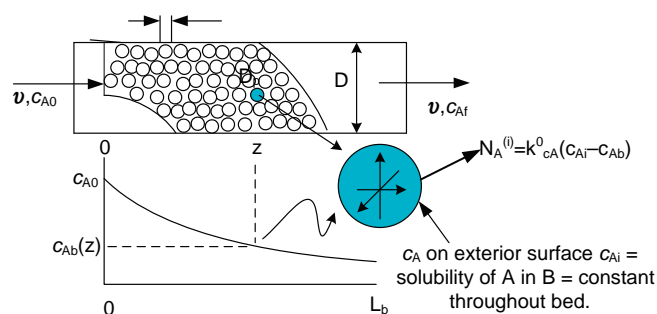


FIGURE 12.6 Measurement of liquid side mass transfer coefficients in a fixed bed.

The diameter of the spheres D_p was 1/16 in. The inside diameter of the tube d_b was 1.25 in. and the packed length was 12 in. The bed porosity was determined to be 0.492. The outlet composition was 75% of saturation. Determine the Sherwood, Schmidt, and Reynolds numbers. Compare with correlation of data for fixed beds given in the following section.

Solution:

Physical properties

Neglect effect of acid on mixture properties: A = benzoic acid, B = water

From Appendix C:

$$\eta = 10^{+1.7730 \times 10^{-2} \times (273.16 + 26.1) - 1.2631 \times 10^{-5} \times (273.16 + 26.1)^2} = 0.88811$$

$$c_P = 0.0088811 \text{ g/(cm s)}$$

$$\rho = 0.3471 \times 0.274 - \left(1 - \frac{26.1 + 273.16}{647.13}\right)^{0.28571} = 1.0264 \text{ g/cc}$$

From Yaws (1999):

solubility (mole basis) = 501.53 ppm at 20 °C. Use this value

$$c_{Ai} = \frac{501.53}{1000000 \times 18.015 / 1.0264} = 2.8575 \times 10^{-5} \text{ gmol/cc}$$

From Poling et al. (2001):

D_{AB} at infinite dilution = $1.38 \times 10^{-5} \text{ cm}^2/\text{s}$ at 298 °K.

Temperature correction: Use Siddiqui–Lucas equation in Chapter 8

$$D_{AB} = 1.38 \times 10^{-5} \frac{273.16 + 26.1}{298} = 1.3858 \times 10^{-5} \text{ cm}^2/\text{s}$$

Mass transfer coefficient

$$a_v = \frac{4(2.54/32)^2}{\frac{4}{3}(2.54/32)^3} (1 - 0.492) = 19.2 \text{ cm}^{-1}$$

$$V = 3.1416(1.25 \times 2.54)^2 \frac{1}{4} 12 \times 2.54 = 241.32 \text{ cm}^3$$

Use mass balance (divided though by solubility = interfacial composition)

$$50(0.75 - 0) = k_c(19.2) \frac{(1-0)-(1-0.75)}{\ln \frac{1-0}{1-0.75}} 241.32, \text{ Solution}$$

is: $k_c = 1.4960 \times 10^{-2} \text{ cm/s}$

Dimensionless groups

$$N_{Sh} = \frac{1.4960 \times 10^{-2} (2.54/16)}{1.3858 \times 10^{-5}} = 171.37$$

$$v = \frac{50}{\pi \frac{(1.25 \times 2.54)^2}{4}} = 6.3153 \text{ cm/s}$$

$$N_{\text{Re}} \frac{1.0264(2.54/16)6.3153}{0.0088811} = 115.87$$

$$N_{\text{Sc}} = \frac{0.0088811}{1.0264 \times 1.3858 \times 10^{-5}} = 624.38$$

Comparison with correlation—Equation (12.37)

$$N_{\text{Sh}} = 2. + 1.1(115.87^{0.6})(624.38^{0.333333333}) = 164.9$$

12.4 FIXED BEDS

A summary of mass transfer data for both gas and liquid systems is given in Figure 12.7. The data have been corrected for dispersion and are represented by

$$N_{\text{Sh}} = 2.0 + 1.1N_{\text{Re}}^{0.6}N_{\text{Sc}}^{1/3} \quad (12.37)$$

The characteristic length is the diameter of the beads and the characteristic velocity is based on the total cross section. For nonspherical particles a number of approaches have been taken. A widely used one is the diameter of a sphere with the same external surface area. The Sherwood number approaches 2 as the Reynolds number approaches zero. The limiting value of 2.0 is the Sherwood number for diffusion into a semi-infinite medium from a spherical surface at a fixed concentration.

12.4.1 Fixed-Bed Adsorption

The adsorption of gases is normally carried out in a fixed bed, which consists primarily of a cylindrical shell with internal supports or screens to maintain the integrity of a charge of

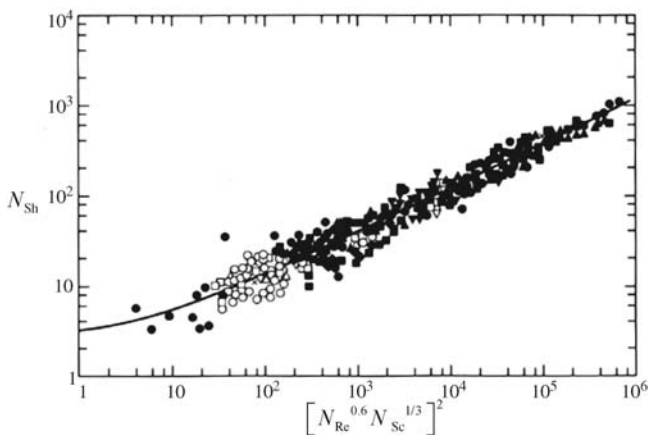


FIGURE 12.7 Mass transfer coefficients in a fixed bed. (from Wakao and Funazkri, 1978.). Reprinted with permission of Elsevier.

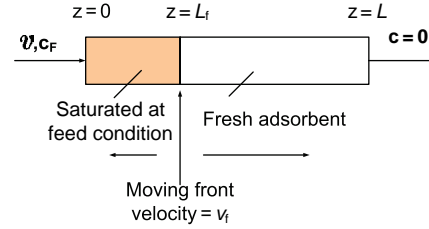


FIGURE 12.8 Ideal adsorption.

adsorbent particles. The gas flow is usually opposite of gravity in order to maintain the stability of the particles bed. The bed removes all of the adsorbate in the feed gas until the adsorption capacity of the bed is approached. The adsorbate then begins to appear at the exit. When the exit concentration reaches the minimum acceptable level, we say that “breakthrough” has taken place. Although much of the following discussion applies to both liquids and gases, the fluid phase will be limited to the latter.

12.4.1.1 Ideal Case Consider the idealized case of a very strong adsorbent that instantly reaches saturation in the presence of the adsorbate. The situation is illustrated in Figure 12.8 where the feed concentration persists up to the moving front. There is plug flow, no dispersion, and no mass transfer resistances.

The following balance equation states that with the elapse of a small quantity of time, all of the adsorbate that enters is adsorbed by the solid.

$$\mathcal{V}c_F dt = w(c_F)\rho_B A_c dz = w(c_F)\rho_B A_c L \frac{1}{L} dL \quad (12.38)$$

$$\mathcal{V}c_F dt = w(c_F)\mathcal{W}_{\text{ads}} \frac{1}{L} dz \quad (12.39)$$

$$v_f = \frac{\mathcal{V}c_F L}{w(c_F)\mathcal{W}_{\text{ads}}} \quad (12.40)$$

The front advances by an amount sufficient to capture enough solid d to accomplish this at the loading in equilibrium with the feed composition, $w(c_F)$. The bed cross section is A_c and the total mass of adsorbent is \mathcal{W}_{ads} with a packing density of ρ_B .

The front reaches the exit after a time t_b given by

$$t_b = \frac{w(c_F)A_c}{\mathcal{V}c_F} \quad (12.41)$$

The concentration at the outlet then appears as illustrated in Figure 12.9 where a more realistic concentration history is also illustrated.

At the instant breakthrough takes place, the bed is taken off stream and the feed is switched to a regenerated bed. Regeneration generally takes place at a higher temperature (temperature swing adsorption—TSA) or a lower pressure (pressure swing adsorption—PSA). PSA is attractive for bulk separations because of the short time cycle

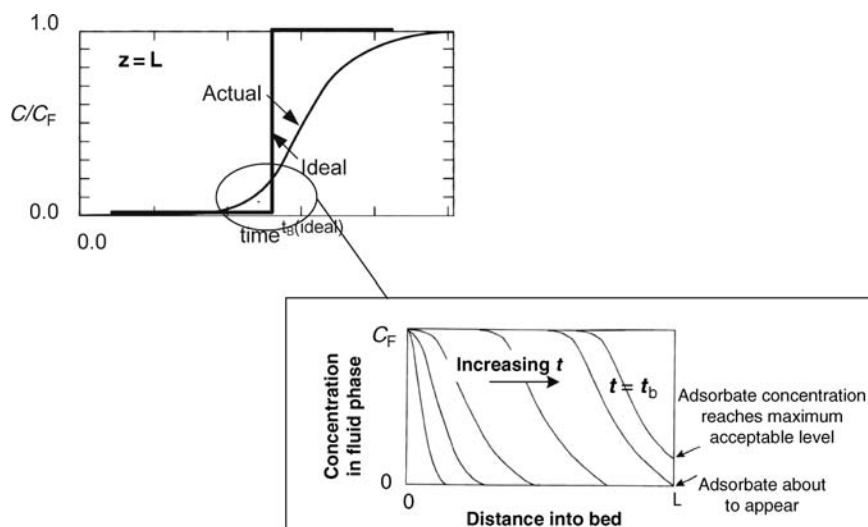


FIGURE 12.9 Evolution of the output concentration profile.

(Couper et al., 2005). Cycle times are sometimes set in multiples of 8 h to coincide with shifts.

A pair of activated carbon adsorbers is illustrated in Figure 12.10 and the parallel connection is illustrated in Figure 12.11.

The ideal view can at best provide a preliminary estimate of the breakthrough time. To be able to predict breakthrough times and concentration profiles with reasonable accuracy requires a more sophisticated model than the ideal case.

12.4.1.2 More General Model A number of models have been proposed for the fixed-bed adsorber (Ruthven, 1984). The basic features of these models may be found in the following formulation.



FIGURE 12.10 Activated carbon adsorbers. Reprinted with permission of Everfilt.

The interstitial fluid with nearly constant density is in plug flow along the axis of a cylindrical bed containing spherical adsorbent particles. The model is expressed in two geometries as per the discussion in Section 8.7.4.

12.4.1.3 Gas Phase The rate of disappearance of adsorbate from the gas phase is interpreted as a homogeneous reaction rate, equal in magnitude to its rate of accumulation in the adsorbent phase. The reaction rate must be scaled and

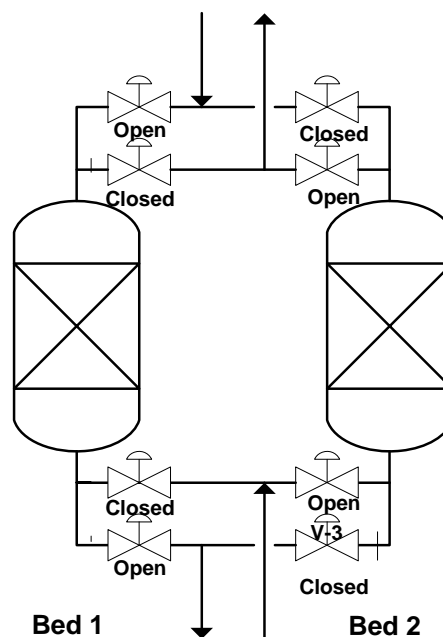


FIGURE 12.11 Parallel connection of adsorption equipment. Valve positions shown for Bed 1 on adsorption cycle and Bed 2 on desorption cycle.

represented per unit volume of the gas phase to be counted properly in the gas-phase material balance.

$$r_{iv} = \underbrace{\frac{1 - \varepsilon_b}{\varepsilon_b}}_{\text{volume of adsorbent per unit volume of bed}} \underbrace{\frac{\partial}{\partial t} \int_{\text{solid volume}} \underbrace{w}_{\text{mass of adsorbate per unit mass of adsorbent}} \underbrace{\rho_p}_{\text{mass adsorbent per unit volume of adsorbent}} \underbrace{r^2 \sin\theta \, dr \, d\theta \, d\phi}_{\text{volume element of adsorbent particle}}}_{\text{mass of adsorbate per unit volume of adsorbent (solid particle)}} \underbrace{\quad}_{\text{rate of change of mass of adsorbate per unit volume of adsorbent particle}} \quad (12.42)$$

The axial (z direction) velocity is the only nonzero component of the velocity. If the density is nearly constant, there is no substantial change in the axial velocity. Under these conditions, the fluid phase model can be extracted from Table 10.1 as

$$\frac{\partial c}{\partial t} + v_z \frac{\partial c}{\partial z} = D \frac{\partial^2 c}{\partial z^2} + \left(\frac{1 - \varepsilon_b}{\varepsilon_b} \right) \rho_p \frac{\partial \bar{w}}{\partial t}, \quad (12.43)$$

$$\text{where } \bar{w} = \frac{24}{D_p^3} \int_0^{D_p/2} w r^2 \, dr \quad (12.44)$$

$$c(z, 0) = 0, \quad c(0, t) = c_F \quad (12.45)$$

Spherical symmetry in the adsorbent (diameter D_p) has been assumed and axial dispersion (coefficient D) is accounted for. The adsorbent bed contains no adsorbate initially.

12.4.1.4 Intraparticle Diffusion The transient mass balance for the adsorbent particle was developed in Section 10.4. The response was found to a sudden rise in the surface concentration, Equation (10.110), to a constant value above a uniform initial composition, Equation 10.114, in the porous solid. The boundary condition will be replaced with continuity in the mass flux at the surface of the adsorbent (M2 in Table 8.13) and the adsorbent will be assumed free of adsorbate initially.

$$D_{eff} \frac{\partial w}{\partial r} \bigg|_{r=\frac{D_p}{2}} = K k_c^0 M \left(c(z, t) - \frac{1}{K} w \left(\frac{D_p}{2}, 0, z \right) \right) \quad (12.46)$$

$$w(r, 0, z) = 0$$

The value of the mass transfer coefficient k_c^0 may be obtained from the correlation in Equation (12.37). A low mass transfer is assumed so that no correction is required (see Section 12.6.1). For a dilute system, Henry's law [Equation (6.136)] may be applied to obtain the gas concentration in the film at the exterior surface of the adsorbent. The value of K in this case is $MkRT$ where M is the molecular weight of the adsorbate.

The analytic solution to a number of models of this general type may be found in Ruthven (1984). In some cases, it is faster to numerically integrate the differential equations than to use the analytical solution. However, it turns out, many of the solutions are remarkably similar in case to the solution of a simpler model called the linear driving force (LDF) model. The LDF has been found [see Ruthven (1984)] provided the system is linear, which very closely approximates more comprehensive versions and is much easier to use.

12.4.1.5 LDF (Linear Driving Force) Model The intra-particle diffusion equations are replaced with

$$\frac{\partial \bar{w}}{\partial t} = k(w^{sat} - \bar{w}) = kK(c - c^{sat}). \quad (12.47)$$

where K is the linear proportionality constant in the equilibrium relation, w^{sat} is the equilibrium loading associated with the bulk-phase concentration and c^{sat} is the bulk-phase concentration in equilibrium with the average loading. The value of k is determined in order that the solution to the LDF for a pulse input is similar to the solution to the general model for the same input. By similar it is meant that the second moments of the solution to a pulse input agree for the more general model and the LDF. An incentive for using moments is that they may be obtained in the Laplace transform domain without need to invert the transform.

The value of k in the LDF model for the case of intra-particle diffusion and external mass transfer is that

$$\frac{1}{kK} = \frac{d_p}{6k_c} + \frac{d_p^2}{60D_{eff}} \quad (12.48)$$

With this equality, the solution to the LDF is very effective for describing the behavior of fixed-bed gas adsorbers. Approximate solutions to the LDF are

$$\frac{c}{c_F} = \frac{1}{2} \operatorname{erfc} \left[\sqrt{\xi} - \sqrt{\tau} - \frac{1}{8\sqrt{\xi}} - \frac{1}{8\sqrt{\tau}} \right],$$

Error < 0.6% for $\xi > 2.0$ (12.49)

$$\frac{c}{c_F} = \frac{1}{2} \operatorname{erfc} \left[\sqrt{\xi} - \sqrt{\tau} \right], \quad \text{Asymptotic form for large } \xi \quad (12.50)$$

where

$$\xi = \frac{kKz}{v_z} \left[\frac{1 - \varepsilon_b}{\varepsilon_b} \right] \quad \text{and} \quad \tau = k \left[t - \frac{z}{v_z} \right] \quad (12.51)$$

The general appearance of the concentration distribution in the bed at fixed times is shown in Figure 12.9.

12.5 PIPES

Mass transfer coefficients inside pipes have been studied by using tubes cast from a slightly soluble material such as benzoic acid. It has also been studied for gas-phase systems with a wetted wall tower where a pure, slightly volatile liquid flows down the inside walls of the pipe and an insoluble gas phase flows countercurrently. A schematic of a wetted wall tower is shown in Figure 9.5.

Mass transfer data between the fluid and wall are represented by Green and Maloney (1997).

$$N_{Sh} = 0.023 N_{Re}^{0.83} N_{Sc}^a, \quad 2100 < N_{Re} < 35000 \quad (12.52)$$

$$\text{Gases: } a = 0.44, \quad 0.6 < N_{Sc} < 2.5 \quad (12.53)$$

$$\text{Liquids: } a = 1/3, \quad 0.6 < N_{Sc} < 3000 \quad (12.54)$$

12.5.1 Turbulent Flow in a Pipe with Catalytic Walls

The correlation in Equations (12.52)–(12.54) may be used to extend the problem considered earlier of laminar pipe flow with catalytic walls to the turbulent regime. We can adapt the model used there as follows. The convection term in

Equation (10.140) for laminar flow can be replaced with a uniform velocity profile. This is referred to as “plug flow” and is often applied in the turbulent regime. The concentration gradients in the r direction are limited to the thin film described by the film-penetration model and the diffusion mechanism is replaced with the mass transfer expression across the film.

$$v \frac{dc_A}{dz} = -k_{cA}^o (c_A - c_{As}) \frac{4}{D} \quad (12.55)$$

The boundary condition at the wall [see Equation (10.141)] does not change. The mass flux from the gas phase is equal to the surface reaction rate:

$$k_{cA}^o (c_A - c_{As}) = k_r c_{As} \quad (12.56)$$

This boundary condition allows the unknown surface concentration of A to be evaluated in terms of the bulk value. The same is true for a single arbitrary reaction,

$$\sum_{\text{all } i} \vartheta_i A_i = 0 \quad (12.57)$$

This can be seen as follows: Because of stoichiometry,

$$k_{ci}^o (c_i - c_{is}) = \frac{\vartheta_i}{\vartheta_A} k_{cA}^o (c_A - c_{As}) \quad (12.58)$$

or, using the mass transfer correlation in Equation (12.55),

$$c_{is} = c_i - \frac{\vartheta_i}{\vartheta_A} \left[\frac{D_A^V}{D_i^V} \right]^{0.56} (c_A - c_{As}) \quad (12.59)$$

This relationship can be used to eliminate all surface composition in the reaction rate expression in favor of the surface composition of A and the bulk composition values. As claimed above, the boundary condition supplies the value of the unknown surface composition in terms of the bulk values. This effectively supplies the mass transfer rate in terms of the bulk-phase conditions only. In the present case, this can be done analytically:

$$k_{cA}^o (c_A - c_{As}) = K c_A \quad (12.60)$$

$$\frac{1}{K} = \frac{1}{k_{cA}^o} + \frac{1}{k_r} \quad (12.61)$$

Note that the overall rate coefficient, K , is bounded by two extremes:

$$K \approx k_r \quad \text{when } k_{cA}^o \gg k_r : \text{Reaction controlled} \quad (12.62)$$

$$K \approx k_{cA}^o \quad \text{when } k_r \gg k_{cA}^o : \text{Diffusion controlled} \quad (12.63)$$

A determination of K , by itself, could not be interpreted as a reaction rate parameter or a mass transfer coefficient. Additional information is required. For example, a plot of $\ln K$ versus $1/T$ would exhibit a change in slope as the process changed from diffusion to reaction controlled. The temperature dependence of the two rate constants can normally be expressed in the Arrhenius form, $k_0 \exp(-E/RT)$. The activation energy, E , is much smaller for mass transfer.

In addition, since the interfacial composition, given by

$$c_{As} = \frac{c_A}{1 + k_r/k_{cA}^o} \quad (12.64)$$

is nearly zero in the diffusion-controlled regime, which would appear as an irreversible first order reaction.

The solution for the concentration profile in dimensionless variables is given by

$$\Gamma = e^{-\frac{4\Lambda}{N_{Re}N_{Sc}}\xi} \quad (12.65)$$

where,

$$\frac{1}{\Lambda} = \frac{\Lambda_l}{\Lambda_r^2} + \frac{2/\Lambda_l}{N_{Sh}} \quad (12.66)$$

The definition of the remaining parameters is the same as in Table 10.6 where the same problem was considered for the case of a laminar velocity profile. The average velocity denoted here by v is $1/2$ of the maximum of the laminar velocity profile. Also, the concentration at the tube entrance is taken here to be uniform at c_{Ao} . The catalyst effectiveness is again given by

$$\mathcal{E} = \frac{[c_{Ao} - c_A(L)]v\pi D^2}{k_r c_{Ao} \pi DL} \quad (12.67)$$

$$\mathcal{E} = \frac{1 - \exp\left[-\frac{4\Lambda}{N_{Re}N_{Sc}}\right]}{\frac{4\Lambda}{N_{Re}N_{Sc}}} \frac{\Lambda\Lambda_l}{\Lambda_r^2} \quad (12.68)$$

The catalyst effectiveness is plotted in Figure 12.12 for a gas-phase reaction at a fixed $L/D = \Lambda_l/2$ for several values of the Reynolds number in the turbulent regime. This is compared to the laminar flow result at a Reynolds number of 2/3.

Figure 12.12 illustrates the beneficial effect of the turbulent mass transfer on the reaction rate. The productivity of the reactor increases with the Reynolds number but the conversion, x , decreases. This means that the separation of the products from the reaction mixture will be more costly since the products are available in a less concentrated mixture at a higher rate of flow. The economic design of the reactor must ultimately account for these competitive features.

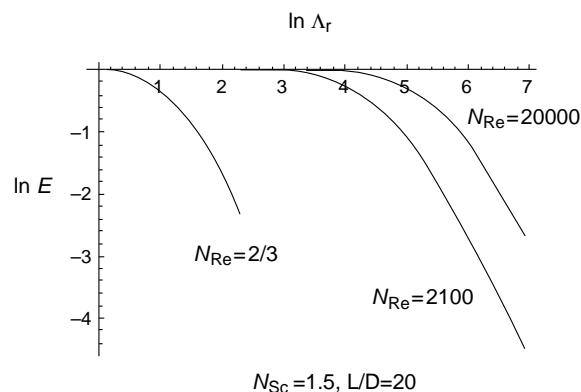


FIGURE 12.12 Catalyst effectiveness as a function of a Reynolds number.

12.6 PARTICLES, DROPS, AND BUBBLES IN AGITATED SYSTEMS

Many chemical engineering operations involve the transfer of mass between two nearly immiscible phases. In such cases, it is desirable to provide as large an interfacial area as possible since the interfacial mass transfer rate is directly proportional to the interfacial area. To this end, one of the phases is finely dispersed in the accompanying phase in nearly spherical forms.

In the acrylic acid process, for example, the DIPE steam is dispersed through perforated plates into the aqueous phase for extraction of the acid components in T-303. In T-305, the dispersion is accomplished with structured packing. Two examples will be considered here: a liquid-solid system for slurry adsorption in an agitated batch process and a packed tower. The following correlation applies to the adsorption process.

For small solid particles, gas bubbles, or liquid drops (in Green and Maloney, 1997):

$$N_{Sh} = 2.0 + 0.31 \left[\frac{D_p^3 |\rho_p - \rho_c| g}{\eta_c D_{AL}} \right]^{1/3} \quad D_p \leq 2.5 \text{ mm} \quad (12.69)$$

where

D_p = diameter of the particle in m

D_{AL} = diffusivity of solute in solution in m^2/s

η_c = viscosity of continuous phase in $\text{kg}/\text{m s}$

ρ_c = density of continuous phase in kg/m^3

ρ_p = density of particle in kg/m^3

$g = 9.80665 \text{ m/s}^2$

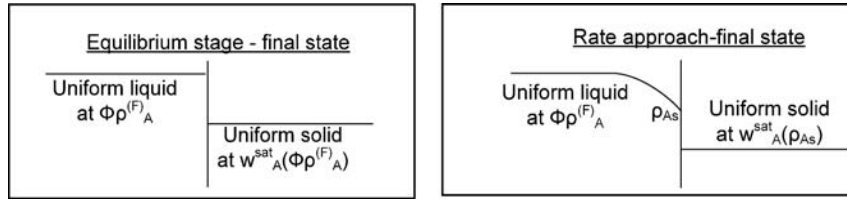


FIGURE 12.13 Concentration profiles for rate and equilibrium stage approaches.

12.6.1 Slurry Adsorption—External Mass Transfer Control

A batch adsorption process was considered in Chapter 6 where a powdered adsorbent was suspended in an agitated liquid containing a solute at an undesirable concentration. The minimum amount of adsorbent was calculated on the basis of a sufficiently long contact time that equilibrium could be assumed. Our objective here is to determine the contact times required for adsorbent charges greater than the minimum.

We will suppose that there is no initial loading of the particles and that the external mass transfer resistance is controlling. The conditions in the liquid and solid phases with the controlling resistance in the liquid phase can be gleaned from Figure 12.4.

A mass balance on each phase may be written as follows, noting that the phase interface is the only input/output and that we must have the accumulation term prescribed by Equation (2.1).

$$\text{Liquid phase } \mathcal{V}_L \frac{d\rho_A}{dt} = -k_{cA}^0 a_m \mathcal{W}_{\text{ads}} (\rho_A - \rho_{As}) \quad (12.70)$$

$$\rho_A(0) = \rho_A^{(F)} \quad (12.71)$$

$$\text{Solid phase } \mathcal{W}_{\text{ads}} \frac{dw_A}{dt} = k_{cA}^0 a_m \mathcal{W}_{\text{ads}} (\rho_A - \rho_{As}) \quad (12.72)$$

$$w_A(0) = 0 \quad (12.73)$$

If Equations (12.70)–(12.72) are added and the result is integrated, we obtain the overall material balance quoted in Chapter 6:

$$\mathcal{V}_L (\rho_A - \rho_A^{(F)}) + \mathcal{W}_{\text{ads}} (w_A - 0) = 0 \quad (12.74)$$

In the equilibrium stage approach, the process is exhausted and the overall material balance and the equilibrium relation are sufficient, for example, to determine the concentration in each phase, given an adsorbent loading. In the rate approach, the interfacial concentration in at least one of the phases is not equal to the bulk value and is required at each instant to

fix the process rate. The distinction between the rate and equilibrium stage approach is shown in Figure 12.13.

The time required in the rate analysis may be determined by following the liquid phase concentration in time.

- Solve the overall material balance, Equation (12.74), for the concentration in the solid.
- Substitute the preceding result into the equilibrium relation and solve for the concentration in the liquid at the interface.
- Substitute the result for the interfacial liquid concentration into the liquid phase material balance and make the result dimensionless.

The results for two isotherms are

Freundlich isotherm:

$$\frac{d\rho^*}{d\tau} = \frac{(1 - \rho^*)^\beta}{\sigma^\beta} - \rho^* \quad \sigma = \frac{\mathcal{W}_{\text{ads}} w_A^{\text{sat}}(\rho^{(F)})}{\mathcal{V}_L \rho^{(F)}} \quad (12.75)$$

Langmuir isotherm:

$$\frac{d\rho^*}{d\tau} = \frac{1}{k\rho^{(F)}} \frac{1 - \rho^*}{[\sigma - (1 - \rho^*)]} - \rho^* \quad \sigma = \frac{\mathcal{W}_{\text{ads}} w_{\text{max}}}{\mathcal{V}_L \rho^{(F)}} \quad (12.76)$$

$$\text{where } \rho^* = \frac{\rho}{\rho^{(F)}}, \rho^*(0) = 1, \text{ and } \tau = k_{cA}^0 a_m \frac{\mathcal{W}_{\text{ads}}}{\mathcal{V}_L} t \quad (12.77)$$

The dimensionless time required achieve a specified concentration level is

$$\text{Freundlich isotherm: } \tau_f = \int_{\phi_f}^1 \frac{dx}{x - ((1 - x)^\beta / \sigma^\beta)} \quad (12.78)$$

Langmuir isotherm:

$$\tau_f = \int_{\phi_f}^1 \frac{dx}{x - ((1/k\rho^{(F)})((1 - x)/(\sigma - (1 - x))))} \quad (12.79)$$

where Φ_f is the fraction of the feed concentration remaining. The result of the Langmuir isotherm in Equation (12.79) may be integrated to give

$$\tau_f = \left[\frac{\sigma + A - \sqrt{A^2 + \sigma}}{2A} \right] \ln \frac{(1 - \phi - \sqrt{A^2 + \sigma} - A)(\sqrt{A^2 + \sigma} - A)}{(1 - \phi - \sqrt{A^2 + \sigma} + A)(\sqrt{A^2 + \sigma} + A)} - \ln \frac{A + \sqrt{A^2 + \sigma} - (1 - \phi)}{A + \sqrt{A^2 + \sigma}} \quad (12.80)$$

$$\text{where } A = \sqrt{\frac{1}{4} \left(\sigma + 1 + \frac{1}{k\rho^{(F)}} \right)^2 - \sigma}$$

If the adsorbent charge corresponds to the equilibrium value associated with Φ , the value of τ_f will be infinite. With the same value of the final concentration, the value of the required time will decrease as the adsorbent charge is increased. This behavior is illustrated in Example 12.6.1-1.

Example 12.6.1-1 Adsorption Time and Batch Integration in Continuous Processes

Consider the adsorption step in the production of hexyl glucoside that is discussed in Chapter 1. The material balance for a proposed continuous process is given in Problem 2.3 in Chapter 2. The adsorbent (alumina) loading for a single-stage batch operation was found in Example 6.5.3-1 to be 199.04 kg. This charge reduced the product concentration to 0.5% of the feed value. The feed was 265.04 L of hexanol containing 4.2823 g/L of hexyl glucoside.

Data required:

$$\rho^{(F)} = 4.2823 \text{ kg/m}^3$$

$$V_L = 0.265036 \text{ m}^3$$

$$D_p = 0.00015 \text{ m}^2 \text{ s}^{-1} = 2.14 \text{ kg/m}^3$$

$$k = 2.14 \text{ kg/m}^3$$

$$w_{\max} = 0.1295$$

From Appendix C:

$$\rho_p = 1500 \text{ kg/m}^3$$

$$\eta = 0.0043085 \text{ kg/(m s)} \text{—see Example 10.4-1}$$

$$D_{AL} = 8.49145 \times 10^{-11} \text{ m}^2/\text{s} \text{—see Example 10.4-1}$$

$$\phi = 0.005$$

$$N_{Sh} = 2.0 + 0.31 \left(\frac{0.0015^3 (1500 - 1043) 9.80665}{8.49145 \times 10^{-11} \times 0.0043085} \right)^{1/3} = 109.19$$

$$\sigma = \frac{0.1295}{0.265036(4.2823)} W = 0.1141 W$$

$$\sigma(W) = 0.1141 W$$

$$A(W) = \left(\frac{1}{4} (\sigma(W) + 1 + \frac{1}{k\rho})^2 - \sigma(W) \right)^{1/2}$$

$$g(W) = \frac{\sigma(W) + A(W) - (A(W)^2 + \sigma(W))^{1/2}}{2A(W)} \times \left(\left(\frac{(1 - \phi - (A(W)^2 + \sigma(W))^{1/2} - A(W))((A(W)^2 + \sigma(W))^{1/2} - A(W))}{(1 - \phi - (A(W)^2 + \sigma(W))^{1/2} + A(W))((A(W)^2 + \sigma(W))^{1/2} + A(W))} \right) \ln \right) - \ln \frac{A(W) + (A(W)^2 + \sigma(W))^{1/2} - (1 - \phi)}{(A(W)^2 + \sigma(W))^{1/2} + A(W)}$$

$$\tau = 109.19 \times \left(\frac{8.49145 \times 10^{-11}}{0.00015} \right) \times \frac{6}{0.00015} \times \frac{1}{1500} \times \frac{1}{0.2665036} W t = 6.18510^{-3} W t$$

$$t(W) = \frac{g(W)}{6.1850 \times 10^{-5} W}$$

Residence time is infinite for equilibrium stage:

$$1/g(W) = 0 \quad W \in (195, 200), \text{ Solution is: } W = 199.04$$

Checks with the single equilibrium stage calculation.

Behavior of dimensionless residence time with loading is shown in Figure 12.14.

Select loading

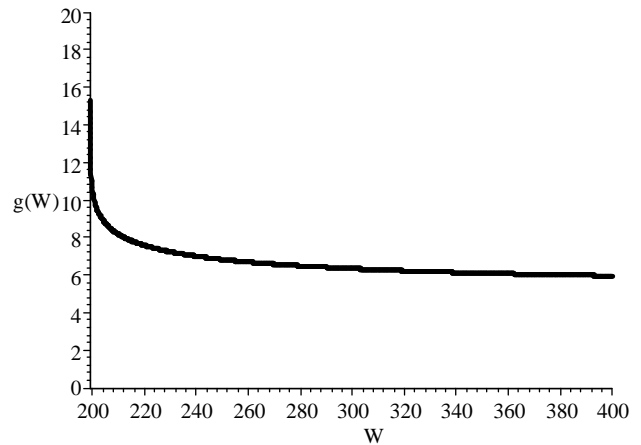


FIGURE 12.14 Behavior of dimensionless loading time with loading.

Choose W just before sharp increase; say $W = 200$

$$t(W) = \frac{g(W)}{6.1850 \times 10^{-5} W}$$

$$t(200) = 851.67 \text{ s} \frac{851.67}{60} = 14.195 \text{ min}$$

On the basis of the 4 h filling period in Example 6.5.3-1, we can assume that the process stream 6 is collected over a 4 h period. Over a period of 4 h, some or all of the following operations are performed:

- Charging of adsorber with collected process fluid.
- Addition of adsorbent.
- Adsorption of hexyl glucoside.
- Discharge slurry.
- Clean adsorber.
- Separation of adsorbent from slurry.
- Recycle of adsorbent for processing of next batch.
- Filling of the hexanol product tank (source of stream 10).
- Transfer of hexyl glucoside to storage.

12.7 PACKED TOWERS—GAS ABSORPTION

An illustration of a packed tower for gas–liquid contacting is given in Figure 1.17. It is the continuous version of the stagewise process for gas absorption in tray towers given in

Section 7.1. The packed section serves to distribute the liquid and gas phases uniformly over the cross section and to present a large interfacial area for mass transfer. Some common packing materials are shown in Figure 12.15.

Packed towers are used in distillation, solvent extraction, quenching, absorption, and stripping. Some basic aspects of the application to gas absorption are considered here.

Packed towers are normally selected for a gas–liquid separation when the required diameter for tray towers is less than 2 ft, which allows little space to access trays. Also, there is greater flexibility in material selection for packing when corrosion is an issue. The pressure drop and liquid holdup are generally lower in packed towers. Also some packing can provide more theoretical stages per unit height than a tray tower.

12.7.1.1 Heuristics for Packed Towers (Couper et al., 2005)

- The optimum value of the absorption factor [see Equation (12.102)] is in the range of 1.25–2.0.
- Random and structured packings are suited especially to towers under 3 ft in diameter. With proper initial and periodic attention to liquid distribution, volumetric efficiencies can be made greater than those in tray towers.
- The ratio of tower diameter to packing (equivalent) diameter should be at least 15.
- Because of deformability, plastic packing should be limited to a depth of 10–15 ft and metal to 20–25 ft.

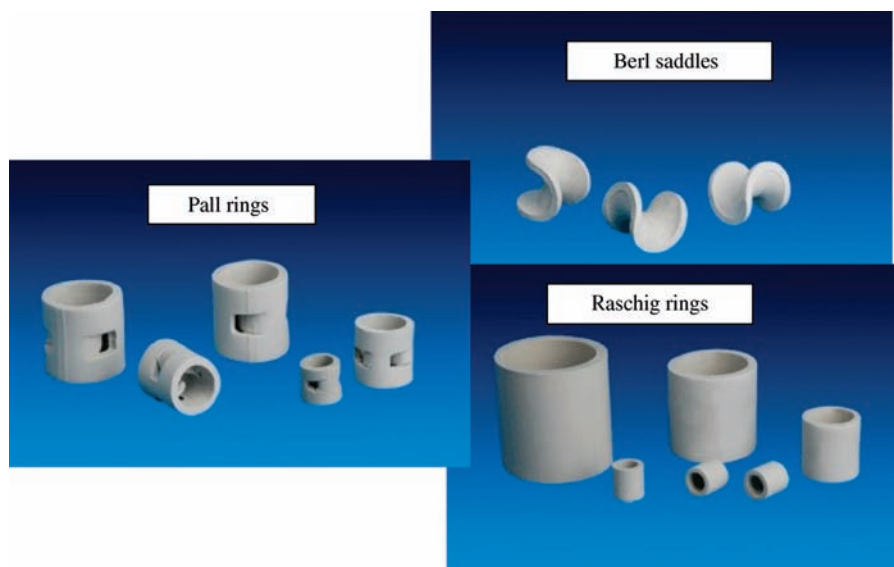


FIGURE 12.15 Random column packing—some examples. Reprinted with permission of Pingxaing Ceramics, Ltd.

- Liquid distributors are needed every 5–10 tower diameters but at least every 20 ft for pall ring (see Figure 12.15) packing. The number of liquid streams should be 3–5/ft² in towers larger than 3 ft in diameter.
- The tower height should not be more than 175 ft because of foundation and wind load considerations. Moreover, the height to diameter ratio for the tower should be less than 30.

The gas and liquid inlets and outlets are situated the same as in tray towers. The arguments in favor of countercurrent operation for tray towers carry over to packed towers. The packing must be carefully loaded and the column oriented vertically to avoid maldistribution of the gas and liquid flows, which generally diminish the mass transfer rate. For gas rates 2000 cfm or more, a packing size of 2 in. is normally used (Couper et al., 2005). A packing size of 1 in. is used down to 500 cfm. The gas flow should be approximately 70% of the flooding value (see Chapter 13).

12.7.2 Mass Transfer Correlations

A number of mass transfer correlations are available for gas absorbers. In some cases, the volumetric coefficient is provided where the mass transfer coefficient combined with area per unit volume. In others, the area and mass transfer correlations are separate. An example of the latter is in Treybal (1980).

$$\text{Gas side: } N_{\text{Sh}} = 1.195(1 - \varepsilon_{\text{Lo}})^{0.36} N_{\text{Re}}^{0.64} N_{\text{Sc}}^{1/3} \quad (12.81)$$

The diameter of a sphere with the same surface area as the packing, d_s , is the characteristic length, which appears in the

Sherwood and Reynolds numbers. The characteristic velocity in the Reynolds number is the superficial velocity of the gas based on the tower cross section.

The operating void fraction in the bed, ε_{Lo} , is the void fraction with no liquid present, ε , less the fraction taken up by both moving and stagnant liquid, ϕ_{Lt} .

$$\varepsilon_{\text{Lo}} = \varepsilon - \phi_{\text{Lt}} \quad (12.82)$$

The void fraction with no liquid present is normally available from the manufacture's data for the particular packing being used. The packing characteristics for Raschig rings are given in Table 12.1 for wet dumped packing from Shulman and coworkers as reported in (Treybal, 1980).

Note that the mass transfer coefficient is proportional to the 2/3 power of the diffusivity, which is consistent with the film-penetration theory but inconsistent with the surface renewal theory.

The total holdup is expressed in terms of the operating and static holdup:

$$\varphi_{\text{Lt}} = \varphi_{\text{Lo}} + \varphi_{\text{Ls}} \quad (12.83)$$

The calculation of the operating and static holdups is based on the values for water: $\varphi_{\text{Ltw}}, \varphi_{\text{Low}}, \varphi_{\text{Lsw}}$. The procedure is summarized in Table 12.2 (from Treybal, 1980).

In contrast to the gas side, the liquid side coefficient is consistent with the surface renewal theory.

$$\text{Liquid side: } N_{\text{Sh}} = 25.1 N_{\text{Re}}^{0.45} N_{\text{Sc}}^{0.5} \quad (12.84)$$

The characteristic length and velocity are the same as those for the gas side.

TABLE 12.1 Characteristics of Random Packings

Packing	Nominal Size, mm (in.)									
	6(1/4)	9.5(3/8)	13(1/2)	16(5/8)	19(3/4)	25(1)	32 (5/4)	38(32)	50(2)	76(3)
Raschig Rings										
Ceramic: Wall thickness (mm)	0.8	1.6	2.4	2.4	2.4	3	4.8	4.8	6	9.5
C_r		1000	1600	380	255	155	125	95	65	37
C_D			909	749	457	301		181.8	135.6	
ε	0.73	0.68	0.63	0.68	0.73	0.73	0.74	0.71	0.74	0.78
a_p : m ² /m ³ (ft ² /ft ³)	787(240)	508(155)	364(111)	328(100)	262(80)	190(58)	148(45)	125(38)	92(28)	62(19)
Metal:										
0.8 mm wall:										
C_r	700	390	300	170	155	115				
ε	0.69		0.84		0.88	92				
a_p : m ² /m ³ (ft ² /ft ³)	774(236)		420(128)		274(83.5)	206(62.7)				
1.6 mm wall:										
C_r			410	290	220	137	110	83	57	32
C_D			688	431	485	304		172.9	133.5	
ε			0.73		0.78	0.85	0.87	0.90	0.92	0.95
a_p : m ² /m ³ (ft ² /ft ³)			387(118)		236(71.8)	186(56.7)	162(49.3)	135(41.2)	103(31.4)	68(20.6)

a_p = specific area of packing; C_D = empirical constant.

TABLE 12-2 Liquid Holdup in Packed Tower

Packing	Nominal Size		d_s (m)	ϕ_{LS}	Water, Ordinary Temperature	η_L (kg/m s)	H
	mm	in.					
Ceramic	13	0.5	0.01774		$\beta = 1.508d_s^{0.376}$	< 0.012	$\frac{975.7L'^{0.57}\mu_L^{0.13}}{\rho_L^{0.84}(2.024L'^{0.430} - 1)} \left(\frac{\sigma}{0.073}\right)^{0.1737-0.262\log L'}$
Raschig	25	1	0.0356				
rings	38	1.5	0.0530	$\frac{0.0486\mu_L^{0.02\sigma^{0.99}}}{d_s^{1.21}\rho_L^{0.37}}$	$\phi_{LSW} = \frac{2.47 \times 10^{-4}}{d_s^{1.21}}$		
	50	2	0.0725		$\phi_{LW} = \frac{(2.09 \times 10^{-6})(737.5L')^\beta}{d_s^2}$	> 0.012	$\frac{2168L'^{0.57}\mu_L^{0.31}}{\rho_L^{0.84}(2.024L'^{0.430} - 1)} \left(\frac{\sigma}{0.073}\right)^{0.1737-0.262\log L'}$
Ceramic	25	1	0.01305		$\beta = 1.104d_s^{0.376}$	< 0.012	$\frac{407.9L'^{0.57}\mu_L^{0.13}}{\rho_L^{0.84}(1.393L'^{0.315} - 1)} \left(\frac{\sigma}{0.073}\right)^{0.1737-0.262\log L'}$
Raschig	38	1.5	0.0543				
rings	50	2	0.0716	$\frac{0.0237\mu_L^{0.02\sigma^{0.23}}}{d_s^{1.21}\rho_L^{0.37}}$	$\phi_{LSW} = \frac{5.94 \times 10^{-4}}{d_s^{1.21}}$		
					$\phi_{LW} = \frac{(7.34 \times 10^{-6})(737.5L')^\beta}{d_s^2}$	> 0.012	$\frac{901L'^{0.57}\mu_L^{0.31}}{\rho_L^{0.84}(1.393L'^{0.315} - 1)} \left(\frac{\sigma}{0.073}\right)^{0.1737-0.262\log L'}$
Ceramic	13	0.5	0.01622		$\beta = 1.508d_s^{0.376}$	< 0.012	$\frac{1404L'^{0.57}\mu_L^{0.13}}{\rho_L^{0.84}(3.24L'^{0.413} - 1)} \left(\frac{\sigma}{0.073}\right)^{0.28177-0.262\log L'}$
Berl	25	1	0.0320				
saddles	38	1.5	0.0472	$\frac{4.23 \times 10^{-3}\mu_L^{0.04\sigma^{0.55}}}{d_s^{1.56}\rho_L^{0.37}}$	$\phi_{LSW} = \frac{5.014 \times 10^{-5}}{d_s^{1.56}}$		
					$\phi_{LW} = \frac{(2.32 \times 10^{-6})(737.5L')^\beta}{d_s^2}$	> 0.012	$\frac{2830L'^{0.57}\mu_L^{0.31}}{\rho_L^{0.84}(3.24L'^{0.413} - 1)} \left(\frac{\sigma}{0.073}\right)^{0.28177-0.262\log L'}$

Only SI units ρ_L : kg/m³, η_L : kg/m s, σ : N/m, and L_p : kg/m² s are used. $\phi_{Lo} = \phi_{LoW}H$, $\phi_{Lt} = \phi_{Lo} - \phi_{Ls}$, ϕ_{Ls} , $\phi_{LW} = \phi_{LoW} - \phi_{LsW}$.

The interfacial area per unit volume is also given in terms of values for water:

$$a_v = a_w \frac{\phi_{Lo}}{\phi_{LoW}} \quad (12.85)$$

The required calculations are summarized in Table 12.3 (Treybal, 1980).

12.7.3 Mass Balances

As the gas flows up through the bed, the soluble component(s) move across the gas–liquid interface and dissolve in the liquid solvent. The amount of soluble material contained in the gas phase *continuously* decreases in contrast to the equilibrium stage model where the composition decreases stepwise. The operating line (mass balance) is the same in both towers. All points, however, are accessed in the packed tower in contrast to discrete points in the tray tower.

An element of gas *continuously* approaches equilibrium with the liquid as it travels up the column. The liquid that contacts the gas element is traveling down the column and is therefore less concentrated with height. A distance from

equilibrium between the gas and liquid phase can thereby be maintained as the gas element travels to the outlet.

A gas absorber is normally designed to provide for a fixed amount of material to be absorbed from a given process stream and therefore the bulk gas composition travels between two well-defined limits. If a large amount of liquid is used, its composition does not increase substantially throughout the column and a distance from equilibrium imposed at the inlet can be maintained throughout the tower. As the liquid flow is decreased, however, and the required tower height increases, and the average composition of the liquid increases until either in the tower or at the liquid outlet the concentration in the liquid falls on both the operating line and then the equilibrium curve. At this point, called a pinch point, the two streams are equilibrated and emerge from a small cross-sectional volume element unchanged. Pinch points are discussed quantitatively in Section 7.1.3

For a liquid flow rate greater than the minimum, the required contact time depends on the rate that the solute crosses the gas–liquid interface. This contact time translates into a required height with a given flow rate. The interfacial mass transfer rate is therefore the central feature in determining the size of the tower.

TABLE 12-3 Interfacial Area for Absorption and Desorption, Aqueous Liquids

Packing	Nominal Size		Range of L'		m	n	p
	mm	in	kg/m ² · s	lb/ft ³ · h			
Raschig Rings	13	0.5	0.68–2.0	500–1500	28.01	$0.2323L' - 0.30$	-1.04
			2.0–6.1	1500–4500	14.69	$0.01114L' - 0.148$	-0.111
	25	1	0.68–2.0	500–1500	34.42	0	0.552
			2.0–6.1	1500–4500	68.2	$0.0389L' - 0.0793$	2-0.47
	38	1.5	0.68–2.0	500–1500	36.5	$0.498L' - 0.1013$	0.274
			2.0–6.1	1500–4500	40.11	$0.0109L' - 0.022$	0.140
	50	2	0.68–2.0	500–1500	31.52	0	0.481
			2.0–6.1	1500–4500	34.03	0	0.362
Berl Saddles	13	0.5	0.68–2.0	500–1500	16.28	0.0529	0.761
			2.0–6.1	1500–4500	25.61	0.0529	0.170
	25	1	0.68–2.0	500–1500	52.14	$0.0506L' - 0.1029$	0
			2.0–6.1	1500–4500	73.0	$0.0310L' - 0.063$	-0.359
	38	1.5	0.68–2.0	500–1500	40.6	0.0508	0.455
			2.0–6.1	1500–4500	62.4	$0.0240L' - 0.0996$	-0.1355

Only SI units are used (see Table 12.2). For condition below loading, $\alpha_{AW} = m(808G'/\rho_G^{0.9})^n L^p$; $L' = \frac{4V^{(l)}}{\pi D^2}$, $G' = \frac{4V^{(g)}}{\pi D^2}$.

The liquid presents a large area for mass transfer because of the packing. The local or microscopic construction of the packed bed is illustrated in Figure 12.16. The interfacial molar fluxes per unit volume of the bed in the gas and liquid phases are also shown. The mass transfer coefficients do not carry the reference to basic experimental conditions (o), indicating that some adjustment may be necessary. Correction factors were introduced at the conclusion of Section 12.1. They are evaluated in Section 12.8 for common applications.

The interfacial conditions as well as the bulk-phase conditions are considered uniform throughout any volume element perpendicular to the vertical z -axis of the tower. The time-averaged microscopic mass balance, Equation (8.76), can then be applied to the gas and the liquid phases at steady state with the proper interpretation of the production term.

$$-\mathcal{V}_L \frac{dc_{ib}}{dV} = R_i \phi_{Lt} + N_i^{(l)} a_v \quad (12.87)$$

12.7.3.2 For the Gas For the gas, we will assume that there are no chemical reactions and that the molar density is constant. The molar average velocity is therefore constant and calculations similar to those above for the liquid phase provide the gas-phase mass balance:

$$N_G \frac{dy_{ib}}{dV} = N_i^{(ig)} a_v \quad (12.88)$$

The flux expressions are

$$N_i^{(g)} a_v = \Phi_{mi}^{(g)} k_{yi}^o a_v (y_{is} - y_{ib}) \quad (12.89)$$

$$N_i^{(l)} a_v = \Phi_{mi}^{(l)} k_{ci}^o a_v (c_{is} - c_{ib}) \quad (12.90)$$

12.7.3.1 For the Liquid

$$\underbrace{\frac{d}{dz}(\rho_i(-v_z))}_{\substack{\text{Assume constant density} \\ \Rightarrow v_z = \text{constant} \\ = \text{volume average velocity} \\ = -\frac{V_L}{\phi_{Lt} A_c} \text{ (based on cross section} \\ \text{occupied by liquid)} \\ \text{Molar basis} = -\frac{V_L}{\phi_{Lt} A_c} c_{ib}}} + \underbrace{j_{iz} + j_{iz}^l}_{\text{Neglect}} = \underbrace{r_{iv}}_{\substack{\text{source term} = \text{rate per unit volume} \\ \text{of liquid} \\ R_{iv} = \text{molar chemical reaction per unit volume} \\ \text{of liquid} \\ + \text{interfacial rate of addition per unit area of} \\ \text{interface} (N_i^{(l)}) \cdot \frac{a_v}{\phi_{Lt}}}} \quad (12.86)$$

In summary $-\frac{V_L}{\phi_{Lt} A_c} \frac{dc_{ib}}{dz} = R_i + N_i^{(l)} \frac{a_v}{\phi_{Lt}}$ or

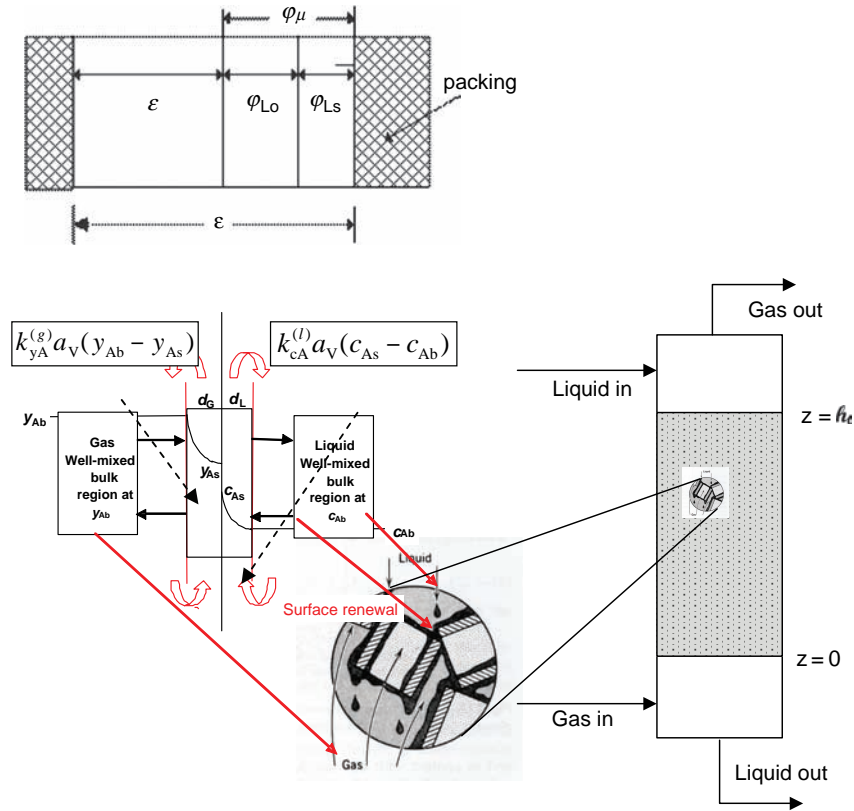


FIGURE 12.16 Microscopic construction of packed bed.

Φ_m are correction factors to account for conditions in the mass transfer film that were not present in the experiments, which determined the mass transfer coefficients. Some examples will be considered in the following section.

If the quantity of gas being absorbed is a large fraction of the feed, the assumption of a constant molar gas flow will not be tenable. In these cases, the flow basis can be taken as the nondiffusing components and the compositions as the mole ratio of the solute to the nondiffusing components, that is, $\mathcal{N}_S^{(g)}$ and $Y_A^{(g)}$, respectively. These scales are discussed in Sections 2.1.1.1 and 6.2.2. Note that the form of the driving force ($Y_{is} - Y_{ib}$) does not change, but a linear equilibrium relation will become nonlinear.

Given the bulk-phase concentrations, the interfacial compositions and hence the interfacial mass transfer rate can be obtained from simultaneous solution of the flux equalities and equilibrium relations given, respectively, by

$$\Phi_m^{(g)} k_{yi}^o (y_{ib} - y_{is}) = \Phi_m^{(l)} k_{ci}^o (c_{is} - c_{ib}) \quad (12.91)$$

$$y_{is} = E(c_{is}, \dots) \quad (12.92)$$

The mass balances provide the means to evaluate the bulk-phase compositions. Consequently, we have sufficient tools

to approximate the behavior of the condensable and volatile components in the tower.

For the noncondensable or nonvolatile components, the flux in the appropriate film at the interface is required to be zero. It may be expedient in some cases to specify the surface composition at the outset and then determine its value to meet the condition of a zero flux.

The given conditions for a new installation are

- Inlet gas stream—flow rate and composition $\mathcal{N}_i(0)$
- Inlet solvent steam—composition: $c_i(h_t)$
- The desired purity is defined: $y_i(h_t)$

12.7.3.3 Unreactive Case with Henry's Law A basic application of the preceding analysis is the case of a single gas being absorbed with no corrections required to the mass transfer coefficients, no chemical reaction in the liquid film, and phase equilibrium described by Henry's law:

$$-\mathcal{V}_L \left[\frac{dc_{Ab}}{dV} \right] = k_{cA}^o a_v (c_{As} - c_{Ab}) \quad (12.93)$$

$$\mathcal{N}_G \left[\frac{dy_{Ab}}{dV} \right] = k_{yA}^o a_v (y_{As} - y_{Ab}) \quad (12.94)$$

$$k_{yA}^o a_v (y_{Ab} - y_{As}) = k_{cA}^o a_v (c_A - c_{Ab}) \quad (12.95)$$

$$y_{As} = H c_{As} \quad (12.96)$$

Addition of the two differential equations eliminates the interfacial flux terms and provides a constant that can be evaluated at the top of the bed to give the relation between the two bulk-phase compositions:

$$y_{Ab} = \frac{\mathcal{V}_L}{\mathcal{N}_G} c_{Ab} + \left[y_{Ab,out} - \frac{\mathcal{V}_L}{\mathcal{N}_G} c_{Ab} \right] \quad (12.97)$$

Compare this result with Equation (7.11). The minimum liquid to gas ratio under the current assumptions is given by the intersection of this operating line with the equilibrium curve at the bottom of the tower (see Figure 7.12):

$$\left(\frac{\mathcal{V}_L}{\mathcal{N}_G} \right)_{\min} = \frac{y_{Ab,in} - y_{Ab,out}}{(y_{Ab,in}/H) - c_{Ab,in}} \quad (12.98)$$

A liquid to gas ratio about 50% higher than this minimum on a molar basis could be used (see the discussion above).

In order to calculate the height of the bed, one of the differential mass balances must be integrated. Choosing the liquid balance requires that the variable concentrations be replaced with functions of c_{Ab} . This can be accomplished by using the flux equality, the equilibrium condition, and the operating line. The result for the interfacial liquid composition is given by

$$c_{As} = \frac{\left[\frac{\mathcal{V}_L}{\mathcal{N}_G} + \frac{k_{cA}^o}{k_{yA}^o} \right] c_{Ab} + \left[y_{Ab,out} - \frac{\mathcal{V}_L}{\mathcal{N}_G} c_{Ab,in} \right]}{H + \frac{k_{cA}^o}{k_{yA}^o}} \quad (12.99)$$

This result can replace the interfacial concentration in the liquid phase mass balance, Equation (12.93), to give

$$\frac{dc_{Ab}}{dV} + \frac{K_{Gy}^o a_v}{\mathcal{N}_G} \left[1 - \frac{1}{A} \right] c_{Ab} = - \frac{\mathcal{N}_G}{\mathcal{V}_L} \frac{K_{Gy}^o a_v}{\mathcal{N}_G} \left[y_{Ab,out} - \frac{\mathcal{V}_L}{\mathcal{N}_G} c_{Ab,in} \right] \quad (12.100)$$

$$A = \frac{\mathcal{V}_L}{H \mathcal{N}_G} \quad (12.101)$$

and

$$\frac{1}{K_{Gy}^o a_v} = \frac{1}{k_{yA}^o a_v} + \frac{H}{k_{cA}^o a_v} \quad (12.102)$$

The quantity A is called the absorption factor. It is a measure of the absorptive capacity of the liquid and is a primarily a function of the liquid flow rate. The value of A ranges from 1.25 to 2.0 with a typical value of 1.4. In the present case,

$$A = \underbrace{\frac{[\mathcal{V}_L/\mathcal{N}_G]_{\text{Actual}}}{[\mathcal{V}_L/\mathcal{N}_G]_{\text{Min}}}}_{\text{Difficulty of separation}} \underbrace{\left[\frac{y_{in} - y_{out}}{y_{in}} \right]}_{\text{Difficulty of separation}} \quad (12.103)$$

if the inlet solvent is pure ($c_{in} = 0$).

The overall mass transfer coefficient was defined earlier (see Section 12.2) and refers to the driving force $(y - y^*)$ where y^* is the gas-phase mole fraction that is in equilibrium with the bulk liquid composition.

The differential equation may be integrated with the boundary condition

$$c_{Ab}(0) = c_{Ab,in} \quad (12.104)$$

to give the liquid concentration profile

$$c_{Ab}(z) = \left[c_{Ab,out} + \frac{1}{H(A-1)} \left(y_{Ab,out} - \frac{\mathcal{V}_L}{\mathcal{N}_G} c_{Ab,in} \right) \right] \times e^{-[(K_{Gy}^o a_v A_c / \mathcal{N}_G A)(A-1)]z} - \frac{1}{H(A-1)} \left(y_{Ab,out} - \frac{\mathcal{V}_L}{\mathcal{N}_G} c_{Ab,in} \right) \quad (12.105)$$

The value of z at the inlet liquid composition gives the height of the packing in the column:

$$h = \frac{\mathcal{N}_G}{K_{Gy}^o a_v A_c} \frac{A}{(A-1)} \ln \left[\frac{(y - y^*)_{\text{bottom}}}{(y - y^*)_{\text{top}}} \right] \quad (12.106)$$

$$y^* = H c \quad (12.107)$$

$$(y - y^*)_{\text{bottom}} = y_{Ab,in} - H c_{Ab,out} \quad (12.108)$$

$$(y - y^*)_{\text{top}} = y_{Ab,out} - H c_{Ab,in} \quad (12.109)$$

The log mean of the overall driving force is defined as

$$(y - y^*)_{\text{LM}} = \frac{(y - y^*)_{\text{bottom}} - (y - y^*)_{\text{top}}}{\ln \left[(y - y^*)_{\text{bottom}} / (y - y^*)_{\text{top}} \right]} \quad (12.110)$$

The expression for the height can be rearranged on this basis to read

$$h_t = \frac{\mathcal{N}_G}{K_{Gy}^o a_v} \frac{4}{\pi D_t^2} \frac{y_{Ab,in} - y_{Ab,out}}{(y - y^*)_{\text{LM}}} \quad (12.111)$$

The first factor on the right-hand side has the units of distance. The second is unitless and represents the number of times the average overall driving force divides into the desired concentration change. It increases with the difficulty of separation. For this reason, the factors have been called the overall height and number of transfer units, respectively.

$$h = N_{OG} H_{OG} \quad (12.112)$$

$$N_{OG} = \frac{y_{Ab, in} - y_{Ab, out}}{(y - y^*)_{LM}} = \int_{y_{Ab, out}}^{y_{Ab, in}} \frac{dy}{(y - y^*)} \quad (12.113)$$

$$H_{OG} = \frac{G}{K_{Gy}^o a_v S} \quad (12.114)$$

Using the definition of the overall mass transfer coefficient, the overall height can be divided between the liquid and gas phases:

$$H_{OG} = H_G + (H \mathcal{N}_G / \mathcal{V}_L) H_L \quad (12.115)$$

Correlations for mass transfer coefficients are sometimes given in terms of the liquid and gas side heights of transfer units.

Example 12.7.2-1: Sulfur Dioxide Absorber

An air stream flowing at 30000 ft³/h contains SO₂ at a mole fraction of 0.075. The mole fraction of SO₂ is to be reduced to 0.01 by countercurrent absorption into pure water. The pure water solvent and the gas stream are at 25 °C and 1 atm. Determine the height of packing required for the separation if 1/2 in ceramic Raschig rings are used.

Equilibrium

Solubility data over the range of operation (7.6–57 mm Hg of SO₂) are listed below and plotted in Figure 12.17 with an approximate straight line:

$$yP(\text{mmHg}) = 54.5c' \left(\frac{\text{gSO}_2}{100\text{gH}_2\text{O}} \right)$$

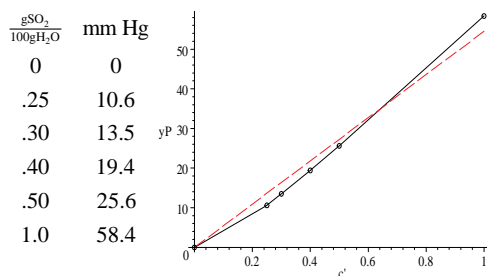


FIGURE 12.17 Linear approximation to sulfur dioxide aqueous solubility data.

The concentration unit can be converted to moles per unit volume with neglecting any volume change on mixing. The desired approximate linear equilibrium relation is then:

$$y_A = \frac{1}{760} 54.5 \frac{64.07}{0.01} = 459.45 c_A$$

$$y_A = 459.45 c_A (\text{gmol/cm}^3)$$

where $M_B = 18.02$, $M_A = 64.07$, and $A = \text{SO}_2$, $B = \text{H}_2\text{O}$

Minimum Liquid Rate:

$$c_{in} = 0.0$$

$$y_{in} = 0.075$$

$$y_{out} = 0.010$$

$$\left(\frac{\mathcal{V}_L}{\mathcal{N}_G} \right)_{\min} = \frac{0.075 - 0.01}{\frac{0.075}{459.45} - 0} = 398.19 \text{ cm}^3/\text{gmol}$$

Assuming the gas is ideal with the molecular weight of air,

$$\rho_G = \frac{MP}{RT} = \frac{29(1)}{0.732(25 + 273.16)1.8} = 7.3818 \times 10^{-2} \text{ lb/ft}^3$$

$$\mathcal{W}_G = 30000(0.073818) = 2214.5 \text{ lb/h}$$

$$\mathcal{N}_G = 2214.5(454/29) = 34668 \text{ gmol/h}$$

Using a factor of 1.5 for the liquid rate and a liquid density of 1g/cc

$$\mathcal{V}_L = 1.5(398.19)34668 = 2.0707 \times 10^7 \text{ cm}^3/\text{h}$$

$$\mathcal{W}_L = 2.0707 \times 10^7 / 454 = 45610 \text{ lb/h}$$

The outlet liquid composition

$$\mathcal{W}_L = 2.0708 \times 10^7 / 454 = 45610 \text{ lb/h}$$

$$\frac{0.075 - 0.01}{c - 0} = 1.5(398.19), \quad \text{Solution is}$$

$$c = 1.0883 \times 10^{-4} \text{ gmol/cm}^3$$

$$c_{Ab, out} = 0.00010883 \text{ gmol/cm}^3$$

Mass Transfer Coefficients

The equivalent particle diameter d_s from Table 12.1 is given by

$$a = \frac{6}{d_s} = 364 \text{ m}^{-1}$$

$$\text{or } d_s = 0.016484 \text{ m.}$$

The tower diameter is determined in Example 13.2.3-1:

$$D = 3.5 \text{ ft} = \frac{3.5}{3.2808} = 1.0668 \text{ m}$$

Liquid Side Mass Transfer Coefficient

$$\eta \approx 1 \text{ cP} = 0.00067197 \text{ lb}_m/\text{ft}$$

$$N_{\text{Re}} = \frac{\rho_L V_L d_s}{\pi D^2/4 \eta} = \frac{\frac{45610}{3600} (1.6484 \times 10^{-2} \times \frac{100}{254 \times 12})}{\frac{31416}{4} (3.5)^2} = 105.98 \quad N_{\text{Sc}} = \frac{\mu}{\rho D_{\text{Am}}} = \frac{(0.01813 \times 0.01)}{\left(\frac{7.381 \times 10^{-2} \times 454}{28317}\right) (0.13066)} = 1.1724$$

Calculation of diffusivity: Tyn–Calus method in Table 8.5.

$$V_{\text{cA}} = 122 \text{ cm}^3/\text{gmol} \text{ (Lange, 1946)}$$

$$V_{\text{cB}} = 56 \text{ cm}^3/\text{gmol}$$

$$V_{\text{A}} = 0.288 V_{\text{cA}}^{1.048} = 0.288 (122)^{1.048} = 44.248 \text{ cm}^3/\text{gmol at n.b.p.}$$

$$V_{\text{B}} = 0.288 V_{\text{cB}}^{1.048} = 0.288 (56)^{1.048}$$

$$\sigma_{\text{A}} = 28.63 \text{ at } 263 \text{ K (n.b.p.) (DIPPR, 2009)}$$

$$\sigma_{\text{B}} = 58.28 \text{ at } 373 \text{ K (n.b.p.) (DIPPR, 2009)}$$

$$P_{\text{A}} = V_{\text{A}} \sigma_{\text{A}}^{1/4} = 44.248 (28.63)^{1/4} = 102.35$$

$$P_{\text{B}} = V_{\text{B}} \sigma_{\text{B}}^{1/4} = 19.566 (58.28)^{1/4} = 54.061$$

$$\begin{aligned} D_{\text{am}} &= 8.93 \times 10^{-8} \left(\frac{V_{\text{A}}}{V_{\text{B}}^2} \right)^{1/6} \left(\frac{P_{\text{B}}}{P_{\text{A}}} \right)^2 \left(\frac{T}{\eta_{\text{B}}} \right) \\ &= 8.93 \times 10^{-8} \left(\frac{44.248}{19.566^2} \right)^{1/6} \left(\frac{54.061}{102.35} \right)^2 \left(\frac{298}{1} \right) \\ &= 5.1817 \times 10^{-6} \text{ cm}^2/\text{s} \end{aligned}$$

$$N_{\text{Sc}} = \frac{\eta}{\rho D_{\text{Am}}} = \frac{0.01}{1.0 (5.1817 \times 10^{-6})} = 1929.9$$

$$N_{\text{Sh}} = 25.1 (105.98)^{0.45} (1929.9)^{0.5} = 8990.7$$

$$k_{\text{CA}}^o = 8990.7 \frac{5.1817 \times 10^{-6}}{0.01648 (100)} = 2.8269 \times 10^{-2} \text{ cm/s}$$

Gas Side Mass Transfer Coefficient:

$$\eta \approx \eta_{\text{air}} \approx 0.01813 \text{ cP}$$

$$N_{\text{Re}} = \frac{W_{\text{G}} d_s}{(\pi D^2/4) \eta} = \frac{\frac{22145}{3600} 454}{\frac{31416 (3.5 + 12 + 2.54)^2}{4}} \frac{1.648 \times 10^{-2} \times 100}{0.01813 \times 0.01} = 284.08$$

Scale the diffusivity of sulfur dioxide in nitrogen at 1 atm and 263 K with the 1.75 power of temperature according to estimation method for binary low-pressure gases in Table 8.5.

$$D_{\text{SO}_2, \text{N}_2} P = 0.105 \text{ at } 263 \text{ K (Poling et al., 2001)}$$

$$D_{\text{Am}} = 0.105 (298/263)^{1.75} = 0.13066 \text{ cm}^2/\text{s}$$

See Table 12.2; row entries for 0.5 in ceramic Rasching rings:

$$N_{\text{Sc}} = \frac{\mu}{\rho D_{\text{Am}}} = \frac{(0.01813 \times 0.01)}{\left(\frac{7.381 \times 10^{-2} \times 454}{28317}\right) (0.13066)} = 1.1724$$

$$L_{\text{p}} = \frac{\frac{2.0707 \times 10^7}{3600} \times \frac{1}{1000}}{3.1416 \frac{(3.5/3.2808)^2}{4}} = 6.4350 = \text{kg/m}^2\text{s}$$

$$\varphi_{\text{Ls}} = \frac{0.0486 (0.001)^{0.02 (0.0583)^{0.99}}}{(1.6484 \times 10^{-2})^{1.21} (1000)^{0.37}} = 0.53752$$

$$\beta = 1.508 (1.6484 \times 10^{-2})^{0.376} = 0.32212$$

$$\varphi_{\text{LsW}} = \frac{2.47 \times 10^{-4}}{(1.6484 \times 10^{-2})^{1.21}} = 3.5486 \times 10^{-2}$$

$$\varphi_{\text{LtW}} = \frac{2.09 \times 10^{-6} (737.5 L_{\text{p}})^{0.32212}}{(1.64684 \times 10^{-2})^2} = 0.11778$$

$\eta < 0.012$ Use first entry in last column of Table 12.2 for calculation of H :

$$\begin{aligned} H &= \frac{975.7 L_{\text{p}}^{0.57} (0.001)^{0.13}}{(1000)^{0.84} (2.024 L_{\text{p}}^{0.43} - 1)} \left(\frac{0.0583}{0.073} \right)^{(0.1737 - 0.262 \log_{10} L_{\text{p}})} \\ &= 0.99765 \end{aligned}$$

See Table 12.2; row entries:

$$\begin{aligned} \varphi_{\text{Lo}} &= \varphi_{\text{LoW}} H = (\varphi_{\text{LtW}} - \varphi_{\text{LsW}}) H \\ &= (0.11779 - 0.035486) 0.99765 = 8.2111 \times 10^{-2} \end{aligned}$$

$$\varphi_{\text{Lt}} = \varphi_{\text{Lo}} + \varphi_{\text{Ls}} = 0.08211 + 0.53752 = 0.61963$$

From Table 12.1, $\varepsilon = 0.63$

$$\varepsilon_{Lo} = \varepsilon - \varphi_{LW} = 0.63 - 0.11778 = 0.51222$$

$$N_{Sh} = 1.195(1 - 0.51222)^{0.36}(284.08)^{0.64}(1.1724)^{1/3} = 36.171$$

$$\frac{k_{yA}^o}{c} = 36.171 \frac{0.13066}{0.01648(100)} = 2.8678 \text{ cm/s}$$

$$k_{yA}^o = 2.8678 \frac{7.3818 \times 10^{-2}(454)\left(\frac{1}{2.54 \times 12}\right)^3}{29}$$

$$= 1.1704 \times 10^{-4} \text{ gmol/(cm}^2\text{s)}$$

Overall Mass Transfer Coefficient

$$\frac{1}{K_{Gy}^o} = \frac{1}{1.1704 \times 10^{-4}} + \frac{459.45}{2.8269 \times 10^{-2}} = 8544.1 + 16253.$$

\Rightarrow Approximately 1/3 of the mass transfer resistance is due to the gas phase and 2/3 is due to the liquid phase.

$$K_{Gy}^o = (8544.1 + 16253.)^{-1} = 4.0327 \times 10^{-5} \text{ gmol/cm}^2\text{s}$$

Area per Unit Volume:

See Table 12.3; second row

Liquid flux (6.435 kg/m² just beyond upper limit of 6.1)

- a) $a_v = a_{AW} \frac{\varphi_{Lo}}{\varphi_{Low}} = 0.99765 a_{AW} \approx a_{AW}$ since the solution is dilute

$$h = \frac{\frac{34668}{3600} (1.3/.3)}{4.0327 \times 10^{-5} \left(\frac{39.086}{100}\right) 3.1416 \frac{1}{4} \left(\frac{3.5}{3.2808}\right)^2 10^4}$$

$$\times \ln \frac{(0.075 - 459.45 \times 0.00010883)}{(0.01 - 459.45 \times 0.)} = 271.37 \text{ cm}$$

$$h = 2.7137 \times 3.2808 = 8.9031 \text{ ft}$$

$$H_{t0G} = \frac{(34668/3600)}{4.0327 \times 10^{-5} (.39086) 3.1416 \frac{1}{4} \left(\frac{3.5}{3.2808}\right)^2 100}$$

$$= 68.35 \text{ cm} = 0.6835 \times 3.2808 : 2.2424 \text{ ft}$$

$$N_{\text{tog}} = (1.3/.3) \ln \frac{(0.075 - 459.45 \times 0.00010883)}{(0.01 - 459.45 \times 0.)} = 3.9703$$

The assumption in this section and the mass transfer results in the preceding sections have largely been limited to low mass transfer rates and a single component being

transferred. In addition, there are many applications in gas absorption where the rate of transfer is enhanced by the presence of a chemical reaction in the liquid phase film. The following section is intended to demonstrate how these limitations can be alleviated analytically in lieu of specific experimentation.

12.8 APPLIFICATION OF EXPERIMENTAL MASS TRANSFER COEFFICIENTS

The mass transfer correlations are based on measurements of unreactive systems at low mass transfer rates (diffusion alone accounts for the mass flux in the film). The film-penetration theory provides the means for extending the applicability of the mass transfer coefficients to systems undergoing physicochemical processes not present in the experimental systems. The basic assumption is that additional processes do not appreciably affect the hydrodynamic and film-replacement parameters (s, L) in the model. It turns out in many cases that only one of the parameters (s, L) is needed and the corrective action can be accomplished at the film-penetration theory limits.

In the film theory, the thickness of the film is the hydrodynamic parameter. Its value is given by the basic mass transfer coefficient as

$$L = \frac{D_A^v}{k_{cA}^o}$$

The additional processes are added to a film of this dimension and the mass transfer rate computed on this basis. Additional data are therefore not required to characterize the mass transfer process.

The penetration theory limits may also be used to make the corrections, but there appears to be no real incentive to face the more complicated mathematics since the corrections are nearly the same at both limits. A comparison will be shown below for the case of an irreversible first order reaction in the film.

12.8.1 Free Fluxes

Consider a liquid-liquid film of constant density. The calculations for this configuration are typical of what would be needed in other circumstances. The mass balance in Equation (8.82) requires that the divergence of the mass flux vector for each component be zero at steady state in an unreactive system. The mass flux must then be constant throughout the unidirectional film:

$$\rho_i v + j_i = \text{constant} = W_i \quad (12.116)$$

The total mass balance in Equation (8.83) states that for constant density

$$\rho v = \text{constant} = \sum W_k \quad (12.117)$$

for unidirectional mass transfer.

Substitution of Equation (8.161) for the diffusion flux in Equation (12.116) and using Equation (12.117) for the convection term gives

$$\frac{d\omega_i}{dz} - \left[\frac{\sum_k W_k}{\rho D_i^V} \right] \omega_i = - \left(\frac{W_i}{\rho D_i^V} \right) \quad (12.118)$$

There are two boundary conditions on the mass fraction,

$$\omega_i = \omega_{is} \quad \text{at} \quad z = 0 \quad (12.119)$$

$$\omega_i = \omega_{ib} \quad \text{at} \quad z = \frac{D_i^V}{k_{\omega i}^0} \quad \text{where} \quad k_{\omega i}^0 = \frac{M_i}{\rho} k_{ci}^0 \quad (12.120)$$

which may appear inconsistent with the order of the differential equation. The differential equation is first order, since one integration has been carried out in arriving at Equation (12.116). Consequently either of the preceding boundary conditions may be chosen or the other regarded as determining the value of W_i . The result is

$$W_i = k_{\omega A}^o \left(\frac{W_i}{\sum_k W_k} \right) \ln \frac{\omega_{ib} - (W_i / \sum_k W_k)}{\omega_{is} - (W_i / \sum_k W_k)} \quad (12.121)$$

or

$$W_i = \Phi_{im} k_{\omega}^o (\omega_{is} - \omega_{ib}) \quad (12.122)$$

where

$$\Phi_{im} = \frac{1}{\left[\left(\frac{1}{W_i} \sum W_k \right) - \omega \right]_{LM}} \quad (12.123)$$

The mass flows may be replaced with total molar flows and the mass fractions with mole fractions for the results pertaining to the assumption of a constant molar density.

A trial-and-error procedure is normally needed to solve for the mass transfer rates. Consider, for example, situations where a second film is present (e.g., liquid-liquid extraction, gas absorption and stripping, distillation, etc.), say, a primed and an unprimed phase. Since the fluxes are equal on both sides of the interface, the preceding result gives

$$\frac{\omega_{ib} - (W_i / \sum_k W_k)}{\omega_{io} - (W_i / \sum_k W_k)} = \left\{ \frac{\omega'_{ib} - (W_i / \sum_k W_k)}{\omega'_{io} - (W_i / \sum_k W_k)} \right\}^{k'_{\omega A} / k_{\omega A}} \quad (12.124)$$

Interfacial equilibrium under isothermal and isobaric conditions can be expressed as

$$\omega'_o = g(\omega_o) \quad (12.125)$$

The bulk-phase compositions are subject to material balances at the equipment level, so they may be considered as known for the present purposes. The objective is then given bulk-phase conditions, determine the associated interfacial mass transfer rates.

Following the (unproven) direct substitution method will illustrate what is needed in the cases where there are no additional restrictions on the fluxes:

- Assume values for the interfacial concentrations in the unprimed phase.

Use the equilibrium relations in Equation (12.125) to compute the interfacial concentrations in the primed phase.

- Solve Equation (12.124) for the $\frac{W_i}{\sum_k W_k}$ (and hence the W_i).
- Solve Equation (12.121) for new values of the interfacial compositions in the unprimed phase.
- Repeat the preceding three steps until the concentrations in the unprimed phase converge.

12.8.2 Constrained Fluxes

The following three examples involve circumstances where the interfacial flows are subject to additional constraints.

12.8.2.1 Diffusion Through a Stagnant Film: Absorption with Constant Flows As an example, consider the unreactive gas absorption system discussed in Section 12.7.2. A constant mass density is assumed for the liquid and a constant molar density is assumed for the gas phase. A single component A moves through the two films. This is the ideal case of a highly selective, nonvolatile solvent with the restrictions $\Phi_{mA} = 1$ and a linear equilibrium relationship, Henry's law. These restrictions are not carried over to the present calculations. Moreover, the assumption of constant flows can usually be removed through the use of mole ratios for the concentration measures. The methodology in that case is that which is followed here.

The sum of the fluxes is the flux of A and the flux expression for the gas film in Equation (12.121) becomes

$$N_A = k_{yA}^o \ln \left[\frac{1 - y_{As}}{1 - y_{Ab}} \right] = \Phi_{mA}^{(g)} k_{yA}^o (y - y_{As}) \quad (12.126)$$

where

$$\Phi_{mA}^{(g)} = \frac{1}{(1 - y_A)_{LM}} = \frac{1}{(y_B)_{LM}} \quad (12.127)$$

The correction factor is the inverse of the log mean mole fraction of the insoluble components.

For the liquid phase, we can again use molar units noting that equilibrium data as a function of molar concentration, for example, can be converted to mole fractions with (see Section 2.1.1.1 for concentration relationships).

$$x_i = \frac{c_i}{\sum c_k} \quad (12.128)$$

$$N_A = k_{xA}^o \ln \left[\frac{1 - x_{Ab}}{1 - x_{As}} \right] = \Phi_{mA}^{(l)} k_{xA}^o (x_{As} - x_{Ab}) \quad (12.129)$$

where

$$\Phi_{mA}^{(l)} = \frac{1}{(1 - x_A)_{LM}} = \frac{1}{(x_B)_{LM}} \quad (12.130)$$

The equality of the interfacial fluxes

$$\left[\frac{1 - y_{As}}{1 - y_{Ab}} \right] = \left[\frac{1 - x_{Ab}}{1 - x_{As}} \right] \frac{\Phi_{mA}^{(l)} k_{xA}^o}{\Phi_{m}^{(g)} k_{yA}^o} \quad (12.131)$$

Given the bulk-phase mole fractions, the preceding equation provides a relationship between the interfacial mole fractions that will guarantee the equality of the interfacial molar fluxes. The intersection of this function with the equilibrium relation between the interfacial concentrations, of course, provides the values that will satisfy both.

The bulk-phase values fall on the operating line, which is the material balance referred to above. The numerical procedure referred to in Section 12.8.1 arises here in the solution for the interfacial concentrations.

Either the liquid or the gas-phase mass balance may be used to determine the packing height. In the latter case (Equation (12.94) with flux correction included.

$$\mathcal{N}_p = \frac{4}{\pi D^2} \frac{\mathcal{N}_G}{k_{yA}^o} \int_{y_{Ab,out}}^{y_{Ab,in}} \frac{dy_{Ab}}{\Phi_m^{(g)} (y_{Ab} - y_{As})} \quad (12.132)$$

The specific steps required to determine the packing height are illustrated in the following example.

Example 12.8.2.1-1: Height of Packed Bed in SO_2 Absorption Using Method Suitable for Nonlinear Equilibrium Data

See Example 12.7.21- for operating conditions and data.

The objective here is to generate values for the kernel of the integral for the packed height

$$\frac{1}{\Phi_m^{(g)} (y_{Ab} - y_{As})}$$

as a function of the bulk-phase mole fraction so that it may be integrated numerically.

Equilibrium Curve

$$y(x) = 459.45 c_A = 459.45 c x = \frac{459.45}{18} x = 25.525 x \quad (A)$$

The equilibrium curve is the locus of all the interfacial concentrations in the bed.

Operating Line

$$y(x) = \frac{\mathcal{N}^{(L)}}{\mathcal{N}^{(G)}} x + y_{out} = \frac{2.0707 \times 10^7}{34668} \frac{1}{18} x + 0.01$$

$$y(x) = 33.183 x + 0.01 \quad (B)$$

The operating line is the locus of all liquid and gas-phase mole fractions (x_{Ab}, y_{Ab}) that satisfy the bulk-phase material balance.

Interfacial Flux Equality

Because of the dilute concentrations, the correction factors in the flux equality will be omitted.

$$\frac{k_{xA}^o}{k_{yA}^o} = \frac{1}{18.02} \frac{2.8269 \times 10^{-2}}{1.1704 \times 10^{-4}} = 13.404$$

$$y(x) = 1 - \frac{(1 - y_{Ab})}{[(1 - x)/(1 - x_{Ab})]^{13.404}} \quad (C)$$

Given a point on the material balance, the flux equality is the locus of all gas-liquid combinations that will result in equal fluxes on each side of the interface. The combination that satisfies the equilibrium condition is required here. Substitution of the equilibrium relation for the gas-phase mole fraction provides a single nonlinear algebraic equation. (See Table 12.4)

Intersection of Flux Equality with Equilibrium Curve

$$25.525 x = 1 - \frac{(1 - y_{Ab})}{[(1 - x)/(1 - x_{Ab})]^{13.404}}$$

$$\int_{y_{Ab,out}}^{y_{Ab,in}} \frac{dy_{Ab}}{\Phi_m^{(g)} (y_{Ab} - y_{As})} \approx$$

$$\begin{aligned} (\text{Trapezoidal rule}) &= (294.43/2 + 266.10 + 243.07 \\ &+ 224.05 + 208.01 + 194.37 + 182.63 + 172.33 \\ &+ 163.39 + 155.38 + 148.33 + 142.00 + 136.29 \\ &+ 83.7/2) 0.005 = 12.125 \end{aligned}$$

TABLE 12.4 Summary of Results

y_{Ab}	x_{Ab}	x_{As}	y_{As}	$\Phi_m^{(g)}$	$\frac{1}{\Phi_m^{(g)}(y_{Ab} - y_{As})}$
0.01	0	2.576×10^{-4}	6.5752×10^{-3}	0.99167	294.43
0.015	1.5068×10^{-4}	4.3847×10^{-4}	2×10^{-2}	0.98687	266.10
0.02	3.0136×10^{-4}	6.1943×10^{-4}	1.5811×10^{-2}	0.98213	243.07
0.025	4.5204×10^{-4}	8.0049×10^{-4}	2.0433×10^{-2}	0.97733	224.05
0.03	6.0272×10^{-4}	9.8165×10^{-4}	2.5057×10^{-2}	0.97248	208.01
0.035	7.5340×10^{-4}	1.1629×10^{-3}	2.9683×10^{-2}	0.96768	194.37
0.04	9.0408×10^{-4}	1.3443×10^{-3}	3.4313×10^{-2}	0.96283	182.63
0.045	1.0548×10^{-3}	1.5257×10^{-3}	3.8943×10^{-2}	0.95804	172.33
0.05	1.2054×10^{-3}	1.7073×10^{-3}	4.3579×10^{-2}	0.95320	163.39
0.055	1.3561×10^{-3}	1.8889×10^{-3}	4.8214×10^{-2}	0.94841	155.38
0.06	1.5068×10^{-3}	2.0707×10^{-3}	5.2855×10^{-2}	0.94357	148.33
0.065	1.6575×10^{-3}	2.2526×10^{-3}	5.7498×10^{-2}	0.93879	142.00
0.07	1.8082×10^{-3}	2.4346×10^{-3}	6.2143×10^{-2}	0.93388	136.29
0.075	1.9588×10^{-3}	2.6166×10^{-3}	6.6789×10^{-2}	0.92911	83.714

See Figure 12.18, letters refer to discussion points in the text.

$$V = \frac{\mathcal{N}_G}{k_{yA}^0 a_v} \int_{y_{Ab,out}}^{y_{Ab,in}} \frac{dy_{Ab}}{\Phi_m^{(g)}(y_{Ab} - y_{As})}$$

$$= \frac{34668}{3690} \frac{1}{0.00011704(0.39)} \frac{35.3145}{10^6} 12.125 = 88.133 \text{ ft}^3$$

$$h = \frac{4(88.133)}{3.1416(3.5)^2} = 9.1603 \text{ ft}$$

12.8.2.2 Equimolar Counter-Diffusion In distillation, there are repeated condensations and vaporizations. The condensation process provides the energy required for the vaporization. When the latent heats are nearly equal, the molar condensation rate is approximately equal to the vaporization

rate. In this case, there is no net molar flux through the film and

$$N_A = k_{yA}^0 (y_{As} - y_{Ab}) \quad \Phi_{mA} = 1 \quad (12.133)$$

No correction is necessary in this case.

12.8.2.3 Heterogeneous Chemical Reaction In this application, as in the previous three cases, there is no reaction in the film. However, the film here shares a boundary with the reaction zone and is the sole means by which reactants and products can enter or leave the otherwise closed zone. Examples are the catalytic pellet and the laminar flow reactor with catalytic walls, discussed in Section 10.5.2.

If in the reaction zone there is a single reaction proceeding at steady state, the molar fluxes through the film must be in the proportions dictated by the reaction

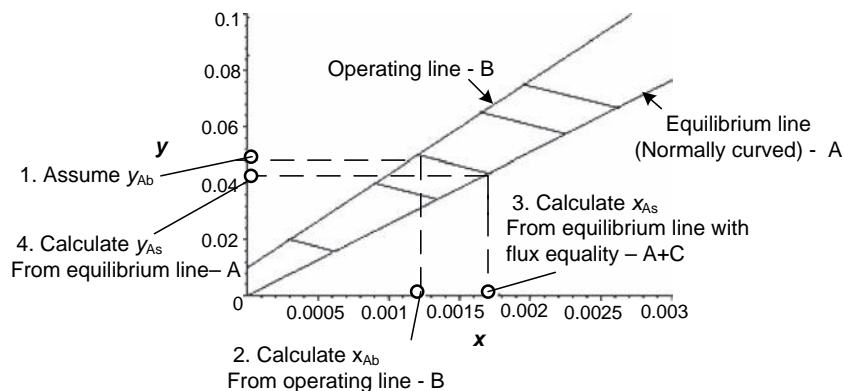


FIGURE 12.18 Graphical illustration with explanations for $y_{Ab} = 0.05$.

stoichiometry:

$$N_i = \frac{\vartheta_i}{\vartheta_\alpha} N_\alpha \quad (12.134)$$

The inert flows are zero. The total molar flow will be nonzero if there is a mole change in the reaction:

$$\sum N_i = \frac{N_\alpha}{\vartheta_\alpha} \sum \vartheta_i = \frac{\Delta n}{\vartheta_\alpha} N_\alpha \quad (12.135)$$

The adjustment factors are given by

$$\Phi_{iy} = \frac{1}{(1 - \frac{\Delta n}{\vartheta_i} y_i)_{LM}} = \frac{1}{\frac{\Delta n}{\vartheta_i} (y_{is} - y_{ib})} \ln \left[\frac{1 - \frac{\Delta n}{\vartheta_i} y_{ib}}{1 - \frac{\Delta n}{\vartheta_i} y_{is}} \right] \quad (12.136)$$

$$N_i = k_{yi}^o \frac{1}{\frac{\Delta n}{\vartheta_i}} \ln \left[\frac{1 - \frac{\Delta n}{\vartheta_i} y_{ib}}{1 - \frac{\Delta n}{\vartheta_i} y_{is}} \right] = k_{yi} \Phi_{iy} (y_{is} - y_{ib}) \quad (12.137)$$

However, in most cases, Equation (12.134) would be used instead of determining the additional steps that are called for in the previous two equations.

These results apply, for example, to the porous catalytic pellet. The mass transfer film surrounds the particle and the two share the exterior surface of the pellet as a boundary and we face the problem of calculating the reaction rate in the pellet given the bulk-phase conditions.

It is shown in Section 11.2.1 that the concentrations and temperature throughout the catalytic pellet can be expressed in terms of the surface concentrations and temperature. For the current discussion, we may take the temperature and pressure as specified and write the total reaction rate in the pellet in terms of the effectiveness factor (also a function of the surface conditions) and the reaction rate if the surface conditions persisted throughout the pellet. This must be equal to the mass transfer rate at steady state. Consequently,

$$k_{iy}^o \Phi_{iy} (y_{ib} - y_{is}) A_p = \vartheta_i \mathcal{E} \mathcal{R}_s (y_{1s}, y_{2s}, \dots, y_{N_{cs}}) V_p \quad (12.138)$$

Because of the stoichiometric relation of the fluxes, Equation (12.134), all of the surface concentrations may be linked to the mole fraction of the key component:

$$k_{iy}^o \Phi_{iy} (y_{is} - y_{ib}) A_p = \frac{\vartheta_i}{\vartheta_\alpha} k_{\alpha y}^o \Phi_{\alpha y} (y_{\alpha s} - y_{\alpha b}) A_p \quad (12.139)$$

or

$$y_{is} = y_{ib} + \frac{\vartheta_i}{\vartheta_\alpha} \frac{k_{\alpha y}^o \Phi_{\alpha y}}{k_{iy}^o \Phi_{iy}} (y_{\alpha s} - y_{\alpha b}) \quad (12.140)$$

Substitution of this result into Equation (12.138) provides a single nonlinear algebraic equation for the surface concentration of the key component, which will in turn provide the reaction rate.

The preceding calculations can be applied, for example, to the reaction rate data and the fixed-bed reactor design.

12.8.2.4 Kinetics Experiments In the determination of intrinsic kinetics, it is important that the concentrations be known at the catalyst surface for model discrimination and parameter determination. The experimental conditions are normally adjusted to the point where it is convincing that the bulk-phase conditions persist up to the catalyst surface. For example, consider the Berty internal recirculation reactor illustrated in Figure 12.19.

A fixed-bed arrangement is situated inside a reaction chamber where a fan, situated over the fixed bed, pulls the contents of the reaction chamber over the bed at a very high rate. The rate is determined by the RPM of the fan. The RPM is increased until the reaction rate, as determined by a material balance over the reactor, does not respond.

In so doing, the fan produces uniform conditions throughout the reaction chamber (a CSTR). If, for example, the catalyst is coated on the exterior surface of the support, Equation (12.138) can be used as follows to calculate the surface concentrations. At this point, the

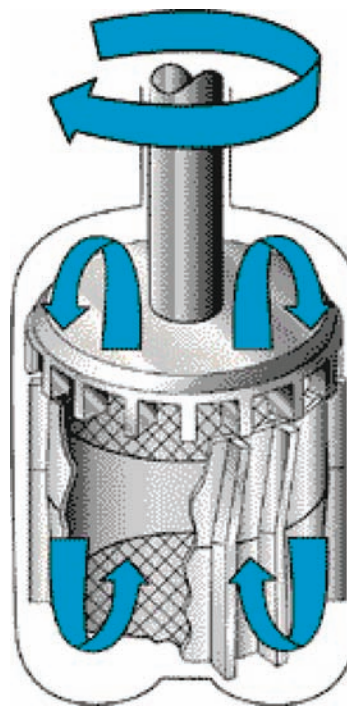


FIGURE 12.19 Berty internal recirculation reactor. Reprinted with permission of Autoclave Engineering.

conditions over the catalyst are uniform and equal to the surface conditions:

$$\underbrace{k_{iy}^o}_{\substack{\text{From performance} \\ \text{characteristics of fan (see} \\ \text{Couper et. al.),} \\ \text{catalyst dimensions, and} \\ \text{obtain gas velocity in bed.} \\ \text{Use Equation (12.4-1).}}} \underbrace{\Phi_{iy}(y_{ib} - y_{is})}_{\substack{\text{Set bulk-phase mole} \\ \text{fractions equal to} \\ \text{measured values in} \\ \text{reactor exit stream.}}} \underbrace{\frac{A}{V}}_{\substack{\frac{6}{D_p} \text{ for} \\ \text{spheres}}} = \underbrace{\mathcal{E}}_{\substack{1 \text{ since} \\ \text{the reaction} \\ \text{is confined} \\ \text{to the exterior} \\ \text{surface}}} \underbrace{\vartheta_i \mathcal{R}_s(y_{1s}, y_{2s}, \dots, y_{N_{cs}})}_{\substack{\text{From material balance over} \\ \text{the reactor = difference between} \\ \text{inlet and outlet molar flows of} \\ \text{species } i.}} \quad (12.141)$$

12.8.2.5 Fixed-Bed Reactor Modeling This basic reactor model can provide estimates of the tube dimensions and the wall temperature required for a specified conversion and can be used for optimization studies as a one-dimensional model. The model is discussed in Chapter 14. Here, the incorporation of the reaction system in the microscopic mass balance for fluid phase is illustrated (refer to Figure 12.20).

The diffusion-reaction process within the catalyst in a fixed bed is envisioned to take place locally at the prevailing bulk-phase conditions at that location (see Section 8.7.4). The interaction of the two phases in this regard is the stoichiometric transfer of mass across the fluid-solid interface. The associated heat effect is discussed in Chapter 14. At steady state, the interfacial mass transfer rate must be equal to the reaction rate as illustrated in Figure 12.22. The interfacial concentration is the linkage between the two processes. Its value adjusts to make the rates of transfer equal.

The equality can, in principle, be used to generate a functional relationship between the surface and bulk-phase concentrations. It may be expedient in this regard to assume values of the surface concentration and to determine the associated bulk-phase concentration with the equality. The relationship can be generated *a priori* followed by integration of the bulk-phase equations. The two processes are thus uncoupled (Tortoriello and DeLancey, 2007).

12.8.3 Homogeneous Chemical Reaction

Chemical reactions are often employed to increase the absorption rate and capacity of a liquid solvent as a solute in gas absorption operations. Some commercial examples are given in Table 12.5.

To appreciate the enhancement of the absorption rate, consider a liquid phase element in a mass transfer film (i.e., film-penetration theory). For the purposes of discussion, fix the concentrations of a solute A at the boundaries and examine the effect of increasing the rate of reaction on the concentration profile (refer to Figure 12.21).

The concentration profile is linear for the case of no reaction. As the reaction rate is increased, the concentration of A is diminished in the liquid phase, remaining subject to the fixed concentrations at the boundaries of the film. The absorption flux of A across the interface is proportional to the slope at $z = 0$, which increases with the reaction rate. The enhancement of the rate by the chemical reaction can then be measured by

$$\text{Enhancement} = \frac{\left. \frac{dc_A}{dz} \right|_{z=0, \text{ with reaction}}}{\left. \frac{dc_A}{dz} \right|_{z=0, \text{ without reaction}}} \quad (12.142)$$

Very slow reactions will not take place to any appreciable extent in the film and will therefore have little effect on the

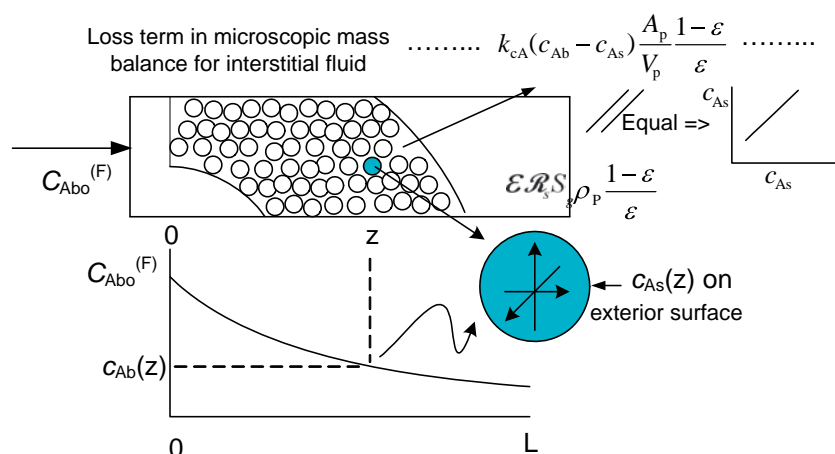
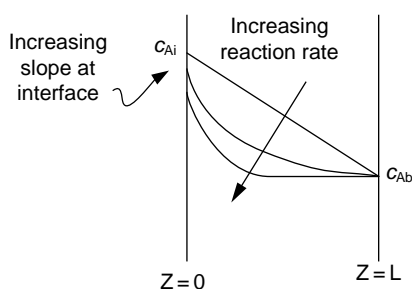


FIGURE 12.20 Communication of solid catalyst with a fluid phase in a fixed bed.

TABLE 12.5 Commercial Examples of Chemical Absorption

Solute–Gas Phase Reactant	Absorbent–Aqueous Phase Reactant	Reaction Type
Carbon dioxide	NaOH	Irreversible
Hydrochloric acid	NaOH	Irreversible
Hydrocyanic acid	NaOH	Irreversible
Hydrofluoric acid	NaOH	Irreversible
Hydrogen sulfide	NaOH	Irreversible
Carbon monoxide	Cuprous ammonium salts	Reversible
Carbon monoxide and hydrogen sulfide	Monoethanolamine or diethanolamine	Reversible
Carbon monoxide and hydrogen sulfide	Diethylene glycol or triethylene glycol	Reversible

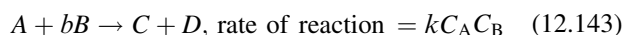
**FIGURE 12.21** Effect of the reaction rate on the concentration profile.

absorption rate. These reactions will be primarily confined to the bulk region. Very fast reactions, on the other hand, will be completed in the film region, and the concentration of the solute gas in the bulk will be zero or at its equilibrium.

The film-penetration theory predicts a much different dependence of the mass transfer coefficient on the solute diffusivity between its two limits. However, the difference in the relative effect of chemical reaction on the mass transfer coefficient is not nearly so dramatic between the two limits. In fact, the difference is often within the error of the physical parameters. The similarity of the predictions of the mass transfer theories will be demonstrated for the first-order irreversible kinetics. Instantaneous reaction kinetics will be considered with the film theory to represent very fast reactions. Approximations for more complicated kinetics are introduced.

12.8.3.1 Irreversible First-Order Kinetics

12.8.3.1.1 Film Theory As an example of the beneficial effects of the chemical reaction, consider the case where



Here A is the gas-phase solute, B is a nonvolatile reactant in the liquid phase, and C and D are nonvolatile reaction products. An example of such a system is the absorption of carbon dioxide (A) by sodium hydroxide ($\text{OH}^- = B$).

If the concentration of B in the bulk liquid is very much greater than the concentration of A at the interface, that is, a low partial pressure of A in the gas phase, the concentration of B in the film may be taken as nearly constant. In this case, the diffusion–reaction problem in the film is given by

$$D_{Am} \frac{d^2 c_A}{dz^2} - k c_{Bb} c_A = 0 \quad (12.144)$$

$$c_A = c_{Ai} \quad \text{at } z = 0 \quad (12.145)$$

$$c_A = c_{Ab} \quad \text{at } z = \frac{D_{Am}}{k c_{Bb}} \quad (12.146)$$

The concentration of B may be replaced with the catalyst concentration in the hydration of carbon dioxide by hypochlorite solutions. The concentration of B may also be replaced with kinetic and other factors as in the absorption of carbon dioxide by buffered solutions of carbonate and bicarbonate. There are a variety of circumstances where the rate of disappearance of a dissolved gas is proportional to the first power of the concentration so that the kinetic factors in the present formulation should be broadly interpreted.

The interfacial flux of A can be obtained by differentiating the concentration profile and evaluating the derivative at the interface. The result is

$$N_{Ao} = k_{cA}^o \sqrt{k c_{Bb} D_{Am}} \frac{c_{Ai} \cosh \sqrt{k c_{Bb} D_{Am}} - c_{Ab}}{\sinh \sqrt{k c_{Bb} D_{Am}}} \quad (12.147)$$

Under the assumed conditions it is likely that the concentration of A in the bulk phase may be neglected in the numerator in which case

$$N_{Ao} = \Phi_{Ar} k_{cA}^o (c_{Ai} - c_{Ab}) \quad (12.148)$$

The enhancement factor is given by

$$\Phi_{Ar} = \frac{N_{Ha}}{\tanh N_{Ha}}, \quad \text{where} \quad (12.149)$$

$$N_{Ha} = \frac{1}{k_{cA}^0} \sqrt{k c_{Bb} D_{Am}} \quad (12.150)$$

The dimensionless Hatta number is denoted by N_{Ha} . Note that the enhancement factor is greater than unity and approaches the value of the Hatta number.

12.8.3.1.2 Penetration Theory The same reaction taking place in the very young elements on the surface is described by unsteady-state unidirectional diffusion without convection. The simplifications of the general mass balance used to arrive at the microscopic balances in Table 10.1 can be followed here without dropping the transient accumulation term. The penetration theory formulation is then given by

$$\frac{\partial c_A}{\partial t} = D_A^y \frac{\partial^2 c_A}{\partial x^2} - k_r c_A \quad (12.151)$$

$$c_A(0, t) = c_{As} \quad t \geq 0 \quad (12.152)$$

$$c_A(x, 0) = 0 \quad x > 0 \quad (12.153)$$

$$c_A(\infty, t) = 0 \quad t \geq 0 \quad (12.154)$$

The bulk concentration has again been taken to be zero to maintain the grounds for comparison. The solution was obtained by Danckwerts (1953). The amplification factor is given by

$$\Phi_{Ar} = N_{Ha} \left[\operatorname{erf} \frac{N_{Ha}}{\sqrt{\pi}} + \frac{e^{-\frac{N_{Ha}^2}{\pi}}}{\operatorname{erf} \frac{N_{Ha}}{\sqrt{\pi}}} \right] \quad (12.155)$$

12.8.3.2 Surface Renewal Theory In the case of the surface renewal theory, the interfacial flux is given by

$$N_{A0} = \int_0^\infty s e^{-st} N_A(0, t) dt \quad (12.156)$$

where $N_A(0, t)$ is the flux into a surface element of age t . This can be obtained from the solution to the penetration theory formulation or advantage may be taken of the equivalence of the preceding equation to the Laplace transform:

$$N_{A0} = -s D_{Am} \left[\frac{\partial c_A}{\partial x} \right]_{x=0} = -s D_{Am} \frac{d\bar{c}_A(x, s)}{dx} \bigg|_{x=0} \quad (12.157)$$

The Laplace transform in time is required, not the inverse. Consequently the calculations may be carried out in the Laplace domain, thereby decreasing the dimensionality of the problem by one.

The penetration theory in the Laplace domain follows from Equations (12.151) to (12.154):

$$\frac{d\bar{c}_A(x, s)}{dx^2} - \left(\frac{k+s}{D_{Am}} \right) \bar{c}_A(x, s) = 0 \quad (12.158)$$

$$\bar{c}_A(0, s) = \frac{c_{Ai}}{s} \quad (12.159)$$

$$\bar{c}_A(\infty, s) = 0 \quad (12.160)$$

The solution is

$$\bar{c}_A(x, s) = \frac{c_{Ai}}{s} e^{-\sqrt{\frac{k+s}{D_{Am}}} x} \quad (12.161)$$

$$N_{A0=D_{Am}} \sqrt{\frac{k+s}{D_{Am}}} c_{Ai} \quad (12.162)$$

The correction or enhancement factor is then

$$\Phi_{rA} = \sqrt{1 + N_{Ha}^2} \quad (12.163)$$

The three results are compared in Figure 12.22, which illustrates the validity of the comments made at the outset concerning the similarity of the three corrections.

12.8.3.3 Instantaneous Reactions A limiting case of very fast reaction kinetics, which finds practical application, is the instantaneous reaction between a soluble gas component (A) and a dissolved solute (B). In the limit, these components cannot coexist. In the unidirectional case, there must exist a reaction plane, which separates two reactants. The plane will be located in the liquid film at the gas-liquid interface at such a position where the stoichiometric quantities of the reactants can be delivered. Note that a flux ratio vanishes at one boundary and is infinite at the other. The situation is illustrated in Figure 12.23.

The stoichiometric requirement of the fluxes is given by

$$\frac{D_{Am} c_{As}}{d_R} = \frac{1}{b} \frac{D_{Bm} c_{Bb}}{(D_{Am}/k_{cA}^0) - d_R} \quad (12.164)$$

This result provides the location of the reaction plane, which gives the absorption rate of component A:

$$N_{A0} = k_{cA}^0 \left[1 + \frac{1}{b} \frac{D_{Am} c_{Bb}}{D_{Bm} c_{As}} \right] c_{As} \quad (12.165)$$

was carried out in a fixed bed of impermeable particles coated with a catalyst at 362°C and atmospheric pressure in the presence of a large excess of nitrogen. At a point in the reactor where the cumene partial pressure was 0.0689 atm, a reaction rate of $0.153\text{ kmol cumene}/(\text{kg cat h})$ was observed. Determine the mole fraction of cumene at the catalyst

surface at this point in the reactor assuming isothermal conditions.

The coated area of the catalyst is a $45\text{ m}^2\text{ cat}/\text{kg cat}$ and the interstitial mass flux is $56.47\text{ kg}/(\text{m}^2\text{ h})$.

See Problem 14.1 for the nonisothermal case.

13

INTERPHASE MOMENTUM TRANSFER UNDER TURBULENT CONDITIONS

The interphase momentum transfer process refers here to the transfer of momentum from a flowing fluid to solid or a nearly rigid liquid interface. The loss of momentum by the fluid is important, for example,

- for steady flow in pipelines, the loss must be replaced with a blower, pump or compressor of appropriate size,
- in operations where submerged objects may be suspended by the fluid, the velocity of the fluid is a primary factor in the momentum transferred to the solid, determining the required process conditions and/or equipment size as well.

The items listed on the right-hand side (terminal points) of Figure 13.1 fall into the circumstances in the preceding list and represent a summary of what is presented in this chapter.

The surface element on the left-hand side of Figure 13.1, dA , represents a solid or fluid phase over which a fluid is flowing with a velocity v . The surface is considered closed to mass transfer or that the contribution of the mass transfer process to the interfacial momentum transfer process across the surface can be neglected.

A local friction coefficient, ϕ , is defined as a fraction of the convective flux of s momentum, which flows to the surface:

$$dF_s = \phi[\rho v_s v_s]dA \quad (13.1)$$

The force, dF_s , is due to the fluid motion. If the physical conditions are approximately constant over the surface, the preceding equation may be integrated to give

$$F_s = \phi[\rho v_s v_s]A \quad (13.2)$$

In the case of empty tubes, dA is located on the inside surface of the tube. The same interpretation holds for the pressure drop in packed beds since these are modeled as bundles of empty capillaries that offer passage through the bed. A momentum balance on the fluid enclosed by A provides a relationship for the pressure drop containing the friction factor, Φ , which is discussed in Section 9.2.1 for laminar flow. The inverse of the relationship for the pressure drop is used to experimentally extend the results to turbulent flow.

For flow in conduits, the area A is taken to be the wetted surface whereas for flow over submerged objects, the area is taken to be the projected area of the solid on a plane perpendicular to the velocity vector. In both cases, a factor of $1/2$ is extracted from the friction coefficient to change the interpretation of the bracketed term to a kinetic energy concentration. This is consistent with the form of the friction loss in pipelines that appears in the mechanical energy balance [see Equation (4.14)]. Friction coefficients for submerged objects are referred to as drag coefficients.

The last three items on the right-hand side of Figure 13.1 are all concerned with the effect of the gas velocity on the

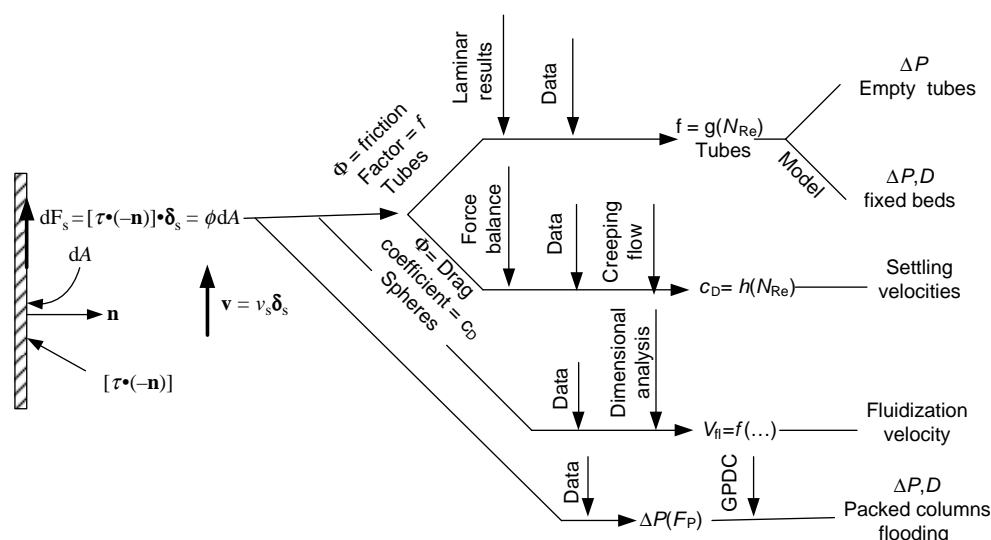


FIGURE 13.1 Overview of this chapter.

entrained particle. In the case of settling velocities, the shear forces do not overcome the body forces and the particle can settle out of a suspension with a steady terminal velocity (see Example 5.3.2.3-1 for power requirements for solid suspensions).

For fluidization and flooding in packed towers, the objective is to determine the fluid velocity that will just suspend the particle. If the velocity is greater than this value, the particles will be carried overhead. In this and the preceding case, a momentum balance on the particle reveals that the quantity

$$\sqrt{\frac{\rho - \rho_f}{\rho_f}}$$

has a significant influence on the flooding velocity. This proves to be the case empirically for the cases considered here as well as other two phase operations [e.g., tray towers, gas liquid separators (see Section 6.3)].

13.1 PRESSURE DROP IN CONDUITS AND FIXED BEDS

Laminar flow in circular conduits was considered in Chapter 9. As the flow velocity approaches a Reynolds number of approximately 2100, a flow instability is presented as a fluctuating component of the velocity field (see Chapter 8). The expressions for the momentum flux change in order to account for the fluctuating component of the velocity. In tube flow, the velocity vanishes at the wall, which gives rise to a laminar regime near the tube wall and a gradual

transition to the turbulent regime upon moving radially to the center of the tube. The extra contribution of eddy momentum transport decreases the gradient in velocity that is observed in laminar flow. The flow regimes are depicted in Figure 13.2.

Experimental data and approximate expressions are available for the turbulent velocity distribution in circular tubes (Bird et al., 2002).

For flow in tubes, the coefficient ϕ in Equation (13.1) is replaced with $f/2$ and dA is identified as a differential element on the wetted cylindrical surface of the pipe with the direction s pointing along the axial direction, z , in the pipe. The development of the friction factor for turbulent flow follows that for laminar flow in Section 9.2.1. The velocity v_s is taken as the average velocity in the pipe, which is constant for a constant density fluid. The friction factor can then be expressed as

$$f = \frac{1}{\pi R L \rho \langle v \rangle} \int_0^L \int_0^{2\pi} \tau_{zr}|_{r=R} R d\theta dz \quad (13.3)$$

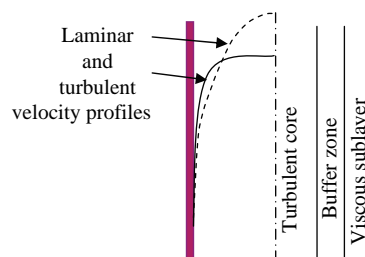


FIGURE 13.2 Flow regimes for turbulent flow in pipes.

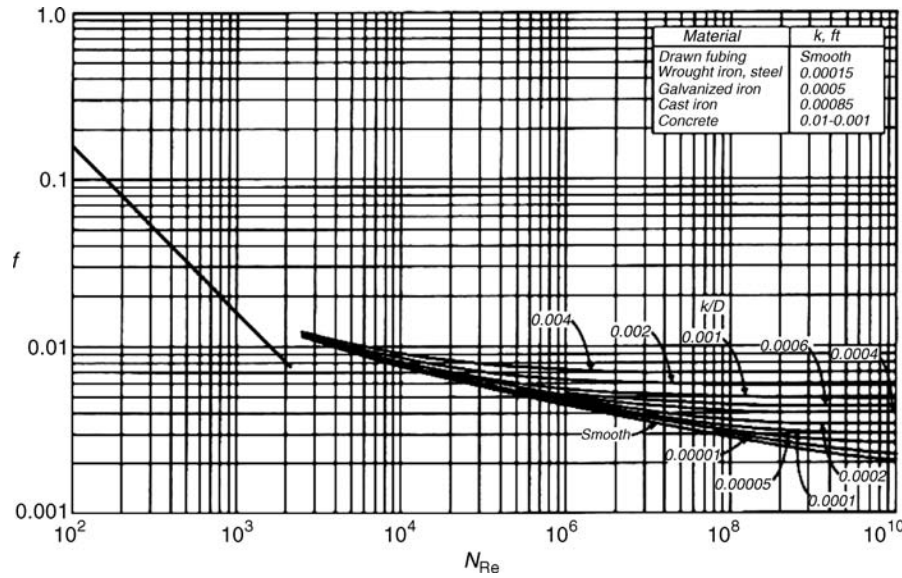


FIGURE 13.3 Correlation of the Fanning friction coefficient for flow in tubes. As reported in McCabe et al. (2001). Reprinted with permission of McGraw-Hill.

and from a momentum balance on an element of fluid of length L ,

$$f = \frac{1}{4(L/D)} \frac{[(P_1 - P_2) + \rho g L]}{(1/2)\rho \langle v \rangle^2} \quad (13.4)$$

In a flow experiment, all of the variables on the right-hand side are measured. The calculated values of the friction factor are then correlated with the Reynolds number. In an application, the pressure drop is calculated with the correlated value of the friction factor.

For a Newtonian fluid, the dimensionless momentum balance in Chapter 8 implies that the dimensionless form of Equation (13.3) is given by

$$f = f(N_{Re}, N_{Fr}, L/D) \quad (13.5)$$

The Froude number and L/D have not been found experimentally to be important.

A well-known correlation is shown in Figure 13.3.

These results are based on isothermal flow. For non-isothermal applications, for example, pressure drop in heat exchanger tubes, a correction factor,

$$\left[\frac{\eta}{\eta_w} \right]^{0.14}$$

is included on the right-hand side of Equation (13.5) (Peters et al., 2003). The viscosity ratio is the value at the bulk temperature relative to the value at the tube wall (heat transfer surface).

The results may also be applied to noncircular cross sections by using an equivalent diameter equal to the ratio

of the open cross section to the wetted perimeter. The ratio is called the hydraulic radius, R_h , for noncircular cross sections. For a circular tube, this ratio is $D/4$. The preceding equations are applied to tubes with noncircular cross sections by everywhere replacing the diameter with $4R_h$.

13.1.1 Turbulent Flow of Gases in Pipelines

The flow of gases in pipelines may be considered incompressible for small changes in pressure and temperature. Otherwise, an equation of state, $P = P(V, T)$, for a pure component must be used for the density to adequately account for these changes. The simplest is the ideal gas equation of state. Cubic forms are introduced in Chapter 5. A truncated virial equation of state will be used below for illustration.

For small Mach numbers (velocity relative to the speed of sound in the gas), the pressure distribution for adiabatic flow is close to that for isothermal flow (McCabe et al., 2001) and the simpler equations for isothermal flow may be used. We will be concerned with subsonic flows of gases under isothermal conditions. The velocity of sound in gases is given by Berry et al. (1980).

$$c^2 = \left(\frac{\partial P}{\partial \rho} \right)_s \quad (13.6)$$

which reduces to

$$c = \sqrt{\frac{RT\gamma}{M}}, \quad \gamma = \frac{c_p}{c_v} \quad (13.7)$$

for ideal gases.

The mechanical energy balance is generally applied to sections of process equipment as indicated in Equation (4.15). Equation (4.15) was the result of a macroscopic thermodynamic argument. The same result can be achieved from the microscopic view adopted at this juncture as expressed by the microscopic mechanical energy balance in Equation (8.92). The integration of Equation (8.92) over a finite volume of equipment is carried out in Chapter 15 (see Section 15.3). The result is Equation (4.14) with the determinations that

$$W_s = \int_V \nabla \cdot (\mathbf{\tau} \cdot \mathbf{v}) dV \quad (13.8)$$

$$E_v = \int_V (-\mathbf{\tau} : \nabla \mathbf{v}) dV \quad (13.9)$$

13.1.1.1 Isothermal Flow in Pipelines The density varies continuously along the pipeline due to the change in pressure so that the differential form of the mechanical energy balance is needed:

$$v dv + \frac{dP}{\rho} + dE_v = 0 \quad (13.10)$$

$$v_2 = \sqrt{\frac{(RT/M)(1/b^2) \left\{ b \left[\frac{1}{(\hat{V}_1 - b)} - \frac{1}{(\hat{V}_2 - b)} \right] + \ln \left[\frac{\hat{V}_2(\hat{V}_1 - b)}{\hat{V}_1(\hat{V}_2 - b)} \right] \right\}}{\ln(\hat{V}_2/\hat{V}_1) + (2L/D)f(N_{Re})}} \hat{V}_2 \quad (13.17)$$

The friction loss term for pipelines is given by Equation (4.22). The Reynolds number is constant since the density and velocity vary in proportion to satisfy the mass balance for a uniform cross section

$$\begin{aligned} \rho v &= \text{constant} = G \\ \text{or} \\ v &= G\hat{V} \end{aligned} \quad (13.11)$$

The friction factor is therefore constant and the differential form of the mechanical energy balance reads

$$\frac{d\hat{V}}{\hat{V}} + \frac{1}{G^2} \left(\frac{\partial P}{\partial \hat{V}} \right)_{T,x} \frac{d\hat{V}}{\hat{V}} + \frac{2}{D} f(N_{Re}) dL = 0 \quad (13.12)$$

If the gas obeys the truncated virial equation of state (see Table 2.3), the mechanical energy balance becomes

$$\frac{d\hat{V}}{\hat{V}} - \frac{RT}{MG^2} \frac{d\hat{V}}{\hat{V}(\hat{V} - b)^2} + \frac{2}{D} f(N_{Re}) dL = 0 \quad (13.13)$$

and the results that follow will be valid up to reduced densities of approximately 0.5. If an upstream position is fixed at “1” integration of Equation (13.13) downstream to a point “2,” a length L away, gives

$$\begin{aligned} \ln \frac{\hat{V}_2}{\hat{V}_1} + \frac{RT}{MG^2} \frac{1}{b^2} \left\{ b \left[\frac{1}{\hat{V}_2 - b} - \frac{1}{\hat{V}_1 - b} \right] + \ln \left[\frac{\hat{V}_1(\hat{V}_2 - b)}{\hat{V}_2(\hat{V}_1 - b)} \right] \right\} \\ + \frac{2L}{D} f(N_{Re}) = 0 \end{aligned} \quad (13.14)$$

The downstream pressure may be determined by substituting the equation of state or by solving the two equations simultaneously. Substitution of the equation of state gives

$$\begin{aligned} \ln \frac{(RT/MP_2) + b}{(RT/MP_1) + b} + \frac{1}{G^2} \frac{1}{b^2} \left\{ b[P_2 - P_1] \right. \\ \left. + \frac{RT}{M} \ln \left[\frac{(RT/MP_1) + bP_1}{(RT/MP_2) + bP_2} \right] \right\} + \frac{2L}{D} f(N_{Re}) = 0 \end{aligned} \quad (13.15)$$

which reduces to the case of an ideal gas as b approaches zero

$$-\ln \frac{P_2}{P_1} + \frac{M}{2RTG^2} [P_2^2 - P_1^2] + \frac{2L}{D} f(N_{Re}) = 0 \quad (13.16)$$

The downstream gas velocity is given by

For an ideal gas the result is

$$v_2 = \sqrt{\frac{(M/2RT) [P_1^2 - P_2^2]}{\ln(P_1/P_2) + (2L/D)f(N_{Re})}} \hat{V}_2 \quad (13.18)$$

Example 13.1.1.1-1: Pressure Drop and Pipe Size for Gas Supply Line

Consider the isothermal flow of natural gas in a pipeline that is to be provided with compressor stations every 20 miles. These compressors are to restore the pressure to 100 psia, the original input pressure. Assume first ideal behavior and check for corrections that may be needed due to nonideality.

a. Ideal Gas Calculations:

Pipe size:

If the flow rate is to be 20 lb mass/s, the optimal pipe size at 100 psia can be estimated with Equation (4.16)

$$M = 12.011 + 4(1.0079) = 16.043$$

$$T = 298 \text{ K}$$

$$P = ((MP)/(RT)) = ((16.043(100/14.7))/(0.0821(298))) \\ = 4.4608 \text{ kg/m}^3$$

$$\mathcal{W} = 20(454/1000) = 9.08 \text{ kg/s}$$

$$\mathcal{V} = ((9.08)/(4.4608)) = 2.035 \text{ m}^3/\text{s}$$

$$D = 0.363(2.0355)^{0.45}(4.4608)^{0.13}(0.0001)^{0.025} \\ = 0.48221 \\ = (((0.48221)(100))/((2.54)12)) = 1.5821 \text{ ft}$$

The optimal diameter will increase with a decrease in pressure. At 50 psia, for example, the optimal diameter is given by

$$P = ((MP)/(RT)) = ((16.043(50/14.7))/(0.0821(298))) \\ = 2.2304 \text{ kg/m}^3$$

$$\mathcal{V} = ((9.08)/(2.2304)) = 4.071 \text{ m}^3/\text{s}$$

Values of the remaining variables remain the same as above.

$$D = 0.363(4.072)^{0.45}(2.2304)^{0.13}(0.0001)^{0.025} \\ = 0.60202 \text{ m} \\ = (((0.60202)(100))/((2.54)12)) = 1.9751 \text{ ft}$$

Say $D = 2.0 \text{ ft}$ and revisit this specification after the pressure drop is calculated.

The velocity at 100 psia is given by

$$v = \frac{W}{\rho\pi(D^2/4)} \\ = \frac{20}{((16.04 \times 100)/(10.73 \times 530))3.416(D^2/4)} \\ = 20.758 \text{ ft/s,}$$

which is well below the sonic velocity given by the ideal gas value:

$$c = \sqrt{\frac{RT\gamma}{M}} = \left[\frac{10.73 \times 539 \times 1.3}{16.04} \times 144 \times 32.175 \right]^{1/2} \\ = 1473.7 \text{ ft/s} \\ \gamma = 1.3 \text{ (Smith et al., 2005).}$$

The pressure drop may be calculated for the ideal case with Equation (13.1.1-7).

Friction factor:

$$G = \rho v = \frac{W}{\pi(D^2/4)} = \frac{20}{3.416(D^2/4)} = 5.8548 \text{ lb mass/ft}^2 \text{ s}$$

$$\eta = 10^{-4} \text{ P (Green and Maloney, 1997).}$$

$$N_{\text{Re}} = \frac{GD}{\eta} = \frac{5.8548 \times D}{10^{-4} \times 0.067197} = 1.7426 \times 10^6$$

$$\frac{1}{\sqrt{f}} = -4 \log_{10} \left[\frac{0.27\varepsilon}{D} + \left(\frac{7}{N_{\text{Re}}} \right)^{0.9} \right], \quad N_{\text{Re}} \geq 4000 \text{ (Green and Maloney, 1997).}$$

$$\varepsilon = 0 \text{ for smooth pipe}$$

$$f = 0.00265$$

Pressure drop for ideal gas:

$$G = 5.8548 \text{ lb mass/ft}^2 \text{ s}$$

$$L = 20 \times 5280 = L = 1.056 \times 10^5 \text{ ft}$$

$$M = 16.04$$

$$T = 530 \text{ R}$$

$$-\ln \frac{P_2}{100} + \frac{M(100)^2(32.175) \times 144}{2 \times 10.73 \times T \times G^2} \left(\left(\frac{P_2}{100} \right)^2 - 1 \right) + \frac{2fL}{D} = 0 \\ P_2 \in (0.001, 100)$$

Solution: $P_2 = 92.366 \text{ atm.}$

b. *Nonideal Gas Calculations:* Truncated virial equation: Equation (13.15)

Equation of state parameters:

$$T_c = 190.6 \text{ K (Sandler, 1999)}$$

$$P_c = 46.0$$

$$\omega = 0.008$$

$$b(T) = \frac{1.8(10.73)T_c}{Mp_c(14.7)} \left(0.083 - \frac{0.422}{(T/1.8T_c)^{1.6}} \right. \\ \left. + \omega \left(0.139 - \frac{0.172}{(T/1.8T_c)^{4.2}} \right) \right)$$

TABLE 13.1 Compressor Applications

Compressor Type	Pressure Range–Upper Limit (psig)	Flow Range ACFM	hp per Compressor	Efficiency (%)
Reciprocating	100,000	5–7,000	20	80–90
Centrifugal	500	100–15,000	2,000	70–75
Screw	400	800–20,000	600	75–85

$$\rho(p) = \frac{1}{(10.73T/Mp) + b(T)}$$

$$x_1(T) = \frac{M(100)}{10.73T}$$

$$\ln \frac{(1/x_2) + b(T)}{(1/x_1(T)) + b(T)} + \frac{1}{G^2 b(T)^2} \frac{49,686T}{M} (b(T)(x_2 - x_1(T)))$$

$$+ \ln \left(\frac{((1/x_1(T)) + b(T)) \left(\frac{x_1(T)}{x_2} \right)}{((1/x_2) + b(T)) \left(\frac{x_1(T)}{x_2} \right)} \right) + \frac{2Lf}{D} = 0$$

$$x_2 \in (0.005, 1)$$

Solution is $\{x_2 = 0.26077\}$

$\frac{MP_2}{10.73T} = 0.26077$, Solution is $\{P_2 = 92.455\}$. The correction for nonideality is negligible in this case (see Problem 13.1).

13.1.1.2 Compressors Some useful rules of thumb for compressors (Couper et al., 2005) are given below:

- Fans are used to raise the pressure about 3% (12 in. water). Blowers raise the pressure to less than 40 psig, and compressors to higher pressures, although the blower range is commonly included in the compressor range.
- To compress air from 100 °F, $k = 1.4$, compression ratio = 3. Theoretical power required = 62 hp/million cuft/day, outlet temperature 306 °F.
- Exit temperature should not exceed 350–400 °F: for diatomic gases ($C_p/C_v = 1.4$) this corresponds to a compression ratio of about 4.
- Compression ratio should be about the same in each stage of a multistage unit, ratio = $(P_n/P_1)^{1/n}$, with n stages.
- Efficiencies of reciprocating compressors: 65% at compression ratio of 1.5, 75% at 2, and 80–85% at 3–6.
- Efficiencies of large centrifugal compressors, 6,000–100,000 ACFM at suction are 76–78%.

- Rotary compressors have efficiencies of 70%, except the liquid liner type, which have 50% of 1.5, 75% at 2.0, and 80–85% at 3–6.

Table 13.1 summarizes some compressor applications. In all cases, the outlet temperature should not exceed 375 °F.

Neglecting changes in potential energy as well as frictional losses across the compressor, the work done by the compressor can be calculated from the mechanical energy balance:

$$W_{mc} = \frac{1}{2} v_1^2 \left[\left(\frac{\rho_1}{\rho_2} \right)^2 - 1 \right] + \int_{P_1}^{P_2} \frac{dP}{\rho} \quad (13.19)$$

13.1.1.2.1 Ideal Gas Essentially three paths are used to determine the work required to compress an ideal gas and each refers to a particular path for the integral in the expression for compressor work:

1. Isothermal
2. Adiabatic
3. Polytropic

Each of these paths are reversible (see Chapter 3). In the first case, $PV = \text{constant}(RT)$. In the second case $PV^\gamma = \text{constant}(\gamma = C_p/C_v)$, and in the third case, $PV^b = \text{constant}(0 < b < \infty)$. In the first case, the process of compression is considered to be much slower than the heat transfer process. In the second case, the heat transfer process is considered to be much slower than the compression process. The last case includes the previous two, all processes in between, and applies to isobaric processes as $b \rightarrow 0$ and isochoric processes as $b \rightarrow \infty$.

Substitution of the polytropic case into the integral in Equation (13.19) gives

$$\int_{P_1}^{P_2} \frac{dP}{\rho} = \frac{P_1^{1/b}}{\rho_1} \int_{P_1}^{P_2} \frac{dP}{P^{1/b}} = \frac{P_1^{1/b}}{\rho_1} \frac{b}{b-1} \left[\left(\frac{P_2}{P_1} \right)^{(b-1)/b} - 1 \right] \quad (13.20)$$

The compressor work is then given by

Polytropic:

$$W_{mc} = \frac{1}{2} v_1^2 \left[\left(\frac{P_2}{P_1} \right)^{-(2/b)} - 1 \right] + \frac{P_1}{\rho_1} \frac{b}{b-1} \left[\left(\frac{P_2}{P_1} \right)^{(b-1)/b} - 1 \right] \quad (13.21)$$

Isobaric:

$$b = 0: \quad W_{mc} = 0 \quad (13.22)$$

Isothermal:

$$W_{mc} = \frac{1}{2} v_1^2 \lim_{b \rightarrow 1} \left[\left(\frac{P_2}{P_1} \right)^{-(2/b)} - 1 \right] + \frac{P_1}{\rho_1} \lim_{b \rightarrow 1} \frac{b}{b-1} \left[\left(\frac{P_2}{P_1} \right)^{(b-1)/b} - 1 \right] \quad (13.23)$$

$$b = 1 \quad W_{mc} = \frac{1}{2} v_1^2 \left[\left(\frac{P_2}{P_1} \right)^{-2} - 1 \right] + \frac{P_1}{\rho_1} \lim_{a \rightarrow 0} \left[\left(\frac{P_2}{P_1} \right)^a \ln \left(\frac{P_2}{P_1} \right) \right] \quad (13.24)$$

$$W_{mc} = \frac{1}{2} v_1^2 \left[\left(\frac{P_1}{P_2} \right)^2 - 1 \right] + \frac{P_1}{\rho_1} \ln \left(\frac{P_2}{P_1} \right) \quad (13.25)$$

Adiabatic:

$$b = \gamma \quad W_{mc} = \frac{1}{2} v_1^2 \left[\left(\frac{P_2}{P_1} \right)^{-(2/\gamma)} - 1 \right] + \frac{P_1}{\rho_1} \frac{\gamma}{\gamma-1} \left[\left(\frac{P_2}{P_1} \right)^{(\gamma-1)/\gamma} - 1 \right] \quad (13.26)$$

Isochoric:

$$b \rightarrow \infty \quad W_{mc} = \frac{P_2 - P_1}{\rho_1} \quad (13.27)$$

Example 13.1.1.2.1-1: Calculation of Compressor Work for Natural Gas Supply Line

See Example 13.1.1.1-1.

Data:

$$\gamma = 1.3$$

$$v_1 = 21 \sqrt{\frac{1}{32.2}} \text{ (ft lb force/lb mass)}^{1/2}$$

$$P_1 = 92.5 \text{ psia}$$

$$P_2 = 100 \text{ psia}$$

$$T = 530/1.8 \text{ K}$$

$$M = 16.04 \text{ lb mass/lb mol}$$

$$R = 1.987 \times 454 \frac{0.7376}{0.23901} \text{ ft lb force/(lb mol K)}$$

$$\rho_1 = \frac{MP_1}{RT}$$

Summary of calculations:

b	$W(b)$ ft lb _f /lb _m	$n(b)$ ft lb _f /lb _m
0.0	0.0	0.0
0.001	44.308	-6.8478
0.01	509.13	-6.8478
0.5	3831.0	-1.8346
0.6	3880.8	-1.5671
0.7	3917.0	-1.3674
1.0	3983.2	-0.98865
1.1	3997.4	-0.90501
1.2	4009.3	-0.83440
1.3	4019.5	-0.77399
1.8	4053.4	-0.56822
3.0	4089.2	-0.34682
5	4110.8	-0.21025
10	4127.2	-0.10595
100	4141.9	-1.0669×10^{-2}
∞	4143.6	0.0

The effect of the kinetic energy change from the inlet to the outlet and the polytropic parameter can be gleaned from the preceding results. Both effects are negligible over the isothermal–isochoric range.

$$W_{mc}(b) = \frac{1}{2} v_1^2 \left[\left(\frac{P_2}{P_1} \right)^{-(2/b)} - 1 \right] + \frac{P_1}{\rho_1} \frac{b}{b-1} \left[\left(\frac{P_2}{P_1} \right)^{(b-1)/b} - 1 \right]$$

$$w = \frac{1}{2} v_1^2 \left(\left(\frac{P_2}{P_1} \right)^{-2} - 1 \right) + \frac{P_1}{\rho_1} \ln \left(\frac{P_2}{P_1} \right)$$

$$n(b) = \frac{1}{2} v_1^2 \left(\left(\frac{P_2}{P_1} \right)^{-(2/b)} - 1 \right)$$

$$\frac{P_2 - P_1}{\rho_1}$$

$$[a] = \begin{bmatrix} 0.2911 \times 10^5 & 0.0861 \times 10^5 & 1.7016 \times 10^3 & 0.001 \times 10^5 & 909.79 \\ 0.2910 \times 10^5 & 0.1004 \times 10^5 & 2.5265 \times 10^3 & 0.0936 \times 10^5 & 1153.80 \\ 0.3336 \times 10^5 & 0.2679 \times 10^5 & 2.6105 \times 10^3 & 0.0890 \times 10^5 & 1169 \end{bmatrix}$$

Example 13.1.1.2.1-2: Power Required for C-301 A/B:
Acrylic Acid Plant

Stream 1 is to be compressed from 1 to 5 atm (see process flow diagram, Figure 1.4).

The compression ratio is 5.0. Specify two stages with equal compression ratio. The interstage pressure can be established as follows:

$$\frac{P}{1} = \frac{5}{P} \text{ or } P = 2.2361 \text{ atm}$$

Interstage pressure = 2.24 atm, which sets the compression ratio at 2.24. The flow rate is given by

$$162.9(1000)(1/60) \times (0.0821) \times (298) \times (35.3145/1000) \\ = 2345.8 \text{ CFM at inlet}$$

Consequently, a centrifugal compressor may be used. The power required per stage can be calculated with the ideal gas result for adiabatic conditions in Equation (13.26).

$\gamma = 1.4$ for air at 1 bar and 300 K (Green and Maloney, 1997).

$$W_c = 8.314 \times 298 \times \frac{1.4}{1.4 - 1} (2.2361^{4/1.4} - 1) \\ \times 1362.9(1000)/(3600 \times 1000) \\ = 848.64 \text{ kW at 100\% efficiency}$$

$$W_c = \frac{848.64}{0.725} = 1170.5 \text{ at 72.5\% efficiency or 2341 kW for} \\ \text{two stages.}$$

The temperature rise may be calculated with the First Law. The specific heats as a function of temperature are formulated as follows:

1 = nitrogen

2 = oxygen

3 = water

$$C(i, T) = a_{i,1} + a_{i,2} \times \left(\frac{a_{i,3}/T}{\sinh(a_{i,3}/T)} \right)^2$$

$$+ a_{i,4} \times \left(\frac{a_{i,5}/T}{\cosh(a_{i,5}/T)} \right)^2$$

$$[N] = \begin{bmatrix} 1056.7 \\ 280.9 \\ 25.3 \end{bmatrix}$$

$$W_c = 3.0551 \times 10^9 \text{ J/h}$$

$$\sum_{i=1}^{i=3} N_i^{(1)} \int_{298}^x C(i, T) dT = 3.0551 \times 10^9, \quad \text{Solution is} \\ \{T = 374.42\} \text{ K}$$

$$\text{Outlet temperature of first stage} = 374.42 - 273.16$$

$$= 101.26^\circ\text{C} = 182.3^\circ\text{F}$$

which is less than 375 °F, the “rule of thumb” maximum.
See Problem 13.2.

13.1.1.2.2 Nonideal Gas The option of a nonideal gas is available in most process simulators. The reversible adiabatic process or isentropic method is generally used and can be implemented as follows:

$$P(V_1, T_1) = P_1 \quad (13.28)$$

Determine the outlet conditions from the equation of state and the requirement of no entropy change:

$$P(V_2, T_2) = P_2 \quad (13.29)$$

$$S(V_2, T_2) = S(V_1, T_1) \quad (13.30)$$

Having the outlet conditions completed, the energy balance can be used to determine the reversible adiabatic work required of the compressor:

$$\hat{W}_c = H(V_2, T_2) - H(V_1, T_1) \quad (13.31)$$

The actual outlet temperature of the compressor can be calculated using an efficiency, η , for the compressor. The efficiency of centrifugal compressors is approximately 65–75%, 80–85% for axial flow compressors, and 70–85% for reciprocating compressors (Branan, 1994). Considering that the extra energy increases the enthalpy of the gas, the actual enthalpy of the outlet can be calculated from

$$\text{isentropic efficiency} = \frac{H(V_2, T_2)_{\text{isentropic}} - H(V_1, T_1)}{H_{\text{actual}} - H(V_1, T_1)} \quad (13.32)$$

The actual outlet conditions follow from the following:

- Calculate isentropic enthalpy and work
- Determine actual work using efficiency
- Determine outlet conditions from

$$W_{\text{actual}} = H(V_2, T_2) - H(V_1, T_1) \quad (13.33)$$

$$P(V_2, T_2) = P_2 \quad (13.34)$$

Expressions for the entropy and enthalpy for a nonideal gas are derived in Chapter 3 for the Redlich–Kwong–Soave equation of state (see Example 3.2.1-1). Using those results gives the desired property changes as

$$\begin{aligned} S(V_2, T_2) - S(V_1, T_1) = R \ln \frac{(V_2 - b)z_2 V_1}{(V_1 - b)z_1 V_2} \\ - \frac{a}{2bT_2^{3/2}} \ln \left[1 + \frac{b}{V_2} \right] + \frac{a}{2bT_1^{3/2}} \ln \left[1 + \frac{b}{V_1} \right] \\ + \int_{T_1}^{T_2} \frac{c_{p0}(T)}{T} dT + R \ln \frac{p_1}{p_2} \end{aligned} \quad (13.35)$$

$$\begin{aligned} S(V_2, T_2) - S(V_1, T_1) = R \ln \frac{(V_2 - b)z_2 V_1}{(V_1 - b)z_1 V_2} \\ - \frac{a}{2bT_2^{3/2}} \ln \left[1 + \frac{b}{V_2} \right] + \frac{a}{2bT_1^{3/2}} \ln \left[1 + \frac{b}{V_1} \right] \\ + \int_{T_1}^{T_2} \frac{c_{v0}(T)}{T} dT + R \ln \frac{V_2}{V_1} \end{aligned} \quad (13.36)$$

$$\begin{aligned} H(T_2, V_2) - H(T_1, V_1) = p_2 V_2 - p_1 V_1 - R(T_2 - T_1) \\ - \frac{3a}{2b} \left[\frac{1}{T_2^{1/2}} \ln \left(1 + \frac{b}{V_2} \right) - \frac{1}{T_1^{1/2}} \ln \left(1 + \frac{b}{V_1} \right) \right] \\ + \int_{T_1}^{T_2} c_{p0}(T) dT \end{aligned} \quad (13.37)$$

The procedures outlined above for nonideal gases were implemented in a Mathematica program with the expressions derived from the Redlich–Kwong–Soave equation of state.

SUMMARY OF RESULTS Isentropic process:

$$\begin{aligned} V_1 &= 0.00379464 \text{ m}^3/\text{mol} \\ V_2 &= 0.00357338 \text{ m}^3/\text{mol} \\ T_2 &= 299.945 \text{ K} \\ W &= 3997 \text{ ft lb}_f/\text{lb}_m \end{aligned}$$

Actual at 80% efficiency:

$$\begin{aligned} V_2 &= 0.0050869 \text{ m}^3/\text{mol} \\ T_2 &= 423 \text{ K} \\ W &= 4996 \text{ ft lb}_f/\text{lb}_m \end{aligned}$$

Note the substantial increase in temperature due to the inefficiency.

13.1.2 Pressure Drop in Fixed Beds

Fixed (or packed) beds of solid particles are common in chemical processes. In adsorption, the particles are porous with a high surface affinity for a restricted range of compounds. Fixed-bed reactors contain solids consisting of a solid support whose surface area is coated with a catalytic material. These are examples of a stationary solid phase, a packed bed of solid particles, over which a single fluid phase flows. Fixed beds of solids are also used in gas absorption, for example, but in these cases, there are two fluid phases that flow countercurrently. Here we consider estimates of the pressure drop in a fixed bed based on a capillary model of the flow of a single fluid phase.

The void space surrounding the particles in the packed bed is envisioned to consist of a collection of straight round capillaries of diameter d and effective length l_c . The total volume of these capillaries is the actual void volume in the bed. The surface or wall area of the capillaries is taken to be the external area of the particles. A characteristic diameter for the particles is defined so that the ratio of the external surface area to the volume of the particle is exact for spheres: D_p . Consequently,

$$\underbrace{\frac{[(1-\varepsilon)V_T]}{\text{Volume of solid}}}_{\text{Volume of solid}} \underbrace{\frac{6}{D_p}}_{\text{External surface area per unit volume of solid}} = \underbrace{\frac{[\varepsilon V_T]}{\text{Volume of void space}}}_{\text{Volume of void space}} \underbrace{\frac{\pi dl_e}{\pi(d^2/4)l_e}}_{\text{Surface area per unit volume of capillaries}} \quad (13.38)$$

$$d = \frac{2}{3} \frac{\varepsilon}{(1-\varepsilon)} D_p \quad (13.39)$$

where the total bed volume is given by V_T .

From the definition of the friction factor in empty tubes,

$$\Delta(P + \rho g l_e) \frac{\pi d^2}{4} = \frac{f_e}{2} (\rho \langle v \rangle \langle v \rangle) \pi dl_e \quad (13.40)$$

Three flow regimes can be identified.

Low Velocities In this case, it is assumed that the effective friction factor follows a relation similar to that for straight round tubes:

$$f_e = \frac{A}{(\rho d \langle v \rangle) / \eta} \quad (13.41)$$

where A was found to be 16 for the case of laminar flow in tubes. The interstitial velocity is $\langle v \rangle$. The superficial velocity is $v_o (= \varepsilon \langle v \rangle)$. Substitution into the definition of the effective friction factor above gives

$$\Delta(P + \rho g l_e) \frac{\pi d^2}{4} = \frac{1}{2} \frac{A \eta}{\rho d \langle v \rangle} (\rho \langle v \rangle \langle v \rangle) \pi dl_e \quad (13.42)$$

$$\Delta(P + \rho g l_e) = \frac{2A\eta}{d^2} \langle v \rangle l_e = \frac{2A\eta}{[(2/3)(\varepsilon/(1-\varepsilon))D_p]^2} \frac{v_o}{\varepsilon} l_e \quad (13.43)$$

$$\Delta(P + \rho g l_e) = \frac{4.5A\eta v_o l_e (1-\varepsilon)^2}{D_p^2 \varepsilon^3} \quad (13.44)$$

The experimental result for a tube of length L is the Blake-Kozeny equation:

$$\left(\frac{D_p}{L}\right) \frac{\rho[\Delta(p + \rho g L)]}{G_o^2} \frac{\varepsilon^3}{(1-\varepsilon)} = 150 \frac{\mu}{D_p G_o} (1-\varepsilon) \quad (13.45)$$

G_o is the superficial mass flux, a constant through the bed. The density and viscosity can be the average of the inlet and outlet values.

High Velocity At high velocities, the friction factor for empty tubes approaches a constant value. On this basis, the effective friction factor is set equal to B and its definition becomes

$$\Delta(P + \rho g l_e) \frac{\pi d^2}{4} = \frac{1}{2} B (\rho \langle v \rangle \langle v \rangle) \pi dl_e \quad (13.46)$$

$$\Delta(P + \rho g l_e) = 2B \left(\rho \frac{v_o}{\varepsilon} \frac{v_o}{\varepsilon} \right) \frac{1}{[(2/3)(\varepsilon/(1-\varepsilon))D_p]} l_e \quad (13.47)$$

$$\Delta(P + \rho g l_e) = \frac{3B \rho v_o^2 l_e (1-\varepsilon)}{D_p \varepsilon^3} \quad (13.48)$$

The experimental result for a tube of length L is the Burke-Plummer equation:

$$\Delta(p + \rho g L) = \frac{7 \rho v_o^2 L (1-\varepsilon)}{4 D_p \varepsilon^3} \quad (13.49)$$

or

$$\left(\frac{D_p}{L}\right) \frac{\rho[\Delta(p + \rho g L)]}{G_o^2} \frac{\varepsilon^3}{(1-\varepsilon)} = \frac{7}{4} \quad (13.50)$$

Full Range of Velocities The addition of these two equations is called the Ergun equation. It is able to correlate the data over the full range:

$$\left(\frac{D_p}{L}\right) \frac{\rho[\Delta(p + \rho g L)]}{G_o^2} \frac{\varepsilon^3}{(1-\varepsilon)} = 150 \frac{\eta}{D_p G_o} (1-\varepsilon) + \frac{7}{4} \quad (13.51)$$

Again note that G_o is a constant through the bed and that the density and average of the inlet and outlet values. Although the basic model is for incompressible flow, applications to gas phase systems have been successful. If the density changes are extremely large, the results can be applied in differential form.

13.2 FLOW OVER SUBMERGED SPHERES

The fluid velocity required to suspend a particle is of interest in a variety of applications. For example:

- In gas-liquid contacting equipment, this velocity determines the condition called flooding where the liquid phase dispersion falling by gravity through an opposing gas is prevented from exiting the equipment and can be found in significant proportions in the exiting gas.
- It is the defining characteristic of fluidized beds.

- In liquid–liquid systems, the relative motion of the droplets is related to this parameter, which bears directly on the mass transfer rate.
- It characterizes the power requirements to suspend solids in agitated tanks (see Figure 5.11).

At the root of all these applications is the flux of momentum to an entrained solid or liquid particle.

13.2.1 Momentum Balance for Single Particle

Assume that the diameter of liquid droplets is sufficiently small so that surface tension can maintain a spherical shape and internal circulation does not affect the momentum transfer process with the surrounding fluid. Under these circumstances, the liquid droplets can be treated in the same way as solid spheres and the fluid medium can be a liquid or gas.

From the analysis of the momentum transfer process for the case of very low gas phase velocities (see Section 9.4.1), we can identify the forces due to gravity and buoyancy. The viscous forces, Stoke's law, can be replaced with a friction or drag coefficient using the terminology for friction factors for submerged objects. The terminal velocity of a spherical object falling through a stagnant medium is the same as the suspension velocity where the particle is stagnant in the grips of a rising fluid. The momentum balance for the particle is given by

$$\underbrace{\left(\frac{4}{3}\pi R_p^3\right)g\rho_f}_{\text{Buoyancy force opposes gravity}} + \underbrace{C_D(\pi R_p^2)\frac{1}{2}\rho_f v_t^2}_{\text{Momentum transfer from fluid to particle drag coefficient in lieu of friction factor and projected area in lieu of actual area as discussed at the outset}} - \underbrace{\left(\frac{4}{3}\pi R_p^3\right)g\rho}_{\text{Gravitational force opposite to motion of surrounding fluid}} = 0 \quad (13.52)$$

$$v_t = \left[\frac{8gR_p}{3C_D}\right]^{1/2} \left(\frac{\rho - \rho_f}{\rho_f}\right)^{1/2} \quad (13.53)$$

The result that the terminal velocity is proportional to the relative density difference has been beneficial in a number of correlations of experimental data.

Example 13.2.1-1: Diameter of Gas–Liquid Separators

The following heuristic (Couper et al., 2005) was stated in Section 6.3 for gas–liquid separators such as the drum in a flash vaporization unit.

The gas velocity in gas–liquid separators may be calculated with

$$v = k\sqrt{\left(\frac{\rho_L}{\rho_V} - 1\right)}$$

For v in ft/s, $k = 0.35$ with mesh de-entrainer; $k = 0.1$ without mesh de-entrainer.

This is a direct adaptation of the terminal velocity analysis where the coefficient of the density factor is taken to be an empirical constant.

13.2.2 Terminal Velocities in Newtonian Fluids: Solid Suspensions

The expression for the terminal velocity derived from the momentum balance may be used to evaluate the drag coefficient from experimental measurements. The expression for the force on the sphere given in Chapter 9 may be used with the definition of the drag coefficient to show that the drag coefficient is a function only of the Reynolds number.

Measurements of the drag coefficient for submerged spheres generally follow the curve shown in Figure 13.4.

The value of the terminal velocity may be determined as follows. In the region of Stoke's law, the drag coefficient is given by

$$6\pi\mu R v_t = C_D(\pi R_p^2)\frac{1}{2}\rho_f v_t^2 \quad (13.54)$$

$$C_D = 24\frac{\eta}{\rho_f v_t d_p} = \frac{24}{N_{Re}} \quad (13.55)$$

This relation is valid up to a Reynolds number of approximately 0.1, although it has been applied to values of the Reynolds number as high as 1.0. The complete range of drag coefficients may be represented as Green and Maloney (1997):

$$c_D = \frac{24}{N_{Re}}, \quad N_{Re} \leq 0.1 \quad (13.56)$$

$$c_D = \frac{24}{N_{Re}}(1 + 0.14N_{Re}^{0.7}), \quad 0.1 \leq N_{Re} \leq 1000 \quad (13.57)$$

$$c_D = 0.44 \quad 1000 \leq N_{Re} \leq 350,000 \quad (13.58)$$

$$c_D = 0.19 - \frac{8 \times 10^4}{N_{Re}} \quad N_{Re} \geq 1,000,000 \quad (13.59)$$

The combination of the preceding four equations constitutes a single functional relation of the drag coefficient to

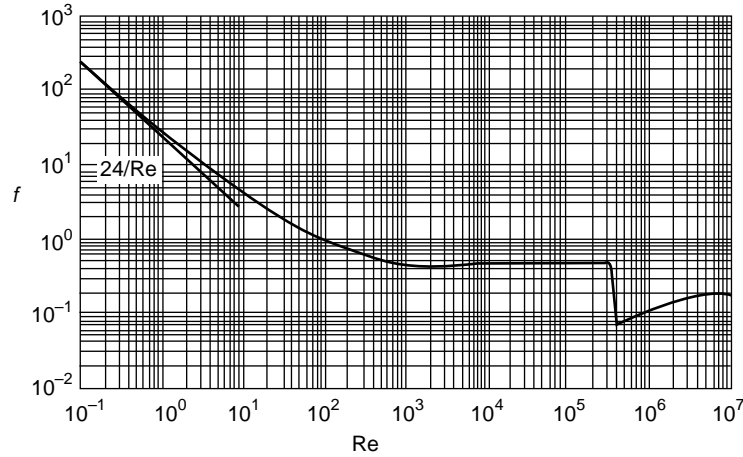


FIGURE 13.4 Drag coefficients for suspended spheres (Middleman, 1998).

the Reynolds number over the full range of values. The momentum balance on the particle provides a second:

$$c_D = \frac{A_D}{N_{\text{Re}}^2} \quad (13.60)$$

where

$$A_D = \frac{4}{3} d_p g \left(\frac{\rho_f d_p}{\eta_f} \right)^2 \left(\frac{\rho}{\rho_f} - 1 \right) \quad (13.61)$$

The value of A being set, we now have two equations and two unknowns, the drag coefficient and the Reynolds number. The desired terminal velocity may be extracted from the Reynolds number.

Example 13.2.2-1: Slurry Adsorption of Hexyl Glucoside

In Chapter 5, a batch adsorption system was considered to capture the hexyl glucoside from a solution with hexanol. The terminal velocity of the adsorbent particles is needed to estimate the power required (see Example 5.3.2.4-1). Assume that the adsorbent particles are 5 mm spheres of activated alumina η_f

Solution:

Refer to the database requested in Problem 1.1c (Yaws, 1999). Say $T = 328 \text{ K}$:

$$\eta_f = 10^{(-9.7166 + 2.0060 \times 1000/328 + 0.0159(328) - 1.2286 \times 10^{-5} \times (328)^2)}$$

$$\times \eta_f = 1.9619 \times 10^{-3} \text{ kg/(ms)}$$

$$\rho_f = 0.268(0.2673)^{-(1 - 328/611.35)^{0.254}} : \rho_f = 793.6 \text{ kg/m}^3$$

Density and diameter of particles:

Estimate the solid density and void volume from Table 6.16.

$$\rho_s = 3100 \text{ kg/m}^3$$

$$V_g = 0.65(0.001) = 0.00065 \text{ m}^3/\text{kg}$$

Calculate the apparent density (not independent of preceding two properties):

$$\rho_P = \frac{\rho_s}{1 + \rho_s V_g}$$

$$\rho_P = \frac{3100}{1 + 3100(0.00065)} = 1028.2 \text{ kg/m}^3$$

$$D_p = 5 \text{ mm spheres} = 0.005 \text{ m}$$

$$A_D = \left(\frac{4}{3} \right) (0.005) \left(\frac{793.6 \times 0.005}{1.9619 \times 10^{-3}} \right)^2 \left(\frac{1028.2}{793.6} - 1 \right) = 8061.7$$

from Equation (13.61)

$$\frac{8061.7}{x^2} = \frac{24}{x} (1 + 0.14x^{0.7}), \text{ Solution is } \{x = 82.473\}$$

$$82.473 = \frac{793.6(0.005)v_t}{1.9619 \times 10^{-3}}, \text{ Solution is}$$

$$v_t = 4.0777 \times 10^{-2} \text{ m/s} = 4.0777 \times 10^{-2} \left(\frac{100}{2.54 \times 12} \right)$$

$$= 0.13378 \text{ ft/s} = 0.13378 \times 60 = 8.0268 \text{ ft/min}$$

TABLE 13.2 Values of K , α , and R for the Equation $v_{mf} = KX^\alpha$

Fluidizing System ρ = Solid Density (g/cm^3) D_p = Particle Diameter (μm)	K	α	Correlation Coefficient R
Metal–gas $3 < D_p < 900$	4.7673×10^{-6}	0.71635 ± 0.02213	0.990
Alumina–gas Low-medium density $0.768 \leq \rho \leq 2.8$	2.7568×10^{-6}	$0.81455 + 0.02845$	0.991
High density $3.3 \leq \rho \leq 4.015$	3.7774×10^{-5}	$0.6301 + 0.03064$	0.991
Glass–gas $23 < D_p < 569$	4.3384×10^{-7}	$0.89029 + 0.01888$	0.992
$569 < D_p < 3000$	2.4624×10^{-3}	$0.46943 + 0.01190$	0.991
Sand–gas $95 < D_p < 800$	9.7119×10^{-7}	$0.84268 + 0.01601$	0.993
$800 < D_p < 2800$	6.4051×10^{-3}	0.42520 ± 0.01339	0.992
Coal–gas $710 < D_p < 1000$	4.7731×10^{-6}	$0.87117 + 0.01513$	0.998
$1000 < D_p < 3578$	8.5557×10^{-3}	$0.46093 + 0.28872$	0.996
Catalysts–gas $25 < D_p < 2250$	1.145×10^{-5}	0.71957 ± 0.01422	0.991
Metallic ores–gas $101 < D_p < 1250$	3.1108×10^{-8}	$0.93283 + 0.03451$	0.994
Gas–polymer air $116 < D_p < 1000$	2.1308×10^{-4}	$0.59460 + 0.01730$	0.995
Mineral–gas Orthorhombic $502 < D_p < 2828$	4.427×10^{-3}	$0.47851 + 0.03930$	0.992
Hexagonal $0.89 < D_p < 2300$	7.9265×10^{-4}	$0.50953 + 0.01379$	0.991
Cubic $106 < D_p < 2474$	7.1187×10^{-5}	$0.61787 + 0.04099$	0.994

Source: Coltters and Rivas (2004).

13.2.3 Fluidization Velocities: Diameter of Fluidized Beds

The rapid movement of immersed solids in fluids has a very favorable effect on the rates of heat and mass transfer to surface of the particles. Temperature gradients are largely reduced or eliminated in such conditions. These features are very attractive, for example, in the design chemical reactors involving heterogeneous vapor phase catalytic reactions with large enthalpy changes.

As the gas velocity through a fixed bed is gradually increased, the pressure drop increases until the point is reached where the particles are no longer in permanent contact with their neighbors. This velocity is called the minimum fluidization velocity and represents the transition from a fixed bed to the first of five fluidization regimes: particulate fluidization, bubbling fluidization, slugging regime, turbulent regime, and fast fluidization (Couper et al., 2005).

From the momentum balance given above, the following parameters may be proposed as the primary players in determining the minimum fluidization velocity:

$$\left\{ \frac{\rho}{\rho_f}, d_p, (\rho - \rho_f), \eta \right\}$$

Coltters and Rivas (2004) used these variables to determine a functional relation between them and the minimum fluidization velocity using dimensional analysis. Their result is

$$v_{mf} = K \left[\frac{d_p^2 g (\rho - \rho_f)}{\eta} \left(\frac{\rho}{\rho_f} \right)^{1.23} \right]^\alpha \quad (13.62)$$

where the values of K and α depend on the system. An extensive set of values is given in Table 13.2.

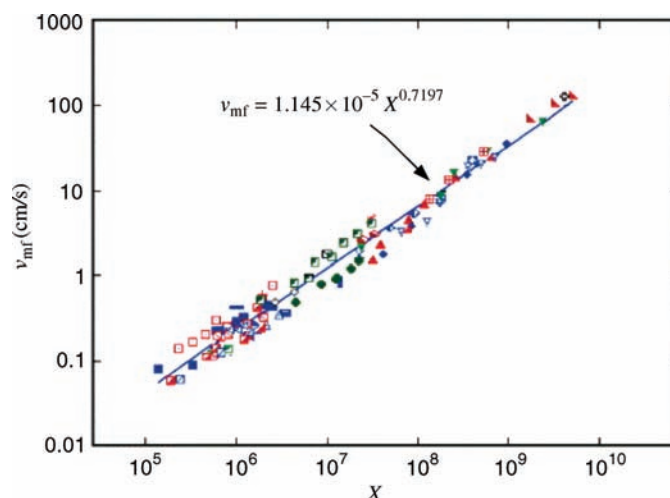


FIGURE 13.5 Comparison of predictions of minimum fluidization velocity with operating data for catalyst–gas fluidized beds (Coltters and Rivas, 2004). Reprinted with permission of Elsevier.

The correlation for catalyst–gas fluidized beds is shown in Figure 13.5.

As the velocity is increased further beyond the minimum fluidization velocity the bed density decreases until the bed particles are found in the exit gas stream. The gas velocity at the onset of this condition is the terminal velocity calculated above.

The following heuristics provide some insight into the operation of fluid beds.

Heuristics for Fluidization (Couper et al., 2005)

- A particle size (diameter) in the range 50–500 μm or a spectrum of sizes with the ratio of the maximum to minimum diameter in the range 10–25 are properties of particles that support smooth fluidization.
- Cracking catalysts generally have diameters in the range 30–150 μm and a density of approximately 1.5 g/ml. Appreciable expansion of the bed takes place before fluidization and the minimum bubbling velocity is greater than the minimum fluidization velocity.
- Cohesive particles and particle with diameters of 1 μm or more do not fluidize well.
- Pilot plant experience is highly recommended.
- Bed operation is normally at two to three times the minimum fluidization velocity.

Example 13.2.3-1: Diameter of R-301 Reactor

A gas flow of two to three times the minimum fluidization velocity may be used to estimate the diameter.

Chemical properties handbook:

Viscosity of N_2 at 583 K = 286×10^{-6} P

Water = 83.2×10^{-6} P

As a rough approximation, ignore pressure correction and give equal weights to each [see Poling et al. (2001) for method to use].

$$\eta = \frac{286 + 83.2}{2} = 184.6 \text{ or } 0.000184 \text{ P}$$

Use medium particle size of 75 μm . Range from Woods (1995) is 60–80 μm

$$\rho_G = \frac{MP}{RT} = \frac{0.5(18 + 28)350}{8.314(583.16)} = 1.6603 \text{ kg/m}^3$$

$$\rho_G = 2 \text{ g/cm}^3 \text{ or } 2000 \text{ kg/m}^3$$

$$X = \frac{(75 \times 10^{-6} \times 100)^2 (2000 - 1.66) 10^{-6} (980)}{0.000184 \times 0.1 \times \left(\frac{1}{100}\right)} \times \left(\frac{2000}{1.6603}\right)^{1.23} = 3.6867 \times 10^6$$

$$v_{mf} = (1.145 \times 10^{-5}) (3.6867 \times 10^6)^{0.71957} = 0.60808 \text{ cm/s}$$

$$\text{Design at } 2 \times 0.60808 = 1.2162 \text{ cm/s}$$

$$\begin{aligned} \mathcal{V}_G &= (15.533 + 53.993 + 1056.7 + 59.707 + 1164.6 \\ &\quad + 6.4762 + 87.247) \frac{1}{350/(8.314(583.16))} \frac{1}{3600} \\ &= 9.4053 \text{ m}^3/\text{s} \end{aligned}$$

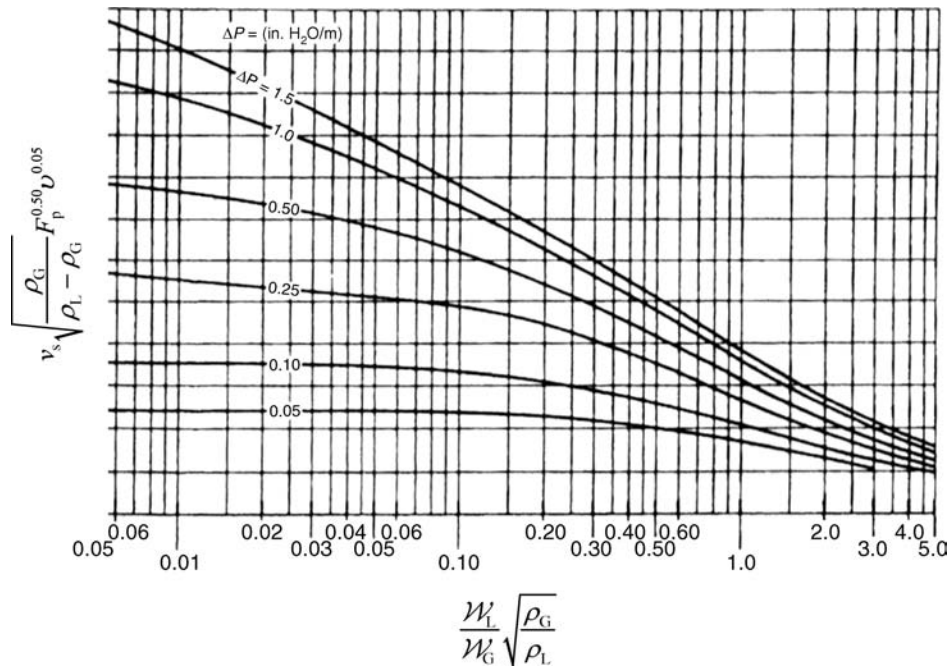


FIGURE 13.6 GPDC chart (Green and Maloney, 1997). Reprinted with permission of McGraw-Hill.

$$\frac{1.2162}{100} \frac{3.1416}{4} d^2 = 9.4053, \text{ Solution is } \{d = -3.4605\},$$

$$\{d = 3.4605\}$$

Diameter = 3.46 m as compared to reported simulator value of 3.6 m.

13.2.4 Flooding Velocity in Packed Towers: Tower Diameter and Pressure Drop

In gas-liquid operations, the liquid phase is dispersed in the gas and wets the 1 in. solid surface of the packing (see Figure 12.16) under normal operating gas velocities. As the gas phase flow rate is increased, the liquid holdup remains nearly constant until a point is reached where the amount of liquid retained in the column changes and begins to increase rapidly (Treybal, 1980). The column is said to be loaded at these conditions and the pressure drop increases rapidly with the gas flow. Further increases in the gas rate will lead to flooding where the amount of liquid contained in the column is very high and the dispersion may even change to gas dispersed from the liquid dispersed. Incipient flooding for most absorbers is taken to be at a pressure drop of 1.5 in. water/ft of packing (Green and Maloney, 1997).

The packed tower adds a third phase to the operation over the fluid-solid systems considered in the preceding section. Although this moves the physical circumstances that much further away from the single particle considerations, the basic interphase momentum flux requirements remain.

However, an even greater reliance on empirical data is necessary. For several decades, the correlation in Figure 13.6 has been used to calculate flooding velocities and pressure drops in packed towers (Kister et al., 1992). It is generally known as the generalized pressure drop correlation (GPDC) and constitutes the summary of extensive experimental data. The following discussion will employ an approximate graphical interpolation. A more extensive and accurate interpolation method using the supporting data is available in Kister et al. (1992).

The superficial gas velocity, v_s , is in ft/s. The packing factor, F_p , is in ft^{-1} , and the kinematic viscosity (centistokes) is obtained by dividing the molecular viscosity in centipoises by the liquid density in g/cm^3 . The packing factor is normally the wetted surface area of the packing divided by the cube of the void volume (a_p and ε in Table 12.1). However, its value may have been adjusted to obtain a better correlation of the pressure drop data. Some examples are given in Table 13.3.

The chart is used by first calculating the abscissa at the end of the column with the highest flow rates. The superficial gas velocity at flooding can then be evaluated from the ordinate of the pressure drop curve at 1.5 in. water/ft packing. This is taken as the flooding velocity. The value of the ordinate is evaluated with a superficial gas velocity at approximately 70% of the flooding value. The pressure drop can then be read directly from the chart. The column diameter is obtained from the relation of the total flow to the superficial flow rate.

TABLE 13.3 Characteristics of Random Packings

Name	Material	Nominal Size (mm)	Surface Area (m ² /m ³)	% Voids	Packing Factor (m ⁻¹)	Vendor
^a Intalox saddles	M	(No. 25)		97	135	Koch-Glitsch, Inc., Wichita, Kansas, USA
"IMTP"		(No. 40)		97	24	
		(No. 50)		98	59	
^a Pall rings	M	16	—	92	266	(Generic)
		25	205	94	184	
		38	130	95	131	
		50	115	96	88	
		90	92	97	59	
^a Pall rings	P	16	340	87	310	(Generic)
		25	205	90	180	
		50	130	91	131	
		90	100	92	85	
Berl saddles	C	13	465	62	790	(Generic)
		25	250	68	360	
		38	150	71	215	
Intalox saddles	C	13	625	78	660	Koch-Glitsch, Inc. Wichita, Kansas, USA
		25	255	77	197	
		50	118	79	98	
		75	92	80	70	
Intalox saddles	P	25	206	91	131	Koch-Glitsch, Inc. Wichita, Kansas, USA
		50	108	93	92	
		75	88	94	59	
Raschig rings	C	13	370	64	1900	(Generic)
		25	190	74	587	
		38	120	68	305	
		50	92	74	213	
		75	62	75	121	
Raschig rings	M	19	245	80	730	(Generic)
		25	185	86	470	
		38	130	90	270	
		50	95	92	187	
		75	66	95	105	

Source: Couper et al. (1997).

^aThrough flow packing.

Example 13.2.4-1: Sulfur Dioxide Absorber

An air stream blowing at 30,000 ft³/h contains SO₂ at a mole fraction of 0.075. The mole fraction of SO₂ is to be reduced to 0.01 by countercurrent absorption into pure water. The pure water solvent and the gas stream are at 25 °C and 1 atm. In determining the height of a packed tower required for the separation using 1/2 in ceramic Raschig rings, the liquid and gas rates were found to be 45,604 lb/h and 2214.5 lb/h, respectively (see Example 12.7.3.3-1).

Solution:

Using the ideal gas law to calculate the gas phase density gives

$$\frac{L'}{G'} \left[\frac{\rho_G}{\rho_L} \right]^{1/2} = \frac{45604}{2214.5} \left[\frac{0.073818}{62.4} \right]^{1/2} = 0.7083$$

Using 1.5 in. water/ft as the pressure drop per feet of packing, the vertical axis is at 0.9. Therefore,

$$\frac{G}{S} = \frac{0.90}{\sqrt{\rho_G/(\rho_L - \rho_G)} F_p^{0.50} v^{0.05}}$$

The value of F_p for 0.5 in. (13 mm) ceramic Raschig rings from Table 13.3 is 1900 m⁻¹. Taking the liquid viscosity to be that of water, 1 cP, and using the equation

$$\frac{22,145/3000}{\pi(D^2/4)} = \frac{0.90}{\sqrt{0.0738/(62.4 - 0.0738)} \sqrt{1900 \times ((2.54 \times 12)/100)(1.0)^{0.05}}},$$

$$D = 0.8489$$

The diameter of the tower is then 0.85 ft or approximately 20 packing diameters, which conforms to the heuristic (see Chapter 11) that it should be at least 15.

PROBLEMS

13.1. Recalculate optimum pipe diameter for Example 13.1.1.1-1. Repeat calculations with a new diameter.

13.2. Determine if water condensation is expected in the compression of Example 13.1.1.2.1-2. We might ask if any of the water condenses. We can compute the temperature at which liquid water has a vapor pressure equal to the

prevailing partial pressure. The temperature is called the dew point. This is an application of Raoult's law.

$$p(T) = 10^{29.861 - 3152.2/T - 7.3037 \times (1/2.3026) \times \log T + 2.4247 \times 10^{-9} \times T + 1.8090 \times 10^{-6} \times T^2}$$

vapor pressure of water in mmHg

At the inlet conditions

$$P(T) = \frac{\mathcal{N}_3^{(1)}}{\sum_{i=1}^3 \mathcal{N}_i^{(1)}} 1 \times 760, \text{ Solution is } \{T = 289.66\}$$

$$\{x = 450.01\} = 450.01 - 273.16 = 177.01^\circ\text{C}$$

INTERPHASE ENERGY TRANSFER UNDER TURBULENT CONDITIONS

Energy transfer under turbulent conditions takes place when a fluid phase in turbulent motion encounters a solid surface at a different temperature. If the surface is open, energy will be transferred with each element of mass that appears or disappears at the interface with the solid phase. This energy flow can be appended to the mass transfer process. However, energy will also flow down a temperature gradient across a closed surface. This mechanism is separately accounted for in this chapter in much the same way that mass transfer coefficients were discussed in Chapter 12.

14.1 HEAT TRANSFER COEFFICIENTS—ANALOGY WITH MASS TRANSFER

The heat transfer coefficient is not measured directly, but is the result of calculations that use temperature and flow measurements at the inlet and outlet. The dependence of the heat transfer coefficient on the system parameters is deduced from the microscopic balance equations for the particular circumstances of the experiment. As we have seen in Chapters 8 and 11 for example, the solution to the microscopic balances in terms of dimensionless variables exposes the relative effects of the combinations of the physical parameters that affect the system behavior. The heat transfer coefficients can thereby be expressed most efficiently in the terms of these dimensionless variables.

It is important to know the temperature at the heat transfer interface in order to extract the heat transfer coefficient from an overall rate measurement of the thermal energy

transferred. To this end we may construct a heat transfer system essentially consisting of two fluids separated by a rigid diathermal solid. One of the fluids is pure and saturated at the desired temperature of the heat transfer interface. The local heat transfer process in the single-phase system can be isolated. The situation is illustrated in Figure 14.1, which may be discussed in terms of a heat transfer experiment to measure h .

The system is therefore similar to that in Figure 12.5 for the determination of a mass transfer coefficient. An overall energy balance corresponding to the mass balance in Equation (12.38) is given by

$$\rho c_p \mathcal{V} dT_b = h(T_s - T_b) \frac{dA_h}{dV} dV \quad (14.1)$$

In keeping with the similarity to the mass transfer case, this result entails averaging the microscopic thermal energy balance over the cross section with a unit normal perpendicular to that of the heat transfer surface (see Problem 15.1). The bulk temperature is therefore an average, but, because of turbulent mixing, the average will be close to the actual over most of the cross section. Equation (14.1) may be integrated between the inlet and outlet to give

$$\rho c_p \mathcal{V}(T_{bf} - T_{bo}) = h a_V (T_s - T_b)_{LM} V \quad (14.2)$$

where

$$(T_s - T_b)_{LM} = \frac{(T_s - T_{bf}) - (T_s - T_{bo})}{\ln \left[\frac{T_s - T_{bf}}{T_s - T_{bo}} \right]} \quad (14.3)$$

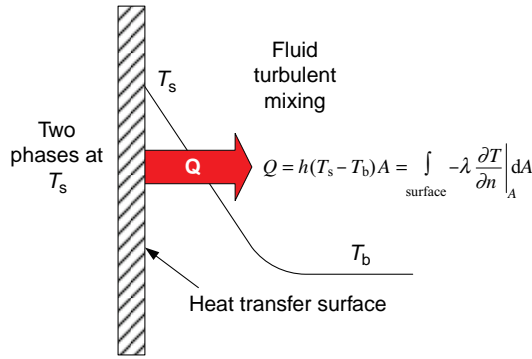


FIGURE 14.1 Local heat transfer surface.

The heat transfer coefficient and therefore the local convective hydrodynamic environment have been assumed to be constant over the surface.

As in the case of mass transfer, the heat transfer coefficient could be calculated from a solution to the transport equations, which would provide the integrand shown in Figure 14.1 for the evaluation of the heat transfer coefficient. The continuity equation, Equation (8.224), and the momentum balance, Equation (8.225), written for the mass transfer scenario apply here as well. The internal energy balance is given by Equation (8.227).

The characteristic temperature difference will most likely be the value at the surface less the inlet value. Additional dimensionless groups may appear in the same way as suggested in Chapter 12 for the mass transfer coefficient. For example, additional dimensionless groups may appear in the boundary conditions required at the inlet, equipment boundaries, and phase interfaces. It is important to note that the system of equations is the same with only a symbolic difference between the dimensionless concentration and temperature and the replacement of the Schmidt number with the Prandtl number. The solution for the concentration field may therefore be used for the temperature field with these replacements.

The heat transfer coefficient may then be calculated from the solution as follows:

$$h\Delta T a_V = \int_V k \nabla T \times \mathbf{n} a_V dV \quad (14.4)$$

$$\frac{hL}{k} = \frac{1}{V} \int_V \nabla^* T^* \times \mathbf{n} dV \quad (14.5)$$

The heat transfer coefficient has been assumed to be constant over the heat transfer surface. If the mean temperature difference is not the characteristic difference used in the transport equations, an adjustment will be needed in the result. The dimensionless form of the heat transfer coefficient (hL/k) is referred to as the Nusselt number for heat transfer and it is the same function of dimensionless groups as the Sherwood number in Equation (12.35) with the replacement of the Schmidt number with the Prandtl number:

$$N_{Nu} = F(N_{Re}, N_{Pr}, N_{Gr}, N_{Fr}, N_{Eq}, \dots) \quad (14.6)$$

Heat and mass transfer correlations are interchangeable to this extent.

14.2 HEAT EXCHANGERS

Chemical processes operate at specific temperatures selected on the basis of safety and material considerations, and the thermodynamic and rate considerations required to obtain the desired product stream. Temperature and phase requirements are affected by heat exchangers. A generic heat exchanger is depicted in Figure 14.2.

The heat exchanger is a device that provides a large internal area that prohibits any mixing of a hot stream with a cold stream and allows the exchange of thermal energy sufficient to achieve the desired outlet phase and temperature conditions in the process stream. The energy transfer rate required to meet the desired conditions is denoted by Q . The exchanger area required is A , which is a primary objective of design calculations. The overall heat transfer coefficient depends on the specific type of heat exchanger.

The stream targeted as the process stream can be the cold or the hot stream. It is most desirable for the second stream to also be a process stream to make the maximum use of the thermal energy available in the process itself. There are effective algorithms available for such heat integration and they can have a substantial effect on the process economics.

If the desired change cannot be (fully) affected by a process stream, a heat exchange medium is employed that is regenerated in the plant. Such streams are called process utilities and are produced by a separate unit in the plant. The process utilities may be cold or hot.

A common coolant is cooling water that is a process utility used very often because it is inexpensive to regenerate. Regeneration is affect in cooling towers where the water

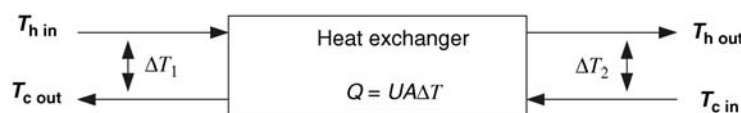


FIGURE 14.2 Generic heat exchanger.

is sprayed over a forced air stream. Some water is evaporated, which takes the heat of vaporization from the falling droplet. If you have not already done so, spin a wet wash rag and sense the cooling. Cooling towers accept water at approximately 115 °F and supply cold water at 80–90 °F (Couper et al., 2005). Because of economics alone, the operating pressure of distillation towers is selected so that cooling water may be used in the overhead condenser.

A common heat source is saturated steam made available by the utility section of the plant at different pressures. The steam is condensed to saturated liquid in the process heat exchanger, thereby supplying the required thermal energy at a constant temperature. Typical low pressure steam is at 5 barg, medium pressure at 10 barg, and high pressure at 41 barg (Turton et al., 2003).

The driving force for the transfer of thermal energy is the local temperature difference between the hot and cold fluids that exists across the heat exchange area. This temperature difference continually decreases through the exchanger when the streams are in parallel flow, since the cooling of the hot steam and the heating of the cold stream take place between aging elements in both streams. In countercurrent flow, the exchange takes place between aging elements in one stream and younger elements in the other, which tends to maintain the temperature driving force. For this reason, countercurrent flow is most often used.

For a given heat duty, a small driving force results in a large investment cost for a high area exchanger. A high driving force results in a smaller exchanger but a higher operating cost. The average driving force is reflected by the values at either end of the exchanger. These temperature differences, ΔT_1 and ΔT_2 , are called the approach temperatures and the minimum of these is normally the minimum driving force in the exchanger. The optimal value for sensible heat exchange is approximately 5–8 °C (Woods, 1995) in the region of ambient temperature.

The optimal approach temperature varies with temperature. The variation can be determined to maintain the efficiency associated with the heat exchange. To be specific about what we mean by efficiency, consider the transfer of heat, Q , between a hot fluid at T_h and a cold fluid at T_c . The greatest amount of work that could be derived from this interchange in an environment at temperature T_o is that of a reversible process such as the one illustrated in Figure 14.3.

The lost work is given by

$$W_{\text{Lost}} = W_h - W_c = QT_o \frac{T_h - T_c}{T_h T_c} = QT_o \frac{\Delta T}{T_h T_c} \quad (14.7)$$

An ideal efficiency, η , can then be defined as

$$\eta = \frac{W_h - W_c}{Q} = T_o \frac{T_h - T_c}{T_h T_c} = T_o \frac{\Delta T}{T_h T_c} \quad (14.8)$$

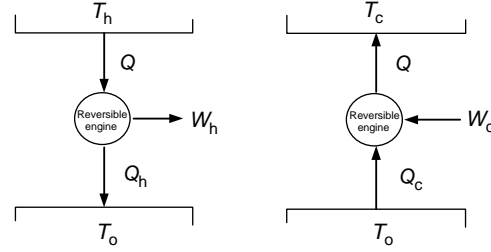


FIGURE 14.3 Lost work scenario.

This result implies that the minimum approach temperature should vary with the square of the root mean temperature of the heat exchange, in order to maintain the efficiency of the exchange. At cryogenic temperatures near 150 °K, the optimum approach temperature decreases to 1–2 °C (Woods, 1995).

Care must be taken in the selection of the minimum approach temperature in the case of phase change operations to avoid temperature crossover. The minimum temperature difference in these cases may occur inside the exchanger. For example, consider the cooling of a pure hot vapor, followed by condensation and subsequent cooling of the liquid. Suppose this is all affected by sensible heating of a cold liquid and that both streams have heat capacities that are independent of temperature.

A transfer of heat dQ from the hot vapor results in a proportional temperature change given by

$$dT_h = -\frac{1}{(mc_p)_h} dQ \quad (14.9)$$

A plot of the hot fluid temperature versus the heat extracted is therefore nearly a straight line in this region. The final cooling zone will also be a straight line, but the slope will be less for the liquid. The intermediate region will be horizontal, since the temperature will not change during the condensation process. The corresponding curve for the cold fluid will be a straight line. The situation depicted in Figure 14.4 could result.

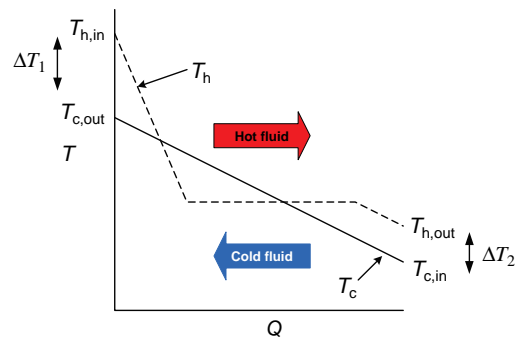


FIGURE 14.4 Temperature crossover.

In spite of the apparently acceptable approach temperatures at either end of the exchanger, a physically impossible condition exists in the exchanger. The cold fluid temperature can never exceed the hot fluid temperature and the hot fluid can never be cooled below the cold fluid temperature.

Film boiling is another important phenomenon in heat exchangers and takes place beyond a maximum allowable heat flux. Below this value, bubbles are formed on the heat exchange surface and are quickly released to the fluid phase in which they promote efficient mixing. Beyond this heat flux, the bubbles remain attached to the surface for a period of time sufficient to maintain a gas film on the heat transfer surface. The bubbles are released in explosions of vapor into the liquid phase. The resistance to heat transfer by the film is substantial and is to be avoided.

A **rule of thumb** is that the heat flux in reboilers should not exceed $31,500 \text{ W/m}^2$ (Peters et al., 2003) or that the temperature driving force should not exceed 45°F (Seader and Henley, 2006).

There are many types of heat exchangers devised for meeting a diverse set of process needs, but there are common analytical threads that unify them. The basic design procedures for heat exchangers can therefore be illustrated with several examples.

14.2.1 Double Pipe Exchangers

The simplest heat exchanger arrangement is the double pipe or concentric tube arrangement, which basically consists of a tube surrounded by a shell with an inlet and an outlet. The heat transfer surface is the surface of the tube. An example is shown in Figure 14.5 with a finned tube to enhance the heat transfer.

Double pipe exchangers are not recommended for phase change operations. The following rules of thumb may be contradictory, so the designer may need to develop alternatives and select the least expensive design for adoption.



FIGURE 14.5 Double pipe heat exchanger with fins. Reprinted with permission of Energy Transfer MDE.

- The stream that has the greatest potential for fouling should be placed in the tube. The tubes are easier to clean and generally less expensive in accommodating corrosive materials or high temperatures.
- The stream with the highest pressure or temperature should be placed in the tube that is more effective in accommodating a high pressure and the heat transfer coefficients will normally be higher.
- The stream with the lowest allowable pressure drop should be placed on the tube side.
- The more viscous stream should be placed in the shell side to increase the heat transfer coefficient.
- A maximum length of approximately 20 ft will avoid sagging.

As a basis for considering a sizing procedure for the double pipe exchanger, we assume that a process stream with a given flow rate and composition is to be cooled by another stream with specified temperature and composition. A reasonable procedure for designing a double pipe exchanger for a particular application is as follows (Smith, 2005):

1. Suppose that the hot process stream is allocated to the tube side and that there is no phase change in either stream. Suppose the minimum approach temperature is at the cold fluid outlet. Set this value to $\Delta T_{\min} = 10^\circ\text{F}$ as noted energy balance. Assuming constant heat capacities, the balance is given by

$$\mathcal{W}_c = \mathcal{W}_h \frac{c_{ph} (T_{h,in} - T_{h,out})}{c_{pc} (T_{c,out} - T_{c,in})} \quad (14.10)$$

2. Determine the tube and shell diameters. Both diameters can be calculated to give a liquid velocity of 2–3 m/s or a gas velocity of 10–20 m/s. Values in this range will provide a reasonable balance between fixed and operating costs (Peters et al., 2003). A nominal diameter of $\frac{3}{4}$ in. or 1 in. is common. The actual dimension of the tube (e.g., the inside diameter and the wall thickness) depends on the schedule, which is selected by Couper et al. (2005).

$$\text{Schedule} \approx 1000 \frac{\text{Internal pressure (psig)}}{\text{Allowable stress (psi)}} \quad (14.11)$$

The actual dimensions of steel pipe as a function of the schedule is shown in Table 14.1.

The smaller diameter will allow a higher surface area per unit volume.

3. Calculate the heat transfer area. The required area is given by

$$Q = U_o \Delta T_{LM} (2\pi r_o L) \quad (14.12)$$

TABLE 14.1 Steel Pipe Dimensions (Couper et al., 2005)

Nominal Pipe Size (in.)	OD (in.)	Schedule No.	ID (in.)	Flow Area per Pipe (in. ²)	Surface per lin ft (ft ²)		Weight per lin ft (lb Steel)
					Outside	Inside	
8-Jan	0.405	40\$	0.269	0.058	0.106	0.07	0.25
		80\$	0.215	0.036	0.106	0.056	0.32
4-Jan	0.54	40	0.364	0.104	0.141	0.095	0.43
		80	0.302	0.072	0.141	0.079	0.54
8-Mar	0.675	40	0.493	0.192	0.177	0.129	0.57
		80	0.423	0.141	0.177	0.111	0.74
2-Jan	0.84	40	0.622	0.304	0.22	0.163	0.85
		80	0.546	0.235	0.22	0.143	1.09
4-Mar	1.05	40	0.824	0.534	0.275	0.216	1.13
		80	0.742	0.432	0.275	0.194	1.48
1	1.32	40	1.049	0.864	0.344	0.274	1.68
		80	0.957	0.718	0.344	0.25	2.17
4-Nov	1.66	40	1.38	1.5	0.435	0.362	2.28
		80	1.278	1.28	0.435	0.335	3
2-Nov	1.9	40	1.61	2.04	0.498	0.422	2.72
		80	1.5	1.76	0.498	0.393	3.64
2	2.38	40	2.067	3.35	0.622	0.542	3.66
		80	1.939	2.95	0.622	0.508	5.03
2 1/2	2.88	40	2.469	4.79	0.753	0.647	5.8
		80	2.323	4.23	0.753	0.609	7.67
3	3.5	40	3.068	7.38	0.917	0.804	7.58
		80	2.9	6.61	0.917	0.76	10.3
4	4.5	40	4.026	12.7	1.178	1.055	10.8
		80	3.826	11.5	1.178	1.002	15
6	6.625	40	6.065	28.9	1.734	1.59	19
		80	5.761	26.1	1.734	1.51	28.6
8	8.625	40	7.981	50	2.258	2.09	28.6
		80	7.625	45.7	2.258	2	43.4
10	10.75	40	10.02	78.8	2.814	2.62	40.5
		60	9.75	74.6	2.814	2.55	54.8
12	12.75	30	12.09	115	3.338	3.17	43.8
16	16	30	15.25	183	4.189	4	62.6
20	20	20	19.25	291	5.236	5.05	78.6
24	24	20	23.25	425	6.283	6.09	94.7

where

$$\frac{1}{r_o U_o} = \frac{1}{r_i h_i} + \frac{1}{k_m} \ln \left[\frac{r_o}{r_i} \right] + \frac{1}{r_o h_o} \quad (14.13)$$

Resistances may be added to Equation (14.13) to account for fouling on the tube or shell side. The log mean temperature difference is defined in Equation (14.3), r_i is the inside diameter of the tube, r_o is the outside diameter of the tube, and L is its length. The overall heat transfer coefficient was determined with Equation (14.13) augmented by the resistances in the hot and cold fluids as illustrated in Figure 14.6. The subscript on the overall heat transfer coefficient indicates that the heat transfer area is being taken as the outside area of the tubes.

Any heat leak from the cold fluid to the surroundings has been neglected. Equations (14.14) and (14.15) are the result of applying the local form of the energy balance to the hot and cold streams:

$$\mathcal{W}_h c_{ph} \frac{dT_h}{dV} = -U_o (T_h - T_c) \frac{dA}{dV} \quad (14.14)$$

$$\mathcal{W}_c c_{pc} \frac{dT_c}{dV} = -U_o (T_h - T_c) \frac{dA}{dV} \quad (14.15)$$

The temperature differences at the ends of the exchanger may then be related and the overall energy balance for each fluid used to eliminate the flow rates. The result is the equation for the area of the exchanger.

The heat transfer coefficients may be calculated with the following correlations of experimental data.

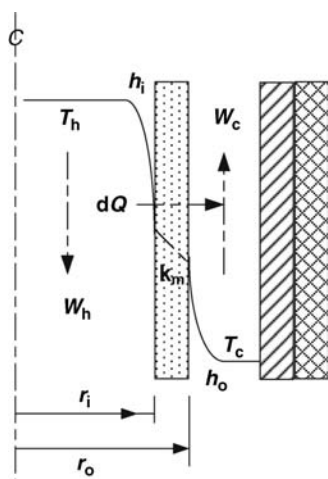


FIGURE 14.6 Temperature field and flow directions.

Tube Side:

A summary of the available correlations has been provided by Krauss et al. (2001). For turbulent flow, the following correlation is often used (Smith, 2005):

$$Nu = AN_{Re}^{4/5} N_{Pr}^{1/3} \left(\frac{\eta}{\eta_w} \right)^{0.14} \quad (14.16)$$

$$A = \begin{cases} 0.021 & \text{for gases} \\ 0.023 & \text{for nonviscous liquids, } N_{Re} \geq 10000 \\ 0.027 & \text{for viscous liquids} \end{cases} \quad (14.17)$$

The subscript w refers to conditions at the tube wall.

Shell Side:

The shell side coefficient can be obtained from the preceding correlations by using an equivalent diameter defined as four times the cross-sectional area for flow divided by the heated perimeter (Kern, 1950):

$$D = \frac{D_o^2 - D_i^2}{D_i} \quad (14.18)$$

where D_i and D_o are the inner and outer diameters of the annulus, respectively.

Typical values of the overall heat transfer coefficient are given in Table 14.2.

TABLE 14.2 Typical Values of Overall Heat Transfer Coefficients Double Pipe Exchangers

Process	U Btu/(h ft ² °F)
Gas (1 atm)–gas (1 atm)	2–6
Gas (250 atm)–gas (250 atm)	25–90
Liquid–gas (250 atm)	35–100
Liquid–liquid	50–250

Source: Adapted from Couper et al. (2005).

If the heat transfer area is greater than 20 m², multiple units as well as a shell and tube exchanger should be considered.

- Calculate the pressure drops on the tube and shell sides.

If the final design does not meet the design requirements from either the technical or the economic points of view, some adjustments within the ranges of the physical ranges discussed in the preceding examples could be made in an attempt to alleviate the discrepancies.

Example 14.2.1-1 Cooling of HCl Product from Adiabatic Mixing

(See Example 3.5.4.1-1.)

The product of an adiabatic dilution process is a 35 mol% HCl stream flowing at 5000 kg/h and 136.3 °C. The stream is to be ultimately cooled to 25 °C. It is first used to generate low pressure steam (lps) at 20 psig and to preheat a reactor feed stream. These heat integration operations result in a stream temperature of 160 °F. Process cooling water (80–115 °F) is available that can cool the stream to 90 °F in a countercurrent exchanger for a minimum approach temperature of 10 °F and not exceed a temperature difference of 45 °F. Determine the size of a double pipe exchanger that would be required.

Data:

$$t_{\text{ave shell}} = \frac{80 + 115}{2} = 97.5^\circ\text{F} = (97.5 - 32)/1.8 = 36.389^\circ\text{C} = 36.39 + 273.16 = 309.55\text{ K}$$

$$t_{\text{ave tube}} = \frac{90 + 160}{2} = 125.0^\circ\text{F} = (125 - 32)/1.8 = 51.667^\circ\text{C} = 51.667 + 273.16 = 324.83\text{ K}$$

Approximate data:

$$\rho = 1,189\text{ kg/L} = 1.189\text{ g/cm}^3$$

$$\eta = 2.10\text{ mPa s} = 0.0210\text{ g/(cm s)} \text{ for mixture} \\ = 0.716\text{ cP} = 0.00716\text{ g/(cm s)} \text{ for water}$$

Specific heat data are available in Example 3.5.4.1-1:
1 = HCl, 2 = H₂O

$$a = \frac{73.993 - 1.2946 \times 10^{-1} - 7.8980 \times 10^{-5} - 2.6409 \times 10^{-6}}{92.053 - 3.9953 \times 10^{-2} - 2.1103 \times 10^{-4} - 5.3469 \times 10^{-7}}$$

$$c_p(i, T) = \sum_{j=1}^{j=4} a_{i,j} T^{j-1} \text{ J/(mol K)}$$

$$\text{Tube side : } T_1 = (90 - 32)/1.8 + 273.16 = 305.38\text{ K} \\ T_2 = (160 - 32)/1.8 + 273.16 = 344.27\text{ K}$$

$$c_{Pm} = \frac{1}{(T_2 - T_1)} \left(0.35 \sum_{j=1}^{j=4} a_{1,j} \frac{1}{j} (T_2^j - T_1^j) + 0.65 \sum_{j=1}^{j=4} a_{2,j} \frac{1}{j} (T_2^j - T_1^j) \right) = 88.914 \text{ J/(mol K)}$$

Shell Side : $T_1 = (80 - 32)/1.8 + 273.16 = 299.83 \text{ K}$
 $T_2 = (115 - 32)/1.8 + 273.16 = 319.27 \text{ K}$

$$c_{Pm} = \frac{1}{(T_2 - T_1)} \sum_{j=1}^{j=4} a_{2,j} \frac{1}{j} (T_2^j - T_1^j) = 75.333 \text{ J/(mol K)}$$

Heat Duty

$$Q = \frac{5000(1000)}{3600} \frac{88.914(344.27 - 305.38)}{0.35(36.4610 + 0.65(18.016))} = 2.8485 \times 10^5 \text{ J/s,}$$

which gives a coolant rate of

$$\mathcal{W}_c = \frac{2.8485 \times 10^5}{75.33(319.27 - 299.83)} 18.016 = 3504.4 \text{ g/s}$$

Diameters: velocity 2–3 m/s—say, 250 cm/s:

Tube:

$$(1.189)(250) \frac{\pi D^2}{4} = \frac{5000(1000)}{3600}, \text{ Solution is: } D = 2.4391 \text{ cm or } 0.9603 \text{ in. Choose 1 in. (Schedule 80) nominal pipe size (Table 14.3).}$$

Shell:

$$(1)(250) \frac{\pi}{4} (D^2 - (2.54 \times 1.32)^2) = 3504. \text{ Solution is: } D = 5.3934 \text{ or } \frac{5.3934}{2.54} = 2.1234 \text{ in. Choose 2 in. (Schedule 40) nominal pipe size (Table 14.3).}$$

Exchanger Length

In applying the correlation in Equation (14.13), an initial estimate of the wall temperature can be made by carrying out the calculations without including the viscosity term. At the conclusion of the calculations, the wall temperature may be estimated by equating the heat transfer rates in the two zones. The calculations are then repeated until the wall temperature converges.

Shell side heat transfer coefficient:

$$\text{Estimate } \lambda = 0.0016 \text{ cal/(s cm K)} = 0.0016/0.23901 = 0.0066943 \text{ J/(s cm K)}$$

$$\text{Dequivalent} = (2.0672 - 1.322)/1.32 = 1.916 \text{ in.} = 4.866 \text{ cm}$$

$$N_{Re} = 4(3505.4)/(3.1416 \times 4.866 \times 0.00716) = 128,104$$

$$N_{Pr} = (75.3333/(18.016))0.00716/0.0066943 = 4.4724$$

$$N_{Nu} = 0.023(128,104)^{1/3} 4.4724^{1/3} = 462.0$$

$$h = 462.0(0.0066943)/4.866 = 0.636 \text{ J/(s cm}^2 \text{ K)}$$

Tube side heat transfer coefficient:

Similar calculations give

$$N_{Re} = 25,116$$

$$N_{Pr} = 16.543$$

$$N_{Nu} = 236.61$$

$$H = 0.325 \text{ J/(s cm}^2 \text{ K)}$$

Neglecting the viscosity correction and the resistance of the metal wall, the overall heat transfer coefficient may be calculated:

$$\frac{1}{1.32U} = \frac{1}{0.957(0.325)} + \frac{1}{1.32(0.636)}, \text{ Solution is: } U = 0.172 \text{ J/(s cm}^2 \text{ K)}$$

$$\Delta T_{lm} = \frac{\frac{160 - 115}{1.8} - \frac{90 - 80}{1.8}}{\ln \frac{160 - 115}{90 - 80}} = 12.928 \text{ K}$$

$$2.8485 \times 10^5 = 0.172(12.93)3.1416(1.32 \times 2.54)L, \text{ Solution is: } L = 1.2162 \times 10^4 \text{ cm or } 1.2162 \times 10^4/(2.54 \times 12) = 399.02 \text{ ft}$$

$$\text{Area} = 3.1416(1.32/12)399.02 = 137.9 \text{ ft}^2$$

Maximum length = 20 ft so that 20 tubes (O.D. = 2.067 in. for tube plus insulation) connected in series with return bends.

14.2.2 Shell and Tube Heat Exchangers

There is a wide variety of shell and tube heat exchangers, all designed to provide a large heat transfer area per unit volume and a high heat transfer rate. If the tubes of a double pipe exchanger with multiple return bends are connected in parallel and made to share a common shell, there results the defining construction of a shell and tube heat exchanger. The tubes are collected in a tube bundle and mounted on a tubesheet. See Figure 14.7 for a 1(shell pass)–1(tube pass) exchanger with two typical layouts for the tube sheet: the square and triangular pitches (distance between tube centers).

Standard tube lengths are 8, 12, 16, and 20 ft. Standard diameters are given in Table 14.3.

The shell sizes required to support some tube bundles of various sizes are given in Table 14.4 for a square pitch.

The sizing of shell and tube exchangers follows along the same general lines as for the double pipe. Some basic differences can arise. Except for the case when one or both fluids undergo an isothermal phase change, a correction must be applied to the log mean temperature difference to obtain the correct average driving force. Different heat transfer correlations apply to the shell side and the pressure drops are computed with different correlations on each side. Typical values of the heat transfer coefficients are given in Table 14.5.

14.2.2.1 Constant Wall Temperature A particularly common application of shell and tube heat exchangers is when a phase change material (such as the process utility, saturated steam) is supplied to the shell. In these cases, a constant tube wall temperature may be assumed and the heat exchanger sized on the basis of the tube alone.

For a constant wall temperature, the correlation of Gnielinski (as reported in Bejan, 1993):

$$N_{Nu} = \frac{\frac{f}{2}[N_{Re} - 1000]N_{Pr}}{1 + 12.87\sqrt{\frac{f}{2}}[N_{Pr}^{2/3} - 1]} \quad 0.5 < N_{Pr} < 1,000,000 \quad (14.19)$$

TABLE 14.3 Heat Exchanger and Condenser Tube Data

Tube OD (in.)	BWG	Wall Thick- ness (in.)	ID (in.)	Flow Area per Tube (in. ²)	Surface per lin ft (ft ²)		Weight per lin ft (lb Steel)
					Outside	Inside	
1/2	12	0.109	0.282	0.0625	0.1309	0.0748	0.493
	14	0.083	0.334	0.0876		0.0874	0.403
	16	0.065	0.37	0.1076		0.0969	0.329
	18	0.049	0.402	0.127		0.1052	0.258
	20	0.035	0.43	0.145		0.1125	0.19
3/4	10	0.134	0.482	0.182	0.1963	0.1263	0.965
	11	0.12	0.51	0.204		0.1335	0.884
	12	0.109	0.532	0.223		0.1393	0.817
	13	0.095	0.56	0.247		0.1466	0.727
	14	0.083	0.584	0.268		0.1529	0.647
	15	0.072	0.606	0.289		0.1587	0.571
	16	0.065	0.62	0.302		0.1623	0.52
	17	0.058	0.634	0.314		0.166	0.469
	18	0.049	0.652	0.334		0.1707	0.401
	8	0.165	0.67	0.355	0.2618	0.1754	1.61
1	9	0.148	0.704	0.389		0.1843	1.47
	10	0.134	0.732	0.421		0.1916	1.36
	11	0.12	0.76	0.455		0.199	1.23
	12	0.109	0.782	0.479		0.2048	1.14
	13	0.095	0.81	0.515		0.2121	1
	14	0.083	0.834	0.546		0.2183	0.89
	15	0.072	0.856	0.576		0.2241	0.781
	16	0.065	0.87	0.594		0.2277	0.71
	17	0.058	0.884	0.613		0.2314	0.639
	18	0.049	0.902	0.639		0.2361	0.545
1 1/4	8	0.165	0.92	0.665	0.3271	0.2409	2.09
	9	0.148	0.954	0.714		0.2498	1.91
	10	0.134	0.982	0.757		0.2572	1.75
	11	0.12	1.01	0.8		0.2644	1.58
	12	0.109	1.03	0.836		0.2701	1.45
	13	0.095	1.06	0.884		0.2775	1.28
	14	0.083	1.08	0.923		0.2839	1.13
	15	0.072	1.11	0.96		0.2896	0.991
	16	0.065	1.12	0.985		0.2932	0.9
	17	0.058	1.13	1.01		0.2969	0.808
1 1/2	18	0.049	1.15	1.04	0.3025	0.3015	0.688
	8	0.165	1.17	1.075		0.3063	2.57
	9	0.148	1.2	1.14		0.3152	2.34
	10	0.134	1.23	1.19		0.3225	2.14
	11	0.12	1.26	1.25		0.3299	1.98
	12	0.109	1.28	1.29		0.3356	1.77
	13	0.095	1.31	1.35		0.343	1.56
	14	0.083	1.33	1.4		0.3492	1.37
	15	0.072	1.36	1.44		0.3555	1.2
	16	0.065	1.37	1.47		0.3587	1.09
	17	0.058	1.38	1.5		0.3623	0.978
	18	0.049	1.4	1.54		0.367	0.831

Source: Kern (1950).

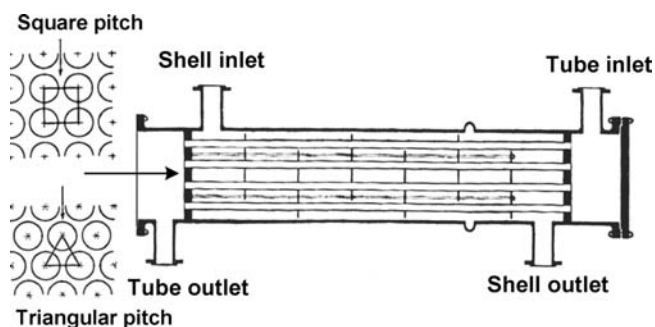


FIGURE 14.7 Fixed head shell and tube heat exchanger with tube pitch illustrations. Adapted from Kern 1950.

where

$$f = 0.046 N_{\text{Re}}^{-1/3} \quad 20,000 < N_{\text{Re}} < 1,000,000 \quad (14.20)$$

or

$$\frac{1}{\sqrt{f}} = 1.737 \ln \left[\sqrt{f} N_{\text{Re}} \right] - 0.396 \quad 2,000 < N_{\text{Re}} < 1,000,000 \quad (14.21)$$

is valid over the entire range.

Example 14.2.2.1-1: Exchanger 309—Solvent Endings

The acid products in the acrylic acid process are separated from the extraction solvent, diisopropyl ether (DIPE), in T-304 and the solvent is returned to the extraction unit, 03. (see Figure 14.8).

Stream Properties

Species 1 = Diisopropyl ether

Species 2 = Water

$$M = \frac{102.2}{18.016} \text{ Molecular weight}$$

$$\omega = \frac{\frac{M_{1,1} 1299.8}{M_{1,1} 1299.8 + M_{2,1} 198.7}}{\frac{M_{2,1} 198.7}{M_{1,1} 1299.8 + M_{2,1} 198.7}} = \frac{0.97376}{2.6241 \times 10^{-2}}$$

Weight fraction

$$x = \frac{\frac{1299.8}{1299.8 + 198.7}}{\frac{198.7}{1299.8 + 198.7}} = \frac{0.8674}{0.13260} \text{ Mole fraction}$$

$$A = \begin{matrix} 73.085 & 92.053 \\ 1.1235 & -3.9953 \times 10^{-2} \\ -3.7356 \times 10^{-3} & -2.1630 \times 10^{-4} \\ 5.2200 \times 10^{-6} & 5.3469 \times 10^{-7} \end{matrix} \text{ Specific heat}$$

parameters; columns = components

$c(j, T) = \sum_{i=1}^4 A_{i,j} T^{i-1}$ J/(mol K) Specific heat of component j

$$c(1, 298.16) = 214.34$$

$$c(2, 298.16) = 75.084$$

Energy Balance

$h(j) = \int_{273.18+13}^{273.16+40} \sum_{i=1}^4 A_{i,j} T^{i-1} dT$ Enthalpy change for component j J/mol

TABLE 14.4 Shell Sizes for Square Pitch

4 in. OD Tubes on 1 in. Square Pitch						1 in. OD Tubes on 1 in. Square Pitch					
ID Shell (n)	1-P	2-P	4-P	6-P	8-P	Shell ID (n)	1-P	2-P	4-P	6-P	8-P
8	32	26	20	20		8	21	16	14		
10	52	52	40	36		10	32	32	26	24	
12	81	76	68	68	60	12	48	45	40	38	36
13%	97	90	82	76	70	13%	61	56	52	48	44
15%	137	124	116	108	108	15%	81	76	68	68	64
17%	177	166	158	150	142	17%	112	112	96	90	82
19%	224	220	204	192	188	19%	138	132	128	122	116
21%	277	270	246	240	234	21%	177	166	158	152	148
23%	341	324	308	302	292	23%	213	208	192	184	184
25	413	394	370	356	346	25	260	252	238	226	222
27	481	460	432	420	408	27	300	288	278	268	260
29	553	526	480	468	456	29	341	326	300	294	286
31	657	640	600	580	560	31	406	398	380	368	358
33	749	718	688	676	648	33	465	460	432	420	414
35	845	824	780	766	748	35	522	518	488	484	472
37	934	914	886	866	838	37	596	574	562	544	532
39	1049	1024	982	968	948	39	665	644	624	612	600

TABLE 14.5 Typical Values of Film and Fouling Coefficients in Btu/(h ft² R)

Fluid and Process	Conditions	P (atm)	(ΔT), _{max} , (°F)	104 h	104 h_f
Sensible					
Water	Liquid			7.6–11.4	6–14
Ammonia	Liquid			7.1–9.5	0–6
Light organics	Liquid			28–38	6–11
Medium organics	Liquid			38–76	9–23
Heavy organics	Liquid heating			23–76	11–57
Heavy organics	Liquid cooling			142–378	11–57
Very heavy organics	Liquid heating			189–568	23–170
Very heavy organics	Liquid cooling			378–946	23–170
Gas		1–2		450–700	0–6
Gas		10		140–230	0–6
Gas		100		57–113	0–6
Condensing transfer					
Steam ammonia	All condensable	0.1		4.7–7.1	0–6
Steam ammonia	1% noncondensable	0.1		9.5–14.2	0–6
Steam ammonia	4% noncondensable	0.1		19–28	0–6
Steam ammonia	All condensable	1		3.8–5.7	0–6
Steam ammonia	All condensable	10		2.3–3.8	0–6
Light organics	Pure	0.1		28–38	0–6
Light organics	4% noncondensable	0.1		57–76	0–6
Light organics	Pure	10		8–19	0–6
Medium organics	Narrow range	1		14–38	6–30
Heavy organics	Narrow range	1		28–95	11–28
Light condensable mixes	Narrow range	1		23–57	0–11
Medium condensable mixes	Narrow range	1		38–95	6–23
Heavy condensable mixes	Medium range	1		95–190	11–45
Vaporizing transfer					
Water		<5	45	5.7–19	6–12
Water		<100	36	3.8–14	6–12
Ammonia		<30	36	11–19	6–12
Light organics	Pure	20	36	14–57	6–12
Light organics	Narrow range	20	27	19–76	6–17
Medium organics	Pure	20	36	16–57	6–17
Medium organics	Narrow range	20	27	23–95	6–17
Heavy organics	Pure	20	36	23–95	11–28
Heavy organics	Narrow range	20	27	38–142	11–45
Very heavy organics	Narrow range	20	27	57–189	11–57

Source: Couper et al. (2005).

Note: h = value in column $\times 10^4$.

Light organics have viscosity <1 cP, typically similar to octane and lighter hydrocarbons. Medium organics have viscosities in the range 1–5 cP, like kerosene, hot gas oil, light crudes, and so on. Heavy organics have viscosities in the range 5–100 cP, cold gas oil, lube oils, heavy and reduced crudes, and so on. Very heavy organics have viscosities above 100 cP, asphalts, molten polymers, greases, and so on. Gases are all noncondensables except hydrogen and helium, which have higher coefficients.

$$Q = 1299.8h(1) + 198.7h(2) = 7.9363 \times 10^6 \text{ kJ/h}$$

Duty required to heat process stream

$$h_{vap} = 2082.6(16 + 2 \times 1.008) = 37520.0 \text{ kJ/kmol}$$

Latent heat of vaporization of 160°C saturated steam

$$\text{duty} = 7.9363 \times 10^6 / 37520.0 = 211.52 \text{ kmol/h}$$

= Steam required

$$\text{duty} = 211.52M_{2,1}/1000 = 3.8107 \text{ tonne/h}$$

Tube diameter and number of tubes (N) required:

Say, tube velocity = 1.5 m/s in a 3/4 in BWG 14 heat exchanger tubes

$$\text{Mass flow rate in tubes} = M_{1,1}1299.8 + M_{2,1}198.7$$

$$= 1.3642 \times 10^5 \text{ kg/h}$$

$$\text{Tube ID} = 0.584 \text{ in.}$$

$$\text{Tube OD} = 0.584 + 2 \times 0.083 = 0.75 \text{ in.}$$

$$\rho(T) = \omega_{1,1}0.26218(0.26974)^{-\left(1-\frac{T}{500.05}\right)^{0.28571}} + \omega_{2,1}0.34710(0.274)^{-\left(1-\frac{T}{647.13}\right)^{0.28571}}$$

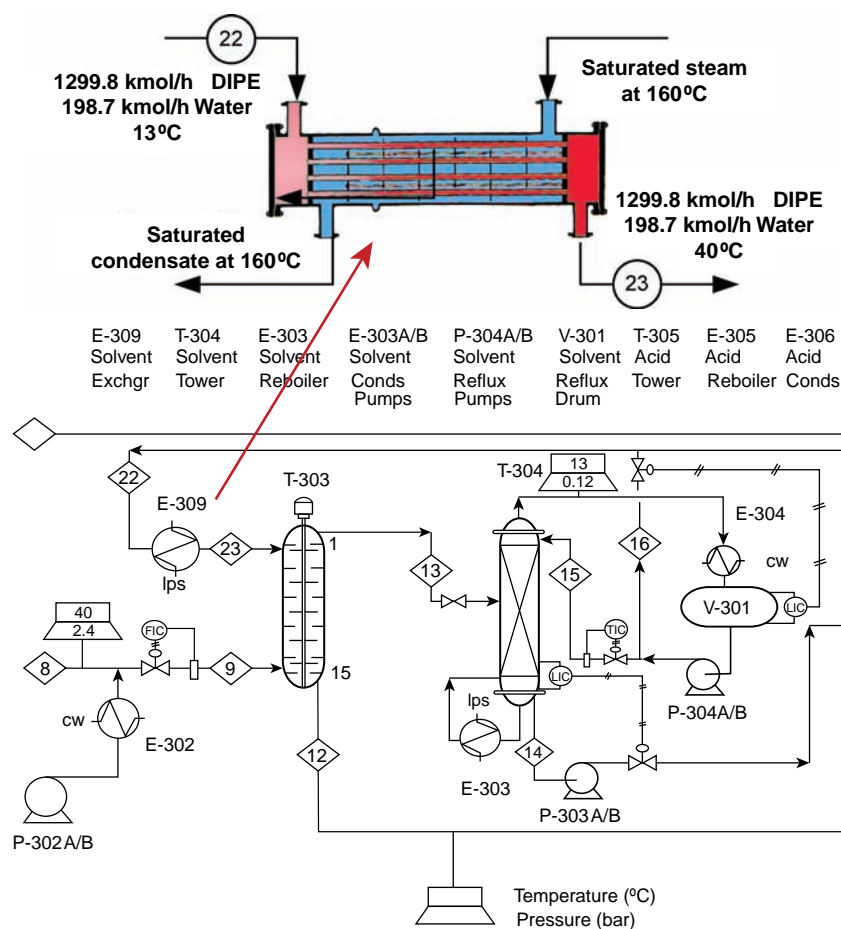


FIGURE 14.8 Heat exchanger E-309.

$$\rho(273.16 + 40) = 0.71307$$

$$\rho(273.16 + 13) = 0.74093$$

Say, average density = $(0.71307 + 0.74093)/2 = 0.727 \text{ g/ml}$

$N \left(\frac{3.1416}{4} \left(\frac{0.584 \times 2.54}{100} \right)^2 \right) 0.727 \times 10^6 \times 1.5 \times 3600 = 1.3642 \times 10^5 \times 1000$, Solution is: $\{N = 201.08\}$, or 202 tubes are needed

Determine the overall heat transfer coefficient.

Viscosity: Average with weight fractions

$$\mu(T) = \omega_{1,1} 10^{-5.535 + \frac{748.94}{T} + 0.013145T - 1.5557 \times 10^{-5} T^2} + \omega_{2,1} 10^{-10.2158 + \frac{1792.5}{T} + 0.01773T - 1.2631 \times 10^{-5} T^2}$$

$$\mu(273.16 + 40) = 0.2902 \text{ cP}$$

$$\mu(273.16 + 13) = 0.39376 \text{ cP}$$

Say, average viscosity = $(0.2902 + 0.39376)/2 = 0.34198 \text{ cP}$

Thermal Conductivity: Average with weight fractions

$$\lambda(T) = \omega_{1,1} \left(0.2894 - 8.7145 \times 10^{-4} T + 9.26 \sum_{i=1}^n X_i 49 \times 10^{-7} T^2 \right) + \omega_{2,1} (-0.2758 + 4.612 \times 10^{-3} T - 5.5391 \times 10^{-6} T^2)$$

$$\lambda(273.16 + 40) = 0.12095 \text{ W/(m K)}$$

$$\lambda(273.16 + 13) = 0.12835 \text{ W/(m K)}$$

Say, average thermal conductivity = $(0.12095 + 0.12835)/2 = 0.12465 \text{ W/(m K)}$

$$N_{Pr}(T) = \frac{\frac{x_{1,1} c(1,T) + x_{2,1} c(2,T)}{x_{1,1} M_{1,1} + x_{2,1} M_{2,1}} (0.01 \eta(T))}{0.01 \lambda(T)} \text{ Prandtl number}$$

$$N_{Pr}(273.16 + 13) = 6.5052$$

$$N_{Pr}(273.16 + 40) = 5.2653$$

Inside Coefficient

$$N_{Re}(T) = \frac{\rho(T)(0.584 \times 2.54)1.5 \times 100}{\eta(T) \times 0.01} \text{ Reynolds number}$$

$$N_{Re}(273.16 + 40) = 54,673.$$

$$N_{Re}(273.16 + 13) = 41,868.$$

$$N_{Nu}(T) =$$

$$\frac{\left(\frac{0.046 \times N_{Re}(T)^{-1/5}}{8}\right)(N_{Re}(T) - 1000)N_{Pr}(T)}{1.00 + 12.7 \sqrt{\frac{0.046 \times N_{Re}(T)^{-1/5}}{8}}(N_{Pr}(T)^{2/3} - 1) \text{ Nusselt number}}$$

$$N_{Nu}(273.16 + 40) = 110.75$$

$$S(273.16 + 13) = 99.666$$

$$h_i(T) = S(273.16 + \frac{53}{2}) \frac{k(T)}{\frac{0.584 \times 2.54}{100}} \text{ Inside heat transfer coefficient J/(m}^2 \text{ s K)}$$

$$h_i(273.16 + 40) = 859.655$$

$$h_i(273.16 + 13) = 912.23.$$

$$\text{Say, } h_i = \frac{859.65 + 912.23}{2} = 885.94 \text{ J/(m}^2 \text{ s K)}$$

Neglecting any additional resistances (tube wall, shell fouling), the overall coefficient based on the outside area of the tube is given by

$$U = \frac{0.584}{0.750} 885.94 = 689.85 \text{ J/(m}^2 \text{ s K)}$$

Average Temperature Difference

$$LMTD = \frac{(160 - 40) - (160 - 13)}{\ln \frac{(160 - 40)}{(160 - 13)}} = 133.04$$

$$= 133.04 \text{ }^\circ\text{K or }^\circ\text{C}$$

Area Required

$$A = \frac{Q}{U\Delta T} = \frac{7.9363 \times 10^6 \times 1000}{3600 \times 689.85 \times 133.04} = 24.02 \text{ m}^2 \text{ (Simulator result = 19.7 m}^2\text{)}$$

$$\text{Tube length } 202(3.1416) \times \frac{0.75 \times 2.54}{100} \times L = 24.02,$$

$$\text{Solution is: } L = 1.9869 \text{ m} = \frac{1.9869 \times 100}{2.54 \times 12} = 6.5210 \text{ ft}$$

The number of tubes may be decreased to reach a standard length of 8 ft. The current number of tubes may be installed in a 19 $\frac{1}{4}$ in. shell with the tubes arranged on a 1 in. square pitch (see Table 14.4).

14.3 MULTI-TUBULAR CATALYTIC REACTORS

The basic design of many chemical reactors involves substantial heat transfer considerations for reactions with large enthalpy changes. If the reaction rate is thought of as a rate or proportionality factor times a distance from equilibrium, it can be seen that for both endothermic and exothermic reactions, heating of the reaction mixture has a beneficial effect on the rate constant. Close to equilibrium, however, the two reaction classes call for completely different heating programs. The endothermic reaction calls for more heat, but the exothermic reaction calls for cooling in order to move the equilibrium target toward the reaction products. Consequently, the heat transfer considerations can be either heating or cooling.

The basic idea of the shell and tube heat exchanger, whereby a high area per unit volume is achieved by distributing the reaction volume over many tubes encased in a heat exchange medium, is an attractive reactor consideration. Some examples are given in Table 14.6.

Reactor illustrations and additional examples are available (Froment and Bischoff, 1979).

We will consider a basic model to gain some experience with the full description of such systems and to illustrate some important operational characteristics.

14.3.1 Fixed-Bed Constant Wall Temperature One-Dimensional Model

In formulating a basic one-dimensional model of a nonisothermal fixed bed, two additional heat transfer coefficients

TABLE 14.6 Examples of Industrial Multi-Tubular Reactors

Product	Catalyst	Reaction Temperature ($^\circ\text{C}$)	Reaction Pressure (atm)
Acetone	Ni	300	1
Cyclohexanone	Cu on pumice	250–350	1
Phosgene	Activated carbon	50	5–10
Phthalic anhydride	V_2O_5	350	1
Styrene	Metal oxides	600–650	1

Source: Couper et al. (2005).

will be needed; one at the tube wall and the other at the particle surface.

A conductive mechanism of radial heat transfer through the fluid persists up to the tube wall in unpacked tubes. In fixed beds, the pathway involves two resistances: the packing as well as the fluid. The thermal conductivity of the packing lowers the resistance up to the region of the wall where a void is encountered with a substantially higher resistance. The energy flux at the wall is expressed as

$$J_e = h_w(T - T_w) \quad (14.22)$$

A correlation due to J. Beek (as reported by Smith, 1981) is

$$Nu_w = \frac{h_w D_p}{\lambda} = 2.58 N_{Re}^{1/3} N_{PrRe}^{1/3} + 0.094 N_{Re}^{0.8} N_{Re}^{0.4} \quad \text{cylinders} \quad (14.23)$$

$$Nu_w = \frac{h_w D_p}{\lambda} = 0.203 N_{Re}^{1/3} N_{PrRe}^{1/3} + 0.220 N_{Re}^{0.8} N_{Re}^{0.4} \quad \text{spheres} \quad (14.24)$$

There is considerable variation in the reported values as indicated in Figures 14.9 and 14.10.

A one-dimensional model of a fixed-bed catalytic converter can be formulated on the basis of the following assumptions and restrictions:

- See Section 8.7.4.
- No axial or radial dispersion or conduction in bulk phase.
- Gas phase with single reaction on internal surface of catalyst particle.
- No temperature gradients in catalyst particle.

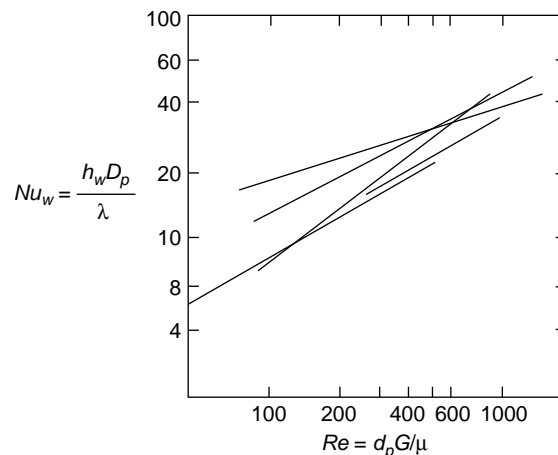


FIGURE 14.9 Wall heat transfer coefficient from various sources (Froment and Bischoff, 1979). Reprinted with permission of John Wiley & Sons.

- No mass transfer resistance between the bulk phase and the surface of the catalyst.
- Ideal gas mixture.

14.3.1.1 Bulk Phase Mass Balance (Molar Units) See Table 10.1 for mass balance in cylindrical system; steady state; axial (z) dependence only; interpret diffusivity as dispersion coefficient and set to zero; see footnote to Table 10.1 reference to the molar unit.

$$\frac{dN_i}{dz} = \mathcal{E}(\mathbf{y}, T_s, P) \vartheta_i \mathcal{R}_s(\mathbf{y}, T_s, P) S_g \rho_p (1 - \varepsilon_b) \quad i = 1, 2, \dots, N_c \quad (14.25)$$

$$N_i = N_{i0} \quad \text{at } z = 0 \quad (14.26)$$

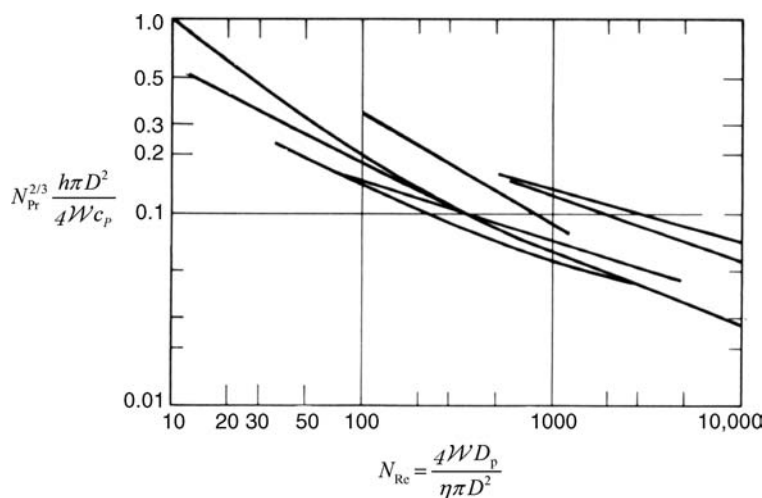


FIGURE 14.10 Heat transfer coefficient to particles in a fixed bed from various sources (Froment and Bischoff, 1979). Reprinted with permission of John Wiley.

There are N_c balances here. By selecting a key component, say α (see Section 2.3.1), the molar fluxes as well as the mole fractions may all be related to the flux of the key:

$$\frac{dN_\alpha}{dz} = \mathcal{E}(\mathbf{y}, T_s, P) \vartheta_\alpha \mathcal{R}_s(\mathbf{y}, T_s, P) S_g \rho_P (1 - \varepsilon_b) \quad (14.27)$$

$$N_\alpha = N_{\alpha 0} \quad \text{at } z = 0 \quad (14.28)$$

$$N_i = N_{i0} + \frac{\vartheta_i}{\vartheta_\alpha} (N_\alpha - N_{\alpha 0}) \quad (14.29)$$

$$y_i = \frac{y_{i0} + \frac{1}{N_o} \frac{\vartheta_i}{\vartheta_\alpha} (N_\alpha - N_{\alpha 0})}{1 + \frac{1}{N_o} \frac{\Delta n}{\vartheta_\alpha} (N_\alpha - N_{\alpha 0})} \quad \text{where} \quad (14.30)$$

$$\Delta n = \text{mole change for the reaction} = \sum_{\text{all components}} \vartheta_i \quad (14.31)$$

$$N_o = \text{Total molar flow to the reactor} = \sum_{\text{all components}} N_{i0} \quad (14.32)$$

14.3.1.2 Particle Phase Mass Balance (Molar Units)

The mass balance equations in Section 10.3.2 apply here also:

$$D_{ae} \frac{d^2 c_\alpha}{dx^2} + \rho_P S_g \vartheta_\alpha \mathcal{R}_s = 0 \quad (14.33)$$

$$c_\alpha = c_{\alpha s} \quad \text{at } x = \frac{V_p}{A_p} \quad (14.34)$$

$$-D_{ae} \frac{dc_\alpha}{dx} = 0 \quad \text{at } x = 0 \quad (14.35)$$

The same equations apply to all components in the mixture. Consequently, the concentrations in the reaction mixture within the catalyst pores are related to the key component value:

$$c_i = c_{is} + \frac{D_{ae} \vartheta_i}{D_{ie} \vartheta_\alpha} (c_\alpha - c_{\alpha s}) \quad (14.36)$$

At the surface of the catalyst,

$$c_{is} = y_i c(\mathbf{y}, T_s, P) \quad i = 1, 2, \dots, N_c \quad (14.37)$$

The assumption that the mole fractions at the exterior surface are equal to the bulk values is actually a statement about the mass transfer coefficients. It means that the mass transfer coefficients (see Section 12.2) are so large that a very small mole fraction difference is required to meet the equality of mass transfer and reaction rate:

$$k_{yi}(y_i - y_{is}) \frac{A_p}{V_p} = \int_{V_p} \rho_P S_g \vartheta_i \mathcal{R}_s dV \quad (14.38)$$

The molar density in Equation (14.37) must be calculated with an equation of state (see Example 2.1.1.1-1). For an ideal gas, Equation (14.37) becomes

$$\frac{dN_i}{dz} = \mathcal{E}(\mathbf{y}, T_s, P) \vartheta_i \mathcal{R}_s(\mathbf{y}, T_s, P) S_g \rho_P (1 - \varepsilon_b) \quad i = 1, 2, \dots, N_c$$

$$N_i = N_{i0} \quad \text{at } z = 0$$

$$c_{is} = y_i \frac{P}{RT_s} \quad (14.39)$$

The pressure, which is assumed to be uniform over each cross section, will be obtained from a momentum balance on the bulk phase. The energy balance on the catalyst will provide a relationship for the temperature at the surface.

14.3.1.3 Particle Phase Energy Balance The total flow of energy to the catalyst must be zero. Since the surface is uniform, the flux [see Equation (8.73)] must vanish at every point on the surface. For an ideal system this requires that

$$J_e^{(g)} = 0 = \sum_{\text{all components}} N_i^{(g)} H_i + h(T - T_s) \quad (14.40)$$

$$T_s = T + \varepsilon(\mathbf{y}, T_s, P) (-\vartheta_\alpha) \mathcal{R}_s(\mathbf{y}, T_s, P) S_g \rho_P \frac{V_p}{A_p} \underbrace{\frac{(-\Delta H_{R\alpha})}{\frac{1}{\vartheta_\alpha} \sum_{\text{all components}} \vartheta_i H_i}}_{\text{}} \quad (14.41)$$

14.3.1.4 Bulk Phase Energy Balance The energy balance for the bulk phase provides the means for determining the reactor temperature profile. It may be obtained by adapting the general formulation in Table 8.12 to the current application (see Problem 14.3). It may also be obtained from the general statement in Equation (8.88) and the energy flux in Equation (8.73). Taking the latter approach,

$$\frac{dJ_e}{dz} = -h_w(T - T_w) \frac{A_t}{V_t} = -h_w(T - T_w) \frac{4}{D_t} \quad (14.42)$$

The loss of thermal energy through the tube wall is not accessible to a unidirectional model that does not recognize the radial direction. The balance equation rests on a volumetric basis so that the loss through the tube wall is placed on a volume basis and included in the energy balance as a source term.

The derivative of the energy flux is

$$\frac{dJ_e}{dz} = \sum_{\text{all species}} N_i \frac{H_i}{dz} + \sum_{\text{all species}} H_i \frac{dN_i}{dz} \quad (14.43)$$

Applying the definition of the specific heat and the results of the material balance in the preceding equation yields the gradient in the total energy flux. Substitution of the flux into

the energy balance gives

$$NC_P \frac{dT}{dz} = (-\Delta H_{R\alpha}) \left[-\frac{dN_A}{dz} \right] - \frac{4}{D_t} h_w (T - T_w) \quad (14.44)$$

where

$$C_p = \sum_{\text{all components}} y_i C_{Pi} \quad (14.45)$$

The boundary condition required for the energy balance is a specified inlet temperature:

$$T = T_o \quad \text{at } z = 0 \quad (14.46)$$

14.3.1.5 Momentum Balance on Interstitial Fluid The Ergun equation [Equation (13.51)] can be applied locally to calculate the pressure.

$$\frac{dP}{dz} = \frac{(1 - \varepsilon_b)}{\varepsilon_b^3} \frac{G_0^2}{\rho D_p} \left[150 \frac{\eta(1 - \varepsilon_b)}{D_p G_0} + 1.75 \right] \quad (14.47)$$

$$P = P_o \quad \text{at } z = 0 \quad (14.48)$$

The mass flux is given by

$$G_0 = \sum M_i N_{io} = \text{constant} \quad (14.49)$$

The bed porosity and particle diameter are presumed to be fixed. An equation of state is required for the density. Table 8.9 provides methods for evaluating the viscosity.

The fixed-bed reactor model developed in this section is relatively sophisticated. It does not include all of the features

required to model every application so that individual cases must be carefully considered. However, the model and some simplified versions can be used to reflect behavior that is present to a greater or lesser extent in all fixed-bed reactors. Some examples are given below.

14.3.2 Some Operational Considerations

Exothermic reactions are best carried under conditions where the temperature is high initially from a rate point of view and decreased later in the reaction path from an equilibrium point of view. Such considerations were addressed in Section 7.4.4. The point here is that the heated feed inevitably leads to a “hot spot” in the reactor, which must be limited from chemical, material, and safety considerations.

As an example (Froment and Van Welsenaere, 1970) consider a single exothermic reaction in a fixed bed with a simplified version of the preceding model. Suppose that the reaction is first order in the key component and all but the key components are present in excess. The reaction rate can then be expressed as

$$\mathcal{R}_s = k_\infty e^{-E/RT} \underbrace{\prod_{i \neq \alpha} P_i^{\alpha_i}(0)}_{\substack{\text{Evaluation at} \\ \text{reactor entrance} \\ = \pi_0}} P_\alpha \quad (14.50)$$

Without any significant effect of mole changes in the reaction and without any important intraparticle or

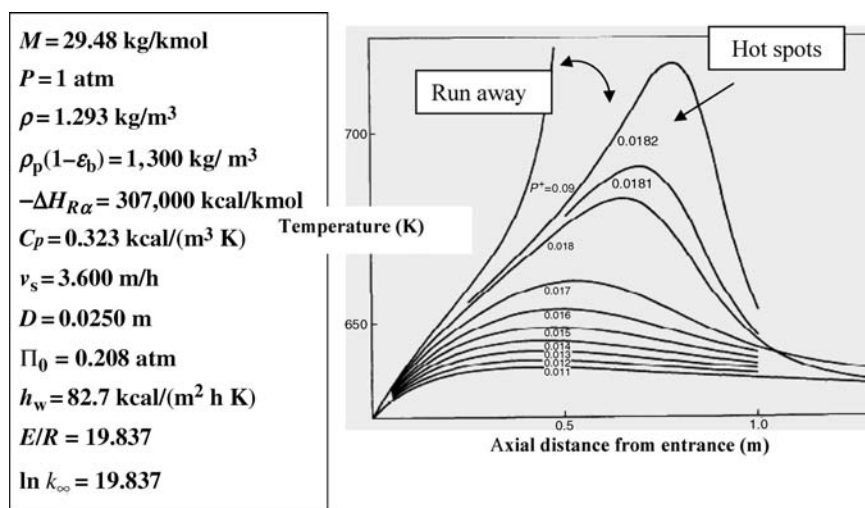


FIGURE 14.11 Temperature profiles—sensitivity to inlet partial pressure (Van Welsenaere and Froment, 1970). Reprinted with permission of Elsevier.

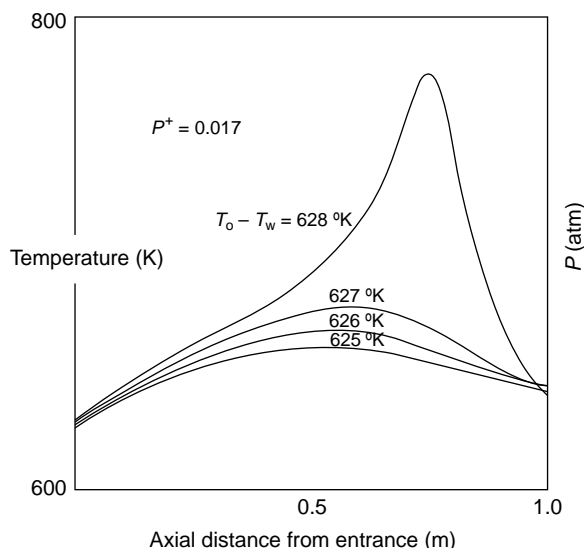


FIGURE 14.12 Temperature profiles—sensitivity to inlet wall temperature (Van Welsenaere and Froment, 1970). Reprinted with permission of Elsevier.

interparticle gradients, the mass balance in Equation (14.27) becomes

$$v_s \frac{dP_\alpha}{dz} = -Ak_\infty e^{-E/RT} P_\alpha \quad (14.51)$$

where

$$A = \frac{MP[\rho_p(1 - \varepsilon_b)]\pi_o}{\rho} \quad (14.52)$$

and v_s is the superficial axial velocity. The energy balance in Equation (14.48) becomes

$$v_s \frac{dT}{dz} = Bk_\infty e^{-E/RT} P_\alpha - C(T - T_w) \quad (14.53)$$

where

$$B = \frac{-\Delta H_{R\alpha}}{C_p} \rho_b \pi_o \quad \text{and} \quad (14.54)$$

$$C = \frac{4}{D} \frac{h_w}{cC_p} \quad (14.55)$$

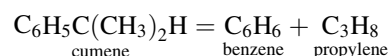
The following parameter values in Equations (14.50)–(14.55) to generate the profiles in Figures 14.11 and 14.12.

The hot spot referred to above is evident in both figures. The magnitude of the hot spot increases with both the wall temperature and the inlet partial pressure of the key reactant. The increase in the hot spot grows until a point is reached where a relatively small increase in the parameter value results in an enormous increase in the hot spot. This is an example of parametric sensitivity, which was first pointed out by Bilous and Amundson (1956). Similar sensitivity is observed in the ignition and extinction behavior of CSTRs (Section 6.6.1.5).

Note that the A/V ratio for this reactor is 160 m^{-1} . Tubular exchanger reactors in the microtechnology have A/V ratios of at least three times this value.

PROBLEMS

14.1. The cracking of cumene into benzene and propylene,



was carried out in a *fixed* bed of impermeable particles coated with a catalyst at 362°C and atmospheric pressure in the presence of a large excess of nitrogen. At a point in the reactor where the cumene partial pressure was 0.0689 atm, a reaction rate of $0.153 \text{ kmol cumene}/(\text{kg cat h})$ was observed. Determine the mole fraction of cumene and the temperature at the catalyst surface at this point in the reactor.

The catalyst surface area is $45 \text{ m}^2/\text{kg cat}$ and the interstitial mass flux is $56.47 \text{ kg}/(\text{m}^2 \text{ h})$.

14.2. A countercurrent, concentric tube heat exchanger is to be designed to cool 7500 lb m/h of benzene from 180°F to 100°F . Water at 70°F is to enter the shell at 5 ft/s . Benzene flows countercurrently through the inside pipe.

The inside pipe is Schedule 40-1 1/4 in. steel with an inside diameter of 1.38 in. and an outside diameter of 1.66 in. The outside pipe is Schedule 40-2 in. steel with an inside diameter of 2.07 in.

- Calculate the length required if the shell is insulated.
- Apply the heuristics presented in this chapter and make any changes that are required for conformity.

MICROSCOPIC TO MACROSCOPIC

The microscopic balance equations for mass—Equation (8.82), energy—Equations (8.92), (8.93), and (8.106), and momenta—Equations (8.84) and (8.87) apply pointwise throughout each phase in any chemical system. The balance equations for each phase are interwoven at phase boundaries by continuity in the flows of mass, energy, and momentum and by local thermodynamic equilibrium between adjoining phases. Similar conditions are applied at the surfaces that define the system (Table 8.7). In this chapter, we will demonstrate what we know intuitively to be correct: namely, that the macroscopic view is the summary of the microscopic views. The calculations have been reported by Bird (1957).

The following two mathematical results will be used repeatedly (Lass, 1950):

G = divergence theorem (Gauss): Suppose that \mathbf{F} and $\nabla \cdot \mathbf{F}$ are continuous over a volume V , which is contained by a finite number of surfaces with well-defined normals. It can be shown that

$$\int_V \nabla \cdot \mathbf{F} dV = \int_S \mathbf{F} \cdot \mathbf{n}_s dS \quad (15.1)$$

where \mathbf{n}_s is an outwardly directed normal to dS .

L = differentiation of a volume integral (Extension of Leibniz's rule) (Kaplan, 1991)

$$\begin{aligned} \frac{d}{dt} \int_V F(x, y, z, t) dV &= \int_V \frac{\partial F(x, y, z, t)}{\partial t} dV \\ &+ \int_S (\mathbf{v}_s \cdot \mathbf{n}_s) F(x, y, z, t) dS \end{aligned} \quad (15.2)$$

The volume V is a single-phase mixture that meets continuity requirements for the integrations (G and L above) over which we will integrate the microscopic balance equations. The volume is defined by a set of surfaces (S) that characterize the interactions of the system within with the surroundings.

- S_f = Portion of system boundary that is fixed; forms interface with surroundings; closed.
- S_w = Moveable portion of boundary; means by which mechanical work can be exchanged with the surroundings.
- S_1, S_2 = Open surfaces by which mass is transferred to the system (inlet) and mass is transferred from the system (outlet), respectively.
- S_m = Surface other than S_1 or S_2 by which mass may be interchanged with the surroundings.

15.1 MACROSCOPIC MASS BALANCE

Integration of the microscopic mass balance, Equation (8.82), is formulated as follows:

$$\int_V \frac{\partial \rho_i}{\partial t} dV + \int_V \nabla \cdot (\rho_i \mathbf{v} + \mathbf{j}_i) dV = \int_V r_{iV} dV \quad (15.3)$$

The first integral on the left-hand side follows from L :

$$\int_V \frac{\partial \rho_i}{\partial t} dV = \frac{d}{dt} \int_V \rho_i dV - \int_S \rho_i \mathbf{v}_s \cdot \mathbf{n}_s dS \quad (15.4)$$

$$= \frac{dm_i}{dt} - \int_S \rho_i \mathbf{v}_s \cdot \mathbf{n}_s dS \quad (15.5)$$

where W_i is the total mass of species in V , \mathbf{n}_s is an outwardly directed unit normal to the surface, and \mathbf{v}_s is the velocity of the surface.

The second integral on the left-hand side of Equation (15.3) follows from G :

$$\int_V \nabla \cdot (\rho_i \mathbf{v} + \mathbf{j}_i) dV = \int_{S_1+S_2+S_w+S_f+S_m} (\rho_i \mathbf{v} + \mathbf{j}_i) \cdot \mathbf{n}_s dS \quad (15.6)$$

which calls for integration over each of the containing surfaces:

S_1 : The magnitude of the integral over the inlet is the total mass flow rate of species i into the system through that portal. If this flow is primarily by convection and in the opposite direction of the normal to S_1 , the integral may be expressed as

$$\int_{S_1} (\rho_i \mathbf{v} + \mathbf{j}_i) \cdot \mathbf{n}_s dS \simeq \int_{S_1} \rho_i \mathbf{v} \cdot \mathbf{n}_s dS = - \int_{S_1} \rho_i v_n dS \quad (15.7)$$

where v_n is the inwardly directed normal velocity on the surface. Assuming that the concentration is constant over the inlet surface,

$$-\rho_i^{(S_1)} \int_{S_1} v_n dS = -\rho_i^{(S_1)} \left[\frac{1}{S_1} \int_{S_1} v_n dS \right] S_1 \quad (15.8)$$

$$= -\rho_i^{(S_1)} \langle v^{(S_1)} \rangle S_1 = -\mathcal{W}_i^{(S_1)} \quad (15.9)$$

The mass flow rate is the rate referred to in Equation (2.9) and $\langle v^{(S_1)} \rangle S_1$ is the volumetric rate referred to in the same equation.

S_2 : Following the same procedure at the outlet where the flow direction is aligned with the outward pointing normal to the integration surface:

$$\int_{S_2} (\rho_i \mathbf{v} + \mathbf{j}_i) \cdot \mathbf{n}_s dS \simeq \rho_i^{(S_2)} \langle v_i^{(S_2)} \rangle S_2 = \mathcal{W}_i^{(S_2)} \quad (15.10)$$

S_w : The integral over the moving surface may be expressed in terms of the flow due to the velocity of the surface and the flow relative to the surface:

$$\int_{S_w} (\rho_i \mathbf{v} + \mathbf{j}_i) \cdot \mathbf{n}_s dS = \int_{S_w} \rho_i \mathbf{v}_i \cdot \mathbf{n}_s dS \quad (15.11)$$

$$= \int_{S_w} \rho_i \mathbf{v}_s \cdot \mathbf{n}_s dS + \int_{S_w} \rho_i (\mathbf{v}_i - \mathbf{v}_s) \cdot \mathbf{n}_s dS \quad (15.12)$$

$$= \int_{S_w} \rho_i \mathbf{v}_s \cdot \mathbf{n}_s dS \quad (15.13)$$

The flow relative to the surface has been set to zero since the surface is assumed to be closed.

S_f : The integral over the fixed surface makes no contribution since it is closed and unreactive:

$$\int_{S_f} (\rho_i \mathbf{v} + \mathbf{j}_i) \cdot \mathbf{n}_s dS = 0 \quad (15.14)$$

In fixed beds, for example, the catalyst surface would be characterized as part of S_m even though it is fixed.

S_m : The mass transfer surface is assumed to be stationary so that

$$\int_{S_m} (\rho_i \mathbf{v} + \mathbf{j}_i) \cdot \mathbf{n}_s dS = \int_{S_m} (\rho_i \mathbf{v}_i \cdot \mathbf{n}_s dS = -\mathcal{W}_i^{(S_m)} \quad (15.15)$$

Otherwise, the velocity of species i relative to the surface velocity would appear in Equation (15.15).

The total reaction rate is given by the homogeneous and the heterogeneous components:

$$r_i = \int_V r_{iV} dV + \int_{S_m} r_{iS} dS \quad (15.16)$$

Equation (15.3) therefore becomes

$$\frac{dm_i}{dt} = \mathcal{W}_i^{(S_1)} - \mathcal{W}_i^{(S_2)} + \mathcal{W}_i^{(S_m)} + r_i \quad (15.17)$$

Equation (15.17) is the unsteady-state version of Equation (2.68) in mass units with one inlet and one outlet.

15.2 MACROSCOPIC ENERGY BALANCE

The macroscopic energy balance follows from the microscopic version with calculations very much the same as those for the mass balance in the preceding section. The microscopic energy flux and balance expression are given by Equations (8.69) and (8.88), respectively. Integration of the energy balance and one application each of the divergence theorem (G), Equation (15.1), and Leibniz's rule (L), Equation (15.2) gives

$$\begin{aligned} & \frac{dE_{\text{total}}}{dt} - \int_{S_1+S_2+S_w+S_f} \rho e \mathbf{v}_s \cdot \mathbf{n}_s dS \\ & + \int_{S_1+S_2+S_w+S_f} \underbrace{(\rho e \mathbf{v} + \mathbf{\Pi} \cdot \mathbf{v} + \sum \bar{h}_i \mathbf{j}_i + \mathbf{q}) \cdot \mathbf{n}_s}_{=\rho \left(\frac{1}{2} v^2 + \psi \right) \mathbf{v} + \sum \rho_i \bar{h}_i \mathbf{v}_i + \mathbf{q}} dS = 0 \end{aligned} \quad (15.18)$$

An external source, if present, must be added to the right-hand side of Equation (15.18).

S_1 : If diffusion and work against shear forces are neglected and the velocity is normal to the inlet surface and inwardly directed:

$$\begin{aligned} \int_{S_1} (\rho \mathbf{e} \mathbf{v} + \mathbf{\Pi} \cdot \mathbf{v} + \sum \bar{h}_i \mathbf{j}_i + \mathbf{q}) \cdot \mathbf{n}_s dS \\ = \int_{S_1} (\rho \mathbf{e} \mathbf{v} + P \mathbf{v} + \mathbf{q}) \cdot \mathbf{n}_s dS \end{aligned} \quad (15.19)$$

If the conditions over the inlet surface are constant except for the velocity,

$$\int_{S_1} (\rho \mathbf{e} \mathbf{v} + P \mathbf{v}) \cdot \mathbf{n}_s dS = -\rho^{(S_1)} e^{(S_1)} \langle v^{(S_1)} \rangle S_1 - P^{(S_1)} \langle v^{(S_1)} \rangle S_1 \quad (15.20)$$

$$Q_1 = - \int_{S_1} \mathbf{q} \cdot \mathbf{n}_s dS \quad (15.21)$$

S_2 : Similarly, at the outlet

$$\int_{S_2} (\rho \mathbf{e} \mathbf{v} + P \mathbf{v}) \cdot \mathbf{n}_s dS = \rho^{(S_2)} e^{(S_2)} \langle v^{(S_2)} \rangle S_2 + P^{(S_2)} \langle v^{(S_2)} \rangle S_2 \quad (15.22)$$

$$Q_2 = - \int_{S_2} \mathbf{q} \cdot \mathbf{n}_s dS \quad (15.23)$$

S_f : The fixed surface is presumed to be closed and unreactive. Consequently,

$$\int_{S_f} (\rho \mathbf{e} \mathbf{v} + \mathbf{\Pi} \cdot \mathbf{v} + \sum \bar{h}_i \mathbf{j}_i + \mathbf{q}) \cdot \mathbf{n}_s dS = \int_{S_f} \mathbf{q} \cdot \mathbf{n}_s dS = -Q_f \quad (15.24)$$

where Q_f is the rate of energy addition to the system by conduction through the fixed surfaces.

S_w : On the moving surface,

$$\begin{aligned} \int_{S_w} (\rho \mathbf{e} \mathbf{v} + \mathbf{\Pi} \cdot \mathbf{v} + \sum \bar{h}_i \mathbf{j}_i + \mathbf{q}) \cdot \mathbf{n}_s dS \\ = \int_{S_w} (\rho \mathbf{e} \mathbf{v}_s + \mathbf{\Pi} \cdot \mathbf{v}_s) \cdot \mathbf{n}_s dS + \int_{S_w} \mathbf{q} \cdot \mathbf{n}_s dS \end{aligned} \quad (15.25)$$

The second term on the right-hand side of Equation (15.25) is the rate at which the system does work on the surroundings so that

$$\begin{aligned} \int_{S_w} (\rho \mathbf{e} \mathbf{v} + \mathbf{\Pi} \cdot \mathbf{v} + \sum \bar{h}_i \mathbf{j}_i + \mathbf{q}) \cdot \mathbf{n}_s dS \\ = \int_{S_w} (\rho \mathbf{e} \mathbf{v}_s \cdot \mathbf{n}_s dS + W_s - Q_w \end{aligned} \quad (15.26)$$

where

$$W_s = \int_{S_w} (\mathbf{\Pi} \cdot \mathbf{v}_s \cdot \mathbf{n}_s dS \quad (15.27)$$

$$Q_w = \int_{S_w} \mathbf{q} \cdot \mathbf{n}_s dS \quad (15.28)$$

S_m : The mass transfer surface is assumed to be stationary. Neglecting work against shear forces as well as potential energy effects and conduction, its contribution may be determined as follows:

$$\begin{aligned} \int_{S_m} (\rho \mathbf{e} \mathbf{v} + \mathbf{\Pi} \cdot \mathbf{v} + \sum \bar{h}_i \mathbf{j}_i + \mathbf{q}) \cdot \mathbf{n}_s dS \\ = \int_{S_m} \left(\rho \left(\frac{1}{2} v^2 + \psi \right) \mathbf{v} + \sum \rho_i \mathbf{v}_i \bar{h}_i + \boldsymbol{\tau} \cdot \mathbf{v} + \mathbf{q} \right) \cdot \mathbf{n}_s dS \end{aligned} \quad (15.29)$$

$$= \int_{S_m} \left(\frac{1}{2} \rho v^2 \right) \mathbf{v} + \sum \rho_i \mathbf{v}_i \bar{h}_i \cdot \mathbf{n}_s dS = -Q_m \quad (15.30)$$

Substitution of the results into the integral of the microscopic energy balance gives

$$\frac{dE_{\text{total}}}{dt} = -\Delta \left[\left(h + \frac{1}{2} v^2 + \Psi \right) \mathcal{W}^{(S)} \right] + Q + Q_m - W_s \quad (15.31)$$

where

$$Q = Q_1 + Q_2 + Q_f + Q_w \quad (15.32)$$

Conduction at the inlet and outlet have been included in the definition of Q but these are often not important. The heat interaction on the fixed surface is likely to be most significant in sizing a heat exchanger

Equations (15.31) and (3.91), derived from macroscopic arguments, are the same for steady-state applications.

15.3 MACROSCOPIC MECHANICAL ENERGY BALANCE

The microscopic mechanical energy balance can be expressed as the sum of the microscopic kinetic and potential energy balances given by Equations (8.92) and (8.93). The internal energy that accounts for thermal effects is excluded for the purpose of considering only the mechanical effects. If gravity is the only external force, the microscopic mechanical energy balance is given by

$$\begin{aligned} \frac{\partial}{\partial t} \left[\rho \left(\frac{1}{2} v^2 + \psi \right) \right] + \nabla \cdot \rho \left[\frac{1}{2} v^2 + \Psi \right] \mathbf{v} \\ = -\nabla \cdot (\boldsymbol{\tau} \cdot \mathbf{v}) - (-\boldsymbol{\tau} : \nabla \mathbf{v}) - \mathbf{v} \cdot \nabla P \end{aligned} \quad (15.33)$$

The macroscopic form of the mechanical energy balance follows from calculations similar to those carried out above for mass and energy.

Application of Equation (15.2) to the first term in Equation (15.33) and noting that the only surface with a nonzero velocity is S_w ,

$$\int_V \frac{\partial}{\partial t} \left[\rho \left(\frac{1}{2} v^2 + \Psi \right) \right] dV = \frac{d(K_{\text{total}} + \Psi_{\text{total}})}{dt} - \int_{S_w} \left[\rho \left(\frac{1}{2} v^2 + \Psi \right) \right] \mathbf{v}_s \cdot \mathbf{n}_s dS \quad (15.34)$$

Application of Gauss's theorem, Equation (15.1), to the next two terms in Equation (15.33):

$$\int_V \nabla \cdot \left[\rho \left(\frac{1}{2} v^2 + \Psi \right) \right] \mathbf{v} dV = \int_{S_1+S_2+S_w+S_f+S_m} \left[\rho \left(\frac{1}{2} v^2 + \Psi \right) \right] \mathbf{v} \cdot \mathbf{n}_s dS = \Delta \left\{ \left[\frac{1}{2} \frac{\langle v^3 \rangle}{\langle v \rangle} + \Psi \right] \mathcal{W}^{(S)} \right\} \quad (15.35)$$

$$+ \int_{S_w} \left(\left[\rho \left(\frac{1}{2} v^2 + \Psi \right) \right] \mathbf{v}_s \right) \cdot \mathbf{n}_s dS + \int_{S_m} \left(\left[\rho \left(\frac{1}{2} v^2 + \Psi \right) \right] \mathbf{v} \right) \cdot \mathbf{n}_s dS$$

$$\int_V \nabla \cdot (\boldsymbol{\tau} \cdot \mathbf{v}) dV = \int_S (\boldsymbol{\tau} \cdot \mathbf{v}) \cdot \mathbf{n}_s dS \quad (15.36)$$

$$= \int_{S_w} (\boldsymbol{\tau} \cdot \mathbf{n}_s) \cdot \mathbf{v} dS + \int_{S_m} (\boldsymbol{\tau} \cdot \mathbf{n}_s) \cdot \mathbf{v} dS$$

$$\int_V \nabla \cdot P \mathbf{v} dV - \int_V P \nabla \cdot \mathbf{v} dV = \int_V \nabla \cdot P \mathbf{v} dV - \int_V P \nabla \cdot \mathbf{v} dV \quad (15.37)$$

$$= \int_{S_w} (\boldsymbol{\tau} \cdot \mathbf{n}_s) \cdot \mathbf{v}_s dS + \int_{S_w} (\boldsymbol{\tau} \cdot \mathbf{n}_s) \cdot (\mathbf{v} - \mathbf{v}_s) dS + \int_S P \mathbf{v} \cdot \mathbf{n}_s dS - \int_V P \nabla \cdot \mathbf{v} dV \quad (15.38)$$

The work against the shear forces due to mass transfer across the interfacial mass transfer surface is neglected.

The next term accounts for the total rate of viscous dissipation in the system:

$$\int_V (-\boldsymbol{\tau} : \nabla \mathbf{v}) dV = E_v \quad (15.39)$$

The last term cannot be integrated in closed form, except for particular circumstances.

15.3.1 Unsteady-State Form

To continue with the unsteady-state analysis, we note that

$$\begin{aligned} \int_V \mathbf{v} \cdot \nabla P dV &= \int_V \nabla \cdot P \mathbf{v} dV - \int_V P \nabla \cdot \mathbf{v} dV \\ \int_V \nabla \cdot P \mathbf{v} dV &= -\Delta \frac{P}{\rho} \langle v \rangle S + \int_{S_{wA}+S_{mA}} P \mathbf{v}_s \cdot \mathbf{n} dS \\ &\quad + \int_{S_{mA}} P (\mathbf{v} - \mathbf{v}_s) \cdot \mathbf{n} dS \end{aligned} \quad (15.40)$$

The second term on the right-hand side of the preceding equation is the work done by the system at the moving surfaces against the normal pressure force, W_n . The third term on the right-hand side contributes to the flux of mechanical energy across the mass transfer surface. Substitution of the preceding results into the integral of the microscopic mechanical energy balance gives

$$\begin{aligned} \frac{d(K_{\text{total}} + \Psi_{\text{total}})}{dt} &= -\Delta \left\{ \left[\frac{1}{2} \frac{\langle v^3 \rangle}{\langle v \rangle} + \Psi + \frac{P}{\rho} \right] \mathcal{W} \right\} \\ &= +B - W - E_v - \int_V (P \nabla \cdot \mathbf{v}) dV \end{aligned} \quad (15.41)$$

where

$$B = - \int_{S_m} \left(\left[\left(\frac{1}{2} v^2 + \Psi + \frac{P}{\rho} \right) \right] \mathbf{v} \right) \cdot \mathbf{n}_s dS \quad (15.42)$$

The integral on the right-hand side vanishes for incompressible systems

15.3.2 Steady-State Systems

Suppose that the volume of the system, at steady state, is formed by small volume elements about streamlines, lines whose tangent, t , is in the direction of the mass average velocity. Consider the volume element about a streamline to have cross-sectional area δA_c , perpendicular to the streamline. The contribution of this streamline to the integral,

$$I = \int_V (\mathbf{v} \cdot \nabla P) dV \quad (15.43)$$

is given by

$$\delta I = \int_{\delta V} (\mathbf{v} \cdot \nabla P) \delta A_c \delta l \quad (15.44)$$

where δl is a differential distance along the streamline. Since the velocity is tangent to the streamline,

$$\delta I = \int_{\delta V} (\mathbf{t} \mathbf{v} \cdot \nabla P) \delta A_c \delta l = \int_{\delta V} (\rho v \delta A_c) \frac{1}{\rho} \frac{dP}{dl} \delta l \quad (15.45)$$

Since there is no net flow of mass relative to the mass average velocity, the term in parentheses is the constant mass flow rate through the volume element about the streamline

$$\delta I = \delta w \int_{P_1}^{P_2} \frac{dP}{\rho} \quad (15.46)$$

For streamlines that begin on a moving surface with velocity v_s directed inward,

$$\begin{aligned} \delta I_m &= \int_{\delta V} (v_s \cdot \nabla P) \delta A_c \delta l = \int_{\delta V} (v_s \delta A_c) \frac{dP}{dl} \delta l \quad (15.47) \\ &= \int_{\delta V} (v_s \delta A_c) P \delta l = \int_{dV} (v_s \delta A_c) \delta P = \int_{\delta V} v_s \delta F = -\delta W_n \end{aligned} \quad (15.48)$$

where the force is positive when pointing into the system and δW_n is work done by the system against the normal pressure force at the moving surface. The final result is that

$$\begin{aligned} I &= \int_V (\mathbf{v} \cdot \nabla P) dV \delta I = \int \delta w \int_{P_1}^{P_2} \frac{dP}{\rho} - \int dW_n \quad (15.49) \\ &= w \int_{P_1}^{P_2} \frac{dP}{\rho} + W_n \end{aligned} \quad (15.50)$$

The integral is an average value over all the streamlines in the system. Substitution of the preceding results into the integral of the microscopic mechanical energy balance gives

$$\Delta \rho_A \left[\frac{\langle v_A^3 \rangle}{2} + \Psi_A \langle v_A \rangle \right] S_A - B + W + E_v + w \int_{P_{1A}}^{P_{2A}} \frac{dP}{\rho} = 0 \quad (15.51)$$

For frictionless adiabatic flow of an ideal gas, $p/\rho^\gamma = \text{constant}$ where $\gamma = \hat{c}_P/\hat{c}_V$ and the integral is given by

$$\int_1^2 \frac{dp}{\rho} = \frac{P_{1A}}{\rho_{1A}} \frac{\gamma}{\gamma - 1} \left[\left(\frac{\rho_{2A}}{\rho_{1A}} \right)^{\gamma-1} - 1 \right] \quad (15.52)$$

Problem 15.4, or part thereof, will serve to review and unify much of the basic material presented throughout this text.

PROBLEMS

15.1. Refer to the general mass transfer experiment discussed in Section 12.3.1. Consider two particular situations, both under isothermal conditions in a straight round tube:

- mass transfer from the tube wall to a homogeneous flowing fluid and
- mass transfer between a homogeneous flowing fluid and a fixed bed of cylindrical particles.

Define the appropriate surfaces and volume elements and carry out the integrations required to arrive at the mass balances.

15.2. Consider the one-dimensional model of a nonisothermal fixed-bed reactor model discussed in Section 14.3.

Define the appropriate surfaces and volume elements and carry out the integrations required to arrive at the applicable energy balance.

15.3. Derive the macroscopic momentum balance.

15.4. Refer to the flow diagram for the acrylic acid process in Figure 1.2. For each of the following items:

- C-301AB—inlet air blower
- T-301—quench tower
- T-303—acid extractor
- T-304—solvent tower
- P-304AB—solvent reflux pump
- E-303—solvent reboiler
- T-305—acid tower
- V-303—waste reflux drum

Describe each of the surfaces S_1 , S_2 , S_m , S_f , and S_w and the contribution of the surface to the macroscopic mass, energy, and momentum balance for the enclosed volume.

APPENDIX A

PERIODIC TABLE

1 H 1.0079																	18 He 4.0026
3 Li 6.941	4 Be 9.0122											5 B 10.811	6 C 12.011	7 N 14.007	8 O 15.999	9 F 18.998	10 Ne 20.180
11 Na 22.990	12 Mg 24.305	3	4	5	6	7	8	9	10	11	12	13 Al 26.982	14 Si 28.086	15 P 30.974	16 S 32.065	17 Cl 35.453	18 Ar 39.948
19 K 39.098	20 Ca 40.078	21 Sc 44.956	22 Ti 47.867	23 V 50.942	24 Cr 51.996	25 Mn 54.938	26 Fe 55.845	27 Co 58.933	28 Ni 58.693	29 Cu 63.546	30 Zn 65.38	31 Ga 69.723	32 Ge 72.64	33 As 74.922	34 Se 78.96	35 Br 79.904	36 Kr 83.798
37 Rb 85.468	38 Sr 87.62	39 Y 88.906	40 Zr 91.224	41 Nb 92.906	42 Mo 95.96	43 Tc (98)	44 Ru 101.07	45 Rh 102.91	46 Pd 106.42	47 Ag 107.87	48 Cd 112.41	49 In 114.82	50 Sn 118.71	51 Sb 121.76	52 Te 127.60	53 I 126.90	54 Xe 131.29
55 Cs 132.91	56 Ba 137.33	57-71 *	72 Hf 178.49	73 Ta 180.95	74 W 183.84	75 Re 186.21	76 Os 190.23	77 Ir 192.22	78 Pt 195.08	79 Au 196.97	80 Hg 200.59	81 Tl 204.38	82 Pb 207.2	83 Bi 208.98	84 Po (209)	85 At (210)	86 Rn (222)
87 Fr (223)	88 Ra (226)	89-103 #	104 Rf (261)	105 Db (262)	106 Sg (266)	107 Bh (264)	108 Hs (270)	109 Mt (268)	110 Ds (281)	111 Rg (272)	112 Uub (285)	113 Uut (284)	114 Uuq (289)	115 Uup (288)	116 Uuh (291)		118 Uuo (294)
* Lanthanide series			57 La 138.91	58 Ce 140.12	59 Pi 140.91	60 Nd 144.24	61 Pm (145)	62 Sm 150.36	63 Eu 151.96	64 Gd 157.25	65 Tb 158.93	66 Dy 162.50	67 Ho 164.93	68 Er 167.26	69 Tm 168.93	70 Yb 173.05	71 Lu 174.97
# Actinide series			89 Ac (227)	90 Th 232.04	91 Pa 231.04	92 U 238.03	93 Np (237)	94 Pu (244)	95 Am (243)	96 Cm (247)	97 Bk (247)	98 Cf (251)	99 Es (252)	100 Fm (257)	101 Md (258)	102 No (259)	103 Lr (262)

APPENDIX B

CONVERSION FACTORS (HVISTENDAHL, 1964)

The conversion factors given in these tables are based on

1 yard = 0.9144 m

1 pound avoirdupois = 0.45359237 kg

1 International Steam Table calorie = 4.1868 J

1 physical atmosphere (standard atmospheric pressure) = 1.01325 bar.

Standard value of the acceleration of gravity, $g_n = 9.80665 \text{ m/s}^2$.

Density of mercury at 0°C and normal atmospheric pressure = 13.5951 kg/dm^3 .

Specific volume of pure water at 4°C and normal atmospheric pressure = $1.000028 \text{ dm}^3/\text{kg}$.

Standard prefixes for decade multiples and decimal submultiples of units

Prefix	Abbreviation	Numerical Value	Example
Tera-	T	10^{12}	1 TWh = 10^{12} Wh
Giga-	G	10^9	1 GW = 10^9 W
Mega-	M	10^6	1 MW = 10^6 W
kilo-	K	10^3	1 kcal = 10^3 cal
(hekto-)	(h)	10^2	1 hl = 10^2 l
(deca-)	(da)	10	1 daA = 10 A
(deci-)	(d)	10^{-1}	1 dl = 10^{-1} l
(centi-)	(c)	10^{-2}	1 cm = 10^{-2} m
milli-	m	10^{-3}	1 mg = 10^{-3} g
micronano-	μ	10^{-6}	1 μ s = 10^{-6} s
nano-	n	10^{-9}	1 nm = 10^{-9} m
pico-	p	10^{-12}	1 pF = 10^{-12} F

Mass				
	Kilogram (kg)	Tonne (Metric Tonne) (t)	Pound (lb)	Imperial or Long Tonne (ton)
kg	1	10^3	2.20462	0.984206×10^{-3}
t	1000	1	2204.62	0.984206
lb	0.453592	0.453592×10^{-3}	1	0.446429×10^{-3}
ton	1016.05	1.01605	2240	1

Note: 1 U.S. ton = 1 short ton = 2000 lb = 907.185 kg.

Length					
	Meter (m)	Inch (in.)	Foot (ft)	Yard (yd)	Imperial Mile
m	1	39.3701	3.28084	1.09361	0.621371×10^{-3}
in.	0.0254	1	0.083333	0.027778	0.015783×10^{-3}
ft	0.3048	12	1	0.333333	0.189394×10^{-3}
yd	0.9144	36	3	1	0.568182×10^{-3}
mile	1609.344	63,360	5,280	1,760	1

Notes: 1 micron ($1 \mu\text{m}$) = 10^{-6} m = 10^{-3} mm. 1 International nautical mile = 1 n mile = 1852 m. 1 English nautical mile = 6080 ft = 1.00064 n mile = 1853.18 m.

Volume Flow Rate					
	Cubic Meter per Second (m ³ /s) (10 ³ s ⁻¹)	Cubic Meter per Hour (m ³ /h)	Cubic Foot per Second (ft ³ /s)	Imperial Gallon per Minute (gal/min)	Imperial Gallon per Hour (gal/h)
m ³ /s	1	3,600	35.3147	13.1981 × 10 ³	791.888 × 10 ³
m ³ /h	0.27777 × 10 ⁻³	1	9.80964 × 10 ³	3.66615	219.969
ft ³ /s	28.3168 × 10 ⁻³	101,940	1	373.729	22.4238 × 10 ³
gal/min	75.7681 × 10 ⁻⁶	0.272765	267,573 × 10 ⁻³	1	60
gal/h	1.26283 × 10 ⁻⁶	4.54609 × 10 ⁻³	445,722 × 10 ⁻⁶	0.016667	1

Notes: 1 U.S. gal/h = 0.832680 Imp. gal/h = 3.78544 × 10⁻³ m³/h.

Specific Mass (Density) and Concentration					
	Kilogram per Cubic Meter (kg/m ³)	Kilogram per Cubic Decimeter (kg/dm ³) or (g/cm ³)	Pound per Cubic Foot (lb/ft ³)	Grain per Cubic Foot (grain(1)/ft ³)	Grain per Imperial Gallon (grain/gal)
kg/m ³	1	10 ⁻³	62.4280 × 10 ⁻³	436.995	70.1569
kg/dm ³ or g/cm ³	10 ³	1	62.4280	436.995 × 10 ³	70.1569 × 10 ³
lb/ft ³	16.0185	16.0185 × 10 ⁻³	1	7000	1123.81
grain/ft ³	2.2883 × 10 ⁻³	2.28835 × 10 ⁻⁶	0.14286 × 10 ⁻³	1	0.160544
grain/gal	14.254 × 10 ⁻³	14.2537 × 10 ⁻⁶	0.88983 × 10 ⁻³	6.22882	1

Note: To avoid confusion with the gram, it is advisable not to use the abbreviation “gr” for grain.

Force					
	Newton (N)	Kilogram-Force (kilopond) kgf(kp)	Tonne-Force (tf)	Pound-Force (lbf)	Imperial Ton-Force (tonf)
N	1	0.101972	0.10197 × 10 ⁻³	0.224809	0.10036 × 10 ⁻³
kgf	9.80665	1	10 ⁻³	2.20462	0.98421 × 10 ⁻³
tf	9806.65	1000	1	2204.62	0.984206
lbf	4.44822	0.153592	0.45359 × 10 ⁻³	1	0.44643 × 10 ⁻³
tonf	9964.0	1016.05	1.01605	2240	1

Pressure or Stress					
	Newton Per Square Meter (Pascal) N/m ² (Pa)	Bar (b)	Kilogram-Force per Square Centimeter (kgf/cm ²)	Pound-Force per Square Inch (lbf/in ²)	Imperial Ton-Force per Square Inch (tonf/in ²)
N/m ² = 1 Pa	1	1 × 10 ⁵	0.101972	0.14504 × 10 ⁻³	0.06475 × 10 ⁻⁶
b (bar)	10 ⁵	1	1.1972	14.5038	6.47490 × 10 ⁻³
kgf/cm ² = 10 ⁴	98.0665 × 10 ³	0.980665	1	14.2233	6.34971 × 10 ⁻³
kgf/m ²					
atm	101.325 × 10 ³	1.01325	1.03323	14.6960	6.56072 × 10 ⁻³
lbf/in. ²	6894.76	0.068948	0.070307	1	0.44643 × 10 ⁻³
tonf/in. ²	15.4443 × 10 ⁶	154.443	157.488	2240	1

Energy or Enthalpy per Unit Mass						
	Joule per Kilogram (J/kg)	Kilogram-Force Meter per Kilogram (kgf m/kg)	Kilocalorie per Kilogram (kcal/kg)	Joule per Pound (J/lb)	Foot Pound-Force per Pound (ft lbf/lb)	British Thermal Unit per Pound (Btu/lb)
J/kg	1	0.101972	0.23885×10^{-3}	0.453592	0.334553	4.299×10^{-3}
kgf	9.80665	1	2.34228×10^{-3}	4.44822	3.28084	0.042161
m/kg						
kcal/kg	4186.8	426.935	1	1899.10	1400.71	1.8
J/lb	2.20462	0.224809	0.52653×10^{-3}	1	0.737562	0.9482×10^{-3}
ft lbf/lb	2.989067	0.3048	0.71393×10^{-3}	1.355818	1	1.285×10^{-3}
Btu/lb	2326.00	237.186	0.555556	1055.056	778.170	1

Power					
	Watt or Joule per Second W (J/s)	Kilogram-Force Meter per Second (kgf m/s)	Metric Horsepower (PS)	Foot Pound-Force per Second (ft lbf/s)	English Horsepower (hp)
W = 1 J/s	1	0.101972	1.3596×10^{-3}	0.737562	1.3410×10^{-3}
kgf m/s	9.80665	1	13.333×10^{-3}	7.233014	13.151×10^{-3}
PS	735.499	75	1	542,476	0.986320
ft lbf/s	1.355818	0.138255	1.8430×10^{-3}	1	1.8182×10^{-3}
hp	745,700	76.0403	1.01387	550	1

Value of the Universal Gas Constant <i>R</i>				
Joule per Kilo-Mole Degree Kelvin (J/kmol K)	Kilogram-Force Meter per Kilo-Mole Degree Kelvin (kgf m/kmol K)	Kilocalorie per Kilo-Mole Degree Kelvin (kcal/kmol K)	Foot Pound-Force per Pound-Mole Degree Rankine (ft lbf/lb mol °R)	British Thermal Unit per Pound-Mole Degree Rankine (Btu/lb mol °R)
8314.66	847.860	1.98592	1545.39	1.98592

APPENDIX C

PARTIAL DATABASE FOR ACRYLIC ACID PROCESS

Data Item	Acrylic Acid	Acetic Acid	Acrolein	Diisopropyl Ether	Preliminary Database			Oxygen	Nitrogen	Carbon Dioxide	Notes
					Propylene	Propane	Water				
Formula	Propenoic acid $\text{CH}_2=\text{CHCO}_2\text{H}$	$\text{CH}_3\text{CO}_2\text{H}$		$\text{C}_3\text{H}_7\text{OC}_3\text{H}_7$	$\text{CH}_3\text{CH}=\text{CH}_2$	$\text{CH}_3\text{CH}_2\text{CH}_3$	H_2O	O_2	N_2		1
Molecular weight	72.065	60.054		102.740	42.081	44.097	18.016	32	28.014		1
Melting point ($^{\circ}\text{C}$)	13-Dec	16.7			-185	-187.1	0	-218.4	-209.86		1
Boiling point ($^{\circ}\text{C}$)	141-142	118.1			-48	-42.2	100	-183	-195.8		1
T_c (K)	615	591.95		500.05	365.57	369.83	647.13	154.58	126.2		2
$P_c \times 10^{-6}$ (Pa)	56.60 bar	5.74			4.63	4.21	21.94	5.02	3.39		2
V_c (m^3/kmol)	208.0 cm^3/mol	0.179			0.188	0.2	0.056	0.074	0.089		2
Z_c	0.23	0.208			0.286	0.273	0.228	0.287	0.288		2
Ω	0.518	0.463			0.137	0.149	0.343	0.02	0.037		2
Ideal gas heat capacity	J/(mol K)	J/(kmol K)	J/(mol K)		J/(kmol K)	J/(mol K)	J/(kmol K)	J/(kmol K)	J/(kmol K)	J/(kmol K)	
$c_1 \times 10^{-5}$	$A = 7.755\text{E}+00$	0.4020	$A = 1.0924\text{E}+02$		0.4339	$A = 2.8277\text{E}+01$	0.3336	0.2910	0.2911	0.2937	3
$c_2 \times 10^{-5}$	$B = 2.9386\text{E}-01$	1.3675	$B = 5.0952\text{E}-01$		1.5200	$B = 1.1600\text{E}-01$	0.2679	0.1004	0.0861	0.3454	3
$c_3 \times 10^{-3}$	$C = 2.0878\text{E}-04$	1.2620	$C = 1.7059\text{E}-03$		1.4250	$C = 1.9597\text{E}-04$	2.6105	2.5265	1.7016	1.4280	3
$c_4 \times 10^{-5}$	$D = 7.159\text{E}-08$	0.7003	$D = -1.807\text{E}-07$		0.7860	$D = -2.327\text{E}-07$	0.0890	0.0936	0.0010	0.2640	3
c_5	$E = 9.0960\text{E}-12$	569.7000	$E = 6.5983\text{E}-10$		623.9000	$E = 6.8669\text{E}-11$	1169.0000	1153.8000	909.7900	588.0000	3
T_{\min} (K)	250.0000	50.0000	250.0000		130.0000	100.0000	100.0000	50.0000	50.0000	50.0000	3
c_p (T_{\min})	28.6360	40.2000	66.33@298		43.8800	74.658@298	3.3360E+04	2.9100E+04	2.9110E+04	2.9370E+04	3
T_{\max} (K)	1500.0000	1500.0000	1000.0000		1500.0000	1500.0000	2273.1500	1500.0000	1500.0000	5000.0000	3
c_p (T_{\max})	*****	157.5600	*****		168.3600	*****	5.2760E+04	3.6530E+04	3.4840E+04	6.3350E+04	3
Liquid heat capacity	J/(mol K)	J/(mol K)	J/(mol K)				J/(mol K)				
A	1.8242E+01	18.944	4.8243E+01	7.3085E+01			9.2053E+01				4
B	1.2106E+00	1.0971E+00	5.8199E-01	1.1235E+00			-3.9953E-02				4
C	3.1160E-03	2.8921E-03	-1.9335E-03	-3.7356E-03			-2.1630E-04				4
D	3.1409E-06	2.9275E-06	2.6860E-06	5.2200E-06			5.3469E-07				4
T_{\min} (K)	288	291	186	189			273				4
T_{\max} (K)	554	533	455	450			615				4
c_p (298 K)	148.96	128.66	121.07	214.32			75.55				4

Data Item	Acrylic Acid	Acetic Acid	Acrolein	Diisopropyl Ether	Propylene	Propane	Water	Oxygen	Nitrogen	Carbon Dioxide	Notes
Gibb's free energy of formation: gas at 298 K (kJ/mol)	-286.06	9.47	-55.98		62.72	-23.47	-228.6	*****	*****	-394.4	5
Enthalpy of formation: gas at 298 K (kJ/mol)	-336.23	-434.84	-81		20.42	-103.85	-241.8	*****	*****	-393.5	6
Liquid density at 25 °C (g/cm ³)	1.046	1.043	0.834				1.027				7
Heat of vaporization at n.b.p. (kJ/mol)	42.52	23.33	29.03				39.5				8
Vapor pressure (mmHg)											
<i>A</i>	2.3067E+01	2.8376E+01	5.7982E+01	15.5992			2.9861E+01				9
<i>B</i>	-3.1437E+03	-2.9734E+03	-3.0933E-03	-2.0276E+03			-3.1522E+03				9
<i>C</i>	-4.8813E+00	-7.0320E+00	-1.9638E+01	-2.8551			-7.3037E+00				9
<i>D</i>	4.3690E-04	-1.5051E-09	1.1486E-02	2.7662E-04			2.4247E-09				9
<i>E</i>	-4.9161E-13	2.1806E-06	-2.3854E+04	-9.9111E-14			1.8090E-06				9
<i>T</i> _{min} (K)	286.65	289.81	592.71	187.65			273.16				9
<i>T</i> _{max} (K)	615	592.71	566	500.05			647.13				9

Data Item	Acrylic Acid	Acetic Acid	Acrolein	Diisopropyl Ether	Propylene	Propane	Water	Oxygen	Nitrogen	Carbon Dioxide	Notes
Liquid viscosity (cP)											
<i>A</i>	-1.5418E+01	-3.8937E+00		-5.5350E+00			-1.0216E+01				10
<i>B</i>	2.3541E+03	7.8482E+02		7.4894E+02			1.7925E+03				10
<i>C</i>	3.3600E-02	6.7000E-03		1.3145E-02			1.7730E-02				10
<i>D</i>	2.7350E-05	-7.5606E-06		-1.5557E-05			-1.2631E-05				10
Value at 25 °C				3.2600E-01			9.1100E-01				10
Liquid density (g/cm ³)											
<i>A</i>				2.6218E-01			0.3471				10
<i>B</i>				2.6974E-01			0.274				10
<i>N</i>				2.8571E-01			0.28571				10
Value at 25 °C				7.2100E-01			1.027				10
Thermal conductivity (W/(m K))											
<i>A</i>				2.8940E-01			-0.2758				11
<i>B</i>				-8.7140E-04			0.004612				11
<i>C</i>				9.2649E-07			-5.5391E-06				11
Value at 25 °C				1.1190E-01			0.607				11
Hitec heat transfer liquid											
Specific heat	0.37 Btu/lb °F										
Density	112 lb/ft ³										
Viscosity	2.1 cP										
Thermal conductivity	0.31 Btu/(h ft °F)										
Heat transfer coefficient	1164 Btu/(h ft ² °F)										

Notes:

1. Tables 2.1 and 2.2 from Green and Maloney (1997) with molecular weight adjustment.
2. Table 2.164 from Green and Maloney (1997) and Yaws (2003).
3. Table 2.198 from Green and Maloney (1997).

$$C_p = c_1 + c_2 \left[\frac{c_3/T}{\sinh c_3/T} \right]^2 + c_4 \left[\frac{c_5/T}{\cosh c_5/T} \right]^2$$

and

Yaws (2003).

$$C_p = A + BT + CT^2 + DT^3 + ET^4$$

4. Yaws (1999), Section 3.

$$C_p = A + BT + CT^2 + DT^3$$

5. Yaws (1999), Section 13: $F(T)$ available.
6. Yaws (1999), Section 12: $F(T)$ available.
7. Yaws (1999), Section 8.
8. Yaws (1999), Section 5.
9. Yaws (1999), Section 7.

$$\log_{10} P = A + \frac{B}{T} + C \log_{10} T + DT + ET^2$$

$$\log_{10} \eta(\text{cP}) = A + \frac{B}{T} + CT + DT^2$$

10. Yaws (1999).

$$\rho = AB^{-(1-(T/T_c))^n}$$

11. Yaws (1999, 2003).

$$\lambda(T) = A + BT(K) + CT^2$$

Kinetics:

The reaction rates at the conditions of the process are taken to be

$$\mathcal{R}_j = k_j P^2 e^{-E_j/RT} y_{\text{C}_3\text{H}_6} y_{\text{O}_2} \text{ kmol/m}^3 \text{ reactor}$$

where

J	E_j (kcal/kmol)	k_j (kmol/(m ³ reactor h kPa ²))
1	15,000	1.59×10^5
2	25,000	1.81×10^5
3	20,000	8.83×10^5

APPENDIX D

SOME MATHEMATICAL RESULTS

D.1 DIVERGENCE THEOREM (GAUSS)

Let D be closed and bounded region with a piecewise smooth boundary, S , that is oriented outward. Let F be a vector field that is continuous and has continuous first partial derivatives; then,

$$\int_S \mathbf{F} \cdot \mathbf{n} dS = \int_V \nabla \mathbf{F} \cdot \mathbf{n} dV$$

Relationship of microscopic kinetic energy accumulation to the momentum balance and continuity equation:

$$\begin{aligned} \frac{\partial \rho \mathbf{v} \cdot \mathbf{v}}{\partial t} &= \mathbf{v} \cdot \frac{\partial \rho \mathbf{v}}{\partial t} + \rho \mathbf{v} \cdot \frac{\partial \mathbf{v}}{\partial t} \\ &= \mathbf{v} \cdot \frac{\partial \rho \mathbf{v}}{\partial t} + \rho \frac{1}{2} \frac{\partial \mathbf{v} \cdot \mathbf{v}}{\partial t} \\ &= \mathbf{v} \cdot \frac{\partial \rho \mathbf{v}}{\partial t} + \frac{1}{2} \frac{\partial \rho \mathbf{v} \cdot \mathbf{v}}{\partial t} - \frac{\mathbf{v} \cdot \mathbf{v}}{2} \frac{\partial \rho}{\partial t} \end{aligned}$$

Derivation of microscopic kinetic energy balance from the equation of motion and the continuity equation:

$$\begin{aligned} \frac{\partial}{\partial t} \left[\frac{1}{2} \rho \mathbf{v} \cdot \mathbf{v} \right] &= \mathbf{v} \cdot [-\nabla \cdot (\rho \mathbf{v} \mathbf{v} + \Pi) - \rho \mathbf{g}] - \left(\frac{\mathbf{v} \cdot \mathbf{v}}{2} \right) (-\nabla \cdot \rho \mathbf{v}) \\ \frac{\partial}{\partial t} \left[\frac{1}{2} \rho \mathbf{v} \cdot \mathbf{v} \right] &= -\mathbf{v} \cdot [\mathbf{v} \cdot \nabla \rho \mathbf{v} + \rho \mathbf{v} (\nabla \cdot \mathbf{v})] - \mathbf{v} \cdot \nabla \cdot \Pi + \rho \mathbf{v} \cdot \mathbf{g} \\ &\quad + \left(\frac{\mathbf{v} \cdot \mathbf{v}}{2} \right) (\nabla \cdot \rho \mathbf{v}) \end{aligned}$$

$$\begin{aligned} \frac{\partial}{\partial t} \left[\frac{1}{2} \rho \mathbf{v} \cdot \mathbf{v} \right] &= -\mathbf{v} \cdot \left[\frac{1}{2} \rho \nabla v^2 + v^2 \nabla \rho + \rho \mathbf{v} (\nabla \cdot \mathbf{v}) \right] \\ &\quad - \mathbf{v} \cdot \nabla \cdot \Pi + \rho \mathbf{v} \cdot \mathbf{g} + \left(\frac{\mathbf{v} \cdot \mathbf{v}}{2} \right) (\nabla \cdot \rho \mathbf{v}) \end{aligned}$$

$$\begin{aligned} \frac{\partial}{\partial t} \left[\frac{1}{2} \rho \mathbf{v} \cdot \mathbf{v} \right] &= -\frac{1}{2} \rho \mathbf{v} \cdot \nabla v^2 - v^2 \mathbf{v} \cdot \nabla \rho - \rho v^2 (\nabla \cdot \mathbf{v}) \\ &\quad - \mathbf{v} \cdot \nabla \cdot \Pi + \rho \mathbf{v} \cdot \mathbf{g} + \left(\frac{v^2}{2} \right) (\nabla \cdot \rho \mathbf{v}) \end{aligned}$$

$$\frac{\partial}{\partial t} \left[\frac{1}{2} \rho \mathbf{v} \cdot \mathbf{v} \right] + \nabla \cdot \rho \frac{v^2}{2} \mathbf{v} = -\mathbf{v} \cdot \nabla \cdot \Pi + \rho \mathbf{v} \cdot \mathbf{g}$$

$$\frac{\partial}{\partial t} \left[\frac{1}{2} \rho \mathbf{v} \cdot \mathbf{v} \right] + \nabla \cdot \rho \frac{v^2}{2} \mathbf{v} = -\nabla \cdot (\Pi \cdot \mathbf{v}) + \Pi : \nabla \mathbf{v} + \rho \mathbf{v} \cdot \mathbf{g}$$

$$\begin{aligned} \frac{\partial}{\partial t} \left[\frac{1}{2} \rho \mathbf{v} \cdot \mathbf{v} \right] + \nabla \cdot \rho \frac{v^2}{2} \mathbf{v} &= -\nabla \cdot ((p\delta + \tau) \cdot \mathbf{v}) \\ &\quad + (p\delta + \tau) : \nabla \mathbf{v} + \rho \mathbf{v} \cdot \mathbf{g} \end{aligned}$$

$$\begin{aligned} \frac{\partial}{\partial t} \left[\frac{1}{2} \rho \mathbf{v} \cdot \mathbf{v} \right] + \nabla \cdot \rho \frac{v^2}{2} \mathbf{v} &= -\nabla \cdot p \mathbf{v} - \nabla \cdot (\tau \cdot \mathbf{v}) \\ &\quad + p \nabla \cdot \mathbf{v} + \tau : \nabla \mathbf{v} + \rho \mathbf{v} \cdot \mathbf{g} \end{aligned}$$

$$\begin{aligned} \frac{\partial}{\partial t} \left[\frac{1}{2} \rho \mathbf{v} \cdot \mathbf{v} \right] + \nabla \cdot \rho \frac{v^2}{2} \mathbf{v} &= -\mathbf{v} \cdot \nabla p - \nabla \cdot (\tau \cdot \mathbf{v}) \\ &\quad + \tau : \nabla \mathbf{v} + \rho \mathbf{v} \cdot \mathbf{g} \end{aligned}$$

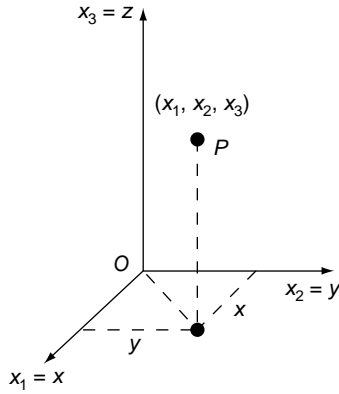


FIGURE D.1 Rectangular coordinates.

D.2 COORDINATE SYSTEMS

Most important to us are rectangular, cylindrical, and spherical. These are orthonormal systems where the coordinate planes are perpendicular and the coordinate vectors are of unit length, normal to the respective coordinate surfaces.

D.2.1 Rectangular

Replace (x, y, z) with (x_1, x_2, x_3) , respectively. The coordinate surfaces are the planes $x_i = \text{constant}$ and the unit vectors, δ_{x_i} are perpendicular to these surfaces (Figure D.1).

D.2.2 Cylindrical

The coordinate surfaces are a cylinder, and two planes (Figure D.2):

$$\begin{aligned} r &= \text{constant} & 0 < r < \infty \\ \theta &= \text{constant} & 0 < \theta < \pi \\ z &= \text{constant} & -\infty < z < \infty \end{aligned}$$

D.2.3 Spherical

The coordinate surfaces are a sphere, a cone, and a plane (Figure D.3):

$$\begin{aligned} r &= \text{constant} & 0 < r < \infty \\ \theta &= \text{constant} & 0 < \theta < \pi \\ \phi &= \text{constant} & 0 < \phi < 2\pi \end{aligned}$$

The representations in the cylindrical and spherical systems can be reset to the rectangular values as

Cylindrical	Spherical
$x_1 = r \cos \theta$	$x_1 = r \sin \theta \cos \phi$
$x_2 = r \sin \theta$	$x_2 = r \sin \theta \sin \phi$
$x_3 = x_3$	$x_3 = r \cos \theta$

These relations can be inverted to give $q_i(x_1, x_2, x_3)$ where the cylindrical or the spherical coordinates are represented by the q set.

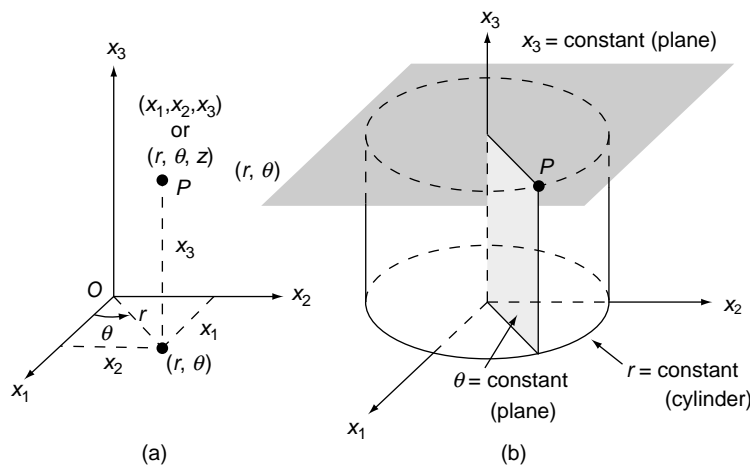


FIGURE D.2 Cylindrical coordinates.

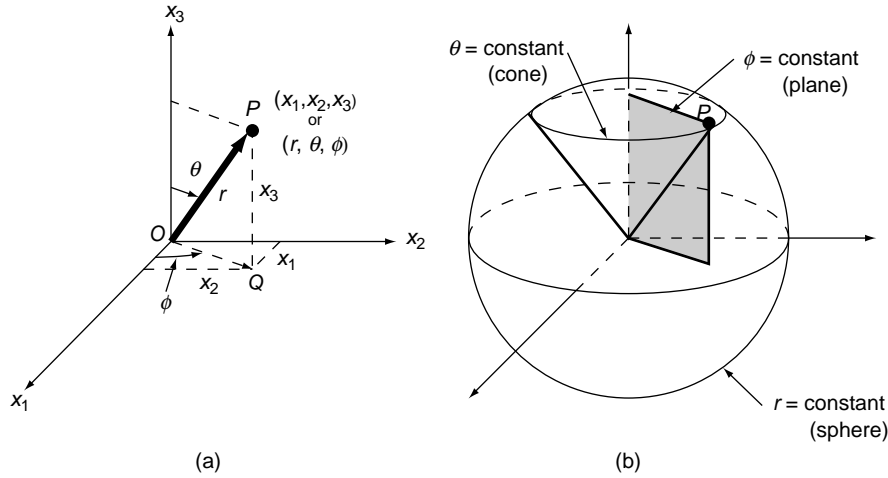


FIGURE D.3 Spherical coordinates.

D.3 UNIT VECTORS AND DISTANCE METRICS

Follow a point on a coordinate curve—the other coordinates held constant: The change in the position vector is tangent to the coordinate curve and therefore points in the same direction as the unit vector δ_α . Consequently, since the magnitude of the change in the position vector is the distance traveled (Figure D.4)

$$\delta_\alpha = \frac{d\mathbf{R}}{|d\mathbf{R}|} = \frac{d\mathbf{R}}{ds_\alpha} = \frac{1}{h_\alpha} \frac{\partial \mathbf{R}}{\partial q_\alpha}$$

The h_α is a metric that converts a change in the associated coordinate to a distance. Since the unit vectors in the basic rectangular configuration are constant, it is convenient to differentiate the position vector in that system. Consequently,

$$h_\alpha = \sqrt{\sum_{i=1}^3 \left(\frac{\partial x_i}{\partial q_\alpha} \right)^2}$$

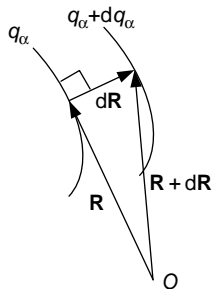


FIGURE D.4 Coordinate curve.

For example, the metric for the angular direction in the cylindrical coordinate system is determined as follows:

$$h_\alpha = \sqrt{(-r \sin \theta)^2 + (r \cos \theta)^2 + (0)^2} = r, \quad ds_\theta = r d\theta$$

Rectangular	Cylindrical	Spherical
$h_{x_1} = 1$	$h_r = 1$	$h_r = 1$
$h_{x_2} = 1$	$h_\theta = r$	$h_\theta = r$
$h_{x_3} = 1$	$h_{x_3} = 1$	$h_\phi = r \sin \theta$

A unit volume in each system is the product the three dimensions: $dV = h_1 dq_1 h_2 dq_2 h_3 dq_3$. The area normal to the i direction is given by $dA_i = h_j dq_j h_k dq_k$. We can now express the unit vectors in terms of the rectangular unit vectors using the preceding results. For example, for the cylindrical system

$$\begin{aligned} \delta_r &= \frac{1}{h_r} \frac{\partial \mathbf{R}}{\partial r} = \frac{1}{r} \frac{\partial}{\partial r} [r \cos \theta \delta_{x_1} + r \sin \theta \delta_{x_2} + x_3 \delta_{x_3}] \\ \delta_r &= \left[\frac{\partial(r \cos \theta)}{\partial r} \delta_{x_1} + \frac{\partial(r \sin \theta)}{\partial r} \delta_{x_2} \right] \\ \delta_r &= \cos \theta \delta_{x_1} + \sin \theta \delta_{x_2} \end{aligned}$$

The same procedure will produce the following results:

Cylindrical	Spherical
$\delta_r = \cos \theta \delta_{x_1} + \sin \theta \delta_{x_2}$	$\delta_r = \sin \theta \cos \phi \delta_{x_1} + \sin \theta \sin \phi \delta_{x_2} + \cos \theta \delta_{x_3}$
$\delta_\theta = -\sin \theta \delta_{x_1} + \cos \theta \delta_{x_2}$	$\delta_\theta = \cos \theta \cos \phi \delta_{x_1} + \cos \theta \sin \phi \delta_{x_2} - \sin \theta \delta_{x_3}$
$\delta_{x_3} = \delta_{x_3}$	$\delta_\phi = -\sin \theta \delta_{x_1} + \cos \theta \delta_{x_2}$

D.4 COMPONENTS OF RECTANGULAR UNIT VECTORS

The cylindrical and spherical components of the rectangular coordinate vectors can be extracted from the preceding results using the scalar product. For example, the components of $\mathbf{\delta}_{x_1}$ in cylindrical coordinates are obtained as follows:

$$\begin{aligned}\mathbf{\delta}_{x_1} \cdot \mathbf{\delta}_r &= \mathbf{\delta}_r \cdot \mathbf{\delta}_{x_1} = \cos \theta \\ \mathbf{\delta}_{x_1} \cdot \mathbf{\delta}_\theta &= \mathbf{\delta}_\theta \cdot \mathbf{\delta}_{x_1} = -\sin \theta \\ \mathbf{\delta}_{x_1} \cdot \mathbf{\delta}_{x_3} &= 0 \\ \Rightarrow \mathbf{\delta}_{x_1} &= \cos \theta \mathbf{\delta}_r - \sin \theta \mathbf{\delta}_\theta\end{aligned}$$

Similar calculations give the remaining components.

D.5 DERIVATIVES OF UNIT VECTORS

The derivatives required in the balance equations and their applications need to account for the variation of the unit vectors in the spherical and cylindrical systems with position. For example, the angular unit vector in the cylindrical system points in exactly the opposite directions at the extreme ends of its path. The rectangular unit vectors

are of course constant. For example, in the cylindrical system

$$\begin{aligned}\frac{\partial \mathbf{\delta}_r}{\partial r} &= \frac{\partial \cos \theta}{\partial r} \mathbf{\delta}_{x_1} + \frac{\partial \sin \theta}{\partial r} \mathbf{\delta}_{x_2} = 0 \\ \frac{\partial \mathbf{\delta}_r}{\partial \theta} &= \frac{\partial \cos \theta}{\partial \theta} \mathbf{\delta}_{x_1} + \frac{\partial \sin \theta}{\partial \theta} \mathbf{\delta}_{x_2} = -\sin \theta \mathbf{\delta}_{x_1} + \cos \theta \mathbf{\delta}_{x_2} = \mathbf{\delta}_\theta\end{aligned}$$

The remaining derivatives are evaluated in this manner:

Cylindrical :

$$\begin{aligned}\frac{\partial \mathbf{\delta}_r}{\partial r} &= 0 \quad \frac{\partial \mathbf{\delta}_\theta}{\partial r} = 0 \quad \frac{\partial \mathbf{\delta}_{x_3}}{\partial r} = 0 \\ \frac{\partial \mathbf{\delta}_r}{\partial \theta} &= \mathbf{\delta}_\theta \quad \frac{\partial \mathbf{\delta}_\theta}{\partial \theta} = -\mathbf{\delta}_r \quad \frac{\partial \mathbf{\delta}_{x_3}}{\partial \theta} = 0 \\ \frac{\partial \mathbf{\delta}_r}{\partial x_3} &= 0 \quad \frac{\partial \mathbf{\delta}_\theta}{\partial x_3} = 0 \quad \frac{\partial \mathbf{\delta}_{x_3}}{\partial x_3} = 0\end{aligned}$$

Spherical :

$$\begin{aligned}\frac{\partial \mathbf{\delta}_r}{\partial r} &= 0 \quad \frac{\partial \mathbf{\delta}_\theta}{\partial r} = 0 \quad \frac{\partial \mathbf{\delta}_\phi}{\partial r} = 0 \\ \frac{\partial \mathbf{\delta}_r}{\partial \theta} &= \mathbf{\delta}_\theta \quad \frac{\partial \mathbf{\delta}_\theta}{\partial \theta} = -\mathbf{\delta}_r \quad \frac{\partial \mathbf{\delta}_\phi}{\partial \theta} = 0 \\ \frac{\partial \mathbf{\delta}_r}{\partial \phi} &= \mathbf{\delta}_\phi \sin \theta \quad \frac{\partial \mathbf{\delta}_\theta}{\partial \phi} = \mathbf{\delta}_\phi \cos \theta \quad \frac{\partial \mathbf{\delta}_\phi}{\partial \phi} = -\mathbf{\delta}_r \sin \theta - \mathbf{\delta}_\theta \cos \theta\end{aligned}$$

APPENDIX E

MASS BALANCE IN CYLINDRICAL COORDINATES AND LAMINAR FLOW IN Z DIRECTION

The mass balance in molar units is given by

$$\frac{\partial c_i}{\partial t} + \nabla \cdot (c_i \mathbf{v} - D_{im} \nabla c_i) = \mathcal{R}_{iv}$$

where the velocity is the mass average velocity. We are concerned here with the reduction of the divergence term for laminar flow in the z direction

$$\mathbf{v} = v(r) \mathbf{\delta}_z = v_{\max} \left[1 - \left(\frac{r}{r_0} \right)^2 \right] \mathbf{\delta}_z$$

The first term of the mass balance becomes

$$\nabla \cdot c_A \mathbf{v} = \left(\mathbf{\delta}_r \frac{\partial}{\partial r} + \mathbf{\delta}_\theta \frac{1}{r} \frac{\partial}{\partial \theta} + \mathbf{\delta}_z \frac{\partial}{\partial z} \right) \cdot c_A v(r) \mathbf{\delta}_z = v(r) \frac{\partial c_A}{\partial z}$$

The second term of the mass balance reduces as follows.

Note that the unit vector in the z direction is constant and orthogonal to the unit vectors in the radial and angular directions, only the third term of the del operator acts on the convective flux vector.

$$\begin{aligned} \nabla \cdot \nabla c_A &= \left(\mathbf{\delta}_r \frac{\partial}{\partial r} + \mathbf{\delta}_\theta \frac{1}{r} \frac{\partial}{\partial \theta} + \mathbf{\delta}_z \frac{\partial}{\partial z} \right) \\ &\quad \cdot \left(\mathbf{\delta}_r \frac{\partial c_A}{\partial r} + \mathbf{\delta}_\theta \frac{1}{r} \frac{\partial c_A}{\partial \theta} + \mathbf{\delta}_z \frac{\partial c_A}{\partial z} \right) \\ &= \frac{\partial}{\partial r} \frac{\partial c_A}{\partial r} + \mathbf{\delta}_\theta \frac{1}{r} \cdot \frac{\partial}{\partial \theta} \left(\mathbf{\delta}_r \frac{\partial c_A}{\partial r} + \mathbf{\delta}_\theta \frac{1}{r} \frac{\partial c_A}{\partial \theta} + \mathbf{\delta}_z \frac{\partial c_A}{\partial z} \right) \\ &\quad + \frac{\partial}{\partial z} \frac{\partial c_A}{\partial z} = \frac{\partial}{\partial r} \frac{\partial c_A}{\partial r} + \left(\mathbf{\delta}_\theta \cdot \mathbf{\delta}_r \frac{1}{r} \frac{\partial}{\partial \theta} \frac{\partial c_A}{\partial r} \right. \\ &\quad \left. + \mathbf{\delta}_\theta \cdot \mathbf{\delta}_\theta \frac{1}{r} \frac{\partial c_A}{\partial r} - \mathbf{\delta}_\theta \cdot \mathbf{\delta}_r \frac{1}{r^2} \frac{\partial c_A}{\partial \theta} + \mathbf{\delta}_\theta \cdot \mathbf{\delta}_\theta \frac{1}{r} \frac{\partial}{\partial \theta} \frac{1}{r} \frac{\partial c_A}{\partial \theta} \right. \\ &\quad \left. + \mathbf{\delta}_\theta \cdot \mathbf{\delta}_z \frac{1}{r} \frac{\partial c_A}{\partial z} \right) + \frac{\partial}{\partial z} \frac{\partial c_A}{\partial z} \\ &= \frac{\partial}{\partial r} \frac{\partial c_A}{\partial r} + \frac{1}{r} \frac{\partial c_A}{\partial r} + \frac{1}{r^2} \frac{\partial}{\partial \theta} \frac{\partial c_A}{\partial \theta} \end{aligned}$$

Substitution of mass units produce the equation quoted in Table 10.1.

NOMENCLATURE

a	Avogadro's number	e^-	charge on electron
a	equation of state parameter	e	total energy per unit mass
a_i	value of a for pure i	e_v	friction loss factor
a_{ij}	i, j binary contribution to a	E	activation energy
a_v	area per unit volume	E_o	overall (column) efficiency
A	area; absorption factor	E_v	rate of dissipation of mechanical energy into heat
A_c	cross-sectional area	E_{vm}	rate of dissipation of mechanical energy per unit rate of mass throughput
A_i	molecular formula for species i	\mathcal{E}	effectiveness factor for porous catalyst
A_{ij}	parameter in activity coefficient model	\mathcal{E}_p	effectiveness factor for catalyst pore
\mathcal{A}_j	affinity of j th reaction	\mathcal{E}_r	enhancement factor for chemical reaction
\mathcal{A}	availability per unit mass	f	friction factor
b	equation of state parameter; parameter in Toth adsorption isotherm	$f(t)$	residence time frequency distribution
b_{ij}	i, j binary contribution to b	\mathcal{f}	turnover frequency for enzymes
\mathcal{B}	availability per mole	\mathcal{F}	Faraday's constant ff
B	molar flow rate of bottom product from distillation tower	F	arbitrary thermodynamic function
B	virial coefficient	$F(t)$	cumulative residence time frequency distribution
c	molar concentration	F_p	packing factor
c_0^\pm	step change in concentration from c_0^- to c_0^+	F_s	force in s direction
c_p	specific heat per unit mass at constant pressure	g	gravitational acceleration; $g(\mathfrak{V}) = \text{function of vapor fraction}$
C_p	molar specific heat at constant pressure	G	Gibbs free energy per mole
d	molecular diameter; gap distance	h	enthalpy per unit mass
d_{ij}	number of atoms of i in molecule j	h_p	height of packing
D	diameter and molar flow rate of distillate	\mathcal{h}	height above datum plane
D_o	hole diameter for sieve trays		
D_{Am}^R	diffusivity of A in mixture; reference frame R		

h_s	height of settling zone in extraction tower	Q_{soln}	molar heat of solution
h_t	height of tower	r_v	total mass rate of production per unit volume
h_{ts}	tray spacing	R	gas constant
H	enthalpy per mole; also height	R_c	radius of curvature
H_i	enthalpy per mole of species i ; also Henry's law constant	R_{sj}	molar rate of reaction j (j omitted for single reaction) per unit area
J_e	total flux of energy	R_v	total molar rate of production per unit volume
k	forward reaction rate constant; adsorption equilibrium constant	\mathcal{R}_j	molar rate of reaction j (j omitted for single reaction)
k_-	reverse reaction rate constant	$\mathcal{R}_j^{(V)}$	molar rate of reaction (j omitted for single reaction) over; finite volume V
k_0	preexponential factor in Arrhenius rate constant	s	entropy per unit mass
k_{ij}	binary interaction parameter	S	entropy per mole or stripping factor
k_{cA}^0	mass transfer coefficient of species A at low rate and with molar concentration in the driving force	S_g	surface area per unit mass
K	vapor-liquid or liquid-liquid or chemical equilibrium constant; overall mass transfer coefficient	S_i	stream i
l	index of limiting reactant	\mathbb{S}	selectivity in liquid-liquid extraction
L	length or film thickness	t	time
\mathcal{L}	phenomenological coefficient	t_{lf}	residence time for plug flow
m_o	mass of tracer injected over a short time	\mathbb{T}	time interval for averaging turbulent fluctuations
M	molecular weight	T	absolute temperature
n	normal direction	u	internal energy per unit mass
\mathcal{N}	molar flow rate also revolutions per minute	$[u]$	upper triangular matrix; row equivalent to $[d]$
N	number of moles	U	internal energy per mole
N_{ads}	moles of adsorbate	\mathcal{U}	unit step function
N_c	number of components	v	mass average velocity
N_D	number of daughter streams from splitter	$v^{(c)}$	superficial velocity of continuous phase
N_F	number of feed streams	$v^{(D)}$	superficial velocity of dispersed phase
N_{Kn}	Knudsen number	v_{mf}	minimum fluidization velocity
N_l	number of elements	V	molar volume of gas (V_G) or liquid (V_L) or fluid (V_f) or drum (V_d)
N_L	number of layers	V_g	pore volume per unit mass
N_P	number of product streams	\mathcal{V}	volumetric flow rate
N_P	power number	\mathcal{V}_L	volume of liquid
N_r	number of reactions	w	mass adsorbate per unit mass adsorbent
N_{rpm}	revolutions per minute	w^R	weighting factor in definition of velocity of reference frame R
N_S	number of subsystems or stages	W	width; mass
$N\pi$	number of phases	W_s	work rate by system through containing surfaces
p	mixture parameter in cubic equation of state	\mathcal{W}	mass or mass flow rate
p_{ij}	i, j binary contribution to p	\mathcal{W}_{ads}	mass of solid adsorbent
P	pressure	x, y, z	Cartesian coordinates; mole fraction liquid, vapor, or mixture, respectively
P_c	critical pressure	X	mole ratio in liquid phase
P_j	parachore	\mathcal{X}	general driving force
\mathcal{P}	power	Y	mole ratio in gas phase
q	conductive energy flux		
Q	general flux in entropy production expression		
Q	heat flow rate into system		

Z	compressibility factor
Z_i	valence of species i

GREEK SYMBOLS

α_{AB}	relative volatility of A to B
α_D	Joule–Thompson coefficient
α_D	thermal diffusivity
α_T	coefficient of thermal expansion
a	function of acentric factor and reduced temperature in cubic equations of state; parameter in Freundlich adsorption isotherm
β	parameter in Freundlich adsorption isotherm
γ_i	activity coefficient for species i ; also specific heat ratio without subscript.
ε_j	fraction of stream j
ε	porosity
ζ	slipping coefficient
η	viscosity
κ	isothermal compressibility
$\Lambda(t)$	intensity function
Λ_{ij}	parameters in Wilson's model
λ	mean free path for gas
ξ_j	extent of reaction ξ_j'' ; extent per unit volume
Π	osmotic pressure
σ_g	specific gravity
∂	vapor fraction; stoichiometric coefficient
ρ	mass density; apparent value if subscript p
ρ_{e0}	initial free enzyme concentration
σ	surface tension
Φ	degrees of freedom
Φ_{ir}	effect of homogeneous reaction on absorption rate of species i
ϕ	friction factor
Ψ	electric potential
φ	fugacity coefficient; fraction not absorbed; fraction not stripped
τ_R	residence time
ω_{ij}	acentric factor for binary ij interaction coefficient in second virial coefficient
ω	acentric factor; mass fraction
χ	conversion
Ψ	potential energy

SUPERSCRIPTS

'	departure function
0	ideal gas or standard state

+	reference state
∞	infinite dilution
','	phase
*	dimensionless
az	azeotrope
Id	ideal solution
(j)	stream, stage, phase j
L	liquid phase
sat	equilibrium conditions
t	turbulent
V	vapor phase

SUBSCRIPTS

b	bulk value or bubble point
c	value at critical conditions
d	dew point
eq	equilibrium
i, j, k	species
imp	impellor
Int	interstitial
L	liquid phase
LM	log mean value
m	per unit mass
na	not absorbed
ns	Not stripped
opt	optimum value
p	particle
r	value relative to critical value
ss	steady state
t	tower
v	value per unit volume
V	vapor phase

OVERSTRIKE

—	partial specific
~	partial molar
^	mixture value

UNDERSCORE

—	extensive variable
---	--------------------

OTHER

Δ	difference between two states
$\langle \rangle$	average value

$[\zeta]$ matrix or vector with ζ_{ij} as the element in the i th row and j th column

VECTOR

f_b body force per unit mass
 j mass diffusion flux
 J_e total flux of energy
 j_s entropy diffusion flux
 N total molar flux

q conductive flux of energy
 u_i i th column of $[u]$
 v mass average velocity
 W total mass flux

TENSORS

Φ total flux of momentum
 Π flux of momentum relative to mass average velocity

REFERENCES

- Abhaya, K., Xu, Q. Kharas, K. C., and McCarty, J. M. (2006) *Catalysis Today*, 111, 9.
- Abramowitz, M. and Stegun, I. A. (1965) *Handbook of Mathematical Functions*. New York: Dover Publications.
- Abulnaga, B. E. (2002) *Slurry Systems Handbook*. New York: McGraw-Hill.
- Aiba, S., Humphrey, A. E., and Millis, N. F. (1973) *Biochemical Engineering*. New York: Academic Press.
- Amrouche, Y., Dave, C., Gursahani, K., Lee, R., and Montemayor, L. (2002) *Chem. Eng. Prog.*, 98, 12, 54.
- Arce, A. and Blanco, M. (1998) *J. Chem. Thermodyn.*, 30, 798.
- Aris, R. (1965) *Introduction to the Analysis of Chemical Reactors*. Englewood Cliffs, NJ: Prentice Hall.
- Arkilic, E. B., Schmidt, M. A., and Breuer, K. S. (1997) *J. Microelectromech. Syst.*, 6, 167.
- Aspen Technology, Inc. (2000) User Guide for Aspen Plus 12.1, 2-03.
- Baker, R. (2001) *Membr. Technol.*, 138, 3.
- Bartholomew, C. H. and Farrauto, R. J. (2006) *AIChE J.*
- Bejan, A. (1993) *Heat Transfer*. New York: Wiley.
- Bejan, A. and Krauss, A. (2003) *Heat Transfer Handbook*. New York: Wiley.
- Berry, S. R., Rice, S. A., and Ross, J. (1980) *Physical Chemistry*. New York: Wiley.
- Bianchini, C., Meli, A., and Vizza, F. (2004) *J. Organomet. Chem.*, 689, 24, 4277.
- Bilous, O. and Amundson, N. R. (1956) *AIChE J.*, 2, 2116.
- Bird, R. B. (1957) *Chem. Eng. Sci.*, 6, 128.
- Bird, R. B., Stewart, W. E., and Lightfoot, E. N. (2002) *Transport Phenomena*. New York: Wiley.
- Boudart, M. (1968) *Kinetics of Chemical Processes*. Englewood Cliffs, NJ: Prentice Hall.
- Branan, C. R. (Ed.) (1994) *Rules of Thumb for Chemical Engineers*. Texas: Gulf Publishing.
- Brandrup, J. (2005) *Polymer Handbook*. New York: Wiley.
- Brian, P. L. T., Vivian, J. E., and Habib, A. G. (1962) *AIChE J.*, 8, 205.
- Brown, L. F., Haynes, H. W., and Manoque, V. H. (1969) *J. Catal.*, 4, 220.
- Callen, H. R. (1960) *Thermodynamics*. New York: Wiley.
- Carrott, P. J. M., Riberio Carrott, M. M. L., Cansado, I. P. P., and Nabias, J. M. V. (2000) *Carbon*, 38, 465.
- Chiang, S. H. and Toor, H. L. (1964) *AIChE J.*, 10, 398.
- Chung, T. H., Ajlan, M., Lee, L. L., and Starling, K. E. (1988) *Ind. Eng. Chem. Res.*, 27, 671.
- Clark, M. M. (1996) *Transport Modeling for Engineers and Scientists*. New York: Wiley.
- Coltters, R. and Rivas, A. L. (2004) *Powder Technol.*, 147, 34.
- Couper, J. R., Penney, W. R., Fair, J. R. and Walas, S. M. (2005) *Chemical Process Equipment: Selection and Design*. New York: Elsevier.
- Cusack, R. W., et al. (1991) *Chem. Eng.*, 98 (2), 66–76.
- Cussler, E. L. (1984) *Diffusion Mass Transfer in Fluid Systems*. Cambridge: Cambridge University Press.
- Cussler, E. L. and Moggridge, G. D. (2001) *Chemical Product Design*. Cambridge: Cambridge University Press.
- Danckwerts, P. V. (1951) *Ind., Eng., Chem.*, 43, 1460.
- Danckwerts, P. V. (1953) *Chem. Eng. Sci.*, 23, 1.
- Danckwerts, P. V. (1970) *Gas-Liquid Reactions*. New York: McGraw-Hill.

- Davis, M. E. and Davis, R. J. (2003) *Fundamentals of Chemical Reaction Engineering*. New York: McGraw-Hill.
- DeLancey, G. B. (1974) *Chem. Eng. Sci.*, 29, 2315.
- DeLancey, G. B. (1999) *Chem. Eng.*, 40.
- Denbigh, K. (1966) *Chemical Reactor Theory*. London: Cambridge University Press.
- Denbigh, K. (1971) *The Principles of Chemical Equilibrium*. London: Cambridge University Press.
- de Roode, B. M., van Beek, J., van der Padt, A., Franssen, M. C. R., and Boom, R. M. (2001) *Enzyme Microb. Technol.*, 29, 513.
- Dettman, J. W. (1962) *Mathematical Methods in Physics and Engineering*. New York: McGraw-Hill.
- Design Institute for Physical Properties (DIPPR). (2009) 801, AIChE, Knovelized update.
- Dodge, B. F. (1944) *Chemical Engineering Thermodynamics*. New York: McGraw-Hill.
- Dongari, N., Agrawal, A., and Agrawal, A. (2007) *Int. J. Heat Mass Transfer*, 50, 3411.
- Drioli, E. and Romano, M. (2001) *Ind. Eng. Chem. Res.*, 40, 1277.
- Drott, D. W. and Aris, R. (1969) *Chem. Eng. Sci.* 24, 541.
- Espenson, J. H. (1981) *Chemical Kinetics and Reaction Mechanisms*. New York: McGraw-Hill.
- Foust, A. S., Wenzel, L. A., Clump, C. W., Maus, L., and Andersen, L. (1960) *Principles of Unit Operations*. Chichester: Wiley.
- Froment, G. F. and Bischoff, K. B. (1979) *Chemical Reactor Analysis and Design*. New York: Wiley.
- Fuller, E. N., Schettler, P. D., and Giddings, J. C. (1966) *Ind. Eng. Chem.*, 58, 18.
- Gad-el-Hak, M. (2003) *Int. J. Heat Mass Transfer*, 46, 3943.
- García-Junceda, E., García-García, J. F., Bastida, A., and Fernandez-Mayoralas, A. (2004) *Bioorg. Med. Chem.*, 12, 1827–1834.
- Gates, L. E., Morton, J. R., and Fondy, P. L. (1976) *Chem. Eng.*
- Geankopolis, C. J. (2003) *Transport Processes and Separation Process Principles*. Upper Saddle River, NJ: Prentice Hall.
- Gogos, C. G. (2010) *Polymer Processing Institute, September*. Newark, NJ: New Jersey Institute of Technology.
- Green, D. W., and Maloney, J. O. (Eds.) (1997) *Perry's Chemical Engineers' Handbook*, 7th ed. New York: McGraw Hill.
- Grunberg, L. and Nissan, A. H. (1949) *Nature*, 164, 799.
- Gunn, D. J. (1987) *Chem. Eng. Sci.*, 42 (2), 363.
- Gupta, V. K., Ali, I., and Saini, V. K. (2007) *J. Colloid Interfacial Sci.*, 315, 87.
- Hadden, S. T. and Grayson, H. G. (1961) *Refiner*, 40, 207.
- Happel, J. and Jordan, D. (1975) *Chemical Process Economics*. New York: Marcel Dekker.
- Hayduk, W. and Minhas, B. S. (1982) *Can. J. Chem. Eng.*, 60, 295.
- Hayes, R. E. and Kolaczowski, S. T. (1999) *Catal. Today*, 47, 295.
- Henley, E. J. and Staffin, H. K. (1963) *Stagewise Process Design*. New York: Wiley.
- Higbie, R. (1935) *Trans. Am. Inst. Chem. Engrs.*, 35, 3659.
- Hikita, H. and Asai, S. (1964) *Int. Chem. Eng.*, 4, 332.
- Hill, C. G. (1977) *An Introduction to Chemical Engineering Kinetics and Reactor Design*. New York: Wiley.
- Hinze, J. O. (1959) *Turbulence*. New York: McGraw-Hill.
- Hirschfelder, J. O., Curtiss, C. F., and Bird, R. B. (1954) *Molecular Theory of Gases and Liquids*. New York: Wiley.
- Hougen, O. A., Watson, K. M., and Ragatz, R. A. (1954) *Chemical Process Principles: Material and Energy Balances*. New York: Wiley.
- Hu, G. and Li, D. (2007) *Chem. Eng. Sci.*, 62, 3443.
- Hvistendahl, H. S. (1964) *Engineering Units*. London: MacMillan.
- Isdale, J., MacGillivray, J. C., and Cartwright, G. (1985) *National Engineering Laboratory Reports*. East Kilbride: National Engineering Laboratory.
- Jeong, B., Hasegawa, Y., Sotowa, K., Kusakabe, K., and Morooka, S. (2003) *J. Membr. Sci.*, 211, 1165.
- Johnson, M. F. L. and Stewart, W. E. (1965) *J. Catal.*, 4, 248.
- Kadlec, B. and Pour, V. (1968) *Coll. Czech. Chem. Commun.*, 33, 2526.
- Kao, C. and Lin, W. (1999) *Fluid Phase Equilib.*, 163, 9.
- Kaplan, W. (1991) *Advanced Calculus*. Berkeley, CA: Addison-Wesley Publishing.
- Kent, J. A. (1983) *Riegel's Handbook of Industrial Chemistry*. New York: Van Nostrand Reinhold.
- Kern, D. Q. (1950) *Process Heat Transfer*. New York: McGraw-Hill Publishing.
- King, C. J. (1980) *Separation Processes*. New York: McGraw-Hill Publishing.
- Kister, H. Z. (1992) *Distillation Design*. New York: McGraw-Hill Publishing.
- Klibanov, A. M. (1986) *Chemtec*, 16, 354–359.
- Kovenkiloglu, S. and DeLancey, G. B. (1979) *Chem. Eng. Sci.*, 34, 841.
- Kramers, H. and Westerterp, K. (1963) *Elements of Chemical Reactor Design and Operation*. New York: Academic Press.
- Krauss, A., Azte, A., and Welty, J. (2001) *Extended Services Heat Transfer*. New York: Wiley.
- Lange, N. A. (1946) *Handbook of Chemistry*. Sandusky, OH: Handbook Publishers.
- Lass, H. (1950) *Vector and Tensor Analysis*. New York: McGraw-Hill Publishing.
- Latini, G., Marcotullio, F., Pierpoli, P., and Ponticciello, A. (1989) *Thermal Conductivity*. New York: Plenum Press, p. 205.
- Lee, S. T. and DeLancey, G. B. (1974) *Chem. Eng. Sci.*, 29, 2325.
- Levenspiel, O. (1999) *Chemical Reaction Engineering*. Hoboken, NJ: Wiley.
- Lloyd-George, I and Chang, T. M. S. (1995) *Biotechnol. Bioeng.*, 48, 706.
- Lucas, K. (1980) *Phase Equilibria and Fluid Properties in the Chemical Industry*. Frankfurt: Dechema, p. 573.
- Luyben, W. L. and Wenzel, L. A. (1988) *Chemical Process Analysis: Mass and Energy Balances*. Englewood Cliffs, NJ: Prentice Hall.
- Manz, A., Graber, N., and Widner, H. M. (1990) *Sens. Actuator*, 8 (1), 244.
- Mason, E. A. and Saxena, S. C. (1958) *Phys. Fluids*, 1, 361.

- McCabe, W. L., Smith, J. C., and Harriot, P. (2001) *Unit Operations of Chemical Engineering*. New York: McGraw-Hill.
- Middleman, S. (1998) *Introduction to Fluid Dynamics*. New York: Wiley.
- Nauman, E. B. (2008) *Chemical Reactor Design, Optimization, and Scaleup*. New York: Wiley.
- Onsager, L. (1931) *Phys. Rev.* 37, 405; Onsager, L. (1931) *Phys. Rev.*, 38, 2265.
- Panintrarux, C., Adachi, S., Araki, A., Kimura, Y., and Matsuno, R. (1995) *Enzyme Microb. Technol.*, 17, 32–40.
- Paul, E. L. (Ed.) (2004) *Handbook of Industrial Mixing: Science and Practice*. New York: Wiley.
- Perkins, L. R. and Geankoplis, C. J. (1969) *Chem. Eng. Sci.*, 24, 1035.
- Perlis, S. (1958) *Theory of Matrices*. Reading, MA: Addison-Wesley.
- Petersen, E. E. (1965) *Chemical Reaction Analysis*. New Jersey: Prentice Hall.
- Peters, M. S., Timmerhaus, K. D., and West, R. E. (2003) *Plant Design and Economics for Chemical Engineers*. New York: McGraw-Hill Higher Education.
- Poling, B. E., Prausnitz, J. M., and O'Connell, J. P. (2001) *The Properties of Gases and Liquids*, 5th ed. New York: McGraw-Hill.
- Rester, S. and Aris, R. (1969) *Chem. Eng. Sci.*, 24, 793.
- Ritter, A., Reisman, B., and Michniak, B. B. (2005) *Biomedical Engineering Principles*. New York: Taylor and Francis.
- Rosevear, A., Kennedy, J. F., Cabral, J. M. S. (1987) *Immobilised Enzymes and Cells*. Philadelphia: Adam Hilger.
- Rothfeld, L. B. (1963) *AIChE J.*, 9, 9.
- Ruthven, D. M. (1984) *Principles of Adsorption and Adsorption Processes*. New York: Wiley.
- Ryon, A. D., Daly, F. L., and Lowrie, S. (1959) *Chem. Eng. Progr.*, 55 (10), 70.
- Sandler, S. I. (1999) *Chemical and Engineering Thermodynamics*. New York: Wiley.
- Sandler, S. and Mason, E. R. (1968) *Chem. Phys.*, 48 (28), 73.
- Satterfield, C. N. (1970) *Mass Transfer in Heterogeneous Catalysis*. Cambridge, MA: MIT Press.
- Satterfield, C. N. and Cadle, P. J. (1968) *Ind. Eng. Chem. Fundam.*, 7, 202.
- Schendel, R. L. (1993) *Oil Gas J.*, 91 (39), 63–68.
- Schweitzer, P. A. (Ed.) (1979) *Handbook of Separation Techniques for Chemical Engineers*. New York: McGraw-Hill.
- Scott, D. S. and Dullien, F. A. L. (1962) *AIChE J.*, 8, 113.
- Seader, J. D. and Henley, E. J. (2006) *Separation Process Principles*. New York: Wiley.
- Senol, A. (2005) *J. Chem. Thermodyn.*, 32, 1104.
- Sherwood, T. K., Pigford, R. L., and Wilke, C. R. (1975) *Mass Transfer*. New York: McGraw-Hill.
- Silla, H. (2003) *Chemical Process Engineering*. New York: Marcel Dekker.
- Slech, G. (1980) *Phys. Rev. B.*, 22, 6.
- Smith, J. M. (1981) *Chemical Engineering Kinetics*. New York: McGraw Hill.
- Smith, R. (2005) *Chemical Process Design and Integration*. New York: Wiley.
- Smith, J. M., van Ness, H. C., and Abbott, M. M. (2005) *Introduction to Chemical Engineering Thermodynamics*. New York: McGraw-Hill Higher Education.
- Speight, J. G. (2002) *Chemical Process and Design Handbook*. New York: McGraw-Hill.
- Straathof, A. J., Panke, S., and Schmid, A. (2002) *Curr. Opin. Biotechnol.*, 13, 548–556.
- Tester, J. S. and Modell, M. (1997) *Thermodynamics and Its Applications*. Upper Saddle River, NJ: Prentice Hall.
- Toor, H. L. and Marchello, J. M. (1958) *AIChE J.*, 4, 97.
- Tortoriello, V. and DeLancey, G. B. (2007) *J. Ind. Microbiol. Biotechnol.*, 34, 475.
- Towler, G. and Sinnott, R. (2008) *Chemical Engineering Design*. New York: Elsevier.
- Treybal, R. (1980) *Mass Transfer Operations*. New York: McGraw-Hill.
- Turton, R., Baile, R. C., Whiting, W. B., and Shaeiwitz, A. (2003) *Analysis, Synthesis, and Design of Chemical Processes*. Upper Saddle River, NJ: Prentice Hall.
- Ullmann, D. G. (1994) *Encyclopedia of Chemical Technology*, English ed. Weinheim, FRG: Verlag, Chemie.
- Van Balken, J. A. M., Kamphuis, J., and Jenkins, R. O. (1997) In: van Balken, J. A. M. and Currell, B. (Eds.), *Biotechnological Innovations in Chemical Synthesis*. Oxford: Butterworth-Heinemann.
- Van Rantwijk, F., van Woudenberg Oosterom, M., and Sheldon, R. A. (1999) *J. Mol. Catal., B* 6, 511.
- Van Welsenaere, R. J. and Froment, G. F. (1970) *Chem. Eng. Sci.*, 25, 1503.
- Verma, S. and DeLancey, G. B. (1975) *AIChE J.*, 21, 96.
- Vignes, A. (1966) *Ind. Eng. Chem. Fundam.*, 5, 189.
- Vision 2020 Catalyst (Workshop) Report. (1997) Joint report of the American Chemical Society, the American Institute of Chemical Engineers, the American Manufacturers Association, the Council for Chemical Research, the Synthetic Organic Chemicals Manufacturers Association. Available from American Chemical Society, Government Relations and Science Policy.
- Wakao, N. and Funazkri, T. (1978) *Chem. Eng. Sci.*, 33, 1375.
- Walas, S. M. (1985) *Phase Equilibria in Chemical Engineering*. Stoneham, MA: Butterworth Publishers.
- Wassermann, G. (1965) *Diels-Alder Reactions: Organic Background and Physicochemical Aspects*. Berlin: Springer-Verlag.
- Wehner, J. F. and Wilhelm, R. H. (1956) *Chem. Eng. Sci.*, 6, 89.
- Whitman, W. G. (1923) *Chem. Met. Eng.*, 29, 147.
- Whitwell, J. R. and Toner, R. K. (1969) *Conservation of Mass and Energy*. Waltham, MA: Academic Press, Blaisdell Publishing.
- Wijmans, J. G. and Baker, R. W. (1995) *J. Membr. Sci.*, 107, 1.
- Woods, W. R. (1995) *Process Design and Engineering Practice*. Englewood Cliffs, NJ: Prentice Hall.
- Yaws, C. L. (1999) *Chemical Properties Handbook*. New York: McGraw-Hill.

- Yaws, C. L. (2003) *Yaws' Handbook of Thermodynamic and Physical Properties of Chemical Compounds*. Online version: Knovel.
- Yaws, C. L., Prasad, K., and Chaitanya, G. (2005) *Yaws' Handbook of Antoine Coefficients for Vapor Pressure*. Online version: Knovel.
- Zhao, Y. and DeLancey, G. B. (2000) *Biotechnol. Bioeng.*, 69, 639.
- Zlokarnik, M. (1991) *Dimensional Analysis and Scale-up in Chemical Engineering*. New York: Springer-Verlag.
- Zwietering, T. (1959) *Chem. Eng. Sci.*, 11, 1.

INDEX

- Absorption and stripping
 - multistage
 - binary gas absorption, 184
 - column efficiency, 196
 - diameter, 197
 - graphical methods, 186
 - height, 197
 - heuristics, 199
 - liquidstripping, 191
 - multicomponent, 194
 - tray tower, 185
 - singlestage, 126–129
- Acrylic acid process
 - catalysis, 7
 - downstream processing, 16
 - feed section, 8
 - process definition, 5
 - reactor section, 12
- Activity, 117
- Adiabatic operation, 72
- Adsorbents, 152
- Adsorption,
 - gas, 154
 - liquid, 157
 - singlestage, 151
- Alkylglucosides, 23
- Availability and lost work, 80
 - for a distillation tower, 82
 - for a shell and tube exchanger, 81
- Axial flow in pipes and tubes, 280
- Balance equations
 - reduction to scalar equations, 270
- Batch reactor, isothermal
 - gas phase, 172
 - liquid phase, 169
 - mass balance, 168
- Boundary conditions, 269
- Characterization of porous solids, 154
- Chemical processing systems
 - active units, 29
 - definition, 28
 - driving force, 3
 - rate processes, 4
 - equilibrium, 4
 - steady state, 3
 - system definition for heat duty and flowrate calculation, 64
- Chemical reaction equilibrium, 174
 - equilibrium constant as a function of temperature, 174–176
 - minimization of the Gibbs function, 174
 - standard Gibbs free energy and enthalpy change for the reaction, 174–175
- Conduction in solids
 - composite walls, 325
- Continuous stirred tank reactor (CSTR) 160. *See also* stirred tank design
 - autothermal operation; stability of steady states, 166
 - energy balance, 166
 - heuristics, 168
 - molar flows in terms of reaction extents, 160
 - reaction rate representation, 160
 - reactor volume for an irreversible, first, second, and arbitrary order reaction in a dilute reactant, 161
 - temperature selection, 163
 - volume flow and molar concentrations for constant density, 160
- Conversion factors, 406
- Coordinate systems, 414
- Corrections to mass transfer coefficients,
 - chemical reaction, 360–365
 - equimolar counter diffusion, 360
 - stagnant film, 358
- Database for acrylic acid process, 409
- Database construction, 24
- Departure functions, 55. *See also* Vapor-liquid equilibrium
- DePriester charts, 126
- Diffusion and average velocities, 244
- Diffusion models for porous solids, 307
 - effective diffusivity of porous catalysts, 307
 - parallel pore model, 309
 - tortuosity factor, 309
- Diffusivities, estimation, 261
- Dimensionless numbers and characteristic times, 272
- Distance metrics, 416. *See also* Unit vectors.

- Distillation, 200
 - efficiency and dimensions, 213
 - energy requirements, 212
 - equipment, 201
 - feed tray analysis, 203
 - graphical construction, 205–20
 - heuristics, 217
 - high purity products, 210
 - intersection of operating lines, 206
 - summary of calculations, 214
- Divergence theorem of Gauss, 414
- Effectiveness factor
 - closed pore, 311
 - catalyst particle, 314
 - irreversible reaction with heat effect, 328
- Energy balances
 - neutralization of acids, 74
 - without reaction, 64
 - with single reaction in an ideal solution, 70
- Energy flux, conduction, 250
- Entropy change, 64
 - for an isothermal liquid pump, 64
 - calculation of minimum work required or maximum work produced, 64
- Enzymatic systems, 21
 - examples of industrial processes, 23
- Equations of state 57. *See also* Vapor-liquid equilibrium
- Equilibrium, 133
- Extent of reaction, 40
- Falling film-short contact times heat transfer 330. *See also* Wetted wall tower
- Flash vaporization, 133
 - common problem specifications, 134
 - mass and energy balances, 133
- Flooding velocity in packed towers, 381
 - tower diameter and pressure drop, 381
- Friction factor, 281
- Fugacity
 - mixture, 114
 - pure component, 112
- Gibbs-Duhem equation, 55
- Heat exchangers
 - double pipe, 387
 - shell and tube, 390
- Heat transfer coefficients
 - analogy with mass transfer, 384
- Henry's Law constants, 128
- Heterogeneous catalysis, 311
 - thermal effects, 327
- Ideal gas mixture, 59
- Independent reactions, 47
 - in the acrylic acid process, 29
 - construction, 48
 - selection, 48
 - tests for, 47
- Kinetics
 - heterogeneous catalytic, 256
 - homogeneous, 255
 - suspensions – enzyme kinetics, 257
- Liquid-liquid extraction in a single stage, 145–151
 - data collection and representation, 146
 - equilibrium in ternary systems, 145
 - interpolation, 146
 - solvent selection, 146
- Liquid-liquid multistage extraction, 221
 - cross flow cascade, 221
 - countercurrent operation, 222
 - equipment, 232
 - heuristics, 234
 - mixer-settler units, 214
 - tower dimensions and efficiency, 233
- Mass transfer coefficients, 335. *See also* Membranes
 - controlling resistance, 338
 - correlation, 340
 - film-penetration theory, 335
 - film theory, 338
 - fixed bed, 342
 - measurement, 339
 - penetration theories, 337
 - pipes, 345
- Mechanical energy
 - flow of liquids in piping systems, 89
 - macroscopic balance, 88
 - optimum pipe diameter, 89
 - pump sizing-system and pump characteristic curves, 93
- Membranes, 296
 - gas separation, 298
 - material balance for generic membrane, 297
 - overall mass transfer coefficient for porous and composite, 303
- Microchannel, model of gas flow, 290
 - momentum and mass balances, 290
 - axial velocity distribution, 291
 - pressure distribution, 292
- Microscopic Conservation of Energy 252. *See also* Boundary conditions
- Microscopic entropy balance and flux expressions, 254. *See also* Boundary conditions
- Microscopic Linear and angular momentum balance, 252. *See also* Boundary conditions
- Microscopic mass balance, 251–252
 - reduction to laminar flow in cylindrical coordinates, 418
- Microscopic mechanical energy equation
 - from continuity and momentum equations, 414
- Mixing of nonideal liquids
 - heat of solution, 60
 - mixing two liquid streams at different temperatures and concentrations, 68
 - partial molar quantities, 68
- Mixture rule, 148
- Mixtures, 59
 - ideal solution, 60
 - nonideal gas mixtures, 60
- Momentum flux: stress tensor, 249
- Momentum, macroscopic, balance, 86
- Moving boundary problem, 332
- Multistage chemical reactors, 235–241
 - comparison of CSTR with batch and plug flow reactors, 235
 - number of stages for given conversion, 236
 - optimal temperature programs for single and multiple reactions CSTR stages, 239
 - staged fixed bed converters (PFRs) for exothermic gas phase reactions, 238
- Nonturbulent isothermal momentum transfer, 276
- Packed towers
 - gas absorption, 34
 - mass balances, 351
 - mass transfer correlations, 350
- Particles, drops, and bubbles in agitated systems, 346
- Periodic table, 405
- Pressure drop
 - compressors, 372
 - in conduits, 368
 - in fixed beds, 375
 - turbulent flow of gases in pipelines, 369
- Reactor
 - constant wall temperature, 395
 - laminar flow, 282
 - multitubular, 395
 - operational considerations, 398
 - with catalytic walls, 320
- Reference state
 - for reactive systems, 71

- for unreactive systems, 66
- Residence time distributions, 95
 - bypassing and dead space, 99
 - definitions and properties, 96
 - macro and micro mixing, 99
 - maximum mixedness, 99
 - step input to a completely mixed system, 99
 - tracer output from arbitrary system, 95
- Reverse osmosis, 301
- Scalar processes, 255
- Slit flow: extrusion of
 - plastics through narrow dies, 276
- Single stage separation operations
 - absorption, 151
 - adsorption, 152–157
 - flash vaporization, 133
 - liquid-liquid extraction, 145
- Standard heat of reaction, 71
- Stirred tank design, 99
 - diameter and impeller specifications, 99
- Substantial derivative, 282
- Superficial velocities, 248
- Terminal velocities
 - in Newtonian fluids, 377
 - in solid suspensions, 377
- Thermal conductivities, estimation, 261
- Thermodynamic models, 78
- Turbulence, 265
- Turbulent flux expressions, 267
- Unit vectors, 416. *See also* Distance
 - metrics
 - derivatives, 417
- Vapor – liquid equilibrium, 111
 - activity coefficient method, 115
 - boiling points and azeotropes, 111–112
 - bounds on bubble and dew points, 135
 - calculation of component and mixture fugacities, 113–115
 - coefficients, 120
 - definition of activity and reference state, 117
 - Depriester charts, 125
 - determination of model parameters from VLE data, 121–125
 - equation of state method, 112
 - estimation, 112
 - evaluation of equilibrium or distribution coefficient, 115
 - evaluation of reference state fugacity, 119
 - excess Gibb's free energy, 120
 - graphical representation in binary systems, 135
 - models of excess free energy in terms of activity, 119
 - representative equations of state, 113
 - summary of equilibrium expressions, 116
 - summary of expressions, 125
- Vector processes: diffusion and conduction, 260
- Viscosity estimation, 265
- Viscous momentum flux, 261
- Volume flow, 255
- Wetted wall towers, 283
 - chemical absorption in, 319
 - physical absorption in, 318
 - short contact time, 318